UNITED STATES DEPARTMENT OF THE INTERIOR

GEOLOGICAL SURVEY

NATIONAL EARTHQUAKE HAZARDS REDUCTION PROGRAM, SUMMARIES OF TECHNICAL REPORTS VOLUME XXIV

Prepared by Participants in

NATIONAL EARTHQUAKE HAZARDS REDUCTION PROGRAM

July 1987

OPEN-FILE REPORT 87-374

Menlo Park, California

1987

INSTRUCTIONS FOR PREPARATION OF SUMMARY REPORTS

1. Use 8 1/2" x 11" paper for both text and figures.
2. Leave at least 1" wide margins at top, sides and bottom.
3. Type headings at top of first page. Headings should include:
    a. Project title
    b. Contract, grant or project number
    c. Name of Principal Investigator(s)
    d. Name and address of institution
    e. Telephone number(s) of Principal Investigator(s)
4. Original copies of text and figures are required. No xerox copies.
5. Type figure captions on the same page as the figure.
6. Only type on one side of the paper.
7. Type all text single spaced.
8. Do not number pages.
9. Do not use staples.
10. All figures must be in black and white. No color figures (color, weak or grey lines will not photo-reproduce).

UNITED STATES
DEPARTMENT OF THE INTERIOR
GEOLOGICAL SURVEY

NATIONAL EARTHQUAKE HAZARDS REDUCTION PROGRAM, SUMMARIES OF TECHNICAL REPORTS VOLUME XXIV

Prepared by Participants in

NATIONAL EARTHQUAKE HAZARDS REDUCTION PROGRAM

Compiled by

Muriel L. Jacobson

Thelma R. Rodriguez

The research results described in the following summaries were submitted by the investigators on October 16, 1986 and cover the 6-months period from October 1, 1986 through May 31, 1987. These reports include both work performed under contracts administered by the Geological Survey and work by members of the Geological Survey. The report summaries are grouped into the three major elements of the National Earthquake Hazards Reduction Program.

Open File Report No. 87-374

CONTENTS

Earthquake Hazards Reduction Program

Southern California Seismic Arrays

Cooperative Agreement No. 14-08-0001-A0257

Clarence R. Allen and Robert W. Clayton
Seismological Laboratory, California Institute of Technology
Pasadena, California 91125 (818-356-6912)

Investigations

This semi-annual Technical Report Summary covers the six-month period from 1 October 1986 to 31 March 1987. The Cooperative Agreement's purpose is the partial support of the joint USGS-Caltech Southern California Seismographic Network, which is also supported by other groups, as well as by direct USGS funding to its own employees at Caltech. According to the Agreement, the primary visible product will be a joint Caltech-USGS catalog of earthquakes in the southern California region; quarterly epicenter maps and preliminary catalogs have been submitted as due during the Agreement period. About 250 preliminary catalogs are routinely distributed to interested parties.

Results

Figure 1 shows the epicenters of all cataloged shocks that were located during the six-month recording period. This was a relatively quiet period, and the preliminary data processing is virtually complete. Some of the seismic highlights of this period were:

Number of earthquakes fully or partially processed: 4731
Number of earthquakes of M = 3.0 and greater: 138
Number of earthquakes of M = 4.0 and greater: 6
Number of earthquakes of M = 5.0 and greater: 2
Largest event within network area: M = 5.4 (7 February, Cerro Prieto area of northern Baja California, Mexico)
Number of earthquakes reported felt: 40
Number of earthquakes for which systematic telephone notification to emergency-response agencies was made: 4

During the first part of the reporting period, aftershocks from the three July 1986 sequences continued at a high level. Aside from these three areas (Fig. 1), the activity was very typical of long-term southern California seismicity. The first three months of 1987 were relatively quiet, although occasional aftershocks continued.

The events of magnitude 4.0 and greater were as follows:

1 October	M = 4.0	Aftershock of 13 July Oceanside shock
9 October	4.3	Aftershock of 21 July Chalfant Valley shock
15 October	4.7	Aftershock of 8 July North Palm Springs shock
29 October	4.1	South of San Diego
7 February	5.4	Northern Baja California, Mexico
14 February	5.1	Coalinga area

The 9 October event in Chalfant Valley and the 14 February event near Coalinga occurred outside of our official coverage area but have been included in the catalog nevertheless. Notification calls were not made for these events.

Data processing efforts continued in an effort to finish the backlog created by the July 1986 sequences. By the end of the reporting period, all of 1986 data except that for September had undergone preliminary processing. This routine analysis includes interactive timing of phases, locations of hypocenters, calculations of magnitudes, and preparation of the final catalog using the CUSP analysis system. A 6-week backlog in November and December 1985, created during a switch of computer systems, remains to be cleared up.

This 6-month reporting period saw the transfer of about 40% of the network from leased telephone-line telemetry to a USGS-operated microwave system. It remains to be seen what effect this change may have on the recording and processing of array data.

Publications

Bent A., and Kanamori, H., 1986, Indian Wells Valley earthquake swarm: 1981-1983 [abstract]: EOS, v. 67, p. 1084-1085.

Given, D. D., Norris, L. M., Jones, L. M., Hutton, L. K., Johnson, C. E., and Hartzell, S., 1986, The Southern California Network Bulletin, January-June 1986: U.S. Geol. Survey Open-File Rept. 86-598.

Given, D. D., 1986, Master event relocations of the North Palm Springs earthquake sequence of July 1986 [abstract]: EOS, v. 67, p. 1089.

Given, D. D., Koesterer, C. L., and Hutton, L. K., 1987, Survivability of the Caltech-USGS seismic network in the event of a major earthquake in southern California [abstract]: Seismol. Research Letters, v. 58, p. 13.

Gross, S. J., and Jones, L. M., 1987, Characteristics of earthquake clusters in southern California [abstract]: Seismol. Research Letters, v. 58, p. 21.

Hauksson, E., and Saldivar, G. V., 1986, The 1930 Santa Monica and the 1979 Malibu, California earthquakes: Seismol. Soc. America Bull., v. 76, p. 1542-1559.

Ho-Liu, P., Kanamori, H., and Clayton, R., 1986, Amplitude tomography: Theory and applications [abstract]: EOS, v. 67, p. 1098.

Hutton, L. K., Allen, C. R., Given, D. D., Johnson, C. E., and Jones, L. M., 1986, DNAG summary of southern California seismicity [abstract]: EOS, v. 67, p. 1235.

Hutton, L. K., and Johnson, C. E., 1987, Routine coda decay measurements from the southern California network [abstract]: Seismol. Research Letters, v. 58, p. 28.

Johnson, C. E., and Hutton, L. K., 1986, A tectonic model for the Imperial Valley and its relation to seismic risk of the southern San Andreas fault [abstract]: EOS, v. 67, p. 1200.

Jones, L. M., Given, D. D., Hutton, L. K., and Allen, C. R., 1986, The North Palm Springs, California, earthquake sequence of July 1986 [abstract]: EOS, v. 67, p. 1089.

Jones, L. M., Hutton, L. K., Given, D. D., and Allen, C. R., 1986, The North Palm Springs earthquake sequence of July 1986: Seismol. Soc. America Bull., v. 76, p. 1830-1837.

Magistrale, H., and Kanamori, H., 1986, Changes in NTS seismograms in the source region of the North Palm Springs earthquake of 7/8/86 [abstract]: EOS, v. 67, p. 1090.

Michael, A. J., and Jones, L. M., 1986, Stress fluctuations due to the July 8, 1986, North Palm Springs earthquake [abstract]: EOS, v. 67, p. 1090.

Nicholson, C., Wesson, R. L., Given, D., Boatwright, J., and Allen, C. R., 1986, Aftershocks of the 1986 North Palm Springs earthquake and relocation of the 1948 Desert Hot Springs earthquake sequence [abstract]: EOS, v. 67, p. 1089-1090.

Nicholson, C., 1987, Seismic slip on the southern San Andreas fault: 1948 and 1946 [abstract]: Seismol. Research Letters, v. 58, p. 14.

Phelps, S., and Kanamori, H., 1987, Seismicity in the Banning area before the 1986 North Palm Springs earthquake [abstract]: Seismol. Research Letters, v. 58, p. 21.

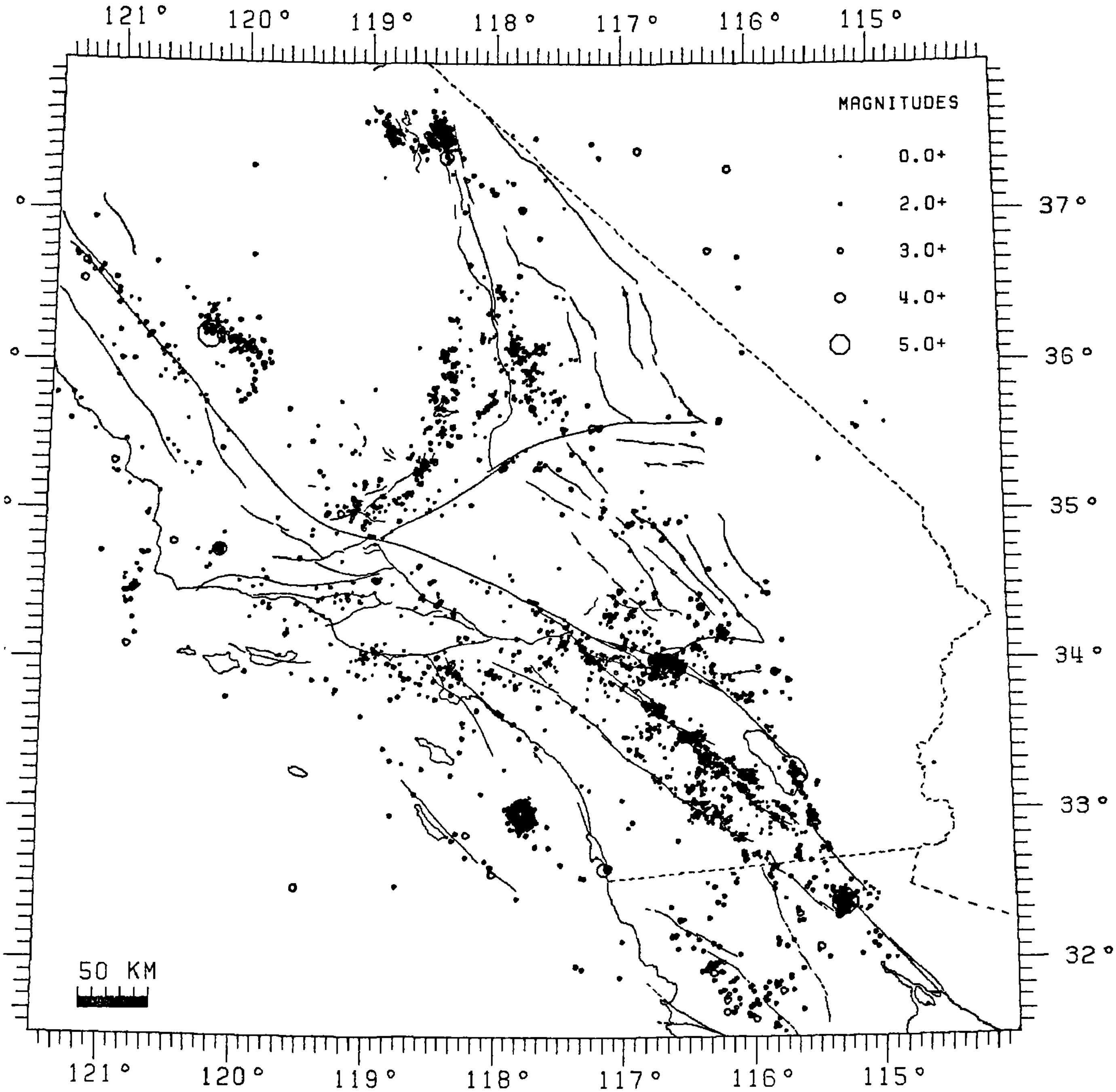

Fig. 1.--Epicenters of larger earthquakes in the southern California region, 1 October 1986 to 31 March 1987.

Regional Seismic Monitoring Along The Wasatch Front Urban Corridor And Adjacent Intermountain Seismic Belt

14-08-0001-A0265

W. J. Arabasz, R.B. Smith, J.C. Pechmann, and E.D. Brown
Department of Geology and Geophysics
University of Utah
Salt Lake City, Utah 84112
(801)581-6274

Investigations

This contract supports "network operations" (including a computerized central recording laboratory) associated with the University of Utah's 80-station regional seismic telemetry network. USGS support focuses on the seismically hazardous Wasatch Front urban corridor of north-central Utah but also encompasses neighboring areas of the Intermountain seismic belt (ISB). Primary products of this USGS contract are quarterly earthquake catalogs and a semi-annual data submission, in magnetic-tape form, to the USGS Data Archive.

Results

1. Network Seismicity

Figure 1 shows the epicenters of 273 earthquakes ($M_L \leq 3.7$) located in part of the University of Utah study area designated the "Utah region" (lat. 36.75°-42.5°N, long. 108.75°-114.25°W) during the six-month period October 1, 1986 to March 31, 1987. The seismicity includes eleven shocks of magnitude 3.0 or greater, several areas of spatial clustering, and ten felt events. The epicenters shown in Figure 1 reflect typical earthquake activity scattered throughout Utah's main seismic region.

The two largest earthquakes during this time period, both M_L 3.7, occurred on February 25 and March 5, 1987, and were located respectively 42 km WNW of Logan in northern Utah and 90 km west of Vernal in eastern Utah. The northern earthquake was reported felt 17 km away in Tremonton, Utah, and other areas of Box Elder County. Three felt earthquakes of about the same magnitude originated in the same source area on October 29, October 31, and December 31, 1987. The March 5 earthquake was felt in areas in and about Duchesne within the Uinta basin.

The source zone of the February 25 shock near Tremonton became active at the end of September 1986, and it generated 78 locatable earthquakes during the report period, including four felt events and five events greater than magnitude 3.0. As part of a special study of this source zone undertaken jointly by the University of Utah Seismograph Stations and the

Utah Geological and Mineral Survey, three temporary telemetry stations were recently installed within 5 km of the localized source.

2. Special Aftershock Study

Figure 2 illustrates results of a special study of an earthquake sequence ($M_L \leq 4.4$) that occurred March 24-31, 1986, in the vicinity of late Quaternary fault scarps in Japanese Valley near the southern end of the Wasatch fault (Brown et al., 1986). A total of 47 earthquakes were located using the permanent regional network and an 8-station portable array deployed March 26-31. The data typify the problematical correlation with first-order faults. Although epicenters cluster in the vicinity of the Japanese Valley graben (Figure 2a), foci are scattered in cross section and do not define a single rupture plane (Figure 2b). Eight single-event focal mechanisms, including that for the main shock (Figure 2c), imply oblique normal slip on planes of moderate dip. The seismicity predominates above a regional detachment, consistent with a working hypothesis (Arabasz and Julander, 1986, GSA Spec. Paper 208) that background seismicity in central Utah is primarily located in the shallow upper crust. Of three fault geometries considered, that involving an antithetic fault system with the main shock rupture fault dipping westward is most consistent with the observations—assuming that seismicity did not occur entirely on secondary fractures not simply expressed in the surface geology.

Reports and Publications

Brown, E.D., Utah earthquake activity, Wasatch Front Forum, v. 3, no. 1, p. 6, 1986.

Brown, E.D., Utah earthquake activity, April through June, 1986, Survey Notes, v. 20, no. 2, p. 10, 1986.

Brown. E.D., W. J. Arabasz, I. Bjarnason, and K. Quigley, The March 1986 M_L 4.4 Japanese Valley, Utah, earthquake sequence: A type-case study for central Utah, EOS Trans. Am. Geophys. Union, v. 67, no. 44, p. 1107.

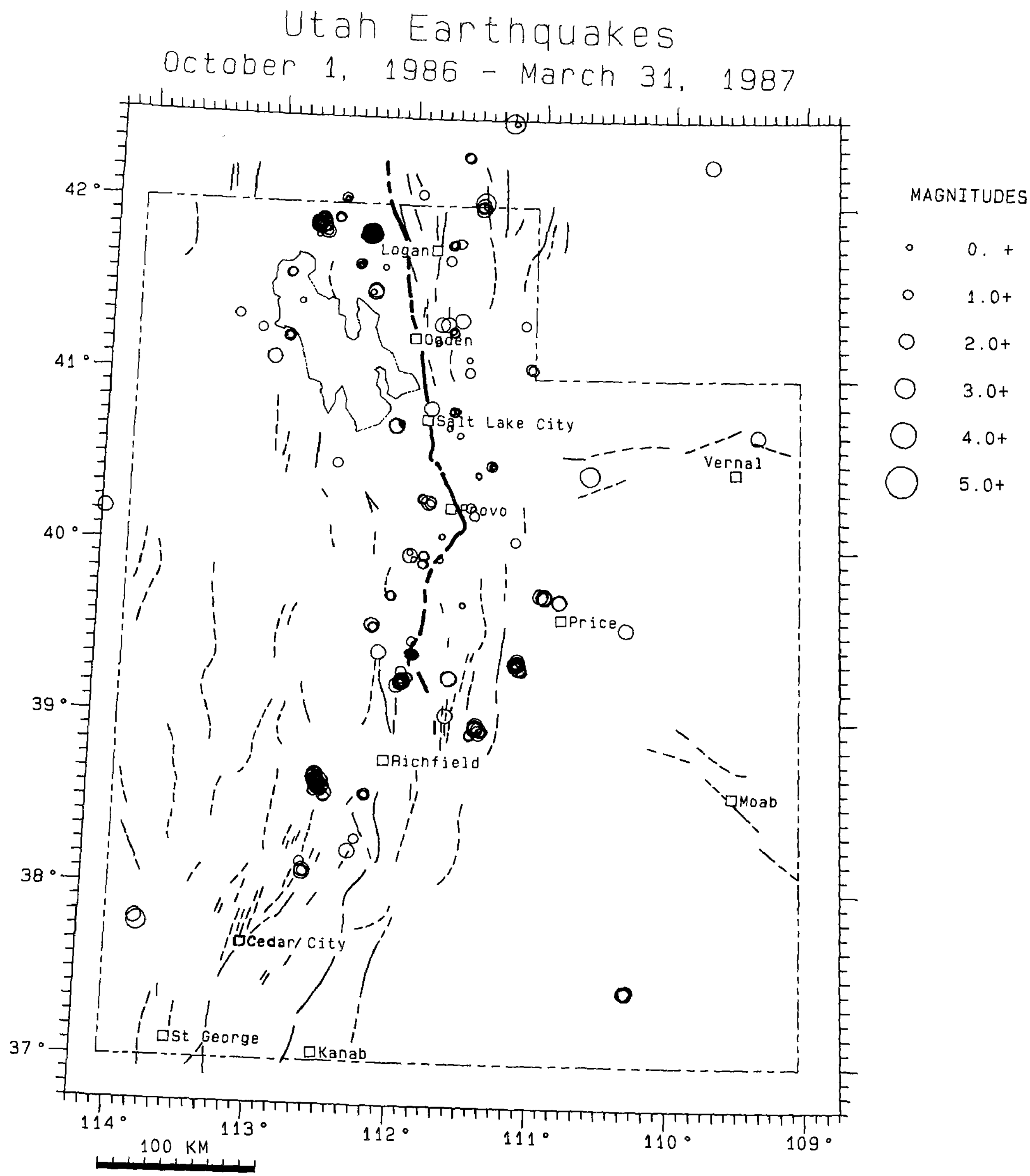
Utah Earthquakes
October 1, 1986 - March 31, 1987
MAGNITUDES
0. +
1.0+
2.0+
3.0+
4.0+
5.0+
42°
41°
40°
39°
38°
37°
114°
113°
112°
111°
110°
109°
100 KM
Logan
Ogden
Salt Lake City
Vernal
Provo
Price
Richfield
Moab
Cedar City
St George
Kanab

Figure 1

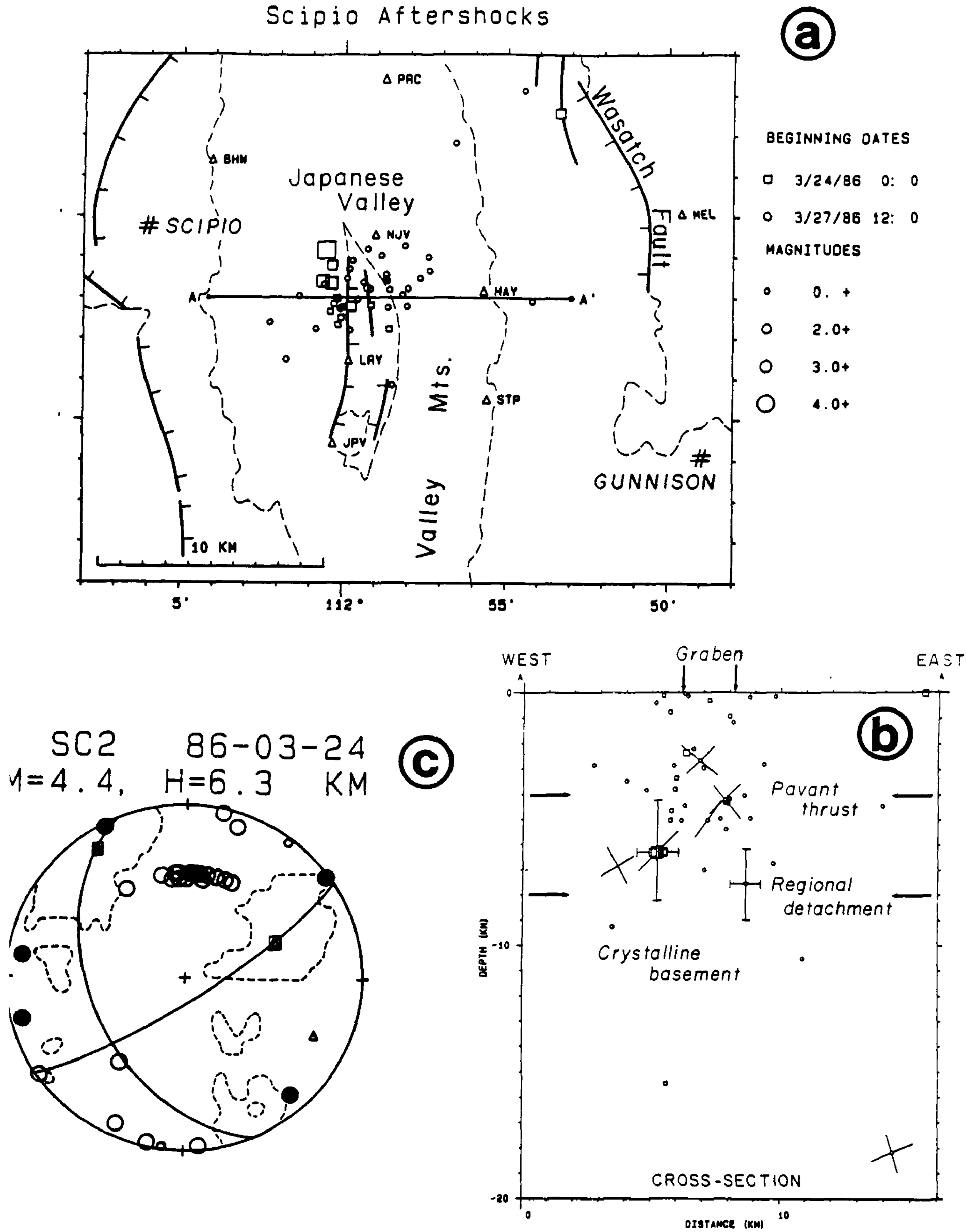

Figure 2. (a) Epicenter map, (b) cross section, and (c) main shock lower-hemisphere focal mechanism (open circles, dilatations) for a March 1986 earthquake sequence near the southern Wasatch fault (Brown and others, 1986), illustrating typical problematical correlation with first-order faults.

Seismological Data Processing

9930-03354

Barbara Bekins and Thomas Jackson

Branch of Seismology
U.S. Geological Survey
345 Middlefield Rd. MS 977
Menlo Park, California, 94025
(415) 323-8111 ext. 2965

Investigations

Data processing, mathematical modeling, electronic communications, and word-processing, using digital computers are now an integral part of seismological research. The purpose of this project is to provide for general purpose and specialized computer systems required by the branch of Seismology and its research collaborators. Some systems are required to meet general computing needs of scientists in the earthquake prediction program. Other specialized systems monitor earthquakes in northern and central California in real-time around the clock or perform specific data acquisition and processing tasks. Lately, there is an increasing need for networking facilities to transfer data, programs, and electronic mail between computers. The project goals have thus expanded to include addressing these networking needs.

To meet the stated project goals, this project has responsibility for maintaining and enhancing existing computer systems and networks in addition to planning and purchasing new systems. Existing systems include a PDP 11/70 UNIX system, a VAX 750 VMS system, one Data General Eclipse system, a Motorola 68020 UNIX system, a VAX 785 VMS system, and two PDP 11/44 RSX systems. These systems presently perform a variety of functions such as digitizing of analog tapes, real-time monitoring of Northern and Central California seismicity, general purpose research computing, and word processing. All of these systems are connected via various networking schemes including Ethernet, phone links to other sites, and dedicated direct connections. This project is also responsible for assessing the need for new network connections, selecting appropriate hardware, and adding and maintaining connections.

Recent work has focused on five main efforts. The first is enhancing performance of the VAX 750 system to handle increased waveform data anticipated as a result of the Parkfield Prediction Experiment. The second is migrating users and real-time monitoring functions from the PDP 11/70 UNIX system to the new Integrated Solutions Motorola 68020 UNIX system. The third is networking the VMS VAX systems and the UNIX systems on ethernet. The fourth is planning for uninterrupted data processing and real-time monitoring while asbestos is removed from the beams in the building. The fifth is conversion of the existing terminal communications lines to the newly installed voice and data phone system.

Results

The effort to enhance the performance of the VAX 750 VMS system is nearly completed. Additional memory and more efficient terminal communication devices were installed. Additional disk space totaling 1.1 billion bytes was also installed. Further efforts will focus on enhancing the processor either by adding third party hardware or by purchasing another VAX.

The migration of users and programs from the PDP 11/70 UNIX system to the Integrated Solutions system is nearly complete. At this point about 75 percent of the users and programs have been moved. The system is still performing very well under this load with an average of six simultaneous users. A laser printer was purchased for the system and software which formats equations, tables, text and graphics for output to the printer was installed. Output destined for the printer may be previewed on the graphics monitor before printing. It is anticipated that the PDP 11/70 system will be retired within the next six months.

The networking of the VMS VAX systems and the UNIX systems is complete. From the VMS VAX 785, VMS VAX 750, and the two new Seismology and Tectonophysics UNIX systems, users may request a connection and login via Ethernet to the other systems. File transfers may also be requested to or from a remote machine. In the next month, an electronic mail facility which will provide electronic mail between the UNIX and VMS systems via the Ethernet will be installed. Other future plans include integrating the two UNIX systems to allow transparent remote file access between the two systems, and incorporating various personal computers into the network.

The removal of asbestos from the computer room ceiling is close to completion. Work on the rest of the building will continue for the next seven months. This project is providing terminal connections as needed to computer users displaced by the work.

Installation of the new data and voice phone system is in progress. Migration of the existing terminal communications lines to the new phone system will be completed in the next few months.

Earthquake Prediction Research in the Anza-Coyote Canyon Gap

14-08-0001-21295

Jonathan Berger
Institute of Geophysics and Planetary Physics
Scripps Institution of Oceanography
University of California, San Diego
La Jolla, CA 02193
(619) 534-2889

We have been developing a number of new spectral analysis techniques to apply to high frequency seismic records. The large dynamic range digital recordings from the three component instruments in the Anza Telemetered Seismic Array have provided data which is of high enough quality to warrant the use of these more sophisticated methods of analysis. Records from the Anza array have therefore been used in our investigations.

The methods which we have been developing are all based on the use of several orthogonal data tapers which minimize spectral leakage (originally suggested by D. J. Thomson, Spectral estimation and harmonic analysis, *Proc. IEEE,* Vol. 70, No. 9, 1982). As using several orthogonal data tapers makes fuller use of the data, multiple taper spectral estimation is superior to conventional single taper spectral analysis, especially when applied to short record segments containing transient signals such as seismic phases.

A segment of the record is multiplied by several orthogonal data tapers, creating several time series from one piece of data. A discrete Fourier transform is applied to each of these tapered time series, creating several "eigenspectra". These eigenspectra are recombined to form more reliable estimates of the true spectrum. Our comparisons of the method with conventional single taper analysis indicate that this multiple taper analysis allows one to more accurately estimate the seismic source spectrum, along with its major features such as corner frequency and seismic rolloff.

We have also formed a multitaper estimate of the spectral density matrix of a given record segment. Analysis of the eigenstructure of this matrix allows us to estimate the polarization as a function of frequency for the wave motion recorded by the three-component seismometers in the Anza array. Preliminary analysis suggests that geological structure in the neighborhood of each instrument strongly contributes to the character of the polarization seen at each site. This promises to be a powerful method for extracting more detailed information from seismic records.

I-1

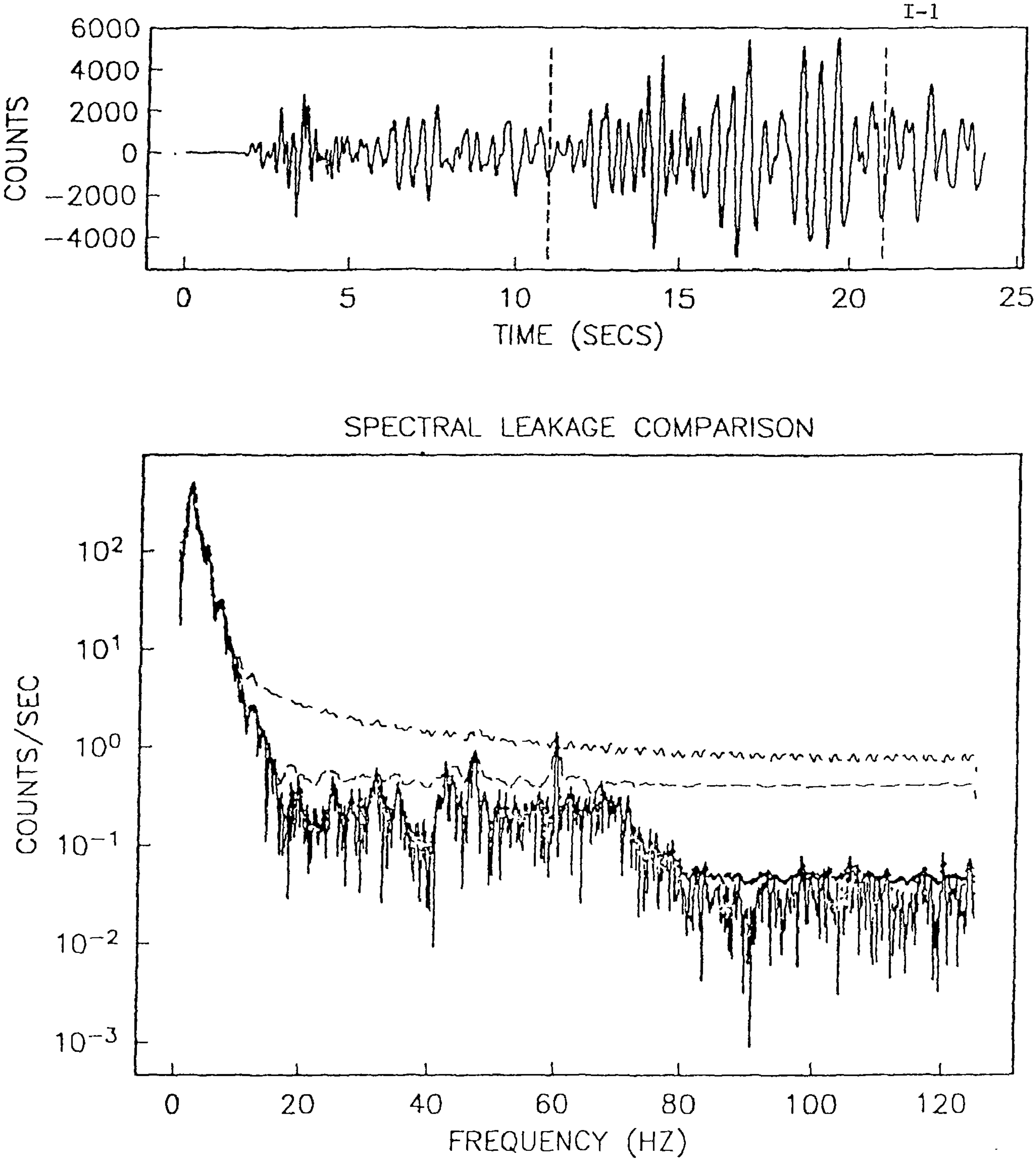

Spectra leakage comparison for vertical seismogram fron N.T.S. explosion 412 km distant. The Hanning tapered spectrum (asterisks) and the multitaper spectrum (solid line) resolve the seismic signal (0 Hz—02 Hz), ground noise (20 Hz—60 Hz).

Central Aleutian Islands Seismic Network

Agreement No. 14-08-0001-A0259

Selena Billington and Carl Kisslinger
Cooperative Institute for Research in Environmental Sciences
Campus Box 449, University of Colorado
Boulder, Colorado 80309

(303) 492-6042

Brief Description of Instrumentation and Data Reduction Methods

The Adak seismic network consists of 13 high-gain, high-frequency, two-component seismic systems and one six-component system (ADK) located at the Adak Naval Base. Station ADK has been in operation since the mid-1960s; nine of the additional stations were installed in 1974, three in 1975, and one each in 1976 and 1977.

Data from the stations are FM-telemetered to recording sites near the Naval Base, and are then transferred by cable to the Observatory on the Base. Data were originally recorded by Develocorder on 16 mm film; since 1980 the film recordings are back-up and the primary form of data recording has been on analog magnetic tape. The tapes are mailed to CIRES once a week.

At CIRES the analog tapes are played back at four-times the speed at which they were recorded into a computer which digitizes the data, automatically detects events, and writes an initial digital event tape. This tape is edited to eliminate spurious triggers, and a demultiplexed tape containing only seismic events is created. All subsequent processing is done on this tape. Times of arrival and wave amplitudes are read from an interactive graphics display terminal. The earthquakes are located using a program developed for this project by E. R. Engdahl, which uses corrections to the arrival times which are a function of the station and the source region of the earthquake.

Data Annotations

A major earthquake (M_S 7.6) occurred immediately to the east of the network coverage area on May 7, 1986 (at 22:47). Thousands of aftershocks of that earthquake occurred within the network coverage area. At the time of this writing, the local catalog of hypocenters is still incomplete for the immediate time period following the mainshock. A discussion of research on that earthquake and its aftershocks is published under the report of Grant. No. G1368 (Kisslinger) elsewhere in this volume.

The network was serviced from mid-July through September, 1986. Because of major logistic problems, three of the westernmost stations could not be reached at that time. Of the 28 short-period vertical and horizontal components, 21 were operating for most of the time period of May through July, 1986. By the end of the 1986 summer field trip to Adak, 23 of the 28 components were operating (AK2z, AK5h, AD3 and AD5 having been brought back up).

Current Observations

458 earthquakes have been located so far with data from the network for the time period between the time (20:43) of the M_S 6.0 foreshock of the May 7 mainshock and 24:00 on May 10. The data report and catalog submitted to the USGS six months ago had most of the aftershocks which occurred on May 8. During the past six months project personnel have located roughly another 75 aftershocks which occurred throughout May 8 and 210 aftershocks occurring on May 9 and 10, as well as having skipped ahead in time and located 192 events which occurred in June and July, 1986. Epicenters of *all* of the events from May 8 through May 10 (including those reported in the previous Data Report), as well as the events in June and July, are shown in Figures 1 and 2, respectively.

So far, 35 of the events located with data from the Adak network for May 8 - May 10 were large enough to be located teleseismically (USGS PDEs), of which 18 occurred on May 8, 10 on May 9, and 7 on May 10. A number of other teleseismically located aftershocks within the network region are difficult for us to locate due to their arrivals being masked by the codas of other aftershocks. Also, 11 of the events located with data from the Adak network so far for June and July, 1986, were large enough to be located teleseismically (USGS PDEs). No attempt is being made to locate aftershocks with duration magnitudes (m_d) of less than 2.3. More detailed information about the network status and a catalog of the hypocenters determined for the time period reported here are included in our semi-annual data report to the U.S.G.S. Recent research using these data is reported in the Technical Summary for U.S.G.S. Grant No. G1368.

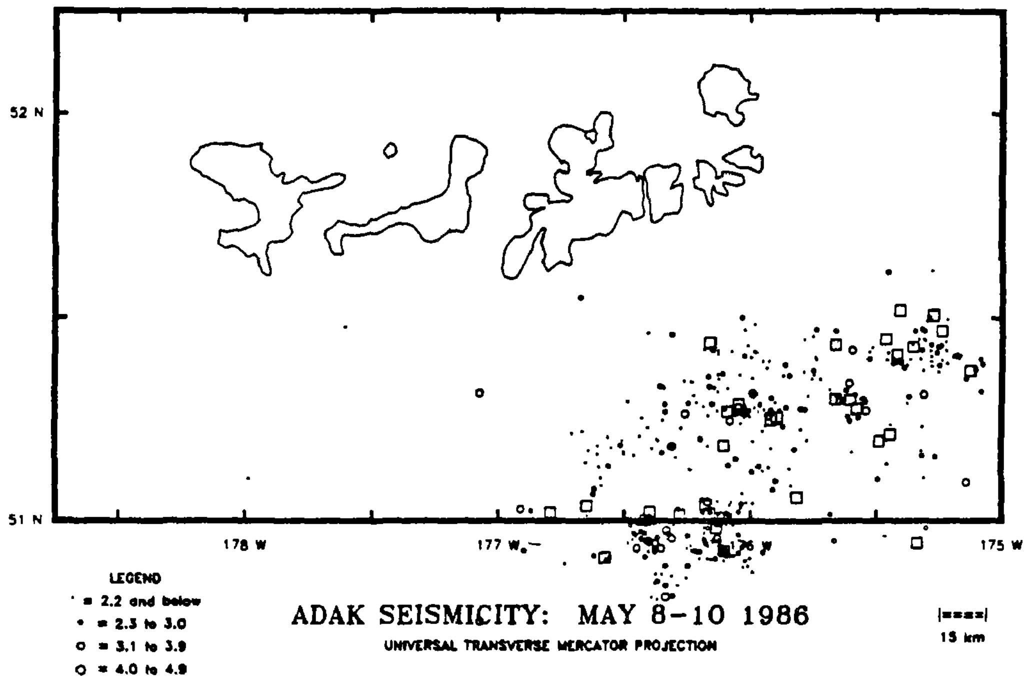

Figure 1: Map of seismicity which occurred from May 8 May 10, 1986. All epicenters were determined from Adak network data. Events marked with squares are those for which a teleseismic body-wave magnitude has been determined by the USGS; all other events are shown by symbols which indicate the duration magnitude determined from Adak network data. The islands mapped (from Tanaga on the west to Great Sitkin on the east) indicate the geographic extent of the Adak seismic network.

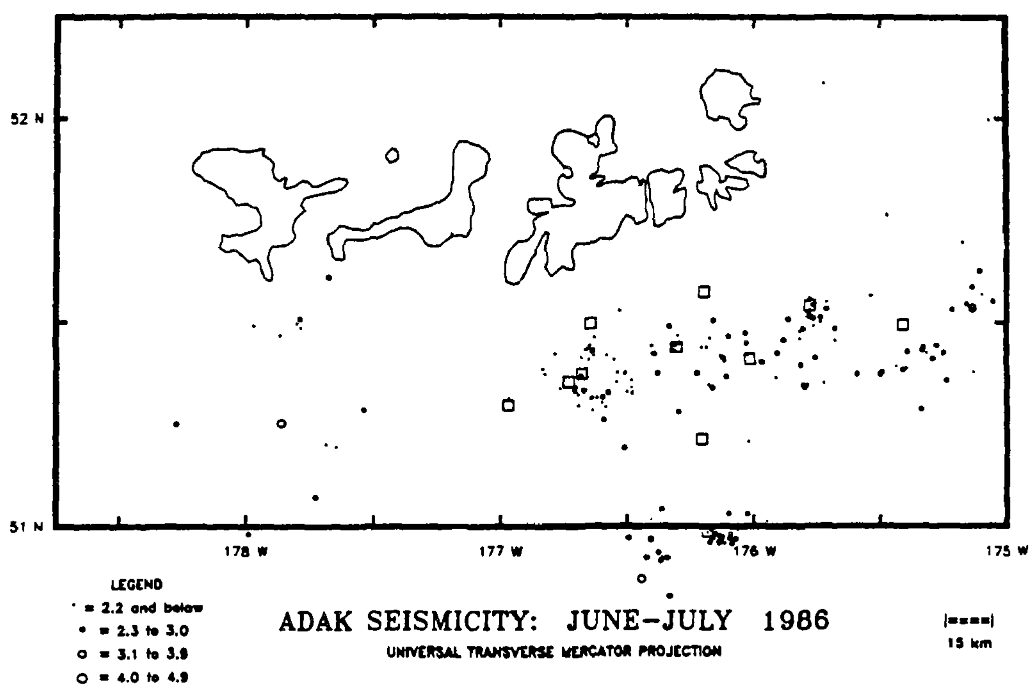

Figure 2: Incomplete map of seismicity which occurred in June and July, 1986. Symbols as in Figure 1.

WESTERN GREAT BASIN-EASTERN SIERRA NEVADA SEISMIC NETWORK

Cooperative Agreement 14-08-0001-A0262

E.J. Corbett and W.F. Nicks
Seismological Laboratory
University of Nevada
Reno, NV 89557
(702) 784-4975

Investigations

This program supports continued operation of a seismographic network in the western Great Basin of Nevada and eastern California, with the purpose of recording and location of earthquakes occurring in the western Great Basin, and acquiring a data base of phase times and analog and digital seismograms from these earthquakes. These data are used for research on: (1) ongoing seismicity in the western Great Basin with emphasis on the Long Valley caldera; (2) source mechanisms studies of these earthquakes; (3) possible precursory seismicity patterns in the White Mountains gap; (4) seismicity near reservoirs in the Lake Tahoe region; and (5) evaluation of the contribution that high-quality digital broad-band seismic stations can make to regional network-seismic studies.

Results

A. *Seismic Network Operation*

Virtually no changes have been made to our seismic network during the six-month period: Nov 86 - Apr 87. The only noteworthy change is the interruption of recording of our Battle Mountain (BMN) station, due to the phone line being cut off by USGS Golden. We may attempt to install radio relays during the summer, if time and resources permit.

B. *Data Analysis*

Our earthquake data have been timed and located through April 30, 1987. Since the beginning of the contract period on November 1, 1986, the University of Nevada Seismological Laboratory registered 2,569 earthquakes (Figure 1). Of these events:

1018 were magnitude 2 or greater;
96 were magnitude 3 or greater;
8 were magnitude 4 or greater.

The largest earthquake was a magnitude 4.3 event that occurred on November 1, 1986, in the Topaz Lake area, halfway between Lake Tahoe and Mono Lake. As Figure 1 shows, the vast amount of seismicity occurs in the Mammoth-Bishop area, with Chalfant Valley aftershocks still occurring at the rate of several a day. The most noteworthy change in seismicity pattern during this period is an increase in small earthquakes in central Nevada. The N-S trending central Nevada seismic belt (longitude 118°) is showing increased seismicity, especially at its northern end in the Stillwater gap. Prior to this period, seismicity north of latitude 40° was rare. In addition, a significant number of events are now occurring east of longitude 117°, especially near the Utah border. Formerly, events in eastern Nevada used to only average about 1 per month. These recent changes in seismicity distribution suggest that ambient stresses may be changing on a Basin-and-Range-wide scale.

EQs Nov 86–Apr 87

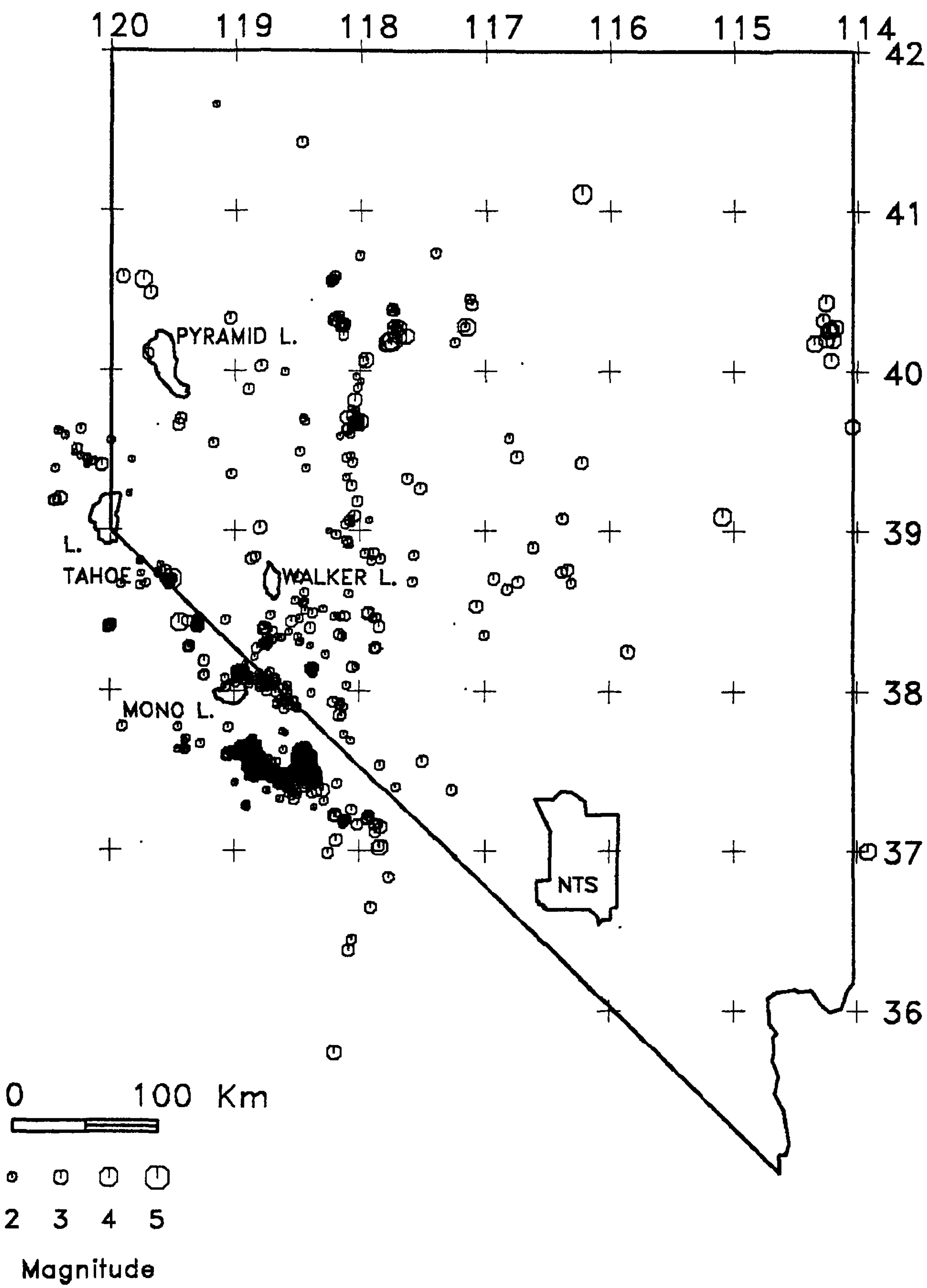

Regional Seismic Monitoring in Western Washington

14-08-0001-A0266

R.S. Crosson and S.D. Malone
Geophysics Program
University of Washington
Seattle, WA 98195
(202) 543-8020

Investigations

Operation of the western Washington regional seismograph network and routine prelimina analysis of earthquakes in western Washington are carried out under this contract. Quarterly cat logs of seismic activity in Washington and Northern Oregon are available for 1984 through 198 and the first two quarters of 1987. These catalogs are funded jointly by this contract and other The University of Washington operates approximately 80 stations west of 120.5°W. Twenty eig are funded under this contract.

Data are provided for USGS contract 14-08-0001-G1390 and other research program Efforts under this contract are closely related to and overlap objectives under contract G1390, als summarized in this volume. Publications are listed in the G1390 summary. This summary cove a six month period from October 1, 1986 through March 31, 1987. During this period the U.W seismic network located 727 events west of 120.5°W. 434 of these were located at Mount S Helens and were associated with the extrusion of a new lava lobe between October 4 and Octob 27. Excluding Mt. St. Helens, 293 earthquakes were located west of 120.5° W, compared to 31 and 309 in the preceding two six-month periods. During the six months covered by this sum mary, the largest earthquake located in western Washington was a M_c 3.2, which occurred o October 12th, at 67 km depth, about 40 km northeast of Longview Washington. The prelimina focal mechanism suggests normal faulting with extension in a NE-SW direction. Only one oth earthquake this deep has been located in southwestern Washington (a magnitude 3.3 in Apr 1984).

Central California Network Operations

9930-01891

Wes Hall
Branch of Seismology
U.S. Geological Survey
345 Middlefield Road, Mail Stop 977
Menlo Park, California 94025
(415) 323-8111, Ext. 2509

Investigations

Maintenance and recording of 325 seismograph stations (432 components) located in Northern and Central California. Also recording 62 components from other agencies. The area covered is from the Oregon border south to Santa Maria.

Results

1. Modified and installed one hundred seventy-one (171) VCO/AMPS for greater frequency stability; temperature stability; and dynamic range.
    - J302ML - 90 ea.
    - J402ML - 6 ea.
    - J402H - 70 ea.
    - J502 - 5 ea.

2. Assembled and tunded 90 J502 VCP/AMPS for the Jordan Project.

3. Installed and began recording low gain FBA's
    - PHOI, PHOJ, PHOK PHOZ
    - PAGI, PAGJ, PAGK
    - PGHI, PGHJ, PGHK
    - PSMI, PSMJ, PSMK
    - PSRI, PSRJ, PSRK

4. Installed and began recording high gain FBA's
    - PCHS, PCHB, PCHC
    - PHOA, PHOB, PHOC
    - PGHA, PGHB, PGHC
    - PMMA, PMMB, PMMC
    - PSRA

5. Deleted and removed following seimsic stations
    - LHO, LBG, LHM

6. Installed new seismic stations at
    - MWB (Warren Bench)
    - NCP (Capay)
    - NRR (Rocky Ridge)
    - NAD, NADN (Allendale)
    - NAP (Atlas Peak)

7. Expanded data base to include helicorder, develocorder, and map quad information.

8. Completed tuning 40 ea. J502 VCO/AMPS for HVO project.

ALASKA SEISMIC STUDIES

9930-01162

John C. Lahr, Christopher D. Stephens, Robert A. Page, Kent A. Fogleman
Branch of Seismology
U.S. Geological Survey
345 Middlefield Road, MS 977
Menlo Park, California 94025
(415) 323-8111, Ext. 2510

Investigations

1) Continued collection and analysis of data from the high-gain, short-perioc seismograph network extending across southern Alaska from the volcanic arc west of Cook Inlet to Yakutat Bay, and inland across the Chugach mountains.

2) Continued monitoring in the region of the proposed Bradley Lake hydroelectric project on the southern Kenai Peninsula, a cooperative effort with the Alaska Power Authority.

3) Cooperated with the Branch of Engineering Seismology and Geology in operating 19 strong-motion accelerographs in southern Alaska, including 13 between Icy Bay and Cordova in the area of the Yakataga seismic gap.

Results

1) During the past six months preliminary hypocenters have been determined for 1,525 earthquakes that occurred between August 1986 and January 1987 (Figure 1). The coda-duration magnitudes (M_D) of these events range from 0 to 4.2, and 94 are M_D 3 and larger. The five largest events ($M_D \geq 4$) were located at depths between 44 and 217 km within the Aleutian Wadati-Benioff zone (WBZ) west of about longitude 149.5°W. Within the northeastward-dipping Wrangell WBZ the largest earthquake (3.9 M_D; 4.7 m_b, NEIC) known to be associated with this zone occurred on September 15, 1986. This event was located at a depth of 52 km near 61.5°N, 143.75° W. and felt reports (NEIC) include MM intensity IV in Chitina at an epicentral distance of about 50 km, and intensity III in Valdez and Cordova at epicentral distances of about 160 km. The deepest event ever located within the Wrangell WBZ by the regional network also occurred during this time period, a 2.4 M_D shock on September 26 near Mt. Wrangell with a depth of 103 km.

Within the aftershock zone of the 1979 St. Elias earthquake, which abuts the eastern edge of the Yakataga seismic gap, over 500 shocks were locate(during the recent six-month period. This number represents a 30 percent increase relative to the previous six-month period. However, at least part of this change is probably due to improved detection capabilities following the re-activation of several local stations that had been offline. In December, an unusual swarm of 27 shocks with magnitudes of u| to 2.1 M_D occurred 60 km eastnortheast of Icy Bay. The location of this swarm is immediately north of an area where a similar cluster of events occurred within six months prior to the 1979 mainshock.

In and around the Yakataga seismic gap the pattern of shallow seismicity during the last six months was not significantly different from that observed for at least the past nine years. One unusual event with a magnitude of 3.1 M_D occurred on September 7 beneath the Bering Glacier at the southern limit of a persistent, diffuse concentration of seismicity near the center of the gap. Only two other events of M_D 3 or larger have occurred within this zone since October 1977. The prodominant frequency (1-2.5 Hz) of the September shock is lower than the typical frequencies of tectonic earthquakes in southern Alaska. A 2.7 M_D shock occurred at nearly the same location in 1985 and also had uncharacteristically low freqencies. At the present time we cannot rule out the possibility that these low-frequency events are icequakes related to the Bering glacier.

Despite a notable increase in the level of microearthquake activity preceding and accompanying the August-September, 1986 eruption of Augustine volcano in southern Cook Inlet (EOS, Transactions, American Geophysical Union, 1986, v. 67, no. 42, p. 804), no shallow (depth less than 30 km) earthquakes were located near the volcano by the USGS regional network for this time period. Earthquakes as small as magnitude 2 M_D that occur in this area are routinely located by the network. Only one shock (2 M_D) associated with the March-April 1986 eruptive episodes was located by the regional network. In contrast, during the 1976 eruption of Augustine, over 250 events with magnitudes between 2.0 and 2.5 were located (Reeder and Lahr, in press).

2) Four event-triggered seismic recorders (ELOG's) were deployed for 14 days in August 1986 to obtain improved locations for two swarms of crustal seismicity which occurred in June and July about 10 km south of Talkeetna. Station spacing was approximately 20 km. A total of 630 individual waveforms of 12.5s duration were recorded. Half of these were earthquakes; the rest were mostly noise from vehicles on nearby roads. Of 189 earthquakes recorded by one or more ELOG's, about 60 had a minimum S-P time interval of 8s or less. Two-thirds of these were crustal shocks (depths shallower than 35 km) concentrated beneath or near the edges of the array. The remainder were 40-70 km deep, south and east of the array within the Aleutian WBZ. Six of the well-recorded shallow ELOG earthquakes were used to develop an improved velocity model and traveltime corrections to simulate the structure of the crust beneath the Talkeetna study area (latitude 61.5°-62.5°N, longitude 149°-151°N). Shallow, crustal earthquakes in the study area from January 1, 1986 through the end of the ELOG deployment were relocated using the new velocity model and station corrections. Most of the ELOG shocks beneath the array range in depth from 10 to 25 km. The swarm events moved about 15 km deeper after being relocated and range in depth from 22 to 32 km. The remaining relocated earthquakes were south and southeast of the array and north of the mapped trace of the Castle Mountain fault, and range in depth from about 5 to 25 km. The depths of the relocated hypocenters agree with the revised depths reported by Lahr and others (1986) for shocks in the study area that occurred between 1971 and the time of the August 1984 Sutton earthquake (5.7 m_b) on the Castle Mountain fault.

Single-event and composite focal mechanism solutions for the swarm and ELOG shocks beneath the array have compression axes oriented NW-SE. Based on the regional NE-SW trend of the closest known faults and the orientation of the compressive stress direction, the June and July swarm earthquakes probably involved reverse faulting on a NE-SW-trending, NW-dipping plane.

3) Based on the performance of the ELOG recorders during the Talkeetna deployment in 1986, it was concluded that frequency domain techniques could be used to good advantage to reduce the recording of false events. For this purpose, the Walsh transform into the sequency domain was chosen because its speed would allow near realtime processing on the RCA 1805 microprocessor currently used in the ELOG. Two techniques are being tested: spectral correlation and sequency shift. The correlation technique involves looking for a typical earthquake sequency spectrum within a time window after an event trigger. The sequency shift technique assumes that the sequency spectrum will shift in time to higher sequencies if an earthquake is present. Although the algorithms are not yet complete, testing on events recorded last summer indicates that 80-90 percent of the noise events (mostly vehicles) could be eliminated while excluding less than 5 percent of the recorded earthquakes of interest.

4) Velocity models derived from TACT (Trans-Alaska Crustal Transect) seismic-refraction profiles are being used in the relocation of earthquakes recorded by the southern Alaska regional seismograph network. Recent investigations have focused on a cluster of 20 earthquakes occurring within 25 km of Glennallen. Routine network location procedures placed these shocks in the depth range 0-40 km, primarily between 10 and 35 km. Phases for 14 of the better-recorded ($1.6 \leq M_D \leq 3.0$) shocks from 1977-1983 were reread. These events were then relocated with a local velocity model derived from TACT refraction profiles and station traveltime corrections obtained from repeated refraction shots at a nearby shotpoint. Most of the 14 relocated shocks fall in the depth range 13-20 km. Seven of the shocks lie in a tight (point) cluster 5 km southeast of Glennallen at about 16 km depth. The first-motion patterns for the cluster earthquakes are consistent with a northwest-southeast-trending nearly horizontal P axis and a vertical to moderately northeast-diping T-axis. Compositing the dihedra for the P and T axes from the seven best-recorded shocks, including five from the cluster, suggests that all the shocks could result from a uniform stress field, characterized by a subhorizontal, northwest-southeast, greatest compressive stress axis and a nearly vertical least compressive stress axis. Convergence of the Pacific and North American plate along the continental margin in the Gulf of Alaska may account for the inferred orientation of the greatest compressive axis.

5) In order to obtain more reliable relative locations for earthquakes within the southern Alaska network, we have been seeking to improve the regional velocity model used. We have adapted the program VELEST (originally written by S. Reocker and W. Ellsworth and then revised by E. Kissling), which inverts arrival time data simultaneously for hypocenters, station delays, and the velocity depth function, for use with HYPOELLIPSE-format data, and have added features to facilitate its use. Preliminary results using this program indicate that a great amount of CPU time is required, in part because the method requires the inversion of a very large matrix. Another approach being studied which substantially reduces the amount of CPU time per iteration is to sequentially invert for hypocenters and the velocity-depth function (Pavlis and Booker, 1980). After the velocity model has been determined the average residual at each station is used to increment the corresponding station delay. Initial tests with simulated data for 125 earthquakes indicate that the sequential approach requires only about one fifth as much CPU time as VELEST.

The computer programs FPFIT, FPPLOT, and FPPAGE (Reasenberg and

Oppenheimer, 1986) have been modified to accept HYPOELLIPSE-format data, to compute both single-event and composite focal mechanism solutions, to allow more options in selecting and weighting observations, and to provide more flexibility in displaying the results. When a focal mechanism is based on sparse data, the P- and T-axes for acceptable solutions cover a very large part of the focal sphere. FPFIT typically generates plots of acceptable P- and T-axes that are misleading and difficult to interpret. This is due in part to the highly non-uniform distribution of the P- and T-axes for the trial mechanisms tested by FPFIT. An alternate version of the program, FPFIT2, is well-suited for sparse data sets such as is characteristic of Alaska data. It uses a set of trial solutions with a uniform distribution of P- and T-axes so that the distribution of accepable axes properly indicates the confidence regions for the axes.

References

Lahr, J. C., Page, R. A., Stephens, C. D., and Fogleman, K. A., 1986, Sutton, Alaska earthquake of 1984: Evidence for activity on the Talkeetna segment of the Castle Mountain fault system, Bulletin of the Seismological Society of America, v. 76, p. 967-983.

Pavlis, G. L., and Booker, J. R., 1980, The mixed discrete-continuous inverse problem: application to the simultaneous determination of earthquake hypocenters and velocity structure, Journal of Geophysical Research, v. 85, p. 4801-4810.

Reasenberg, P. A., and Oppenheimer, David, 1985, FPFIT, FPPLOT and FPPAGE: Fortran computer programs for calculating and displaying earthquake fault-plane solutions, U.S.G.S. Open-File Report, 85-739, 109 p.

Reeder, J. W., and Lahr, J. C., Seismological aspects of the 1976 eruption of Augustine volcano, Alaska, U.S. Geological Survey Bulletin 1768, in press.

Reports

Biswas, N. N., Lahr, J. C., and Page, R. A., 1986, Some results on the seismicity of Alaska [abs.], EOS, v. 67, p. 1236.

Fogleman, K. A., Page, R. A., Lahr, J. C., and Stephens, C. D., 1987, Earthquake activity around Valdez, Alaska, for 1983-1984, U.S. Geological Survey Open-File Report 87-58, 44 p.

Fogleman, K. A., and Rogers, J. A., 1987, ELOG: Design and deployment of a digital earthquake recorder in study of the 1986 Talkeetna, Alaska earthquake swarms, (Abs.), Seismological Research Letters, v. 58, no. 1, p. 12.

Lahr, J. C., Stephens, C. D., Page, R. A., and Fogleman, K. A., 1986, Summary of seismic monitoring by the USGS southern Alaska network - October 1971 through June 1985, Symposium and workshop, regional seismographic networks, past-present-future [abs.], Earthquake Notes, v. 56, p. 93.

Lee, W. H. K., Lahr, J. C., and Habermann, R. E., 1986, Application of personal computers in geophysicsl [abs.], EOS, v. 67, no. 46, p. 1321-1

Stephens, C. D., Page, R. A., and Lahr, J. C., 1987, Evidence for a mid-crustal seismic velocity discontinuity beneath the southern Kenai Peninsula, Alaska, (abs.), Seismological Research Letters, v. 58, no. 1 p. 27.

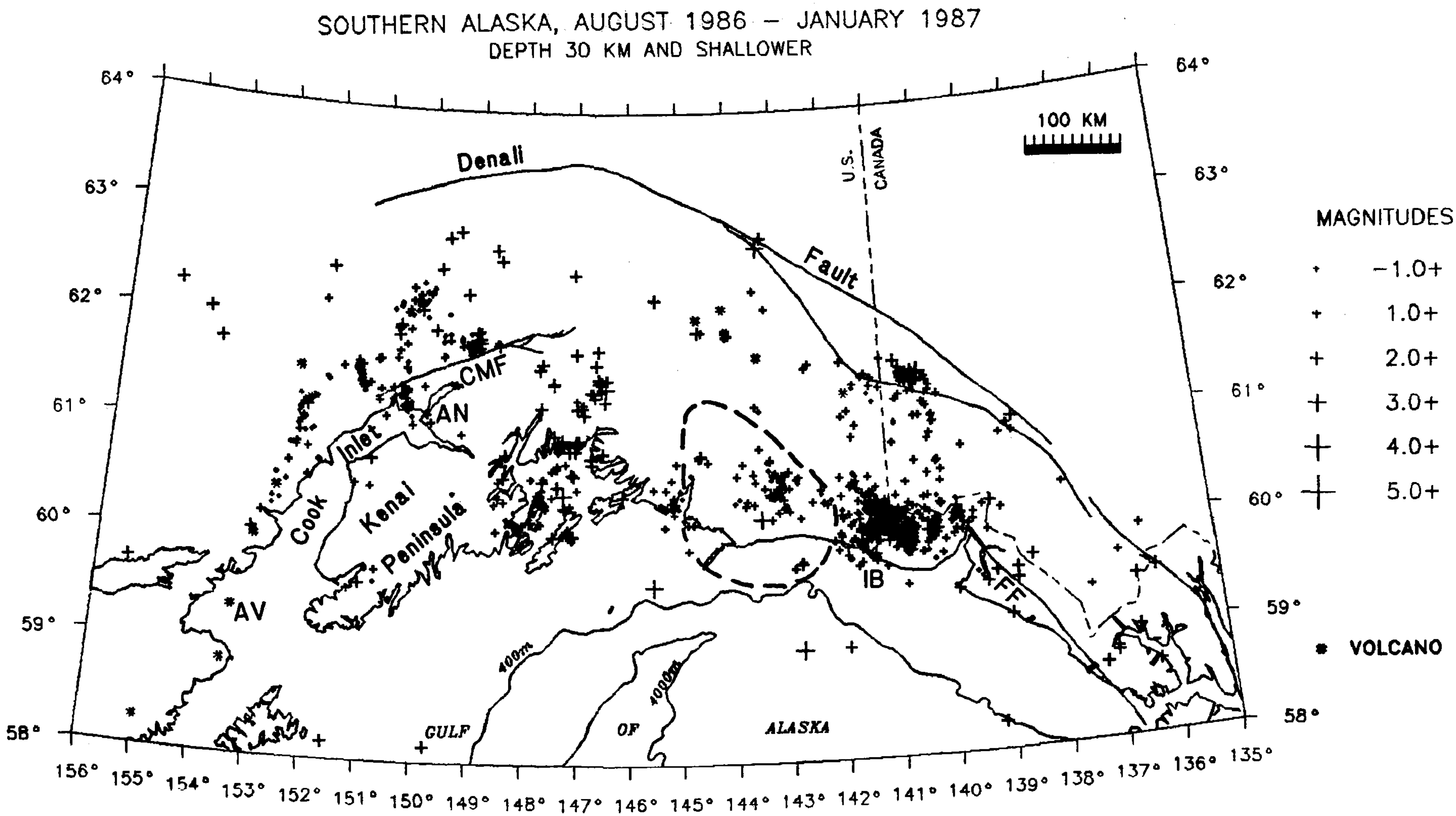

Figure 1a. Epicenters of 1060 earthquakes located using the USGS southern Alaska seismograph network for the period August 1986 - January 1987. Magnitudes are determined from coda duration or maximum amplitude, and events of magnitude 3 and larger can be as much as one unit smaller than the corresponding teleseismic m_b magnitude. The lowest magnitude level to which data is processed varies across the network due to uneven station spacing and changes in processing criteria. Heavy dashed contour indicates inferred extent of Yakataga seismic gap. Abbreviations are: AN - Anchorage, AV - Augustine volcano, CMF - Castle Mountain fault, FF - Fairweather fault, IB - Icy Bay.

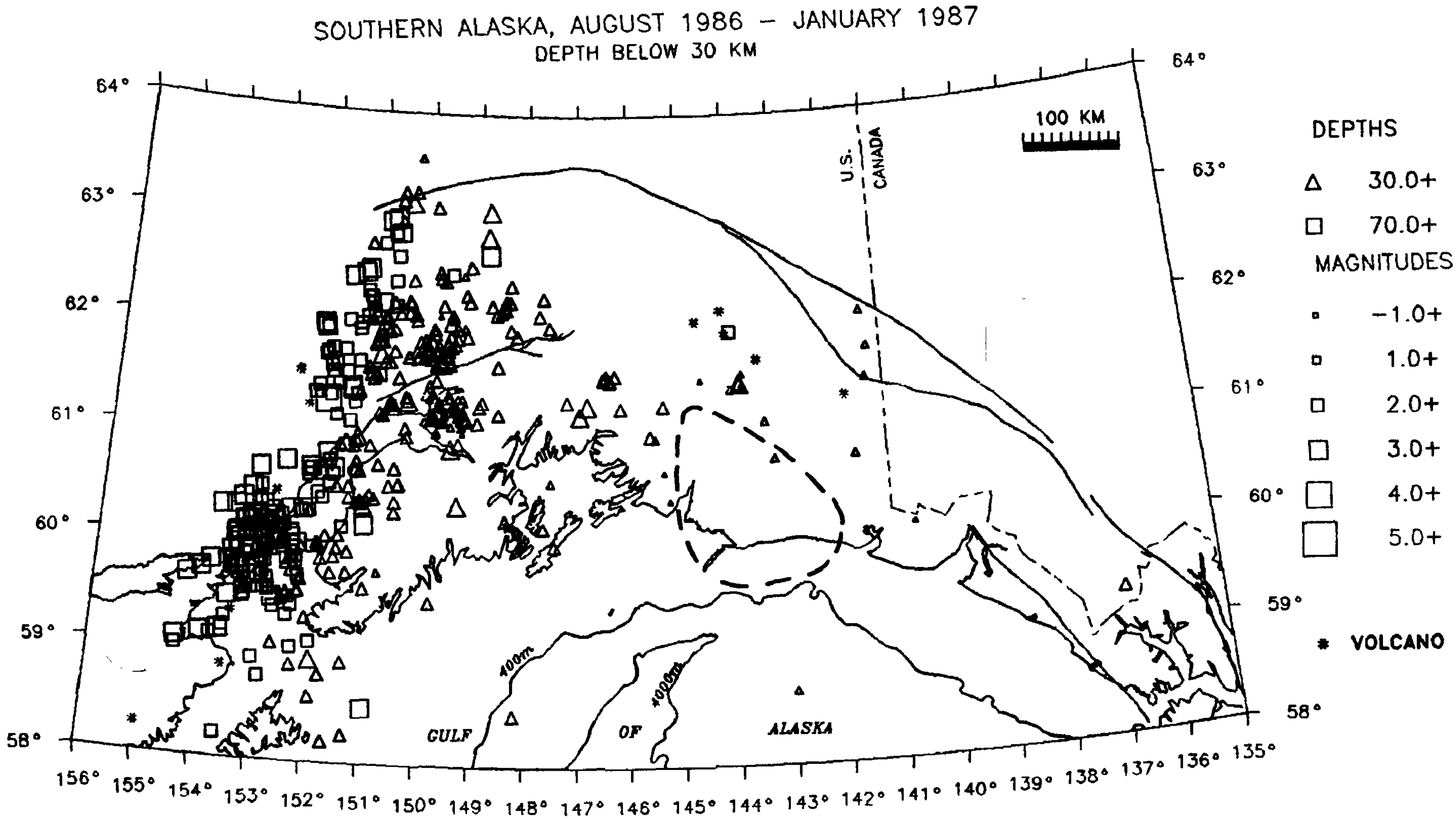

Figure 1b. Epicenters of 465 earthquakes deeper than 30 km located using the USGS seismograph network for the period August 1986 - January 1987. See Figure 1a for details about magnitudes and for identification of map features.

Seismic Data Library

9930-01501

W. H. K. Lee
U.S. Geological Survey
Branch of Seismology
345 Middlefield Road, Mail Stop 977
Menlo Park, California 94025
(415) 323-8111, Ext. 2630

This is a non-research project and its main objective is to provide access of seismic data to the seismological community. Ths Seismic Data Library was started by Jack Pfluke at the Earthquake Mechanism Laboratory before it was merged with the Geological Survey. Over the past ten years, we have built up one of the world's largest collections of seismograms (almost all of them on microfilm) and related materials. Our collection includes approximately 4.5 million WWNSS seismograms (1962 - present), 1 million USGS local earthquake seismograms (1966-1979), 0.5 million historical seismograms (1900-1962), 20,000 earthquake bulletins, reports and reprints, and a collection of several thousand magnetic tapes containing (1) a complete set of digital waveform data of the Global Digital Seismic Network (Data Tapes), and (2) a complete set of digital archive data of Calnet (CUSP archive tapes).

Northern and Central California Seismic Network Processing

9930-01160

Fredrick W. Lester
Branch of Seismology
U.S. Geological Survey
345 Middlefield Road M/S 977
Menlo Park, California 94025
(415) 323-8111, ext. 2149

Investigations

1. In 1966 a seismographic network was established by the USGS to monitor earthquakes in central California. In the following years the network was expanded to monitor earthquakes in most of northern and central California, particularly along the San Andreas Fault, from the Oregon border to Santa Maria. In its present configuration there are over 350 single and multiple component stations in the network. There is a similar network in southern California. From about 1969 to 1984 the primary responsibility of this project was to manually monitor, process, analyze, and catalog the data recorded from this network. In 1984 a more efficient and automatic computer-based monitoring and processing system (CUSP) began online operation, gradually replacing most of the manual operations previously performed by this project. For a more complete description of the CUSP system see the project description "Consolidated Digital Recording and Analysis" by S. W. Stewart.

   Since the introduction of the CUSP system the responsibilities of this project have changed considerably. The main focus of the project now is that of finalizing and publishing preliminary network data from the years 1978 through 1984. We also continue to manually scan network seismograms as back-up event detection for the CUSP system. We then supplement the CUSP data base with data that were detected only visually or by the other automatic detection system (Real-Time Processor, RTP) and digitized from the continuously recording analog magnetic tapes. Project personnel also act as back-up for the processing staff in the CUSP project. As time permits some research projects are underway on some of the more interesting or unusual events or sequences of earthquakes that have occurred within the network.

   This project continues to maintain a data base for the years 1969 - present on both a computer and magnetic tapes for those interested in research on the network seismic data. As soon as the older data are finalized they are exchanged for the preliminary data existing in the data base.

Results

1. Figure 1 illustrates the more than 8100 earthquakes located by this office for northern and central California during the time period October 1986 through March 1987. The largest earthquake recorded was a M5.6 shock that occurred on November 21 along the Mendocino coast, approximately 75 km south of Eureka. It was accompanied by a modest rise in local seismic activity. The second largest earthquake to occur during that time was a magnitude 5.0 event that occurred on February 14, near Coalinga. There

was also a slight rise in the level of seismic activity in that area associated with that event. However the highest rate of aftershock activity was in Chalfant Valley as the aftershocks continued following the M6.5 quake that occurred on July 21, 1986. The largest aftershock in that area during this reporting period was M4.3 on January 27. Due to the large number of aftershocks from the M6.5 event there is still a small back-log in the CUSP processing for July 20-21.

2. Final processing of data for the second half of the calendar year 1982 is complete and those data are ready for publication, as are the data from the Lake Shasta area for 1981-1984. Work is currently underway on the final processing of data for the areas around Mt. Shasta, and Lassen Volcanic National Park. Some of these data are very preliminary and need extensive reprocessing and analysis, but it is expected that this work will be completed by mid-1987.

3. Since June 1986 this project has been involved in a combined effort with personnel from many different projects. The first purpose of this group endeavor is to collect all available seismic data pertaining to the more than 150,000 earthquakes that the USGS has located in northern and central California, mainly from 1969 to the present. Those data will then be combined, checked for errors and omissions, reprocessed as necessary, and finalized for publication. It is estimated that this job will take at least one year, which is much less time than would be necessary for this project alone. Personnel in this project will be responsible for coordinating much of this group effort. To date all but a small portion of the data have been collected, had gross errors corrected, and have been rerun through the location program.

4. For the time period October 1986 - March 1987 there were an average of 3 to 6 events per day missed by the CUSP automatic detection system. These will be added to the existing CUSP data base from the back-up magnetic tape and processed using standard CUSP processing techniques. Most of the earthquakes that were missed occurred in northern California, north of latitude 39 degrees. This is a particular problem in the north because of telemetry noise that exists on those circuits. To avoid producing an abnormally large number of false triggers in the detection system the trigger thresholds are often set higher than normal and therefore some of the real events are missed.

5. Steve Walter is currently investigating some unusual low frequency events that he has detected in Lassen Volcanic National Park over the last four years (Walter, 1986). Most of these are deep events, between 15 and 20 kilometers, and most are concentrated west of Lassen Peak. These events are of interest because they resemble events seen in other volcanic regions, particularly Hawaii, that have been associated with magma transport. Some results of this investigation were presented at the Fall AGU meeting in San Francisco.

6. Quarterly reports were prepared on seismic activity around Monticello Dam, Warm Springs Dam, the Auburn Dam site and, New Melones Dam for the appropriate funding agencies. Quarterly reports on seismic activity in the Mount Shasta area and in Lassen Volcanic National Park were also prepared and distributed to interested agencies and individuals.

7. For the past 2 or 3 years Mari Kauffmann has been involved in the development of an automatic system to pick p-phases off magnetic tapes

from portable 3-component seismographs. The system is now operational an is being utilized with Mari as the chief operator (Kauffmann, 1986). There are several other people involved and they have made improvements s that digital seismograms can also be produced on magnetic tape. These seismograms can then be processed and analyzed using CUSP software. To date Mari has processed a large volume of data from numerous California earthquake sequences from areas that include Long Valley, Coalinga, Kettleman Hills, Morgan Hill, Chalfant Valley, and Palm Springs.

8. Steve Walter has been playing a key role in the development of a new off-line automatic computer-based digitizing system to replace the old on that broke down in March 1986. That system was the back-up digitizer for CUSP. The new one is now operational, with a few bugs, but is not as automatic as it will be in the near future. There is presently a 10 mont backlog of data to be digitized.

Reports

Kauffman, M. L., 1986, A users guide to the automatic phase picking system for portable 3-component seismograph 5-day tapes, U.S. Geological Survey Open-File Report 86-109, 28 p.

Walter, S. R., 1986, Long period earthquakes at Lassen Peak - evidence for magma movement, (abs.), EOS, v. 67, no. 44.

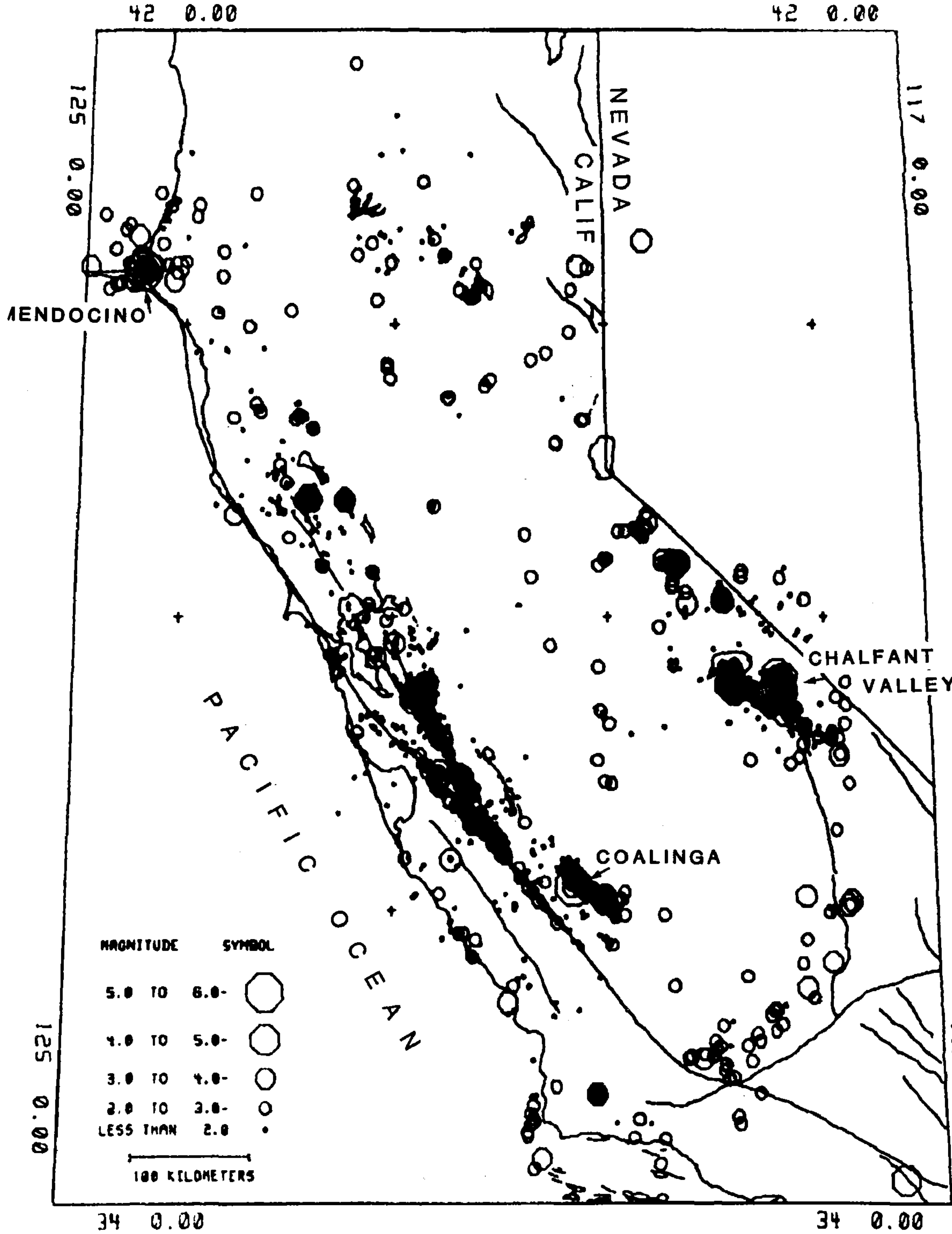

Figure 1. Northern and central California seismicity October 1986 - March 1987.

Regional Microearthquake Network in the Central Mississippi Valley

14-08-0001-A0263

William V. Stauder and Robert B. Herrmann
Department of Earth and Atmospheric Sciences
Saint Louis University
P.O. Box 8099 Laclede Station
St. Louis, MO 63156
(314) 658-3131

Investigations

The purpose of the network is to monitor seismic activity in the Central Mississippi Valley Seismic zone, in which the large 1811-1812 New Madrid earthquakes occurred. The following section gives a summary of network observations during the last six months of the year 1986.

Results

In the last six months of 1986, 140 earthquakes were located and 45 other nonlocatable earthquakes were detected by the 42 station regional telemetered microearthquake network operated by Saint Louis University for the U. S. Geological Survey and the Nuclear Regulatory Commission. Figure 1 shows 137 earthquakes located within a 4° x 5° region centered on 36.5 °N and 89.5°W. Seismograph stations are denoted by triangles and are labeled by the station code. The magnitudes are indicated by the size of the open symbols. Figure 2 shows the locations and magnitudes of 117 earthquakes located within a 1.5° x 1.5° region centered at 36.25°N and 89.75°W. Figures 3 and 4 are similar to Figures 1 and 2, but the epicenter symbols (squares) are scaled to focal depth.

In the last six months of 1986, 80 teleseisms were recorded by the PDP 11/34 microcomputer. Epicentral coordinates were determined by assuming a plane wave front propagating across the network and using travel-time curves to determine back azimuth and slowness, and by assuming a focal depth of 15 kilometers using spherical geometry. Arrival-time information for teleseismic P and PkP phases has been published in the quarterly earthquake bulletin.

The significant earthquakes occurring in the last six months of 1986 include the following:

1. 11 July 1986, UTC 1426, 35.11°N, 84.98°W: felt (V) at Chattanooga, (IV) at Apison, Ocoee and Ooltewah. Also felt (IV) at Blue Ridge, Cisco, Fort Oglethorpe and Rocky Face, Georgia. Felt (III) at Birchwood, Calhoun, Cleveland, Copperhill, Etowah and Soddy-Daisy, Tennessee. m_{Lg}(10Hz) = 3.3(SLM), m_{Lg} = 3.3(NEIS).

2. 12 July 1986, UTC 0819, 40.43°N, 84.43°W: felt in much of Ohio and parts of Michigan, Indiana, Kentucky and West Virginia. Slight damage in St. Marys, Ohio. m_{Lg}(10Hz) = 4.6(SLM), M_B = 4.5(PDE).

3. 26 August 1986, UTC 1641, 38.32°N, 89.79°W: felt (IV) at New Athens and Belleville, Illinois. Felt (III) in the St. Louis, Missouri area and many parts of southern Illinois. m_{Lg}(10Hz) = 3.6(SLM), m_{Lg} = 3.7(NEIS), m_{Lg}(3Hz) = 2.9<FVMZ>.

4. 24 October 1986, UTC 0557, 36.17°N, 89.66°W: felt (IV) in Caruthersville, Missouri. m_{Lg}(10Hz) = 2.9(SLM), m_{Lg}(3Hz) = 2.6 <FVMZ>.

5. 6 November 1986, UTC 1921, 38.11°N, 90.42°W: felt (II) in Crystal City, Missouri. m_{Lg}(10Hz) = 2.7(SLM), m_{Lg}(3Hz) = 2.3 <FVMZ>.

6. 30 December 1986, UTC 0715, 36.42°N, 89.58°W: felt (IV) at Hayti, Malden, Caruthersville and Pt. Pleasant, Missouri. Felt (III) at Blodgett, Dexter, Harviel, Portageville and Sikeston. Also felt (III) at Finley, and Tigrett, Tennessee. m_{Lg}(10HZ) = 3.4(SLM), m_{bLg} = 3.5(NEIS), m_{Lg}(3Hz) = 3.1<FVMZ>.

Acknowledgements

The cooperation of the Tennessee Earthquake Information Center, National Earthquake Information Service, and the University of Kentucky is gratefully acknowledged for providing station readings, magnitude data, and felt information. The results reported were supported by the Department of the Interior, U. S. Geological Survey, under Contract 14-08-0001-A0263 and the U.S. Nuclear Regulatory Commission under Contract NRC-04-81-195-03.

References

Central Mississippi Valley Earthquake Bulletin, Department of Earth and Atmospheric Sciences, Saint Louis University. 1986 No. 47

PDE Preliminary Determination of Epicenters, Monthly Listings, U.S. Geological Survey, 1986

TEIC Quarterly Seismological Bulletin, Tennessee Earthquake Information Center, Memphis State University. 1986, Vol. 7, No. 1.

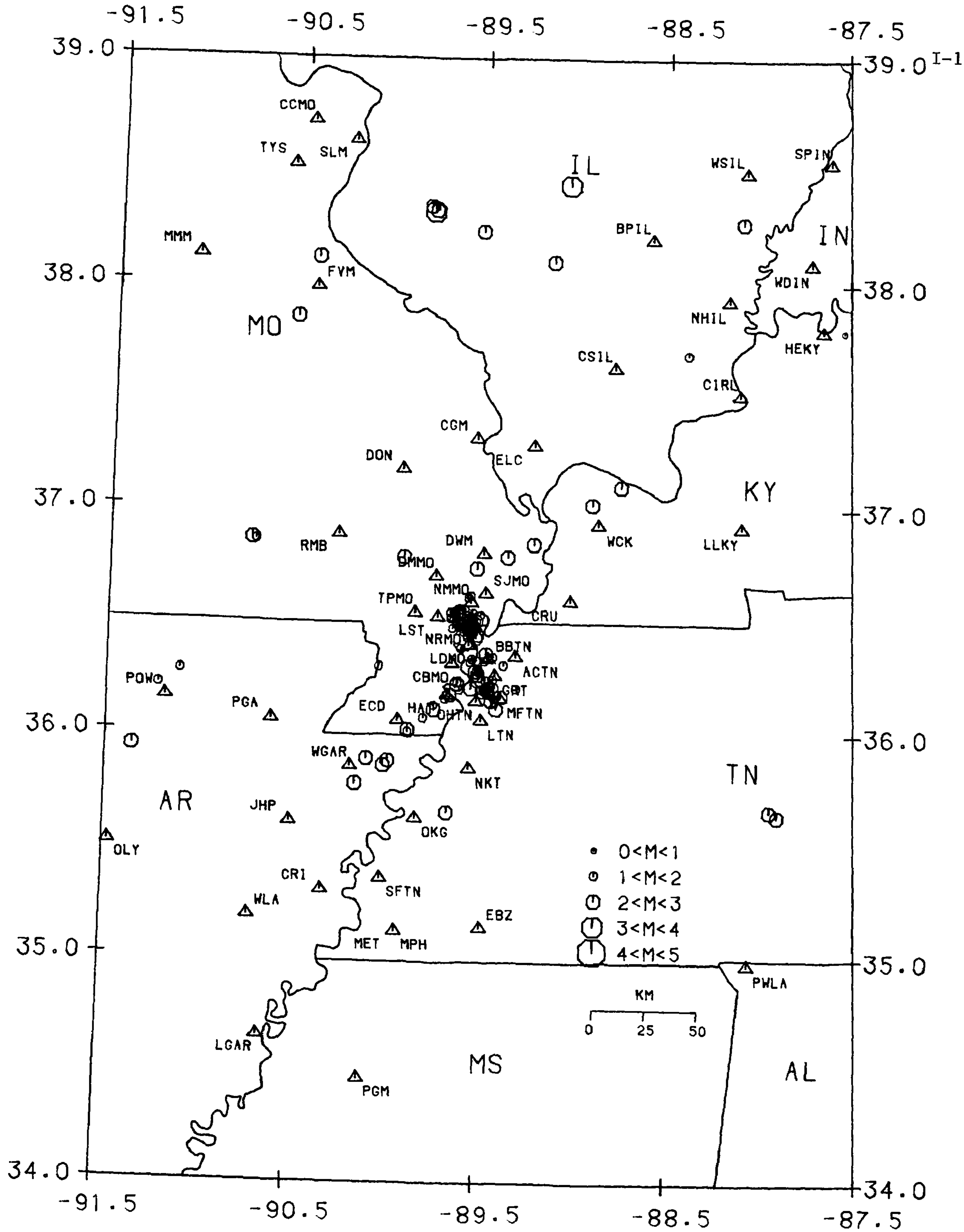

FIGURE 1

CUMULATIVE EVENTS 01 JUL 1986 TO 31 DEC 1986

LEGEND . STATION EPICENTER

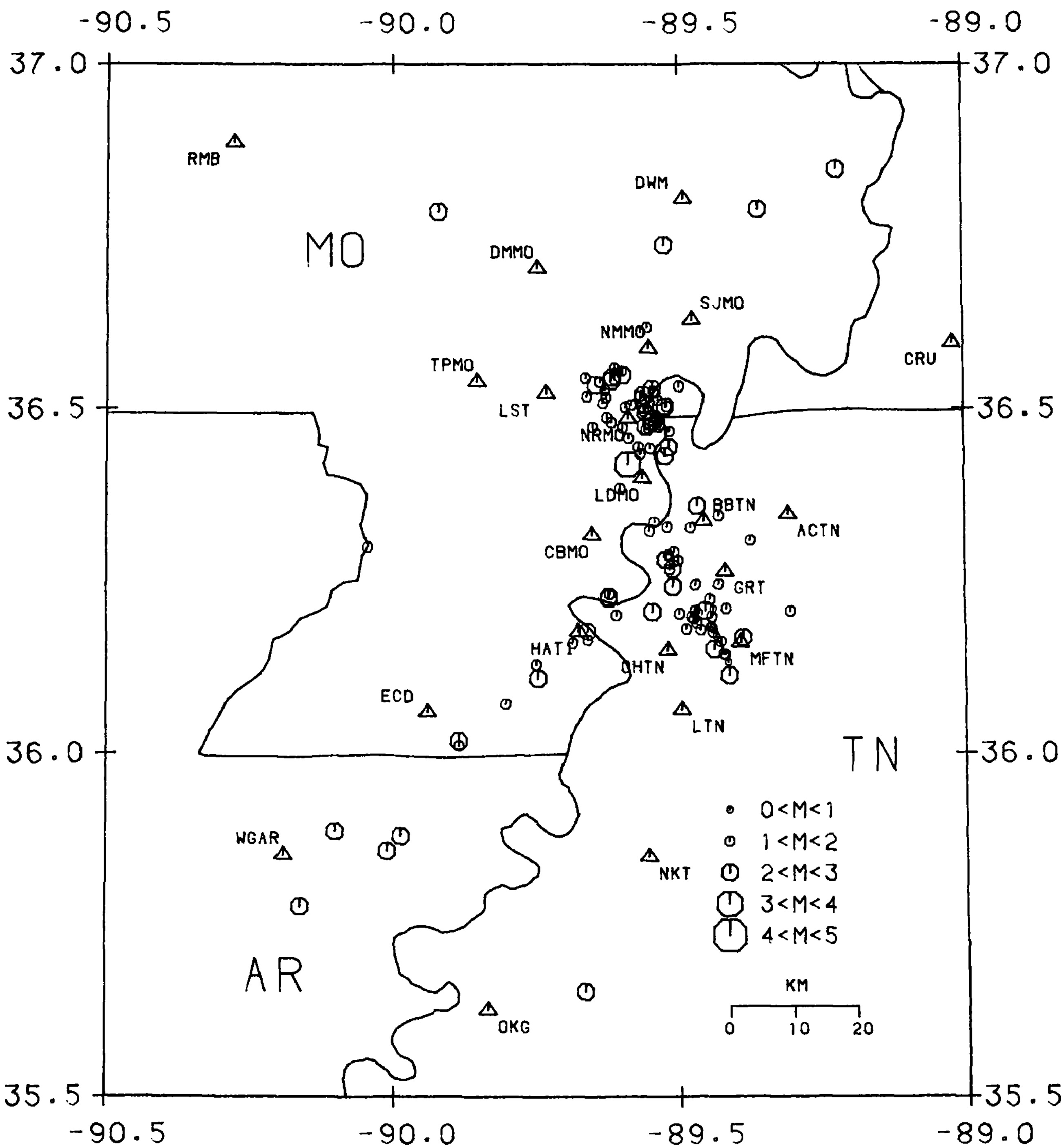

FIGURE 2
CUMULATIVE EVENTS 01 JUL 1986 TO 31 DEC 1986
LEGEND . △ STATION ⊙ EPICENTER

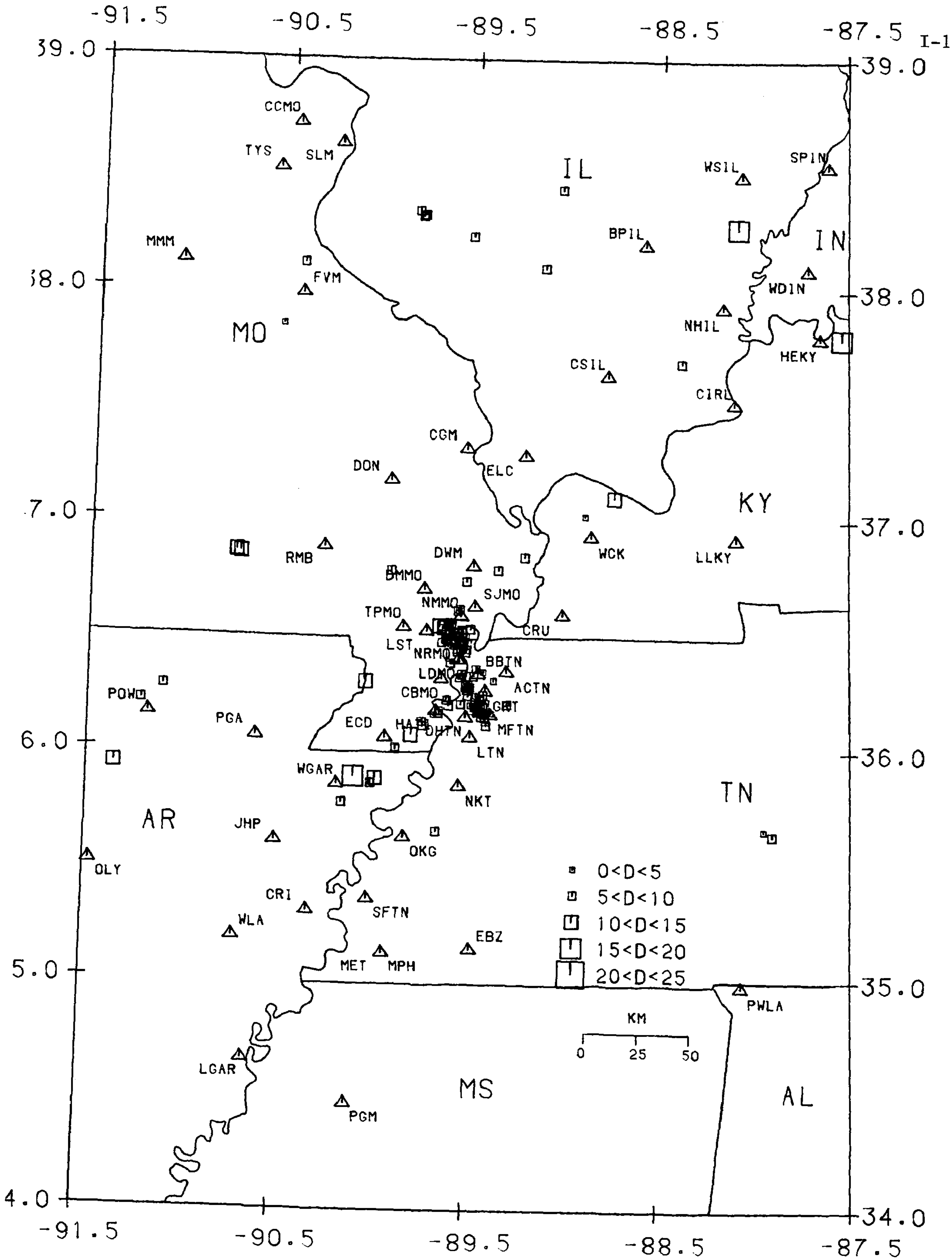

FIGURE 3
CUMULATIVE EVENTS 01 JUL 1986 TO 31 DEC 1986
LEGEND . △ STATION ▫ EPICENTER

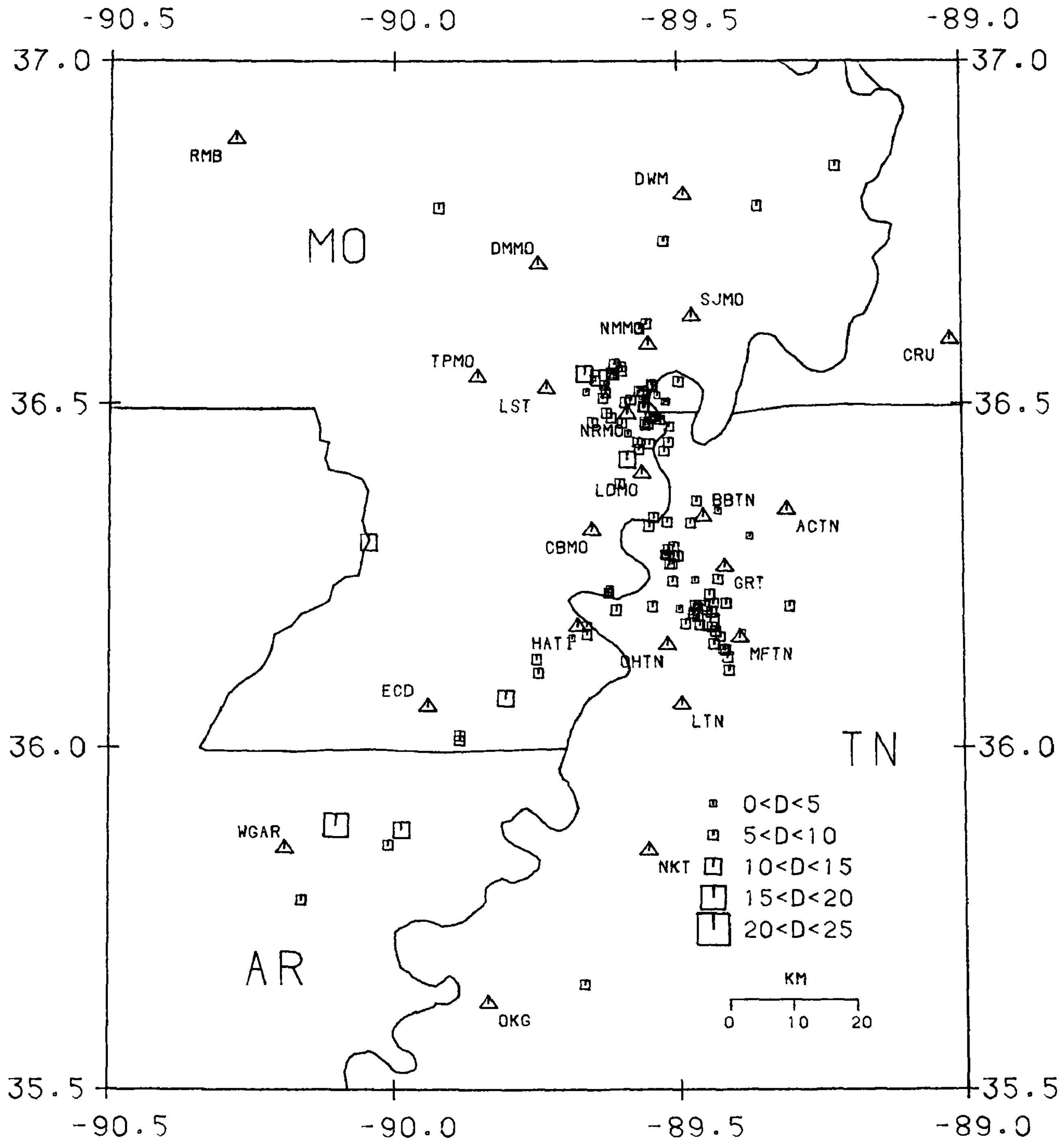

FIGURE 4
CUMULATIVE EVENTS 01 JUL 1986 TO 31 DEC 1986
LEGEND . △ STATION ◻ EPICENTER

Consolidated Digital Recording and Analysis

9930-03412

Sam Stewart
Branch of Seismology
U.S. Geological Survey
345 Middlefield Road, Mail Stop 977
Menlo Park, California 94024
(415) 323-8111 x 2577

Investigations

The goal is to operate, on a routine and reliable basis, a computer-automated system that will detect and process earthquakes occurring within the USGS Central California Earthquake Network (also known as CALNET). Presently, the output from more than 460 short-period seismic stations is telemetered to a central recording point in Menlo Park, California. Two DEC PDP11/44 computers, and a VAX/750, are used on this project. The 11/44A is dedicated to the task of online, realtime detection of earthquakes and storing the waveforms for later analysis. The 11/44B is used for offline processing and archiving of earthquakes. Both computers have a 512 channel analog-to-digital converter, so the 11/44B can serve as backup to the online system whenever necessary. (One of the a/d converters can be connected to the VAX/750 computer as well, to be used both for Calnet realtime monitoring experiments, and for offline digitizing from analog magnetic tapes.) The two 11/44 computers communicate with each other via a simple digital-bit I/O "semaphore" system, and transfer large amounts of data via a dual-ported disk subsystem or a dual-ported magnetic tape subsystem.

The VAX/750 is a general purpose computer used by the Branch of Seismology. We use it as the primary "research" computer for the CUSP system. It holds the primary data base of earthquake summary data and phase card data, which is available for research purposes. We update and maintain the CALNET data on this computer.

Both 11/44 computers use the RSX11M-PLUS (v2.1) operating system. The VAX/750 uses the DEC VMS operating system. Software has been developed largely by Carl Johnson in Pasadena, but with considerable modification by Peter Johnson, Bob Dollar and Sam Stewart, to meet Menlo Park's specific needs. Our applications are written in Fortran-77, but with heavy use of system functions unique to the RSX or VMS operating systems.

Results

1. The CUSP system processed approximately 7600 earthquakes that occurred within or near the CALNET network during the period October 1986 through March 1987. The usual few thousand non-seismic noise events had to be examined and deleted from the system as well.

   In addition, we are still processing aftershocks from the Chalfant Valley earthquake of July 1986.

2. The Parkfield Earthquake Prediction Experiment has added many instruments to the CUSP realtime earthquake monitoring task. There is a total of 111 instruments designated as within or near the Parkfield area. Of these, 11

are the 3-component Force Balance Accelerometers (resulting in 33 instruments to monitor), and 5 are Dilatometers. We are watching for earthquakes sufficiently large in the Parkfield area to record useful signals on these low gain instruments. The job has just started, and so far there are no results to report.

3. Project personnel and Alaska Network personnel have been trying to make necessary modifications to CUSP analysis software so that Alaska data can be digitized from their telemetry tapes and processed on the 750 CUSP system. The main delay now is to get a noise glitch problem out of the 750 digitizing process.

Reports

None.

Seismic Monitoring of the Shumagin Seismic Gap, Alaska

USGS 14-08-0001-A0260

John Taber
Lamont-Doherty Geological Observatory of Columbia University
Palisades, New York 10964
(914) 359-2900

Investigations

Seismic data from the Shumagin seismic network were processed to obtain origin times, hypocenters, and magnitudes for local and regional events. The processing resulted in files of hypocenter solutions and phase data, and archive tapes of digital data. These tiles are used for the analysis of possible earthquake precursors, seismic hazard evaluation, and studies of regional tectonics and volcanicity (see Analysis Report, this volume). Yearly bulletins are available starting in 1984.

Results

The Shumagin network was used to locate 611 earthquakes in 1986. The seismicity of the Shumagin Islands region for this time period is shown in map view and cross section in figure 1. The largest event in this period within the network had a magnitude of 4.5 and was located over the main thrust zone at a depth of 4.5 km. A magnitude 4.1 earthquake occurred at a depth of 201 km. This was the first deep event larger than magnitude 4 since 1981. Otherwise the overall pattern over this time period is similar to the long term seismicity. Concentrations of events occur at the base of the main thrust zone and in the shallow crust directly above it. The continuation of the thrust zone towards the trench is poorly defined. West of the network (which ends at 163°) the seismicity is more diffuse in map view and extends closer to the trench. Nine of the 13 located events larger than magnitude 4 occurred in this western region. Below the base of the main thrust zone (~45 km) the dip of the Benioff zone steepens. Part of the double plane of the lower Benioff zone is evident near 100 km depth.

The network is capable of digitally recording and locating events as small as Ml = 0.4 with uniform coverage at the 2.0 level. Onscale recording is possible to ~Ms=6.5 on a telemetered 3 component force-balance accelerometer. Larger events are recorded by one digitally recording accelerometer and on photographic film by 12 strong-motion accelerometers.

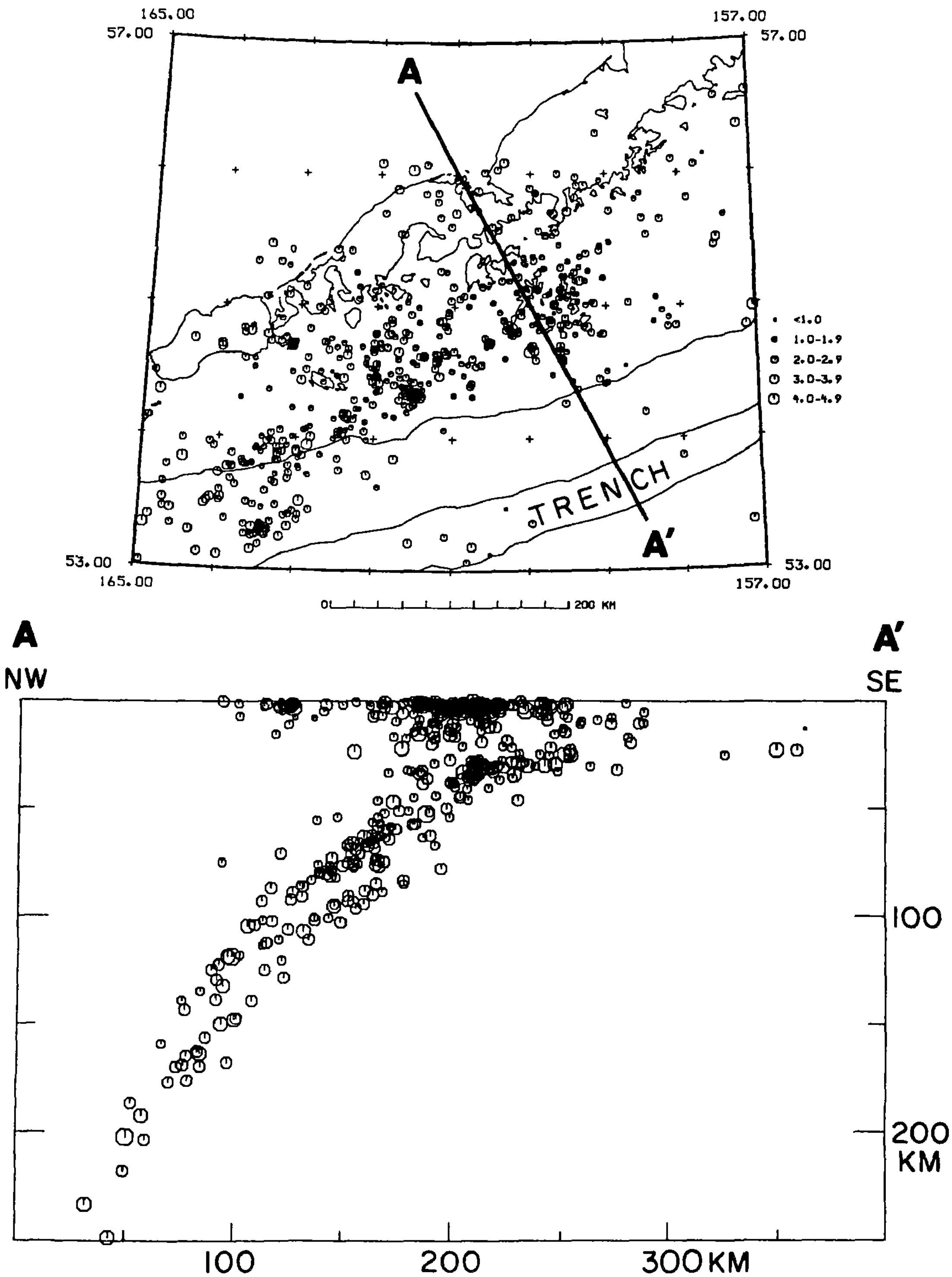

Figure 1. Top: Seismicity recorded by the Shumagin seismic network during 1986. Bottom: Cross section of seismicity projected along the line A-A' in the upper figure.

Earthquake Hazard Research in the Greater Los Angeles Basin and Its Offshore Area

#14-08-0001-A0264

Ta-liang Teng
Thomas L. Henyey
Egill Hauksson

Center for Earth Sciences
University of Southern California
Los Angeles, CA 90089-0741
(213) 743-6124

INVESTIGATIONS

(1) Monitor earthquake activity in the Los Angeles Basin and the adjacent offshore area.

(2) Upgrade of telemetry electronics used by remote field stations. The microprocessor-based Optimal Telemetry System has been deployed for field testing at three seismic stations.

RESULTS

(1) The earthquake activity that occurred in the Los Angeles basin and the southern California coastal zone during 1986 is shown in Figure 1. The seismicity rate during 1986 is similar to the rate that was recorded during the previous three years. The earthquake activity in the Los Angeles basin is characterized by single shocks that are scattered throughout the region. Several spatial clusters are observed in the monitoring region. Clusters of seismicity are observed at the northern segments of both the Newport-Inglewood fault as well as the Palos Verdes fault during 1986. The adjacent offshore area in Santa Monica Bay is also characterized by a moderate level of seismic activity. A cluster of earthquakes is observed near the aftershock zone of the 1973 Point Mugu earthquake. The largest earthquake to occur within the Los Angeles basin had a magnitude of 3.9 and was located near the Newport-Inglewood fault, just south of the City of Long Beach. In summary, although the 1986 seismicity in the southern California coastal zone and the Los Angeles basin is characterized by several spatial clusters of seismicity, the overall level of activity is moderate to low as compared with the last 10 years of seismicity.

Five earthquakes of M>3.0 occurred in the greater Los Angeles basin during 1986. Their respective focal mechanisms are shown in Figure 2. The event of March 20, 1986 that shows reverse faulting on the Palos Verdes fault was a part of a small spatially clustered swarm. A M=3.9 quake (April 5, 1986) that was the largest earthquake reported during 1986 in the Los Angeles basin had a strike slip mechanism and is located near the southern segment of the Newport-Inglewood fault. A reverse mechanism (March 9, 1986) and a strike-slip mechanism (July 7, 1986) are two of the larger events in a swarm that occurred near Claremont, eastern San Gabriel Valley. Two events near Manhattan Beach show strike-slip faulting near the northern end of the Palos Verdes fault (June 16, 1986) and reverse faulting onshore (May 19, 1986). The largest offshore event (August 16, 1986) shows strike-slip faulting 15 km to the northeast of Santa Barbara Island.

In summary, strike slip faulting mixed with reverse faulting is observed for M>3.0 local earthquakes in the greater Los Angeles basin.

(2) A second generation of the Optimal Telemetry System (OTS) is currently being designed and built. The front-end anti-aliasing filters have been upgraded to 7 poles. To minimize electronic noise the microprocessor has been placed on a separate circuit board. The design goals are to achieve a background noise level of 1 mV or less. Field testing of the new OTS is planned to begin in summer 1987.

A new seismograph station (SAT) was installed in a 1300 ft. deep borehole in the City of Santa Ana in Orange County. The station that began operating in February 1987 is located near the Newport-Inglewood fault and fills an important gap in the station distribution between Long Beach and San Onofre.

REPORTS

Hauksson, E., T. L. Teng, T. L. Henyey, J. K. McRaney, L. Hsu and G. Saldivar, Earthquake Hazard Research in the Los Angeles Basin and Its Offshore Area, U.S.C. Geophysics Laboratory Technical Report #87-1, 1987.

Teng, T. L. and M. Hsu, A Seismic Telemetry System of Large Dynamic Range, Bull. Seism. Soc. Amer. 76, 1461-1471, 1986.

Hauksson, E. and G. Saldivar, The 1930 Santa Monica and the 1979 Malibu, California, Earthquakes, Bull. Seism. Soc. Amer. 76, 1542-1559, 1986.

Hauksson, E., Seismotectonics of the Newport-Inglewood Fault Zone in the Los Angeles Basin, Southern California, Bull. Seism. Soc. Amer. 77, 539-561.

Hauksson, E., T. L. Teng and T. L. Henyey, Near-Surface Attenuation of Waveforms of Local Earthquakes: Results from a 1500 m Deep Downhole Seismometer Array, submitted to Bull. Seism. Soc. Amer., January, 1987.

Saldivar, G. V., E. Hauksson and T. L. Teng, Seismotectonics of the Santa Monica and Palos Verdes Fault Systems in the Santa Monica Bay, Southern California, to be submitted to BSSA, May, 1987.

Hauksson, E., T. L. Teng and T. L. Henyey, Near-surface Attenuation of Waveforms of Local Earthquakes: Results From a 1500 m Deep Downhole Seismometer Array, EOS Trans., Amer., Geophys. Union 67, p. 1091, 1986.

Saldivar, G. V., E. Hauksson and T. L. Teng, Seismotectonics of the Santa Monica and Palos Verdes Fault Systems in the Santa Monica Bay, EOS Trans., Amer. Geophys. Union 67, p. 1085, 1986.

Hauksson, E., Seismotectonics of the Newport-Inglewood Fault Zone and the 1933 Long Beach Earthquake (M_L = 6.3) in the Los Angeles Basin, Southern California, presented at S.S.A. Meeting Santa Barbara, March, 1987.

st/87-363

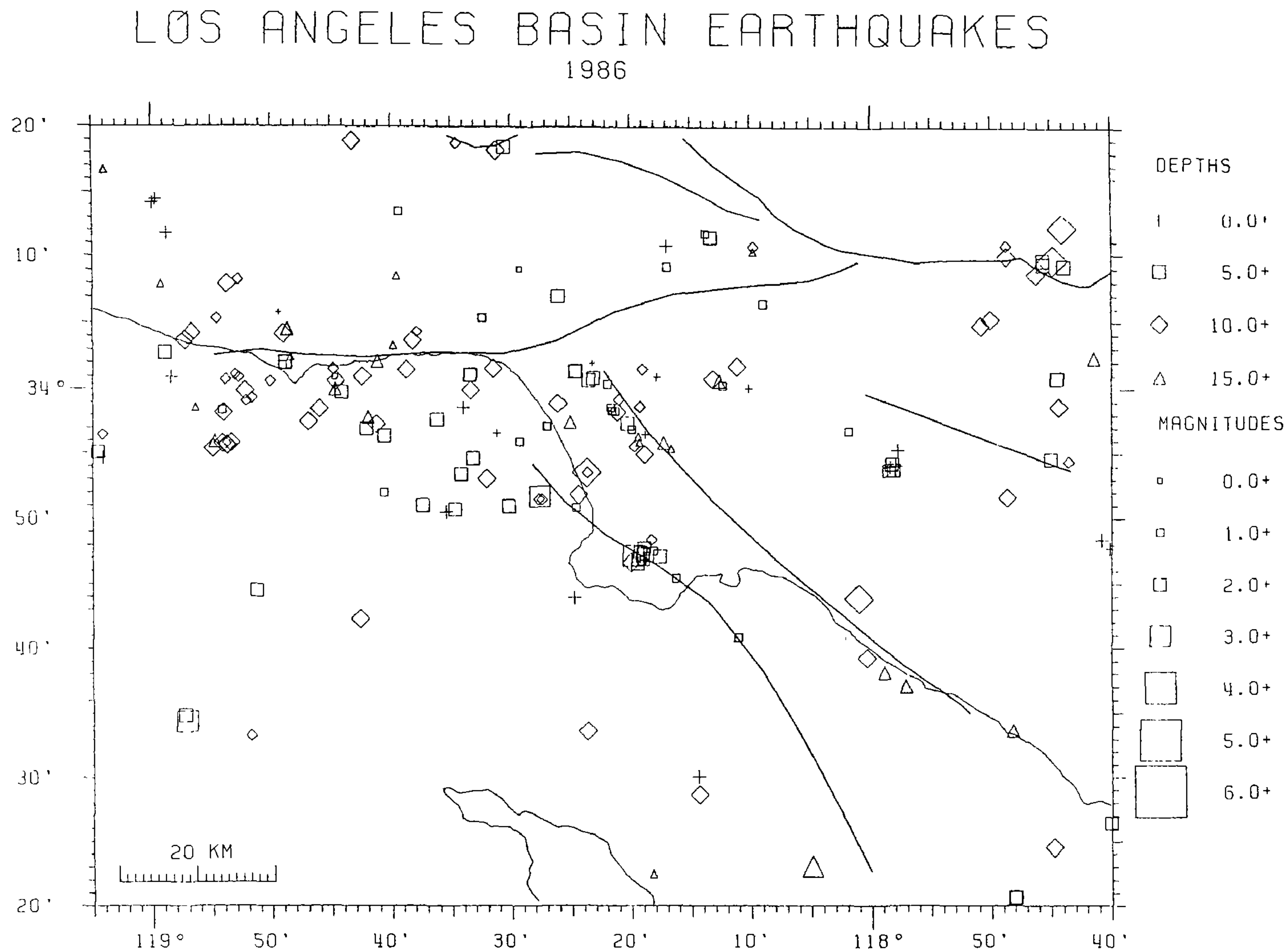

Figure 1. Seismicity 1986 recorded by the U.S.C. seismic network in the Los Angeles Basin.

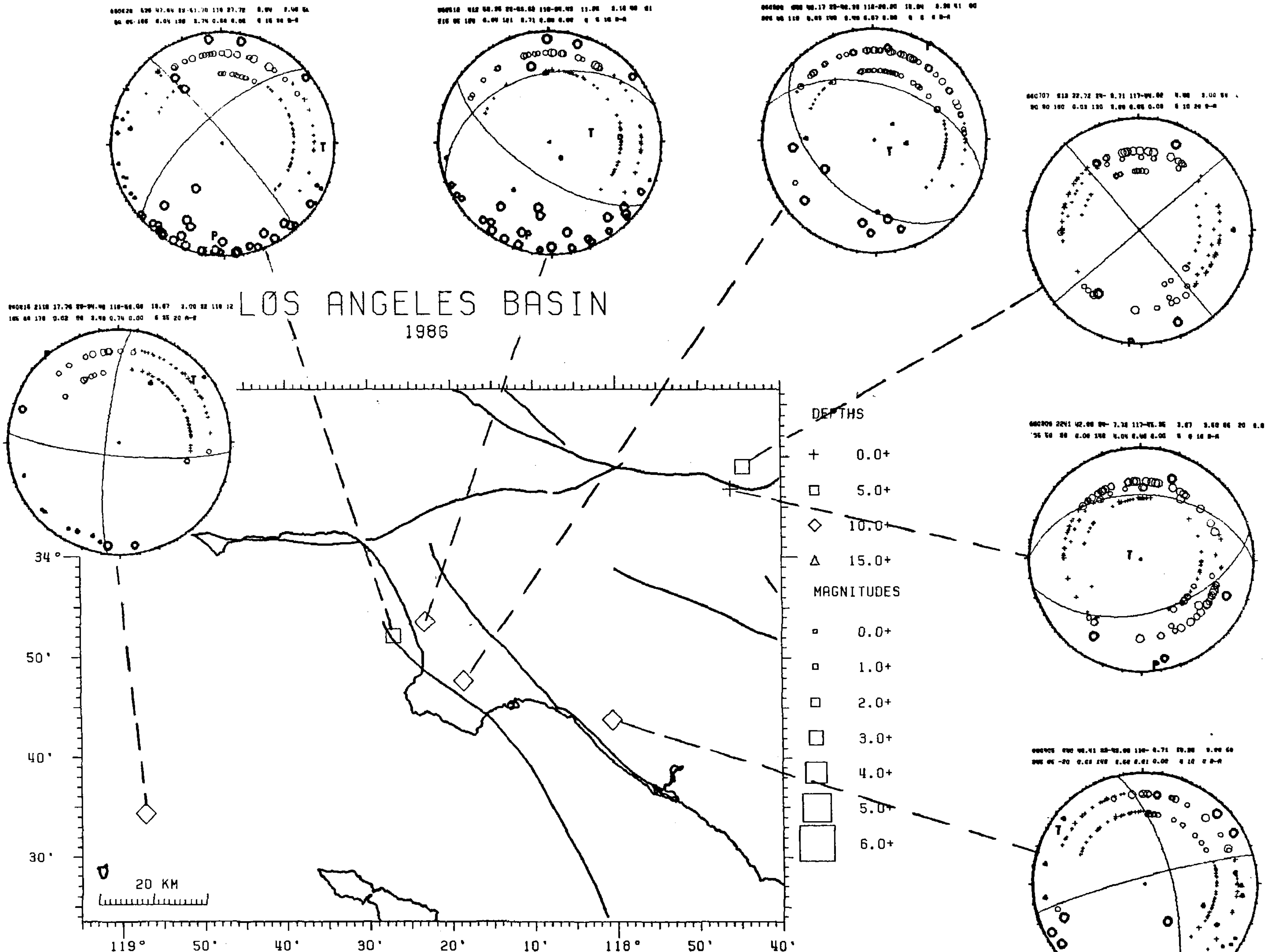

Figure 2. Focal mechanisms of M≥3.0 earthquakes reported during 1986 in the Los Angeles basin.

Field Experiment Operations

9930-01170

John Van Schaack
Branch of Seismology
U. S. Geological Survey
345 Middlefield Road MS-977
Menlo Park, California 94025
(415) 323-8111, ext. 2584

Investigations

This project performs a broad range of management, maintenance, field operation, and record keeping tasks in support of seismology and tectonophysics networks and field experiments. Seismic field systems that it maintains in a state of readiness and deploiys and operates in the field (in cooperation with user projects) include:

a. 5-day recorder portable seismic systems.
b. "Cassette" seismic refraction systems.
c. Portable digital event recorders.
d. Smoked paper recorder portable seismic systems

This project is responsible for obtaining the required permits from private landowners and public agencies for installation and operation of network sensors and for the conduct of a variety of field experiments including seismic refraction profiling, aftershock recording, teleseism P-delay studies, volcano monitoring, etc.

This project also has the responsibility for managing all radio telemetry frequency authorizations for the Office of Earthquakes, Volcanoes, and Engineering and its contractors.

Results

Seismic Refraction

One hundred twenty seismic cassette recorders were used in two seperate experiments. The first experiment was carried out near San Luis Obispo CA. in conjunction with a seismic refraction experiment being conducted for Pacific Gas and Electric Co. by an independent contractor. We recorded two profiles, one running approximately East West and one running North South. There were considerable problems firing the shots and results were disappointing. The second experiment was a cooperative experiment conducted with the University of Southern California. This experiment consisted of a single profile across the Tehachapi Mountains Southeast of Bakersfield CA. The record quality on this experiment was good.

Telemetry Networks

We have completed the installation of a six station seismic network near Lake Berryessa in Central California for The Bureau of Reclamation and the data are being monitored by CUSP. We have installed a total of seven Force balance Accelerometers each operating at multiple gains seperated by 20 db. These data are being telemetered to Menlo Park. We have also instrumented 4 Dilatometer sites for telemetry, these are also operating at multiple gains. All of these sensors will be monitored by the CUSP and RTP automatic earthquake detection systems in Menlo Park.

Portable Networks

For the first time in approximately 20 years there were no 5-day recorders deployed anywhere.

Geothermal Seismotectonic Studies

9930-02097

Craig S. Weaver
Branch of Seismology
U. S. Geological Survey
at Geophysics Program AK-50
University of Washington
Seattle, Washington 98195
(206) 442-0627

Investigations

1. Continued analysis of the seismicity and volcanism patterns of the Pacific Northwest in an effort to develop an improved tectonic model that will be useful in updating earthquake hazards in the region. (Weaver, Yelin, with Guffanti of IGP branch)

2. Continued acquisition of seismicity data along the Washington coast, directly above the interface between the North American plate and the subducting Juan de Fuca plate. (Weaver, Zollweg, UW contract)

3. Continued seismic monitoring of the Mount St. Helens area, including Spirit Lake (where the stability of the debris dam formed on May 18, 1980 is an issue) and Elk Lake, and the southern Washington-northern Oregon Cascade Range. The data from this monitoring is being used in the development of seismotectonic models for southwestern Washington. (Weaver, Grant, Yelin, UW contract)

4. Study of Washington seismicity, 1960-1969. Efforts are underway to determine magnitudes based on a revised, empirical Wood-Anderson-coda duration relation. Earthquakes with magnitudes greater than 4.5 are being re-read from original records and will be re-located using master event techniques. Focal mechanism studies are being attempted for all events above magnitude 5.0. (Yelin, Weaver)

5. Detailed analysis of the seismicity sequence accompanying the May 18, 1980 eruption of Mount St. Helens. Earthquakes are being located in the ten hours immediately following the onset of the eruption, and the seismic sequence is being compared with the detailed geologic observations made on May 18. Re-examination of the earthquake swarms that followed the explosive eruptions of May 25 and June 13, 1980, utilizing additional playbacks of 5-day recorder data. (Weaver, Zollweg, Norris, UW contract)

6. Study of earthquake catalogs for the greater Parkfield, California region for the period 1932-1969. Catalogs from the University of California (UCB) and CalTech (CIT) are being compared, duplicate entries noted, and the phase data used by each reporting institution are being collected. The study is emphasizing events greater than 3.5, and most events will be relocated using station corrections determined from a set of master events located by the modern seismographic networks. (Meagher, Weaver, with Lindh, Ellsworth)

7. Analysis of a swarm of over 500 sub-edificial (depths 3 - 14 km) earthquakes that occurred at Mt. St. Helens prior to the 1980 eruption. Sub-edifical earthquakes have recently been found to be useful in mapping the overall geometry of the magma feeder system, and the pre-May 18 data set is probably the best available to us in terms of numbers of events, numbers and distribution of stations recording them, and

background noise level. (Zollweg, UW contract)

8. Analysis of the sequence of high frequency earthquakes that followed the eruption of Nevado del Ruiz in Colombia, South America. (Zollweg, with Colombian investigators)

9. Detailed study of a swarm of tectonic earthquakes near Darrington in the Washington North Cascades, and the geometry of the recently-recognized Darrington Seismic Zone. Cross-correlation and cross-spectrum techniques are being used to resolve the spatial relationships of the swarm events. (Zollweg, UW contract)

10. Comparison of spatial features of aftershock seismic moment release with surface faulting for the 1983 Borah Peak, Idaho earthquake. (Zollweg)

Results

1. The interagency agreement between the U.S. Geological Survey and the Bonneville Power Administration to allow the transmission of seismic data over existing BPA microwave facilities was completely implemented. Nine commercial phone lines were replaced by microwave transmission during the past 6 months; in all 14 phone lines have been replaced by 18 microwave links. The additional microwave links are expected to be used to re-instrument the Oregon Coast and Cascade Ranges in the last half of FY87 and during FY88.

2. A small-diameter (~ 1 km), near-vertical seismogenic region beneath Mt. St. Helens was defined by sub-edificial earthquakes occurring before the 1980 eruption. The structure as presently known extends from 4 to 13 km in depth. It is interpreted as a zone of brittle failure which occurred in response to magmatic pressure variations in a narrow feeder conduit. Resolution of this structure is the first indication that has been found in the seismographic data that deep magma transport at Mt. St. Helens may be confined to small, well-defined structures.

3. Mt. St. Helens sub-edificial activity between May 18 and June 14, 1980, indicates the existence of a second tightly-clustered zone of activity at depths of 6 to 12 km lying 1 to 2 km west of the seismogenic structure we have tentatively identified as the main feeder conduit. This second zone seems to have been active only between those dates rather than persistently through time like the the first zone identified. Its relation to the rest of the system is presently unclear; it may represent an older feeder conduit that is no longer directly connected to the surface but can still respond to pressure variations in the rest of the system.

4. High frequency earthquakes at Nevado del Ruiz volcano, Colombia, occur over a wide geographical area (at least 150 square km) and cannot be related in a predictive sense to the minor eruptive activity that has occurred at the volcano since late 1985. Some linear trends are evident from epicenter plots, and a few of these trends appear to be directly related to mapped faults. Seismic activity in any one area is usually highly non-stationary in time. We infer that the sub-surface magmatic system is complex and of large areal extent, and that these features will make attempts to use the high frequency activity in prediction efforts very difficult under a much better understanding of the system is achieved.

5. A swarm of earthquakes having magnitudes as high as 3.6 occurred near Darrington in the Washington North Cascades in early 1986. This was the second-most intense swarm to occur in northwest Washington since 1970. Cross-correlation and cross-spectral analysis of digital data from the UW net indicates that the source region was a

400 by 700 meter area at a depth of about 9 km. The earthquakes tended to occur in tight clusters within this area, probably at asperities along a fault. Reanalysis of regional seismicity with station corrections developed in the investigation of this sequence shows evidence for an east-west striking fault structure dipping to the south. The Darrington sequence would fall on this structure and the computed focal mechanisms agree well in both strike and dip. A rough draft of a paper on this structure, which we have named the Darrington Seismic Zone, has been completed.

6. Relative location bias caused by using different subsets of a given "master" station network causes significant scatter in the resultant patterns of hypocenters and interferes with identification of small structures. The 95% confidence ellipses have been found to enclose roughly 90% of the possible solutions for single events using different station subsets; solutions tend to stabilize near their "best" locations using the full network when data from at least 7 stations are available. The network bias effect is quasi-systematic and can be computed and corrections for it made.

Reports

Shemeta, J. E. and Weaver, C.S., 1986, Seismicity accompanying the May 18, 1980 eruption of Mount St. Helens, Washington, *in, Proceedings, Mount St. Helens Five Years Later,* Eastern Washington University Press, Cheney, WA., (still in press).

Grant, W. C. and Weaver, C. S., The 1958-1962 earthquake sequence near Swift Reservoir, Washington, *Bulletin of the Seismological Society of America, 76,* 1573-1587, 1986.

Grant, W. C. and Weaver, C. S., Seismicity of the Spirit Lake area: Estimates of possible earthquake magnitudes for engineering design, in *The formation and significance of major lakes impounded during the 1980 eruption of Mount St. Helens, Washington, U. S. Geological Survey Professional Paper,* edited by R. L Shuster and W. Meyer, (still in press).

Weaver, C. S. and G. E. Baker, Geometry of the Juan de Fuca plate beneath Washington: Evidence from seismicity and the 1949 South Puget Sound earthquake, *Bulletin of the Seismological Society of America,* (in press).

Baker, G. E. and C. A. Langston, Source parameters of the magnitude 7.1, 1949, South Puget Sound, Washington, earthquake *Bulletin of the Seismolgical Society of America,* (in press).

Weaver, C. S., Shemeta, J. E., and W. C. Grant, Crustal spreading at Mount St. Helens, Washington, *J. Geophys. Res., 92,* (in press).

Guffanti, M. and C. S. Weaver, Distribution of late Cenozoic volcanic vents in the Cascade Range and northwestern Basin and Range province, (abs), *EOS, Trans. Am. Geophys. Union., 67,* 1226, 1986.

Ludwin, R. S., L.L. Noson, A. I. Qamar, R. S. Crosson, C. S. Weaver, S. D. Malone, W. C. Grant, and T. S. Yelin, Seismicity in the northwestern U.S., (abs), *EOS, Trans. Am. Geophys. Union., 67,* 1084, 1986.

Atwater, B. F. and W. C. Grant, Holocene subduction zone earthquakes in coastal Washington, (abs), *EOS, Trans. Am. Geophys. Union, 67,* 906, 1986.

Jonientz-Trisler, C. and J. Zollweg, Sub-edificial Seismicity at Mt. St. Helens Prior to the 1980 Eruption, (abs), *Abstract volume, Hawaii Symposium on How Volcanoes Work,* 126, 1987.

Zollweg, J., F. Munoz, H. Meyer, D. Harlow, and F. Guendel, Post-eruptive High Frequency Seismicity at Nevado del Ruiz, Colombia, (abs), *Proceedings, Hawaii Symposium on How Volcanoes Work,* 282, 1987.

P. Johnson-Browne and J. Zollweg, The 1986 Darrington, Washington earthquake swarm: evidence for tightly clustered asperities?, (abs), *EOS, Trans. Am. Geophys.*

Union, 68, 46, 1987.

P. Johnson-Browne and J. Zollweg, High precision relative locations for a northwestern Washington earthquake swarm, (abs), *Seismological Research Letters, 58,* 28, 1987.

J. Zollweg, Seismic monitoring at active silicic volcanoes: hypocentral accuracy and its importance in interpretation of volcanic processes, (abs), *Proceedings, IAVCEI 1987 Meeting,* in press.

Weaver, C. S. and J. E. Zollweg, Seismological studies at Mount St. Helens, USA: Implications for forecasting other volcanic events, (abs), *Proceedings, 1987 IUGG Workshop on Global Change,* (in press).

Meagher, K.L., C. S. Weaver, A. G. Lindh, and W. L. Ellsworth, Seismicity in Central California, 1932-1969: Initial results of a catalog study, (abs), *EOS, Trans. Am. Geophys. U., 68,* (in press).

G. Clayton and J. Zollweg, Tertiary-Quaternary faults and the 1981 magnitude 5 earthquake in the Goat Rocks Wilderness, south-central Cascade Range Washington, (abs), *Programme and Abstracts, A Symposium on Crustal Movements in the Pacific Northwest,* Pacific Geoscience Centre, Sidney B.C., Canada, 29-31, 1987.

STRONG GROUND MOTION OF LARGE INTRAPLATE EARTHQUAKES ESTIMATED FROM TELESEISMIC RECORDINGS

9910-new

John Boatwright
U.S. Geological Survey, MS 977
345 Middlefield Road
Menlo Park, CA 94025
FTS 467-2485 or 415-329-5609

George L. Choy
U.S. Geological Survey, Box 25046, MS 967
Denver Federal Center, CO 80225
FTS 776-1506

Investigations

1. Teleseismic analysis of the 1985 Nahanni earthquakes, which occurred in the Canadian Northwest Territories for rupture characteristics.

2. Teleseismic analysis of a set of nine large (m_b = 5.5 to M_s = 7.4) intraplate earthquakes to deduce the appropriate scaling characteristics for high-frequency ground motion radiated by large shallow thrust earthquakes in intraplate environments.

Results

1. Boatwright and Choy (1986) developed an analysis technique which corrects teleseismic recordings for the focal mechanism of the events, the interference of the depth phases, and the teleseismic attenuation, in order to estimate the acceleration source spectrum of the earthquake in the frequency band from 50 sec to 2 Hz. The analysis uses a frequency dependent Q determined by Choy and Cormier (1986) and a finite source description which permits an unbiased estimate of the acceleration spectral level for frequencies above the corner frequency. The near-field strong ground motion can be estimated by appropriately scaling the acceleration source spectrum for hypocentral distance and site effects.

2. We have analyzed a set of nine large intraplate earthquakes to determine the maximum expectable acceleration spectral level for near-field strong ground motion. The nine events range in size from the m_b = 5.5 aftershock of the 1982 Miramichi earthquake to the M_s = 7.4 Tabas, Iran, earthquake. The most surprising result of the analysis is the average spectral shape of the events; eight of the nine events show a pronounced intermediate slope, between the low-frequencies where the acceleration spectra increase proportional to the square of the frequency, and the high-frequencies, where the acceleration spectra are approximately flat, or decrease slightly as a function of frequency.

Publications

Boatwright, J., and G.L. Choy, 1986, Acceleration spectra for subduction zone earthquakes, EOS 67, 310.

Boatwright, J., and G.L. Choy, 1987, Acceleration spectra for subduction zone earthquakes, in preparation.

Choy, G.L., and J. Boatwright, 1987, Teleseismic analysis of the Nahanni earthquakes in the Canadian Northwest Territories, in preparation.

Boatwright, J. and G.L. Choy, 1987, Acceleration spectra for large earthquakes in North Eastern North America, in preparation.

Intensive Studies of Source Zone and Crustal Structure of the Arkansas Swarm Region using a 40-station Three-Component, Telemetry, Portable, Digital Array

Contract Number : 14-08-0001-G1327

Jer-Ming Chiu, Jose Pujol, and Arch Johnston

Memphis State University
Tennessee Earthquake Information Center
Memphis, TN 38152
Tel: 901-454-2007

The PANDA (Portable Array for Numerical Data Acquisition) array has been deployed and is fully operationalin the Arkansas earthquake swarm regio (Figure 1) from early January to late April, 1987 after about 5 months of field testing and trouble shooting. The configuration of the PANDA array, the field experiment, and data processing techniques are briefly discussed below.

1. The PANDA Array

The design criteria of the PANDA array includes the following: (1) portability, (2) high dynamic range, (3) three-component recording within 0.1 to 40 Hz frequency ranges, (4) small power consumption and solar power for each station, (5) telemetry with capability of transmitting seismic signals over 100 miles after one repeat station, (6) synchronized digital recording at a central station, (7) ease of installation and maintenance that can be performed by a two-man crew, and (8) capability for on-site data analysis during the experiment. All these design goals are accomplished with several minor modifications as discussed in the following.

The PANDA array consists of 40 three-component stations telemetered to a central recording station by standard FM radio links. The common recording base assures the precision of inter-station timing. The high dynamic range of 96 dB is achieved by using two channels per component with offset gains (high- and low-gain channels). The powerful central recording computer described below is capable of on-line data acquisition, off-line data analysis, and tape archiving.

Seismic signals from each station are transmitted via radio back to the recording center, stored in a 474 Mbyte Winchester disc and later archived to magnetic tape. Seismic signals from 20 outer stations are repeated once by the other 20 inner stations as shown in Figure 1 to allow broader extent of the network coverage and to overcome topographic constraints in a telemetry system. Before April 1987, eighty Mark Products TDC-1 tripod L28 (4.5 Hz) seismometers were used. Ten Kinemetric FBA (1 Hz) sensors were delivered and installed in the field in early April to replace the ten L28's. Two three-component L28 seismometers are co-sited at each of the 30 stations. A FBA unit and a L28 unit are co-sited at the other 10 stations. The 10 stations with FBA seismometers are located near the center of the swarm zone and are capable of on-scale recording of up to 2 g ground acceleration. Each station consists of an SX-20 solar panel, VCO's and amplifiers, and a radio transmitter. The VCO, designed by TEIC's Technical Director, has been proved to be very stable in the field with almost no frequency drift. With such a reliable VCO at least 60 DB dynamic range system can be achieved through FM radio links. Input seismic signals are filtered using Butterworth bandpass filters for a frequency range from 0.1 to 40 Hz. Although the overall system response tends to be low at the lower frequency band important for teleseismic and converted seismic phase studies, low frequency information can be recovered by digital filtering techniques.

After demultiplexing, 240 data channels are input into an analogue-to-digital converter in the main central recording computer, a MASSCOMP MC5600 32-bit machine, for trigger threshold detection and on-line digital recording. Since seismic signals from all stations are telemetered to a common recording center, a much more sophisticated trigger algorithm is possible than with single, independent stations. The MC5600 system consists of 8 Mbyte memory, 4 Gbyte user-addressable space, UNIX operating system with FORTRAN and C compilers, a 256 channel A/D converter, a 16-bit high speed digital I/O interface, a data acquisition system, a floating point accelerator, a streaming tape drive, two 1 Mb floppy disk drives, a 71 Mb Winchester hard disk, a 474 Mb Winchester disk, a line printer, a high resolution color graphics terminal, a high resolution ink-jet color copier, and a 16-bit array processor. The A/D converter is capable of sampling 1024 channels data at a maximum rate up to 1 MHz. The PANDA array is currently operated at 100 samples/second. This integrated field computer system allows very efficient data acquisition as well as extensive preliminary data analysis in the field.

An IRIG H coded time signal output from a portable satellite clock is input to three of the unused A/D channels of the computer for accurate timing. Two internal clocks in the data acquisition system (DACP) are gated in the way that frame rate for the first clock (frame clock) is set to 100 Hz and burst rate for the second clock (burst clock) is set to 50,000 Hz. Output of the burst clock is input to the input of the frame clock. Output of the frame clock is then input to the A/D converter to control the sampling operation of the A/D converter. The burst clock will start to control the actual sampling at 0.5 MHz when voltage of the frame clock changes from low to high. Therefore an almost synchronized sampling can be achieved. In addition, a global positioning system (GPS) is used to accurately locate station coordinates : latitude, longitude, and elevation to within $\pm 5m$ (plus time, if necessary).

2. On-Line Digital Recording System

240 seismic channels after discriminators and three time channels from satellite clock are input into the DACP system of the MASSCOMP computer. A large ring buffer with forty 51,200 byte buffers is set up in the CPU to temporarily store the incoming digital data from 256 channels. Each buffer in the ring buffer can store 1 second of digital data from 256 channels at 100 samples/second sampling rate. Incoming digital data fills up one buffer after another on a real-time basis. After the last buffer is filled, the first buffer will be filled again, and the cycle repeats. Vertical high-gain channels from 10 stations are selected for trigger detection. Ratios of short term average (STA) and long term average (LTA) for the 10 selected stations are continuously evaluated to determine the status of the incoming seismic signals. We are experimentally testing the selection of trigger stations and the determination of trigger threshold. It is an event if the STA/LTA value of three

stations out of the 10 trigger stations reach or beyond the given trigger ratio. When an event occurs, the on-line digital recording system will first retrieve pre-event memory from the ring buffer and then continue to store 2 minutes of incoming digital data from all 256 channels into a disk file created at the time of trigger. After the event has been successfully stored, the STA/LTA ratio trigger evaluation resumes. The field test of this on-line trigger detection program has been very successful. During the 3 months experiment period, fourteen swarm earthquakes were large enough to trigger the PANDA array (some less than magnitude 0). All parameters, including frame clock rate, burst clock rate, number of trigger stations, STA and LTA windows, STA/LTA ratio, pre-event memory, and total recording time for each event can be changed by editing one of the input files.

After data files have been stored in the 474 Mb Winchester disk, a graphics display program, "LOOK," is available immediately to display the data in the EURORA color graphics terminal in order to check the signal quality and determine whether it is an earthquake or a false trigger, and to determine the time window within the two minutes of data to be demultiplexed and to be archived to a magnetic tape. The archived tape can be either processed with the MASSCOMP or sent back to TEIC to be processed in the VAX 11/785 where a powerful NUMERIX 432 array processor is available to analyze such a big data bank.

A program, "BLAST," is set up in the MASSCOMP system. This program will allow the on-line digital recording system to turn on and continuously store the incoming digital data into a file for the given time period. This program has been used successfully to record four dynamite explosions during the dismantling of one Titan missile silo .

One analogue seismic channel from one selected station is also recorded at the recording center by an MEQ-800 drum recorder to visually see the background activity in the region. In case a large earthquake swarm sequence occurs or the disk space is filled up faster than the process of archiving data to tape, the on-line digital recording system can be switched to write the triggered data to tape instead of the 474 Mb Winchester disk. The tape will be read back into MASSCOMP for preliminary processing, demultiplexing, and archiving in a later time.

Since the MASSCOMP computer system is a UNIX based multi-user, multi-task, and multi-processor system, all processing on the on-line digital recording system mentioned above can be executed simultaneously. We have not yet developed much of the processing software in the MASSCOMP system due to delay in the delivery of the array processor. Since the PANDA array will be shipped and deployed in the San Juan, Argentina for about a one-year period beginning in the coming summer of 1987, we expect that processing of the Arkansas swarm data collected by the PANDA array in the current project will be carried out mainly on the VAX 11/785 at TEIC.

3. Examples of Data Collected by the PANDA Array

(a) Explosion from Titan Missile Silo Dismantling

Figure 2 shows some examples of vertical-component seismograms recorded by the PANDA array during a field test period in December 1986 from a dynamite explosion at the 373-9 Titan missile site (#2 in Figure 1). Complicated waveforms can be seen in these examples. Large amplitude surface waves follow the P waves and show a very large moveout in time as the station distance from the source increases. Another feature shown in these seismograms is the large amplitude and high-frequency late arrivals. This portion of seismic energy can be interpreted as air coupled sonic waves from the explosion source. These air waves can best be seen on the vertical component in all examples indicating that these waves must be polarized along the radial plane and travel with very low velocity (air velocity $0.3 \sim 0.5$ km/sec). There are two distinct arrivals with almost constant time separation on all seismograms which can be interpreted as (1) air-coupled body waves (possibly P waves), and (2) air-coupled surface waves. In all there were four explosions from the same location and recorded by portions of the PANDA array and by eleven MEQ800 single component recorders. The 11 MEQ800 recorders were deployed directly over the swarm source zone with station spacing as small as 0.5-1 km. Three explosions were large enough to produce visible air-coupling waves as shown in Figure 2. A detailed analysis and modeling of air coupled sonic waves is in progress.

(b) Earthquakes from Arkansas Swarm Region

Figure 1 shows also examples of vertical-component seismograms recorded by many PANDA array stations from an earthquake located in the swarm source region. Unambiguous P and S arrival times can be read from the vertical and the two horizontal components. Accurate earthquake location can therefore be achieved. The S arrival, marked by an arrow above each seismogram, has been identified from the horizontal component. Seismograms are displayed in the direction coinciding with the azimuth between the stations and the source. Strong secondary arrivals dominate most of the vertical component seismograms in almost all directions. The complicated secondary arrivals between the P and S waves seem consistent with, but more complicated than, our previous observations. A systematic study of the occurrence of these strong crustal converted phases and their tectonic implications is in progress.

(c) Regional Earthquakes

During the deployment of PANDA array, two regional earthquakes from New Madrid seismic zone and one from Oklahoma were recorded. Two of the events were triggered by their S waves but not by P waves due to the longer travel distance and therefore emergent P arrivals. These events, however, can provide very unique opportunities to calibrate the array response to the incoming seismic waves. Study of array response to regional earthquakes is also in progress.

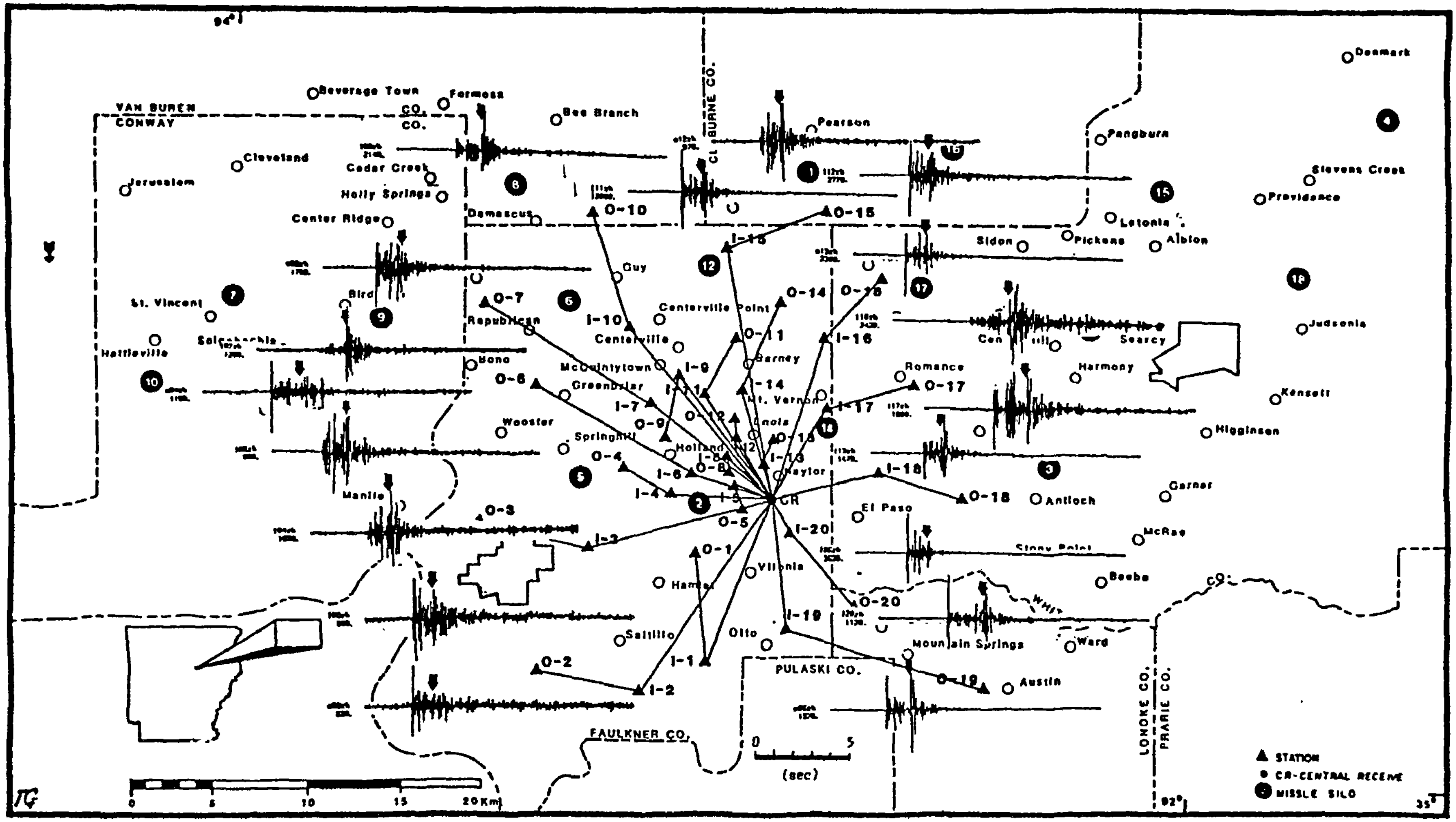

Figure 1. The PANDA array and some displays of the vertical component seismograms from an earthquake occurred in February 7, 1987. Epicenter is marked by the solid star. Radio links from outer stations ("0") to inner stations ("I") and to central recording site ("CR") are drawn. Seismograms are displayed roughly in correspondent to the azimuth of the stations from the epicenter. The S arival time is picked up from the two horizontal components and is marked by the arrow above each trace. Complicated waveforms between the P and S arrivals are apparent in all the seismograms shown here.

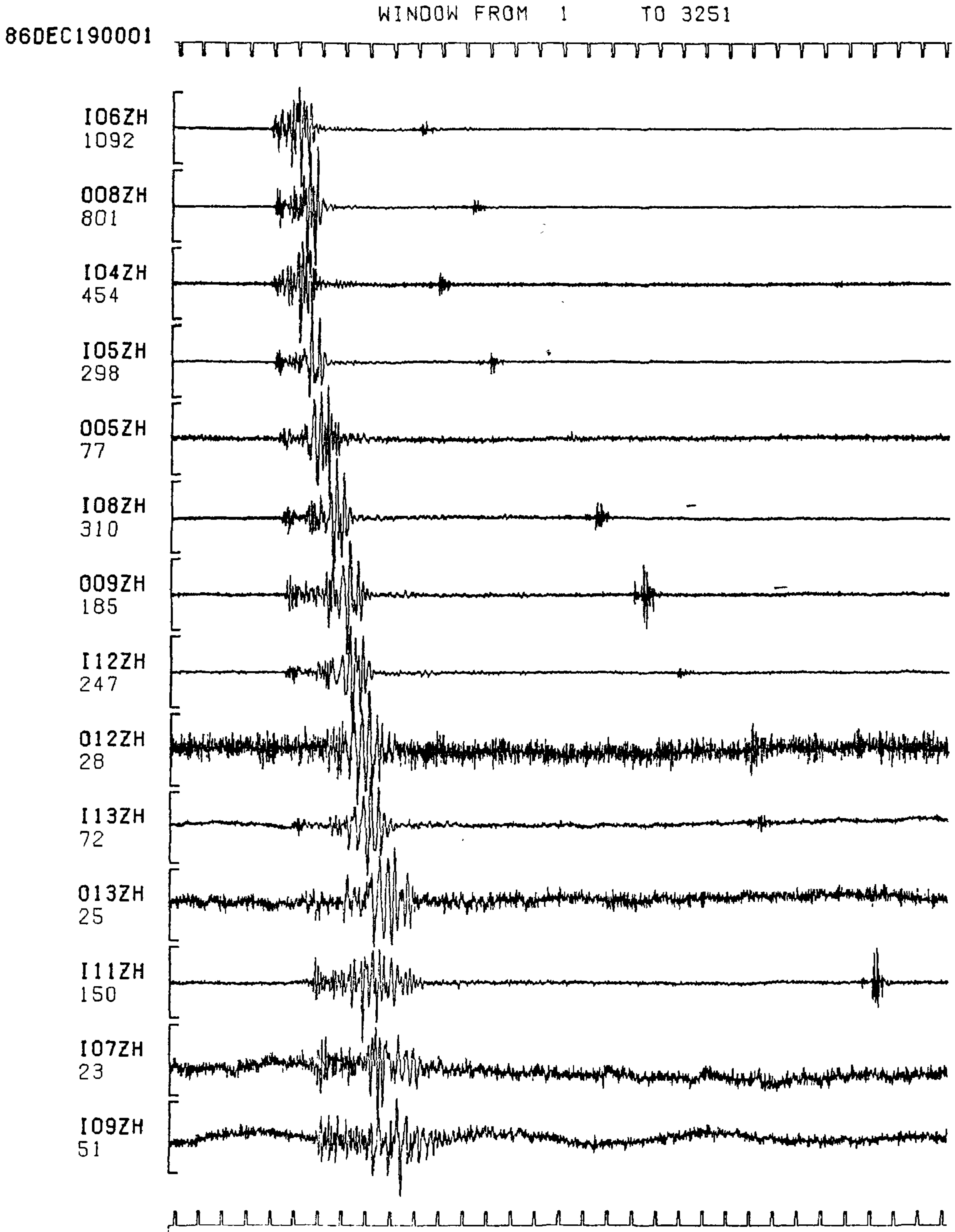

Figure 2. Examples of vertical seismograms from one of the explosions from the missile silo # 2 in Figure 1. Station code and maximum amplitude are printed in front of each trace. The large amplitude surface waves immediately after the first P arival and the later air-coupled sonic waves can be identified most clearly in the vertical component. Interpretation of seismograms recorded by the PANDA array is in progress.

Comparative Earthquake and Tsunami Potential for Zones in the Circum-Pacific Region

9600-98700

George L. Choy
Stuart P. Nishenko
William Spence
Branch of Global Seismology and Geomagnetism
U.S. Geological Survey
Denver Federal Center
Box 25046, Mail Stop 967
Denver, Colorado 80225
(303) 236-1506

Investigations

1. Prepare detailed maps and text of comparative earthquake potential for west coasts of Mexico, Central America and South America.

2. Develop a working model for the interaction between forces that drive plate motions and the occurrence of great subduction zone earthquakes.

3. Develop methods for the rapid estimation of the source properties of significant earthquakes.

4. Conduct investigations of the historic repeat-time data for great earthquakes in the northern Pacific Ocean margin.

5. Compile tsunami data for the circum-Pacific and the corresponding seismic source zones.

Results

1. The probabilistic work for northern Mexico has been completed and published in three papers by Nishenko and Singh in 1987. Two regions have the highest probabilities for the recurrence of large earthquakes within the next two decades: the central Oaxaca gap and the Acapulco-Marco gap. With the occurrence of the catastrophic earthquake of September 19, 1985, the Michoacan seismic gap now has a very low probability for recurrence of a great earthquake within 20 years. However, plate motions related to this earthquake could cause stress to transfer to the seismic gap at Acapulco and trigger a great earthquake there within the next few years. A study of aftershocks of the great 1979 Colombia earthquake has been accepted for publication (Mendoza, 1987). The study of this event in the context of the great 1906 and 1958 earthquakes will help the probabilistic assessment for the recurrence of great earthquakes in this region.

2. An evaluation of the ridge-push and slab-pull forces in the context of stresses that lead to great subduction zone earthquakes has been completed

(Spence, 1986, 1987). An important conclusion is that specific parts of a subducting plate may be monitored for precursors to seismic gap-filling earthquakes.

3. We have been integrating techniques of analyzing broadband data in the data flow of the NEIC. Broadband data are now used routinely to increase the accuracy of some reported parameters such as depth. By mid-1987, we hope to implement a semi-automated package to compute radiated energy from digitally recorded broadband data for all earthquakes with $m_b > 5.8$.

4. Data on the occurrence of great earthquakes and tsunamis from the Queen Charlotte Islands to the Aleutian Islands have been collected and the evaluation of probabilistic recurrence is being conducted by Drs. Nishenko and Jacob.

5. Several tsunami catalogs have been gathered prior to compilation of a comprehensive tsunami catalog. Dr. Nishenko has designed a form for systematically gathering and analysing tsunami data. Currently, there is no uniform approach to this data acquisition.

Reports

Choy, George, L., and Engdahl, E.R. (in press), Analysis of broadband seismograms from selected IASPEI events: Physics of the Earth and Planetary Interiors.

Langer, C.J., and Spence, W., Deformation of the Nazca Plate related to the gap-filling earthquake series of October-November 1974: Submitted to the Journal of Geophysical Research.

Mendoza, C., 1987, Aftershock source properties using digital surface wave data--The 1979 Colombia sequence: Bulletin of the Seismological Society of America, v. 76, in press.

Nishenko, S.P., and Buland, R.P. (in press), A generic recurrence interval distribution for earthquake forecasting: Bulletin of the Seismological Society of America.

Nishenko, S.P., and Singh, S.K. (in press), Relocation of the great Mexican earthquake of 17 January 1903: Bulletin of the Seismological Society of America.

______(in press), The Acapulco-Ometepec earthquakes of 1907-1982: Bulletin of the Seismological Society of America.

Nishenko, Stuart P., and Singh, S.K., Conditional probabilities for the recurrence of large and great interplate earthquakes along the Mexican subduction zone: Submitted to the Bulletin of the Seismological Society of America.

Spence, William, 1986, The 1977 Sumba earthquake series--Evidence for slab pull force acting at a subduction zone: Journal of Geophysical Research, v. 91, p. 7225-7239.

Spence, William (in press), Slab pull and the seismotectonics of subducting lithosphere: Reviews of Geophysics.

Analysis of Earthquake Data from the Greater Los Angeles Basin and Adjacent Offshore Area, Southern California

#14-08-0001-G1328

Egill Hauksson
Ta-liang Teng
Center for Earth Sciences
University of Southern California
Los Angeles, CA 90089-0741
(213) 743-7007

INVESTIGATIONS

Analyze earthquake data recorded by the USC and CIT/USGS networks during the last 12 years in the Los Angeles basin to improve earthquake locations including depth and to determine the detailed patterns of faulting in the study region.

RESULTS

A study of the seismotectonics of the Santa Monica bay-Offshore area has been completed.

One of the more difficult problems in southern California seismotectonics is the relationship between left-lateral slip or underthrusting at the Transverse Ranges and ongoing right-lateral strike-slip faulting in the greater L.A. basin and adjacent offshore areas. To investigate this relationship we have examined the seismicity from 1973 to 1985 for the central and northern Santa Monica bay and the central Santa Monica mountains in southern California (Saldivar *et al*., 1987).

The results of relocating 38 earthquakes ($M_L \geqslant 2.5$) show scattered seismicity in central and northern Santa Monica bay. No obvious spatial clustering is observed around the surface traces of the numerous mapped faults except near the north-northwest branch of the Palos Verdes fault (Figure 1). The Santa Monica mountain block appears to be almost aseismic since only two small events ($M \geqslant 2.5$) are reported north of the Malibu coast. The spatial distribution of background seismicity in Santa Monica bay, therefore, suggests that the bay is a broad zone of crustal deformation and the transition from strike-slip to reverse faulting does not cause anomalous spatial clustering of seismicity.

To continue the search for the transition from strike-slip to reverse faulting 20 single-event focal mechanisms have been determined. These mechanisms show that strike-slip faulting mixed with some reverse faulting is dominant in central Santa Monica bay while almost pure reverse faulting is occurring in northern Santa Monica bay (Figure 2). The transition from mixed strike-slip and reverse faulting to almost pure reverse faulting occurs approximately along a north-south boundary that coincides with the aftershock zone of the 1979 Malibu (M_L = 5.0) earthquake. Hence the Anacapa-Dume fault may form the southern boundary for almost pure reverse faulting to the south of the Malibu coast. As the Anacapa-Dume fault approaches the Santa Monica bay shelf, it probably joins up with the northwest extension of the Palos Verdes fault through a series of en echelon discontinuous fault segments (Figure 1). Some crustal shortening thus appears to be taking place throughout Santa Monica bay with somewhat higher rate of shortening occurring between the Anacapa-Dume fault and the Santa Monica fault.

REPORTS

Hauksson, E., T. L. Teng and G. Saldivar, Analysis of Earthquake Data from the Greater Los Angeles Basin and Adjacent Offshore Area, Southern California, U.S.C. Annual Technical Report #87-2, prepared for the U.S.G.S., 31 pp., 1987.

Hauksson, E. and G. Saldivar, The 1930 Santa Monica and the 1979 Malibu, California, Earthquakes, Bull. Seism. Soc. Amer. 76, 1542-1559, 1986.

Hauksson, E., Seismotectonics of the Newport-Inglewood Fault Zone in the Los Angeles Basin, Southern California, Bull. Seism. Soc. Amer. 77, 539-561, 1987.

Hauksson, E., T. L. Teng and T. L. Henyey, Near-Surface Attenuation of Waveforms of Local Earthquakes: Results from a 1500 m Deep Downhole Seismometer Array, submitted to Bull. Seism. Soc. Amer., January, 1987.

Saldivar, G. V., E. Hauksson and T. L. Teng, Seismotectonics of the Santa Monica and Palos Verdes Fault Systems in the Santa Monica Bay, Southern California, to be submitted to BSSA, May, 1987.

Hauksson, E., T. L. Teng and T. L. Henyey, Near-surface Attenuation of Waveforms of Local Earthquakes: Results From a 1500 m Deep Downhole Seismometer Array, EOS Trans., Amer., Geophys. Union 67, p. 1091, 1986.

Saldivar, G. V., E. Hauksson and T. L. Teng, Seismotectonics of the Santa Monica and Palos Verdes Fault Systems in the Santa Monica Bay, EOS Trans., Amer. Geophys. Union 67, p. 1085, 1986.

Hauksson, E., Seismotectonics of the Newport-Inglewood Fault Zone and the 1933 Long Beach Earthquake (M_L = 6.3) in the Los Angeles Basin, Southern California, presented at S.S.A. Meeting Santa Barbara, March, 1987.

st-86/363

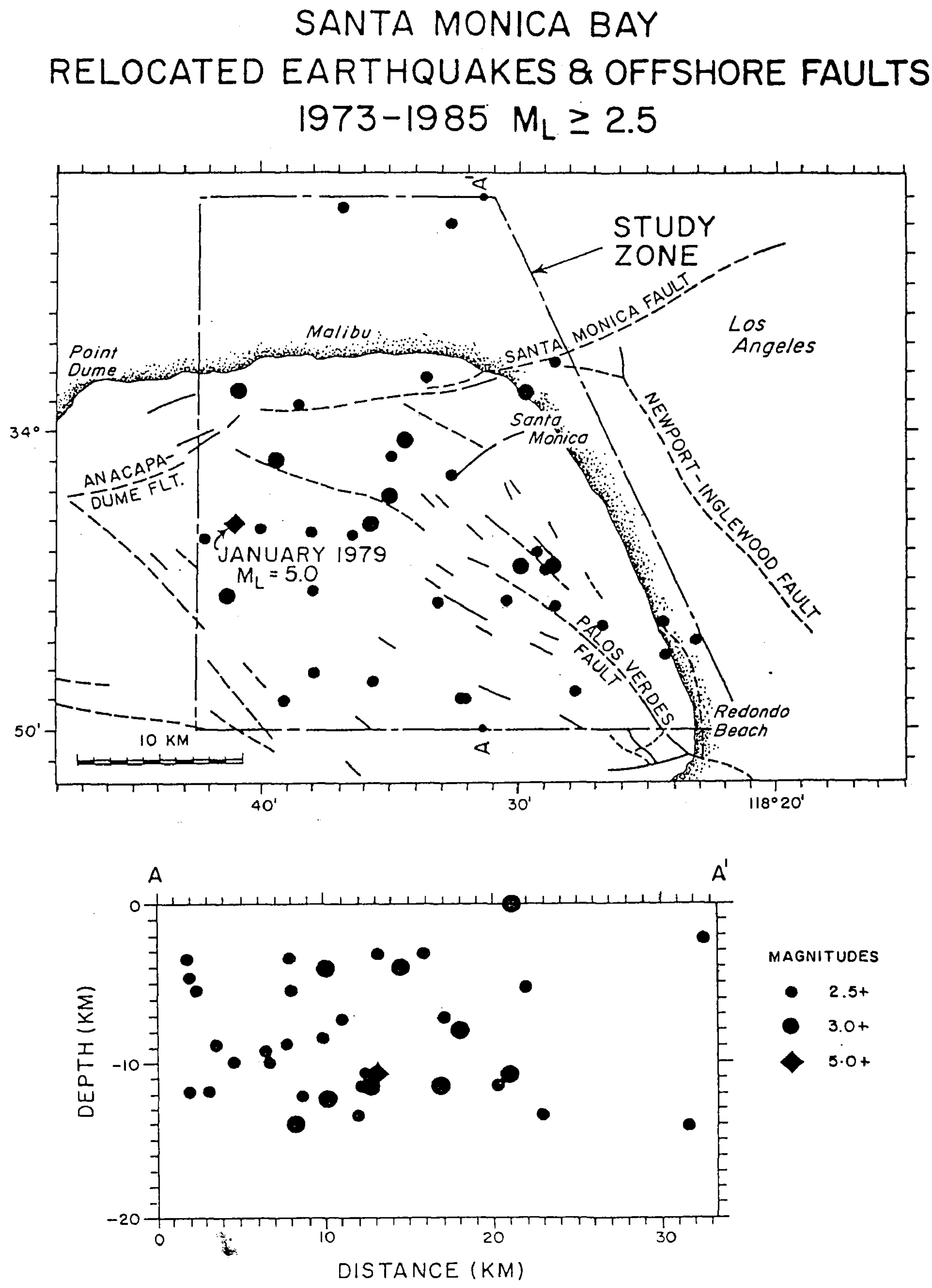

Figure 1. Relocated seismicity 1973-1985, M≥2.5 in Santa Monica bay. (Bottom) North-south cross section A-A[1].

SANTA MONICA BAY FOCAL MECHANISMS (M ≥ 2.5)

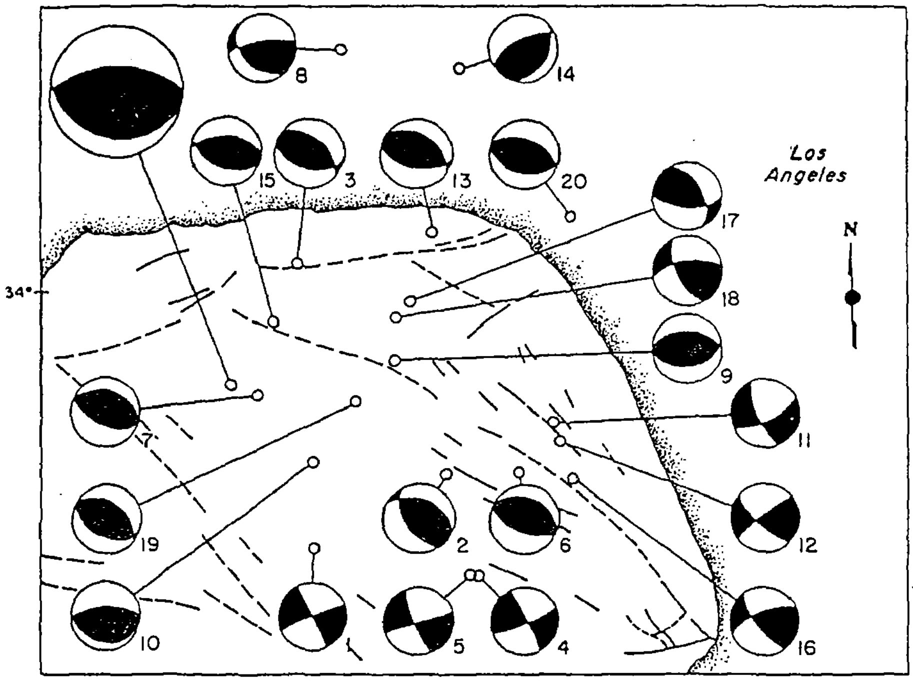

Figure 2. Lower-hemisphere focal mechanisms for earthquakes in Santa Monica bay 1978-1985. (Bottom) The actual data where open circles indicate dilatation and closed circles indicate compression.

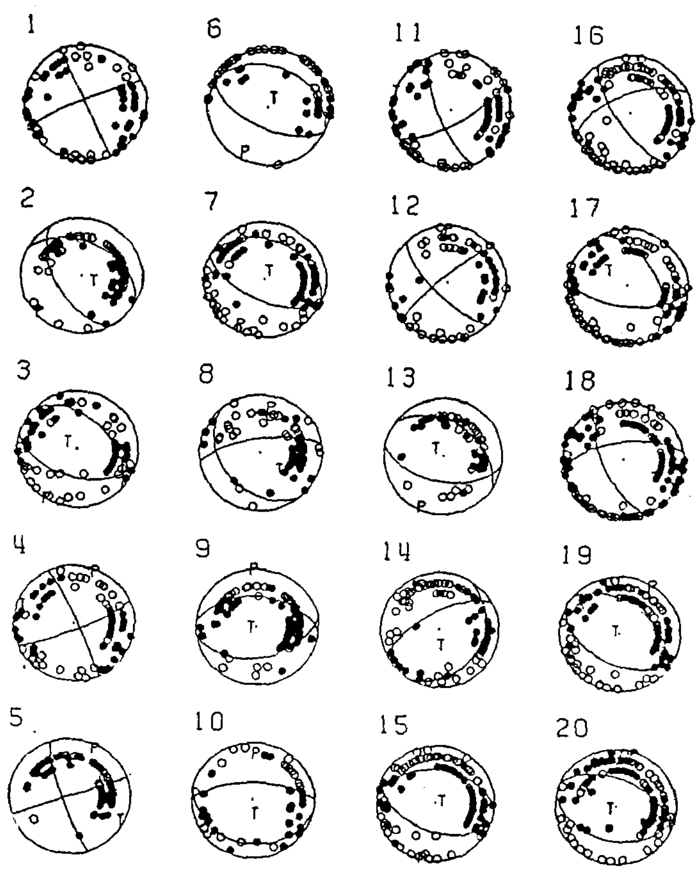

Seismic Source Characteristics of Western States Earthquakes

Contract No. 14-08-0001-21912

Donald V. Helmberger

Seismological Laboratory
California Institute of Technology
Pasadena, California 91125
(818) 356-6998

Investigation

A study on the characteristics of pre and post- 1962 Western U.S. earthquakes is in progress, with special emphasis on clusters. The study has begun with well recorded modern events (post-1962) and will proceed to (pre-1962) events later. Four major tasks will be addressed over a two-year funding cycle. These tasks are:

1.) Extended analysis of low-gain recordings of earthquakes occurring in the Imperial Valley and Northern Baja; to fix the depths of main energy release (asperity concentration).
2.) Analysis of body waves at all ranges using direct inversion for fixed earth models, application of the intercorrelation method to measure differences between events and develop master events per region.
3.) Analysis of historic events (pre-1962) using the same methods (masters) but on a more regional basis.
4.) Reassessment of events with sparsely recorded strong motions using more accurate Green's functions computed from laterally varying earth models.

Results

Some characteristics of earthquakes in the Big Bend region of California were reported on at the spring SSA (87) meeting where we investigated a few dozen events between Coalinga and Palm Springs. Most of these events range in magnitude from 5 to 6 and sample a limited portion of the crust. Accurate epicentral depth estimates were obtained for post-WWSSN (1962) events from teleseismic short-period depth phases and local array data. Source parameter estimates were obtained by modeling P_{nl} as well as regional and teleseismic body wave data.

Relative stress drops were estimated from the relative amount of short period strength m_b and M_L, relative to M_o. Stress drop showed no depth dependence on a regional or local scale. On a regional scale, 15 strike-slip Southern California events were modeled. On a local scale the 1983 m = 6.7 Coalinga earthquake and 6 of its largest aftershocks were modeled. All of these were thrust events. It was also determined that the results were not affected by an independent depth dependence of either moment or magnitude. The stress drop appears to be more a function of fault roughness and repeat time rather than depth.

Some preliminary results of pre-1962 events can be obtained by comparing modern events recorded by the 3 component broad-band Galitzin instrument operated at DeBilt, Netherlands since the early 1920's. Excellent records have been collected for a number of modern events, such as, Coalinga and its larger aftershocks, the Santa Lucia bank events, Santa Barbara, San Fernando and the 1927 Lompoc earthquake. All these events have a strong thrusting component implying overall compression of the region.

In the remainder of this report we will discuss in some detail progress made in modeling events in the 4 to 5 magnitude class which have been neglected in recent years largely because of our recording habits. These events are too large for local arrays to remain on scale and too small to be seen on the global networks. Fortunately, these events have been well recorded at regional three-component long-period stations as displayed in Figure 1. This figure displays a portion of the 1979 Imperial Valley mainshock along with a series of smaller aftershocks. This event had about 12 aftershocks with magnitudes over 5 and hundreds of smaller events. The strong arrival near the upper right of the records shown has a magnitude of 5.5. The event labeled C has magnitude 4.8. Events A (m = 4.6) and B (m = 4.1), which look much alike on the longer period records, are not so similar on the broad-band (1-90) recording. Since the paths from events A, B and C to PAS are so similar, we can assume that the differences are probably due to variations in source depth and source parameters. However, in order to retrieve these source characteristics, we must separate the propagational distortions caused by complex crustal structures. In short, we require effective Green's functions.

To derive such Green's functions requires at least one master event or an event with known source properties in the general region. The 1976 Brawley earthquake, with magnitude 4.9, serves this purpose. The strong motion study done by Heaton and Helmberger (1978) determined a complete set of source parameters so that we were able to study the effects of propagation separately.

In general, flat layered and dipping layered models did not work for modeling the seismograms with the proper timing. Thus, we used a finite-difference scheme discussed by Helmberger and Vidale (1987) to assure proper handling of the heterogeneity. A starting model was obtained from a compilation of crustal studies (Hadley and Kanamori, 1977 and 1979; Fuis et al, 1982) followed by adjustments made by fitting the waveforms and travel times of synthetics to whole seismograms. Only one parameter of the model was adjusted at a time so that we could systematically estimate the sensitivity of the synthetic to each parameter. We first adjusted the structure in order to obtain the correct waveforms, and then allowed variations in velocities to obtain the correct arrival times. The best fitting model to date is displayed in Figure 2 along with a profile of synthetics for a pure dip-slip and strike-slip source at a depth of 7 km. The sensitivity to depth is given in Figure 3.

Following the modeling formalism discussed in previous papers, we propose to explain long-period records occurring in the region by a linear combination of the synthetics in Figure 3. A total of nine events with unknown parameters, including the three 1979 Imperial Valley aftershocks A, B, C, were digitized and rotated in SH-SV motions in a test of the above hypothesis. The best fitting mechanisms and corresponding synthetics are presented in Figure 4. Note that the source depths are confined to be 3.5, 7, 10.5 or 14 km in the synthetics but that none of these events appear to be deeper than 10.5 km. The moment estimates are 3.5, 2.5 and 20.0 X 10^{22} dym-cm for the three A, B, C events discussed earlier which does not agree with their local magnitude very well. We are presently examining the other components as well as refining the model to explain the secondary arrival that appears for the shallow events, see aftershock B. This feature is associated with shallow energy release which travels as a very slow Love wave to the edge of the basin and then as a high speed Love wave. This arrival is not seen in short period observations.

References

Fuis, G. S., W. D. Mooney, J. H. Healy, G. A. McMechan and W. J. Lutter, 1982, Crustal structure of the Imperial Valley region in the Imperial Valley, California earthquake of October 15, 1979, U. S. Geol. Survey Prof. Paper, **1254**, 25-49.

Hadley, D. and H. Kanamori, 1977, Seismic structure of the Transverse Ranges, California, Bull. Geol. Soc. Am., **88**, 1469-1478.

Hadley, D. and H. Kanamori, 1979, Regional S-wave structure for southern California from the analysis of teleseismic Rayleigh waves, Geophys. J. R. astr. Soc., **358**, 655-666.

Heaton, T. H. and D. V. Helmberger, 1978, Predictability of strong ground motion in the Imperial Valley: Modeling the M4.9, November 4, 1976 Brawley earthquake, Bull. Seism. Soc. Am., **68**, 31-48.

Helmberger, D. V. and J. Vidale, 1987, Modeling strong motions produced by earthquakes with 2-D numerical codes, submitted to Bull. Seism. Soc. Am.

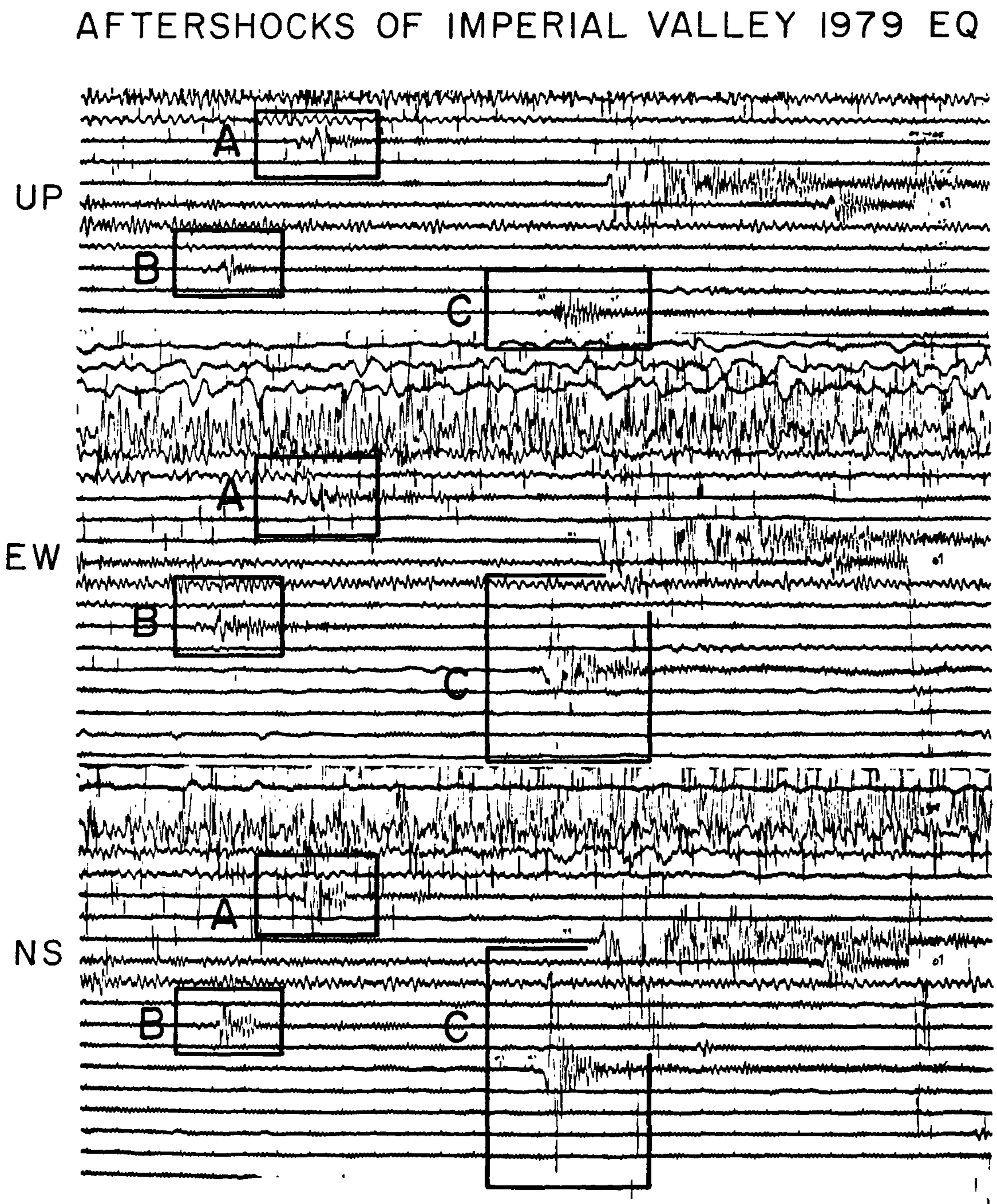

Figure 1: Aftershocks of the 1979 Imperial Valley Earthquake as recorded at PAS on the long period (30, 90) instruments. Events A, B, and C were assigned M_L's of 4.6, 4.1 and 4.8 respectively.

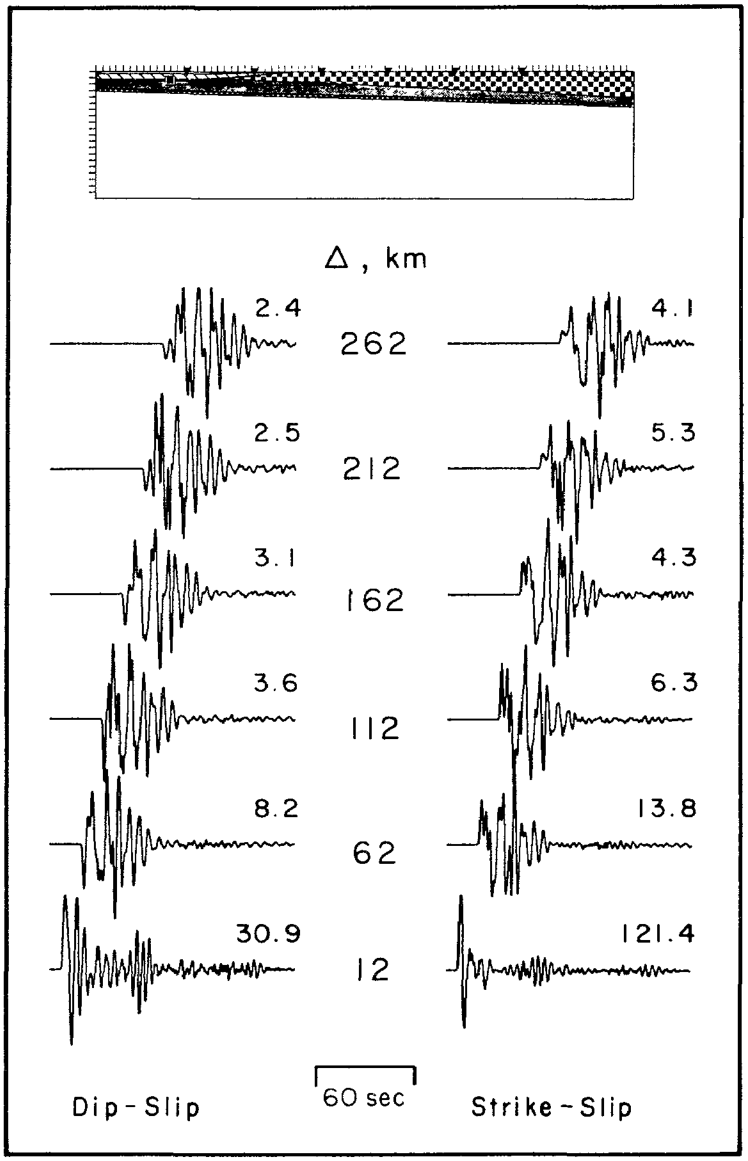

Variations of Green's Functions with Distance

Figure 2: Top panel displays a structural model (cross-section) from Imperial Valley to PAS. The velocities are: $\beta_1 = 1.0$ km/sec, $\beta_2 = 2.3$ km/sec, $\beta_3 = 3.18$ km/sec, $\beta_4 = 3.38$ km/sec, $\beta_5 = 3.78$ km/sec, $\beta_6 = 4.18$ km/sec, $\beta_7 = 4.2$ km/sec. The crust thickens from 15 to 30 km at PAS. The Green's functions are appropriate for a smoothed delta function with amplitudes above each trace (x 10^{-6}) cm for an assumed moment of 10^{20} ergs.

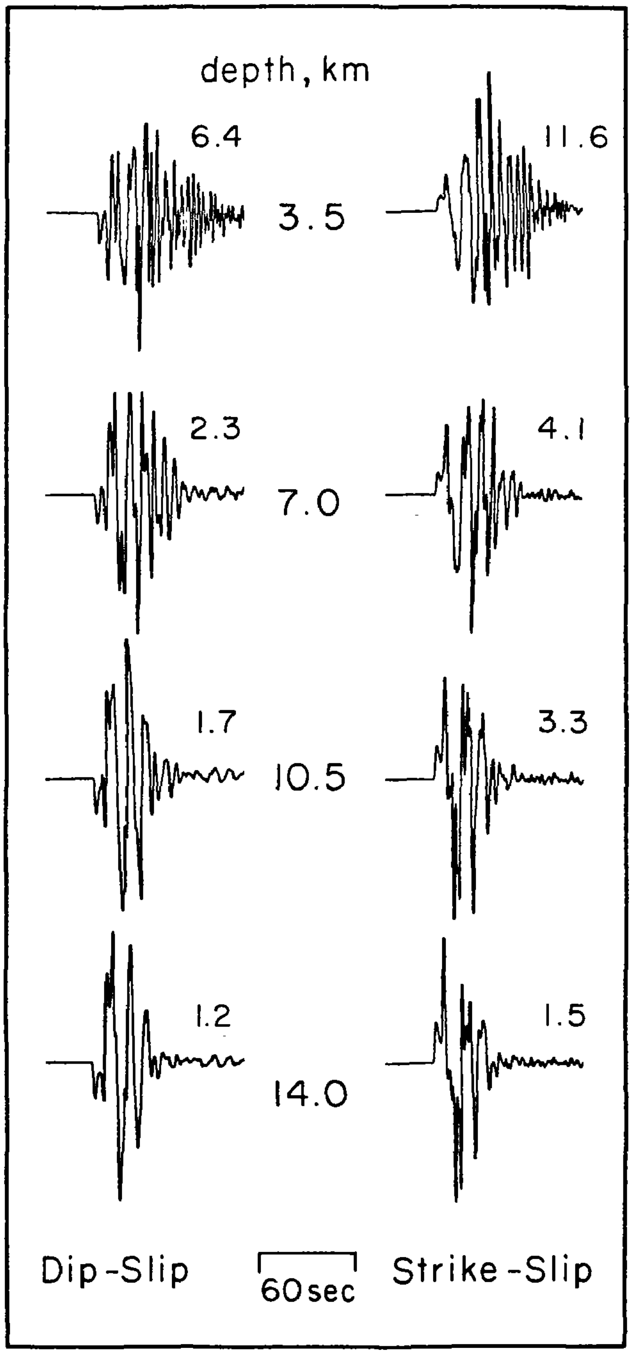

Figure 3: Green's functions displaying the source depth sensitivity, namely 3.5, 7, 10.5, and 14 km as recorded at the range of 262 km. Note the rather large changes in amplitudes.

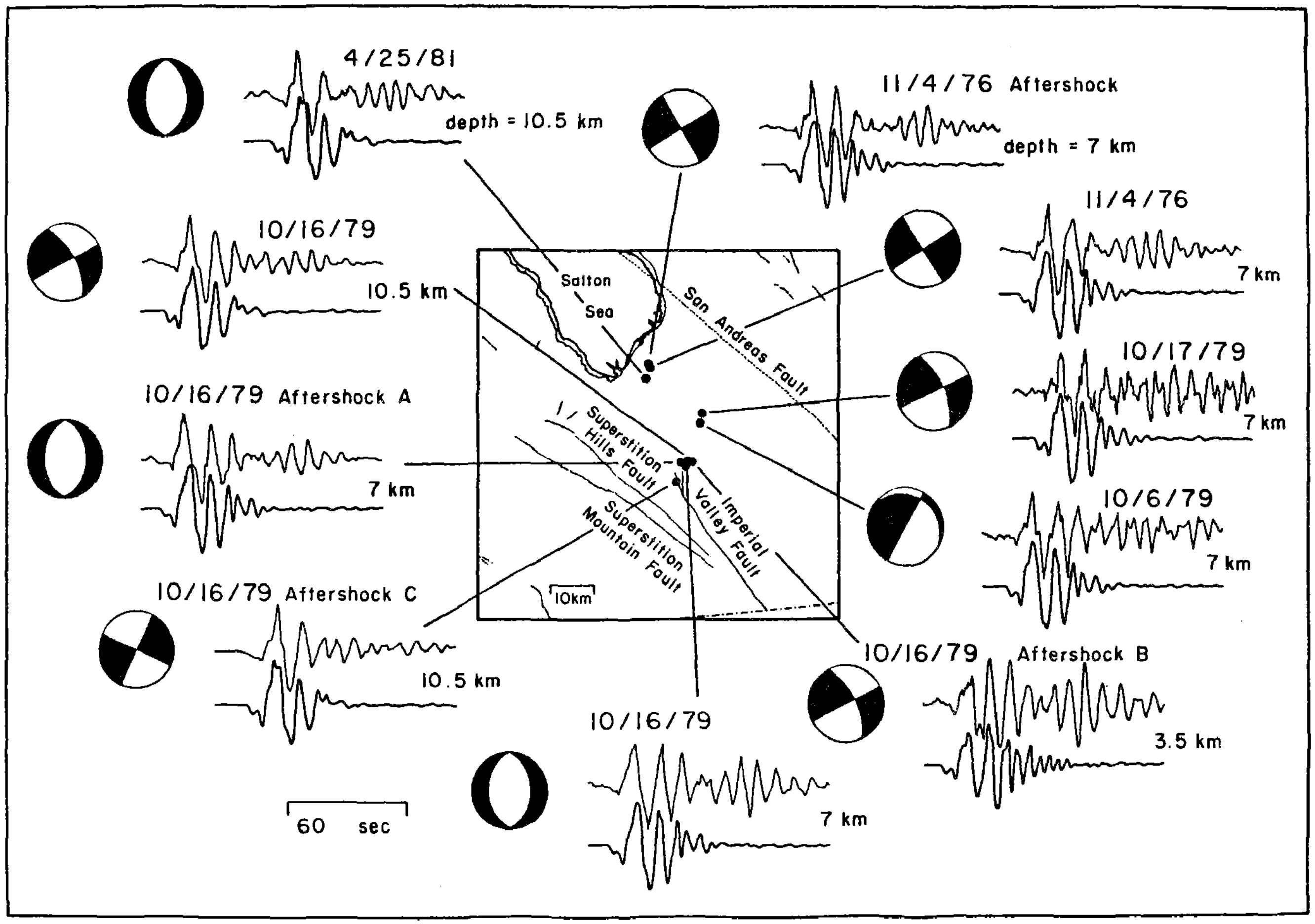

Figure 4: Comparison of some observed Love waves with synthetics where the traces are aligned with respect to absolute time.

Earthquake Source Parameters Using Regional Seismic Network Data: Application to California and Eastern United States

14-08-0001-G1391

Robert B. Herrmann
Department of Earth and Atmospheric Sciences
Saint Louis University
P.O. Box 8099 Laclede Station
St. Louis, MO 63156
(314) 658-3131

Goals

1. Perform research on the earthquake process in the New Madrid Seismic Zone to delineate the active tectonic processes.

2. Perform more general research relating to the problems of the eastern U. S. earthquake process and of the nature of eastern U. S. earthquakes compared to western U. S. earthquakes.

3. Acquire USGS CALNET data for comparative seismic source studies with New Madrid data.

Investigations

1. A reinvestigation of spectral scaling of earthquakes in the Central Mississippi Valley Seismic zone is nearing completion. Spectral data from 5 magnetic tapes of digitized LRSM data provided by EPRI have been processed. In addition, data from digitized old seismograms, pre 1941, have been obtained from R. Street, University of Kentucky, for reanalysis.

Using Q values inferred from the observed spectra, Lg-wave corner frequencies are correctly obtained. Corner frequency-seismic moment scaling of the Lg wave does not differ significantly from scaling based on short distance digital recordings or from teleseismic studies.

2. Work continues on the January 31, 1986 Painesville, Ohio earthquake, with effort directed toward understanding the strong motion record at a distance of 10 km away. The surface-wave focal mechanism can explain the horizontal components of the strong motion record but the synthetic vertical motion is much smaller than observed. An examination of USGS GEOS data, shows that some aftershocks have a vertical to horizontal ratio much less than 1, as expected form the modeling, but others very close to 1, as seen on the strong motion record, in spite of the almost identical location of aftershocks.

A trip to USGS Menlo Park was fruitful in obtaining the GEOS digital data set for cooperative research.

3. A sample CALNET data set was obtained from USGS, Menlo Park, for use in the comparative study. Effort will be directed temporarily to extend a generic set of computer programs for handling different types of data sets.

Publications

Shin, T.-C. and R. B. Herrmann (1987). Lg attenuation and source studies using 1982 Miramichi data, *Bull. Seism. Soc. Am.* **77,** 384-397.

Peters, K. E. and R. B. Herrmann, editors (1986). First-hand observations of the Charleston earthquake of August 31, 1886, and other earthquake materials, *Bulletin 41,* South Carolina Geological Survey, 116pp.

Tectonics of Central and Northern California

9910- 01290

William P. Irwin
Branch of Engineering Seismology and Geology
U. S. Geological Survey
345 Middlefield Road, MS-977
Menlo Park, CA 94025
(415) 323-8111, ext. 2065

Investigations

1. Tertiary crustal extension in northern California; in collaboration with R. A. Schweickert.

2. A chapter titled "Geology and Plate Tectonic Development" for a multi-authored bulletin on the San Andreas fault was completed and submitted to Branch for review.

3. Distribution of radiolarian faunas in cherts of the Coast Ranges of California, with special attention to Early Jurassic faunas and evidence for northward translation of coastal terranes; in collaboration with C. D. Blome and M. J. Rymer

Results

1. The Trinity arch in the Klamath Mountains of northern California is believed to be the first example of a structural feature involving ultramafic (ophiolitic) rocks that is analogous to a metamorphic core complex. Northeast-trending normal faults and associated features in the Klamath Mountains provide evidence that significant crustal extension occurred during Tertiary (Oligocene-Miocene) time. These faults cut across the older accretionary structural grain of the region, forming grabens and half-grabens in which Tertiary continental beds (Weaverville Formation) are preserved. Development of these faults is thought to be related to broad arching of the Trinity ultramafic sheet along a northeast-trending axis--the ultramafic sheet and associated rocks of the central metamorphic belt being analogous to the domed metamorphic core complexes of the eastern Cordillera. The Paleozoic rocks of the Redding section and the Yreka terrane lie to the southeast and northwest of the Trinity sheet, respectively, and are thought to be extensional allochthons that are detached from their original positions overlying the Trinity sheet. Evidence for the detachment nature of the faulting is seen at the La Grange gold-placer mine on the southeast side of the arch, where the Tertiary beds dip northwest 15° into the mylonitic footwall surface of the La Grange fault that dips southeast 22°. The mylonitic footwall surface of the fault was exposed during hydraulic mining of the overlying Tertiary beds of the hanging wall, and now is spectacularly exposed for one-half mile along U. S. Highway 299 a few miles west of Weaverville. Large down-dip displacement of the upper

plate of the La Grange fault is suggested not only by the mylonite but also by significant changes in bedrock across the fault. In addition, the northeastern extension of the La Grange fault, which bounds the southeastern side of the Trinity ultramafic sheet for more than 60 km, locally cuts out much of the lower part of the Paleozoic strata of the Redding section. Faults on the northwestern side of the Trinity arch juxtapose stacked plates of lower Paleozoic strata of the Yreka terrane against the Trinity ultramafic sheet, and suggest a detachment origin for the Yreka terrane that is complementary to that of Redding section on the opposite side of the arch. The overall geometric relations suggest that the crustal extension was in northwest-southeast directions. Preparation of a paper describing these relationships is nearly completed.

Reports

No reports published this period.

Seismicity Patterns and the Stress State in Subduction-Type Seismogenic Zones

Grants Number 14-08-0001-G-1099/1368

Carl Kisslinger
Cooperative Institute for Research in Environmental Sciences
Campus Box 449, University of Colorado
Boulder, Colorado 80309-0449
(303) 492-6089

The research during the six months, December, 1986, through April, 1987, was concentrated on several types of follow-on studies of the May 7, 1986 Andreanof Islands Earthquake. The data set acquired by the Central Aleutians Seismic Network and teleseismic stations provides an excellent base for a variety of investigations of earthquake processes and precursory phenomena in subduction zones.

Aftershocks of the May 7, 1986 Earthquake and Other Aleutian Islands Events

The aftershock sequence of the M_W 8.0 earthquake has been analyzed to determine the parameters of the time decay function and to learn if any of the larger aftershocks were preceded by detectable changes in the aftershock occurrence rate. The analysis has been based on the event catalogue reported in the Monthly Listings of the U.S.G.S. through August, 1986, supplemented by the weekly PDE reports for events greater than magnitude 5 through February, 1987. A lower magnitude cut of m_b 4.6 was used as the bound for completeness of the Monthly Listing. The resulting data set consists of 247 events, m_b 4.6 or greater in the 105 days after the main event, 104 events, m_b 5 and greater in 243 days. Eventually, the catalogue based on the local network data will be analyzed also, but over an order of magnitude more events have been logged and the hypocenter locations are now complete only for the first few days after the main event.

The methods developed by Y. Ogata, Institute of Statistical Mathematics, Tokyo, Japan, and applied by Ogata and Shimazaki, Matsu'ra and others, have been used to estimate the parameters in the Modified Omori relation for aftershock occurrence: the number of events per unit time $n(t) = K/(t+c)^p$, which leads on integration to the cumulative number of events:

$$N(t)=K[(t+c)^{(1-p)}-(S+c)^{(1-p)}]/(1-p)$$

where S is the starting time for the sequence. The original Omori relation is a special case, with p=1 and c=0. N(t) follows a logarithmic growth curve in that case. The time of the main shock is taken as t = 0, but a later starting time, S, is usually used because some events are often missed in the time immediately after a very strong main shock, so the early part of the event list is incomplete. Ogata has developed a method for deriving maximum likelihood estimates of K, c, and p, which can be calculated for the whole time sequence or any part of it. He has also extended the method to accommodate secondary aftershock sequences following strong aftershocks of the original mainshock. Then, the time variable is replaced by the "frequency linearized time" (FLT), which is the value of N(t) calculated from the above relation. When the observed cumulative number is plotted against the FLT, departures of the sequence from the modified Omori relation are easily detected. A simplified version of Ogata's program has been developed for use on a PC and applied in this research.

The results for the PDE catalogue are summarized in Figures 1 and 2. The sequence with m_b 5 and greater was started at 0.018 days, with event 10, that for m_b 4.6 and greater at 0.206 days, with event 50. The starting times are different because the data indicate that the list is complete for the larger events at an earlier time. The results are:

for $m_b \geq 5$, K=10.03, p=0.989, c=0.000665 (Figure 1, top)
for $m_b \geq 4.6$, K=26.52, p=0.887, c=0 (Figure 2, top)

The plots show a drop in the occurrence rates, after event #77, 11.19 days, in Figure 1, and after event #190, 21.855 days, Figure 2. The Omori parameters were calculated for the intervals ending at these times and used to generate FLT plots for the entire data set, the bottom part of the two figures. As measured by the Akaike Information Criterion, the early parts of both curves are modeled much better and the decreased rates are emphasized in the resulting plots, bottom of Figures 1 and 2. The parameter values are:

for $m_b \geq 5$, K=10.97, p=0.950, c=0
for $m_b \geq 4.6$, K=27.19, p=0.877, c=0

The reason for the difference in onset time of the rate decreases in the two data sets is not fully understood, but may indicate the limits of time resolution possible with these data when such a large total aftershock zone is involved. Further work, in which the zone is subdivided into smaller sections, may clarify this point.

No changes in aftershock occurrence rates are found to be associated with the strong aftershocks of May 15 (M_S 6.4), May 17 (M_S 6.6), or June 19 (M_S 6.3). The clear decrease at day 11.19 (May 19) for the stronger events and day 21.855 (May 29) for the other data set precede the June 18 event, but recovery does not follow shortly after the occurrence and there is no basis for associating the two observations.

Various seismicity models that predict p values do not indicate that p should be dependent on the lower magnitude cutoff. More work is needed to determine if the difference found here is real, and, if so, whether it is a general phenomenon.

One objective this research is to examine is whether the p value is a useful indicator of basic mechanical properties of the fault, as suggested by seismicity models. The aftershock sequence of the M_S 6.7 event of November 4, 1977, in the eastern part of the Adak zone was also analyzed. The Adak catalogue data gave a value of p=0.666, the PDE data (only 5 aftershocks) gave p=0.707. The smaller p value for this event, which occurred within the aftershock zone of the May 7, 1986 earthquake, suggests that the rupture surface for that event was characterized by a more heterogeneous strength distribution than the much larger 1986 fault surface. This result is probably explained by the fact that the properties for the larger event are averaged over a much greater area.

As a first test for variations in aftershock behavior along the Aleutian subduction zone, the aftershocks of a M_S 6.6 event in the Shumagin Islands, October 9, 1985, within the region well monitored by the Shumagin Islands network of Lamont-Doherty Geological Observatory, were examined. This sequence does not fit the Modified Omori relation very well. The p value for the data from the time of the main shock until the end of 1986 (446 days) is 0.709, close to the value for the November 4, 1977 Adak sequence. However, a clear second sequence of aftershocks began with a strong event on November 14, 1985, and efforts to fit this combined sequence have not been successful. In addition, the b-value for this Shumagin sequence is unusually low, 0.35 to 0.45 for different time segments, suggesting that either many smaller events are missing from the data set (not indicated by the recurrence graphs) or that this fault has some very unusual properties.

Coda Q in the Adak region Before and After the 1986 Andreanof Earthquake

The digital recordings of 330 microearthquakes during January 1981 to April 1986 as well as 40 aftershocks in June and July 1986 in the Adak region were selected for this coda Q study. The aim was to search for any spatial and temporal Q variations related to the May 7, 1986 earthquake.

60 seconds of the seismograms after the S arrival were first passed through a digital zero-phase-shift band-pass filter. The center frequencies were 1.5, 3, 6, and 12 Hz, with band width 1, 2, 4, and 8 Hz respectively. In each frequency band the rms amplitudes in consecutive two second windows were calculated, then corrected for the background noise and geometrical spreading. The coda Q values were calculated from the coda decay rate by using Aki's single back scattering model. We used two windows for measuring Q in order to achieve better spatial resolution. The first one, hereafter called Window 1, started from 6.5 seconds after the S arrival and lasted for 30 seconds. Window 2 measured the coda between 12.5 and 60.5 seconds after S. According to the single scattering model Window 1 samples roughly a 120 km-wide segment of the subduction zone. Window 2 samples a segment twice as wide; i.e. about the same dimension as the rupture zone of the mainshock. When the multiple scattering effect is considered, the sampling volumes are likely to be smaller.

The resulting data set consists of approximately 1000 data points. Figure 3 shows that the coda Q values in 6 Hz band increase as a function of mean longitude eastward to about longitude 177°W, and then are roughly constant in the eastern part. This could be interpreted as the eastern part of Adak seismic zone having higher Q value relative to the western part. The extent of this high Q region could not be well defined. The west boundary was a little west of Adak Canyon. The data from Window 2 were slightly peaked between longitudes 176.5°W and 177°W. This may suggest that the high Q zone extended deeper at this longitude range. We divided the stations and events into three groups. The western group includes stations AD6, AD7, AK1, and events west of 177°W. The central group includes station AD4 and AD5, and events between 176.2°W and 177.2°W. The eastern group includes AD1, AD2, AD3, and events east of 176.5°W. In Window 1 the coda Q of the central and eastern groups was about 20% higher than that of the western group. In Window 2 the Q of the central group was 20% higher than both the eastern and western groups. These differences were statistically significant at very high confidence level. To exclude the possibility that the coda Q differences were merely caused by the station site effect, we compared the coda Q of events from the east and west region recorded on the same group of stations. The results showed that the near-station site effect contributed less than half of the spatial difference in Q. If we relate high Q with high stress, this study agrees with our earlier work localizing seismic asperities.

The temporal coda Q variations were also studied carefully. In spite of large data scattering, the one year average Q values were very stable for various station-event groupings. In Window 1 the mean values fluctuated generally within the range of $\pm$ 10% of the mean. The variation in Window 2 was even smaller. No consistent change in pattern can be identified as the precursor to the mainshock. So if the precursory coda Q change existed in our case, it might be less than 10% of the mean when averaged over one year and over the sampling volume. Figure 4 shows an example of the temporal variation. After the mainshock the coda Q decreased about 10% in the east region. The comparison between the pre- and post-mainshock Q values in the west region is not available at the present stage of analysis.

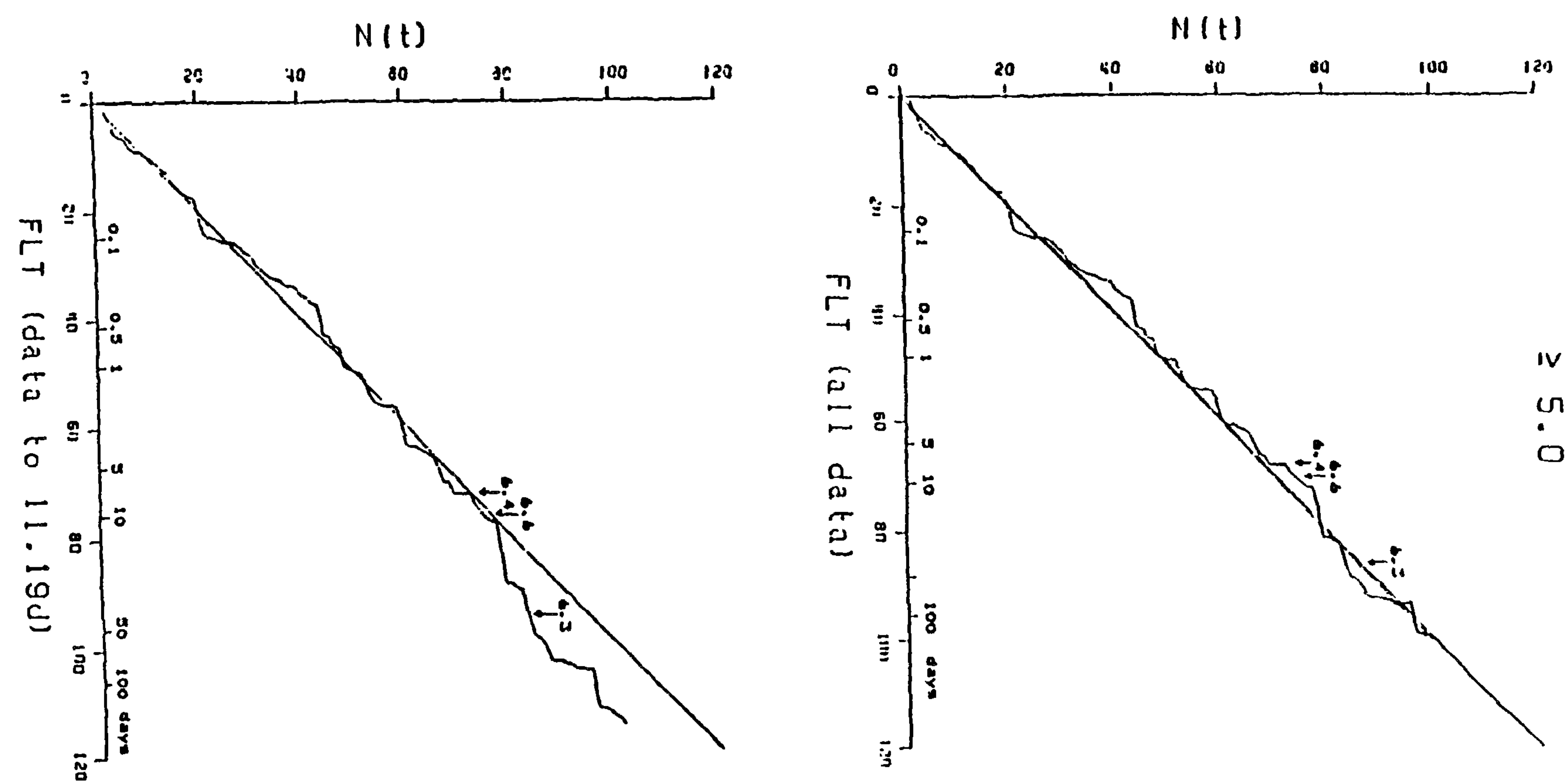

Figure 1. Cumulative number of aftershocks vs. frequency linearized time, for PDE catalogue with $m_b \geq 5$. In top figure, the Modified Omori parameters were found for the whole data set. In lower figure, the parameters were found for data to day 11.19 and then applied to whole data set. The first 9 events were not included in the parameter determinations.

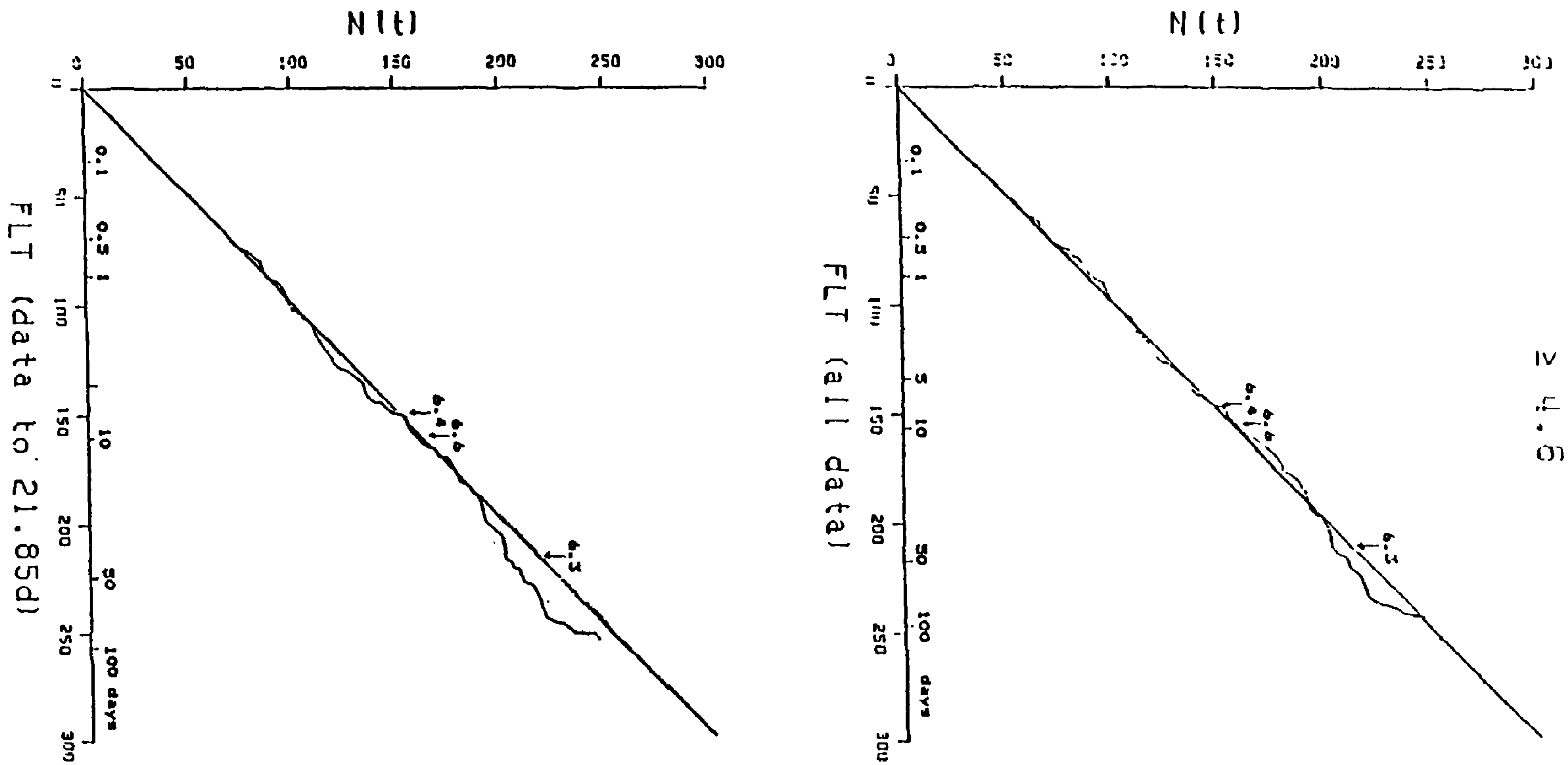

Figure 2. Cumulative number of aftershocks vs. frequency linearized time, for PDE catalogue with $m_b \geq 4.6$. In top figure, the Modified Omori parameters were found for the whole data set. In lower figure, the parameters were found for the data to day 21.85 and then applied to the whole data set. The first 49 events were not included in the parameter determinations.

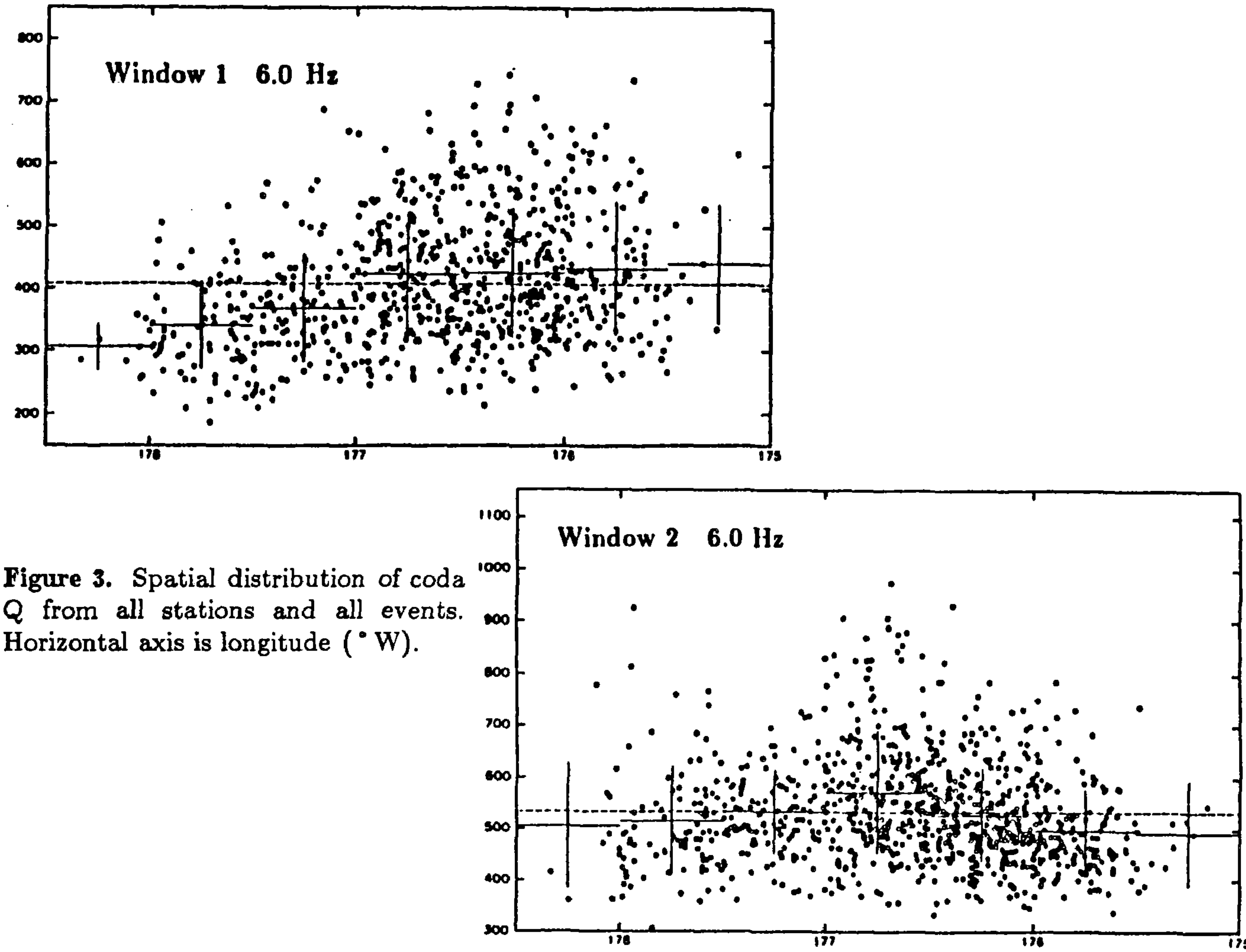

Figure 3. Spatial distribution of coda Q from all stations and all events. Horizontal axis is longitude (°W).

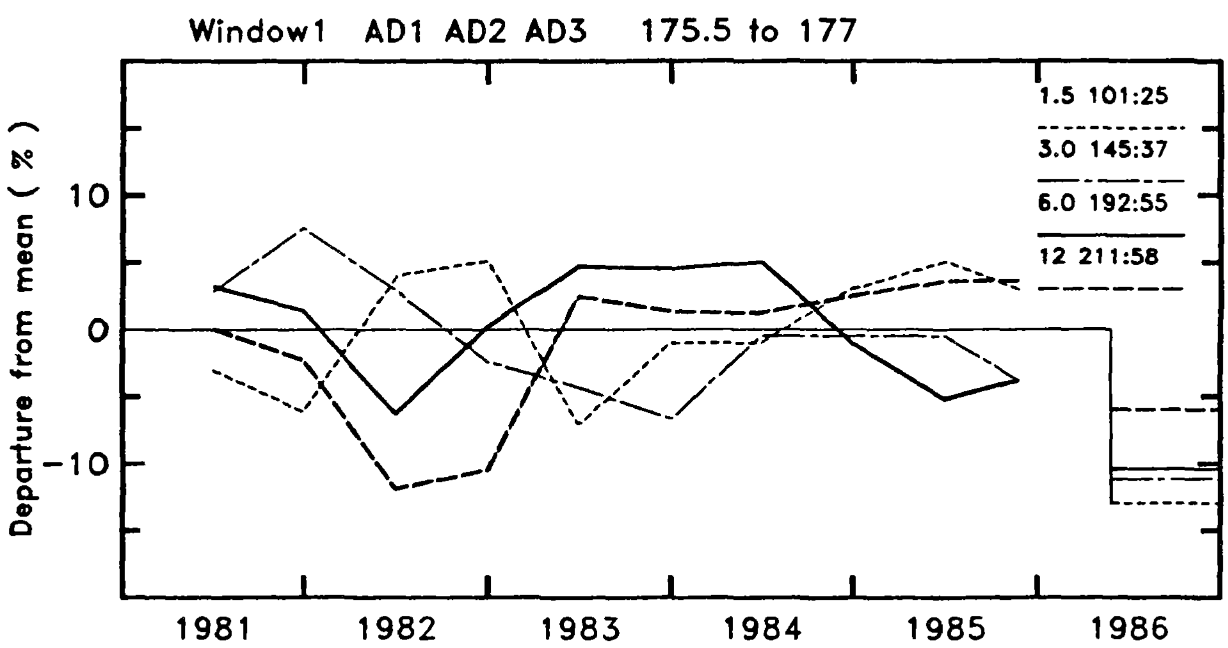

Figure 4. Temporal variation of coda Q.

Seismological Field Investigations

9950-01539

C. J. Langer
Branch of Geologic Risk Assessment
U.S. Geological Survey
Box 25046, MS 966, Denver Federal Center
Denver, CO 80225
(303) 236-1593

Investigations

1. Peru postearthquake study--local/regional investigation of aftershocks resulting from an M_S 7.8 earthquake of October 3, 1974.

2. Carbondale, Colorado, earthquake swarm--local investigation of an earthquake swarm, April-May, 1984.

Results

1. Nearly all aftershocks of the October 3, 1974, Peru thrust-faulting earthquake (M_S 7.8) lie south of the main shock epicenter. The largest aftershocks for which the regional network data are complete ($3.6 \leq M_{bd} \leq 5.3$), define a 'T'-shaped zone of about 13,000 km^2 in area. A northwest-trending subzone (NWSZ) of aftershocks which includes the location of the main shock and largest aftershock, is midway between the coast and the axis of the Peru-Chile trench. The NWSZ is 40-50 km wide, about 220 km long, and extends subparallel to the coast, filling a previously identified seismic gap between about 12° and 14°S latitude. Hypocentral cross sections suggest that the NWSZ consists of two shallow dipping (~7°NE) layers of aftershocks. The upper layer appears to be near the interface between the Nazca and South American plates, and the lower layer may be related to the base of the crust. A northeast-trending subzone (NESZ) of aftershocks is perpendicular to the NWSZ at its approximate midpoint, and extends landward for about 140 km to beneath the coastal town of Chilca. Hypocenters in the more oceanward part of the NESZ are principally confined to a 15 km thick zone, probably interior to the Nazca plate, that dips about 30°NE until it terminates in a dense cluster of aftershocks (Chilca cluster). In vertical section, the Chilca cluster is tabular in shape and is comprised of aftershocks that occur in both the Nazca and South American plates. Aftershock depths range from shallow crustal for the most oceanward events, to a maximum of about 65 km for hypocenters located beneath the coast. A composite focal mechanism solution for 25 aftershocks in the NESZ is well-constrained, and the preferred nodal plane parameters suggest reverse and right-lateral differential motion within the subducting plate along the northeasterly trend of NESZ aftershocks.
2. During the Carbondale, Colorado, earthquake swarm, a total of 34 earthquakes were located using regional data or local data from a temporary network installed in the epicentral area. These earthquakes were relocated with the method of Joint Hypocenter Determination (JHD) in order to better delineate the source zone of the swarm. The majority of

the earthquakes occurred about 7 km south-southwest of Carbondale, at the northern terminus of the Elk Mountain anticline. The hypocenters do not appear to lie on a single plane, but rather show a scattered distribution between depths of about 2 and 7 km. Two first-motion composite focal mechanisms were constructed from local data. One of these mechanisms corresponds to normal faulting and the second suggests reverse faulting.

Ten of the JHD-relocated epicenters of the locally-recorded earthquakes occurred about 7 km south-southwest of Carbondale, just north of Thompson Creek and east of the Grand Hogback monocline. The epicenters are situated at the northern terminus of the mapped axis of the northwest-trending Elk Mountain anticline (Poole, 1954) and form a slightly elongated cluster, 5 km by 3 km. Four epicenters are located within a kilometer of the mapped axis of the west-dipping Grand Hogback monocline (Tweto and others, 1978). These four are not considered to be in the same seismic source zone, and so they will not be further discussed. Similarly, the two epicenters just southwest of Redstone do not appear to be related to the major cluster of earthquakes. These southernmost earthquakes may be possibly related to coal mining activities in the area.

The distribution of seismicity as a function of depth show a diffuse distribution between depths of 3.2 and 6.5 km. The scatter of the hypocenters along the crest of the anticline suggests that the earthquakes did not occur along a single plane, such as a bedding plane, but perhaps more closely represent a volumnar source.

Similarities between the Elk Mountain anticline, which is the locality of the 1984 earthquakes, and the nearby Cattle Creek anticline lead us to speculate about the possible role of the Eagle Valley Evaoprite in the earthquake series. The Cattle Creek anticline is described by Mallory (1966) as a salt diapir west-southwest of Glenwood Springs. It is northwest of, and subparallel to, the Elk Mountain anticline. The crest of the Cattle Creek anticline, like the Elk Mountain anticline, is characterized by exposures of the Maroon formation overlying the Eagle Valley Evaporite. Below the Eagle Valley Evaporite in the Cattle Creek anticline is halite, interbedded with anhydrite and siltstone (Mallory, 1966). Though the time of initial movement of the Cattle Creek anticline is uncertain, it is believed that as arching progressed, erosion removed surficial strata, thereby exposing Eagle Valley Evaporite to meteoric stream water, and anhydrite was hydrated to gypsum (Mallory, 1966). Expansion accompanying the hydration of anhydrite to gypsum ranges from about 30 to 58 percent, and thus the pressure exerted by hydration has been estimated at 300 to 10,000 pounds per square inch (Brune, 1965). The three factors that Mallory has suggested as favoring flowage of halite at depth from marginal into crestal areas of the Cattle Creek anticline are these: (1) removal of overburden from the crest of the anticline, (2) weight of thousands of feet of Maroon Formation on the flanks of the structure, and (3) the high hydration pressure of anhydrite. Mallory (1966) further notes that upwelling of halite at depth has tilted the terraces in post-Pleistocene time, and that movement may still be taking place.

The similar geologic settings of the Elk Mountain anticline and the Cattle Creek anticline suggest similar mechanics of deformation. For this reason, we should consider the potential role of the Eagle Valley Evaporite in the 1984 earthquake series. Of particular interest, and possible significance, is that the 1984 earthquake swarm occurred during the spring following an unusually wet winter. The Colorado Climate Center (Nolan Doesken, pers. commun., 1985, from Doesken and McKee, 1985) reported levels of precipitation nearly one and a half times average during the winter of 1983 and spring of 1984. This substantial departukre from the long-term average is mostly accounted for by record levels of snowfall in November and December 1983, as well as above-normal precipitation during March and April 1984. Of further interest is a new spring of water that developed during, or shortly after, the time of the earthquake series (Bill Perry and Bruce Stover, pers. commun., 1985), near Edgerton Creek, about 5 km southwest of Carbondale. Because the winter-spring of 1983-1984 was characterized by above-normal precipitation, ponding of additional runoff might have caused water to enter cracks and joints in the Evaporite. As water reached anhydrite beds, the expansion accompanying the hydration process would begin, as gypsum was produced. The pressures generated by this expansion could have been sufficient to generate the swarm of earthquakes which were observed.

Because the spatial and temporal relationships, albeit somewhat circumstantial, between the Eagle Valley Evaporite, the above-normal precipitation and the earthquake swarm, we consider that to be a possible cause for the events which occurred near Carbondale in April and May, 1984. However, we are reluctant to attach any great regional, or even local, tectonic significance to what is in all ways a minor swarm of seismic activity.

References:

Brune, Gunnar, 1965, Anhydrite and gypsum problems in engineering geology: Engineering Geology, v. 2, no. 1, p. 103-106.

Doesken, Nolan, and McKee, Thomas, 1985, Colorado climate summary water-year series (October 1983-September 1984), Colorado Climate Center, Department of Atmospheric Science, Colorado State University: Climatology Report 85-1.

Mallory, W.W., 1966, Cattle Creek anticline, a salt diapir near Glenwood Springs, Colorado: U.S. Geological Survey Professional Paper 550-B, p. B12-B15.

Poole, F. G., 1954, Geology of the southern Grand Hogback area, Garfield and Pitkin Counties: Colorado Unniversity M.S. thesis, 128 p.

Tweto, Ogden, Moench, R. H., and Reed, J.C., Jr., 1978, Geologic map of the Leadville 1° X 2° quadrangle, northwestern Colorado: U.S. Geological Survey Miscellaneous Investigation Series Map I-999.

Reports

Bollinger, G. A., and Langer, C. J., 1987, Development of a velocity model for locating aftershocks in the Sierra Pie de Palo region of western Argentina: U.S. Geological Survey Bulletin No. 1795, 28 p.

Langer, C. J., and Bollinger, G. A., 198__, Aftershocks of the western Argentina (Caucete) earthquake of 23 November 1977--Some tectonic implications: (Submitted to Tectonophysics, April 1987).

Goter, S. K., Presgrave, B. W., Henrisey, R. F., and Langer, C. J., 198__, The Carbondale, Colorado, earthquake swarm of April-May, 1984. (Submitted to Seismological Research Letters, March 1987).

Cranswick, E., Deshpande, V. C., Harmsen, S. C., Langer, C. J., and Butler, D. 1987, Procedure of a micro-array experiment on earthquake swarm activity near Crested Butte, Colorado [Abs.]: Seismological Research Letters, v. 58, p. 12

San Andreas Fault Slip History Near Cholame, California

9910-NEW

J.J. Lienkaemper
Branch of Engineering Seismology and Geology
U.S. Geological Survey
345 Middlefield Road, MS 977
Menlo Park, California 94025
(415) 323-8111, ext. 2759

Investigations

1. Slip histories of the Parkfield and Cholame segments of the San Andreas fault.

Results

1. Special aerial photography was flown between Cholame Valley and Bitterwater Canyon in October during low afternoon sun and at a sun azimuth selected to preferentially illuminate stream channel walls and shadow fault scarps. The large scale of the photos, 1:2400 (RF), makes it possible to reconstruct the smallest offset channels (1 to 12 meters) with at least as much reliability as ground inspection. The photos give the advantage of a synoptic view of the entire offset channel segment without the disadvantage of image foreshortening experienced by the ground observer.

   The three highest quality offset channels were pre-paneled and surveyed to 1-cm accuarcy for the purpose of producing detailed (0.25-m contour) topographic maps for making a more quantitative reconstruction of the 1857(?) slip at these sites. The first of these maps was actually produced from 1966 photography by transferring the 1986 survey control by analytical plotter at the USGS Western Mapping Center at Menlo Park. The older photography was necessary because agricultural disking over the last 20 years had largely destroyed the offset.

   I am nearly done with the task of interpreting the smallest offsets between Cholame Valley and Bitterwater Canyon on enlarged (approx. 1:400 scale) stereo pairs of air photos. The least equivocal sites have offsets between 5 and 7 meters, and have no geomorphic evidence (e.g., lateral bevels, rather than an abrupt offset) suggesting multiple events. Thus, I believe, because they are widely spaced along the fault, that they probably do represent the upper boundary values of slip distribution associated with the great 1857 earthquake for the Cholame segment.

Reports

None during this report period.

Charleston Project: Geologic and engineering Studies

9950-03868

Stephen F. Obermeier
Br. of Geologic Risk Assessment
U.S. Geological Survey
National Center, MS 926
Reston, VA 22092
(703) 648-6791

9510-01343

Gregory S. Gohn
Br. of Eastern Regional Geology
U.S. Geological Survey
National Center, MS 926A
Reston, VA 22092
(703) 648-6901

Investigations

Investigations were undertaken to: 1) determine more completely the areal extent of sand blows in South Carolina; 2) determine the ages of sand blows using ^{14}C analysis of wood fragments in craters; 3) attempt to determine relative strength of pre-1886 earthquakes, based on diameters and areal extent of pre-1886 craters; and 4) back-calculate 1886 accelerations at sand blow sites.

Results

1. Sufficient field data have been collected in coastal South Carolina to show that: a) pre-1886 sand blow craters are substantially larger than 1886 craters beyond a radius of about 15-20 miles from Charleston airport; b) at Hollywood, at least three different generations of pre-1886 craters (all Holocene) are widely separated in time, and are much larger than sand blows produced by the 1886 earthquake; and c) near the epicentral region of the 1886 earthquake, there are multiple generations of very large, pre-1886 Holocene sand blows. Thus, it tentatively appears that 1) earthquakes stronger than the 1886 event have probably struck repeatedly during the Holocene, and 2) the epicentral region(s) for these strong quakes is in the general vicinity of the epicenter(s) for the 1886 earthquake. More field data are needed to prove this model.

2. Sand blows have been found near Southport, N.C. The sand blows are probably older than 5,000 years, as judged solely on the basis of the degree of weathering in the filled crater.

3. An effort was made to locate ditches and pits in fluvial terrace deposits along the Savannah River in the area between I-95 and the Barnwell nuclear plant. No sand blows were found in the very few pits that were located, but ditches and pits are so rare that it is impossible to make conclusions about previous earthquakes. It is planned to take a boat down the Savannah River and examine freshly exposed banks undercut by the river.

4. Lateral spreads have originated by liquefaction and shearing within shell beds at many places in the Mount Pleasant, S.C. area. This unexpected source bed appears to be associated with zones of intense weathering in

shells, and thus weakening of the shells, apparently making them susceptible to collapse and development of high pore pressure.

5. Two trips were made to the Hollywood ditch to collect cone penetration data. The purpose of the data collecting is to back-calculate 1886 accelerations. This undertaking is a cooperative venture with Professor Wayne Clough of Virginia Polytechnic Institute and State University.

Reports

None

Array Studies of Seismicity

9930-02106
David H. Oppenheimer
Branch of Seismology
U.S. Geological Survey
345 Middlefield Road, MS 977
Menlo Park, California 94025
(415) 323-8111, Ext. 2791

Investigations

1. Analyze fault-plane solutions of aftershocks of the M6.2 Morgan Hill earthquake which occurred on April 24, 1984 to gain understanding of regional stress field.

2. Continue consolidation and clean up phase data of central California Seismic Network (CALNET) from 1969 through 1984.

3. Analysis of P- and S-velocity structure at Coalinga, California.

4. Continue investigation of 10 characteristic earthquake sets (M > 4.0) in the Stone Canyon/Bear Valley region of the San Andreas fault.

Results

1. An expanded set of 946 fault plane solutions was computed for aftershocks ($M \geq 1.5$) of the 1984 Morgan Hill earthquake which ruptured the Calaveras fault. This suite of data presents a complete picture of the aftershock deformation throughout the region. In addition to the results reported in Volume 23 of the Summaries of Technical Reports, we have considered in greater detail possible explanations for the deviation of the stress field inferred from the fault plane solutions from the field inferred from regional geodetic data. We are collaborating with Robert Simpson of the USGS who is modeling the elastic fields resulting from various dislocation scenarios and are attempting to use these quantitative results to assess the likelihood that the respective dislocations would give rise to the slip directions observed from the fault plane solutions. Models under active consideration are the following: 1) the 3 degree bend in the trace of the Calaveras east of San Felipe Valley, 2) a detachment surface represented by the reverse fault plane solutions that dips to the east and which intersects the Calaveras at a depth near 7 km, 3) rotation of the block between the Calaveras and the San Andreas faults, 4) the effects of a mismatch of Pacific-North American plate motion directions from the local orientation of the Calaveras, 5) the left step of the Hayward fault which bifurcates from the Calaveras to the north of Halls Valley, and 6) variations in failure conditions on and off the Calaveras fault. We hope these investigations will place limits on the absolute stress levels at seismogenic depths. A preliminary manuscript was prepared describing the calculation of the fault plane solutions, their interpretation in terms of fault structure, and the implications of the solutions for the state of stress.

2. A substantial effort was devoted to the collection, organization, relocation, archiving, and documentation of all the CALNET earthquake data since 1969. Programs were written to detect gross errors in the phase

data and all data prior to 1985 were reprocessed using this program. A program was written to merge phase data from separate networks into a common set based upon the accompaning earthquake locations. Merging will occur following the renaming of all the stations in CALNET to the new "rational" names.

3. Existing computer programs which simultaneously invert local earthquake traveltime data for the 3-dimensional velocity structure and hypocentral parameters have been modified to generate output that can be used to compute fault-plane solutions. Accompanying graphics software has been developed to display the 3-D solution in perspective view.

   The primary effort was devoted to refining the 3-dimensional velocity model calculated from inversion of traveltime data recorded in the vicinity of Coalinga, California. Data exhibiting large traveltime residuals were investigated, and a series of inversions to examine the effect of variable model scale were carried out. Seismic refraction interpretations of the upper 5 km of the crust are being incorporated into the model as "a priori" information.

4. High precision scaling of S-wave and coda wave amplitudes was completed for a subset of the Stone Canyon characteristic earthquakes to determine the temporal stability of coda waves. The 28 events studied occurred between 1/34 and 6/86 and group into 8 source sets. Results from the scaling of Wood-Anderson seismograms from Mt. Hamilton show that the ratio of maximum shear wave amplitude to coda wave amplitude varies by as much as 60 percent within a given characteristic set. The patterns of changes have no obvious temporal association with the M 5.5 earthquakes occurring in the region between the sources and receiver. It was also found that the coda shape varied between source sets despite their separation of only a few kilometers. An Open-File Report discribing these results is in press.

   The earth tidal stress and phase was calculated for the origin time of each of the 37 earthquakes in the 10 Stone Canyon characteristic sets. No consistent relationship was found between the event time and the phase of the tidal stress. We conclude that variations in the earth's tidal stress play little or no role in triggering the rupture of these sources. Present efforts were directed toward the collection and processing of digital seismograms for the characteristic event pairs from 1965 to 1986. Spectral analysis will be carried out to determine the coherence of the earthquakes as well as other similarities and differences in the sources.

Reports

Ellsworth, William L., Lynn D. Dietz, J. Frechet, and G. Poupinet, 1987, Preliminary results on the temporal stability of coda waves in Central California from high-precision measurements of characteristic earthquakes: Redbook for USGS Conference on Intermediate-Term Precursors, in press.

Eberhart-Phillips, D., 1986, Three-dimensional P- and S-velocity structure at Coalinga, California: possible evidence for high pore pressure in the hypocentral zone, EOS, Tran. Am. Geophys. Union, 67, 1222-1223.

Dietz, L. D., and W. L. Ellsworth, 1986, A characteristic earthquake source at Stone Canyon, California, EOS, Tran. Am. Geophy. Union, 67, 905.

Ellsworth, W. L., and L. D. Dietz, 1986, Are all earthquakes Characteristic?, EOS, Tran. Am. Geophy. Union, 67, 905.

R. W. Simpson, S. S. Schulz, and L. D. Dietz, Response of Creepmeters on the San Andreas fault to the 26 January 1986 Tres Pino earthquake, EOS, Tran. Am. Geophy. Union, 67, 1206.

Mountain Run Fault Zone of Virginia

9510-03680

Louis Pavlides
Branch of Eastern Regional Geology
U.S. Geological Survey
National Center, MS 928
Reston, Virginia 22092
(703) 648-6925

Investigations

Mapping within the Mountain Run Fault Zone (MRFZ) southwest of its "type area" in the Unionville quadrangle of Virginia indicates it is polymictic; it contains both mylonite and phyllonite as well as a late breccia phase. Some of the foliated rocks contain two generations of chloritoid. In thin section, this is demonstrated by early chloritoid alined along folded foliation and late chloritoid along cleavage that is axial planar to the folded foliation with early chloritoid. Thus, a complex picture of polydeformation and polymetamorphism is emerging from this fault zone. Phyllonite that holds up linear scarps is cut by unmetamorphosed and undeformed Mesozoic dikes, which indicates that a large part of this fault had formed in pre-Jurassic(?) time. However, as described last year, faulting occurred northwest of the scarp area several times since the MRFZ formed and probably in the Tertiary as well as possibly into fairly recent time.

During field conferences with geologists of the Virginia Geological Survey, the MRFZ and its possible southwestward extension into Virginia were discussed and evaluated by geologic reconnaissance. Since then, the MRFZ has been extended by Conley (1987, Geological Society of America Abstracts with Programs, v. 19, no. 2, p. 80) into southcentral Virginia. He notes that a 2.4 magnitude earthquake epicenter near Carters Bridge, central Virginia, is located along the trace of the Mountain Run Fault Zone.

Reports

Kolata, D. R., and Pavlides, Louis, 1986, Echinodums from the Arvonia Slate, Central Virginia Piedmont: Geologica et Paleontologica, vol. 20, p. 1-9.

Seismotectonics of the Central Calaveras Fault

14-08-0001-G1084

Gary L. Pavlis
Department of Geology
Indiana University
Bloomington, Indiana 47405
(812) 339-4872

Atilla Aydin
Department of Earth and Atmospheric Sciences
Purdue University
West Lafayette, Indiana 47907
(317) 494-3696

Objective

To improve our understanding of the nature of the process leading to moderate sized, strike slip earthquakes in California through combined geologic and seismological investigations.

Investigation

This is a cooperative effort between groups at Indiana University and Purdue University. We have combined surface fault data mapped by Aydin with extremely precise earthquake hypocenter location estimates for the source region of the 1984 Morgan Hill, California, earthquake (Figure 1).

Results

Comparison of the seismicity data to the mapped fault structures lead to three major conclusions.

1. Seismicity is highly nonuniform along this section of the Calaveras fault. Statistical analysis of the seismicity patterns indicate significant clustering of earthquakes in space for both the preshock and aftershock seismicity. (Eneva and Pavlis, 1988). Correlation of the seismicity with the surface fault geometry indicate this clustering is due to a concentration of activity at major stepovers in the fault zone. Activity is concentrated at major right (extensional) stepovers in Halls Valley and San Felipe Valley, and at the left (compressional) stepover southeast of Anderson Reservoir (Figure 1).

2. Strong motion data (Hartzell and Heaton, 1986) and the aftershock data (Cockerham and Eaton, 1984) indicate the Morgan Hill mainshock rupture terminated a few kilometers southeast of Anderson reservoir. The 1979 Coyote Lake earthquake rupture also appears to have terminated in this region (Reasenberg and Ellsworth, 1982). The surface fault map shows a major left step in this area which apparently acted as a barrier to both earthquake ruptures.

3. There is a suggestion that two separate segments of the Calaveras separated by the right step at San Felipe Valley formed the Morgan Hill event. The aftershock and strong motion data indicate the initial rupture ran along an area from 6 to 10 km in depth from Halls Valley to San Felipe Valley. From there the rupture appears to have expanded vertically to rupture through almost the entire seismogenic zone (Hartzell and Heaton, 1986) until the rupture terminated southeast of Anderson reservoir. We suggest this change may have been caused by the rupture jumping to another strand of the Calaveras at the stepover forming San Felipe Valley. We note, however, that other stepovers in the Halls Valley section do not appear to show a similar behaviour.

References

Cockerham, R.S. and J.P. Eaton (1984). The April 24, 1984, Morgan Hill earthquake and its aftershocks: April 24 through September 30, 1984, in The 1984 Morgan Hill, California, Earthquake, Calif. Dept. of Conser., Div. Mines and Geology, Spec. Pub. 68, 215-236.

Eneva, M.G. and G.L. Pavlis (in review). Application of pair analysis statistics to aftershocks of the 1984 Morgan Hill, California, earthquake, J. Geophys. Res.

Hartzell, S.H. and T.H. Heaton (1986). Rupture history of the 1984 Morgan Hill, California, earthquake from the inversion of strong motion records, Bull. Seism. Soc. Amer, 76, 649-674.

Reasenberg, P. and W.L. Ellsworth (1982). Aftershocks of the Coyote Lake, California, earthquake of August 6, 1979: A detailed study, J. Geophys. Res., 87, 10637-10655.

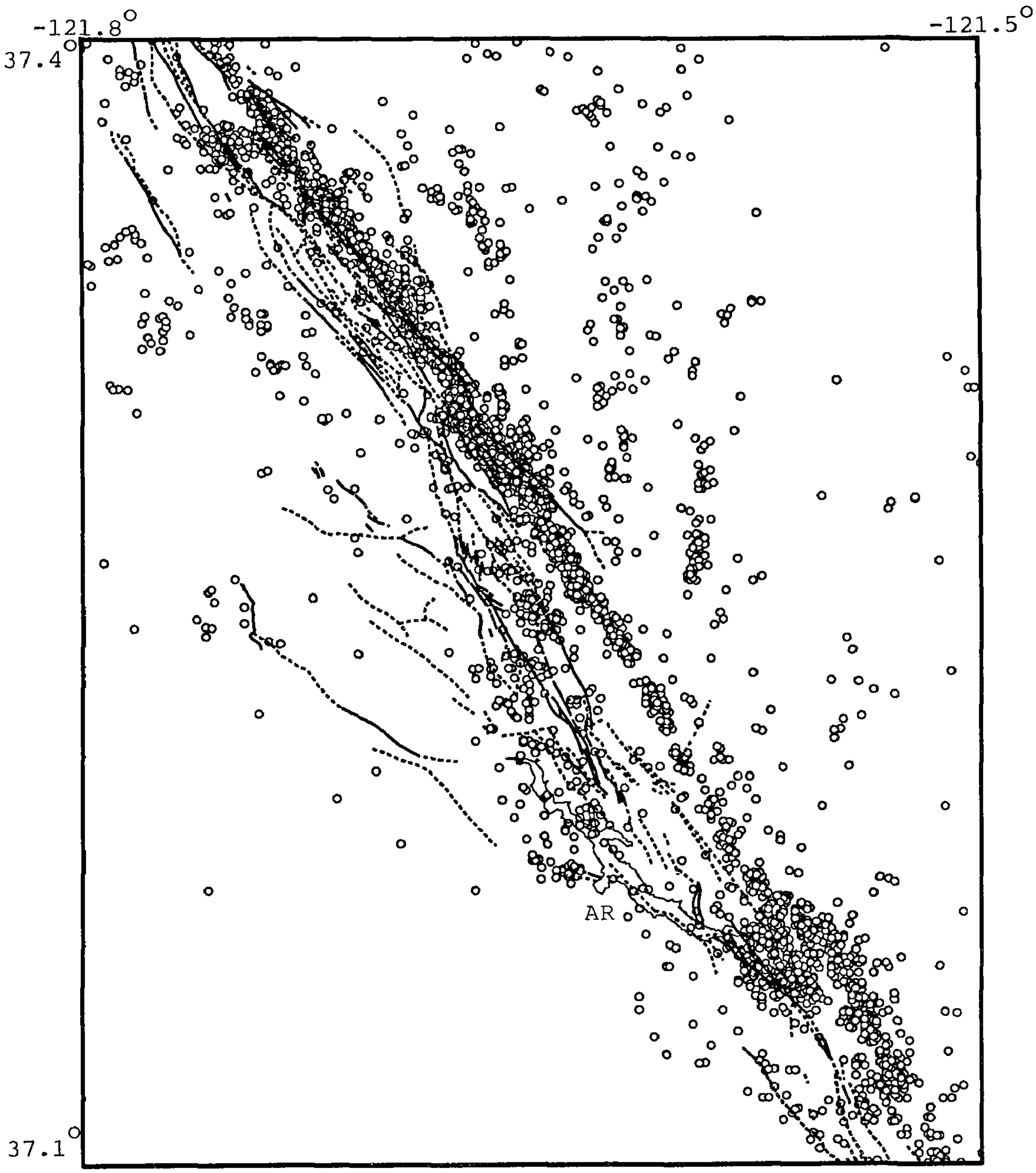

Figure 1. *Fault map and seismicity of the source region of the 1984 Morgan Hill earthquakes.* All earthquakes from 1978 to March 1986 were relocated using the velocity model from Cockerham and Eaton (1984). These are plotted as small circles on this map. Mapped faults shown are all strike slip. Dashed traces are less certain. Dip slip faults were also mapped, but are not plotted here. Anderson Reservoir (AR) is also shown for a geographic reference point.

INTEGRATED ANALYSIS OF SOURCE PARAMETERS FOR A BASIN AND RANGE EARTHQUAKE SEQUENCE

14-08-0007-G1326

Keith F. Priestley and Kenneth D.Smith
Seismological Laboratory, Mackay School of Mines
University of Nevada, Reno, Nevada 89557
(702)-784-4975

INVESTIGATIONS:

Our objective is to determine source parameters for the main shock and many of the aftershocks of the 1984 Round Valley, California earthquake sequence, and interpret this with respect to the details of the aftershock development. We have determined the source paramters of 26 aftershocks, M_L>2.7, using a pulse width technique (Frankel and Kanamori; 1983) and the short period clipped records. Source parameters for the Round Valley mainshock have been determined incorporating local strong motion records, region surface waves, teleseismic body waves, and short period first motion data. Also. we have pursuded analysis of the foreshock sequence of the 1986 Chalfant, California earthquake.

RESULTS:

The 1984 Round Valley earthquake has been one in a series of moderate size $M_L \approx 6$ earthquakes to have occurred in the Mammoth Lakes-Bishop, California area since 1978. The most recent of this series, the 1986 Chalfant, California sequence, took place 15 km to the northeast of the Round Valley epicentral area and included 5 events over M_L 5. These sequences have occurred within the U.S. Geological Survey-University of Nevada local short period network, which has provided an excellent data set for determining the character of earthquake activity in this area.

Source Parameters of the Mainshock

We have determined several source parameters for the mainshock. Telseismic body waves (phases P, PP, PcP, PKP, PS, S, SS, SSS, ScS, and SKS) have been inverted for the moment tensor representation of the source, and the Round Valley mainshock can be represented by a simple double couple. Our moment tensor solution is similar to that obtained by Barker and Wallace (1985) using P and SH teleseimic body waves. Both of these studies have determined the mechanism to have been left-lateral nearly pure strike slip on a vertical northeast striking plane. This is important in terms of the controversy that has surrounded several of the M_L 6 events in the Mammoth Lakes area that have shown a significant non-double couple component in the moment tensor solution. These non-double couple solutions have been interpreted by Julian (1985) to have resulted from magma injection. A strong motion instrument, operated by the California Division of Mines and Geology (CDMG), recorded the mainshock at an epicentral distance of 3 km. This trace has been digitized and used to determine the high frequency spectra. Surface waves at regional distances have been fit to synthetics in a forward sense to determine the long period level, and give a seismic moment of 7.94 x 10^{24}. A composite spectra has been constructed from the the high frequency spectra from the strong motion record and the long period level determined by surface wave fitting. The spectra has a corner frequency of .4 Hz and assuming a circular source and a Brune (1970) model this returns a stress drop of 89 bars. This is in reasonable agreement with the stress drop determined by estimating the source area from the aftershock distribution. An approximately 36 km^2 area free of aftershock activity on the mainshock fault plane is the apparent slip surface of the event. Using this area and the surface wave moment the stress drop is 49 bars and the slip is 73 cm for the mainshock. The short period focal mechanism, the early aftershock activity and the moment tensor solution all indicate that the Round Valley mainshock took place on a near vertical northeast striking plane, and the focal mechanism and moment tensor solution agree on the sense of motion as nearly pure strike slip.

Round Valley Aftershock Sequence

The Round Valley sequence is characterized by two conjugate planes of seismicity; one nearly vertical plane striking N30°E associated with the mainshock and the other striking N40°W and dipping 55° to the NE which conforms to a suggested extension of the Hilton Creek fault, a major holocene fault (Malcom Clark, unpublished research). The mainshock occurs near the intersection of these two planes. This is the first activity that has been directly associated with the Hilton Creek fault since the Mammoth Lakes-Bishop, California sequence began in 1978. Focal mechanisms indicate nearly pure left-lateral strike slip faulting on the deeper vertical plane and right- lateral strike slip to obique slip on the N40°W plane. The mode of slip was left-lateral strike slip in the first day of aftershock activity and became dominantly right-lateral strike slip as the sequence progressed.

Source Parameters of Aftershocks (Pulse Width Technique)

We have selected the pulse technique of Frankel and Kanamori (1983) and O'Neill and Healy (1973) to determine source parameters of a number of aftershocks between $M_L \approx 3$ and 4. This technique is applied to the clipped velocity records of the local short period network. Although first pulses are generally clipped for this magnitude range and distance (≈10 km), pulse widths are preserved (Ellis and Lindh, 1976). The technique involves substracting the pulse width of small events (< M_L 2) from that of the larger events, effectively deconvolving the path and instrument effects. The small event should be as close as possible in space (≈1 km or less for this study) to the larger event so as to have nearly the same travel path. The corrected pulse width is then assumed to represent the source process time, and the source radius can then be calculated directley (Boatwright, 1980). To apply this technique, assumptions must also be made about the source geometry and the rupture velocity. The stress drop is then calculated by scaling source radius measure to the seismic moment. We have used a moment magnitude scale (Chavez and Priestley, 1985), and magnitudes have been determined from the short period records using a duration magnitude scale or from regional broadband recordings converted to Wood-Anderson equivalents. This has been somewhat of a problem. Duration magnitudes are not consistent with regional magnitude determinations. In fact the duration magnitude has been systematiclly .4 M_L higher than the Wood-Anderson equivalents. Duration magnitudes have been calibrated to the California Richter magnitude and this difference is apparently due to different attenuation properties in the Basin and Range. Therefore stress drops of individual events are considered at this time to be only relative values.

We have determined the source parameters of 24 aftershocks and 2 foreshocks of the Round Valley sequence using this technique (Table 1). There is no correlation between stress drop and M_o in the events studied to date, but there is a relationship between stress drop and depth (Figure 1). Higher stress drops are associated with those events located at the edge of the apparent slip area of the mainshock where higher stresses would be expected (Das and Sholz, 1981). The two events with the highest stress drop values occur at the southern end of the mainshock rupture surface at a depth of 13 km. Focal mechanisms for these events are not consistent with the general trend for events located on the N30°E mainshock fault plane, but indicate fault planes striking N60°E.

Chalfant Foreshock Sequence

The M_L 6.4 July 21, 1986 Chalfant, California was preceded by a distinct foreshock sequence. The largest foreshock, M_L 5.7 occurred 24 hours before the mainshock and within a dense cluster of activity which began on July 3. This cluster was confined to a very small volume of the crust, depth 7 km, and included 8 events over M_L 3. As at Round Valley, two nearly conjugate planes of seismicity are also the character of the Chalfant sequence. One conforms to the slip area of the M_L 5.7 foreshock striking N30°E and dipping 55°NW and the other is associated with the mainshock, striking N25°W and dipping 70°SW. The hypocenter of the mainshock is located within an off-fault cluster of activity perpendicular to the slip area of the M_L 5.7 event. Not only is there an increased shear stress at the edge of a ruptured surface but there is also an predicted increase perpendicular to the faulted area (Das and Scholz, 1981). This appears to have been the triggering mechanism of the mainshock. Aftershocks of the M_L 5.7 foreshock indicate that this event ruptured exclusively in the upper 10 km of the crust. This sequence is similar to the 1980 Mammoth Lakes sequence in that shallow clustering which preceded a shallow $M_L \approx 6$ event was followed by continued activity at the M_L 6 level.

Reports

Priestley, K.F. and K.D. Smith (1987). The 1984 Round Valley, California earthquake earthquake, submitted to G.J.R.A.

Smith K.D. and K.F. Priestley (1986). Rupture duration and stress drop for aftershocks of the November 23, 1984 Round Valley California earthquake, Earthquakes Notes (abstract) 57, 23.

Smith, K.D., K.F. Priestley, and R.S. Cockerham (1987). Spatial and temporal variations in the 1984 Round Valley, California earthquake sequence, submitted to Geology.

Smith, K.D. and K.F. Priestley (1987). Foreshock sequence of the 1986 Chalfant, California sequence, submitted to Bull. Seism. Soc. Am.

Smith, K.D., U.R. Vetter, and K.F. Priestley (1986). Focal mechanisms of the July 1986 Chalfant, Claifornia earthquake sequence, EOS Trans. (abstract) 44, 1106.

Smith, K.D. and K.F. Priestley (1987). Foreshock sequence of the 1986 Chalfant, California earthquake, Seism. Res. Lett. (abstract) 58, 20.

References

Barker J.S. and T.C. Wallace (1985). A note on the teleseismic body waves from the 23 November 1984 Round Valley, California, earthquake, Bull. Seism. Soc. Am. 76, 883-888.

Boatwright, J. (1980). A spectral theory for circular seismic sources: simple estimates of source dimension, dynamic stress drop and radiated energy, Bull. Seism. Soc. Am. 70, 1-28.

Brune, J.N. (1970). Tectonic stress and the spectra of seismic shear waves from earthquakes, J. Geophys. Res. 75, 4997-5009.

Chavez, D.E. and K.F. Priestley (1985). M_L observations in the Great Basin and M_o of the 1980 Mammoth Lakes, California, earthquake sequence, Bull. Seism. Soc. Am. 75, 1583-1598.

Das, S. and C.H. Scholz (1981). Off-fault aftershock clusters caused by shear stress increase, Bull Seism. Soc. Am. 71, 1669-1675.

Ellis, J. and A. Lindh (1976). Linearity of VCO-discriminator system with respect to zero crossing times, U.S. Geol. Survey Open-File Rept. 76-873.

Frankel, A. and H. Kanamori (1983). Determination of rupture duration and stress drop for earthquakes in southern California, Bull.Seism Soc. Am. 73, 1527-1551.

O'Neill, M.E. and J.H. Healy (1973). Determination of source parameters of small earthquakes from P-wave rise time, Bull. Seism. Soc. Am. 63, 599-614.

Event	Lat	Lon	Depth	ML	Log Mo (dyne/cm)	Source Radius (m)	Stress Drop (bars)
840802 1626	37-29.87	118-33.31	7.74	2.9	20.97	595	2
841123 1808	37-27.57	118-35.38	10.42	2.8	20.85	131	91
841123 2342	37-23.76	118-36.71	6.93	3.1	21.81	391	47
841124 0246	37-26.50	118-38.00	5.54	3.0	21.21	160	173
841124 0510	37-27.40	118-36.91	8.40	3.0	21.09	234	41
841124 0740	37-27.20	118-36.84	7.10	3.0	21.09	333	14
841124 0748	37-26.18	118-36.69	7.82	3.1	21.21	171	141
841124 0800	37-27.51	118-36.81	8.41	2.8	20.85	204	35
841124 0841	37-27.23	118-36.84	7.62	2.7	20.73	221	21
841124 0852	37-27.26	118-36.83	7.50	2.9	20.97	308	13
841124 0921	37-28.44	118-35.15	9.00	3.7	21.93	324	109
841124 1013	37-26.75	118-37.12	6.44	3.2	21.33	210	100
841124 1122	37-28.41	118-34.19	8.50	2.9	20.97	143	136
841124 1215	37-27.30	118-36.78	7.28	3.4	21.57	318	50
841124 1301	37-27.70	118-37.07	8.25	3.1	21.21	153	196
841125 2148	37-26.56	118-38.35	5.22	3.0	21.09	249	34
841125 2254	37-27.15	118-36.52	6.77	3.3	21.45	238	90
841125 2309	37-27.19	118-36.56	7.34	4.0	22.29	877	12
841125 1731	37-27.56	118-35.91	12.72	3.4	21.57	475	15
841125 1042	37-25.66	118-36.84	12.51	3.5	21.69	189	314
841125 1045	37-25.68	118-36.99	12.47	3.4	21.57	153	416
841201 0455	37-27.62	118-41.30	3.64	3.5	21.69	811	4
841201 2014	37-25.44	118-37.01	7.7	3.1	21.21	224	63
841203 2038	37-27.56	118-40.58	4.02	2.9	20.97	164	91
841207 2205	37-25.73	118-37.10	8.8	2.9	20.97	96	346
850103 0921	37-27.89	118-38.72	4.31	3.6	21.81	536	16

Table 1. Source parameters of Round Valley aftershocks determined from pulse width method.

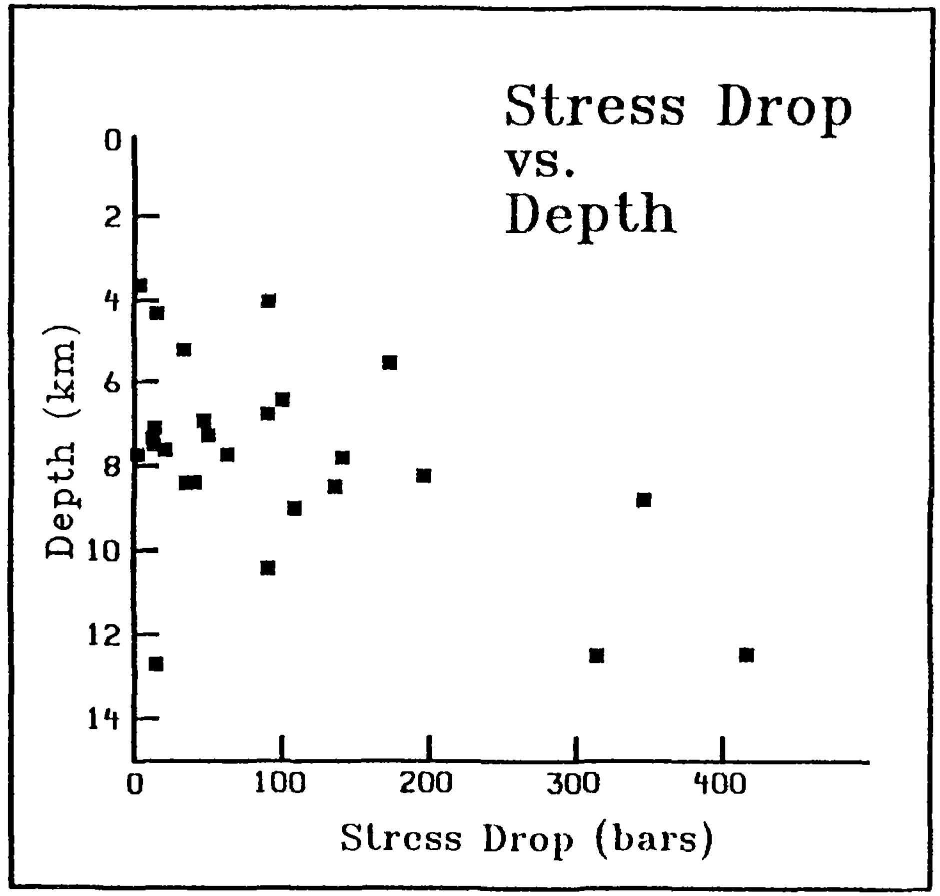

Figure 1: Stress drop as a function of depth for events in Table 1.

Basement Tectonic Framework Studies
Southern Sierra Nevada, California

9910-01291

Donald C. Ross
Branch of Engineeriing Seismology and Geology
345 Middlefield Road, MS 977
Menlo Park, California 94025
(415) 323-8111 ext. 2341

Investigations

1. Preparation, and revision following technical review, of report summarizing data on mafic rocks of the southern Sierra Nevada.

2. Preparation of summary text and description of map units to accompany reconnaissance geologic map of basement rocks of the southern Sierra Nevada (at a scale of 1:250,000).

3. Compilation of data from some 1600 modal analyses of granitic rocks from the southern Sierra Nevada and preparation of a report that summarized the data by rock type for the entire area and for each of some 67 granitic bodies.

Results

1. Mafic and ultramafic rocks (exclusive of the large gneissic complex in the Sierran tail) in the southern Sierra Nevada fall into possibly three age groups. Most are probably Cretaceous, are largely gabbro and gabbronorite, and form generally small remnants engulfed by granitic bodies. This group is concentrated along the west side of the batholith near latitude 36° 00' north, but smaller, possibly related patches are scattered elsewhere throughout the batholith. Many of these bodies are altered in part, or completely, to amphibolite composed chiefly of intermediate plagioclase and amphibole (variously represented by dark colored hornblende and lighter colored acicular antinolitic and cummingtonitic types).

   A body of olivine gabbro near Bodfish, much altered to amphibolite and fragmented by lateral movement of the Kern Canyon fault, is cut by dark dikes that may be related to the Independence dike swarm of possibly Jurassic age. Dated Jurassic gabbroic rocks also occur at Eagle Rest Peak north of the San Emigdio Mountains, but these outcrops are separated from the Sierran basement by younger rocks and they may be structurally separate from the Sierran basement, as they are different from other Sierran mafic basement rocks.

   Probable dikes of the Triassic quartz diorite of Walker Pass intrude the Summit gabbro on the east side of the southern Sierra Nevada. These sparse data suggest Triassic (or older), Jurassic, and Cretaceous pulses of mafic plutonism in the southern Sierra Nevada.

2. The areal distribution of granite, granodiorite, tonalite, and quartz diorite in the southern Sierra Nevada has been determined using the modal averages of some 67 granitic bodies (based on the IUGS igneous rock classification).

   Granite, which occurs in many relatively small bodies, is widely scattered through the eastern and central part of the study area.

   Granodiorite is by far the most abundant rock type, underlying more than 2700 km^2, mostly in the east and central part of the batholith.

   Tonalite forms an almost continuous belt along the west side of the batholith. Tonalitic granitic rocks are also common in the gneissic complex of the Sierran tail, where they are less commonly in readily mappable discrete bodies, and more commonly mixed with gneissic and mafic rocks.

   Quartz diorite is only sparsely represented, but some relatively large bodies, seemingly anomalous is the eastern part of the batholith, are old Triassic remnants engulfed in the younger, more felsic plutons. Quartz diorite is also abundant in the gneissic complex of the Sierran tail but not readily separable into discrete bodies.

Reports

Ross, D.C. 1987, Metamorphic framework rocks of the southern Sierra Nevada, California: *U.S. Geological Survey Open-File report 87-18*, 74 p.

EARTHQUAKE HAZARD STUDIES USING NETWORK AND GEOLOGIC DATA IN NEW YORK STATE

USGS 14-08-0001-22024

Leonardo Seeber and Lynn R. Sykes
Lamont-Doherty Geological Observatory of Columbia University
Palisades New York 10964

Purpose

This project is concerned with fundamental aspects of intraplate neotectonics and seismogenesis along the Atlantic Seaboard and the Appalachians, with special emphasis on New York State and surrounding areas.

Data

Earthquake data provide the main basis for the work in this project. These data include hypocentral data from the New York-New Jersey Seismic Network operated by the Lamont-Doherty Observatory (L-DGO) during the last 15 years and from temporary networks of portable seismographs, early instrumental data, and historic data on felt reports. Geologic and geophysical information also play an important role in this research, but most of the work dealing with those data falls within the scope of other projects which are complementary to the project discussed here.

Investigations

1. Detailed investigations are being carried out of recent important earthquake sequences in the northeastern U.S. The 1985 earthquake sequence in Westchester County (Figure 1) is being investigated for the geometry of the seismogenic faults and their relation to surface faults. The time-space migration of events in this sequence may yeald evidence of aseismic deformation. A detailed intensity data set was compiled for the main shock of the Westchester sequence; these data are being compared to surface geology and morphology to establish a basis for seismic zonation and to serve as calibration for deriving source parameters from preinstrumental earthquakes. Other earthquake sequences being investigated include: the ML=4.1 Martic 1984 sequence in eastern Pennsylvania; the Ms=5.3 Goodnow 1983-85 sequence in the central Adirondacks; and the Ms=5.0 January 1986 sequence near Cleveland, Ohio.

2. The study of seismicity induced by flooding in an abandoned deep iron mine in the Adirondacks.

3. Possible changes in the distribution of earthquakes over time and over the magnitude range are being investigated by comparing seismicity as derived from network data in the last 15 years, and as derived from preinstrumental data in the last 250 years. This comparison includes improvements of the macroseismic data base and a new interpretation of these data for source parameters.

4. Development of MACRO, an algorithm that fits the intensity data from an earthquake with a prescribed intensity distribution by parametrizing the epicenter coordinates, felt area, and the rate of intensity fall off with epicentral distance. Magnitudes are derived from felt areas. This algorithm is being tested using recent data and is being applied to preinstrumental data.

Results

The Newark Basin is associated with a prominent seismic zone (the NBSZ) and is one of the best examples of seismicity controlled by preexisting features along the Appalachians and Atlantic Seaboard. Following a pattern noticed for other basins along the Atlantic Seaboard, seismicity is clustered around the Basin, while few reliable epicenters fall within it. This is surprizing, since similar Paleozoic crystalline rocks surround and floor the Basin. In the NBSZ, coverage of seismicity starts in the mid 1700s and the 1737 New York City earthquake is the first known prominent event. We improved constraints on preinstrumental events by examining archival sources and by applying MACRO (see above).

Generally, the NBSZ maintains similar characteristics through the historic and the recent instrumental periods. Several persistent sources of historic seismicity, such as Lancaster Co., Pa., Willmington, Dl., and the New York City metropolitan area, are found to correlate with clusters of recent epicenters. Both historical and modern epicenters form two belts on either side of the Basin. But, while most of the modern instrumental epicenters are adjacent to the Ramapo border fault (Figure 2), the more prominent earthquakes ($M \geq 4$) are on the southeast side of the Basin and are broadly associated with the Martic-Cameron's Line, a lower Paleozoic suture (Figure 3).

Our working hypothesis is that this difference between the long term and the short term distributions of seismicity reflect a difference in the tectonic regime on the two sides of the Basin rather than temporaral variations. Seismicity on the northwest side of the Basin is confined within a relatively thin allochthonous slab of crystalline rocks, the Reading-Hudson highlands Prong, and therefore tends to be shallow, to produce small magnitude events, and, possiby, have a low maximum-magnitude cut off. In contrast, seismicity on the sowtheast side of the Basin is associated with deeper reaching faults and therefore has a lower b-value and higher maximum-magnitude cut off.

The large scale pattern of seismicity in the NBSZ follows major structural trends, but contrasts with the geometry of faulting in recent events. The ruptures inferred for the Mblg=4.0, April 23, 1984 Martic earthquake in Lancaster Co., Pa. and for the Mblg=4.0, October 19, 1985 Ardsley earthquake in Westchester Co., N.Y. are transverse to the border faults of the Basin and to Paleozoic structures that control them. Secondary faults of Mesozoic or later age are correlated with these ruptures. In particular, the Dobbs Ferry fault which had been identified before 1985 and the inferred rupture of the Ardsley earthquake are coincident by a 5 km extrapolation (mostly in depth), within a small (0.5 km) margin of error.

The structural control of seismicity may occur by reactivation of preexisting faults which are still zones of weakness, or by concentration of stress around pockets of ductile rocks distributed along these faults. Results from detailed geological and aftershock investigation in the Goodnow epicentral region of the Adirondacks suggest that the latter hypothesis applies in that region. We are now testing this hypothesis in the Manhattan Prong.

Reports

1986 L. Seeber, Seismicity of the New York City area, The Geology of Southern New York, p. 13-14, Hofstra University Symposium, April 1986.

1986 J. G. Armbruster, L. Seeber, and K. Locke, Historical and Modern Seismicity around the Newark Basin, Northern New Jersey and Southern New York (Abstract), Eastern SSA, Ottawa, Oct. 1986.

1987 Armbruster, J. G., and L. Seeber, The April 23, 1984 Martic Earthquake and the Lancaster Seismic Zone in Eastern Pennsylvania, Bull. Seismol. Soc. Amer., in press.

1987 Seeber, L., and J. G. Armbruster, Seismicity along the Atlantic Seaboard of the U.S. intraplate neotectonics and earthquake hazard, DNAG Volume on the Atlantic Margin, in press.

SOUTHERN WESTCHESTER CO. SEQUENCE, 1985

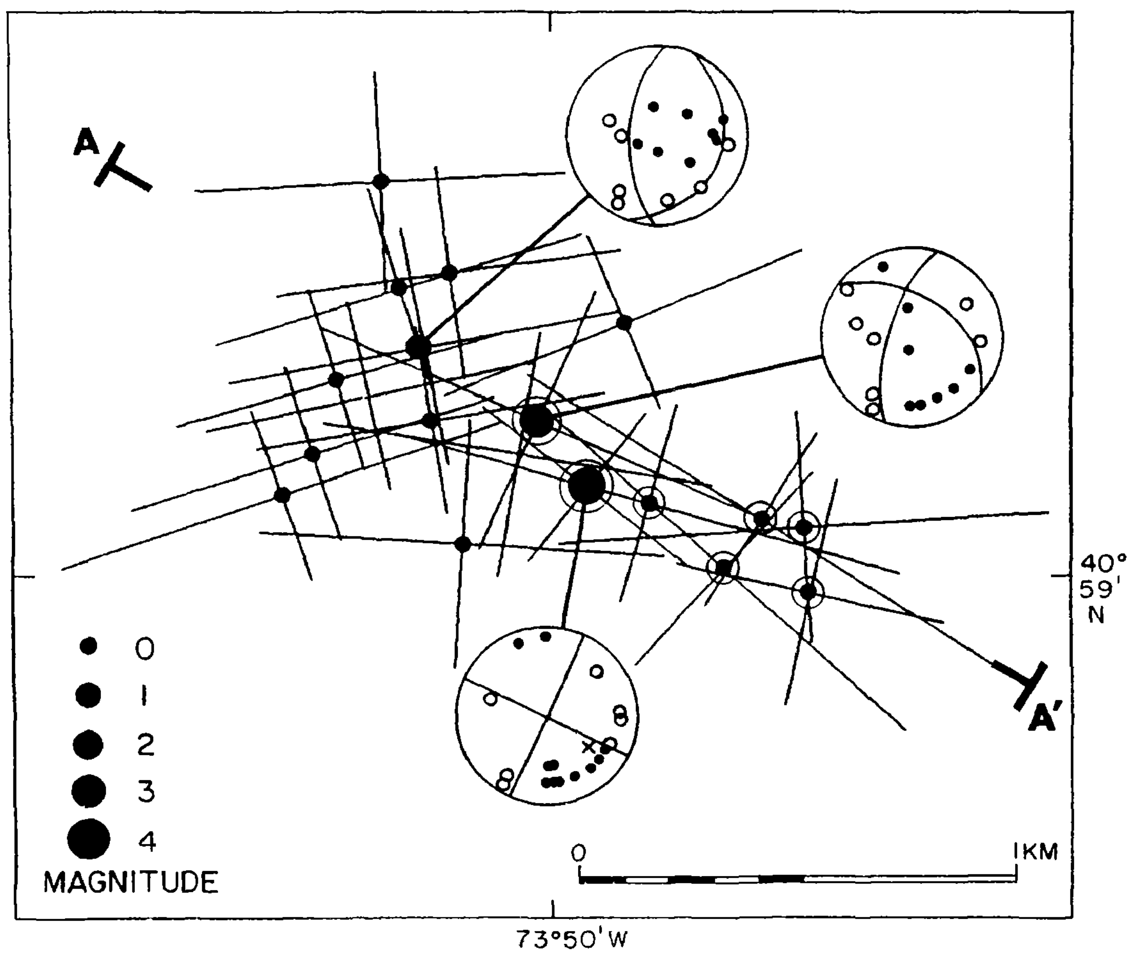

Fig. 1 . Detailed epicenter map of the Ardsley earthquake sequence and focal mechanisms for the mainshock and the two largest aftershocks. Hypoellipse errorbars are indicated for each epicenter.

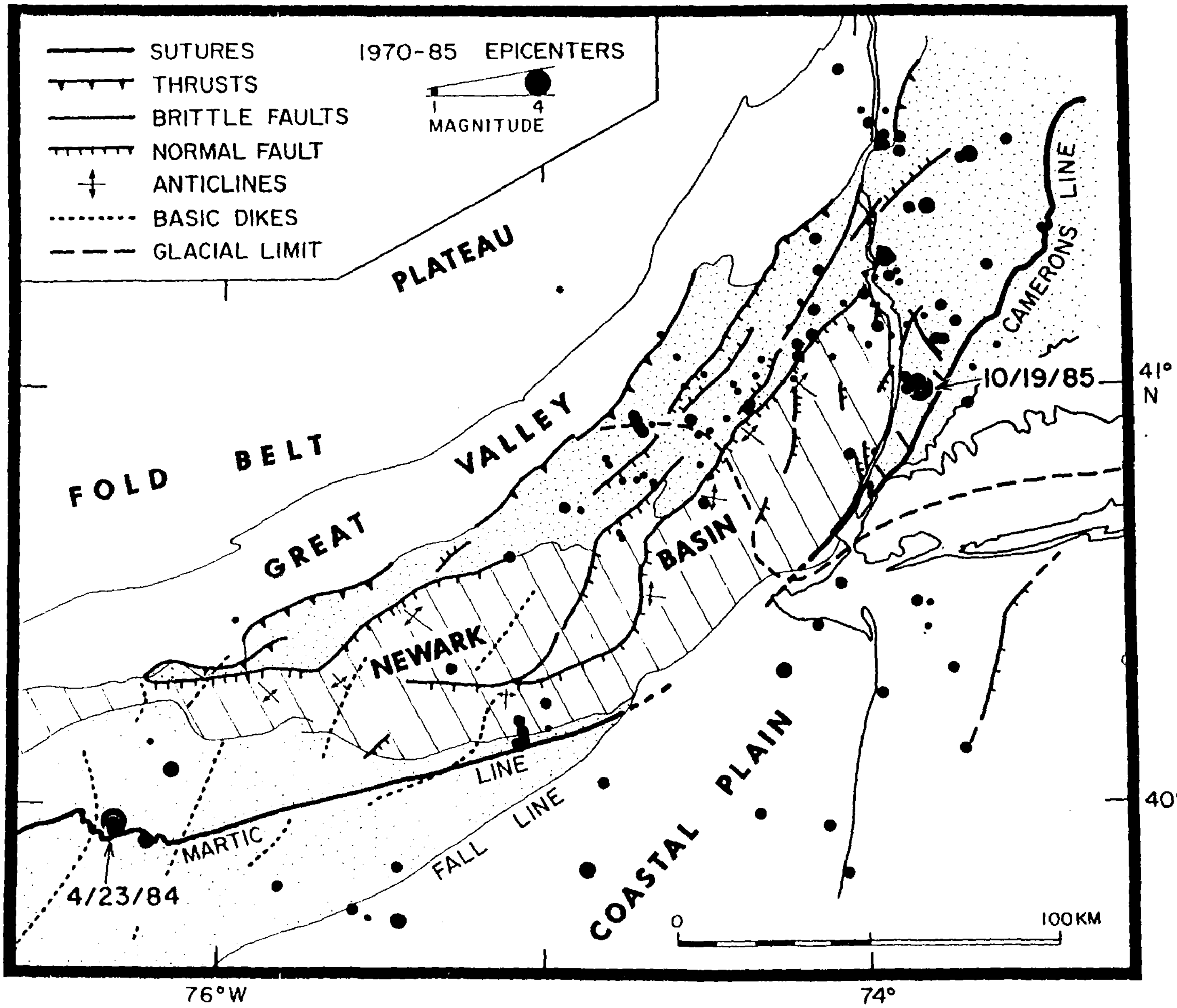

Figure 2. Seismicity detected by the regional network and the Newark Triassic- Jurassic Basin. Location uncertainties for most of the epicenters are smaller than the size of the symbols. Seismicity is concentrated in crystalline rocks adjacent to the Basin, but is absent within and below the Basin. This relatively short sample contains mostly small earthquakes which are concentrated along and northwest of the Ramapo Border fault. However, the two largest (M=4) earthquakes in the period covered by these data (1970-1985), the 4/23/84 earthquake in Lancaster Co. southwest of the Newark Basin and the 10/19/85 earthquake in Westchester Co., are located south and east of the Basin. Both these events occurred near the Lower Paleozoic suture (Cameron's -- Martic Line), on the belt of seismicity, that is prominent in the revised historic catalog (Figure 3.). These events ruptured faults transverse to this suture and to the trend of the Basin.

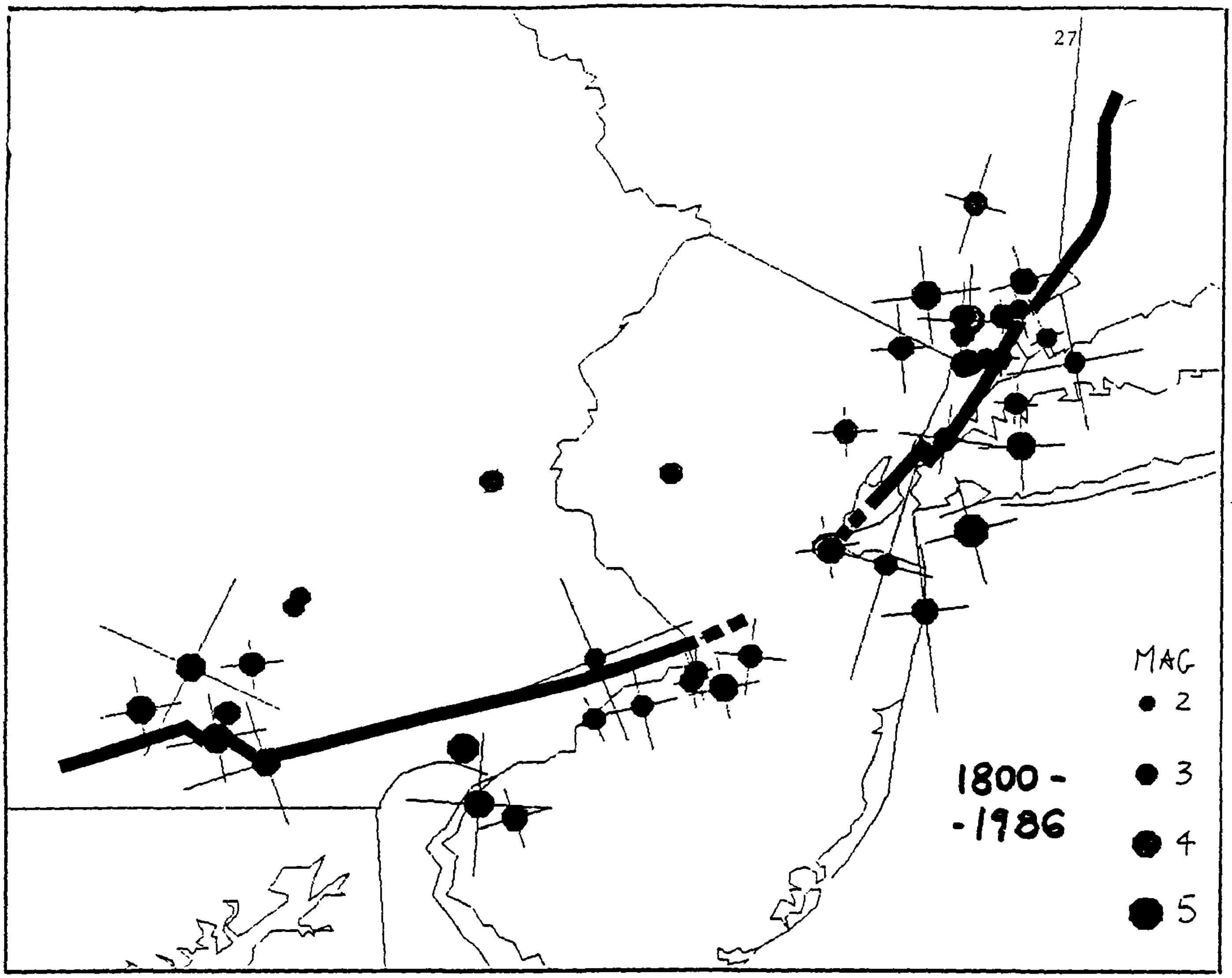

Figure 3. Result of a reexamination of archival data and MACRO relocations of the seismicity 1800-1986, from Lancaster County, Pennsylvania to New York City. Error estimates are shown. After this reexamination of the catalog the pattern of seismicity is much simpler. Compare to Figure 1. Most of the epicenters are on a belt that appears to be associated with Martic/Cameron's line (dark line), a Paleozoic suture.

SALTON TROUGH TECTONICS AND QUATERNARY FAULTING

9910-01292

Robert V. Sharp
Branch of Engineering Seismology and Geology
U.S. Geological Survey
345 Middlefield Road, MS 977
Menlo Park, CA 94025
415-323-8111, ext. 2596 or (415) 329-5652

Investigations

1. Lake Cahuilla calibration of scarp degradation dating method of Andrews and Bucknam.

2. Field check of Imperial fault for surface movement triggered by the M_L 5.4 earthquake of 6 February 1987 near Cerro Prieto, Mexico.

3. Paleomagnetic sampling of the Imperial and Coyote Creek faults for evidence of non-brittle deformation of young sediments near the fault traces (with R. Weldon).

4. Preliminary trenching of San Andreas-related young faulting near Bombay Beach (with M. Rymer).

5. San Jacinto fault zone structural mapping of Pleistocene sediments between Borrego Valley and Salton Sea.

6. Resumption of measurement of near-field vertical surface deformation at Harris Road on the Imperial fault.

7. Geometry of stepover dome between *en echelon* eastern breaks of the Imperial fault at the U.S.-Mexico boundary.

Results

1. For application of the Andrews-Bucknam dating method to scarps in the Salton trough, a local calibration to augment calibrations already provided by Lake Lahontan and Lake Bonneville shorelines is needed. An extensive field reconnaissance of the latest Lake Cahuilla shoreline was made to identify sites where degradation of the approximately 300-year old feature could be measured in unconsolidated alluvial deposits. The search yielded negative results in the sense that no sites appeared to have had the initial geometry employed in their degradation model, *i.e.*, a planar surface extending upslope to the base of the shoreline embankment. Until a local calibration is obtained, dating scarps in the Salton Trough by this method appears to be inappropriate.

2. No obvious surface features reflecting triggered creep were observed along the fault trace on the U.S. side of the border 1.5 days after this event--the strongest in this region since the 1981 Westmorland earthquake. Another check for delayed creep made on March 17 yielded a similar result. The cumulative slip on the fault since the 1979 Imperial Valley earthquake may now have reached asymptotic levels and further movement in surficial materials appears to be inhibited even during strong shaking. The maximum cumulative right-lateral slip since 15 October 1979 is now about 1.0 meter at a site where 1979 coseismic slip was on the order of 0.4 meter at the ground surface (at McCabe Road about 9 km north of the border).

3. Late Holocene sediment samples were collected at sites adjacent to and at distance from the two traces of the Imperial fault at the U.S.-Mexico border and at the Coyote Creek fault a few kilometers southwest of Ocotillo Badlands. The samples are now being prepared for measurement of paleomagnetic orientation.

4. Young fault traces discovered and previously trenched near Bombay Beach southeast of the known surface expression of the San Andreas fault (Sharp, 1979) have been investigated with new reconnaissance trenches at sites where surface expression is absent. The faults were found in the shallow subsurface, and stratigraphic contrasts revealed on opposite sides of the fault indicate strike slip movement. A detailed trenching study to establish the movement history and to determine the extent and relation of these breaks to the San Andreas fault will proceed.

5. 1:24,000-scale structural mapping of the late Pleistocene and Holocene folding and faulting in the complex deformational zone east and southeast of the Clark and Coyote Creek faults is nearly complete.

6. The Harris Road leveling line was destroyed by repaving in the spring of 1986, ending an unbroken 10-year record of vertical deformation across the Imperial fault trace. A new line was constructed in October and the first remeasurement in March 1987 indicated no obvious shallow or surface fault movement. This measurement confirmed the absence of triggered faulting for the 6 February earthquake in Mexico mentioned above for this site.

7. Stratigraphic and structural details of a fragmented stepover dome have been determined by additional trenching for this fault strand. This information agrees with the history established for the southwestern trace: strata above an erosional surface have been offset once, during the 1940 earthquake, and strata beneath it have recorded the horizontal movements of many events. The cumulative offset for both strands below this surface probably exceeds 30 meters.

Detailed Geologic Studies, Central San Andreas Fault Zone

9910-01294

John D. Sims
Branch of Engineering Seismology and Geology
U.S. Geological Survey
345 Middlefield Road, MS 977
Menlo Park, California 94025
(415) 323-8111, ext. 2252 or (415) 329-5653

Investigations

1. Continued investigations of Holocene movement along the San Andreas and Hayward-Calaveras-Paicines faults (Perkins, Sims, Barclay).

2. Investigation of the long-term (10-5 Ma) slip history of the San Andreas fault in central Caliofrnia (Perkins).

3. Calibrate fault scarp morphology dating technique to alluvial deposits for use in slip-rate studies along strike-slip faults.

4. Detailed mapping of fault and alluvial deposits along a 70-kn-long reach of the San Benito River in the Hollister region.

Results

1. The initial study of Holocene slip along the San Andreas fault at Melendy Ranch (San Juan Bautista area) is complete, and the final written report has Director's Approval. Fieldwork commenced on the second phase of the Melendy Ranch study, which proposes to determine two additional Holocene slip rates for the San Andreas fault. The second phase of study will concentrate on age determination of the Qa_2 and Qa_3 alluvial deposits at Melendy Ranch. These age data will be used to date displaced Qa_2 and Qa_3 riser. The Melendy Ranch studies have the potential to produce three independent Holocene slip rates for the San Andreas fault in central California.

   Continuing studies along the Calaveras and Paicines faults in the Hollister region concentrate on two study sites; the Windfield Ranch along the Calaveras fault and the Roberts Ranch along the Paicines fault. Trenching and geomorhic studies at Windfield Ranch have resulted in a nearly 14-ka-long average slip rate of 9.1 mm/yr for the Calaveras fault. Preliminary results of trenching and geomorphic study at Roberts Ranch suggest a slip rate of 20-30 mm/yr for the Paicines fault.

   Additional work along the Calaveras fault north of Hollister, and along the Hayward fault, concentrated on aerial photographic reconnaissance for study sites likely to produce Holocene slip rates along these fault segments. The reconnaissance was conducted using pre-1975 photographs. Field investigations of the three most likely revealed that these sites have been destroyed by urban development or access is denied.

2. Investigations of the Etchegoin Formation in regard to tectonism and slip along the San Andreas fault is nearly complete. A 7.5 Ma average slip rate of about 28 mm/yr for the San Andreas fault in central California has been determined on the basis of a displaced hornblende-quartz gabbro source terrace and age constraints emplaced by tephrachronoplogy. The Open-File Report that contains the data and conclusions is complete. The subsequent final written report went through review during this reporting period.

3. Fault scarp morphologic dating technqiues have proven successful in slip-rate studies of active dip-slip faults. This age-dating technique is not readily amenable to studies of strike-slip faults, because vertical displacement is usually a minor component in strike-slip faulting events. The lack of radiometric age data for displaced alluvial deposits along the Paicines fault prompted an investigation on calibrating this technique to alluvial formed scarps.

   During this reporting period, we have obtained additional scarp profiles from alluvial deposits of knwon age along the San Benito River. The resulting diffusivities have thus far varied by a factor of two. Applying these diffusivities to displaced alluvial deposits along the Paicines fault produces imprecise slip-rate estimates, the most reasonable of which range from 20-30 mm/yr.

4. Detailed mapping of faults and alluvial deposits along a 70-km-long reach of the San Benito River was the basis for our fault investigation in the Hollister region. Approximate 95 percent of the fieldwork and 50 persent of the final drafting is complete.

Reports

Perkins, J.A., Sims, J.D., and Sturgess, S.S., Director's Approval, Late Holocene movement along the San Andreas fault at Melendy Ranch: Implication for the distribution of fault movement in central California: *Journal of Geophysical Research*.

Perkins, J.A., Branch Chief's Approval, Provenance of the upper Miocene and Pliocene Etchegoin Formation: Implications for paleogeography of the late Miocene of Central California: *U.S. Geological Survey Open-File Report 87-____.*

Seismotectonic Framework and Earthquake Source Characterization (Continued)--Wasatch Front, Utah, and Adjacent Intermountain Seismic Belt

14-08-0001-G1349

R.B. Smith, W.J. Arabasz, and J.C. Pechmann*
Department of Geology and Geophysics
University of Utah
Salt Lake City, Utah 84112
(801)581-6274

Investigations

1. Statistical analysis of the University of Utah earthquake catalog.

2. Moment-magnitude relations for the Intermountain seismic belt.

3. Synthetic Wood-Anderson seismograms from digital network data.

Results

1. A collaborative project underway with Daniele Veneziano, Professor of Civil Engineering at M.I.T., involves: (1) initiation of multi-step "conditioning" (that is, accounting for homogeneity of size estimates, event independence, and completeness) and processing of the University of Utah's catalog of more than 11,000 earthquakes for the Utah region and Intermountain seismic belt (ISB); and (2) preliminary processing of the post-1962 seismicity catalog for the Utah region with the cluster-analysis code of Veneziano and Van Dyck (1985, Electric Power Res. Inst. Project P101-29). The purpose of (2) is to segregate independent and dependent events and to investigate space-time-size behavior, especially in the vicinity of the Wasatch fault. The procedure differs in two main respects from other existing methods: (1) it automatically identifies the region in space and time occupied by each cluster, and (2) it uses rigorous statistical methods to flag groups of earthquakes that constitute significant clusters. The analysis is "local" in time and space, so that real clustering is confounded neither with spatial nonhomogeneity of seismicity nor with temporal variations in the rate of events due to incomplete reporting or long-term nonstationarity.

Figure 1 shows preliminary results of the application of this clustering method to the University of Utah catalog by D. Veneziano and Y. Shimizu of M.I.T. for the period 1962-1985. Of the 3003 events $\geq$ M2.0, 2053 were classified as secondary and 950 as main events. As a group, the

*Graduate students K. Quigley and J. Shemeta also contributed significantly to this project during the report period.

secondary events were found to have a substantially higher b-value than the main events.

The space-time distribution of the mainshocks and dependent events as a function of latitude shows that independent mainshocks (Figure 1b) define a horizontal band of less intense seismicity between roughly 39.5°N and 41.5°N—encompassing the most active segments of the Wasatch fault. Remarkably, dependent events for that same space-time compartment (Figure 1d) are even more notably sparse. The behavior of dependent events clearly provides a new perspective—and raises the critical question of whether or not this apparently suppressed aftershock behavior in the vicinity of the Wasatch fault could represent a contemporary anomaly.

2. The validity of existing moment-magnitude relations for the ISB remains open to question and has been the focus of ongoing study. The most commonly used moment-magnitude relation for applications in the ISB is the relation $\log M_o = 1.1 M_L + 18.4$ developed by Doser and Smith (1982, BSSA, v. 72, p. 525-551) for 15 earthquakes in the Utah region, ranging in magnitude from M_L 3.7 to M_L 6.0. Using P-wave spectra from indirectly calibrated stations of the University of Utah network, Peinado and Arabasz (1985, EOS, v. 66, p. 954) determined values of M_o for a set of 16 earthquakes in the ISB in the magnitude range 2.5 to 5.0. The resulting M_o-M_L relation of $\log M_o = 1.0 M_L + 17.7$ is similar in slope to that of Doser and Smith (1982) but has a clearly different intercept.

The earthquakes analyzed by Doser and Smith (1982) all pre-date digital recording by the University of Utah seismic network, so direct comparison of measurements of M_o is impossible. The following test, however, was made. Using the technique of Bolt and Herraiz (1983, BSSA, v. 73, p. 735-748), amplitude and duration measurements were made on Wood-Anderson seismograms (4 different stations) for earthquakes including those for which Doser and Smith (1982), Peinado and Arabasz (1985), and also Dziewonski and others (1984, Phys. Earth Planet. Int., v.34, p. 129-136), had determined values of M_o. A quantity "psi" was determined for each Wood-Anderson recording which is a product of an amplitude measurement, a duration measurement, and epicentral distance. This quantity has been shown by Bolt and Herraiz (1983) to provide an empirical estimate of M_o. Results show that there are clear systematic deviations from the curve calibrated for California, which is intermediate in prediction of M_o between the data of Peinado and Arabasz (1985) and Doser and Smith (1982). Moment estimates of Dziewonski et al. (1984) appear to relate more closely to the data of Doser and Smith (1982). Thus, there remains an evident need for more detailed study of M_o-M_L relations in the ISB.

3. We have developed and tested a simple procedure for creation of synthetic digital Wood-Anderson seismograms using data from horizontal component Geotech S-13 seismometers, which we are installing at seven high-quality recording sites in Utah. Data from these stations will provide greatly improved local magnitude (M_L) determinations for Utah earthquakes, after appropriate calibration of station corrections and distance corrections. The free period (T_o) and damping constant (h) of the S-13 seismometers are set to match those of a standard Wood-Anderson seismometer: $T_o = 0.8$ sec and $h = 0.8$. Because the S-13 is a velocity transducer while the Wood-Anderson seismograph essentially records

displacement, the frequency response of the S-13 is approximately equal to that of the Wood-Anderson instrument multiplied by iw, where w is angular frequency. This applies to the complete recording system as well up to about 12.5 Hz, where the amplifier gain begins to decrease. Thus, to create a synthetic Wood-Anderson seismogram from an S-13 record, it is necessary only to perform a numerical integration in the time domain or, equivalently, divide by iw in the frequency domain. The latter is easily accomplished by filtering with a lowpass, first-order, recursive Butterworth filter with a corner frequency well below the frequency range of interest, for example 0.2 or 0.02 Hz. We have tested these two techniques using digital records from S-13 seismometers located next to the photographically-recording Wood-Anderson seismograph in the vault at Dugway, Utah. Comparison between synthetic and real Wood-Anderson records demonstrates that these techniques work quite well.

Although this synthetic Wood-Anderson scheme can easily be implemented digitally, we are currently planning to implement it in the hardware of the recording system by adding analog filters between the discriminators and the A/D converter on our PDP-11/34. The advantages of this plan are: (1) it will simplify the routine determination of M_L from the S-13 data, (2) the filters will remove much of the high-frequency noise introduced by the telemetry system, and (3) the filters will prevent aliasing of the recorded signals, even for small, nearby earthquakes.

Reports and Publications

Arabasz, W.J., and E.D. Brown (1987). Observational seismology and the evaluation of earthquake hazards and risk in the Wasatch front area, Utah, submitted to U.S. Geol. Surv. Prof. Pap. on "Assessment of Regional Earthquake Hazards and Risk Along the Wasatch Front, Utah."

Benz, H.M., and R.B. Smith (1986). Kinematic source modeling of normal faulting earthquakes in inhomogeneous velocity structures, EOS, Trans. Am. Geophys. Union, 67, 1112.

Bjarnason, I.T. (1987). Contemporary tectonics of the Wasatch front region, Utah, from earthquake focal mechanisms, M.S. thesis, University of Utah, Salt Lake City, Utah, 79 pp.

Bjarnason, I.T., and J.C. Pechmann (1986). Contemporary tectonics of the Wasatch front region, Utah, from earthquake focal mechanisms, EOS, Trans. Am. Geophys. Union, 67, 1107.

Brown, E.D., W.J. Arabasz, I. Bjarnason, and K. Quigley (1986). The March 1986 M_L 4.4 Japanese Valley, Utah, earthquake sequence: A type-case study for central Utah, EOS, Trans. Am. Geophys. Union, 67, 1107.

Eddington, P.K., R.B. Smith, and C. Renggli (1987). Kinematics of Basin-Range intraplate extension, in Continental Extensional Tectonics, M.P. Coward, J.F. Dewey, and P.L. Hancock, Editors, Geological Society Special Publication, 371-392.

Pechmann, J.C., and L.L. Leu (1986). Focal mechanisms for aftershocks of the 1983 Borah Peak, Idaho, earthquake: Complex faulting within a simple aftershock zone, EOS, Trans. Am. Geophys. Union, 67, 1107.

Smith, R.B., and W.J. Arabasz (1987). Seismicity of the Intermountain seismic belt, EOS, Trans. Am. Geophys. Union, 68, 101.

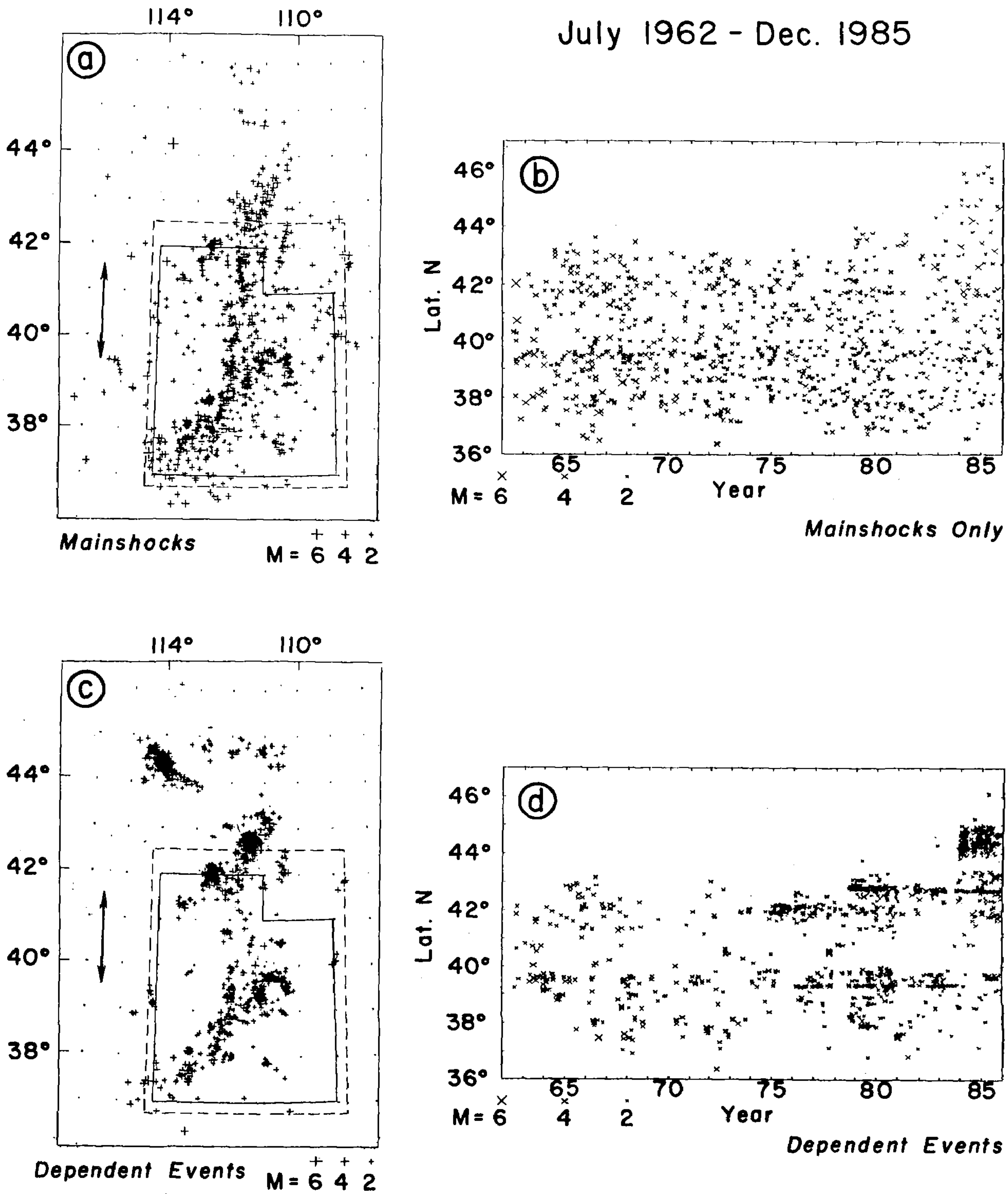

Figure 1. Results from D. Veneziano and Y. Shimizu (M.I.T.) of preliminary cluster analysis of the University of Utah's earthquake catalog for 1962-1985. The catalog is complete only within the area of the dashed rectangle. Arrows indicate a band of latitude along the main seismic belt, encompassing most of the Wasatch fault, in which the rate of occurrence of dependent events and, to a lesser extent, independent mainshocks, appears to be suppressed (see text).

Great Earthquakes and Great Asperities, Southern California: A Program of Data Analysis

USGS 14-08-0001-G-1096

Lynn R. Sykes and Leonardo Seeber
Lamont-Doherty Geological Observatory of Columbia University
Palisades, New York 10964
(914) 359-2900

Investigations

During the period of this grant the principal investigators and their colleagues have carried out a number of major studies of earthquakes and tectonics of southern California. This work has resulted in three papers being published, one in press that will soon be published, one in preprint form that is nearly ready for journal submission and the final study "Fault mechanisms associated with the southern San Andreas fault: Seismicity of the eastern Transverse Ranges" by Williams, Sykes, Nicholson and Seeber is also in preprint form.

Results

The paper "Great earthquakes and great asperities, San Andreas fault, southern California" by Sykes and Seeber was published in *Geology* in December 1985. They find that the big bend region of the southern San Andreas fault consists of two great asperities that rupture infrequently in great earthquakes. The eastern knot near San Gorgonio Pass, which has not ruptured historically in a great event, is the main locus of plate motion, appears to break in great events every few hundred years and is more advanced in the cycle of strain accumulation than the western knot. The large size of these asperities results in the properties of these earthquakes being nearly invariant over many cycles of great shocks. An unusual sequence of moderate-size shocks within the eastern knot from 1940 to 1948 is an example of the type of precursory phenomena that might precede a great earthquake.

The paper "Seismicity and fault kinematics through the eastern Transverse Ranges, California : block rotation, strike-slip faulting and shallow-angle thrusts" by Nicholson, Seeber, Williams and Sykes, was published in the *Journal of Geophysical Research* in April 1986. This paper uses data from the southern California seismic network to study focal mechanisms and detailed distribution of earthquakes in the major tectonic knot in southern California near San Gorgonio Pass. Surprisingly, little seismic activity can be directly associated with major throughgoing faults. Seismicity is generally absent in the upper 5 km. This pattern of behavior appears to be typical of the inter-seismic period between great earthquakes. Great earthquakes in this area, which appear to have a repeat time of 300 to 500 years, are thought to mainly rupture the throughgoing faults. The predominant style of faulting above 10 to 12 km is oblique slip with a large reverse (thrust) component. The spatial distribution of relocated hypocenters and first-motion data suggest the presence of left-slip faults striking northeast. The pattern of faults in conjunction with an unusual set of normal and reverse focal mechanisms is interpreted as the clockwise rotation of the small set of crustal blocks subjected to regional right-lateral shear. At depths of greater than about 10 km seismicity defines a wedge-shaped volume undergoing pervasive internal deformation and a combination of strike-slip and low-angle thrust faults. A low-velocity seismic zone beneath the San Bernardino Mountains and the transition between block rotation and the deeper style of deformation may correspond to a major detachment under much of the region and would imply that the overthrust San Bernardino Mountains are allochthonous. The present pattern of seismic deformation may change systematically as a region prepares to accommodate large right-lateral displacements in an eventual future great earthquake.

The paper "Seismic evidence for conjugate slip and block rotation within the San Andreas fault system, southern California" by Nicholson, Seeber, Williams and Sykes was published in *Tectonics* in August 1986. This paper expands a number of the ideas developed in the previous paper for the region near San Gorgonio Pass to other areas of southern California. Again, the pattern of seismicity for small to moderate size earthquakes of the past ten years indicates that much of that activity is presently occurring on secondary structures, several of which are oriented nearly orthogonal to the strikes of major throughgoing faults. Slip along these secondary transverse features is predominantly left-lateral and is consistent with the reactivation of conjugate faults by the current regional stress field. A number of small to moderate size crustal blocks are defined which are undergoing contemporary rotation in response to the regional stress field. A rotational block model accounts for a number of structural styles characteristic of strike-slip deformation in California including; variable slip rates and alternating transtensional and transpressional features observed along strike of major wrench faults; domains of evenly-spaced antithetic faults that terminate against major fault boundaries; continued development of bends and faults with large lateral displacements; anomalous focal mechanisms; and differential uplift in areas otherwise expected to experience extension and subsidence. Low-angle structures like detachments may be involved in the contemporary tectonics of southern California. Changes in the translation of small crustal blocks and their relative rotation parts could represent important premonitory changes prior to large to great earthquakes along major throughgoing faults.

The paper "Block rotation along the San Andres fault system in California: long-term structural signature and short-term effects in the earthquake cycle" by Seeber and Nicholson, which is in preprint form, describes the rotation of small crustal blocks located between closely spaced subparallel strike-slip faults. Block rotation can allow one of these strands to grow at the expense of the other. Not only structural and paleomagnetic data, but also recent small earthquakes provide evidence for block rotation of this type. Associated seismicity often occurs on left-lateral secondary faults that strike northeast and are symptomatic of block rotation. Examples of this phenomena are illustrated for Coyote ridge, which is located between branches of the San Jacinto fault zone of southern California and the complex rupture involved in the Coyote Lake earthquake of 1979 along the Calaveras fault of northern California.

Bogen and Seeber (preprint) in their paper "Late Quaternary block rotation within the San Jacinto fault zone, southern California" report abundant structural and seismological evidence for block rotation during the past 0.94 million years or less in the region between two major branches of the San Jacinto fault zone between Anza and Borrego in southern California.

Williams, Sykes, Nicholson and Seeber (in preparation) examined fault mechanisms and seismicity in the vicinity of the southernmost San Andreas fault and the eastern Transverse Ranges of southern California. Data from the southern California seismic network for the period 1977 to 1985 were used to study precise locations of small earthquakes, focal mechanisms and the state of stress. The southernmost San Andreas fault in the Coachella Valley is essentially quiescent at the microearthquake level. Relocation of earthquakes using only stations northeast of the San Andreas fault, proximal to the activity but outside the Salton trough does not seriously effect epicentral locations, suggesting the observed offset of epicenters from the San Andreas fault is not an artifact of the velocity models used. Many of the earthquakes in the broad region to the northeast of the San Andreas fault occur along steeply dipping, left-lateral faults striking northeasterly. Focal mechanisms involve strike-slip, normal fault or a combination of the two mechanisms. In contrast, reverse and strike-slip faulting characterize San Gorgonio Pass and the region to the west within the big bend region of southern California. These observations imply that relatively high normal stresses of tectonic origin are present across the San Andreas fault in San

Gorgonio Pass, while lower normal stresses are found across the southernmost San Andreas fault from Palm Springs to the Salton Sea. One stress regime appears to be associated with long repeat times for great earthquakes within the two major tectonic knots in southern California whereas shorter repeat times are indicated for the other stress regimes near the southernmost San Andreas fault.

The paper "Secondary faults associated with the 7 July 1986 Palm Springs earthquake rupture on the San Andreas fault" (in preparation) by Seeber, Armbruster, and Tuttle discusses a well defined aftershock zone that delineates the 10 km long NW rupture of the 1986 Palm Springs earthquake. Fault plane solutions in the main zone of aftershocks show consistently oblique right-lateral and reverse slip on a NW plane dipping northeasterly, and reflect the geometry of slip in the main shock. The sharp boundaries of the aftershock zone appear to coincide with the intersection between the main strand and secondary faults. Several secondary reverse and left-lateral faults were recognized primarily from seismicity during the aftershock sequence. They observed that the lower limit of the Palm Springs earthquake, about 13 km deep, coincides with the upper limit of a widespread zone of midcrustal seismicity in the San Gorgonio Pass area and is bounded by the Palm Spring earthquake, locally, and the Mission Creek fault, regionally. This zone may be associated with a detachment as observed on fault plane solutions.

Pacheco and Nabelek (preprint) studied the source processes of three moderate California earthquakes which occurred in July 1986. They determined that the July 8, 1986 M_L=5.9 Palm Springs earthquake had a simple rupture with most of the seismic moment released in the first three seconds by a single pulse. The faulting mechanism is right-lateral strike-slip with a sizable reverse component consistent with uplift of the Banning fault. The M_L=5.3 earthquake offshore of Oceanside on July 13, 1986 consists of 2 pulses that released most of the moment in the first 3 sec. The source mechanism indicates reverse faulting and is consistent with the missing component of plate convergence not taken up by the onshore strike-slip systems. The source function of the M_L=6.2 Chalfant Valley earthquake which occurred on July 21, 1968 indicates that in a 4 sec time window three asperities were broken. The average parameters for this rupture indicate right-lateral strike-slip motion, with a sizable normal component.

Continuing Studies

Continuing work on earthquakes and tectonics of southern California includes the following studies: examination of regional time-space patterns of seismicity for the period 1932 to 1986 (Seeber, Armbruster, Williams and Sykes); analysis of teleseismic source mechanisms of July 1986 earthquake (M_L>5) (Pacheco and Nabelek); documentation of triggered slip on the southern San Andreas after the July 8, 1986 North Palm Springs earthquake (Williams, Fagerson, and Sieh); and secondary faults and the 1986 North Palm Springs rupture on the main strand of the San Andreas (Seeber and Armbruster).

Publications

Bogen, N., and L. Seeber, Late Quaternary block rotation within the San Jacinto fault zone, southern California, submitted for publication, 1987.

Nicholson, C., L. Seeber, P. Williams, and L. R. Sykes, Seismicity and fault kinematics through the eastern Transverse Ranges, California: Block rotation, strike-slip faulting and shallow-angle thrusts, *J. Geophys. Res., 91*, 4891-4908, 1986.

Nicholson, C., L. Seeber, P. L. Williams, and L. R. Sykes, Seismic deformation along the southern San Andreas fault, California: Implications for conjugate slip and rotational block tectonics, *Tectonics, 5*, 629-649.

Pacheco, J., and J. Nabelek, Source mechanisms of three moderate southern California earthquakes of July 1986 (abstract), *EOS, Trans. AGU, 67*, 1091, 1986.

Seeber, L., and C. Nicholson, Block rotation along the San Andreas fault system in California: Long term structural signature and short term effects in the earthquake cycle, prerprint, 1987.

Seeber, L., J. G. Armbruster, P. Williams, and L. R. Sykes, Faults antithetic to the San Andreas delineated by seismicity in the San Gorgonio Pass of southern California (abstract), *EOS, Trans. AGU, 67*, 1200, 1986.

Seeber, L., J. G. Armbruster, M. Tuttle, Secondary faults associated with the 7 July 1986 Palm Springs earthquake rupture on the San Andreas fault (abstract), *Seismol. Soc. Am. Abstracts with Programs*, pp. 20, 1987.

Seeber, L., and J. Armbruster, Secondary faults as agents for segmentation of the master strands in southern California (abstract), *IUGG Conference* , Vancouver, Canada, Aug. 17-22, 1987.

Sykes, L. R., and L. Seeber, Great earthquakes and great asperities, San Andreas fault, southern California, *Geology, 113*, 835-838, 1985.

Williams, P., S. Fagerson, and K. Sieh, Triggered slip of the San Andreas fault after the July 8, 1986 North Palm Springs earthquake (abstract), *EOS, Trans. AGU, 67*, 1090, 1986.

Williams, P. L., L. R. Sykes, C. Nicholson, and L. Seeber, Seismicity and state of stress in the eastern Transverse Ranges: Implications of seismic potential of the southern San Andreas fault, California, in preparation.

Source and Path Effects for Northeastern U. S. Earthquakes—Implications for Earthquake Hazards

14–08–0001–G1092

M. Nafi Toksöz and Anton M. Dainty
Earth Resources Laboratory
Dept. of Earth, Atmospheric and Planetary Sciences
Massachusetts Institute of Technology
Cambridge, MA 02139
(617) 253–7857

Investigations:

1). Separation of the effect of anelastic attenuation and scattering on the attenuation with distance of pseudo velocity in the northeastern United States.

2). Total attenuation of the phase Rg as a function of frequency in the northeastern United states.

Results:

1). The mechanisms contributing to the attenuation of earthquake ground motion in the distance range 10–200 km have been studied with the aid of laboratory data, coda waves and strong motion attenuation measurements in the northeast United States and Canada, together with theoretical models. The relative contributions to attenuation of anelasticity of crustal rocks (constant Q), fluid flow and scattering have been evaluated. Scattering was found to be strong with albedo $B_0 = 0.9$ and scattering extinction length (mean free path) about 17 km. The intrinsic attenuation in the crust can be explained by a high constant Q ($500 \leq Q_0 \leq 2000$) and a frequency dependent mechanism most likely due to fluid effects in rocks and cracks. A fluid-flow attenuation model gives a frequency dependence ($Q \simeq Q_0 f^{0.5}$) similar to those determined from the analysis of coda waves of regional seismograms.

2). We have begun measuring Q for Rg as a function of frequency by the two station method. The data set consists of USGS refraction data from explosions set off in Maine in 1986. Preliminary results show Q *decreasing* from 60 to 20 as frequency increases from 1 to 4 Hz. This is in the opposite sense compared to most other studies. The Q at 1 Hz is consistent with the results for scattering mean free path cited in (1) above, i.e., it is a total Q.

Paper:

Toksöz, M. N., R. S. Wu and D. P. Schmitt (1986). Physical mechanisms contributing to seismic attenuation in the crust. *Submitted to* Proc. NATO ASI "Strong Ground Motion Seismology", Ankara, Turkey.

Tectonic Analysis of Active Faults

9900-01270

Robert E. Wallace

Office of Earthquakes, Volcanoes, and Engineering
345 Middlefield Road, MS 977
Menlo Park, California 94025
(415) 323-811, ext. 2751

Investigations

1. Tectonics of the San Andreas fault system.

2. Tectonics of the central Nevada and eastern California seismic belts.

3. International Geological Correlation Program (IGCP)--Project 206--Active Faults of the World.

Results

1. Organized a group of authors to prepare a U.S.G.S. professional paper on the San Andreas fault. Chapters are being written; some first drafts are completed.

2. As member of panel on Seismic Hazard Assessment for NRC/NAS, participated in several writing sessions and have in progress a chapter on "how probabilistic seismic hazard assessment techniques capture earth-science information."

3. Have in progress a joint paper comparing the San Andreas, Tan Lu, Alpine, and North Anatolia faults and the Median Tectonic Line under IGCP project 206.

Reports

1. Wallace, Robert E., and Morris, Hal T., 1986, Characteristics of Faults and Shear Zones in Deep Mines: PAGEOPH, v. 124, nos. 1/2, P. 107-125.

2. Wallace, Robert E., 1987, Variations in Slip Rates, Grouping, and Migration of Slip Events on Faults in the Great Basin Province: Seismological Society of America Bulletin, v. 77.3, no. __, P. ___.

Development of a Prediction Model for a Possible 1994± 1.5 Kaoiki (Hawaii) Mainshock

USGS 14-08-0001-G1325

Max Wyss
University of Colorado, CIRES
Boulder, CO 80309
(303-492-5642)

Objective: In the Kaoiki fault zone main-shocks ranging in magnitude from 5.5 to 6.6 seem to occur at regular intervals of 10.4 years. The last one happened in November 1983. The current part of the project aimed at improving the knowledge about historic earthquakes in the Kaoiki source area, and to arrive at source parameters for these mainshocks.

Task 1: Macroseismic location of historic Kaoiki earthquakes are being derived from a compilation of felt reports. This investigation is done jointly with R. Koyanagi of HVO. Preliminary isoseismal maps have been drawn for earthquakes which occurred in Southeastern Hawaii between 1868 and 1986. The intention is to use the macroseismic data of recent shocks to approximately calibrate the location and size of the older events by comparison of the isoseismal maps.

The availability of data is surprisingly good. The local newspaper(s) often provide considerable detail on damage and felt reports. We have completed a thorough search of newspaper accounts for all Hawaiian earthquakes listed in US-Earthquakes. Combining this information with the felt reports filed at HVO the isoseismal maps for many events allow a reasonable estimate of seize and location.

In addition we came across a new and extensive source of information on 19th and early 20th century seismic activity in Hawaii. The Lyman Memorial Museum is holding an earthquake diary kept over decades by Mrs. Lyman and continued by her daughter in law. Collaborating with the museum we have typed this earthquake list in camera ready form, and we are in the stage of proofreading it.

We have also searched the Volcano Letter for additional earthquakes with intensity V not mentioned in US-Earthquakes. It appears that the endproduct of the above mentioned efforts will be a new catalog of historic Hawaiian earthquakes, with macroseismic maps for the bigger events.

Task 3: Relative size of all mainshocks. Up to now we have concentrated on the most recent 1983 event. This earthquake may have had a fairly complex source mechanism. By analyzing the polarization of individual pulses on the strong motion records we are identifying individual P- and S-phases. From these we will then calculate the origin of multiple rupture events and try to estimate their individual fault plane solution. This task is difficult, and only in its beginning stage.

Task 4: Seismicity patterns can only be well defined if the earthquake catalog is homogeneous. We have made an analysis of the reporting quality and consistency in the Kaoiki area. Using the magnitude signature technique we confirm changes of reporting which were already known, but we also find some unexpected changes. These will be discussed with HVO staff before we interpret them.

Geologic Studies for Seismic Zonation of the Puget Lowland

9540-04004

Brian F. Atwater
U. S. Geological Survey at Department of Geological Sciences
University of Washington AJ-20
Seattle, Washington 98195
(206) 442-2927 FTS 399-2927

INVESTIGATIONS

Analysis of samples and other findings from last summer's paleoseismic field work along Washington's outer coast. The goal is to test the hypothesis that great earthquakes have occurred in the Cascadia subduction zone during the Holocene.

RESULTS

Plant remains from buried lowlands yield radiocarbon dates for four episodes of rapid coastal subsidence in southwestern Washington. Corrected for variations in atmospheric ^{14}C, these dates indicate that rapid subsidence occurred about 300, 1700, 2700, and 3000-3400 years ago. The dates of about 300 sidereal years (17th century A.D.) come from roots and sticks along both the Niawiakum River (Willapa Bay) and the Copalis River--sites that are 60 km apart along the strike of the Cascadia subduction zone. Synchrony between the Niawiakum and Copalis sites, if exact, would suggest some of the regionality that one should be expect of coseismic subsidence from a great subduction earthquake. The earlier episodes were dated only at the Niawiakum River. More work is needed to determine whether these episodes had great coastwise extent and, if they did, whether they represent the only four great earthquakes in southwestern Washington during the past 3000-3400 years.

As for northwestern Washington, new dates confirm an age of about 1100 years for what appears to be the most recent episode of rapid coastal subsidence along the Waatch River, near Neah Bay. The dates from the Niawiakum River indicate that this subsidence did not extend to Willapa Bay; conversely, the most recent episode of rapid coastal subsidence in southwestern Washington does not appear to be represented--unless as uplift--at Neah Bay. Such asynchrony could signify the division of the Cascadia subduction zone into patches that are capable, at least sometimes, of independent rupture.

REPORTS

Atwater, B. F., and Grant, W. C., 1986, Holocene subduction earthquakes in coastal Washington [abstract]: EOS, v. 67, p. 906.

Atwater, B. F., 1987, Evidence for great Holocene earthquakes along Washington's outer coast: Science (in press).

Nelson, A.R., Atwater, B. F., and Grant, W. C., 1987, Estuarine record of Holocene subduction earthquakes in coastal Oregon and Washington, USA: INQUA 12th International Congress, Ottawa (in press).

DATING MARINE TERRACE DEFORMATION NORTH OF THE MENDOCINO TRIPLE JUNCTION

CONTRACT no.: 14-08-0001-G1332

Glenn W. Berger, Don J. Easterbrook
Department of Geology
Western Washington University
Bellingham, WA 98225
(206) 676-3582

OBJECTIVES

This project began Feb. 15, 1987. The goal is to date suitable eolian and waterlaid sediments by thermoluminescence (TL) methods (eg. Berger, 1986), and thereby infer temporal relations between observed uplift and displacement features in the area of Humboldt County, northern California (eg. Carver et al., 1986). The applicable age range of the method is from early Holocene to middle Pleistocene. To assist in rejecting deposits that are too old for the TL method, we are also employing some paleomagnetic analyses.

PROGRESS TO DATE

In late February we collected several samples with the assistance of Drs. Burke and Carver from Humboldt State University. Principal areas sampled were the mouth of the Mad River, Table Bluff terraces, Centerville Beach terraces, and Trinidad Headland terraces.

Presently, samples are being prepared for TL analyses and for paleomagnetic measurements. Analyses for potassium, uranium and thorium have begun.

REFERENCES

Berger, G. W., 1986, Dating Quaternary deposits by luminescence--recent advances: Geoscience Canada, v. 13, p. 15-21.

Carver, G. A., Burke, R. M., and Kelsey, H. M., 1986, Deformation of late Pleistocene marine terraces along the California coast north of Cape Mendocino: Geol. Soc. Amer. Absts. with Programs, v. 18, p.

Frequency and Magnitude of Late Quaternary Faulting, Sierra Nevada, California

14-08-0001-G1334

Peter W. Birkeland and Margaret E. Berry
Department of Geological Sciences
University of Colorado
Boulder, Colorado, 80309
(303) 492-6985

Investigation

The history of late Quaternary faulting along the eastern mountain front of the Sierra Nevada is being evaluated in the area between Bishop and McGee (N) Creeks. One objective of the project is to map the glacial sequences in valleys where deposits have been offset by faulting. Materials suitable for radiometric dating of the deposits are scarce; therefore, soil development and rock weathering parameters are being used extensively to give approximate ages to the deposits. Data obtained from this work should allow the establishment of a time frame for faulting from which rates of offset along the faults can be approximated. The other objectives of the project are to study soil development on the fault scarp slopes to gain information about timing of fault events, and to excavate trenches across two of the fault scarps to try to evaluate frequency of faulting and amounts of offset associated with each displacement event at these sites.

Prior work on the project has included mapping glacial deposits in Bishop, McGee (S), Pine, and McGee (N) Creeks, describing soils and collecting rock weathering data for each deposit, profiling the fault scarps in the areas, and describing soils on the fault scarp slopes. Work during the first four months of the U.S.G.S.-funded project period includes 1) continuation of the analyses of field data and calculation of numerical indices that rank weathering by degree of development, 2) preparation of soil samples for laboratory analyses, 3) preparation and submittal of charcoal for ^{14}C dating by accelerator mass spectrometry, and 4) planning and preparation for the excavation of the two trenches which will be dug during May and June of the 1987 field season.

Results

1) The Harden Index (Harden, 1982) is being calculated for 48 soil profiles which have been described and sampled in the field thus far. Use of the index allows soils to be ranked numerically by their relative degree of development, and thus provides a method for comparing overall soil development from one site to another. These values are being used to help group deposits by age, and to help assess the length of time soils on

fault scarp slopes have been developing. Rock weathering data have been collected at 39 sites for a variety of parameters, including rock fresh/weathered ratios, percent pitted rocks and depth of pits, percent rocks with weathering rinds and thickness of rinds, height of mafic inclusions weathered into relief, surface boulder frequency, and ratios of oxidized/partially oxidized/unoxidized boulders. To help evaluate the degree of surface rock weathering at each site within a valley, z-scores have been calculated for each parameter that increases in value through time (z-score= individual value minus the mean devided by the standard deviation). Z-scores are summed and devided by the number of parameters used to give the z-score index. The method allows many weathering parameters to be used together, expressed as a single number for each site, to differentiate between deposits of varying age. Use of the index results in statistically significant groupings of glacial deposits in each valley studied. Deposits fall into two groups in Bishop, McGee (S), and McGee (N) Creeks, and are correlated with the Tioga and the Tahoe glaciations. In Pine Creek, a three-fold subdivision of glacial deposits is suggested. Deposits within two of the groups are also correlated with the Tioga and the Tahoe glaciations, however the age of the third group is debatable. Laboratory analyses of the soils should help with the age estimation. Groupings suggested by the surface weathering data are supported by the soil field data.

2) Soil samples collected in the field are being processed for particle-size, iron, pH, organic carbon, soluble-salts, and moisture factor analyses. Processing includes sieving bulk samples to remove particles larger than 2-mm in size, and splitting out representative samples for each analysis using a soil sample splitter. Data obtained in the laboratory analyses should help establish relative ages of the faulted deposits, as well as relative ages of soils developed on the scarp slopes or buried at the base of the scarps. It is expected that ages based on laboratory data will provide tighter age control than those from the field data.

3) A small sample of charcoal was found at the base of a fault scarp in McGee Creek (S) during the investigation of soil development on fault scarp slopes. The charcoal was discovered in a sand unit within a recessional Tioga outwash deposit. The outwash had been offset by faulting and subsequently buried by fault scarp colluvium. The charcoal, which was in sand-size and smaller pieces, has been picked out and submitted for ^{14}C dating. Because of the small sample size, it will be analyzed by accelerator mass spectrometry. The sample is important because it is the only material found thus far which is suitable for radiometric dating. The ^{14}C date of this sample should provide both an age for latest-Tioga glaciation in the valley, and a maximum age for the faulting which created the scarp. The date should also provide some age control for soil development in the valley.

4) Arrangements have been made for the excavation and mapping of the two trenches, which will take place in May and June of 1987. One trench will be located in the Bishop Creek area, across a fault scarp which displaces a Tahoe age moraine. Study of fault scarp soils from hand dug soil pits suggests that this scarp is pre-Tioga in age, and was formed during at least two faulting events. A buried soil separates two colluvial units at the fault scarp footslope. The lower unit contains many grussified biotite-rich clasts. In contrast, biotite-rich clasts are rare in the overlying unit. These characteristics of the fault scarp colluvium suggest that enough time separated the events to allow the biotite-rich lithology to be grussified and thus depleted from parent materials of the upper colluvium. The trench should reveal additional information about the history of faulting at this site. The other trench site will be located in McGee Creek (N) area, across a fault scarp which displaces a recessional Tioga moraine. Field studies suggest that displacement along this fault has occurred several times during the Holocene.

References Cited

Harden, J. W., 1982, A quantitative index of soil development from field descriptions: examples from a chronosequence in central California: Geoderma, v. 28, p. 1-28.

Surface Faulting Studies

9910-02677

M.G. Bonilla
Branch of Engineering Seismology and Geology
U.S. Geological Survey
345 Middlefield Road, MS 977
Menlo Park, CA 94025
(415) 323-8111, ext. 2245 or (415) 329-5615

Investigations

1. Minimum earthquake magnitude associated with coseismic surface faulting.

2. Appearance of active faults in exploratory trenches.

3. Preparation of reports.

Results

1. The scope of the study of minimum earthquake magnitude associated with coseismic surface faulting was expanded by adding more events of magnitude <6 and compiling data on focal depths, intensities, and fault damage to structures. The basic finding is unchanged--the smallest earthquakes with reported coseismic surface faulting are of about M_L 5; however, a combined empirical and theoretical analysis suggests that under ideal conditions, coeseismic surface faulting of a few millimeters associated with earthquakes having moment magnitudes as small as 3 could be recognized by simple field methods. Among the ideal conditions are a fault plane at shallow depth having a steep dip, timely and detailed field examination, good exposures, and situations unfavorable for compaction, liquefaction, landsliding, and other surficial effects of earthquakes. Earthquakes in the M_L 5 to 6 range have produced maximum reported intensities ranging from IV to IX; the associated surface faulting has damaged pipelines and house foundations, and some of it was large enough to have damaged more important structures had they been present.

2. Some recently compiled data from exploratory trenches were analyzed by J.J. Lienkaemper. Statistically significant differences at the 95% confidence level were found in the frequency of occurrence of concealed ruptures on different types of faults and in different materials. Concealment of segments of fault strands is most common on strike-slip faults, intermediate on reverse-slip faults, and least common on normal-slip faults; soil horizons and sand more commonly conceal strand segments than do gravel or clay.

3. Manuscripts on a) minimum earthquake magnitude associated with coseismic surface faulting, b) faulting and seismic activity related to engineering projects, and c) the 1983 Guinea earthquake and faulting were revised after technical review by journal editors.

Reports

Bonilla, M.G., *in press*, Faulting and seismic activity, Chapter 10 in Kiersch, G.A., ed., The heritage of engineering geology--the first hundred years: *Geological Society of America Centennial Special Volume CSV-3*.

Crone, A.J., Machette, M.N., Bonilla, M.G., Lienkaemper, J.J., Pierce, K.L., Scott, W.E., and Bucknam, R.C., *in press*, Surface faulting accompanying the Borah Peak earthquake and segmentation of the Lost River fault, central Idaho: *Seismological Society of America Bulletin*, v. 77, no. 3.

Harms, K.K., Clark, M.M., Rymer, M.J., Bonilla, M.G., Harp, E.L., Herd, D.G., Lajoie, K.R., Lienkaemper, J.J., Mathieson, S.A., Perkins, J.A., Wallace, R.E., and Ziony, J.I., 1987, The search for surface faulting, in Hoose, S.N., ed., The Morgan Hill, California, earthquake of April 24, 1984: *U.S. Geological Survey Bulletin 1639*, p. 61-68.

Langer, C.J., Bonilla, M.G., and Bollinger, G.A., *in press*, Aftershocks and surface faulting associated with the intraplate Guinea, west Africa, earthquake of December 22, 1983: *Seismological Society of America Bulletin*.

SOIL DEVELOPMENT AND DISPLACEMENT ALONG THE HAYWARD FAULT

14-08-0001-21929

Glenn Borchardt
California Department of Conservation
Division of Mines and Geology
380 Civic Drive
Pleasant Hill, CA 94523-1997

(415) 671-4926

Investigations

1. Fremont City Hall study site

Phase two of the trench exploration will continue in May in collaboration with Jim Lienkaemper and Dave Schwartz of the U.S. Geological Survey. We will excavate a short perpendicular trench for determining the exact location and width of the fault zone and two long trenches that will be parallel the fault and as close to it as the shearing within the zone will allow. We hope to uncover both the northern and southern margins of the paleostream channel that we found offset by the Hayward fault in the first phase of the investigation. We expect this to give us a relatively precise match and corresponding offset measurement. Three earlier trenches may be lengthened a few meters to determined the southern margin of the channel in each.

2. Point Pinole study site.

The East Bay Regional Park District has approved the trench exploration plan for Point Pinole Regional Shoreline, with the work scheduled to begin in June. Two small trenches about 50 m apart will be excavated perpendicular to the strike of the mapped trace of the fault immediately southeast of the Southern Pacific fuel oil line. Two long trenches will be excavated parallel the fault on the margin of a late Holocene alluvial fan. Other trenches will be dug along strike to the northwest in an effort to precisely locate the fault and to determine if the fault offsets the 1,360 B.P. bay mud unit that overlies a paleosol at the 38-cm depth. We will also explore the subsurface configuration of the fine sand deposits that exist along the fault in the tidal marsh.

Results

1. Slip rate for the Fremont Segment of the Hayward fault, Fremont City Hall

The first phase of this project, conducted during September of 1986, has been extremely successful in that we have identified a buried paleostream channel that has been displaced between 28.5 and 39 meters by the Hayward fault. The poorly drained soil on the northeast side of the fault is at least 4,040 years old as calculated from an MRT (mean residence time) of 2,020 B.P. determined on representative soil carbon from the A horizon. This soil also had a Bk horizon high in pedogenic calcite which had formed throughout the last 1,620 years (calculated from an MRT date of 810 B.P.). The existence of the Bk horizon of this age implies that this southern portion of the Niles alluvial cone has had no significant alluvial deposition during the last 1,620 years.

The above soil information was used to calculate a local downwarp rate of 0.4 to 0.6 mm/yr. Assuming a constant rate of downwarping, the offset channel could be a much as 7,691 years old. Until we determine the precise measurements of the offset in May and receive the C-14 dates for charcoal from above and below the paleostream channel, the geologic slip rate for this section of the fault remains poorly constrained between 3.7 and 9.7 mm/yr.

2. Point Pinole Study Site

Work on this site will resume with the trench exploration phase scheduled for June.

Geologists Kim Seelig of San Francisco State University and Dave Wagner of the California Division of Mines and Geology are collaborating in the preparation of a 1:12,000 scale geologic map of the Point Pinole area as part of this project. This will advance our knowledge of this most important portion of the fault and its possible connection with the Rogers Creek-Healdsburg fault on the other side of San Pablo Bay.

Oliver Chadwick and Harvey Doner of the University of California at Berkeley are cooperating in the investigation of the mineralogy of the extremely well developed Mn oxide-coated horizon that appears to mark the top of the water table in soils at the site.

A field trip was held with personnel of the East Bay Regional Park District. They are especially interested in the public educational value of our studies of the fault. We propose to assist them in preparing an earthquake exhibit and self-guided trail for the park.

Reports

Borchardt, Glenn, 1987(in press), Smectites, in J. B. Dixon and S. B. Weed, eds., Minerals in soil environments (2nd edition): Soil Science Society of America, Madison, WI.

Borchardt, Glenn, Lienkaemper, Jim, and Schwartz, David, 1988 (in preparation), Slip rate for the Fremont segment of the Hayward fault, Fremont City Hall, California: Bulletin of the Seismological Society of America.

Borchardt, Glenn, and Manson, M. W., 1986, Magnitude 5.9 North Palm Springs earthquake, July 8, 1986, Riverside County, California: Lifeline damage: California Geology, v. 39, p. 248-252.

Steinbrugge, K. V., Lagorio, H. J., Davis, J. F., Bennett, J. H., Borchardt, Glenn, and Toppozada, T. R., 1986, Earthquake planning scenario for a magnitude 7.5 earthquake on the Hayward fault, San Francisco Bay area: California Geology, v. 39, p. 153-157.

Steinbrugge, K. V., Bennett, J. H., Lagorio, H. J., Davis, J. F., Borchardt, Glenn, and Toppozada, T. R., 1987, Earthquake planning scenario for a magnitude 7.5 earthquake on the Hayward fault in the San Francisco Bay area: California Division of Mines and Geology Special Publication 78, 243 p.

Northern San Andreas Fault System

9910-03831

Robert D. Brown
Branch of Engineering Seismology and Geology
U.S. Geological Survey
345 Middlefield Road, MS 977
Menlo Park, California 94025
(415) 323-8111, ext. 2461 or (415) 329-5620

Investigations

1. Continuing research on Quaternary deformation in the San Andreas fault system for a planned volume summarizing current geologic and geophysical knowledge of the fault system.

2. Research and review of work by others on the tectonic setting and earthquake potential at Diablo Canyon Power Plant (DCPP), near San Luis Obispo, California. Activities are in an advisory capacity to the Nuclear Regulatory Commission (NRC) and are chiefly to review and evaluate data and interpretations obtained by Pacific Gas and Electric (PG&E) through its long-term seismic program.

3. Serve (*ex-officio*) as vice-chairman on Policy Advisory Board, Bay Area Earthquake Preparedness Project (BAREPP). A joint project of the State of California and the Federal Emergency Management Agency, BAREPP seeks to further public awareness of earthquake hazards and to improve mitigative and response measures used by local government, businesses, and private citizens.

Results

1. First draft of San Andreas Quaternary paper is about 90% complete; text, except for conclusions, is complete, but some illustrations remain to be done.

2. Participated in several field and workshop reviews related to DCPP and provided oral and written review comments to NRC. Coordinated USGS review and data acquisition efforts related to DCPP.

3. Provided informal oral and written data, analysis, and recommendations to BAREPP and other Policy Advisory Board members on geologic, seismologic, and management issues relating to earthquake hazard mitigation in the San Francisco bay region.

Reports

Brown, Robert D. Jr., and Kockelman, William J., 1987, Using geologic knowledge for the public welfare: *California Geology*, v. 40, no. 2, p. 38-44.

Characteristics of Active Faults

9950-03870

Robert C. Bucknam
Branch of Geologic Risk Assessment
U.S. Geological Survey
Box 25046, MS 966, Denver Federal Center
Denver, Colorado 80225
(303) 236-1604

Investigations

1. Completed field mapping and analysis of data pertaining to earthquake hazards in the Tooele, Utah, 1°X1° quadrangle. (Barnhard)

2. Compilation of data for Great Basin part of DNAG Neotectonic Map of North America. (Bucknam)

3. Collaboration with D. J. Andrews on diffusion modelling of fault-scarp degradation. (Bucknam)

Results

1. Ten zones of fault scarps were identified in the Tooele, Utah, 1°X1° quadrangle. The scarps are formed on unconsolidated basin-fill deposits of late Quaternary age. The lengths, locations, and relative displacement directions of the scarp zones have been mapped and transferred to a 1:250,000-scale base map. Ages of the scarps in 8 of the 10 zones have been determined, relative to the highstand of Lake Bonneville (15 Ka), using fault-scarp geomorphology and crosscutting relationships of the fault scarps with shoreline features of Lake Bonneville. Surface faulting in one of the eight zones is younger than Lake Bonneville (<15 Ka), and surface faulting in the other seven zones is older than Lake Bonneville (15 Ka) but of late Pleistocene age (<150 Ka). The age of faulting in 2 of the 10 zones is indeterminate relative to the highstand of Lake Bonneville but the scarps are believed to be late Pleistocene (150 Ka) or younger.

2. Compilation of faults and slip rates in the Great Basin for the DNAG Neotectonic Map was about 50 percent complete at end of report period. Data collected in western Utah for this compilation will also be a contribution for a Quaternary fault map of Utah to be published by the Utah Geological and Mineral Survey.

Reports

Andrews, D.J., and Bucknam, R.C., 1987, Fitting degradation of shoreline scarps by a model with nonlinear diffusion: Journal of Geophysical Research (in press).

Barnhard, T.P., and Dodge, R.L., 1987, Map of fault scarps formed in unconsolidated sediments, Tooele 1°X1° quadrangle, Utah: U.S. Geological Survey Miscellaneous Field Studies Map, scale 1:250,000 (in press).

Late Quaternary Slip Rates on Active Faults of California

9910-03554

Malcolm M. Clark
Branch of Engineering Seismology and Geology
345 Middlefield Road, MS 77
Menlo Park, CA 94025
(415) 323-8111, ext. 2591 or (415) 329-5624

Investigations

1. Late Quaternary activity along the Lone Pine fault, Owens Valley, California (L.K. Lubetkin [USFS], M.M. Clark, S. Beanland [NZGS], K.K. Harms, and S.K. Pezzopane).

2. Slip rates on the Paicines fault near Tres Pinos, California (K.K. Harms, J.W. Harden, M.M. Clark).

Results

1. Remeasurement of the north wall of the oldest former channel of Lone Pine Creek that has been offset by the Lone Pine fault shows 13 to 17 m of right slip after abandonment. As reported earlier, the associated scarp indicates 3 slip events, including that of 1872, since 10-21 ka. Hence, the average component of right lateral slip at this channel is 4.3 to 5.7 m, which overlaps the range of average right slip at an abandoned debris flow about 200 m to the north along the scarp, 5.1 to 6 m.

   Horizontal offset of this channel has been debated for years. Hobbs in 1910 reported W.D. Johnson's observations of this scarp, and included Johnson's photo of this channel with a caption that described 20 feet of right offset of it. Paul Bateman in 1961 published some of Johnson's field notes and manuscripts that established 4.9 m of right slip on the nearby main Owens Valley fault trace, but which also denied that any horizontal slip occurred along the Lone Pine fault. However, we have found the letters from Johnson to Hobbs that formed the basis for Hobb's 1910 report. The letters are in the University of Michigan Library, and include Johnson's description that this channel shows about 20 feet of right offset, contradicting his later statement, published by Bateman. We think horizontal offset of this channel is clearly supported by field evidence. An intriguing possibility is that Johnson saw a 20-foot offset of a young, ephemeral part of the channel. A 20-foot (approx. 6 m) horizontal offset is close to our 3-event average horizontal offset of 4.3 to 5.7 m at this channel.

2. We determined late Quaternary slip rates at two sites along the right-lateral, northwest-trending Paicines fault, the southernmost extension of the Calaveras-Hayward fault zone. Our primary dating method is soil development, which is calibrated from dated soils in the San Joaquin Valley and the San Francisco Bay area. At our sites we quantified soil development on fault-affected terraces along both the present and abandoned courses of Tres Pinos Creek.

We derive one slip rate from an offset terrace riser that could have formed any time after the deposition of the terrace that it cuts. The displaced riser could have been eroded upstream from the fault after it was offset; thus it preserves only a minimum offset. These measurements yield a minimum slip rate of 3.5 mm/yr.

We base the second slip rate on a hill that probably blocked the present course of the stream at a time when the more northerly (abandoned) course was active. The hill moved northwestward enough for the present drainage to be established at some time before 70 ka (the youngest age of the oldest terrace along the present drainage). This minimum age, combined with the maximum displacement of 900 m, yields a maximum slip rate of about 13 mm/yr. We find no geomorphic evidence for significant uplift on the west side of the fault, a possibility previously reported.

We could not determine additional slip rates by correlating the degree of soil development across the fault, because the soils on the southwest side of the fault have been modified by stripping.

Reports

Beanland, Sarah, and Clark, M.M., 1987, The Owens Valley fault zone, eastern California, and surface rupture associated with the 1872 earthquake [abs.]: *Seismological Research Letters*, v. 58, p. 32.

Harms, K.K., Harden, J.W., and Clark, M.M., 1987, Use of quantified soil development to determine slip rates on the Paicines fault, northern California [abs.]: *Geological Society of America, Abstracts with Programs*, in press.

Lubetkin, L., and Clark, M.M., 1987, Late Quaternary activity along the Lone Pine fault, eastern California [abs.]: *Seismological Research Letters*, v. 58, p. 32.

Lubetkin, L., and Clark, M., Late Quaternary activity along the Lone Pine fault, eastern California: *Geological Society of America Bulletin*, in press.

EARTHQUAKE RESEARCH IN THE WESTERN GREAT BASIN

Contract 14-08-0001-21986, April 1987

E.J. Corbett, W.A. Peppin, and U.R. Vetter
Seismological Laboratory
University of Nevada
Reno, NV 89557
(702) 784-4975

Investigations

This program supports continued studies with research focused on: (1) seismicity in the White Mountains Gap; (2) magmatic processes in Long Valley Caldera; (3) relocations of Mammoth Lakes earthquakes; (4) analysis of digital waveforms. The most interesting new results are described below.

The White Mountains seismic gap.

In **Figure 1** is shown a map of the UNR catalog locations from 1970 to 1986 for the area around Mammoth Lakes and the White Mountains seismic gap, a zone which has been identified as having potential for a major earthquake in the near future (Wallace, 1978). Also plotted are the faults showing Holocene/Quaternary evidence of movement, based in part on original fieldwork and analysis of aerial photos by Craig dePolo and Alan Ramelli, UNR grad students. With faulting and seismicity at this level of detail, some striking patterns and relationships emerge which have not been seen so clearly before. Note in particular the lack of seismicity along the west side of the White Mountains north of Chalfant Valley. Also note the cluster of seismicity at the north end of the northern Death Valley - Fishlake Valley fault. Each of these regions, within the White Mountains seismic gap, are obvious target zones for the next major earthquake in the western Great Basin. Instrumental coverage to the east of this zone is being augmented to cover such events.

Another noteworthy seismic trend in Figure 1 was identified by dePolo and dePolo (1986) and is of interest three ways. First, it also is in the White Mountains seismic gap (i.e., between the ruptures of the major 1932 and great 1872 earthquakes); second, it passes right beneath the town of Bishop, California, posing potentially serious seismic hazard to this regional population center; third, it is about 30 km in length, and so capable of a sizable earthquake. Seismicity associated with the trend is shown in **Figure 2**, and focal mechanisms in **Figure 3**. The latter shows how the mechanisms line up fairly closely (NW right-lateral strike slip motion) with the epicenters comprising the Bishop trend. We are monitoring activity on this trend carefully following migration of activity into the seismic gap with the 1986 Chalfant sequence.

REFERENCES

dePolo, C.M. and dePolo, D.M., 1986. Seismicity of northern Owens Valley from August 1984 to mid-July 1986, *EOS, Trans. Am. Geophys. Un.*, **67**, 1106.

Wallace, R.E., 1978. Patterns of faulting and seismic gaps in the Great Basin province, in *Proceedings of Conference VI, Methodology for Identifying Gaps and Soon-to-Break Gaps*, edited by J.F. Evernden, U.S.G.S. Open-File Report, 78-943, 858-868.

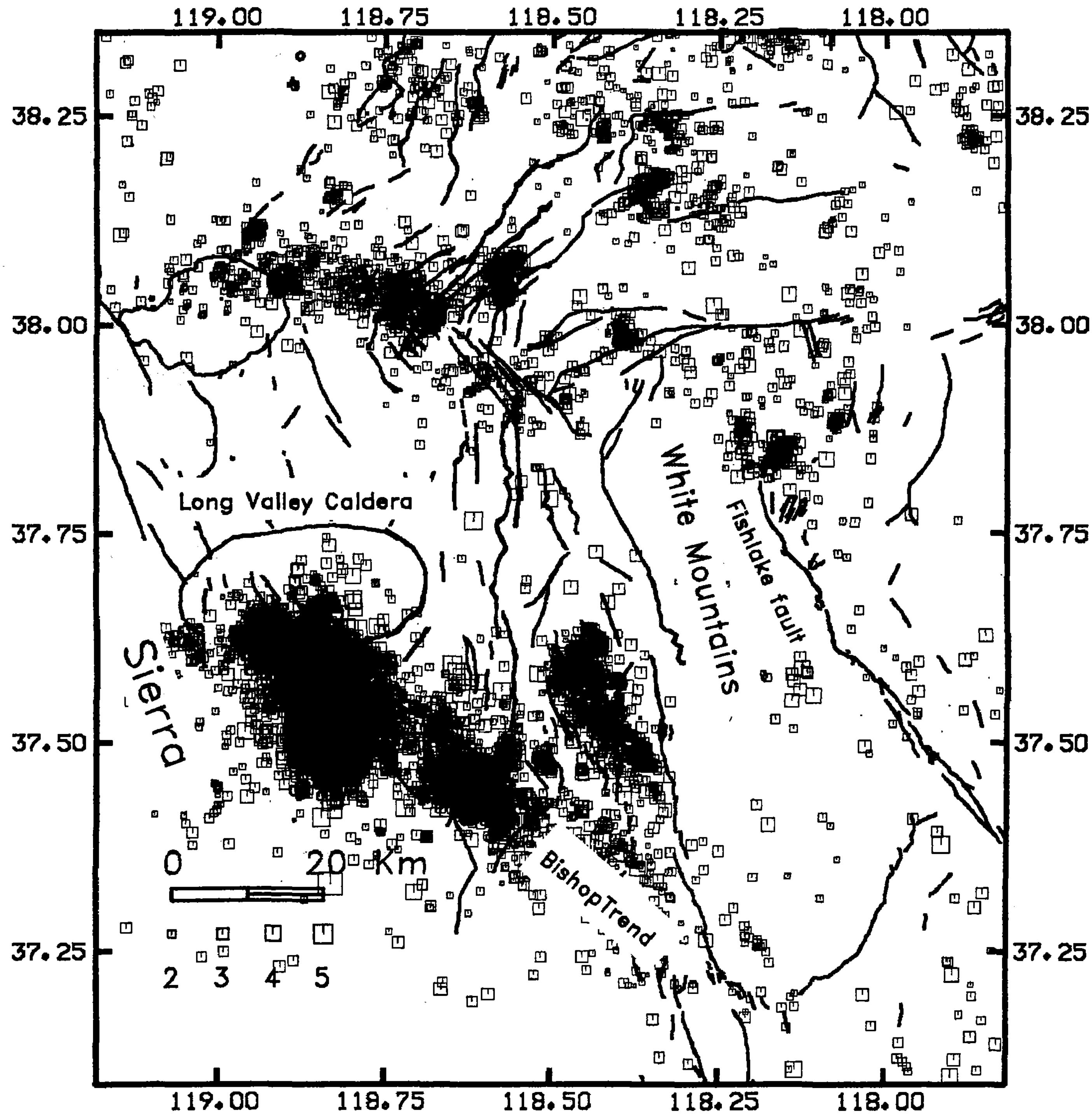

Figure 1. Seismicity, 1970 to 1986 from the UNR earthquake catalog. The large zones of seismicity near and east of the Long Valley caldera are the 1980 aftershocks, the 1984 Round Valley sequence, and the 1986 Chalfant Valley sequence.

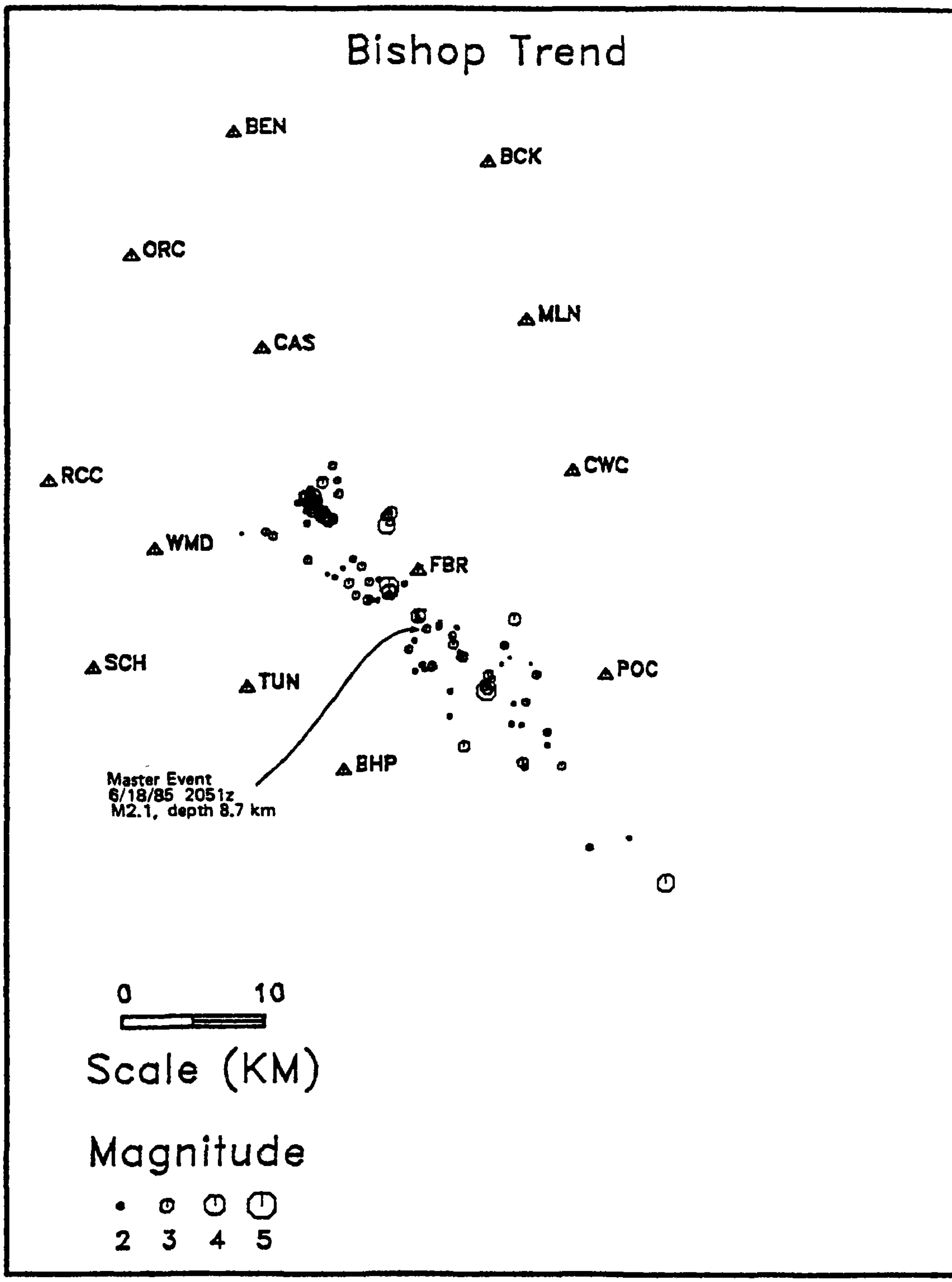

Figure 2. Seismicity comprising the lineup of epicenters, trending through Bishop, California, and herein called the "Bishop Trend," together with the location of the master event used in the locations and of the station array. Coverage is good except at the south end of the trend.

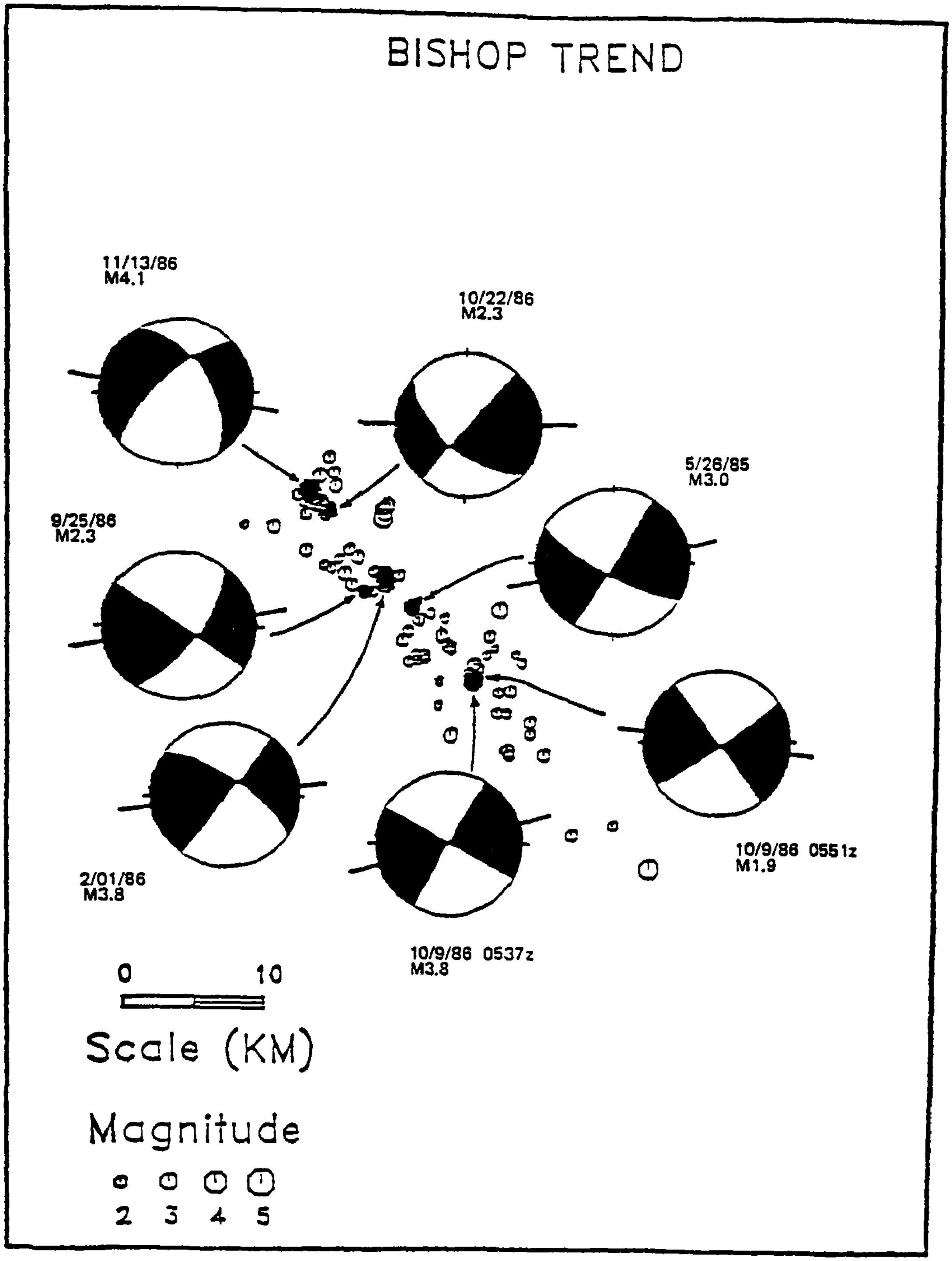

Figure 3. Mechanisms for events occurring along the Bishop trend. The NW-striking planes are fairly close in strike to the trend of the epicenters itself.

THOMAS L. DAVIS
GEOLOGICAL CONSULTANT
3937 RODERICK ROAD
LOS ANGELES, CA 90065
U.S.A
213-259-3086

Objectives: Subsurface Study of the Late Cenozoic Structural Geology of the Los Angeles Basin:

a)Detection or postulation of concealed late Cenozoic faults in the basin.

b)Determine subsurface geometry, sense of slip, and displacement history for the concealed faults and already known late Cenozoic faults of the basin.

c)Principal format for this study is the construction of retrodeformable cross sections using subsurface data from oil and gas wells and surface geologic mapping. Limited subsurface mapping will be completed between the cross sections to understand the three-dimensional aspects of the basin.

Results:
This project commenced on Feb.1,1987 and has accomplished phases I-IV(data collection, construction of cross section, structural interpretation and integration) for a cross section from Eagle Rock to Gardena (Figure 1). Phase I(data collection) has been accomplished on a west Los Angeles cross section. The Eagle Rock to Gardena cross section was constructed at 1:24,000 scale and reduced for Figure 2.The restoration is shown in Figure 3. The cross section is tentative and will need to be refined as additional subsurface data becomes available. The cross section is also highly interpretative below the drilling depth in the basin. The interpretation is based largely on the fold models of Suppe(1985) and the principles of restorable cross sections. It should be understood that at least several retrodeformable solutions may be possible for this particular set of surface and subsurface data. The following is a short outline of the assumptions and implications of the cross section.

1)It is assumed that the edges of the Los Angeles Basin were controlled by normal faulting during middle Miocene through early Pliocene(Delmontian) time. Extensional structures include the Newport-Inglewood fault trend(fault 1) and faults 2-4. All of these faults were growth structures. Fault scarp deposits of middle and late Miocene age have been mapped by Lamar(1970) along faults 3 and 4, and well data show that late Miocene through early Pliocene strata are much thicker on the downthrown side of the Newport-Inglewood fault(Figure 2). Along faults 3 and 4 distinctive detritus within the scarp deposits indicate the local crystalline basement was exposed and shedding debris at this time(L.T.Silver,personal communication). Figure 3 is the cross section restored to earliest Pliocene time(end of Delmontian or about 4.0 Ma, M.B.Lagoe, personal communication). Figure 3 shows the structural setting at the end of extension and just before the start of thrust faulting.

2)Thrust faulting and folding began about 4.0 Ma. This is documented by the northward thinning out of the Repettian age(4.0 to 2.6 Ma, M.B.Lagoe, personal communication) strata on the south flank of the Elysian Park anticline. Delmontian and older rocks are equally deformed by folding.

3)It is assumed in Figure 2 that the Elysian Park anticline is due to two thrust faults(B&C) that make a stacked set of fault-bend folds. The total fault slip on faults B&C is about 12,960m which gives an average slip rate of 3.24mm/yr. It might be possible to make the Elysian Park anticline a fault-propagation fold or just one fault-bend fold and this would reduce the total fault displacement considerably. Work on such a structural solution is now in progress. Regardless of the structural solution the total uplift rate for the Elysian Park anticline for the last 4.0 Ma is about 1.7mm/yr which is about 1.7 times faster than growth at the Coalinga anticline(Namson and Davis,1986). Thus if the Elysian Park anticline is being uplifted by Coalinga-sized earthquakes the recurrence interval for these events would be about 0.6 times shorter than that estimated for Coalinga or about 125 to 225 years.

References:

Lamar,D.L.,1970, Geology of the Elysian Park-Repetto Hills area, Los Angeles County, California: California Division of Mines and Geology Special Report 101, 45p.

Namson,Jay and Davis,Thom,1986,Estimation of Recurrence Interval for the May 2,1983 Coalinga Earthquake Using the Fault Bend Fold Method: Transactions of the American Geophysical Union (abstract), v.67, no.44, p1222.

Suppe,J.,1985, Principles of Structural Geology, Prentice-Hall, Englewood Cliffs, New Jersey, 537p.

Yerkes,R.F.,McCulloh,T.H.,Schoellhamer,J.E.,and Vedder,J.G.,1965, Geology of the Los Angeles Basin, California-an introduction: U.S.Geological Survey Professional Paper 420A, 57p.

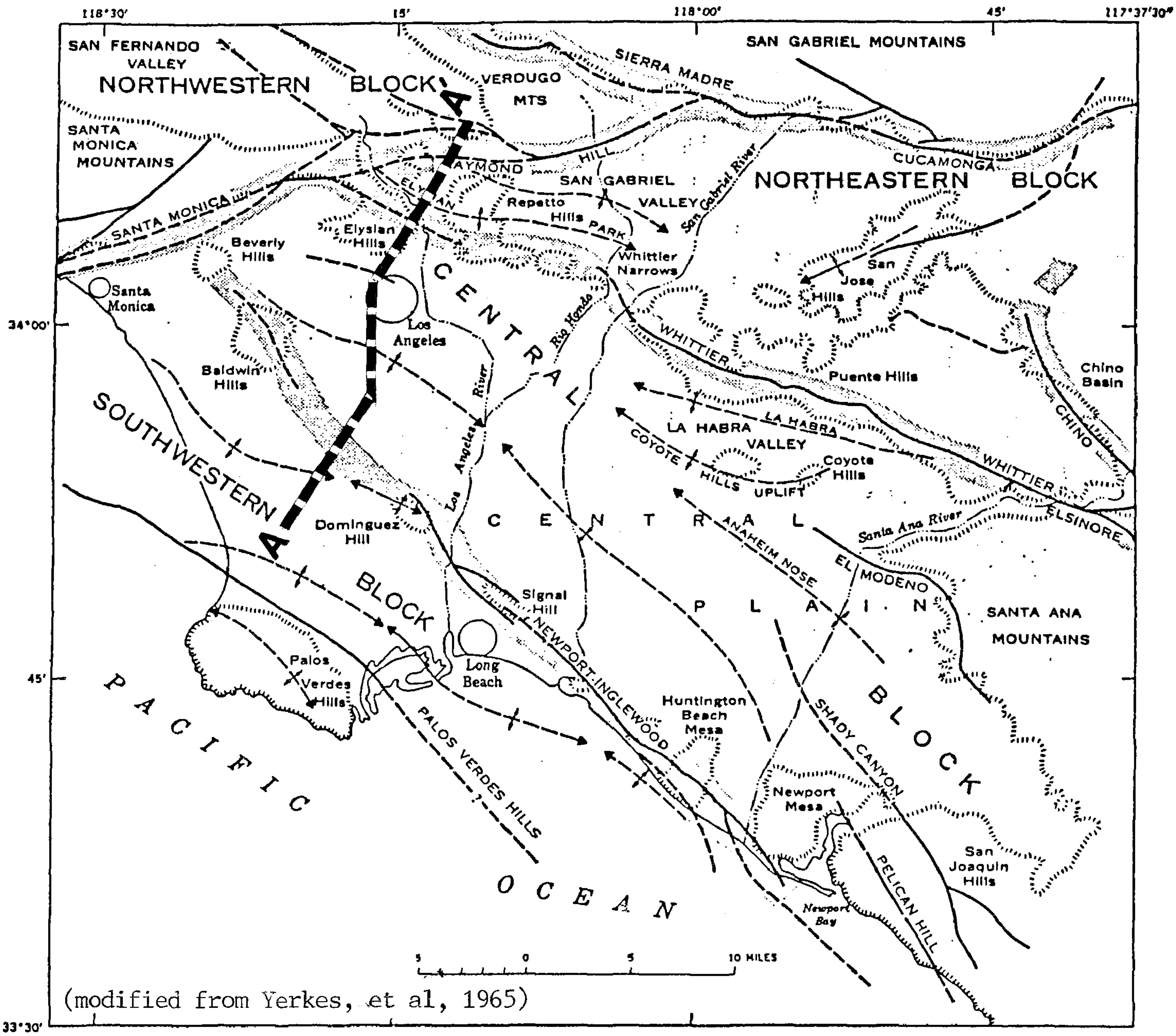

(modified from Yerkes, et al, 1965)

Figure 1. Location map for Los Angeles Basin cross section study.

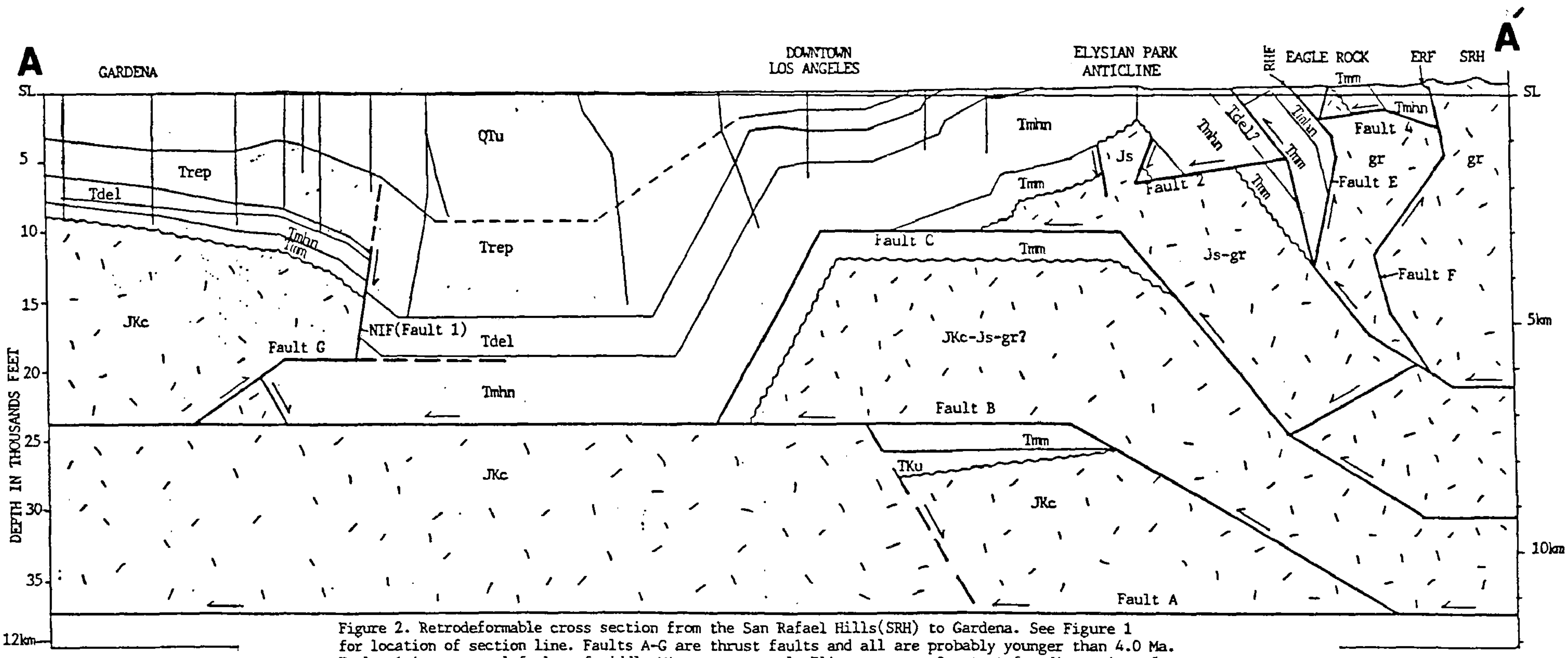

Figure 2. Retrodeformable cross section from the San Rafael Hills(SRH) to Gardena. See Figure 1 for location of section line. Faults A-G are thrust faults and all are probably younger than 4.0 Ma. Faults 1-4 are normal faults of middle Miocene to early Pliocene age. See text for discussion of section. NIF=Newport-Inglewood fault; RHF=Raymond Hill fault; ERF=Eagle Rock fault; QTu=late Pliocene and Quaternary age strata; Trep=Repettian age(Pliocene) strata; Tdel=Delmontian age(late Miocene to early Pliocene); Tmhn=Mohnian age(late Miocene); Tmm=middle Miocene age strata; TKu=undifferentiated strata of late Cretaceous(?) to early Miocene age; JKc=Catalina Schist; Js=Santa Monica Slate; gr=Wilson quartz diorite.

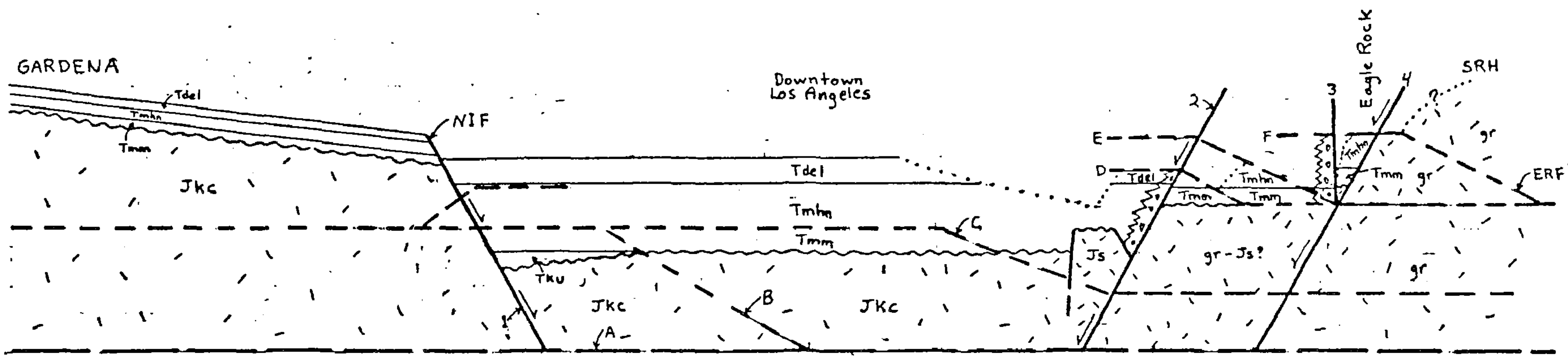

Figure 3. Cross section retrodeformed to end of Delmontian time(4.0 Ma). See text for discussion. Symbols are explained in Figure 2.

VERY PRECISE DATING OF PREHISTORIC EARTHQUAKES IN SOUTHERN CALIFORNIA USING TREE-RING ANALYSIS

Gordon C. Jacoby
Tree-Ring Laboratory
Lamont-Doherty Geological Observatory of Columbia University
Palisades, New York 10964
(914) 359-2900

USGS 14-08-0001-G 1329

We further documented the effects of the 1857 earthquake in the tree-ring record near Wrightwood, California (Sheppard and Jacoby 1987) to complement an earlier study (Meisling and Sieh 1980). These studies confirm the ability of tree-ring analysis to be useful as a paleoseismological method. Efforts over the past year have also produced a hypothesis that the reported earthquake of 8 December 1812 (Toppozada et al. 1981) occurred on the San Andreas fault.

In the vicinity of Wrightwood, California, a town that straddles the San Andreas fault northeast of Los Angeles, many Jeffrey pine (Pinus jeffreyi) and ponderosa pine (Pinus ponderosa) samples were collected along with three of white fir (Abies concolor) and one incense-cedar (Libocedrus decurrens). The average extent for the samples was back to around 1600, although one Jeffrey pine extended back to 1382. Unfortunately this particular tree sits about 100 m off the fault, and its tree-ring series is quite complacent, with no missing rings or unique growth anomalies. All rings of all samples were dated (using rigorous dendrochronological techniques) to the exact year of growth and annual ring widths measured to $\pm$0.01 mm. Most of the sampled trees are currently near homes or other developments, and tree growth since at least 1900 probably reflects that disturbance. Some show effects of the known 1857 earthquake. One particular white fir section shows a tree-ring response to two disturbances (Figure 1). Prior to 1857, this tree had a healthy growth rate, though it still responded to the drought years of the 1840s with slightly narrower rings. The 1857 ring, however, is missing, and the growth rate for several years after that is quite reduced compared to pre-1857. Clearly this tree responded to something more than just climate, which is expressed by a control chronology created from undisturbed trees from the Wrightwood area (Figure 1); we consider this to be an excellent example of the theoretical tree-ring response to earthquakes. There is also evidence (less obvious but still clear) of an earlier disturbance between the growing seasons of 1812 and 1813.

Additionally, we found similar responses, starting with the 1813 ring, in eight other fault-zone trees along a 12 km segment of the fault zone in or near Wrightwood (Figure 2). In two of these trees (Figure 3), the growth suppression was so severe that many rings were missed. In others, all rings are accounted for through crossdating, but the suppressed post-1812 ring growth does not follow the standardized climate response as shown by other, undisturbed trees from in or near Wrightwood (Figure 1).

Because the set of off-fault, control trees shows the undisturbed climate pattern of the Wrightwood area, and the only trees showing a disturbance after 1812 are virtually on the fault, we hypothsize that some

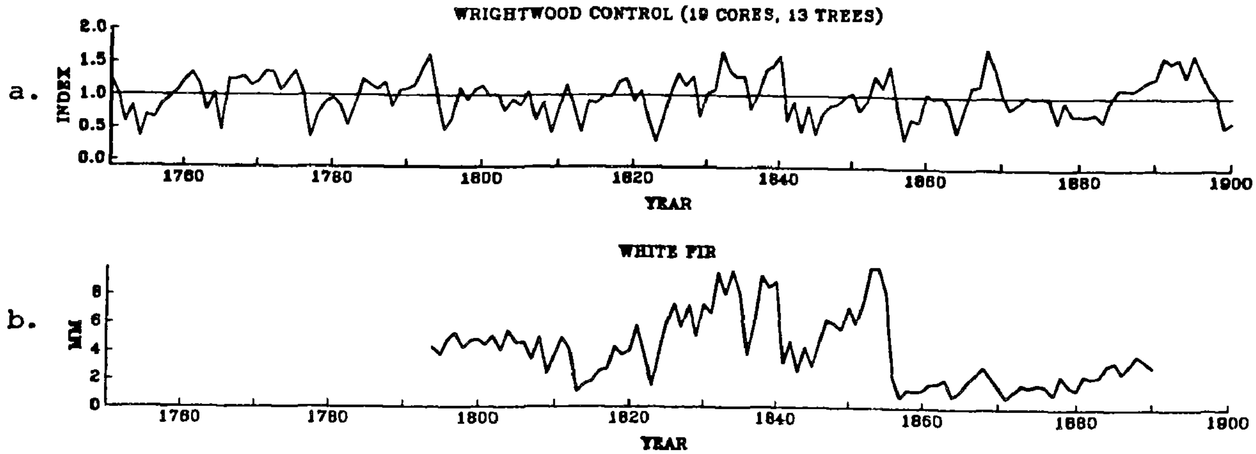

Figure 1: a. Ring-width indices for undisturbed trees near Wrightwood, California. The main cause of variation is moisture stress due to variations in precipitation.

b. Ring widths from a white fir that is moderately sensitive to drought. Many of the narrower rings match but the extended sequences of narrow rings beginning in 1813 and 1857 indicate more than merely moisture stress. The tree was very young and small in 1812 and not as damaged as in 1857.

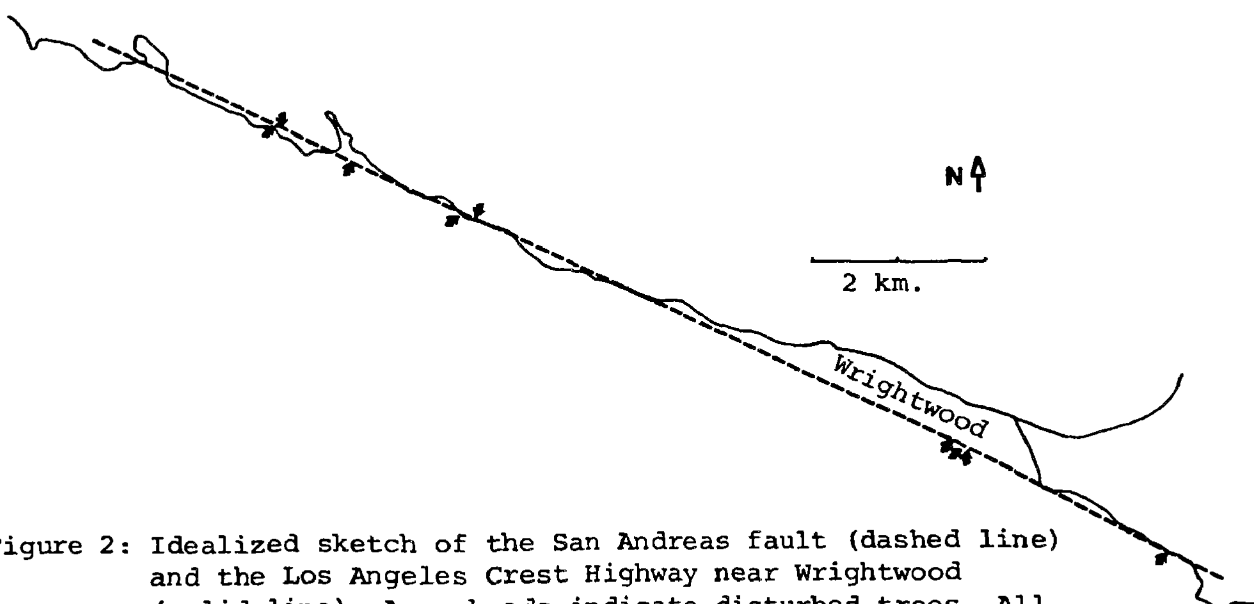

Figure 2: Idealized sketch of the San Andreas fault (dashed line) and the Los Angeles Crest Highway near Wrightwood (solid line). Arrowheads indicate disturbed trees. All are within about ten meters of the fault. All the control trees are farther away. None of the trees farther away show the 1813 decrease in ring widths.

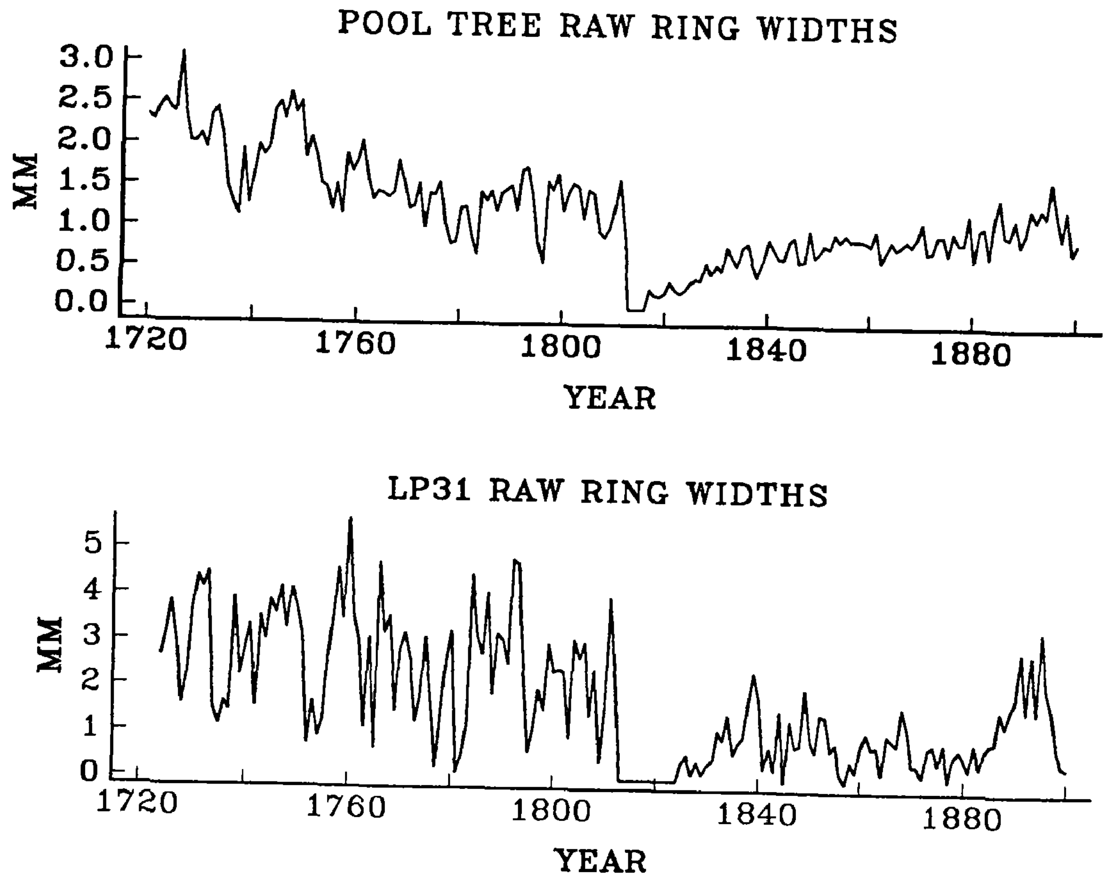

Figure 3: Plots of raw ring widths of two trees from near Wrightwood that were traumatized just after the 1812 growing season. The ring-width declines begin with 1813 and, followed by several years of slow recovery.

earth movement occurred on that section of the San Andreas fault between the 1812 and 1813 growing seasons. This time period pre-dates any recorded history in the immediate area, there are no documents to indicate that an earthquake actually occurred there. There were, however, missions to the south and west of the Wrightwood area, primarily on the coast, and several of them recorded large earthquakes on 8 and 21 December 1812 (Toppozada et al. 1981). Estimated isoseismal lines for both of these events do not include the Wrightwood area, and neither event has been previously interpreted as being epicentered on the San Andreas fault. However, the isoseismal line for the 8 December event comes close to including Wrightwood, and therefore we feel that it could have been the event that caused earth movement in that area and the subsequent tree-ring response in nine fault trees. Although there was severe damage to one structure plus associated deaths at the San Juan Capistrano mission to the south, a careful reading of the mission report and later information indicates at least one adobe building survived with only minor damage (Toppozada et al. 1981). The paucity of reports from that time period prevents close constraint of the epicenter location.

References

Meisling, K.E. and K.E. Sieh. 1980. Disturbance of trees by the 1857 Fort Tejon earthquake, California. Journal of Geophysical Research 85(B6):3225-3238.

Sheppard, P.R. and G.C. Jacoby. 1987. Dating earthquakes along the San Andreas fault system in California. In: Proceedings of the International Symposium of Ecological Aspects of Tree-Ring Analysis, G.C. Jacoby and J.W. Hornbeck, compilers. 17-21 August 1986, Marymount College, Tarrytown, New York. 700p.

Toppozada, T.R., C.R. Real, and D.L. Parke. 1981. Preparation of isoseismal maps and summaries of reported effects for the pre-1900 California earthquakes. Calif. Div. Mines Geol., Sacramento, CA Open File Rep., 81-11 SAC. 182pp.

Coastal Tectonics, Western United States

9910-01623

Kenneth R. Lajoie

Branch of Engineering Seismology and Geology
U.S. Geological Survey
345 Middlefield Road, MS 977
Menlo Park, California 94025
(415) 329-5641

Investigations:

1. Age and deformation of Pleistocene marine strandlines and sediments in the Los Angeles Basin.

2. Theoretical modeling of co-seismic uplift in coastal areas.

3. Preliminary summary of Quaternary vertical crustal movements west coast U.S.

4. Feasability studies of ESR (Electron Spin Resonance) dating of marine shells.

Results:

1. Amino-acid racemization analyses of fossil mollusks from type localities of the Palos Verdes Sand (PVS), San Pedro Sand (SPS), Timms Point Silt (TPS), and Lomita Marl (LM) provide a means of correlating these classic Pleistocene formations to the aminostratigraphic sequence recently developed in the western Los Angeles Basin. The amino-acid data support the relative ages proposed originally by Woodring (1946), but indicate these formations are younger than originally proposed. Most significantly, the type SPS, TPS, and LM are roughly coeval and are middle Pleistocene in age, not lower Pleistocene as previously estimated. Consequently, the rates of tectonic deformation (vertical displacement, folding, faulting) recorded by these stratigraphic units are also more rapid than previously estimated.

2. The two main aspects of paleoseismology are 1) identifying and dating the geologic record of past earthquakes, and 2) interpreting that record to predict the size and time of future earthquakes. Ideal theoretical models of coseismic uplift (both time- and displacement-predictable patterns) recorded by flights of emergent Holocene strandlines have been developed to provide insight and establish constraints for both aspects of paleoseismoloy. These models are general, so should also be useful in studies of episodic fault displacement (both horizontal and vertical). The models indicate that if there is any post-earthquake recovery, a displacement-predictable pattern cannot be demonstrated from the geologic record. In fact, the geological record of a displacement-predictable uplift pattern may actually appear to represent a time-predictable uplift. In general,

the models indicate that even under ideal geologic conditions (clear geologic expression and precise dating of each uplift event), no meaningful pattern can be established if there has been significant post-earthquake recovery.

3. An initial summary of vertical crustal movements along the Pacific Coast of the U.S. confirms earlier predictions based mainly on tectonic setting. In general, emergent Pleistocene strandlines along the entire coast record coastal uplift typically at rates of 0.1 - 2.0 m/ka. Extremely high rates of 4.0 - 14.0 m/ka occur only locally on anticlinal structures (Ventura, California) or in areas of complex plate interactions (Cape Mendocino, California). Coastal subsidence occurs only in local structural basins (San Francisco Bay, Los Angeles Basin). South of the Mendocino triple junction, uplift is probably caused in part by crustal thickening related to horizontal compression (up to 9 mm/yr) normal to the San Andreas fault. North of the triple junction, a region dominated by oblique subduction, net coastal uplift is low (0.0 - 0.4 m/ka), but coseismic uplift may be large if followed by subsidence; this pattern is seen along subduction zones in southern Alaska and in parts of Japan.

4. A major need in Quaternary geology is a widely applicable absolute dating technique with a range beyond that of ^{14}C (0 - 40 ka). In our studies of coastal tectonics we have developed relative dating techniques based on paleontology, amino-acid racemization and sea-level fluctuations that partially fill this need under suitable conditions. However, because of limitations in these techniques, we continually attempt to develop and apply new dating techniques. A limited experiment to investigate the feasability of using NMRT (nuclear magnetic resonance) to date marine shells produced discouraging results. However, a similar experiment using ESR (electron spin resonance) has produced very encouraging results. This technique, like TL (thermoluminescence dating), is based on measuring accumulated natural radiation damage to a crystal lattice. Preliminary work in Europe and Japan shows the technique may be applicable to various materials (shell, gypsum, wood, travertine, quartz, fault gouge) over an age range of 10^3 - 10^7 years. Our preliminary work is through informal co-operation with Stanford University Department of Chemistry (ESR spectrometry) and Lawrence Livermore Laboratory (cobalt-60 irradiation). If shell dating becomes routine, more formal arrangements will be made.

Reports

Ponti, D.J., Lajoie, Kenneth R., and Appel, S.H., 1987, Aminostratigraphic classification of the type Quaternary marine formations from the San Pedro-Palos Verdes area, Los Angeles Basin, California [abs.]: *Geological Society of America Abstracts with Program*, 19867.

NEOGENE MAGNETIC STRATIGRAPHY AND TECTONIC ROTATIONS, TRANSVERSE RANGES, CALIFORNIA: TIMING AND DEFORMATION RATES OF POTENTIALLY ACTIVE FAULTS

14-08-0001-G1353

Shaul Levi

Geophysics, College of Oceanography
Oregon State University
Corvallis, Oregon 97331
(503) 754-2915

PALEOMAGNETIC RESULTS FROM SOLEDAD CANYON

Objectives: The purpose of this sudy is to establish the control of the San Gabriel fault (SGF) on the tectonics of this area since the deposition of the Saugus Formation, which occurred from about 2.3 to 0.4 Ma (Levi, et al., 1986). Toward this end we have been studying the paleomagnetism (PM) of the Saugus Formation in Soledad Canyon located in the San Gabriel block just northeast of the SGF. These results will be compared with our previous PM investigations of the Saugus Formation near Castaic, only 6-8 km to the west of Soledad Canyon, but off the San Gabriel block.

Results: Fourteen Saugus sites were sampled at the western end of Soledad Canyon (Figure 1) along the Southern Pacific Railroad just east of the intersection of the Sierra Highway and San Fernando Road. The sampling sites have east-southeast bedding attitudes and were distributed along approximately 1 km of the southeasterly trending railroad tracks, representing a vertical section on the order of 0.4 km.

Sites were chosen at the finer grain sedimentary interbeds, typically between 0.5 and 3 m in thickness. Three oriented hand samples were obtained at each site, and two specimens were cut from each sample. All specimens were stepwise demagnetized in alternating fields (AF) to 80 or 100 mT in 8 to 10 steps. For each site stable PM directions were determined by vector averaging the remanence vectors for 2 to 5 consecutive AF levels, chosen independently for each site. Within a site the same AF steps were used to obtain the stable direction of each specimen. The progression of PM directions during AF demagnetization for all six specimens from one normal and one reversed site are shown in Figure 2.

The stable PM directions for all sites are listed in Table 1 in *stratigraphic order:* Site 1 represents the oldest, first deposited material, and Site 15 is the uppermost, youngest sediment so far sampled in the section. All sites yielded polarity information, as well as characteristic PM directions. The oldest two sites are reversed. Of the overlying five sites, four are normal, with a reversed site sandwiched in the middle. The upper seven sites are reversed. Based on the predominantly reversed polarity of this section and in analogy with the reference section near Castaic, we conclude that the sampled sites in Soledad Canyon were deposited during the Matuyama, 0.7-2.5 Ma. However, it is not known at present which of the several normal subchrons in the Matuyama might be represented by the normal sites in the measured sequence.

Site mean PM directions were determined using 78 of the 84 demagnetized specimens (Table 1, Figure 3). The mean PM direction, treating the14 sites as reversed polarity, has $\overline{D}$ (declination) = 183°, $\overline{I}$ (inclination) = -49° with α_{95} = 10° and k = 18. This value is not significantly different from the expected geocentric axial dipole value at the sampling site, which is $\overline{I}$ = ±54°. Interestingly, the mean PM direction of the four normal sites has the expected dipole inclination, but $\overline{D}$ = 31°, probably because there are insufficient sites for proper averaging of the secular variation. However, the overall mean PM direction of the Soledad Canyon sites shows no significant tectonic rotation. This is in marked contrast with the Castaic section about 6-8 km to the west and southwest of the SGF, where a clockwise rotation of 30° has been recorded in Matuyama sites (Levi et al.,1986). The northern hemisphere virtual geomagnetic poles (VGPs) corresponding to the site mean PM directions are shown in figure 4. The mean VGP of the 14 sites, where all sites were considered as normal polarity, is at 86° N, 15°E (α_{95} = 11° and k = 14). Although the mean VGP is somewhat farsided, it does not deviate significantly from the Earth's rotation axis with respect to the α_{95} value.

The contrast between 1) the unrotated Saugus section in Soledad Canyon on the San Gabriel block and 2) the clockwise rotated Saugus near Castaic a mere 6-8 km to the west suggests that there has been an active tectonic boundary between the two sampling areas during the last 2.3 Ma, probably associated with the SGF or the Holser fault.

References:

Jennings, C.W., and Strand, R.G., 1969, Los Angeles sheet: Geologic map of California 1:250,000: Calif. Div. Mines and Geology.

Levi, S., Schultz, D.L., Yeats, R.S., Stitt, L.T., and Sarna-Wojcicki, A.M., 1986, Magnetostratigraphy and paleomagnetism of the Saugus Formation, near Castaic, Los Angeles County, California, in P.E. Ehlig, editor, Field Trip Guidebook and Volume on Neotectonics and Faulting in Southern California and Baja California, Cordilleran Section, GSA, 82nd Annual, Los Angeles, California, p. 103-108.

Treiman, J. and Saul, R., l986, The mid-Pleistocene inception of the Santa Susana Mountains, in P.E. Ehlig, editor, Fieldtrip Guidebook and Volume on Neotectonics and Faulting in Southern California and Baja California, Cordilleran Section, GSA, 82nd Annual, Los Angeles, California, p. 7-12.

TABLE 1

SOLEDAD CANYON, SUMMARY OF PALEOMAGNETIC RESULTS

Site No.	N/n	D_R°	I_R°	k	α_{95}(°)	Levels (mT)	Bedding Strike/Dip	VGP-northern hemisphere pole Long	Lat
SOC 15	6/6	190.2	-18.2	37	11.2	60-80(2)	106.5°/44.5°S	38.6	63.2
SOC 14	6/6	176.7	-47.0	128	5.9	50-80(3)	125°/59°SW	86.7	83.2
SOC 13	4/6	169.1	-37.5	50	13.2	40-80(4)	117°/32°S	99.9	73.5
SOC 12	6/6	174.9	-48.6	113	6.3	50-80(3)	119°/57.5°S	104.5	83.5
SOC 11	6/6	145.9	-52.2	406	3.3	50-80(3)	119°/57.5°S	-202.1	61.7
SOC 10	6/6	173.1	-58.9	66	8.3	50-80(3)	127°/57°SW	-163.0	82.4
SOC 9	6/6	194.3	-46.3	241	4.3	40-80(4)	124°/58°SW	-3.3	76.0
SOC 8	4/6	32.5	71.9	33	16.2	40-100(5)	114°/58.5°S	-84.1	58.6
SOC 6	5/6	29.9	43.9	54	10.5	20-50(4)	94.5°/36°S	-18.0	62.8
SOC 5	6/6	150.1	-30.9	16	17.5	50-100(4)	94.5°/36°S	125.5	57.9
SOC 4	5/6	25.5	46.3	19	18.2	50-100(4)	91.5°/49.5°S	-18.2	67.2
SOC 3	6/6	39.1	59.4	87	7.2	50-80(3)	99°/54°S	-50.8	58.6
SOC 2	6/6	186.5	-50.5	62	8.6	30-60(4)	78°/53°S	-0.1	83.7
SOC 1	6/6	177.3	-48.7	106	6.5	30-50(3)	78°/53°S	87.8	84.7
MEAN	14	182.9	-49.0	18	9.6				
MEAN	14			14	11.0			15.1	85.7

N/n, number of specimens used in calculations/number of specimens measured.

D_R, I_R, structurally corrected declination (D) and inclination (I); rotated to horizontal using measured bedding attitude (strike/dip).

k, best estimate of precision parameter of Fisher distribution.

α_{95}, radius in degrees of the 95 percent cone of confidence about the mean direction.

Levels, range of consecutive AF demagnetization steps in millitesla; number of steps are given in ( ).

VGP Long., positive (negative) east (west) of Greenwich.

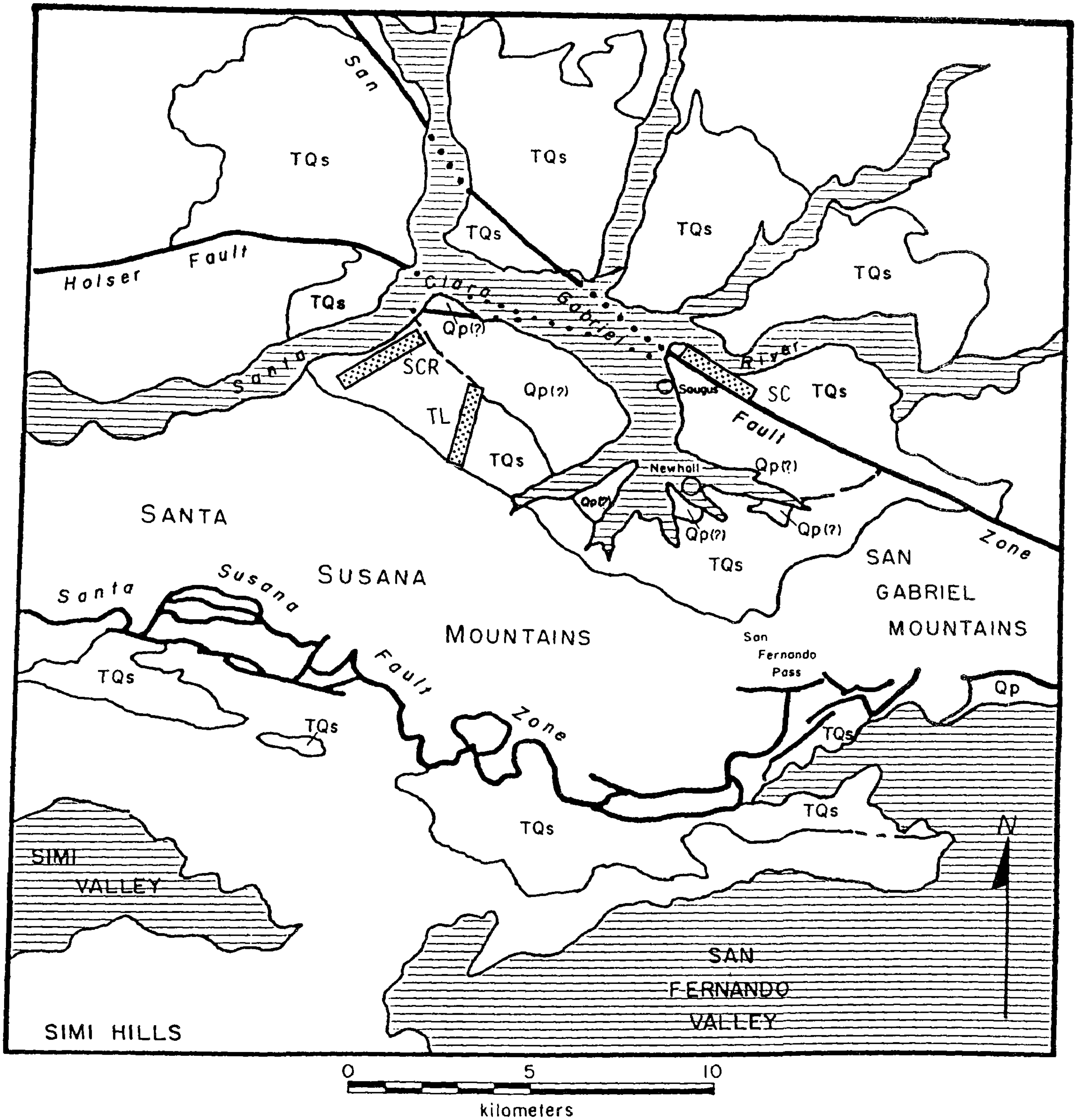

Figure 1. Generalized geologic map (modified from Jennings and Strand, 1969).
From Treiman and Saul, 1986

- alluvial valleys
Qp - Pacoima Formation, queried where correlation is tentative
TQs - Saugus Formation
- Paleomagnetic sections (SCR, TL, SC)

Areas not labeled include Tertiary and older rocks.

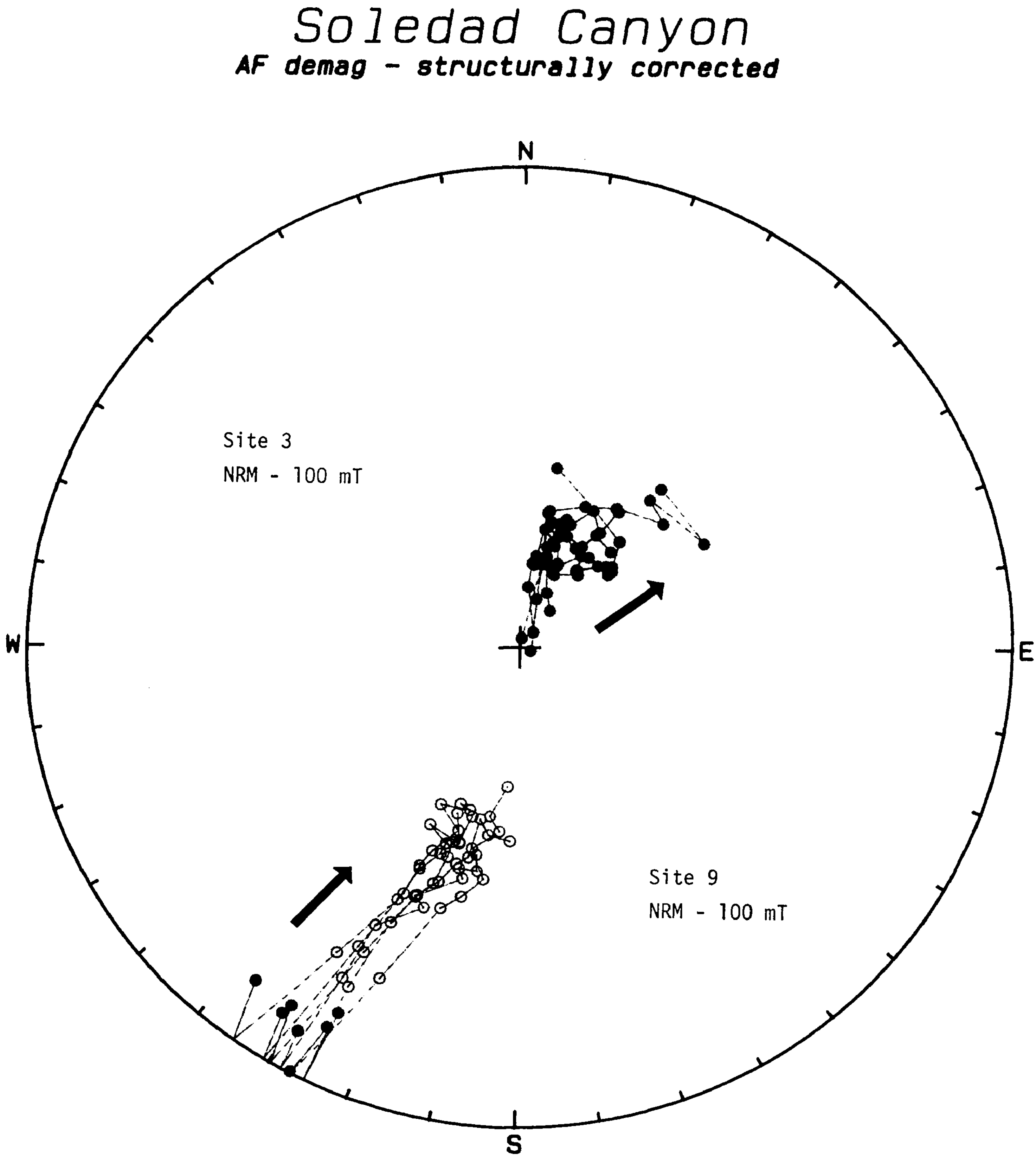

Figure 2. Stereogram of structurally corrected PM directions during AF demagnetization for all six specimens from normal site 3 and reversed site 9. Solid (open) symbols represent lower (upper) hemisphere directions. The arrows indicate the trend of movement of the remanence directions during demagnetization in progressively increasing AF

Soledad Canyon

Site mean directions - structurally corrected

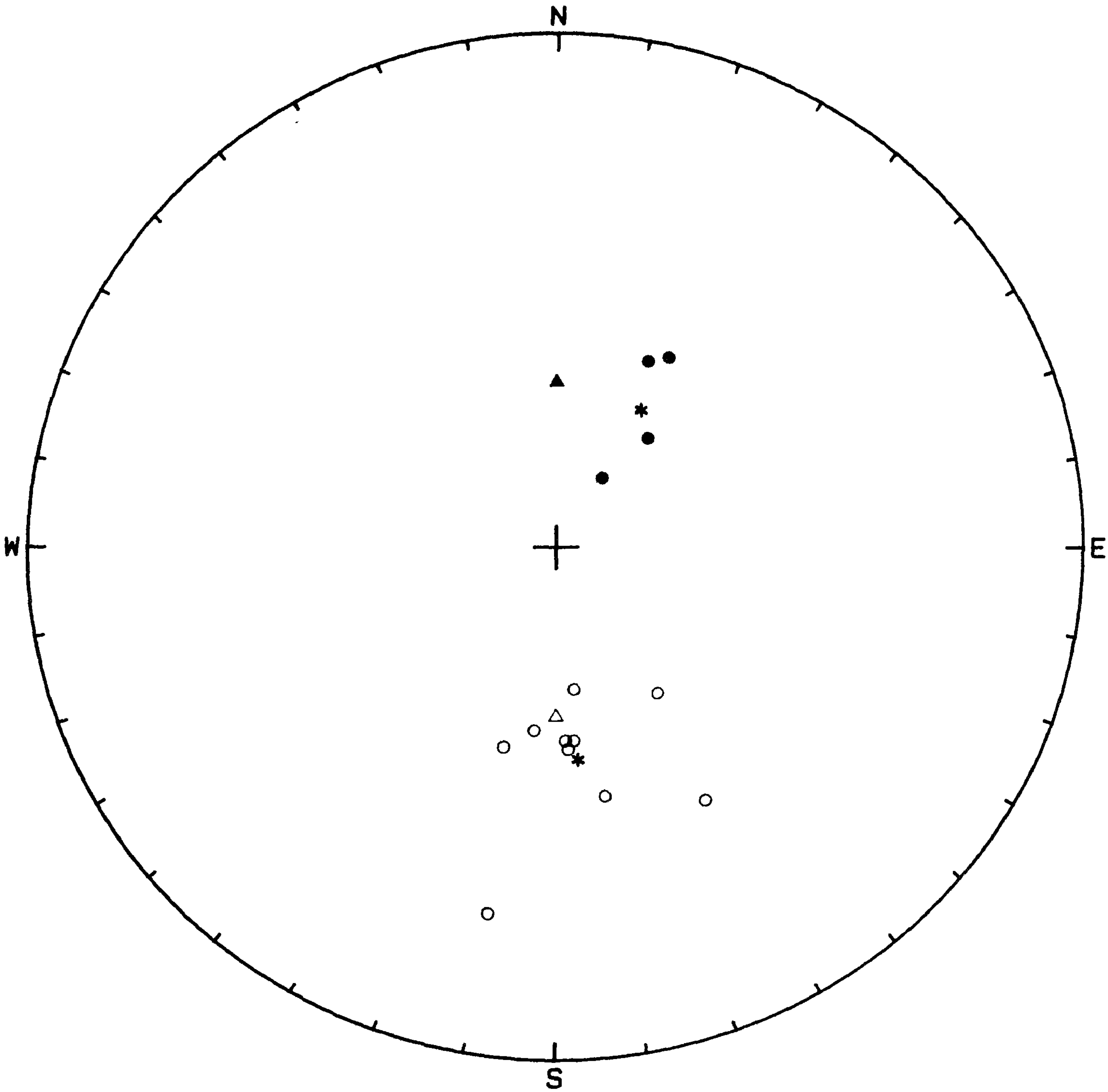

Figure 3. Stereogram of structurally corrected site mean PM directions (circles). Solid (open) symbols represent lower (upper) hemisphere directions. Triangles represent the expected geocentric axial dipole directions. The stars represent the mean PM directions of the normal and reversed sites separately.

Soledad Canyon

Site VGP's

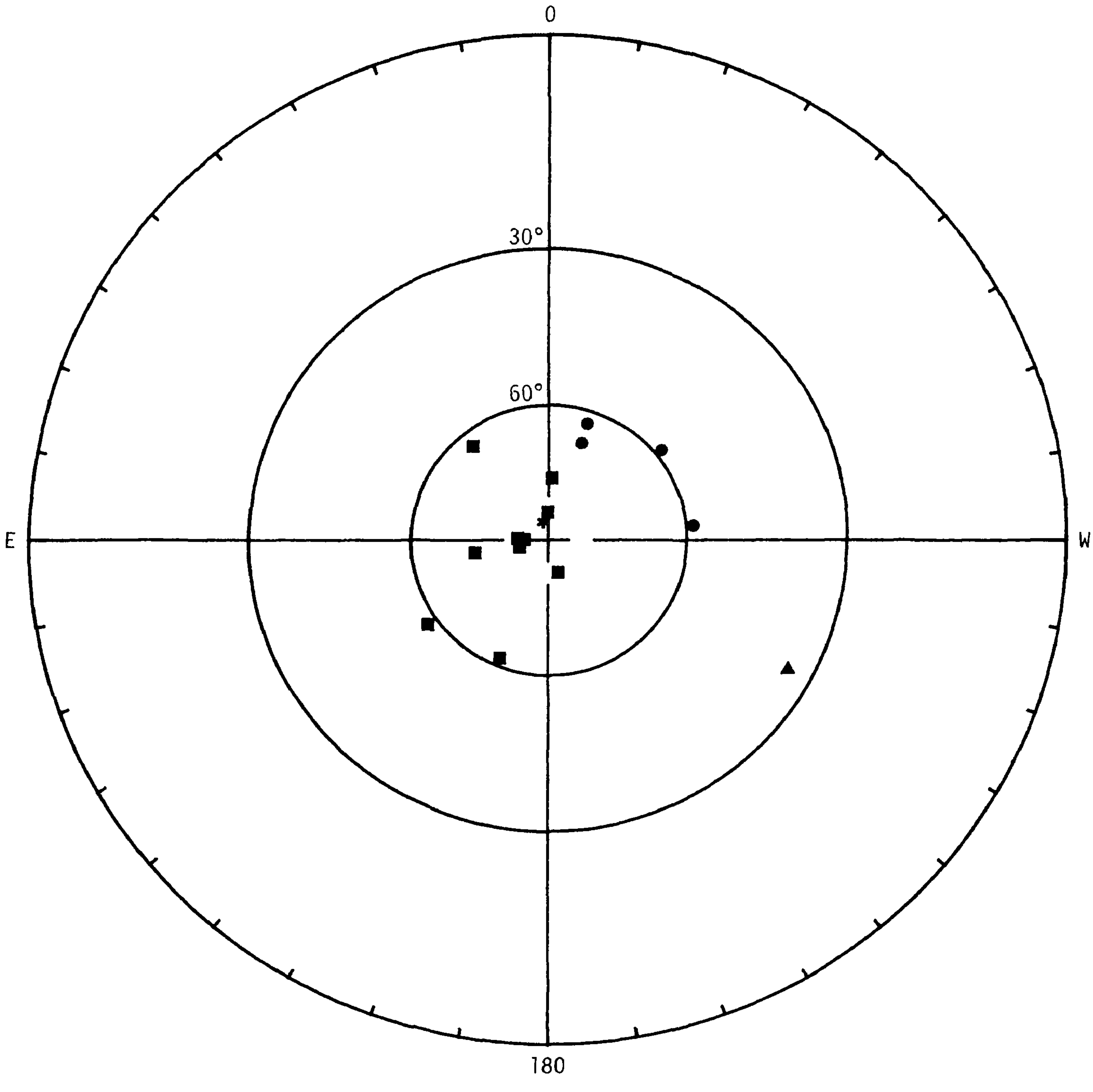

Figure 4. Northern hemisphere VGPs of structurally corrected Soledad Canyon sites. Triangle represents the sampling area at Soledad Canyon (34°25'N 118°32'W); the star denotes the mean VGP.

Earthquake Hazards Studies, Upper Santa Ana Valley and Adjacent Areas, Southern California

9540-01616

Jonathan C. Matti
Office of Régional Geology
U.S. Geological Survey
National Center, MS 908
12201 Sunrise Valley Drive
Reston, Virginia 22092
(703) 648-6966

Investigations

1. Studies of the Quaternary history of the upper Santa Ana River valley. Emphasis currently is on: (a) generation of a liquefaction susceptibility map, and (b) the three-dimensional distribution of the valley fill and its lithologic, lithofacies, and pedogenic character.

2. Neotectonic studies of the San Andreas fault zone and associated fault complexes. The study has focussed on: (a) mapping fault strands that deform crystalline basement rocks, Tertiary sedimentary rocks, and Quaternary surficical units; (b) identification of Quaternary units to establish Quaternary depositional patterns, relative ages of displacements along various fault strands, and rates of Quaternary fault slip; and (c) interpreting kinematic relations between the Crafton Hills fault complex, the San Gorgonio Pass fault complex, and the modern trace of the San Andreas fault.

Results

1. J.C. Matti and S.E. Carson completed an investigation of earthquake-induced liquefaction susceptibility in alluvial sediments of the San Bernardino valley and vicinity, southern California. The study includes maps that zone the region into areas having high to low susceptibility for each of three scenario earthquakes: a M_s=8.0 earthquake on the San Andreas fault, a M_s=7.0 earthquake on the San Jacinto fault, and a M_s=6.75 earthquake on the Cucamonga fault.

A M_s=8.0 earthquake on the San Andreas fault is accompanied by elevated (H, MH) susceptibilities in the San Bernardino valley region wherever ground water is shallow. Within 0 to 4 miles of the fault, the overall susceptibility of sands and silty sands is H, even where ground water is as deep as 30 to 50 ft subsurface. For areas 4 to 8 miles from the fault, overall susceptibilities remain H where ground water is shallower than 10 ft subsurface but decline to M where ground water is deeper. At all distances from the fault populations of silty samples have lower susceptibility than sand samples, but the numerical abundance of susceptible sand samples pulls the overall susceptibility rating up to H even at deeper ground-water levels.

A M_s=7.0 earthquake on the San Jacinto fault is accompanied by elevated susceptibilities (H, MH) wherever ground water is shallower than 20 ft within 0 to 4 miles of the fault and wherever ground water is shallower than 10 ft within 4 to 8 miles of the fault. Within 0 to 4 miles of the fault, susceptibilities decline to M wherever ground water is between 20 and 50 ft subsurface; within 4 to 8 miles of the fault, susceptibilities decline to M and L where ground water is between 30 and 50 ft subsurface. In general, populations of silty samples appear to be less susceptible than sand samples, especially at ground-water levels below 30 ft subsurface.

Elevated susceptibilities accompanying a M_s=6.75 earthquake on the Cucamonga fault are not as widespread as those for larger earthquakes on the San Andreas and San Jacinto faults. Within 0 to 4 miles of the fault susceptibilities probably are H and MH where ground water is shallow, but because penetration data from this fault-distance interval were not available for our investigation the susceptibility ratings are inferred based on their comparison with susceptibility results from equivalent ground-water intervals at greater distances from the fault. At all distances between 4 and 15 miles of the fault H or MH susceptibility occurs wherever ground water is shallower than 10 ft, but susceptibilities decline to M and L where ground water is deeper than 10 ft subsurface.

The shape and size of the susceptibility zones largely are controlled by depth to ground water and distance to the causative fault, although the age and type of sediment also influence its susceptibility. The main zones of elevated susceptibility accompanying earthquakes on the San Andreas, San Jacinto, and Cucamonga faults are associated with shallow ground-water zones which occur under the modern flood plains of Cajon Creek, Warm Creek, and the Santa Ana River. These areas are underlain by recently deposited Holocene sediments which would be expected to have lower penetration resistance and higher susceptibility than older sediments. However, even the older Holocene and latest Pleistocene sediments have elevated susceptibilities comparable to those in the younger deposits, and this fact accounts for zones of H and MH susceptibility which extend away from the modern flood plains and into adjacent areas underlain by older deposits. Additional areas of elevated susceptibility occur in isolated zones downstream from the mouths of canyons along the base of the San Bernardino Mountains.

The widespread distribution of susceptible conditions within near-surface alluvial sediments of the San Bernardino valley region can be attributed to the strong ground-shaking conditions accompanying the large-magnitude earthquakes specified by our analysis. The large peak-acceleration values posed by these scenario earthquakes are greater than those based on probabilistic seismic-potential analyses. The latter scale down ground-motion parameters by using peak-acceleration values that are likely to be exceeded by earthquakes within a specified return period (such as 50 years). If large earthquakes occur in the San Bernardino valley region in the next few decades, as some workers have proposed, then a large-magnitude scenario-earthquake approach to regional hazard analysis is appropriate for evaluating liquefaction susceptibility in the San Bernardino valley region.

Although the evaluation of hazards resulting from liquefaction-induced ground failure is beyond the scope of our investigation, the susceptibility maps indicate where ground failures are most and least likely to occur. Within zones of high and moderately high susceptibility, liquefaction-induced ground failures are most likely, at least on a regional basis. These areas require special attention during land-use planning and future development, and mitigation of existing hazards may be advisable. In areas having moderate to low susceptibility, liquefaction-induced ground failures are less likely.

2. J.C. Tinsley and J.C. Matti completed the initial phase of trenching and stratigraphic studies designed to reconstruct the history of faulting in the San Gorgonio Pass fault zone--a zone of thrust and wrench faults that bounds the southeastern margin of the San Bernardino Mountains. The faults form scarps in Holocene alluvial-fan deposits, and this setting provides an opportunity to evaluate rates of faulting recurrence and fault slip within a region where slip apparently steps left between the Coachella Valley and Mojave Desert segments of the San Andreas fault and leads to crustal convergence within the San Gorgonio Pass fault zone.

Our investigation has focussed on east-trending fault scarps that traverse young alluvial deposits on the Millard Canyon alluvial fan north of Cabazon, California. One scarp in Sec. 5, T. 3 S., R. 2 E., traverses at least two different-aged alluvial deposits and has a different surface offset in each. The scarp is about 20 m high in deposits whose soil-profile characteristics are similar to those of deposits dated at less than 5,000 years elsewhere in the Transverse Ranges. Along strike, where it traverses a younger Holocene alluvial unit having weak A and C_{ox} horizons, this 20-m scarp has only 1.5 to 2 m of surface offset.

Backhoe excavations across both scarp segments provide outstanding examples of thrust-fault geometries in young coarse-grained alluvial sediments. The 20-m-high scarp was trenched at a point about 150 m west of Millard Canyon wash; the trench was 32 m long and about 4 m deep, and extended from the downthrown block northward to a point about two-thirds of the way up the scarp face. The deposits of sandy cobble-boulder gravel are well stratified and are cut by four discrete fault planes that dip north at 15° to 25°. The gravels also are warped in the vicinity of the scarp face. The 2-m-high scarp was excavated by cleaning off the east-facing wall of Millard Canyon wash, thereby providing excellent exposures of the well-stratified sandy gravel and two north-dipping thrust-fault planes that dip 25° to 27°. Measurable dip-slip offsets amount to 173 cm, with an additional amount of strain taken up by warping. The low scarp and its associated fault planes probably represent one ground-rupture event, although more than one rupture cannot be ruled out by the observed relations. Radiocarbon samples (detrital charcoal) were obtained from two levels in the excavation, above and below a disconformity.

We described and sampled soil profiles from these two excavations, from soil pits on the alluvial-fan surface of the upthrown and downthrown blocks, and from excavations across a 4-m-high thrust-fault scarp about one mile north in Sec 32, T. 2 S., R. 2 E. The samples will be analyzed by L.D. McFadden at the University of New Mexico, Albuquerque.

3. Continued regional investigations by R.J. Weldon and J.C. Matti have led to the recognition that the southern San Andreas fault between Palmdale and the Coachella Valley may be segmented by regional patterns of secondary faulting. Most active secondary faults within 20 km of the fault in this region exhibit principal components of either normal or reverse slip. These faults define alternating regions of secondary extension or compression. Boundaries between these regions correspond to geometric complexities in the fault system, including the northern termination of the San Jacinto fault and each end of the east-trending part of the San Andreas in the San Gorgonio Pass region. The fact that the 1857 rupture on the San Andreas fault terminated at a boundary between compressional and extensional regions suggests that they can be useful for defining future rupture segments. Because the 1857 rupture included several compressive regions but ended at an extensional region in the south and the creeping zone to the north, "weak" regions may limit rupture--not "strong" regions as is widely thought. The location of the 1986 Palm Springs M_s=6.0 earthquake--at the boundary between reverse faulting in San Gorgonio Pass and secondary normal faulting to the east--suggests that the boundaries between compressional and extensional domains also may influence the distribution of moderate-sized earthquakes.

Publications

Matti, Jonathan C., and Carson, Scott E., 1986, Liquefaction susceptibility in the San Bernardino Valley and vicinity, southern California: a preliminary evaluation: U.S. Geological Survey Open-File Report 86-562, 40 p., scale 1:48,000

Weldon, Ray, and Matti, Jonathan, 1986, Geologic evidence for segmentation of the southern San Andreas fault: American Geophysical Union Transactions, EOS, v. 67, p. 905-906.

Structural Framework of the Peninsular Ranges

9540-04040

Douglas M. Morton
Branch of Western Regional Geology
U.S. Geological Survey at Dept. of Earth Sciences
University of California, Riverside
Riverside, California 92521
(714) 787-3429

Investigations

Continued study of tectonic history of the San Jacinto Graben area and San Jacinto fault geomorphology along the west side of the San Timoteo Badlands. Mapped ground fracturing and landsliding produced by the July 8, 1986 North Palm Springs earthquake. Began revision of the Devore and Cucamonga Peak 7.5' quadrangles.

Results

The July 8, 1986 North Palm Springs earthquake produced a considerable array of fractured ground and landslides. Most of the fractured ground, nascent landslides, was located within 200 m of the Banning fault, on which the earthquake probably occurred. A minority of the fractures along the fault are probably tectonic ruptures on the fault. Most are fault related, not produced merely from ground shaking, but are probably a result of seismogenic displacement at depth. Thoroughly shattered ridge tops were common near the Banning fault. Landslides, mainly debris slides and rock falls occurred over an area of 300 km^2. Weak materials, mainly fractured basement and unconsolidated sediments, on steep slopes were particularly landslide prone.

Reports

Gilmore, T. D., 1986, Historic vertical displacement in the Salton Trough and some adjoining parts of southeastern California: U.S. Geological Suvey Open File Report 86-380, 183 p., 11 plates.

Harding, S, T., Wesson, R. L., Nicholson, C., and Morton, D., 1986, Shallow reflection profiling across the trace of the southern San Andreas fault: AGU Transactions, vol. 67, no. 44, p. 1200.

Morton, D. M., 1986, Contrasting pultons in the northern Peninsular Ranges batholith, southern California: Geological Society of America Abstracts with Programs, vol 18, no. 2, p. 161.

Morton, D. M., Matti, J. C., Tinsley, J. C., 1987 (in press), Banning fault, Cottonwood Canyon, San Gorgonio Pass, southern California, Geological Society of America DNAG vol., Centennial Field Trip Guide, Cordilleran Section.

Morton, D. M., Matti, J. C., and Tinsley, J. C., 1987 (in press), Cucamonga fault zone scarps, Day Canyon alluvial fan, eastern San Gabriel Mountains, southern California: Geological Society of America DNAG vol., Centennial Field Trip Guide, Cordilleran Section.

Morton, D. M. and Miller, F. K., 1987 (in press), K/Ar apparent ages of plutonic rocks from the northern Peninsular Ranges batholith, southern California: Geological Society of America Absracts with Programs, vol. 19, no. .

Rymer, M. J., Sharp, R. V., and Morton, D. M., 1986, Surface fractures on the Banning fault associated with the North Palm Springs earthquake of 8 July 1986: AGU Transactions, vol. 67, no. 44, p. 1090.

Sharp, R. V., Rymer, M. J., and Morton, D. M., 1986, Trace fractures on the Banning fault created in association with the 1986 North Palm Springs earthquake: Bulletin Seismological Society of America, vol. 76, no. 6, p. 1838-1843.

Todd, V. R., Erskine, B. G., and Morton, D, M., in press, Metamorphic and tectonic evolution of the northern Peninsular Ranges batholith, southern California: Rubey Vol., 73 p.

Wesson, R. L., Jibson, R. W., Morton, D., Campbell, R. H., and Nicholson, C., 1986, Intepretation of surface cracks and other fault-line surface deformation associated with the North Palm Springs earthquake of July 8, 1986: AGU Transactions, vol. 67, no. 44, p. 1090.

Holocene Displacements of the Alvord Fault and the Steens Fault Zone, Southeastern Oregon

Grant No. 14-08-0001-G1333

William D. Page, Mark A. Hemphill-Haley
Woodward-Clyde Consultants
100 Pringle Avenue, Suite 300
Walnut Creek, CA 94596-3564

Gary A. Carver, Raymond (Bud) Burke
Department of Geology
Humboldt State University
Arcata, CA 95521

Steens Mountain in southeastern Oregon is the northwestern most range in the Basin and Range tectonic province. It is a 90-km-long, west-tilted range that is bounded on the east by normal, range-front faults of the Steens fault zone (SFZ).

Recent studies by Hemphill-Haley (1987) on the Alvord fault within the SFZ found fresh scarps extending 20 km along the range front. The scarps displace deposits and shorelines of pluvial Lake Alvord correlated with the 12,000-year-old pluvial Lake Lahontan stand (Hanks and Wallace, 1985; Thompson, et al., 1986). Degradational analysis of the scarp and presence of a basal graben along one segment of the fault indicates late Holocene movement. This evidence of late Holocene rupture on the Alvord fault contrasts with the fact that no significant historical earthquakes are known in this part of southeastern Oregon.

Favorable trench sites have been located where the style of faulting and chronology of the most recent events have a strong likelihood of being established.

Objectives

The proposed study has four objectives: 1) to better characterize the SFZ and the Alvord fault; 2) to obtain data for scarp degradation analysis; 3) to contrast and compare the results to tectonically similar faults in more densely populated areas of Nevada and Utah; and 4) to add information to the fault length and displacement relationships for normal faults in the Basin and Range province (Bonilla and Buchanan, 1970; Slemmons, 1977). Investigations proposed for this study will be done by professionals from Woodward-Clyde Consultants (WCC) and Humboldt State University (HSU). The proposed program includes aerial reconnaissance and taking of low-sun-angle aerial photographs, mapping of the Steens fault zone using the new photographs, excavation of at least two trenches across the Alvord fault, and estimating the ages of the Holocene deposits associated with the faulting using correlations and, if suitable materials are found, C-14 and tephrochronology.

Results

This grant commenced on 15 January 1987, and only preparatory work has been conducted to date. Low-sun angle aerial photographs will be taken in May 1987. Trenching will take place July and August 1987.

References

Bonilla, M. G., and Buchanan, J. M., 1970, Interim report on worldwide historic surface faulting; Geological Survey Open-File Report, 31 p.

Hanks, T. C., and Wallace, R. E., 1985, Morphological analysis of the Lake Lahontan shoreline and beachfront fault scarps, Pershing County, Nevada; Bull. Seismological Society America, v. 75, no. 3, pp. 835-846.

Hemphill-Haley, M., (1987), Quaternary stratigraphy and late Holocene tectonics along the eastern escarpment of Steens Mountain, southeastern Oregon; Humboldt State University Masters thesis.

Slemmons, D. B., 1977, Faults and earthquake magnitude in State-of-the-art for assessing earthquake hazards in the United States; U. S. Army Waterways Experiment Station Miscellaneous Paper 5-73-1, no. 6.

Thompson, R. S., Benson, L., and Hattori, E. M., 1986, A revised chronology for the last Pleistocene lake cycle in the central Lahontan basin; Quaternary Research, v. 25, pp. 1-9.

Detailed Geomorphic Studies to Define Late Quaternary Fault Behavior and Seismic Hazard, Central Nevada

14-08-0001-G136

Philip Pearthree, Karen Demsey, W.B. Bull, Oliver Chadwick, Julia Fonseca, Steve Slaff
Department of Geosciences
University of Arizona
Tucson, AZ 85721
(602) 621 2219

Project goals

The primary *objective* of this project is to better define Quaternary fault behavior in the region including the large historic earthquakes of Nevada--the central Nevada seismic belt (CNSB). Our approach combines several detailed geomorphic studies of faulting along individual mountain fronts, reconnaissance studies of young faulting over a broad region in central Nevada, and analyses of landforms and stream gradients to assess rates of late Quaternary fault activity. The goals of this project are to compare historic, Holocene, and longer-term patterns of fault activity, assess geologic (>100 yrs.) rates of large earthquake occurrence, and estimate the rate of extension across central Nevada.

Investigations

Detailed geomorphic studies along parts of the 1915 Pleasant Valley surface rupture, the Stillwater seismic gap, the 1954 Dixie Valley surface rupture, and the Wassuk Range have been summarized in earlier project summaries (also, Hecker, in press; Fonseca, in review; Demsey, in prep.; Pearthree et al, 1986). Reconnaissance studies in progress will cover the area from the CNSB east to the Toiyabe and Cortez ranges. All field studies have involved acquisition of fault scarp profiles and soil profile data to constrain as closely as possible age estimates for large Holocene earthquakes in central Nevada. When field studies are completed, we anticipate being able to delineate spatial and temporal patterns of Holocene faulting across a broad region in central Nevada. These data may permit estimation of the Holocene rate of extension across this region. Topographic maps and aerial photos are being used in quantitative analyses of landforms and stream gradients to determine relative rates of late Quaternary activity along faults with primarily dip-slip movement. The Holocene record will supply relatively short-term, high-resolution information on regional patterns of individual faulting events; the late

Quaternary record will not identify individual faulting events well but will identify consistently active faults.

Preliminary Results

Studies conducted to date have defined some patterns of Holocene faulting and the most active dip-slip faults in the CNSB. The most recent large prehistoric surface ruptures identified in the CNSB occurred in the mid- to late Holocene along the Wassuk Range, the Stillwater Range in Dixie Valley, the Sulphur Springs fault in Pumpernickel Valley (see also Wallace, 1979), and possibly the east side of the Tobin Range in Buffalo Valley. Earlier Holocene activity is less thoroughly defined, but ruptures occurred along the Wassuk Range and the west side of the Tobin Range in Pleasant Valley (along part of the 1915 rupture). Faults involved in the 1954 Fairview Peak surface rupture were last active in the late Pleistocene. We have found no clear evidence of prehistoric analogs to the belt-like historic pattern of surface ruptures.

Tectonic landform and stream gradient analyses indicate that the Stillwater Range in Dixie Valley and the Wassuk Range along Walker Lake have been the most active predominantly dip-slip fault zones in the CNSB area during the late Quaternary; the Tobin Range in Pleasant Valley may be only slightly less active. This is consistent with our interpretation that these fault zones have had recurrent movement in the last ~13 ky (post-Lahontan highstand) while other fault zones either have not been active or have been active only once.

References

Demsey, Karen, in prep, Holocene faulting and tectonic geomorphology along the Wassuk Range, west-central Nevada: Prepub ms, Dept of Geosci, Univ of Arizona.

Fonseca, Julia, in review, The Sou Hills--a barrier to faulting in the Central Nevada Seismic Belt: **J Geoph Res.**

Hecker, S, in press, Timing of Holocene faulting in part of a seismic belt, west-central Nevada: **Bull Seis Soc Am.**

Pearthree, P.A., Fonseca, Julia, Hecker, Suzanne, 1986, Patterns of Holocene and Quaternary faulting in the central Nevada seismic belt: Implications for fault behavior in the northern Great Basin: **GSA Abstr with Progams, 18.**

Wallace, R.E., 1979, Map of young fault scarps related to earthquakes in north-central Nevada: **USGS Open-file Rpt 79-1554.**

EVALUATION OF ACTIVITY OF THE SAN GABRIEL FAULT ZONE, LOS ANGELES AND VENTURA COUNTIES, CALIFORNIA

14-08-0001-21928

F.H. Weber, Jr.
California Department of Conservation
Division of Mines and Geology
107 South Broadway, Room 1065
Los Angeles, CA 90012
(213) 620-3560

Investigations

Two sites along the fault are to be trenched in late April to June 1987 involving the portion of the contract funds released for expenditure by the State of California. The first site is on the Bermite property in the Saugus area, 6 km southeast of the site where displacement of Holocene alluvial materials was observed in a trench dug by W. Cotton, P. Ehlig and A. Seward. The second site is about 1 km west of Clear Creek guard station of the U.S. Forest Service in the western San Gabriel Mountains.

Results

Since preparation of the last report, very detailed geologic mapping has been done in the Smith Fork area, near the northwestern terminus of the San Gabriel fault. The mapping substantiates conclusions reached in previous mapping by the writer that the San Gabriel fault is not overlapped by nonmarine sedimentary rocks of the Hungry Valley Formation as concluded by previous workers. Strata typical in clast content of all but uppermost Hungry Valley Formation extend along the fault for 8 km southeast of the terminus. These strata would extend against, and abut the fault if not interrupted by Violin Breccia.

An article by the writer (Weber, 1987, in press) was submitted for publication to California Geology in January 1987. This article is partially in reply to a rebuttal by J.C. Crowell (Crowell, 1986) to a previous article by the writer (Weber, 1986).

References Cited

Crowell, J.C., 1986, Geologic history of the San Gabriel fault, central Transverse Ranges, Kern, Los Angeles, and Ventura Counties, California: California Geology, v. 39, no. 12, p. 276-281.

Weber, F.H., Jr., 1986, Geologic relationships between the San Gabriel and San Andreas faults, Kern, Los Angeles, and Ventura counties: California Geology, v. 39, no. 1, p. 5-14.

Weber, F.H., Jr., 1987 (in press), Geologic relationships along the San Gabriel fault between Hardluck Canyon and Castaic, Los Angeles and Ventura counties, California: California Geology.

Earthquake Hazards Reduction Program
9560-01568
Stephen W. Robinson
U.S. Geological Survey
345 Middlefield Drive, MS 937
Menlo Park, CA 94025

Investigations

In the first half of FY87 the following radiocarbon dating investigations related to earthquake hazards reduction have been conducted: (with the cost to the Branch of Isotope Geology).

1. Alaskan Coastal Earthquake Hazards Investigation - S. Bartsch-Winkler and H. Schmoll ($3000).

2. California Coastal Disaster Area Study - K. Lajoie ($6500).

3. Puget Lowland Seismic Hazards - B. Atwater ($3000).

4. Wasatch Front seismic Hazards Reduction - M. Machette ($4000).

On the horizon we have:

5. Palmdale Seismic Hazards - Dave Schwartz (perhaps $15,000).

6. Earthquake Potential of Fold Belts - Dave Trumm ($7000-8000).

Thus we see that the annual radiocarbon dating requirements of the Earthquake Hazards Reduction Program are still at the 'normal' level of $40,000 per year.

The Role of Block Rotation in Wrench Tectonics Along the San Jacinto Fault Zone, Southern California

USGS 14-08-0001-G-1330

Leonardo Seeber
Lamont-Doherty Geological Observatory of Columbia University
Palisades, New York 10964
(914) 359-2900

April 30, 1987

During recent field work on the southern San Jacinto Fault Zone, Lamont graduate students Ken Hudnut and Pat Williams found evidence that the Superstition Mountain Fault has been active in the Late Holocene. Their main evidence is that the highest and most prominent berm deposits of the ancient Lake Cahuilla are vertically offset by about 2 m (NE-down) across the fault zone (see Figure 1). In addition, a well-developed, subsequently deposited, recessional berm is not significantly offset. Thus, it appears that the displacement occurred rapidly (presumably in a large earthquake) between the times of deposition of the two berm deposits.

Date of Slip Event: Our present best estimate is that the high berm, which is offset, was deposited during the latest lake filling, circa 290 yr. B.P. (Sieh, 1985), and that the recessional berm was deposited some 20 years or so later. Thus we might constrain the date at 300 ± 10 yr. B.P. It is possible, however, that the offset berm was deposited during an earlier filling of the Salton Trough (there have been several lakes in the past millenia whose shorelines were at about the same elevation), in which case the event may be considerably older. Microstratigraphic analysis, carbon dating, and determining the absolute elevation of the berm deposits (for comparison to the known 290 yr B.P. lake level) should eventually resolve this ambiguity.

Amount of Slip in Event: Work so far indicates up to 2 m of dip-slip (NE-down) at the SE end of the rupture, and about 1.1 m of right-lateral slip along the southeastern 10 km of the Superstition Mtn. Fault. The dip-slip component is obtained from offset shoreline deposits, whereas the lateral component is obtained from preliminary statistical analysis of about 70 offset stream channels along part of the fault zone (see Fig. 2). For now, we presume that the offset channels correlate to the same event as the offset shoreline deposits, yet this remains unproven. Our study of the shoreline morphology indicates a surprisingly narrow zone of deformation, perhaps suggesting that the large dip-slip component is localized and involves shallow sediment deformation in response to predominantly lateral slip at depth. Dislocation and boundary-element modeling are being used to constrain our interpretation of the narrow deformed zone. Modeling and further field study of channel offsets should allow an estimate of moment release for this presumably seismic event. Rupture included at least the southeast 7 km of the Superstition Mtn. Fault, but we do not yet have data on the total rupture length, so our next step for field study is to do further channel-offset work towards the northwest along the Coyote Creek Fault strand. We also will study the Lake Cahuilla shoreline crossings at the northwest end of the Superstition Mtn. Fault and at the south side of Ocotillo Badlands. One of our 'working hypotheses' is that the event may have ruptured the southern half of the 1968 zone, or perhaps even further to the northwest.

Seismic Hazard: This report presents the first evidence for seismic slip on the Superstition Mtn. Fault, which is one of the two main strands of the southernmost San Jacinto Fault Zone. Previous to this work, Wesnousky's (1986) hazard analysis of the Superstition Mountain Fault estimated a 1 mm/yr seismic slip rate, a magnitude of 6.4 (from fault-length), and a repeat time of 468 years. We currently suspect that the magnitude of the event we are studying is larger than 6.4, considering that the M=6.4 Borrego Mtn.

earthquake in 1968 had a maximum lateral surface displacement of about 40 cm. It has been at least about 300 years since the shoreline-offsetting event. There is a suggestion from the channel offset data that this event was preceded by another event with a similar rupture. Since the previous event is not dated we cannot yet revise the recurrence interval; also, we cannot revise the slip rate estimate without further investigation.

If substantiated, our preliminary results on large prehistoric displacements on the Superstition Mtn. Fault may have fundamental implications about earthquake hazard and tectonics along the southern San Andreas and San Jacinto Fault system. Using intensity data and the available seismograms, we will be re-investigating the possibility that a M=6.5 earthquake in 1942 may have been on the Superstition Mtn. Fault. Field and office studies will be concerned with further constraints on the timing and spatial extent of the displacements, and on modeling to help explain the observed deformation. Hudnut and Williams are planning to weather the summer heat of the Imperial Valley for an additional ten days in early June.

Other accomplishments include mapping of cross-folds and faults west of the Coyote Creek Fault, south of the Borrego Sink, in the Superstition Hills, and along the Superstition Mtn. Fault, analysis of geodetic data from the Clark Lake Radio Observatory experiment, and analysis of paleomagnetic data from Borrego Badlands, south of the Inspiration Point Fault.

References:

Sieh, K., 1985. USGS Open-File Report #86-580, pg. 165 [Table 1-2].

Wesnousky, S., 1986. Earthquakes, Quaternary Faults, and Seismic Hazard in California, J. Geophys. Res., V. 91, p 12587-12631.

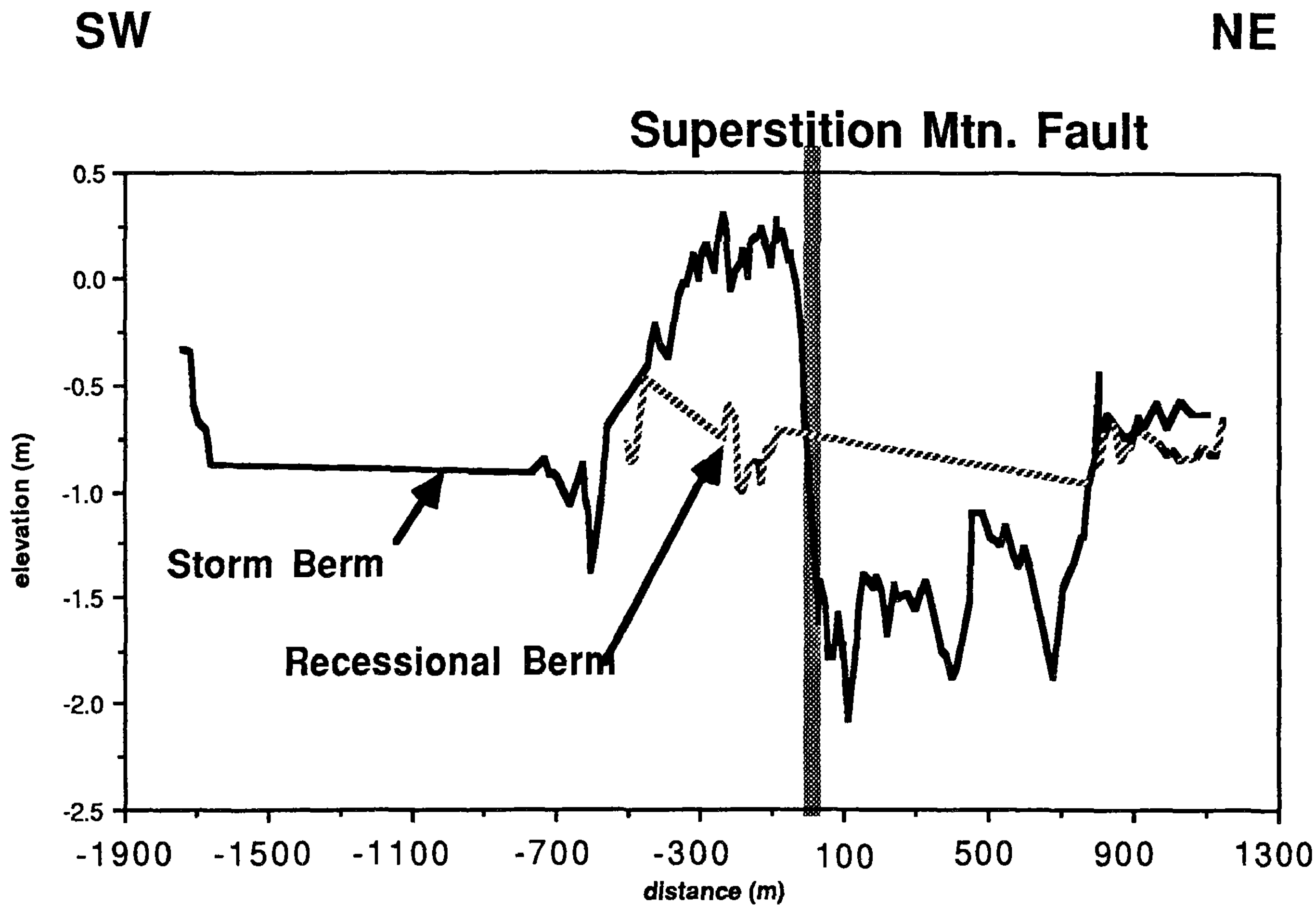

Figure 1. Plot of Lake Cahuilla shoreline deposit morphology near the intersection of the shoreline with the Superstition Mountain Fault. The storm berm is the highest in elevation of the shoreline deposits, and is the most prominent morphologically. It is offset by ~2 meters across the fault zone, with the NE side dropped down. The recessional berm was deposited later, and is not offset. This figure shows the main evidence for a slip event between the times of deposition of the two berm deposits.

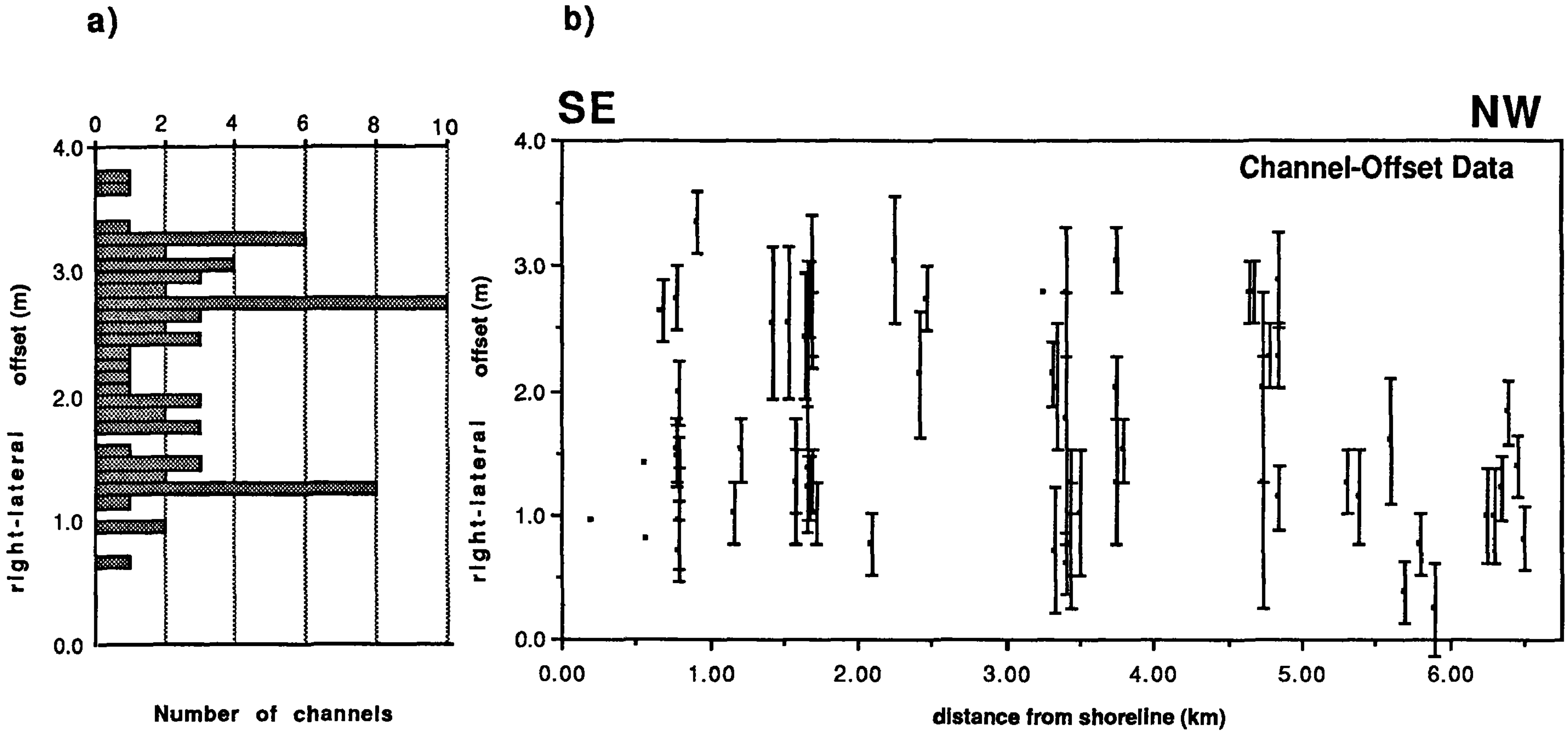

Figure 2. Plots showing a) bimodal distribution of channel-offset data, and b) channel offsets against distance along the Superstition Mtn. Fault from the shoreline crossing. Preliminary analysis shows a bimodal distribution in the offsets,with one mode at 1.14 m and another at ~2.48 m. Our interpretation is that this represents two seperate events of similar slip distribution along this segment of the fault. We infer that the more recent 1.14 m slip correlates to the same event which produced a 2 m dip-slip displacement of the Lake Cahuilla shoreline deposits. Clearly further study is needed to extend the study area towards the northwest, and to increase the number of observations.

Modeling of Induced Seismicity and Implications for Earthquake Prediction

USGS 14-08-0001-G-1358

D. W. Simpson
Lamont-Doherty Geological Observatory of Columbia University
Palisades, New York 10964
(914) 359-2900

Investigations:

A methodology has been developed, in cooperation with T.N. Narasimhan of University of California, Berkeley, for carrying out simple model simulations of the influence of reservoir loading on a deformable, porous, fluid-filled medium.

Studies of earthquakes at Aswan reservoir, Egypt, have provided a number of new insights into the mechanism of induced seismicity.

Monitoring of water levels in deep boreholes near Aswan Reservoir has provided information on the infiltration of water into the sandstone underlying the reservoir. Because of the virtual absence of external influences (precipitation, pumping, flow) on these wells, other than seepage from the reservoir, they also provide a set of very high quality data to study the influence of tidal stress and atmospheric pressure on water levels in piezometer wells.

Results:

Induced seismicity can result, on a short time scale, from a) the influence of increased elastic stress, either through the direct effect of increased shear stress, or b) through increased pore pressure from the reduction of pore space due to compaction. Diffusion of pore pressure to hypocentral depths is a longer term process and may be reponsible for those cases of induced seismicity where the onset of major seismic activity is delayed for some years after initial impoundment. Many of the temporal and spatial characteristics of cases of induced seismicity can be explained by the influence of inhomogeneities in the elastic and hydraulic properties of porous media beneath a reservoir. The presence of zones at depth of material with anomolous strength (Young's modulus) or pore pressure response (Skempton's constant) can concentrate the influence of the compaction effect on increasing pore pressure. This provides a mechanism by which the reservoir can act rapidly to decrease strength at depth, without the time necessary for diffusion from the surface. It also provides an explanation for the transient response and dependence on the rate of reservoir loading that is observed at some reservoirs. If the strength contrasts at depth are sufficient, the transient increases in pore pressure at depth can exceed the pressure increase at the base of the reservoir.

Flow of water into unsaturated pore space may have a significant influence on induced seismicity in areas where the water table is significantly raised by the filling of the reservoir. At Aswan reservoir, the water table in the Nubian sandstone rose more than 60 m after the area of induced seismicity was flooded. The influence of the water in the sandstone exceeded the effect of the lake alone, which had an average water depth of less than 10 m in the same area.

Reports:

Simpson, D. W., Triggered earthquakes, *American Review of Earth and Planetary Sciences, 14*, 21-42, 1986.

Kebeasy, R. M., M. Maamoun, E. Ibrahim, A. Megahed, D. W. Simpson, and W. S. Leith, Earthquake studies at Aswan Reservoir, *Journal of Geodynamics,* in press, 1987.

Simpson, D. W., R. M. Kebeasy, C. Nicholson, M. Maamoun, R. N. H. Albert, E. M. Ibrahim, A. Megahed, A. Gharib, and A. Hussain, Aswan telemetered seismograph network, *Journal of Geodynamics*, in press, 1987.

Simpson, D. W., and T. N. Narasimhan, Reservoir induced earthquakes and the hydraulic properties of the shallow crust, *EOS, Trans. AGU, 67*, 242, 1986.

Simpson, D. W., W. S. Leith,and C. H. Scholz, Two types of reservoir induced seismicity, preprint (to be submitted to *Bulletin of the Seismological Society of America*), 1987.

Comparative Study of the Neotectonics of the Xianshuihe Fault, China

Grant No. 14-08-0001-G1088

Clarence R. Allen
Seismological Laboratory, California Institute of Technology
Pasadena, California (818-356-6904)

Objectives

The purpose of this study is to investigate, together with Chinese colleagues from the Bureau of Seismology of Sichuan Province, the Xianshuihe fault of western Sichuan. This structure is among the world's most active faults, having producing 3 earthquakes during this century exceeding magnitude 7 along a 200-km length of the zone. At least 6 such events have occurred since 1725. In the more limited 60-km-long segment between Luhuo and Daofu, major earthquakes in 1923, 1973, and 1981 ($M = 7\frac{1}{2}$, 7.6, 6.9) were associated with overlapping surficial fault ruptures, and with individual left-lateral displacements as large as 3.6 m. Specific objectives of the study include the questions of (1) whether the current burst of activity is typical of late Quaternary activity, (2) whether the high degree of activity of the fault could be readily ascertained from physiographic features even in the absence of the historic record, and (3) a comparison of neotectonic features of the Xianshuihe fault with those of other active strike-slip faults in China and elsewhere.

Results

The principal results of the study were reported in the previous 6-month technical summary, and the study is now nearing its conclusion. During November and December 1986, co-investigators Luo Zhuoli, Qian Hong, and Wen Xueze visited the United States, and we spent much of the time working on the manuscript resulting from the study. In addition, field visits were made to various parts of the San Andreas fault system, and the visitors attended the annual fall meeting of the American Geophysical Union in San Francisco.

Carbon-14 dates from samples along the Xianshuihe fault have become available during the reporting period, and they support the indirect evidence of a high slip rate along at least parts of the fault. One sample from near Luhuo, in a locality somewhat analogous to that at Wallace Creek on the San Andreas fault, indicates that a channel has been displaced at least 54 m in 5630 ± 80 yr, yielding a minimum slip rate of 9.6 mm/yr. At a locality near Gelu, 20 km northwest, a Holocene terrace riser has been offset 138 m, representing a probable minimum slip rate of some 13 mm/yr. Four latest Pleistocene glacial moraines are cleanly offset in the mountainous region farther southeast near Kangding, suggesting slip rates of 5-7 mm/yr. Our overall conclusion from these and other data is that the Xianshuihe fault zone is characterized by a slip rate of 15 ± 5 mm/yr in its northern segment, decreasing to about 5 mm/yr in its southern segment.

Late Pleistocene and Holocene Paleoseismicity of the San Gabriel Fault

14-08-0001-G1196

William R. Cotton
William Cotton and Associates
318-B North Santa Cruz Avenue
Los Gatos, California 95030
(408) 354-5542

Investigations:

Studies directed toward establishing a chronology of the Late Pleistocene and Holocene faulting along the Rye Canyon segment of the San Gabriel fault near Valencia, California are continuing. Fault-dislocation measurements for a variety of geologic piercing points, in conjunction with radiocarbon age dates of Holocene alluvial horizons, have provided preliminary slip-rate determinations. In addition, the sense of slip on the fault during Holocene time has also been established.

Current efforts are directed toward confirming and expanding our preliminary findings at an adjacent site. The adjacent site has the potential to provide offset paleogeomorphology of a younger age (i.e., less than 6000 years) than that exposed at our first site. If successful, such findings would provide a good opportunity to determine the slip-rate for the last half of the Holocene epoch and also serve as an interesting comparison with the slip-rate determined at our first site.

Results:

1. In our previous semi-annual technical report (Cotton, 1986), fault-dislocated paleogeomorphic features were described and a preliminary slip-rate determination and sense of fault offset reported. Our findings suggested a slip-rate of approximately 0.6 mm/yr for the post-Pleistocene epoch. The sense of offset during the Holocene appeared to have been predominantly right-lateral with a dip-slip component of 20 degrees (+ or - 6 degrees) to the south as indicated by striae and slickensides preserved in gouge along the fault surface.

2. Inclement weather in our field area has prevented additional subsurface exploratory efforts over the past six months. Consequently, no new findings are available for reporting at this time. We anticipate, however, that additional results will be available for the next reporting period.

Publications:

Cotton, W.R., 1986, "Holocene Activity of the San Gabriel Fault, Valencia, California", The Geological Society of America, Cordilleran Section, Abstracts with Programs, 18 (2):96.

Cotton, W.R., 1986, "Holocene Paleoseismology of the San Gabriel Fault, Sangus/Castaic Area, Los Angeles County, California", in Neotectonics and Faulting in Southern California (Guidebook and Volume), GSA, Cordilleran Section, 82nd ann. met., p. 31-41.

Source and Seismic Potential Associated with Reverse Faulting and Related Folding

14-08-0001-G1165

Edward A. Keller
Department of Geological Sciences
University of California
Santa Barbara, California 93106
(805) 961-4207

Objective: Investigate tectonic framework, geometry, and uplift rates associated with folding on upper plates of buried reverse faults. Study sites are Wheeler Ridge, San Emigdio Canyon, and the Los Lobos folds near Bakersfield, California.

Results: Active tectonics at the southern end of the San Joaquin Valley is demonstrated near the piedmont area of the San Emigdio Mountains at Wheeler Ridge and San Emigdio Canyon. Latest Pleistocene and Holocene rates of uplift along the piedmont derived from 14-C dates on deformed geomorphic surfaces are 3-5 mm/yr.

Wheeler Ridge anticline is actively forming on the upper plate of a buried thrust fault. The latest Pleistocene to Holocene uplift of the surface topography is about 1.4 mm/yr. Uplift based on subsurface structural relief is greater, perhaps as much as 4 mm/yr. (Medwedeff personal communication, 1987). South of Wheeler Ridge on the Pleito fault Hall (1984) has determined an average Holocene rate of uplift of 0.5 mm/yr. The combined rate of uplift along the piedmont is less than 5 mm/yr. Assuming that the 1 m (Stein and Thatcher, 1981) uplift associated with the 1952 Kern County earthquake (M=7.3) is a characteristic event, then the recurrence interval is most likely between 200 and 700 years.

Twenty km west of Wheeler Ridge at San Emigdio Canyon the mountain front has migrated about 5 km north since late Pleistocene time. As a result, the mountains are being thrust over the southern San Joaquin Valley consuming alluvial fans. The Pleito fault is no longer active at San Emigdio Canyon. Active deformation is along the present range bounding Wheeler Ridge and Los Lobos buried reverse faults (Figure 1), which are delineated by active surficial folding and subsurface data. Holocene rates of uplift due to folding above the concealed Wheeler Ridge and Los Lobos faults are respectively 2.0 and 1.6 mm/yr., providing a combined rate of 3.6 mm/yr. Assuming that a characteristic earthquake will produce approximately 1 meter of uplift at San Emigdio Canyon, then the recurrence interval for such an event is approximately 300 years. Stream terraces at San Emigdio Creek are much more common at the mountain front than either upstream or downstream (Figures 2 and 3). I hypothesize that the greater number of terraces at the mountain front is related to active tectonism and specifically the timing of moderate to large earthquakes. The radiocarbon date for the Q-2 terrace is less than 1000 years and there may have been one earthquake event during that time. Between Q-2 and Q-3 time (approximately 3000 years) there were at least 3 events. Therefore the terrace history in San Emigdio Canyon suggests a recurrence interval of less than 1000 years for moderate to large earthquakes, a result consistent with that calculated from the rate of uplift and an assumed characteristic earthquake.

REFERENCES CITED:

Hall, N. T., 1984, "Late Quaternary history of the eastern Pleito thrust fault, northern Transverse Ranges, California": unpublished Ph.D. thesis, Stanford University, California.

Stein, R. S. and Thatcher, W., 1981, Seismic and aseismic deformation associated with the 1952 Kern County, California, earthquake and relationship to the Quaternary history of the White Wolf fault: Journal of Geophysical Research 86: 4913-4928.

PUBLICATIONS:

Laduzinsky, Dennis M., Seaver, Din B., and Keller, Edward A., 1986. Tectonics of an active fold-thrust belt. The Geological Society of America Abstracts with Programs 18 (2): 126.

Seaver, D. B., 1986, Quaternary evolution and deformation of the San Emigdio Mountains and their alluvial fans, Transverse Ranges, California. Unpublished M.A. thesis, Department of Geological Sciences, University of California, Santa Barbara.

Seaver, D. B., Zepeda, R. L., Keller, E. A., Laduzinsky, D. M., Johnson, D. L., and Rockwell, T. K., 1986, Active folding: southern San Joaquin Valley, California. EOS, Trans. Amer. Geophysical Union 67 (44): 1223.

Zepeda, Ricardo L., Keller, Edward A., and Rockwell, Thomas K., 1986, Rates of active tectonics at Wheeler Ridge, southern San Joaquin Valley, California. The Geological Society of America, Abstracts with Programs 18 (2): 202.

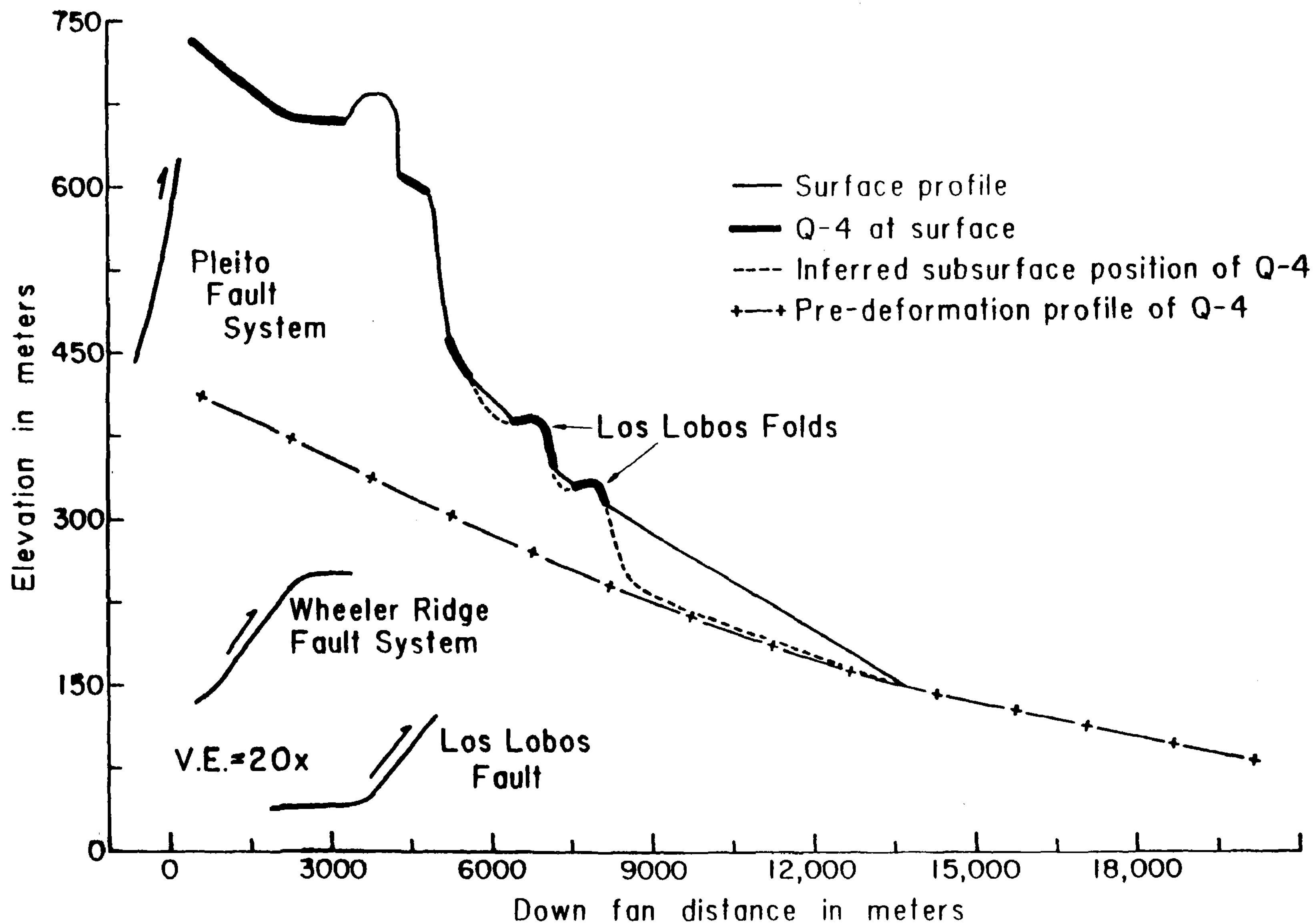

Figure 1. Topographic profile down San Emigdio Canyon showing location of buried reverse faults. The age of Q-4 is estimated at Late Pleistocene (~130 Ka). From Seaver, 1986.

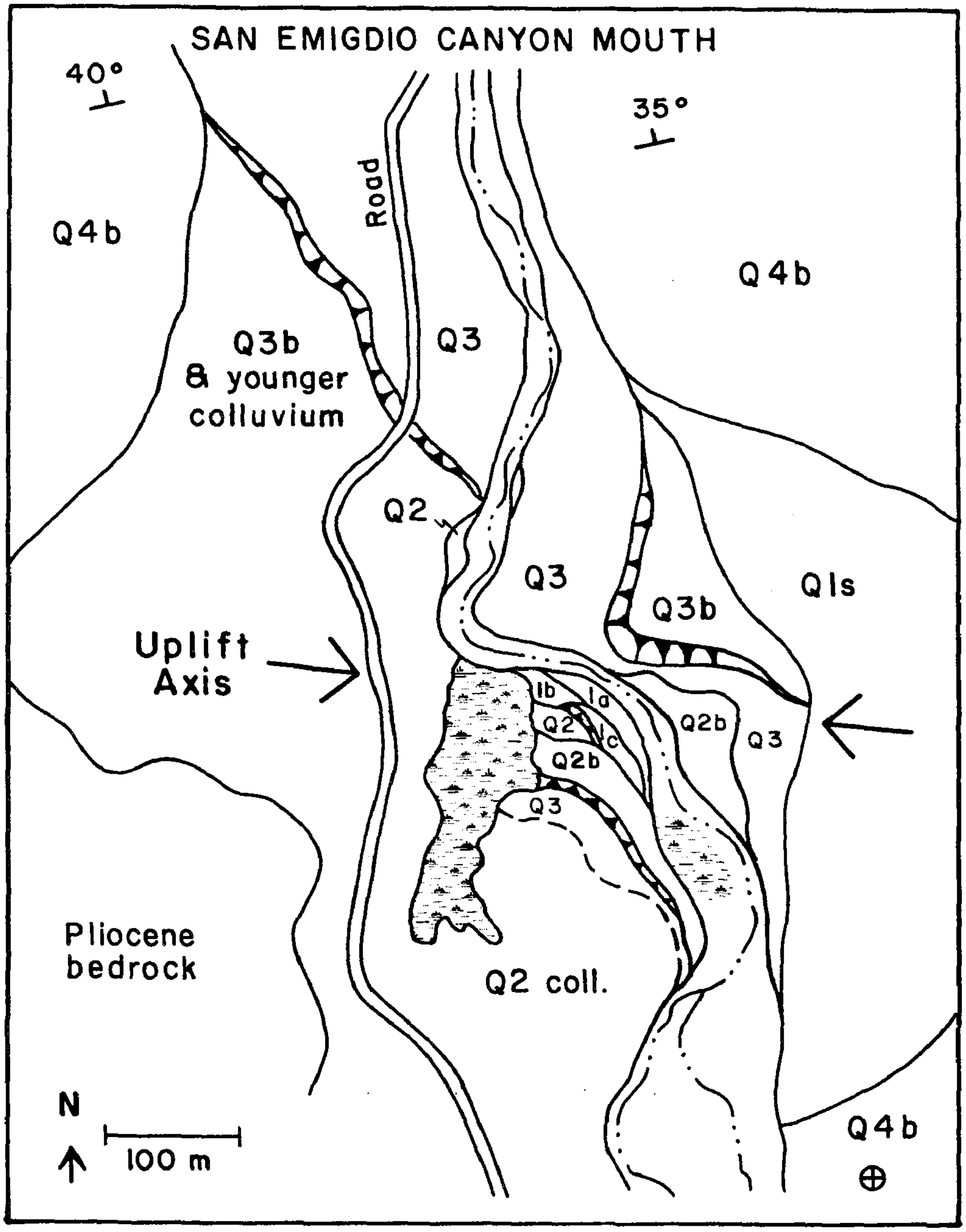

Figure 2. Sketch map of the range front at San Emigdio Canyon. The approximate ages of the major terraces are: Q-4b (130 Ka); Q-3b (6-7 Ka); Q-3 (4 Ka) and Q-2 (1 Ka). Dates are based on 14-C dates and rate of uplift. From Laduzinsky (in preparation).

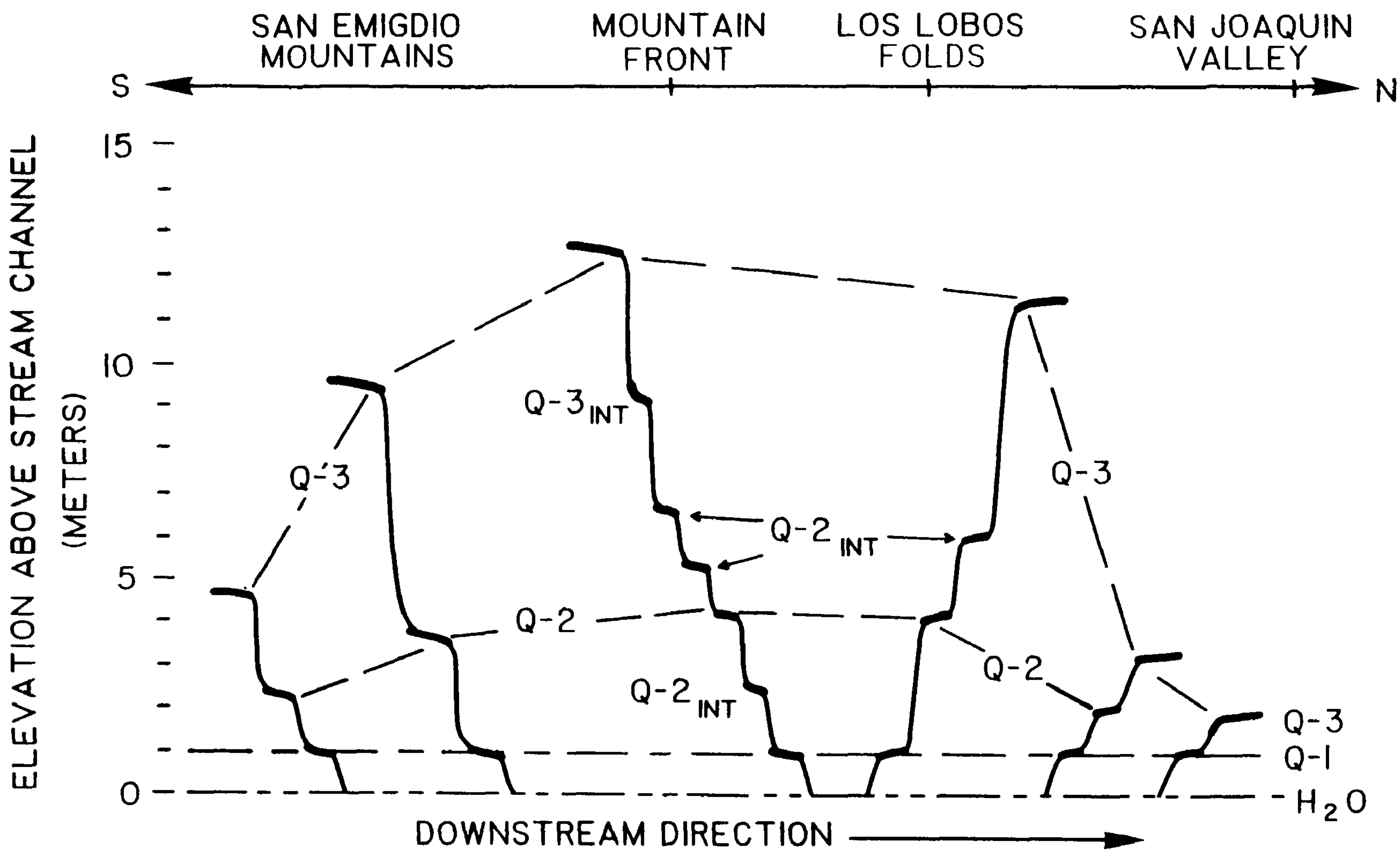

Figure 3. Profiles of terraces in the San Emigdio Canyon, mountain front area. The age of Q-3 is approximately 4 Ka and Q-2 is about 1 Ka. From Seaver, 1986.

ANALYSIS OF RECURRENT HOLOCENE FAULTING
NORTHERN ELSINORE FAULT
Grant No. 14-08-0001-G1164

T.K. Rockwell
J.F. Brake
R.S. McElwain
Department of Geology
San Diego State University
San Diego, CA 92182

Objectives

The objectives of this investigation are to further constrain the timing of slip events, the displacement per event, and a slip rate on the Glen Ivy North strand of the Elsinore fault zone in Temescal Valley through a detailed study of the faulted late Holocene stratigraphy at Glen Ivy Marsh.

Results

Recent work has concentrated on determining lateral offset of specific fluvial and pond deposits and historical features that have been displaced. The previously reported offset pre-1910 cement flume is laterally displaced about 35 cm (includes ductile deformation)(Figure 1), most if not all of which apparently occurred in the May 15, 1910 earthquake. A terracota pipe, emplaced across the fault in 1914 to drain a well that was dug adjacent to the fault, was reported in the previous technical summary to be laterally displaced. The pipe has collapsed in the vicinity of the fault zone due to vertical displacement of about 75-100 cm, resulting in an apparent lateral deflection (Figure 2). Detailed survey of the two sides of the pipe as they cross the fault zone, taking into account the collapse, results in no more than a maximum of a few centimeters of right lateral slip. A concrete pipe that overlies the terracota pipe was emplaced in about 1940 and is displaced 25-30 cm vertically by the fault. The vertical displacement of both the terracota and concrete pipes apparently results from groundwater withdrawal induced subsidence due to pumping of the well that fed the terracota pipe: the subsidence is very localized in the area of the well only. These data support the idea that the M6 1910 earthquake did rupture the surface and produced significant lateral slip.

PRE-1910 CEMENT FLUME CONSTRUCTED ACROSS FAULT ZONE

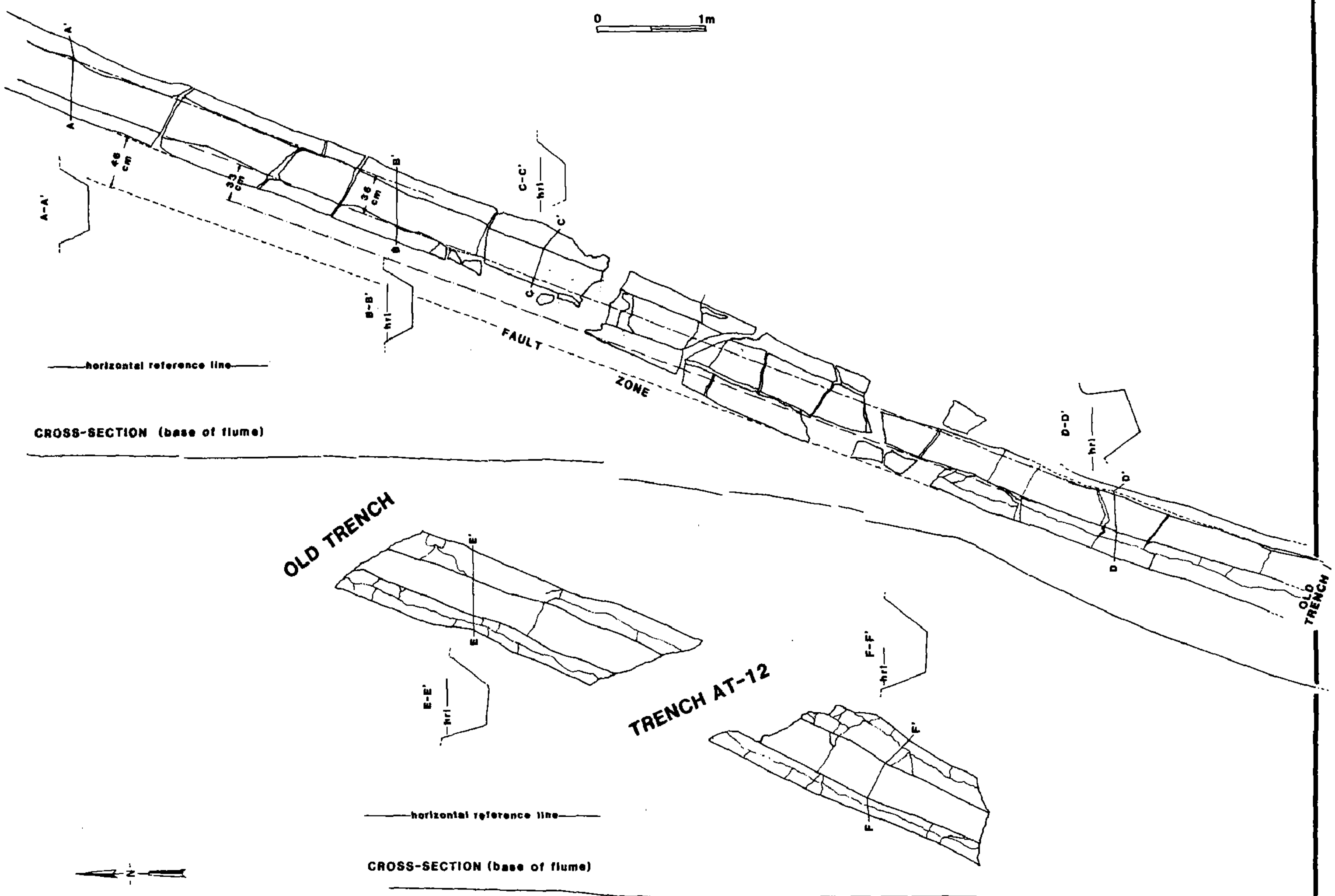

CIRCA 1914 TERRACOTA PIPE CONSTRUCTED ACROSS FAULT ZONE

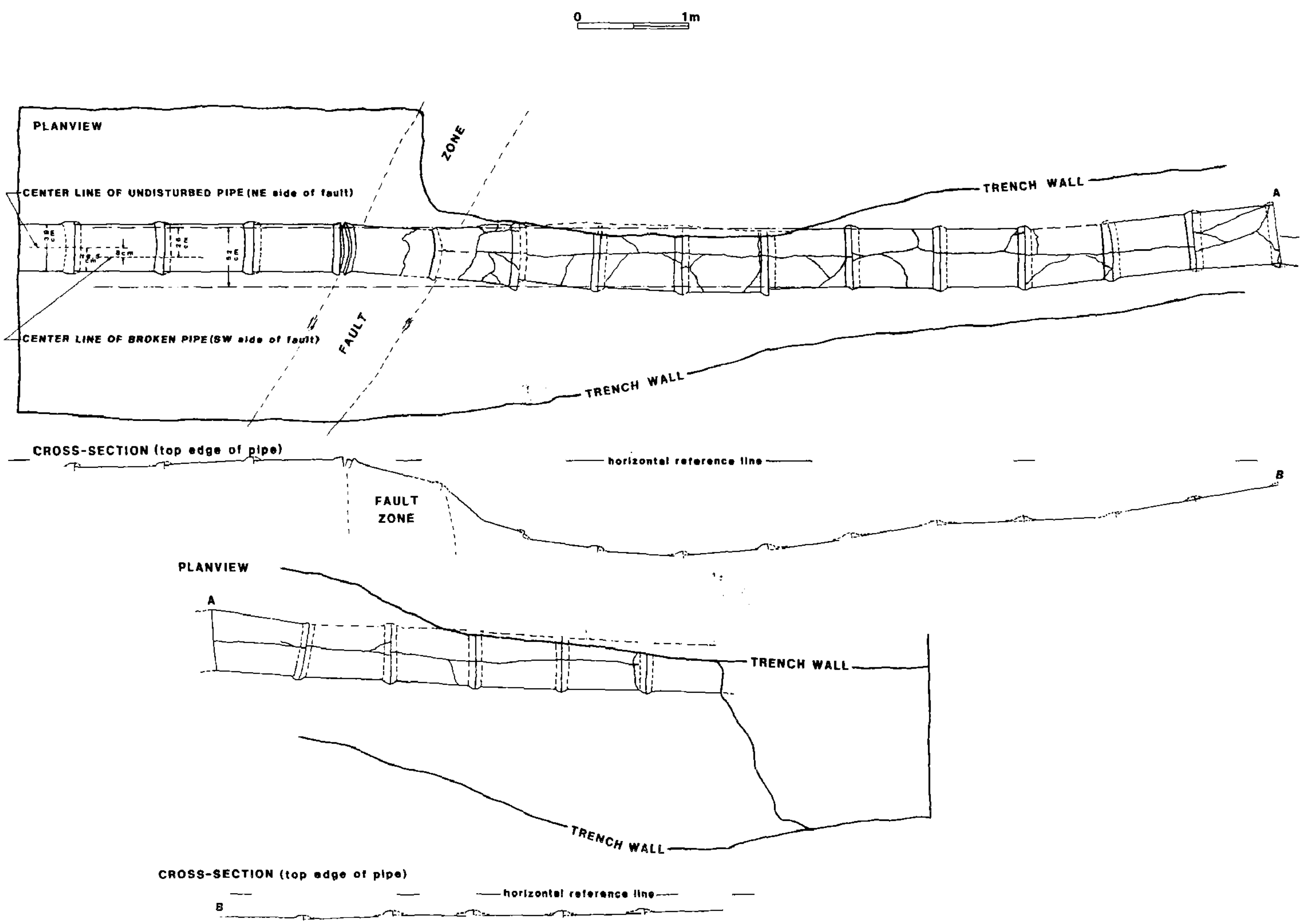

Very Precise Dating of Earthquakes at Pallett Creek and Their Interpretation

Contract # 14-08-0001-G1086

Kerry Sieh
California Institute of Technology 170-25, Pasadena, CA 91125
(818) 356-6115

The purpose of this investigation is to date as precisely as possible the ancient earthquakes recorded in the sediments at Pallett Creek. Advances in radiocarbon analysis now allow determination of ^{14}C ages with 2-σ precisions much smaller than those obtained nearly a decade ago. Refinement of the ages of the earthquakes will make patterns of earthquake irregularity or regularity more apparent and hence enable a more accurate estimate of earthquake probability for the San Andreas fault.

I am now in the second year of this study. At the time of this writing, I have completed collection of the second suite of samples at Pallett Creek, and Minze Stuiver (Univ. of Washington) has completed analysis of the first suite of samples, which we collected in 1985. Calendar-year precisions of about three decades have been achieved for several earthquakes.

Within a few months I expect analysis of the remaining samples will be completed and interpretation of the sample ages will begin. David Brillinger (Univ. of California, Berkeley) has already written computer programs and developed the methodology for statistical analysis of the samples.

Aspects of the Behavior of the San Andreas and Related Faults in Southern California

Contract # 14-08-0001-G1098

Kerry Sieh
California Institute of Technology 170-25, Pasadena, CA 91125
(818) 356-6115

This grant funds paleoseismological research along the southern, south-central and northern segments of the San Andreas fault and in the Mammoth-Mono Lake region of eastern-central California.

In the past six months, Ph.D. students Carol Prentice, Steve Salyards, Marcus Bursik and Pat Williams have continued to collect and interpret data for their individual projects.

Prentice is continuing to pursue late Pliocene and late Pleistocene slip rates along the northern San Andreas fault near Fort Ross and Point Arena. She has also discovered evidence of three late Holocene slip events on the fault in a trench excavated near Point Arena, and is awaiting completion of radiocarbon analyses.

Salyards has recently completed paleomagnetic analysis of our first suite of samples from Pallett Creek. Dextral near-fault warping documented by paleomagnetic rotations is substantial—more than the brittle offset recorded across the faults for the past three large earthquakes. Additional sampling and analysis will be completed this spring and summer.

Bursik has continued to analyze data bearing on the pattern of late Quaternary activity on the Sierran Range front faults in the Mono Basin. As we reported earlier, he seems to be confirming the hypothesis that dike intrusion beneath the Mono Craters volcanic chain has replaced shear along the normal frontal faults as the means of extension in this portion of the Basin Ranges.

Williams's field work near the southern terminus of the San Andreas fault continued during February through April of this year. Evidence of at least two episodes of prehistoric late Holocene slip of the southern San Andreas fault is preserved at the Salt Creek site, located 15 km northwest of Bombay Beach and 45 km southeast of Indio along the San Andreas fault. Two en echelon fault traces are believed to be the primary locus of displacement at the Salt Creek trench site. Near-shore lacustrine sedimentary features have provided good opportunities to measure fault displacement. Survey data documenting the three-dimensional position of those features is now being reduced. The ages of the lacustrine strata offset by fault displacement are believed to be ca. 1,200 and ca. 1,050 years before present. These ages are based on radiocarbon dating of detrital charcoal fragments within near-shore lacustrine strata.

Lacustrine strata deposited during the human-caused accidental filling of the Salton Sea in 1907 are offset between 90 and 190 mm along a fault trace located about 30 m northwest of the primary Salt Creek trench site. The offset is believed to reflect aseismic slip during the last 80 years at Salt Creek. This result indicates that the modern slip rate determined from alignment array and creepmeter data is characteristic of the faults' behavior over the last 80 years. Williams installed an alignment array spanning the historically offset Salt Creek fault trace on April 10. Five closely spaced bench marks were established in proximity to the historically active trace, and four more bench marks were established approximately 40 m and 90 m from the fault.

Additional work scheduled for May 1987 is expected to provide constraints on displacement of ca. 300-year-old recessional shorelines of the latest filling of Lake Cahuilla. These features cut across the San Andreas fault at an oblique angle 2 km north of Salt Creek. We believe that displacement of these features is less than or equal to 1 m. Measurement of the offset of these features will provide additional evidence for evaluation of the mechanism and role of aseismic displacement along the southern San Andreas fault.

Very Precise Dating of Earthquakes at Pallett Creek, and Their Interpretation

14-08-0001-C1083

Minze Stuiver

Department of Geological Sciences and Quaternary Research Center
University of Washington, Seattle, WA 98195, (206)545-1735

Objective: High precision radiocarbon dating, with age errors less than two decades for samples up to 5000 yrs old, is applied to the organic deposits of the stratigraphic section at Pallett Creek. This section contains the record of twelve large earthquakes. The radiocarbon dating project is part of the Kerry Sieh and David Brillinger project described elsewhere in this volume. The ultimate goal is to discern patterns of earthquake recurrence and to determine more precisely any variability in actual recurrence intervals and the probability of a great earthquake in the next couple of decades.

Data Acquisition and Analysis: Some forty odd samples have been measured so far. For most samples, the radiocarbon age errors (one standard deviation) are between 12 and 18 yr. These errors are based on the reproducibility of the measurements, and thus represent the full uncertainty of the measuring process. Realistic error assignment is important because the prevalent use of counting statistics to calculate radiocarbon errors may underestimate the error by up to a factor of two. To determine recurrence intervals in calendar years, a radiocarbon age calibration curve is used for the conversion of the radiocarbon ages. A high precision calibration curve is needed (Stuiver and Pearson, Radiocarbon 28,805-838,1986). For our Pallett Creek samples, the maximum range of calendar years compatible with one standard deviation in the radiocarbon age averages 45 calendar years. Probability distributions within these ranges also play a role. A more detailed assessment of these distributions on earthquake prediction will be made by D. Brillinger and K. Sieh.

Oak Ridge Fault, Ventura Basin, California: Slip Rates and Late Quaternary History

14-08-0001-G1194

Robert S. Yeats
Department of Geology
Oregon State University
Corvallis, Oregon 97331-5506
(503) 754-2484

David A. Gardner
Staal, Gardner & Dunne, Inc.
121 N. Fir Street, Suite F
Ventura, California 93001
(805) 653-5556

Thomas K. Rockwell
Department of Geology
San Diego State University
San Diego, CA 92183
(619) 265-4441

Investigations

Staal, Gardner & Dunne, Inc. described a new trench more than 300 m long and up to 6 m deep at Saticoy, east of Saticoy Avenue, extending from Telephone Road southeast across the Southern Pacific railroad tracks to the terrace riser cut by the modern Santa Clara River. This trench is located in the gap between two right-stepping traces of the Oak Ridge fault as shown in Figure 6 of Yeats and others (1981) about 250 m west of the west end of the fault where it can be traced upward to within 40 m of the surface. In addition, the western prow of Oak Ridge was remapped in detail. Both projects were done without use of USGS funds, but their results were contributed to the USGS project.

Gary Huftile completed detailed mapping of the Chaffee Canyon area where the Oak Ridge and Torrey faults were believed to intersect. Russ Van Dissen completed a geomorphic study of the western end of Oak Ridge, including an interpretation of data from the Ventura County Soil Survey (Edwards and others, 1970).

Results

The Oak Ridge fault was not found in the trench near Saticoy Avenue although several sand dikes in overbank silts in the trench may be related to seismic shaking. The soil developed in the unfaulted sediments was described by T. Rockwell and correlated to the dated soil chronosequence of Rockwell and others (1985). The moderately well-developed argillic horizon and mollic epipedon classify this soil as a typic argixeroll and, when compared to the dated soils, is estimated at 40-60 ka in age. The sediments upon which the soil is developed are nearly horizontal, indicating little or no deformation over this time period. The mapping at the western end of Oak Ridge showed that two westward-inclined surfaces previously mapped as tilted terrace deposits are part of large landslides, and thus they are not related to tectonic tilting.

At Chaffee Canyon, the Torrey fault probably does not intersect the Oak Ridge fault as previously believed. "Windows" of Pico formation are exposed locally as much as 550 m south of the previously-mapped surface trace of the Oak Ridge fault at the base of Oak Ridge at Guiberson Road. This strongly suggests that the Guiberson Road trace is a landslide, and that the Oak Ridge fault comes to the surface 150-550 m south of the road beneath the landslide.

Russ Van Dissen compared the soils on several prominent terraces on the southern flank of Oak Ridge, as reported in Edwards and others (1970), with the soils chronosequence constructed by Rockwell and others (1984) and concluded that these soils were no older than about 40,000 years. The most mature soils (Huerhuero and Chesterson) have a hue of 7.5 to 10 YR, a chroma of 2-4, a color index of 4-6, and a clay film index of 6-7. The older soils predominate downstream from the range front on dissected alluvial fans, whereas the subsequently-entrenched valley fill upstream from the mountain front has developed much younger soils. It is difficult, therefore, to isolate tectonic tilting from other variables affecting longitudinal stream profiles such as changes in stream power and changes in climate. The Oak Ridge drainage divide makes a southward shift near the west end of Oak Ridge, apparently due to under-cutting of the northwestern flank of the ridge by the Santa Clara River. The southward migration of the drainage divide has been accomplished by capture of the headwaters of south-flowing streams by the more vigorous north-flowing streams in addition to massive landslides. Furthermore, archeological evidence suggests that the Santa Clara River flowed south into the Oxnard Plain fairly recently in its history, trimming the western end of Oak Ridge and the lower ends of southwest-flowing alluvial fans.

References

Edwards, D.R., Rabey, D.F., and Kover, R.W., 1970, Soil survey of Ventura area, California: Soil Conservation Service, United States Department of Agriculture, 148 p.

Rockwell, T.K., Keller, E.A., and Johnson, D.L., 1984, Tectonic geomorphology of alluvial fans and mountain fronts near Ventura, California, in Morisawa, M. and Hack, J.T., eds., Tectonic Geomorphology: The Binghamton Symposia in Geomorphology, International Series, No. 15, p. 183-207.

Rockwell, T.K., Johnson, D.L., Keller, E.A., and Dembroff, G.R., 1985, A late Pleistocene-Holocene soil chronosequence in the central Ventura basin, southern California, U.S.A., in Richards, K., Arnett, R., and Ellis, S., eds., Geomorphology and Soils: George Allen and Unwin, p. 309-327.

Yeats, R.S., Clark, M.N., Keller, E.A., and Rockwell, T.K., 1981, Active fault hazard in southern California: Ground rupture versus seismic shaking: Geological Society of America Bulletin, part I, v. 92, p. 189-196.

Reports

Yeats, R.S., 1986, Faults related to folding with examples from New Zealand: Royal Society of New Zealand Bulletin 24, p. 273-292.

Yeats, R.S., 1987, Changing tectonic styles in Cenozoic basins of southern California, in Ingersoll, R.V. and Ernst, W.G., eds., Cenozoic Basin Development of Coastal California: Rubey Volume VI, Prentice-Hall, Inc., Englewood Cliffs, N.J., p. 284-298.

Analysis of Southern California Seismic Network Data for Earthquake Prediction

14-08-0001-G1381

Keiiti Aki
Department of Geological Sciences
University of Southern California
Los Angeles, CA 90089-0741
(213) 743-3510

INVESTIGATIONS

The goals of this study are to use data from China and California to (1) look for the relation between coda Q and long-term seismicity; (2) look for the spatial-temporal variation of coda Q in finer scale; and (3) understand the physical meaning of coda Q and its spatial-temporal variation.

RESULTS FROM MAINLAND CHINA

By the use of Herrmann's method (1980) of assuming $Q(f)=Q_0f^n$ and the coda amplitude decay method (Aki and Chouet, 1975) considering the distance between source and receiver, we determined coda Q at 80 stations throughout the mainland China. The resultant Q value at 1 Hz (Q_0) averaged for each station is plotted at the center of midpoints between the station and epicenters. It varies smoothly enough from place to place to draw a contour map. Figure 1 shows contours for constant Q_0 at Q_0 = 100, 200, 400, 600 and 1000.

The resultant contour map shows much more detailed variation of Q than that obtained by Singh and Herrmann (1983) for the United States, because our results are based on the coda data for the lapse time window from $2t_s$ to 100 sec, much shorter than their time window 100 to 1000 sec.

A. Relation Between Coda Q and Historic Earthquakes in China

Figure 1 also shows the epicenters of historic great earthquakes in China. It is remarkable that the high Q_0 regions are devoid of the epicenters, and the low Q_0 regions are full of them. In order to find a more quantitative relation between the coda Q_0 and seismicity, we calculated the area that was sampled by coda waves for each station (assuming the single back-scattering model). We then find the maximum earthquake that ever occurred in the area. Figure 2 shows a remarkable relation between Q_0 and the maximum magnitude. The relation becomes even better defined if we exclude regions in which the maximum earthquake occurred before 1700. Roughly speaking, if Q_o is 1000, M_{max} is about 4, and if Q_o is 100, M_{max} is about 8. This relation will be very useful for siting critical facilities such as nuclear power plants and waste disposal sites.

B. Migration of Low Q-High Seismic Region

It has been well known among Chinese seismologists that the active zone of large earthquakes in northeastern China migrated toward the east in the past several hundred years. Figure 2 shows that the pre-1700 active zone has about a factor of 2 higher Q_o than the currently active zone. If the relation between Q_o and M_{max} for more recent earthquakes should hold universally, Q_o might have been lower than the current value in the pre-1700 active zone.

RESULTS FROM CALIFORNIA

A. Preliminary Map of Coda Q for Central California

About 500 earthquakes recorded by the USGS central California network during a 3-month period (April-June) in 1984 were analyzed by the procedure described by Lee et al. (1986), and the resultant Q values are assigned to the mid-point of earthquake epicenter and station location.

In order to show the spatial distribution of coda Q, we divided California into rectangular blocks with the sides equal to 0.2 degree in longitude and latitude. We then averaged the values of Q^{-1} for the midpoints which lie in each block. Figure 3 is the map of coda Q for the time window 50-100 sec and the frequency 1.5 Hz. This map is the closest to our Chinese map shown in Figure 1, in terms of the time window and frequency. Since coda Q shows greater variabilitey for short lapse time because of the effect of forward-scattered waves, the time window 50-100 sec should give the most stable results. The pattern of Q distribution is very systematic. It shows the lowest Q in the northern extension of the Hayward-Calaveras fault zone and near the big bend of the San Andreas fault. Interestingly, the trend of low Q zone in the latter area is not along the San Andreas fault, but along the Garlock, Big Pine, and White Wolf faults, and may be due to the after effect of the Kern County earthquake of 1952. The low Q in the former area may be due to the Geysers-Clear Lake geothermal activity.

These low Q zones, on the other hand, can invite strain concentration because they are probably weak regions. They may be the easiest place to absorb the relative motion between the North American and the Pacific plates.

Between the above two lowest Q regions, the map shows a clear low Q zone along the San Andreas-Calaveras-Hayward fault zone, sandwiched between high Q regions. We find a relatively high Q region in the area between San Luis Obispo and Santa Barbara, including the Diablo Canyon nuclear power plant site.

The presentation of the map of Q shown in this progress report is still preliminary. We must have some measure of accuracy to go with the Q distribution. In any case, the map should be used only for a quick inspection. The reality of spatial and temporal variation should be examined by the use of a statistical significance test.

LIST OF PUBLICATIONS

Jin, A., and K. Aki, Spatial and Temporal Correlation Between Coda Q and Seismicity in China. Submitted to Bull. Seis. Soc. Am., April 1987.

Peng, J. Y., K. Aki, B. Chouet, P. Johnson, W. H. K. Lee, S. Marks, J. T. Newberry, A. S. Ryall, S. W. Stewart, and D. M. Tottingham, Temporal Change in Coda Q Associated with the Round Valley, California, Earthquake of November 23, 1984, J. Geophys. Res. (in press), 1987.

REFERENCES

Aki, K. and Chouet, B., 1975, Origin of coda waves: Source, Attenuation, and Scattering Effects, J. Geophys. Res., 80, 3322-3342.

Herrmann, R. B., 1980, Q estimates using the coda of local earthquakes, Bull. Seism. Soc. Am., 70, 447-468.

Lee, W. H. K., et al., 1986, A preliminary study of coda Q in California and Nevada, Bull. Seism. Soc. Am., 76, 1143-1150.

Singh, S. K., and R. B. Herrmann, 1983, Regionalization of crustal coda Q in the continental United States, J. Geophys. Res., 88, 527-538.

MAP OF CODA Q AT 1HZ AND EPICENTERS OF MAJOR EARTHQUAKES

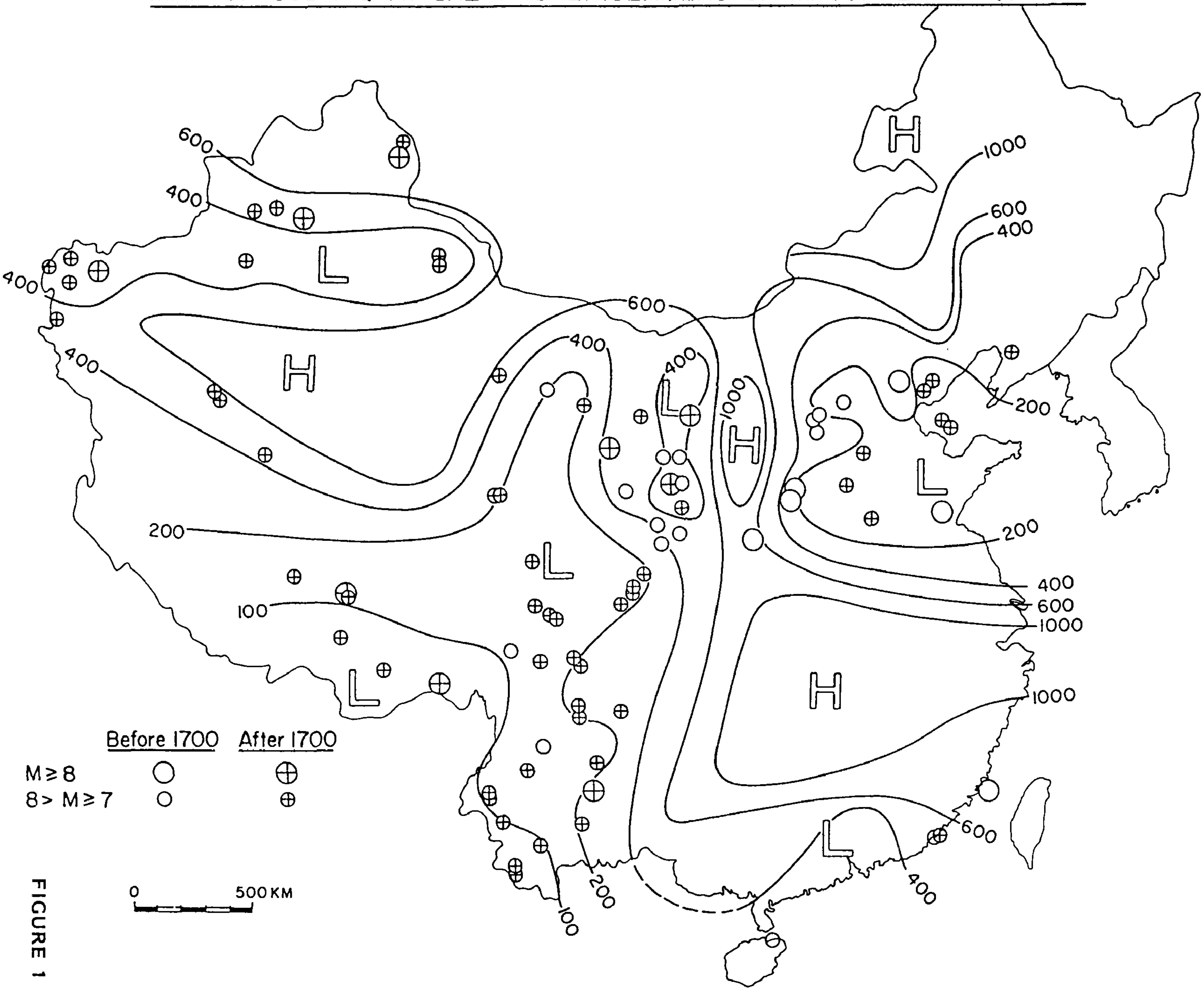

FIGURE 1

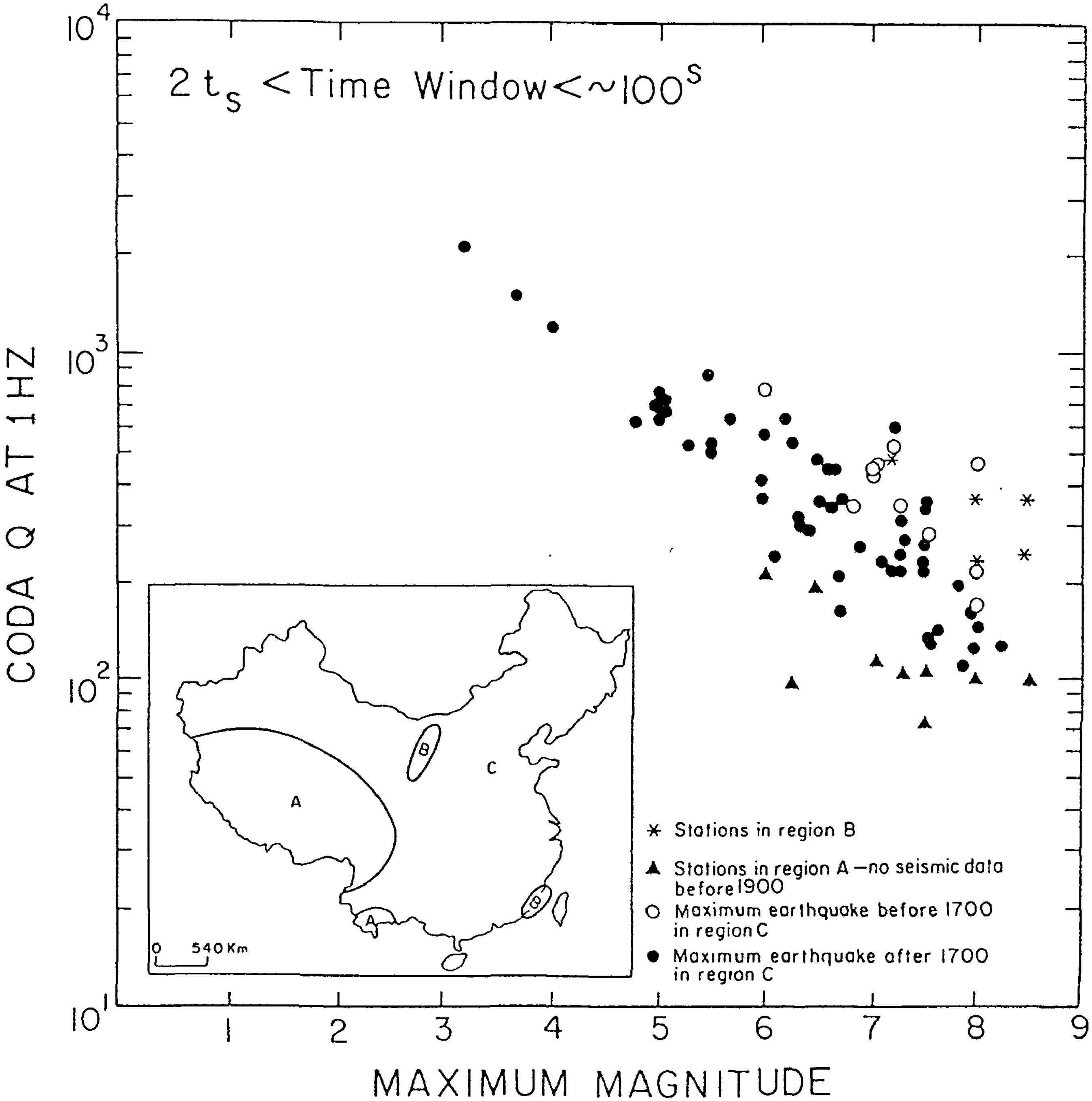
2 t_s <Time Window<~100^s
CODA Q AT 1 HZ
MAXIMUM MAGNITUDE
10^4
10^3
10^2
10^1
1
2
3
4
5
6
7
8
9
A
B
C
0 540 Km
✳ Stations in region B
▲ Stations in region A — no seismic data before 1900
○ Maximum earthquake before 1700 in region C
● Maximum earthquake after 1700 in region C

FIGURE 2

50–100 Sec (1.5 Hz)

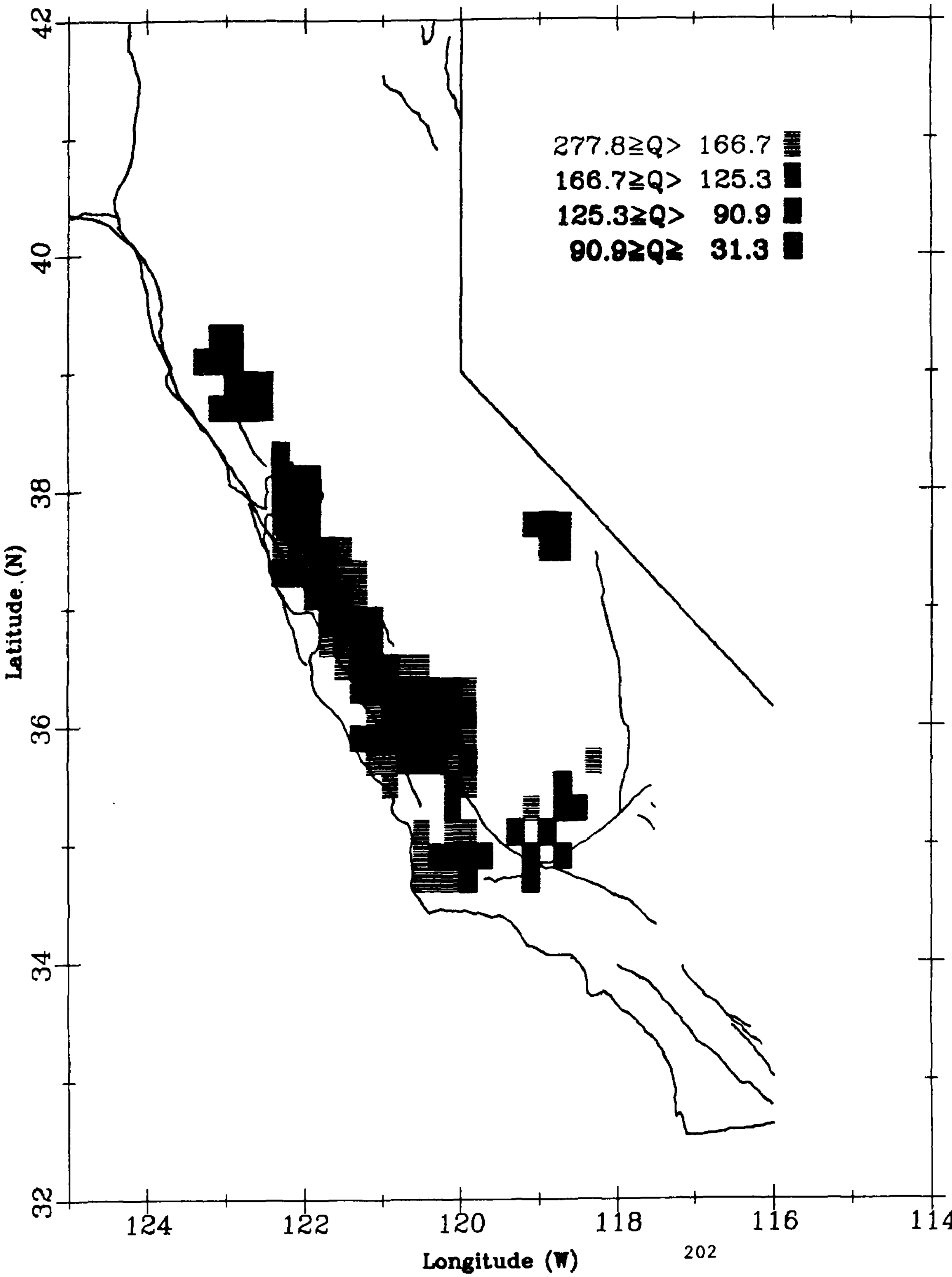

FIGURE 3

On-Line Seismic Processing

9930-02940

Rex Allen
Branch of Seismology
U.S. Geological Survey
345 Middlefield Road, MS 77
Menlo Park, California 94025
(415) 323-8111 ext 2240

Investigations and Results

The basic 'vanilla-flavored' RTP algorithm has been adapted to the new development system based on the 68020 processor. Operating in a mode in which it simply emulates the Mark I RTP the new system can process 48 stations with a single 68020. This single processor is filling both the picker and associator functions. The system currently does not save the digital traces for later use, but the offline version for use with the fiveday tapes does save them, and the techniques, both hardware and software, should be directly applicable to the online system when the requirement arises.

Another 68020 system has been ordered for use in the Parkfield experiment. It will be used as a backup for the current system, and will also allow the use of more elaborate warning algorithms.

Jim Ellis has continued work on the multiproject effort to develop new digital field instruments.

The Mk I RTP's here at Menlo Park and at the University of Washington and the University of Utah have continued to operate satisfactorily.

Crustal Deformation Observatory Part F

14-08-0001-G1355

John Beavan, Roger Bilham

Lamont-Doherty Geological Observatory
Palisades, New York 10964
914-359-2900

Investigations

We operate a 535 m long-baseline half-filled water tube tiltmeter at Pinon Flat Observatory. This is used in conjunction with a similar instrument operated by the University of California, San Diego, to investigate:

(1) sources and magnitudes of noise affecting the tilt signal;
(2) water level sensor design and reliability;
(3) methods of referencing tiltmeter to depth.

Results

The LDGO tiltmeter differs from the UCSD tiltmeter in several fundamental ways although its length and operating principle are the same (Figure 1). Tilt is monitored by measuring the height of the air-water interface at each end of a long horizontal pipe half-filled with water. Tilt is derived by differencing the two signals; this also eliminates gross thermal effects from the measurement and residual thermal signals are removed by measuring the temperature of the sensors at each end and applying a correction factor to the resulting data.

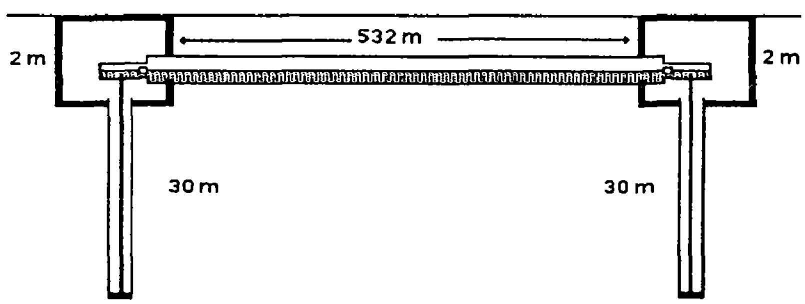

Figure 1. Schematic of PFO long baseline tiltmeter. The tiltmeters are referenced to fiducial points at 30 m depth.

The sensors of the UCSD tiltmeter consist of an equal-arm white light fringe-follower interferometer to monitor water motion, and a stabilised-laser interferometer to monitor motion of the water level transducer relative to the base of a 30 m deep borehole. In the LDGO tiltmeter we use an approximately equal arm unstabilised laser interferometer to monitor water level and an invar rod extensometer to monitor to the base of the borehole. Water levels are also monitored periodically by a micrometer accurate to $\pm$ 2 micron. This provides an independent estimate of the interferometer signal, or supplies an absolute datum in the event of the interferometer losing count for any reason.

The end vaults and monitoring systems of the LDGO tiltmeter are essentially passive while the end vaults of the UCSD system are temperature controlled and the fringe servo system is mechanically active during operation.

The past year has been devoted to interconnecting the two (UCSD and LDGO) long baseline tiltmeters at Pinon Flat in order to better understand the observed differences in their signals, and to improving our interferometer sensor in support of a forthcoming (Summer 1987) deployment of a two-component tiltmeter at Mammoth Lakes that we are undertaking jointly with the University of Colorado. A year of recent data from the tiltmeter is shown in Fig. 2. Prior to the long gap (which occurs at the time of the tiltmeter interconnection), the long term tilt rate is -0.32 µrad/yr.

1. Tiltmeter interconnection

Both the long-baseline half-filled tube tiltmeters at PFO perform very well, but unexplained discrepancies remain at the 0.1µrad/yr level. We believe these are related to the way the tiltmeters are referenced at depth. As part of the investigation into this effect we have introduced a half-filled tube connection between the LDGO tiltmeter end vaults and the nearby UCSD end vaults. Micrometer measurements of these water levels will enable us to track relative vertical motion of the LDGO and UCSD end piers at the micron level. The interconnections were installed during May and June 1986, with the work taking substantially longer than expected. The interconnection required 6 man-weeks of effort from Lamont personnel, as well as very considerable backup support from the UCSD group. Work on the micrometer sensors required for measuring the water levels has been delayed as a result of the effort expended on the interconnection. The micrometer sensors are designed and partially built; they are scheduled for installation in June 1987.

2. Improved sensors

The LDGO tiltmeter end units and interferometer fringe-counting electronics at PFO are still our original prototype instruments constructed in 1977, with a few lash-up modifications added since then. These units need fairly frequent attention, which they are able to receive in the PFO environment. However, we believe there is no reason why this type of sensor should not run for many months unattended without failure or loss of count (and therefore tilt datum). To this end, and with a view to field deployment, we have completely redesigned the mechanics and electronics of our sensors, taking into account the lessons we have learned from the years of operation at PFO. The new unit has a stainless steel reservoir and superior quality, easily aligned optics. The electronics use an HP $\lambda/4$ counter, and automatic level control that compensates for wide fluctuations in beam intensity and fringe contrast. The new units are presently under test at LDGO. They will be installed in the Mammoth Lakes tiltmeter in August 1987.

The new electronics will be installed on the existing PFO instrument in May 1987, as will an uninterruptible power supply for the laser. We expect that this will result in far more continuous operation of the LDGO tiltmeter than hitherto.

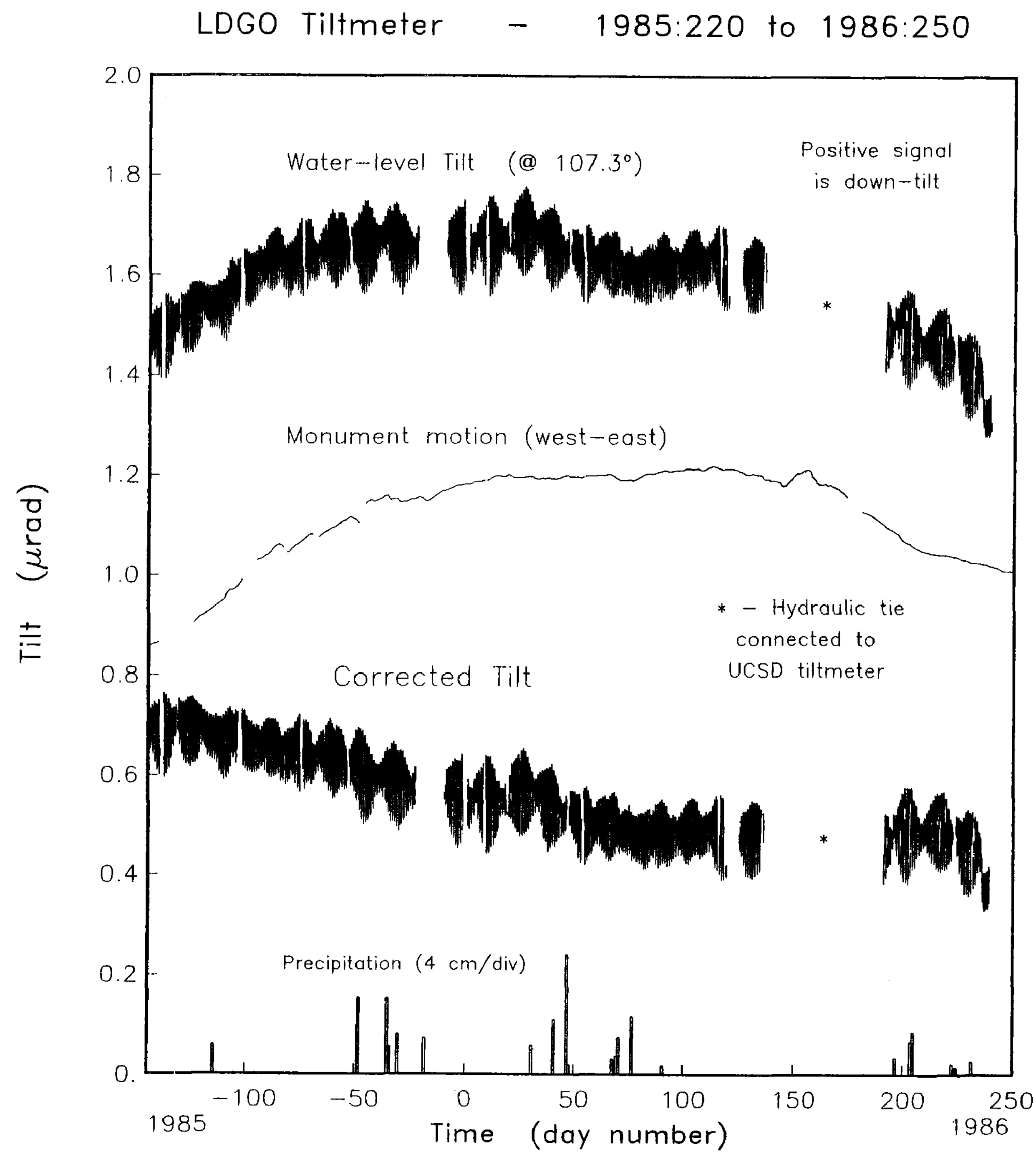

Figure 2. Thirteen months of tilt data from the LDGO titlemter at PFO. The upper trace is the tilt between the near surface monuments. The datum is transferred across gaps by using absolute micrometer measurements of the water heights. The central trace is tilt of the surface monuments relative to the 30 m deep fiducial points; this is derived from the vertical strainmeter records. The lower trace is the corrected ground tilt referenced to depth. Prior to the long data gap (when the LDGO-UCSD connection was installed), the long-term tilt was 0.32 μrad/yr down to the west. Plot provided courtesy of Frank Wyatt.

Crustal Deformation Measurements in the Shumagin Seismic Gap

14-08-0001-G1379

John Beavan

Lamont-Doherty Geological Observatory of Columbia University
Palisades, New York 10964
(914) 359-2900

Investigations

1. Nine short (~1 km) level lines are measured approximately annually within the Shumagin seismic gap, Alaska (Fig. 1). Surface tilt data are interpreted in terms of tectonic deformation at the Pacific-North American plate boundary.

2. Five absolute-pressure sea-level gauges are operated in the Shumagin Islands in an attempt to measure vertical deformation associated with the Aleutian subduction zone. A two-component short-baseline tiltmeter is operated at one site.

3. Data from the sea-level and tilt sensors are transmitted to Lamont by satellite in near real time, and are examined for possible tectonic signals. Studies of noise level as a function of frequency are used to determine the relative usefulness of different types of measurement, and to evaluate the minimum size of tectonic signal that will be visible above the noise. Our data are compared with other crustal deformation data from the Shumagin gap.

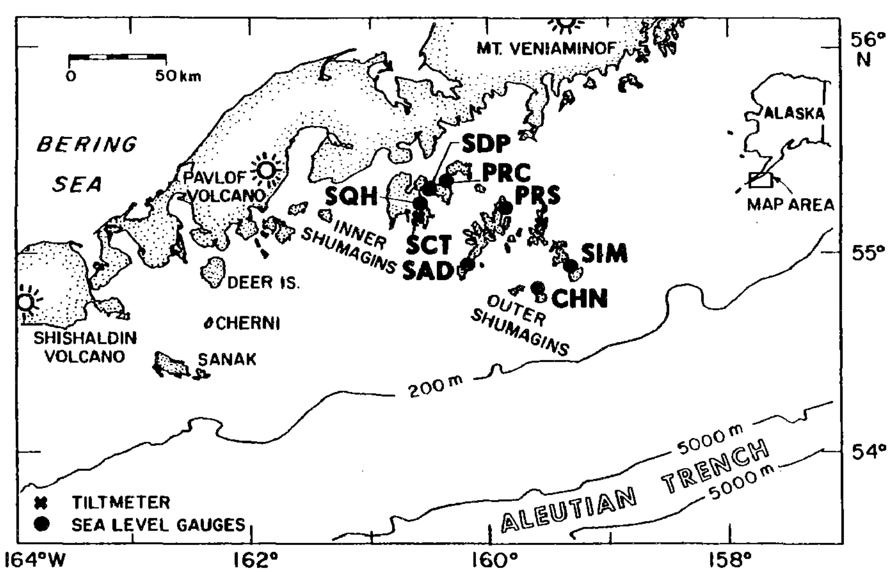

Figure 1. Location of the Shumagin Islands with respect to the trench and the volcanic arc. Depth contours are in metres. Also shown are the sites of sea-level gauges operated by Lamont-Doherty and by the National Ocean Survey (SDP). Station SAD is no longer operated because of repeated storm damage. PRS is not operating this year. CHN failed after 2 months due to a (rare) pressure sensor failure. SQH failed in October 1986 after 26 months of low-maintenance operation. All sites now use Paroscientific quartz pressure sensors.

Results

Sea level gauge and level line locations are given in Figures 1 and 2. The level line data are shown in Figure 3, and the 1980-86 tilt rates derived from these data are given in Table 1. The pre-1984 level data, including the apparent 1978-80 tilt reversal, are discussed by Beavan *et al.* [1983, 1984].

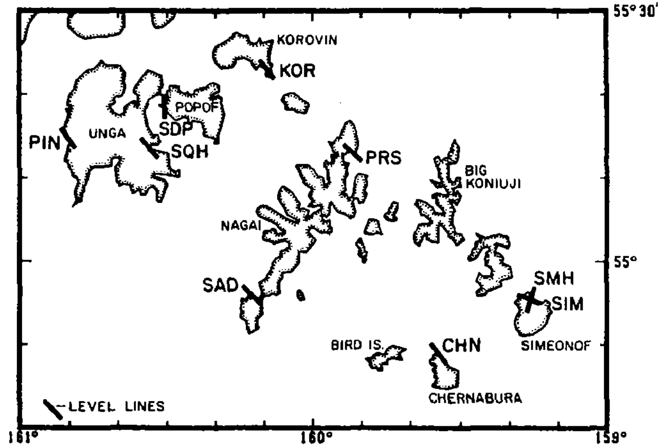

Figure 2. Locations and directions of first-order level lines, whose lengths vary from 600 - 1200 m. The resultant of data from SDP and SQH is used to estimate the tilt direction in the Inner Shumagins. The resultant of SIM and SMH is used for the Outer Shumagins.

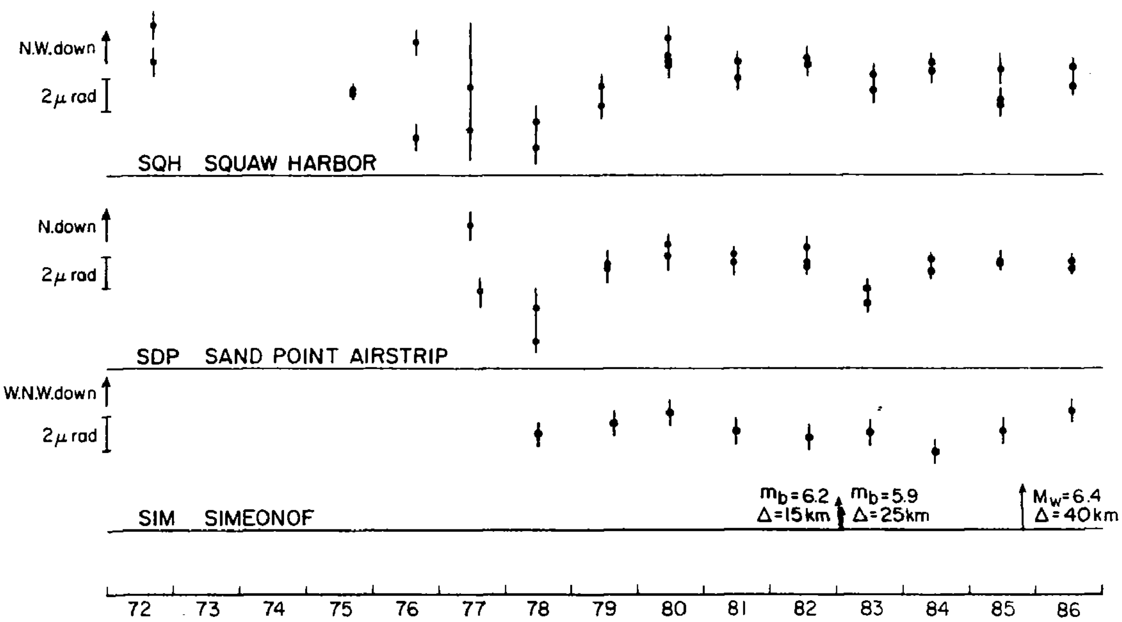

Figure 3a. See also Figure 3b. All data (1972-1986) from level lines in the Shumagin Islands. All lines except SMH are oriented approximately in the direction of relative plate motion. The two data points each year represent the forward and backward runs of leveling. The error bars are $\pm 1\sigma$, based on variations in multiple readings of each stadia rod from each tripod position. The height differences between the ends of the lines have been converted to slope by dividing by the line length; changes in slope from year to year are due to ground tilt (or noise in the data). Several benchmarks are set at each end of each line to guard against benchmark instability. Lines SIM and SAD have only one data point plotted for each year; this is because they have benchmarks between almost every tripod position and the overall tilt is estimated by averaging tilts between adjacent benchmarks.

Figure 3b. See also Figure 3a. Most of the NW-SE oriented lines show tilt rates since 1980 that are not significantly different from zero (see Table 1). Clusters of microseismicity at shallow depths below KOR in 1978 through 1980 may contribute to its noisy behavior. The 1980 measurement on CHN was made immediately after setting the benchmarks, so there may be some settling error due to hardening of the concrete. CHN shows a significant tilt rate, with tilting down towards the north. However, this is controlled largely by the initial measurement. The 1986 measurement may also be affected by the Oct - Nov 1985 earthquakes, whose aftershock zone extended beneath CHN.

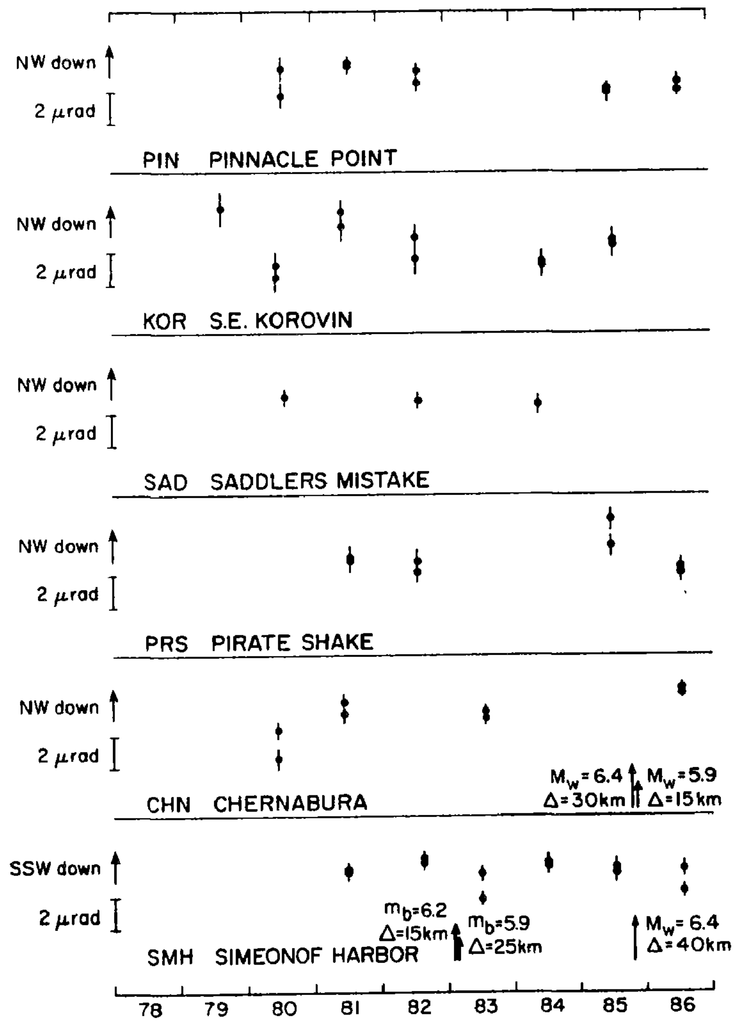

Table 1. Shumagin 1980-86 tilt rates

Site	Interval	Rate (μrad/yr)*	Azimuth*	Confidence
Inner Shumagins				
SDP/SQH	1980-86	-0.34±0.17	-60°±35°	-
PIN	1980-86	-0.16±0.12	NW†	-
KOR	1980-85	0.09±0.15	NW†	-
Central Shumagins				
PRS	1981-86	0.09±0.16	NW†	-
SAD	1980-84	-0.14±0.25	NW†	-
Outer Shumagins				
SIM/SMH	1980-86	-0.06±0.15	31°±153°	-
CHN	1980-86	0.43±0.15	NW†	95%

* Positive rates indicate tilt is down towards the given azimuth
† Level line in only one azimuth, so tilt only determined in that azimuth
Errors quoted are 1 standard deviation

None of the leveling data, with the exception of CHN, show tilt rates that are different from zero at the 95% confidence level.

Beavan *et al.*, [1986] describe in detail the sea level data through 1984, and the processing methods used. Briefly, the best-fitting ocean tide is subtracted from each data series, and the residual signals from two stations are differenced. The differencing removes any non-tidal signal common to both gauges. The resulting time series is a record of the differential vertical movement of the one station with respect to the other, plus any differential oceanographic signal and instrument drift. It typically has an rms amplitude of about 4 cm. Figure 4 shows the operational status of the array since 1984.

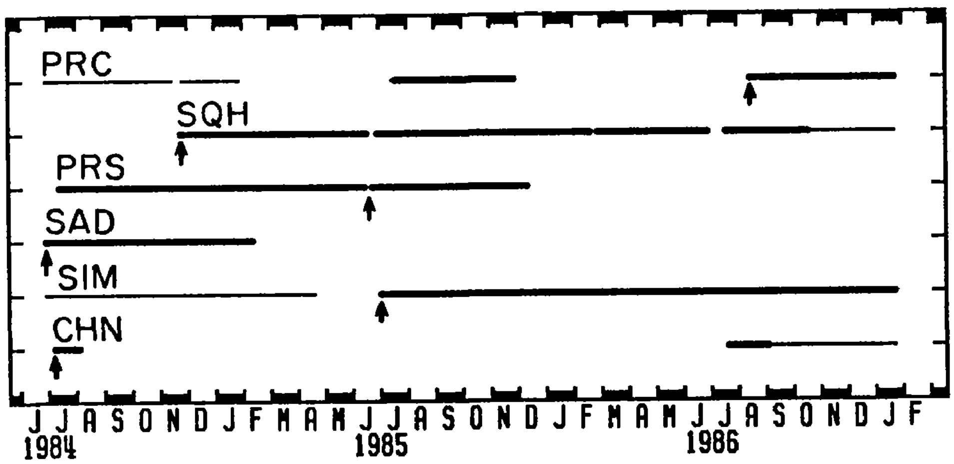

Figure 4: Operational status of sea level gauge array since 1984. Installation of quartz gauges is shown by vertical arrows. Thick lines indicate good quality sea level data was collected. Thin lines indicate data transmission but poor quality or missing sea level data. Station SAD was discontinued in 1985 due to repeated storm damage.

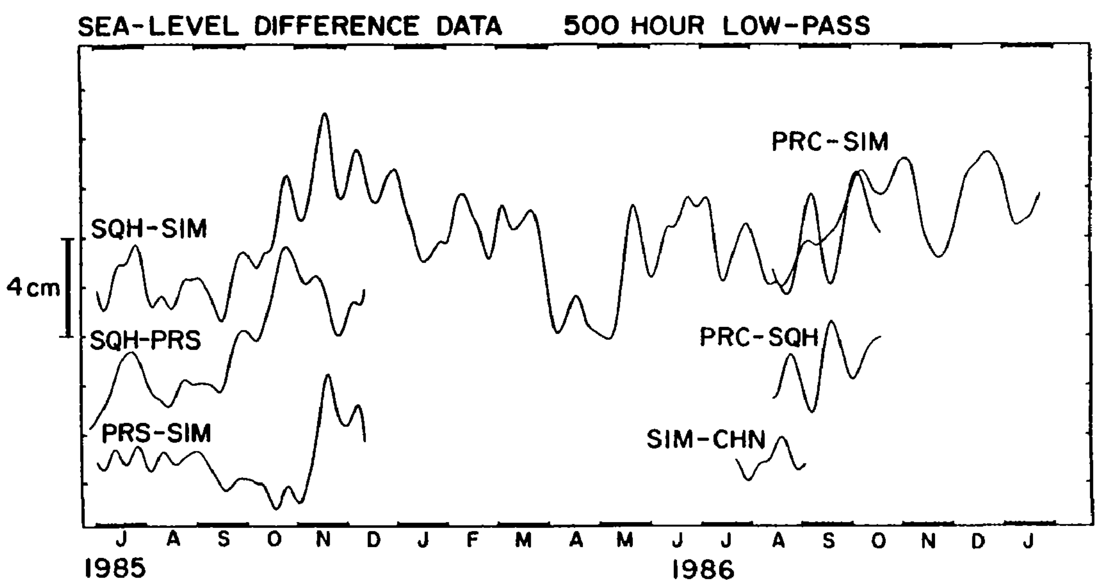

Figure 5. Low-pass filtered sea-level difference data since 1985 from pressure-sensor gauges that use Paroscientific quartz transducers. Top trace shows sea level difference between inner and outer islands (see Fig. 1), where we have overlayed the SQH-SIM and PRC-SIM curves to give a continuous record. PRC and SQH are both in the inner islands, hence should experience similar signals. The rms noise level is less than 20 mm.

Figure 5 shows several such difference series since 1985. An annual cycle of about 4 cm remains, presumably because the amplitude of the annual signal (which is an edge effect due to longshore currents along the coastal shelf), varies as a function of distance from the coast. Nevertheless, the very fact that we can see such signals gives us confidence in the stability of the gauges. We estimate that precursory (or other) signals greater than about 5 cm in relative sea level should be recognisable in our data in near real-time. This corresponds to 0.5 μrad tilt over the baseline of the array. We note that even with the long data gaps that we have experienced to date, we are still able to derive scientifically valuable results from our sea level data (see Figure 6 and associated discussion). We therefore expect even better results as the reliability of the gauges improves.

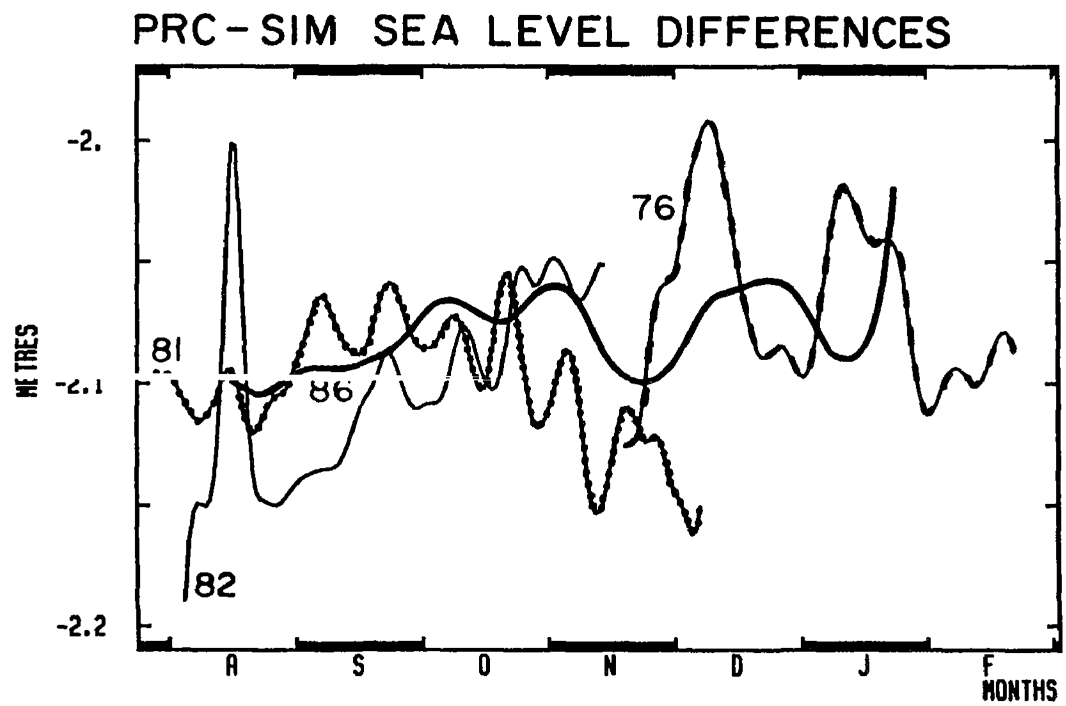

Figure 6: A 1 year stack of all good quality sea level difference data between PRC and SIM. The data are stacked on the same 1 year time axis in order to facilitate comparison between years. No significant differential vertical movement appears to have taken place between PRC (inner islands) and SIM (outer islands) since 1976.

In Figure 6 we show a plot of several years of sea level differences between a site in the inner islands (PRC) and one in the outer islands (SIM). These sites have the longest history of data due to an earlier 1976-77 occupation with float-type gauges [Bilham, 1977]. The data for each year are plotted on the same time axis, so that the difference for a given year may be compared easily with the differences for previous years in the presence of the several cm annual oceanographic signals. The differences have all been low pass filtered with a cutoff at 21 days. From this plot we conclude that differential vertical movement between PRC and SIM in the time period from 1976 to 1986 has been 0.0 ± 0.4 cm/yr.

Comparison of data from ceramic and quartz pressure transducers

Since we are attempting to measure very long period (months to years) deformation of the crust, the long term stability of the gauges used to measure the pressure generated by the sea is of utmost importance. Since 1984, we have been upgrading the array to use Paroscientific quartz pressure transducers, rather than the ceramic transducers we used earlier. This has resulted in a marked data improvement [Hurst and Beavan, 1987].

The sea level difference signals are converted to apparent tilt by dividing by the baseline length between the stations. A comparison of the power spectra of the tilt measurements using the ceramic and the quartz gauges demonstrates the superiority of the quartz gauges at periods greater than 2 months (Figure 7). The data for the ceramic gauges were taken from stations SAD and SIM during the periods August 1982 to March 1983, and July 1983 to December 1983. The data for the quartz gauges were taken from stations SQH and SIM during the period July 1985 to July 1986.

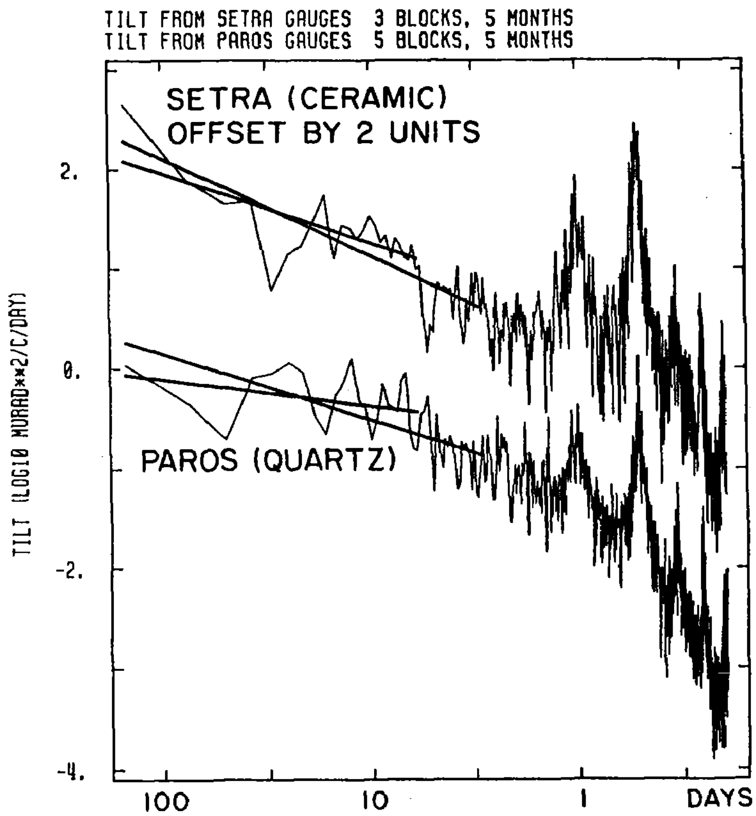

Figure 7: Power density spectra of apparent tilt derived from sea level differences using the two types of pressure gauges. The "quartz" spectrum is at the correct position relative to the vertical scale. The "ceramic" spectrum has been offset vertically by 2 units for presentation purposes. The heavy lines are least squares best fits to the spectra in log-log space between periods of (i) 5 months and 6 days, (ii) 5 months and 3 days. The steeper fit to the "quartz" spectrum is used in the analysis described in the text. At periods longer than ~2 months, the data from the quartz gauges are quieter, with the two spectra diverging by ~1 dB/octave.

The spectra are smoothed by section averaging with 10% cosine taper windows applied to the detrended sections of data, and about 50% overlap between sections; other statistics are given on the Figure. The power in the two spectra are about equal at 2 months period, but the spectrum derived from the ceramic sensors rises about 1 dB/octave faster until the longest period in the spectrum is reached at 5 months. Since we are investigating instrumental noise, we have taken the baseline length to be the same (85 km) in both cases even though the true SAD - SIM distance is only 55 km. This is to avoid biasing upwards the instrumental noise of the ceramic gauges. Any true ground tilt in the data will therefore be biased negatively in the "ceramic" spectra, so that our noise analysis favors the ceramic rather than the quartz gauges; even so, the quartz gauges prove superior. The effect of the different time periods involved is probably small as both data sets include approximately equal durations of data from the noisier winter months. We therefore interpret the differences in the spectra as unequivocal evidence of better intermediate to long term (> 2 months) stability of the quartz gauges.

Comparison of vertical measurement capabilities

Since we have three independent methods of measuring tilt in the Shumagins, (leveling, tiltmeters, and sea level) it is natural to ask which method is best for measuring deformations at various frequencies.

Figure 8 shows spectra of one component of the tiltmeter and a sea level difference (converted to tilt) using the quartz pressure gauges. For periods of ~1 month the noise levels are similar, and for shorter periods the tiltmeter spectrum becomes relatively quieter by ~4 dB/octave. For longer periods the sea level spectrum is essentially flat, while the tiltmeter spectrum continues to rise at ~7 dB/octave. Thus, the short-baseline tiltmeter is more sensitive to signals with periods less than ~1 month.

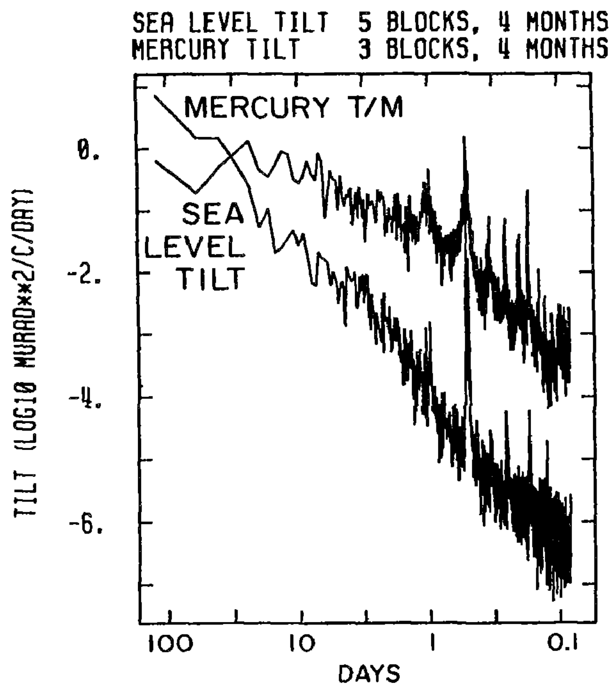

Figure 8: Power density spectra from one component (255 degree azimuth) of the tiltmeter at SCT, and from tilt derived from the sea level difference between SQH and SIM using quartz gauges. The tiltmeter is quieter at shorter periods (less than ~1 month).

Assuming errors between surveys are uncorrelated, leveling has a white spectrum whose power spectral density is given by $P = 2\sigma^2 t$ where σ is the standard error of the survey and t is the time interval between surveys. For a 1 km level line measured annually with a standard error of 0.5 mm/km$^{1/2}$ the power is ~1.8×10^2 μrad^2/c/day. The heavy lines in Figure 7 are least squares estimates of the sea level derived tilt spectra that we assume may be extrapolated to longer periods. The more conservative (steeper) estimate of the long period quartz spectrum has a power of 1 μrad^2/c/day at 2 month period, and rises at 2 dB/octave towards longer periods. If the power spectral density can be represented by $P(f)=K/f^{\alpha}$, then we can follow a discussion by Agnew

(1987) to calculate the period T at which the leveling data become quieter than the sea level difference data:

$$T = \left(\frac{2\,\sigma^2\, t}{K} \right)^{\frac{1}{\alpha}} .$$

Using the values K = 0.0676 and α = 0.658 from Figure 3, we find T = 450 years, with T becoming substantially longer for less conservative choices of K and α, or for less frequently repeated leveling. Thus sea level differences over an 85 km baseline will give better measures of tilt than annually repeated conventional leveling on 1 km baselines at all periods less than 450 years.

While it is not really fair to compare 1 km leveling lines with sea level differences having an 85 km baseline, it is still an interesting comparison since these are the data sets which we have available in the Shumagins. The unavoidable fact that leveling lines are restricted to the islands dictates that they can not achieve the 85 km baseline that the sea level differences can.

The new GPS technology offers a way of measuring the vertical deformation over 85 km baselines in spite of the water separating the islands. Using the same equations as above, we find that annual GPS surveys would require a standard error of 1.2 cm in order to match the noise level of the sea level differences at 10 year periods. Estimates of the eventual vertical precision of GPS when water vapor radiometers are used are about 2-3 cm [Kroger et al., 1986]. These imply values for T of 45 - 130 years, with T increasing if surveys are less frequent than once per year. The same reasoning and conclusions are valid for VLBI measurements. Thus, assuming our extrapolation of the spectra to lower frequency is valid, sea level differences will continue to provide the most reliable data on vertical deformations with periods from longer than 1 month up to a substantial fraction of the earthquake repeat time.

References

Agnew, D. C., On noise levels in deformation measurements: comparison in the frequency domain, *USGS Conference on Intermediate-Term Earthquake Precursors, Monterey, Ca., November 1986, USGS Open File Report,* in press, 1987.

Beavan, J., E. Hauksson, S. R. McNutt, K. Jacob, and R. Bilham, Tilt and seismicity changes in the Shumagin seismic gap, *Science, 222,* 322-325, 1983.

Beavan, J., R. Bilham, and K. Hurst, Coherent tilt signals observed in the Shumagin seismic gap: Detection of time-dependent subduction at depth?, *J. Geophys. Res., 89,* 4478-4492, 1984.

Beavan, J., K. Hurst, R. Bilham, and L. Shengold, A densely spaced array of sea level monitors for the detection of vertical crustal deformation in the Shumagin seismic gap, Alaska, *J. Geophys. Res., 91,* 9067-9080, 1986.

Bilham, R., A sea level recorder for tectonic studies, *Geophys. J. R. astr. Soc., 48,* 307-314, 1977.

Hurst, K. and J. Beavan, Improved sea level monitors for measuring vertical crustal deformation in the Shumagin seismic gap, Alaska, *submitted to Geophys. Res. Lett.,* 1987.

Kroger, Peter M., J. Davidson, and E. Gardner, Mobile Very Long Baseline Interferometry and Global Positioning System Measurement of Vertical Crustal Motion, *J. Geophys, Res., 91,* 9169-9176, 1986.

Tectonic Tilt Measurement: Salton Sea

14-08-0001-G1392

John Beavan

Lamont-Doherty Geological Observatory of Columbia University
Palisades, New York 10964
(914) 359-2900

Investigations

1. Historical water level measurements at three sites on the Salton Sea are being investigated to determine tectonic tilting, taking account of as many noise and error sources as possible.

2. The tectonic tilt derived from Salton Sea records is being carefully compared with leveling data from the area.

3. LDGO-designed pressure sensor gauges are being installed at several sites around the Sea to measure water level continuously, to investigate noise sources, to determine the level of detectability of tectonic tilt signals in the data, and to measure tectonic signals.

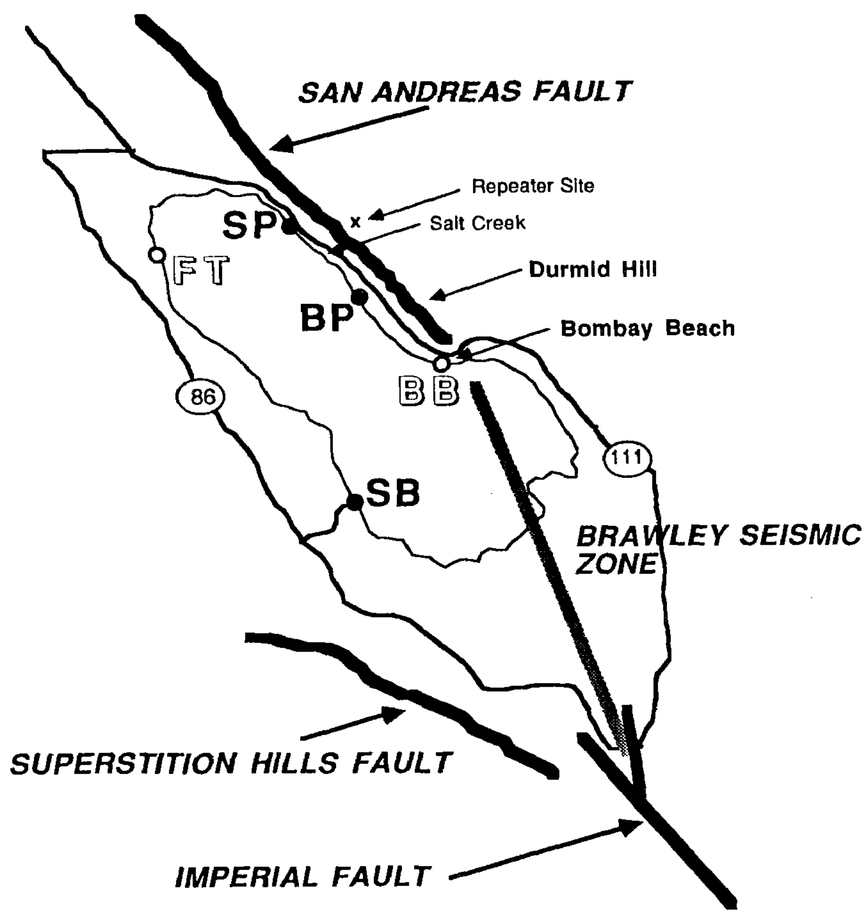

Figure 1. Map of the study region, showing the tectonic setting and the sea-level gauge network. Historical sea-level data have been collected at FT and SB since 1950, and at SP since 1970. Continuously recording pressure gauges have operated at SP since May 1985, at SB since January 1986, and at BP since December 1986. Gauges will be installed at BB and FT in May 1987.

Results

1. Historical data

We have completed re-analysis and updating of the historical (1950 - 1986) sea level records. By careful review of the historical data we found several datum changes in the data processed by Wilson and Wood (1980), and we also improved on their method of differencing the data. The resulting tilt curve (Fig. 2) shows essentially steady tilt down to the SE at ~0.1 µrad/yr between 1950 and about 1974. Between about 1974 and about 1979, the tilt is zero. Since then, it has been down to the W at ~0.3 µrad/yr. The changes in tilt direction coincide approximately with the 1974 Brawley swarm, and with the 1979 Imperial Valley earthquake, though we presently do not understand the causal relationship, if any.

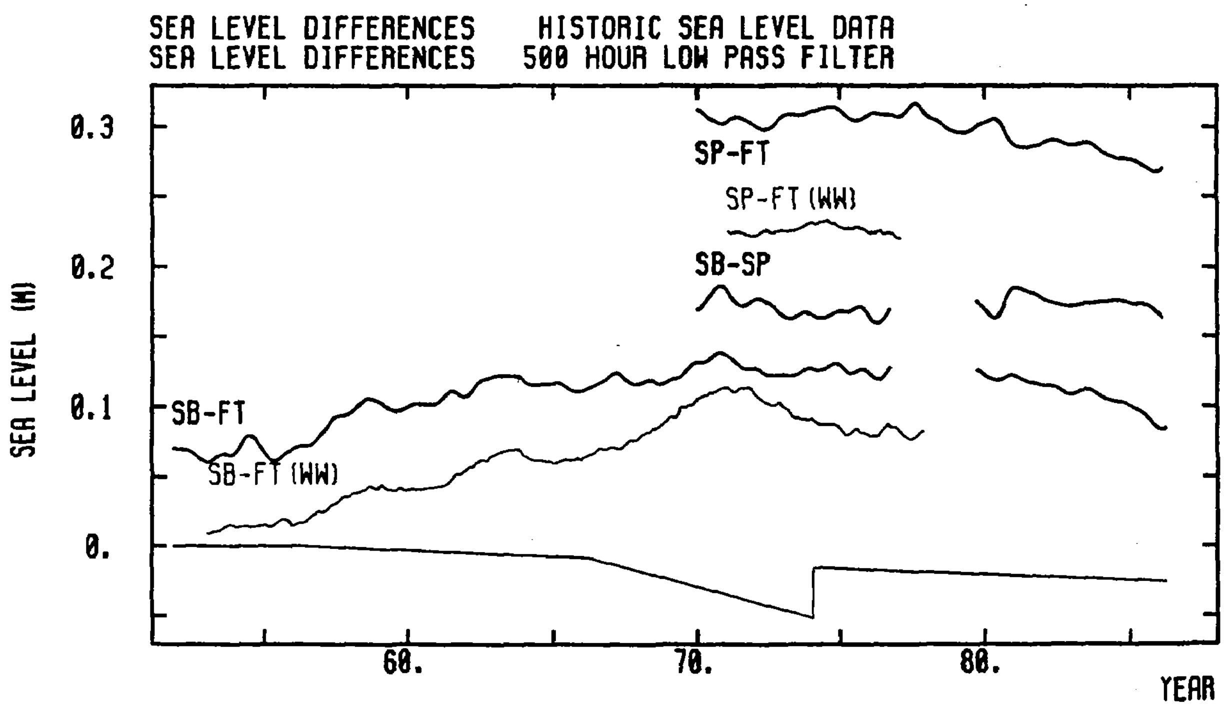

Figure 2. Differences between historical sea-level records. These are obtained by fitting smoothing splines to the unevenly sampled, low resolution raw data; differencing the resulting evenly sampled series; then low-pass filtering the differences. The clearest results are the ~0.1 µrad/yr ground tilt down to the SE prior to about 1970, the change to approximately zero tilt in about 1974, and the ~0.3 µrad/yr tilt down to the W since about 1980. The Wilson and Wood [1980] curves (WW) are shown for comparison. The curves are offset vertically for clarity. Tick marks on the time axis are at the start of the labelled year. The curves differ in detail from similar plots that have appeared in earlier reports. This is principally because of a Jan 1974 error in the SB raw data that we have located and corrected. The lowest trace shows the correction signal that has been added to the SB raw data.

Stability of the gauges used to derive the tilt curve is a serious concern. At site FT (Fig. 1) two gauges ran independently between 1951 and 1970. They show only a few mm offset over this time period, when the bulk of the observed tilting took place; thus we have confidence in the stability of this gauge. Leveling to 3 km distant benchmarks showed stability within 1 cm between 1956 and 1976. We will relevel this line in May 1987 as a final check on the stability of the data. At site SB, the local benchmark used for setting the tide gauge had not been tied to bedrock benchmarks since 1956. Since the local mark was rather suspect, we releveled it to several benchmarks up to 4 km away in December, 1986. This first-order leveling showed that the local mark had changed in elevation by 2.6±0.3 cm, in such a sense as to slighty decrease the slope of the raw tilt curve (Fig. 2).

We have compared the sea-level derived tilt curve with the tilt derived from repeated leveling surveys. We used only raw data from non-magnetic levels, and only from sections of line that approximately coincide with the sea-level baselines. There is only fair agreement, and where there are significant differences we prefer the sea-level data, on the basis of its continuity and smoothness. Castle et al. (1984) and Gilmore (1986) report rapid tilt changes in this region, based on adjusted regional leveling data. Their tilt rates are up to three times those we report, and include rapid changes in direction. Our sea-level data do not support their interpretations in the vicinity of the Salton Sea.

2. *Instrumental installations*

Continuous recording gauges using Paros differential pressure sensors have been installed at SP, SB and BP (see Fig. 1). Two more gauges are built and tested and will be installed at BB and FT in May 1987. An example of recent data is given in Fig. 3.

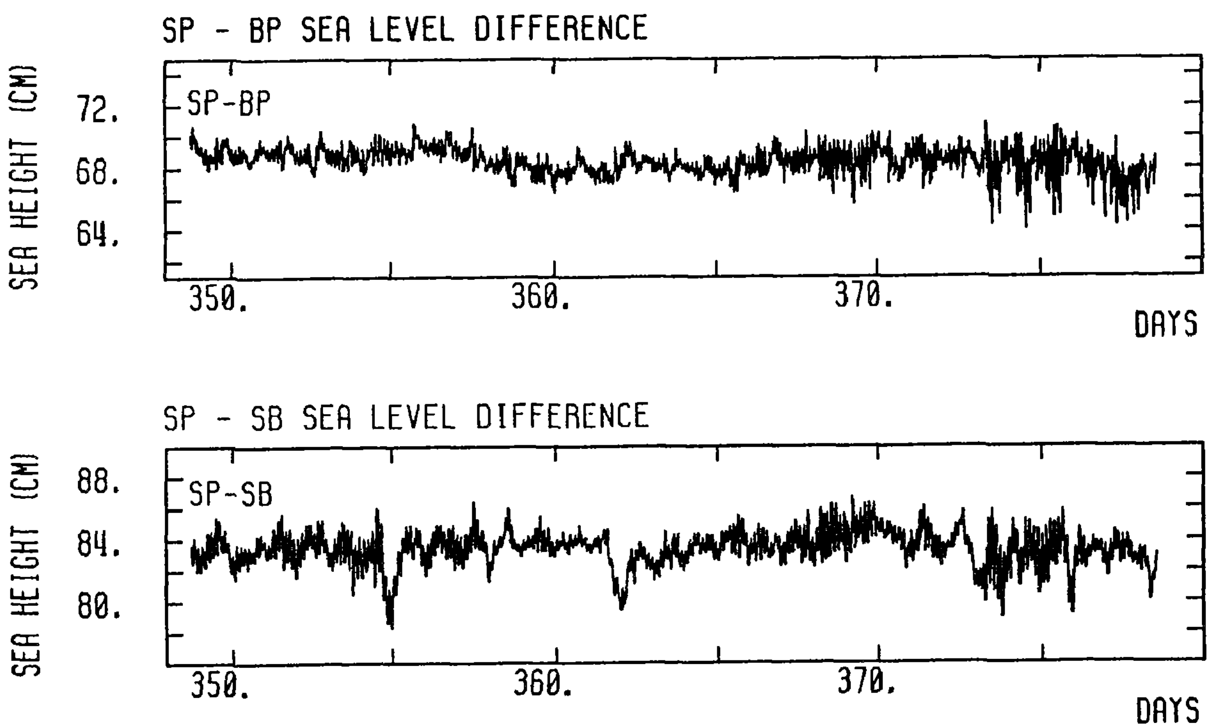

Figure 3. A 1 month (Dec 15 1986 - Jan 14 1987) sample of recent unfiltered data from the Lamont-designed pressure sensor gauges. Shown are the difference signals between SP and SB (upper), and SP and BP (lower). The 3 hour seiche is clearly visible.

Data are sampled every 12 minutes, and are digitally transmitted to a central recording site every hour. All data are transmitted twice to guard against short power outages or transmission errors. The recording system is an IBM-PC powered via an uninterruptible power supply, with a watchdog timer to ensure clean power-up. The recording system has worked very reliably, with less than 1% data loss over the past year. Several weeks of data were lost from the remote site SB due to fouling of the solar panel by birds, and by a gel-cell failure at the radio repeater. Data are presently forwarded to us by mail every two weeks. In May 1987, we will instal a modem so that data can be transferred to Lamont on a daily basis. This will allow us to identify technical problems rapidly, and correct them in a timely fashion.

Arrays of local benchmarks have been installed and measured near all three gauges. These are used to check gauge elevations at every visit. SB and SP have also been tied to more remote benchmarks on the main leveling routes; these ties will be repeated every few years to check the stability of the local array. BP will be tied to the main leveling route in the near future, as will the new gauges at BB and FT.

3. Instrumental data

We now present analysis of our instrumental data to show: (i) tilt derived from Salton sea level differences is quieter than that derived from leveling at all periods up to at least decades; (ii) the sea level array is best suited for detecting intermediate to long-term anomalies (weeks and longer). Its ability to detect shorter period precursors is poor unless they are of substantial magnitude (several cm); (iii) salinity and temperature variations do not significantly affect the tilt signal at the longer periods of interest.

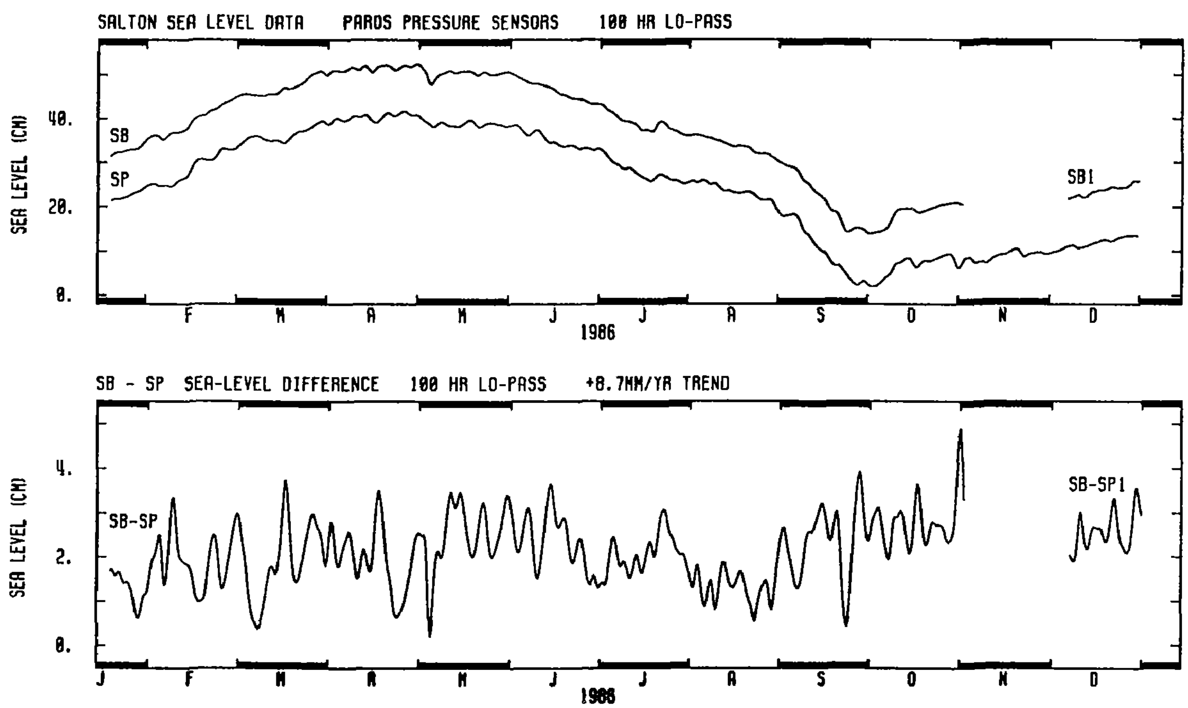

Figure 4. A year of data from gauges SB and SP, low-pass filtered at 0.01 c/hr. The slope of the difference curve is 8.7 mm/yr, corresponding to ~0.25 μrad/yr tilt down towards the south. The rms value of the difference signal is < 8 mm.

(i) Long-period noise. Figure 4a shows almost a year of data from the gauges at SB and SP, low-pass filtered at 100 hr period. Figure 4b shows the difference signal, which has a trend of 8.7 mm/yr, corresponding to ~0.25 µrad/yr down to the south. This is not very consistent with the trend of the historical data over the past several years (~0.3 µrad/yr down to the west). However, the historical plot in Fig. 2 ends in February 1986 so it is not possible to directly compare that plot with the instrumental data. We are acquiring additional data from the staff gauges so that the staff gauge - instrumental comparison can be properly made.

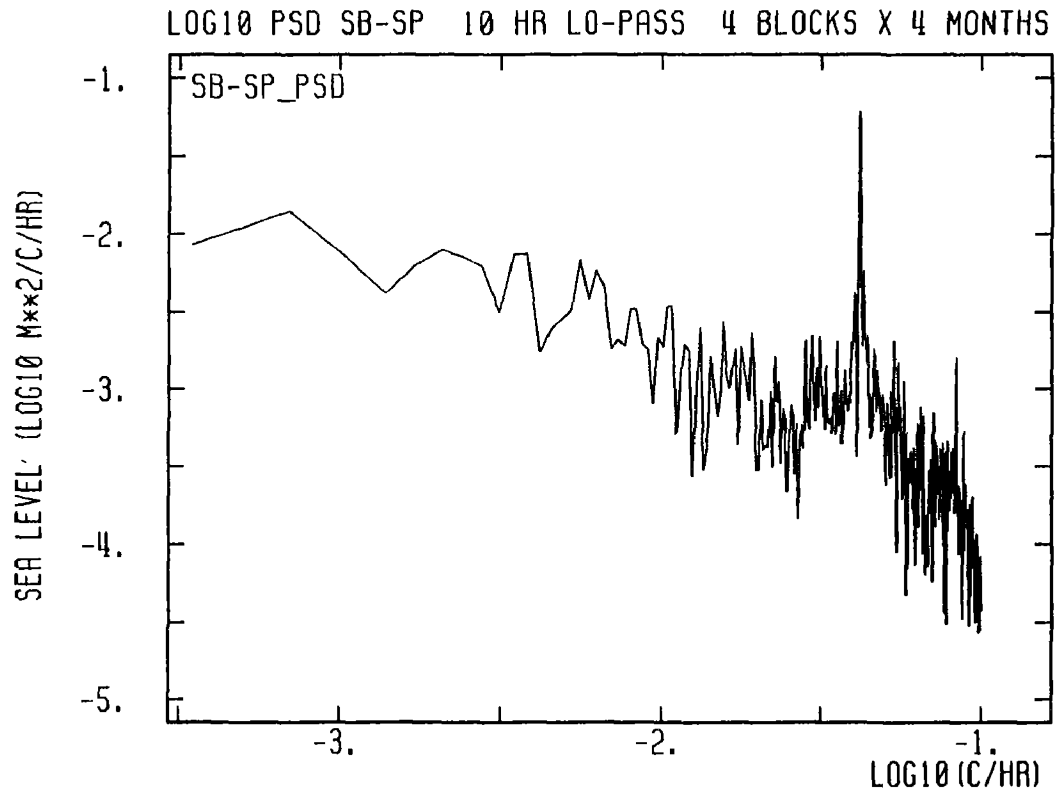

Figure 5. Logarithm of power spectral density of the difference signal of Fig. 4, but with the time series low-pass filtered at 0.1 rather than 0.01 c/hr. Note the relatively small spectral slope at low frequencies. The minimum frequency in this spectrum is 0.25 c/month.

Fig. 5 shows a section-averaged spectrum of the difference data low-passed at 10 hour period. The lowest frequency in the spectrum corresponds to a 4 month period. The prominent peak corresponds to 1 c/day, and occurs because of <1 cm amplitude thermally-induced water-level variations that are unequal at different sites. The important feature of this spectrum is its low frequency slope, which we estimate as -0.6±0.1 by fitting a straight line to the spectrum at frequencies lower than 0.5 c/day. We assume that this slope may be extrapolated to lower frequencies. This is much less "red" than typical geophysical time series, and means that the sea level difference data remain quieter than leveling data to much longer periods than if the spectrum were "redder". In order to compare noise levels of instrumental data with leveling data, they must be expressed in the same way (e.g. Agnew, 1987). Assuming that leveling errors are uncorrelated between surveys, then leveling data have a white spectrum whose power spectral density is given by $P_0 = \sigma^2/f_n = 2\sigma^2 t$ where σ is the rms error in each level survey, and f_n is the Nyquist frequency corresponding to the interval between surveys, t. If the sea-level difference spectrum is expressed as $P(f) = K/f^{\alpha}$ then the period, T, at which the leveling data become quieter than sea-level data is $T = (2\sigma^2 t/K)^{1/\alpha}$. From Fig. 5, we use $K = 1.3\times10^{-4}$ m^2/c/hr and $\alpha = 0.6$ for the sea-level data. Using 0.7 mm/km$^{1/2}$ as the error in first-order leveling, and assuming annual repetition of a 40 km level survey, we have $\sigma = 4.2\times10^{-3}$ m and t = 8760 hr, leading to T = 50 years. More realistic assumptions about the leveling would imply considerably larger T. Thus, our data suggest that the Salton Sea level difference data are a much more powerful tool than leveling with which to study the earthquake cycle in this region, particularly for detecting possible intermediate or long-term precursors. This does not, of course, undermine the importance of leveling, since the sea-level measurements are necessarily restricted to the coastline.

(ii) Short-term precursors. Fig. 6 shows a four month continuous section of difference data from Jun - Oct 1986, low-passed at three different frequencies. It is clear that a precursor that occurred over a time scale of a week would have to be > 2.5 cm in order to be recognised. At two days the corresponding figure would be about 4 cm. At shorter periods, the sea-level data become contaminated by thermal (~1 day) and seiche (< 3 hr) signals of up to 15 cm amplitude.

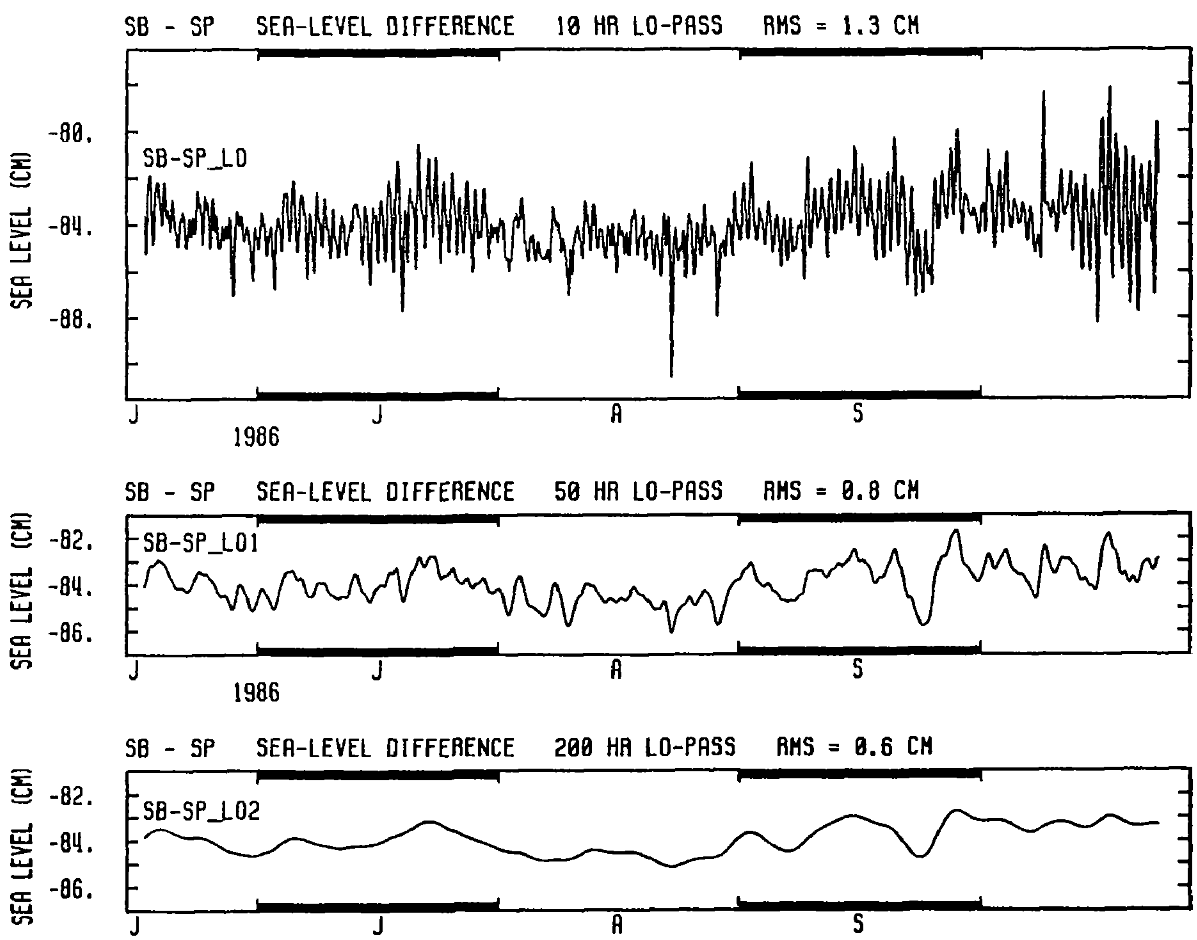

Figure 6. Four months sea level difference data, low-passed filtered at different frequencies. Short term precursors smaller than a few cm are unlikely to be recognised at periods shorter than several weeks.

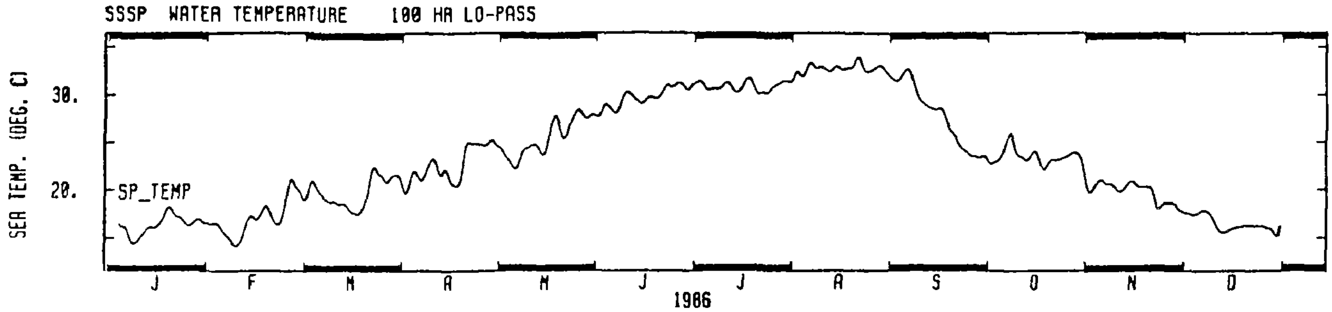

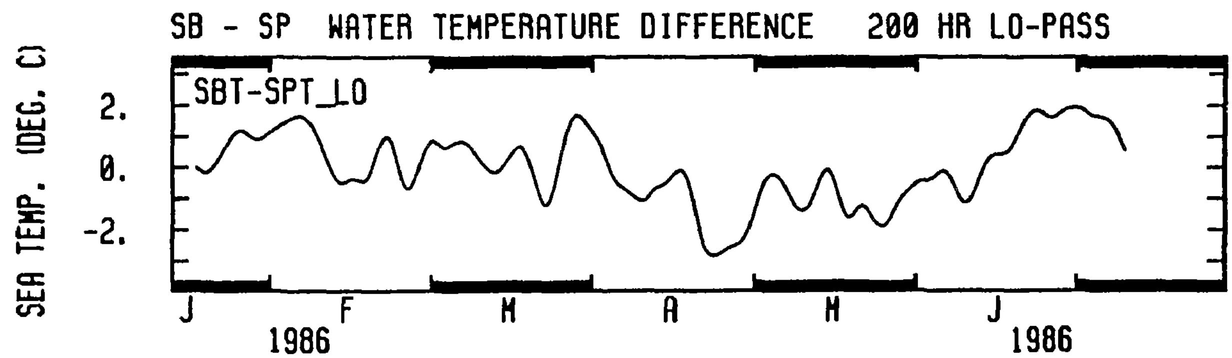

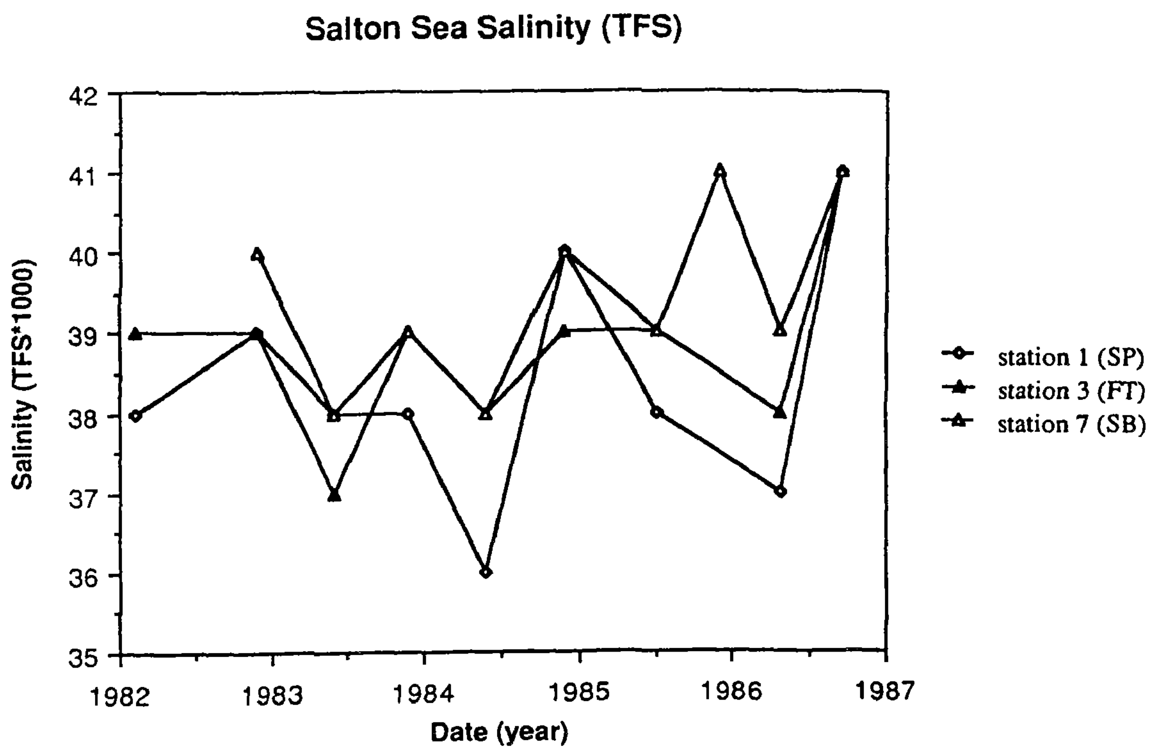

Figure 7. (a) Sea temperature at SP, showing the approximately 20°C annual cycle. (b) Temperature difference between SB and SP. When low-pass filtered at .005 c/hr (~8 days), the maximum deviation is ±3°C, and the rms is 1°C. (c) Salinity samples taken twice yearly at sites SP, SB and FT show evidence for an annual cycle that is similar at different sites around the sea.

(iii) Density effects. Fig. 7b shows that at periods greater than a week, the temperature at two sites on opposite sides of the sea track very closely. Similarly, salinity data (Fig. 7c) though sparse, track fairly well throughout the year. The maximum possible density variations that we expect vary from 1.030 gm/cm^3 (corresponding to 15°C and 4.1% salinity) to 1.022 gm/cm^3 (33°C and 3.6% salinity). We would therefore expect to see annual density-induced signals of up to 8 cm at each site, assuming a 10 m water depth, and that the density variations occur throughout the depth of the sea. However, temperature differences *between* sites (Fig. 7b) rarely exceed 2°C at periods longer than a few days, so that errors in the difference data should be less than 1 cm at weekly and monthly periods, and only a few mm at longer periods.

In summary, the noise characteristics of the recent instrumental data demonstrate that the current network of gauges can provide very useful data for earthquake prediction efforts.

References

Agnew, D.C., 1987. On noise levels in deformation measurements: comparison in the frequency domain, *USGS Conference on Intermediate-term earthquake precursors, Monterey, Ca., Nov. 1986, USGS Open File Rept., in press.*

Castle, R., M. Elliot, J. Church, and S. Wood, 1984. The evolution of the southern California uplift, 1955 through 1976, *U.S.G.S. Prof. Paper*, **1342.**

Wilson, M.E. and S.H. Wood, 1980. Tectonic tilt rates derived from lake-level measurements, Salton Sea, California, *Science*, **207** (11 Jan), *183-185.*

Remote Monitoring of Source Parameters for Seismic Precursors

9920-02383

George L. Choy
Branch of Global Seismology and Geomagnetism
U.S. Geological Survey
Denver Federal Center
Box 25046, Mail Stop 967
Denver, Colorado 80225
(303) 236-1506

Investigations

1. Enhancement of NEIC reporting services. We are integrating techniques of analyzing broadband data into the data flow of the NEIC. Broadband data can then be used routinely to increase the accuracy of some reported parameters such as depth and to compute additional parameters such as radiated energy.

2. Teleseismic estimates of radiated energy and strong ground motion. On a world-wide basis, the relative paucity of near-field recording instruments hinders the prediction of strong ground motion radiated by earthquakes. We are developing a method of computing radiated energy and acceleration spectrum from direct measurements of teleseismically recorded broadband body waves. From our method, the maximum expectable spectral level of acceleration and lower bounds of stress drops can be made for any event large enough to be teleseismically recorded.

3. Rupture process of large- and moderate-sized earthquakes. We are using digitally recorded broadband waveforms to characterize the rupture process of selected intraplate and subduction zone earthquakes. The rupture processes thus delineated are used to complement seismicity patterns to formulate a tectonic interpretation of the epicentral regions.

Results

1. The advantages of using broadband data to determine the differential arrival times of direct P and depth phases was demonstrated in Choy and Engdahl (1987). Differential times are much more accurate in determining depth of an earthquake than arrival times of P waves alone. The processing of Choy and Boatwright (1981) and Harvey and Choy (1982) are being applied routinely to digital data from the GDSN and RSTN to obtain broadband data. The NEIC now uses broadband waveforms to routinely: (1) resolve depths of all earthquakes with $m_b > 5.8$; (2) resolve polarities of depth phases to help constrain first-motion solutions; and (3) present as representative digital waveforms in the PDE's. We are in the process of implementing the algorithm of Boatwright and Choy (1986) to routinely compute radiated energy for all earthquakes with $m_b > 5.8$.

2a. Subduction zone events. We have applied our algorithm for the computation of radiated energy to a number of large subduction-zone earthquakes. Generally, indirect estimates of energy (e.g., those using simplistic relations with moment) may overestimate energy if the rupture process involves a sizeable component of aseismic slip. In the frequency range 0.1-1.0 Hz, a teleseismically derived acceleration spectrum compares well with the spectra from near-field accelerograms. This implies we can make routine estimates of strong ground motion from large earthquakes with teleseismic data.

2b. Intraplate events. We have applied our algorithm for the computation of acceleration spectra to a series of shallow intraplate earthquakes. Most of these events are characterized by a flat spectral level at high frequencies but an intermediate slope before an ω^2 falloff at low frequencies.

3. A study of the Yemen earthquake of 13 December 1982 has been completed. This event was found to consist of two events that occurred 3 s apart on a steeply dipping fault that trended NNW. Correlation with aftershock distribution confirms the hypothesis of Langer and others (1987) that conjugate faulting occurred. We are in the process of examining the Valparaiso earthquake of March 1985, and its aftershocks. Preliminary findings are that the event was complex. The dominant energy release occurred 17 s after the initial nucleation as a point which marks the termination of the 1971 Chilean earthquake.

Reports

Boatwright, J., and Choy, G.L., 1986, Acceleration spectra for subduction zone earthquakes [abs.]: EOS (American Geophysical Union, Transactions), v. 67, p. 310.

Choy, G.L., and Engdahl, E.R., 1986, Analysis of broadband seismograms from selected IASPEI events: Physics of the Earth and Planetary Interiors, in press.

Choy, G.L. and Kind, R., 1986, Rupture complexity of a moderate-sized (m_b 6.0) earthquake--Broadband body-wave analysis of the North Yemen earthquake of 13 December 1982: Bulletin of the Seismological Society of America, v. 77, p. 28-46.

Seismic Analysis of Large Earthquakes and Special Sequences in Northern California

9930-03972

Robert S. Cockerham
Jerry P. Eaton
A.M. Pitt
Branch of Seismology
U.S. Geological Survey
345 Middlefield Road, Mail Stop 977
Menlo Park, California 94025
(415) 323-8111, Ext 2963

Investigations:

1. Compilation of a combined California - Neveda microearthquake catalog from four seperate contiguous regional networks in California and Nevada. (Eaton and Dave Hill)

2. Continued monitoring and analysis of the seismicity of the Mono Lake to Bishop area of Eastern California. (Cockerham)

3. Completion of a USGS Yellowstone seismic catalog covering the years 1964 through 1984. (Pitt)

4. Collection and analysis of data from large earthquakes recorded by the Central and Northern California telemetered seismic network in support of:

   (a) Developement of better velocity models and associated station travel time corrections, (Eaton, Cockerham and Katie Poley)

   (b) Evaluation of magnitude calculation based on maximum amplitude and associated period. (Eaton)

   (c) Calculation of regional variations in focal mechanisms of large (M > 4) California earthquakes. (Cockerham and Eaton)

Results:

1. Earthquake catalogs generated by four contiguous telemetereed seismic networks in California and Neveda were merged to show the 5-year regional pattern of seismicity in the entire California - Neveda seismic zone. Contributing networks were: (1) the Nothern and Central California USGS network, (2) the Southern California USGS/CIT cooperative network, (3) the Central and Western Neveda network operated by University of Neveda at Reno, and (4) the Southern Great Basin (Southwestern Neveda) USGS network. Boundaries between networks were drawn on the basis of station distribution; and contributions of each network catalog to the combined catalog were based on those boundaries. See report by Dave Hill and Jerry P. Eaton (this volume) for more information.

2 The overall spatial distribution of epicenters (Figure 1) within the Mono Lake - Bishop area remained unchanged compared with one previous six month

period. Analysis of these data during this six month period has concentrated on (1) the Chalfant sequence and (2) focal mechanism calculations for several thousand earthquakes in this area. From an analysis of fault plane solutions and calculated P- and T- axes the results are (Figure 3): (1) faulting mechanism does not systematically change with depth; (2) although the general style of faulting is strike slip (both right and left lateral) significant variations occur, e.g., in Long Valley Caldera (LVC), earthquakes occuring around Mammoth Mtn. consistently show normal slip, earthquakes in the wet moat (west of Hwy 395) exhibit both dip-slip (normal and reverse) and right-lateral strike slip movement, and earthquakes east of Hwy 395 exhibit predominantly left-lateral strike slip motion; (3) the T-axes, mostly within 30° of horizontal, show a significant rotation from NNE to ESE in a west to east direction: NNE to NE in LVC, NE to ENE to EW within the Sierran block south and southeast of LVC, and EW to ESE in the Chalfant Valley area north of Bishop; and (4) the P-axes, although showing a greater degree of variation in plunge that the T-axes, also are mostly within 30° of horizontal. (The P-axes for earthquakes of M>5.5 in this area in 1978, 1980 and 1981 also are nearly horizontal). In contrast to the present day nearly horizontal P-axis, the curvilinear Sierran frontal fault system from Owens Valley to Lundy lake, which includes the Round Valley and Hilton Creek segments (see Figure 2), exhibits only vertical offset during the Late Quaternary, implying a nearly verical P-axis. Thus, a rotation of the P-axis from nearly vertical to nearly horizontal has occured since the last major normal-slip events in this area. However, the very linear White Mountains frontal fault system and the Ownes Valley fault exhibit predominantly horizontal motion (implying near-horizontal P-axis) during the Late Quaternary and, in particular, the last 115 yrs. as evidenced by the 1872 earthquake (Beanland and Clark, abstracts of the SSA Annual Mtg., 1987) and the 1986 Chalfant Valley earthquakes. Therefore, the data summarized here suggest that $\sigma 1$ (P-axis) and $\sigma 2$ are close in magnitude and that one fault system geometry and small fluctuations in the magnitudes of $\sigma 1$ and $\sigma 2$ together, influence (control?) which fault (faults) will rupture.

3. A 1:250,000 scale map of the seismicity in the Yellowstone Park-Hebgen Lake region from 1964 to 1981 was completed and submitted for review. The map shows epicenters of approximately 700 earthquakes from 1964 to 1972 and over 6000 earthquakes from 1973 to 1981. The events were sorted into 4 groups based on epicenter uncertainty (Fig. 3). The map will probably be released in the USGS "I series" with the earthquake epicenter symbol indicating the 4 classes of epicenter reliability. The map will also show cultural features, topography, and traces of Quaternary faults. A histogram of number of events per month and a cumulative moment plot for the years 1973 to 1981 will be inculded along with focal mechanisms for 56 events.

   The 56 focal mechanisms are a representative sample from mechanisms for 320 earthquakes determined using the computer program FPFIT (Reasenberg and Oppenheimer, U.S. Geol. Survey Open-File Rept. 85-739, 1985). This is approximately 10 times the number of single event machanisms determined for the region in all previous studies. The focal mechanisms indicate predominately extensional tectonics with a mixture of normal and strike-slip faulting. A small number of thrust fault solutions were obtained but they are in areas of the network with poor focal depth control and may have unreliable takeoff angles. Generally, T-axis orientations vary from NNS clockwise to EW. This variation exists across the entire network and may indicate that earthquakes are occuring on pre existing faults that trend at optimum angles to the present stress regime. Focal mechanisms for 23 events in the inset on Figure 3.

Reports:

Cockerham, R. S., Focal mechanisms of earthquakes in one Mammoth Lakes - Bishop area, eastern California, (abs.), Seismol. Res. Lett., 58 (1), p19, 1987.

Cockerham, R. S., and Corbett, E. J., The July 1986 Chalfant Valley, California, Earthquake sequence: Preliminary results, Bull. Seismoc. Soc. Amer., 77 (1), 280-289, 1987.

Pitt, A. M., Tectonics of The Hebgen Lake - Northwest Yellowstone Park region from earthquake hypocenters and focal mechanisms, (abs.) Seismol. Res. Lett., 58 (1) p. 29, 1987.

Savage, J. C., and Cockerham, R. S., Quaisperiodic occurance of earthquakes in the 1978-1986 Bishop-Mammoth Lakes sequence, eastern California, (abs.) Seismol. Res Lett., 58 (1), p. 1987.

Savage, J. C., Cockerham, R. S., Estrem, J. E., and Moore, L. R., deformation near One Long Valley caldera, eastern California, 1982-1986, Jour. Geophys. Res., 92 (B3), 2721-2746, 1987.

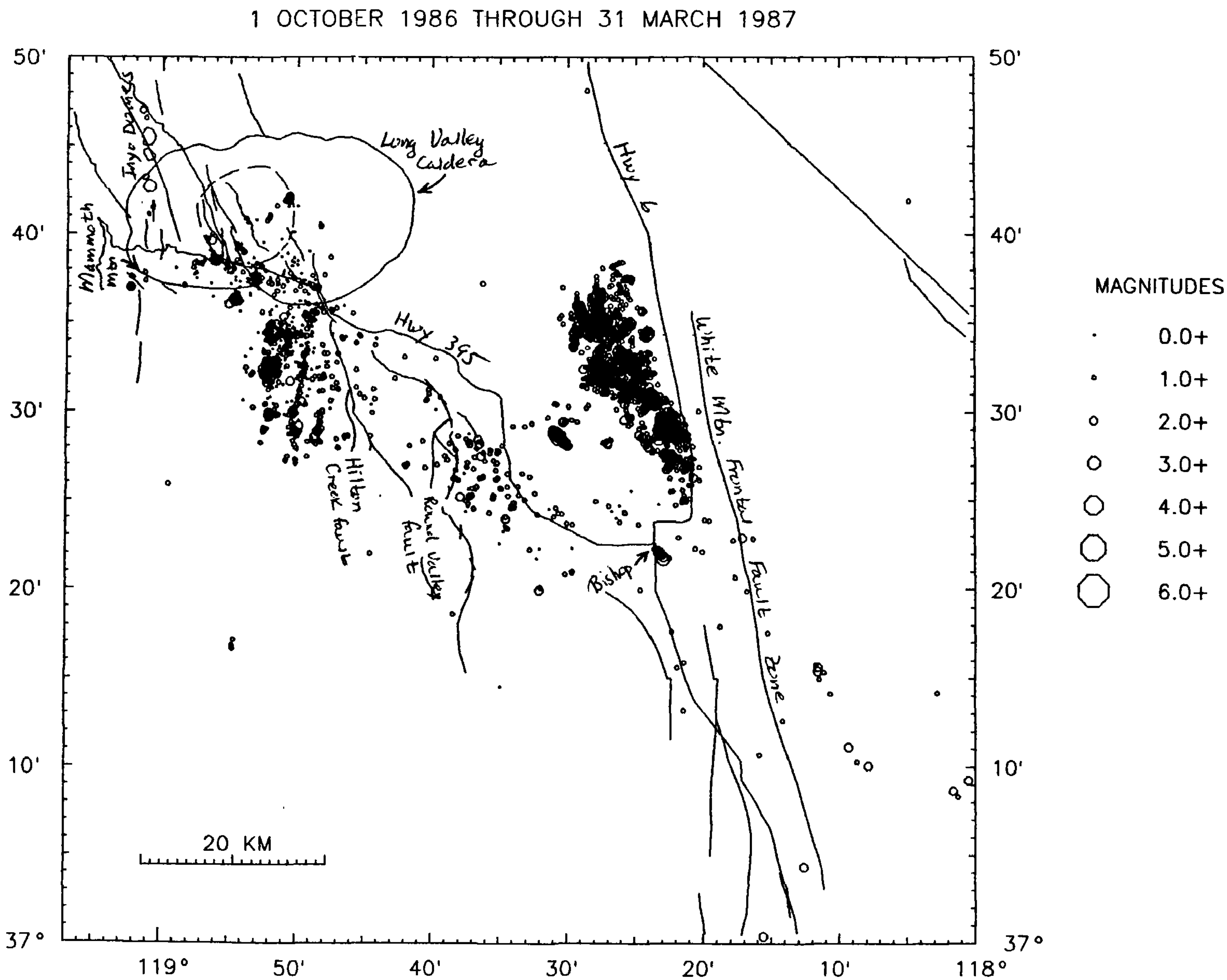

Figure 1. Map of earthquake epicenters (M 0.5) in the Mammoth Lakes-Bishop area of eastern California for the period 1 Oct. 1986 through 31 March 1987. The heavy concentration of epicenters west of the White Mtn. Frontal Fault Zone represents the continuing high level of aftershock activity within the July 1986 Chalfant earthquake rupture zone.

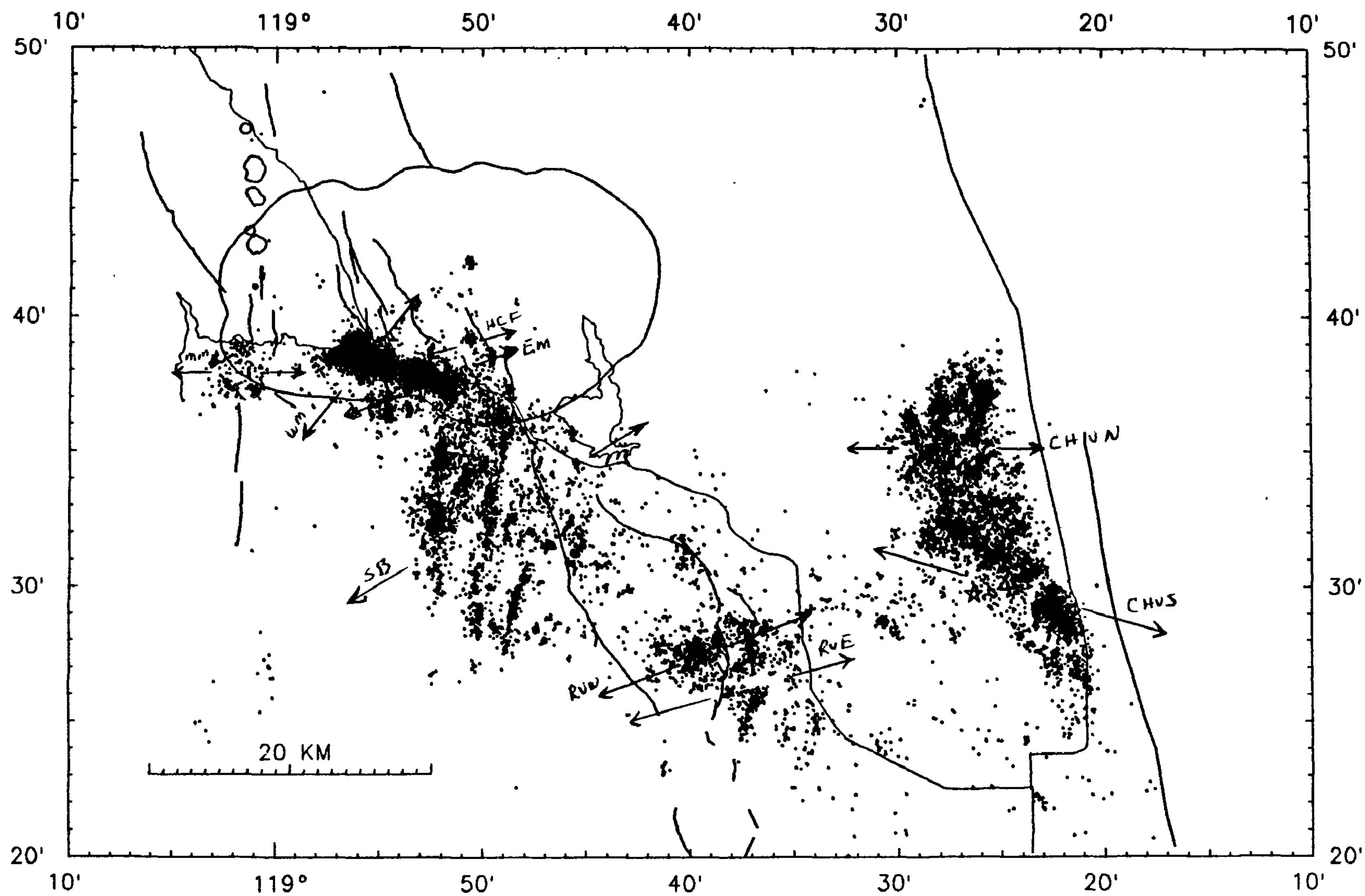

Figure 2. Map of earthquake epicenters from the period 1 Jan. 1983 to 1 April 1987 from which several thousand focal mechanism solutions were calculated. The arrows represent approximate horizontal projections of the T-axis for the groups as indicated. MM - Mammoth Mtn.; WM - west moat; EM - east moat; HCF - Hilton Creek fault (caldera only); SB - Sierran block; RVW - Round Valley west; RVE - Round Valley east; CHVN - Chalfant Valley north; CHVS - Chalfant Valley south. The geographical and geological features are the same as Figure 1. See text for discussion of the T-axes orientation.

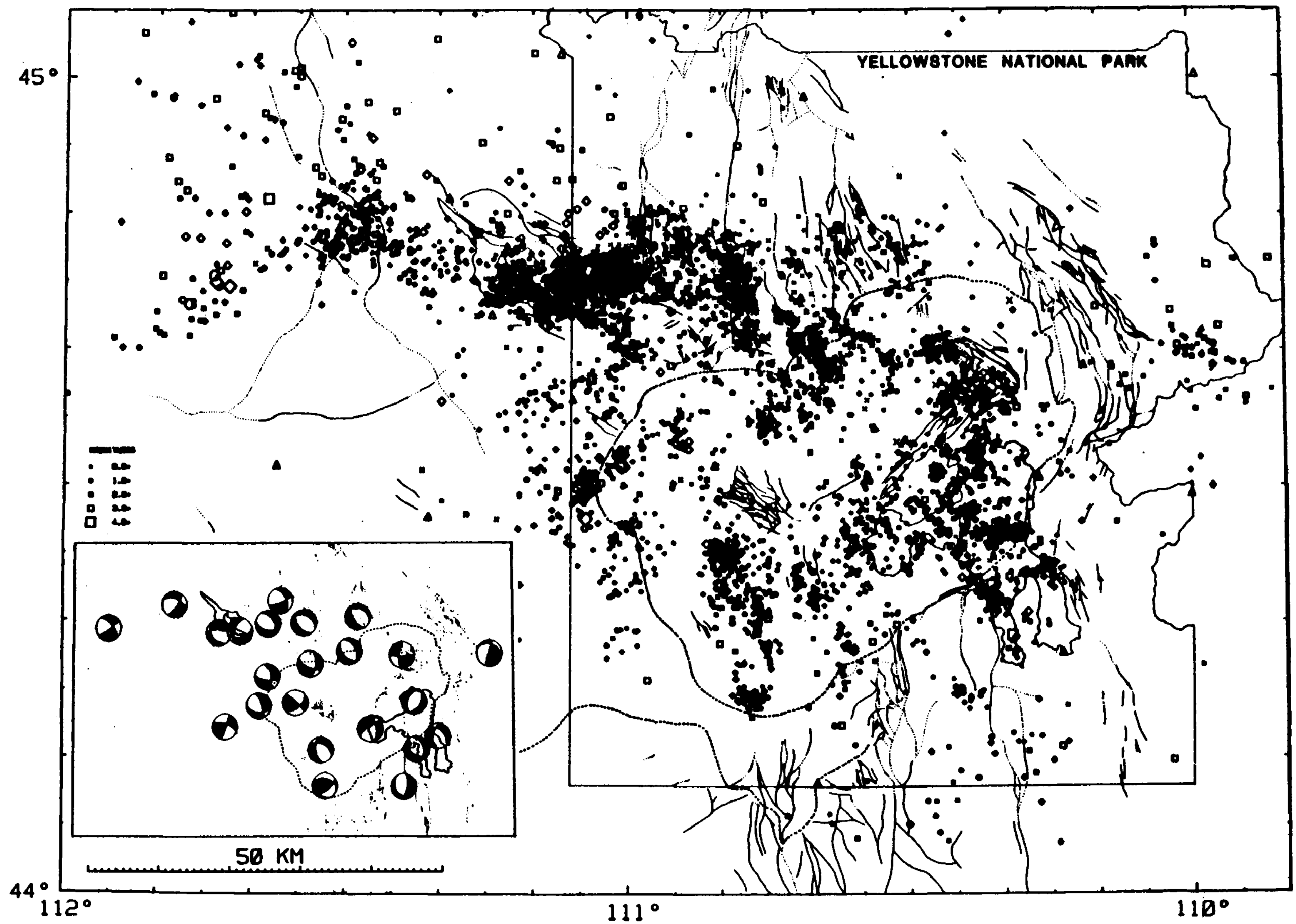

FIGURE 3. Map of earthquake epicenters in the Yellowstone Park region from 1964 to 1981. Symbols show epicenter uncertainty: ✱ 1km, ⬮ 1-3km, ◆ 3-5km, ◘ 5-25km. Triangles mark seismograph stations. Heavy dotted lines are caldera boundaries, light solid and dotted lines are faults showing evidence of Quaternary movement. Inset shows lower hemisphere fault plane solutions; compressional quadrents are solid.

Stress Transfer, Nonlinear Stress Accumulation and Seismic Phenomena at a Subduction-Type Plate Boundary

14-08-0001-G1203

R. Dmowska and J.R. Rice (P.I.)
Division of Applied Sciences and
Department of Earth and Planetary Sciences,
Harvard University
Cambridge, MA 02138
(617) 495-3452, 3445

(For period Oct. 1, 1986 - April 30, 1987)

1. Investigations. We have formulated and run some cases for one-dimensional model of subducting slab, which is slightly more complicated than our previous version (see our previous summary reports). The model allow us to investigate space- and time distribution over the earthquake cycle of stresses in oceanic lithosphere, adjacent to zone of main thrust subduction events, in the zone itself, and down-dip from this zone as well. The model is applicable to coupled subduction zones (where great subduction earthquakes occur) up to the depths of approximately 300 km.

2. Results. Fig. 1a schemetically shows the gravitationally sinking elastic slab with thickness H, the sinking being moderated and opposed by viscoelastic asthenosphere. The slab is locked at part of the marked thrust contact zone, which breaks in periodic large subduction events.

With reference to fig. 1b, the thickness average extensional stress σ and displacement u satisfy

$$H\partial\sigma(x,t)/\partial x + H\, f(x) = \tau_t(x,t) + \tau_b(x,t),$$

$$\sigma(x,t) = [2\mu/(1-\nu)]\partial u(x,t)/\partial x\ .$$

Here f is the slab-parallel gravitational body force component from density contrast; τ_t and τ_b are resistive shear stresses on the top and bottom of the slab. The shear coupling represented by τ_b is approximated as satisfying a generalized Elsasser viscoelastic coupling relation

$$\partial u(x,t)/\partial t - V_b(x) = (b/\mu)[\partial\tau_b(x,t)/\partial t + \tau_b(x,t)/t_r]$$

for appropriately chosen elastic coupling length scale b and relaxation time t_r. The time-invariant nearby mantle flow rate $V_b(x)$ agrees with the plate convergence rate V_{pl} as x approaches + or $-\infty$, and V_{pl} and the implied viscosity factor are assumed to be consistent with long term balance of the gravitational driving force. The coupling τ_t vanishes along the ocean plate, $x<o$, and is likewise approximated as satisfying a generalized Elsasser form, similar to that above, along the subducting slab, $x>z$. Here the thrust zone contacts the subducting plate over length z, i.e., over the zone $o<x<z$. Consistently with the above coupling, we write

$$u(x,t) - \Delta(x,t) = (b/\mu)\ \tau_t(x,t)$$

along the thrust contact zone, where $\Delta(x,t)$ is the thrust slippage along the contact.

In the simplest modeling we assume that $\Delta(x,t)$ jumps by $V_{pl}T$ everywhere along the thrust contact zone after each lapse of earthquake cycle time T, but remains constant in the inter-seismic period. However, more elaborate spatially non-uniform slip histories $\Delta(x,t)$ may be considered which are still consistent with periodic earthquake cycles. In these Δ has net increase $V_{pl}T$ at each location x after a lapse of cycle time T, but has different detailed time histories by which that common increase accumulates at different locations x along the thrust contact zone.

The variables σ, τ_t and u of interest have the form

$$u = V_{pl}t + u''(x) + u'(x,t),$$

$$\sigma = \sigma''(x) + \sigma'(x,t) \ , \quad \text{and} \quad \tau_t = \tau_t''(x) + \tau_t'(x,t)$$

where σ', τ_t' and u' are periodic in t with zero mean throughout the cycle, and are independent of the detailed form of the driving functions $f(x)$, $V_b(x)$, and $V_t(x)$ (the latter defined for $x>z$).

The subsequent plots of shear coupling stress τ_t' along the thrust contact and extensional stress σ' along the oceanic and subducting plates are only the periodic parts of the stresses. The magnitude and spatial distribution of the mean stresses τ_t'' and σ'' is unknown, and hence comparison of the stresses as plotted at different locations x should not be used to draw inferences on differences of absolute stress levels at those locations.

The example for which detailed results are shown is illustrated in fig. 2. There we chose the thrust contact zone width z as 3H (and $H \approx 30$ km would be representative for the Middle American Trench off Mexico). Guided by the observation that the lower portions of some MAT thrust zones become highly active relatively late in the cycle, we have examined the possibility that such seismicity reflects some pre-slip, prior to the large scale thrust instability, in the lower, and hence hotter, portion of the thrust contact zone. Such is much like what occurs in the Tse and Rice (1986) simulations of slip development throughout the strike-slip earthquake cycle, based on slip-rate and slip-history (and temperature) dependent friction.

We have subdivided the lower half of the contact zone into four segments (A,B,C,D), starting from its base, which "break" at respective times (16,17,18,19)T/20 during each cycle. Breaking means that τ_t is suddenly reduced by an amount $\Delta\tau$. In these calculations, we assume that once a zone breaks, it stays broken such that the stress τ_t there remains at the reduced level for the remainder of the cycle. As part of what then turns out to be a rather elaborate calculation, we calculate the slip history $\Delta(x,t)$ at each broken segment which is necessary to keep τ_t reduced there. However, to save computing and programming time, we readjust the stresses back down to their proper level only after each time interval T/20, so that the pre-slip accumulates in 4 rather sizeable steps over the last 20% of the cycle, rather than continuously.

Figure 3 shows the results for τ_t at the four locations (A,B,C,D), of fig.2 through which the pre-slip propagates, and at location E at the center of the remaining part of the thrust contact that ruptures only during the great earthquake at t=T. In that figure and the three which follow the upper and lower diagrams represent the respective cases of modest and large stress drop $\Delta\tau$ in the pre-slip. In the large $\Delta\tau$ case the stress τ_t after pre-slip is reduced nearly to its level just after the great earthquake (at $t=T^+$, corresponding also to $t=o^+$ in the periodic model).

Fig. 4 shows corresponding histories of extensional stress σ' at various locations x updip in the slab and along the ocean plate (negative x values) towards the outer rise. Fig. 5 shows the same at locations along the descending slab downdip from the bottom of the thrust contact ($x \geq z = 3H$). Fig. 6 shows the same set of plots as 5, but with σ' plotted also at $x=2H$. The latter location is traversed by the pre-slip episode, which creates a large transient stress pulse there.

We note from fig. 5 that pre-slip episodes like those considered can appreciably reduce the rate of growth of extensional stress in the slab, and if large enough can even reverse the late-cycle build-up of extensional stress downdip and compressional stress updip (fig. 4, bottom) in the plate. This reversal happens while the still locked thrust zone segment (E of fig. 2) continues to experience an ever rising shear stress, as seen in fig. 3.

The scenario just described provides a possible mechanism for seismic quiescence before great subduction zone earthquakes. What seems to be required is a pre-slip episode, which significantly drops shear stress in the slipped region, over a relatively short fraction of the whole cycle time, but whose continued propagation updip in the thrust zone (and hence, one assumes, continued generation of thrust zone seismicity) is blocked by encounter with a strong asperity. The interactive reductions of downdip extension and updip compression in the plate, described above, stop the seismicity from those regions too. The blocking asperity may, in fact, simply be a zone of cooler (shallower) and hence stronger but more brittle material, whose eventual penetration by accumulating shear stress triggers the final instability.

Work is in progress, and we are now preparing the manuscript (Dmowska et al., 1987).

References

Dmowska R., J.R. Rice, L.C. Lovison and D. Josell, Stress transfer and seismic phenomena in coupled subduction zones during the earthquake cycle, in preparation.

Tse, S. and J.R. Rice, Crustal earthquake instability in relation to the depth variation of frictional slip properties, J. Geophys. Res., Vol 91, pp. 9452-9472, 1986.

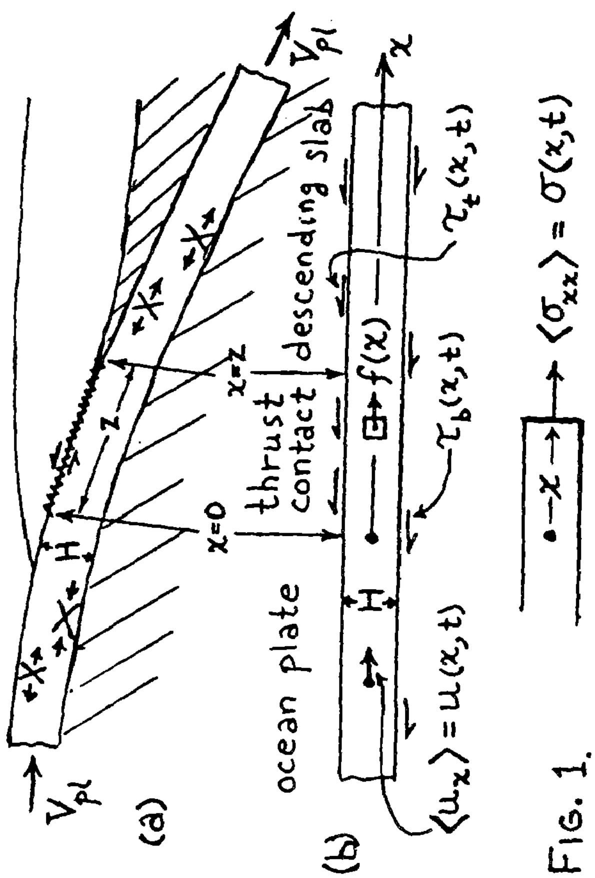

Fig. 1.

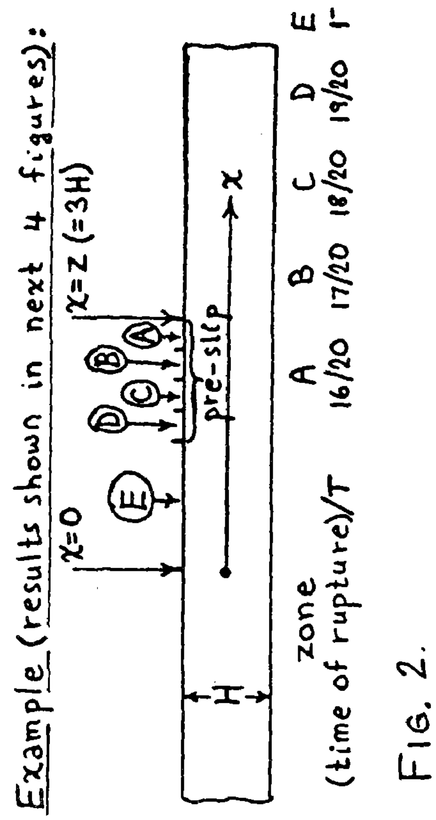

Fig. 2.

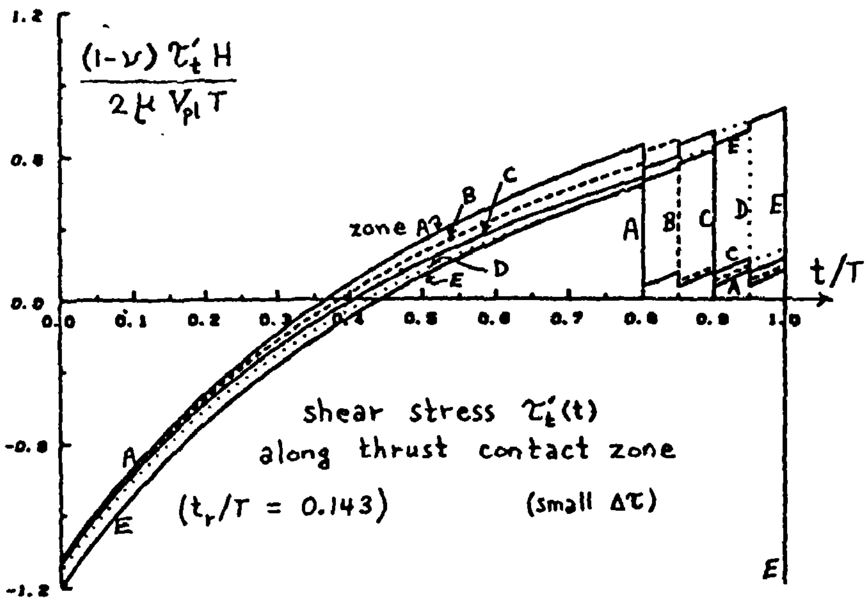
$\frac{(1-\nu)\,\tau_t'\,H}{2\mu V_{pl} T}$
zone A
B
C
D
E
t/T
shear stress $\tau_t'(t)$
along thrust contact zone
$(t_r/T = 0.143)$
(small $\Delta\tau$)

FIG. 3.

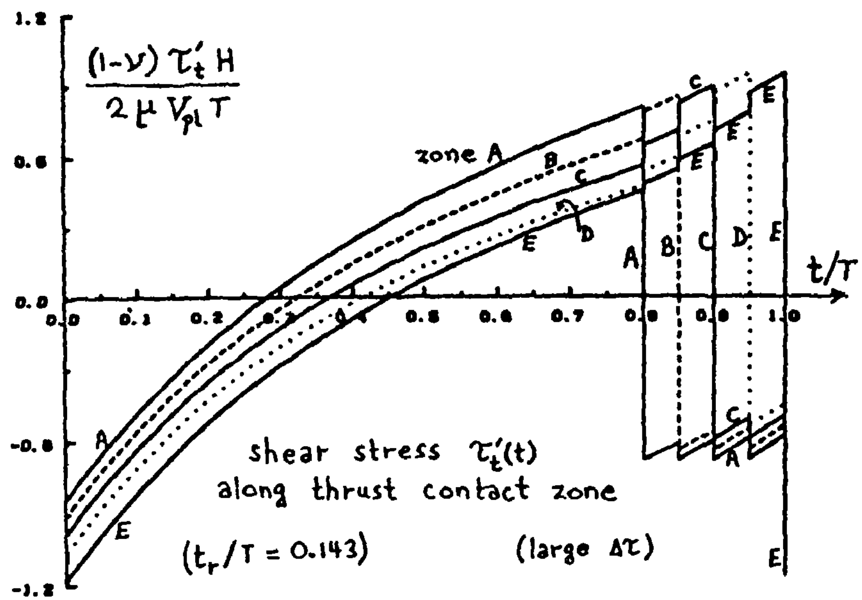
$\frac{(1-\nu)\,\tau_t'\,H}{2\mu V_{pl} T}$
zone A
B
C
D
E
t/T
shear stress $\tau_t'(t)$
along thrust contact zone
$(t_r/T = 0.143)$
(large $\Delta\tau$)

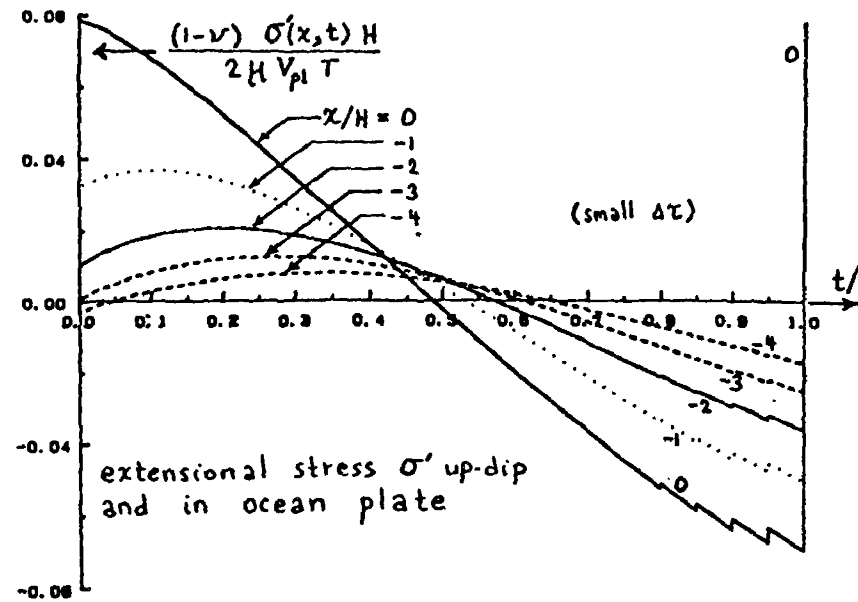
$\frac{(1-\nu)\,\sigma'(x,t)\,H}{2\mu V_{pl} T}$
x/H = 0
-1
-2
-3
-4
(small $\Delta\tau$)
t/T
extensional stress σ' up-dip
and in ocean plate

FIG. 4.

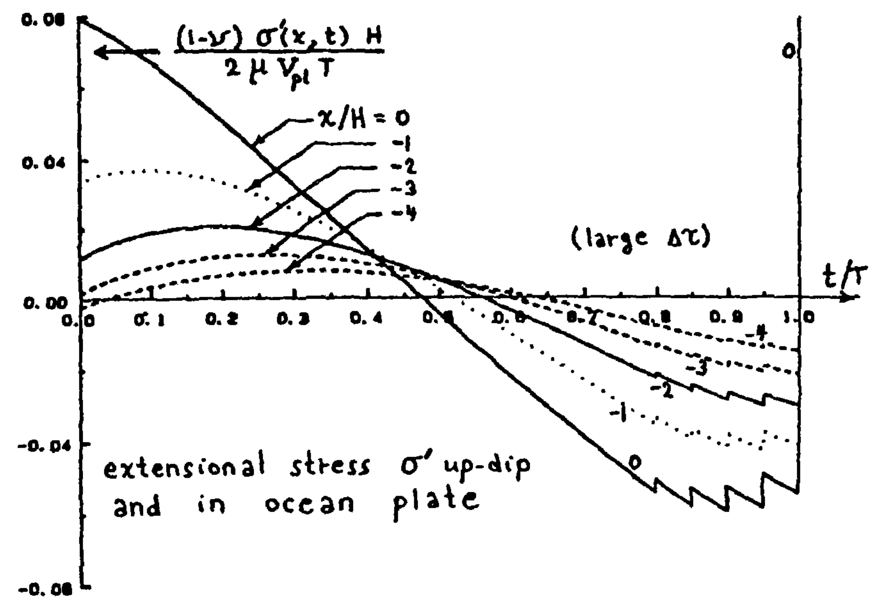
$\frac{(1-\nu)\,\sigma'(x,t)\,H}{2\mu V_{pl} T}$
x/H = 0
-1
-2
-3
-4
(large $\Delta\tau$)
t/T
extensional stress σ' up-dip
and in ocean plate

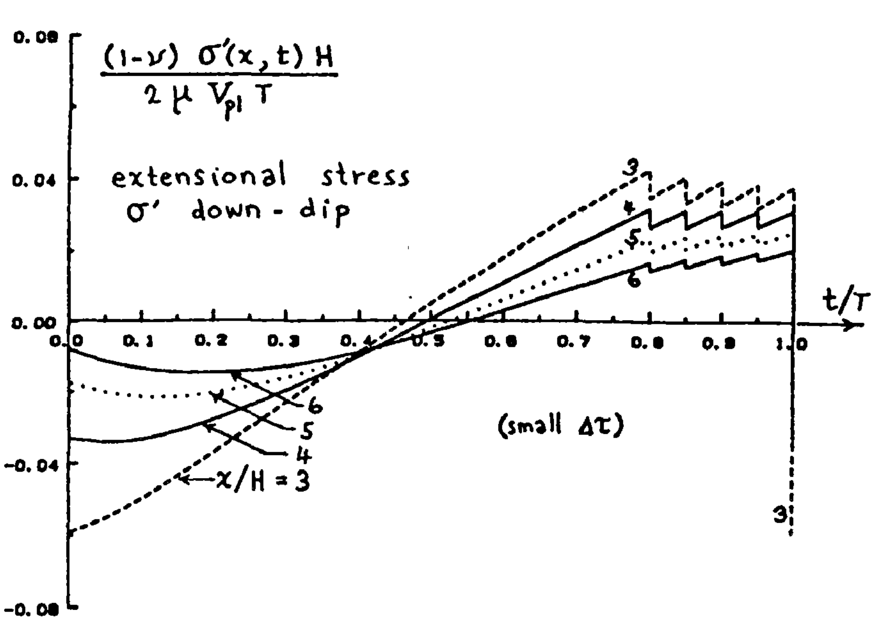

$\frac{(1-\nu)\ \sigma'(x,t)\ H}{2\mu\ V_{pl}\ T}$
extensional stress
σ' down-dip
(small Δτ)
χ/H = 3
t/T
0.08
0.04
0.00
-0.04
-0.08
0.0 0.1 0.2 0.3 0.4 0.5 0.6 0.7 0.8 0.9 1.0

FIG. 5.

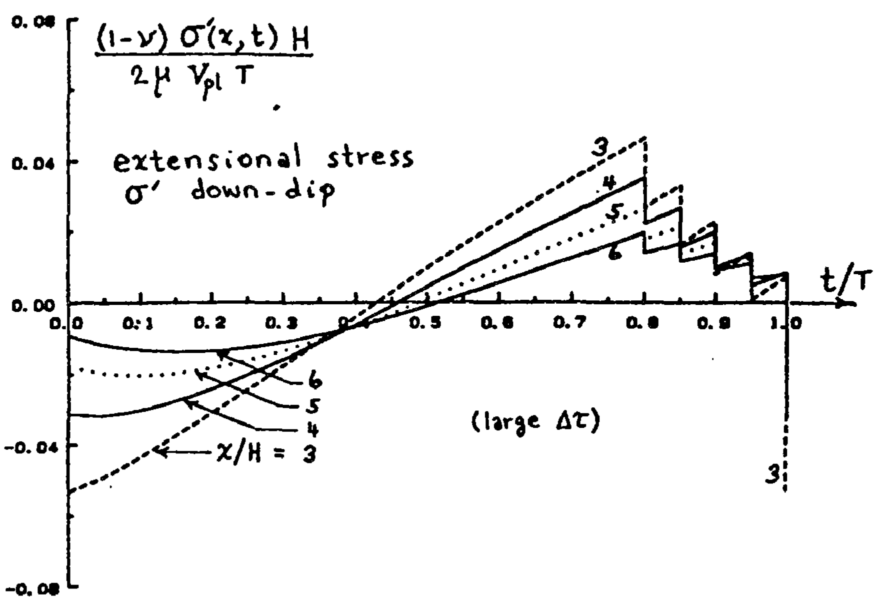

$\frac{(1-\nu)\ \sigma'(x,t)\ H}{2\mu\ V_{pl}\ T}$
extensional stress
σ' down-dip
(large Δτ)
χ/H = 3
t/T
0.08
0.04
0.00
-0.04
-0.08
0.0 0.1 0.2 0.3 0.4 0.5 0.6 0.7 0.8 0.9 1.0

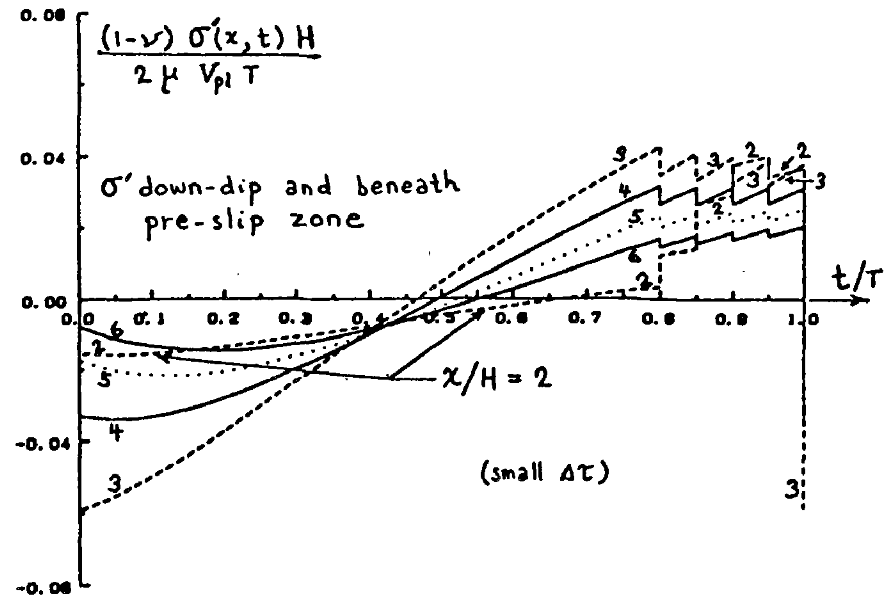

$\frac{(1-\nu)\ \sigma'(x,t)\ H}{2\mu\ V_{pl}\ T}$
σ' down-dip and beneath
pre-slip zone
(small Δτ)
χ/H = 2
t/T
0.08
0.04
0.00
-0.04
-0.08
0.0 0.1 0.2 0.3 0.4 0.5 0.6 0.7 0.8 0.9 1.0

FIG. 6.

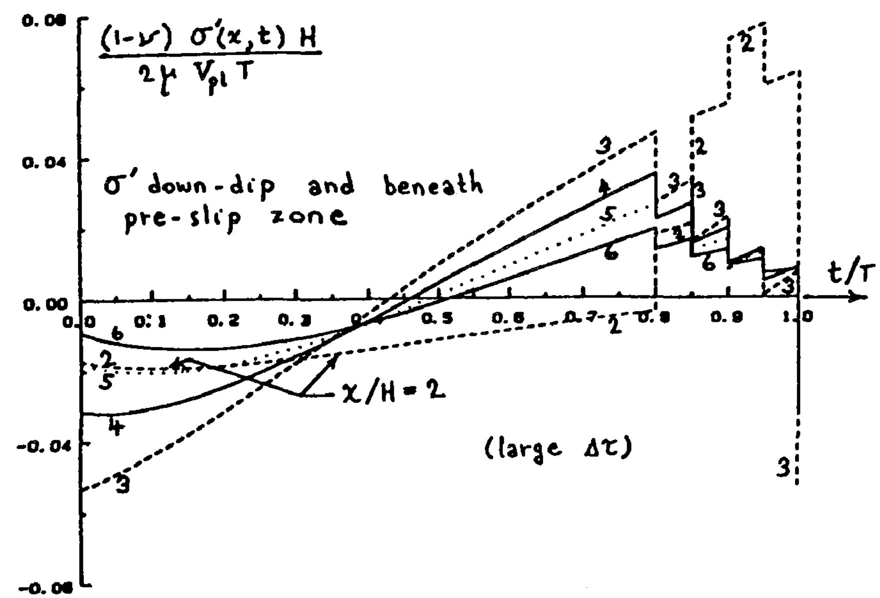

$\frac{(1-\nu)\ \sigma'(x,t)\ H}{2\mu\ V_{pl}\ T}$
σ' down-dip and beneath
pre-slip zone
(large Δτ)
χ/H = 2
t/T
0.08
0.04
0.00
-0.04
-0.08
0.0 0.1 0.2 0.3 0.4 0.5 0.6 0.7 0.8 0.9 1.0

Earthquake Prediction - Helium and Groundwaters

9570-00382

Irving Friedman
U.S. Geological Survey, MS 963
Box 25046, Federal Center
Denver, CO 80225-0046
(303) 236-7886

Investigations

During this year difficulty in maintaining our satellite telemetering platform plus the requirement to change satellite communication frequencies forced a change in telemetering methods from our helium earthquake prediction station near Gardiner, Montana.

Instrumentation at the Miller well has also been expanded from measurements of dissolved helium in the continuously pumped well to include water temperature, electrical conductivity and depth-to-water in the well. The later three parameters are measured and recorded by an on-the-site micrologger. The helium mass spectrometer sampling system is now controlled by an Apple IIe computer. Data is recorded on floppy disk, and telemetered via phone to Denver, where the data is plotted - see fig. 1. We can either operate in an automatic made where sampling occurs periodically, with the data stored on site until requested via modem, or in on-line mode where we can initiate sampling and analysis from Denver and observe data in real time. We have been operating in the first (automated) made in order to reduce phone charges.

The new system has been operating without interruption for over four months. It is far less expensive than the former system and is more flexible in that changes in sampling program can be made easily in software rather than in hardware as formerly.

We may increase the telemetry to include the well data now recorded on site.

Results

The helium abundance has remained constant during this period. Seismic activity within ~100 km has also remained low with no events with a magnitude greater than 4.

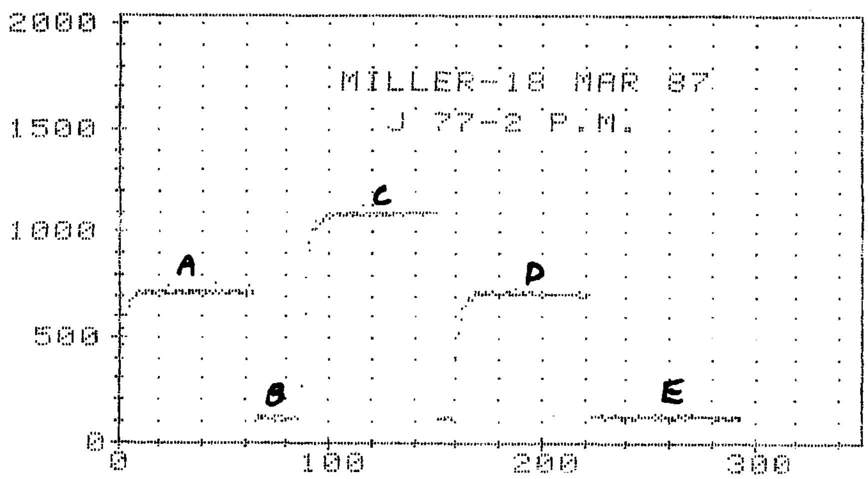

Fig. 1. A and D are helium abundance measurements on a standard tank gas containing 10,000 ppm of helium. C is the helium analysis in the well water. E is the helium - in air (5.2 ppm), while B is instrumental background.

Analysis of Natural Seismicity at Anza

9910-03982

Joe Fletcher, Art Frankel, Leif Wennerberg, and Linda Haar
Branch of Engineering, Seismology, and Geology
U.S. Geological Survey
345 Middlefield Rd.
Menlo Park, CA. 94025
(415) 323-8111

Investigations:
1). Several investigators have suggested recently that the dependence of stress drop on moment for earthquakes at Anza with moments $\leqq 10^{20}$ dyne-cm. may be due to attenuation in the upper crustal layers under the receiver. Although such arguments are plausible, only directly measuring the attenuation at Anza stations will answer these questions. We have drilled boreholes at stations KNW and PFO and both shear wave generators as well as earthquake waves will be used to determine the site response in the upper 300m at these two sites.
2). Another approach to determining the effect of the propagation path on source spectra is to stack spectra from a group of events that have roughly the same moment and compare stacked spectra at each station. Site specific characterisitics of the stacked spectra are then associated with the ray path to that station. These results are important if we are to infer source properties from surface recordings. A refinement of this method, confirming its usefulness, is to use particularly small events as empirical green functions to deconvolve path effects from the seismograms of larger events.

Results:
1). The first site to be instrumented is station KNW, where we have observed seismograms that appear high in frequency content compared to other stations in the Anza net. Boreholes, 300 and 150m. deep were instrumented with a three-component package designed by Hsi-Ping Liu. The geophones have natural frequencies of 2 Hz. and are leveled downhole. The sensor packages are emplaced at the bottom of each of the two holes and packed with sand: they should be retrieveable. Logging for shear wave velocity using a shear-wave generator was performed in the 300m hole and shows that a velocity of about 2.9 km/sec is reached at 30m and is constant to the maximum depth of 300m. Televiewer logs show that the rock formation has zones that are heavily fractured but otherwise is devoid of cracks.

Seismograms recorded on the downhole sensors (see fig.1) are clearly higher in frequency content then the surface record. Additionally the coda for the P wave is usually larger and dies off much slower downhole then at the surface. In fact some of the smaller events that have S-P times of about 2 sec. do not have a corner frequency inside of 100 Hz. We have computed spectral ratios of a suite of these events (e.g. fig. 2) and have found that while the ratios are highly variable most show resonances in the surface records compared to those downhole. These resonances are strongest between 5 and 40 Hz, but there may be some attenuation above that frequency.

Initially we were sampling at 200 samples/s and we are now at 400 samples./s to avoid the aliasing we found in the first records obtained from this experiment. Moments of events are mostly in the $10^{17}$to 10^{18}dyne-cm range: no large events have been recorded yet.

2). Eighty-one small events with moments of about 10^{18} dyne-cm. were subdivided into source regions and then stacked by source region. Corner frequencies and high frequency asymptotes of S-wave spectra were found to be strongly dependent on site and less so on depth or range. For instance, one set of six events had average corner frequencies of 19 Hz at station KNW and 5 Hz at station SND. One event which had an unusually shallow depth had lower corners then most other events which are deeper. High attenuation in the shallow material near the fault zone may be causing this difference. A small event was used as a green function and deconvolved from a larger event. The deconvolved spectra then had remarkably consistent shapes between stations. Form this deconvolution, resonances were found at at station KNW. There was no indication below 60 Hz of a corner frequency for the small event (again consistent with the downhole results) suggesting the small earthquake spectra (to 60 Hz) reflects propagation rather than source effects.

Abstracts:

Haar, L.C., Fletcher,J.B., Liu,H.-P., Warrick,R.E., and Westerlund,R.E., (1987) Near-surface effects at Anza: comaprisons of surface and borehole data,Seis. Res. Let,vol.58, p26..

Haar, L.C., Fletcher,J.B., Liu,H.-P., Warrick,R.E., and Westerlund,R.E.,(1987) Preliminary results from a borehole experiment at Anza, CA, to investigate near-surface effects of seismic wave propagation, submitted to the Spring AGU meeting, Baltimore, MD.

Liu, H.-P., Warrick, R.E., Fletcher,J.B., and Westerlund,R.E.,(1987) A three-component borehole seismometer for controlled-source and earthquake seismology, submitted to the Spring AGU, Baltimore, MD.

Liu, H.-P., Warrick, R.E., Fletcher,J.B., and Westerlund,R.E.,(1987) A three-component borehole seismometer for controlled-source and earthquake seismology, Seis. Res. Let.,vol.58,p11.

Wennerberg, L., and Frankel,A., (1987) Site response and spectra of earthquakes determined from the Anza network, Seis. Res. Let., 58, p25.

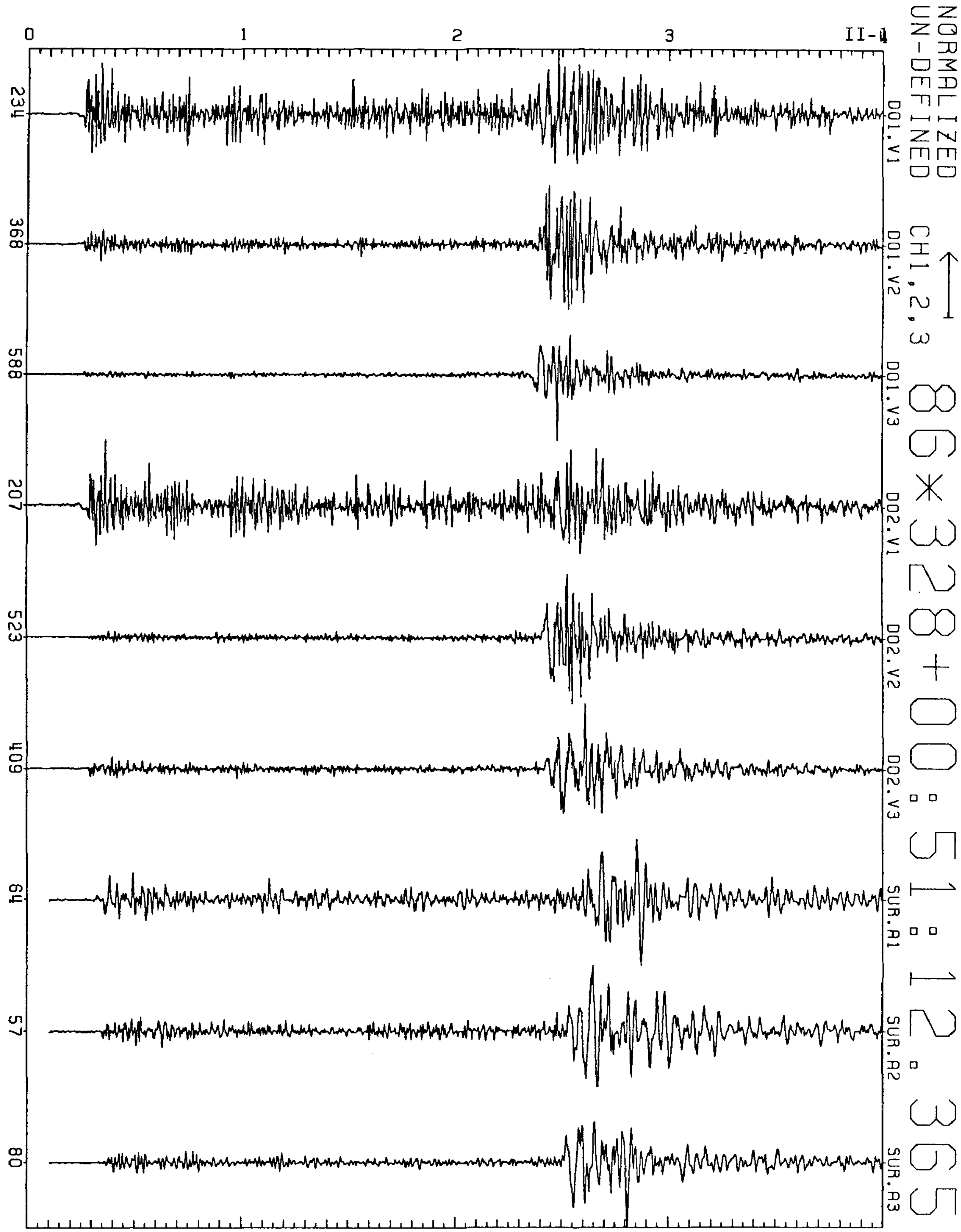

Figure 1: Time series for November 23, 1986 event. The top three traces are from the 300m deep instrument, the next three are from the 150m deep instrument, and the last three are from the surface instrument. The first trace in each group of three is the vertical component and the remaining two are the horizontal components.

328:00:51

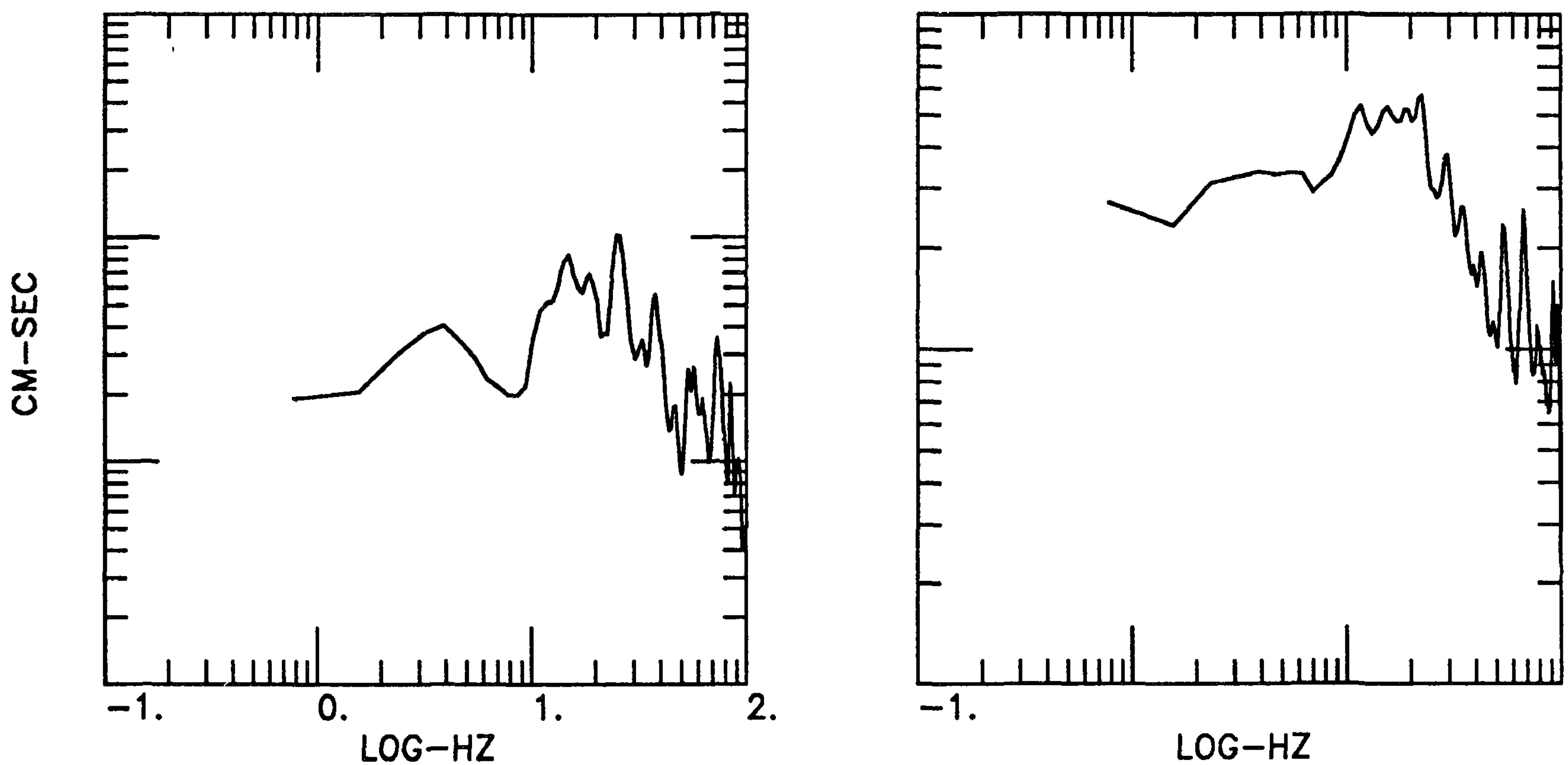

FIGURE 2 : Spectral ratios of surface to downhole for event of November 23, 1986.
A) Ratio of vertical components. B) Ratio of horizontal power.

Quantitative Determination of the Detection History of the California Seismicity Catalog

14-08-0001-G-992

R.E. Habermann
School of Geophysical Sciences
Georgia Institute of Technology
Atlanta, Georgia 30332
(404) 894-2860

We have made progress on several aspects of this work during the last six months. First, we have initiated and made substantial progress on a careful evaluation of the significance levels which we ascribe to changes in seismicity rates. Second, we have nearly finished our comparison of Berkeley and CALNET magnitudes for six regions of Central California. Each of these tasks are described in more detail below.

Significance Levels

Our analysis of seismicity data involves searching for changes in seismicity rates using various statistical tests and windowing schemes. Matthews and Reasenberg recently proposed that the process of searching changes the significance level which is associated with a given statistic. We search for anomalies using the function AS(t) which was designed to answer two questions: 1) When is the most significant rate change between two points in time? and 2) How significant is that change? Matthews and Reasenberg agree that the function finds the times of the most significant change, but they disagree with the interpretation of the significance of those changes.

We have examined this question using several thousand sets of data with uniform, Poisson, and normal distributions. We calculated statistics for these data in the same way as we would for real data and examined the resulting distributions of the statistics. There are two distributions which we are interested in. First, the distribution of all AS(t) values and second, the distribution of maxima of each set of AS(t) values. In addition, there are two lengths that are important. The first is the set length, which is the number of samples in each series. The second is the minimum sample length.

The distribution of all AS(t) values was found to be normal in all cases, as expected. Table 1 shows the critical levels determined from the distribution of maxima for a series of set lengths ranging from 332 to 900 and for minimum sample lengths ranging from 10 to 100. Each critical level is calculated by examining the cumulative frequency distribution from 1000 sets with the listed lengths and minimum sample sizes. One can make several interesting observations from these data.

First, it is clear that for small minimum sample lengths (10) the critical value is erratic regardless of the set length. The values range from 3.97 to 4.40. For longer minimum sample lengths (100) the range of the critical levels is much smaller and is not dependent on the length of the set. These observations indicate that shorter anomalies are more likely to be random fluctuations and therefore are more difficult to recognize without false alarms, in accordance with our experience. These results indicate that a critical level of 3.5 is appropriate for minimum sample lengths longer than 50.

Table 1. 99% Critical Levels From Sets of 1000 Simulations

Minimum Sample Length	Set Length 332	400	500	600	700	800	900
10	4.27	4.40	4.40	4.00	3.97	4.23	3.98
25	3.60	3.80	3.90	3.56	3.58	3.80	3.67
50	3.75	3.67	3.70	3.65	3.54	3.58	3.60
60	3.47	3.35	3.45	3.50	3.52	3.56	3.56
75	3.40	3.55	3.52	3.48	3.50	3.50	3.50
100	3.43	3.45	3.40	3.50	3.46	3.50	3.50

These preliminary findings suggest that our significance estimates for anomalies shorter than 50 samples may have to be reassessed. Many of these anomalies, however, have z values that are above 3.5, so they remain significant at the 99%+ level. This suggests that while the significance estimates that we made were incorrect, the change in critical level will not strongly influence our conclusions.

Comparison of Berkeley and CALNET Magnitudes.

We have recently completed a comparison of magnitudes in the Berkeley and CALNET catalogs. This comparison is limited to larger events because the Berkeley catalog contains only events which are larger than ML = 2.5. We carried out this comparison in seven different regions. The results for six of these regions are shown in Figure 1 (the Northern California region could not be reasonably studied because of the low level of reported activity at these magnitude levels). The differences between USGS and Berkeley magnitudes are shown as a function of time. Changes in the mean difference are thought to reflect changes in the USGS magnitudes because the Berkeley magnitudes are calculated using a stable set of seismometers.

The most obvious observation that can be made from these data is that rather strong systematic changes in USGS magnitudes are apparent in all but the Parkfield region. A common feature appears to be a period of relatively high magnitudes starting during the early 1970's and lasting until 1976 (East Bay), 1977 (N. Calaveras and San Juan Bautista), or 1979 (Bear Valley and S. Calaveras). The decrease in magnitudes at the end of this period is probably associated with decreases in gains in the develocorders at Menlo Park during April, 1977.

We are presently in the process of comparing the information gained from an analysis of these data with that gained from the analysis of magnitude signatures, the technique we developed for examining detection histories and magnitude stability. The primary difference between the two techniques is in the magnitude bands examined, as mentioned above. The ability to include smaller events in the analysis, provided by the magnitude signature approach, gives one a much larger data set to work with and permits one to recognize apparent changes which affect only the smaller events. Good examples of such changes are those associated with the installation and adjustment of the RTP system. In addition, the magnitude difference approach provides less resolution in the time domain because of the scarcity of larger events. Finally, the statistical basis of the magnitude difference approach is weakened by the small number of events which one has to examine. The small number of events also restricts one to examination of relatively large regions using this approach.

ORAL PRESENTATIONS

Consistency of magnitudes in the CALNET catalog, EOS, 67, 1086.

A test of two techniques for identifying systematic errors in magnitudes using data from Parkfield, California, EOS, 67, 1087.

PAPERS PUBLISHED

Man-Made Changes in Seismicity Rates, BSSA, 77, 141, 1987.

A test of two techniques for identifying systematic errors in magnitudes using data from the Parkfield, California region, BSSA, 76, 1660, 1986.

PAPERS IN PRESS

Reply to Comment by Matthews and Reasenberg (to JGR, with M. Wyss)

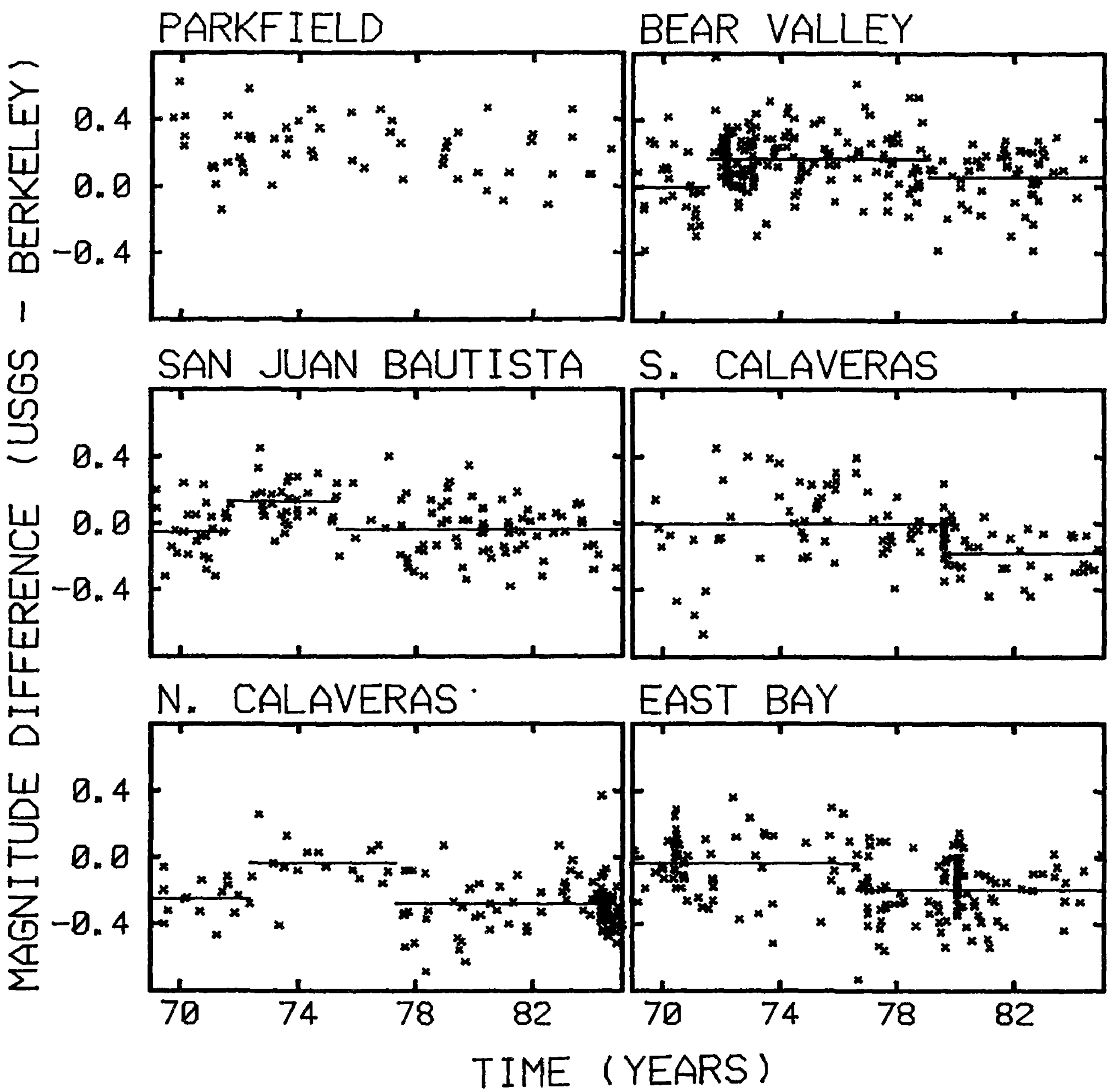

Figure 1. Magnitude differences as a function of time for six regions of California.

SEISMICITY AND THE SEISMOTECTONIC FABRIC OF CALIFORNIA AND WESTERN NEVADA: 1980-1985

9930-01496

David P. Hill and Jerry P. Eaton

Branch of Seismology
U.S. Geological Survey
345 Middlefield Road, MS 977
Menlo Park, California 94025
(415) 329-4795

Investigations

We are in the process of describing detailed seismicity patterns over the six-year interval 1980-1985 based on data compiled from the telemetered seismic networks operated in California and western Nevada. This represents a cooperative effort with contributions from principal scientists involved with seismic network operations in southern California (Caltech and USC), central and northern California (U.S.G.S., Menlo Park; U.C. Berkeley) western Nevada (the University of Nevada, Reno), and southern Nevada (U.S.G.S., Golden, Colorado). The core of this investigation will involve publication of a series of seismicity maps for each of the six years with associated cross-sections emphasizing spatial-temporal variations in the occurrence of M>1.5 earthquakes across the entire San Andreas transform boundary between the Pacific and North American plates and the adjacent (western) section of the Basin and Range intraplate extensional province.

Results

We (with Bill Ellsworth, Rob Cockerham, Rick Lester, and Ed Corbett of UNR) have completed an initial draft manuscript focused on central California seismicity for the 1980-1986 period that will appear as a chapter in the DNAG associated volume GSMV-1, Neotectonics of North America edited by Slemmons and others. Figure 1 shows the annual spatial-temporal variation in seismicity for central/northern California and western Nevada for the six-year period covered in the paper, and Figure 2 summarizes the associated frequency-magnitude statistics. The latter indicates a completeness threshold of M = 1.5-2.0 throughout most of northern California. The curves in Figure 2 also support the view that a self-similar source scaling applies to events as small as M = 1.5 in northern California. Particularly noteworthy at the scale of Figure 1 is the stability of the overall seismicity pattern from year to year marked by persistent clusters of activity at the Mendocino triple junction just off Cape Mendocino and in Mammoth Lakes-Bishop region of eastern California superimposed on two subparallel bands of seismicity: one along the San Andreas fault system in the Coast Ranges and the other extending northwestward from the Mammoth Lakes-Bishop cluster through Lake Tahoe and beyond toward Lassen

Peak and Mount Shasta of the southern Cascades. More diffuse seismicity patterns extend across the northern and central sections of the otherwise seismically quiescent Great Valley-Sierra Nevada block.

Equally noteworthy are the marked changes in detail from one year to the next within the outline of the stable seismicity patterns. The most pronounced of these changes are associated with major earthquakes and the decay of their aftershock sequences. Two examples stand out in Figure 1. The rapid decay of the aftershocks to the November 1980 M=7 earthquake off Cape Mendocino leaves little trace of the distinctive northeast lineation of epicenters (Figure 1a) beginning only two months later in 1981 (Figure 1b). In contrast, the slowly decaying aftershocks to the May 1983 M=6.7 Coalinga earthquake have persisted as a dense cluster of epicenters east of the San Andreas fault in central California for more than three years (Figure 1d,e, and f).

Figure 3 shows the pattern of M>1.5 earthquakes throughout the California-western Nevada region for 1980-1984. We, in collaboration with colleagues at Caltech, USC, UNR, and Golden, are working on the early stages of a manuscript describing the seismicity data represented in this map and its relation to major aspects of the seismotectonic fabric of the greater San Andreas fault system and its junction with the Basin and Range province.

<u>Reports</u>

None published

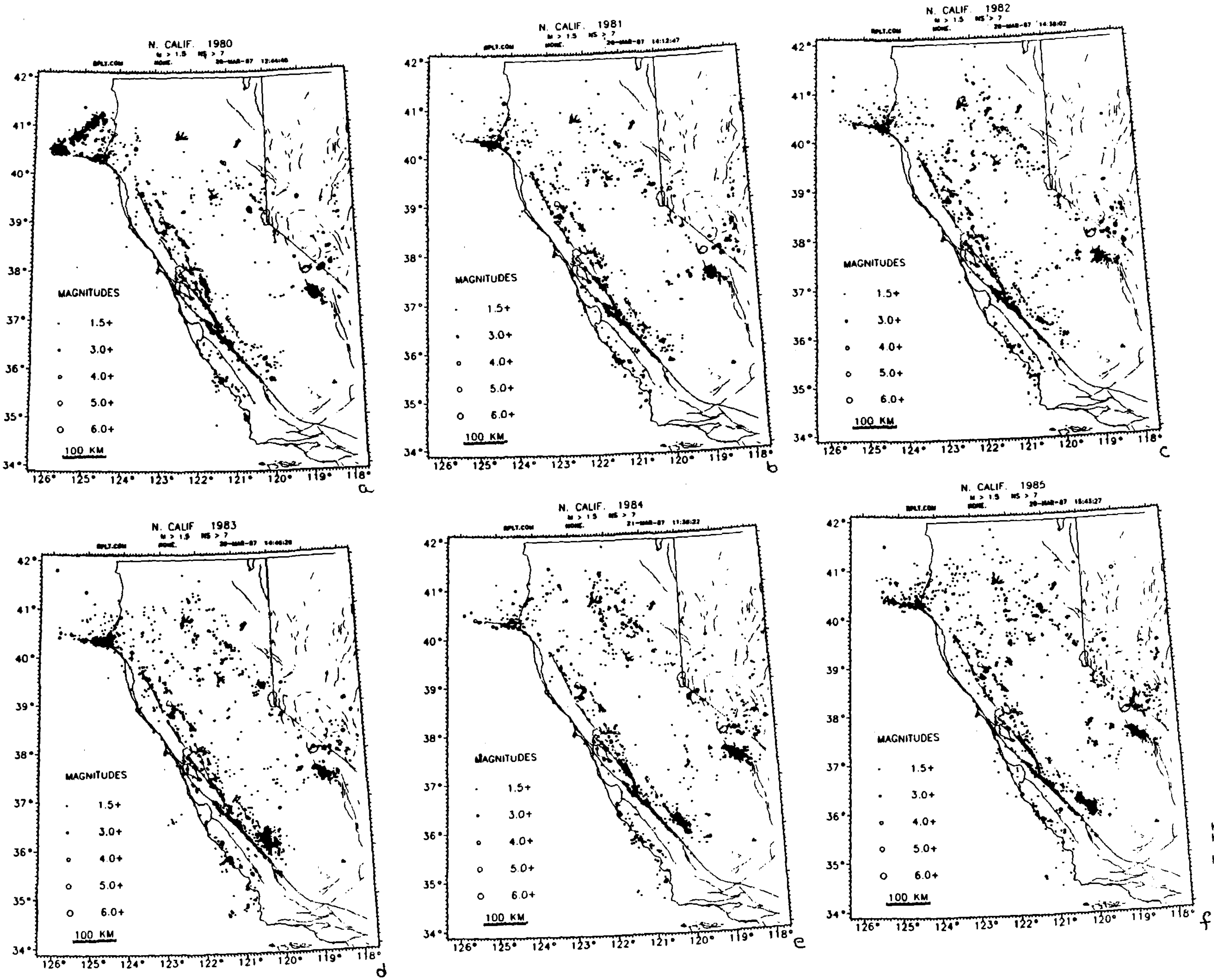

Figure 1. Seismicity patterns for M>1.5 earthquakes in northern California and western Nevada for 1980 through 1985.

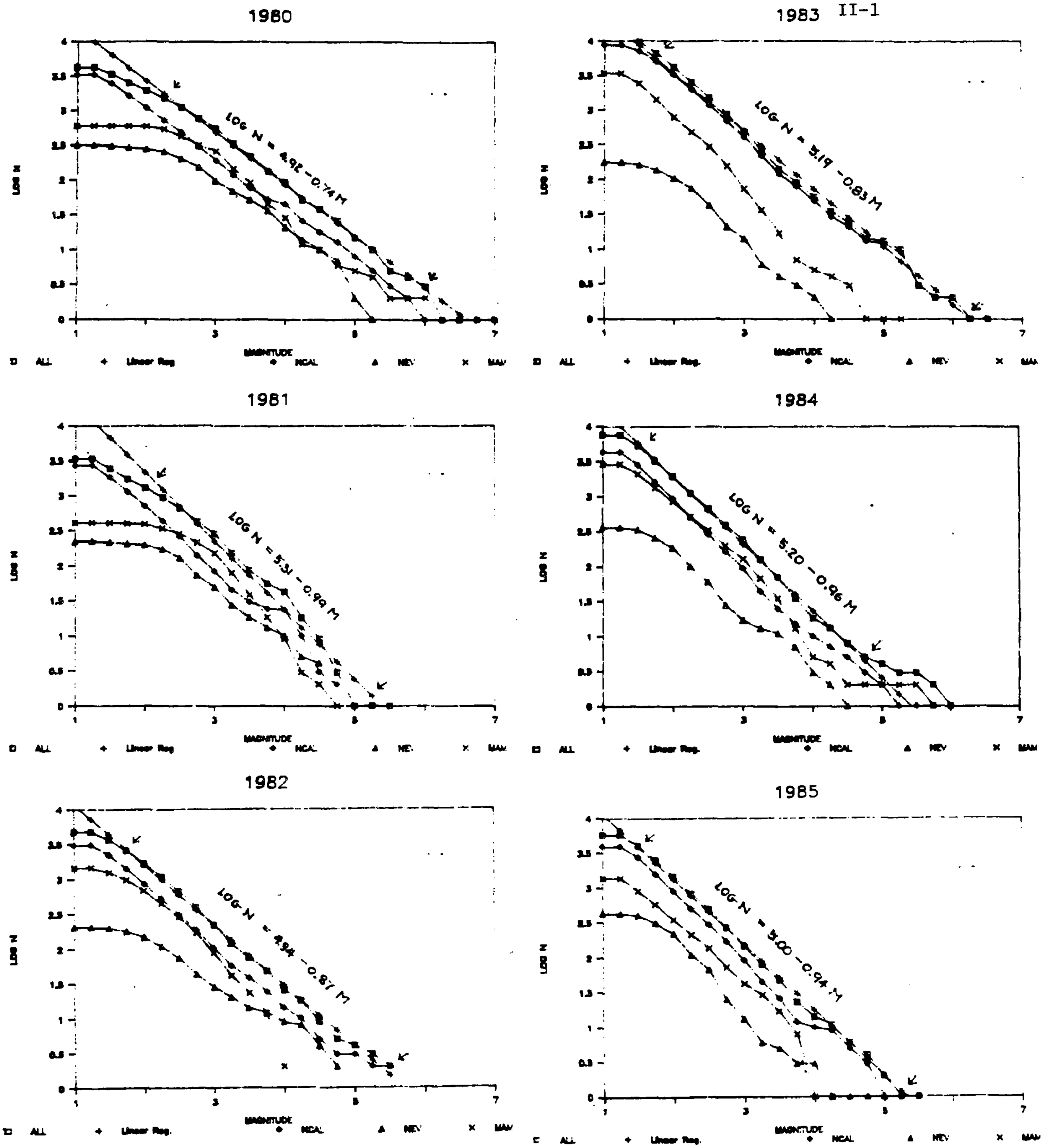

Figure 2. Annual frequency-magnitude curves for the earthquakes plotted in Figure 1. N is the cumulative number of events of magnitude M>Mo. Data from contributing networks indicated by NCAL = northern California (USGS), NEV = western Nevada (UNR), MAM = Mammoth Lakes-Long Valley region (USGS, UNR). ALL is combined data from all three networks, and Linear Reg. is the best-fitting line Log N = a + bM over the interval between the arrows through ALL.

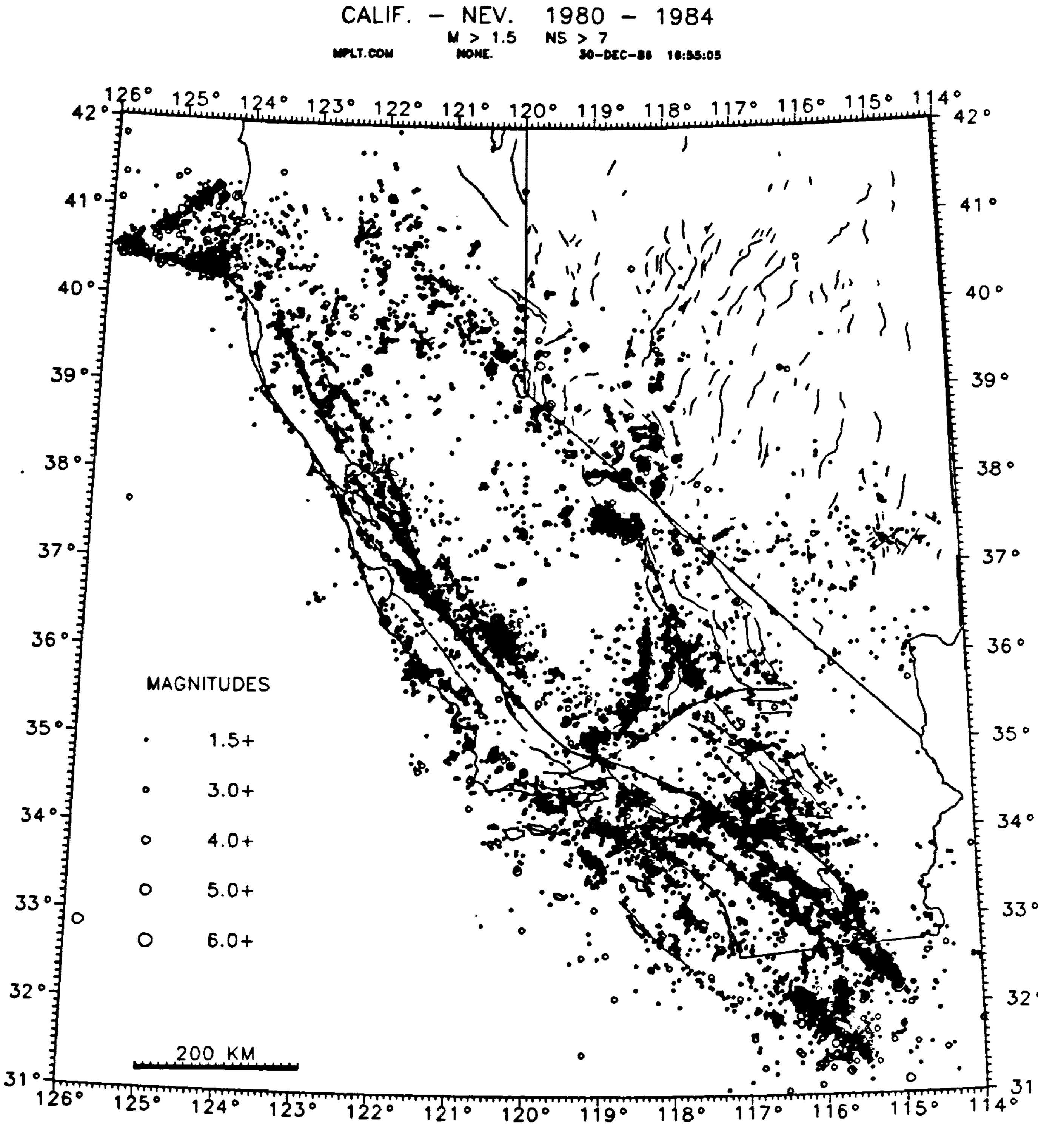

Figure 3. Seismicity for M>1.5 earthquakes throughout California and western Nevada for the period 1980-1984.

Instrument Development and Quality Control

9930-01726

E. Gray Jensen
Branch of Seismology
U.S. Geological Survey
345 Middlefield Road - Mail Stop 977
Menlo Park, California 94025
(415) 323-8111, Ext. 2050

Investigations

This project supports other projects in the Office of Earthquakes, Volcanoes and Engineering by designing and developing new instrumentation and by evaluating and improving existing equipment in order to maintain high quality in the data acquired by the Office.

Results

A clock board and an input amplifier board for the J1000 digital seismic recorder / telemetry station were built. An IBM compatible laptop computer, which will be used to program J1000 field units, set their clocks and collect their data, was modified with a very stable oscillator to allow accurate transfer of time. Also a new floating-point amplifier module was received permitting development of a gain-ranged analog-to-digital converter board for the system. Current effort is on software development.

Six one-inch tape recorders which continuously record all seismic data telemetered to the Menlo Park office were moved along with their associated equipment and time rack to the telemetry center. This move was required because of asbestos removal in the building. The transfer went smoothly and data recording was interrupted for only a few hours. Digitizing of one-inch tapes by the VAX 11/750 computer through the Tustin digitizer became operational. This group implemented the hardware changes required to transfer this operation from the Eclipse computer. More recently, the addition of Parkfield stations to the network required that Tustin input connections be changed to accommodate both the CUSP network digitizing and tape digitizing. The newly completed solution is a ribbon cable patch panel which permits users to easily switch control of the two Tustin digitizers to any of three computers (VAX or two PDP 11/44's) and to switch their analog inputs to either the CalNet or the tape output.

In January, as part of an agreement between the Seismological Bureau of Yunnan Province and the USGS, a geophysicist from this project travelled to Kunming, PRC. While there he assisted their scientific staff in maintaining and upgrading a system of PDR-2 seismic data recorders and associated playback computers.

Approximately 350 more J120 discriminators have been tuned bringing the total to 430. The Hawaii Volcano Observatory is currently using 100 units, a few are installed here and most of the rest will be going to Cal Tech. There has been a lot of activity in Parkfield. About 9 three-component force-balanced accelerometers stations have been installed with specially adapted VCO's for FM telemetry to Menlo Park. Several dilatometers have been similarly set-up for telemetry. A set of ultra-low-noise amplifiers for buffering down-hole seismometer outputs were constructed. The J502A preamp/VCO design was modified to improve its low temperature response.

As usual a lot of time has been spent augmenting and maintaing the microwave telemetry network. Preparations have been made for installation of a new backup power generator at Menlo Park and transfer of the old one to Parkfield. Many CalNet and Parkfield seismic stations were visited for maintenance, repair and upgrading. Also, numerous telemetry radios and seismometers were repaired, adjusted or calibrated. Support was provided for Seismic Cassette Recorder operations in San Luis Obispo.

Southern California Earthquake Hazard Assessment

7-9930-04072

Lucile M. Jones and Douglas D. Given
Branch of Seismology
U.S. Geological Survey
Seismological Laboratory 252-21
California Institute of Technology
Pasadena, California 91125

INVESTIGATIONS

1. Routine Processing of Southern California Network Data.

Routine processing of seismic data from stations of the cooperative southern California seismic network was continued for the period October 1986 through March 1987 in cooperation with scientists and staff from Caltech. Routine analysis includes interactive timing of phases, location of hypocenters, calculation of magnitudes and preparation of the final catalog using the CUSP analysis system. About 800 events are detected in most months with a regional magnitude threshold of 2.0. The three month backlog (July to September 1986) created by the large number of earthquakes in the July 8, North Palm Springs, July 13, Oceanside and July 21, 1986 Chalfant Valley sequences has been reduced. At present, only the last two weeks of September remain unprocessed. The six week backlog in November and December 1985 created during a switch in computer systems remains untimed. We plan to eliminate this backlog by October 1987.

2. Foreshocks in Southern California

Analysis of the characteristics of immediate foreshocks (those that occur within hours or days of their mainshocks) in southern California is continuing. The probability as a function of magnitude and time that any southern California earthquake will be a foreshock has been determined as well as a site-specific result for possible foreshocks on the San Andreas, San Jacinto and Hayward faults. The site-specific results have been determined by combining the increased probability of a large earthquake occurring after a possible foreshock with the conditional probability of a large earthquake determined from recurrence intervals using Utsu's probability gain formulation. These results are also applied to real time earthquake hazard assessment.

3. Focal Mechanisms and State of Stress in Southern California.

The state of stress in southern California is being analyzed from focal mechanisms of small and moderate earthquakes. Two projects are currently underway. First, the state of stress as a function of position along strike of the southern San Andreas fault has been determined from earthquakes of $M \geq 2.6$ with epicenters within 10 km of the surface trace of the fault. In addition, temporal changes in the state of stress on the San

Andreas fault are being examined by comparing the aftershocks of the North Palm Springs earthquake to background seismicity in the same region recorded in the last 8 years. In both studies, focal mechanisms are determined from local network data and then inverted for information about the stress state.

4. The North Palm Springs Earthquake of July 1986.

The M = 5.9 North Palm Springs earthquake of July 08, 1986 and its aftershocks are being analyzed. Focal mechanisms are being determined for the $M \geq 3.0$ aftershocks. All of the aftershocks are being relocated using a master event technique. The results are compared to the geologic structures to better understand the deformation occurring on the southern San Andreas fault.

5. Characteristics of Earthquake Clusters in Southern California.

The properties of earthquake sequences in southern California are being analyzed. Earthquakes in the southern California catalog from 1932 to 1986 have been grouped into spatial-temporal clusters using Reasenberg's (1985) clustering algorithm. The spatial extent, b-value, and magnitude gaps (the difference between the largest and the second and third largest events) have been determined and the regional variations in these quantities studied.

6. Southern California Network Survivability

The potential for impairment of the data recording and processing capability of the Caltech-USGS seismographic network by large damaging earthquakes in southern Caifornia has been studied. The primary goal of this work is to identify weaknesses in the data collection and processing stream and propose measures to mitigate those weaknesses. First, the telemetry, recording and processing components of the network were defined. Information on the potential for shaking damage to hardware components was gathered from equipment manufacturers, utilities, technicians, and published sources. Possible data loss due to high station gain and software saturation were also considered. Finally, recommendations for increasing the survivability of the network were made based on the weakness and importance of each component.

RESULTS

1. Foreshocks in Southern California.

We estimate that an earthquake in western California increases the probability of a larger earthquake occurring at the same site within 3 days to 4%. The probability that the mainshock will have a magnitude Mm or greater decreases as Mm - Mf (the magnitude of the possible foreshock) increases. Thus a M5 earthquake has a .8% chance of being a foreshock to a M6 event and a .1% chance of being a foreshock to a M7 event. The probability of a M6 earthquake being a foreshock to a plate boundary ruptuing event is highest on the Indio segment of the San Andreas fault.

We estimate the M=5.9 1986 North Palm Springs earthquake had approximately a 5% chance of being followed by a large earthquake. A moderate earthquake at Point Arena, by contrast, has less than a 0.1% chance of being a foreshock. These probabilities are shown by position along the fault in Figure 1. Most foreshocks occur near their mainshock's hypocenters at the ends of ruptures and have focal mechanisms similar to those of their mainshocks. Therefore, moderate strike-slip earthquakes at the ends of segments of the San Andreas are assumed to be twice as likely to be foreshocks while events elsewhere are taken to be half as likely. Based on these (unproven) assumptions, the occurrence of a moderate strike-slip event at Cajon Pass or Bombay Beach is estimated to abruptly increase the probability of the Indio earthquake occurring within 3 days to 10%.

2. Focal Mechanisms and the State of Stress in Southern California.

Focal mechanisms have been determined for background seismicity ($M \geq 2.6$) in the region of the North Palm springs earthquake between 1978 and 1985 and for $M \geq 3.0$ aftershocks of that 1986 M=5.6 event. By inverting the focal mechanisms of the background seismicity, we can obtain the uniform component of the deviatoric stress field that existed before the earthquake. The same can be done for the aftershocks in order to find the stress regime after the earthquake. Any statistically significant differences are most likely due to the mainshock, because it represents the majority of moment released in the area. The 22 mechanisms of earthquakes from 1978 to 1985 indicate that the most compressional stress axis is oriented nearly horizontal with an azimuth 9° west of north. Preliminary inversion of 20 aftershocks during the first day show that the most compressional stress axis has shifted to an azimuth 20° west of north. The application of non-parametric bootstrap statistics shows that this rotation shows that this rotation is significant at the 93% confidence level.

3. The North Palm Springs Earthquake.

The mainshock and aftershocks of the North Palm Springs earthquake sequence have been relocated using the master event technique. The aftershock distribution clearly delineates a planar structure that strikes N65°W and dips 45° northeast. This structure is most likely the down-dip extention of the Banning fault. The aftershocks are distributed symetrically about the mainshock but tend to cluster. They occur through a depth range of 2 to 18 km with a peak in activity at 11 km; the depth of the mainshock. The aftershock pattern northwest of the mainshock is markedly different from that to the south-east. Northwest of the mainshock most events lie on the dipping planar structure and gradually peter out with distance along strike. In contrast, the events to the southeast are diffuse, shallower on average, and cease abruptly at a distance of about 7 km along strike from the mainshock. The different pattern of aftershocks on either side of the mainshock coincides with the southern kink of the "big bend" in the San Andreas fault zone and a persistent boundary between high activity in San Gorgonio Pass and low activity in the Coachella Valley. This suggests that the earthquake occurred at a point where the fault zone undergoes a significant change in regime.

4. Characteristics of Earthquake Clusters in Southern California.

B-values were calculated for the larger earthquake clusters and most were found to be normally distributed between 0.6 and 1.4 with no significant regional variation. In addition there were 5 sequences with very high b-values that were preferentially located in the geothermal areas of the Owens Valley. Magnitude gap is large for mainshock-aftershock sequences and small for swarms and can be considered a discriminator for swarms. Magnitude gap showed considerable regional variation with swarms being more common in the Imperial and Owens Valleys and mainshock-aftershock sequences being more common in Santa Barbara and along the San Jacinto fault. Magnitude gap also increased with magnitude such that no $M \geq 5.5$ earthquakes have been part of swarms during the 50 years of the catalog. The spatial extent of the sequences of course increased with magnitude of the mainshock. For a given mainshock magnitude, however, swarms (small magnitude gaps) had greater spatial extents than mainshock-aftershock sequences.

5. Survivability of the Southern California Network

Evaluation of the survivability of the Caltech-USGS seismic network has lead to a clearer understanding of the relative weakness of network components and the potential for data loss that the failure of each of those components would cause. The most important result of this study is a set of recommendations that, when implemented, will increase the likelihood of uninterrupted data gathering and processing. The results of this study will also be used for long term planning to insure that survivability of future network components is optimized.

REPORTS

1. Jones, L.M., L.K. Hutton, D.D. Given, and C.A. Allen, The North Palm Springs earthquake sequence of July 1986, Bull. Seismol. Soc. Amer., 76, 1830-1837, 1986.

2. Gross, S. J., and L.M. Jones, Characteristics of earthquake clusters in southern California, Seismol. Res. Let., 58, p. 21, 1987.

3. Jones, L.M., and A.G. Lindh, Foreshocks and time-dependent conditional probabilities of damaging earthquakes on major faults in California, Seismol. Res. Let.., 58, p. 21, 1987.

4. Given, D.D., L.K. Hutton, and C. Koesterer, Survivability of the Caltech-USGS seismic network in the event of a major earthquake in southern California, Seismol. Res. Let., p. 13, 1986.

5. Given, D.D., R. Norris, L.M. Jones, L.K. Hutton, C.E. Johnson, and S. Hartzell, The Southern California Network Bulletin, III, January - June, 1986, U.S. Geol. Surv. Open-File Report 86-598, 1986.

6. Jones, L.M., Focal mechanisms and the state of stress on the San Andreas fault in southern California, in review, J. Geophys. Res., 1987.

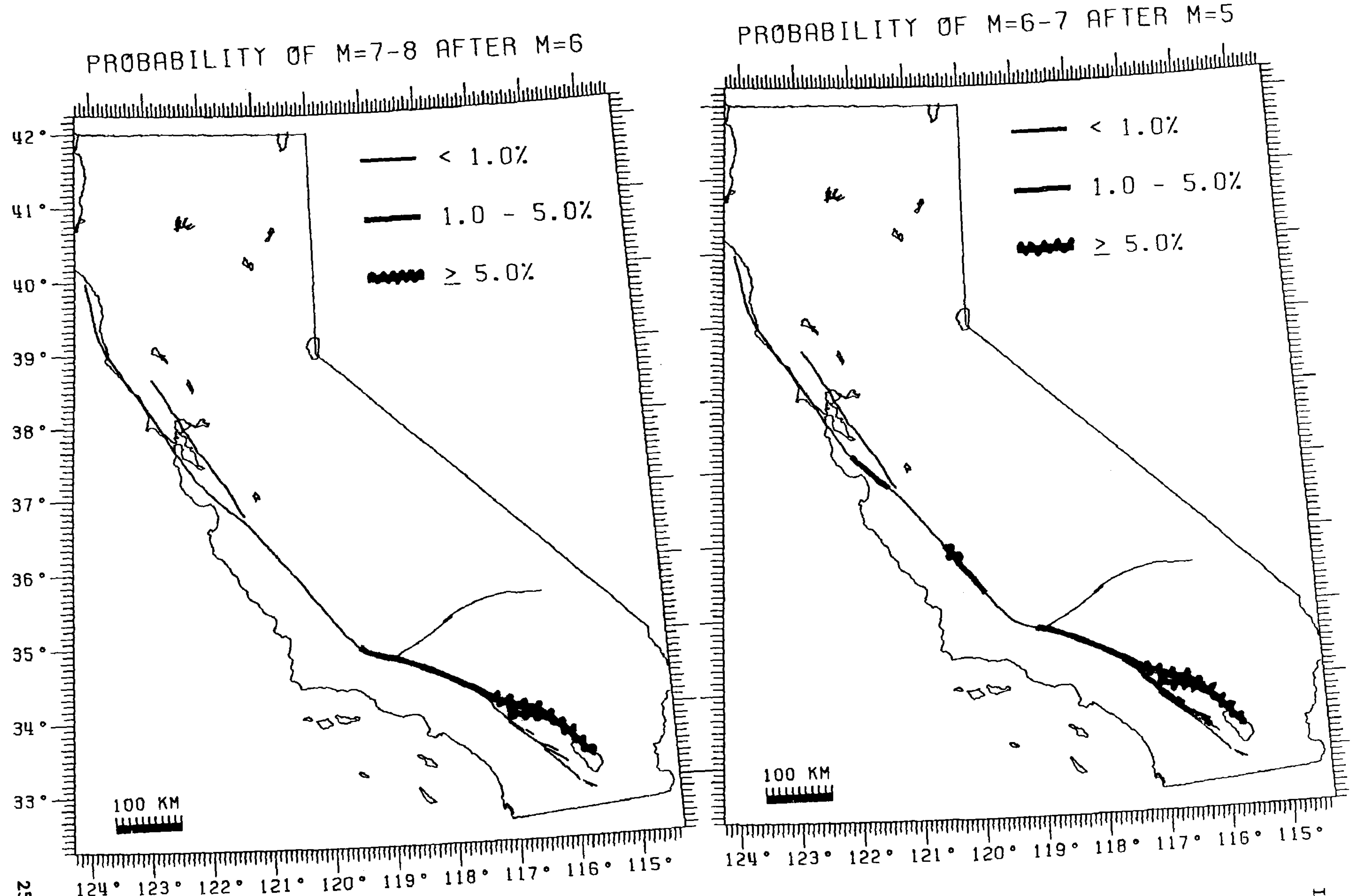
PROBABILITY OF M=7-8 AFTER M=6
< 1.0%
1.0 - 5.0%
≥ 5.0%
100 KM
42°
41°
40°
39°
38°
37°
36°
35°
34°
33°
124° 123° 122° 121° 120° 119° 118° 117° 116° 115°
PROBABILITY OF M=6-7 AFTER M=5
< 1.0%
1.0 - 5.0%
≥ 5.0%
100 KM
124° 123° 122° 121° 120° 119° 118° 117° 116° 115°

Fig 1

State of Stress Near Seismic Gaps

Grant No. 14-08-0001-G1356

Hiroo Kanamori
Seismological Laboratory, California Institute of Technology
Pasadena, California 91125 (818-356-6914)

Investigations

1) Source Parameters of the May 7, 1986 Andreanof Islands Earthquake
Lorraine J. Hwang and Hiroo Kanamori

2) Source Characteristics of Earthquakes in the Michoacan Seismic Gap in Mexico
Luciana Astiz, Hiroo Kanamori and Holly Eissler

Results

1) Source Parameters of the May 7, 1986 Andreanof Islands Earthquake

Source characteristeristics of the May 7, 1986 earthquake (51.412°N, 174.830°W, NEIC) are investigated from WWSSN, GDSN and IDA records. First motions from over 60 stations determine one steeply dipping nodal plane. We constrained this nodal plane and inverted long-period surface waves at a period of T=256 sec and determined the second nodal plane to be dip 18°, rake 116°, and strike 257°. This shallowly dipping thrust mechanism is consistent with plate motions in this region. Seismic moment from surface-wave inversion is 1.3×10^{28} dyne-cm corresponding to M_w=8.0. Amplitudes of body and surface waves from short-period instruments yield magnitudes of $\hat{m}_b$=6.8 and M_s=7.7. The teleseismic average P-wave moment rate spectrum from 17 short- and intermediate-period instruments is slightly lower than that of an average M_w=8.0 subduction-zone event. We constrained the fault plane as determined above to deconvolve the first 90 secs of the long-period body wave at 11 teleseismic stations to determine the source time function and the spatial distribution of moment release. The source time function consists of 4 moment-releasing episodes which have a total moment release of 9.4×10^{27} dyne-cm. The fault ruptured bilaterally with the largest moment releasing subevent occurring between 30-45 sec. This subevent nucleates approximately 75-90 km west of the determined epicenter. This region corresponds to the epicentral area of the 1957 Great Aleutian earthquake which is one of the largest earthquakes in recorded history.

2) Source Characteristics of Earthquakes in the Michoacan Seismic Gap in Mexico

We investigated the source characteristics of large earthquakes which occurred in the Michoacan, Mexico, seismic gap during the period from 1981 to 1986 in relation to historical seismicity in the region. The rupture pattern of the Michoacan gap during this period can be characterized by a sequential failure of five distinct aspertities. Before 1981, the Michoacan gap had not experienced a large earthquake since 1911 when an M_s=7.8 earthquake occurred. The recent sequence started in October 1981 with the Playa Azul earthquake which broke the central part of the gap. Body-wave modeling indicates that the Playa Azul earthquake is 27 km deep with a seismic moment of 7.2×10^{27} dyne cm. It is slightly deeper than the recent Michoacan earthquakes and its stress drop is higher suggesting a higher stress level at depths in the Michoacan gap. The seismic moment of the September 19, 1985 (M_w=8.1) earthquake was released in two distinct events with the rupture starting in the northern portion of the seismic gap and propagating to the southeast with low moment release through the area already broken by the 1981 Playa Azul earthquake. The rupture propagated further southeast with an M_w=7.5 event on September 21, 1985. Another aftershock occurred on April 30, 1986, to the northwest of the September 19 mainshock. Body-wave modeling indicates that this event has a simple source 10 s long at 21 km depth, and fault parameters consistent with subduction of the Cocos plate (θ=280°, δ=12°, λ=70°) and M_o=2.0–3.1$\times10^{26}$ dyne cm (M_w=6.8–6.9). Although this distribution of asperities is considered characteristic of the Michoacan gap, whether the temporal sequence exhibited by the 1981-1986 sequence is also characteristic of this gap or not is unclear. It is probable that, depending on the state of stress in each asperity, the entire gap may fail in either a single large event with a complex time history or a sequence of moderate to large events spread over a few years. The seismic moment and the time since the last earthquake in Michaocan (in 1911) fit an empirical relation between moment and recurrence time found for the Guerrero-Oaxaca region of the Mexico subduction zone.

References

Hwang, Lorriane J. and Hiroo Kanamori, Source parameters of the May 7, 1986 Andreanof Islands Earthquake, *Geophys. Res. Lett. 13*, No. 13, p. 1426-1429, 1986.

Astiz, Luciana, Hiroo Kanamori and Holly Eissler, Source characteristics of Earthquakes in the Michoacan Seismic Gap in Mexico, Bulletin of the Seismological Society of America, in press.

CALIFORNIA AND HAWAII SEISMICITY STUDIES

Project 9930-03563

Fred W. Klein
Branch of Seismology
U.S. Geological Survey MS 977
345 Middlefield Rd.
Menlo Park CA 94025

Investigations

The overall objective is to look for long-term seismicity and tectonic patterns in the Northern California and Hawaii earthquake catalogs. The two catalogs are in very different states of self-consistency and usefulness for research, however. Accordingly, the Hawaiian work uses a completely reprocessed catalog and focuses on research. The Northern California effort presently involves cleaning up the raw phase data and developing methods for reprocessing this data into a self-consistent catalog. This reprocessing is necessary before many types of research become meaningful. The emphasis is on applying methods developed for Hawaiian processing and earthquake display to the California catalog.

The Hawaiian seismic investigation is a detailed study of the vertical magma conduit feeding Kilauea Volcano's shallow (3-7 km depth) magma reservoir. The seismically active conduit extends downward to about 55 km to the top of the magma source region.

The work on the Northern California earthquake catalog is being shared by several colleagues in the branch. This project has assumed responsibility in several areas: (1) Develop a data base of seismic stations including a new systematic set of station codes and apply it to the reprocessing of the earthquake catalog. (2) Develop a computer file system or data base for storing both raw and processed earthquake phase data. (3) Divide the state into geographic regions for examining seismicity and using different crustal models, and implement the regions in several computer programs. (4) Develop and modify the HYPOINVERSE earthquake location program to handle the various tasks needed for Northern California processing. These include archival storage of various data, implementation of a revised coda magnitude procedure, ability to obtain interactive locations in the CUSP processing envirnment, and use of regionalized crustal and station delay models. (5) Revise the QPLOT geophysical data plotting program as necessary for real-time and other display tasks needed for research, monitoring and reprocessing of seismicity data.

Results

The research on Kilauea's magma conduit suggests that the earthquakes require external sources of stress and are not simply generated by excess magma pressure, as with rift zone intrusions. Dramatic evidence for an external stress cause is the major drop in earthquake rate following the M=7.2 Kalapana earthquake in 1975. This event thus released stress in the entire volcanic system in addition to the rupture zone in Kilauea's south flank. Seismic gaps occur along the conduit centered at about 5, 13 and 20 km depths. The 3-to-7-km gap is the main magma reservoir, the 13 km gap appears to result from the layer of buried ocean sediments at the base of the volcanic pile, and the 20-km gap is present under the whole island. The latter may be a depth of low or "neutral" stress within the flexing lithosphere. Lateral extension is characteristic of the focal mechanisms within the volcanic pile (above the 13 km gap) and lateral compression occurs just below. Stresses are thus decoupled at the boundary of the volcanic pile with the underlying oceanic crust. Focal mechanisms below 20 km depth are similar to those in Kilauea's south flank and show southward motion of the upper block on a near-horizontal plane. Stresses do not reverse above and below 20 km depth, so this gap is more complex than simply a plane of neutral stress within the flexing lithosphere.

The reprocessing of the Northern California earthquake catalog is underway. Contributions from this project to date include: (1) A growing data base of seismic stations has been assembled, including assignment of unique 5-letter codes to each station ever used in our phase data. Several programs use the station data base, including one that converts all of the chaotic station codes in our phase data to the new system. (2) The state has been divided into regions for seismic monitoring. These same regions are being incorporated into HYPOINVERSE as a means of chosing an appropriate crustal model for relocation. (3) The QPLOT plotting program has been continually revised, and now plots both maps and time-series in real-time to monitor both seismicity and the status of real-time processing.

Reports

Klein, F.W., R.Y. Koyanagi, W. Tanigawa, J. Nakata (1987), Earthquakes near Kilauea's vertical magma conduit between 7 and 36 km depth (abs.), Hawaii Symposium on How Volcanoes Work, Hilo HI, January 1987.

FAULT MECHANICS AND CHEMISTRY

9960-01485

C.-Y. King
Branch of Tectonophysics
U.S. Geological Survey
345 Middlefield Road, MS/977
Menlo Park, California 94025
(415) 323-8111, ext. 2706

Investigations

1. Water temperature and radon content were continuously monitored at three water wells in San Juan Bautista and Parkfield, California.

2. Water level was continuously recorded at six other wells.

3. Water temperature and electric conductivity were periodically measured, and water samples were taken from most of these wells and two springs in San Jose for chemical analysis.

4. Radon content of ground gas was continuously monitored at Cienega Winery, California, and at Nevada Test Site.

5. Predictability of slip events along a laboratory fault was studied.

Results

Radon levels recorded at a 350-ft deep water well in the Miller Ranch located about 0.5 km west of the San Andreas fault near Parkfield, CA, apparently increased by about a factor of 2 in mid-February, 1987. The significance of this change is difficult to assess because of several gaps in the data.

Reports

King, C.-Y., 1986, Gas geochemistry applied to earthquake prediction: an overview: Journal of Geophysical Research, v. 91, p. 12,269-12,281.

King, C.-Y., 1986, Preface to special section on gas geochemistry of volcanism, earthquakes, resource exploration, and earth's interior: Journal of Geophysical Research, v. 91, p. 12,157.

King, C.-Y., 1986, Predictability of slip events along a laboratory fault: Geophysical Research Letters, v. 13, no. 11, p. 1165-1168.

King, C.-Y., 1986, Predictability of slip events along a laboratory fault (abs.): EOS (Transactions of the American Geophysical Union), v. 67, no. 44, p. 1187.

King, C.-Y., and Basler, D., 1987, Ground-water observation, in The Morgan Hill, California, earthquake of April 24, 1984, U.S. Geological Survey Bull. 1639, p. 135-138.

SOUTHERN CALIFORNIA CO-OPERATIVE SEISMIC NETWORK

7-9930-01174

Charles Koesterer
Branch of Seismology
525 S. Wilson Avenue
Pasadena, CA 91106

Investigations

1. Continuation of operation, maintenance, and recording of the southern California seismic network consisting of 189 U.S.G.S. short period seismograph stations and 66 other agency instruments. All of the stations are being recorded onto the CUSP analysis system and 100 stations recorded on FM tape units for back-up of digital recording.

2. Continuation of computer support for the Pasadena field office.

3. Continuation of logistics and management for co-projects within the Pasadena field office.

Results

1. Completed the first phase of conversion on the U.S.G.S. microwave radio telemetry system. Presently 110 stations are on the new system.

2. Continued construction of new and modifications on the old AMP/VCO units for network upgrades.

3. Installed a 3 component station at the Pasadena field office for testing of analog and telemetry inputs into the on-line processing system. To date, results have aided in necessary modificaton needed on all low gain instruments in the field.

4. Continued operation and maintenance of field stations and office recording systems with very little failure during this reporting period.

Microearthquake Data Analysis

9930-01173

W. H. K. Lee
U.S. Geological Survey
Branch of Seismology
345 Middlefield Road, Mail Stop 977
Menlo Park, California 94025
(415) 323-8111, Ext. 2630

Investigations

The primary focus of this project is the development of state-of-the-art computation methods for analysis of data from microearthquake networks. For the past six months I have been involved in:

(1) a project called "Investigation of signal characteristics of quarry blasts, nuclear explosions, and shallow earthquakes for regional discrimination purposes" for the Defense Advanced Research Projects Agency. The objective is to collect high-frequency seismic data generated by quarry blasts, controlled explosions, and shallow earthquakes, to study their signal characteristics, and to develop a method to discriminate between these three different sources.

(2) a collaborative project with Kei Aki and others on coda Q study in California. The objective is to use seismic coda waves recorded by Calnet for investigating the spatial and temporal variations of seismic attenuation.

Results

At the 1986 Fall AGU Meeting, three papers describing some of our results were presented:

(1) Aviles and Lee discussed the variations in signal characteristics of small quarry blasts and shallow earthquakes in central California. They found large differences between quarry and earthquake spectra, and quantified them by ratios of spectral amplitudes. Results indicated that quarry blasts and earthquakes could be separated into two distinct populations by spectral amplitude ratios. Quarry blasts were observed to be richer in low frequency signals at short distances than earthquakes. This observation is opposite to the well established fact for explosion/earthquake at teleseismic distances. Several explanations are possible: (1) signals from quarry blasts at short distances traveled through mostly the near surface rocks where fractures are common and thus effectively filter out the high-frequency signals, (2) the staggering of shots in quarry blasts stretches out the source-time function and the high-frequency signals are more likely subjected to destructive interferences, and (3) for small magnitude events, the source dimension for an earthquake is much smaller than that for a quarry blast.

(2) Phillips, Lee, and Newberry presented their results on spatial variation of crustal coda Q in California. They found strong variations in coda Q at the high end of the frequency band between Franciscan and Salinian regions of central California, and Long Valley in the Sierra Nevada; at 24 Hz, crustal Q for these areas is 525, 910, and 2100 respectively.

(3) Peng, Aki, and Lee presented their results on scattering and attenuation of high-frequency (1-25 Hz) seismic waves in the lithosphere with application to earthquake prediction. They found that measurements of coda Q^{-1} for earthquakes that occurred after the Round Valley earthquake (M=5.7) were higher than for those earthquakes that occurred prior to the mainshock in regions near the mainshock epicenter. The opposite behavior was found for regions farther away from the mainshock. This result is consistent with Mogi's doughnut model for earthquake activity before a large event.

Reports

Aviles, C. A., and W. H. K. Lee, 1986, Variations in signal characteristics of small quarry blasts and shallow earthquakes. (Abstract) EOS (Transaction Am. Geophys. Union), v. 67, p. 1093.

Lee, W. H. K., 1987, Observational seismology, in "Encyclopedia of Physical Science and Technology", v. 12, p. 491-518.

Lee, W. H. K., Lahr, J. C., and Habermann, R. E., 1986, Applications of personal computers in geophysics, EOC, Am. Geophys. Un. Transaction, v. 67, p. 1321-1323.

Peng, J. Y., K. Aki, and W. H. K. Lee, 1986, Scattering and attenuation of high-frequency (1-25 Hz) seismic waves in the lithosphere with application to earthquake prediction (Abstract), EOS, v. 67, p. 1086.

Peng, J. Y., Aki, K., Chouet, B., Johnson, P., Lee, W. H. K., Marks, S., Newberry, J. T., Ryall, A. S., Stewart, S. W., and Tottingham, D. M., 1987, Temporal changes in coda Q asociated with the Round Valley, California, earthquake of November 23, 1984, J. Geophys. Res., in press.

Phillis, W. S., W. H. K. Lee, and J. T. Newberry, 1986, Spatial variation of crustal coda Q in California, EOS, v. 67, p. 1093.

MAGNETIC FIELD OBSERVATIONS 9960-03814

R. J. Mueller
Branch of Tectonophysics
U. S. Geological Survey
345 Middlefield Rd, MS-977
Menlo Park, Ca. 94025
(415) 323-8111 ext. 2533

INVESTIGATIONS

1. Investigation of total field magnetic intensity measurements and their relation to seismicity and strain observations along active faults in central and southern California.

2. Recording and processing of synchronous 10 minute magnetic field data and maintenance of the 14 station telemetered magnetometer network.

RESULTS

1) Routine processing and monitoring of differential magnetic field data in an effort to identify local anomalies. Data are monitored daily with particular attention to the seven stations operating in the Parkfield region of central California.

2) A large portion of time and effort, this reporting period, was spent installing bore-hole strainmeters. Three tensor strainmeters and five dilatometers were installed in the Parkfield region of central California.

3) Equipment was retrieved from eleven magnetometer stations which were shut down at the beginning of FY86.

4) Processing and analysis of differential magnetic field and intermediate-baseline geodetic data from nets near the northern end of the Red River fault in Yunnan Province, China.

5) A lake level monitoring experiment, designed for measuring tilt, is operational and data is being collected from four stilling wells located around Crowley lake which lies on the boundary of the Long Valley caldera in east-central California. Water depth is measured every 10 minutes using pressure transducers, and water temperature, air temperature, and wind speed are recorded hourly. All data are transmitted by satellite telemetry to Menlo Park, California. Presently three of the four stations are using absolute pressure transducers. Future plans are to exchange the absolute transducers with differential transducer to enable easy cancellation of atmospheric

pressure.

REPORTS

Mueller, R.J., and Johnston M.J.S., Seismomagnetic Observations During the July 8, 1986, M 5.9, North Palm Springs Earthquake in Southern California: EOS (Am. Geophy. Un. Tran), v. 67, p. 1090,1986.

"Variations in Electrical Properties Induced by Stress Along the San Andreas Fault at Parkfield, California"

USGS Grant No. 14-08-0001-G1357

Stephen K. Park and Tien-Chang Lee
Institute of Geophysics and Planetary Physics
University of California
Riverside, CA 92521
(714) 787-3438

Introduction

We plan to monitor variations in resistivity at Parkfield using telluric currents. Our methods and instrumentation are virtually identical to the experiments by Madden in Hollister and Palmdale, with a few modifications. We will use shorter (5 km) dipoles and thus will be sensitive to variations in smaller volumes of crust. The mechanism producing earthquakes in Parkfield is known, so we have our experiment on the region most likely to deform.

Monitoring Array

The array is not installed yet because we have been building the electronics and arranging for telephone lines. Tom Burdette of the U.S.G.S. has been invaluable in helping us get the telephone lines. We anticipate that the array will be functional by June, 1987. Locations of the dipoles are shown in Figure 1. The array has been shifted northward from our originally proposed location so that it is centered within the region monitored by the U.S. Geological Survey for deformation.

Field Survey

We are proceeding with a telluric-magnetotelluric survey of the region surrounding Parkfield to provide the electrical structure. This survey will help us locate where the changes are occurring when we detect them with our array. The installation of the array will take priority over this survey, however.

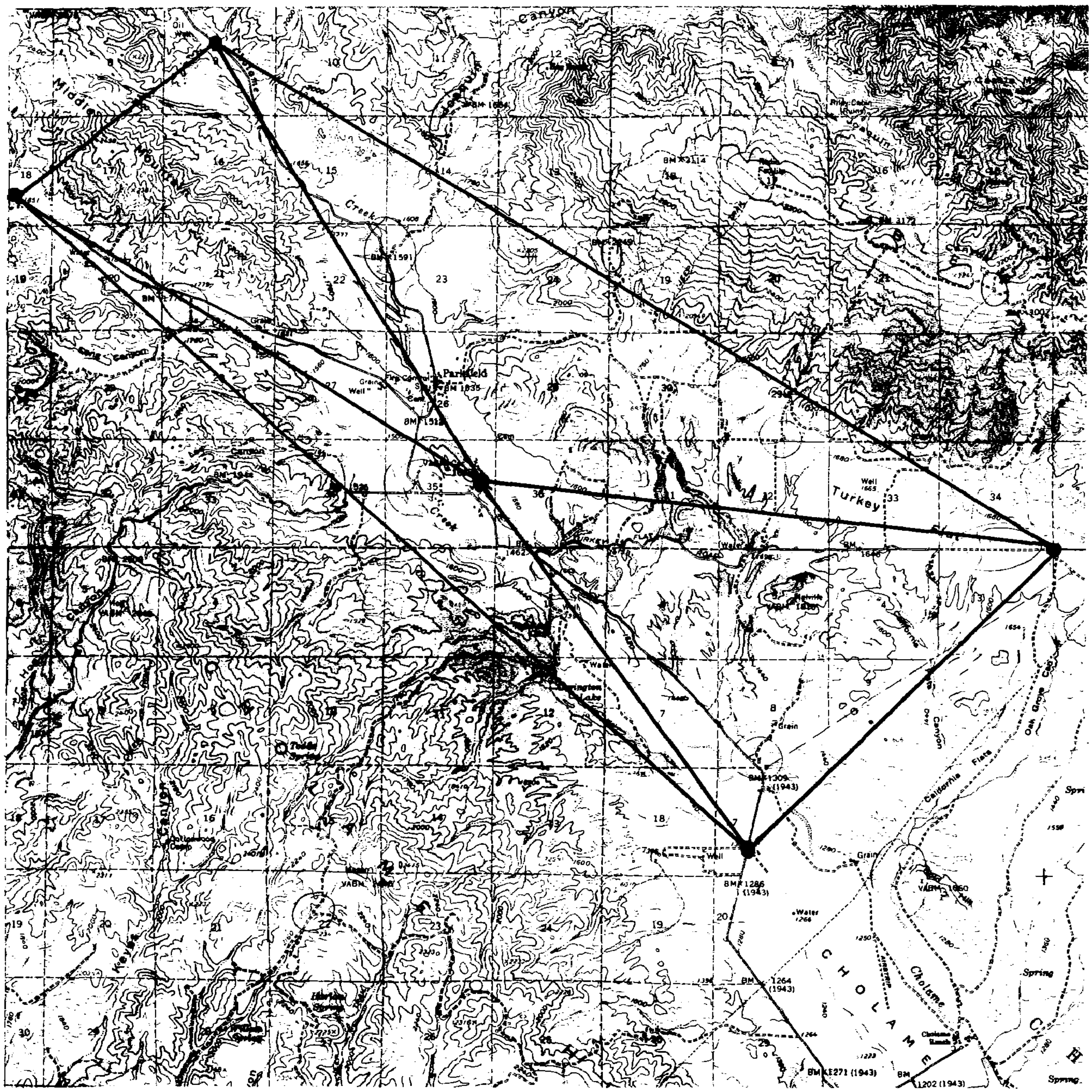

Figure 1 - Map showing locations of electrodes (solid dots) and telluric dipoles (heavy lines). Town of Parkfield is one mile northeast of center of array. (map from USGS 15' quadrangle)

Project Title: Structural Studies of the Allegheny Plateau
Project number: 9380-02646
Principal Investigator: Howard A. Pohn
Name and Address: MS 927, USGS, Reston, VA 22092
Telephone numbers: 703-648-6378, FTS 959-6378

Earthquakes and Lateral ramps in the central and southern Appalachians

Investigations

Studies have been undertaken in the last six months into the distribution of modern earthquakes as they might relate to the positions of lateral ramps in the central and southern Appalachians. Although no sophisticated analyses of first motions, magnitudes, or hypocenters have been attempted as yet, it appears that there is a definite correlation between the two phenomena. Lateral ramps as here defined are areas where decollements (large, flat faults) change stratigraphic level along strike. The positions of lateral ramps were first recognized here by a combination of field investigations and analysis of side-looking airborne radar data. Criteria for the positions of lateral ramps include: 1) abrupt terminations of folds, 2) dramatic changes in fold wavelength along strike, 3) long, straight river segments in the Piedmont, Coastal Plain, and Appalachian Plateau Provinces, 4) changes in the frequency of faults or disturbed zones mapped in the field and, 5) discontinuities in the Blue Ridge Province. Lateral ramps are suspected to be commonly connected to basement because of the presence of cross-strike igneous intrusions along several ramp zones. Furthermore, the ramps are thought to have been seismically active in the past for the following reasons. First, proprietary strike-line seismic reflection profiles show growth faults from the Precambrian basement through Middle Ordovician times. Second, Paleozoic units frequently show dramatic changes in both thickness and lithology across lateral ramps. Third, "Mesozoic basins" show the presence of east-west border faults or Precambrian topographic highs which interrupt the basins.

Results

I have plotted the positions of all of the earthquakes in the Eastern Overthrust Belt from 1698 through December, 1985. These data were overlayed on a map of lateral ramps as determined from the above mentioned radar data and field investigations. More than 45% of all modern seismic events are coincident with the positions of lateral ramps.

Reports

Abstract published - Pohn, H. A., 1987, Appalachian Folds, lateral ramps, and basement faults: A modern engineering problem?; National Research Council, Transportation Research Board Meeting, Washington, D.C., Jan. 12, 1987.

CRUSTAL STRAIN

9960-01187

W.H. Prescott, J.C. Savage, M. Lisowski
Branch of Tectonophysics
U.S. Geological Survey
345 Middlefield Road, MS/977
Menlo Park, California 94025
(415) 323-8111, ext. 2701

Investigations

The principal subject of investigation was the analysis of deformation in a number of tectonically active areas in the United States.

Results

1. Deformation Across the Salton Trough, Southern California

The Salton trilateration network was resurveyed in early 1987 using a Geodolite to measure the distances. The average station velocities over the past 15 years are shown in Figure 1 (top). The Salton sea is outlined near the center of that figure. The 95% confidence error ellipse is shown at the tip of each arrow. In the lower part of Figure 1 is shown the northwest component of velocity as a function of distance measured from southwest to northeast. In that plot the velocities of stations to the southeast are shown by a point with error bars whereas the velocities of stations to the northwest are indicated by just error bars. The error bars extend one standard deviation on either side of the observed velocity. About 38 mm/yr of relative motion parallel to fault strike is shown in the velocity profile. The velocity profile in Figure 1 shows a constant velocity at either end of the profile. Thus, it appears that most of the motion on the San Andreas fault system itself has been captured. The additional 17 mm/yr of right-lateral motion expected for the North American-Pacific plate motion must be distributed over a broad region or concentrated on faults not spanned by the Salton network. Notice the absence of any evidence for spreading normal to fault strike in Figure 1 (top) and the difference in velocity distribution between the northwestern part of the network where the San Jacinto and San Andreas faults are farther apart and the southeastern part of the network where the faults converge Figure 1 (bottom).

2. Global Positioning System Observations

The U.S. Geological Survey has begun a series of experiments designed to investigate the application of Global Positioning System (GPS) technology to the measurement of crustal deformation. Experiments in progress involve lines with lengths between 2 and 350 km. The most carefully examined line is 43 km long and extends from Loma Prieta to Allison, stations located near the San Andreas, Hayward and Calaveras faults in central California. The results of 13 GPS observations of this line are shown in Figure 2. The data for all of these observations were processed with both the "broadcast orbits" and orbits calculated by the Naval Weapons Center in Dahlgren, Virginia. Also shown in the figure are the results of Geodolite measurements of the same line over the same time period. From these and other GPS observations, we have found that the north component of position difference has an uncertainty of about 0.7 ppm, the east component about 1.3 ppm and the vertical component about 2.3 ppm. All three uncertainties are expressed as a fraction of line length. The largest single source of error in these observations is probably contributed by uncertainties in the satellite orbits. The east component is less well-determined than the north component because the satellite orbit geometry produces primarily north-south ground tracks. The vertical component is the most poorly determined of the three essentially because the earth is not transparent to the microwave satellite signals. Much of the error in the horizontal components cancels out because the receivers can see satellites in both directions, north and south or east and west, but at no stations can the receiver see down.

3. Deformation Across the Big Bend Section of the San Andreas Fault Near Palmdale, California

Repeated Geodolite surveys of the Tehachipi, San Gabriel, and Palmdale strain networks were used to determine the average rate of strain accumulation and average station velocities across the San Andreas fault. Principal strain rates from homogeneous data sets are as follows:

Network	Interval	$\dot{\varepsilon}_1$ µstrain	$\dot{\varepsilon}_2$ µstrain	ϕ ° from N
Tehachipi	1977-86	0.129 ± 0.013	-0.122 ± 0.011	71 ± 2
San Gabriel	1977-86	0.176 ± 0.021	-0.132 ± 0.018	73 ± 2
Palmdale	1971-85	0.219 ± 0.014	-0.195 ± 0.012	71 ± 1

where ϕ is the azimuth of $\dot{\varepsilon}_1$ and extension is reckoned positive. The observed deformation is right-lateral shear parallel to the N65°W local strike of the San Andreas fault. The 0.044 ± 0.032 ppm/yr rate of dilational strain ($\varepsilon_1+\varepsilon_2$) in the San Gabriel network is not significant at the 2σ level. Station velocities for a subset of stations from all three networks were determined from the average rates of line-length change. Shown in Figure 3 are station velocities from an outer-coordinate solution and shown in Figure 4 are the fault-parallel station velocities as a function of the distance in a N25°E direction from the center of mass of the combined network. Across the 84-km-wide zone covered by this combined network the fault-parallel relative velocity amounts to 17±2 mm/yr. The average rates of line-length change were used to invert slip on a number of dislocation models of the San Andreas and Garlock faults. The best fitting model that includes only the San Andreas fault has the fault slipping at 27 mm/yr below 19 km. The best-fitting model that includes the San Andreas and Garlock faults has the San Andreas faulting slipping at 21 mm/yr below 16 km and the Garlock fault slipping at 9 mm/yr below 10 km. A wide range of models fit the data almost equally well.

4. Strain Accumulation Across the Strait of Juan de Fuca, Washington and British Columbia

A joint GPS survey by the USGS and Canadian Geodetic Survey in 1986 recovered 19 existing triangulation stations located on both sides of the Strait of Juan de Fuca. Strain accumulation calculated from angle changes between the triangulation surveys and the 1986 GPS survey is shown by the principal deviatoric strain rates, and summarized by average rate of engineering shear ($\dot{\gamma}$) and the direction of the axis of maximum contraction (β) in Figure 5. Also shown in Figure 5c are the average strain rates between 1982 and 1986 in the Olympic trilateration network. Except for the 1954-86 interval, engineering shear strain accumulated at a rate of between 0.09 and 0.36 μrad/yr with the axis of maximum contraction oriented ENE, approximately parallel to the direction of convergence of the Juan de Fuca plate with the North American plate. The best determined rates of strain accumulation are remarkably consistent: 1982-1986, $\dot{\gamma} = 0.19 \pm 0.13$ μrad/yr, β = N70°E ± 9°; 1942-86, $\dot{\gamma} = 0.14 \pm 0.05$ μrad/yr, β = N71°E ± 9°; and 1982-86, $\dot{\gamma} = 0.14 \pm 0.04$ μrad/yr, β = N59°E ± 10°. The actual rate of contraction is uncertain because only shear is determined from the angle changes and the dilatation is not well determined in the Olympic trilateration network. These measurements imply a loading that must eventually be released by a major thrust event along the Cascadia subduction zone.

5) Deformation Associated with the North Palm Springs, California, Earthquake of July 8, 1986

Trilateration surveys show that coseismic horizontal surface deformation associated with the $M_L = 5.6$ North Palm Springs earthquake of 8 July 1986 is concentrated around the Banning fault near Whitewater Canyon. The coseismic displacement of the geodetic stations in the 8-km-wide Whitewater network, as inferred from the observed line-length changes indicates 60 ± 10 mm of distributed right-lateral shear displacement across the Banning fault at the surface. One station, located 1 km north of the Banning fault, had an anomalous 70 mm northward displacement, which we suspect is due to monument instability. No significant coseismic deformation occurred within a 1.5-km-wide network that crosses the Mission Creek fault near the epicenter, nor within a regional network that crosses the Coachella Valley near Palm Springs. The data only weakly delimit possible slip across the rupture surface defined by the distribution of aftershocks. The best-fit dislocation model indicates 0.230 ± 0.070 m of right-lateral slip and 0.080 ± 0.060 m of normal slip on the buried rupture surface that extends between depths of 5 and 15 km on a plane striking N60°E and dipping 50° to the northeast.

6. Effect of Crustal Layering Upon Dislocation Modeling

Slip distribution at depth on a fault may be inferred from the deformation observed on the surface. Generally, in inverting the surface deformation data to obtain the slip distribution, the earth is approximated by an elastic half-space. Slip distributions inferred from a half-space model may contain artifacts, including even zones of reversed slip, due solely to effects of layering in the real earth. This effect is demonstrated for a vertical strike-slip fault in an earth consisting of an elastic layer overlying an elastic half-space. Slip on the fault is taken to be independent of the along-strike coordinate (i.e., antiplane strain is assumed). For a given slip distribution in this model, the slip distribution on a similar fault in an elastic half-space is found that produces the identical surface deformation. Comparison of the two slip distributions reveals structure introduced into the half-space-equivalent slip profile by crustal layering. The comparisons suggest that low resolution inversion schemes (e.g., single-screw-dislocation models) are not drastically affected by earth structure, but attempts at detailed inversion are likely to produce profiles badly contaminated by artifacts of earth structure.

7. Quasiperiodic Occurrence of Earthquakes in the 1978-1986 Bishop-Mammoth Lakes Sequence, Eastern California

In December 1984 Ryall and Hill noted that the five principal events in the Bishop-Mammoth Lakes earthquake sequence occurred at intervals of about 1.5 yr with a standard deviation for an individual event of 0.25 yr. Some data selection was involved in identifying the principal events, although the choices seemed reasonable. The recent Chalfant Valley earthquake (M_L = 6.4; July 21, 1986) followed the last prior principal event in the Bishop-Mammoth Lakes sequence by 1.65 yr, and no important activity intervened except one aftershock from the prior event. Thus, the Chalfant Valley earthquake could have been forecast from the observed periodicity. However, the precision of the forecast (±0.8 yr for the 95% confidence interval) is not sufficient to furnish convincing evidence that the Bishop-Mammoth Lakes sequence is quasiperiodic. Extrapolation of the trend established by the six previous events suggests that the next event in the Bishop-Mammoth Lakes sequence would be expected in December 1987 ±0.7 yr (95% confidence interval). The regularity of the Bishop-Mammoth Lakes sequence is comparable to that of the Parkfield, California, sequence (average interevent interval 20.8 yr with a standard deviation for an individual interval of 6.2 yr). Both sequences consist of six events. There is a plausible physical explanation for the periodicity observed at Parkfield; such an explanation for the Bishop-Mammoth Lakes sequence is lacking.

Reports

Gross, W.K., and J.C. Savage, Deformation associated with the 1986 Chalfant Valley earthquake, eastern California, Bull. Seismol. Soc. Am. 77, 306-310, 1987.

King, N.E., P. Segall, and W. Prescott, Geodetic Measurements near Parkfield, California, 1959-1984, J. Geophys. Res., 92 (B3), 2747-2766, 1987.

Prescott, W.H., M.D. Zoback, and S.W. Krueger, Comment on "Horizontal Deformation in New York and Connecticut: Examining Contradictory Results from the Geodetic Evidence", J. Geophys. Res., 92 (B3), 2805-2806, 1987.

Savage, J.C., R.S. Cockerham, J.E. Estrem, and L.R. Moore, Deformation near Long Valley caldera, eastern California, 1982-1986, J. Geophys. Res., 92, 2721-2746, 1987.

Outer Coordinate Solution

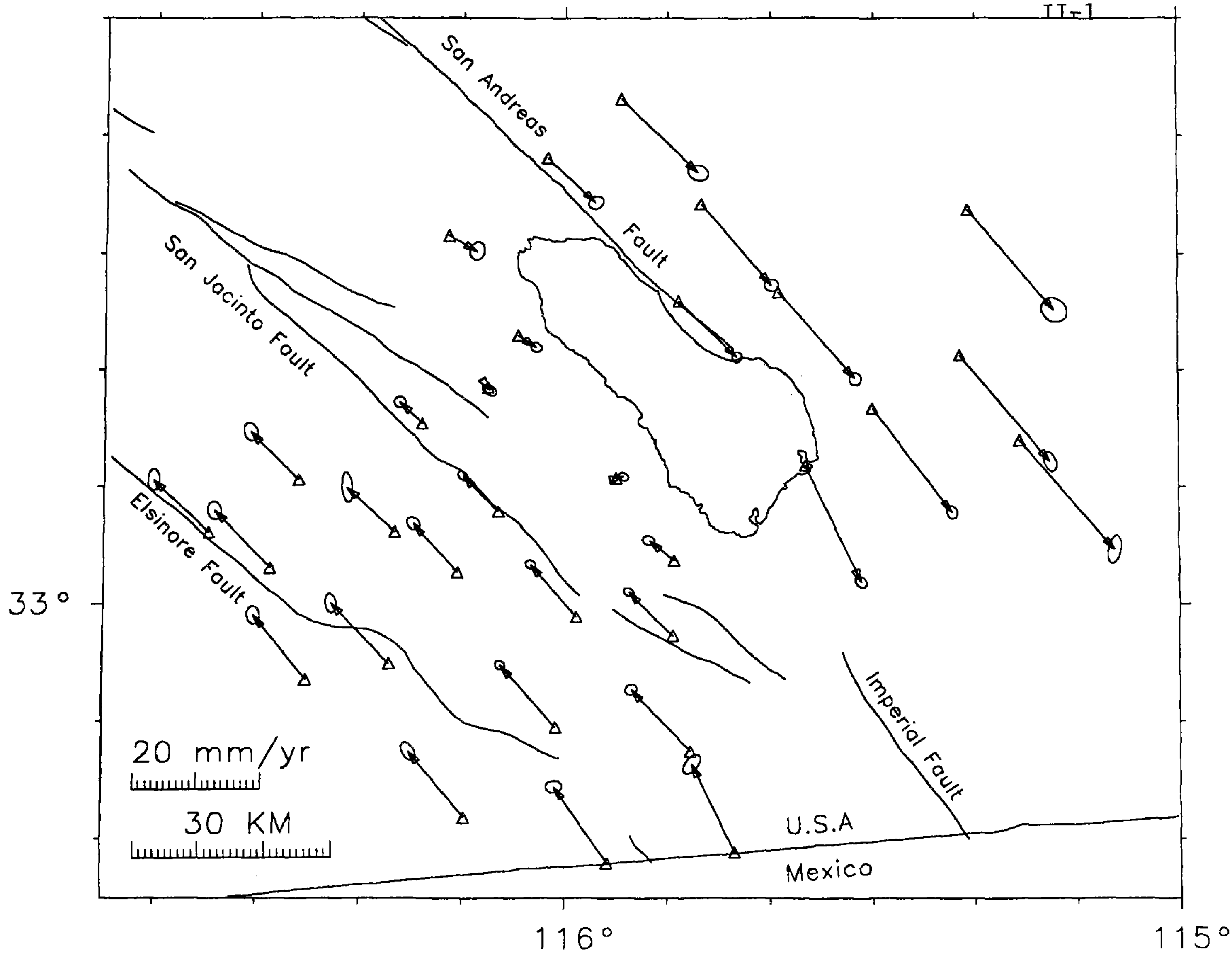

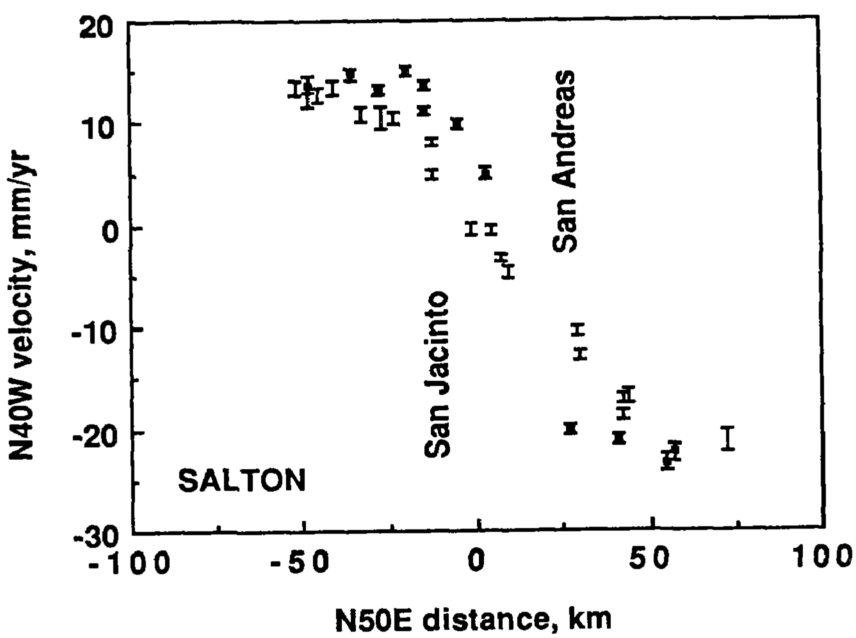

FIGURE 1

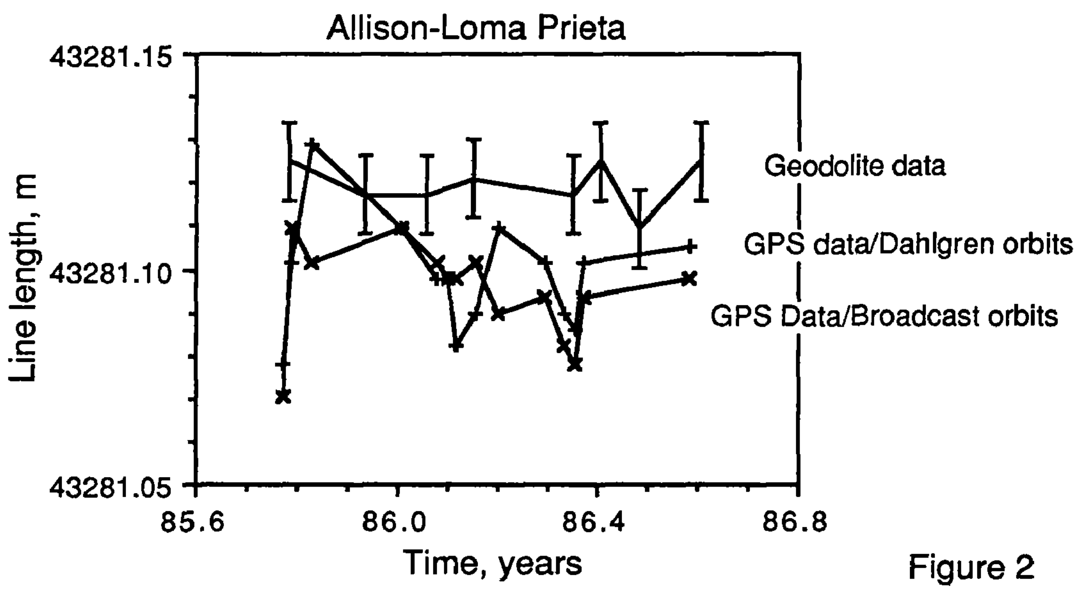
Allison-Loma Prieta
43281.15
43281.10
43281.05
Line length, m
85.6
86.0
86.4
86.8
Time, years
Geodolite data
GPS data/Dahlgren orbits
GPS Data/Broadcast orbits

Figure 2

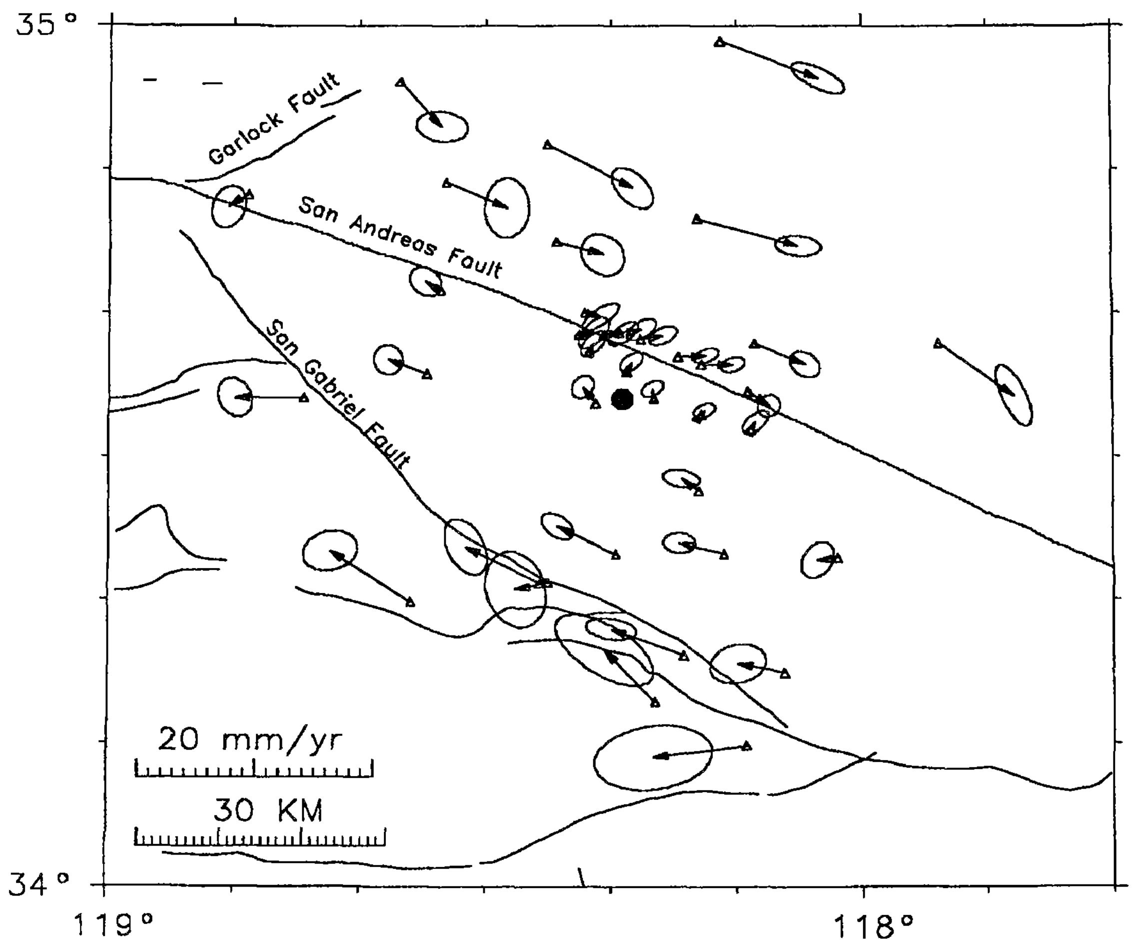

Figure 3. Map showing the average velocities of a subset of stations from the Tehachipi, Palmdale, and San Gabriel strain networks. The velocities are from an outer-coordinate solution and are relative to the center of mass of the network, which is marked by a solid circle near the center of the map. A 95% confidence error ellipse is shown at the tip of each vector. Major faults are shown by the solid lines.

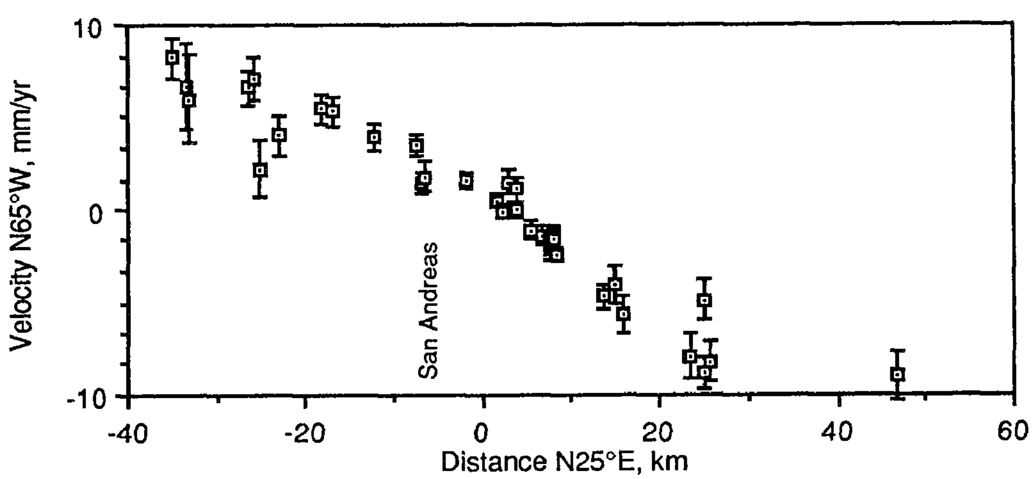

Figure 4. Plot of the component of velocity parallel to the strike of the San Andreas fault (N56°W) as a function of the distance from the center of mass of the network. The location of the San Andreas fault is -6.5 km. The error bars are 1σ on either side of the plotted point.

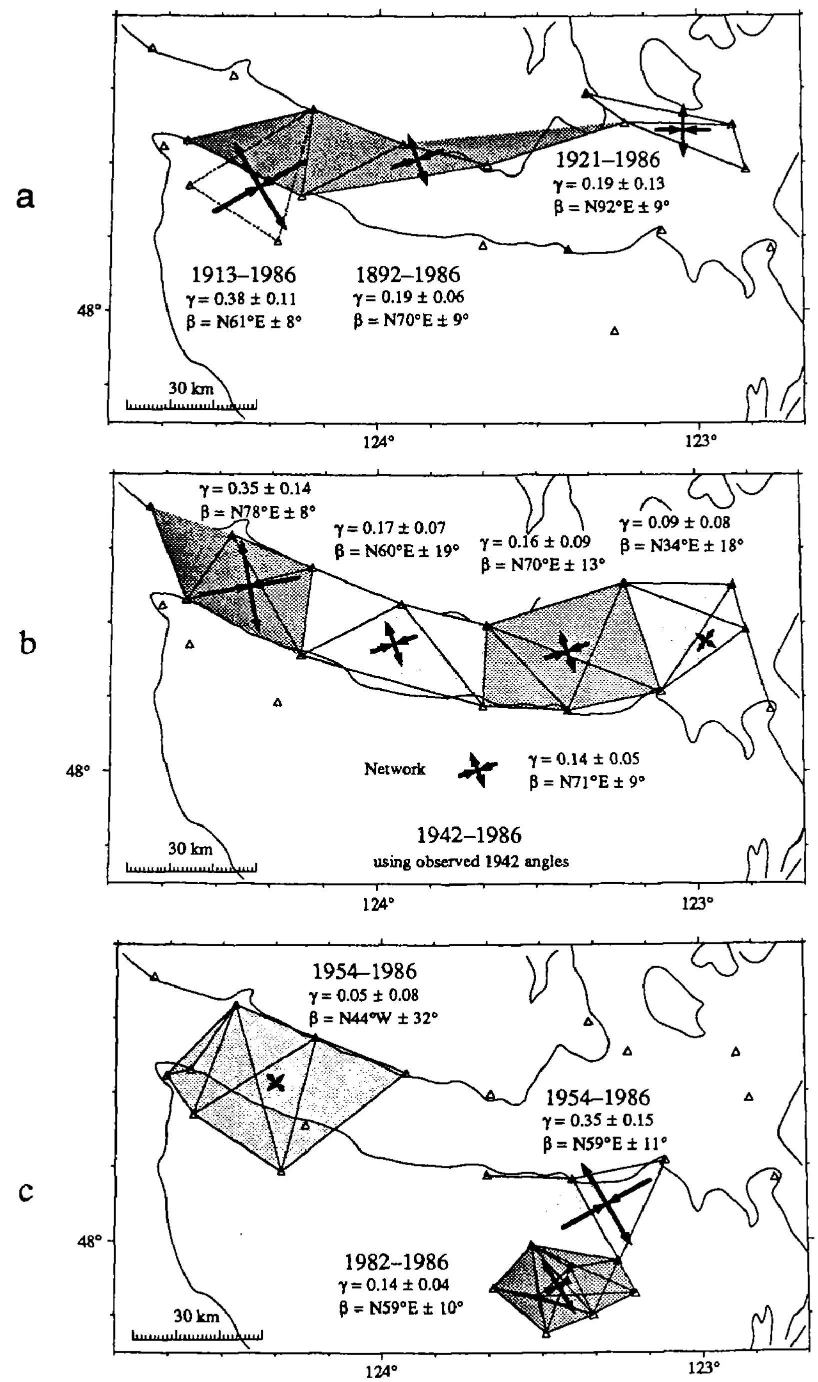

Figure 5. Maps showing the average rate of strain accumulation across the Strait of Juan de Fuca as calculated from the change in observed angles within the shaded areas. The arrows represent the directions and magnitudes of the principal deviatoric strain rates ($\dot{\epsilon}'_1$ and $\dot{\epsilon}'_2$) for the given intervals. Also shown for each interval are the engineering shear strain rate $\dot{\gamma}$ in μrad/yr ($\dot{\gamma} = \dot{\epsilon}'_1 - \dot{\epsilon}'_2$) and β the bearing of the axis of maximum contraction ($\dot{\epsilon}'_2$). (a) Strain accumulation calculated from angle changes between the early triangulation surveys and the 1986 GPS survey. (b) Strain accumulation between 1942 and 1986. (c) Strain accumulation between 1954 and 1986 near the Strait of Juan de Fuca and between 1982 and 1986 within the Olympic trilateration network. Strain accumulation in the Olympic network is calculated from line-length changes and is represented by the principal strain rates.

Seismic Studies of Fault Mechanics

9930-02103

Paul A. Reasenberg
Mark V. Matthews

Branch of Seismology
U.S. Geological Survey
345 Middlefield Road, MS 977
Menlo Park, California 94025
(415) 323-8111, Ext. 2049

Investigations

Our activity in this reporting period continues to focus on a problem in statistical seismology often referred to as the "precursory seismic quiescence hypothesis". The quiescence hypothesis states that decreases in the rate of seismicity within earthquake source regions precede the mainshocks in a systematic, non-random way, such that an observation of a rate decrease provides information about the time and location (and possible magnitude) of a future earthquake. Numerous cases of precursory seismic quiescence have been reported in recent years. Some investigators have interpreted these observatons as evidence that seismic quiescence is a somewhat reliable intermediate-term precursor to moderate or large earthquakes. However, because failures of the pattern to predict earthquakes are generally not reported, and because numerous earthquakes are not preceded by quiescence, the validity and reliability of the quiescence precursor have not been established.

In our previous report we presented preliminary results of a baseline study of seismicity rate fluctuations prior to, and in the source regions of, 37 shallow earthquakes (M 5.3 - 7.0) in central California and Japan. No evidence was found for the existence of a systematic, widespread or reliable pattern of quiescence prior to the mainshocks studied, in the intermediate term. We concluded that the body of reported cases of precursory seismic quiescence may satisfactorily be explained by a model in which random rate fluctuations are preferentially reported when they conform to the hypothesis (i.e., successes are reported preferentially over failures).

While the body of mainshocks studied failed to establish the reliability of the quiescence hypothesis for earthquake prediction, we feel that some individual cases are so strong as to compel further analysis. Our aim now, however, is not toward earthquake prediction through a simple statistical hypothesis. Rather, we seek to understand the detailed structure of one or more individual cases of precursory seismic quiescence in order to gain insight into possible physical processes in the source volume that may have led to the quiescences.

Results

We have selected for study the seismicity preceding the 1983 (M_s 6.6) earthquake at Kaoiki, Hawaii. A strong quiescence beginning 2.4 years before the mainshock was reported by Wyss (1986). We are currently collaborating with Max Wyss in a more detailed analysis of the multi-dimensional structure of this strong quiescence event. No results to report at this time.

Reports

Reasenberg, P. A., and M. V. Matthews, Precursory seismic quiescence: a preliminary assessment of the hypothesis, PAGEOPH, (in press).

Matthews, M. V., and P. A. Reasenberg, Statistical methods for investigating quiescence and other temporal seismicity patterns, PAGEOPH, (in press).

Reference

Wyss, M., Seismic quiescence precursor to the 1983 Kaoiki, Hawaii (M_s = 6.6) earthquake, Bull. Seism. Soc. Am., 76, 785-800, 1986.

Hydrogen Monitoring (9980-02773)

Motoaki Sato and Susan Russell-Robinson (FTS 959-6766)
Branch of Igneous and Geothermal Processes
U.S. Geological Survey, MS 959, Reston, VA 22092

Investigations

Hydrogen (H_2) in soil along the San Andreas and Calaveras faults is continuously monitored at nine sites by using fuel-cell sensors and data are telemetered to Menlo Park, CA. Goals are (1) to accumulate valid data, (2) to find patterns of correlation of the hydrogen data with seismic data, (3) to understand the tectonic mechanism of H_2 emission along active faults, and (4) to constantly improve the monitoring method.

Results

General: There was one M>5 earthquake in the vicinity of the monitored area (Feb. 13, 1987, M=5.0, 7 km NE of Coalinga) during this reporting period. To obtain a better perspective of relative magnitudes of H_2 changes at all monitored sites, multi-site plots covering the one year period from April 1, 1986, to April 1, 1987, are shown in Fig. 1 (northern sites) and Fig. 2 (southern sites). Also shown in the plots are daily rain fall data from Flinge Flat (Wffr, 3 inches full scale). The patterns of H_2 changes vary from site to site, indicating a very complex nature of H_2 emission control at depth. However, this complexity is not limited to hydrogen; other monitored parameters such as creep also show non-uniformity of response patterns.

The following descriptions of individual events at each site covers only the 6-month period starting on October 1, 1986, although the plots cover a longer period.

Calaveras Fault

Shore Road (H2SH): A 150-ppm peak followed by a depletion of H_2 occurred on Jan. 16. There was no rain during this event. An oddly shaped 300-ppm peak occurred on Feb. 13, but this peak coincided precisely with a peak period of a large oscillatory slip recorded by the creepmeter (XSH1). It was probably caused by rain-induced ground movement. The same correlation was also found for the 150-ppm peak of Mar. 6. The Shore Road site is located on a strip of land between two stream beds, and may thus produce this strange behavior.

Wright Road (H2WR): This site recorded a broad increase, the maximum occurring in late December. The broad gradual change was unusual. The effect of seasonal temperature variations on electronics is suspected because this site is the only site that has an above-ground instrument vault. Other than this no noteworthy events were recorded.

San Andreas Fault

San Juan Bautista (H2SJ): As usual, no clear anomalies were recorded.

Cienega Winery (H2CW): No unambiguous events were recorded in this period.

Melendy Ranch (H2MR): There was a break in the record between Jan. 16 and Feb. 12 due to telemetry receiver problem. There were no events.

Slack Canyon (H2SC): No recognizable events occurred throughout the period. The sensor may not be working well because the conductivity test indicated a questionable performance in January.

Middle Mountain (H2MM): Prior to May 1986, this site had not worked satisfactorily for more than one month. After several repair attempts, we finally traced the problem to the original solar panel, which was of dubious quality. The site was brought into a good working order after overhauling of the power supply system in mid-May and replacement of the sensor system in mid-November.

There was a 550-ppm H_2 event starting about 11 a.m. on Feb. 13 (time and date all in GMT) and reaching the maximum about 2 a.m. on Feb. 14. The M5.0 earthquake occurred 5.5 hours later (Fig. 3) at about 30 km to NE. Heavy rain (2") fell between 8:30 a.m. and 7 p.m. on Feb. 13. Rain could have caused the depression that occurred just before the start of the composite peak. This is inferred from the observation that the heaviest rain of the season (Mar. 5, 2.6") clearly depressed the hydrogen level. As evident in Figs. 2 and 3, the correlation of hydrogen events with rain is poor at all sites except Shore Road.

Parkfield (H2PK): Compared with the same period in 1985-86, this site has relatively been quiet ever since the M5.3 Mount Lewis earthquake of Mar.31, 1986. There were ca. 100-ppm events on Oct. 8, Dec. 7 , Feb. 10, and Feb. 26.

Gold Hill (H2GH): There was a 700-ppm peak on Sep. 30 followed by a depression of H_2 with an intervening 100-ppm peak on Oct. 5-6. This complex event coincided with changes in hydrogen (H2PK, Oct. 8) and creep (XPK1, Oct. 2-9) at Parkfield and also with a creep event at Middle Ridge (XMD1, Oct. 3).

Another similar but more prolonged chain of events began on Nov. 21 with a brief 650-ppm peak followed by a week-long 200-ppm peak. Irregular changes including five ca. 100-ppm peaks followed the events until the M5.0 earthquake. The hydrogen level returned to a steady pattern after the earthquake.

Work Ranch (H2WK) and Twisselman Ranch (H2TW): Although the data are not shown, these two new hydrogen monitoring sites were installed in November. These sites are currently undergoing testing and debugging.

Reports

Sato, M., A. J. Sutton, K. A. McGee, and S. Russell-Robinson (1986) Monitoring of hydrogen along the San Andreas and Calaveras faults in central California in 1980-1984: J. Geophys. Res. , v. 91, No. B12, 12,315-12,326.

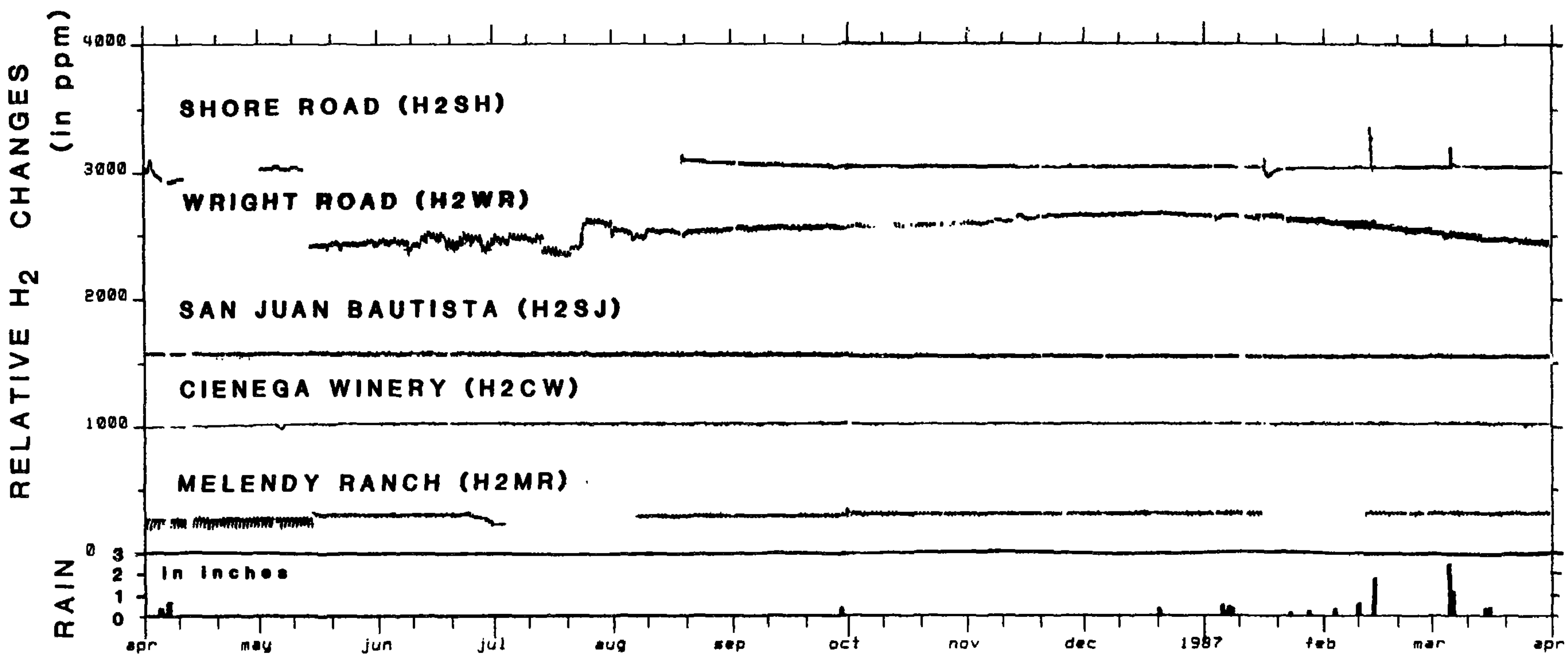

Fig. 1. One-year compositeplots showing <u>relative</u> changes in H_2 concentration in fault-zone soil at northern sites and daily rain fall in the area. The rain data prior to July 1, 1986, were recorded in Hollister, and those after this date were recorded in the Parkfield area (Flinge Flat).

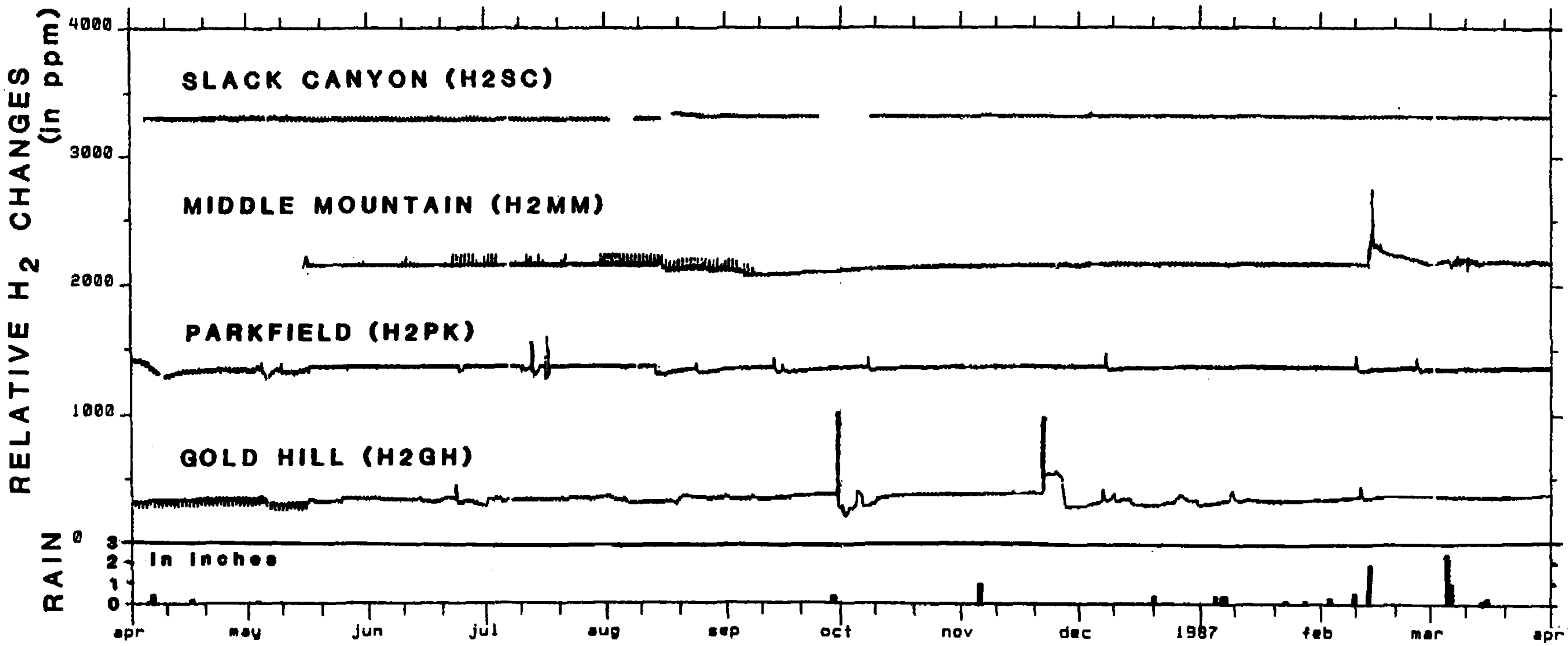

Fig. 2. One-year composite plots showing relative changes in H_2 concentration in fault-zone soil recorded at southern sites and daily rain fall in the area. The rain data prior to July 1, 1986, were recorded in Priest Valley, and those after this date were recorded in the Parkfield area (Flinge Flat).

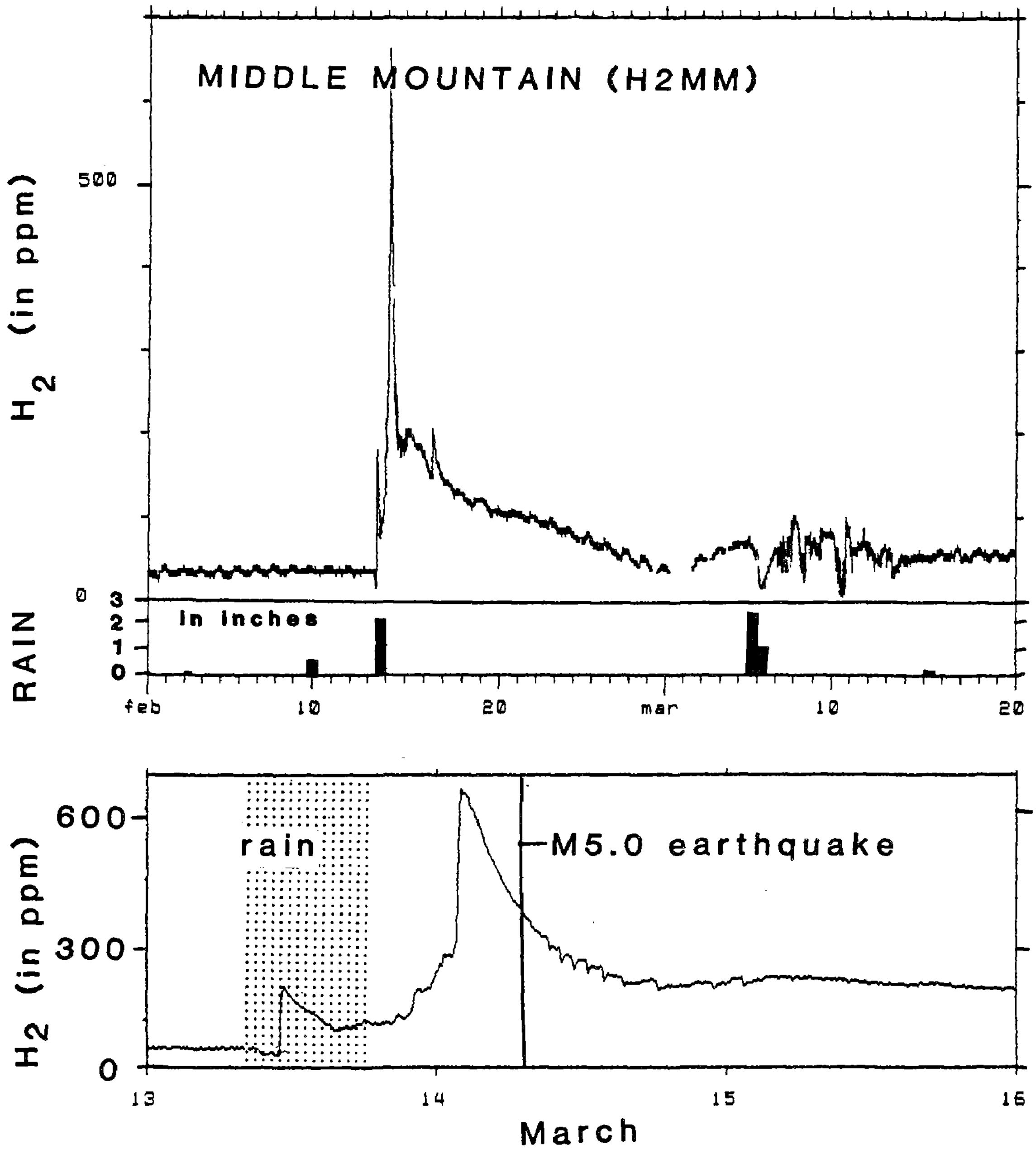

Fig. 3. Expanded plots of H_2 changes recorded at Middle Mountain around the time of an M5.0 earthquake that occurred at 7 km NE of Coalinga at 11:26 p.m. PST on February 13, 1987. The time and date in the plots are in GMT.

FAULT ZONE TECTONICS

9960-01188

Sandra S. Schulz
Branch of Tectonophysics
U.S. Geological Survey
345 Middlefield Road, MS/977
Menlo Park, California 94025
(415) 323-8111 x 2763

Investigations

1. Directed maintenance of creepmeter network in California.

2. Updated archived creep data on PDP 11/44 computer.

3. Continued to establish and survey alinement array network on California faults.

4. Monitored creepmeter and alinement array data for retardations or other possible earthquake precursors, and to better understand near-surface fault action. Submitted for review a catalog of alinement array data collected from 1983 through 1986.

Results

1. Currently 31 extension creepmeters operate; 23 of the 31 have on-site strip chart recorders, and 21 of the 23 are telemetered to Menlo Park (Figure 1).

2. Fault creep data from USGS creepmeter sites along the San Andreas, Hayward, and Calaveras faults have been updated through March, 1987, and stored in digital form (1 sample/day). Telemetry data are stored in digital form (1 sample/ten minutes, updated every ten minutes, and merged with daily-sample data files to produce timely data.

3. James Wilmesher, Project Surveyor, installed and surveyed four new alinement arrays in Parkfield (see Figure 2). HST4, on the main trace between XDR2 and WKR1 creepmeters; KEN4, on the main trace between WKR1 and CRR1 creepmeters and a few hundred feet southeast of the irrigation pipeline that broke before the 1966 earthquake; HSW4, on the southwest trace near site F32 of the USGS Professional Paper on the 1966 earthquake (Brown et al., 1967); and HAR4, at the proposed southern junction of the southwest trace and Parkfield-Cholame Road. Although surface fractures were not

seen at HAR4's site in 1966, topography suggests the fault trace may be active here (see Figure 2).

Two more sets of surveys of five Parkfield alinement arrays were completed by the private contractor during the reporting survey. The other 13 Parkfield arrays were resurveyed periodically by Project personnel.

4. During an initial survey of the new KEN4 array mentioned above, a creep event apparently passed through the line. Remeasurement of the line showed right-lateral movement of approximately 3.5 mm between ends of the 72-meter line, but complicated movement between the 7 deflection monuments.

Preliminary calculations from surveys of the four arrays on the southwest fracture zone in Parkfield show alternate right- and left-lateral movement occurring, perhaps reflected by opposite movement on the nearby main trace. Creepmeter data from the main trace will be compared to array data on the southwest fracture as soon as more surveys are completed.

Two examples of creep propagation showed up on the creepmeters spaced along Middle Ridge in Parkfield. The first event was a surge on XPK1 creepmeter (see Figure 1) that started October 2 and moved 2 mm before subsiding on the 9th. Coinciding with the movement was a 1.2 mm event on the new XMD1 creepmeter, 6 km northwest of XPK1. The rate of movement at XPK1 subsided somewhat after the event at XMD1 (Figure 3). The second example was a 1.7 mm event on XMD1 on October 19. Ten hours into the event, XMM1, 2.4 km northwest of XMD1, moved 0.5 mm. Movement at XMD1 dropped off shortly after the event at XMM1 (Figure 4).

In December, a 0.26 mm right-lateral creep event was recorded at X461, the new instrument installed 2 km south of Highway 46 south of Parkfield. X461 is a few hundred yards north of Quad QH that was placed beyond the end of surface fractures in 1966.

By January, 1987, the creep rate at XPK1 (Parkfield) creepmeter reached its pre-Coalinga trend, the slip deficit apparently having been completely recovered in the months following the August, 1985, Kettleman Hills earthquake. None of the other Parkfield creepmeter data sets show such a complete recovery to date (Figure 5).

Products

1. Wilmesher, J.F. and F.B. Baker, Catalog of Alinement Array measurements in central and southern California from 1983 through 1986, U.S. Geological Survey Open-File Report, in review.

References

Brown, R.D. Jr., J.G. Vedder, R.E. Wallace, E.F. Roth, R.F. Yerkes, R.O. Castle, A.O. Waananen, R.W. Page, and J.P. Eaton, 1967, The Parkfield-Cholame California earthquakes of June-August 1966 - Surface Geologic Effects, Water Resources Aspects, and Preliminary Seismic Data, U.S. Geological Survey Professional Paper 579, 66 pp.

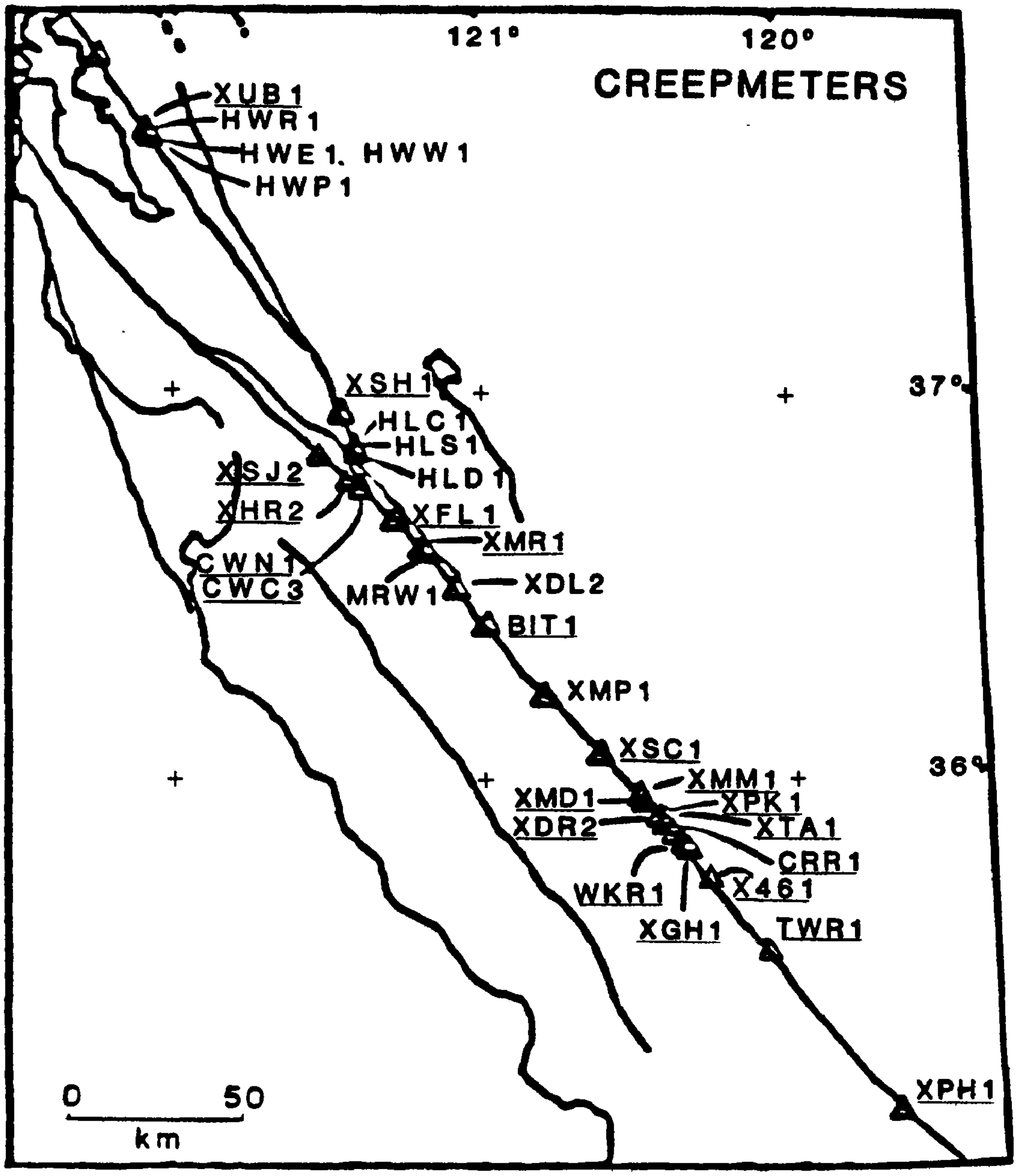

FIGURE 1. USGS creepmeter stations in Northern and Central California. Instruments with underlined names transmit on telemetry.

Creep and Alinement : Parkfield , CA

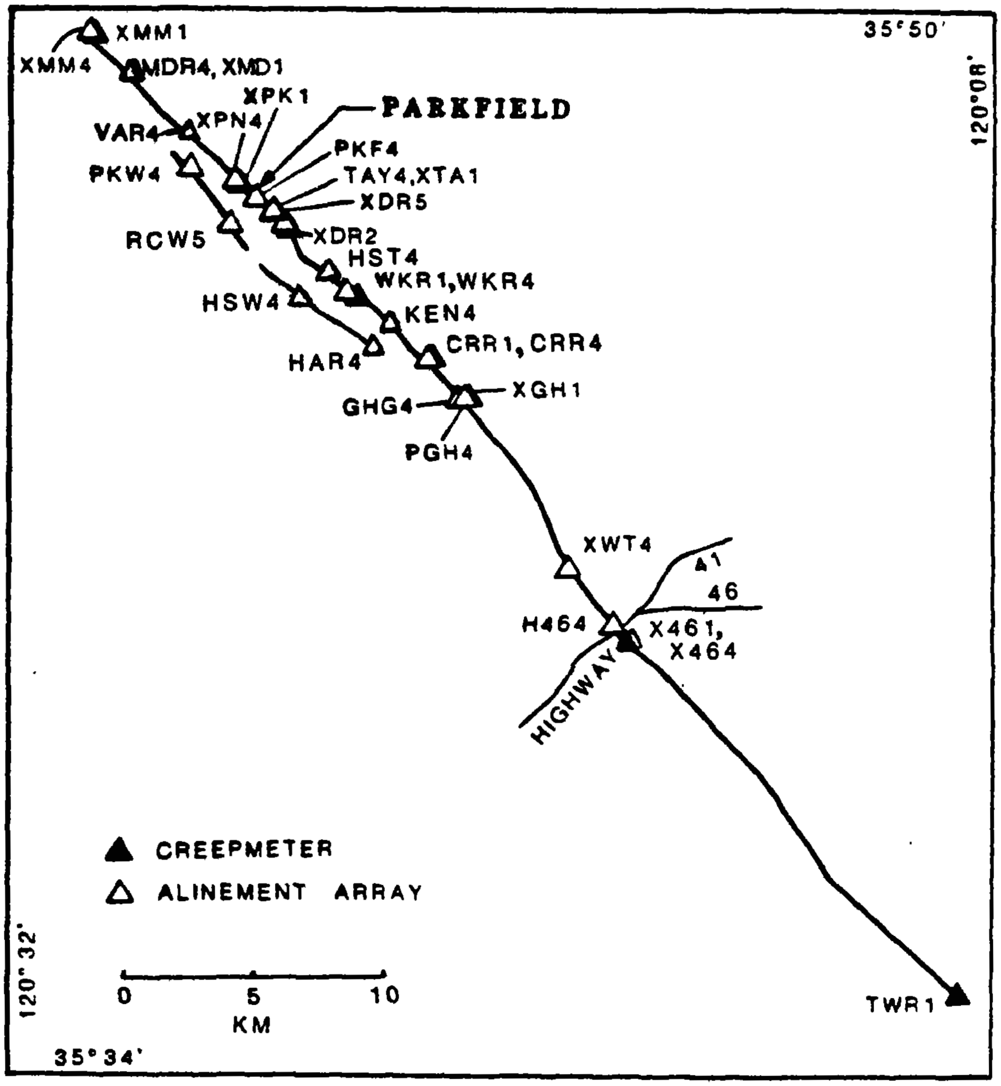

FIGURE 2. Creepmeter and alinement array sites in Parkfield

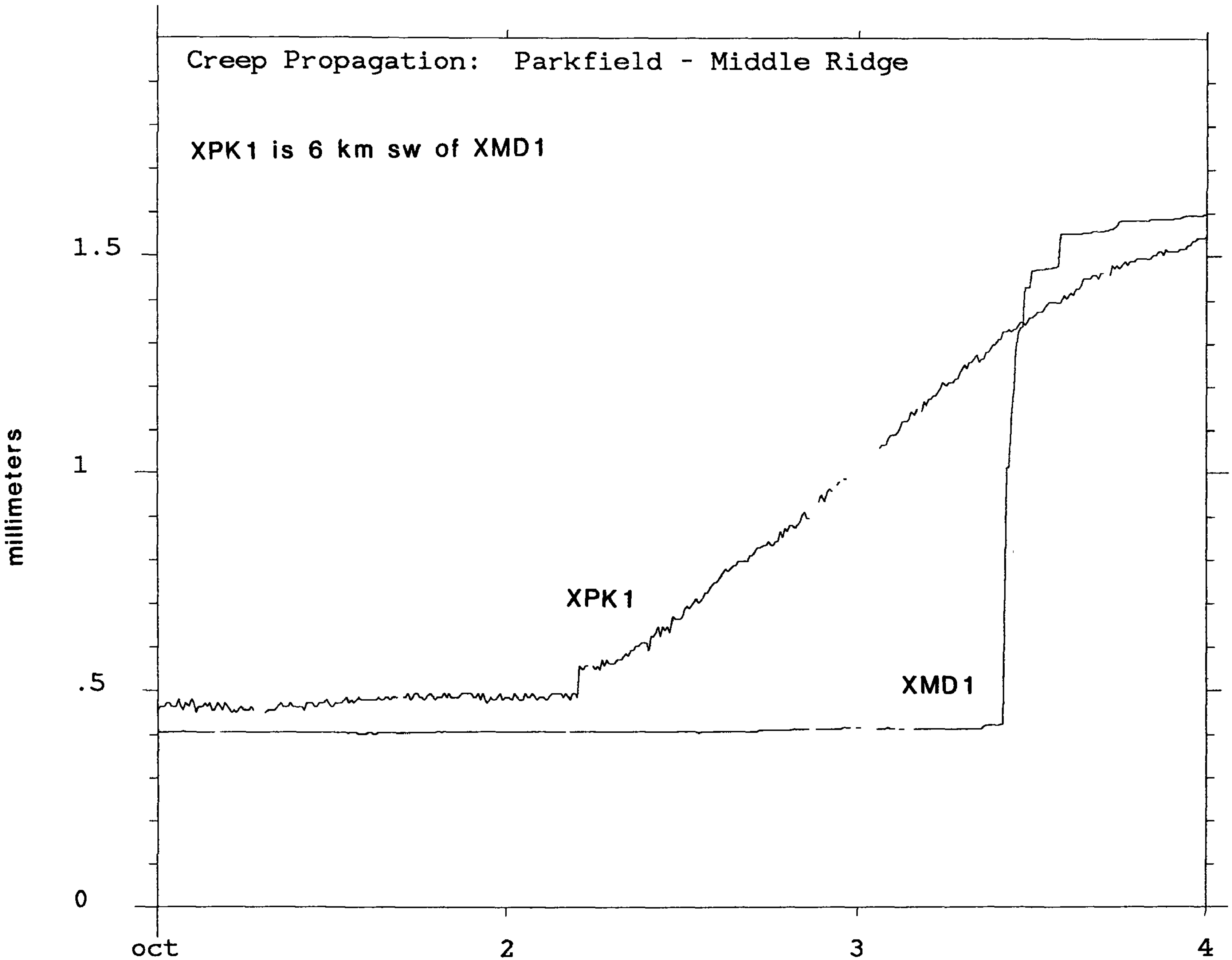
Creep Propagation: Parkfield - Middle Ridge
XPK1 is 6 km sw of XMD1
XPK1
XMD1
millimeters
0
.5
1
1.5
oct
2
3
4

FIGURE 3

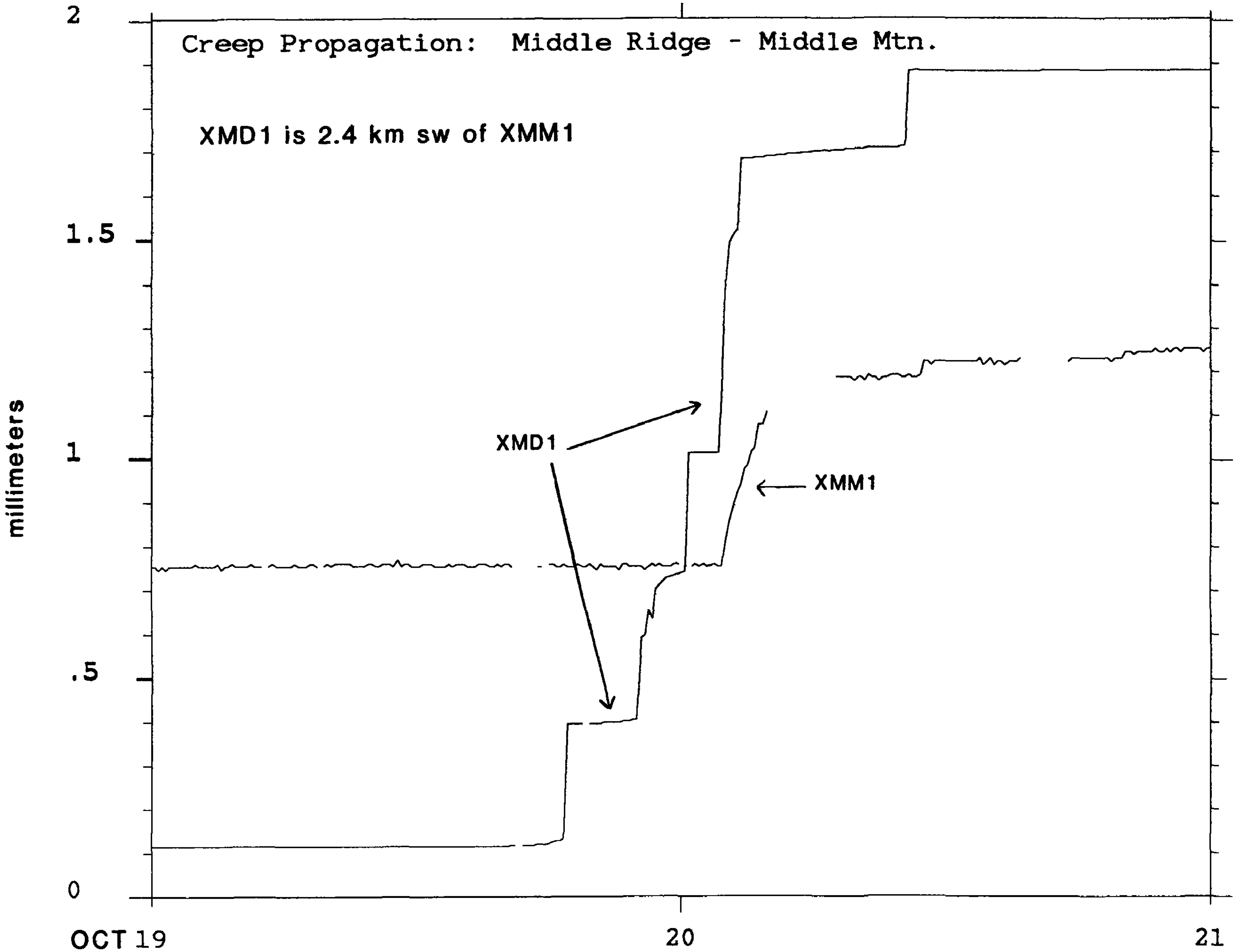
Creep Propagation: Middle Ridge - Middle Mtn.
XMD1 is 2.4 km sw of XMM1
XMD1
XMM1
millimeters
2
1.5
1
.5
0
OCT 19
20
21

FIGURE 4

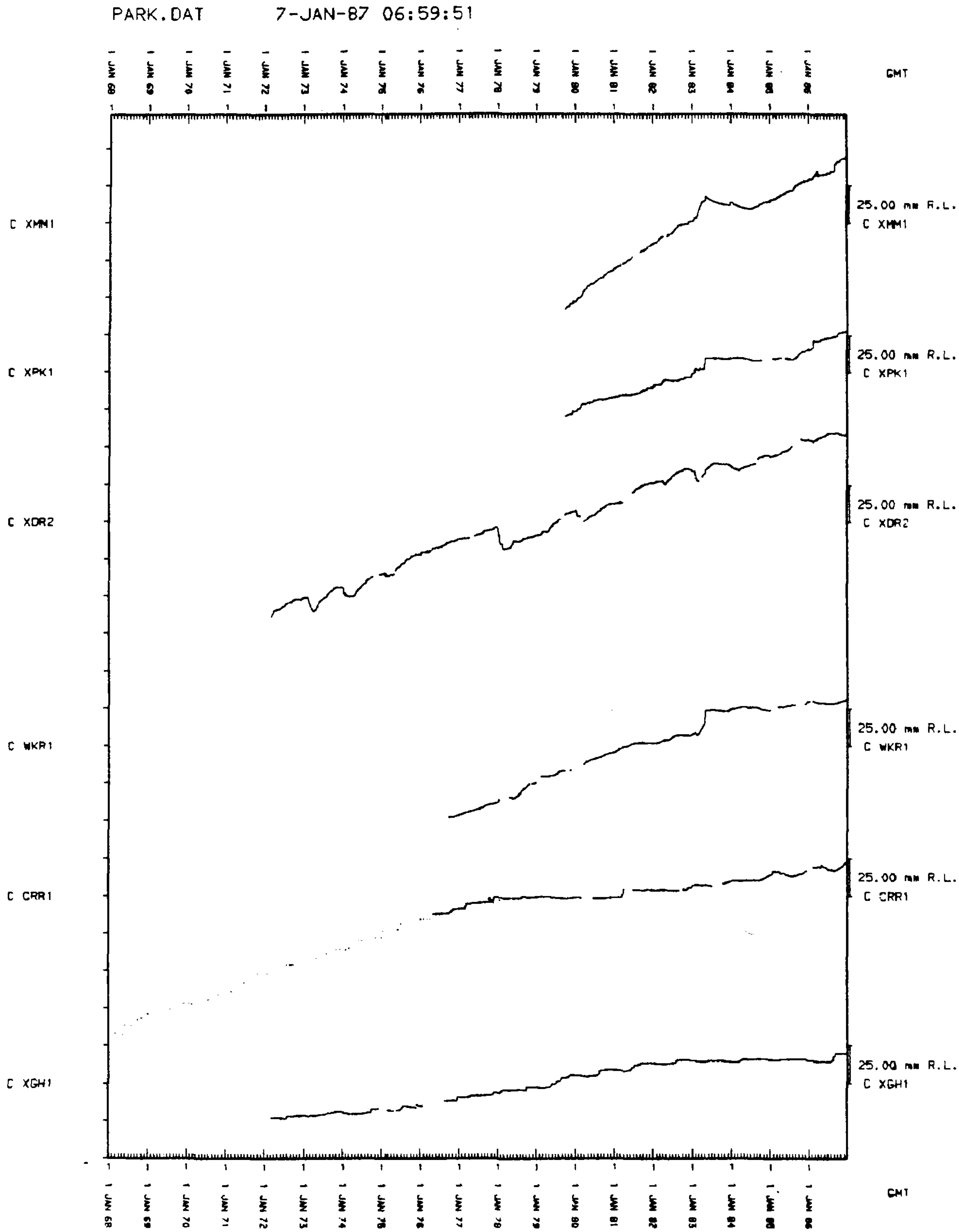

FIGURE 5. **LONG-TERM PLOTS FOR PARKFIELD CREEP**

FORESHOCKS AND THE NUCLEATION OF LARGE EARTHQUAKES

14-08-0001-G1339

Sean C. Solomon and Eric A. Bergman

Department of Earth, Atmospheric, and Planetary Science
Massachusetts Institute of Technology
Cambridge, MA 02139
(617) 253-3786

Investigation

The purpose of this project is to conduct a detailed study of foreshocks in order to investigate the nucleation process of large earthquakes. The study emphasizes multiple event relocation of all foreshocks in a sequence and, for the larger foreshocks, source studies with body waveform inversion techniques. A quantitative theoretical framework in which to interpret our investigations of the spatial-temporal patterns and source characteristics of foreshocks has been suggested by *Das and Scholz* (1981). In this model, which is based on the concept of subcritical crack growth, foreshocks arise from the interaction of a slowly-expanding nucleation zone with strength heterogeneities in the earthquake source zone. One of the goals of this project is to evaluate the utility of this model in characterizing actual foreshock-mainshock sequences.

Results

We have assembled a catalog of foreshock-mainshock sequences which are suitable for the analysis techniques of this study. Of most interest are foreshock sequences with many events, regardless of size, and sequences containing large ($m_b \geq 5.5$) events which are suitable for detailed source studies.

A significant amount of our effort to date on this project has involved development of the software for the multiple-event relocation algorithm described in detail by *Jordan and Sverdrup* (1981). We have begun the testing of this code and we expect to begin analysis of selected foreshock sequences shortly.

In parallel with event relocation, we are conducting detailed source studies of large foreshocks. For most such events, we are using the long-period P-SH waveform inversion method of *Nabelek* (1984). From our initial list of foreshock-mainshock sequences, we selected the Kurile Islands earthquake sequence of January-March 1978 to begin our investigation. The 1978 sequence contains numerous small events and a larger number of events suitable for body-waveform inversion than any other sequence in our list of foreshock sequences. The mainshocks of this sequence are two of only 18 events in the years 1977-1980 with moments in excess of 10^{27} dyn-cm (*Giardini et al.*, 1985). Another prominent sequence with large foreshocks occurred a short distance to the southwest in August 1969 (*Fukao and Furumoto*, 1975; *Schwartz and Ruff*, 1985) and another M_s 7.0 event occurred nearby in February 1980. Combining studies of all these events may clarify the nucleation process in this particular source region. A major fracture zone is known to collide with the trench very near the source region for these sequences, and its role in the nucleation process is deserving of study. The ISC epicenters of the largest events in this sequence reveal that the earliest large foreshocks occur 70-100 km to the northeast of the epicenters of the mainshocks. The final large foreshocks are located very near the epicenters of the mainshocks. Several large events occuring during the 40 hour period between the two mainshocks once again are located in the northeastern cluster. The area between these two clusters experienced no large foreshocks or aftershocks.

Preliminary results are available for five of these events. All the centroid depths are shallower than the ISC depth estimates, which are based on reported pP-P delay times. We surmise that most of the pP phase identification are incorrect. The five events studied have centroid depths ranging from 15 to 27 km below sealevel, whereas the ISC depths are generally between 40 and 60 km (Figure 1). The centroid depths are more consistent with rupture occurring at the interface between the subducting and overthrust plates, extrapolated from the dip of the subducting plate at the trench axis. The narrow range of centroid depths, the tendency for events further from the trench axis to be deeper, and the tendency for deeper events to have steeper dip angles all suggests that these events delineate the interface between the two plates.

The strikes of the likely fault planes for three of the events are close to the average strike of the trench axis, about N235°E. The slip angles (101-109°) of these events deviate somewhat from that for pure dip-slip motion in the sense appropriate for the horizontal projection of the slip vector to be parallel with the direction of relative convergence at this part of the Pacific-Eurasia plate boundary. The other two events, including the M_s 7.3 foreshock, have fault strikes of 201° and 209°, but the slip angles of their mechanisms (80° and 82°) also lead to horizontally projected slip vectors close to the direction of plate convergence. This suggests that there is some complexity in the geometry of the plate interface, but that the earthquakes are still strongly controlled by the overall plate motions in the region.

We plan shortly to complete our source studies of the events in this sequence, including the two mainshocks. For all events studied with waveform inversion we will estimate fault areas from the shape and duration of the source time functions. For the larger events we shall locate the centroid with respect to the nucleation point (which is the reference point for the multiple event relocation) and improve our ability to associate a given event with a specific portion of the plate boundary interface. With the multiple event relocation technique, we will then construct a detailed picture of the spatial-temporal evolution of the sequence. We will test the earthquake nucleation model of *Das and Scholz* (1980) against these results. Our ultimate objective is the development of criteria for the seismic identification of the nucleation of a large earthquake.

References Cited

Das, S., and C. Scholz, Theory of time-dependent rupture in the earth, *J. Geophys. Res., 86,* 6039-6051, 1981.

Fukao, Y., and M. Furumoto, Foreshocks and multiple shocks of large earthquakes, *Phys. Earth Planet. Int., 110,* 335-368, 1975.

Giardini, D., A. M. Dziewonski, and J. H. Woodhouse, Centroid-moment tensor solutions for 113 large earthquakes in 1977-1980, *Phys. Earth Planet. Int., 40,* 259-272, 1985.

Jordan, T. H., and K. A. Sverdrup, Teleseismic location techniques and their application to earthquake clusters in the southcentral Pacific, *Bull. Seismol. Soc. Amer., 71,* 1105-1130, 1981.

Nabelek, J. L., Determination of earthquake source parameters from inversion of body waves, Ph.D. thesis, Mass. Inst. of Technol., Cambridge, MA, 1984.

Schwartz, S. Y., and L. J. Ruff, The 1968 Tokachi-Oki and the 1969 Kurile Islands earthquakes: Variability in the rupture process, *J. Geophys. Res., 90,* 8613-8626, 1985.

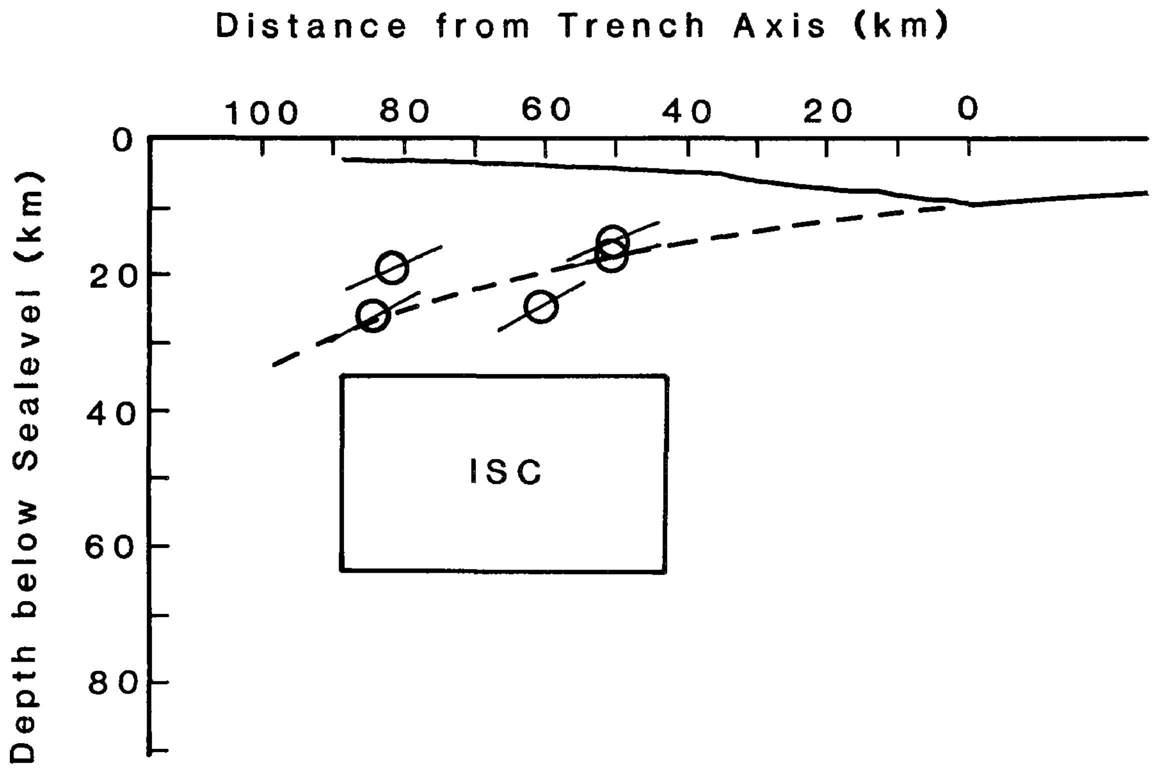

Figure 1. Cross section through the source region of the 1978 Kurile Islands earthquake sequence, showing the range of focal depths indicated by the ISC from reported pP-P times and the centroid depths obtained from body-waveform inversion studies of 5 of the events. Dip angles are shown by lines through the circles representing the centroids. No vertical exaggeration.

Analysis of Seismic Data from the Shumagin Seismic Gap, Alaska

14-08-0001-G-1388

John Taber and Klaus H. Jacob
Lamont-Doherty Geological Observatory of Columbia University
Palisades, New York 10964
(914) 359-2900

Investigations

Digitally recorded seismic data from the Shumagin seismic gap in eastern Aleutian arc, Alaska, are analyzed for detecting space-time variations in the seismicity, focal mechanisms, and dynamic faulting parameters that could be precursory to a major earthquake expected in this seismic gap. The seismic results obtained from the network data are being integrated with crustal deformation data that are independently collected, with volcanicity data of nearby Aleutian volcanoes, and with teleseismic information to identify basic tectonic processes which may be precursory to a great earthquake.

Results

Instrumental evidence that a great earthquake occurred within the Shumagin Gap in 1917 has been discovered. The location and magnitude of the event had been uncertain because it does not appear in the catalogues of Gutenberg and Richter (1954) or Gutenberg (1956). Arrival times for the mainshock (Ms=7.9 according to Abe and Noguchi, (1983)) on May 31, 1917 and 5 aftershocks were used by Boyd and Lerner-Lam (1987) to recalculate the epicenters (Figure 1). While the mainshock is near the boundary between the Shumagin gap and the 1938 rupture zone, three of the five aftershocks clearly show that the mainshock ruptured westward within the Shumagin gap. In addition, the only known felt report is in the Shumagin Islands. We plan to search local newspapers to see if we can obtain more details about the intensity of shaking. Other earthquakes between 1899 and 1903 which Davies et al. (1981) considered possible gap rupturing events have been relocated outside the gap by Boyd and Lerner-Lam (1987) using the added constraint that events must lie along the arc.

The 1917 event is significant because it establishes unquestionably that a great earthquake has occurred within the Shumagin gap and thus the entire gap can't be aseismic as has been suggested by Savage and Lisowski (1986). Previous great earthquakes that probably ruptured the Shumagin gap occurred in 1788 and 1847 (Davies et al., 1981). The unexplainably long time period between 1847 and 1987 was one of the reasons the earthquake potential for the Shumagins was in question. With the addition of the 1917 earthquake, the recurrence intervals become quite regular. Between the great earthquakes in 1788, 1847, and 1917 there are 59 and 70 years, and it has been 70 years since 1917. The maximum probability of an event within the next few years (which was near 99%) will decrease because of the shortened time since the last earthquake, but the uncertainty is greatly reduced. The 1788 and 1847 events probably ruptured the adjoining region of the 1938 earthquake. Such an extended rupture could occur again, based on the high probability of an event within the 1938 zone (Nishenko and Jacob, 1986).

The possibility also exists that the Shumagin gap can be divided into 2 parts with the western portion of the Shumagin Gap most likely to rupture in the future (Hudnut and Taber, 1987). The size of the 1917 event is consistent with the rupture of the western segment. After correcting for the mislocation due to the subducting slab, the location of the mainshock is very near the edge of the western region in the expected nucleation zone. Segmentation of the gap is based on along-arc changes in the seismicity pattern at all depths within the subduction zone.

The 1917 event also helps explain some of the strain measurement results of Savage and Lisowski (1986). They compared their measurements with a survey in 1913 and found no appreciable strain accumulation over the 70 year period. Since the 1913 survey was taken just 4 years before the 1917 earthquake the lack of strain accumulation suggests that the Shumagins are in the approximately the same state they were before the previous earthquake.

Seismicity and volcanicity in the past year increases the short term probability of a gap rupturing event. There has been increased seismicity along the Aleutian arc since the Ms 7.9 Andreanof Island earthquake in May, 1986. Much of the activity could be interpreted as being caused by a largely aseismic strain pulse propagating eastward along the arc. There have been higher than normal levels of seismicity near Unalaska both in the upper plate and along the main thrust zone. The most recent event in the Shumagins (Ml=4.9 on May 2, 1987) appears to have caused local slumping in Sand Point which resulted in broken water and sewer lines.

Volcanic activity seems to have increased across the arc, though this may be due partially to increased reporting because of the Augustine eruption in 1986. Pavlof volcano (near the middle of the Shumagin gap) experienced its most intense eruption in at least 15 years in 1986 and Shishaldin, Akutan, and Mt. Cleveland all have erupted for the the first time in 4-10 years. In March and April, 1986 there were 9 moderate events (Mb 4.6-5.3) near Bogoslof volcano though we have no reports of volcanic activity. Veniaminof, which is near one end of the Shumagin gap, erupted in March 1987 for the first time since 1984.

References

Abe, K., and S. Noguchi, Revision of magnitudes of large shallow earthquakes, 1897-1912, *Phys. Earth Planet Inter. 33*, 1-11, 1983.

Boyd, T.M., and A. Lerner-Lam, The spatial distribution of turn of the century seismicity along the Aleutian Arc, in preparation, 1987.

Davies, J., L. Sykes, L. House, and K. Jacob, Shumagin seismic gap, Alaska Peninsula; History of great earthquakes, tectonic setting and evidence for high seismic potential, *J. Geophy. Res., 86*, 3821-3856, 1981.

Gutenberg, B., Great earthquakes 1896-1903, *Transactions, American Geophysical Union 37*, 608-614, 1956.

Gutenberg, B., and C. Richter, *Seismicity of the Earth*, 2nd ed., Princeton Univ. Press, 310 pp, 1954.

Hudnut, K.W., and J.J. Taber, Transition from double to single Wadati-Benioff zone in the Shumagin Islands, Alaska, *Geophys. Res. Lett. 14*, 143-146, 1987.

Nishenko, S.P. and K. Jacob, Hazards evaluation for large and great earthquakes along the Queen Charlotte-Alaska-Aleutian seismic zone: 1985-2005, *USGS Open File Report 86-92*, 91-102,1986.

Savage J.C., and M. Lisowski, Strain accumulation in the Shumagin seismic gap, Alaska, *J. Geophys. Res. 91*, 7447-7454, 1986.

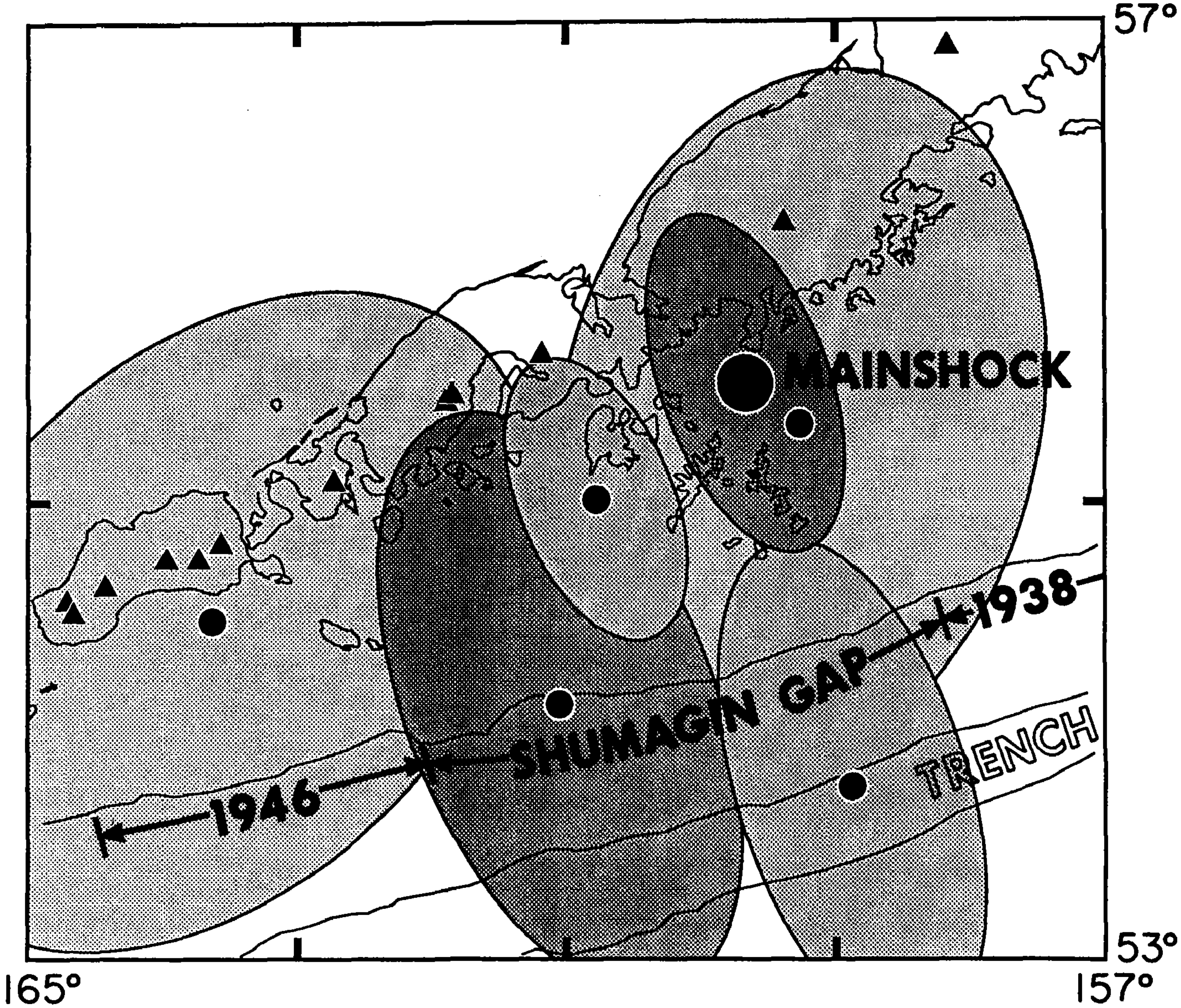

Figure 1. Locations and 75% error ellipses of the May 31, 1917 (Ms=7.9) earthquake and 5 aftershocks. Rupture zones of earthquakes in 1938 and 1946 are also shown. Bathymetric contours are at 400 and 5200 meters. Triangles mark quaternary volcanoes.

Seismic Evidence for Tectonic Process

9930-03353
Peter L. Ward
Branch of Seismology
U.S. Geological Survey
345 Middlefield Road, Mail Stop 977
Menlo Park, California 94025
(415) 323-8111, Ext. 2838

Investigations

Determine the relationship between volcanism on land and plate motions of oceanic plates.

Results

Major databases for radiometric ages of igneous rocks have been merged for the western U.S. (U.S.G.S. Radiometric Age Data Bank), Arizona (Arizona Bureau of Geology and Mineral Technology), Alaska (U.S.G.S. Branch of Alaskan Geology), and western Canada (University of British Columbia) providing data for 13,353 rocks. Almost 12,000 of the ages are younger than Triassic. A comparison of maps of the western U.S. showing location of dated rocks compare quite closely with regional maps of outcrop patterns for the Miocene to Recent. In order to test the homogeneity of sampling, I subdivided the map area into a rectangular grid and determined the percentage of grid cells that contained data and whose center point occurred within the plotted outcrop areas to the total number of grid cells whose centerpoints occurred within the outcrop area. This percentage was only 48% for a 10 x 10 km grid, 80% for a 20 x 20 km grid, 92% for a 30 x 30 km grid and 97% for a 40 x 40 km grid. Thus we can conclude that sampling at least in the Late Cenozoic is relatively homogeneous in a statistical sense when the symbol size is on the order of 40 x 40 km. A few larger gaps do exist where publication of radiometric ages has been slow and some care must be used to check trends observed against other data sources. This comparison also shows that the mapped outcrop area of igneous rocks has increased by about 25% since these detailed outcrop maps were prepared in the late 1970's.

This new, expanded data source provides a basis for a first-order characterization of igneous activity during the Cenozoic and much of the Mesozoic throughout all of western North America. I am in the process of testing more fully the concepts in global tectonics discussed in the last semi-annual report. One observation emerging that is of importance to the Earthquake Program is the apparently close relationship between periods of fundamentally basaltic volcanism and of major strike-slip faulting.

Reports

Ward, P. L., 1986, Volcanism and plate tectonics of the Western United States: EOS Trans. Amer. Geophys. Union, v. 67, p. 1226.

Ward, P. L., 1986, Volcanism and plate tectonics of western North America: Abstract Volume, Hawaii Symposium on How Volcanoes Work, p. 264.

WATER VAPOR RADIOMETER CORRECTIONS AND GPS BASELINE ACCURACY

14-08-0001-G1179

Randolph H. Ware

Cooperative Institute for Research in Environmental Sciences
University of Colorado
Boulder, CO 80309-0449
(303) 492-1586

INVESTIGATIONS

Tropospheric effects can be a limiting factor in the accuracy of baselines determined using the Global Positioning System (GPS), particularly for the vertical component. Since GPS measurements are being used increasingly to determine crustal movements associated with earthquakes, an evaluation of the accuracy of such measurements is useful for earthquake research.

Corrections for tropospheric delay are commonly calculated using a tropospheric model based on surface meteorological (met) data. A more accurate correction can be obtained by augmenting surface met data with water vapor radiometer (WVR) observations of atmospheric water vapor. However, WVRs are not often used in GPS baseline measurement campaigns because the currently existing instruments are cumbersome, expensive, and are not widely available.

For GPS signals, radio path delays of several meters result from transmission through the troposphere to receivers located near sea level. Most of this delay, attributed to atmospheric constituents other than water vapor, can usually be modeled to an accuracy of about one centimeter using surface pressure data. The remaining delay, resulting from water vapor (wet path delay) can be as large as several decimeters in magnitude and is difficult to accurately model using surface met measurements. It is also possible to solve for a zenith troposphere delay as a parameter in the GPS least squares baseline analysis. This approach can reduce the error associated with corrections based on surface met data, but the extra parameter reduces the strength of the GPS solution. The most accurate approach is the estimation of wet path delays using WVR data, which should allow tropospheric errors to be reduced to the one centimeter level.

In order to estimate typical errors associated with surface met corrections, we analyzed GPS data using surface met and simultaneous WVR data from a number of sites with climates ranging from humid to dry. We generated synthetic GPS data which introduced wet path delays computed from WVR observations at one end of a baseline, and then proceeded with baseline determination including delays computed from surface met data which were observed simultaneously with the WVR data. The wet path error at the other end of the baseline was assumed to be zero. If the surface met data were able to predict the delays based on WVR data, then no errors would remain in the GPS baselines. If not, actual errors could be as large as two times the computed errors, depending on the degree of correlation between the wet path delays for the two baseline ends. During disturbed weather conditions associated with local thunderstorms, wet path delays can be poorly correlated for baselines as short as several km. However, high correlation is common for 50 km baselines during stable weather conditions. The computed GPS baseline errors characterize the accuracy limitations resulting from wet path delays in GPS measurements for a variety of climate and weather conditions when surface met corrections are applied.

RESULTS

Simultaneous WVR and surface met data were obtained at three humid sites (Cabo San Lucas, Baja California; Mazatlan, mainland Mexico; and Grand Turk Island in the Caribbean) and two dry sites (Mojave, California; and Denver, Colorado). Average magnitudes of humidity are shown worldwide for ocean zones in Figure 1. Our three humid sites fall within the second most humid zone with an average of 3 to 4 grams per square cm of precipitable water, corresponding to zenith wet path delays of 19.5 to 24 cm. The conversion factor is 6.5 cm/grams per square cm (Hogg et al., 1981). Surface met measurements included pressure measurements accurate to 0.1 millibars, dry bulb temperatures accurate to 0.1 degrees C, and wet bulb temperatures. The relative humidities inferred from the wet and dry bulb temperatures are generally held to be accurate to within 10%. Water vapor radiometers were either the J-01 prototype (Cabo and Grand Turk), the R-Series (Mazatlan), the R-Series Bendix retrofit (Mojave), or the NOAA unit (Denver). Specifications for these WVRs can be found in Elgered et al., 1985. We assume the path delays calculated from WVR data are accurate to 1 cm rms.

For all of the Cabo, Mazatlan, Grand Turk, Mojave, and Denver data analyzed, the horizontal baseline errors were in no cases greater than 1 cm. This was not surprising since the azimuthal variations in path delay observed by WVRs for the data analyzed were also less than 1 cm. However, much larger azimuthal variations have been observed in other data, such as those shown in Figure 2, from the Kokee Park Observatory, Kauai, in the Hawaiian Islands. This particular site is situated between a mountain receiving an average of 300 inches of rain per year and a canyon receiving less than 20 inches per year. The gradient is seen to be as large as one third of the total zenith path delay of 3.5 cm. Azimuthal variations as large as 4 cm have been observed in Colorado (Ware et al., 1986).

The most significant baseline errors were found to be in the vertical component, which were as high as 11.5 cm rms in the humid areas (Figure 3). In the dry areas, the vertical errors were as large as 5.4 cm rms (Figure 4). Precision dilution of precision (Spilker, 1978), or PDOP, resulting from the geometric relationship of the observed satellites, contributed a factor of 2 to 3 to these vertical errors. Real GPS data will have a higher PDOP until the total constellation of 18 satellites are available. Our synthetic GPS data assumed the total constellation.

Zenith wet path delay errors in the surface met data from all of the dry and wet sites are shown in Figure 5. The delays range from less than 4 cm in Denver to more than 32 cm at Grand Turk. This total set of data has an rms of 0.08(SMT) + 1.1 cm, where SMT is the zenith wet path delay estimated from surface met measurements. This expression may be used as a rule of thumb in estimating errors resulting from surface met corrections for tropospheric delays.

REFERENCES

Elgered, G., B. Ronnang, E. Winberg, and J. Askne, Satellite-Earth Range Measurements: Correction of the Excess Path Length due to Atmospheric Water Vapor by Ground Based Radiometry, Research Report No 147, Onsala Space Observatory, Chalmers University, Gothenburg, Sweden, 1985.

Hogg, D. C., F. O. Guiraud, and M. T. Decker, Measurement of Excess Radio Transmission Length on Earth-Space Paths, **Astronomy and Astrophysics, 95**, 304-307, 1981.

Spilker, J. J., GPS Signal Structures and Performance Characteristics, **Navigation, 25**, 121-146, 1978.

REPORTS

Ware, R. H., C. Rocken, and K. J. Hurst, Global Change, GPS, and Water Vapor Radiometers, submitted for the XIX IUGG Meeting, August, 1987.

Ware, R. H., K. J. Hurst, and C. Rocken, Global Change and GPS, **EOS**, abstract submitted for Spring AGU Meeting, May, 1987.

Ware, R. H., K. J. Hurst, and C. Rocken, GPS Baselines: Comparing Tropospheric Corrections Based on WVR Data to Those Based on Surface Met Data, **EOS, 44**, 911, 1986.

Ware, R. H., C. Rocken, and K. J. Hurst, A GPS Baseline Determination Including Bias Fixing and Water Vapor Radiometer Corrections, **Journal of Geophysical Research, 91**, 9183-9192, 1986.

Ware, R. H., C. Rocken, K. J. Hurst, and G. W. Rosborough, Determination of the OVRO-Mojave Baseline During the Spring 1985 GPS Test, **Proceedings of the Fourth International Symposium on Satellite Positioning**, Austin, Texas, April 28 - May 2, 1986.

Ware, R. H., C. Rocken, and J. B. Snider, Experimental Verification of Improved GPS-Measured Baseline Repeatability Using Water Vapor Radiometer Corrections, **IEEE Transactions on Geoscience and Remote Sensing, GE-23**, 467-473, 1985.

Ware, R. H., C. Rocken, and K. J. Hurst, Water Vapor Radiometer Corrections for Tropospheric Errors in a GPS Baseline Determination, **EOS, 46**, 844, 1985.

Figure 1. Average precipitable water over Earth's oceans, measured by Seasat.

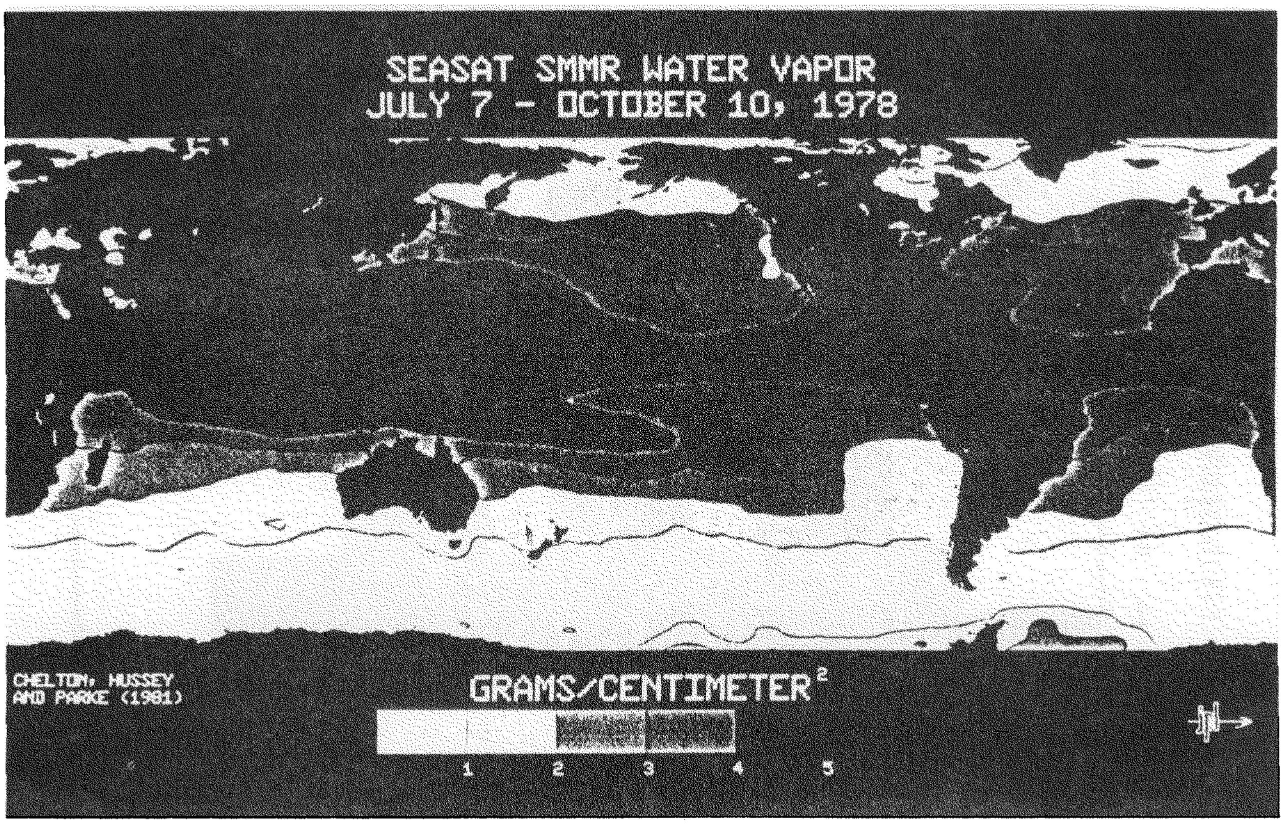

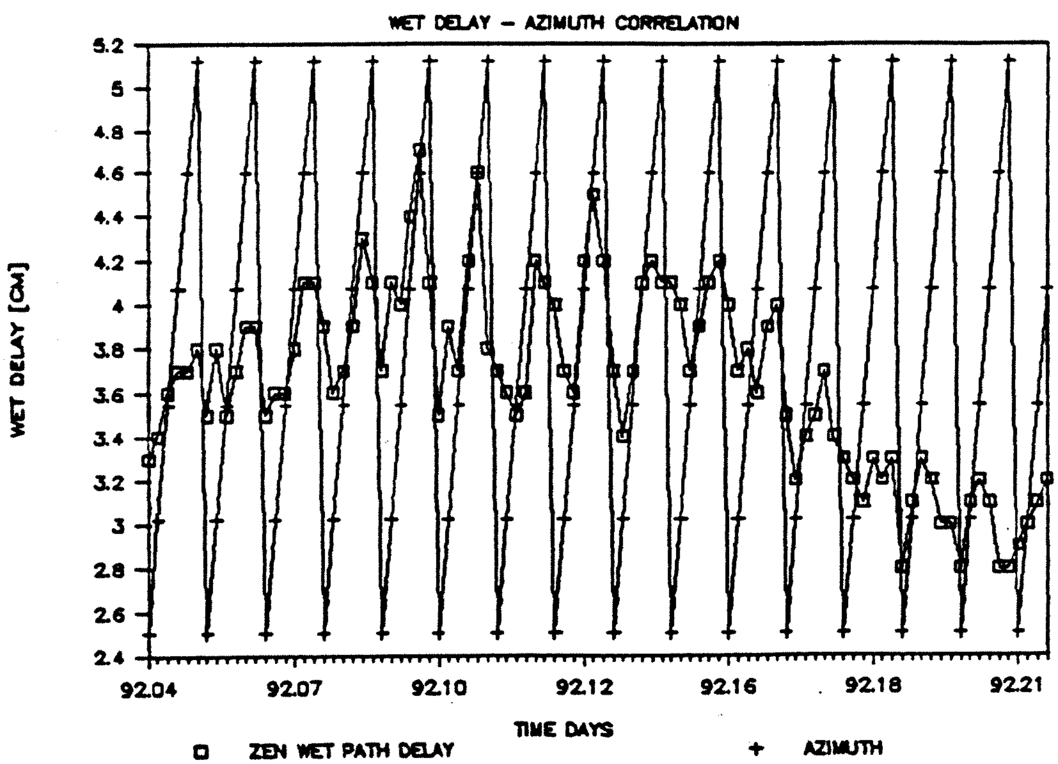

Figure 2. Azimuthal variations in wet path delay observed at Kokee Park, Kauai, in March, 1987.

Figure 3. Computed baseline errors, vertical component, for humid sites at Mazatlan, Cabo San Lucas, and Grand Turk.

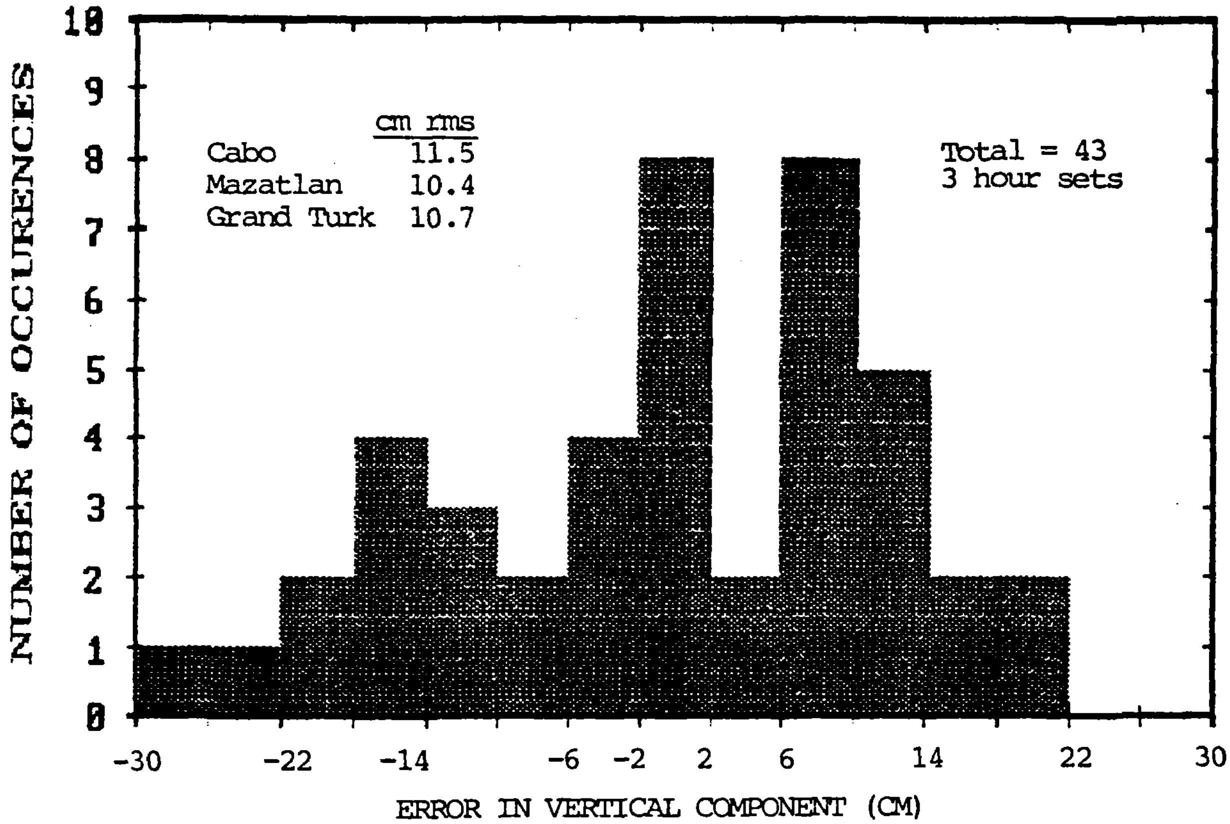

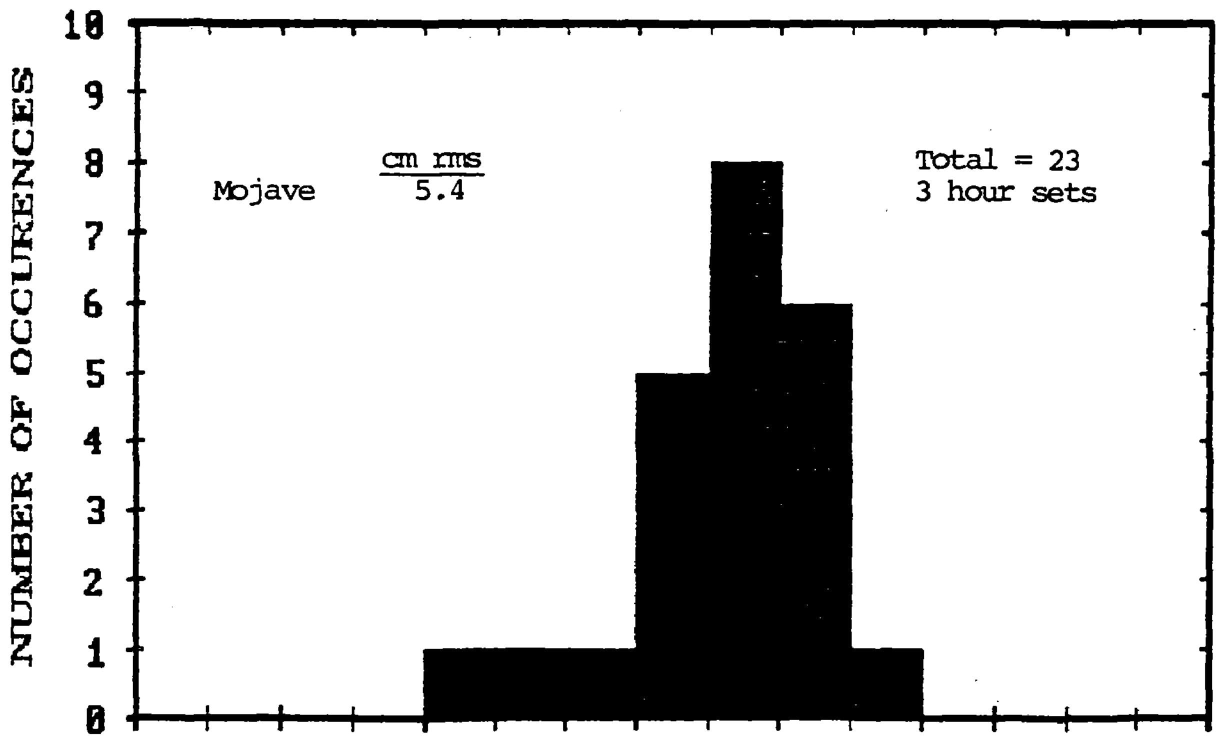

Figure 4. Computed baseline errors, vertical component, for the dry site at Mojave.

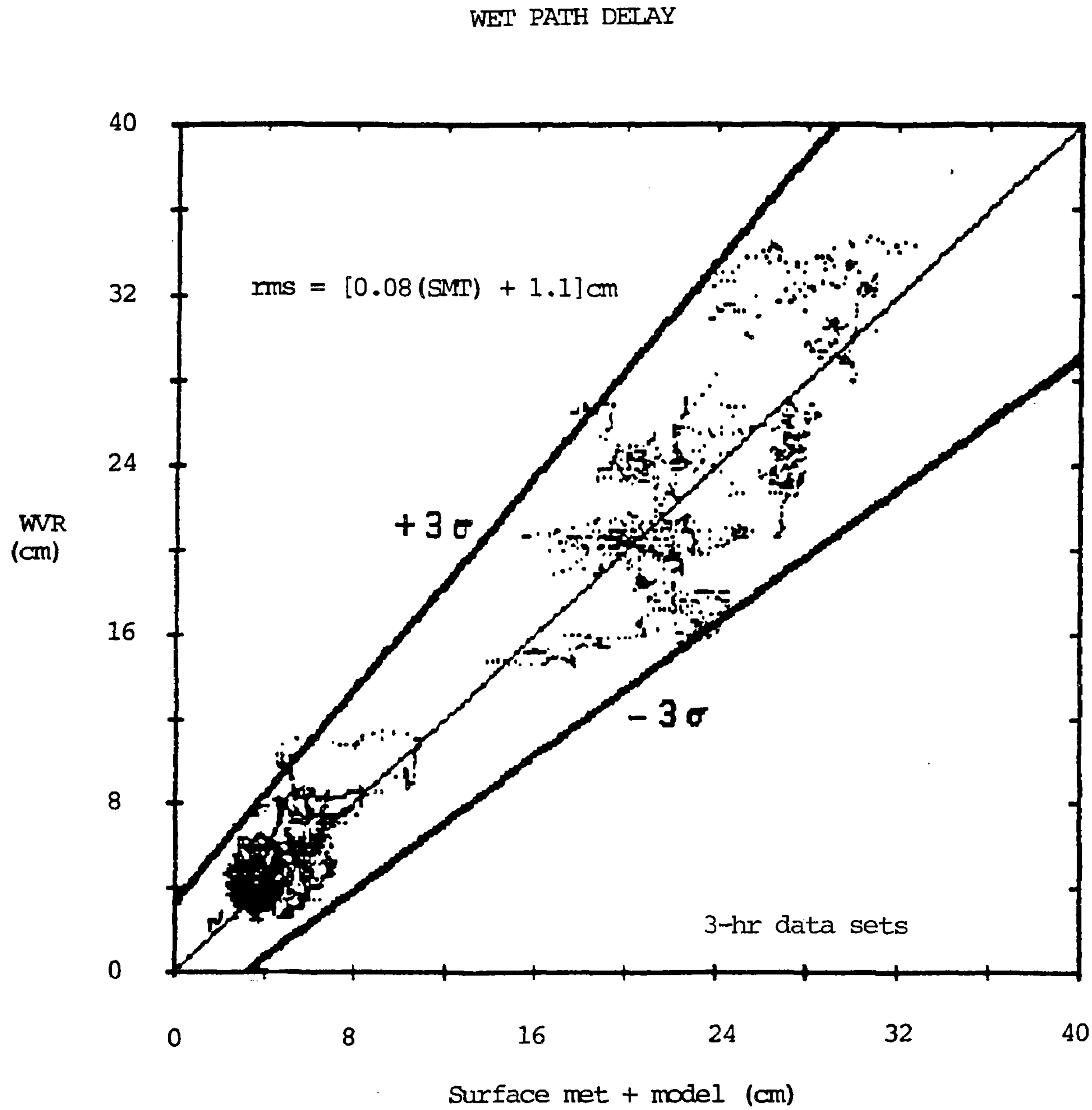

Figure 5. Wet path delays from WVR observations and modeling based on surface met data.

Latin American Seismic Studies

9930-01163

Randall A. White, David H. Harlow
U.S. Geological Survey
Branch of Seismology
345 Middlefeild Road, Mailstop 977
Menlo Park, California, 94025
(415) 323-81111. Ext. 2570

Investigations

San Salvador Earthquake of October 10, 1986. One of us (Harlow) accompanied a team assembled by the Earthquake Engineering Research Institute (EERI) to study the effects of the earthquake. The purpose of the trip was to assist Salvadoran scientists in the interpretation of data collected by an 11-station seismograph network and to provide information on the earthquake to U.S. State Department officials.

Results

The magnitude Ms 5.4 San Salvador earthquake of 10 October 1986 resulted in 1500 deaths, 10,000 injuries, and 250,000 people left homeless. The earthquake was caused by near-surface, left-lateral rupture on a N25 E trending fault located directly beneath the city of San Salvador. Strong ground motion lasted for only 3 to 5 seconds, but the shallow focus and amplification of seismic waves by surface deposits of volcanic tuff combined to produce horizontal ground accelerations up to 0.72g at a period of about 0.8 sec. These somewhat high near-field accelerations at the natural period of low- to mid-rise structures appear to have been a major cause of locally intense destruction in San Salvador that is high for such a small magnitude earthquake. Since 1710, the city has been severely damaged eleven times by similar local earthquakes that have originated on several nearby faults. Such shallow-focus earthquakes are common along the Central American volcanic chain and pose a major seismic risk to numerous cities and towns.

Reports

1. Harlow, D.H., Rymer, M.J., and White, R.A., 1986, The San Salvador Earthquake of October 10, 1986, and Implications of the Regional Earthquake History, Preliminary Report, submitted to U.S. Agency for International Development, October 26, 1986.

2. Harlow, D.H., White, R.A., Martinez, C., and Alverez, S., 1986, The San Salvador Earthquake of 10 October 1986, Seismol. Res. Letters, 58, p. 9.

3. White, R.A., 1986, Statistics of Volcanic Chain Earthquakes in and near San Salvador, Seismol. Res. Letters, 58, p. 9.

Crustal Deformation Observatory Part J: Askania Borehole Tiltmeter

14-08-0001-G1153

Frank Wyatt and Duncan Carr Agnew
Institute of Geophysics & Planetary Physics
University of California, San Diego
La, Jolla, California 92093
(619) 534-2411

Walter Zürn
Geowissenschaftliches Gemeinschaftsobservatorium Schiltach
Universitäten Karlsruhe
D-762 Wolfach, Heubach 206, FRG

This grant supports the operation of an Askania biaxial borehole tiltmeter (S/N 11) at Piñon Flat Observatory (PFO) and the analysis of observations from it. This effort is part of the overall Crustal Deformation Observatory (CDO) program to understand vertical deformations and is a cooperative enterprise with Dr. Walter Zürn of Karlsruhe University (West Germany). The goals of this project are to:

- Establish techniques (and costs) for emplacing and orienting removable tiltmeters in boreholes of various depths, with special emphasis on developing methods that may be applied at greater depths.
- Compare these borehole tilt measurements with those from adjacent tiltmeters, including both long-base surface instruments and other borehole installations. Such comparisons will enable us to establish sources of instability and noise, and test the accuracy of different techniques.
- Monitor the signals produced by this high-quality borehole instrument to accurately record tilt in this tectonically active area.

During this period the instrument was operated at a depth of 25 m in a cased hole, near other borehole tiltmeters and the UCSD long-base tiltmeter (535 m long). Figure 1 shows data from the Askania and long-base instruments. Several offsets of order 0.1 μrad have been removed from the Askania data. Some of these were caused by nearby drilling (15 m away) in early 1986, and by experimental work; one was coincident with the North Palm Springs earthquake of 1986. This last signal was probably caused by cable shaking; the modeled coseismic tilts are only about 1-2 nrad. Both components of the borehole tiltmeter show an initial transient tilt, settling down over the next few months. (The instrument was installed only 21 days after cementing the casing, so we can't be certain about the cause of this signal.)

For a direct comparison with the long-base instrument, we resolved the Askania tilt data along the axis parallel to the long-base instrument. The difference between the two is shown in Figure 1. Each of the series has been scaled according to their own calibration factors; the small tidal residual (possibly caused by different frequency responses) indicates that our gain estimates are very nearly correct. Aside from a deformational event caused by well drilling, the Askania data are well behaved, with a possible annual signal of 0.25 μrad. We plan several experiments for 1987 in an attempt to understand this difference signal.

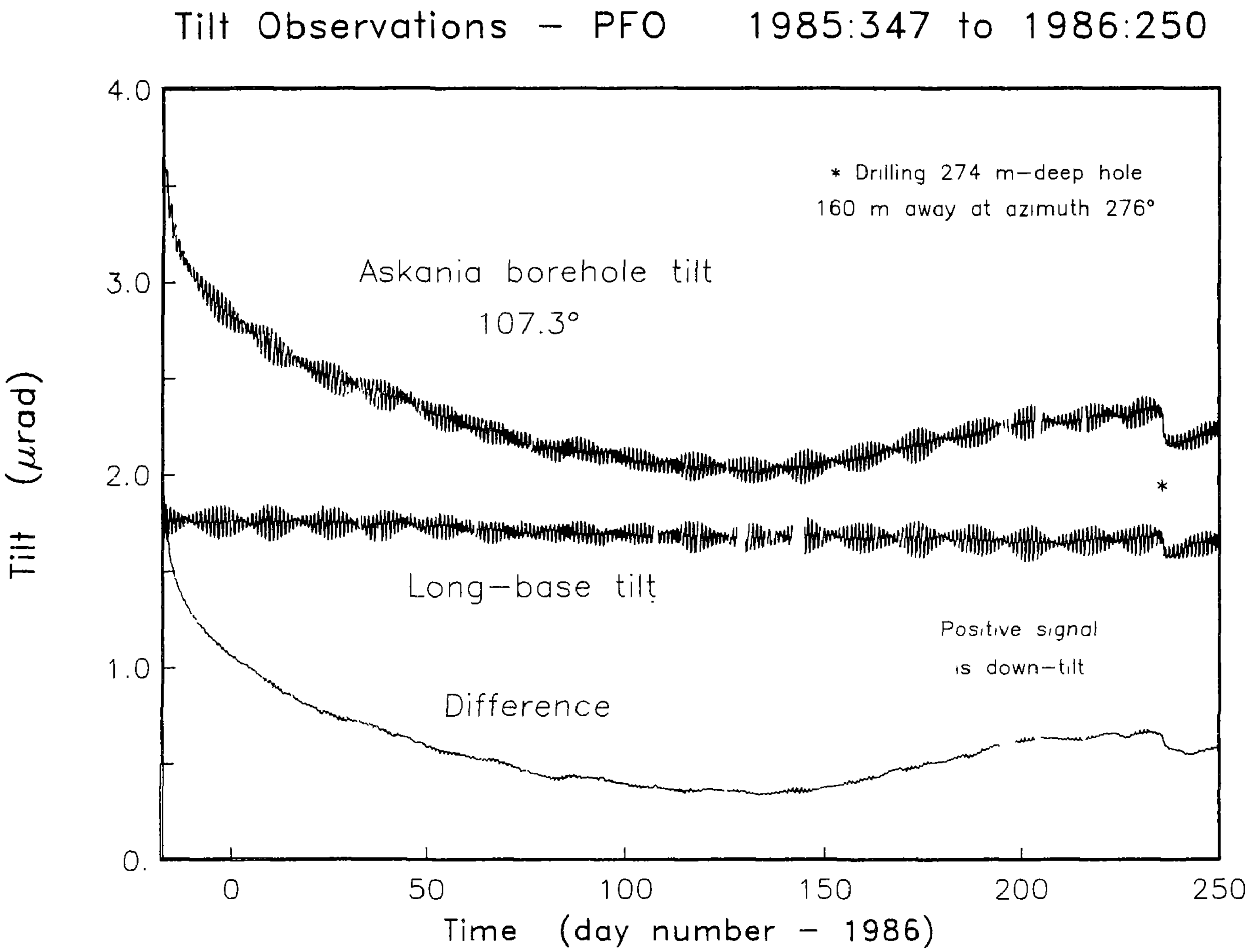
Tilt Observations - PFO 1985:347 to 1986:250
4.0
3.0
2.0
1.0
0.
Tilt (μrad)
* Drilling 274 m-deep hole
160 m away at azimuth 276°
Askania borehole tilt
107.3°
*
Long-base tilt
Positive signal
is down-tilt
Difference
0
50
100
150
200
250
Time (day number - 1986)

Figure 1.

Piñon Flat Observatory: A Facility for Studies of Crustal Deformation

14-08-0001-G1178

Frank Wyatt, Duncan Carr Agnew,
Mark A. Zumberge, Jonathan Berger
Institute of Geophysics & Planetary Physics
Scripps Institution of Oceanography
University of California, San Diego
La Jolla, CA 92093
(619) 452-2019

This grant supports the operation of Piñon Flat Observatory (PFO) by providing one-half the funds needed for running the shared facility. Matching funds are provided by the National Science Foundation. The work done at PFO includes establishing the accuracy of instruments designed for measuring various geophysical quantities by comparing results from them with data from "reference standard" instruments. This comparison also allows reliable monitoring of strain and tilt changes in the area near the observatory, between the active San Jacinto fault and dormant southern San Andreas fault systems. All of this effort is intended to foster development of precision geophysical instrumentation.

This report presents results from the reference standard instruments. The three laser strainmeters provide the reference for strain measurement, and especially for detecting fluctuations in strain. We have suspected that much of the low frequency noise in these instruments came from changes in the frequencies (wavelengths) of the lasers: length changes of the quartz cavities that control these frequencies would cause apparent strain changes. Cavity length variations from 10^{-7} to 10^{-6} per year seemed not unlikely. We began occasional measurements of the laser frequencies relative to an iodine stabilized laser in 1984. Since this involved transporting delicate equipment from our lab to the field, it was not done very often. More recently we installed a system for routine laser frequency measurement. Optical fibers carry light coherently from each of the three strainmeter lasers to a central location where the transmitted beams are beat against light from a reference laser. The beat frequencies are recorded approximately weekly and the results are used to correct the strain data.

Figure 1 shows the records used to produce the corrected strain data. for the Northwest-Southeast strainmeter. The top trace is the observed strain, the next two are the corrections for motion of the end-monuments, the fourth is the partially corrected strain, and the squares show the laser frequency-drift. This strainmeter is tied to a depth of 25 m using optical anchors, so the end-monument correction should be very good. Figure 2 shows the effect of the frequency corrections for the period over which both optical anchors have been operating. The fully-corrected strain (bottom trace) is computed assuming a linear drift between the discrete frequency-correction measurements. (The sparseness of the data before mid-1985 makes this speculative, and the secular rates given below were determined by a fit only to those dates with frequency measurements.) For the fully-corrected series, the trend in the strain rate over the past two years on this instrument drops from a few tenths of a $\mu\epsilon$/a to less than 0.03 $\mu\epsilon$/a, and shows variations about this trend no larger than 0.1 $\mu\epsilon$ with monthly strain rates limited to 0.3 $\mu\epsilon$/a.

Table 1 summarizes the secular strain results from all three laser strainmeters and from single-wavelength EDM measurements, (provided by Dr. James Savage) for a net around PFO.

Table 1
Pinyon Flat Strain Rates ($\mu\epsilon$/yr)

e_{11} (e_{EW})	$e_{NW/SE}$	e_{22} (eNS)	Δ ($e_{11}+e_{22}$)	γ_1 ($e_{11}-e_{22}$)
Geodetic Strain 1973-1985				
0.094	0.032	−0.023	0.071	0.117
±0.015	±0.019	±0.017	±0.021	±0.021
Laser Strainmeter Strain 1984−1986 (frequency corrections made)				
0.094	−0.024	−0.244	−0.170	0.360
±0.099	±0.034	±0.110	±0.075	±0.186
Laser Strainmeter Strain 1974−1986 (no frequency corrections)				
0.049	−0.321	−0.139	−0.090	0.187

Note that "standard errors" for the laser strainmeter data are actually the rms fluctuations about the linear trend, not strain-rate uncertainties.

The geodetic and observatory strain rates in this table agree fairly well for all but the north-south strain, which has severe end-monument instabilities. Strain-rates of this size can usually be determined only by precise geodetic measurements made over many years. The extreme stability and high resolution of the corrected laser strainmeter data give new hope of being able to detect changes in the secular strain rate.

A second, and equally good "reference standard" instrument at PFO is the 535 m-long fluid tiltmeter. Figure 3 shows the record from this instrument. With nearly four years of data, evidence for a secular trend in tilt of 0.12 μrad/a down to the west is becoming quite convincing. Variations about the trend are little more than 0.15 μrad (rms of 0.065 μrad) and generally correspond to some known influence (e.g., nearby well drilling, or a failure of the temperature control). Figure 3 also shows that for high-quality tilt measurement, as for strain, it is essential to anchor the end-monuments to depth properly. The monument motion shown is actually the difference in vertical displacement between the two end-monuments; each of those is measured relative to a depth of 25 m.

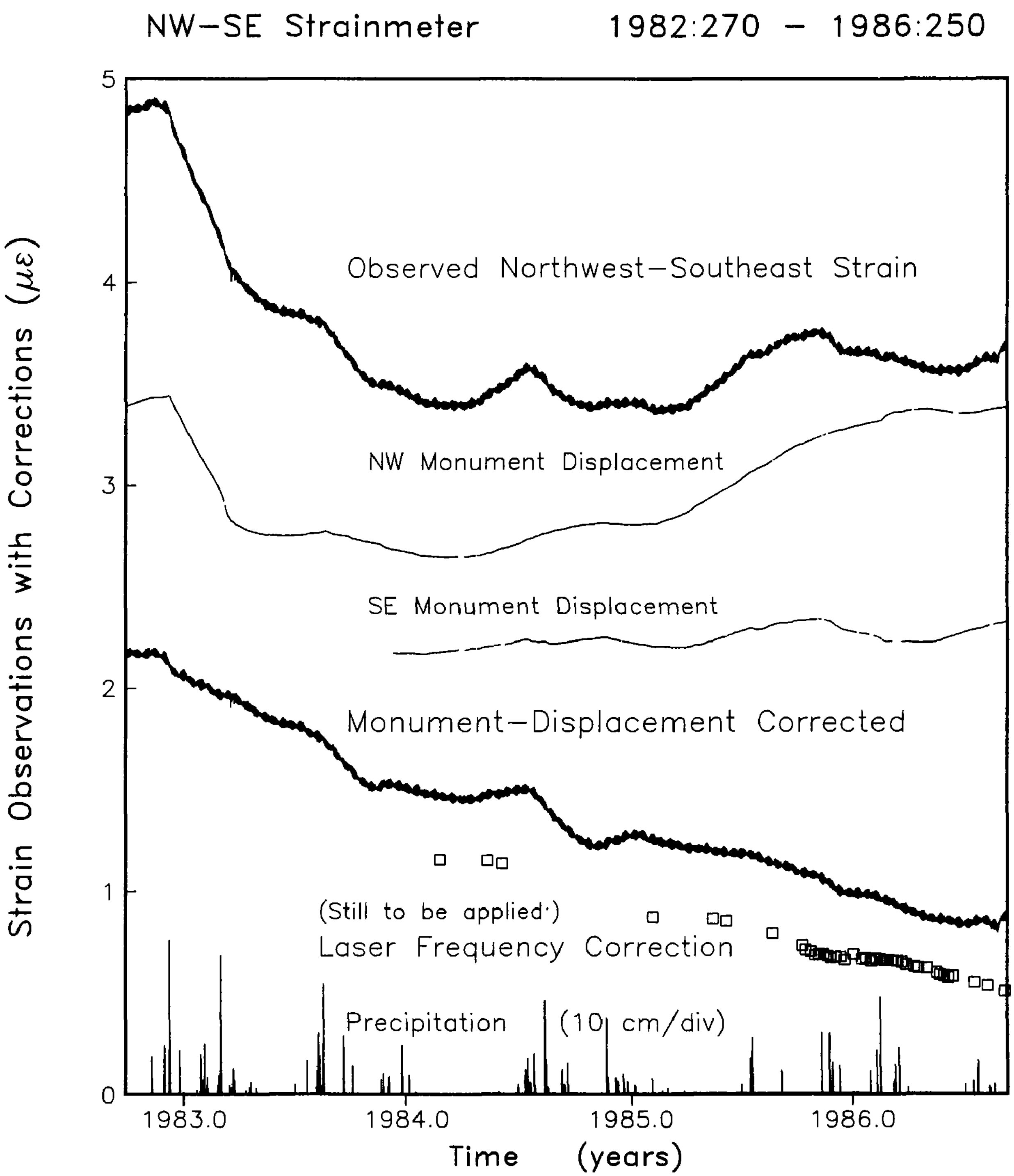
NW-SE Strainmeter 1982:270 - 1986:250
Observed Northwest-Southeast Strain
NW Monument Displacement
SE Monument Displacement
Monument-Displacement Corrected
(Still to be applied')
Laser Frequency Correction
Precipitation (10 cm/div)
Strain Observations with Corrections ($\mu\varepsilon$)
Time (years)
0
1
2
3
4
5
1983.0
1984.0
1985.0
1986.0

Figure 1.

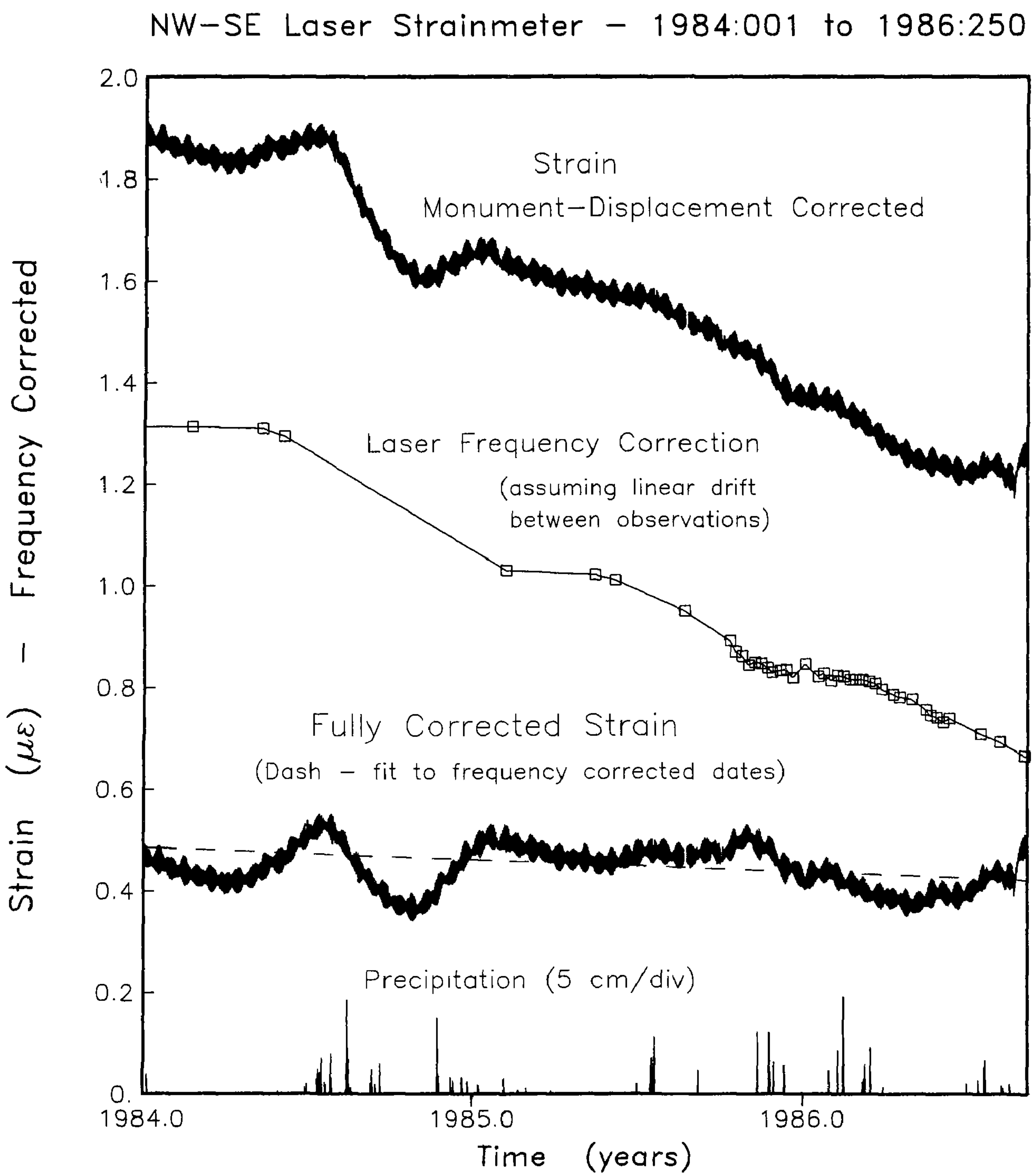
NW-SE Laser Strainmeter - 1984:001 to 1986:250
Strain
Monument-Displacement Corrected
Laser Frequency Correction
(assuming linear drift
between observations)
Fully Corrected Strain
(Dash - fit to frequency corrected dates)
Precipitation (5 cm/div)
Strain (με) - Frequency Corrected
Time (years)
2.0
1.8
1.6
1.4
1.2
1.0
0.8
0.6
0.4
0.2
0.
1984.0
1985.0
1986.0

Figure 2.

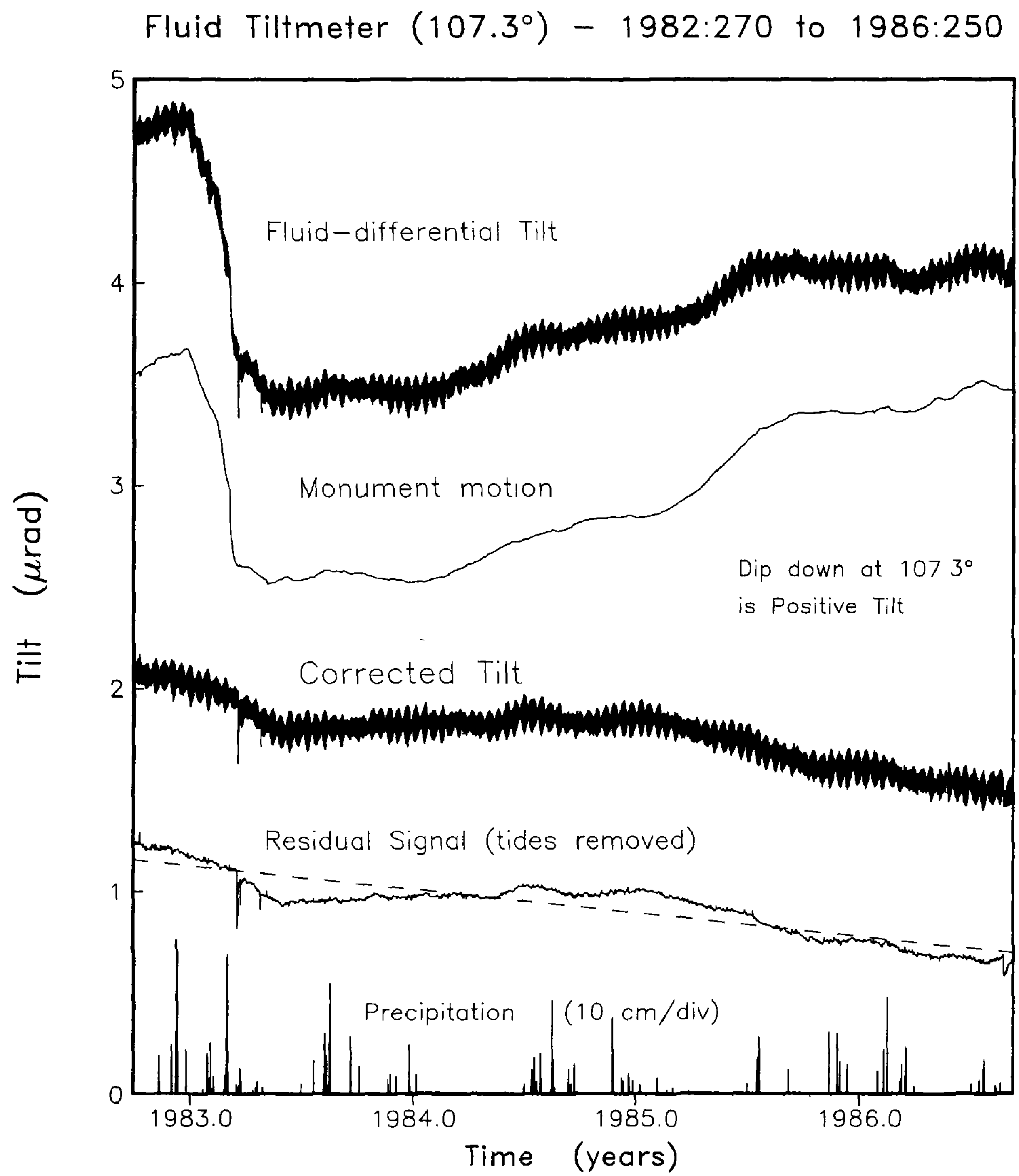
Fluid Tiltmeter (107.3°) – 1982:270 to 1986:250
Fluid–differential Tilt
Monument motion
Dip down at 107 3°
is Positive Tilt
Corrected Tilt
Residual Signal (tides removed)
Precipitation (10 cm/div)
Tilt (μrad)
Time (years)
5
4
3
2
1
0
1983.0
1984.0
1985.0
1986.0

Figure 3.

Piñon Flat Observatory: Cooperative Studies with Outside Investigators

14-08-0001-G1197

Frank Wyatt and Duncan Carr Agnew
Institute of Geophysics & Planetary Physics
Scripps Institution of Oceanography
University of California, San Diego
La Jolla, CA 92093
(619) 452-2019

This grant provides assistance for independent investigators working at Piñon Flat Observatory (PFO) under the auspices of the U.S. Geological Survey. This assistance includes research coordination, instrument operation and testing, data logging, preliminary data reduction, and collaborative data analysis. Part of this is a cooperative program (the Crustal Deformation Observatory Project) to evaluate instruments for measuring long-period ground deformation. Such evaluation involves understanding and reducing noise in the instruments and also developing improved methods to describe measurement error. Most of the studies currently underway are conducted independently, with investigators establishing their own associations to compare results; in the Crustal Deformation Project there is a more formal agreement to share observations.

Most of the sensors operated by outside investigators have continued to work well with only occasional attention, notably the various borehole tiltmeters, which include an Askania tiltmeter (ASK, at 24 m depth) run in cooperation with Walter Zürn of Karlsruhe University; two tiltmeters (BOA, at 24 m, and BOB at 36 m) designed by Judah Levine and Charles Meertens of the University of Colorado; and three St. Louis University tiltmeters (STLA, STLB, and STLD, all at 4.5 m) developed by Sean-Thomas Morrissey.

These tiltmeters, along with other instruments at PFO, recorded extremely large deformations in August 1986, caused by drilling of a deep borehole for a USGS project on near-surface effects on high-frequency seismic signals. Drilling of the three boreholes (called, in order of drilling, GSB, GSC, and GSD) began on 1986:221. The first two holes were only 153 m deep and drilling them did relatively little to deform the ground, though there is some evidence for deformation on 224:20 as the drilling of GSC went below 100 m. Drilling of GSD began on 233, and by 235:18 the hole had reached 217 m, inducing the large event shown in Figures 1 and 2. This hole was drilled to a final depth of 275 m. We suspect that this hole must have intersected a permeable zone near 217 m, allowing an upper aquifer to drain. This interconnection would have reduced the pressure in the upper fracture, causing it to close slightly and produce the observed signals. For some days after completing the hole the water level in it was below the reach of our measuring tape (61 m); it recovered slowly over the next month while the adjacent wells (GSB and GSC) recovered much more quickly.

Figure 1 shows the records from the long-base instruments at PFO, along with the water-well records from the nearby wells CIA and UQA (128 m and 216 m to the ENE). As a general rule, localized deformation events cause less apparent strain or tilt on long-base instruments than on short ones; the only exception is a case (such as this one) where the perturbation is located next to the end of the long-base instrument. Because the deformation is localized (as shown by its absence on more distant short-base sensors), the remote ends of the long-base instruments are unaffected, and we may present the data from these instruments as displacements of the near ends (horizontal for the strainmeters, vertical for the tiltmeter). The long-base tiltmeter (whose near end is 139 m to the NE) shows subsidence of 0.05 mm; the NS strainmeter (84 m to the NW) gives a similar movement towards the south, while the NW/SE strainmeter (66 m NE) first shows south-east motion and then reverses. This would seem to indicate that the center of the water-table depression shifted with time to the north or north-west. Curiously, the water level in borehole CIA, about 128 m distant, shows the greatest response on 224:20, as the drilling of GSC went below 100 m. We have no explanation for this.

Figure 2 shows borehole tiltmeter data (STLD was too distant to display any effect). For these instruments we have plotted only the component of tilt toward the borehole. The tilts are of order 0.3 μrad, with closer sensors showing larger signals. There is a slight though surprising difference in the records from the Askania and JILA tiltmeters, which are all located at about the same distance east of the drilling. The middle instrument (BOA), behaves differently from the others in its recovery. We presume this reflects some perturbing effect of the borehole casings. The most striking results come from another short baselength instrument: the 3-component borehole strainmeter developed by Dr. Michael Gladwin. On this instrument (311 m to the ENE), the induced shear strains are quite large (0.12 $\mu\epsilon$), whereas the dilatation (areal) strain was unaffected. This is just the result expected for the Boussinesq problem of a point load on a half space. We might expect a conical surface depression caused by drilling to look like a point load in the far field—and it does.

One other possibility is that this disturbance represents thermoelastic effects driven by changes in ground temperature that would occur when water flows between different depths. We cannot rule this out quantitatively, but do not think it was the cause, for two reasons. First, the time constant for equilibration in such a case would be much longer than what we observed; underground temperature changes should take years, not months, to settle in. The second is the absence of dilatational strain on the borehole strainmeter; a volume dilatation (such as a temperature change would cause) would have a far-field dilatational component, which is not observed.

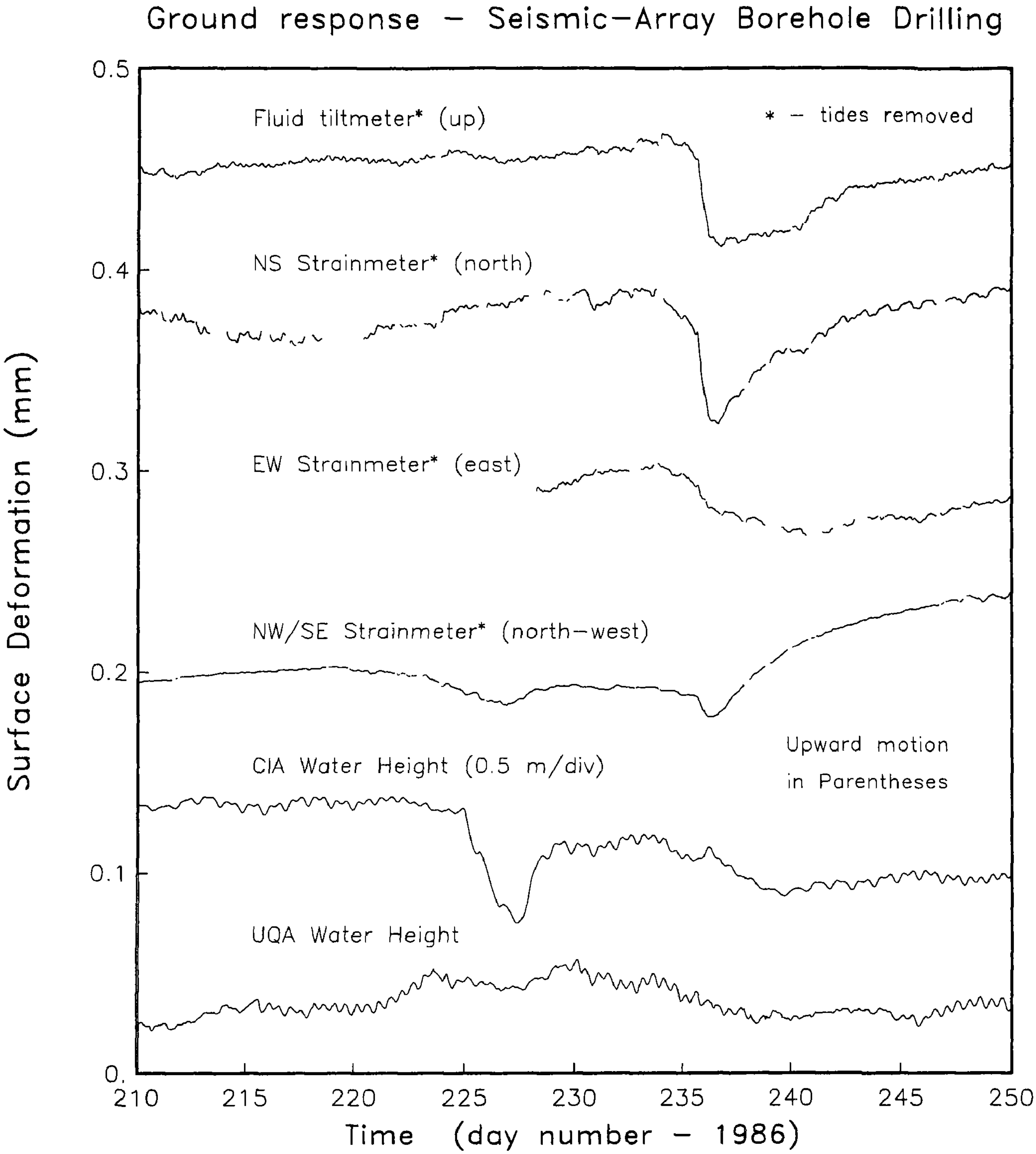
Ground response – Seismic–Array Borehole Drilling
Surface Deformation (mm)
0.5
0.4
0.3
0.2
0.1
0.
Fluid tiltmeter* (up)
* – tides removed
NS Strainmeter* (north)
EW Strainmeter* (east)
NW/SE Strainmeter* (north–west)
Upward motion
in Parentheses
CIA Water Height (0.5 m/div)
UQA Water Height
210
215
220
225
230
235
240
245
250
Time (day number – 1986)

Figure 1.

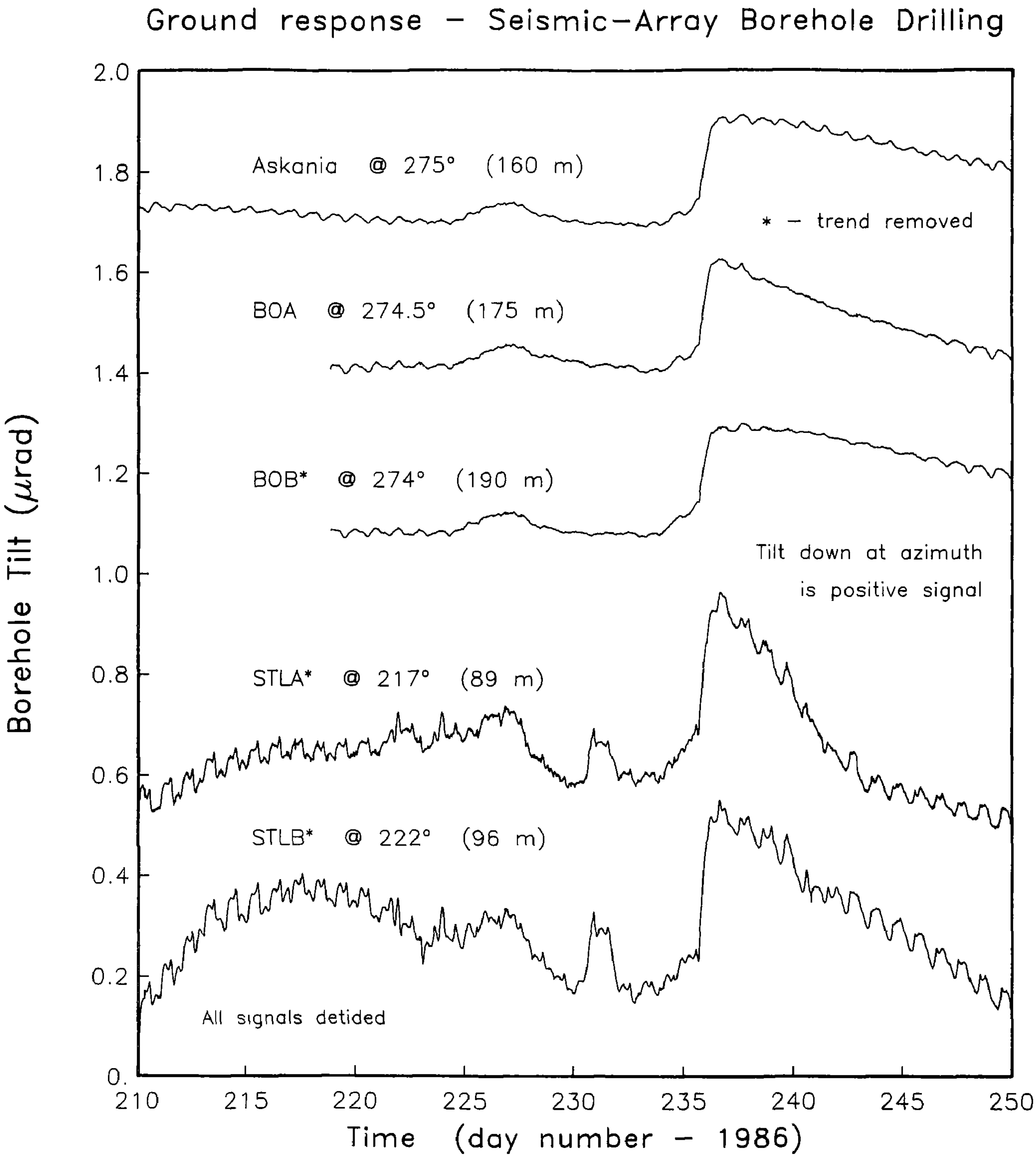
Ground response - Seismic-Array Borehole Drilling
Borehole Tilt (μrad)
2.0
1.8
1.6
1.4
1.2
1.0
0.8
0.6
0.4
0.2
0.
Askania @ 275° (160 m)
* - trend removed
BOA @ 274.5° (175 m)
BOB* @ 274° (190 m)
Tilt down at azimuth
is positive signal
STLA* @ 217° (89 m)
STLB* @ 222° (96 m)
All signals detided
210
215
220
225
230
235
240
245
250
Time (day number - 1986)

Figure 2.

Towards a Widely-Deployable Long-base Tiltmeter: Sensors and Anchors

14-08-0001-G1200

Frank Wyatt, Mark Zumberge, Duncan Carr Agnew
Institute of Geophysics & Planetary Physics
University of California, San Diego
La Jolla, California 92093
(619) 534-2411

For long-base tiltmeters to be generally useful in measuring crustal deformation, they must be engineered for easy use, and widely-applicable installation procedures must be devised. Under this grant we have designed and constructed new tiltmeter systems to be tested against an existing long-base tiltmeter at Piñon Flat Observatory. This new design incorporates two important improvements over our earlier long-base tiltmeter. One is an improved absolute water-height gauge; the other is the use of optical fibers in vertical anchoring, to attempt to ease the greatest problem of observatory-based instruments: attaching the sensor to the underlying crust. Initial results are encouraging and have convinced us that the techniques we have developed are well worth pursuing.

Our basic plan for testing the new equipment is to install the combination of water-height gauge and optical anchor in a new vault so we could experiment with different arrangements. Extending the equipotential surface fluid for the existing tiltmeter over to the new vault allows us to compare our old system (very accurate and very elaborate) with our new one. In the absence of large tilts, we will not accumulate much signal between the new vault and the nearer of the original tiltmeter vaults, and we can correct for any tilt that does occur using the measurements from the present system.

Figure 1 shows the arrangement of the new vault together with details of the optical fiber anchor (all completed in January 1987). The fiber is pulled taut at the surface and used as one arm of Michelson interferometer. As the fiber strains (presumably indicating ground movement) the effective optical path length changes, and causes the interference pattern to change. Unfortunately optical fiber is very sensitive to temperature variations, and may not prove stable over very long periods of time, so we are conducting a number of experiments to identify its limitations.

The other half of the project is to develop an improved sensor to monitor the water height at each end of the tiltmeter unambiguously. We are using a microprocessor controller to hold an optics stage a fixed distance above the fluid surface (using a white light interferometer); measuring from the stage to the top of the optical fiber gives the local height change; and the difference of the measurement from each end provides the tilt. The microprocessor keeps the stage aligned automatically. Figure 2 shows results from the new gauge (UPL). RHO and TAU are records of the water height along the original 535 m long tiltmeter; UPL is at the end of a 116 m extension. The tides at RHO and UPL should be identical and 180° out of phase, while TAU should be a scaled-down version of UPL. The bottom curve of Figure 2 presents an expanded view of the error signal from the controlling electronics of the new gauge. It shows that the automated device follows the fluid height to 0.2 μm, or 0.3 nrad for the 651 m instrument.

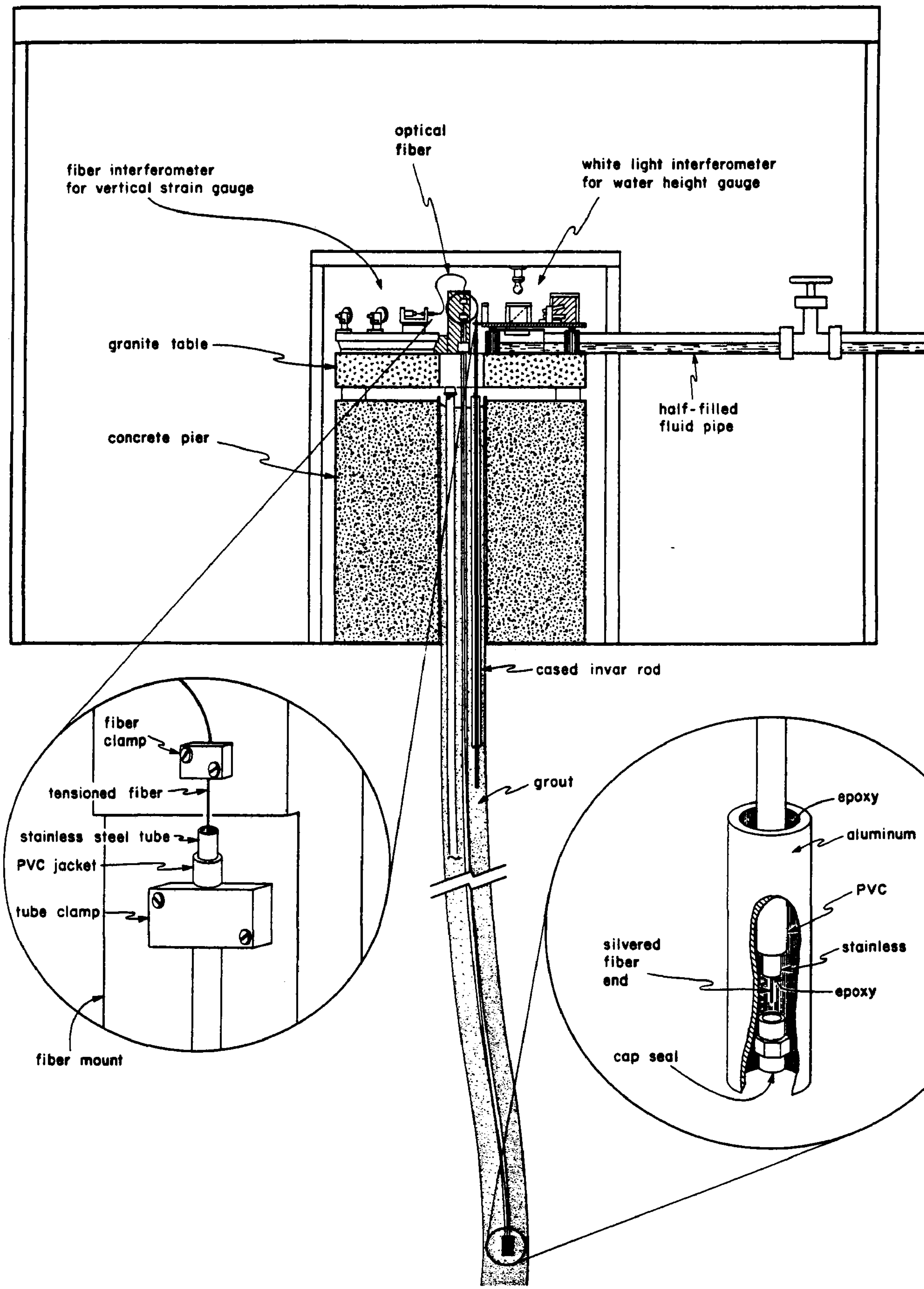
optical
fiber
fiber interferometer
for vertical strain gauge
white light interferometer
for water height gauge
granite table
half-filled
fluid pipe
concrete pier
cased invar rod
grout
fiber
clamp
tensioned fiber
stainless steel tube
PVC jacket
tube clamp
fiber mount
epoxy
aluminum
PVC
stainless
silvered
fiber
end
epoxy
cap seal

Figure 1.

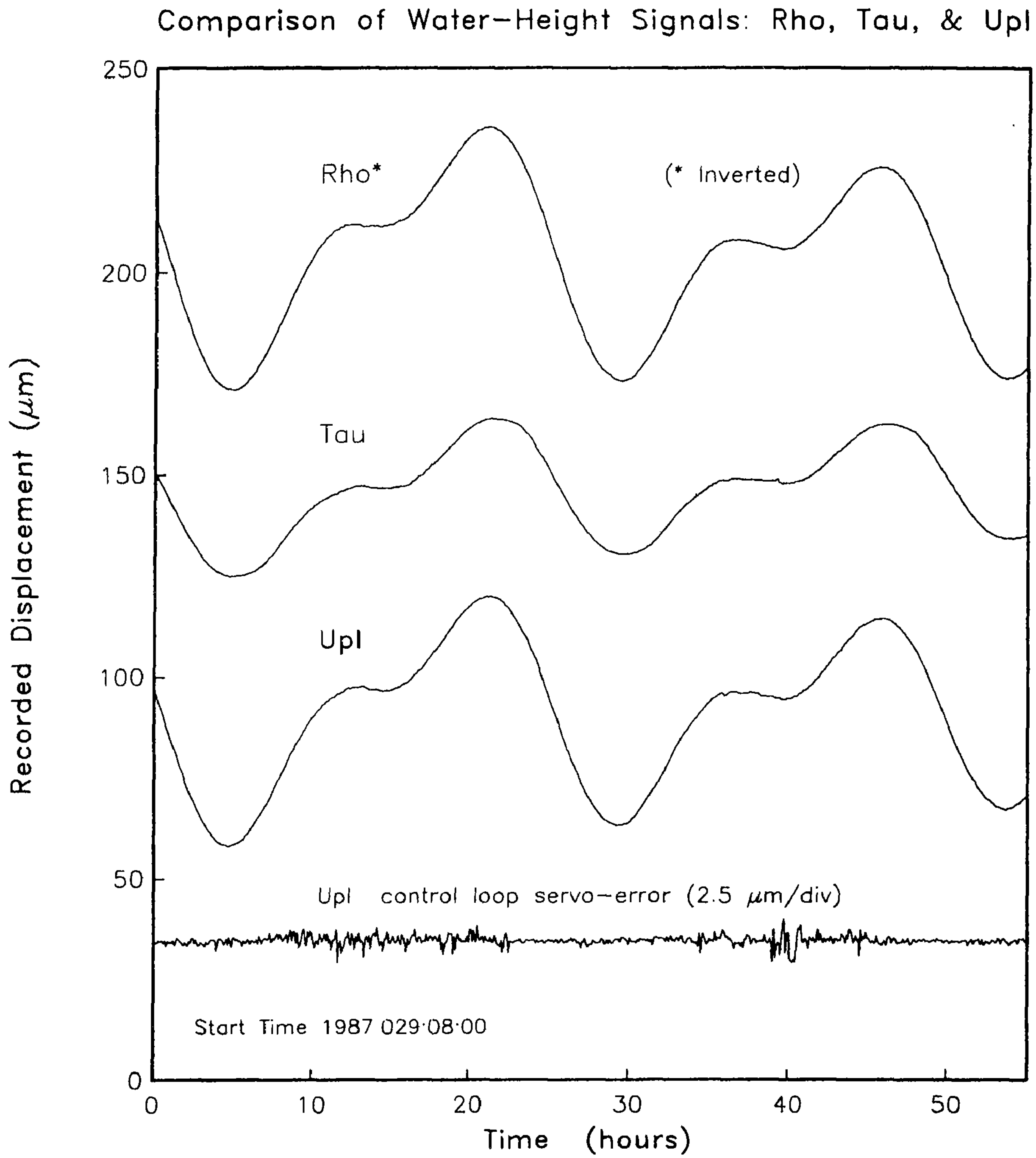

Comparison of Water-Height Signals: Rho, Tau, & Upl
Rho*
(* Inverted)
Tau
Upl
Upl control loop servo-error (2.5 μm/div)
Start Time 1987 029:08:00
Recorded Displacement (μm)
250
200
150
100
50
0
0
10
20
30
40
50
Time (hours)

Figure 2.

THE RELATIONSHIP BETWEEN CREEP AND SEISMICITY RATE ALONG THE CENTRAL SAN ANDREAS FAULT

14-08-0001-G1089

Max Wyss
University of Colorado, CIRES
Boulder, CO 80309
(303-492-5642)

Objective

To determine whether there exists a relationship between seismic quiescence and fault creep, and to define the characteristics of examples of precursory seismic quiescence before mainshocks along the creeping segment of the San Andreas fault.

Results

We correctly predicted an earthquake along the San Andreas fault based on seismic quiescence and creep-retardation. We also defined the characteristics of a new example of precursory seismic quiescence in the same area. These two quiescences preceded the mainshocks of 10 August 1982 (M_L=5.0) and of 31 May 1986 (M_L=4.7), lasting for 18 and 35 months before the respective mainshocks. The decrease of the average seismicity rate was 60 and 70% respectively, and these anomalies were unique. That is, within a 100 km segment of the San Andreas fault we could not find any segment that showed as significant a rate decrease as that in the segments ruptured in these shocks. In the first of these cases the quiet volume included only part of the subsequent aftershock zone, with the rupture initiating in a volume of constant seismicity rate. In the second case the quiet volume coincided with the aftershock zone.

Comparing the characteristics of these two cases of quiescence with all other reliable quiescence precursors, we found that the anomaly durations on the creeping segment of the San Andreas fault were unusually long. They were as long as precursor times for magnitude 6.5 to 7 reported for subduction zone earthquakes. This contradicts the expectation of some researchers that the precursor time should be a function of magnitude and independent of tectonic environment.

The available evidence suggests that seismic quiescence and fault creep may correlate. During the precursory quiescence before the May 1986 Stone Canyon earthquake the nearest creep-meter registered creep-retardation, while other creep-meters continued to record the usual creep-rate. This positive correlation can be interpreted to indicate that the fault is locked temporarily before local mainshocks.

Occurrence of a predicted earthquake on the San Andreas fault, Central California

In May 1985 we predicted that an earthquake of magnitude M_L = 5.0± 0.5 would occur near Stone Canyon within a year. A mainshock of M_L = 4.6 occurred on May 31, 1986, rupturing exactly the specified segment of the San Andreas fault. This is the first successful prediction of an earthquake along the San Andreas fault. The probability for the prediction to have come true by chance is less than 5% (Wyss and Burford, 1987).

Precursory seismic quiescence before the August 1982 Stone Canyon, San Andreas fault earthquakes

The Stone Canyon earthquake sequence started during August 1982 and lasted for about four months. The sequence contained four mainshocks with $M \geqslant 4$, each with an aftershock zone about 4 km long. These mainshocks ruptured a segment of the fault approximately 20 km long from the south to the north leaving two gaps, which later produced the $M_L = 4.6$ mainshocks of January 14, and May 31, 1986.

Precursory seismic quiescence could be identified in: (1) The northernmost 10 km of the aftershock zone which contained three of the mainshocks; and (2) the southern gap in the aftershock zone. The fault segment containing the first mainshock and its aftershocks did not show quiescence. This pattern of precursory quiescence is very similar to two cases in Hawaii where the rupture initiation points of the mainshocks ($M_S = 7.2$ and 6.6 respectively) were located in volumes of constant seismicity rate, surrounded by volumes with pronounced precursory quiescence.

The precursory quiescence before the August 1982 Stone Canyon earthquakes lasted for 76 weeks, amounted to a reduction in rate by about 60%, and could be recognized without any false alarms, that is the anomaly was unique within the 60 km study segment of the fault and in the years 1975 through August 1982. Eighteen foreshocks occurred between July 27 and August 07, 1986. We conclude that the August 1982 mainshocks could have been predicted based on seismic quiescence and foreshocks.

Characteristics of precursory seismic quiescence

Seventeen reliable cases of precursory seismic quiescence to mainshocks with magnitudes from M_L=4.7 to M_S=8.0 have been reported in the literature. The amount of rate decrease ranges from 45% to 90%. The significance of these changes are mostly very high, with the standard deviate z-value exceeding 3.2. The assumption that the background rate is approximately constant is fulfilled in most crustal volumes studied. All quiescence anomalies seem to have abrupt beginnings, and the rate during the anomalous time is fairly constant. The duration of the precursors range from 15 to 75 months, but it is not clear what factors determine that time. At least three successful predictions have been based on seismic quiescence. These cases have shown that mainshocks can be predicted based on quiescence, but they have also shown that the interpretation of the data in real time is difficult and non-unique. The false alarm rate appears to be low, probably less than 50%. Failure to predict may be expected in perhaps 50% of mainshocks even in carefully monitored areas. Quiescence cannot be used as a precursor in tectonic environments with low microseismic activity. Most characteristics of the phenomenon are still poorly defined, but data exist which probably permit at least a doubling of the presently available data on case histories.

Publications

Wyss, M., and R. O. Burford, Occurrence of a predicted earthquake on the San Andreas fault, Central California, Nature, submitted, 1987.

Wyss, M., and R. E. Habermann, Precursory quiescence before the August 1982 Stone Canyon, San Andreas fault, Earthquakes, PAGEOPH, submitted, 1987.

Wyss, M., and R. E. Habermann, Precursory seismic quiescence, PAGEOPH, submitted, 1987.

Creep and Strain Studies in Southern California

Grant No. 14-08-0001-G1177

Clarence R. Allen and Kerry E. Sieh
Seismological Laboratory, California Institute of Technology
Pasadena, California 91125 (818-356-6904)

Investigations

This semi-annual Technical Report Summary covers the six-month period from 1 October 1986 to 31 March 1987. The grant's purpose is to monitor creepmeters, displacement meters, and alignment arrays across various active faults in the southern California region. Primary emphasis focuses on faults in the Imperial and Coachella Valleys.

Results

During the reporting period, alignment arrays were resurveyed across the San Andreas fault at UNA LAKE, PALLETTE CREEK, and CAJON, across the Superstition Hills fault at SUPERSTITION HILLS, across the Imperial fault at HIGHWAY 80, and across the Garlock fault at CHRISTMAS CANYON. Creepmeters were serviced at MECCA BEACH (four times), SALT CREEK, SUPERSTITION HILLS, HARRIS ROAD, and HEBER ROAD. Initial work on a new creepmeter, to be telemetered to Pasadena via SS-GOES satellite, was carried out at ROSS ROAD, to replace the former instrument there. The nail-file arrays were resurveyed at ROSS ROAD and ANDERHOLT ROAD.

No significant creep or strain episodes were noted during the reporting period, in contrast to the high activity during the preceding period (covered in the previous 6-month report.) Fresh cracks along the Superstition Hills fault were reported to us by other observers, but field inspection of these by C. R. Allen in late November did not reveal anything grossly unusual, inasmuch as tensile cracks often form adjacent to the fault trace near Imler Road. Resurvey on 12 January of the SUPERSTITION HILLS alignment array, as well as re-observation of the nearby dial-gauge creepmeter, revealed nothing significant.

Digital Signal Processing of Seismic Data

9930-02101

William H. Bakun
Branch of Seismology
U.S. Geological Survey
345 Middlefield Road - Mail Stop 977
Menlo Park, California 94025
(415) 323-8111, Ext. 2777

Investigations

Coordination of activities in the Parkfield prediction experiment. Analysis of USGS coda-duration measurements for magnitude determination.

Results

A real-time earthquake prediction experiment is underway at Parkfield.

Reports

Poley, C. M., A. G. Lindh, W. H. Bakun, and S. S. Schulz, 1987, Temporal changes in microseismicity and creep near Parkfield, California, Nature, in press.

Michaelson, C. A., and W. H. Bakun, 1986, Spatial and temporal trends in coda duration magnitude residuals in central California (abs), EOS, Trans. Amer. Geophys. Un., 67, p. 1093.

Bakun, H. H., J. Bredehoeft, R. O. Burford, W. L. Ellsworth, M. J. S. Johnson, A. G. Lindh, P. Olds, E. Roeloffs, S. Schulz, P. Segall. R. Simpson, and W. Thatcher, 1986, Parkfield, Ca. earthquake prediction experiment a status report (abs.), EOS, Trans. Amer. Geophys. Un., 67, p. 904-905.

ATTACHMENTS: following are the synopses from each of the Parkfield Data Review meetings held during the reporting period.

PARKFIELD OCTOBER 1986 DATA REVIEW MEETING Held 11/10/86

On OCT 1, it rained at Parkfield: 0.01" at Vineyard Canyon, 0.08" at Turkey Flat, 0.19" at Gold Hill, and nil recorded at Flinge Flat or Joaquin Canyon.

On OCT 10, a mag. 1.6 shock occurred at 14 km depth within the Middle Mtn. alert zone, constituting a level d seismic alert.

The new Middle Ridge creepmeter (XMD1) provided some intriguing signals. First, a 1.2 mm event on OCT 3 coincided with the 2 mm creep serge at XPK1 on OCT 2-9. Secondly, a 1.7 mm event on OCT 19 was followed by 0.5 mm of slip at XMM1. While both sequences imply NW propagating creep, only the XPK1 slip on OCT 2-9 constitute a d level creep alert.

No unusual signals were recorded on the water level dilatometer, magnetometer, or tiltmeter networks. Instrumentation problems at Vineyard Canyon and Gold Hill water wells have been corrected. Much work is in progress to install additional water level, dilatometer, and tensor strainmeter systems before the end of the field season.

-W.H. Bakun

NOVEMBER 1986 PARKFIELD MONTHLY DATA REVIEW MEETING Held: 12/3/86

There were no seismic alerts at Parkfield in NOVEMBER. Seismicity was low, with 13 shocks in the Parkfield area.

There has been a D-level creep alert at CRR1 since OCT 25. To date, CRR1 has shown 4 mm of right-lateral slip since OCT 25, occurring as a steady surge of creep rather than as events. At present, it is not clear that the CRR1 movement is tectonic in origin: Plowing near the instrument and/or an unexplained (no rainfall yet!) seasonal effect are possible causes.

There were no unusual signals of tectonic origin on the borehole dilatometers, the water wells, the magnetometers or the tiltmeters. Four new borehole strainmeters were installed, and there are plans to install several more soon, weather permitting. There are now 6 water well monitoring sites, with the Middle Mtn. well being monitored at 830' and 270' depths. Eight additional core holes have been perforated and will be instrumented when ordered transducers are received.

- W.H. Bakun

December 1986 Parkfield Monthly Data Review Meeting held 1/12/87

Seismicity in the Parkfield region was relatively high in the 11/29/86-1/6/87 time period, particularly around Middle Mountain. There were two D-level alerts, both due to 2 M>1 events within 72 hours in MM3 - on 12/24/86 and on 1/2/87.

Creep rates were relatively low in December, although XPK1 is now fully resumed its pre-1983 Coalinga earthquake rate. A ~3 day event with cumulative amplitude of about 1.7 mm occurred at XDR1 beginning 12/19/86 and a smaller, 0.26 mm event occurred south of Highway 46 at X461 beginning 12/12/86. The larger of these events constituted a D-level alarm. Revised criteria for long (~10 day) creep event alarms were devised using pre-Coalinga earthquake data and the rationale for these changes is included in the monthly report.

Aside from a rainfall-related jump on 12/6/86 at Middle Mountain there were no notable signals observed on the water level array. However, the tidal signals recorded at Middle Mountain indicate a good strain sensitivity at this well being 40% larger in amplitude than those at Flinge Flat. A new well at Bourdieu Valley began recording water level in December, and several of the other pilot coreholes drilled for borehole strainmeter site prospecting have been perforated for use in water level monitoring and will be coming on line soon.

To date 3 new three-component (Gladwin) borehole strainmeters and 3 new borehole dilatometers have been installed and two more holes should be instrumented with dilatometers during the next week.

No alarms were generated by the two-color laser strainmeter, the borehole strain array, the magnetometers, or the tiltmeters.

- W. Thatcher

JANUARY 1987 Parkfield Data Review Meeting **Held 2/9/87**

The Parkfield area was seismically active (M ≤ 1-3/4) during January 1987. There was one D-level seismic alert, the result of two M > 1.0 shocks within 72 hours (12/31 and 1/2).

There were not creep alerts in January, although there were two creep surges at CRR1 and small creep events at XMM1 and at XMD1. Alignment array surveys over a 50-day interval along the southwest fracture zone indicate 1 mm of left-lateral movement at Koester on the northwest and 3 mm of left-lateral movement at Harlan on the southern end.

The tentative water level D alert on 1/17 is now ascribed to a malfunctioniong transducer at Vineyard Canyon so that it goes into the record books as an E-level alert. The Middle Mtn. well showed a 1 cm rise in conjunction with the small creep event on 1/9. The water level in the Bourdieu Valley well apparently rose rapidly between 1/12 and 1/14, although the track record for this well is too short to confidently interpret this as a tectonic event.

No unusual signals were recorded during January on the Parkfield tiltmeters, magnetometers, or borehole strainmeters.

Based on new preliminary criteria for two-color geodimeter alerts, the length changes on lines CAN, GOLD, CREEK, LANG, and POMO produced a D-level alert during 1/25-29. However, these changes do not constitute an alert under the current criteria. Work is continuing to evaluate pier tilt problems in the two-color network.

One hydrogen peak, similar to peaks in November-December 1986, occurred on 1/8 on the Gold Hill monitor.

- W. H. Bakun

PARKFIELD FEBRUARY 1987 DATA REVIEW MEETING   Held 3/9/87

The story of the month is the Parkfield alerts of Feb. 1-6, 1987. The sequence of events is summarized in the attached memorandum (dated 2/17/87) to John Filson.

Seismic activity at Parkfield was high in Feb., with 11 shocks larger than M 1.5. There were two seismic alerts; the level C seismic alert of Feb. 1 and the level D seismic alert of Feb. 3. (see attached memo)

In addition to the creep events of Feb 1-2 (see attached memo), there were 2 creep alerts in Feb. Work Ranch (WKR1) recorded a creep surge (1 mm total movement) from Feb 13-27 that resulted in a level D(1) creep alert from Feb 23-27. On Feb. 21, XMM1 recorded a creep event (0.7 mm total movement) that reached 0.5 mm in 30 minutes. This corresponds to a level D(4) creep event from Feb 21-24.

Although there is no water well report this month (E. Roeloffs is in China), there was a level D water well alert on Feb. 1.

There were no alerts on the other prediction networks in the Parkfield experiment, although the ~2" of rain and the M 5 Coalinga aftershock on Feb. 13 were apparent on the records. The Feb. 13 magnetic field change at Hog Canyon (HGCM) was an instrument malfunction and not a result of tectonic activity. There are available revised criteria for Parkfield 2-color geodimeter alert levels (included in this packet of monthly summaries).

- W. H. Bakun

United States Department of the Interior

GEOLOGICAL SURVEY
OFFICE OF EARTHQUAKES, VOLCANOES AND ENGINEERING
Branch of Seismology
345 Middlefield Road - Mail Stop 977
Menlo Park, California 94025

February 17, 1987

MEMORANDUM

To: John Filson, Chief, OEVE

From: Bill Bakun, Parkfield Coordinator

Subject: Parkfield Alerts of February 1 - 6, 1987

Summary

A sequence of anomalous signals were observed near and within the Parkfield preparation zone that constituted d-, c-, and d-level alerts. The correlation of the signals suggests that a tectonic event did occur, and that unambiguous strain changes clearly preceeded the M=2.7 shock that constituted the C-level alert.

Jan 25-29, 1987

The first unusual signals observed were changes on Jan. 25-29 in the lengths of 2-color geodimeter lines CAN, GOLD, CREEK, LAND, and POMO. While these changes do not constitute an alert under the current alert level criteria, they would constitute a d- level geodetic alert under the provisional revisions of the alert level criteria.

February 1, 1987

At 0559GMT, an M=1.2 shock (shock #1 on Fig. 1) occurred at 8.45 km depth to the northwest of the MM3 alert zone.

At 0800-1300GMT, there was a 10 centimeter drop in the 772'-810' monitor level of the Middle Mountain water well, constituting a d- level alert. The change corresponds to ~ 0.20 μstrain dilatation, well above the 0.05 μstrain threshold for d-level water well alerts.

At 0950-1000GMT, a 0.22 mm right-lateral creep event began at XMM1.

At 1125GMT, an M=2.0 shock (#2 on Fig. 1) occurred at 5.1 km depth above the MM3 alert zone. A right-lateral coseismic creep event with 0.01 mm amplitude was recorded on the XMD1 creepmeter.

At 1143GMT, an M=1.1 shock (#3 on Fig. 1) occurred at 0.5 km depth above the MM3 alert zone.

February 2, 1987

At 0445GMT, an M=2.7 shock (#4 on Fig. 1) occurred at 10.0 km depth in MM3, constituting a c-level alert. Right-lateral coseismic steps were recorded on the XMM1 (0.5 mm), XMD1 (0.14 mm), and XPK1 (0.06 mm) creepmeters.

At 0909GMT, an M=1.3 shock (#5 on Fig. 1) occurred at 6.5 km depth northwest of MM3.

February 3, 1987

At 0250-0300GMT, a 0.02mm right lateral creep event occurred at XMM1.

At 1252GMT a magnitude 1.5 shock (#6 on Fig. 1) occurred at 6.0 km depth northwest of MM3.

At 1449GMT a magnitude 1.7 shock (#7 on Fig. 1) occurred at 9.7 km depth in MM3, constituting a d-level seismic alert that lasted until 1449GMT on February 6, 1987.

cc: Ellsworth
Thatcher

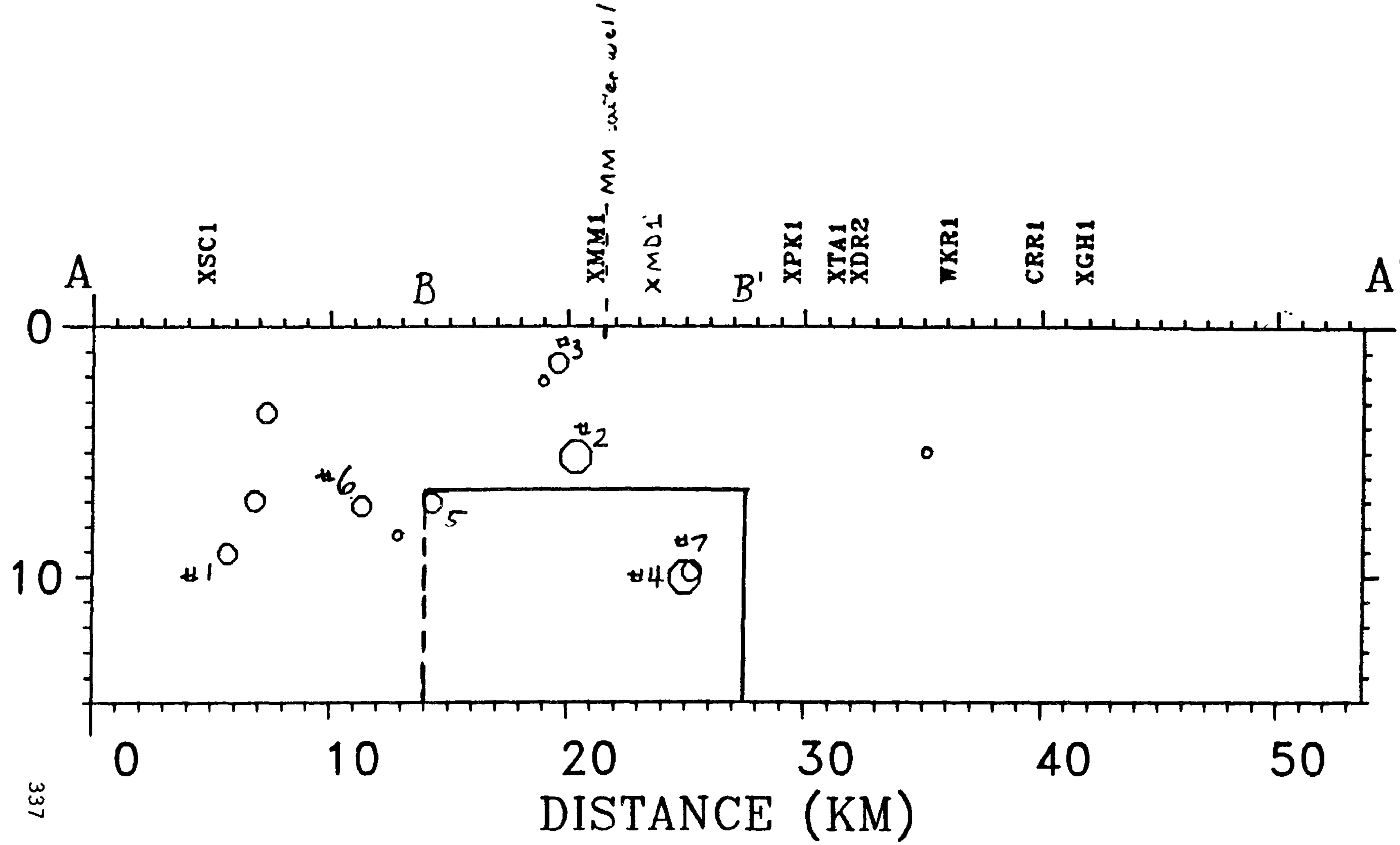

Fig. 1

FEBUARY 1-13, 1987

PARKFIELD DATA REVIEW FOR MARCH 1987 Held 4/13/87

Although seismic activity was low at Parkfield in March, there were **two D-level seismic alerts** resulting from a M=1.8 shock at 11 km depth in MM3 on 3/14 at 1417 UTC and a M=1.5 shock at 11.7 km depth in MM3 on 3/27 at 1303 UTC. (The magnitude of the 3/27 shock was initially just below the M 1.5 threshold; subsequent processing resulted in a revised magnitude of 1.51.)

March was a very active month for creep happenings. The XPK1 and XMM1 instruments responded to rainfall of 3/5-3/6 with 1.0 mm and 0.7 mm of right-lateral movement respectively. The long-running **D-level creep alert at XMD1 (2/23-3/25)** due to 8.25 mm of continuing left-lateral movement, possibly due to rainfall and/or activity on the southwest fault trace, ended on 3/25 with a 1.0 mm right-lateral creep event, resulting in a **D-level creep alert** from 3/25-3/28. (A 0.3 mm right-lateral creep event occurred at XMM1 12 hours after the XMD1 creep event.) In addition, XTA1 had a **D-level creep alert** (3/15-3/18) due to 0.9 mm of left-lateral movement from 3/5-3/16, possibly related to rainfall and/or activity on the southwest fault trace. Finally, WKR1's 1.1 mm of right-lateral movement on 3/5-3/19, resulted in a **D-level creep alert on 3/15-3/19**; this alert was arbitrarily terminated on 3/19 by maintenance at the site. Reports of cracking along the southwest fault trace and felt reports of shocks by residents of Parkfield suggest that there is cause for increased awareness of the Parkfield monitoring networks.

The D-level seismic and creep alerts described above resulted, according to the combination rules, in **C-level alerts on 3/14-3/17 and on 3/27-3/30.** These C-level alerts were not recognized as such until after the fact: (1) The creep alerts from 3/14-3/17 were initially interpreted as effects of rainfall; (2) The seismic alert on 3/27 resulted from a late minor adjustment of a magnitude estimate.

There were no alerts on any of the continuous strain monitoring networks. The eight dilatational strainmeters are now recorded via the satellite telemetry and onsite by GEOS recorders. The tensor strainmeters at Eades and Froelich are now clearly showing north-south compression and east-west extension. There are now 7 water wells on satellite telemetry with 3 of the wells monitored at more than one perforation depth.

There were no alerts on the two-color geodolite network. (A level D alert would have been in effect on 3/19-3/24 using the proposed revised geodolite alert level criteria.) Loss of power on the blue laser coupled with poor visibility prevented some measurements early in the month; the blue laser failed completely on 3/14, was overhauled and returned to service on 3/16. (Some measurements early in March may have been biased owing to the weak return of the blue wavelength signal.) The effects of a strong areal dilatational trend are clear for early February through late March; this trend is similar to the beginning of the 3-month pattern preceding the 8/5/1985 Kettleman Hills shock.

Radon levels at the Miller Ranch located west of the San Andreas near Parkfield apparently changed by about a factor of 3 from mid-February to mid-March. Severe gaps in the data make interpretation difficult.

W.H. Bakun

PARKFIELD TWO-COLOR LASER STRAIN MEASUREMENTS

9960-02943

Robert Burford
Branch of Tectonophysics
U.S. Geological Survey
345 Middlefield Road, MS/977
Menlo Park, California 94025
(415) 323-8111, ext. 2574

and

Larry Slater
CIRES
University of Colorado
Boulder, Colorado 80309
(303) 492-8028

Investigations

Operation of the CIRES two-color laser geodimeter at the Car Hill Observatory near Parkfield, California was continued during the period October 1, 1986 through March 31, 1987. Lines to permanent reflector sites that were monitored for length changes during this period are shown in Figure 1. Additional measurements were made occasionally to monumented points without permanent reflectors as well as to reference marks adjacent to the permanent reflectors.

Results

Plots of detrended length-change histories for the 18 lines to permanent reflector points are shown in Figure 2. The average rate of length change determined by linear least-squares approximation for each line is given in Table 1. Average station velocities relative to Car Hill for motion constrained to be parallel to the strike of the San Andreas fault zone are also given in Table 1 (negative values denote apparent left-lateral motion).

Reports

Segall, P., Burford, R.O., and Harris, R., 1986, The earthquake cycle at Parkfield: Comparing recent strain measurements with a long-term interseismic slip model (abs.): EOS, v. 67, p. 904.

Table 1

Summary of Monitoring Results
Two-Color Laser Geodimeter Network at Parkfield
October 1, 1986 to March 31, 1987

Permanent 2-Color Reflector Sites	Measurements Started	Location Relative to Car Hill	Average Extension Rate, mm/yr	Fault Parallel R.L. Station Velocities
1. Can	10/09/84	5.7 km N03°W	-10.97 ± 0.55	14.12 ± 0.71
2. Norm	11/14/85	1.1 km N45°E	-00.15 ± 0.24	2.53 ± 4.05
3. Table	10/09/84	6.2 km N69°E	+02.54 ± 0.60	7.29 ± 1.72
4. Hunt	07/28/85	2.7 km S72°E	+08.59 ± 0.34	10.01 ± 0.40
5. Mel-S	10/14/84	5.4 km S68°E	+02.80 ± 0.62	3.13 ± 0.69
6. Flat	09/25/85	1.8 km S60°E	+08.89 ± 0.27	9.37 ± 0.28
7. Gold	04/18/86	9.2 km S49°E	+03.35 ± 1.19	3.38 ± 1.20
8. Creek	06/27/84	5.7 km S36°E	-04.00 ± 0.60	4.02 ± 0.60
9. Mason-W	06/26/84	6.3 km S11°W	-02.43 ± 0.65	3.97 ± 1.06
10. Todd	08/07/85	3.7 km S15°W	-12.50 ± 0.50	22.41 ± 0.90
11. Hog-S	07/25/84	5.0 km S62°W	-02.37 ± 0.50	-10.08*± 2.13
12. Lang	07/25/84	4.1 km N72°W	-02.28 ± 0.62	- 2.63*± 0.72
13a. Pomo	04/29/86	5.6 km N51°W	-01.40 ± 0.58	- 1.42*± 0.59
13b. Pitt**	10/09/84	5.7 km N47°W	not determined	-------------
14. Mid	08/23/84	5.0 km N43°W	-05.50 ± 0.51	-05.50*± 0.51
15a. Mid-E	08/21/84	4.5 km N35°W	-09.94 ± 0.46	10.01 ± 0.46
15b. Buck	07/31/86	3.1 km N32°W	-10.06 ± 0.34	10.19 ± 0.34
16. Bare	10/09/84	4.8 km N12°W	-07.35 ± 0.49	8.44 ± 0.56

NOTE: (*) Indicates apparent left-lateral station movement (column 5)
(**) Routine measurements discontinued after June, 1986.

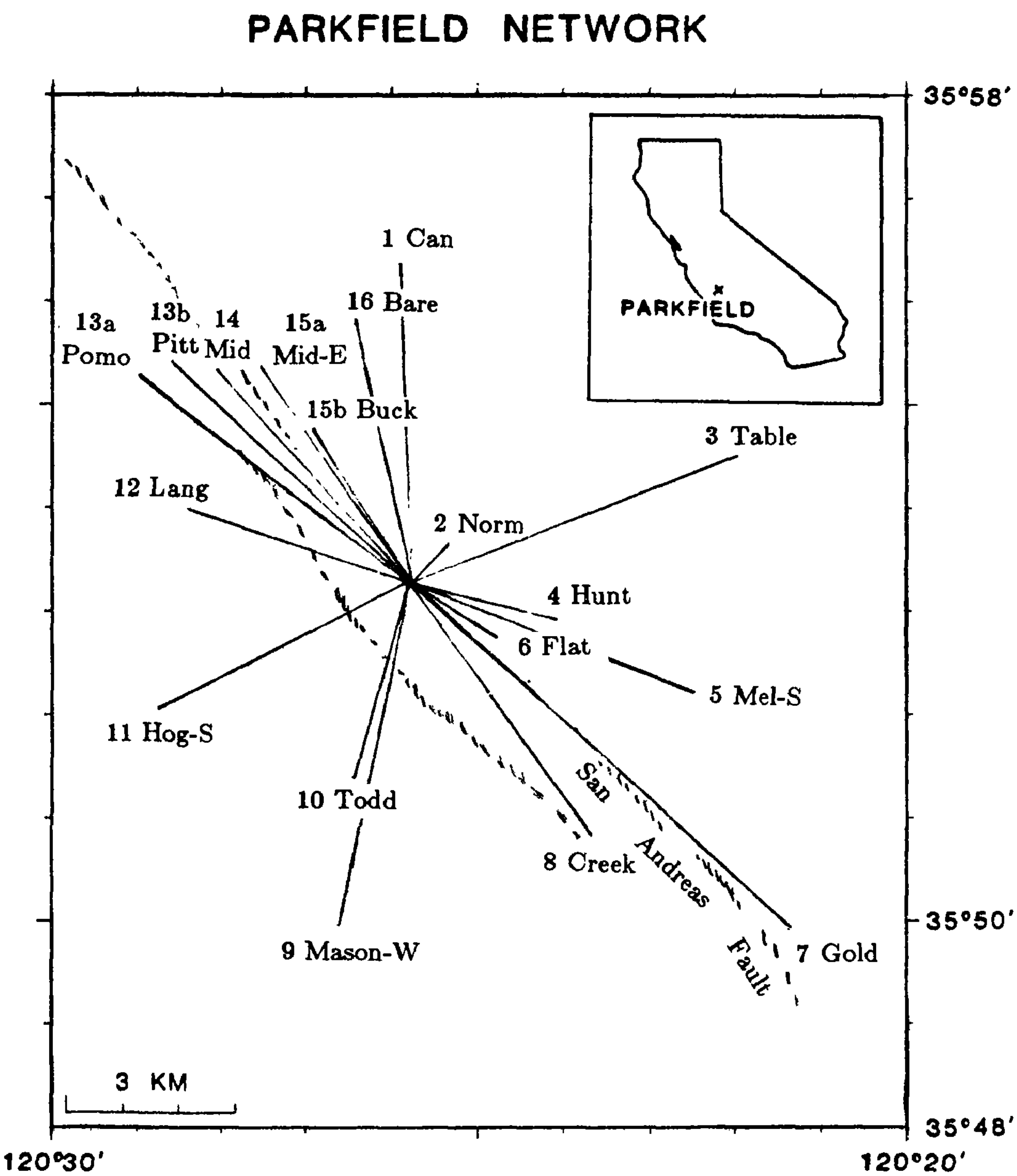

Figure 1. Two-color geodimeter network at Parkfield.

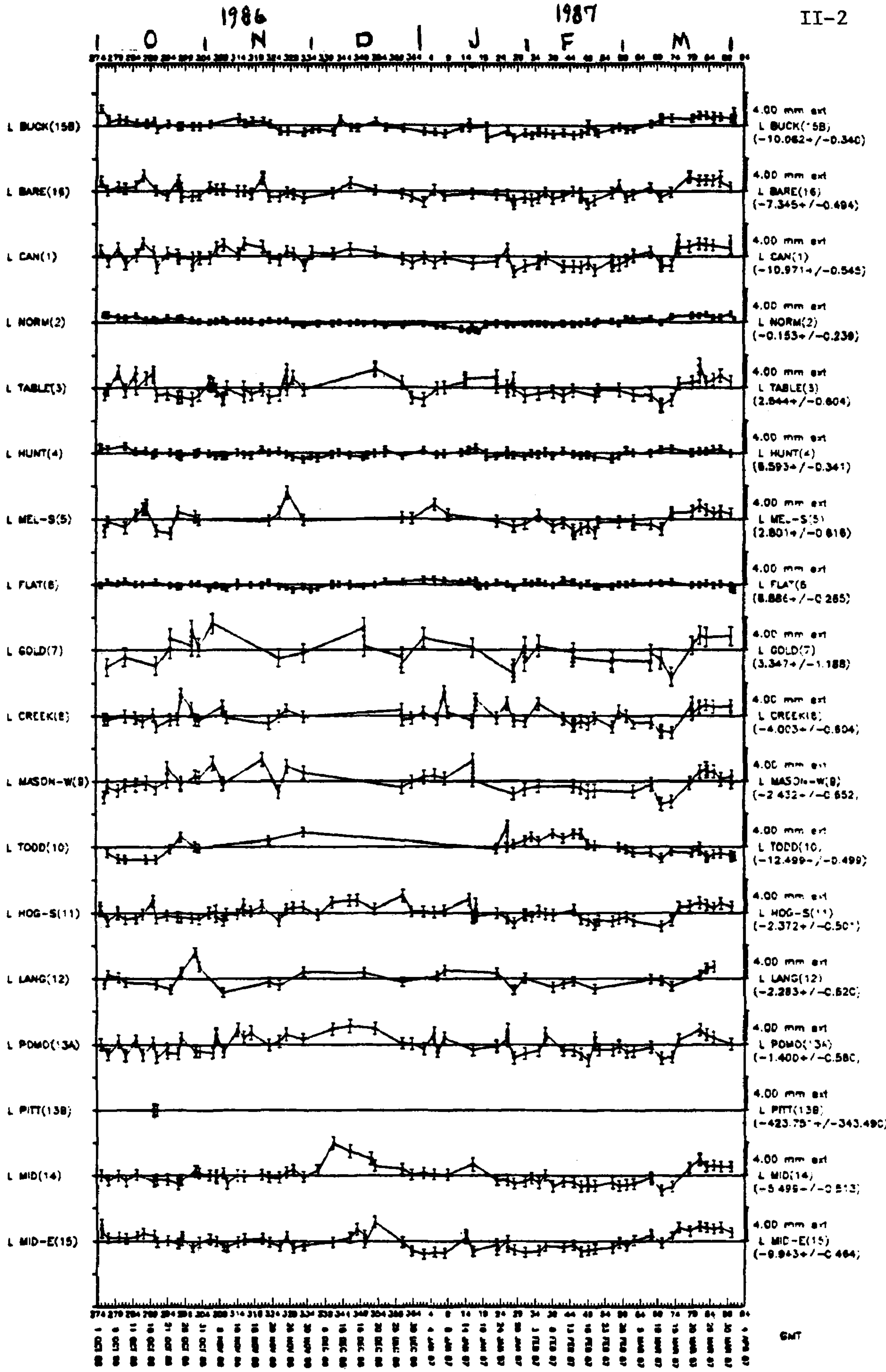

Figure 2. Detrended line-length histories, Parkfield two-color network, October 1986 through March 1987.

Theodolite Measurements of Creep Rates
on San Francisco Bay Region Faults
14-08-0001-G1186

Jon S. Galehouse
San Francisco State University
San Francisco, CA 94132
(415) 338-1204

We began measuring creep rates on San Francisco Bay region faults in September 1979. Amount of slip is determined by noting changes in angles between sets of measurements taken across a fault at different times. This triangulation method uses a theodolite to measure the angle formed by three fixed points to the nearest tenth of a second. Each day that a measurement set is done, the angle is measured 12 times and the average determined. The amount of slip between measurements can be calculated trigonometrically using the change in average angle.

We presently have theodolite measurement sites at 20 localities on ten active faults in the San Francisco Bay region (see location map). Most of the distances between our fixed points on opposite sides of the various faults range from 75-215 meters. The precision of our measurement method is such that we can detect with confidence any movement more than a millimeter or two between successive measurement days. We remeasure most of our sites about once every two months.

The following is a brief summary of our results thus far.

San Andreas fault - Since March 1980 when we began our measurements across the San Andreas fault in South San Francisco (Site 10), no net slip has occurred. Our Site 14 at the Point Reyes National Seashore Headquarters has also shown virtually no net slip since we began measurements in February 1985. Our Site 18 (not shown on location map) in the Point Arena area has averaged about one millimeter per year of right-lateral slip in the 6 years from January 1981 to January 1987. These results indicate that the northern segment of the San Andreas fault is virtually locked, with very little, if any, creep occurring.

Hayward fault - Since we began our measurements on the Hayward fault in September 1979 in Fremont (Site 1) and Union City (Site 2), the average rate of right-lateral slip is 5.1 millimeters per year in Fremont and 4.5 millimeters per year in Union City. It is interesting to note that U.S. Geological Survey creepmeter data from an area between these two sites show an average of about 4.2 millimeters per year from 1978 to 1982 (Schulz, et al., 1982, p. 6979).

Since we began measuring two sites within the City of Hayward in June 1980, the average annual rate of right-lateral movement is 4.6 millimeters at D Street (Site 12) and 5.3 millimeters at Rose Street (Site 13).

Since we began measurements in San Pablo (Site 17) near the northwestern end of the Hayward fault in August 1980, the average rate of movement has been about 4.0 millimeters per year in a right-lateral sense. However, superposed on this overall slip rate are changes between some measurement days of up to nearly a centimeter in either a right-lateral or a left-lateral sense. Right-lateral slip tends to be

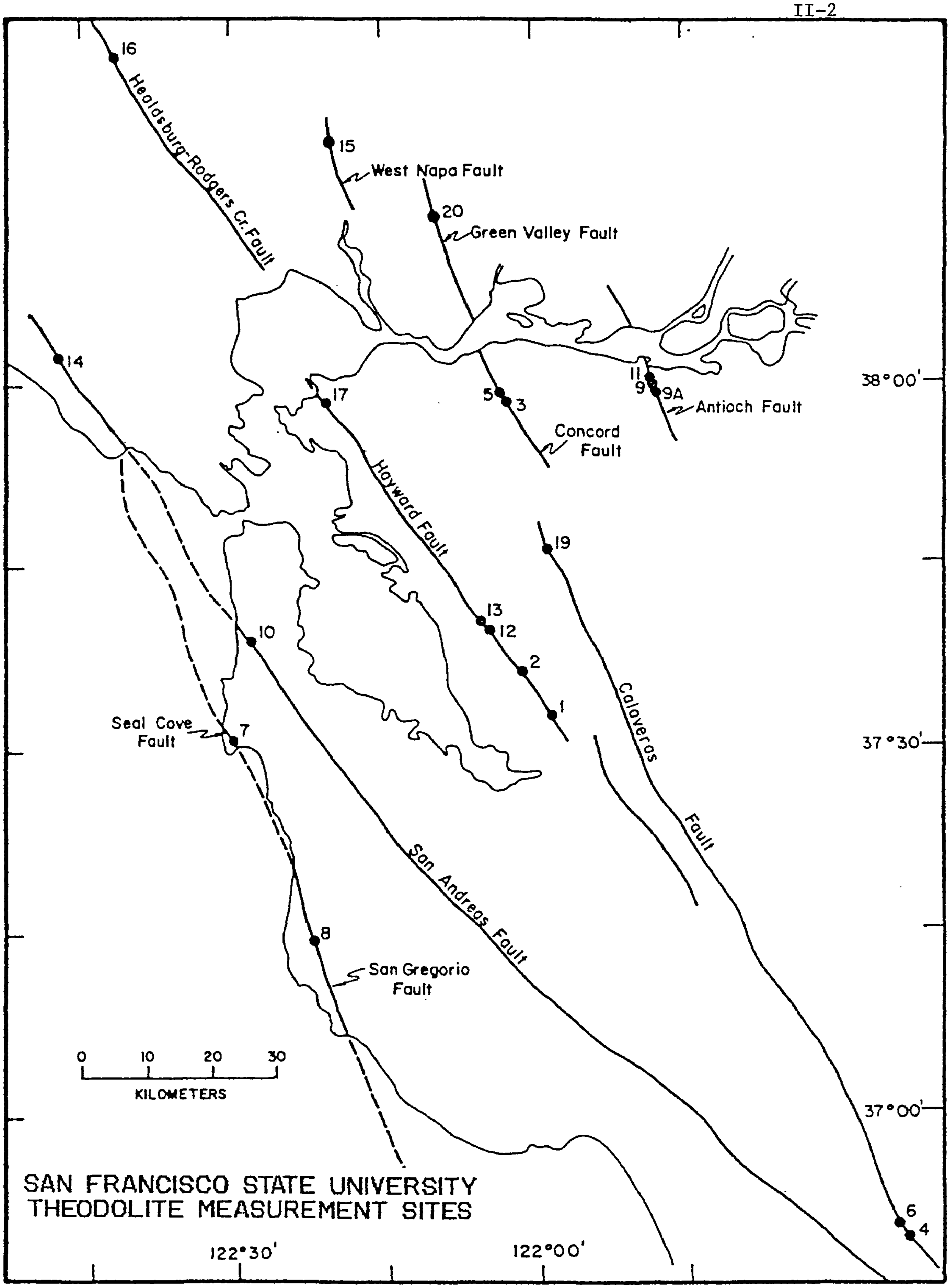

SAN FRANCISCO STATE UNIVERSITY
THEODOLITE MEASUREMENT SITES

measured during the first half of a calendar year and left-lateral during the second half. U.S. Geological Survey creepmeter results also show occasional aberrations in apparent direction of movement on the Hayward fault (Nason, Phillippsborn, and Yamashita, 1974; Schulz, Burford, and Nason, 1976; Schulz and Burford, 1979).

In summary, the average rate of right-lateral movement on the Hayward fault is about 4 to 5 millimeters per year over the past 7 years.

Calaveras fault - We have three measurement sites across the Calaveras fault and the nature and amount of movement are different at all three. We began monitoring our Site 4 within the City of Hollister in September 1979. Slip along this segment of the Calaveras fault is quite episodic, with times of relatively rapid right-lateral movement alternating with times of little net movement. For the past 7.4 years, the fault has been moving at a rate of 6.4 millimeters per year in a right-lateral sense.

At our Site 6 across the Calaveras fault just 2.3 kilometers northwest of our site within the City of Hollister, the slip is much more steady than episodic. In the 7.4 years since October 1979, the Calaveras fault at this site has been moving at a rate of 12.8 millimeters per year in a right-lateral sense, the fastest rate of movement of any of our sites in the San Francisco Bay region.

U.S. Geological Survey creepmeter results in the Hollister area are quite similar to our theodolite results (Schulz, et al., 1982). Creepmeters also show a faster rate of movement at sites on the Calaveras fault just north of Hollister (13.5 millimeters per year between 1971 and 1982) than within the city of Hollister itself (7.3 millimeters per year between 1970 and 1982). This striking comparison between our theodolite triangulation data and U.S. Geological Survey creepmenter data helps increase confidence in the validity of both methods for accurately determining creep rates.

In contrast to the relatively high creep rates in the Hollister area, our Site 19 in San Ramon near the northwesterly terminus of the Calaveras fault has shown virtually no net movement for the past 6.4 years.

Based on our theodolite data and field observations of the Calaveras fault, we contributed two papers (Galehouse, 1987; Galehouse and Brown, 1987) to the U.S. Geological Survey Bulletin 1639 on the Morgan Hill earthquake.

Concord fault - We began our measurements at Site 3 and Site 5 on the Concord fault in the city of Concord in September 1979. Both sites showed about a centimeter of right-lateral slip during October and November 1979, perhaps the greatest amount of movement in a short period of time on this fault in the past three decades. Following this rapid phase of movement by about two months were the late January 1980 Livermore area moderate earthquakes on the nearby Greenville fault (see Galehouse, et al., 1982, for a discussion of this relationship).

After the relatively rapid slip on the Concord fault in late 1979, both sites showed relatively slow slip for the next four and one-half years at a rate of about one millimeter per year right-lateral. However, in late Spring-early Summer 1984, both sites again moved relatively rapidly, slipping about seven millimeters in a right-lateral sense in a few months. The rate has again slowed since late August 1984.

The overall rate of movement on the Concord fault (combining the two periods of relatively rapid movement with those of slower movement) is about 3.7 millimeters per year (Site 3) and 3.0 millimeters per year (Site 5) of right-lateral slip in the past 7.5 years.

Other faults - The Seal Cove fault (Site 7) and the San Gregorio fault (Site 8) have been averaging about one to two millimeters per year of right-lateral slip for the past 7.4 and 4.9 years respectively. However, both sites often show large variations in the amounts and directions of movement from one measurement day to another.

Seasonal and/or gravity-controlled mass movement effects are also present at our sites on the Antioch fault (9A and 11), Rogers Creek fault (16), and West Napa fault (15). Although there have been large variations from one measurement day to another, all these sites show net movement of less than one millimeter per year for the past 5 to 7 years. Because our line of sight at Site 16 on the Rodgers Creek fault became obscured, we had to abandon the site in early 1986. We have recently established a new site on the Rodgers Creek fault and will give our results in subsequent reports.

Since we established Site 20 on the Green Valley fault in June 1984, measurements show right-lateral slip at a rate of about 5 millimeters per year. Large variations also tend to occur between measurement days here. Continued monitoring over a longer period of time will confirm whether or not this apparently high rate of slip is real.

References Cited

Galehouse, J.S., 1987, Theodolite measurements: in Geodetic Observations section of "The Morgan Hill, California Earthquake of April 24, 1984"; U.S. Geol. Survey Bull. 1639, pp. 121-123.

Galehouse, J.S. and Brown, B.D., 1987, Surface displacement near Hollister: in Geological Observations section of "The Morgan Hill, California Earthquake of April 24, 1984"; U.S. Geol. Survey Bull. 1639, pp. 69-72.

Galehouse, J.S., Brown, B.D., Pierce, B. and Thordsen, J.J., 1982, Changes in movement rates on certain East Bay faults: in Proceedings-Conference on Earthquake Hazards in the Eastern San Francisco Bay Area; Hart, E.W., Hirschfeld, S.E., and Schulz, S.S., editors; Special Publication 62, Calif. Div. Mines and Geology, pp. 239-250.

Nason, R.D., Phillippsborn, F.R., and Yamashita, P.A., 1974, Catalog of creepmeter measurements in central California from 1968 to 1972: U.S. Geol. Survey Open-File Report 74-31, 287 pp.

Schulz, S.S., Burford, R.O. and Nason, R.D., 1976, Catalog of creepmenter measurements in central California from 1973 through 1975: U.S. Geol. Survey Open-File Report 77-31, 480 pp.

Schulz, S.S. and Burford, R.O., 1979, Catalog of creepmeter measurements in central California for 1976 and 1977: U.S. Geol. Survey Open-File Report 79-1609, 375 pp.

Schulz, S.S., Mavko, G.M., Burford, R.O., and Stuart, W.D., 1982, Long-term fault creep observations in central California: J. Geophys. Res., v. 87, no B8, pp. 6977-6982.

Spatial and Temporal Patterns of Seismicity in the Garm Region, USSR: Applications to Earthquake Prediction and Collisional Tectonics

14-08-0001-G1382

Michael W. Hamburger
Department of Geology
Indiana University
Bloomington, Indiana 47405
(812) 335-2934

Investigations

This report summarizes the first four months of a new NEHRP research program, which focuses on the highly active seismic zone between the Pamir and Tien Shan mountain belts in Soviet Central Asia. The Garm region, shown in Figure 1, is located directly atop the collisional boundary between the Indian and Eurasian plates. Active deformation of this mountainous area is marked by a complex tangle of thrust and strike-slip faults, and by the densest concentration of earthquakes in the USSR. As the home of the Complex Seismological Expedition (CSE), whose primary mission is the prediction of earthquakes in the USSR, Garm has been the site of some of the most intense observation of earthquake related phenomena in the world (Nersesov et al., 1979). Since 1975, the USGS, in cooperation with the CSE, has operated a telemetered seismic network nested within a stable CSE network that has operated in the area since the early 1950's. The fundamental aims of this research are twofold: (1) to elucidate the structures and processes involved in active deformation of the broad collisional boundary of the Indian and Eurasian plates and their influence on the earthquake generation process, and (2) to examine the temporal variations in seismicity near Garm, in the form of changing spatial, depth, and stress distribution of microearthquakes that precede larger events. The data base is the combined resources of the global, regional, and local seismic networks.

Results

This phase of the project, prior to planned field work at Garm during the summer of 1987, has focused on the compilation and evaluation of the earthquake catalogs that will provide a basis for all subsequent investigations. We now have compiled data from the following earthquake sources: (1) Historical earthquake catalogs of central Asia, including events of $M_s \geq 6$, from Gutenberg and Richter (1954), Rothe (1969), Kondorskaya and Shebalin (1977), and subsets of the global earthquake catalogs; (2) global seismicity catalogs, from the International Seismological Center shown in Figure 1, the USGS Preliminary Determination of Epicenters and their precursors, the International Seismological Summary and US Coast and Geodetic Survey; (3) the Soviet regional catalog ("Earthquakes in the USSR," Acad. Sci. USSR) has been compiled in computer-readable form by David Simpson (Lamont-Doherty Geological Observatory), and is shown in Figure 2; (4) the CSE network based at Garm has recorded over 70,000 events since the early 1950's. All available arrival times and event locations from this network will be made available as part of the Soviet-American exchange; (5) the USGS/CSE network data provide the most detailed spatial information on earthquake distribution. This network includes 13 radio-telemetered stations operated jointly by the USGS and the CSE since 1975 (Wesson et al., 1976). We have begun examining earthquake locations from the first two years of network operation, reported by Pelton and Fischer (1981).

The large shallow earthquakes within Soviet Central Asia are concentrated near the edges of the Pamir and Tien Shan mountain belts; near Garm, these two zones coalesce into a single dense nest of activity. Earthquake depths in the Garm region are largely restricted to the upper crust (3-16 km), with isolated, well located events as deep as 26 km (Pelton and Fischer, 1981). There is no evidence for deeper crustal events (to 44 km depth) suggested by waveform inversion of teleseismically recorded events (Nelson el al., 1987). It is the crustal seismicity of the Pamir/ Tien Shan region that provides the primary basis for our seismotectonic and earthquake prediction studies. However, this area is also the site of the world's densest concentration of intracontinental intermediate-focus seismicity. The Pamir-Hindu Kush zone, shown by filled circles in Figures 1 and 2, provides an extremely reliable supply of subcrustal earthquake sources that may be used for studies of spatial and temporal variations of seismic properties of the crust.

The Soviet regional catalog (Figure 2A) which includes events to magnitude 3, provides an extremely stable, long-term basis for examining seismicity of the Garm region. However, the vast size of this catalog, which includes over 30,000 earthquake locations in the Central Asian region since the early 1950's, has required us to consider alternative methods of presenting the data. Figure 2B shows the seismicity level (in earthquakes/km^2) for the Garm region, and Figure 2C shows the energy release (in joules/km^2) for the same area. Comparison of these two maps reveals several first-order patterns of Central Asia seismicity: (1) earthquake locations, when shown in map view, appear to be somewhat evenly distributed throughout the Central Asia region. In fact, earthquakes are tightly clustered along discrete zones that can be related to specific seismogenic features; (2) there is a striking contrast between earthquake *distribution and energy distribution*: small earthquakes are concentrated in the Tadzhik Depression fold/thrust belt (southwest of Garm), while energy release (i.e., large events) are concentrated along the major fault systems that bound the Pamir and Tien Shan blocks; (3) earthquake distribution and energy release for intermediate-depth events are very tightly concentrated in the Pamir-Hindu Kush nests.

We have also compiled the available published teleseismic focal mechanisms for shallow earthquakes in the Central Asia region, using solutions from Molnar et al. (1973), Ni (1978), Nelson et al. (1987), unpublished solutions by M. Nelson (pers. *comm.*, 1987), and centroid-moment tensor solutions published by PDE, 1981-1987. There are now over 40 solutions available. These are shown in map view in Figure 3A; a summary of inferred stress directions is given in Figure 3B. Despite the obvious geological complexity of the region, the focal mechanisms of shallow earthquakes (Figure 3) document an overall pattern of north-south shortening along east-striking thrust shown and reverse faults.

References

Gutenberg, B., and C.F. Richter, 1954, Seismicity of the Earth, 2nd ed., Princeton, N.J., Princeton Univ. Press, 310 pp.

Keith, C., D.W. Simpson, and O.V. Soboleva, 1982, Induced seismicity and deformational style at Nurek Reservoir, Tadjik SSR, J. Geophys. Res., 87, 4609-4624.

Kondorskaya, N.V., and N.V. Shebalin, 1977, New Catalog of Strong Earthquakes in the USSR, Nauka, Moscow.

Molnar, P., T. Fitch, and F. Wu, 1973, Fault plane solutions and contemporary tectonics in Asia, Earth Planet. Sci. Lett., 9, 101-112.

Nelson, M.R., R. McCaffrey, and P. Molnar, 1987, Source parameters for 11 earthquakes in the Tien Shan Central Asia, determined by P and SH waveform inversion, submitted to J. Geophys. Res.

Nersesov. I.L., Yu, P. Skovorodkin, and T.V. Guseva, 1979, Results of complex studies in the Garm geodynamic polygon, Izvestiya, Physics of the Solid Earth, 15:4, 47-55.

Ni, J., 1978, Contemporary tectonics in the Tien Shan region, Earth Planet. Sci. Lett., 41, 347-354.

Pelton, J., and F.G. Fischer, 1981, An earthquake catalog and velocity model for the USGS Peter the First Range seismic array, Tadzhikistan, USSR. U.S. Geol. Surv. Open-File Rept. 81-1150, pp. 221-246.

Rothe, J.P., 1969, Seismicity of the Earth, 1953-1965, UNESCO, Paris, France, 336 pp.

Wesson, R.L., 1986, Seismicity of the Pamir-Alai region, Soviet Central Asia. Submitted to J. Geophys. Res.

Wesson, R.L., V.G. Leonova, A.B. Maksimov, I.L. Nersesov, and F.G. Fischer, 1976, Results of cooperative field seismological investigations in 1975 in the Peter I Range region [in Russian], in Collection of Soviet-American Works on Earthquake Prediction, v. 1, book 1, pp. 43-69.

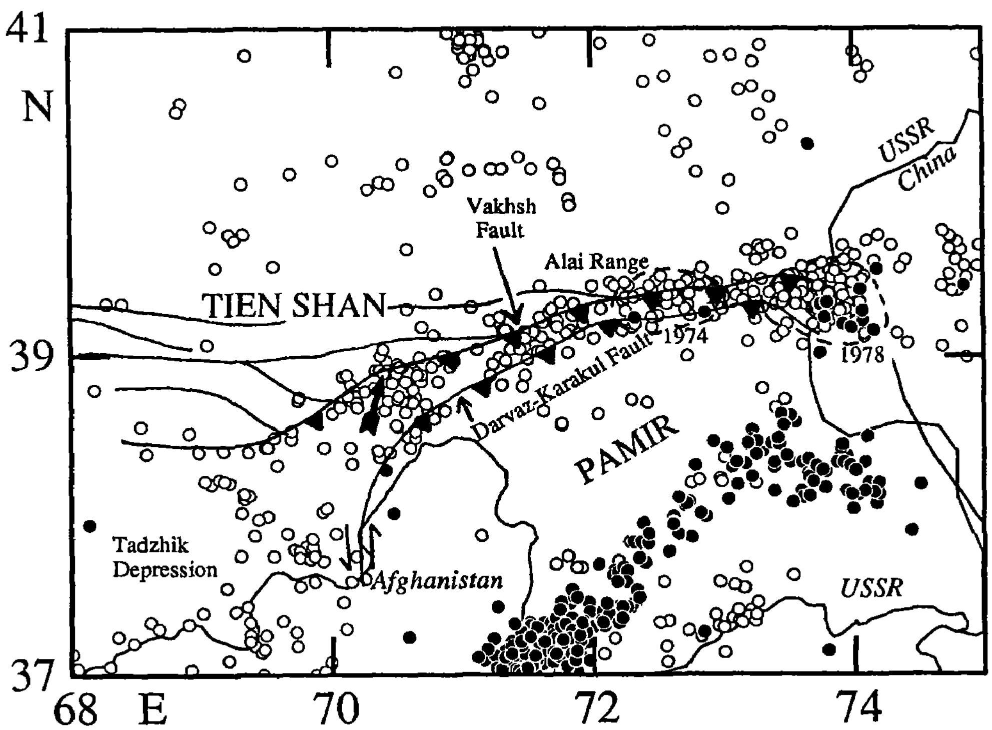

Figure 1. Teleseismically located earthquakes and active faults of the Garm region. Earthquakes recorded from 1964-1984 and located by $\geq$ 20 stations, are from the ISC catalog. Open circles represent earthquakes at $\leq$ 70 km depth; filled circles: h > 70 km. Fault maps are adapted from Keith et al. (1982) and Wesson (1986). Dashed ellipses indicate aftershock zones of 1974 Markansu and 1978 Daraut-Kurgan earthquakes. Heavy arrow shows the location of Garm.

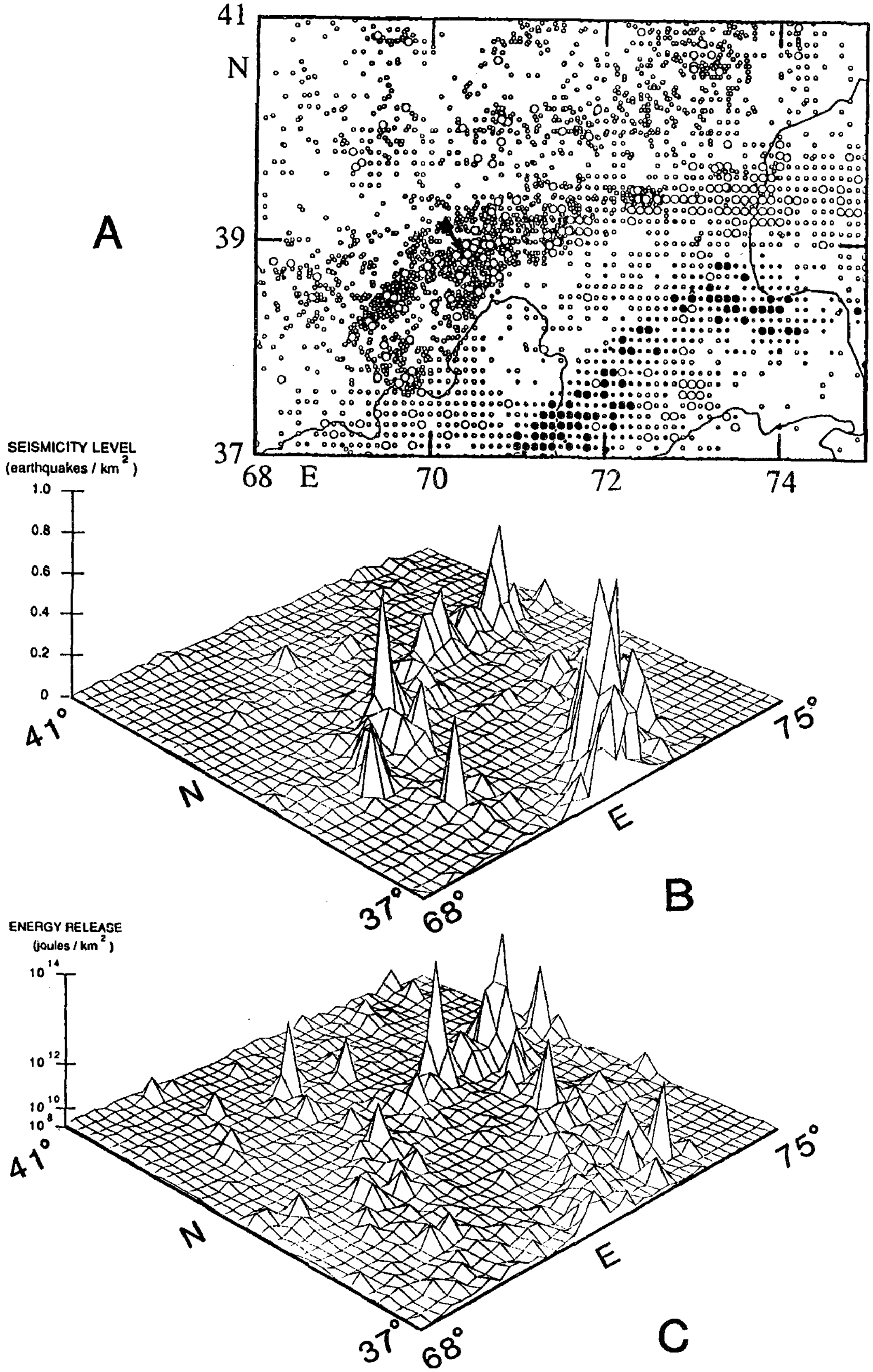

Figure 2. Earthquakes located by the Soviet regional network, 1964-1980. (A) Earthquakes classified by magnitude and depth: open circles: h $\leq$ 70 km; filled circles: h > 70 km. Small symbols: $M_L \leq 4.0$; large symbols: $M_L > 4.0$. The apparent gridding results from poorly located events whose position is given in 0.1 degree increments. Data are from D.W. Simpson, Lamont-Doherty Geological Observatory. The heavy arrow indicates the location of Garm. (B) normalized seismicity level for the same area, presented as a three-dimensional surface, viewed from the southwest. (C) normalized seismic energy release, presented as in (B).

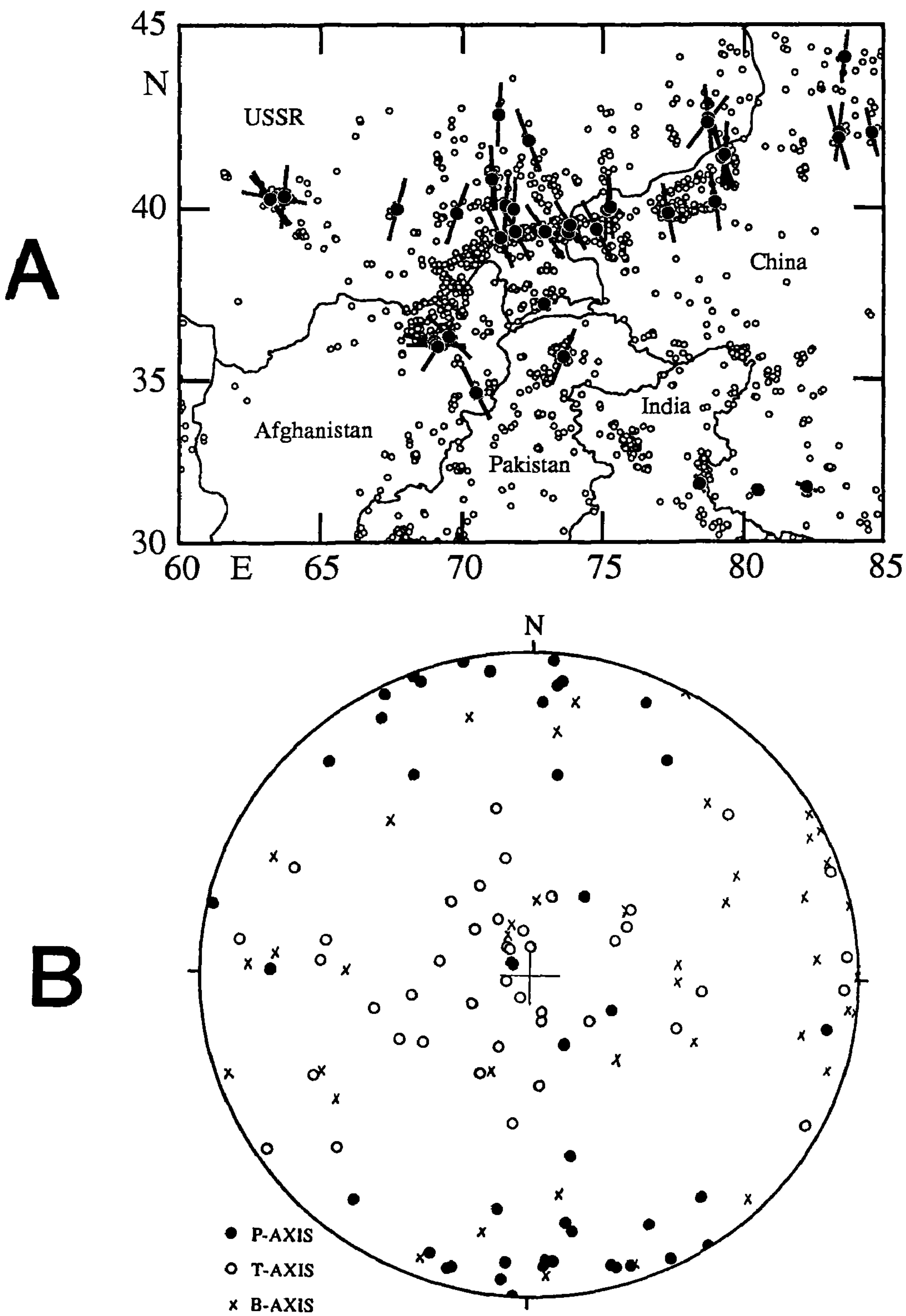

Figure 3. Teleseismically determined focal mechanisms of shallow earthquakes in central Asia. (A) Earthquake focal mechanisms (solid circles) superimposed on shallow seismicity, from ISC. (B) Stereographic projection of principal stress directions inferred from focal mechanism solutions. See text for data sources.

DEEPWELL MONITORING ALONG THE SOUTHERN SAN ANDREAS FAULT

14-08-0001-G1377

Thomas L. Henyey and Steve P. Lund
Center for Earth Sciences
University of Southern California
Los Angeles, California 90089-0741
213-743-6123

INTRODUCTION

Over the past several years, we have reclaimed a set of abandoned deep wells along the San Andreas fault in the Palmdale region (Figure 1) in order to monitor groundwater level and search for variations that might be related to strain changes along the fault. Results of our monitoring program have clearly established the long-term base line of regional water-level variability within the Palmdale region. Also, time series analysis of our water-level data has clearly indicated that the wells are very sensitive to solid-earth tides and atmospheric pressure variations, and therefore should be ideally suited to record regional strain events. However, prior to 1986, we had only once identified a water-level anomaly that could be convincingly related to a local strain event (other than the solid-earth tides), or that could be correlated between two or more wells within the Palmdale array. The only notable exception to this lack of apparent strain-related activity was a water-level anomaly recorded in the Phelan well (Figure 2) that was co-seismic with the 1983 Coalinga earthquake more than 400 km away. We suggested (McRaney et al., 1983) that this water-level anomaly was caused by local creep along the San Andreas fault in sympathy to the Coalinga earthquake. Unfortunately, no other type of strain recorder along the San Andreas fault noted evidence for such a creep event.

NEW RESULTS

During 1986, however, we have recovered much more convincing evidence that the Phelan well, in particular, is sensitive to local strain events. The Phelan well recorded a water-level anomaly co-and post-seismic to the July 8 Palm Springs earthquake (M=5.9) that was similar in waveform to the 1983 Coalinga co-seismic anomaly (McRaney et al.; 1986). In the current case, however, there is abundant evidence (McRaney et al., 1986; Williams et al., 1986; Fagerson et al., 1986) that creep along the southern part of the San Andreas fault occurred co- and post-seismically to the Palm Springs earthquake. The similarity of our water-level anomaly and the Mecca Beach creepmeter record (Fagerson et al., 1986) suggests that both measurements document perhaps 1-2 weeks of intermittent aseismic strain events subsequent to the Palm Springs earthquake. This anomaly, and the entire 1986 water level variation of Phelan well are shown in Figure 3. A filtered version of the anomaly, with solid-earth tides and atmospheric pressure effects removed, is also shown in Figure 3; the 1986 anomaly (filtered to removed solid-earth tides & daily pressure effects only) is superimposed on the 1983 co-seismic anomaly (similarly filtered) in Figure 4.

Both the short and long-term response of the Phelan well to the Palm Spring earthquake are remarkable. The 1983 (Figures 2,4) Coalinga anomaly and previously noted aseismic anomalies in 1985 (Figures 2,5) have a simple waveform (sharp downward drop over less than one day followed by a slow return to the previous base level) that is suggestive of single simple creep events (e.g. Lippincott et al., 1985). The Palm Springs anomaly (Figures 3,4), however, has a much more extended period of water level drop - fast for the first 48 hours followed by a slower drop for the next 2 weeks. This suggests that aseismic strain along the San Andreas fault 80 km north of Palm Springs may have been occurring intermittently for up to 2 weeks after the Palm Springs earthquake. Similar indications of aseismic strain along the San Andreas fault up to 80 km south of Palm Springs has been noted by others as well. Williams et al. (1986) have noted aseismic surface crack development within 2 weeks after the Palm Springs earthquake along three different intervals of the San Andreas fault between 43 and 86 km south of the earthquake epicenter. Also, Fagerson et al. (1986) noted 2 aseismic creep events at the Mecca Beach creepmeter 33 hours and 5 days after the Palm Springs earthquake (see Figure 3). Both of these observations strongly corroborate our interpretation of the Phelan water-level anomaly.

An additional aspect of the Phelan anomaly which must be considered is the fact that the water level changed base-line after dissipation of the anomaly. This is the first time that such a base-line change has occurred at the Phelan well (Figures 2,3). It is possible that this relates to an altered state of stress in the crystalline rocks of the Phelan region as a result of the Palm Springs earthquake. The sense of the base-line change is most consistent with an increased regional stress state. If this can be validated, it would be very important for estimates of the long-term likelihood of a major earthquake in this region.

SUMMARY

The Phelan well has recorded a large-amplitude co-and post-seismic water-level anomaly related to the July 9, 1986 Palm Springs earthquake. Similar waveforms anomalies have been noted at Phelan well in the past. One of these previous anomalies was coseismic with the 1983 Coalinga earthquake. The 1986 Phelan anomaly suggests aseismic strain activity for perhaps 2 weeks subsequent to the Palm Springs earthquake; other studies have indicated similar asiesmic strain activity south of Palm Springs subsequent to the Palm Springs earthquake. A new base-line of water level at Phelan well has been noted subsequent to the Palm Springs earthquake; we tentatively ascribe this to a new level of stress in the crystalline rocks near Phelan well along the San Andreas fault. No other anomalous water level variability was noted in 1986 within the Palmdale array.

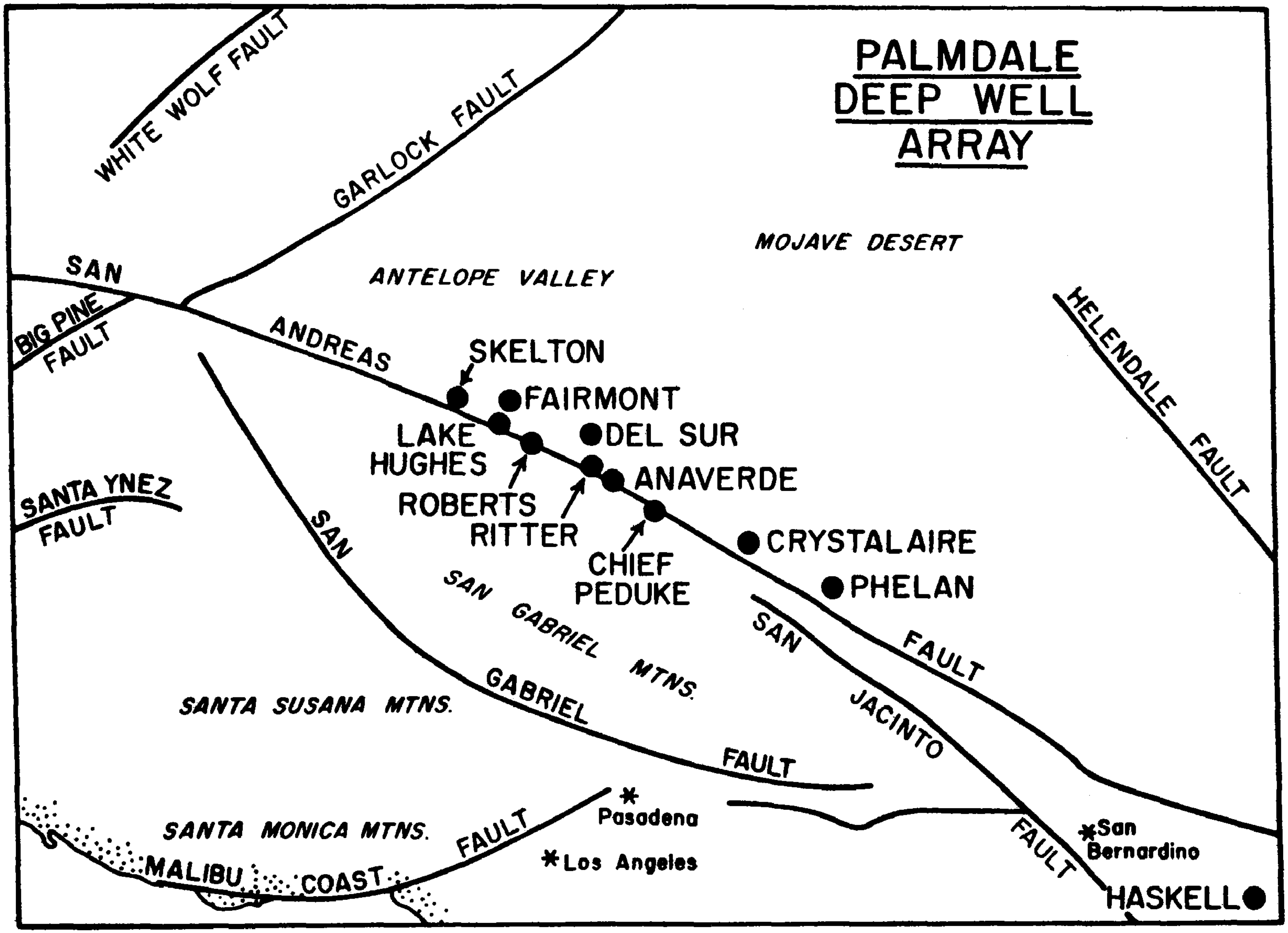

Figure 1. Map showing the location of our deep-well network in relation to major faults.

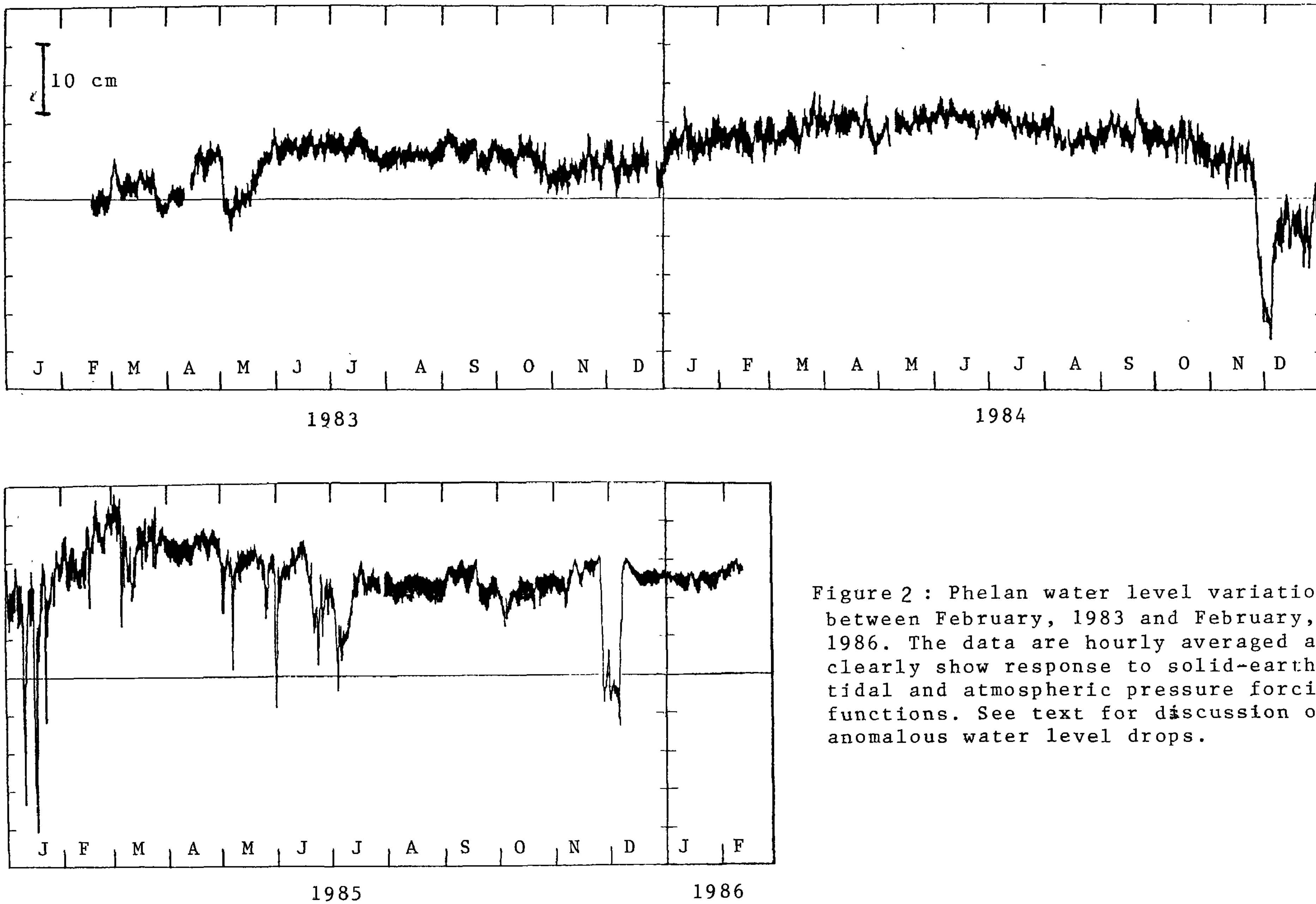

Figure 2 : Phelan water level variation between February, 1983 and February, 1986. The data are hourly averaged and clearly show response to solid-earth tidal and atmospheric pressure forcing functions. See text for discussion of anomalous water level drops.

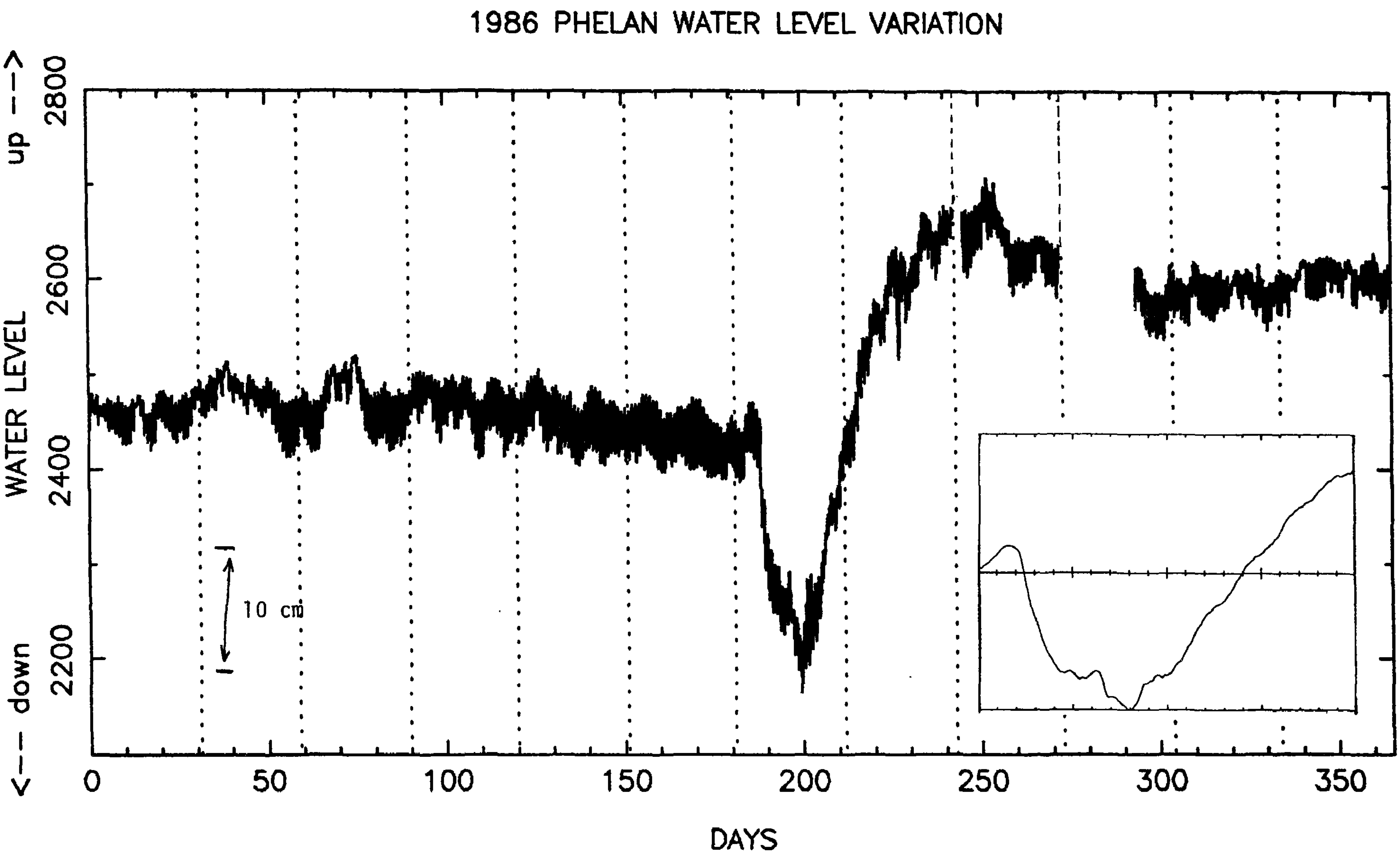

Figure 3: 1986 Phelan water level variation. The July 8 Palm Springs earthquake is noted by an asterisk. The filtered co- and post-seismic water level anomaly is shown in the inset. Filtering removed

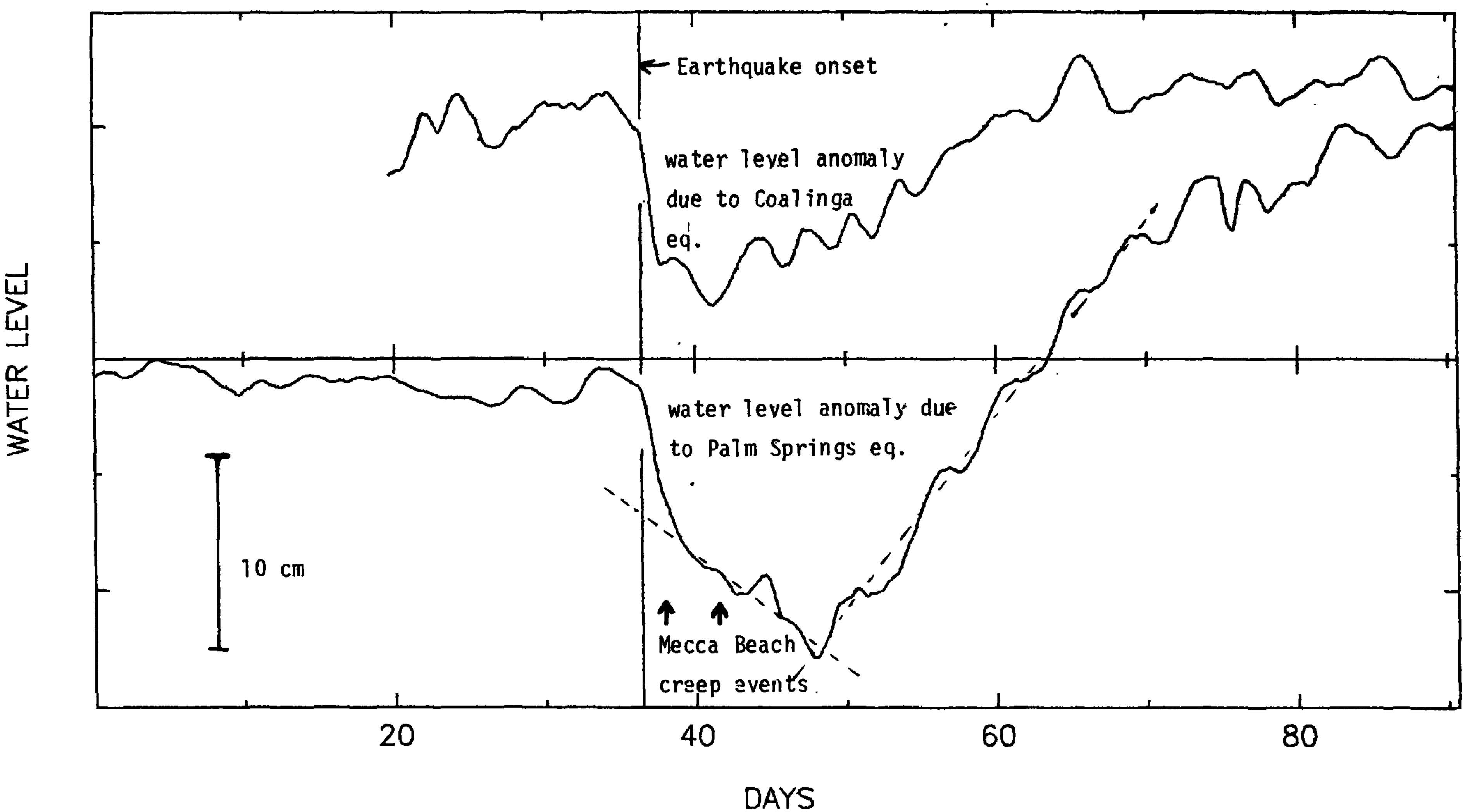

Figure 4: 1983 and 1986 water level anomalies filtered to remove solid-earth tides and daily pressure effects.

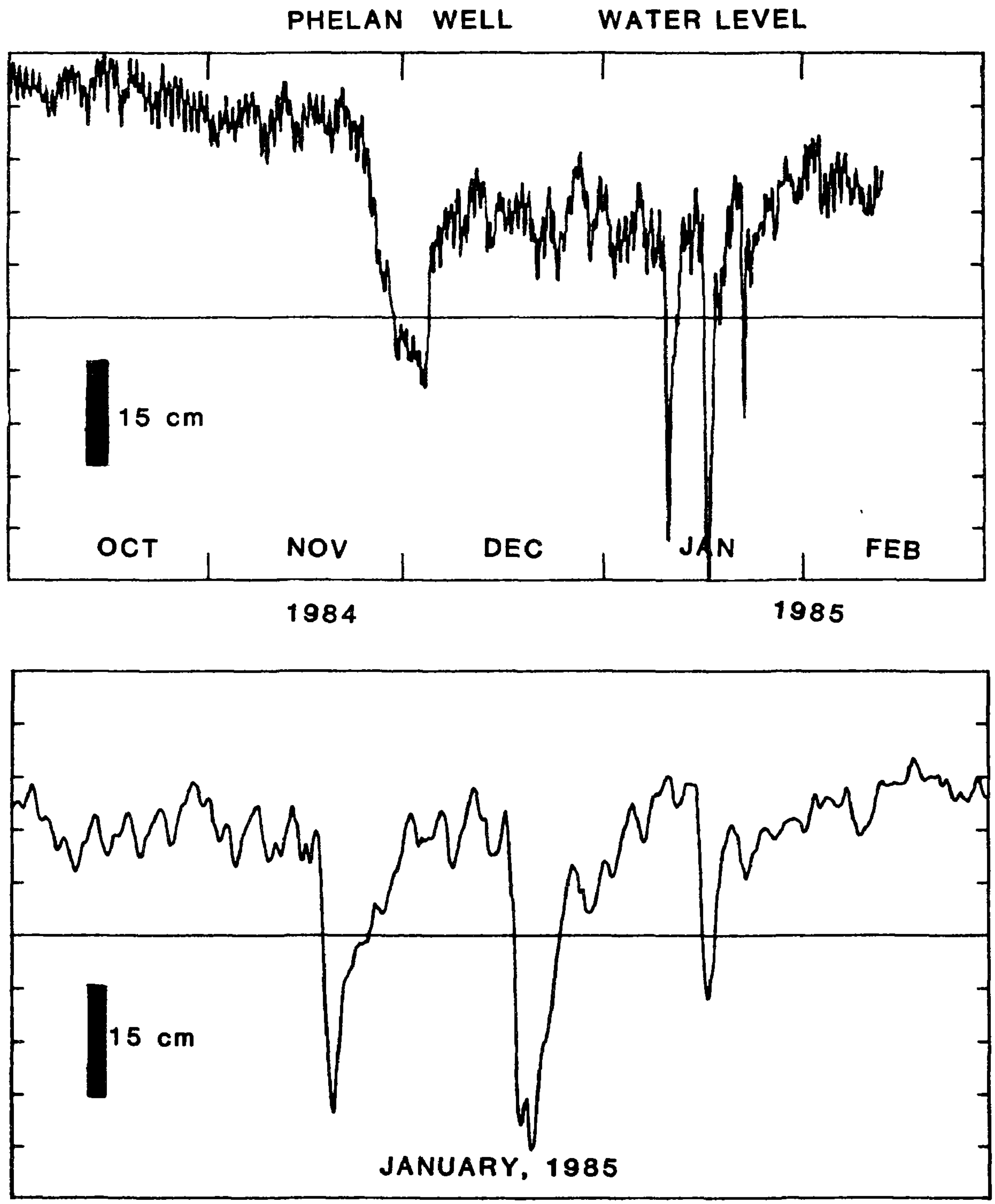

Figure 5: Anomalous water-level variations at Phelan well during late 1984 and early 1985. Four distinct short-term anomalies (one to two weeks) are supperposed on a longer-term apparent offset in the vater level.

San Andreas Earthquake/Parkfield Geophysics

9380-03074

Robert C. Jachens and Carter W. Roberts
U.S. Geological Survey, MS 989
345 Middelfield Road, Menlo Park, CA 94025
(415) 329-5300

Investigations

1. Repeat precision gravity surveys were conducted in January and covered:
   (a) the southern California high precision base station network
   (b) a 170-km-long profile perpendicular to the San Andreas fault and passing through Cajon Pass
   (c) the two-color laser site at Holcomb Ridge

2. With Andrew Griscom, worked on a comprehensive look at the implications of regional gravity and magnetic data on the geometry, properties, and displacement history of the San Andreas fault system. The resulting paper is intended for the San Andreas Professional Paper being assembled by Bob Wallace.
3. Began 3-dimensional modeling of the magnetic field in the area of the Parkfield experiment.

Results

1. The repeat gravity surveys showed only small changes from previous surveys at most stations of the network and profile. Exceptions occurred at the four easternmost stations of the network (Lavic, Amboy, Twentynine Palms, and Cottonwood Pass) which all showed that the gravity increased by 30-40 microGals during the past year. Various consistency checks suggest that these changes are real. The next reoccupation is scheduled for May, 1987, and special attention will be devoted to these stations to see if the changes persist.
2. At a number of locations along faults of the San Andreas system, the juxtaposition of large rock masses with contrasting densities and/or magnetic properties causes characteristic potential field anomalies that reflect the attitudes of the faults. We examined such anomalies at 14 sites along the San Andreas and associated faults through published reports and quantitative modeling. The results indicate that, although the faults generally appear to be vertical, a significant number of locations exist where the faults dip less than 90°. The faults tend to be nonvertical at places where the fault trace changes direction. Examples along the San Andreas fault include: (i) the region just north of Point Arena where the fault dips eastward; (ii) south of Hollister where the fault dips steeply to the west; (iii) at the west end of the "big bend" where the fault dips westward; and (iv) at the east end of the "big bend" where some splays of the fault dip northward.

   A number of authors have suggested that fracturing of the rock in few-km-wide zones surrounding faults of the San Andreas system should significantly decrease the bulk density within the fault zone and should, therefore, be reflected as gravity lows centered on the faults. We have examined gravity profiles crossing the faults in a number of areas where pre-Tertiary basement is continuously exposed across the fault and found that local gravity lows, if present at all, rarely exceeded a few mGal. These results imply that, in general, fracturing within the country rock surrounding the faults causes density decreases of only a few percent. Andrew Griscom pointed out that this finding is in marked contrast to the pronounced zones of low seismic wave velocity that have been found at some places along the San Andreas fault, velocities that would imply gravity anomalies of 20 mGal or more if standard velocity/density relationships obtain. The probable resolution of this paradox is that the standard velocity/density relationships do not apply to fractured rock, a suggestion that is supported by borehole gravity, velocity, and density measurements in the Stone Canyon well south of Hollister reported by Stierman and Kovach. These showed velocity decreases of about 40% were accompanied by density decreases of only about 4%.

3. Magnetic surveys in the area of Parkfield indicate the presence of a large magnetic source northeast of the fault that abuts the fault just southeast of the rupture zone. Bill Hanna modeled the magnetic anomaly from this source and concluded that the body is composed of serpentinite and that it extends to a great depth. Recent 3-D modeling agrees with Hanna's interpretation and yields a source that is about 25 km long, 15 km wide, extends from near the surface to mid-crustal depths, and has sides that dip outward except along the fault. The body does not cross the fault and probably extends as deep as the inferred top of Great Valley crystalline basement (about 15 km) defined by seismic investigations along SJ-6. Although the serpentinite body appears to have been cut by the fault, no comparable anomaly is present southwest of the fault at a location compatible with known slip. A possible explanation is that the body was not cut by the San Andreas, but rather was emplaced directly against the fault. Mobile serpentinite may have migrated upward to fill a zone of extension resulting from right-lateral slip past the right step in the fault that occurs at the southeast end of the Parkfield reach.

TILT, STRAIN, AND MAGNETIC FIELD MEASUREMENTS

9960-2114
M. J. S. Johnston
Branch of Tectonophysics
U. S. Geological Survey
Menlo Park, California 94025
415/323-8111, ext. 2132

Investigations

[1] To investigate the mechanics of failure of crustal materials using data from both deep borehole tensor and dilational strainmeters and near surface strainmeters, tiltmeters, and arrays of absolute magnetometers.

[2] To develop physical models of incipient failure of the earth's crust by analysis of real-time records from these instruments and other available data.

Results

[1] **Review of Tectonomagnetic, Seismomagnetic, and Volcanomagnetic Observations in Western U.S.A., 1974-1986**

Synchronized measurements of geomagnetic field have been recorded along the San Andreas fault since 1974. Along 800 km of the San Andreas fault, in Long Valley Caldera, and on Mount St. Helens more than 27 magnetometers telemeter data in digital form once every 10-minutes to a central location. Repeat measurements have also been made at several hundred additional sites of special interest. Since 1974, a summary of the major tectonic and volcanic activity in the regions monitored includes one major explosive volcanic eruption, numerous minor extrusive eruptions, one episode of aseismic uplift, and four moderate earthquakes for which magnetometers were close enough to expect observable signals ($\approx$ 3 source lengths). The eruption of Mount St. Helens generated large oscillatory fields and a 9 ± 2 nT offset on the only surviving magnetometer. A large-scale traveling magnetic disturbance passed through the San Andreas Array from one to two hours after the eruption. Subsequent extrusive eruptions generated small precursory magnetic changes in some cases. These data are consistent with a simple volcanomagnetic model, MHD effects, and a blast excited traveling ionospheric disturbance. Correlated changes in gravity, magnetic field, areal strain, and uplift occurred during episodes of aseismic deformation in southern California primarily between 1979 and 1983. Because the relationships between these parameters approximately agrees with those calculated from simple deformation and tectonomagnetic models, the preferred explanation appeals to short-term strain episodes independently detected in each data set. A less likely explanation appeals to a common source of meteorologically generated crustal noise in the strain, gravity, and uplift data and a simultaneous disturbance in the magnetic data of unknown origin. Surface observations of fault creep events have no associated magnetic signature, consistent with near-surface failure, but are sometimes associated with longer term perturbations. Of the four earthquakes with $M_L > 5$ for which at least one magnetometer was within the epicentral area, seismomagnetic effects of -1.3 nT and 0.3 nT were observed for only one. For this event, magnetometers were closest to the epicenter and were most optimally located. These observations are consistent with a simple seismomagnetic model of the event. Similar models for the other three events indicate that expected seismomagnetic effects are below the signal resolution of the nearest magnetometer.

[2] **Large Scale Magnetic Field Perturbation Arising from the May 18, 1980, Eruption from Mount St. Helens**

A travelling magnetic field disturbance generated by the May 18, 1980, eruption from Mount St. Helens at 1532 UT was detected on a 800-km linear array of recording magnetometers installed along the San Andreas fault system from San Francisco to the Salton Sea. The arrival times of the disturbance field from the most northern of these 23 magnetometers (992 km south of the volcano) to the most southern (1521 km S23E) is consistent with the generation of a traveling ionospheric disturbance stimulated by the blast pressure wave in the atmosphere. The first arrival at the north and the south ends of the array occurred 43 min and 59 min, respectively, after the initial eruption. Apparent average wave velocities vary from 384 m/s at the north to 430 m/s at the southern end of the array. The periods of the disturbance signals at each site decrease with time after the first arrival and the period of the main disturbance increases linearly with distance from the source. Simple models of point source excitation of ionospheric disturbances can be fit to these data. The subset of ionospheric disturbances generated by trapped atmospheric pressure waves (also termed gravity waves and/or acoustic waves) that are excited by earthquakes and volcanic eruptions are common and propagate to great distances. Some radio frequency disturbances associated with earthquakes may be explained by this mechanism. Magnetic transients (precursive tectonomagnetic effects) were recorded on two independent instruments only before the first of these earthquakes. Traveling ionospheric disturbances (TID's), generated by earthquake related atmospheric pressure waves, may explain many electromagnetic disturbances apparently associated with earthquakes. Differential magnetometer array measurements strongly discriminate against these ionospheric disturbances. Local near-fault magnetic field transients rarely exceed a few nT.

[3] **Static and Dynamic Strain during the July 8, 1986, M 5.9 North Palm Springs, Ca, Earthquake**

Crustal strain during the July 8, 1986, North Palm Springs earthquake (M 5.9) was recorded on several Sacks-Evertson dilatometers (PUBS at 125 km, AMSS at 127.2 km, BBSS at 121 km and others at greater distances), a 3-component (tensor) strainmeter (MPFS - 24.3 km distant), all installed at depths of about 200 m, and 3-component surface seismic velocity transducers at the PUBS and more distant dilatometer sites. Dynamic strain and velocity for the foreshock, mainshock, and aftershocks were recorded at a 300 Hz sampling rate and high gain on digital recorders (GEOS). The moment of the earthquake was estimated from displacement spectra generated using the dynamic strain and velocity seismograms and also from the static strain offsets recorded on the strainmeters. The seismic moments determined from the surface velocity tranducers at the dilatometer locations are between 0.6-$1.4*10^{25}$ dyne-cm. The static moments are larger (between $2\text{-}3*10^{25}$ dyne-cm). Post-seismic strain, consistent with continued failure on the rupture plane, continued for about 30 minutes. This was followed by apparent rebound for several days after the earthquake. The post-seismic moment was less than 10% of that of the earthquake. Precursive strains during the period days to 10 minutes before the event are not apparent in the data from the closest instrument, MPFS. The coseismic shear strain decrease and normal strain increase at this 3-component strainmeter site was 0.06 and 0.02 μ strain, respectively. The North Palm Springs earthquake decreased the effective strength (σ_p-0.6σ_n) for right-lateral failure in nearby sections of the San Jacinto fault and, therefore, increases the probability of earthquakes in sections of this fault.

[4] **Seismomagnetic Observation during the July 8, 1986, M_L 5.9 North Palm Springs, California, Earthquake.**

A differentially connected array of 24 proton magnetometers has been operated along the San Andreas fault since 1976. Seismomagnetic offsets of 1.2 nT and 0.3 nT were observed at two of these array sites following the July 8, 1986, M_L 5.9 North Palm Springs earthquake. These observations, at epicentral distances of 3 km and 9 km, respectively, from the earthquake, are the first obtained of this elusive but long-anticipated effect. The data are consistent with a seismomagnetic model of the earthquake in which right-lateral rupture is assumed on a 16 km segment of the Banning fault at a depth between 3 km and 10 km. The rupture segment is assumed to have 20 cm of displacement in a direction N60°W and dip at 45° down to the north in a region with average magnetization of 1 A/m. Alternate explanations in terms of electokinetic effects and earthquake generated electrostatic charge redistribution seem unlikely since the changes are permanent and complete within a 20 minute period.

[5] **On the Use of Volumetric Strainmeters to Infer Additional Characteristics of Seismic Waves**

Theoretical descriptions of volumetric and displacement fields for radiated seismic energy predict that simultaneous observations of each on colocated sensors permit inferences regarding the radiated fields that cannot be inferred from either sensor alone. Volumetric strain is not dependent on angle of incidence nor azimuth and shows amplitude and phase modulation dependent on intrinsic material absorption. Simultaneous observations on colocated sensors allow; 1) the resolution of superimposed P and S radiation fields, and in particular, superimposed P and S waves reflected at the free surface, 2)angle of incidence and apparent phase velocity based on amplitude on amplitude ratios and, 3) intrinsic material absorption and characteristics of low-loss inhomogeneous wave fields. Several hundred local, regional and large teleseismic events have been observed on colocated volumeteric strain meters and seismometers using broad-band high-resolution recorders (GEOS) at four sites near the San Andreas fault, CA. These observations, in the passband common to the two types of sensors show features which are consistent with the theoretical predictions.

[6] **Structural Implications of Strain and Magnetic Measurements in the Long Valley/Mono Craters Region**

Repeated magnetic measurements have been made since 1972 with a 32-site array in upper Owens Valley. The array extends through Long Valley, around Mono Lake, across the Excelsior Mountains, and down Owens Valley. One or two sets of data have been obtained each year at each of the site pairs. Following the first Mammoth Lakes earthquakes in 1978, telemetered and portable recording magnetometers were also installed from Round Valley through the Long Valley Caldera. The primary feature in data from all sites between Round Valley and Mono Lake is a systematic and linear increase in field with time but with slightly different rates in different places. After correction for geomagnetic field secular variation, the rates peak to the north of Mono Craters at about 1 nT/a and fall off to the north and to the south through Long Valley. These data can be simple interpreted in terms of thermal remagnetization as a result of migration of the Curie point isotherm. A migration rate of about 1 m/a at a depth of 5 km will satisfy the data. At shallower depths the rate will be correspondingly less. A minor change in rate may have occurred in the south moat region starting in 1978. Simple tectonomagnetic models which incorporate either a pressure source at a depth of about 5 km or pressure triggered shear stress release on the Hilton Creek could explain this change. Borehole strain measurements recorded at the Devil's Postpile during the Chalfant earthquake do not indicate attenuated strain expected if a large solid/liquid plexus existed beneath Long Valley.

[7] **Crowley Lake Level Monitoring**

Four water level monitoring sites have been installed on Lake Crowley in the Long Valley/ Mammoth Lakes region (Fig 1). These stills provide differential water level measurements (tilt) equivalent to 6 independent tiltmeters with baselines of up to 8 kilometers at varying angles to the center of the resurgent dome. Each site has been surveyed into the existing level line routes around the lake by John Estrum and NGS. The time constants of the stills are approximately 40 minutes to minimize effects from the primary sieche periods at 18 minutes and 13 minutes, respectively. The water level data, together with water temperature, wind speed, and other parameters, are being transmitted by the low frequency satellite data collection system to Menlo Park at a sample period of 2 minutes.

[8] **Parkfield Strainmeter Array**

As part of a cooperative program with Alan Linde of the Carnegie Institution of Washington, and M. Gladwin of the University of Queensland, Australia, 5 dilatometers and 3 tensor strainmeters were installed in boreholes at depths between 500 and 1000 feet in the Parkfield region. The locations are shown in Figure 2. At each dilatometer location the data are transmitted by 16-bit digital telemetry to Menlo Park, CA, to provide a real time monitoring capability. The data are also recorded on site on 16-bit digital recorders at sample rates of between 100 and 200 sps. Figure 3 shows data recorded at one of the new sites (Donnalee) in Joaquin Cyn from an earthquake near Kettleman Hills.

Reports

Mueller, R.J., and M. J. S. Johnston, 1986, Seismomagnetic Effect during the July 8, 1986, M_L 5.9 North Palm Springs, California, Earthquake, Trans A. G. U., 67, 1090.

Bakun, W.H, Bredehoeft, J., Burford, R. O., Ellsworth, W. L., Johnston, M. J. S., Lindh, A. G., Olds. P., Roeloffs, E., Schulz, S., Segall, P., Simpson, R., and W. Thatcher, 1986, Parkfield, CA. Earthquake Prediction Experiment - A Status Report, Trans A. G. U., **67**, 904.

Gladwin, M. T., Gwyther, R. L., Hart, R., Francis, M., and Johnston, M. J. S., 1986, Borehole Vector Strain Measurements in California, J. Geophys. Res. (in press).

Borcherdt, R. D., Johnston, M. J. S. and G. D. Glassmoyer, 1987, On the Use of

Volumetric Strainmeters to Infer Additional Characteristics of Seismic Waves, Seis. Res. Lett., **58**, 24.

Johnston, M. J. S., Tectonomagnetism and Tectonoelectricity, 1987, Reviews of Geophysics, (in press).

Johnston, M. J. S., Borcherdt, R. D., Glassmoyer, G. D., and A. T. Linde, 1987, Static and Dynamic Strains during the July 21, 1986, Chalfant Earthquake near the Long Valley Caldera, California, Seismol. Res. Lett., **58**, 24.

Mueller, R. J., and M. J. S. Johnston, 1987, Magnetic Field Measurements in The Morgan Hill, California, Earthquake of April 24, 1984, U.S. Geological Survey Bulletin 1639, 129-133.

Johnston, M. J. S., 1987, Structural Implications of Strain and Magnetic Measurements in the Long Valley/Mono Craters Region, 1987, Abs. Long Valley Symposium, Lawrence Berkeley Laboratories, Mar 17-18.

Johnston, M. J. S. Review of Tectonomagnetic, Seismomagnetic, and Volcanomagnetic Observations in Western U.S.A., 1974-1986, 1987, Abs. IUGG, Vancouver, Canada, August, 1987, (in press).

Mueller R. J., and M. J. S. Johnston, Large-Scale Magnetic Field Perturbations Arising from the May 18, 1980, Eruption from Mount St. Helens, 1987, Abs. IUGG, Vancouver, Canada, August, 1987, (in press).

LEVEL MONITORING SITES AT CROWLEY LAKE

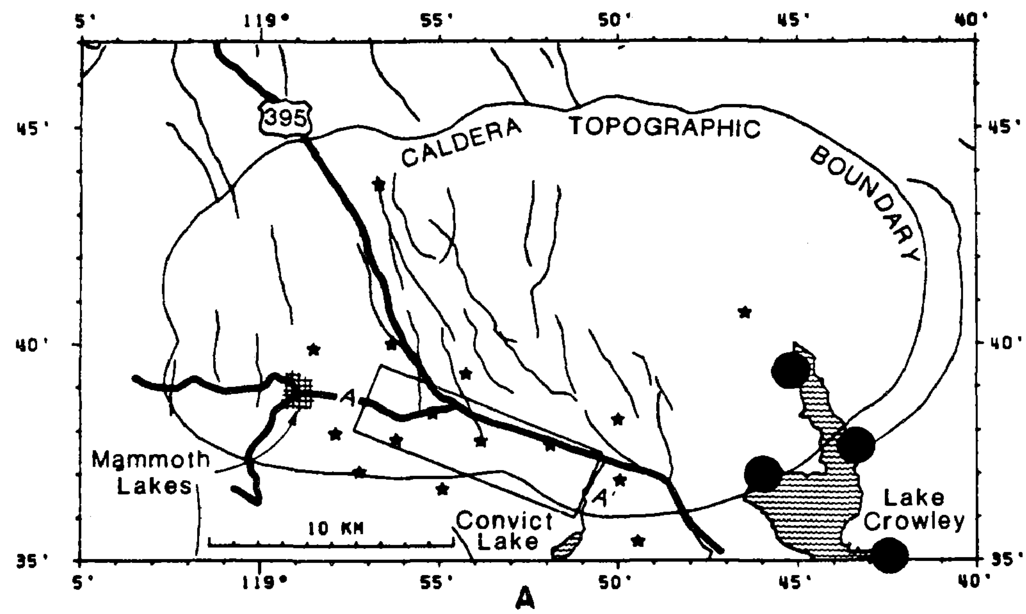

FIGURE 1

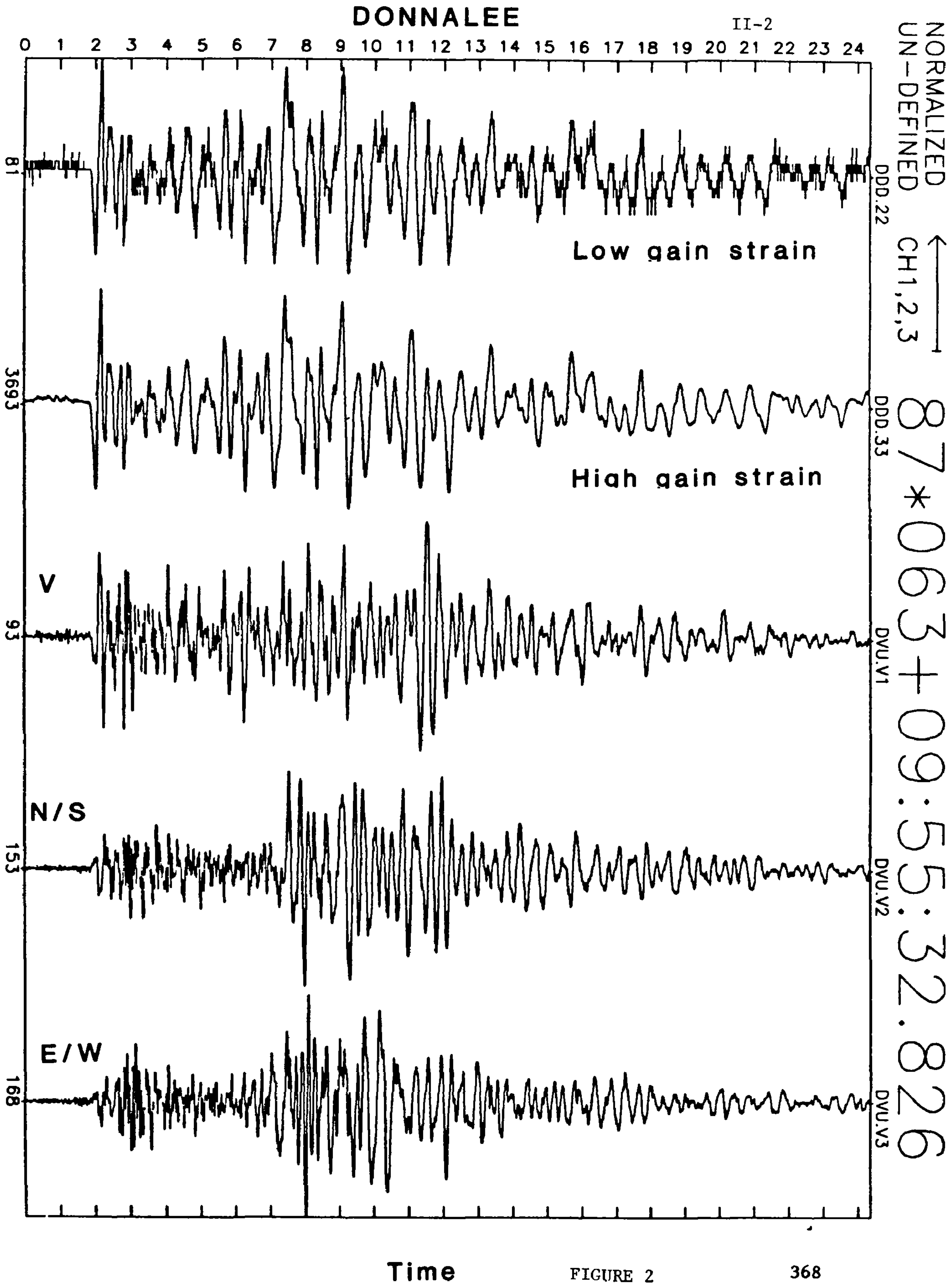
DONNALEE
0 1 2 3 4 5 6 7 8 9 10 11 12 13 14 15 16 17 18 19 20 21 22 23 24
NORMALIZED
UN-DEFINED
CH1,2,3
87*063+09:55:32.826
81
DDD.22
Low gain strain
3693
DDD.33
High gain strain
V
93
DVU.V1
N/S
153
DVU.V2
E/W
168
DVU.V3
Time

FIGURE 2

Earthquake and Seismicity Research Using SCARLET and CEDAR

Grant No. 14-08-0001-G1354

Hiroo Kanamori, Clarence R. Allen, Robert W. Clayton
Seismological Laboratory, California Institute of Technology
Pasadena, California 91125 (818-356-6914)

Investigations

1. Applications of Attenuation Tomography to Imperial Valley and Coso-Indian Wells Region, Southern California
   Phyllis Ho-Liu, Hiroo Kanamori and Robert W. Clayton

2. Seismicity in the Banning Area Before the 1986 North Palm Springs Earthquake
   Scott Phelps and Hiroo Kanamori

Results

1. Applications of Attenuation Tomography to Imperial Valley and Coso-Valley Wells Region, Southern California

Spatial variations in seismic wave attenuation were tomographically imaged from observed S-to-P wave amplitude ratios in the Imperial Valley and Coso-Indian Wells regions of southern California. In the Coso-Indian Wells region, a highly attenuating body (S-wave quality factor $Q_\beta \approx 30$) coincides with a slow P-wave anomaly mapped by Walck and Clayton (1987). This coincidence suggests the presence of a 3 to 5 km depth magmatic or hydrothermal body in the Indian Wells region. In the Imperial Valley, slow P-wave travel-time anomalies and highly attenuating S-wave anomalies were found in the Brawley seismic zone at a depth of 8 to 12 km. The effective S-wave quality factor is very low ($Q_\beta \approx 20$) and the P-wave velocity is 10% slower than the surrounding areas. These results suggest either magmatic or hydrothermal intrusions, or fractures at depth, possibly related to active shear in the Brawley seismic zone. This attenuation tomographic technique is shown to be useful in delineating the spatial variations in seismic wave attenuation and in estimating the effective seismic quality factor of attenuation anomalies.

2. Seismicity in the Banning Area Before the 1986 North Palm Springs Earthquake

Approximately 1000 earthquakes which occurred during the four years before the July 8, 1986 North Palm Springs earthquake in the epicentral area were relocated using the Joint Hypocenter Determination technique. A cross section taken perpendicular to the strike of the Banning fault indicates that nearly all of the activity during this preseismic period occurred beneath the plane defined by the aftershocks. When only events with $M_L \geq 2.5$ are plotted, a linear trend is revealed which is nearly perpendicular to the aftershock zone and extends from the mainshock hypocenter at about 11 km to a depth of 19 km. Focal mechanisms obtained from previous studies in the area include four with very shallow-dipping nodal planes. Three of these four are clustered below the aftershock zone at depths of 15-17 km. These events can be interpreted as evidence for a decollement along which the upper crust moved southward relative to the lower crust, thereby reducing the normal stress on the Banning fault. Topographic loading by the nearby San Bernardino Mtns. is investigated as a possible physical mechanism for such a decollement.

References

Ho-Liu, Phyllis, Hiroo Kanamori and Robert W. Clayton, Applications of Attenuation Tomography to Imperial Valley and Coso-Indian Wells Region, Southern California. Submitted to the Journal of Geophysical Research, February, 1987.

Magistrale, Harold and Hiroo Kananmori, Changes in NTS Seismograms Recorded in the Source Region of the North Palm Springs Earthquake of 7/8/86. American Geophysical Union, Fall Meeting, 1986.

Phelps, Scott and Hiroo Kanamori, Seismicity in the Banning Area Before the 1986 North Palm Springs Earthquake. Seismological Society of America, Annual Meeting, Spring 1987.

GEODETIC STRAIN MONITORING

9960-02156

John Langbein
Branch of Tectonophysics
U.S. Geological Survey
345 Middlefield Road, MS/977
Menlo Park, California 94025
(415-323-8111, ext. 2038

Investigations

Two-color geodimeters are used to survey, repeatedly, geodetic networks within selected regions of California that are tectonically active. This distance measuring instrument has a precision of 0.1 to 0.2 ppm of the baseline length. Currently, the crustal deformation is being monitored within the south moat of the Long Valley Caldera in eastern, California, near Pearblossom, California on a section of the San Andreas fault that is within its Big Bend section and on Middle Mountain near Parkfield, California. Periodic comparisons with the proto-type, 2-color geodimeter are also conducted near Parkfield, California. These inter-comparison measurements serve as a calibration experiment to monitor the relative stabilities of the portable and proto-type geodimeters.

Results

1) Instrument Breakdowns

During the 6 month period from October 1986 through April 1987, we experienced several failures with the two-color geodimeter. These included numerous cable problems, one bad integrated circuit, failure of the Rb clock or time-base, and failure of the blue laser. These problems were tackled as they appeared, but caused the instrument to be down for a number of weeks. The longest delay was caused by replacing the blue laser with a newer model. We had to do some modification of the geodimeter in order to install the new laser. Although a faulty time-base for frequency measurement is cause for concern regarding the stability of the distance data, independent check with another time-base indicated that the faulty time-base had long-term stability but was unstable for periods of less than 30 seconds.

2. Instrument Inter-comparison

Since January 1986, we have completed 4 intercomparison experiments at Parkfield, California using both the portable and prototype two-color geodimeter. Each instrument is set up over an adjacent monument on Carr Hill and length measurements are made on 14 baselines which uniformly cover a 360° range in azimuth. Using the differences in observed baseline lengths, we have deduced both the stability of the geodimeters and the monuments to within 0.2 mm and 0.4 mm respectively.

Previous to January 1986, we conducted this experiment on a reduced set of baselines using only 150° range in azimuths. Data from these experiments, which go back to June 1984, indicate that both the geodimeters and monuments have changed relative to each other. For instance, the inferred instrument length scale have fluctuated as much as 0.4 ppm and fluctuations in monument displacements were on the order of 2 mm. However, the limited range in azimuthal control precluded us from resolving the ambiguity of change in instrument length scale and monument displacement.

The measurement of the instrument length scale (Figure 1) in January 1987 indicated that the distances measured by the portable instrument lengthen by 1.1 ± 0.2 mm relative to the portable instrument. Although the calibration network was not measured completely in January due to intense fog causing reduced visibility, the measurements are consistent with the 1.1 mm change. It is not known whether the change is within the portable or the prototype instrument or a combination of both.

Optical realignment of the portable instrument after replacing the blue laser is one probable cause for the inferred change in length-scale. However, detailed examination of the line-length changes observed in Long Valley taken immediately before and after the laser failure do not reveal any significant offset. A 1.0 mm change would be detectable. A secular drift of either instrument over the 4 month interval from September 1986 through January 1987 is also a distinct possibility but is difficult to unambiguously detect.

3. Long Valley

Measurements made of length changes for the baselines using station CASA (Figure 2) as a common endpoint are shown in Figure 3 for the interval between June 1983 and April 1987. The secular changes for the past 6 months show relatively low strain rate relative to the rates of 3 years ago. The exceptions, however, are the baselines to Krakatau and to Miner.

In the following Table, the strain rates for the Casa baselines are calculated for the 8 month interval before and the 8 month interval following the 21 July 1986 Chalfant Valley earthquake. With the exception of the coseismic compression due to the earthquake, these 16 baselines show secular extension ranging from 0.0 ppm/a to 2.0 ppm/a. Of the 16 baselines, 5 baselines significantly increased their extension rates following the Chalfant earthquake, 4 baselines decreased their extension rates, and the remainder to not show any significant change in rate coinciding with the Chalfant earthquake.

Table

Strain Rates Before and After the Chalfant Earthquake, July 21, 1986

Baseline	Strain Rates ppm/a Nov. 15, 1986-July 20, 1986	July 20, 1986-Apr. 2, 1986
Pile	0.01 ± 0.22	-.44 ± 0.19
Tilla	0.40 ± 0.10	-0.02 ± 0.08
Taxi	0.77 ± 0.14	0.23 ± 0.09
Convict	0.38 ± 0.12	0.43 ± 0.19
Whitmore	0.49 ± 0.17	0.23 ± 0.15
Mike	2.54 ± 0.85	0.65 ± 0.35
Lookout	0.51 ± 0.18	1.07 ± 0.20
Krakatau	0.21 ± 0.06	1.50 ± 0.04
Rodger	0.79 ± 0.50	1.48 ± 0.45
Hot	0.33 ± 0.07	0.78 ± 0.05
Shank	1.35 ± 0.14	-0.13 ± 0.11
Miner	-0.19 ± 0.11	1.92 ± 0.04
Sherwin	1.09 ± 0.09	1.02 ± 0.07
Knolls	0.71 ± 0.06	0.97 ± 0.05
Sewer	1.37 ± 0.21	0.74 ± 0.43
Lomike	1.26 ± 0.26	1.34 ± 0.44

4. Parkfield

In November, 1986 we measured the network established on Middle Mountain during August 1986. The map of the new network and the "Parkfield" network, which is surveyed with the prototype, two-color geodimeter, is shown in Figure 4.

Reports

Langbein, J.O., M.F. Linker, and D.L. Tupper, Analysis of two-color geodimeter measurements of deformation within the Long Valley caldera, June 1983 - October 1985, Journ. of Geophys. Res., in press, 1987.

Figure Captions

Figure 1. Results from instrument intercomparison at Parkfield. The top plot shows the inferred displacement of the monument used by the portable geodimeter relative to the monument used by the prototype instrument. The lower plot shows the inferred change in length scale of the portable instrument relative to the prototype.

Figure 2. Map showing the location of the baselines that comprise the two-color geodimeter network within the Long Valley caldera.

Figure 3. Line-length changes observed for the baselines from station CASA (Figure 2). The length changes have been normalized to the nominal length of each baseline; hence the displacements are plotted as strain changes. The error bars represent one standard deviation. Time of the 21 July, 1986 Chalfant earthquake is indicated with a vertical line.

Figure 4. Map showing the location of the baselines that comprise the two-color network on Middle Mountain and near Parkfield, California.

RELATIVE DISPLACEMENT OF CENTRAL MONUMENTS

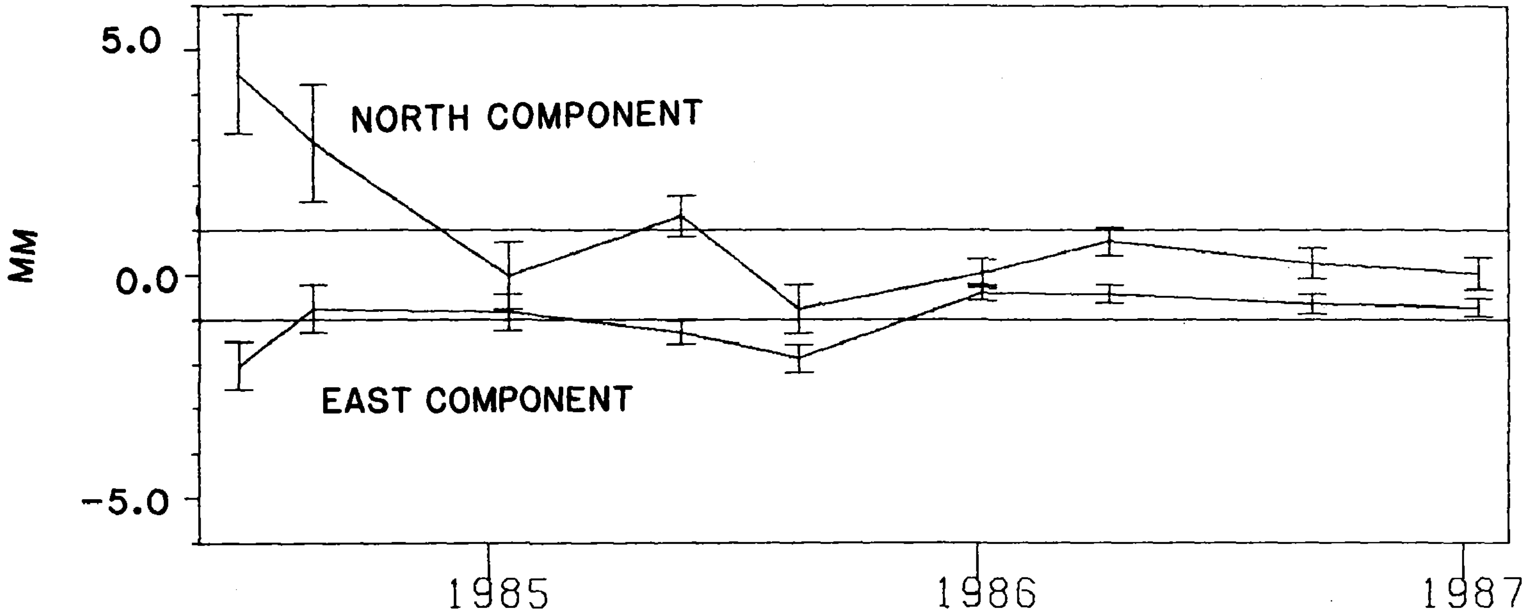

CHANGE IN LENGTH SCALE OF PORTABLE, TWO-COLOR GEODIMETER

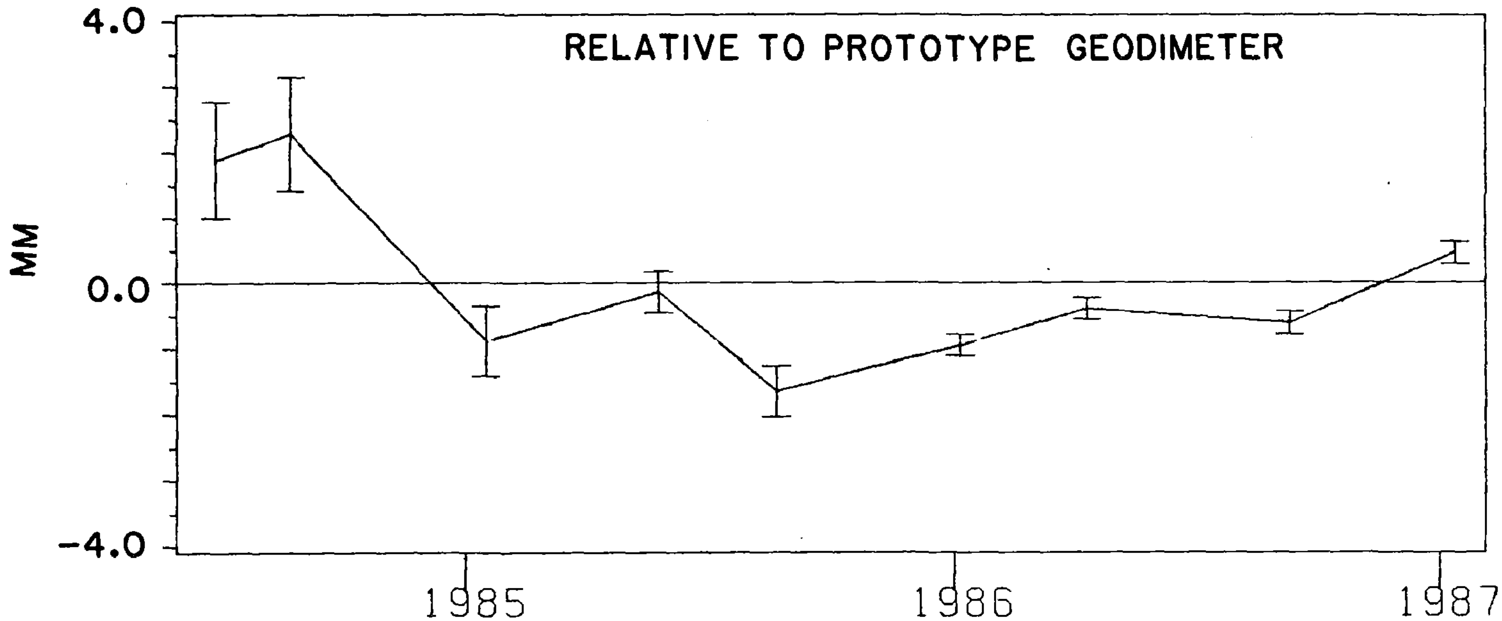

mammoth net

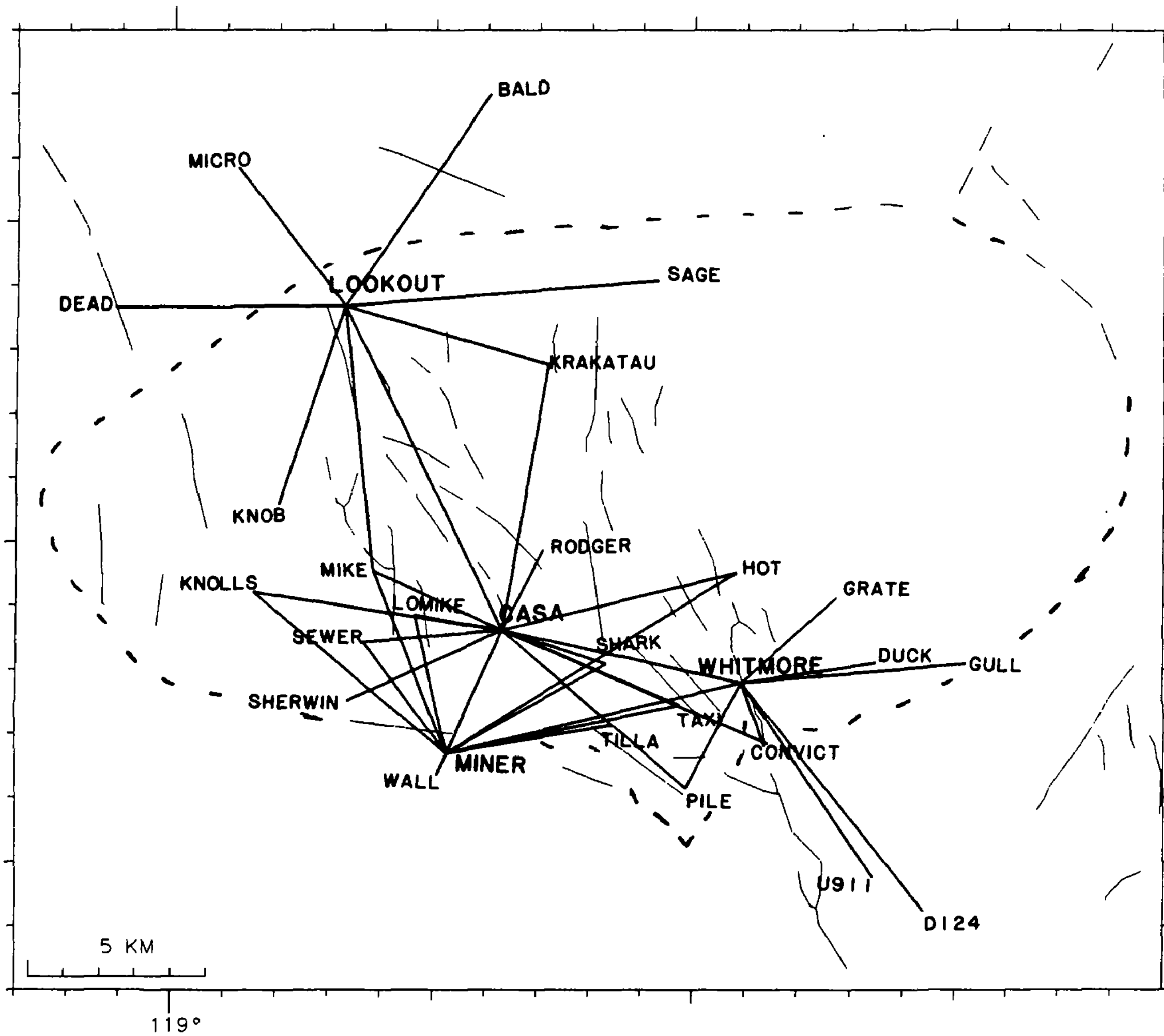

BALD
MICRO
LOOKOUT
SAGE
DEAD
KRAKATAU
KNOB
RODGER
MIKE
KNOLLS
HOT
GRATE
LOMIKE
CASA
SEWER
SHARK
WHITMORE
DUCK
GULL
SHERWIN
TAXI
TILLA
CONVICT
MINER
WALL
PILE
U911
D124
5 KM
119°

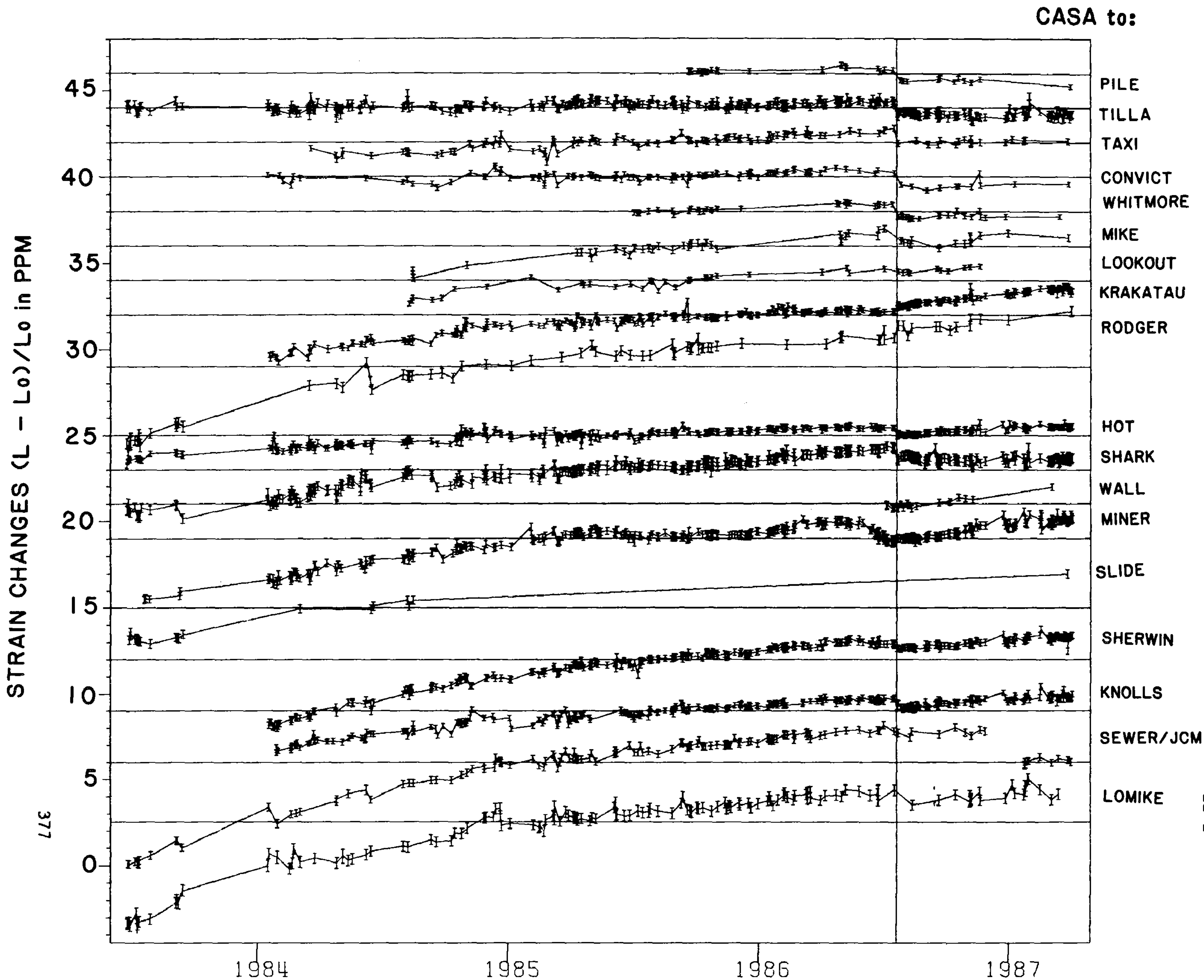
CASA to:
STRAIN CHANGES (L - Lo)/Lo in PPM
45
40
35
30
25
20
15
10
5
0
1984
1985
1986
1987
PILE
TILLA
TAXI
CONVICT
WHITMORE
MIKE
LOOKOUT
KRAKATAU
RODGER
HOT
SHARK
WALL
MINER
SLIDE
SHERWIN
KNOLLS
SEWER/JCM
LOMIKE

parkfield 2 color nets

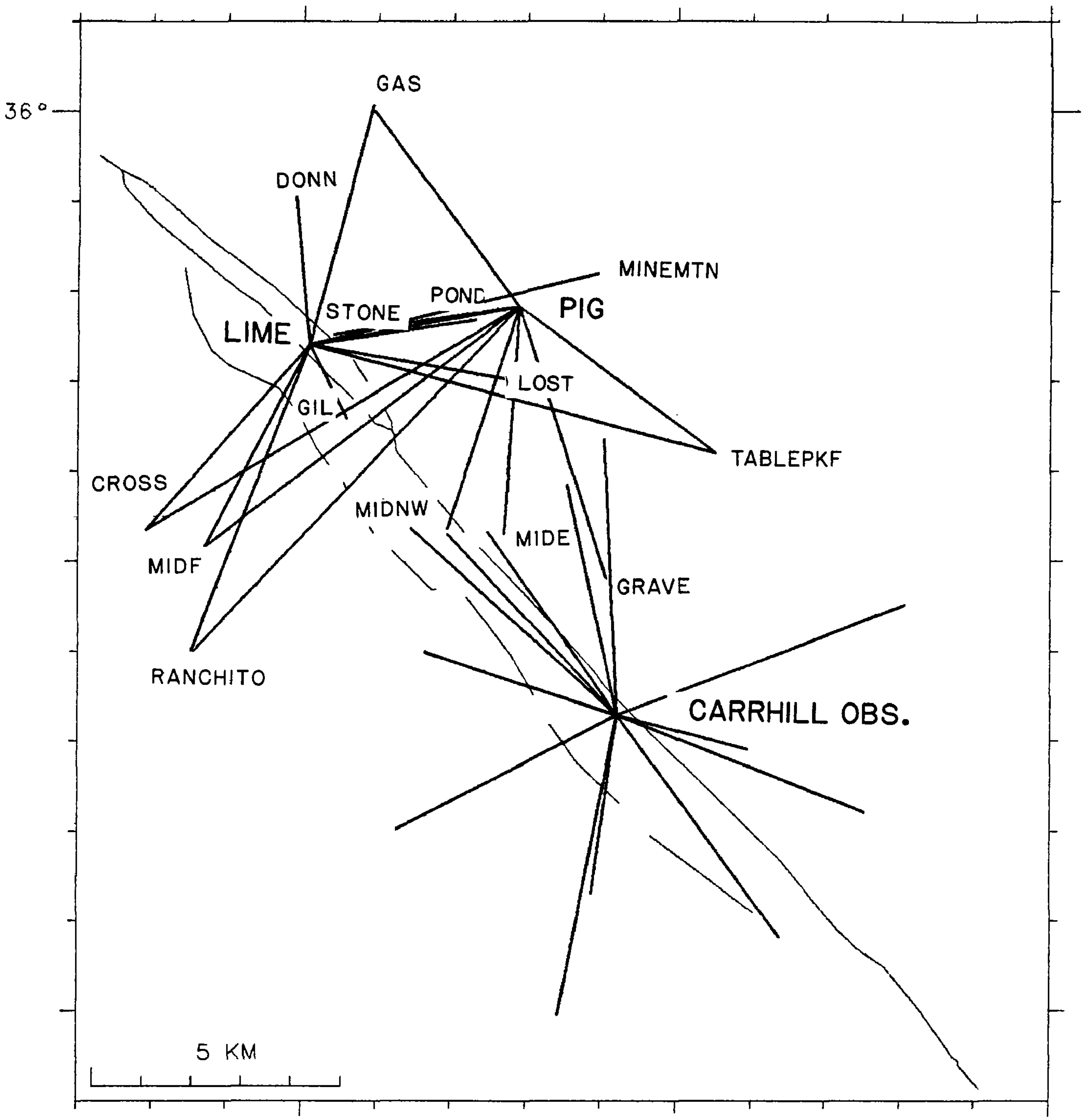

"Acquisition and Analysis of Data from Sacks - Evertson Borehole Strainmeters in California"

Contract Number 14080001 G 1172
Investigators: A.L. Linde and I.S. Sacks
Department of Terrestrial Magnetism
Carnegie Institution of Washington
5241 Broad Branch Road N.W.
Washington, D.C. 20015
(202) 966 0863

The program of installing borehole strainmeters and recording and analyzing the data from these instruments has had minor difficulties in California. Reliable data acquisition requires that the instrument be situated in a region of competent rock relatively free of major fractures. It is difficult to find such rocks close to areas of major interest along the San Andreas fault system. Additionally, this program has been hampered by the fact that we do not yet have a good network of instrumental sites in any area in California. For various good reasons, the Geological Survey has required that several areas be instrumented more or less concurrently; available funds have thus limited the number of sites in each area. Under these conditions, it is difficult or impossible to make significant progress in understanding strain changes associated with seismic activity. Nevertheless a number of important observations and interpretations have been made. In some cases, as discussed below, we have been able to supplement the dilatometer data from California with other local data and also with data from different areas in order to suggest models of tectonic activity which are consistent with the data. These studies have been in collaboration with the Geological Survey (in particular M. Johnston has been very active in this program) and foreign institutions.

Coseismic Effects:

The dynamic range of the instrument is now better (although not fully) exploited by the use of the 16 bit GEOS recording system. Faithful recording of strain steps and seismic waves has allowed determination of seismic moments as well as strain changes immediately following nearby earthquakes. For example, the January 26, 1986, Quiensabe earthquake was recorded by S-E dilatometers (as well as other instruments), the closest being SRLS at 27.1 km. The static moment calculated from the strain offsets was $2\text{-}3 * 10^{24}$ dyne-cm, which may be compared with the seismic moment determined from velocity transducers at the surface of $1.7 * 10^{24}$. Post-seismic strain, consistent with continued fault failure occurred for several days after the earthquake. Its moment is about 20% that of the earthquake. Short term precursive strains were not apparent. (Ref. Johnston et al, 1986 EOS).

High resolution strain recordings have now been made of the May, 1983, Coalinga (M 6.7, Dist 51 km) earthquake, Kettleman Hills (M 5.5, dist 34 km) earthquake, the April 1984, Morgan Hill (M 6.1 dist 55 km) earthquake, the November 1984, Round Valley M 5.8 dist 54 km) earthquake and several other smaller earthquakes. Observed co-seismic effects are generally in good agreement with expectations from elastic dislocation theory. Post seismic deformation which occurred in some cases, had moments comparable to that of the main shock. Pre-seismic slip (minutes to hour), if any occurred, must have had a moment less than a few % that of the main event. (Johnston et al, 1987).

The Parkfield Array:

All the above earthquakes were outside the rather sparse array of strainmeters. It was therefore not possible to recognize or identify any possible precursory deformation which might have occurred in the days to months preceding the earthquake. This should not be the case in the Parkfield area. Eight dilatometers have been installed ranging from the initiation region (VC) in the north to the termination offset in the south (JC, RH). While some of the northern sites are in somewhat marginal rock, we expect that the proximity to the initiation will make up for the expected reduced stability. Fig. 1 shows the installed sites in the Parkfield region.

Longer Term (month to year) Changes:

Stress redistribution in earthquake zones can be complex, and non-linear in space and time (e.g. Sacks et al., 1978). In many regions one cannot consider a fault as an isolated system, subject only to steady loading and episodic release. In some cases concentration of stress on a fault may be due to aseismic slip (or slow earthquakes) on adjacent orthogonal faults. In this situation, genuine precursors may occur substantially away from the eventual earthquake location. It is also possible that the locking of a fault system prior to an earthquake will cause stress redistribution in the surrounding faults which can cause detectable strain changes at these faults.

Ishibashi has named this class of event "tectonic" precursors to differentiate them from "physical" precursors, i.e. those occurring in the preparation zone of the earthquake. With only a sparse network of instruments able to record these signals, it is difficult to determine with confidence which you have. This is further complicated by a possibly complex slip function on whichever fault is yielding.

Fig. 2 is such an example. It shows six months of data from two different types of borehole strainmeters, spaced about 7 km apart. The large strain increase in early October is the co-seismic strain change due to the Morgan Hill (m = 6.5) earthquake. The instruments had only recently been installed and the large initial drifts have been removed. The similarity of the waveforms suggest that they are responding to the same strain change. It is beyond the scope of this discussion to interpret these signals in terms of a model, rather we note that

a) The strain field changes are coherent over a substantial distance (7 km).

b) There are many sub-events: 1) A step-wise decrease about 2 weeks before the earthquake; 2) a gradual further increase for 2 weeks following the quake; 3) a gradual decrease for about 3 weeks; 4) a rapid and substantial decrease for the next 2 months. In the last month shown the two sites are presumably responding to other, more local, changes. Note that if we were not fortunate enough to have two instruments within range, it would be impossible to estimate whether these events were in fact due to continuing (and precursory) substantial motion on the Morgan Hill and adjacent faults, and therefore significant, or due to small slip events on a micro-fault very near an instrument. In the latter case, if the source is very near, the strain changes recorded may have no tectonic significance. However, in the common situation of sparse arrays, we cannot disregard strain signals which appear on one instrument only. To summarize, we have the twin complications that slow strain changes may be complex, and that there may be motion on adjacent faults.

Episodic Changes:

In the first example, shown in Fig. 3, the precursors are clearly of the "tectonic" type. Slow strain changes were recorded by two instruments of different type for about five months prior to the Yamanashi earthquake, m = 5.5. Both the borehole dilatometer at Shizuoka and the extensometer at Fujiwara are within a few km and on opposite sides of the Fossa Magna (aseismic) fault. The polarity of strain change is opposite on the two instruments. The events terminated shortly after the earthquake. Since the events did not occur at the same time on the two stations, they may indicate strain propagation up the fault.

Episodic slow strain changes have been recorded in the Parkfield area on the two instruments operating there at that time (Fig. 4). Similar changes were also recorded in the water level in a nearby well (Fig. 5). Note that although there are similarities in the water level and strain data which confirm the nature of the long duration ($\sim$2 - 3 weeks) signals, that there are also significant differences; the water level data does not reflect longer term changes as detected by the strainmeters and also the noise level appears to be higher at short periods. During this period, there was an increase in the seismicity level as indicated by the occurrence of events in Fig. 4. These strain signals are consistent with aseismic slip on a patch of the San Andreas fault.

By themselves, these data from the sites at Gold Hill cannot be regarded as being necessarily significant, even though the Parkfield area is expected to experience a moderate earthquake soon. However, in other cooperative programs, we have recorded similar strain excursions in two other areas. In Iceland we are working with the Iceland Meteorological Office in monitoring the southern Iceland transform fault where there is an enhanced potential for a moderate earthquake. In 1982/83 (Fig. 6) a series of strain events were recorded at SAU, the station nearest the transform. Minor seismicity, in this normally aseismic area, accompanied these strain events. More recently a magnitude 4 event occurred in this region. Again, these strain events are consistent with aseismic slip on a small section of fault near the station. Fig. 7 shows representative signals produced by slip on such a patch in which the only parameters to change for the different signals is the start and end positions of the rupture.

In the Tohoku area of northern Honshu, Japan, the station GJM nearest the epicenter of the 1983 Japan Sea earthquake (m 7.8) also showed a series of strain events which are certainly correlated with that large earthquake (Fig. 8).

This project is in cooperation with Tohoku University. Again these strain events are consistent with aseismic slip on a fault, in this case an extension of the seismic fault plane (Fig. 9). Fig. 10 shows a fit of the model calculation to the data. The fit is very good and also we see that the predicted amplitudes at the other station (TA2 and SWU) would be too small to observe.

Thus we now have recorded in three different areas, slow, episodic strain signals. In one case (Tohoku) these signals have been associated with a large earthquake. In the other two cases, Parkfield and Iceland, the events were associated with minor seismicity and in both areas there is an expectation that a moderate earthquake will take place.

From these different cases we may make a new hypothesis: stress redistribution which occurs before an earthquake may be at least partially in the form of episodic aseismic slip which is detectable if we have wide frequency, band, high dynamic range strainmeters sufficiently close to these areas. Thus we suggest that a search should be made for this class of episodic strain events as a possible precursory phenomenon.

5 May 1987

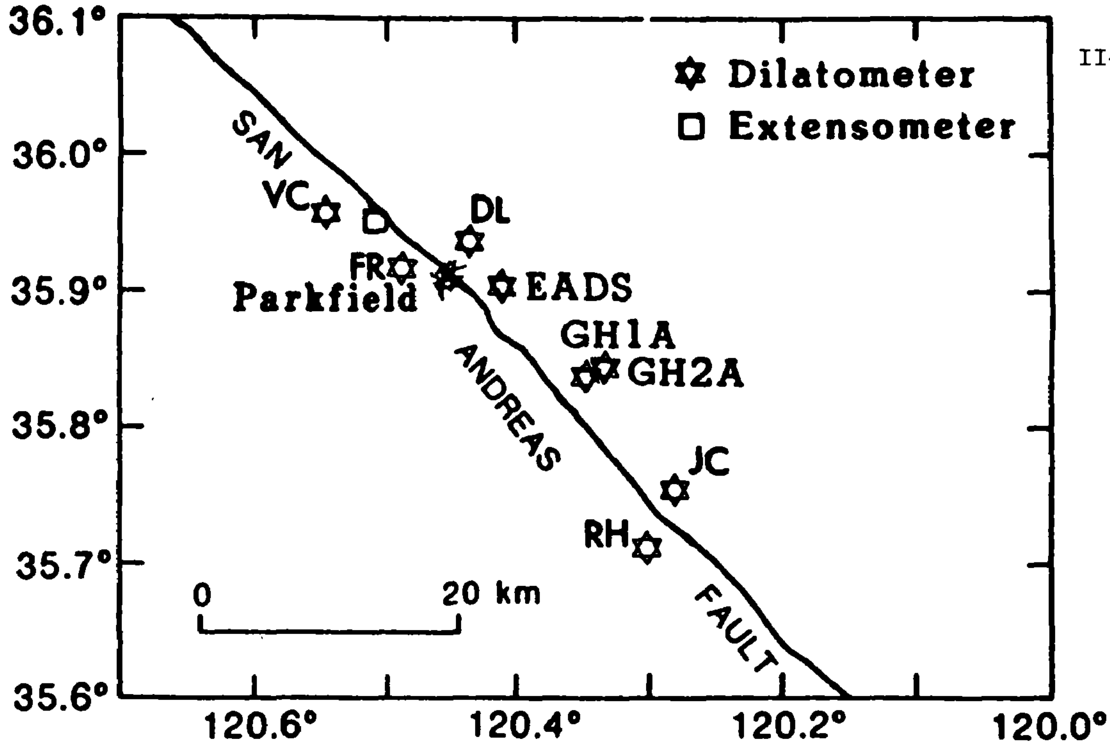

Fig. 1. Dilatometers in the Parkfield area.

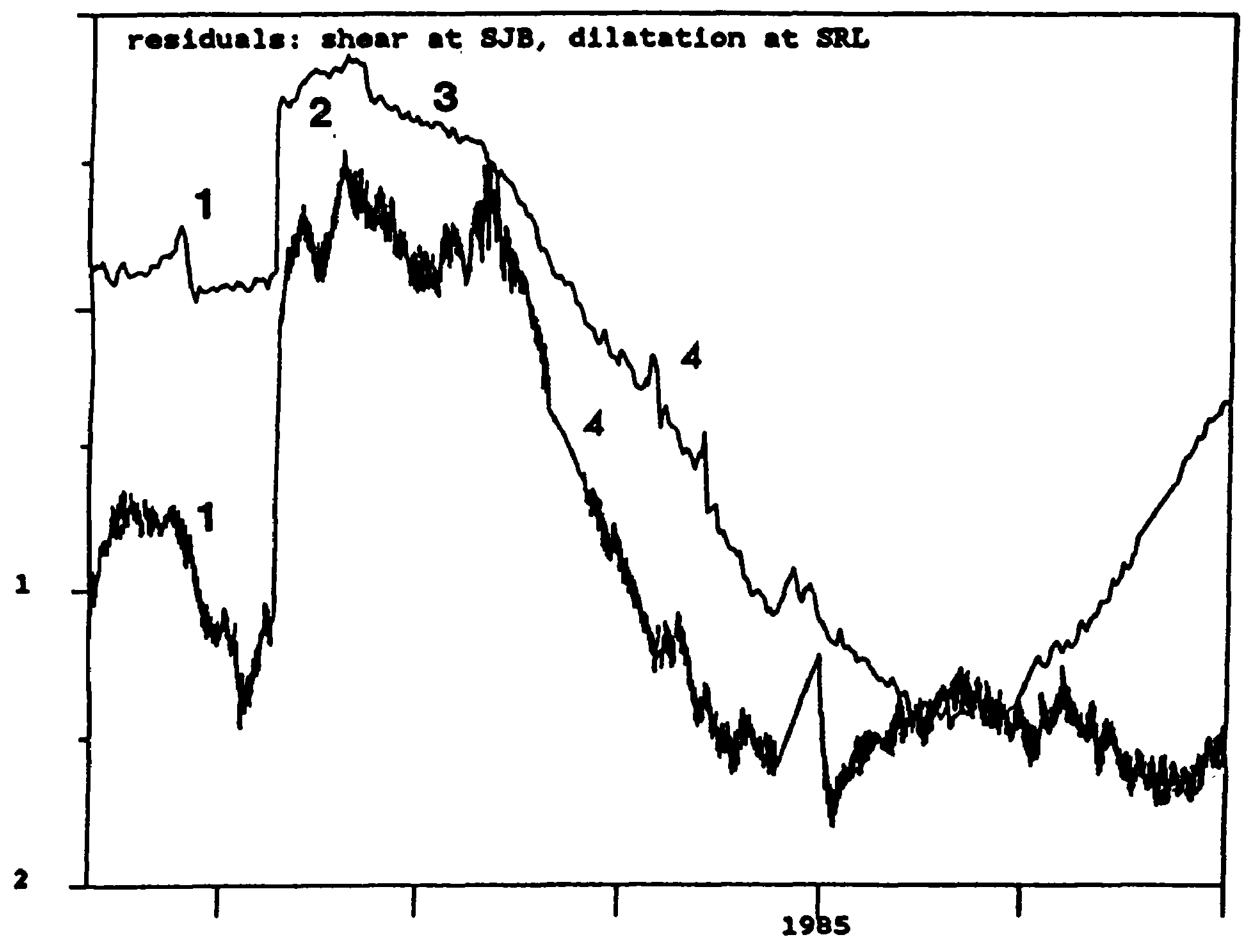

Fig. 2. Detrended strain recorded at San Juan Bautista (borehole tensor strainmeter, Gladwin 1984) and (upper trace) at Searles Road (dilatometer). Ordinate units are microstrain and time marks are months.

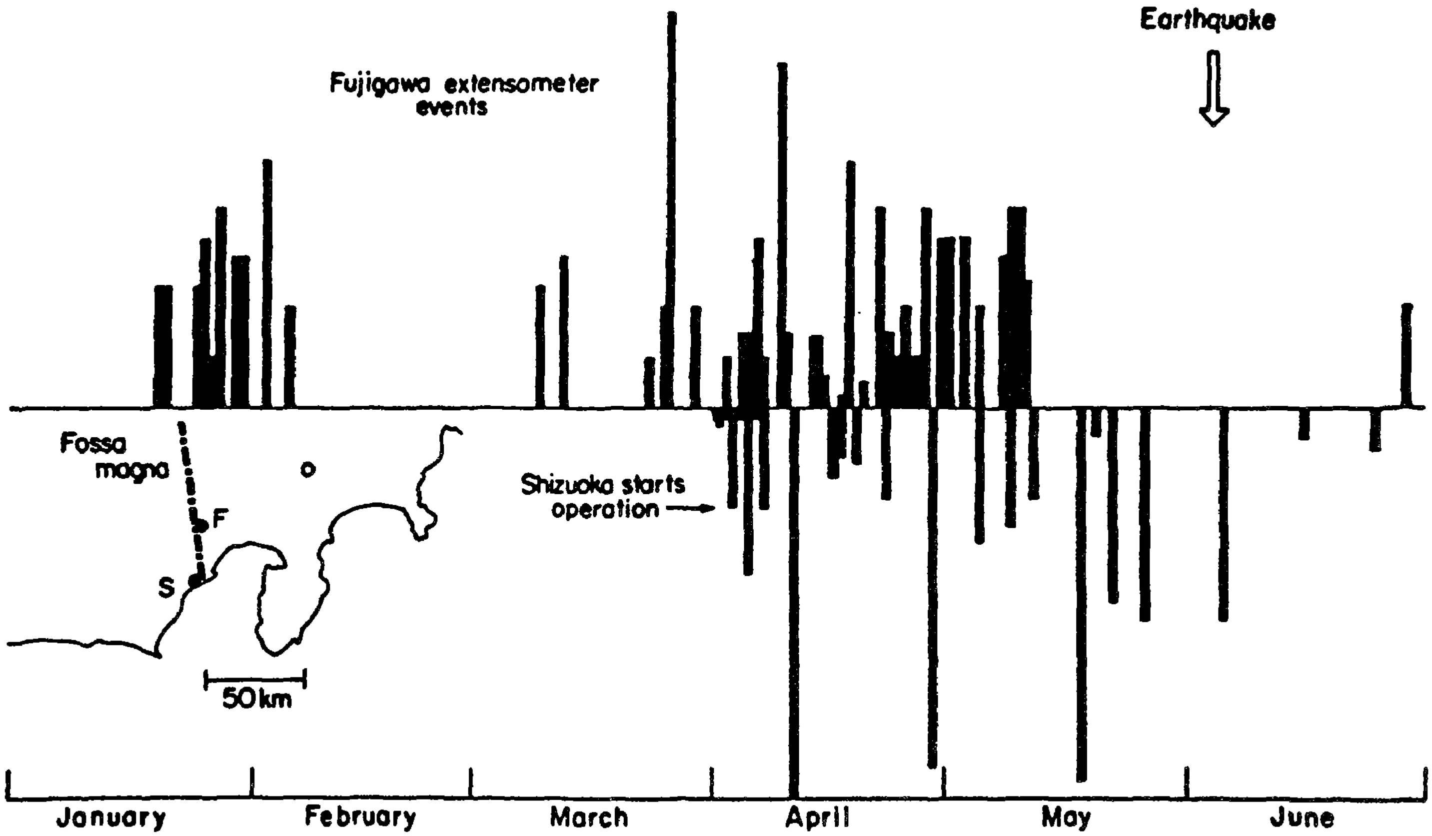

Fig. 3. Time history of the slow earthquakes (recorded on the borehole strainmeter at Shizuoka and on the Fukigawa extensometers) preceding the m = 5.5 Yamanashi earthquake. The Shizuoka observatory began operation in April 1976. The amplitude scales for the two instruments are not the same, but the relative polarity of the strain steps is as indicated. Also included is a map showing the relative locations of the two observatories, the epicentre (O) and the Fossa Magna.

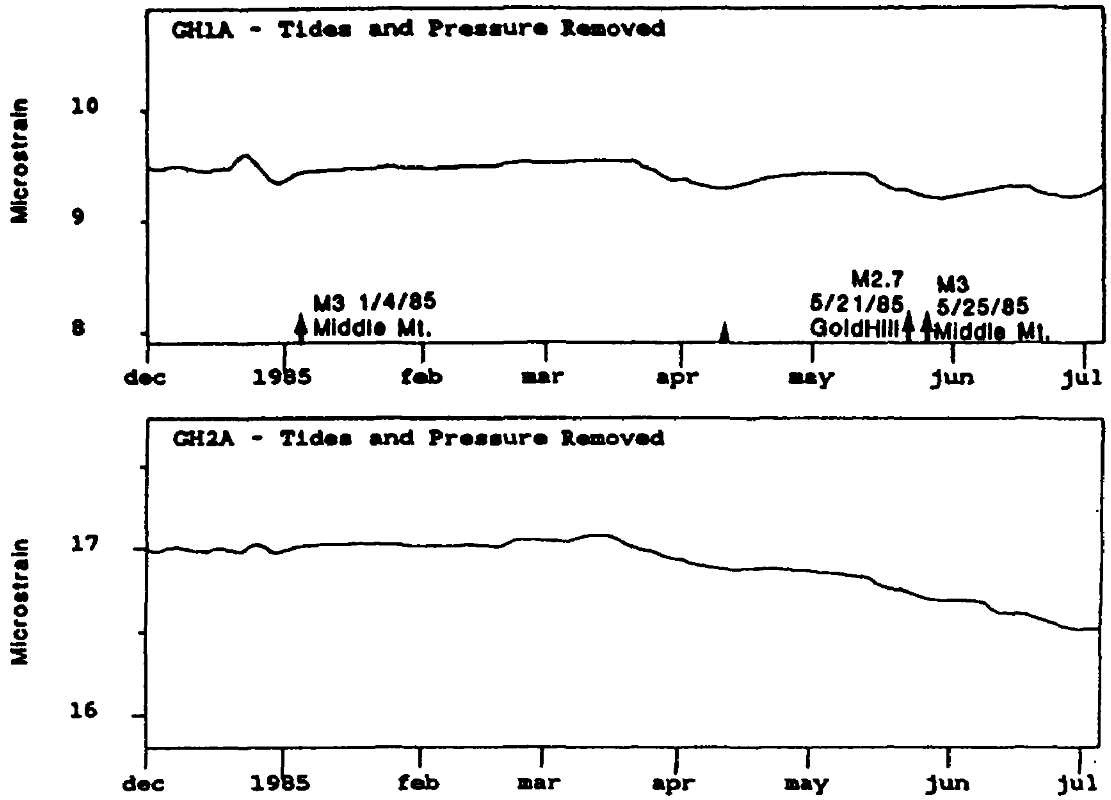

Fig. 4. Strain changes recorded by nearby dilatometers GH1A and GH2A.

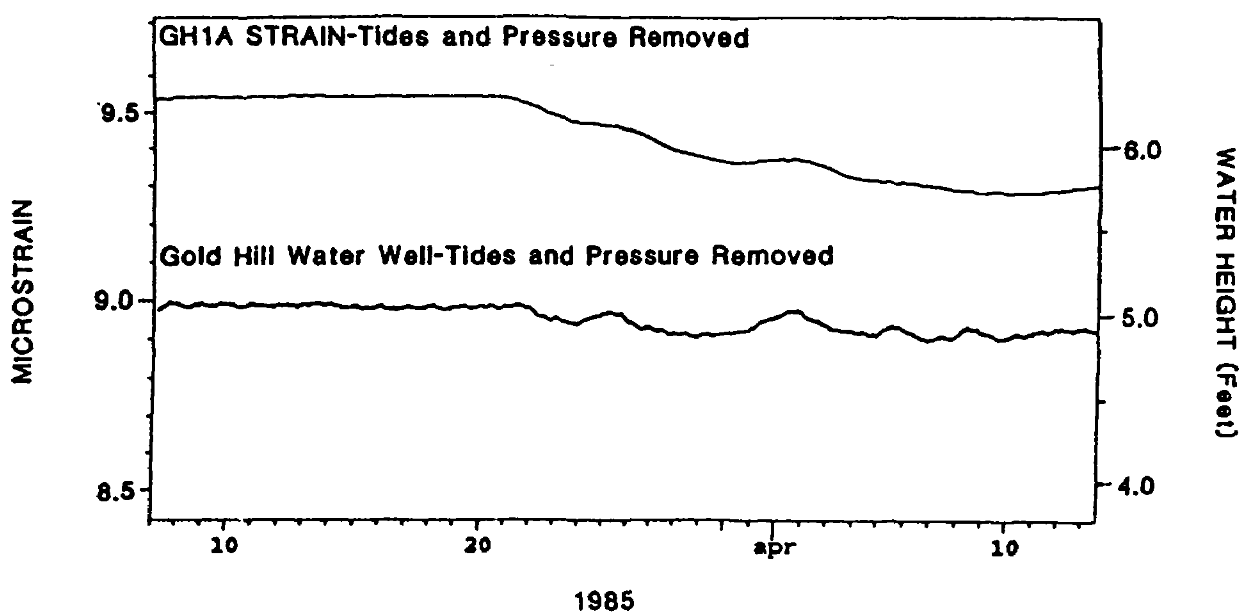

Fig. 5. GH1A strain compared with well water level.

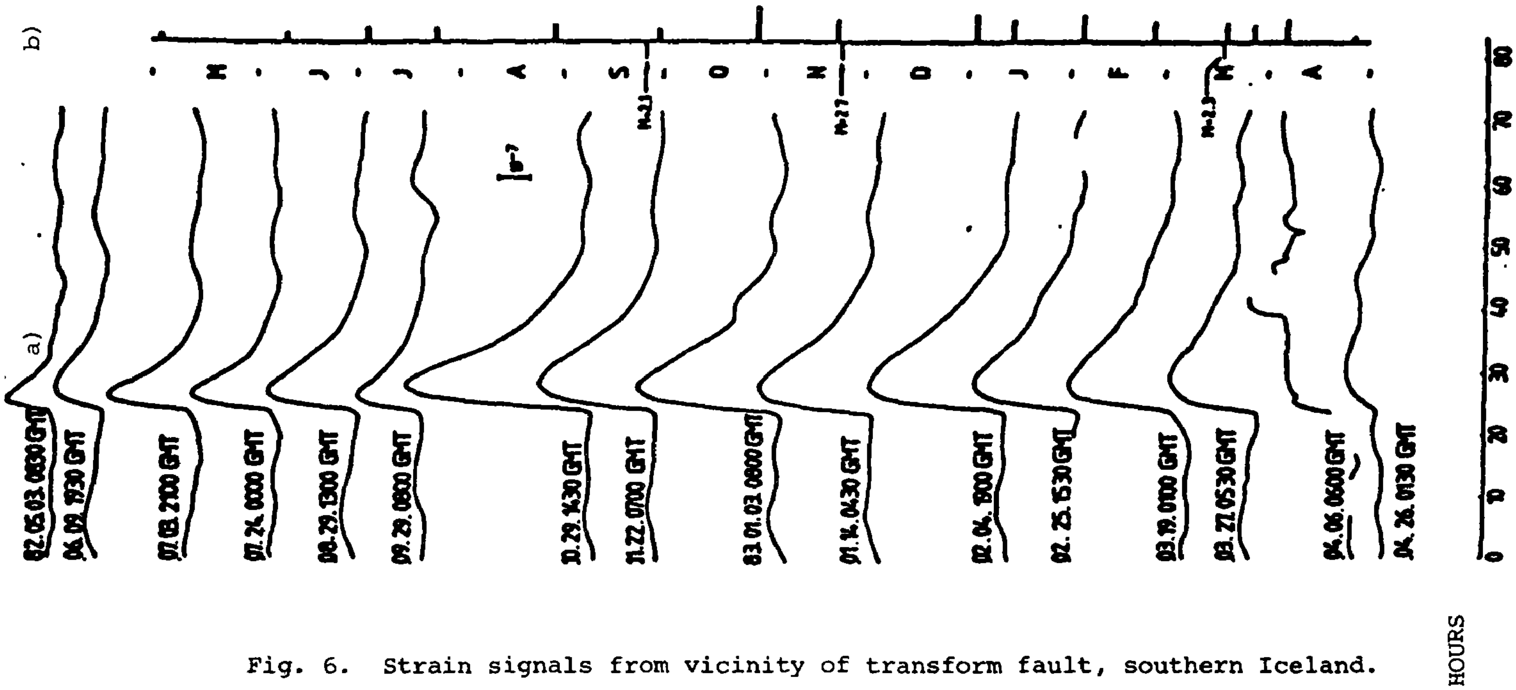

Fig. 6. Strain signals from vicinity of transform fault, southern Iceland.

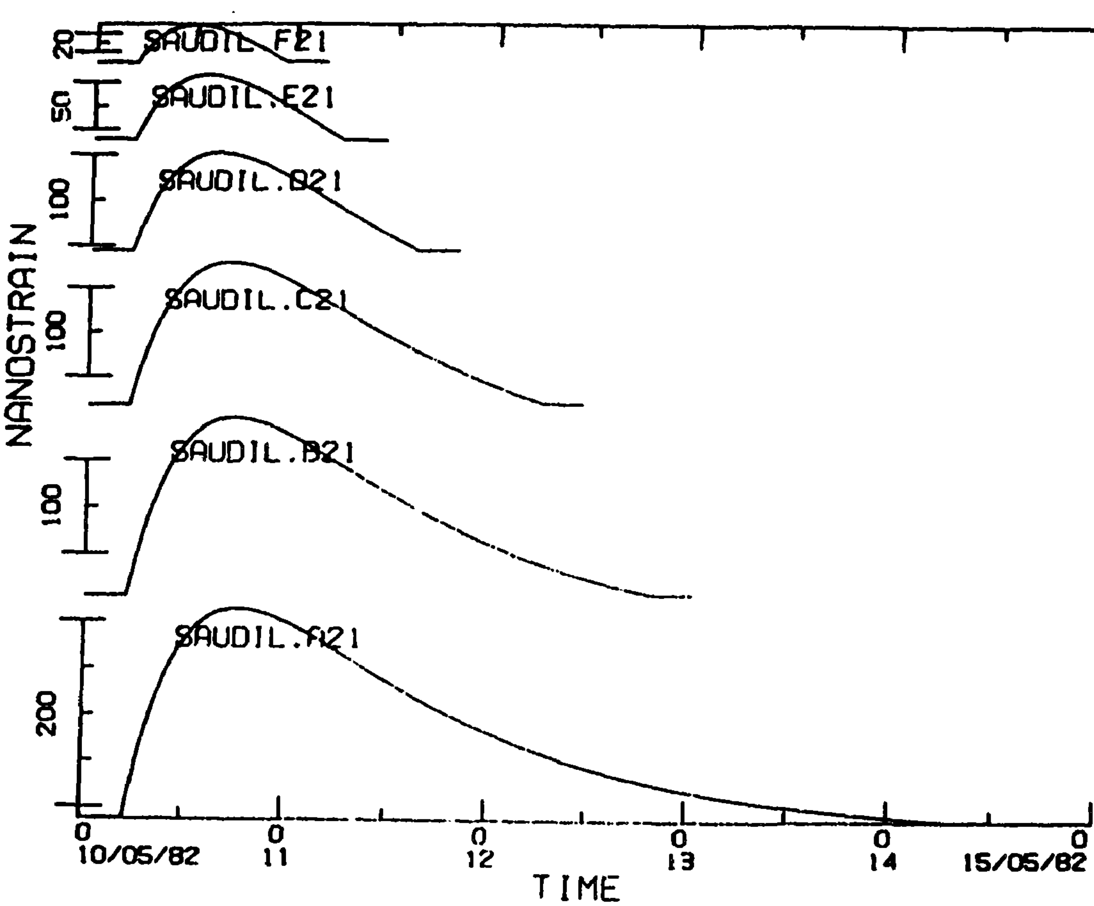

Fig. 7. Strain resulting from slip on transform fault - for various start and end positions.

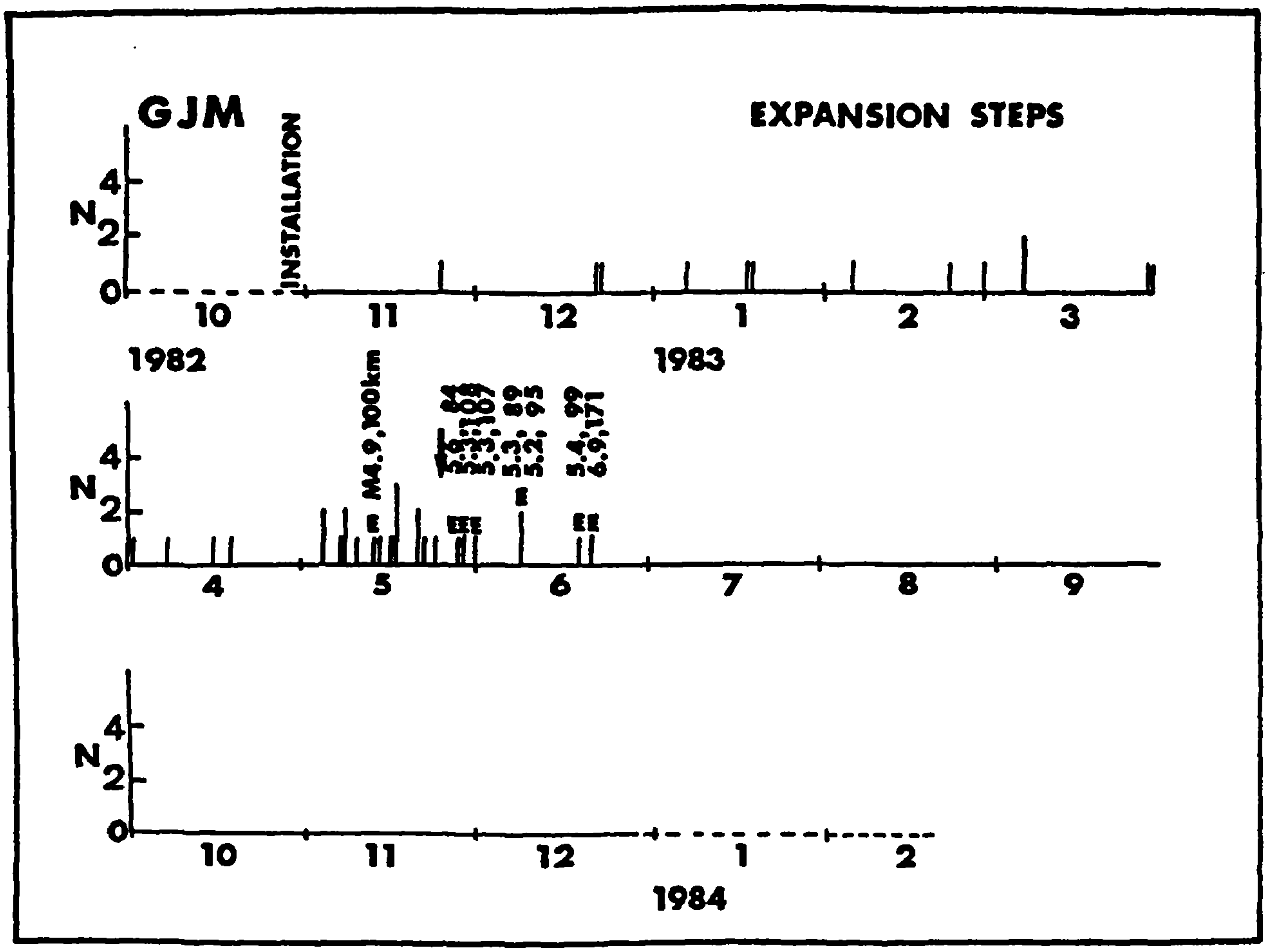

Fig. 8. Calendar of pulses preceding Japan Sea earthquake of 1984, mag 7.8.
Pulses cease after the m = 6.9 aftershock.

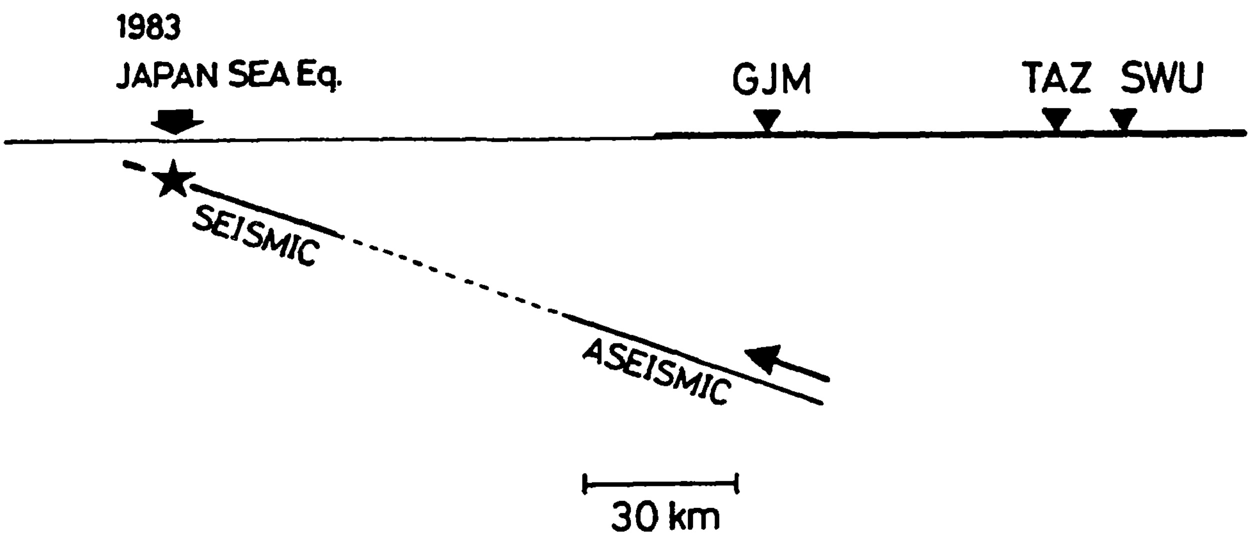

Fig. 9. Pulses can be modelled as slip on the extension of the main shock.

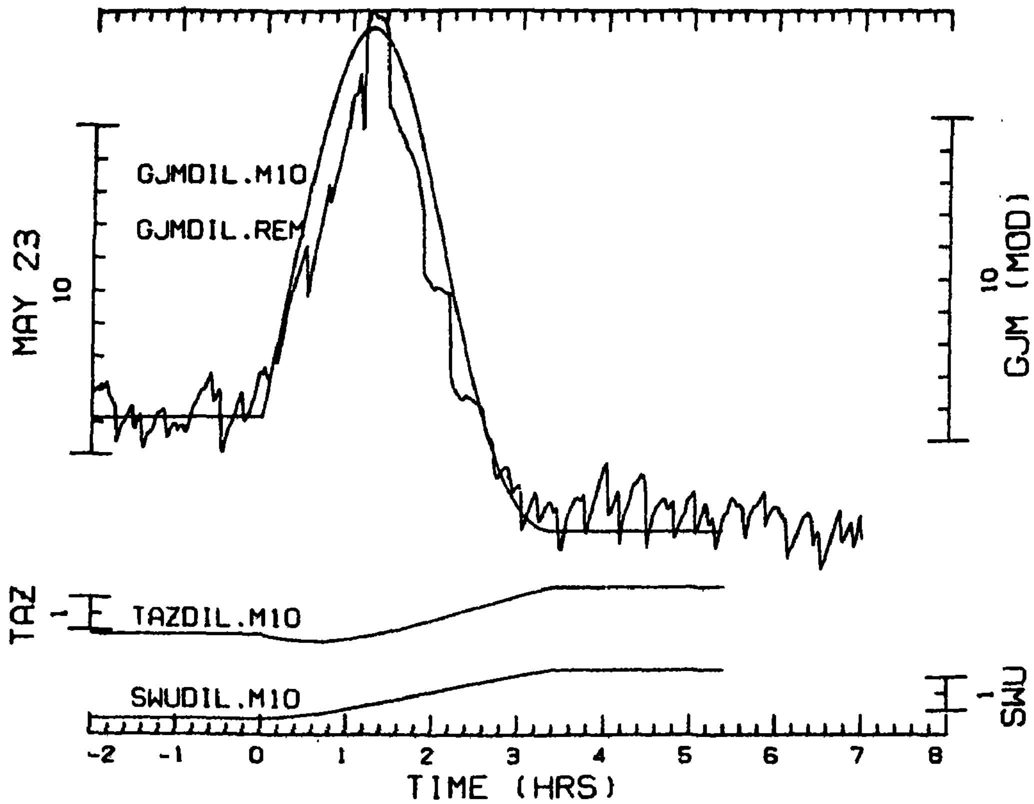

Fig. 10. Strain calculated from geometry in Fig. 9, compared with observed strain pulse.

Parkfield Seismic Experiment

9930-02098

Allan G. Lindh, Catherine M. Poley
John Estrem, and Barry Hirshorn
Branch of Seismology
U.S. Geological Survey
345 Middlefield Road, MS-977
Menlo Park, California 94025
(415) 323-8111, Ext. 2042

Investigations

1. Real-time monitoring and analysis of Parkfield seismicity, as part of the Parkfield Prediction Experiment, with special attention given to seismicity near Middle Mountain.
2. Continued work on long-term earthquake probabilities along the San Andreas system.
3. Relocation and spatio-temporal analysis of central California coastal seismicity.
4. Coda-magnitude and "envelope magnitude" study.
5. Daily reprocessing and maintenance of RTP data, with an eye to seismicity changes. Bi-weekly review of station and network performance.
6. Continued work on incorporation of RTP and CUSP data into one database.
7. Monitoring of Parkfield leveling network and analysis of leveling data, as part of the Parkfield Prediction Experiment.

Results

1. Overall seismicity at Parkfield for the time period 1 October 1986 - 31 March 1987 was normal with 99 events. Activity near Middle Mtn. was slightly higher than normal with 33 events. Nine (9) of these events resulted in seismic alerts (see Figure 1). Six (6) were level D and one (1) was level C; this matches the anticipated rate for level C alerts and exceeds the anticipated rate for level D alerts by 3 alerts (see Bakun, this volume).

   Events of interest include:

   (1) A magnitude 2.66 in MM3 (the zone under Middle Mtn. below 6.5 km) on 2 February 1987. This event was associated with an increase in activity at Middle Mtn. during 29 November 1986 - 2 February 1987 (see Figure 2b). This is similar to the seismicity pattern observed there during December 1985 - January 1986.

   (2) The creeping section (NW of Middle Mtn.) had more activity than usual, particularly in February when sixteen (16) events occurred. A magnitude 2.3 on 22 October 1986 and a magnitude 2.0 on 21 February 1987 occurred in this region (see Figure 2c).

Catherine Poley, with Allan Lindh, Bill Bakun and Sandy Schulz, has completed work on analysing the effects of the 2 May 1983 M=6.7 Coalinga earthquake on the Middle Mtn. section of the San Andreas fault. Coincident changes in surface creep and deep seismicity near the Parkfield Preparation Zone (PPZ) following the Coalinga earthquake suggest that both respond to the same stimuli. These changes were concentrated near the point of initiation of the magnitude-6 characteristic Parkfield earthquakes, lending credence to the hypothesis that this section of the San Andreas fault is characterized by a unique set of physical properties. The term "enhanced stress sensitivity" seems to us to adequately describe the PPZ. We believe that evidence for enhanced stress sensitivity beneath Middle Mtn. provides a basis on which to begin to seek a physically plausible unifying concept for earthquake prediction. A paper discussing this work is in press with NATURE.

Events from Parkfield are now being loaded into the VAX750 Parkfield disk for routine analysis of the seismograms.

2. Allan Lindh, using the different approaches used to calculate foreshock probability gains for Parkfield, has extended his study to determine the likelihood that the next characteristic Parkfield earthquake will be a foreshock to a larger earthquake on the southern section of the San Andreas. Efforts continue, to refine the probability estimates of the next characteristic Parkfield earthquake. A paper concerning these questions is in preparation.

3. Catherine Poley, with Allan Lindh and Jerry Eaton, has collected all the phase data from coastal California from San Francisco to the Transverse Ranges. Relocation and analysis of these data are underway and include systematic relocation, focal mechanism determination and stereo-plot projections of the seismicity.

   A subset of this coastal region is the seismicity which occurs in the San Ardo region. The November 24-25 1985 San Ardo earthquake sequence has been studied and is the subject of a paper in preparation by Catherine Poley.

4. Barry Hirshorn, with Allan Lindh, has developed a coda-magnitude relation by taking the RTP codas form the low-gain stations for all the M3+ events in the Coast Ranges, and regressing them against Berkeley's preliminary M_L estimates for the same events. Allan Lindh has used this formula, with station corrections determined by Caryl Michaelson, as the basis for a new computer program which allows rapid determination of magnitudes (M_z) from low-gain station coda lengths using RTP and Prototype online phase data. For events between M3 and M6, M_z appears to be a quite stable estimate of M_L (see Figure 3). An open-file report concerning this subject is in preparation.

5. Allan Lindh meets with John Van Schaak twice a week to review station performance. Barry Hirshorn, in conjunction with reprocessing of RTP data, runs weekly station quality meetings.

6. Successful efforts continue to incorporate RTP data in the CUSP database. RTP data is now reprocessed within the CUSP database.

7. John Estrem continues to keep the leveling network at Parkfield functional, and routine analysis of the leveling data continues. A fault-crossing leveling line has been installed at Gold Hill.

Reports

Poley, C.M., Lindh, A.G., Bakun, W.H. and Schulz, S.S., 1987, Temporal changes in microseismicity and creep near Parkfield, California, NATURE, in press.

Jones, L.M. and Lindh, A.G., 1986, Foreshocks and earthquake prediction at Parkfield, California, in branch review.

Bakun, W.H., et al., 1987, Parkfield Earthquake Prediction Scenarios and Response Plans, U.S. Geological Survey Open-File Report 87-###.

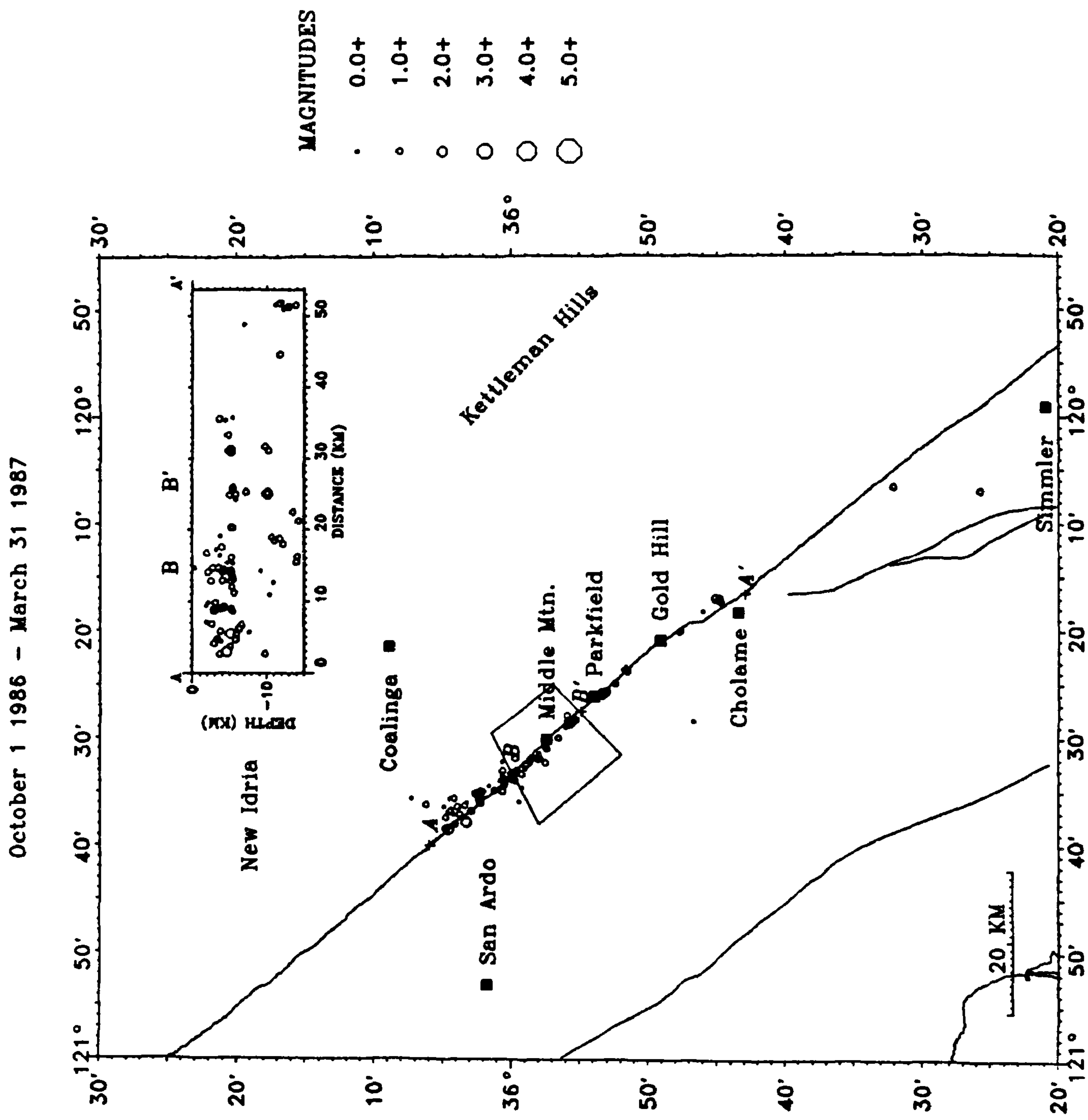

Figure 1. Map of epicentral locations, all magnitudes, from October 1, 1986 thru March 31, 1987. Inset is cross-section along A-A'. The Middle Mtn. region is indicated by the quadrilateral and by B-B' in the inset.

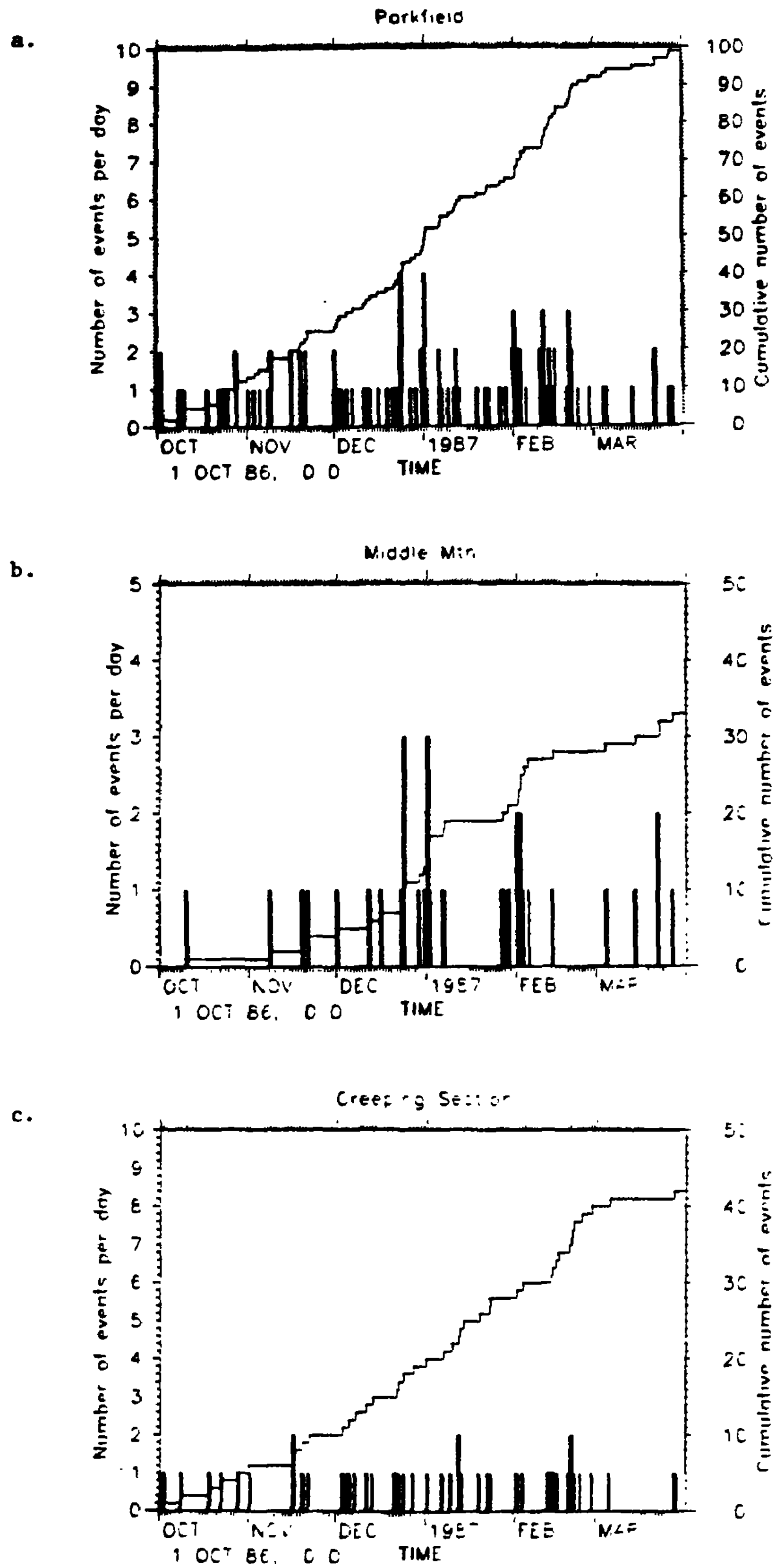

Figure 2. Histograms and cumulative number plots of seismicity, all magnitudes, form October 1, 1986 thru March 31, 1987. a) Parkfield seismicity. b) Middle Mtn. seismicity. c) Creeping section seismicity.

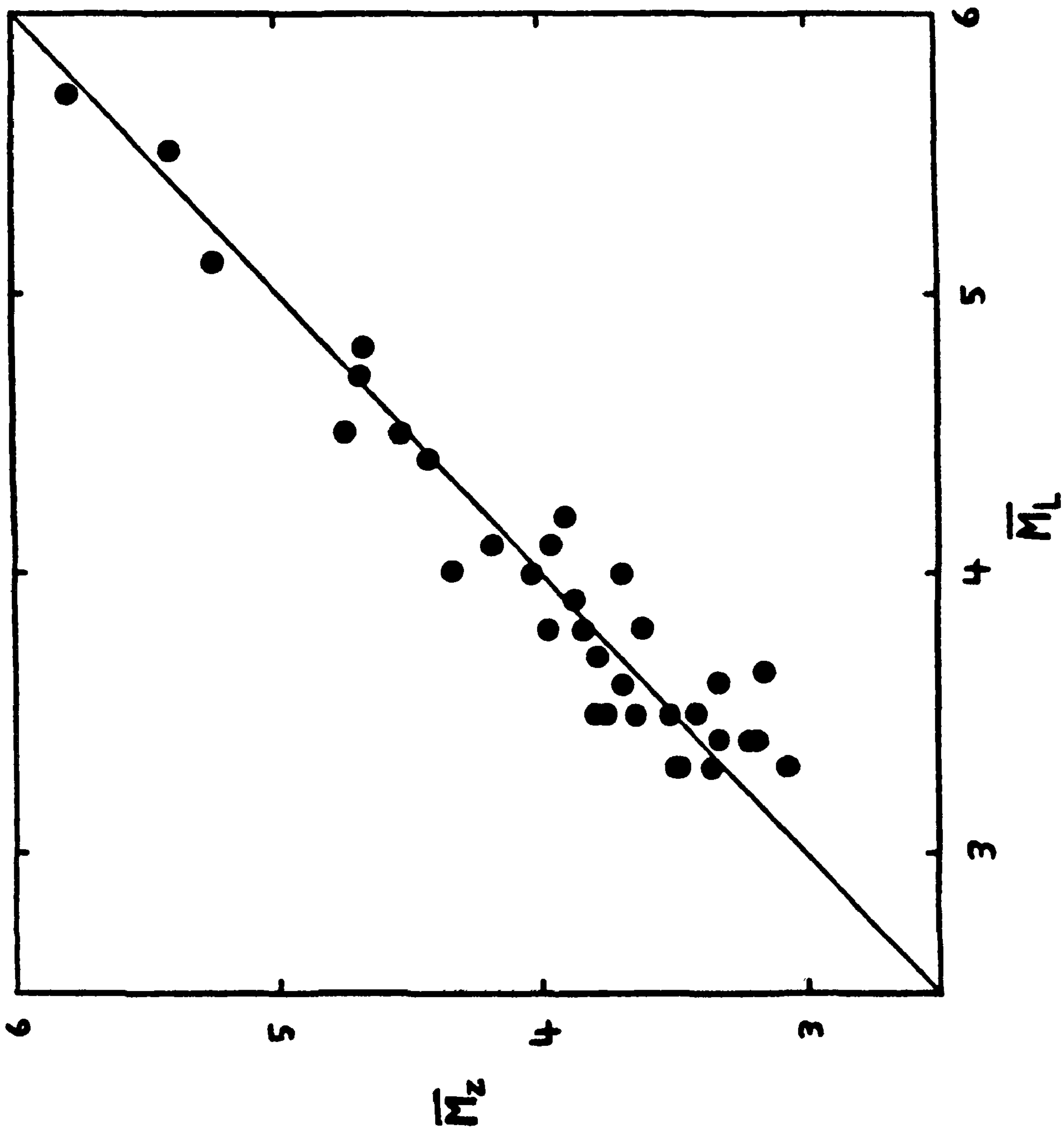

Figure 3. Derived M_Z values vs. M_L. The slope of the line is 1.00 and the intercept is 0.00.

High Sensitivity Monitoring of Resistivity and Self-Potential Variations in the Palmdale and Hollister area

14-08-0601-G109

T.R.Madden
Department of Earth Atmospheric and Planetary Science
Massachusetts Institute of Technology
Cambridge,MA 02139

A large effort during this and the previous reporting period has gone into reconstituting the telluric arrays. Cultural developments and telephone system changes have forced us to make several changes in the array. Thanks to some very significant help from Pacific Bell and further help from GTE and AT&T we should have our arrays in good working order for the foreseeable future. In the Palmdale area Pacific Bell replaced a cable across the San Gabriels with a fully digital cable but worked in two all metal pairs in order to keep our measurements from Palmdale to Placerita and Palmdale to Castaic intact. GTE closed several substations in the Azusa area and had to reconfigure our line from Pasedena to Azusa. In the Hollister area AT&T, due to the divestiture agreements, was required to close a cable that connected us from SanJuan Bautista to Wattsonville but they are arranging to jump us over to a Pacific Bell cable that can keep us connected. We also had to relocate two electrodes. The Castaic electrode was swallowed up by a condominium development and the Hollister electrode was eliminated when a cable post from which we had a drop was mistakenly taken out. We have been able to relocate both these electrodes short distances away from their original locations. We have also been changing all the electrodes in order to make the array more robust. The Cu:$CuSO_4$ electrodes have now been all replaced by Cu electrodes and new and more rugged cabling installed between the electrodes and the telephone line terminals. The original electrodes had worked very well, but the need to keep the fluid level up in the electrodes required more frequent checks than was feasable. We are hoping that the greatly increased area of the new electrodes will actually help reduce electrode rectification of A.C. noise.

Finally and perhaps the most important issue of the reconstitution of the telluric arrays is the matter of the data recording. For many years the array data has been recorded and stored for us by Cal Tech. At one time they were servicing quite a few data collecting projects with their system, but in recent years only a few stations were still in operation. With the installation of a new computer at the Seismo-Lab it was decided not to reprogram the data collecting system and as of the first of April Cal Tech ceased supporting the data collecting. The lead time on this decision was a bit short but fortunately we had been considering making some improvements in the system with onsite data editing which is only a step removed from data recording and we should have a new system up and going this month.

Our plans call for a computer to be installed at each of the two recording sites which will digitize, edit, and store the data. The data can periodically be transfered to floppy disks for transmission to our laboratory. The computer will also carry out a first order analysis of the data and each day the results of this analysis will be transfered onto a network in order to keep us up to date on the array performance. We will also experiment with onsite editing of data glitches and if this works well we will modify the electronic averaging in order to expose the glitches more clearly.

Figure 1 shows the last half year of results from the Palmdale array. The Go-Fp and Az-Su data is telemetered and will require more careful analysis to deal with noise problems. We believe the variance estimates are too small and that the variations shown are not significant. Dipole G is formed from the sum of the two reference dipoles and is therefore only a test of the electronics. The rest of the array was a bit noisy but holding to its historic relationships.

The Hollister data is showing problems which we have traced to the digitizer and this was the reason we had started to design a new recording system. Until the new system is in place and a finite amount of its data has been analysed we will have to hold off on our previous declaration that resistivity variations had occurred in the region prior to the Tres Pinos earthquake.

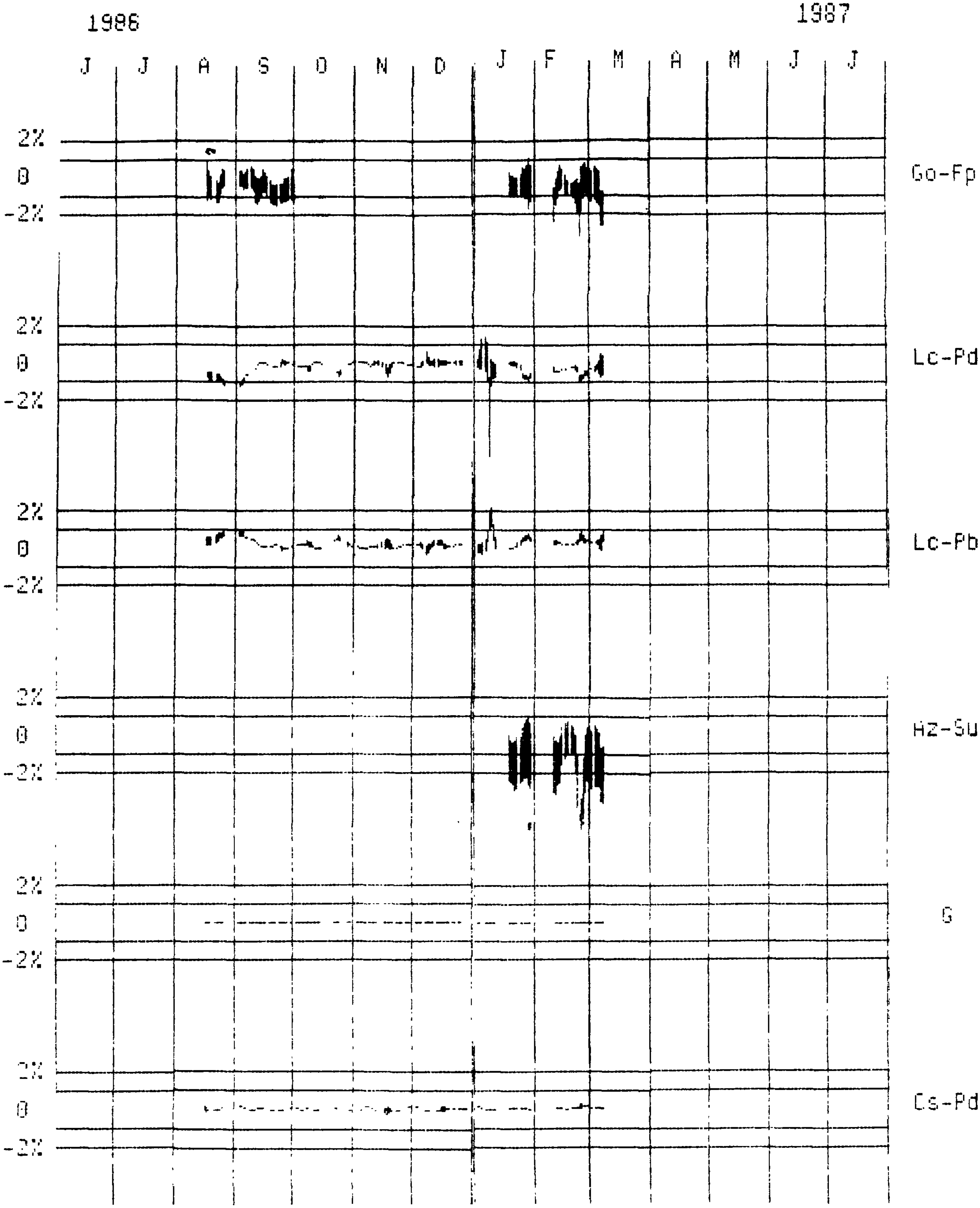

Fig 1 PALMDALE TELLURIC ARRAY

SEISMIC WAVE MONITORING IN CENTRAL CALIFORNIA

14-08-0001-G1149

T.V. McEvilly
R. Clymer
Seismographic Station
Berkeley, California 94720
415/642-3977

INTRODUCTION

Our primary objective is to carry out a program of seismic wave measurements which will be used to analyze properties of the San Andreas fault zone at Parkfield, California. We are using an array of three-component borehole seismometers surrounding the epicenter of the 1966 M5.6 Parkfield earthquake, and a multi-channel data acquisition system featuring digital telemetry and computer-based recording with 9-track tape output in a conventional format. Two types of measurements are being made:

1) Controlled source: Regular, repeated recordings of controlled-poliarization signals from a shear-wave vibrator to detect changes in anisotropy, attenuation, and velocity.

2) Earthquake source: Continuous recording of local micro-earthquakes. Results will be used a) in an attempt to study asperities, and b) to assess the use of small repeating (characteristic) earthquakes to detect temporal changes in source parameters and fault-zone properties.

Secondarily, we are attempting to maintain the long-standing P-wave monitoring program at Hollister, California. However, measurements there have been much reduced to free resources for the Parkfield study.

During the first half of FY 86-87, considerable effort was expended on site instrumentation and maintenance, and on continued acquisition system debugging. Preliminary controlled-source measurements were made and a limited monitoring program was begun. Continuous recording of earthquakes was begun.

GOALS AND INVESTIGATIONS

1. Site instrumentation

Instrumentation of the Parkfield seismometer sites with data acquisition equipment continues as seismometers are installed and equipment becomes available. We and U.C. Santa Barbara have made and maintained temporary installations, and the U.S.G.S. (Menlo Park) has been responsible for the permanent (low-maintenance) installations.

2. Acquisition-system development

We have continued to test and debug the new Ref Tek/Wescomp data acquisition system assembled for the Parkfield study.

3. Preliminary controlled-source studies

Five to ten short profiles are being carried out, recording signals from the entire borehole array and operating the vibrator with several polarizations at 100 m intervals at sites shown in Figure 1. The results will be used to establish target events for monitoring and to assess our capability to detect changes in shear-wave anisotropy and attenuation.

4. Earthquake studies

Recording of local Parkfield micro-earthquakes has begun. This is a cooperative effort involving U.C. Santa Barbara, U.C. Berkeley, and the USGS.

5. Hollister project

We are attempting to continue a reduced set of measurements at Hollister.

RESULTS

1. Nine seismometer sites are now available, shown by the solid circles in Figure 1. All but site SM have been instrumented with acquisition equipment. The permanent installations (involving solar panels, trenched cables, proper housing of instruments, etc.) at the other eight sites are nearly complete.

2. The acquisition system is operational. System reliability has been significantly improved and noise levels significantly reduced by our efforts and those of the equipment manufacturers. False triggers in earthquake recording have been markedly reduced. Some bugs remain and further improvements are expected. Upgrades presently ordered will improve the earthquake trigger algorithm and will add trigger time and date to the tape headers.

3. Two profiles have been recorded (the vibrator sites are shown by the two numbered squares in Figure 1), with two orientations of the shear-wave vibrator. Examples of results are shown in Figures 2, 3, and 4. Clear arrivals with usable signal-to-noise (S/N) ratios are seen at all sites except the two with the greatest source-receiver offsets. We believe we can improve S/N by another factor of four by summing more source sweeps and reducing remaining system noise. These data are being further processed and compared to reprocessed COCORP Parkfield results.

   These measurements mark the beginning of the monitoring program; they will be repeated at regular intervals.

4. We have been recording earthquakes with seven to eight sites operating since mid-December, 1986. After experimentation with triggering parameters and amplifier gain, the system is now reliably recording local events of roughly zero magnitude to M3.0+.

   An example of a local earthquake recorded in December, 1986 is shown in Figure 5. In Figure 6, we compare seismograms from the Middle Mountain (MM) site for the event shown in Figure 5 with a second, nearly idéntical event. Magnitudes are roughly M = 0.5-1.0. We believe these are "characteristic", i.e., repeating, earthquakes from a common source point.

5. No measurements were made at Hollister during this period.

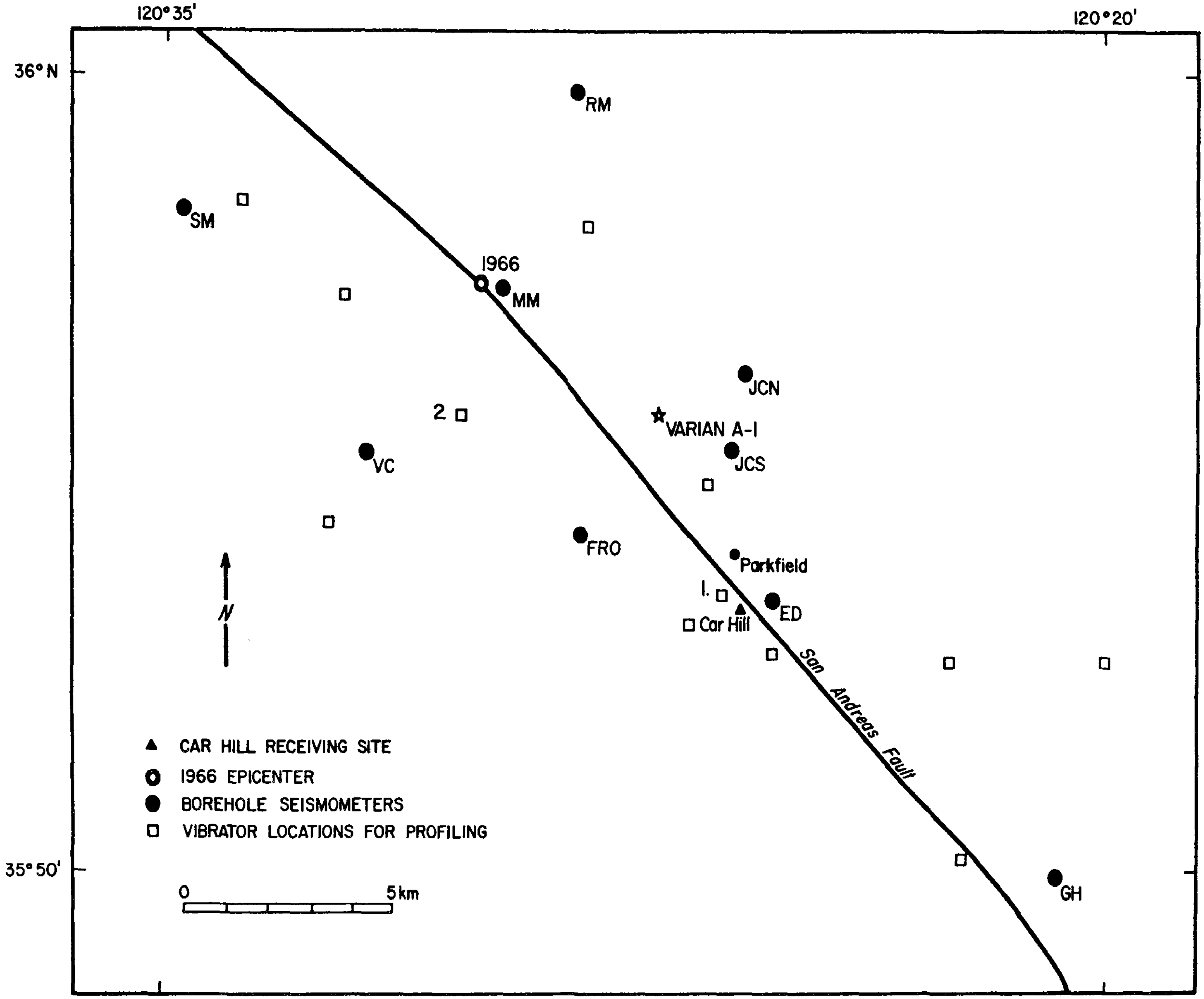

Figure 1. Parkfield area location map. Closed circles show sites of 3-component, borehole seismometers. All but site SM are presently operating. Open squares show sites of short lines of vibrator positions for profiles; numbered squares are those accomplished.

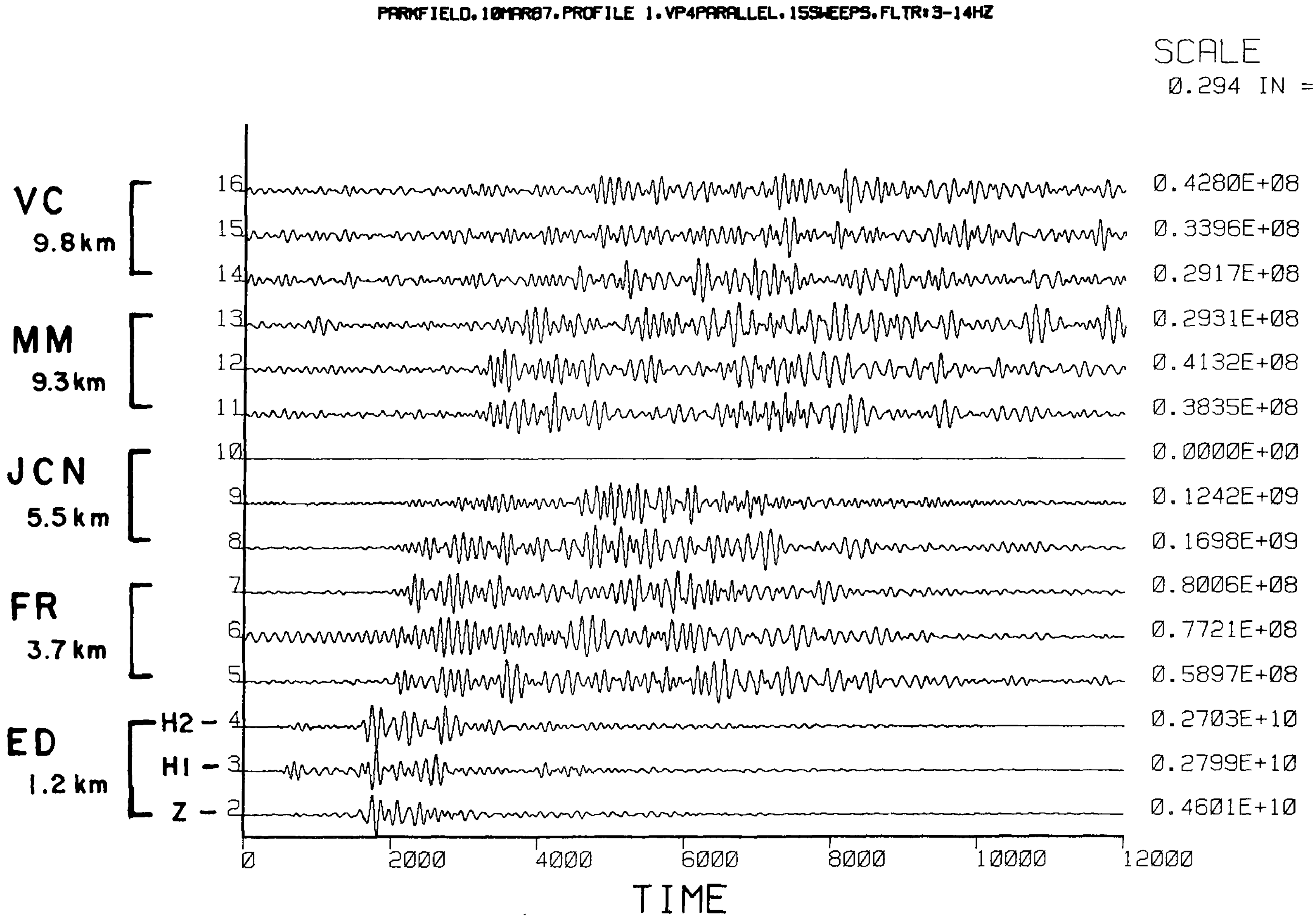

Figure 2. Controlled-source, correlated signals from five of the 3-component borehole seismometers, with the vibrator at one of the source positions of profile 1, near Car Hill (Figure 1). The vibrator baseplate motion was roughly east-west (N101°E). Sites SM and JCS were not operational at the time. Not shown are recordings for sites RM and GH, which were too weak to be usable due to the long offsets. To the left are site and component identifications and source-receiver offsets.

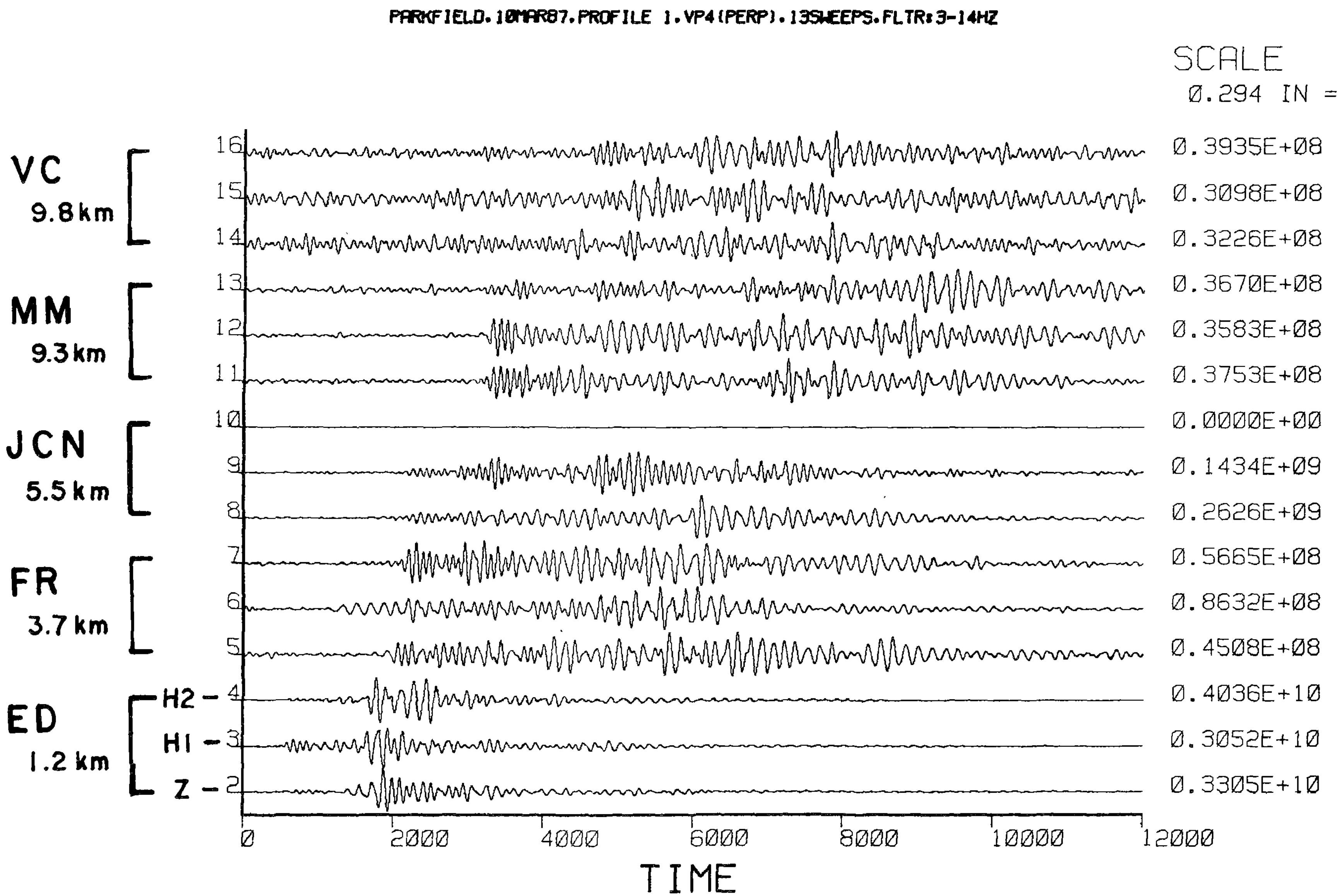

Figure 3. Similar to Figure 2, but with vibrator baseplate oriented roughly north-south (N11°E).

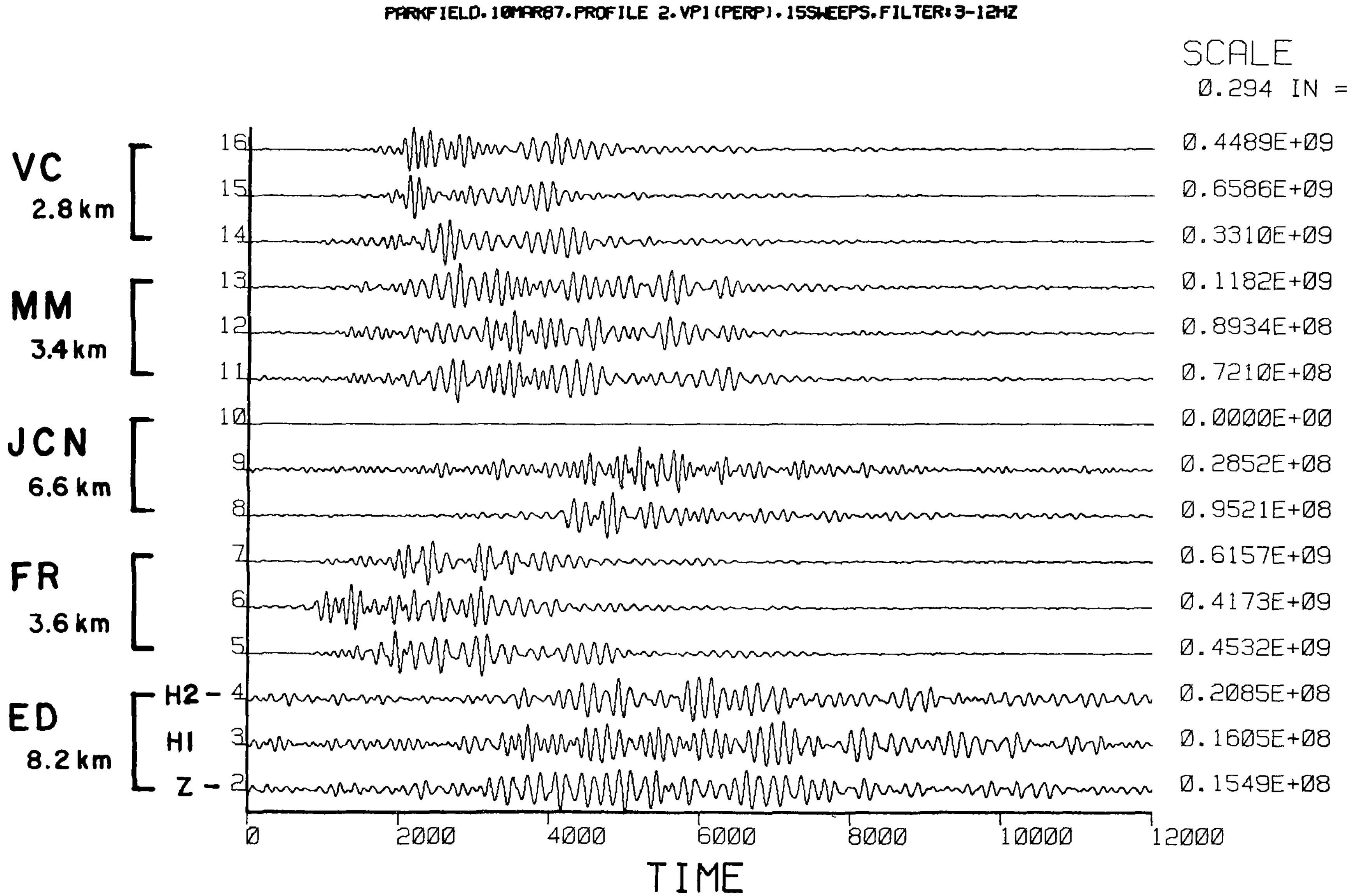

Figure 4. Similar to Figure 2, but with the vibrator at one source position of profile 2, near site VC. The vibrator baseplate orientation was roughly northeast-southwest (N43°E).

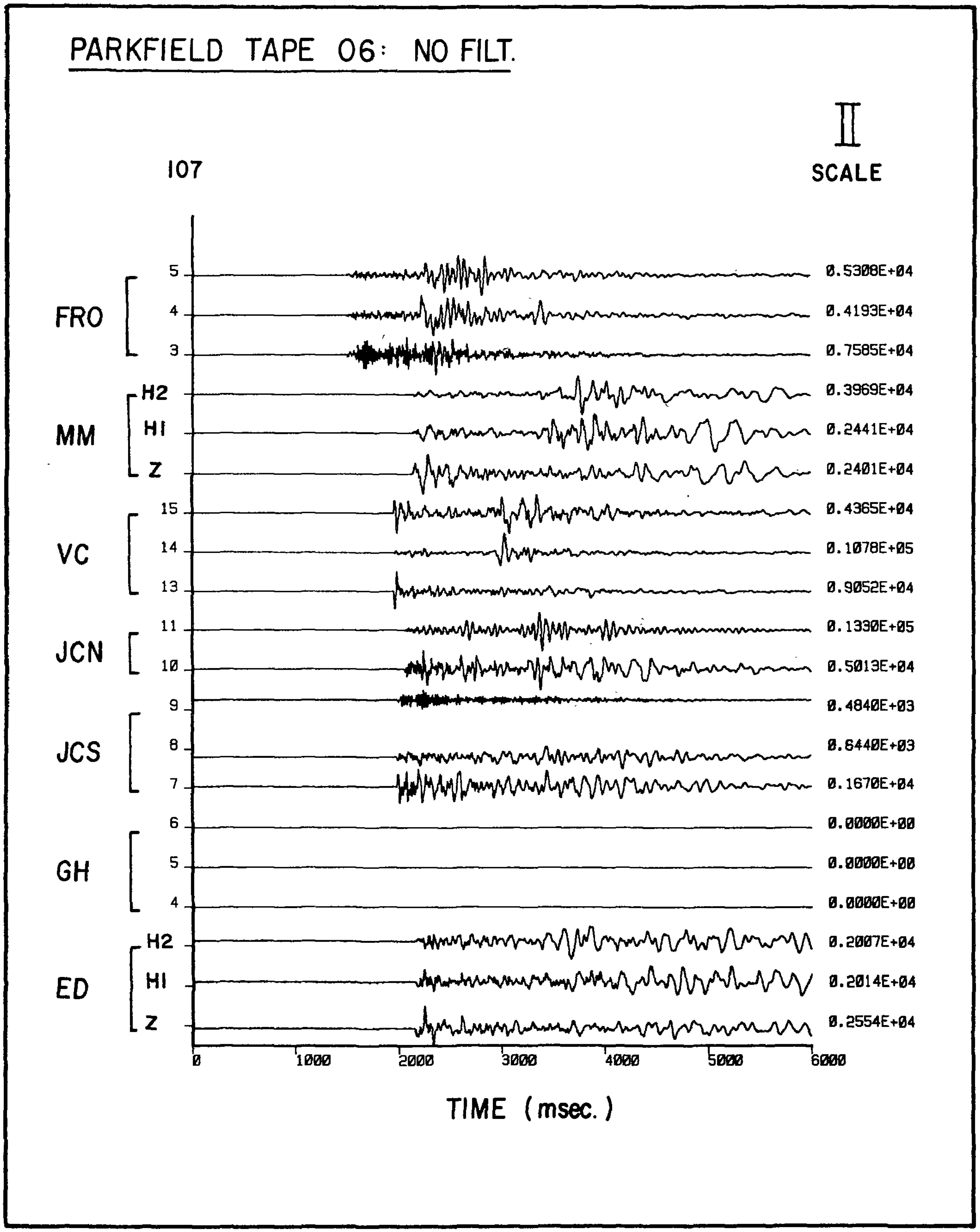

Figure 5. A local Parkfield earthquake, recorded on the Ref Tek/Wescomp acquisition system. Local magnitude is in the range .5-1.0. Site and component identifications are on the left. Amplitude is scaled trace-by-trace; on the right are the number of counts between trace centers.

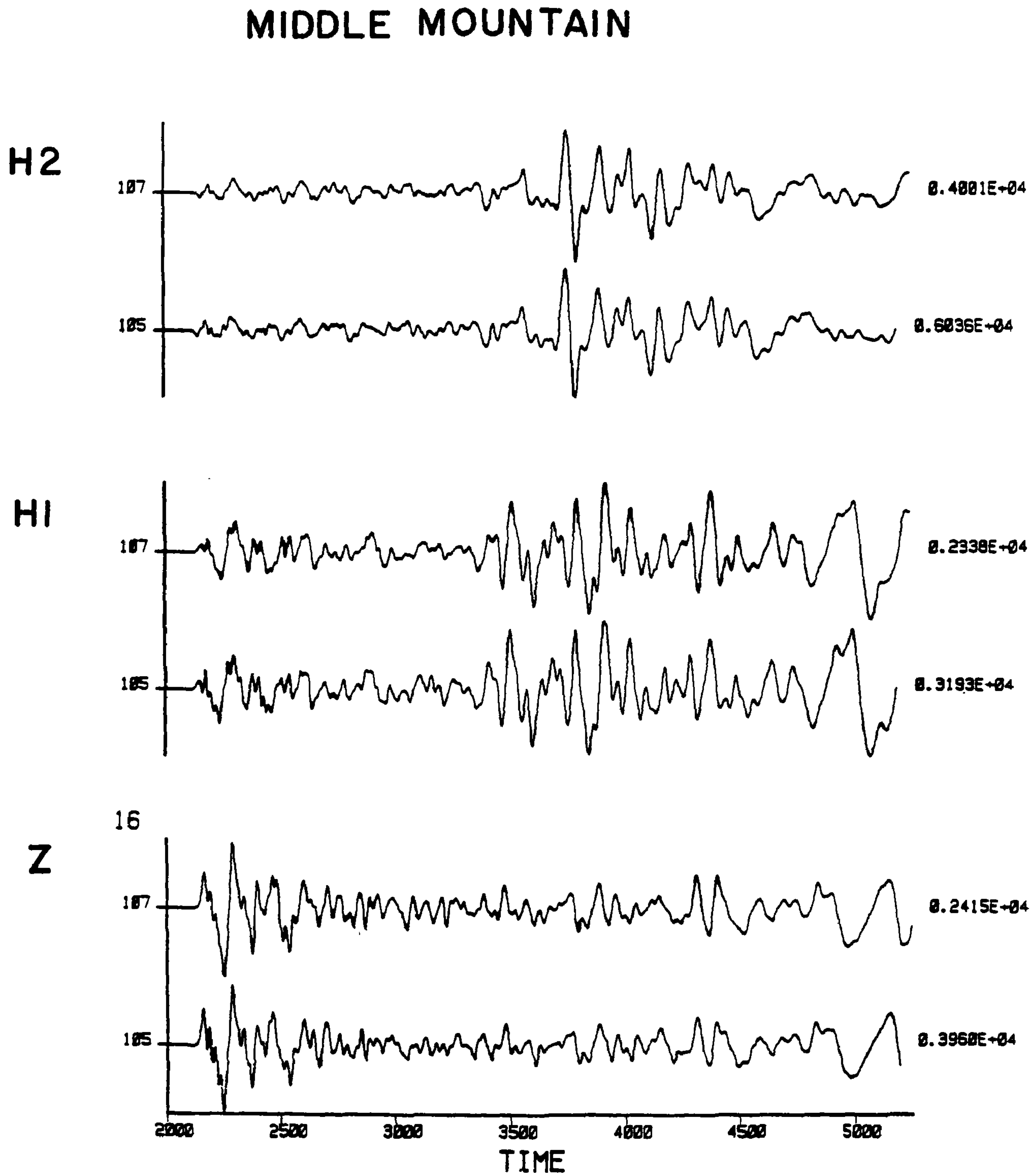

Figure 6. Comparison of seismograms from the Middle Mountain (MM) site for two nearly identical events (one of which was shown for all sites in Figure 5).

Crustal Studies

9930-02102

Walter D. Mooney
Gary S. Fuis
Branch of Seismology
United States Geological Survey
345 Middlefield Road - MS 977
Menlo Park, California 94025
415-323-8111 X2476/2569

Investigations

1. Continued analysis of seismic-refraction data from southern Alaska. This is part of the Trans-Alaska Crustal Transect (TACT) (Fuis, Ambos, Mooney, Page).

2. Preliminary analysis of seismic-reflection data from southern Alaska. This is part of the Trans-Alaska Crustal Transect (TACT) (Brocher, Page, Fuis).

3. Analysis of seismic-refraction data from western Arizona - southeastern California. This is part of the Pacific to Arizona Crustal Experiment (PACE) from seismic refraction data (Fuis, McCarthy, Wilson).

4. Interpretation of seismic-refraction data from Columbia Plateau, Washington (Catchings, Mooney).

5. Continued analysis of seismic refraction data from Maine and Quebec (Luetgert, Murphy, Mann).

6. Acquisition of seismic refraction data near San Luis Obispo, California (Walter, Sharpless).

7. Seismicity investigation in Jordan (Kohler).

8. Lithospheric studies in Nevada (Catchings, Mooney, Whitman).

Results

1. In 1984, the U.S. Geological Survey initiated the Trans-Alaska crustal Transect (TACT) program-- a coordinated geological and geophysical study of the structure, composition, and evolution of the Alaskan crust along a corridor parallel to the Trans-Alaska oil pipeline, from Valdez to Prudhoe Bay and across the adjacent Pacific and Arctic continental margins. TACT is a major element of the multi-institutional Trans-Alaska Lithosphere Investigation (TALI). The TACT project was launched in southern Alaska: in succeeding years the investigations will shift northward with the goal of completing the transect by the end of the decade.

A summary of the results from TACT are given in Page et al. (1986). Geologic, seismic, gravity, and magnetic data from the northern Chugach Mountains and southern Copper River Basin, Alaska indicate that the Chugach terrane (CGT) and the composite Peninsular/Wrangellia terrane (PET/WRT) are thin (<10 km), rootless sheets bounded on the south in both cases by north-dipping thrust faults that sole into a shallow, horizontal, low-velocity zone. The CGT has been thrust at least 40 km beneath the PET/WRT along the Border Ranges fault system (BRFS). Adjacent to the BRFS, uplift and erosion of 30-40 km since Jurassic time have exposed blueschist-facies rocks in the CGT and mafic and ultramafic cumulate rocks in the PET/WRT. Four paired north-dippping layers of low and high seismic velocities extend beneath the northern CGT and southern PET/WRT and may be slices of subducted oceanic crust and upper mantle; the upper two pairs may now be joined to the continental plate. Refraction data recorded along structure in the Prince William Terrane shows that the velocity structure south of the Chugach is different in that the velocities are much slower overall and there is no evidence of an imbricate stack of low high velocity pairs as is seen to the north.

Velocity models derived from the seismic refraction data are being used in the relocation of earthquakes recorded by the southern Alaska regional seismograph network. Beneath the Chugach Mountains relocated earthquakes fall into two groups: a few at less than 10 km depth within the accreted Chugach terrane and the majority between 29-44 km within the regional NNE-dipping Wadati Benioff zone associated with the Wrangell Mountains. The deep group lies within the lowermost of the four pairs, or duplexes, of high and low velocity rocks, suggesting that the deepest duplex was subducted most recently and the three overlying duplexes were emplaced earlier.

2. The USGS acquired 180 km of seismic reflection data along two lines in south central alaska for TACT. One line crosses the Denali Fault, the other the Border Ranges fault. The reflection line across the Denali fault shows little structure near the fault, but north of the fault, reflections are mostly sub-horizontal except for one conspicuous reflection which dips north to 12 s, where it intersects a flat-lying band of reflections which could correspond to the Moho.

   The Border Ranges fault also is not evident in reflection record, but south of this fault, alternating reflective and non-reflective bands may correspond to the alternating higher and lower velocity layers modeled from the refraction data. Reflection events between 0 and 5 seconds undulate suggesting antiformal deformation of the rocks by thrusting, but those below 5 seconds can be divided into three major sub-horizontal bands. These bands could indicate mid-crustal decollements since the deepest of these bands appears to correlate in depth with the Benioff zone associated with the downgoing Pacific plate.

3. <u>PACE</u>

   During 1985, the U.S. Geological Survey initiated the Pacific to Arizona

Crustal Experiment (PACE), a multidisciplinary transect across western Arizona, southern California, and the offshore Pacific continental margin. Two hundred and sixty km of reversed seismic-refraction/wide-angle reflection data were recorded as a part of PACE across the Whipple Mountain metamorphic core complex in southeastern California (Fig. 1). The data were acquired along two perpendicular profiles consisting of 30 shots, 20 shotpoints, and station spacing of 500 m on one profile and 1000 m on the other. Collectively, these data represent one of the most detailed geophysical studies to date across a metamorphic core complex and provide an understanding of the crustal and geologic history of these isolated regions of unusually large extension.

Although analysis of the PACE seismic-refraction data is still underway, several significant results are already evident. First, on the NE-oriented profile a sharp velocity discontinuity is present throughout the survey at a depth of 16-18 km. This discontinuity separates a 6.0-km/s upper crust from a 6.5- to 7.2-km/s middle crust. In addition to this high-velocity layer, laterally discontinuous 6-8-km-thick low-velocity zones (LVZs) are evident both above and below it. The upper crustal LVZ is analogous to those previously identified in the northern Basin and Range province, but the lower-crustal LVZ has no counterpart in the Basin and Range. The data recorded on the perpendicular profile indicate a markedly different structure: a fairly monotonous 6-km/s crust with no high- or low-velocity layers that are continuous over large distances (more than 10 km). It is interesting to speculate that the absence of a high-velocity mid-crustal refractor on the NW-oriented line may be influenced, at least in part, by velocity anisotropy. Jones and Nur (1982) have shown that velocity anisotropy of as much as 20Δ can occur in many phyllosilicate-rich mylonitic rocks and that velocities are typically fastest in the direction of elongation in the core complexes, as is found in the midcrustal layer of Whipple Mountains. Another possible explanation for the midcrustal layer is intermediate to mafic sills. The crust must have been thickened by magma injection or some as-yet-unknown process of crustal convection beneath the Whipple Mountains, because, in spite of extreme extension in this mountain range compared to adjacent ones, the crust is of uniform thickness throughout the region.

5. Interpretation of a 260-km long seismic refraction profile across the Columbia Plateau reveals upper to mid- crustal velocities between 5.0 and 6.8 km/s, a lower crustal velocity of 7.5 km/s and an upper mantle velocity of 8.4 km/s. The upper crust above the crystalline basement consists of between 5 and 12 km of basalt and underlying sediments. The thickest accumulation of these rocks is beneath the Pasco basin which is interpreted to be a graben. In this graben, a top of the crystalline basement (6.3 km/s) lies at 10-12 km depth and the crustal velocities increase to 6.8 km/s and 7.5 km/s at depth of 18 and 25 km respectively. The 6.8-km/s layer is thinest beneath the graben where it is apparently replaced by the 7.5 km/s layer.

The "high-velocity pillow" structure beneath the Columbia Plateau is similar to that found under recognized continental rifts. The upper crustal graben and the lower crustal rift pillow when interpreted together with the available geologic data suggest that Eocene and possibly later rifting occurred prior to the deposition of the Columbia River basalts. Although small fault displacements have occurred since the deposition of the basalts, reactivation of the rift faults can not be excluded, particularly since a similar rift structure, the Mississippi embayment rift, has historic seismicity which has been associated with the reactivation of older rift faults.

6. In recent years, the northern Appalachians have been recognized as being composed of several distinct terranes, having distinguishably separate orogenic histories prior to coalescence in their present form. Recently, active seismic experiments (both reflection and refraction) have been undertaken crossing the Appalachians in Maine and Quebec to characterize the crustal velocity structure. Among the results of this transect are a characterization of four principal terranes of the northern Appalachians. To the northwest, Grenville basement is overlain by as much as 24 kilometers of Taconian thrust sheets obducted over a lateral distance of 100 km. In central Maine, high grade metamorphic crust accreted to North America during the Taconic orogeny has subsequently been covered by up to 12 km of Silurian and Devonian turbidites of the Merrimack Synclinorium. Just west of the coast, we find crust with 9-12 km of highly reflective Paleozoic cover sequences; the coastal Avalon terrane contains reflections throughout the crust. The Meguma terrane, closest to the continental margin, is characterized by few reflections above 5 s, consistent with an upper crust formed by granitic intrusions.

   Preliminary results show upper crustal velocities that range from 5.7-6.3 km/sec with localized regions of low velocity within the upper crust. Secondary arrivals provide evidence for a higher velocity lower crust (6.8-7.2 km/sec) below 22 km. A particularly fruitful approach to the analysis of the refraction data has been the examination of wide-angle reflections from the Moho and from horizons in the lower crust through the use of normal moveout corrected record sections. This examination has provided (1) regional measures of crustal thickness; (2) a measure of variation from region to region of the reflective character of the crust; and (3) evidence for local abrupt changes in depth to the Moho. The latter may be, in some instances, related to the boundaries between recognized terranes. Determinations of crustal thickness show a stepwise regional thinning of the crust from 38-40 km in the northwest to 30-33 km at the coast.

7. In November of 1986, our 120 seismic cassette recorders were deployed along a 100-km long NW-SE profile between San Simeon and Santa Maria, California. Shots were recorded from three shotpoints in-line with these stations, as well as from three shotpoints east of the profile and from several marine shotpoints west of the profile (the in-line shots have reversed coverage of 70 km). The deployed profile is both within and parallel to the structure of the Sur-Obispo terrane, a deformed remnant of the accretionary wedge which resulted from the Late Jurassic to Early

Tertiary subduction off the western coast of North America. The terrane is comprised of Franciscan-type rocks (graywackes, cherts, melanges, volcanics, and ophiolites) which are locally unconformably overlain by Cretaceous and/or Tertiary marine sandstones and shales. Interpretation of the recorded refraction data will provide additional insights into velocity structure of accretionary prisms and can be directly compared to the velocity structures derived from our seismic studies of similar terranes within the Diablo Range of central California as well as within the Chugach terrane of southeastern Alaska.

8. The USGS, in cooperation with the US Agency for International Development and the Jordanian Nataural Resources Authority is currently operating an eight-station seismic network in Jordan, which is being upgraded to a 32-station network. Over the past three years, approximately 2000 events have been recorded and located, which are supplying critical data about the crustal structure and the state of tectonic stress in the vicinity of the Dead Sea Rift Zone. In October, 1986, Will Kohler traveled to Jordan to install and test new computer programs for real-time detection of earthquakes using a PDP 11/23 computer. The new programs are currently operating in Jordan and are expected to supply more accurate and timely information about events detected by the Jordanian network.

9. PASSCAL Northern Nevada Lithospheric Experiment

With funding from the USGS, the Air Force Geophysical Lab, and PASSCAL (Program for Array Seismic Studies of the Continental Lithosphere - NSF funded), the USGS participated in a major seismic investigation in northern Nevada.

Northwestern Nevada has long been identified as an area of unusually thin crust (Eaton, 1963), but recent COCORP data (Klemperer et al., 1986) suggest that this may not be the case. A re-evaluation of the older USGS refraction data (Fallon-Eureka profile) suggests that the area may has a velocity structure much like that observed in many continental rifts. This interpretation is supported by a second refraction data set (Stauber, 1980), which crosses the older USGS (Fallon-Eureka) profile. In a new study, H. Patton and K. Priestley have located an area of high LG-wave attenuation associated with the Carson Sink. In addition, they note an increase in P-wave velocity and a decrease in S-wave velocity over the Carson Sink. Northwestern Nevada has also experienced large historic earthquakes and a relatively greater amount of Quaternary normal faulting (Smith, 1978) than most of the rest of the Basin and Range. Our primary objective is to better determine the lithospheric velocity structure of the area in order to better understand many of the anomalous geological and geophysical characteristics of the Basin and Range Province.

Other objectives of this experiment include an evaluation of: (1) the effectiveness of combining refraction and reflection recording and processing, (2) the effectiveness of sources (e.g. vibroseis vs explosives) in conducting crustal studies, (3) explosive shot sizes vs frequency content of the signal, (4) how efficiently explosive sources yield S-wave energy in the Basin and Range, and (5) strong ground motion from explosive sources.

Participating institutions: Stanford University; U. C. Santa Barbara; University of Utah; University of Nevada, Reno; United States Geological Survey; Air Force Geophysical Lab.; Air Force Weapons Lab.; Princeton University; University of Wisconsin - Oshkosh; M. I. T.; Boston College; SUNY-Binghamton; Werdlinger Assoc., University of Texas, El Paso; Texas A and M; BLM.

REPORTS

Brocher, T. M., and W. D. Mooney, A comparison of the lower oceanic and continental crust and upper mantle based on coincident seismic reflection/refraction profiles, 1987 I.U.G.G. abstract, in press

Catchings, R. D, and W. D. Mooney, Crustal structure of the Columbia Plateau: Evidence for Continental Rifting, Journal of Geophysical Research, in press.

Colburn, R. H., and Fuis, G. S., 1986, Velocity structure across the northern boundary of the Peninsular terrane, Copper River Basin, Alaska, EOS Transactions American Geophysical Union, v. 67, p. 1198.

Fisher, M. A., G. Plafker, T. M. Brocher, R. A. Page, W. J. Nokleberg, D. L. Campbell, G. S. Fuis, and G. L. Smith, Seismic-reflection images of the crustal structure of the northern Chugach terrane, Alaska: Preliminary results of a survey for the Trans-Alaska Crustal Transect (TACT), submitted to Journal of Geophysical Research.

Fisher, M. A., Brocher, T. M., Page, R. A., Plafker, G., Fuis, G. S., Nokleberg, W. J., and Campbell, D. L., 1986, Seismic Reflection images of deep-crustal features of south-central Alaska: preliminary results of a survey for TACT, EOS Transactions America Geophysical Union, v. 67, p. 1196.

Fuis, G. S., Ambos, E. L., Mooney, W. D., Page, R. A., Fisher, M. A., Brocher, T. M., and Taber, J. J., Crustal structure beneath exposed accreted terranes of southern Alaska, Geophysical Journal of the Royal Astronomical Society, in press.

Goodwin, E. B., Ambos, E. L., Fuis, G. S., Mooney, W. D., Page R. A., and Campbell, D. L., 1986, The crustal structure of Wrangellia, southern Alaska, from seismic refraction measurements, EOS Transactions American Geophysical Union v. 67, p. 1196.

Kohler, W. M. and Fuis, G. S., 1986, Travel-time, time-term, and basement depth maps for the Imperial Valley region, California, from explosions, Bull. Seis. Soc. Am., 76, 1289-1303.

Luetgert, J. H., and C. Bottcher, 1987, Seismic refraction profiles within the Merrimack Synclinorium, central Maine, EOS Transactions of the American Geophysical Union, in press.

McMechan, G. A., and G. S. Fuis, 1987, Ray-equation migration of wide-angle reflections from southern Alaska, Journal of Geophysical Research, v. 92, p. 407-420.

McCarthy, J., Fuis, G. S., Wilson, J., Crustal structure of the Whipple Mountain, southeastern California, a refraction study across a region of large continental extension, Geophysical Journal of the Royal Astronomical Society, v. 89, in press.

Meador, P. J., Ambos, E. L., and Fuis, G. S., 1986, Data report for the north and south Richardson highway profiles, TACT, seismic-refraction survey, southern Alaska, U.S. Geological Survey Open-file Report 86-274.

Mooney, W. D. and Brocher, T. M., Coincident seismic reflection/refraction studies of the continental lithosphere: A Global Review, Reviews of Geophysics, in press.

Mooney, W. D., E. L. Ambos, T. M. Brocher, R. D. Catchings, M. E. Fisher, G. S. Fuis, J. H. Luetgert, J. McCarthy, and R. A. Page, Composition of the lower crust: Inferences from coincident seismic reflection/refraction profiles, (abstract) 1987 I.U.G.G., in press.

Murphy, J. M., and J. H. Luetgert, 1987, Data report for the 1984 Maine along-strike seismic-refraction profiles, U.S. Geological Survey Open-file Report 87-133.

Murphy, J. M., J. H. Luetgert, and W. E. Doll, 1987, Seismic refraction and wide-angle reflection profiles in western Maine: The northern Appalachian orogen, Earthquake Notes, v. 58.

Page, R. A., Plafker, George, Fuis, G. S., Nokleberg, W. J., Ambos, E. L., Mooney W. D., and Campbell, D. L., 1986, Accretion and subduction tectonics in the Chugach Mountains and Copper River Basin, Alaska: Initial results of the Trans-Alaska Crustal Transect: Geology, v. 14, 501-505.

Page, R. A., Fuis, G. S., Ambos, E. L., and Stephens, C. D., 1986, Relocated earthquakes along the TALI corridor in the Chugach Mountains, southern Alaska, EOS Transactions American Geophysical Union v. 67, p. 1197.

Spencer, C., A. Green and J. H. Luetgert, 1987, The search for the edge of the Grenville in the Quebec-Maine region, Geophysical Journal of the Royal Astronomical Society, in press.

Taber, J. J., Fuis, G. S., Ambos, E. L., Mooney, W. D., Page, R. A., 1986, Seismic velocity structure of the Prince William terrane, Alaska, EOS Transactions American Geophysical Union, v. 67, p. 1196.

Walter, A. W. and W. D. Mooney (eds.), 1987, Interpretations of the SJ-6 seismic reflection/refraction profile, south central California, USA, U.S. Geological Survey Open-file Report 87-73, 132 p.

Wilson, J. M. and G. S. Fuis, 1987, Data report for the Chemehuevi, Vidal, and Dutch Flats lines, PACE seismic-refraction survey, southeastern California and western Arizona, U.S. Geological Survey Open-file Report 87-86.

Wolf, L. W., Levander, A. R., and Fuis, G. S., 1986, Upper crustal velocity structure of the accreted Chugach terrane, Alaska, EOS Transactions American Geophysical Union, v. 67, p. 1195.

EXPERIMENTAL TILT AND STRAIN INSTRUMENTATION

9960-01801

C.E. Mortensen
Branch of Tectonophysics
U.S. Geological Survey
345 Middlefield Road, MS/977
Menlo Park, California 94025
(415) 323-8111, ext. 2583

Investigations

1. The satellite telemetry system has been brought to a state of relative reliability and stability. There are currently 91 Data Collection Platforms (DCPs) that transmit a variety of data through the GOES-6 spacecraft to the Direct Readout Ground Station (DRGS) in Menlo Park. Forty of these DCPs transmit data at 10-minute intervals on an exclusively assigned random channel, which is being utilized under a special agreement with NESDIS. The remainder of the DCPs report at standard 3 or 4-hour intervals as assigned by NESDIS.

   After the failure of the launch of a GOES satellite in May 1986, a successful launch was finally achieved on 26 February, 1987. This GOES-7 spacecraft will replace GOES-5 in the east position at 75 degrees west longitude. GOES-5 will be moved to the central position (108 degrees west longitude), while GOES-6 will be moved to the west position (135 degrees west longitude). In January the DRGS antenna in Menlo Park was reaimed from GOES-3 (the west satellite) to GOES-6 (the central satellite) in order to get more consistent reception of data from the field. During the period when the satellites are being moved the DRGS antenna will be realigned to GOES-3 until GOES-6 is again available.

2. From 14 September through 1 October, and again from 5 December through 31 January, Carl Mortensen acted as scientific host to Dr. He Shi-hai from the Center for Analysis and Prediction, State Seismological Bureau, Beijing, PRC. Dr. He carried home with him several modeling programs that should be helpful in analyzing strainmeter data in China. He was able to become familiar with the use of these programs by working with them on a VAX machine similarly configured to the one he will be using in China. During his stay in the U.S., Dr. He also visited UC San Diego, Carnegie Institute, and Lamont-Doherty.

3. A system to affect emergency communications and routine operational message traffic in the Parkfield area has been partially implemented. Four wide-band, digitally-synthesized Midland radios have been delivered and installed - three in field-service vehicles and one at the Car Hill laser observatory. Three hand-held King radios with similar capabilities are still on order. These radios can communicate over the USGS repeater frequency, on commercial mobile radio-telephone frequencies, on the California Emergency Services Radio System, and through the USGS microwave to the telephone system at Menlo Park. Additional capabilities are available with the Midland units including access to a large number of local emergency and operational radio nets. It is also planned to establish a capability to link directly to the telephone system locally by installing a phone-patch (already procured) at Car Hill.

4. Networks of tiltmeters, creepmeters and shallow strainmeters have been maintained in various regions of interest in California. A network of 14 tiltmeters located at seven sites monitor crustal deformation within the Long Valley caldera. Other tiltmeters are located in the San Juan Bautista and Parkfield regions. Creepmeters located along the Hayward, Calaveras and San Andreas faults between Berkeley and the Parkfield area are maintained in cooperation with the Fault Zone Tectonics project. A shallow strainmeter is located near Parkfield, while observatory type tiltmeters and strainmeters are sited at the Presidio Vault in San Francisco, and a tiltmeter is installed in the Byerly Seismographic Vault at Berkeley. Data from all of these instruments are telemetered to Menlo Park via the GOES satellite, by phonelines and radio links, or both.

Results

1. In 1983 the U.S. Geological Survey instrumented the Long Valley caldera, near Mammoth Lakes, California, with an array of borehole tiltmeters, whose purpose is to detect rapid deformation that might accompany incipient volcanic activity, such as the intrusion of a dike at shallow depth. The array consists of seven sites, within and surrounding the zone of the 1983 earthquake swarm. Five sites have the instruments installed at a depth of 6 m and consist of two installations that are closely spaced, one containing a Rockwell/Kinemetrics instrument and the other an instrument designed by James Westphal of the California Institute of Technology. A sixth site consists of two of Westphal's instruments and one of the Rockwell/Kinemetrics instruments, and the final site consists of two of the latter instruments only, installed at a depth of 2 m. Since July

1985, all but one site have been equipped with a telemetry system that uses the GOES satellite. Most sites are also equipped with a telemetry system based on telephone lines and radio links.

This tiltmeter array affords a unique opportunity to compare the relative merits of different instrument types and installation techniques, under similar settings. In general, the results are similar for the two different instruments and installations, but local geologic conditions substantially effect the performance at each site. The records from the 6-m boreholes have better long-term stability and lower noise across the frequency response of the sensors than those from the 2-m boreholes. At one site the tilt record appears to be dominated by perturbations related to local geothermal production. Performance at most other sites indicates that sudden deformation, with time spans shorter than about one week and amplitudes of about 5-10 microradians or greater, should easily be detected by the instruments within this array.

Reports

Mortensen, C. E., and A. C. Jones, 1986, Tiltmeter measurements that reflect deformation rates in the San Francisco Bay Area, California, EOS, American Geophysical Union Transactions, v. 67, no. 44, p. 1223.

Mortensen, Carl E., and Douglas G. Hopkins, 1987, Tiltmeter measurements in the Long Valley caldera, California: Abstract Volume, Hawaii Symposium on How Volcanoes Work, p. 182.

Tiltmeter and Earthquake Prediction Program in S. California and at Adak, AK

14-08-0001-21244

Sean-Thomas Morrissey
Saint Louis University
Department of Earth and Atmospheric Sciences
P.O. Box 8099 - Laclede Station
St. Louis, MO 63156
(314) 658-3129

I. Introduction

Yes, Virginia, there is Giardia, and believe it or not, the noxious parasite can apparently be imbibed in the waters of the western Aleutians. Back country hiking sorts would not think that this modern pestilance of the outdoors would have made its way to Adak, Alaska, a thousand miles from anywhere; not quite the end of the earth, but the locals claim that they can see it from there on a clear day. While the previous technical summary related the saga of a deteriorating boat and unprecedented bad weather at Adak in the course of the P.I.'s extended 3 month effort in servicing the multi-island Adak seismic network,the problem did not end there. Modern medicine has serious problems with modern diseases, like giardiasis, and this P.I. spent most of the winter trying to get cured of it. (P.S. We did have the proper filters for drinking water, but did not use them (in the Aleutians!!?); a word to the wise!?)

II. Task 1: The Tiltmeter System

Objective: To continue to improve the performance of bubble sensor tiltmeter systems and to investigate other sensor systems for use in moderate depth boreholes, seeking relatively low-cost, readily deployed instrumentation.

Accomplishments: While we had no problem with the tiltmeters at Adak last summer, on our return we found power supply problems in the former Southern California units running in "standby" waiting to be installed at Pinon Flat. These units were powered in the lab from AC-DC supplies, rather than batteries, and one supply's regulation failed, applying 28 VDC to the tiltmeter converter/regulators. These would have been saved had the fuse lamp been installed properly (we use a 6 volt, 200 ma lamp in 12 volt, 50 ma circuits, where it stays cold and has low resistance; a temporary *faux pas* will flash the lamp momentarily; a real short burns it out in an hour or so). The lamps were relocated on all the new converter boards, and a low power status indicator was added, an LM3909 LED flasher that operates from the 3 volt drop across the reverse-polarity protection diodes. The flashing LED is an immediate visual indication that power is available and being used properly.

III: Task 2: The Installation Method

Objective: To improve the installation methods for borehole instruments with a goal of installing them as deep as 100 meters.

Accomplishments: Work on the new installation system remained on standby, with the P.I.'s health problems complicated by the uncertain future of the work at

Pinon Flat and Parkfield. Two installation concerns were addressed, though, namely the need to achieve calibration and orientation of the sensors within 1% and 1 degree, respectively. The electrolytic sensor does not have an *in situ* calibration ability, but we do have a sufficiently precise and portable tilt table (constructed by this program) that can check the calibration in the field immediately before installation. As for the installation azimuth problem, we have successfully experimented with a disposable compass - LED - photo-sensor arrangement wherein the compass needle eclipses the slit-colliminated light between an LED below and a photo-transistor above the compass case. Of course, this scheme will only work in uncased holes and non-magnetic installation equipment, which is our situation.

IV: Task 3: The Digital Data Systems

Objective: To continue to develop and operate a digital data acquisition system to acquire geodetic data and to thoroughly monitor the environment of the instrument installations.

Accomplishments: The Adak digital data continues to be acquired, although currently two of the five remote digitizers are not operating, and our (unfortunately inept) observer there is unable to solve the problem, even though he has a full set of spare units on hand. The units not working are for the North site, where the data loss is not of concern, and the pier, where we are concerned about not getting the water tide data. We have also acquired the components to assemble five more of our 16-bit replacements for the out-of-date 12-bit units that we have been using.

V: Task 4: Data Interpretation

Objective: To process the digital data and make efforts to remove the environmental noise from the data, so as to establish the intrinsic long-term stability of the tiltmeters. Various analysis techniques are then utilized to present the data in meaningful formats such that any precursory tilt events would become evident.

Accomplishments: In order to assure continuous data quality, routine data analysis is always done on each 8-day floppy disk as they arrive in St. Louis. Of particular interest is the data relating to the M_S 7.7 earthquake that occurred at 22:47 z on 7 May 1986, approximately 2 degrees southeast of the tiltmeter array. Aftershocks have defined a rupture zone that spans about 3°, ending south of Adak. All the tiltmeters showed similar co-seismic tilts, but the most consistent data is from the three-instrument West site, which shows a net tilt of 2.46 ± 0.64 micro-radians down to the east-southeast, the direction of the epicenter. This data is shown in Figure 1. Any evidence of precursory tilting will have to wait until linear thermal corrections are made on the data.

Also of interest is the tide gauge data from our self-contained differential pressure unit as well as from the NOAA nitrogen bubbler. Figure 2 shows the original water tide data, and the detail of the tsunami waves that showed up within minutes of the earthquake. An attempt was made to detect any net change of elevation of the pier, as independent evidence of co-seismic tilting, and statistical analysis of the month of data before and after the event shows a subsidence of 32.5 ± 2.1 mm after the tides and barometric pressure are removed. This, of

Figure 1

ADAK TILTMETER ARRAY, RAW DATA
West site, east tiltmeter

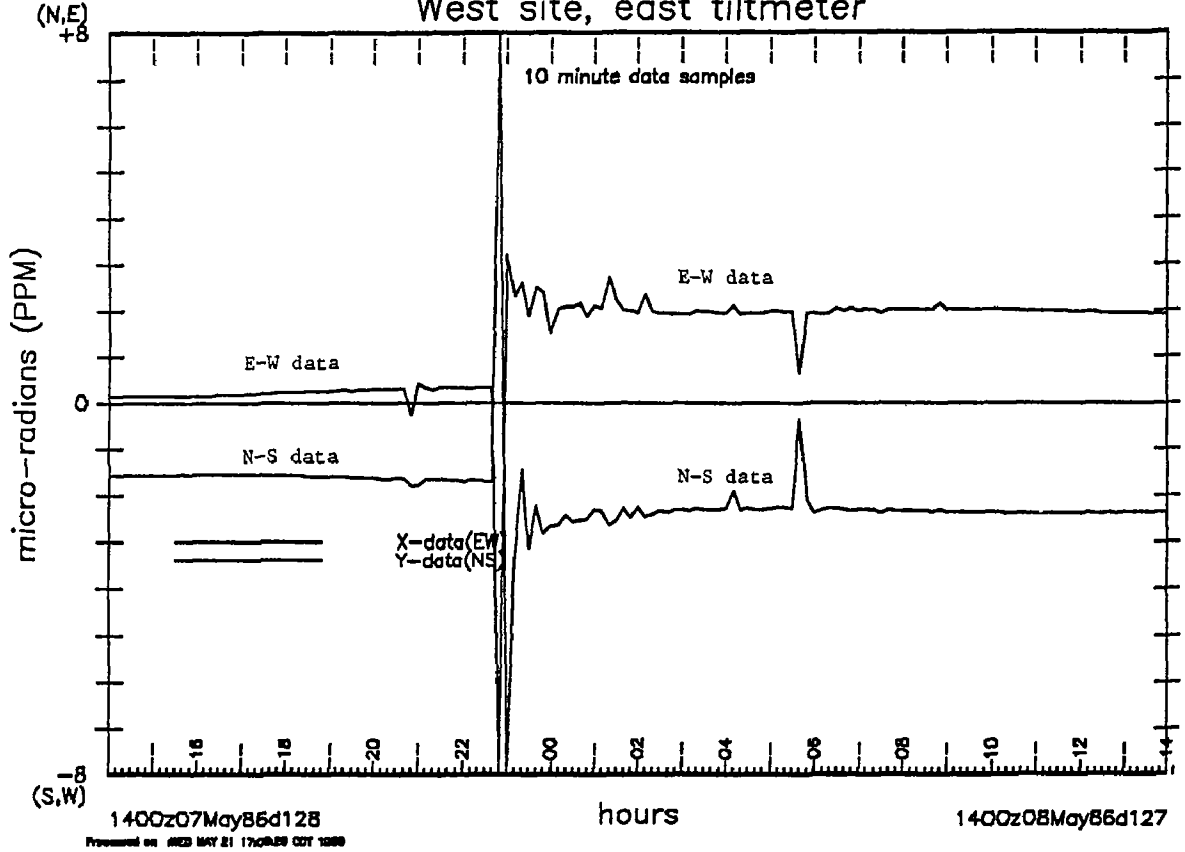

Figure 3h

ADAK TILTMETER ARRAY, RAW DATA
West site, west tiltmeter

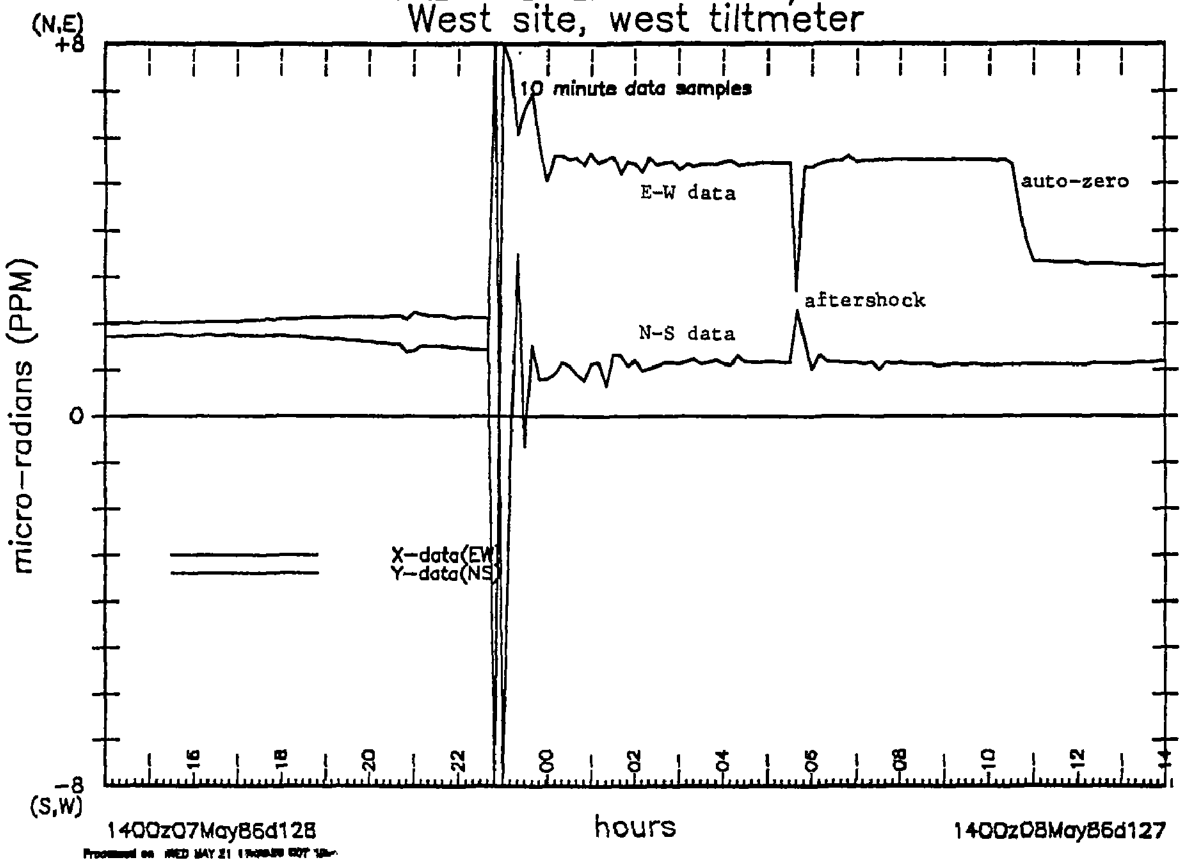

Figure 2

Adak Tide Gauge Data

SLU/CIRES differential pressure gauge

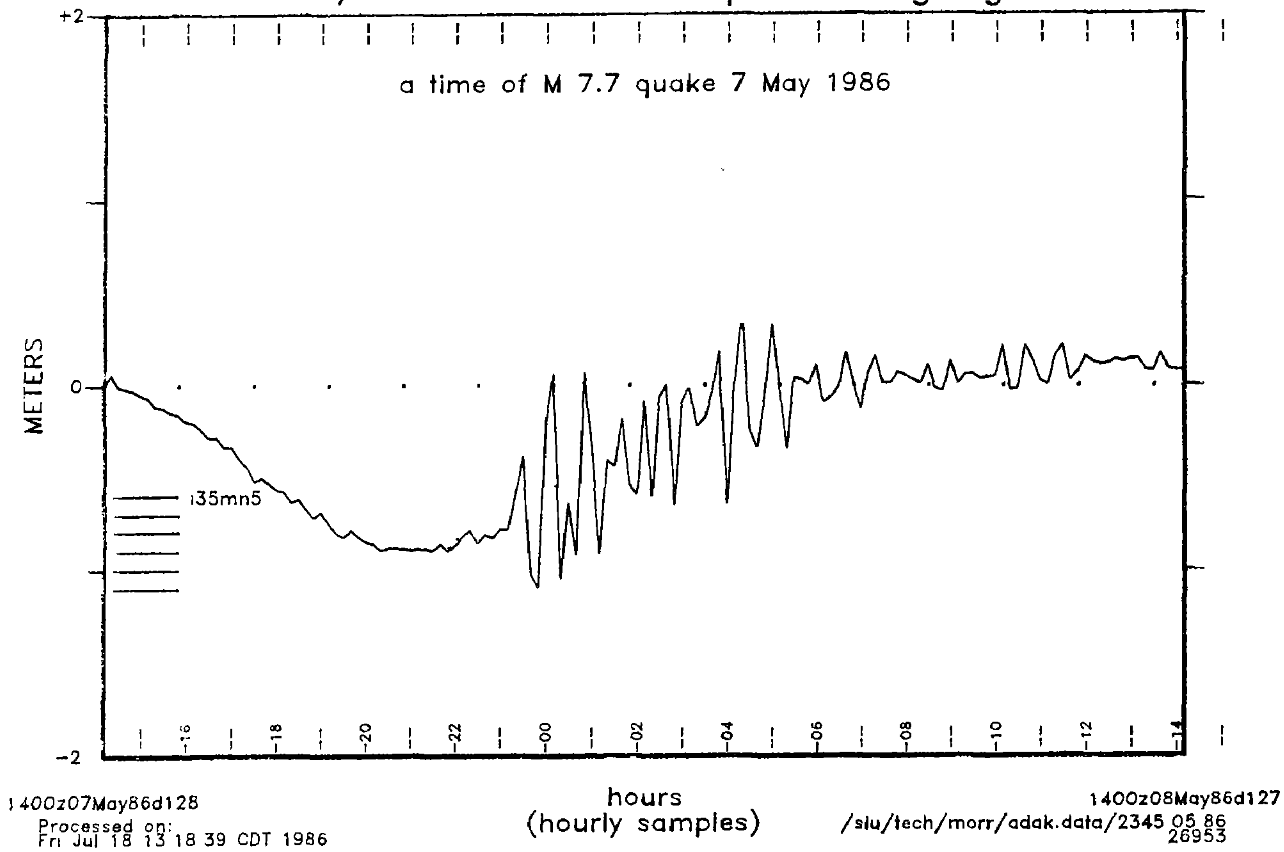

Figure 6b

Adak Tide Gauge Data

NOAA bubbler gauge

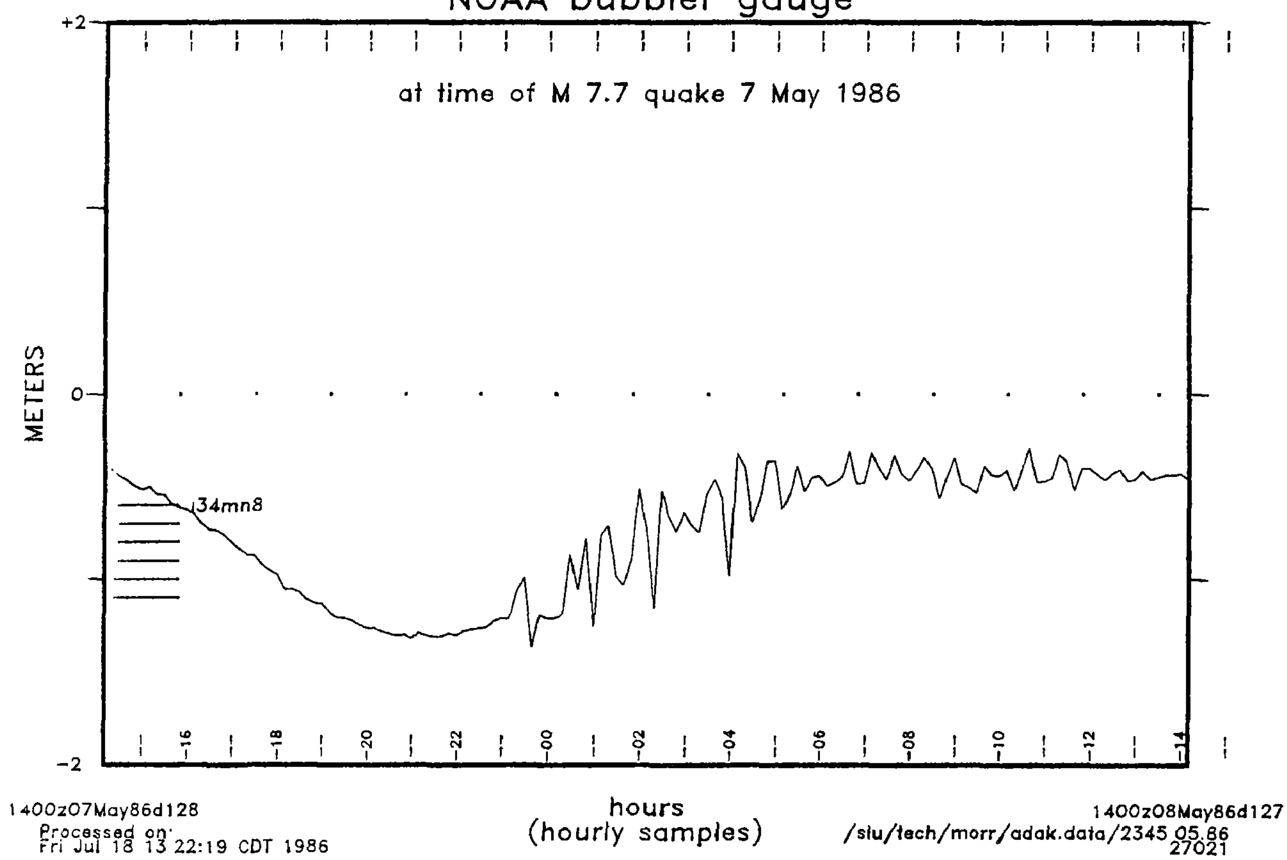

course, could be entirely a seasonal effect, so longer data sets about the event were analyzed, as shown in Figure 3, with similar results.

VI: Problems and Plans

No further funding for this program has been provided, and the present contract ended October 31, 1986. As long as this Principal investigator has to go to Adak to maintain the CIRES seismic network, we will probably continue to run the tiltmeter array, since the cost is minimal, unless, of course, someone comes up with a more urgent funded need for the units.

VI: Reports

A report, "Near-Field Tilt and Water-Tide Gauge Data from Adak, Alaska, Associated with the M = 7.7 Western Aleutian Earthquake of May 7, 1986," was presented at the fall AGU meeting.

Sean-Thomas Morrissey
Senior Research Scientist
30 April 1987

Figure 3b: Recovery of Residual Sea Level.

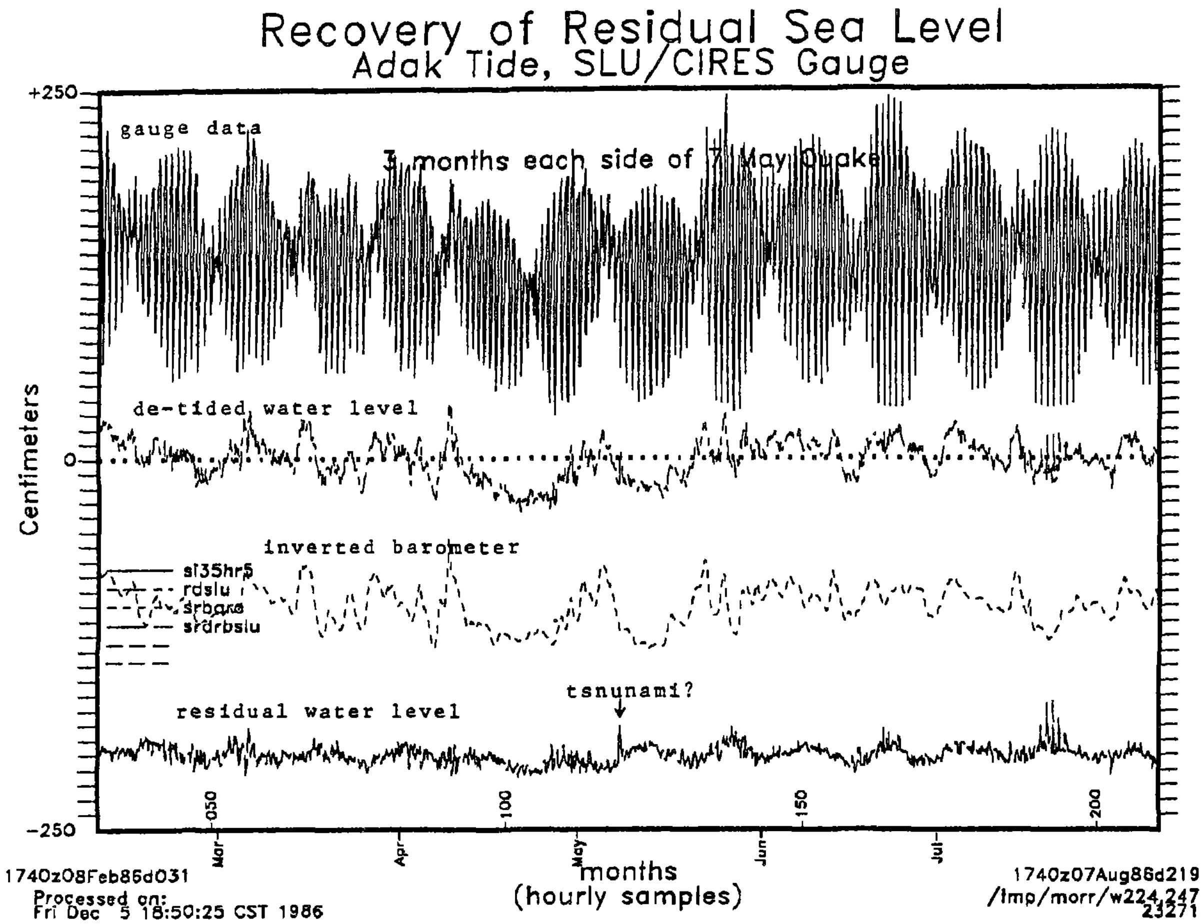

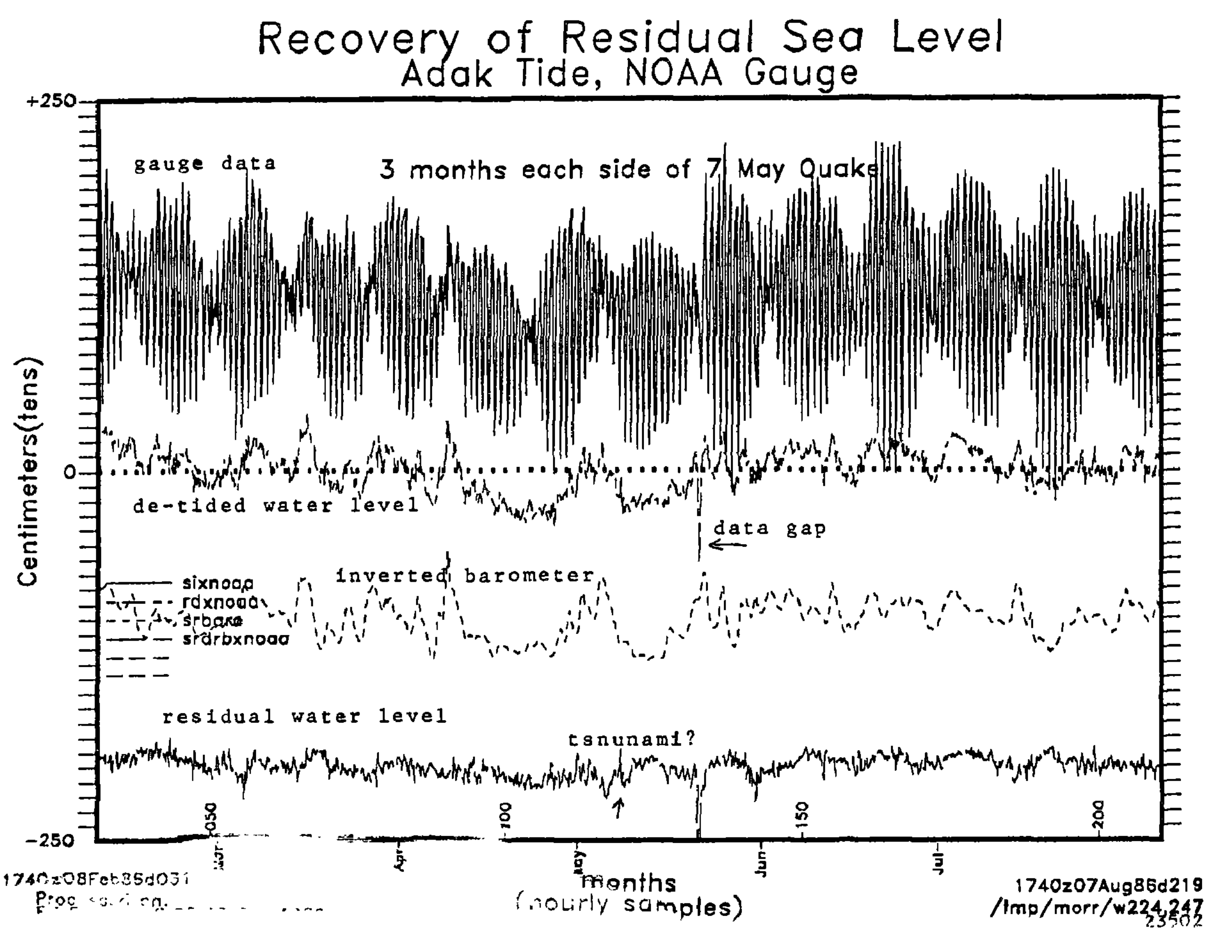

Crustal Deformation Observatory, Part (i)
Shallow Borehole Tiltmeters

14-08-0001-21939

Sean-Thomas Morrissey
Saint Louis University
Department of Earth and Atmospheric Sciences
P.O. Box 8099 - Laclede Station
St. Louis, MO 63156
(314) 658-3129

Objective: To apply the latest innovations and technology of instrumentation and installation methods to the shallow borehole tiltmeters at Pinon Flat such that their performance, particularly with regard to longterm stability, will compare more favorably with the data from the long baseline tiltmeters. Remotely pre-leveled installations in 10 and 20 meter deep holes are planned.

Accomplishments and Problems: Work on completing and testing the new installation system remained mostly on standby, with the P.I.'s health problems complicated by the uncertain future of the work at Pinon Flat. (Refer to the Southern California/Adak summary for a discussion of the problems that continued after the Adak effort of last summer.)

Two installation concerns were addressed, though, namely the need to achieve calibration and orientation of the sensors within 1% and 1 degree, respectively. The electrolytic sensor does not have an *in situ* calibration ability, but we do have a sufficiently precise and portable tilt table (constructed by this program) that can check the calibration in the field immediately before installation. As for the installation azimuth problem, we have successfully experimented with a disposable compass - LED - photo-sensor arrangement wherein the compass needle eclipses the slit-colliminated light between and LED below and a photo-transistor above the compass case. Of course, this scheme will only work in uncased holes and with non-magnetic installation equipment, which is our situation. We have also acquired the components to assemble five more of our 16-bit replacements for the out-of-date 12-bit units that we have been using, of which we will use two of these 14-channel units at CDO in conjunction with their data system.

A proposal to continue the work at Pinon Flat was submitted in response to the latest RFP. It is actually a request for minimum salary funding just to get caught up. The P.I. is only partially funded for tiltmeter work, but since we cannot replace the technician who resigned last May, the P.I. also has had to do all the nitty-gritty technical work, as well as the basic data analysis.

Results: A positive result of the shallow tiltmeter reinstallations at Pinon Flat is the clear indication that the thermal noise is in the shallow rock structure, and not in the instruments. Figure 1 shows the current data from the Alpha unit. The very clear correlation of the NS data with the borehole temperature (vis. the rock at 4 meter depth) is quite clear. Figure 2 (courtesy of Frank Wyatt, 1987) shows over 9 years of data from the shallow instruments. The reinstallation time is indicated. Note that the shallow surface noise continues almost undisturbed,

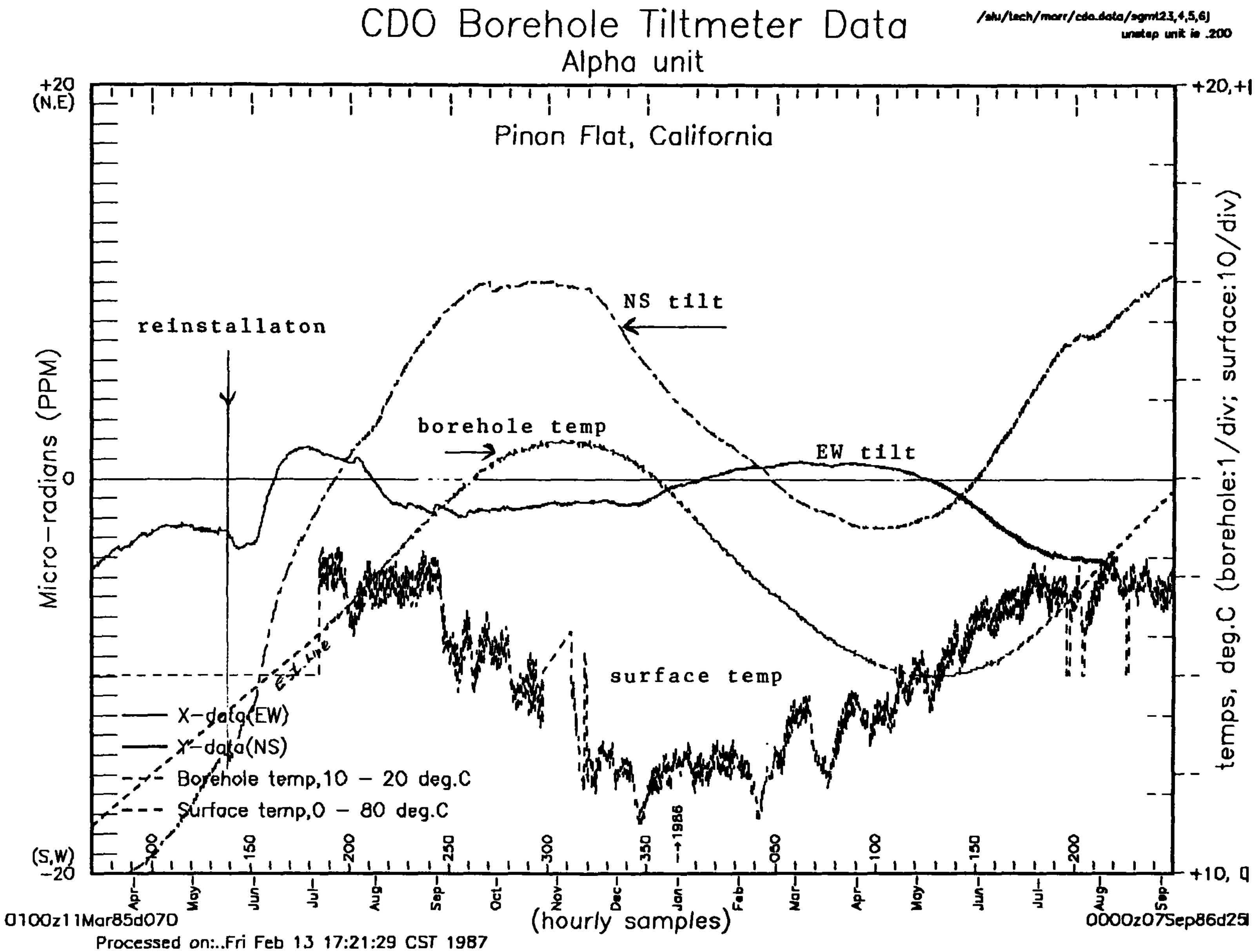

Figure 1: Alpha tilt data since reinstallation.

Figure 2: Shallow borehole tiltmeters at Pinon Flat; 1976 - 1986.

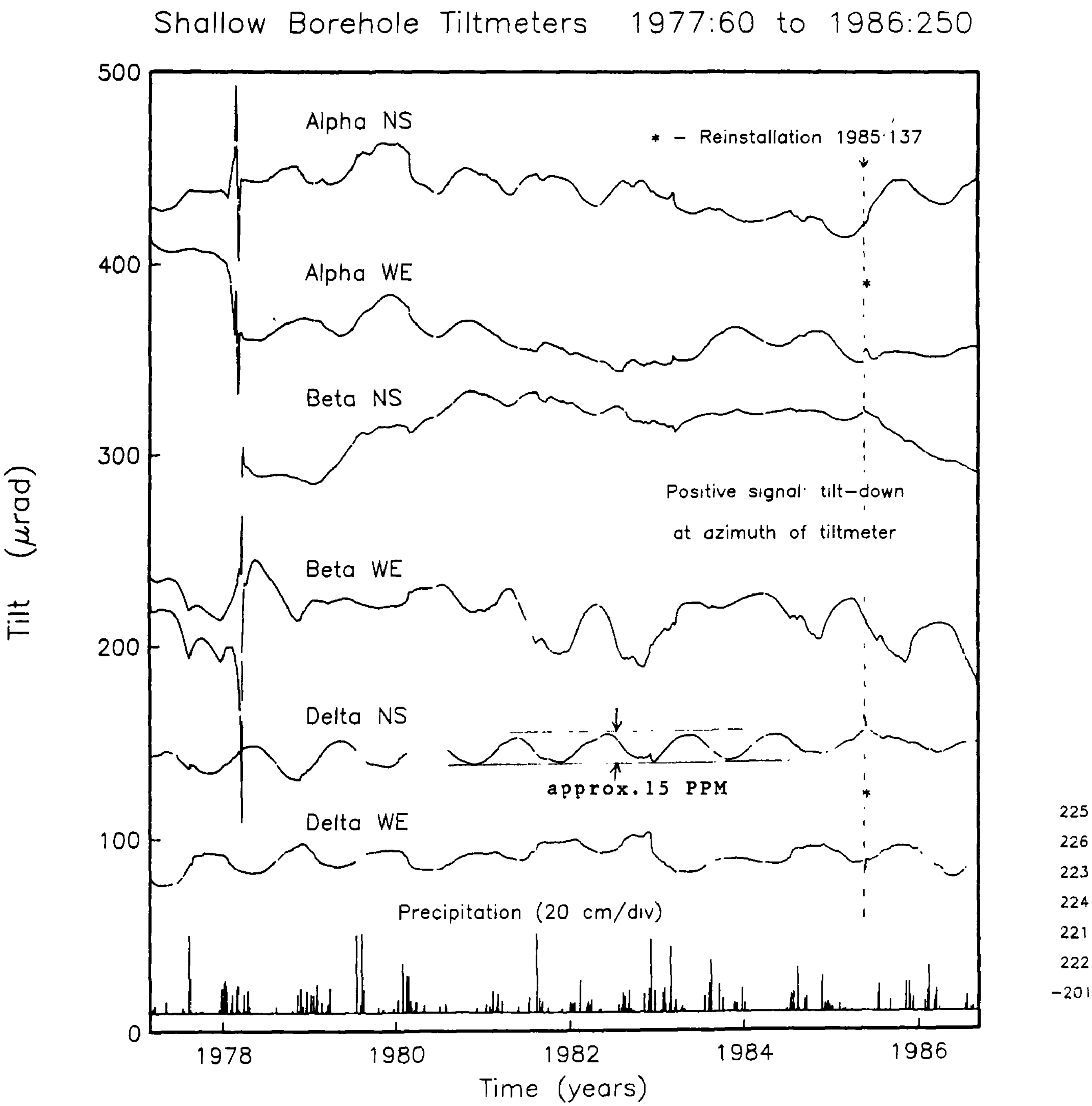

even though the tiltmeter borehole pipes were rotated 90° in the reinstallation, effectively interchanging the NS and EW sensors. Thus it is clear that the sensor can be removed and reinstalled such that annual and secular trends are continued to be recorded exactly as before with better than 1 PPM resolution within a few days after reinstallation. There is no "settling in" or asymtotic aging curve, as is common for many other tiltmeters. This is particularly evident in the Delta instrument data, where an annual cycle of about 15 PPM amplitude shows a longterm stability approaching 1 PPM/year in the NS component.

We expect that the installations in 10 and 20 meter holes, using the same installation concept, except doing it by remote control, will result in the equivalent rapid stabilization while being significantly removed from the surface thermal noise, which attenuates as r^3, that the annual thermal noise will be less than 1 PPM.

Sean-Thomas Morrissey
Senior Research Scientist
30 April 1987

Cooperative Tiltmeter Program at Parkfield, California

14-08-0001-G1204

Sean-Thomas Morrissey
Saint Louis University
Department of Earth and Atmospheric Sciences
P.O. Box 8099 - Laclede Station
St. Louis, MO 63156
(314) 658-3129

Objective: To apply the latest state-of-the-art technology to shallow borehole tiltmeter installations and data acquisition in the Parkfield area, which is forecast to be the locale of a moderate earthquake in the near (3-8 years) future. Considerations of the current failure model, based on known creep data and fault-constituitive models, allows locating the tiltmeters such that the probability of acquiring large coherent signals during the precursory stages is enhanced. The cooperative aspect involves the assistance of the U.S. Geological Survey in site selection, preparation, maintenance, and data acquisition.

Accomplishments: A proposal to continue this work was submitted last year in response to Announcement 1721, but was not funded because this program has been delayed. The panel has recommended that installations at the Turkey Flat site await completion of the 10 and 20 meter installations at Pinon Flat. These have been delayed because the irreplaceable technician resigned, and the Principal Investigator had to devote most of his effort last summer to a major maintenance trip for the Adak seismic network, a cooperative program with CIRES at the University of Colorado, an effort which ran from June to mid-October. Repercussions of the Adak effort continued to be a problem throughout the winter (see the other report). A no-cost extension of the program was granted in order to complete these installations.

Sean-Thomas Morrissey
Senior Research Scientist
30 April 1987

Dilatometer Operations

9960-03815

G. Douglas Myren
Branch of Tectonophysics
U.S. Geological Survey
345 Middlefield Road, MS/977
Menlo Park, California 94025
415-323-8111, ext. 2705

Investigations and Results

In November of 1986 we began the installation of eight borehole strainmeters in the Parkfield, California area. Five of these instruments are volumetric (dilatometers) strainmeters and three were 3-component (tensor) strainmeters.

These instruments were installed using a truck mounted hydraulic hoist and mast at sites selected from previously drilled core holes. The following is a list of the strainmeters installed by us in the past six months.

Site	Instrument	Lat.	Long.	Depth(m)	Date
DLTS	Tensor	35.94	120.43	174.0	11/08/86
DLDS	Dilatometer	35.94	120.43	176.5	11/19/86
EATS	Tensor	35.89	120.42	271.4	11/13/86
VCDS	Dilatometer	35.92	120.53	204.1	11/24/86
FRDS	Dilatometer	35.91	120.49	323.4	12/06/86
FRTS	Tensor	35.91	120.49	237.3	12/07/86
JCDS	Dilatometer	35.71	120.20	169.1	01/18/87
RHDS	Dilatometer	35.54	120.25	229.2	01/19/87

The above sites are currently recording strain data on site, and via satellite in Menlo Park, California. GEOS 16-bit data recorders are collecting seismic data from the dilatometers. (The GEOS recorders are being operated by Tom Noche under Roger Borcherdt's direction.)

At VCDS and FRDS the Seismic Branch is collecting seismic information from the dilatometer for transmission over microwave to Menlo Park, California. This is also being done at the previously installed GH1 (Gold Hill) site.

One of the accompanying maps shows all dilatometer sites in operation in California. The map of Parkfield shows pre-existing sites as a +, and (tensor and volumetric) strainmeters installed since November of 1986 as a *.

Installation of the dilatometers and tensor strainmeters was accomplished with the help of the following people:

Malcolm Johnston	U.S.G.S.
Dale Evertsen	Carnegie Institute of Washington
Selwyn Sacks	Carnegie Institute of Washington
Bob Mueller	U.S.G.S.
Doug Hopkins	U.S.G.S.
Rich Liechti	U.S.G.S.
Jeff Hamilton	U.S.G.S.
Mick Gladwin	University of Queensland, Brisbane, Australia
Rhodes	University of Queensland, Brisbane, Australia
Doug Myren	U.S.G.S.

Temperature testing and final preparation of dilatometer electronics for field installation was done by Doug Hopkins and Doug Myren. Electronics installation at the site was done by Doug Myren and Doug Hopkins with help from Rich Liechti and Andy Records.

By the end of May 1987 the dilatometers installed at VCDS, RHDS and JCDS will be cemented to the surface thus completing the installation process.

The purchase of a truck mounted hydraulic hoist with mast made these instrument installations easier and safer. It also saved both the State and Federal Government money that would have been spent renting similar equipment.

Routine maintenance at existing dilatometer strainmeters continued as required.

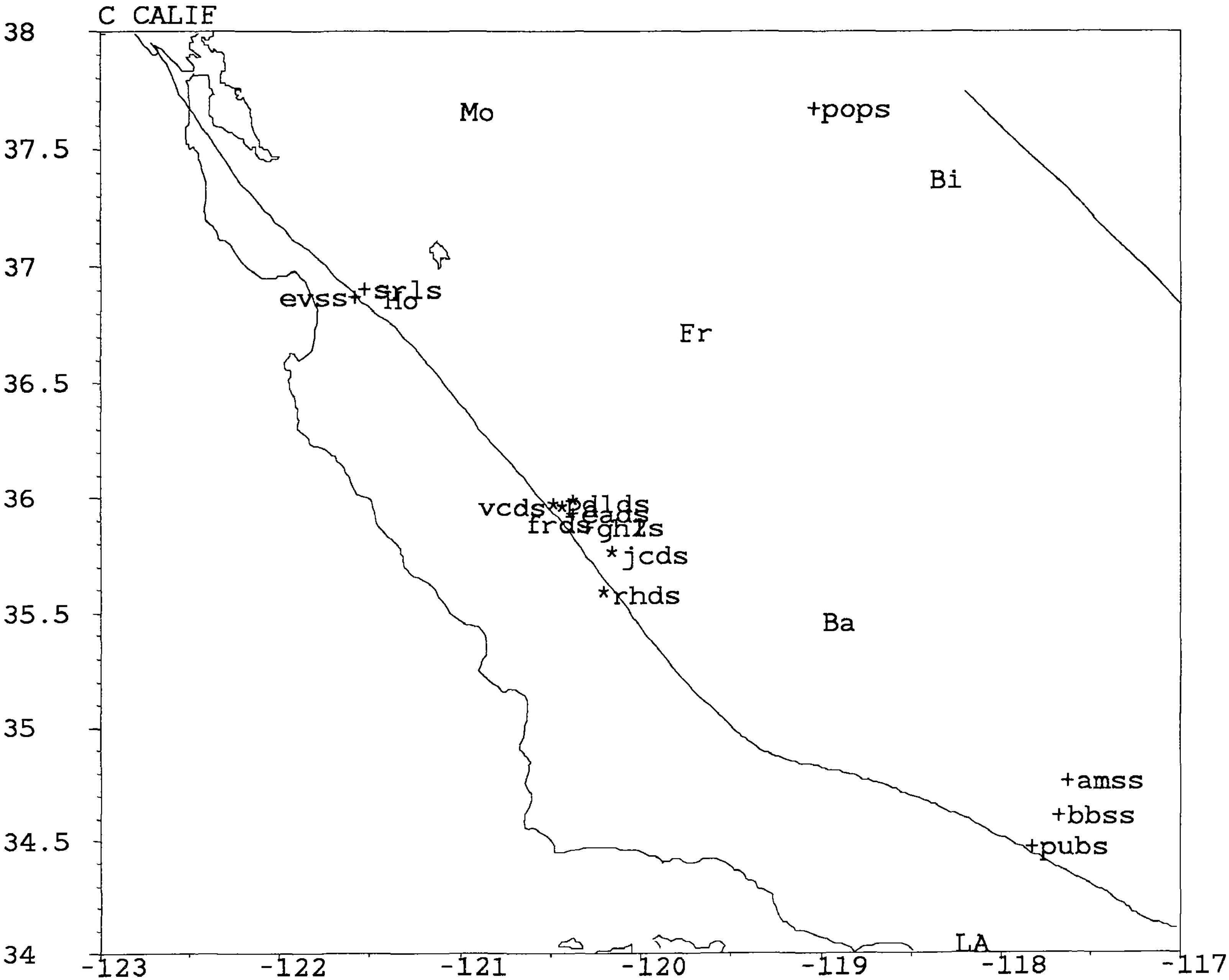
C CALIF
38
37.5
37
36.5
36
35.5
35
34.5
34
-123
-122
-121
-120
-119
-118
-117
Mo
+pops
Bi
+srls
evss+
Ho
Fr
vcds
frds
*jcds
*rhds
Ba
+amss
+bbss
+pubs
LA

PARKFIELD

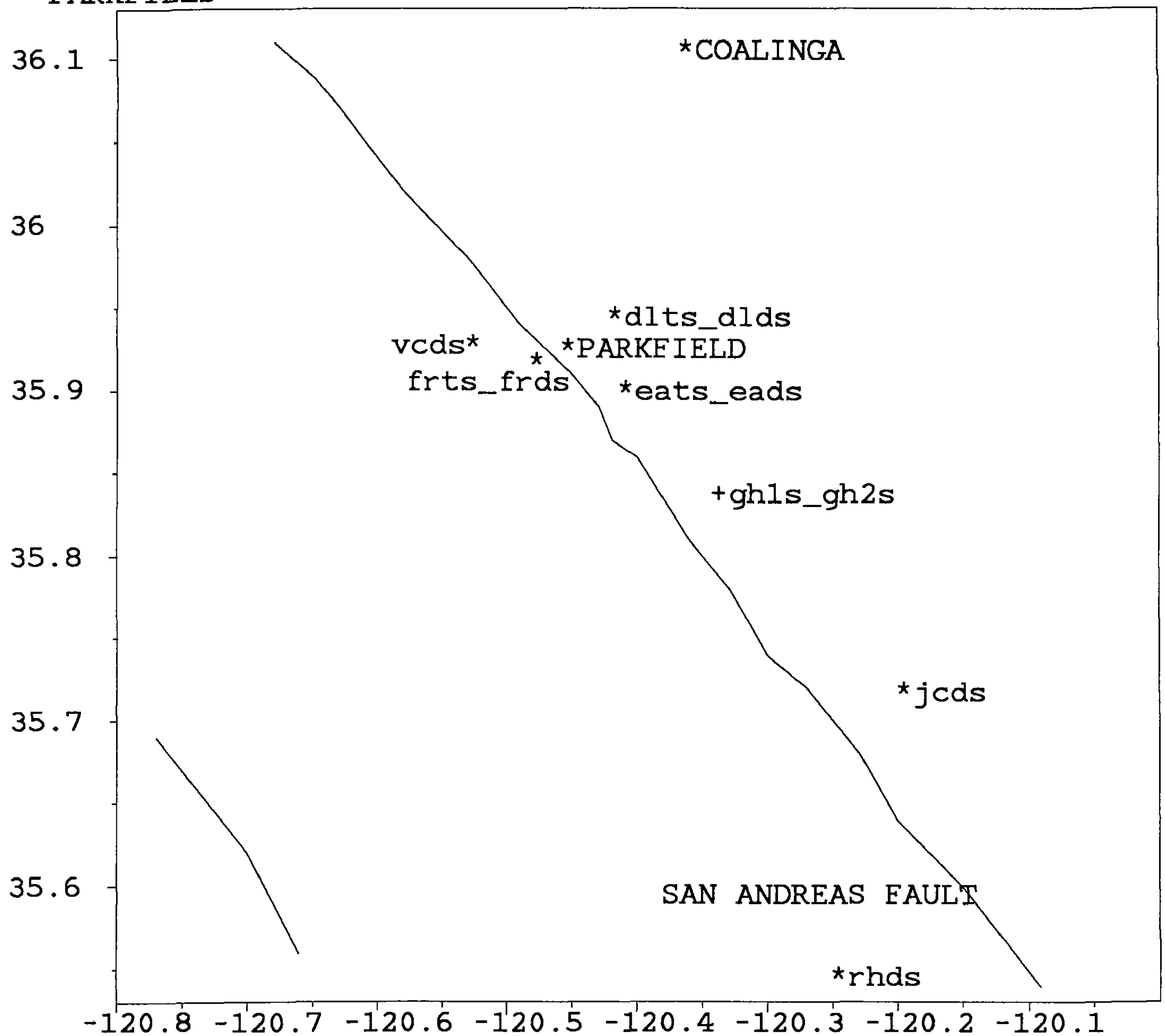

*COALINGA
*dlts_dlds
vcds*
*PARKFIELD
*
frts_frds
*eats_eads
+gh1s_gh2s
*jcds
SAN ANDREAS FAULT
*rhds
36.1
36
35.9
35.8
35.7
35.6
-120.8
-120.7
-120.6
-120.5
-120.4
-120.3
-120.2
-120.1

Helium Monitoring for Earthquake Prediction

9570-01376
G. M. Reimer
U.S. Geological Survey, MS 963
Denver Federal Center
Denver, CO 80225
(303) 236-7886

Investigations

The variations of helium in soil-gas from sample collecting stations along the San Andreas fault from Hollister to San Benito continue to be observed and related to nearby seismic activity. A system to monitor soil temperature and soil moisture is collecting data to see if seasonal helium variations can be corrected by these measurements. It is theorized that temperature and moisture are the two major factors controlling the seasonal variations and these data should help to evaluate that theory.

Results

The accompanying figure shows the helium variations through March 23, 1987. There were no data for a two month period January 15 to March 15, 1987. There were four helium decreases during the last six month period. We feel that decreases correspond to the seismic events as noted in the following table:

Helium decrease begins	Seismic event
mid-August, 1986	Sept. 3, 1986 M=4.2 near San Jose
first November, 1986	December 29, 1986 M-4.5 near San Jose
first January, 1987	January 19, 1987 M-4.3 near Morgan Hill
last March, 1987	no event yet

We did not observe a decrease for the October 11, 1986 M=4.7 event near Walnut Creek. Data are not available for the time that would have marked the February 14, 1987 M=5.2 event near Coalinga but, in the past, helium has been insensitive to seismic events in that area.

Future Studies

Over the past eight years, helium soil-gas monitoring has revealed an 80 per cent correlation between helium decreases and seismic events in the San Benito-Hollister area. We plan to relocate much of the network to near Parkfield during the late summer of 1987. The remaining stations will not be sufficient to maintain a "forecasting" capability but should reveal large changes if they occur. The reason for relocation is to include helium in the Parkfield monitoring experiment and to see if soil-gas helium responds similarly to seismic events along other sections of the San Andreas fault.

Reports

None this period.

HELIUM SOIL-GAS CONCENTRATIONS NEAR HOLLISTER, CA.

3-POINT MOVING AVERAGE THROUGH 87082.

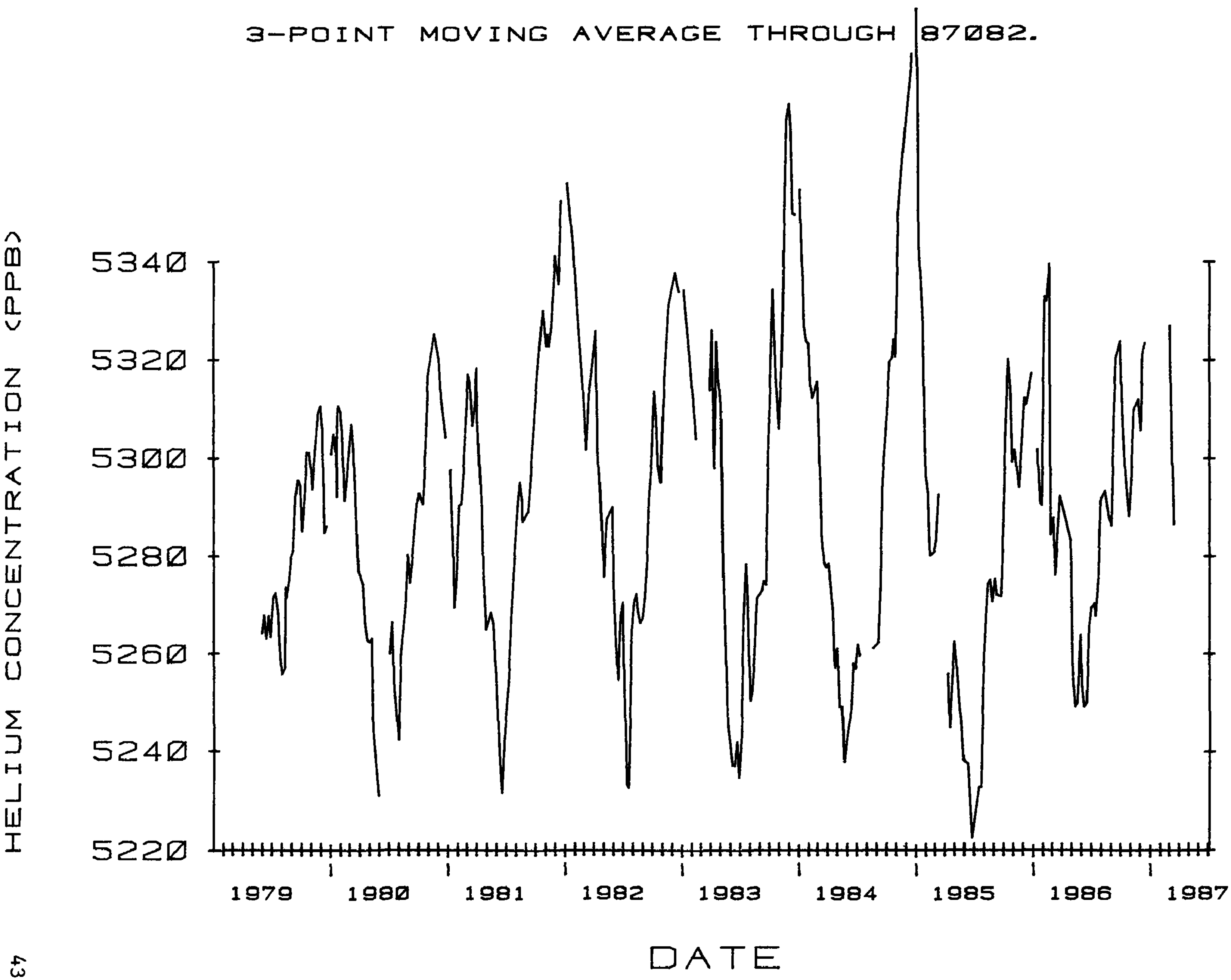

Mechanics of Faulting and Fracturing

9960-02112

Paul Segall
Branch of Tectonophysics
U.S. Geological Survey
345 Middlefield Road, MS/977
Menlo Park, California 94025
415-323-8111, ext. 2635

Investigations

1. Analysis of crustal deformation and the earthquake slip cycle on the San Andreas fault near Parkfield, California.

Results

1. Six moderate earthquakes are thought to have ruptured the Parkfield segment of the San Andreas fault since 1857. The similar characteristics of the three seismically recorded events, together with the quasi-regular 22 ± 3 year recurrence interval, have led to the forecast of a similar event in 1988±5 years. In this study the potential for the hypothesized earthquake is assessed by estimating the time required for interseismic straining to recover the strain energy released by the most recent, June 1966, Parkfield earthquake. For a simple model of the earthquake cycle this interval is proportional to the ratio of the 1966 seismic moment to the interseismic moment-deficit-rate. Baseline lengths measured before and after the 1966 earthquake are inverted to estimate the magnitude and distribution of the combined coseismic and transient postseismic slip. Although the geodetic data determine only broad spatial averages of the fault slip, they do require that slip at depth exceeded the surface offsets measured in 1966. Inversions with extreme prior models are calculated to assess the range of seismic moment and moment-deficit-rate consistent with the available geodetic data. Inversions assuming only that the slip distributions are to some degree smooth yield strain energy recovery intervals of 14 to 25 years. Extreme values range from considerably less than 10 years to nearly 30 years. In comparison, historic recurrence intervals of Parkfield earthquakes range from 12 to 32 years. The present results support our initial findings (Segall and Harris, 1986), and are consistent with the expectation of a magnitude 5-1/2 to 6 earthquake near Parkfield by 1993.

2. We are expanding our analysis of deformation in the Parkfield area to include data collected by the two-wavelength

geodimeter located at Carr Hill. The two-color data will be inverted against our long-term interseismic slip model (Segall and Harris, 1986) to search for coherent temporal changes in fault slip and associated deformation. The goal of this research is to develop methods for detecting changes in fault slip that might preceed the expected earthquake. Previously we compared the rates of line-length change predicted by the long-term model with the two-color measurements. We found that the average trends in the data were consistent with the expected rates on a majority of the baselines. However, there are significant fluctuations about the average trends that are not explained by the steady interseismic model.

We are also generalizing our analysis to include alternate data types. Our goal is to be able to analyze transient deformation episodes recorded by the full spectrum of strain instrumentation currently in place in the Parkfield area.

Reports

Segall, P. and R. Harris, Slip deficit on the San Andreas fault at Parkfield, California, as revealed by inversion of geodetic data, Science, 233, 1409-1413, 1986.

King, N. E., P. Segall, and W. Prescott, 1986, Geodetic Measurements Near Parkfield, 1959-1984, Jour. Geophys. Res., v. 92, pp. 2747-2766, 1987.

Harris, R. and P. Segall, Detection of a locked zone at depth on the Parkfield, California segment of the San Andreas fault, J. Geophys. Res., in press, 1987.

Segall, P. and R. Harris, The earthquake deformation cycle on the San Andreas fault near Parkfield, submitted to Jour. Geophys. Res., January 1987.

Segall, P., R.O. Burford, and R. Harris, The earthquake cycle at Parkfield: Comparing recent strain measurements with a long-term interseismic slip model, Trans. Amer. Geophys. Union (EOS), p. 904.

Martel, S.J., P. Segall and D.D. Pollard, Cataclastic overprinting of ductile deformation textures associated with the development of strike-slip fault zones in granite, Trans. Amer. Geophys. Union (EOS), p. 1188.

Low Frequency Data Network

Semi-Annual Report

S. Silverman, K. Breckenridge, J. Herriot
Branch of Tectonophysics
U. S. Geological Survey
Menlo Park, California 94025
415/323-8111, ext 2933
April 1, 1987

9960-01189

Investigations

[1] Real-time monitoring, analysis, and interpretation of tilt, strain, creep, magnetic, and other data within the San Andreas fault system and other areas for the purpose of understanding and anticipating crustal deformation and failure.

[2] Enhancements to satellite-based telemetry system for reliable real-time reporting and archiving of crustal deformation data.

[3] Compilation and maintenance of long-term data sets free of telemetry-induced errors for each of the low frequency instruments in the network.

[4] Development and implementation of backup capablities for low frequency data collection systems.

[5] Specialized monitoring and display of data relevant to the Parkfield region.

Results

[1] Data from low frequency instruments in Southern and Central California have been collected and archived using the Low Frequency Data System. In the six months over four million measurements from approximately 160 channels have been received via telephone telemetry and subsequently transmitted to the Low Frequency 11/44 UNIX computer for archival and analysis. In the same period, more than 60 satellite platforms have been monitored, accounting for an additional four million measurements on the 11/44 system.

[2] The project has operated a configuration of one PDP 11/44 computer running the UNIX operating system and one PDP 11/03 computer running real-time data collection software. Two AT&T PC 7300 computers have been used as backup machines for collection of satellite and telephone telemetered data. In addition, a new Integrated Solutions V24S computer has been collecting all telemetered data in a test mode. The 11/44 has been operational with less than 1% down time. Data from the Network are made available to investigators in real-time and software for data display and analysis has been enhanced. Tectonic events, such as creep along the fault, can be monitored while still in progress. Also, periodic reports are produced which display data collected from various groups of instrumentation.

[3] The project continues to use a five meter satellite receiver dish installed in Menlo Park for retrieval of real-time surface deformation data from California and South Pacific islands. The GOES geostationary satellite together with transmit and receive stations make possible a greatly improved telemetry system. Due to orbital problems with the current satellite

however, modifications to platforms in the field and software in the system have increased the use of redundant data to provide more complete data sets. Launch and availability of a new GOES satellite should improve data acquisition in the near future. Additional reporting platforms containing waterwell and climate data are being added to the collection end of the system. Further expansion of the number of platforms monitored is anticipated.

[4] Software has been modified and developed to operate a new Integrated Solutions V24S computer system. This system will become the primary data collection and analysis machine for low frequency data within the next six months.

[5] The project continues to take an active part in the Parkfield Prediction activities. New programs to plot low frequency data have been developed for the Parkfield region. These plots can be used to monitor and display ongoing activity. Kate Breckenridge is the associate monitor for Parkfield creep events, which includes contact via paging system during periods of increased activity. Stan Silverman is the alternate monitor for Parkfield strainmeter data.

[6] Computer equipment has been purchased and modified to provide coverage during periods of asbestos removal from USGS facilities.

[7] The project has continued to provide real-time monitoring of designated suites of instruments in particular geographical areas. Terminals are dedicated to real-time color graphics displays of seismic data plotted in map view or low frequency data plotted as a time series. During periods of high seismicity these displays are particularly helpful in watching seismic trends. The system is used in an ongoing basis to monitor seismicity and crustral deformation in Central California and in special areas of interest such as Mammoth Lakes.

Parkfield Area Tectonic Framework

9910-04101

John D. Sims
Branch of Engineering Seismology and Geology
U.S. Geological Survey
345 Middlefield Road, MS 977
Menlo Park, California 94025
(415) 323-8111, ext. 2252 or (415) 329-5653

Investigations:

1. Field investigations of structural and stratigraphic relationships between late Cenozoic sedimentary units and underlying Franciscan and Late Cretaceous units in the Parkfield-Cholame area.

2. Field investigations of late Holocene and historic slip rates in the Parkfield-Cholame area.

3. Geologic consultation and field examination of borehole instrumentation sites in the Parkfield prototype earthquake prediction experiment.

Results:

1. Consultation with other Branch geologists and joint field examination of geomorphic evidence for the amount of offset on the San Andreas fault along the Cholame-Bitterwater Valley segment. This entailed reexamining sites originally described in Sieh (1977) and reinterpreted in Sieh and Jahns (1984) as well as additional sites described by Jim Lienkaemper and Bob Wallace. The final conclusion of the joint group is that there is considerable uncertainty in the amount of offset attributed to the 1857 earthquake. Offset streams can be observed but the right-lateral offsets may be attributable to several non-earthquake processes.

2. Sims has continued a search of the Cholame to Carrizo Plain segment of the San Andreas for possible trench sites. Particular attention was paid to the Bitterwater Valley part of the fault zone which yielded one potential site that was later determined to have been trenched by Kerry Sieh in 1985. The site yielded no data on long term offset rate owing to thick modern deposits and extensive bioturbation (Sieh, oral communication, 1987).

   Additional sites examined on the Carrizo Plain with the collaboration of Eikichi Tsukuda (visiting from Geological Survey of Japan) yielded an interesting site originally described by Wallace (1967). Here a pair of streams are offset 204 m and 162 m. The most recent offsets of the stream are unequal amounts -- 11 m for the northern one and 18 m for the southern one. The latter offset was probably modified by recent stream channel entrenchment and erosion.

3. Consultation with Malcolm Johnston, Paul Spudich, Bill Bakun, Bill Ellsworth, and Wayne Thatcher about geological conditions at potential instrument sites, boreholes, *etc.* Preparation of borehole data base begun for the Parkfield area -- includes location, depth, condition, use, type of instrument(s) installed, and formations penetrated. Data to be used in conjunction with geologic mapping as well as made available for general use.

Reports:

Sims, J.D., 1987, Late Holocene slip along the San Andreas fault near Cholame, California: *Geological Society of America Abstracts with Programs*, v. 19, p. ___ - ___.

Sims, J.D., accepted, Clear Lake, Lake County, California--a 450,000-year-long continual record of climate change and tectonism: *International Union for Quaternary Research*, XII Congress Abstracts.

Sims, J.D., submitted to Branch Chief, Geologic map of the San Andreas fault zone in the Cholame Valley and Cholame Hills, 7-1/2 minute quadrangle, San Luis Obispo and Monterey Counties, California: *U.S. Geological Survey Miscellaneous Field Investigation Map MF-___*.

O'Day, P.A., and Sims, J.D., Director's Approval, Sandstone composition and peleogeopgraphy of the Temblor Foundation, central California--evidence for early to middle Miocene right-lateral displacement on the San Andreas fault system: *Geological Society of America Bulletin*, submitted.

Dense Seismograph Array at Parkfield, California

9910-03974

Paul Spudich
J.B. Fletcher
Branch of Engineering Seismology and Geology
U.S. Geological Survey
345 Middlefield Road, MS 977
Menlo Park, California 94025
(415) 323-8111, ext. 2395 or (415) 329-5654 or (415) 329-5628

Investigations

1. Design and installation of a dense seismograph array at Parkfield.

Results

The basic instrumental parameters of our proposed array have been described in the previous Semi-Annual Technical Report. During this reporting period, we installed permanent cables for velocity geophones to be co-sited with the accelerometers in the dense accelerograph array operated by the Electric Power Research Institute (EPRI) at the Scobie Ranch at Parkfield, California. It is intended to deploy portable recorders and geophones temporarily at the EPRI site in order to record local micro-earthquakes. This will yield information about the weak motion response of the EPRI site.

Reports

None.

MODELING AND MONITORING CRUSTAL DEFORMATION

9960-01488

Ross S. Stein, Wayne Thatcher
Branch of Tectonophysics
U.S. Geological Survey
345 Middlefield Road, MS/977
Menlo Park, California 94025
(415) 323-8111, ext. 2120

Investigations

1. Review of crustal movement investigations carried out in the U.S. during the past 4 years, for the Geodesy contributions to the U.S. National Report to International Union of Geodesy and Geophysics 1983-86.

2. Continued analysis of 1981 Saugus-Palmdale leveling refraction experiment, in response to comments submitted by Craymer and Vanicek (reply submitted) and by Reilinger (reply in progress). This work was carried out in conjunction with the correction of 1979-83 leveling in Southern California for refraction, rod, and magnetic errors.

3. Comparative study of extensional faulting in the Basin and Range province of the western United States from geodetic leveling and geologic data (1959 $M = 2.3$ Hebgen Lake, MT, and 1983 $M = 7.0$ Borah Peak, ID, earthquakes). Examination of the potential of the Peninsular San Andreas fault for $M \simeq 7$ earthquakes, from geodetic strain and geologic data.

Results

1. Contemporary Plate Motion and Crustal Deformation.

   Perhaps the most important advance in geodesy during the past half century was achieved during the past 4 years: direct measurement of global plate motion. The measurement of relative plate velocities is a signal accomplishment in earth science, leading to refinement of the precepts of steady motion of plate interiors and cyclic deformation along plate margins. Regrettably, deformation premonitory to an earthquake has yet to be detected with confidence. Delineation of the spatial and temporal buildup of strain between earthquakes, however, has put limits on models of the earthquake cycle. A diverse set of fault structures and crustal rheologic conditions can explain the pattern of surface strain accumulation and release along strike-slip faults. In contrast, the geometry of thrusts and normal faults, revealed by earthquake deformation, has been found to differ markedly from expectations. Geodetic observations have proved vital to monitor the ascent of magma through the Earth's crust and to predict volcanic eruptions at the Earth's surface. Episodic vertical and horizontal deformation in southern California remains a subject of dispute; if anything, it is less certain than it once seemed. The establishment of the Pinon Flat Observatory in California has been vital for redundant testing and intercomparison of virtually all short- and long-baseline deformation measurement systems at a stable site on crystalline bedrock. Efforts to monitor the approach of the next earthquake on the San Andreas fault along the Parkfield segment and to watch for signs of a potential eruption at Long Valley caldera have also created two concentrated instrument deployments. Evaluation of a dozen competing and ancillary measurements will improve our confidence in some instruments and remove our faith in others.

2. <u>1981 Leveling Refraction Experiment: Reply to Craymer and Vanicek</u>.

In 1981 we conducted a field test of atmospheric refraction error in historical leveling surveys and found that refraction was six times larger than random error and could be modeled and removed [Stein et al., 1986]. Craymer and Vanicek [1986] performed a multiple linear regression on the 1981 data; in addition to confirming the refraction, they reported equally large errors associated with the number of turning points (or rod supports) and the height difference between bench marks. In response, we pointed out [Stein et al., 1986] that their regression was not robust: by design, the number of turning points was positively correlated with height difference. When 2 out of the 60 obervations are removed from the sample, the two independent variables are correlated with each other at the 99.9% confidence level. In their Comments, Craymer and Vanicek [this issue] argue that no observations may be removed from the sample, and that in any case the correlation (r=0.5) is too small to invalidate their coefficients. We reply here that parameters that depend on two points are suspect, which prompted us to examine their regression further. We find that the dependent variable is uncorrelated with the two disputed independent variables, and that Craymer and Vanicek improperly constrained the intercept in their regression to be zero. Removal of the two influential points and the zero-intercept constraint causes the dependences on both the number of turning points and height difference to disappear, leaving only the refraction.

Reports (submitted or published since 12/86, excluding abstracts)

Barrientos, S. E., R. S. Stein, and S. N. Ward, A comparison of the 1959 Hebgen Lake, Montana, and the 1983 Borah Peak, Idaho, earthquakes from geodetic observations, submitted to Bull. Seismol. Soc. Am., v. 77(3), special issue on the Borah Peak earthquake, 1987.

Stein, R. S., Contemporary plate motion and crustal deformation, U.S. National Report to I.U.G.G. 1983-86 Quadrennium, Reviews of Geophysics, v. 25, in press.

Stein, R. S., C. T. Whalen, S. R. Holdahl, W. E. Strange, and W. Thatcher, Reply to Craymer and Vanicek, submitted to J. Geophys. Res., 1987.

Thatcher, W., Geodetic measurements of active-tectonic processes, in Active Tectonics, pp. 155-163, Nat. Acad. Press, Wash., D.C., 1986.

Thatcher, W., Cyclic deformation related to great earthquakes at plate boundaries: Models and observations, in Recent crustal movements of the Pacific Region, pp. 245-272, Bull. 24, Roy. Soc. New Zealand, 1986.

Thatcher, W., and M. Lisowski, Long-term seismic potential of the San Andreas fault southeast of San Francisco, California, J. Geophys. Res., v. 92, in press.

NEARFIELD GEODETIC INVESTIGATIONS OF CRUSTAL MOVEMENTS, SOUTHERN CALIFORNIA

Contract No. USDI-USGS 14-08-0001-G1081

Arthur G. Sylvester
Department of Geological Sciences, and
Marine Science Institute
University of California
Santa Barbara, California 93106
(805) 961-3156

INVESTIGATIONS

Resurveys of 2 of 58 existing precise leveling arrays across active faults were done during the first part of 1987. Both of them, in Indian Wells Valley and near Oildale in the San Joaquin Valley (Fig. 1), were resurveyed at the request of and in part with funds provided by the landowners upon whose land the arrays are located.

The purpose of this investigation is to search for and monitor the spatial and temporal nature of vertical displacement across active and potentially active faults. Thus, we document pre-, co- and post-seismic displacement and creep, if any, especially where seismographic, paleoseismic and geomorphic data indicate current or recent fault activity. The investigations are intermediate in scale between the infrequent, regional geodetic surveys traditionally done by the National Geodetic Survey, and point measurements by continually recording instruments such as creepmeters, tiltmeters, and strainmeters. All surveying is done according to First Order, Class II standards.

RESULTS

Precise leveling arrays SNORT (Fig. 2) and Airfield (Fig. 3) in Indian Wells Valley were releveled 15-16 February to determine if fault movement or tilt had occurred since the last survey in 1985, movements which would affect the alignment of permanent facilities constructed across the faults. Height changes among all benchmarks in both arrays are less than 0.5 mm (Figs. 4 and 5) which is within our allowable error of 1 mm ($L^{-1/2}$), where L equals the length of the leveled segment in kilometers. Thus the faults have not experienced statistically significant movement since 1985 or since they were established in 1983.

A large, box-shaped leveling array was established across the surface trace of the Kern Front fault in mid August 1986 (Fig. 6) at the request of and with partial support from Texaco, USA. The array, which is 1306 m in length, has 106 permanent bench marks. Several of them are spaced as closely as 2 meters where they straddle the fault. We also established a new tilt beam across the surface trace of the fault on November 19, 1986 to replace that which operated there in1968-1974 (Nason et al, 1974) and has been long since vandalized and stolen. The south leg of the array was resurveyed on 22 March 1987. Analysis of that data shows that 3 mm of relative down-to-the-west height change occurred between bench marks FSW and FSE, which straddle the fault next to the tilt beam, and between bench marks KF01 and KF106 about 10 m north of the tilt beam, between 19 August 1986 and 22 March 1987 (Fig. 7). The tilt beam showed no permanent change of height in the time period 24 November 1986 and 23 March 1987. Thus, the movement detected by the leveling occurred between 19 August and 24 November 1986, and the principal offset took place right at the surface trace of the fault.

The rate and direction of movement we determined by precise leveling, 10 mm/yr and down to the west, are the same as were measured by the tilt beam in 1969-1974 (Nason et al, 1974) and determined by Castle et al (1983) from geologic evidence and visual recollections of geologists who first noted the surface fractures in 1949. If the maximum offsets measured by Castle et al (1983) are inverted against the rate of height change across the fault, then the present historic episode of movement began in the late 1920's when both the Kern River and Kern Front oil fields came into significant production. This is one of the reasons Castle et al (1983) maintained that the movement across the fault is primarily induced by withdrawal of fluids by pumping in those two oil fields. They emphasized that even if the movement is tectonic or has a tectonic component, it will be very hard to determine or separate it simply because of the potential for subsidence, given the great magnitude of fluids that are extracted annually.

We intend to resurvey the entire array in early summer, to establish additional lines of 4-6 bench marks elsewhere along the length of the fault, and perhaps construct and install another tilt beam across the fault. All of these endeavors should yield more information on the timing and distribution of the movement along the length of the fault. The geometry of the 106 monument array also affords the opportunity to determine tilt of each of the fault blocks, although the proximity of parts of the arrays to producing oil wells may obscure the tilt record because of the surficial effects of episodic pumping.

REFERENCES CITED

Castle, R. O., J. P. Church, R. F. Yerkes, and J. C. Manning, 1983. Historical surface deformation near Oildale, California. U.S. Geological Survey Professional Paper 1245, 42 p.

Nason, R. D., F. R. Philippsborn, and P. A. Yamashita, 1974. Catalog of creepmeter measurements in central California from 1968 to 1972. U.S. Geological Survey Open File Report 74-31, 287 p.

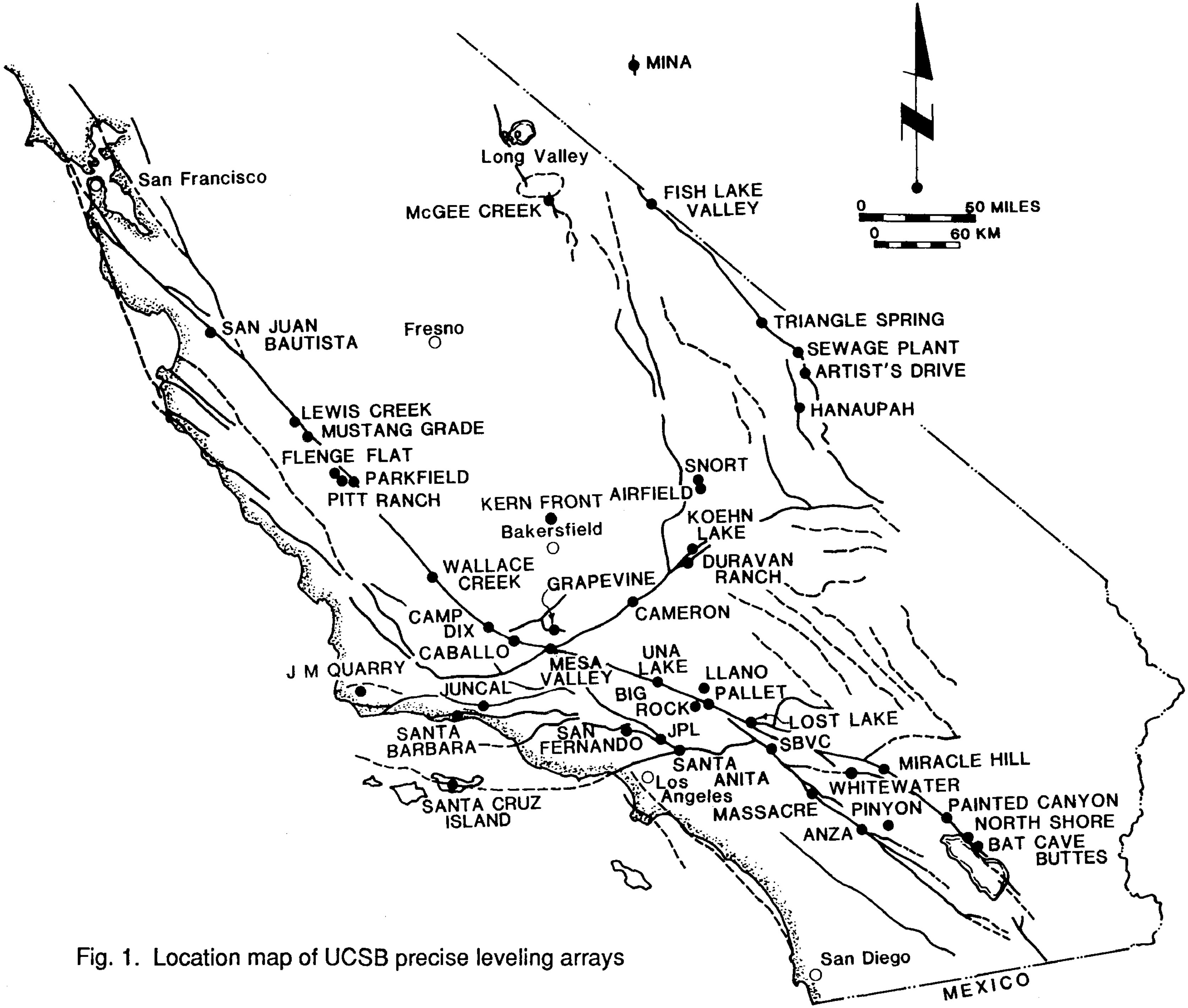

Fig. 1. Location map of UCSB precise leveling arrays

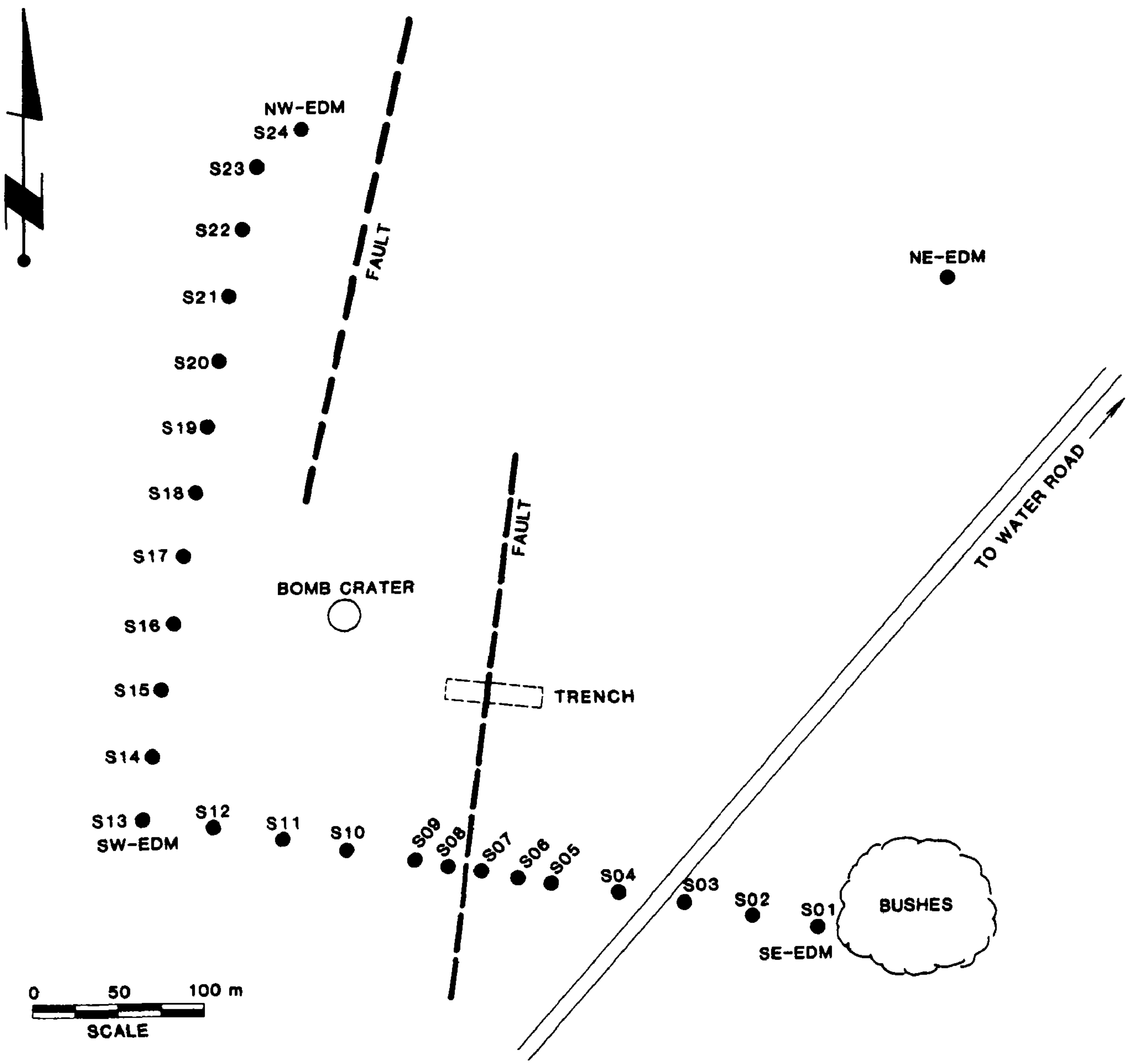

Fig. 2. Site map of UCSB precise leveling and trilateration arrays across fault pair at stations SNORT, Indian Wells Valley.

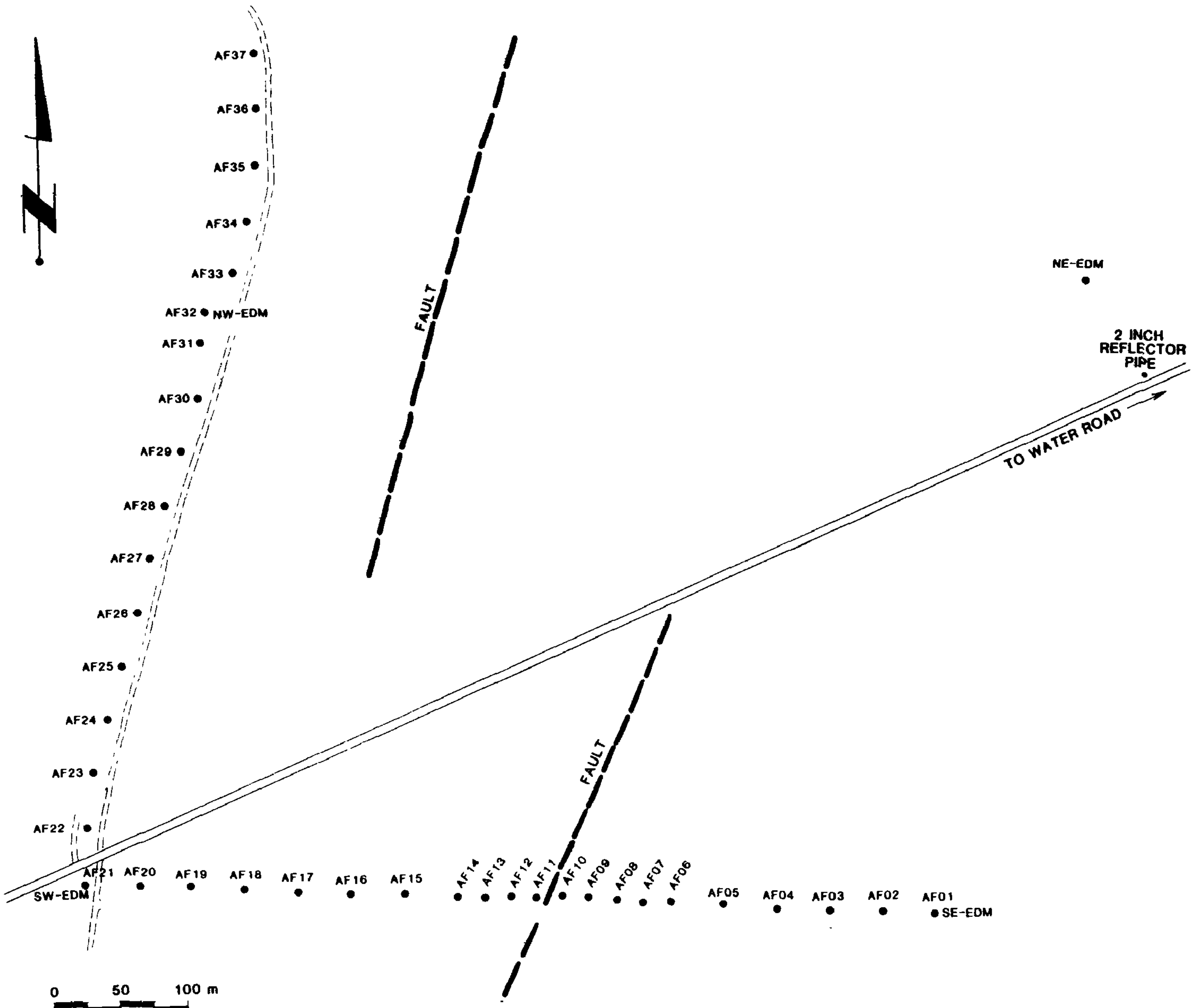

Fig. 3. Site map of UCSB precise leveling and trilateration array across fault pair at station Airfield, Indian Wells Valley.

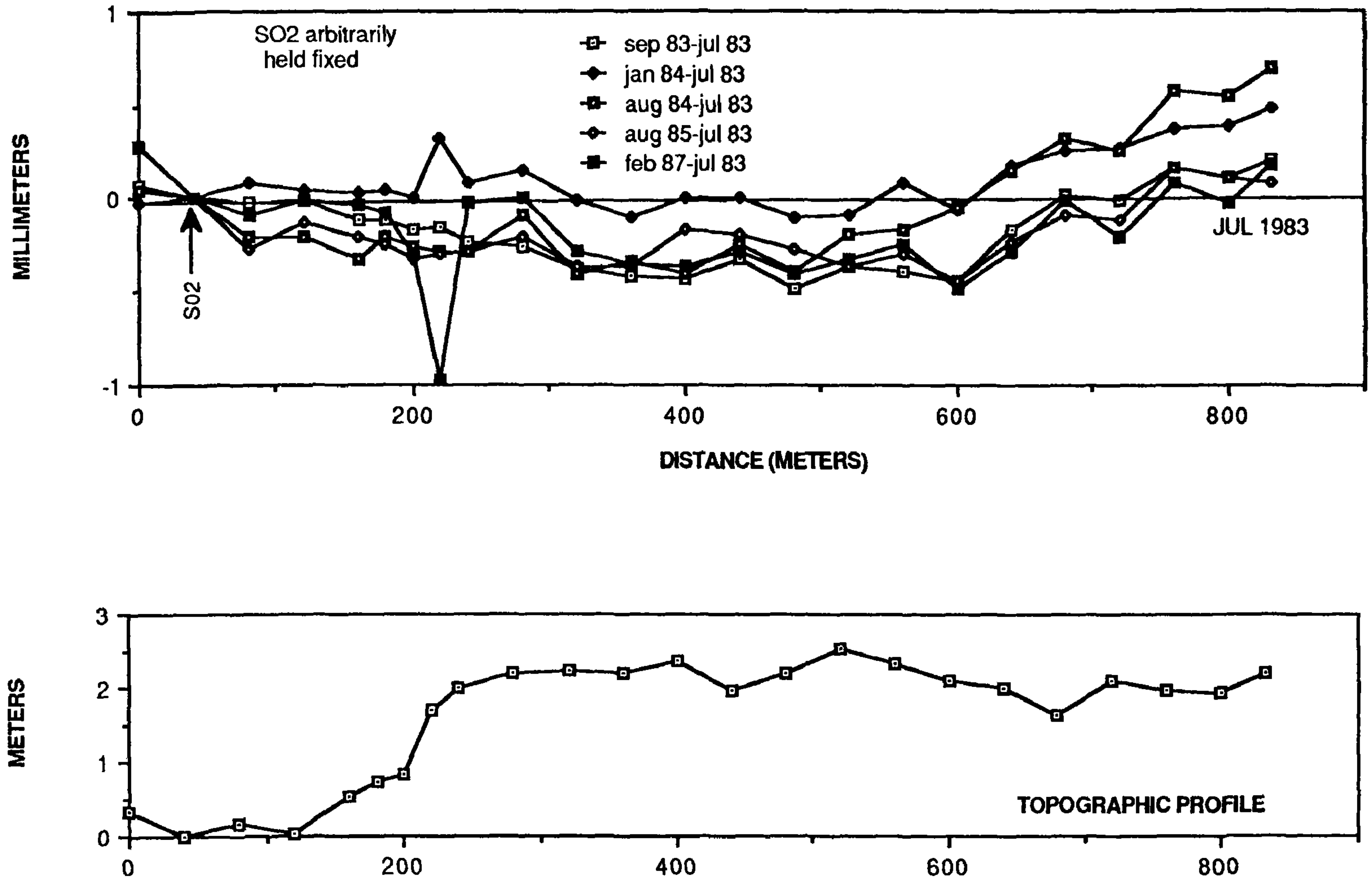

Fig. 4. Height changes of bench marks in the SNORT leveling array for six surveys from July 1983 to February 1987.

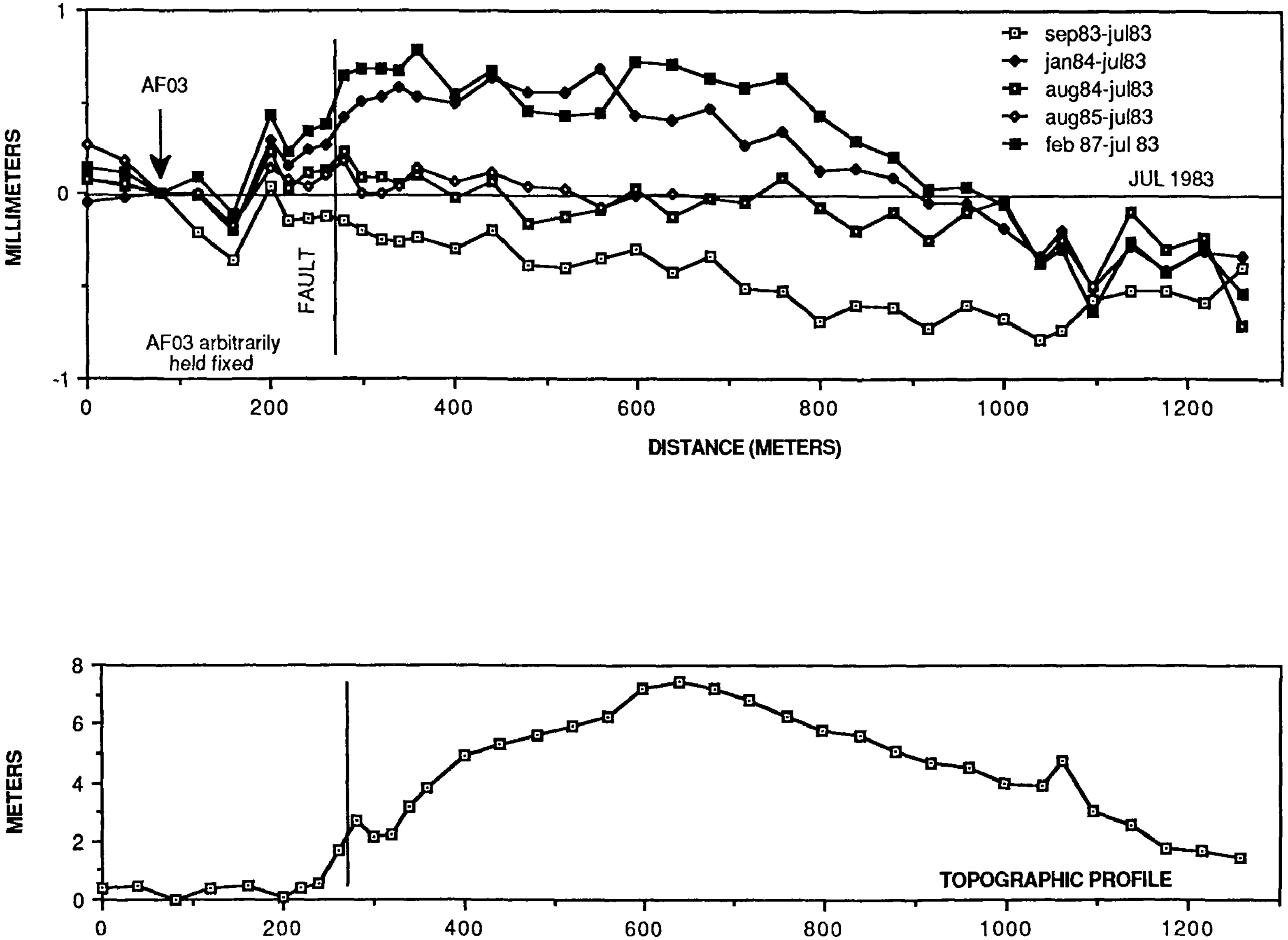

Fig. 5. Height changes of bench marks in the Airfield leveling array for six surveys from July 1983 to February 1987.

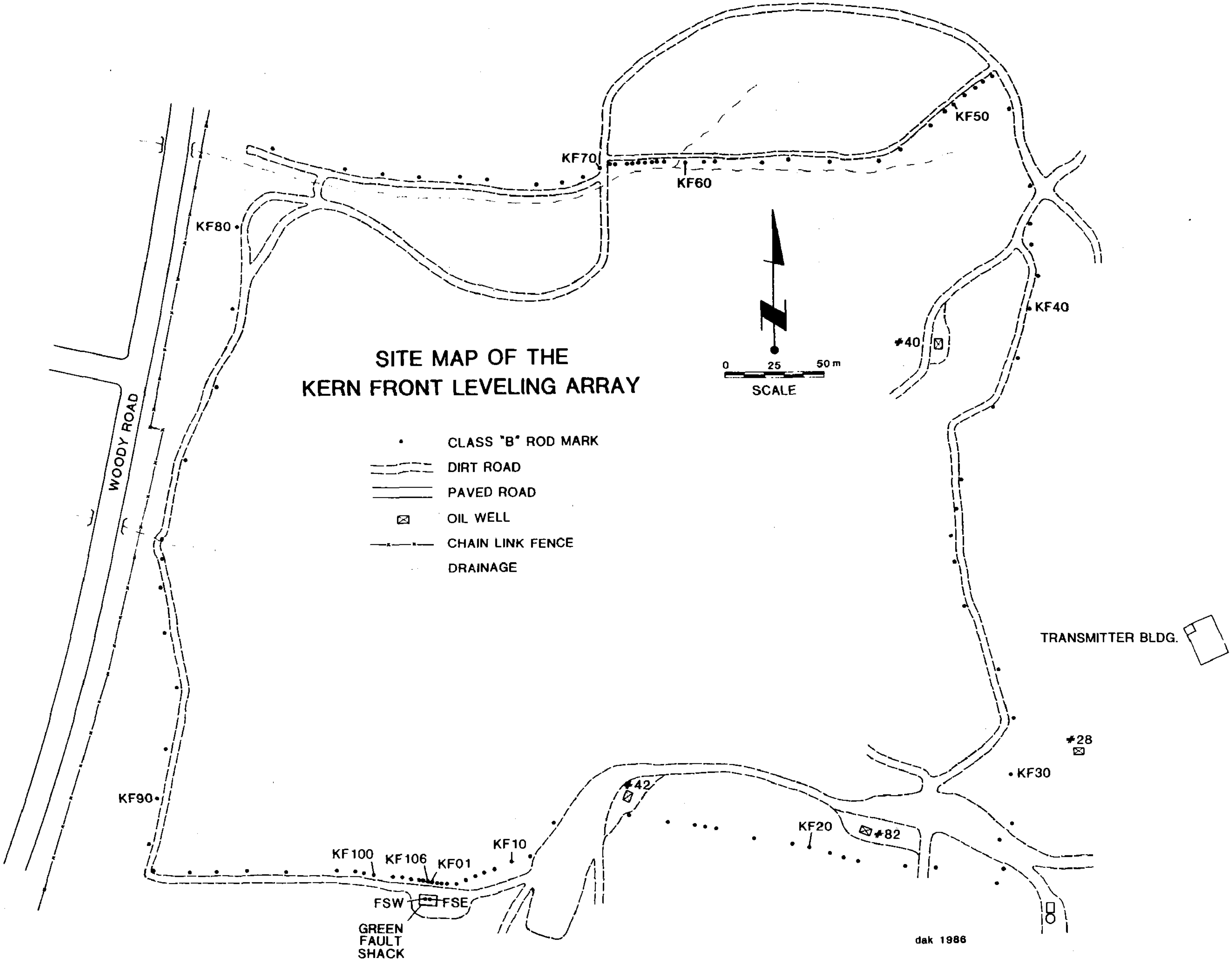

Fig. 6. Site map of UCSB precise leveling array across Kern Front fault near Oildale. The surface trace of the fault is precisely located between bench marks FSW and FSE along the south leg of the array, and less precisely between KF60 and KF70 on the north leg.

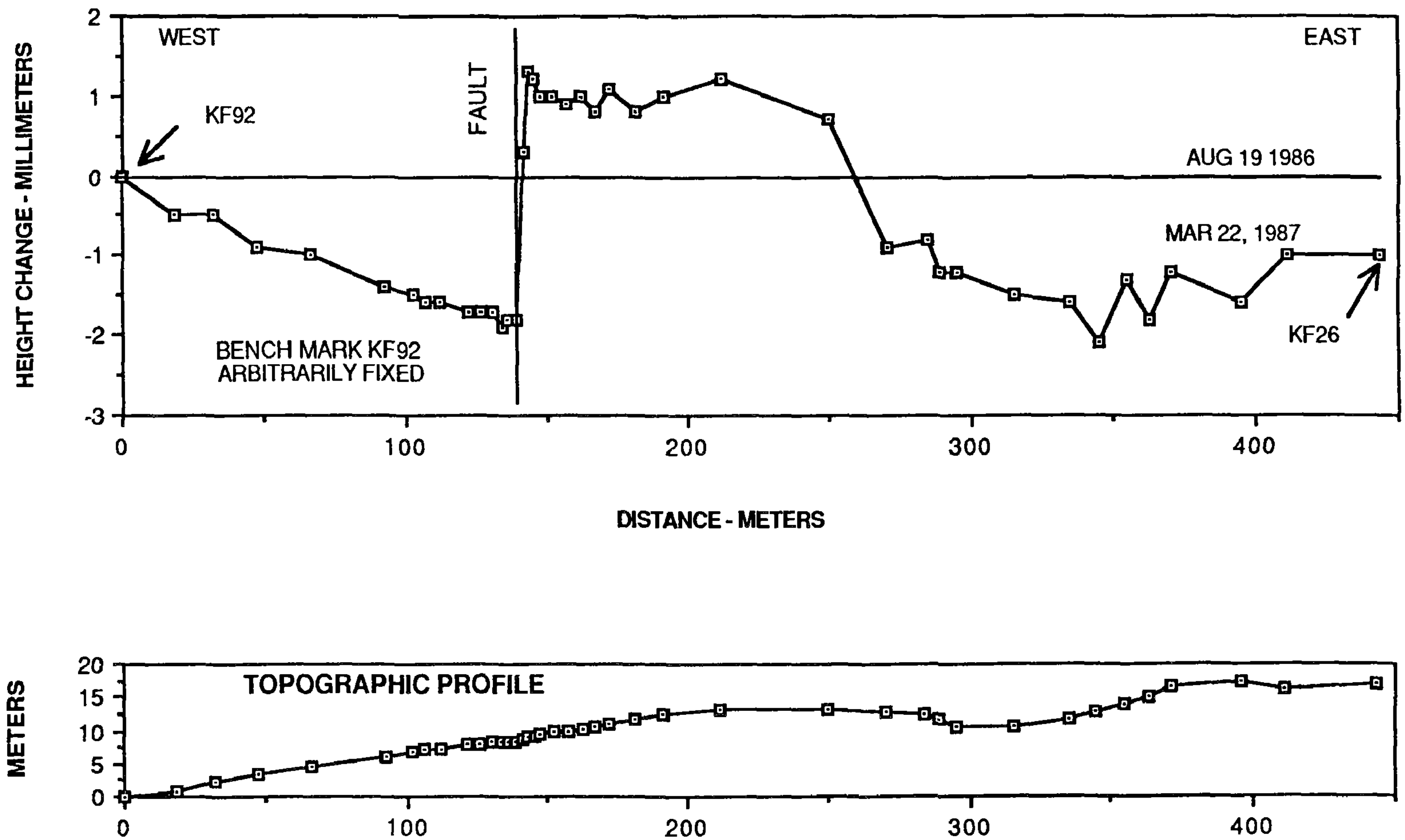

Fig. 7 Height changes of bench marks in the Kern Front leveling array for two surveys from August 1986 to March 1987.

Fault Kinematics in the Imperial Valley, California: Implications for Earthquake Prediction on the Imperial, San Jacinto and Southern San Andreas Faults

14-08-0001-G1337

M.N. Toksoz and R.E. Reilinger
Earth Resources Laboratory
Dept. of Earth, Atmospheric, and Planetary Sciences
Massachusetts Institute of Technology
Cambridge, Massachusetts 02142
(617) 253-7852

INVESTIGATIONS

This project involves using available geodetic observations in conjunction with other geophysical and geological information to investigate contemporary tectonic processes along the southernmost segment of the San Andreas fault system. Specific studies include:

(1) Fault behavior in the Imperial Valley as evidenced by the 1940 and 1979 earthquakes,

(2) Implications of the 1986 NGS GPS observations for seismic and aseismic faulting in the Imperial Valley,

(3) Impact of near surface, nontectonic subsidence on interpretation of regional deformation in Southern California (i.e., Palmdale Bulge),

(4) Earthquake deformation and geologic/topographic structure,

(5) Postseismic viscoelastic deformation following the 1959 M=7.5, Hebgen Lake, Montana earthquake.

RESULTS

1. Fault Behavior in the Imperial Valley, California: Evidence from the 1940 and 1979 Earthquakes. Geodetic and geophysical observations in the Imperial Valley provide information on the spatial and temporal distribution of seismic and aseismic faulting along the Imperial-Brawley fault system and within the Brawley Seismic Zone. The geodetic observations, which span the 1940, M=7.1 and the 1979, M=6.6 earthquakes on the Imperial fault, suggest that the largest coseismic fault slip for these events occurred along approximately the same 20-30 km section of the Imperial fault. The 1940 and 1979 events apparently initiated just north and south of this section of the fault respectively. North and south of this "stick-slip" section of the Imperial fault, failure occurs, at least in part, by aseismic creep. This interpretation is supported by the distribution of small earthquakes along the Imperial fault as well as by direct observations of fault creep at the surface. The Brawley Seismic Zone, which is a complex zone of seismicity between the north end of the Imperial fault and the south end of the San Andreas fault, is characterized by increased seismic activity and rapid deformation during the postseismic period for earthquakes on the Imperial fault. Our preferred interpretation of the nature of faulting in the Brawley Seismic Zone, based on the geodetic and seismic observations, involves right lateral aseismic slip (with a component of down to the west dip-slip) on a northwest striking fault along the east side of the Brawley Seismic Zone and conjugate left lateral slip along northeast striking faults (associated with major aftershocks). Buried creep on this same right lateral fault in the Brawley Seismic Zone may also account for vertical deformation during the interseismic period between the 1940 and 1979 earthquakes. Substantial right lateral slip in the Brawley Seismic Zone suggests that a significant part of the shear strain released by earthquakes on the Imperial fault is transferred to the southern end of the San Andreas fault.

2. GPS Measurements in the Imperial Valley, California. During the summer of 1986, the National Geodetic Survey completed a dense GPS survey in the vicinity of the Imperial fault-Brawley Seismic Zone. Essentially all of the GPS observations were made at preexisting geodetic control points which were observed with conventional methods (trilateration and/or leveling) prior to and closely following the 1979 earthquake. Using conservative estimates for the precision of both the GPS and conventional base line measurements, we show that comparison of these data sets should provide further information on the nature of 1979 coseismic and postseismic fault slip in the Brawley Seismic Zone and along the Imperial fault. We will present the results of our preliminary processing of these data at the Spring AGU. (This work is being done in cooperation with Richard Snay, NGS.)

3. Comment on Stein et al.(1986; JGR, 91,9031-9044). Stein *et al.* (1986) report on the results of field tests designed to determine the effects of atmospheric refraction on historic leveling surveys in Southern California. They use these results to test refraction error models and to correct historical leveling between Saugus and Palmdale for the effects of atmospheric refraction. Stein *et al.* (1986) conclude that the corrected uplift near Palmdale reached 56 ± 16 mm with respect to Saugus during the period 1955-1965. They further state that this relative uplift is tectonic in origin and does not result from subsidence near Saugus.

This comment questions the conclusion of Stein *et al.*, that uplift of Palmdale relative to Saugus does not result from nontectonic subsidence near Saugus. For the most part, the arguments presented here reiterate results published by Reilinger (1980; *Geophys. Res. Lett., 11, 1017-1019).* In particular, we show that:

1) In addition to the Saugus-Palmdale route, two other leveling routes from Saugus indicate subsidence of Saugus relative to the periphery of the Saugus basin during the period 1953 to 1964.

2) Observed elevation changes in the Saugus area correlate spatially with aquifer geometry and temporally with the history of the inferred decline in the potentiometric water surface within the aquifer.

3) Subsidence of individual benchmarks above the Saugus aquifer is roughly proportional to the product of aquifer thickness and inferred decline of the potentiometric surface (relation predicted by compaction theory).

4) The compressibility of the sediments derived from (3) is quite comparable to that reported for other confined aquifers in Southern California.

4. Earthquake Deformation and Geologic/Topographic Structure. An important element of the earthquake deformation cycle is the permanent deformation that accumulates as a result of many earthquakes. This deformation takes the form of mountains and basins in dip-slip fault environments, transverse offsets along strike-slip faults (as well as topographic relief in areas of compression or extension) and folding of the rocks adjacent to the faults. For the most part, these permanent deformations occur over too long a time period to be directly investigated with geodetic techniques and require geologic studies. However, in many cases there is a clear relationship between the geodetically measured, short term deformation associated with particular earthquakes and longer term deformation indicated by geologic and topographic structure. These relationships suggest that the geodetic observations can provide direct, quantitative information on the mountain building process. Furthermore, understanding the contribution of permanent deformation to the earthquake cycle is necessary to effectively use geodetic observations to estimate earthquake repeat times.

In this investigation we attempt to draw some generalizations and identify some unresolved problems concerning the relationship between earthquake deformation and deformation indicated by geologic/topographic structure. The primary information comes from earthquakes in a variety of contrasting tectonic settings and includes an intraplate thrust event in the Precordillera of western Argentina, a normal fault event in the Basin and Range of the western U.S. for which there is a long history of postseismic deformation measurements, and a series of predominantly strike-slip earthquakes along the southernmost segment of the San Andreas fault system in the Imperial Valley, California. Other examples from the literature are used to a limited extent to further examine possible relationships between short and long term deformation.

Our analysis emphasizes the following points:

1) The earthquake deformation cycle provides a useful framework for investigating geodetically measured surface movements as well as deformation indicated by geologic and topographic structure in seismically active areas.

2) While there is often a clear relationship between coseismic deformation and long term deformation, the differences between the spatial patterns of deformation over these time scales require large (i.e., similar amplitude to coseismic) postseismic and/or interseismic movements. Comparison of the coseismic and long term deformation patterns provides direct information on the character of these inter-earthquake movements.

3) Geodetic observations near two intraplate, dip-slip earthquakes suggest that postseismic viscoelastic relaxation in the asthenosphere is an important mechanism responsible for at least a part of the observed inter-earthquake deformation.

4) The established relationship between earthquake deformation and relatively subtle topographic relief, even in predominantly strike-slip environments, indicates that topography can reflect detailed fault behavior.

5. Evidence for Postseismic Viscoelastic Relaxation Following the 1959, M=7.5 Hebgen Lake, Montana Earthquake. A 1983 releveling survey conducted by the National Geodetic Survey, combined with previous surveys in 1923, 1960, 1967 and 1975, provides evidence for ongoing vertical deformation of a broad region (diameter ~150 km) surrounding the site of the 1959 Hebgen Lake earthquake. Deformation consists of relative uplift centered roughly on the coseismic fault and a smaller amplitude zone of relative subsidence south of the fault. Maximum observed elevation change during the postseismic period (1960 to 1983) exceeds 30 cm. Assuming that the entire uplift (i.e., 1923 to 1983) occurred following the 1959 earthquake (i.e., uplift measured between 1923 and 1960 was entirely postseismic), the rate of vertical deformation appears to have decreased exponentially with a characteristic decay time of about 10 years.

The spatial pattern and time behavior of the observed movements are consistent with simple models of postseismic deformation following normal faulting in an elastic layer (thickness ~30-40 km) overlying a viscoelastic half-space (viscosity ~ 10^{19} Pa s). This model may also account for the anomalously large horizontal strain around the Hebgen Lake region measured by repeated trilateration surveys during the period 1973 to 1984. The releveling measurements in the Hebgen Lake region appear to provide the first observations of viscoelastic relaxation in the asthenosphere following an intraplate earthquake in the U.S.

PUBLICATIONS

Reilinger, R.E., Comment on "Saugus-Palmdale, California, field test for refraction error in historical leveling surveys, by Ross S. Stein, Charles T. Whalen, Sanford R. Holdahl, William E. Strange, and Wayne Thatcher," *J. Geophys. Res.*, in press, 1987.

Larsen, S., and R.E. Reilinger, Constraints on the age of the present fault configuration in the Imperial Valley, California, *J. Geophys. Res.*, submitted, 1986.

Reilinger, R.E., and S. Larsen, Crustal deformation associated with the 1979, M=6.6 Imperial Valley, California earthquake: Implications for fault geometry and slip distribution, *J. Geophys. Res.*, *91*, 14,044-14,056, 1986.

Reilinger, R., The earthquake deformation cycle: Examples from South America and the western United States, *Proceedings of China-United States Symposium on Crustal Deformation and Earthquakes*, Wuhan, China, in press, 1986.

Reilinger, R.E., Evidence for postseismic viscoelastic relaxation following the 1959, M=7.5 Hebgen Lake, Montana earthquake, *J. Geophys. Res.*, *91*, 9488-9494, 1986.

Brown, L.D., and R.E. Reilinger, Epeirogenic and intraplate movements, in *Active Tectonics--Impact on Society*, ed. R.E. Wallace, National Academy of Sciences, Washington, D.C., 30-44, 1986.

ABSTRACTS

Reilinger, R.E., K. Kadinsky-Cade, and S. Larsen, The earthquake deformation cycle: Examples from South America and the western United States, *EOS, Trans. Am. Geophys. Union*, *67*, 904, 1986.

Larsen, S., and R. E. Reilinger, Fault behavior in the Imperial Valley, California: Evidence from the 1940 and 1979 earthquakes, *EOS, Trans. Am. Geophys. Union*, *67*, 1200, 1986.

Reilinger, R.E., R. Snay and H.C. Neugebauer, 1986 NGS GPS observations in the Imperial Valley, California: Implications for fault behavior, *EOS, Trans. Am. Geophys. Union*, in press, 1987.

ROCK MECHANICS

9960-01179

James Byerlee
U.S. Geological Survey
Branch of Tectonophysics
345 Middlefield Road, MS/977
Menlo Park, California 94025
(415) 323-8111, ext. 2453

Investigations

Laboratory experiments are being carried out to study the physical properties of rocks at elevated confining pressure, pore pressure and temperature. The goal is to obtain data that will help us to determine what causes earthquakes and whether we can predict or control them.

Results

Layers of artificial granite gouge have been deformed on saw-cut granite surfaces inclined 30° to the sample axes. Samples were deformed at a constant confining pressure of 250 MPa and temperatures of 22 to 845°C. The velocity dependence of the steady-state coefficient of friction (μ^{ss}) was determined by comparing sliding strengths at different sliding rates. The results of these measurements are consistent with those reported by Solberg and Byerlee (1984) at room temperature and Stesky (1975) between 300 and 400°C. Stesky found that the slip-rate dependence of μ^{ss} increased above 400°C. In the present study, however, the velocity dependence of μ^{ss} was nearly independent of temperature.

Reports

Lockner, D., J. Byerlee, V. Kuksenko and A. Ponomarev, 1986, Stick-slip charge separation and decay, PAGEOPH, v. 124, no. 3, p. 601-608.

Lockner, D., R. Summers, J. Byerlee, 1986, Effects of temperature and sliding rate on frictional strength of granite, PAGEOPH, v. 124, no. 3, p. 445-449.

Moore, D., R. Summers, J. Byerlee, 1986, The effects of sliding velocity on the frictional and physical properties of heated fault gouge, PAGEOPH, v. 124, no. 112, p. 31-52.

Morrow, C., J. Byerlee, 1986, The effect of velocity dependent consolidation on the frictional strength of fault gouges, EOS, Trans. Am. Geophys. Union, v. 67, no. 44, p. 1187.

Morrow, C., D. Lockner, J. Byerlee, 1986, Velocity and time-dependent stress transients in simulated fault gouge, Proceedings of the International Symposium on Engineering in Complex Rock Formations, Beijing, China, p. 142-148.

PERMEABILITY OF FAULT ZONES

9960-02733

James Byerlee
Branch of Tectonophysics
U.S. Geological Survey
345 Middlefield Road, MS/977
Menlo Park, California 94025
(415) 323-8111, ext. 2453

Investigations

Laboratory studies of the permeability of rocks and gouge are carried out to provide information that will assist us in evaluating whether in a given region fluid can migrate to a sufficient depth during the lifetime of a reservoir to trigger a destructive earthquake. The results of the studies also have application in the solution of problems that arise in nuclear waste disposal.

Results

As part of the scientific drilling experiment at Cajon Pass, we plan to measure the permeability of rock cores recovered from the hole. The results of this study will be used in the interpretation of the heat flow and in-situ stress measurements. The laboratory equipment that will be used in this study has been overhauled and recalibrated. Cores from the well will be available sometime in April and the results of our studies will be available by year end.

High Frequency Seismic and Intensity Data

9910-03973

Jack Evernden
Branch of Engineering Seismology and Geology
U.S. Geological Survey
345 Middlefield Road, MS 977
Menlo Park, California 94025
(415) 323-8111, ext. 2243 or (415) 329-5627

Investigations:

1) Investigating *via* quantitative modeling of earthquake and explosion spectra the roles of elastic velocity structure, depth of focus and anelastic attenuation on the amplitude and spectral content of both compressional and shear phases (P_n, P_g, S_n, and S_g-L_g, *etc.*) as a function of distance.

2) Investigating *via* large data sets the P-wave spectral content of earthquakes and explosions, the intent being to place in the literature a definitive analysis of this relationship.

Results:

Both investigations in progress.

Reports:

Have prepared documents for presentation at OTA Meetings in April-May 1987 on detection and identification of underground nuclear explosions.

Constitutive Relations for Frictional Rock Sliding and Computer Modelling of the Elastic-Sliding Interactive System

14-08-001-G1191

Bruce E. Hobbs
CSIRO Division of Geomechanics
Box 54, Mt. Waverley, 3149
(03) 23-1355

Objective: This project is aimed at (i) generalizing the constitutive relations for frictional sliding already developed by Dieterich (1979, 1981) and Ruina (1980, 1983) by including a dependence upon normal stress and at (ii) modelling the interaction between constitutive behavior of a fault and the elastic response of the surrounding rocks using hybrid distinct element-boundary element codes.

Modelling Studies: Effort in the past six months has concentrated on exploration of the simple and multiple spring-slider systems with Dieterich-Ruina rate and state dependent friction (see Gu et al., 1984) using an explicit, time marching, finite difference code, UDEC (Cundall, 1971, 1974). In this code the effect of inertia of the sliding block is taken into account. For this report only the single block system is considered.

1. One state variable constitutive law

Figures 1, 2, 3 and 4 show the changes in behavior within this system (with constant normal stress) for various step increases, ΔV, in the load point velocity, V, and for various values of the spring stiffness, k.

Figures 1 and 2 show the effect of step increases in load point velocity ranging from 1.1 in (a) to 10.0 in (h) of each of the figures for a stiffness where according to the analysis of Gu et al (1984) sliding should be stable for low ΔV and unstable for high ΔV. This is indeed shown by Figures 1 and 2. However the transition from stable to unstable is not as straightforward as is indicated by the linear, inertialess analysis of Gu et al (1984). Figure 2 shows a point attractor for ΔV up to 2.8 with the system spiralling inwards to this attractor. Above $\Delta V = 2.8$ the system continues to spiral inwards but now to a set of nested limit cycles whose sizes gradually grow as ΔV increases. The shape of these limit cycles also gradually changes as ΔV increases from a circle for relatively low ΔV to that shown in Figure 2(h) for high ΔV (some numerical instability is shown in the early parts of Figures 2g and h).

Figure 1, however, shows that instability (i.e., the development of stick-slip events) is not to be associated with the bifurcation from a point attractor to stable limit cycles. A large stick-slip event is shown as the first event for $\Delta V = 2.8$ (Figure 1c) but then the system evolves towards stable sliding. For $\Delta V = 2.9 - 3.5$ (Figures 1d,e,f) the first two events are stick-slip and the system evolves towards smooth oscillatory sliding. For $\Delta V = 5,10$ (Figures 1g, h) all of the events are stick-slip but the system evolves towards stable limit cycles.

Thus, for the one-state variable system initial stick-slip events can evolve into stable, oscillatory or continued stick-slip behaviour depending on the value of ΔV.

Figures 3 and 4 are drawn for various step increases in velocity but for a relatively low stiffness correspnding to a situation where the system should always be unstable according to Gu et al (1984). This is indeed the case and two examples are shown in Figure 3 for a low and high ΔV. Figure 4 shows the phase portraits for various ΔV ranging from 1.005 to 10.0. In all cases a stable limit cycle is developed, however for low values of ΔV the system spirals outwards to the limit cycle whereas for high values of ΔV the system spirals inwards to the limit cycle.

2. Two state variable constitutive law

Figures 5 and 6 are drawn for a step increase in load point velocity of 1.5 but for various values of k (decreasing from (a) to (e) in each figure). As in the analysis of Gu et al (1984) for the two state variable constitutive law the system shows a progression from a point attractor to stable limit cycles as k decreases. A birfurcation between inward and outward spiralling systems exists between Figures 6(c) and (d). This coincides with the development of stick-slip (albeit very small) events but which gradually grow in magnitude as k decreases.

Figure 7 shows the two state variable system at high stiffness for two step changes in velocity of 1.3 (Figures 7a,b) and 2.5 (Figures 7c,d). For both examples the system spirals inwards but to a point attractor for low ΔV and to a stable limit cycle for high ΔV. For both examples the first event is stick-slip. Thus, again, in this system, unstable events can evolve into stable sliding.

For the two-state variable examples presented here one state variable remains approximately an order of magnitude smaller than the other. Strict periodicity is always maintained. Examples are now being examined where both state variables are similar in magnitude and more complicated behavior is evident.

References

P.A. Cundall. A computer model for simulating progressive large scale movements in blocky rock systems. Proceedings of the Symposium of the International Society of Rock Mechanics, (Nancy, France, 1971), Vol. 1, Paper No. II-8, 1971.

P.A. Cundall. *Rational design of tunnel supports:* *A computer model for* rock mass behavior using interactive graphics for the input and output of geometrical data, Tech. Report MRD-2074, Missouri River Division, U.S. Army Corps of Engineers, 1974; NTIS Report No. AD/A-001 602, 1974.

J.H. Dieterich. Modelling of rock friction, 1, Experimental results and constitutive equations, J. Geophys. Res., 84, 2161-2168, (1979).

J.H. Dieterich. Constitutive properties of faults with simulated gouge. In Mechanical Behavior of Crustal Rock, Vol. 24, pp.103-120. Geophysical Union Monograph, 1981.

J.-C. Gu, J.R. Rice, A.L. Ruina and S.T. Tse. Slip motion and stability of a single degree of freedom elastic system with rate and state dependent friction. J. Mech. Phys. Solids, 32, 167-196 (1984).

A.L. Ruina. Friction laws and instabilities: A quasi-static analysis of some dry frictional behavior. Ph.D. Thesis, Division of Engineering, Brown University (1980).

A.L. Ruina. Slip instability and state variable friction laws, J. Geophys.Res., 88, 10359-10270 (1983).

Figure Captions

Figure 1. Shear stress (Pa) vs displacement (m) plots for the single block system with one-state variable friction constitutive law. Stiffness > k_{crit}. ΔV for each diagram is (a) 1.1, (b) 1.5, (c) 2.8, (d) 2.9, (e) 3.1, (f) 3.5, (g) 5.0, (h) 10.0.

Figure 2. Shear stress (Pa) vs velocity (ms^{-1}) plots (phase portraits) for the single block system with one-state variable friction constitutive law. Conditions as in Figure 1.

Figure 3. Shear stress vs displacement plots for the single block system with one-state variable friction constitutive law. Stiffness < k_{crit}. ΔV = 1.005 in (a) and ΔV = 10.0 in (b).

Figure 4. Shear stress vs velocity (phase portraits) for the single block system with one-state variable friction constitutive law. Stiffness < k_{crit}. ΔV is (a) 1.005, (b) 1.5, (c) 3.0, (d) 4.0, (e) 5.0, (f) 10.0.

Figure 5. Shear stress vs displacement plots for the single block system with two state variable friction constitutive law. ΔV = 1.5 in all diagrams and k progressively decreases in going from (a) to (e).

Figure 6. Shear stress vs velocity plots (phase portraits) for the single block system with two state variable friction constitutive law. ΔV = 1.5 in all diagrams and k progressively decreases in going from (a) to (e).

Figure 7. One block system with two state variable friction constitutive law. ΔV = 1.3 in a,b and ΔV = 2.5 in c,d. (a) and (d) are plots of shear stress (Pa) against displacement (m) whereas (b) and (c) and phase portraits of shear stress (Pa) against velocity (ms^{-1}).

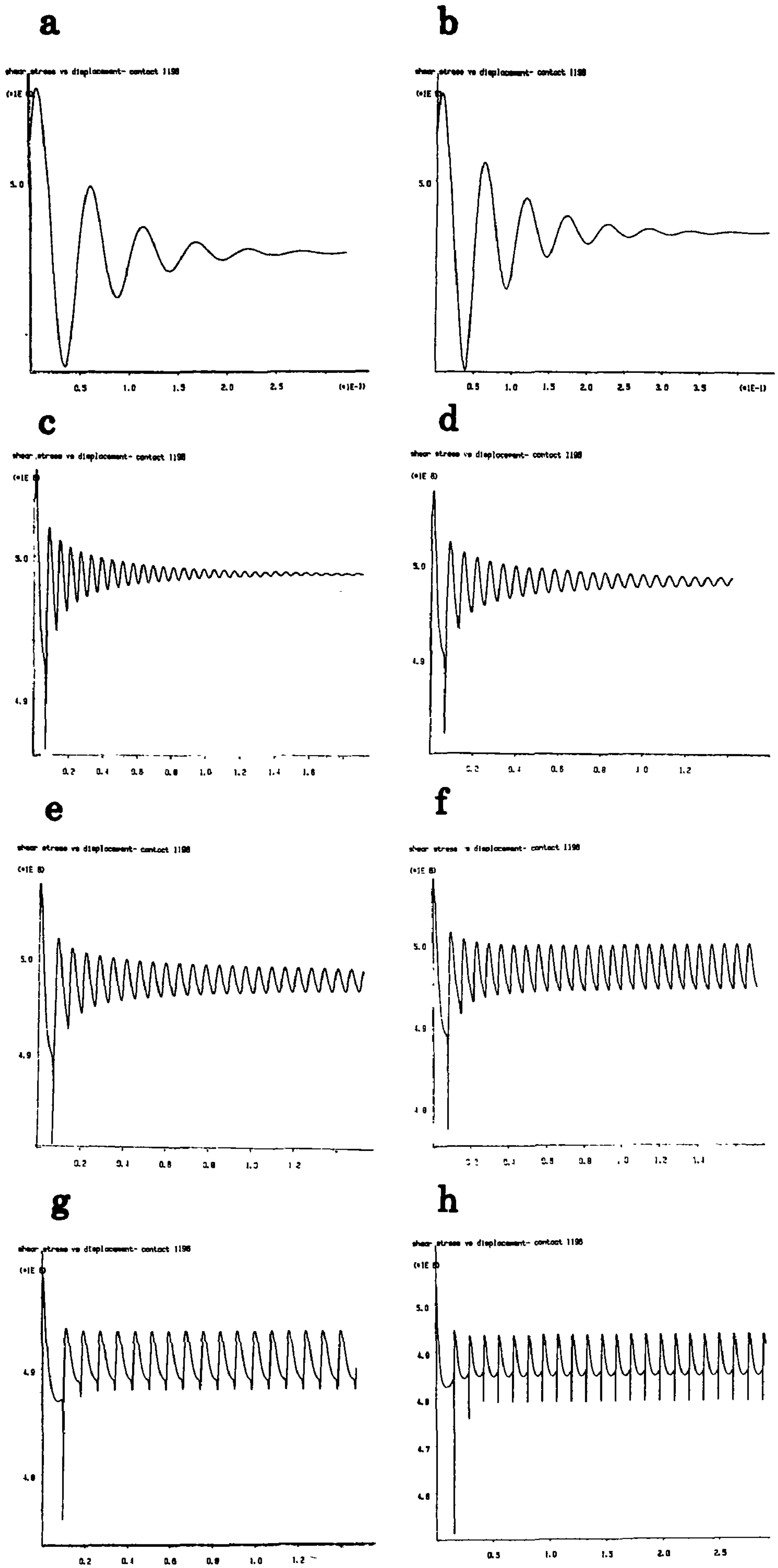

FIGURE 1

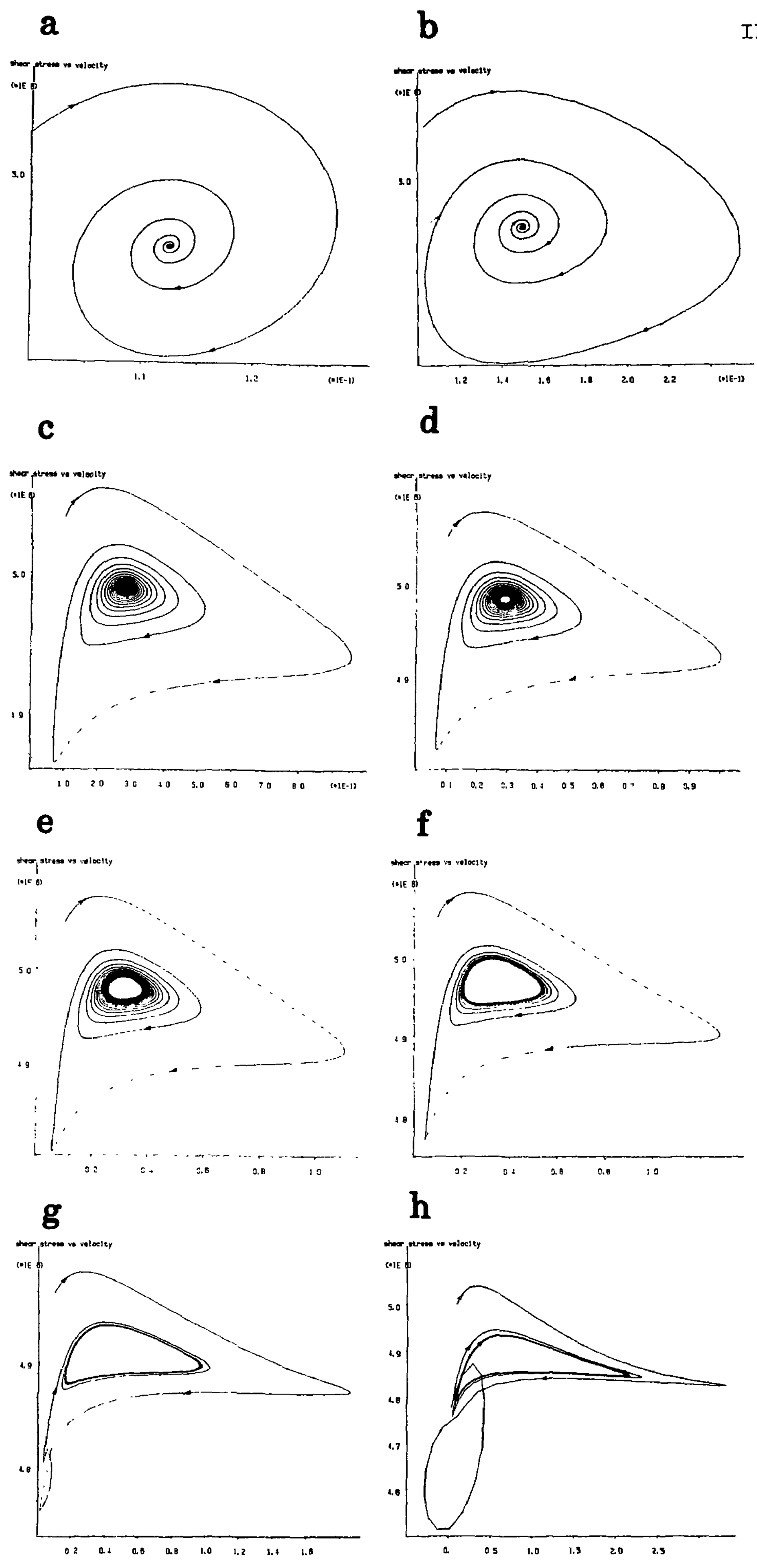

FIGURE 2

a

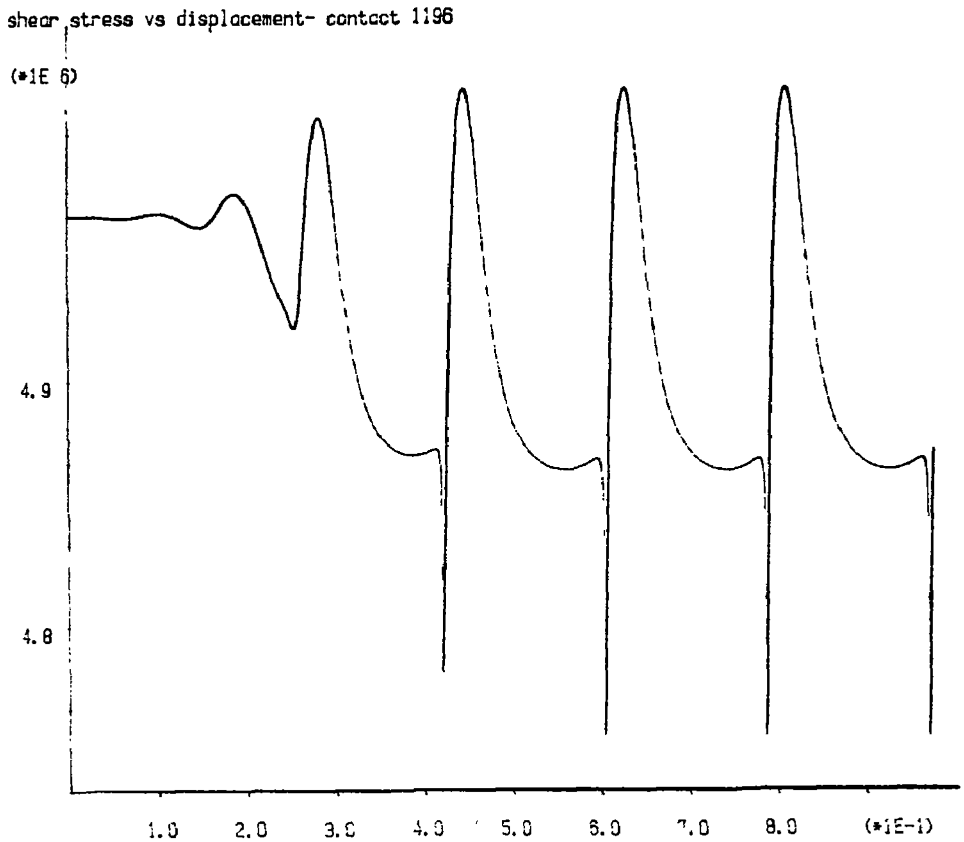
shear stress vs displacement- contact 1196
(*1E 6)
4.9
4.8
1.0
2.0
3.0
4.0
5.0
6.0
7.0
8.0
(*1E-1)

b

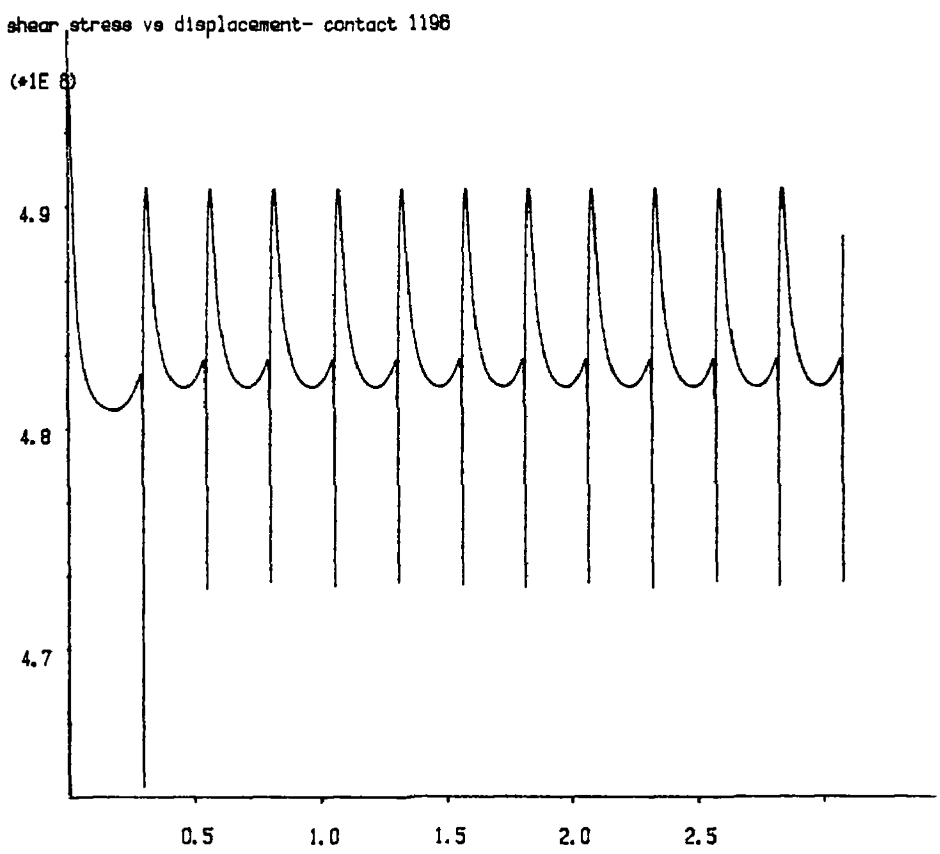
shear stress vs displacement- contact 1196
(*1E 6)
4.9
4.8
4.7
0.5
1.0
1.5
2.0
2.5

FIGURE 3

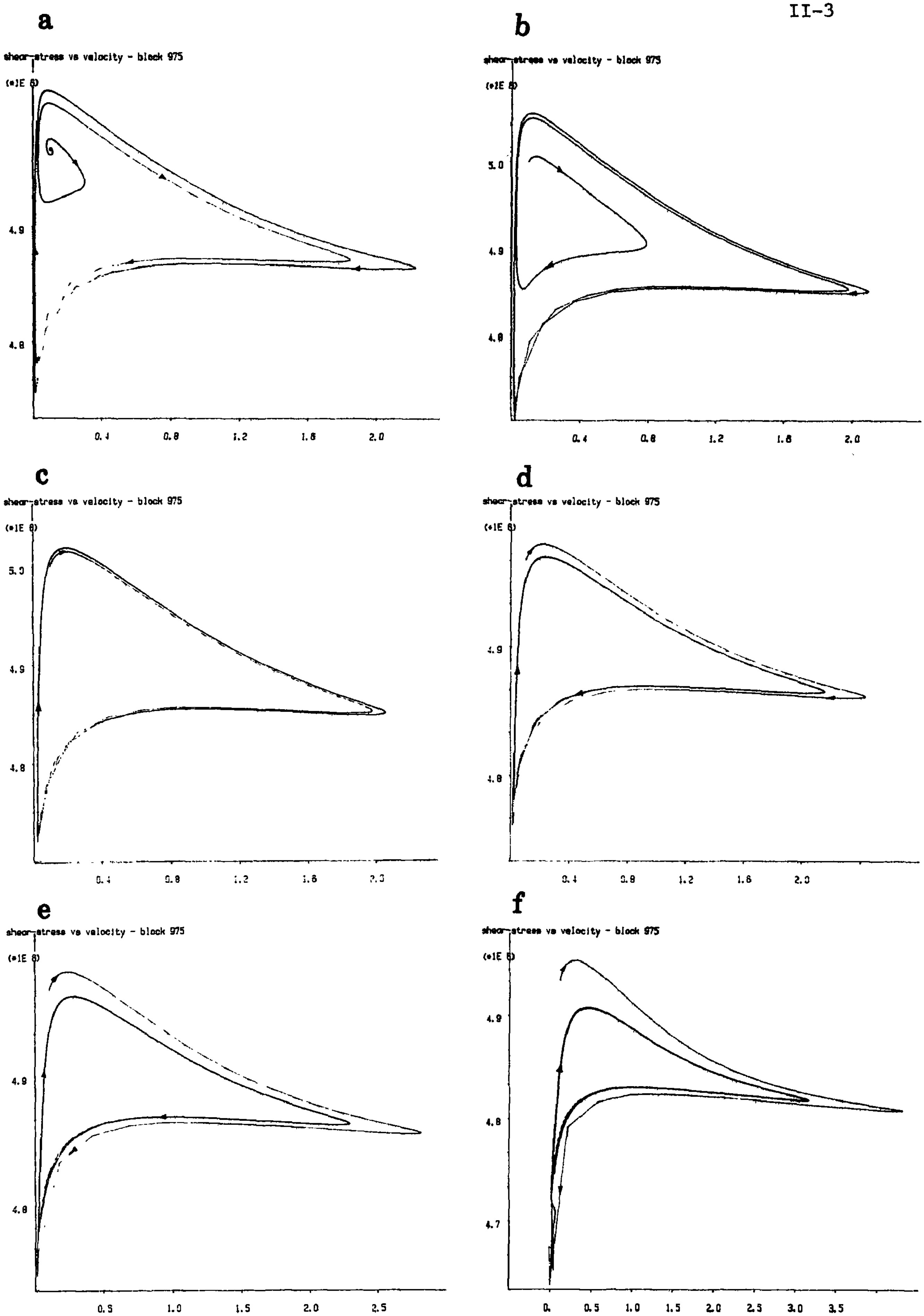
a
shear-stress vs velocity - block 975
(*1E 6)
4.9
4.8
0.4
0.8
1.2
1.6
2.0
b
shear-stress vs velocity - block 975
(*1E 6)
5.0
4.9
4.8
0.4
0.8
1.2
1.6
2.0
c
shear-stress vs velocity - block 975
(*1E 6)
5.0
4.9
4.8
0.4
0.8
1.2
1.6
2.0
d
shear-stress vs velocity - block 975
(*1E 6)
4.9
4.8
0.4
0.8
1.2
1.6
2.0
e
shear-stress vs velocity - block 975
(*1E 6)
4.9
4.8
0.5
1.0
1.5
2.0
2.5
f
shear-stress vs velocity - block 975
(*1E 6)
4.9
4.8
4.7
0.
0.5
1.0
1.5
2.0
2.5
3.0
3.5

FIGURE 4

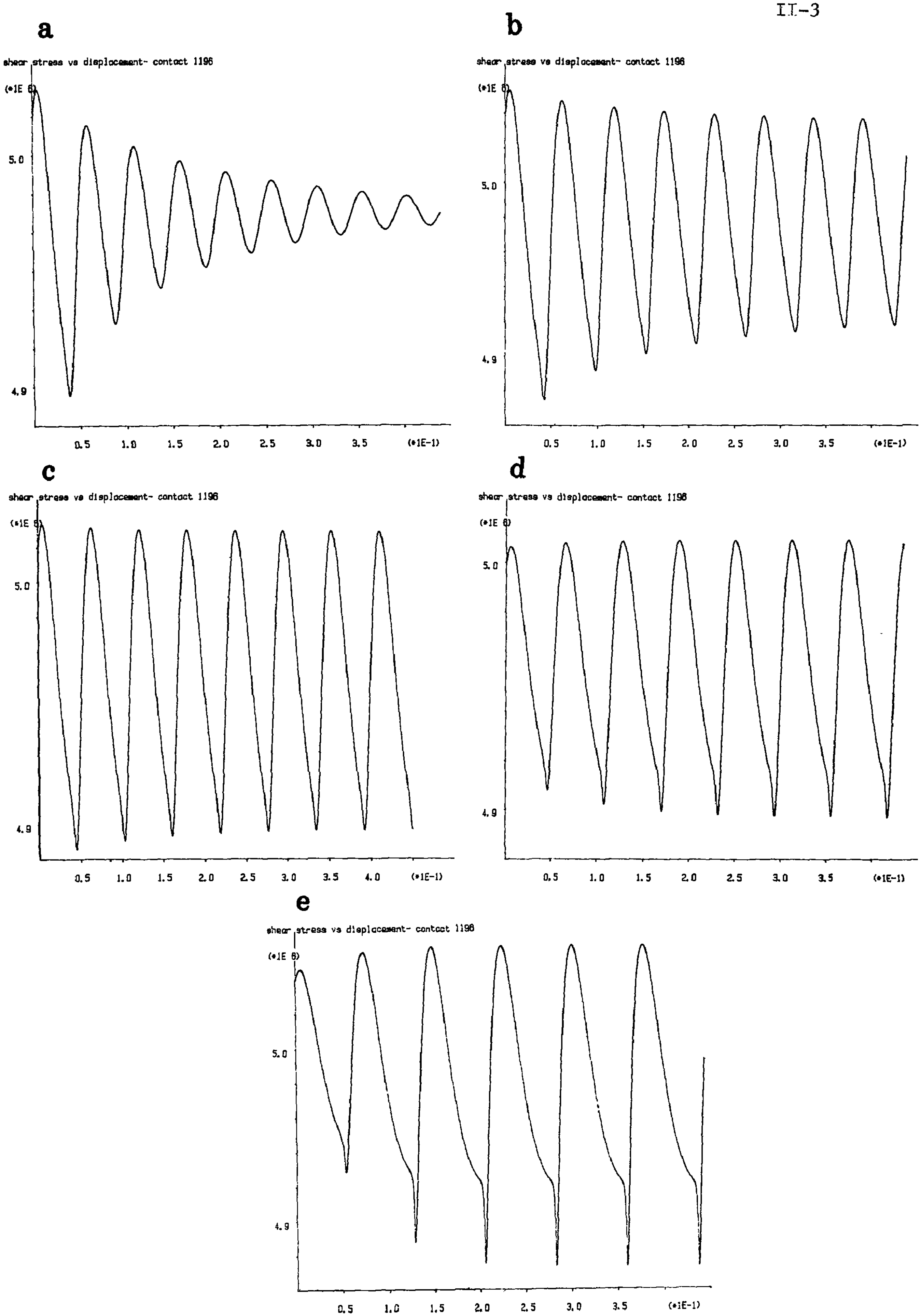

a
shear stress vs displacement- contact 1196
(*1E 6)
5.0
4.9
0.5 1.0 1.5 2.0 2.5 3.0 3.5 (*1E-1)
b
shear stress vs displacement- contact 1196
(*1E 6)
5.0
4.9
0.5 1.0 1.5 2.0 2.5 3.0 3.5 (*1E-1)
c
shear stress vs displacement- contact 1196
(*1E 6)
5.0
4.9
0.5 1.0 1.5 2.0 2.5 3.0 3.5 4.0 (*1E-1)
d
shear stress vs displacement- contact 1196
(*1E 6)
5.0
4.9
0.5 1.0 1.5 2.0 2.5 3.0 3.5 (*1E-1)
e
shear stress vs displacement- contact 1196
(*1E 6)
5.0
4.9
0.5 1.0 1.5 2.0 2.5 3.0 3.5 (*1E-1)

FIGURE 5

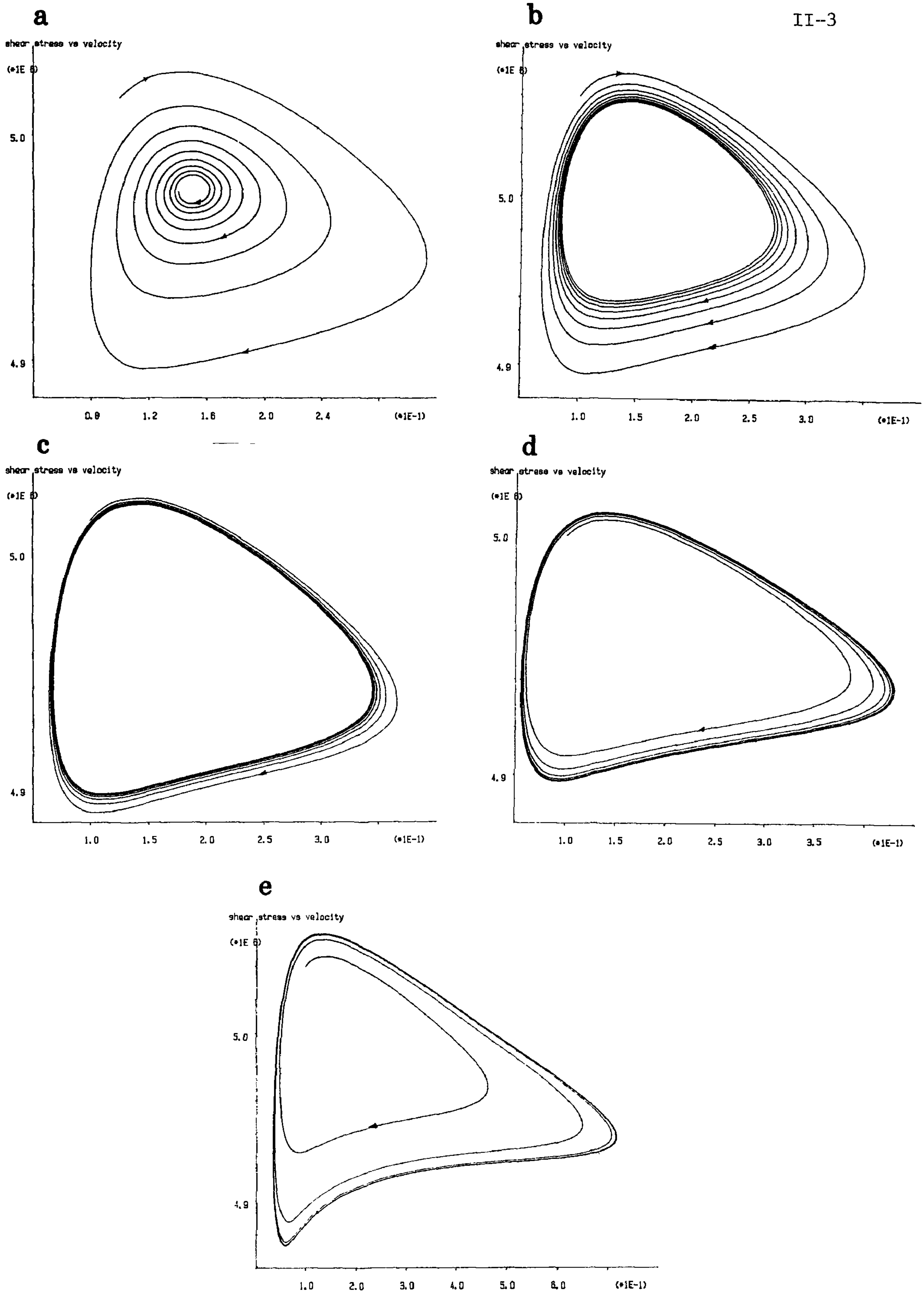
a
shear stress vs velocity
(*1E 6)
5.0
4.9
0.8
1.2
1.6
2.0
2.4
(*1E-1)
b
shear stress vs velocity
(*1E 6)
5.0
4.9
1.0
1.5
2.0
2.5
3.0
(*1E-1)
c
shear stress vs velocity
(*1E 6)
5.0
4.9
1.0
1.5
2.0
2.5
3.0
(*1E-1)
d
shear stress vs velocity
(*1E 6)
5.0
4.9
1.0
1.5
2.0
2.5
3.0
3.5
(*1E-1)
e
shear stress vs velocity
(*1E 6)
5.0
4.9
1.0
2.0
3.0
4.0
5.0
6.0
(*1E-1)

FIGURE 6

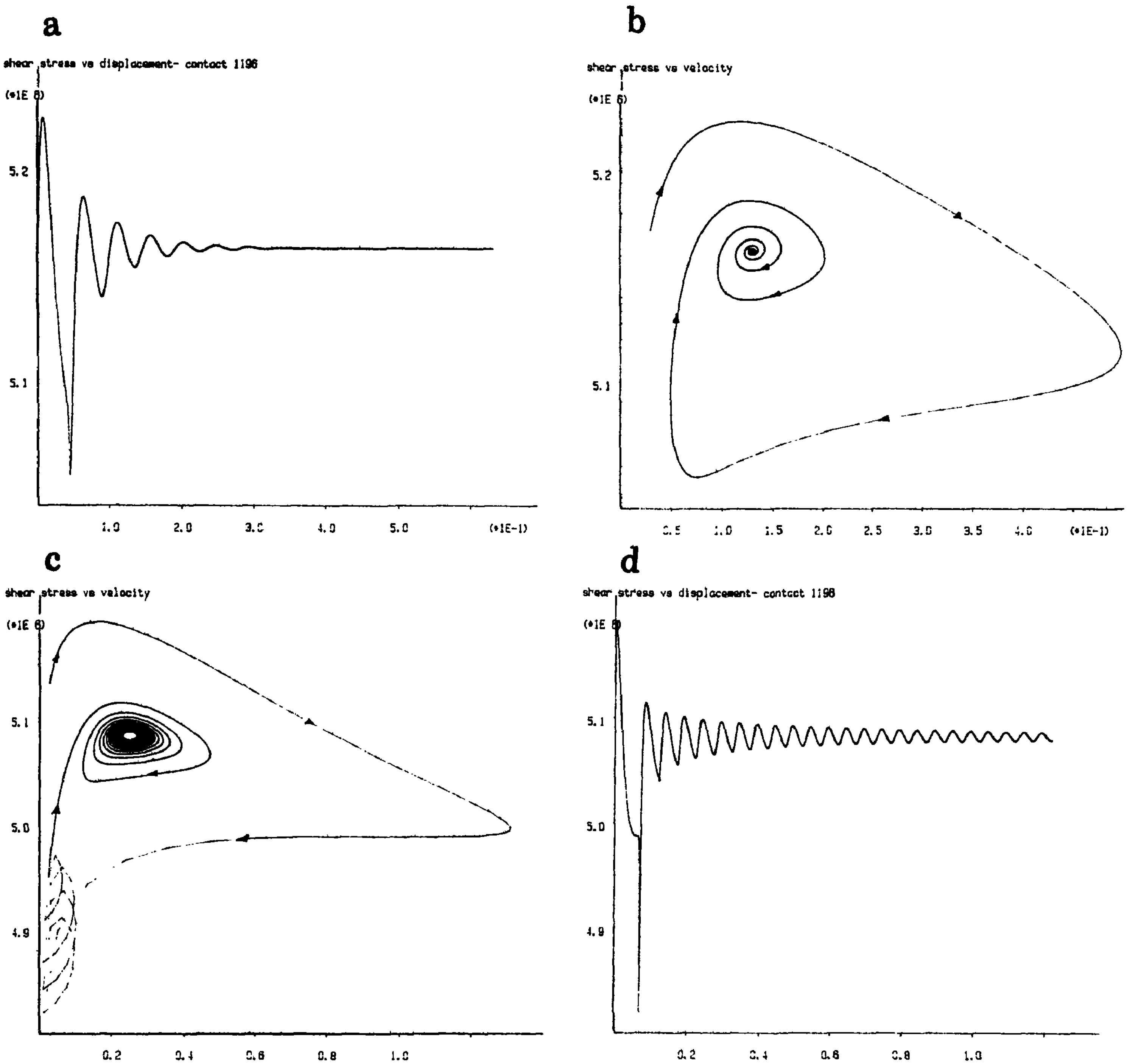
a
shear stress vs displacement- contact 1196
(*1E 6)
5.2
5.1
1.0
2.0
3.0
4.0
5.0
(*1E-1)
b
shear stress vs velocity
(*1E 6)
5.2
5.1
0.5
1.0
1.5
2.0
2.5
3.0
3.5
4.0
(*1E-1)
c
shear stress vs velocity
(*1E 6)
5.1
5.0
4.9
0.2
0.4
0.6
0.8
1.0
d
shear stress vs displacement- contact 1198
(*1E 6)
5.1
5.0
4.9
0.2
0.4
0.6
0.8
1.0

FIGURE 7

Earthquakes and the Statistics of Crustal Heterogeneity

9930-03008

Bruce R. Julian

Branch of Seismology
U.S. Geological Survey
345 Middlefield Road - MS77
Menlo Park, California 94025
(415) 323-8111 ext. 2931

Investigations

Both the initiation and the stopping of earthquake ruptures are controlled by spatial heterogeneity of the mechanical properties and stress within the earth. Ruptures begin at points where the stress exceeds the strength of the rocks, and propagate until an extended region ("asperity") where the strength exceeds the pre-stress is able to stop rupture growth. The rupture termination process has the greater potential for earthquake prediction, because it controls earthquake size and because it involves a larger, and thus more easily studied, volume within the earth. Knowledge of the distribution of mechanical properties and the stress orientation and magnitude may enable one to anticipate conditions favoring extended rupture propagation. For instance, changes in the slope of the earthquake frequency-magnitude curve ("b-slope"), which have been suggested to be earthquake precursors and which often occur at the time of large earthquakes, are probably caused by an interaction between the stress field and the distribution of heterogeneities within the earth.

The purpose of this project is to develop techniques for determining the small-scale distributions of stress and mechanical properties in the earth. The distributions of elastic moduli and density are the easiest things to determine, using scattered seismic waves. Earthquake mechanisms can be used to infer stress orientation, but with a larger degree of non-uniqueness. Some important questions to be answered are:

** How strong are the heterogeneities as functions of length scale?

** How do the length scales vary with direction?

** What statistical correlations exist between heterogeneities of different parameters?

** How do the heterogeneities vary with depth and from region to region?

Scattered seismic waves provide the best data bearing on these questions. They can be used to determine the three-dimensional spatial power spectra and cross-spectra of heterogeneities in elastic moduli and density in regions from which scattering can be observed. The observations must, however, be made with seismometer arrays to enable propagation direction to be determined. Three-component observations would also be helpful for identifying and separating different wave types and modes of propagation.

The stress within the crust is more difficult to study. Direct observations require deep boreholes and are much too expensive to be practical for mapping small-scale variations. Earthquake mechanisms, on the other hand, are easily studied and reflect the stress orientation and, less directly, its magnitude, but are often not uniquely determined by available data.

This investigation uses earthquake mechanisms and the scattering of seismic waves as tools for studying crustal heterogeneity.

Results

Automatic real-time earthquake monitoring

Over the last several years, the USGS has developed a system for monitoring central and northern California earthquakes automatically in real time, using phase arrival information generated by the Real-Time Processor (RTP). The arrival data are processed by a separate computer system, which automatically computes earthquake hypocenters locations and magnitudes, maintains a data base of this information, and displays maps of current activity on interactive graphics terminals. This computer system includes an alarm facility, which detects large earthquakes and swarms and automatically notifies seismologists by means of a radio paging system, and a seismicity monitoring facility, which detects changes in regional rates of earthquake occurrence. The RTP and the associated computer system have become the main tool used by the USGS to monitor earthquakes in central and northern California, and in particular play a critical role in the current Parkfield earthquake prediciton.

During the last six months, we have improved the computation of earthquake magnitudes, added facilities for monitoring the performance of individual seismograph stations, and added several data-management utilities. Previously, reliable magnitudes could not be determined for earthquakes larger than about magnitude 3, because the coda durations exceeded the RTPs measurement ability. This is a serious limitation, for example for identifying the expected magnitude 5 to 6 foreshocks of the predicted Parkfield earthquake. We now compute magnitudes for large earthquakes from 10 low-gain stations, using formulas and station corrections determined by Allan Lindh and Barry Hirshorn. This change enables us to estimate magnitudes up to about 5.5 reliably.

To monitor station performance, we now automatically collect statistics on the number of usable readings provided by individual seismograph stations. Weekly inspection of these statistics has proven valuable for detecting many types of instrumental, telemetry, and processing problems.

Array Observations of Chalfant Valley aftershocks

We are now analyzing data from two dense seismic arrays (aperture about 1 km) that were deployed briefly in the aftershock zone of the magnitude 6.4 Chalfant Valley earthquake of 21 July 1986. The purpose of the experiment was to learn about the mode of propagation of coda waves, and about the spatial distribution in the crust of the scatterers that produce them. High-quality recordings were obtained of several dozen aftershocks, mostly at epicentral distances of less than 10 km. These data are being subjected to "high-resolution" (maximum likelihood) frequency-wavenumber spectral analysis. We also plan to analyze them with recently developed "Multiple Signal Characterization" (MUSIC) algorithms. In addition to high-quality recordings of the coda waves, visual inspection of record sections shows other interesting phenomena, including extreme variations in site response and probable S-to-P converted waves from the top of the crystalline basement rocks.

Mechanism of volcanic tremor

Most of our effort in the last six months has been devoted to continued investigations of a proposed new mechanism for the generation of volcanic tremor by nonlinear flow-induced vibration of the walls of channels transporting magmatic fluids. We have extended the theory to include the effects of acoustic resonance in the network of fluid-filled cracks and chambers within a volcano. Such resonance can enable tremor to occur at lower flow rates than if it were absent, and in addition can lead to non-periodic and chaotic vibration, similar to what is usually observed. A journal article describing this work is nearly finished.

Reports

Sammis, Charles G., and Julian, Bruce R., 1987, Fracture instabilities accompanying dike intrusion: J. Geophys. Res., v. 92, no. B3, pp. 2597-2605.

Julian, Bruce R., 1986, Volcanic tremor: Flow-induced vibration?: EOS Trans. Amer. Geophys. Union, v. 67, no. 44, p. 1264.

Julian, Bruce R., 1987, Flow-induced vibration: A model for volcanic tremor: Hawaii Symposium on How Volcanoes Work, Hilo, Hawaii, 1972, Abstracts, p. 128.

Experimental Rock Mechanics

9960-01180

Stephen H. Kirby
Branch of Tectonophysics
U.S. Geological Survey, MS/977
345 Middlefield Road
Menlo Park, California 94025
(415) 323-8111, Ext. 2872

Investigations

1. Phase changes and shear zones in the crust and upper mantle.

2. Localized phase transformations and the physical mechanisms of deep earthquakes.

3. Fracture in the mantle.

4. Rheology of the lithosphere.

Results

1. Phase changes and the sliding resistance of olivine at elevated pressure and temperature.

   We continue to follow up on our discovery of unusually low sliding resistance of dunite under hydrothermal conditions (Pinkston et al., 1986). We have determined that the weakness spans the temperature range 250 to 450°C and that this corresponds to the temperature range where a hydrothermal alteration reaction occurs on the sliding surface. This supports our hypothesis that the low sliding resistance is governed by hydrothermal reactions at stressed asperities, solute transport, and precipitation of chrysotile in fluid-filled cavities on the sliding surface. Current work focuses on determining the strain-rate and temperature sensitivity of the process as well as SEM study of the sliding surface. We speculate that similar reactions may occur on fault surfaces in the upper crust at quite modest temperatures and these may be responsible for the low inferred deviatoric stress in the continental crust.

2. Localized phase transformations and the physical mechanism of deep earthquakes.

   The discovery paper on high pressure faulting, phase transitions localized in fault zones and the origin of deep earthquakes has been accepted by JGR for publication in the special issue on deep earthquakes. Lisa Dell'Angelo, a USGS postdoctoral fellow, is following up on this work by studying several additional polymorphic phase transformations under non-hydrostatic stress at low to intermediate temperatures where phase changes are ordinarily sluggish.

3. Fracture in the mantle.

Howard Wilshire and Kirby (1987) have submitted a paper to JGR on the evidence for *in situ* fracture in the mantle based on the study of fracture surfaces in mantle-derived xenoliths and alpine peridotites obducted from the mantle. Especially noteworthy are smooth often polished and slickensided surfaces that are undoubted shear fractures which may be connected with mantle earthquakes. We plan a more intensive study of these surfaces to explore the role of plastic deformation in the sliding surface.

4. Rheology of the lithosphere.

Kirby and Kronenberg (1987) have completed their IUGG report for the period 1983-1986 on the subject of the rheology of the lithosphere. It focuses on five "hot" topics: 1) flexure of the oceanic lithosphere, 2) deformation of the continental lithosphere due to forces applied to plate boundaries, 3) rheological stratification of the continental lithosphere, 4) strain localization and shear-zone development, and 5) deformation and seismic anisotropy. This massive undertaking involved reviewing over 700 papers published in the four-year period and was greatly facilitated by Beverly Monroe's handling of the references and production of the camera ready copy.

Reports

Kirby, S. H., 1986, Localized polymorphic phase transformations in high-pressure faults and applications to the physical mechanism of deep earthquakes, Journal of Geophysical Research (accepted, in press).

Kirby, S. H., Hearn, B. C., Jr., He, Yongnian, and Lin, Chuanong, 1986, Geophysical evidence of mantle xenoliths: evidence for fault zones in the deep lithosphere of eastern China: U.S. Geological Survey Circular, Kirby, S. H., Nielson, Jane, and Noller, J., eds. (in press).

Kirby, S. H., Nielson, J., and Noller, J., eds., 1986, Geophysics and petrology of the deep crust and upper mantle: Introduction to the Workshop Proceedings, U.S. Geological Survey Circular (accepted, in press).

Kronenberg, A. K., and Kirby, S. H., 1986, Ionic conductivity of quartz: DC time dependence and transition in charge carriers: American Mineralogist (accepted, in press).

Kronenberg, A. K., Kirby, S. H., Aines, R. D., and Rossman, G. R., 1986, Solubility and diffusional uptake of hydrogen in quartz at high pressures: implications for hydrolytic weakening: Journal of Geophysical Research, 91, 12,723-12,744.

Pinkston, J., Stern, L., and Kirby, S., 1986, Sliding resistance at elevated temperatures of polycrystalline olivine with trace hydrothermal alteration and implications for fault-zone rheology, Trans. A.G.U. (EOS), 67, 1186.

Pinkston, J., Stern, L., and Kirby, S., 1987, Hydrothermal reactions on artificial fault surfaces in dunite: fibrous mineral growth, slickensides and temperature sensitivity of reaction weakening, Trans. A.G.U. (EOS), 68 (accepted, in press).

Wilshire, H. G., and Kirby, S. H., 1987, Brittle fracturing and related magmatic phenomena in the lower lithosphere, Journal of Geophysical Research (submitted).

Rupture Mechanics of Slip-Deficient Fault Zones

14-08-0001-G1167

J.R. Rice (P.I.) and R. Dmowska
Division of Applied Sciences and
Department of Earth and Planetary Sciences,
Harvard University
Cambridge, MA 02138
(617) 495-3445,3452

(for period October 1, 1986 to April 30, 1987)

Investigations

1. Studies are underway on interactions between adjacent fault zones along strike, in particular on interactions between the presently locked zones of the 1906 and 1857 earthquakes and the creeping central section of San Andreas fault, with special emphasis on the Parkfield area.

2. Three dimensional shear crack mechanics is being examined through a perturbation technique that allows study of slightly non-uniform fault advance.

Results

1. We have examined interactions between the Central California creeping zone and adjacent presently locked zones of the 1857 and 1906 ruptures, including the frequently rupturing transition regions at San Juan Bautista and Parkfield (fig. 1). The recent work by Li and Rice (1986) enables us to reasonably constrain parameters for a plate loaded by drag from mantle flow. Thus an issue of interest for the Central California zone is the modeling of the response of a plate which is loaded in that way but whose fault zone is locked non-uniformly along strike and apparently, in places, is not locked at all. Using procedures of Lehner, Li and Rice (1981) and Tse, Dmowska and Rice (1985), those become two dimensional plane stress problems for a plate coupled to a generalized Elsasser foundation.

The mathematical difficulties have not yet been fully dealt with and thus far we have an exact solution within that framework only for the geometry shown in fig. 2a: An infinite plate is loaded from below by drag from mantle flow and has two adjoining semi-infinite fault zones. One slips at constant resistive stress (freely slipping). The other is locked (unfortunately, over its entire depth in the modeling of this type done thus far) between periodic earthquakes, but slips by $V_{pl}T$ after each cycle time T. This gives a complicated solution which we have extracted by Wiener-Hopf procedures based on those of Lehner, Li and Rice (1981). It has the mathematical form

$$\dot{\delta} = V_{pl}\ F_1(t/T, x/H;\ t_r/T)$$

for the thickness averaged slip rate $\dot{\delta}$ along the creeping zone. Here H = plate thickness, t_r = asthenosphere relaxation time.

This solution was used to deal with the geometry of interest shown in fig. 2b, incorporating effects of the 1857 and 1906 ruptures, in the following approximate manner. We write F_1 above as $F_2(t,x)$ for short and then calculate

$$\dot{\delta} \approx V_{pl}\ F_2(t-1857,x)\ [\frac{1}{2} + \frac{1}{\pi} \arcsin\ (\frac{170-2x}{170})\ ]$$

$$+\ V_{pl}\ F_2(t-1906,170-x)\ [\frac{1}{2} - \frac{1}{\pi} \arcsin\ (\frac{170-2x}{170})\ ]$$

(x in km, t in yr). The bracketed spatial attenuation factors go from unity to zero as one goes from one end to the other of the creep zone. They are the factors needed in the corresponding classical plane stress sliding crack solution for a plate that is not coupled to an asthenosphere, and hence would be correct in the relaxed limit.

The simple solution just developed does not include the locked patch at Parkfield but, approximately, it gives the long term slip rate history which must be accommodated at Parkfield when one averages out the additional stick-slip-like contributions from the Parkfield seismic events themselves. Figs. 3 and 4 show the slip rates respectively at the Parkfield nucleation site at Middle Mountain (x=35 km) and at the middle of the creeping zone, each for three elastic plate thicknesses and for a range of relaxation times which are reasonable in terms of geodetic data fits. Li and Rice suggest H = 20 to 30 km and t_r = 10 to 16 yr. The calculations are based on a cycle time T = 150 yr.

We notice that the transients in slip rate near the center of the creep zone are small in all cases. However, as an effect which becomes more notable the greater the plate thickness, there are significant transients in the predicted slip rate which has to be accommodated near the Parkfield nucleation site. This is due primarily to its coupling to the 1857 earthquake zone but a very small transient also shows from coupling to the 1906 zone.

A tacit assumption in using the average recurrence time of past Parkfield earthquakes to predict the time of the next one is that tectonic loadings there accumulate uniformly from one Parkfield event to the next. Our modeling suggests that this assumption is not strictly justified.

Since measured values of the slip rate at the middle of the creep zone for a time window centered around 1975 are 32 to 34 mm/yr, we can use the calculations in fig. 4 to infer V_{pl} and then those in fig. 3 to infer what the slip rate should be for an idealized non-stick-slipping Parkfield region. The results, using t_r = 13 yr as representative, are as follows

elastic thickness H (km)	15	21	30
V_{plate} (mm/yr)	32-34	33-35	34-36
$V_{Parkfield}$ (mm/yr)	28-30	27-29	26-28

The inferred V_{plate} values are sensible in terms of geologic data. The velocities at Parkfield are generally higher than the recently measured values, 20 tc 26 mm/yr. However, the predictions should be compared to measurements which average in the co-seismic, and short-term post-seismic, effects of the Parkfield earthquakes. Thus geodetic data following the next earthquake may allow some further constraints to be placed on the parameters of such crustal loading models.

Sometimes the predicted effects are delayed many years. For example, in fig. 4 a the maximum transient effect of the 1857 and 1906 ruptures reaches the center of the creep zone only about 15 years after those events.

2. The elastic crack perturbation technique, discussed in an earlier summary (Gao and Rice, 1986) for the half-plane crack, has now been applied to somewhat circular shear cracks (Gao,1987). Expressions for stress intensity factors and energy release rate have been derived. Details will be provided in a subsequent summary.

References

Gao, H. and J.R. Rice, Shear stress intensity factors for a planar crack with slightly curved front, J. Appl. Mech., **53**, 774-778, 1986.

Gao, H., Nearly circular shear mode cracks, in review for J. Appl. Mech., submitted 1987.

Lehner, F.K., V.C. Li and J.R. Rice, Stress diffusion along rupturing plate boundaries, J. Geophys. Res., **86**, 6155-6169, 1981.

Li, V.C. and J.R. Rice, Crustal deformation in great California earthquake cycles, in review for J. Geophys. Res., submitted 1986.

Tse, S.T., R. Dmowska and J.R. Rice, Stressing of locked patches along a creeping fault, Bull. Seismol. Soc. Amer., **75**, 3, 709-736, 1985.

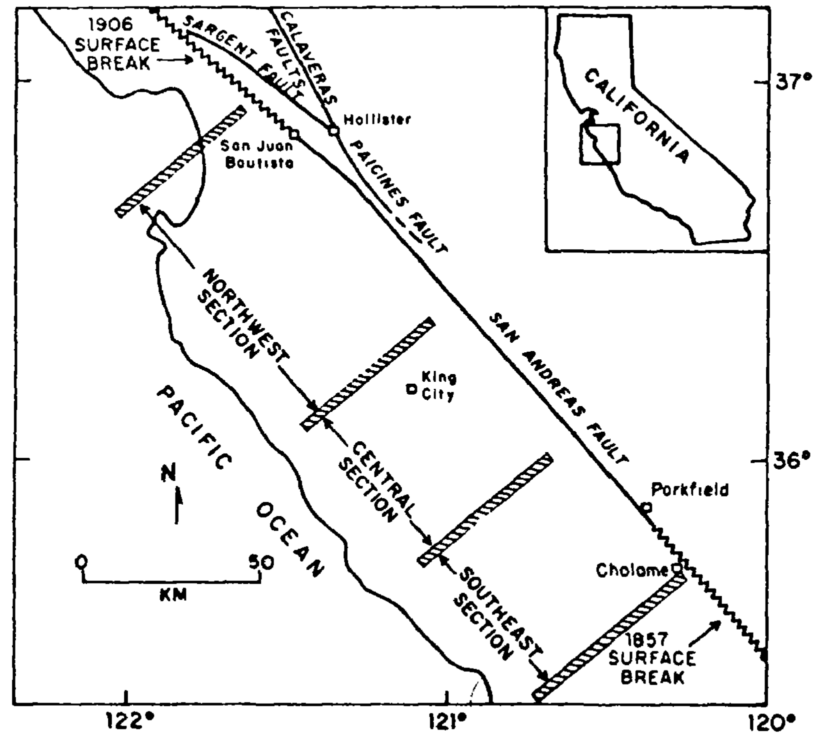

FIG. 6. Creeping section of the San Andreas fault (after Burford and Harsh. 1980).

FIG. 1.

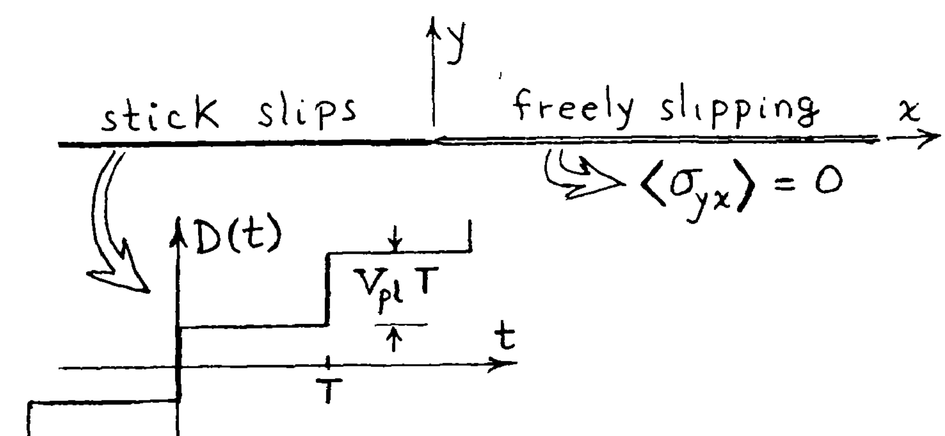

FIG. 2a.

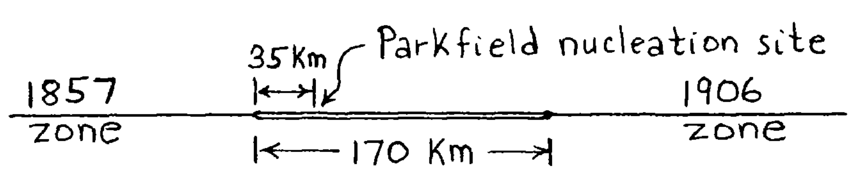

FIG. 2b.

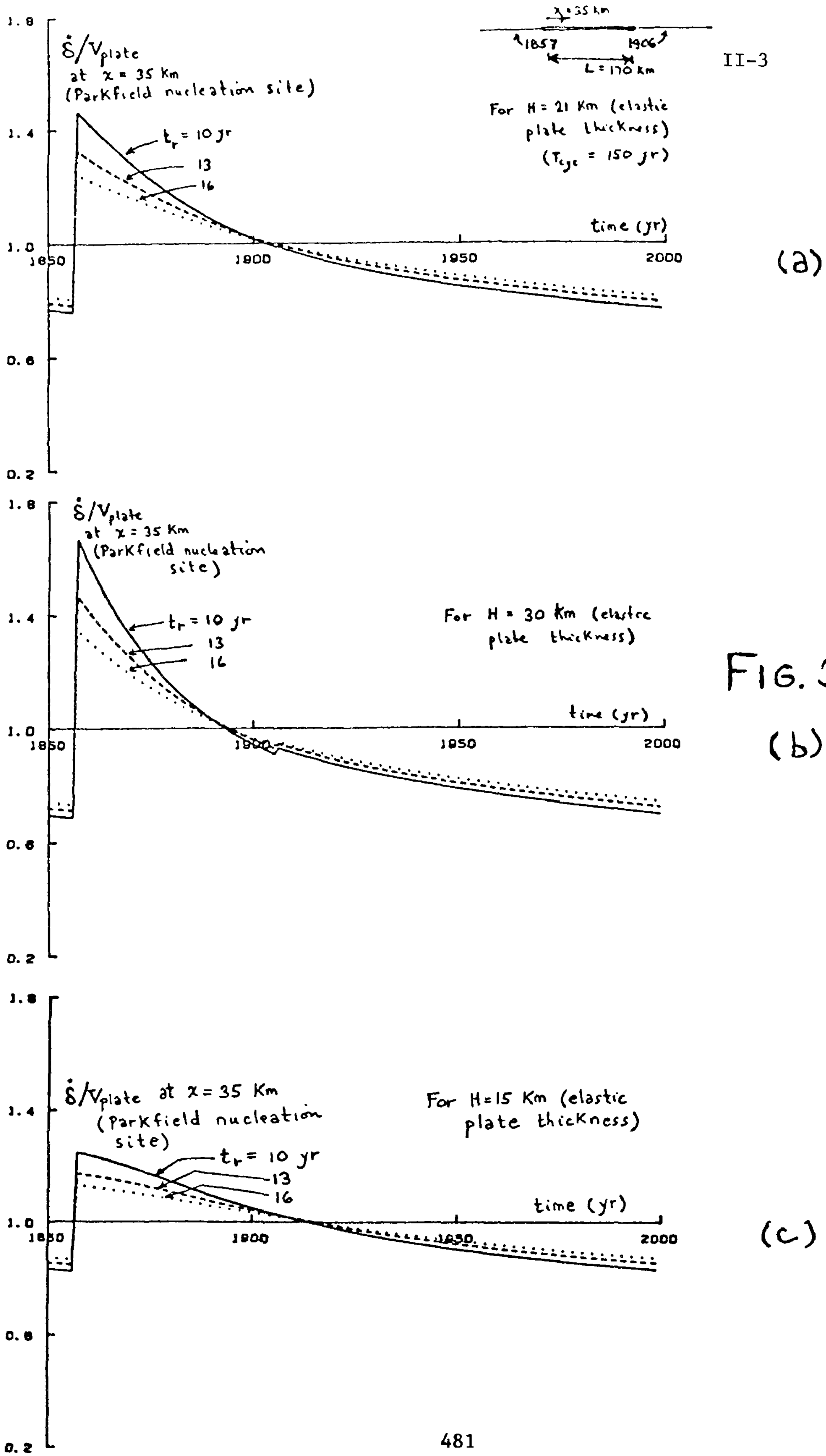

$\dot{\delta}/V_{plate}$ at $x = 35$ Km (Parkfield nucleation site)
$x = 35$ km
1857
1906
$L = 170$ km
For $H = 21$ Km (elastic plate thickness) ($T_{cyc} = 150$ yr)
$t_r = 10$ yr
13
16
time (yr)
1.8
1.4
1.0
0.6
0.2
1850
1900
1950
2000
(a)
$\dot{\delta}/V_{plate}$ at $x = 35$ Km (Parkfield nucleation site)
For $H = 30$ Km (elastic plate thickness)
$t_r = 10$ yr
13
16
time (yr)
(b)
$\dot{\delta}/V_{plate}$ at $x = 35$ Km (Parkfield nucleation site)
For $H = 15$ Km (elastic plate thickness)
$t_r = 10$ yr
13
16
time (yr)
(c)

FIG. 3.

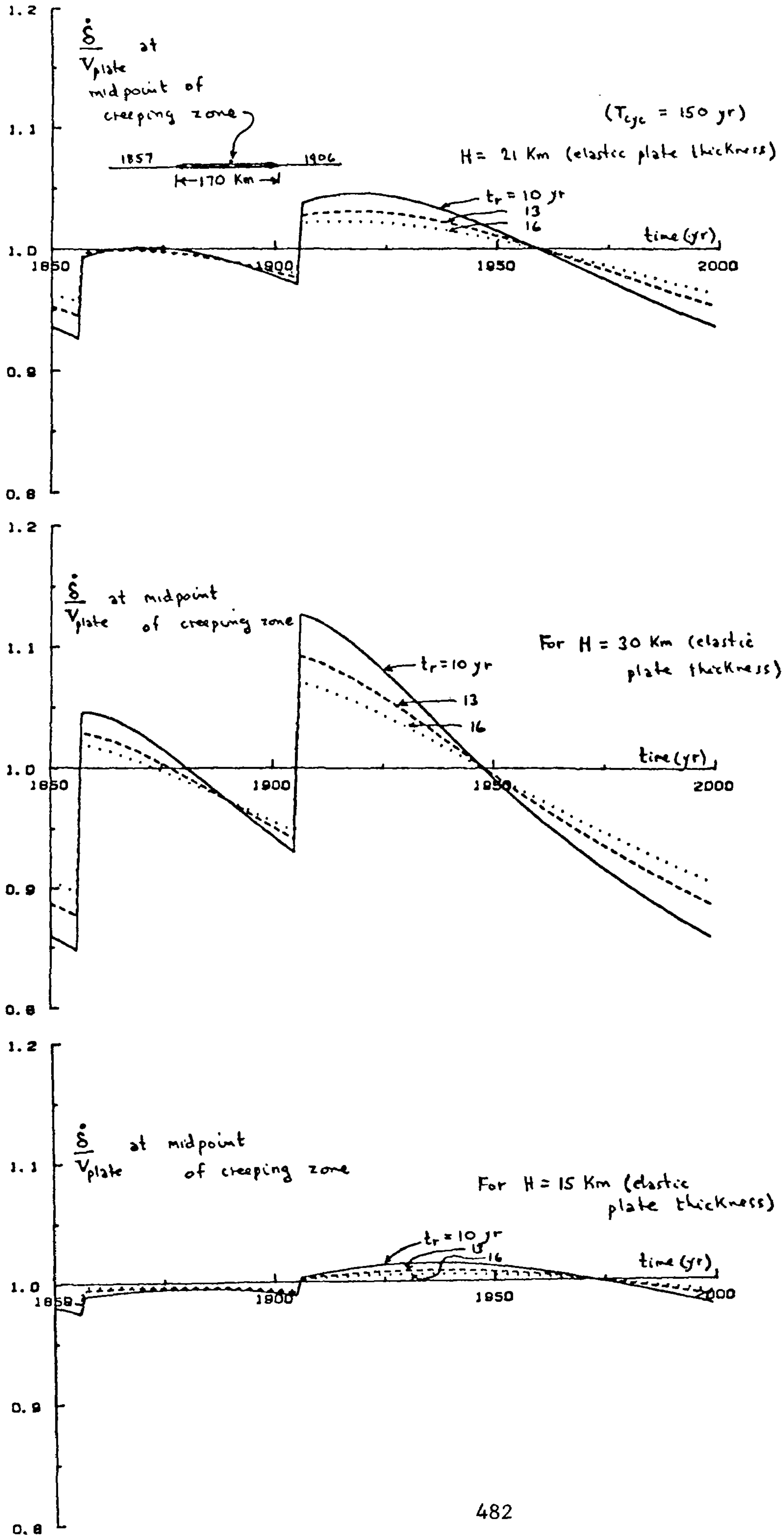

$\dot{\delta}$ / V_{plate} at midpoint of creeping zone
1857
1906
170 Km
(T_{cyc} = 150 yr)
H = 21 Km (elastic plate thickness)
t_r = 10 yr
13
16
time (yr)
1.2
1.1
1.0
0.9
0.8
1850
1900
1950
2000
$\dot{\delta}$ / V_{plate} at midpoint of creeping zone
For H = 30 Km (elastic plate thickness)
t_r = 10 yr
13
16
time (yr)
1.2
1.1
1.0
0.9
0.8
1850
1900
1950
2000
$\dot{\delta}$ / V_{plate} at midpoint of creeping zone
For H = 15 Km (elastic plate thickness)
t_r = 10 yr
13
16
time (yr)
1.2
1.1
1.0
0.9
0.8
1850
1900
1950
2000

(a)

FIG. 4.

(b)

(c)

ROCK DEFORMATION

9950-00409

Eugene C. Robertson
Branch of Geologic Risk Assessment
U.S. Geological Survey
MS 922, National Center
Reston, Virginia 22092
(703) 648-6792

Investigation

Observations have been made underground in mines to determine differences in amount of breccia formed by fault movement in several types of rock.

Results

Based on the rough validity of the log-log relation between displacement (d) and breccia and gouge thickness (t) (Robertson, 1982, 1983), analysis of additional data and review of old data indicates that amount of brecciation does vary uniformly in perceptible amounts among several rocks. Inherent differences among faults at different localities and of varying displacement and length can be accounted for if we assume that fault displacement is acceptable as a normalizing factor for thickness of breccia and gouge. Discussions of the problems with obtaining acceptable measurements of d and t, taking into account splitting and dying out of faults, and estimating averages of d and t are given in Robertson (1983, 1984).

In Figure 1 the d and t data for faults in quartz monzonite in mines at Butte, MT (marked "B") plot nominally as a group on the high t side of the trend line (dashed line in Fig. 1), whereas the data for faults in quartzite in mines at Coeur d'Alene, ID (marked "C") plot nominally at lower t's. The difference in t's between quartzite and quartz monzonite can be demonstrated by normalizing them to d at 1 m, that is, numerically by dividing t by d for each fault. The range in these ratios, t/d is from about 10^{-3} to 10^{-1}; the average ratio for the quartzite is 0.011 and for the quartz monzonite is 0.038. In other words, the average t of breccia if the displacements of the faults are all projected to 1 m would be 11 mm for quartzite and 38 mm for quartz monzonite.

Similarly in Figure 2, the d and t data are shown for faults in shale (circles) and for those in sandstone, limestone, schist, and a few felsic igneous rocks (X's). (Data are from mines in coal, fluorspar, copper, gold, and asbestos in Illinois and various western states.) The points for shale group on the high t side of the trend line, whereas those for the other rocks nominally make up a group at lower t's. The average ratios, t/d, project to a thickness of shale of 51 mm for a projected d of 1m, and of 18 mm for the other rocks. The sampling of about 20 faults for each of the 4 groups of rock in Figures 1 and 2 is considered to be adequate to draw these tentative conclusions.

An anomalous lack of faults of $d > 1$ m was found throughout the workings of the Homestake gold mine at Lead, SD, an observation verified by the mine geologists there. Regional forces have been operative, however, as shown by the large-scale folding of the Precambrian Homestake formation and the large faults in the surrounding quartz-mica schist. The Homestake formation is an unusual schist composed of chlorite, cummingtonite, quartz, and ankerite with minor stilpnomelane; the schist shows ubiquitous small-scale kink-banding and tight drag folding. Apparently regional stresses have been accommodated by large- to very small-scale cataclastic ductility and not brittle rupture. A very similar occurrence of gold in unfaulted chlorite schist is found in the Morro Velho and Raposos mines in Brazil, and a similar accommodation of regional stresses by cataclastic folding is an acceptable explanation. In both Homestake and Morro Velho mines, large stopes stand open without caving and even at nearly 3 km depth there have been no rockbursts in either mine, indicating accommodation by the wall rock to high mining stresses.

The amount of breccia formed by displacement of a fault can also be correlated inversely with uniaxial compressive strength according to rock type; quartzite is stronger (400 MPa) by a factor of 5 to 10 than shale (40-70 MPa) and by a factor of 2 to 3 than quartz monzonite and other rocks listed (150-200 MPa), about the same factors as for the t/d ratios. Laboratory and field studies may eventually explain the effects not only of rock type but also of strain rate, confining pressure, water content, and deformation history on d and t.

Reports

Robertson, E. C., 1982, Continuous formation of gouge and breccia during fault displacement, In Issues in rock mechanics, Goodman, E. R. & F. E. Heuze, (eds.), 23rd Symp. Rock Mech., Amer. Inst. Min. Met. Petrol. Engr., New York, p. 397-404.

------ 1983, Relationship of fault displacement to gouge and breccia thickness, Amer. Inst. Min., Met. Petrol. Engr., Mining Engineering, v. 35, p. 1426-1432.

------ 1984, Discussion of "Relationship of fault displacement to gouge and braccia thickness". Amer. Inst. Min. Met. Petrol. Engr., Mining Engineering, v. 36, p. 1677-1678.

------ 1987, Fault breccia, displacement, and rock type, 28th Smyposium on Rock Mechanics, Proceedings (in press).

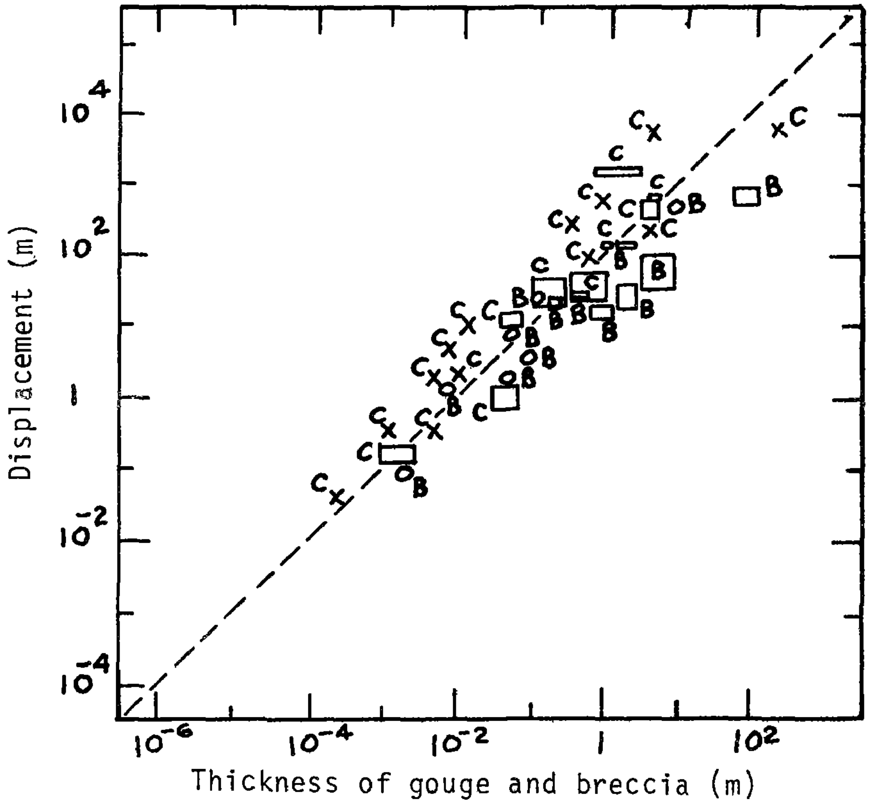

Figure 1. Displacements(d) and thicknesses (t) for faults in quartz monzonite at Butte, (B) and in quartzite at Coeur d'Alene, (C).

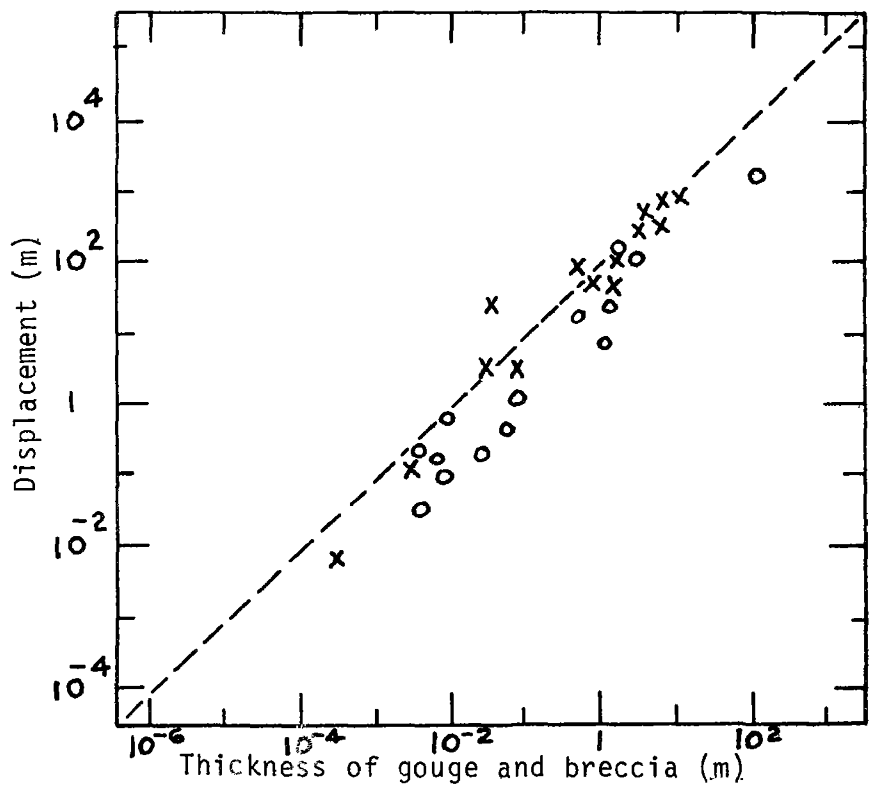

Figure 2. Displacements (d) and thicknesses (t) for faults in shale (circles) and other rocks (X's).

Heat Flow and Tectonic Studies

9960-01177

John H. Sass
Branch of Tectonophysics
U.S. Geological Survey
2255 North Gemini Drive
Flagstaff, AZ 86001
(602) 527-7226
FTS: 765-7226

Arthur H. Lachenbruch
Branch of Tectonophysics
U.S. Geological Survey
345 Middlefield Road
Menlo Park, CA 94025
(415) 323-8111, ext. 2272
FTS: 467-2272

Investigations:

Interpretation of FY 1985 and FY 1986 PACE heat-flow studies was completed.

Preliminary temperature logs and a reconnaissance of thermal conductivity were obtained from the Cajon Pass well.

Work resumed on completion of heat-flow determinations and their interpretation for the Mojave-Sonoran region of California and Arizona.

A study of thermal conductivities was completed, and a report on heat flow begun, for the area of scientific well VC-1, southwestern Valles Caldera.

Heat flow was calculated for the "conductive cap" of the Salton Sea scientific well.

Results:

PACE Studies. Final heat-flow calculations were performed for both the FY 85 wells drilled in southeastern California (and reported in preliminary form in volume 23) and the FY 86 in the Arizona Transition zone. As previously reported, the California data result in significant changes to the previous contours; by contrast, the Arizona results strengthen our previous interpretation of the region.

Cajon Pass. Repeated temperature logs were made when drilling was interrupted at 6000', 6250', and 6935'. The temperatures seem to recover from the effects of drilling about as one would anticipate from simple thermal models, and they are consistent with previously measured values from the Arkoma well only 175' away. Thermal conductivity measurements have been made by the half-space or needle-probe method on samples from all core runs and drill cuttings are being tested by the chip method. A distinctive high conductivity zone at about 4000' in the Arkoma well correlates with a similar one at about the same depth in the Cajon Pass well; this imposes a constraint on vertical displacement on a fault postulated to exist between the two holes.

Mojave-Sonora. Graphing and tabulation of heat-flow data acquired over the past decade in this region is virtually complete. The major variations in heat flow seem to be structurally, topographically, and perhaps, hydrologically controlled.

VC-1, Valles Caldera. The thermal conductivities of 55 carefully preserved core samples from borehole, VC-1, Valles Caldera, New Mexico, were measured using a combination of methods, the steady-state divided bar and two transient line-source methods. The choice of method was dictated by the physical condition and mechanical strength of the core. Because the well encountered high temperatures (∿160°C at the bottom), the room-temperature values of thermal conductivity were corrected using published values for the temperature coefficient of conductivity. A few samples were measured at temperatures of ∿100°C as a check on the validity of the published corrections. A near-equilibrium temperature profile from the well has linear segments that correlate negatively with thermal conductivity suggesting that heat flow from the upper ∿750 m at this site is primarily by conduction. Our preliminary estimate of heat flow is 450 mW m^{-2}.

Salton Sea. Temperature logs were made repeatedly during breaks in drilling and both during and after flow tests in the Salton Sea Scientific Drilling Program (SSSDP) well. The purpose of these logs was to assist in identifying zones of fluid loss or gain and to characterize reservoir temperatures. At the conclusion of the active phase of the project, a series of logs was begun in an attempt to establish the equilibrium temperature profile. Initially, we were able to log to depths below 3 km, but, beginning in late May of 1986, we were unable to log below about 1.8 km because of damage to the liner. Our best estimates of formation temperature below 1.8 km are 305±5°C at 1,890 m and 355±10°C at 3,170 m. For the upper 1.8 km, the last temperature log, using a digital "slickline" (heat-shielded downhole recording) device, appears to be within a few degrees Celsius of equilibrium. As in most other wells in the Salton Sea geothermal field, there is an impermeable, thermally conductive "cap" on the hydrothermal system; this cap extends to a depth of more than 900 m at the State 2-14 well. Thermal conductivities of 19 samples of drill cuttings from this interval were measured at room temperature. The conductivity values were corrected for in situ porosity as determined from geophysical logs, and for the effects of elevated temperature. Thermal gradients decrease from about 250 mK m^{-1} (same as degrees Celsius per kilometer) in the upper few hundred meters to just below 200 mK m^{-1} near the base of the conductive cap. Thermal conductivities increase with depth (mainly because of decreasing porosity) resulting in component heat flows that agree reasonably well with the mean of about 420 mW m^{-2}. This value agrees well with heat flows measured in shallow wells within the Salton Sea geothermal field.

Reports:

DeRito, R. F., 1987, The effects of weak crust upon the strength of the continental lithosphere (extended abstract): U.S. Geological Survey Circular, in press.

Lachenbruch, A. H., and Marshall, B. V., 1986, Changing climate: Geothermal evidence from permafrost in the Alaskan Arctic: Science, v. 234, p. 689-696.

Lachenbruch, A. H., Sass, J. H., Lawver, L. A., Brewer, M. C., Marshall B. V., Munroe, R. J., Kennelly, J. P., Jr., Galanis, S. P., Jr., and Moses, T. H., Jr., Temperature and depth of permafrost on the Alaskan Arctic Slope: Pacific Section - SEPM Special Publication and U.S. Geological Survey Professional Paper 1399 (Branch approval, March 1986).

Langseth, M. G., Lachenbruch, A. H., and Marshall, B. V., 1987, Geothermal observations in the Arctic region: Decade of North American Geology volume, in press.

Munroe, R. J., and Sass, J. H., Thermal conductivity of samples from borehole VC-1, Valles Caldera, New Mexico: U.S. Geological Survey Open-File Report (Branch approval, March 1987).

Pollack, H. N., and Sass, J. H., 1987, Thermal regime of the lithosphere, in Haenel, R., Rybach, L., and Stegena, L., eds., Handbook of Terrestrial Heat-Flow Density Determination (Guidelines and Recommendations of the International Heat Flow Commission), in press.

Sass, J. H., 1987, Salton Sea Scientific Drilling Program: U.S. Geological Survey Yearbook, in press.

Sass, J. H., Hendricks, J. D., Priest, S. S., and Robison, L. C., Temperatures and heat flow in the State 2-14 well, Salton Sea Scientific Drilling Program: EOS (Branch approval, February 1987).

Fractal Heterogeniety of Faults

14-08-0001-G1161

C.H. Scholz
Lamont-Doherty Geological Observatory
Columbia University
Palisades, New York 10964
(914) 359-2900

The fractal nature of the San Andreas fault was evaluated, using the 1:24,000 Alquist-Priolo series of fault hazard maps. The complete map series was digitized, and analized using both the spectral technique and the ruler method. Both methods show that the fault is fractal, but that it is inhomogeneous in two ways. Firstly, like other surfaces we have studied, fractal dimension is a function of wavelength. In the case of the fault D is smaller at long wavelenths than at short (<10 km) wavelengths. D also varies as a function of position along the fault (Scholz and Aviles, 1986; Aviles et al., 1987).

A joint project with Brown University was carried out in which natural slickensided fault surfaces were measured with profilometers. This study showed that the fault surfaces were fractal over the band 10 M - 10^{-5} M, but that they were highly anisotropic. The direction parallel to slip is much smoother at all wavelengths studied (Power et al., 1987).

An analysis was made of the change in aperture that is expected to result from shear offset of two mated fractal surfaces (Wang et al., 1987). This is interesting both from the viewpoint of fracture permeability and friction.

A new model of wear and gouge formation was also developed (Scholz, 1987). This result has led us to become more interested in gouge formation and its relationship to fault topography.

Publications resulting from G1161

Scholz, C. H., and C. A. Aviles, Fractal Geometry of faults and faulting, in Earthquake Source Mechanics (eds. S. Das, J. Boatwright, C. Scholz) AGU geophys. mono. 37, Washington D.C., 147-156, 1986.

Aviles, C. A., C. H. Scholz, and J. Boatwright, Fractal analysis applied to characteristic segments of the San Andreas fault, J. Geophys. Res., 92, 331-344, 1987.

Power, W., T. Tullis, S. Brown, G. Boitnott, and C. Scholz, Roughness of natural fault surfaces, Geophys. Res. Lett., 14, 29-32, 1987.

Scholz, C. H., Wear and gouge formation in brittle faulting, Geology, 15, in press, 1987.

Wang, J. S., T. N. Narisimhan, and C. H. Scholz, Aperture correlation of a fractal fracture, J. Geophys. Res., subm. 1987.

Scholz, C. H., Mechanisms for seismic quiescences, PAGEOPH, subm. 1987.

Systems Analysis of Geologic Rate Processes

9980-02798

Herbert R. Shaw and Anne E. Gartner
Branch of Igneous and Geothermal Processes, U.S. Geological Survey
MS-910, 345 Middlefield Road, Menlo Park, CA 94025
(415) 329-5245, 5209

Objective: The work on this project has the objective of summarizing multifractal sets of seismic and fault data using one region of California as an example.

Results: In earlier technical summaries, and in Shaw and Gartner (1986), we have described evidence to suggest that the fractal geometry of fault sets is variable both in time and size domains. This is confirmed by other studies of differing geographic scope by Aviles and Scholz (1985) and by Okubo and Aki (1987). As a consequence, our approach to the fractal geometry of faulting has been expanded to include the possibility that there may be complex domains of fracture patterns over many length scales in a manner that metaphorically resembles the theory of critical phenomena (e.g., geometric states near the liquid-gas transition or near the Curie temperature of magnetic materials where both short- and long-range order and disorder exist simultaneously; see Wilson, 1979). For the sake of simplicity, we assume in this discussion that there is a direct correspondence between the geometries of faulting and of earthquake sources. That is, we do not discuss concepts of asperities, barriers, and nucleation patches. In other words, we discuss relations among sets of characteristic faults, or fault segments, in the sense of Wesnousky and others (1983) and Scwartz and Coppersmith (1984). To the extent that self-similarity is found to be a property of fault dynamics, it is anticipated that it will provide intra- as well as interfault criteria for dimensional relations among the differing dynamical properties of fracture surfaces.

In general, if faulting within a specified region is not a self-similar fractal object characterized by a single-valued fractal dimension, two limiting alternatives might be examined: (1) Systems of faulting even within the same tectonic domain, whether described in terms of continuous line traces or as discontinuous sets of line segments, are not self-similar (scale invariant) fractal objects at any scales of time and size. (2) Fractal self-similarity exists, but it requires at least two and possibly many fractal dimensions to describe interrelated sets of faulting in time and space. In the first instance there is no universality in the dynamical space-time behavior of fault motions. In the second instance there may be dynamical universality at all scales of motion, but the consequent geometries of faulting can only be described in terms of multifractal sets. Universality is used in the approximate sense that there are proportionality constants that describe the geometry of complex fracture patterns regardless of scale or provenance (more generally, the constants may be independent of dynamical process, as in dimensional comparisons between fluid turbulence and solid state processes; see Bak, 1986; Shaw and Chouet, 1987).

An approach to (1) might be to prove global geometric randomness and stochastic behavior, but this is notoriously difficult and does not explain those aspects of earthquake behavior that have elements of regularity over some scales of time and(or) space. On the other hand, if (2) is assumed to be true as a working hypothesis it suggests the possibility of descriptive hierarchies that can be subjected to classical tests of falsifiability. This has already been accomplished with respect to the possibility that faulting represents a simple fractal object.

Pursuing this second approach, concepts of ordered sets can be examined at several levels of complexity. In the long run this also would automatically constitute a test of interpretation (1) above if no evidence of ordering is found. Without attempting to be complete, we can identify the following types of possible fractal sets (interimly we use "dimension" as shorthand for a self-similar fractal subset of a multifractal set): (a) two or more discrete dimensions lacking evidence of numerical order or dynamical coordination, (b) ordered sets of dimensions with or without evidence of dynamical coordination, (c) sequences of dimensions that themselves can be subdivided without limit into sequences of dimensions (i.e., sets of fractal objects the dimensions of which themselves form a fractal object), (d) continuously differentiable sequences (spectra) of fractal sets of continuously differentiable fractal densities, (e) combinations of any of the above with or without nonfractal intervals of fixed periodic or aperiodic behavior, and (f) uniform (white) distributions over all topologically possible sets.

Several of the above types of sets could be illustrated in terms of results found in other fields of nonlinear dynamics (e.g., Shaw and Chouet, 1987). The results of Shaw and Gartner (1986) suggest that the complexity of faulting behavior in California and at the continental scale is at least at the levels of categories (b), (c), or (d). In this report we illustrate some data at the simplest level, (a), using catalogs of earthquake occurrences in California for surface wave magnitudes equal to or greater than five (Real and others, 1978; Toppozada and others, 1979a,b; Sherburne and others, 1985). This restriction to frequency-magnitude data, as distinguished from our previous discussions of fault-map data, means that the geometric hierarchies outlined refer to the possibilities for ordered b-value subsets, and implicitly to c-value subsets of moment-magnitude correlations.

In keeping with graphical methods described in prior reports and in Shaw and Gartner (1986), we wish to illustrate counts of recurrences at various length scales. In order to use earthquake events, we need a function to convert from magnitudes to lengths. We have done this in two ways: (1) We generated fictive lengths from arbitrary exponential functions of magnitude ("fictive" meaning an artificial construction; that is, such functions are not constrained to fit any particular topologic assumptions). (2) We used an empirical function based on regression correlations of fault lengths and earthquake magnitudes. The reason for the hypothetical scale in (1) is that there may be effects in (2) related to the nature of map data and to the averaging effects of linear regressions that bias the scaling. The use of (1) permits us to examine the effects of variable scaling coefficients of magnitude. These are analogous to scaling indices in renormalization methods (e.g., Halsey and others, 1986).

Examples of these two graphical constructions, respectively, are shown in Figures 1 and 2 for the Los Angeles vicinity (this is an arbitrary selection from diagrams we have constructed for eight different subregions of California). The arbitrary scale relation for length is given by the function:

$$L^*_s = 2^{M/q} \qquad (1)$$

where M is magnitude, q is an adjustable index, and base 2 is used to emphasize the special definition of L^*_s. For example, varying the value of q permits the adjustment of the length-magnitude relation to differing relations between moment, length, and magnitude. We find that for the typical value $c = 3/2$ in moment-magnitude correlations, the value $q = 4/3$ satisfies empirical correlations for both length vs. magnitude and length vs. moment.

The relations in Figure 1 are rescaled to fit a particular relation between magnitude and fault length in Figure 2 based on the empirical relation discussed in Shaw and Gartner (1986):

$$M = 4.964 + 1.243 \log_{10} L_f \quad (L_f \text{ in km}), \qquad (2)$$

where L_f without asterisk represents length data from fault maps. Length conversions between Figures 1 and 2 are made by substituting Eq. (2) in Eq. (1), giving the relation:

$$\log_{10} L^*_f = 3.56 \log_{10} L^*_s - 4, \qquad (3)$$

where L^*_f refers to the fictive length from Eq. (1) normalized to an empirical scale relation based on actual fault lengths. Thus, Eq. (3) includes adjustments for the empirically defined preexponential constant in Eq. (2) and the foreshortening effect of base 2 in Eq. (1); e.g., Figure 1 expands the dimensional relations at small lengths relative to Figure 2, resulting in an amplification of the fractal dimensions for the fictive sets based on L^*_s, as defined below (see Figure 2B). The increase in fractal dimension is not exactly a factor of $1/\log_{10} 2 = 3.32...$ because of the constants in Eqs. (1) and (2); conversions are illustrated for corresponding b-values in Figure 2B, which also shows ratios of derived fractal dimensions on each basis, including the definition $D_s = 3b/c$ given by Aki (1981) for a specific fault segmentation model.

The asterisk in these conventions signifies the fictive basis, where subscript "s" refers to simple exponential scaling of seismic data, and subscript "f" refers to that scaling normalized to a chosen fault-length calibration such as Eq. (2). Fractal dimensions D^*_s and D^*_f correspond to L^*_s and L^*_f, while D_s represents Aki's (1981) seismic fractal model. In such graphical constructions the fractal dimension is defined by the slope, S_i, according to $D_i = (1-S_i)$ for a particular scale relation, where D_i refers to the fractal dimension of one subset within a multifractal set. As a very rough rule-of-thumb, D^*_f is about $D_s/2$, and D^*_s is about $2D_s$ relative to the same values of b and c.

Although the purpose of this report is to suggest a descriptive approach to fractal scale relations based on earthquake data, the results can also be used to discuss questions of universality. We have found that there are crude correspondences among fractal sets found in different subregions of California. These might represent common multifractal sets, or they might represent special samples of ordered or random distributions over longer times. Such distinctions partly relate to the completeness of the seismic catalog and can be tested using paleoseismic data (work in progress).

In the historical data we notice the following features: (1) Fractal subsets are sometimes dominated by low-dimensional and high-dimensional trends (i.e., D^*_f near 0 and near 3) and sometimes also show concentrations near $D^*_f = 1$ and $D^*_f = 2$. (2) There are typically between five and ten distinguishable subtrends based on alignments of three or more points. (3) Where there are pre-1900 data (e.g., Los Angeles vicinity) the pre- and post-1900 subsets are similar (see Figure 1). (4) There are suggestions of continuous spectra in cases where subtrends are not clearly distinguishable. (5) as a whole the distributions tend to form triangular arrays in which the bases of triangles correspond to high fractal dimensions over roughly a decade in frequencies at low magnitudes, and the apices correspond to a convergence of low to intermediate fractal trends toward a single frequency and maximum earthquake magnitude (i.e., although the same fractal subsets are seen at all magnitudes, there is a progressive preponderance of subsets with low fractal dimensions at the higher magnitudes).

Figure 2A shows grid lines for fractal trends 0, 1/2, 1, 3/2, 2, and 3. Numbers at the nodal intersections of grid lines represent values of recurrence times 1/f expressed in years (N represents the numbers of events per 10,000 years). Magnitudes corresponding to values of $\log_{10}L^*_f$ (km) are shown at the top of the figure. The overall triangular shape of the arrays can be interpreted to imply area-filling to volume-filling fracture sets at the lowest magnitudes, and point-like fracture sets (i.e., geographically discontinuous earthquake sources) at the highest magnitudes. In several instances the convergences of the triangular arrays represent arrows pointing toward the maximum historic earthquakes. In the Los Angeles vicinity this convergence occurs at about M = 7, but in all other California subregions we examined of comparable geographic area the apex is at magnitudes of 7.5 and greater.

Average b-values can be defined in different ways, one of which is by regressions over selected data sets in frequency-magnitude diagrams. Figure 2 indicates, however, that b-values might also be subdivided according to spatial and(or) temporal fractal regimes. For example, if the orientation of the bisector of the triangular array is taken to represent an effective b-value for convergences toward a maximum earthquake, the average trend corresponds roughly to b = 0.5 in Figure 2A, and cross-trends represent very high b-values. These relations are similar in other subregions, but the average bisector b-value is less than 0.5 in subregions that include the largest historical earthquakes (this occurs without significantly changing the more distributed trends of high b-values and high fractal dimensions).

It seems possible that the similarities in fractal arrays for different regions may be reflecting some universal scale relation corresponding to continuous fractal spectra of the sorts being investigated by Shaw and Chouet (1987). Regardless of such possibilities, however, the time evolution of these arrays may be applicable to investigations of regional recurrence patterns. In this regard we notice that the Owens Valley - White Mountains - Southern Sierra vicinity is the least dense in fractal subsets among all subregions of comparable area in California. We might infer either that this vicinity has a uniquely discrete and relatively tenuous population of active faults, or it has the least complete population of earthquake occurrences within historic time among fault sets of areal densities comparable to other seismogenic regions of California. The latter possibility seems more likely in view of the distributions of mappable faults, but we have not tested this conclusion at several map scales, as should be done. According to the second interpretation, the paucity of subsets constitutes the existence of fractal seismic gaps which can be characterized according to length scales, magnitudes, and recurrence times with the aid of diagrams such as Figure 2. Of particular value would be analogous constructions at smaller areal scales for smaller earthquakes.

References Cited:

Aki, K., A probabilistic synthesis of precursory phenomena, in Simpson, D.W., and Richards, P.G. (eds.) Earthquake Prediction, Washington, DC, American Geophysical Union, p. 566-574, 1981.

Aviles, C.A., and Scholz, C.H., Fractal analysis of characteristic fault segments of the San Andreas fault system, EOS, 66, 314, 1985.

Bak, P., The Devil's Staircase, Phys. Today, 39, 38-45, 1986.

Halsey, T.C., M.H. Jensen, L.P. Kadanoff, I. Proccacia, and B.I. Shraiman, Fractal measures and their singularities: The characterization of strange sets, Phys. Rev. A, 33, 1141-1151, 1986.

Okubo, P., and Aki, K., Fractal geometry in the San Andreas fault system, Jour. Geophys. Res., 92, 345-355, 1987.

Real, C.R., T.R. Toppozada, and D.L. Parke, Earthquake epicenter map of California, Calif. Div. Mines and Geol., Map-sheet 39, 1978.

Schwartz, D.P., and Coppersmith, K.J., Fault behavior and characteristic earthquakes: Examples from the Wasatch and San Andreas fault zones, Jour. Geophys. Res., 89, 5681-5698, 1984.

Shaw, H.R., and Gartner, A.E., On the graphical interpretation of paleoseismic data, U.S. Geol. Survey, Open-file Report 86-394, 1986.

Shaw, H.R., and Chouet, B., Kilauean volcanic tremor as a case study of multifractal attractor dynamics, Abstracts, Symposium on How Volcanoes Work, Hilo, HI, January 19-25, 1987.

Sherburne, R.W., R.T. Boylan, and D.L. Parke, Seismicity of California, April, 1979 through October, 1982, Calif. Geology, 38, 75-80, 1985.

Toppozada, T.R., C.R. Real, S.P. Bezore, and D.L. Parke, Compilation of pre-1900 California earthquake history, Calif. Div. Mines and Geol., Open-file Report OFR 79-6 SAC, 1979a.

Toppozada, T.R., C.R. Real, and D.C. Pierzinski, Seismicity of California, January, 1975 through March, 1979, Calif. Geology, 32, 139-142, 1979b.

Wesnousky, S.G., C.H. Scholz, K. Shimazaki, and T. Matsuda, Earthquake frequency distribution and the mechanics of faulting, Jour. Geophys. Res., 88, 9331-9346, 1983.

Wilson, K.G., Problems in physics with many scales of length, Sci. Am., 241, 158-179, 1979.

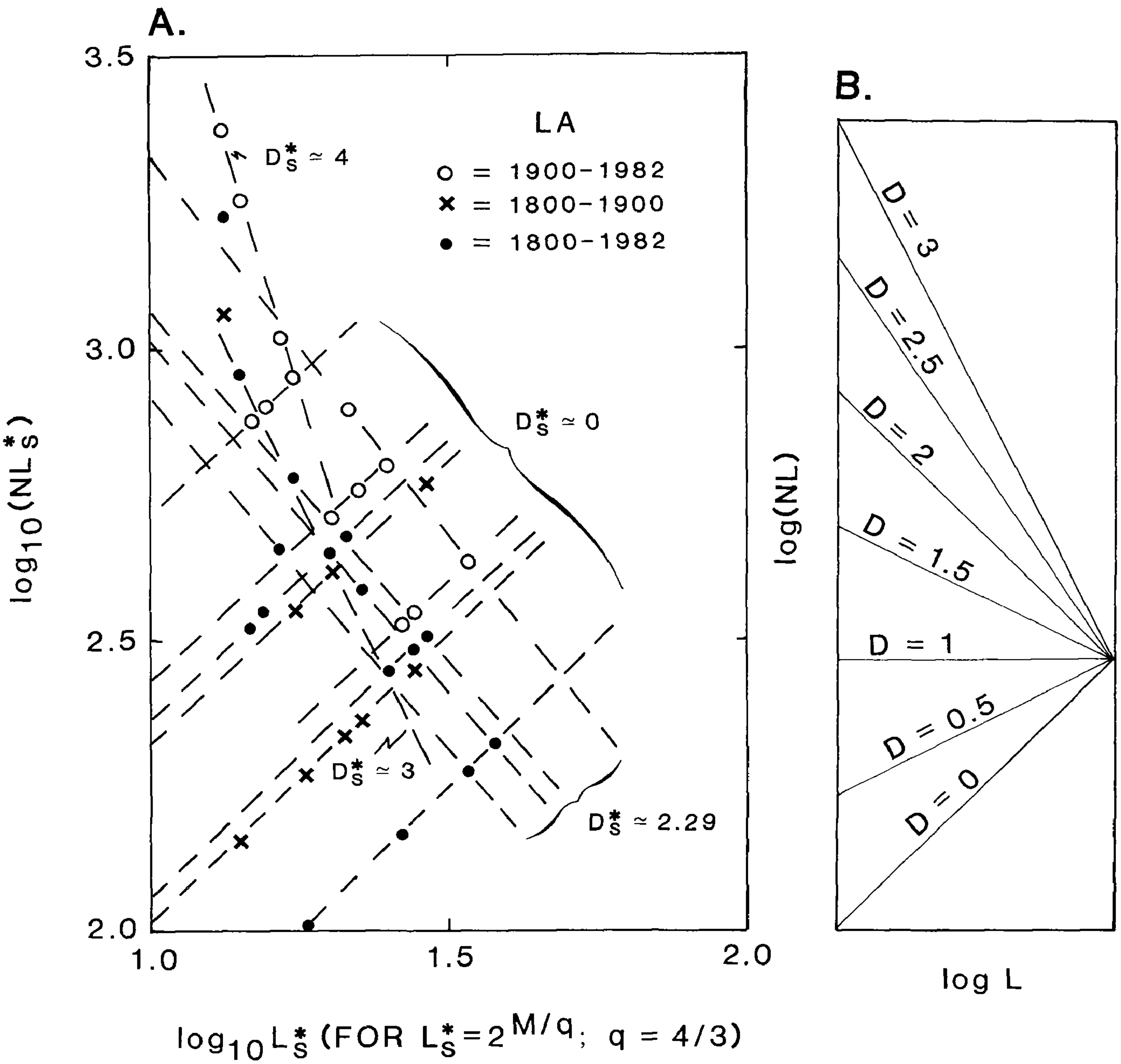

Figure 1. A. Fractal subsets, D^*_s, based on use of Eq. (1) with catalogs of earthquake magnitudes for the Los Angeles vicinity. In this study the Los Angeles subregion is defined by a rectangular area roughly two degrees on a side between 32.5 and 34.5 degrees N. Latitude, and between 116.5 and 121.0 degrees W. longitude. Data are subdivided into three groups: pre- and post-1900 earthquakes and the total historic catalog from 1800-1982 (symbols defined in legend). Frequencies, N, are based on yearly temporal frequencies, f, normalized to 1000 years (i.e., log N = log f + 3). See text for data sources and definitions.

B. The fractal dimension, D, is defined by D = (1-S), where S is the slope (units on ordinate and abscissa are same).

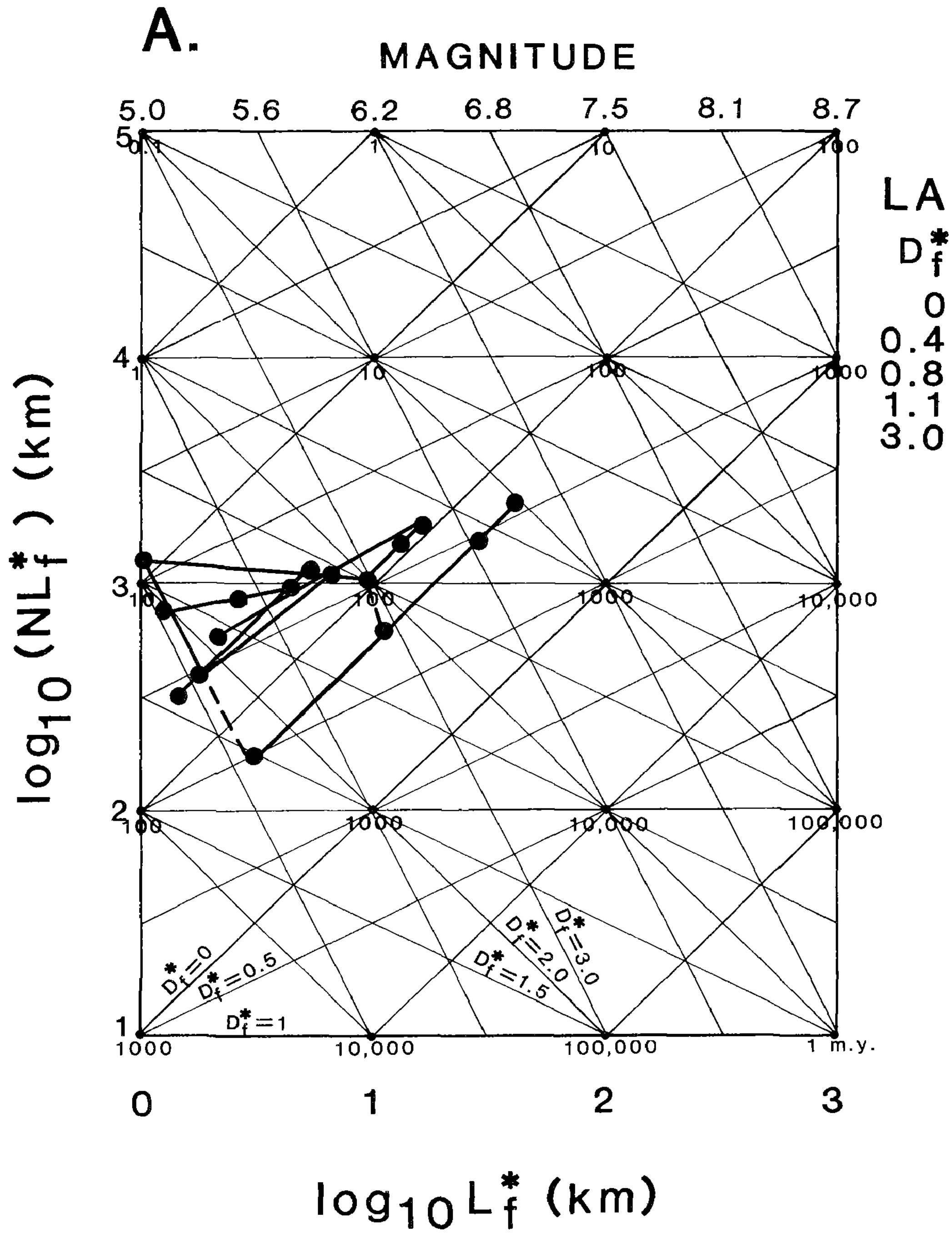

Figure 2. A. All historic earthquakes from Figure 1A rescaled according to calibration of fault lengths. Values of L^*_s, based on Eq. (1) are rescaled according to fault-length calibration defined by Eq. (2), as given by Eq. (3). Frequencies, N, represent numbers of events per 10,000 years, a 10-fold increase of time frame from Figure 1 (i.e., log N = log f + 4). Fractal dimensions, D^*_f, are shown by the grid lines; numbers at nodal points give values of recurrence times (1/f = 10,000/N, years). Magnitudes calculated from Eq. (2) are shown at the top. The estimated fractal subsets are listed at the right.

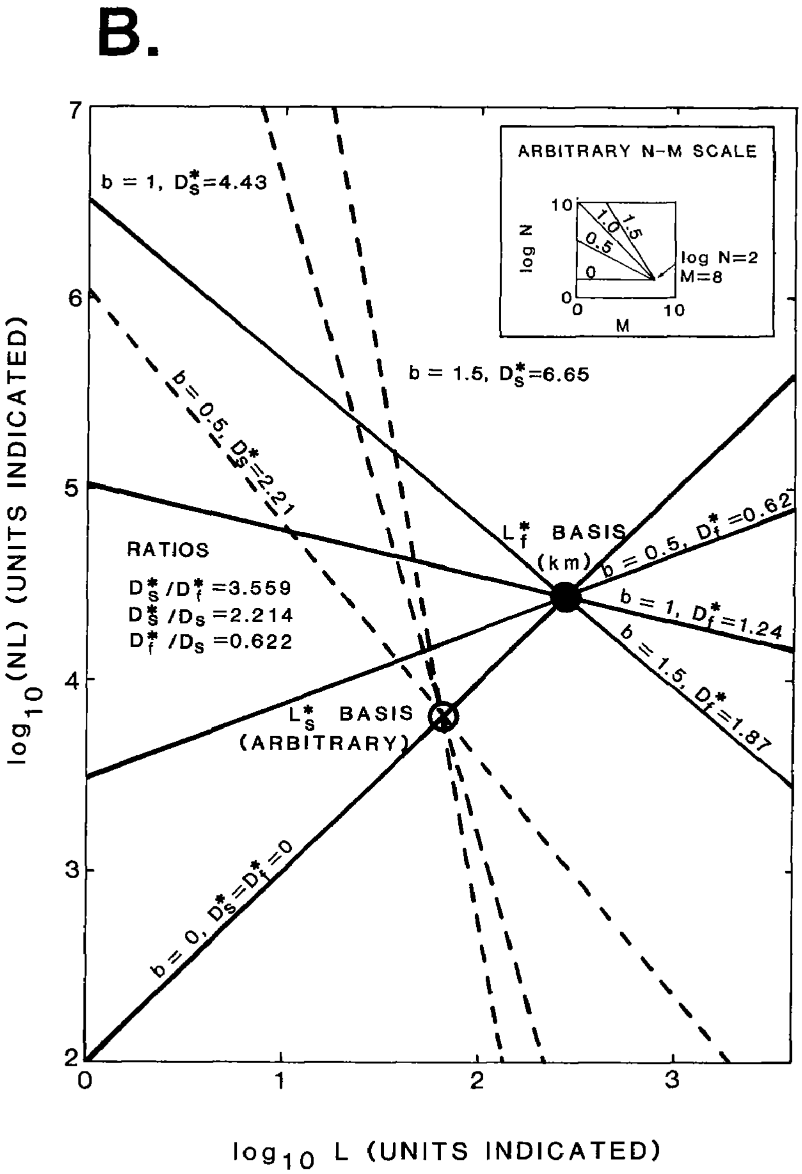

Figure 2. B. Relation of fractal dimensions as defined in A (solid lines) vs fractal dimensions as defined in Figure 1 (dashed lines) for the arbitrary frequency-magnitude relations shown in the inset (representing b-value sets converging at the point M = 8, N = 100 events per 10,000 years). The ratios shown at the left indicate proportionalities among the fractal definitions, D^*_s, D^*_f, and D_s, the latter representing the fractal segmentation model of Aki (1981), D_s = 3b/c, where c is the coefficient in moment-magnitude correlations.

EVALUATION OF DEFORMATION PROCESSES IN FAULT ZONES AT DEPTHS CORRESPONDING TO THE BRITTLE-DUCTILE TRANSITION

14-08-0001-G1341

CAROL SIMPSON
Department of Geological Sciences
Virginia Polytechnic Institute & State University
Blacksburg, VA 24061.
(703) 961 6521.

Investigations

Field and laboratory studies have been made and are underway of deformation in the Striped Rock Pluton, southwest Virginia, that is associated with the nearby Fries Thrust Zone. Field studies will document the sequence and geometry of brittle and crystal plastic events that affect the plutonic rocks by mapping on scales of 1:10 to 1:100. Electron microprobe studies, scanning electron microscopy, transmission electron microscopy and optical microscopy are being used to determine the deformation conditions for the several deformation episodes that have occurred in this exhumed fault zone.

Results

The Fries Thrust Zone (FTZ) in southwest Virginia is a km-scale, gently SE-dipping exhumed fault zone that contains complexly deformed metasedimentary and meta-igneous rocks. The northwestern boundary of the Fries Thrust Zone abuts the Striped Rock Pluton, a composite granite/syenite pluton of the Late Proterozoic Crossnore Plutonic-Volcanic suite of the southern Appalachians. Deformation associated with the FTZ has variably affected the Striped Rock Pluton and it is an objective of this project to carefully document this deformation, in particular the sequence of brittle and crystal plastic events and their conditions of formation. Field work commenced in late Fall, 1986 and laboratory studies commenced in Winter, 1986. Both aspects of the research are continuing at present.

Adjacent to the FTZ, both the Striped Rock Pluton and the surrounding Cranberry Gneiss country rock are deformed into mylonitic augen gneisses. As far as 2km to the northwest of (i.e. structurally below) the FTZ, the plutonic rocks are cut by numerous cm-scale cataclasite zones and mm- to decimeter-scale mylonite zones. This deformation is heterogeneously distributed, becoming less well developed with distance from the FTZ. The pluton extends to a distance of 4km northwest of the FTZ and at its northernmost boundary, the granitic rocks contain an extremely weakly developed tectonic fabric that has comparable strike and dip to that in the FTZ.

Preliminary field and microstructural investigations indicate that four significant deformation events are recorded in the plutonic rocks, at least the first two of which are directly related, geometrically, and spatially with deformation along the FTZ. Deformation commenced with a brittle cracking event, followed by two mylonite-forming events of opposite movement sense, and terminated by another phase of brittle deformation (Simpson and Kalaghan, 1987).

Original igneous textures are only locally preserved in the Striped Rock Pluton; nowhere is the rock completely undeformed. Almost all feldspar grains contain abundant intergranular fractures that are usually dilatant and oriented along (001) or (010) cleavage planes. These fractures are the earliest deformation signature observed in the plutonic rocks and are either sealed with the same mineral as the host grain, in optical continuity, or filled with quartz and/or green biotite or with host grain mineral and green biotite (Simpson, 1986). Both microcline and plagioclase (An13) grains commonly contain cracks filled with plagioclase (An10). Healed intragranular cracks in original igneous quartz grains are defined by fluid inclusion arrays. The composition, and temperatures and pressures of entrapment of these fluids is currently under investigation.

Millimeter- to centimeter-scale quartz veinlets that are parallel to the early transgranular cracks contain abundant evidence for later crystal plastic deformation (Simpson and Kalaghan, 1987). Undulose extinction, subgrains and evidence for both rotational recrystallization and grain boundary migration recrystallization are observed. Rotation of previously formed microcracks was concomitant with subgrain rotation. Non-symmetrical strain distribution in the wall rocks adjacent to the veinlets is common (cf. Segall & Simpson 1986). Alteration of feldspars to white mica plus quartz is most intense adjacent to the filled fractures. These alteration minerals commonly define an anastomosing fabric, consistent in geometry with the sense of shear as inferred from grain shape preferred orientations in the deformed quartz grains.

Two sets of mylonite zones have been found in the Striped Rock Pluton and its surrounding country rocks. The first set has northwest-directed overthrust movement and the second set has southeast-directed normal fault movement (Simpson and Kalaghan, 1987). Relative timing of the two mylonite sets is under investigation. Deformation conditions for both sets belong to lower greenschist facies; detailed petrography and microprobe analysis is in progress to better constrain these conditions. All mylonite fabrics have been overprinted by a late-stage set of stilpnomelane-, chlorite- and quartz-filled cracks that have orientations compatible with late-stage movement on the Fries Thrust Zone.

References

Segall, P. and Simpson, C. 1986. Nucleation of ductile shear zones on dilatant fractures. *Geology* 14: 56-59.

Simpson, C. 1986. Fabric development in brittle-to-ductile shear zones. *Pure and Applied Geophysics* 124: 269-288.

Simpson, C. and Kalaghan, T. 1987. Deformation in the Striped Rock Pluton, N.W. margin of the Fries Thrust Zone, S.W. Virginia. *Geol. Soc. Am. Abstracts with Programs* 19 (2): 129.

Reports

Simpson, C. and Kalaghan, T. 1987. Deformation in the Striped Rock Pluton, N.W. margin of the Fries Thrust Zone, S.W. Virginia. *Geol. Soc. Am. Abstracts with Programs* 19 (2): 129.

Fault Patterns and Strain Budgets

9960-02178

Robert W. Simpson
U.S. Geological Survey
Branch of Tectonophysics
345 Middlefield Road, MS/977
Menlo Park, California 94025
415-323-8111, ext. 4256

Investigations

Purpose is to understand the interactions of faults and fault segments through time using very simple elastic dislocation models. Investigations have included looking at the effects of the Coalinga and Kettleman Hills earthquakes on creeping sections of the San Andreas fault, looking at creepmeter responses to the Tres Pinos earthquake, exploring reasons for the horizontal offset of the surface trace of the San Andreas fault from the 1986 aftershocks at Parkfield, and most recently examining the pattern of aftershocks of the Morgan Hill earthquake in collaboration with Paul Reasenberg and David Oppenheimer.

Results

A paper summarizing the Coalinga and Tres Pinos investigations has been prepared for publication. The recent work on Morgan Hill aftershocks has resulted in several new programs to display stress tensor orientations as beachballs superimposed on a colored or contoured field that represents the change in the Coulomb failure criterion. It is hoped that the distinctive pattern of aftershocks to this earthquake will lead to some inferences about the regional stress field.

References Cited

Simpson, R. W., Schulz, S. S., and Dietz, L. D., 1986, Response of creepmeters on the San Andreas fault to the 26 January 1986 Tres Pinos earthquake: EOS, Transactions American Geophysical Union, v. 67, p. 1206.

Simpson, R. W., Schulz, S. S., Dietz, L. D., and Burford, R.O., 1987, The response of creeping parts of the San Andreas fault to earthquakes on nearby faults - two examples: Redbook for USGS Conference on Intermediate Term Precursors. (Also submitted to PAGEOPH).

Earthquake Forecast Models

9960-03419

William D. Stuart
Branch of Tectonophysics
U.S. Geological Survey
Pasadena, California 91106
(818) 405-7816

Investigations

1. An earthquake instability model for the Nankai Trough subduction zone in Japan has been formulated and tested with geodetic data associated with the 1946 Nankaido earthquake. The model is two-dimensional and represents fault zone constitutive behavior by a slip and velocity dependent fault law. Forcing is by a constant rate of relative plate motion applied at depth. The model resembles earlier models by Mavko (unpubl. ms., 1984) and Tse and Rice (J. Geophys. Res., 1986). This work is now completed.

2. Work has begun on two new projects. The first project is to find a mechanical explanation for seismic quiescence and creep retardation before moderate earthquakes on the San Andreas fault in central California. Wyss, Habermann, and Burford have identified several such areas, one of which has been fulfilled by a predicted earthquake.

   The second new project is to construct new models of tectonic plate interaction. Part of this effort is a study of Cenozoic and current tectonics in southern California. Another part is a study of the causes of motion of the actual plates as they and the mantle interact on a sphere.

3. I helped organize (with K. Aki) a USGS Red Book Conference on intermediate-term earthquake prediction. The meeting was held last November in Monterey, California, and was attended by about 50 scientists.

Results

1. The Nankai Trough model simulates repeated earthquake cycles, including post-, inter-, pre-, and coseismic stages of each cycle. For plausible values of constitutive and geometric parameters the model is able to reproduce most of the main features of elevation changes reported in Thatcher (J. Geophys. Res., 1984). In model simulations, accelerating pre-instability fault slip occurs where the fault zone is brittle. The accelerating slip occurs on two time scales. The first time scale is several years long and is interpreted as an intermediate-term precursor; the second time scale is several days long and is interpreted as a short term precursor. Both kinds of precursory slip produce anomalous elevation changes which are largest near the fault

trace and are as much as 10 cm in amplitude. These results would seem to justify making a three-dimensional instability model for the Tokai gap where a large earthquake is expected.

2. Some exploratory work has been done on the two new projects, but no firm results are available.

3. Technical papers presented at the Red Book Conference described a variety of old and new precursors on the intermediate-term time scale. Some papers attempted to give mechanical explanantions of certain observed or observable precursory phenomena. The meeting proceedings will be published in a USGS Open File Report soon, and many of the papers will appear in a special issue of Pure and Applied Geophysics.

Reports

Stuart, W. D., Forecast model for large and great earthquakes in southern California, J. Geophys. Res., 91, 13771-13786, 1986.

__________________, Review of Earthquake Source Mechanics, Edited by Das, Scholz, and Boatwright, Pure and Applied Geophysics, 1987, in press.

An Experimental and TEM Study of Cataclastic Flow in Quartzo-Feldspathic Rocks

Contract 14-08-0001-G-1363

Jan Tullis and Richard Yund

Department of Geological Sciences
Brown University
Providence, RI 02912
(401) 863-1921

Investigations

1. We have continued work on determining the locations in P-T space of the transitions from brittle faulting to ductile cataclastic flow, and from cataclastic flow to dislocation creep, for natural monomineralic aggregates of plagioclase and of quartz; we find significant differences between the two materials.

2. We have made detailed TEM investigations of the micromechanical processes operating within the cataclastic flow regime, for both materials, and the changes associated with the transitions to shear fracture and to dislocation creep. The cause of the stabilized, distributed cracking in the cataclastic flow field appears to be quite different for the two materials. For quartzite we have made a detailed investigation of how the processes and microstructures in the cataclastic flow regime evolve with increasing strain, as well as an investigation of the effect of initial porosity.

3. We have begun TEM investigations of the gouge developed in rotary shear friction experiments of T. Tullis and J. Weeks, with the goal of correlating microstructural features with constitutive behavior so as to allow more accurate extrapolations to natural conditions. Initial observations have been made on granite, calcite marble, dolomite marble, and quartzite samples.

Results

1. *Cataclastic flow field for feldspar and quartz:* In anorthosite, cataclastic flow occurs at temperatures of ~300-800°C at 1000-1500 MPa, for a strain rate of 10^{-5}/sec. Brittle faulting occurs at all temperatures tested (20-700°C) at 500 MPa, and at low temperatures (20-200°C) at higher pressure (1000-1500 MPa). Dislocation creep occurs >900°C at 1000-1500 MPa. The *transitions* between these regimes are gradual, and occur over a temperature interval of about 100-200°C. In quartzite, the cataclastic flow regime is limited to a much narrower temperature interval, from 700-850°C at 1000-1500 MPa, for a strain rate of 10^{-5}/sec. Brittle faulting is observed at temperatures of 20-700°C at 500 MPa, just as for feldspar, but in strong contrast to feldspar it is also observed at temperatures up to 600°C at 1000-1500 MPa. Dislocation creep occurs at >850°C at 1000-1500

MPa. In both materials, in contrast to predictions, cataclastic flow appears to involve steady state flow rather than strong work hardening (to 40-50% strain).

2. *Micromechanical processes:* In anorthosite, the transition from brittle faulting to ductile cataclastic flow requires modest temperature (>300°C) as well as high pressure (>500 MPa), but dislocations are *not* involved in the stabilization of the cracking; cataclastic flow involves cracking on the two cleavages and the development of very fine fragments (<0.1 μm) due to their intersection. Dislocations are first observed in samples deformed at 700°C (at 10^{-5}/sec), and steady state dislocation creep requires temperatures of 1000°C. Therefore the role of temperature is somehow related to cleavage cracking itself, but the exact mechanism remains unknown at present. In quartzite the situation is very different: new dislocations are first observed at quite low temperature (~300°C) but obviously their mobility is extremely limited, because samples undergo brittle faulting at temperatures up to and including 600°C. The type of cataclastic flow exhibited by quartzite (at 700-850°C) is quite different from that exhibited by the anorthosite; it involves both dislocations and microcracks. Detailed optical and TEM analysis of samples deformed to many different strains at 700°C, 1500 MPa and 10^{-5}/sec shows that at ~5% sample strain locally high dislocation densities are observed, but no cracks; at ~10% strain optical deformation bands are observed to consist of zones of extremely high densities of tangled dislocations; at ~20% strain these bands develop cracks and crush zones with extremely fine grain size (<0.1 μm); at ~30% strain more cracking and crushing occurs; and at ~50% strain there is evidence that some of the very finely crushed regions have undergone some grain growth, as the grains appear more uniform in size and somewhat polygonal.

Thus in anorthosite the ease of cracking on the two cleavages, plus the difficulty of dislocation glide and climb, produce a relatively wide field of cataclastic flow which results from distributed cracking, the stability of which does not result from or cause dislocation motion. In quartzites, in contrast, the absence of cleavages means that at low temperatures where dislocation glide and climb are limited, the stress rises much higher and crack propagation is unstable; at higher temperatures where dislocation glide and climb are limited dislocation pile–ups generate locally high stresses which nucleate cracks, but these cracks are stabilized in part because the stress decays rapidly away from the pile-ups and in part because the presence of other dislocation arrays and cracks form barriers to continued propagation.

The effect of porosity on the cataclastic flow field is being investigated in quartzites. Hadizadeh and Rutter (1983) found that a quartzite with 7% porosity exhibited a transition from brittle faulting to ductile cataclastic flow at room temperature and about 600 MPa (at 10^{-4}/sec), whereas we found that a non-porous quartzite undergoes brittle faulting up to at least 1500 MPa. We have obtained a piece of the porous quartzite used by Hadizadeh and Rutter, and have performed further experiments to higher strain. We find that at room temperature and 1000 MPa, this quartzite does indeed show cataclastic flow for the first ~30% strain, but at 40-50% strain the sample develops a brittle fault. Thus it appears that the cataclastic flow is a transient phenomenon, with cracking initially stabilized by the 'damage' resulting from pore collapse, but that with increasing strain the behavior reverts to that which is inherent to these conditions for non-porous material.

3. *Microstructures in experimental fault gouge:* We have used TEM to examine the gouge from four of the rotary shear samples used by T. Tullis and J. Weeks (USGS 14–08–0001–G–11) to obtain constitutive laws for frictional sliding. The goals are to see whether it is possible to establish correlations between microstructural features and constitutive behavior which would aid in extrapolating the experimental results to natural conditions; in addition we are interested to see what similarities there are with the gouge and crush zones produced in our higher pressure compression experiments. In all of these rotary shear experiments the gouge was generated by sliding on initially bare rock surfaces, to which some water had been added. All four samples had a complex sliding history including many different sliding velocities; the TEM observations are therefore preliminary. More meaningful observations will come later from examination of samples with simpler sliding histories.

Westerly granite: (Normal stress 50 MPa, displacement 376 mm, gouge layer 185-400 μm thick.) The gouge shows some larger fragments, all of quartz; these are embedded in extremely fine-grained material, consisting mostly of feldspar, much of which is <0.1 μm in diameter and ~10-25% of which is amorphous. (We have previously observed that at low temperatures quartz is more resistant than feldspar to cracking, in compression experiments on aplite at higher pressures.) The amorphous nature of portions of the gouge was determined by convergent beam electron diffraction, and its composition determined by analyzing the energy dispersive x-ray spectra from submicron size areas. The amorphous material mostly has the composition of feldspar, but some is essentially pure silica. Despite the locally high stresses in the gouge, no dislocations were observed in the larger fragments of quartz, again in agreement with our observations of room temperature samples deformed in compression at higher pressures.

Carrara calcite marble: (Normal stress 15 MPa, displacement 200 mm, gouge layer 185-450 μm thick.) There are several differences between the gouge in this marble and that in granite: the gouge in this sample is much thicker, it consists of more uniform fine particles, high dislocation densities are observed in some of the larger fragments (higher than in the starting material), and there is little if any amorphous material. The presence of crushed fragments and their equant shape indicate that the dislocations did not accomodate much of the strain, although they might have allowed local flow at point contacts on sliding surfaces.

Dolomite marble: (Normal stress 75 MPa, displacement 55 mm, gouge layer 10-40 μm thick.) Despite the striking difference in the thickness of the gouge layer between the calcite and the dolomite marbles, there is very little difference in the TEM microstructure of the two.

Cheshire quartzite: (Normal stress 7-50 MPa, displacement 386 mm, gouge layer 10-40 μm thick.) The quartzite gouge is very similar to the granite gouge: it shows larger, often somewhat rounded fragments, embedded in extremely fine-grained material, about 10-25% of which is amorphous. There is no evidence that dislocations were generated during the experiment. The gouge layer is even thinner than in the granite sample, and the transition from large, original, unfractured quartz grains into the fine gouge is very sharp, occurring over a distance of only a micron.

Because these four samples all had a complicated sliding history, we do not yet know how the microstructures are related to different experimental conditions; in particular we do not yet know whether certain microstructures are associated with velocity strengthening and others with velocity weakening behavior. However, our initial observations already suggest a possibly important role for amorphous material in the constitutive laws for frictional sliding, and a very minor role for crystal plastic processes. The gouge in these room temperature rotary shear experiments is very similar on the TEM scale to the gouge in uniaxial compression experiments on as-is anorthosite and quartzite at higher pressures, except for the apparent absence of amorphous material in the latter. Clearly it is important to determine whether the percentage of amorphous material correlates with the amount of water added.

Reports

Hirth, G., and Tullis, J., 1986, Cataclastic flow in dry, non-porous quartzites: Trans. Amer. Geophys. Union, 67, 1186.

Tullis, J., and Hadizadeh, J., in preparation, Transitions from faulting to cataclastic flow to dislocation creep in anorthosite: An experimental study: to be submitted to Tectonophysics.

Tullis, J., and Yund, R.A., 1987, Transition from cataclastic flow to dislocation creep of feldspar: mechanisms and microstructures: Geology, in press.

Tullis, J., and Yund, R.A., 1987, Mechanisms of cataclastic flow in anorthosite: Trans. Amer. Geophys. Union, 68, 404.

Yund, R.A., and Tullis, J., in preparation, Micromechanical processes of experimental cataclastic flow in anorthosite: to be submitted to Journal of Structural Geology.

Yund, R.A., Tullis, T.E., Weeks, J.D., and Blanpied, M.L., 1987, Microstructures in experimental fault gouges: Trans. Amer. Geophys. Union, 68, 405.

EXPERIMENTS ON ROCK FRICTION CONSTITUTIVE LAWS APPLIED TO EARTHQUAKE INSTABILITY ANALYSIS

USGS Contract 14-08-0001-G-1185

Terry E. Tullis
John D. Weeks
Department of Geological Sciences
Brown University
Providence, Rhode Island 02912
(401) 863-3829

Investigations

1. We have continued work on determining the detailed constitutive behavior for frictional sliding of several rock types. We have completed one extensive experiment on a pure quartzite and are presently conducting another.

2. We have cooperated with R. Yund and J. Tullis in a TEM study of our experimentally produced gouges.

3. We have continued our numerical investigation of unstable sliding by modelling different types of high velocity constitutive behavior and by including inertial effects.

4. We have conducted a numerical study of temporal and spatial variations in strain and displacement associated with the model earthquake cycle of Tse and Rice (1986).

Results

1. Knowledge of the frictional properties of a variety of rock types is crucial to understanding the earthquake mechanism. Accordingly, the micromechanics controlling the frictional behavior of polyphase rocks (e.g., granite) may be understood better if the contributions of their individual components (e.g., quartz) can be identified. With these goals in mind, we have begun to investigate the frictional properties of pure quartz rock over a range of velocity covering 7.0 orders of magnitude. In our high pressure apparatus, we have performed a rotary shear friction experiment during which we slid initially bare samples of pure quartzite at normal stresses of 7–50 MPa and slip rates of $10^{-3.5}$ to $10^{3.5}$ μm/sec, to over 386 mm total displacement. The sliding surfaces were initially roughened with 80 grit alumina and moistened with distilled water. During the experiment, a 10–40 μm thick layer of gouge developed, containing a single sharp sliding surface. A second experiment is now in progress. We find that the frictional resistance depends on velocity, and the nature of this dependence is different from that previously observed for silicates. The value of **a–b**, the change in steady-state coefficient of friction per e-fold change in slip rate, is positive (velocity strengthening) at the lowest velocities and decreases with increasing velocity such that there is a transition to velocity weakening above ~0.1 μm/sec. This decrease in **a–b** caused unstable sliding in the velocity range 10–1000 μm/sec. We infer from stable sliding at the highest velocities that **a–b** was again increasing, but we were unable to measure the value. The increase in **a–b** at low velocity is similar to a transition observed in halite (Shimamoto and Logan, 1986), and differs from our observation that for granite, **a–b** becomes independent of velocity at low velocities. Numerical simulations using a two-state-variable constitutive law (Ruina, 1983) indicate that the value of **a**, the term measuring the instantaneous direct dependence of friction on slip velocity, and the values of the characteristic decay distances L_1 (~3 μm) and L_2 (~150 μm), are independent of normal stress and slip rate. These observations suggest that the changes in **a–b**, and, therefore, in stability, are due to changes in $\mathbf{b_1}$ and $\mathbf{b_2}$, the constitutive parameters that measure the magnitude of exponential fading memory of previous slip velocities. The differences between these experiments and previous experiments on quartz and granite suggest that different micromechanical processes are operating at the lowest velcocities. This could be very important in extrapolating laboratory data to the longer times of natural earthquake cycles.

2. Our petrographic study of the gouges produced in our experiments on granite, quartzite, calcite marble and dolomite marble is being complemented by a transmission electron microscope (TEM) study of these samples conducted by R. Yund as part of a study of cataclastic flow being undertaken by J. Tullis and R. Yund. A summary of their TEM results is presented elsewhere in this volume (contract 14-08-0001-G-1363) and will not be duplicated here.

3. We have continued our efforts to develop constitutive laws that accurately reflect frictional behavior, and to study the consequences of these steady state functions for unstable slip. We have studied three different forms of constitutive laws: the log-linear law used by Ruina, and two laws that have modified steady state response at high velocity. At low velocity both of these modified laws display steady state velocity weakening, and at high velocity they display either no steady state velocity effect ("zero slope function") or velocity strengthening ("positive slope function"). The former model has been assumed by various workers, but experimental observations of the behavior of several rock types suggests that the second model is more accurate (Blanpied et al. 1987). In the positive slope model we assume that the steady state coefficient of friction is proportional to ln(V) with the slope at high velocity equal to the magnitude of the "direct effect" ("**a**" in Ruina's (1983) law) while at low velocity the slope in both cases is **a–b** as in the simple log-linear Ruina law. Both of these models will arrest an unstable event even in the absence of inertia, the positive slope model yeilding stress drops that are more consistent with our experimental observations of unstable events during sliding on granite. We have also done numerical modelling with all three steady state functions with inertia included, using inertial parameters appropriate to our apparatus. With the addition of inertia, unstable events are arrested even with the log-linear steady state function, but using this function, the stress drops are much larger than we observe in our experiments on granite. For the range of velocities used in our experiments, numerical modelling indicates that it is necessary to use the positive slope function to reproduce both the magnitude of stress drops and their variation with load point velocity. For this particular combination of parameters, the transition to veloctiy strengthening is more important than inertia in determining the stress drop. Other combinations of parameters yield simulations in which the peak velocity is not much different, but dynamic overshoot becomes important in determining the stress drop.

4. In order to design a rational program of earthquake prediction, it is important to know the best places to make measurements of those quantities whose changes can signal a coming earthquake, and how large the signals can be expected to be, in order to determine whether they can be detected with existing or future instruments. The principal problem of earthquake prediction is the difficulty of placing a dense array of instruments at focal depths. If we had complete knowledge of the stress and displacement field we could probably predict nearly all earthquakes, but with only the incomplete knowledge available it is a much more difficult task. A good model of what to expect can provide much insight into how to deploy the appropriate instruments. Although a large number of uncertainties exist concerning the extrapolation of the laboratory data to natural faults, fault models such as those of Tse and Rice (1986), based on laboratory-derived constitutive laws, match the behavior of natural faults undergoing earthquake cycles in a remarkable number of details. We have used the calculated distributions of displacement and velocity from the model fault of Tse and Rice (1986) as input to calculate the distribution of strain, displacement, strain rate, and velocity away from the fault in two dimensions, both at the earth's surface and at depth, using the boundary element displacement discontinuity method. As expected, we find that changes in strain and displacement prior to the earthquake are most obvious at the focal depth because it is there that the earthquakes nucleate. The changes in stress (or, equivalently, strain in the elastic surroundings) that occur at the surface are of insufficient magnitude and occur over the wrong time scale to be very useful for earthquake prediction, but changes in displacement rate that occur at the surface should allow a prediction to be made. The most useful overview of the nature of the earthquake cycle at a variety of depths is provided by Figure 1, which shows strain (or stress) vs. velocity of five points at various depths 500 m away from the fault plane. Careful study of Figure 1 reveals many interesting facts concerning the earthquake cycle. The stress changes during a cycle are progressively larger at depth due to the simple fact that the increasing normal stress causes larger changes in frictional slip resistance. Less obviously, the increase in the shear stress following the previous earthquake ceases much earlier at the surface than it does at depth. Also during the final year prior to the earthquake the changes in strain at the surface are small relative to those at depth. (In Figure 1 compare the changes between 0.8 years and 1 minute prior to the earthquake. Although the shear strain changes at the surface are not very useful for

prediction of the earthquake, Figure 1 shows that the velocities at the surface as well as at depth will increase rapidly prior to the earthquake and could be useful for prediction purposes. It is also apparent, however, that the velocities at the surface lag those at depth and so less warning is provided by having only surface measurements. The changes in velocity predicted from the model fault (Figure 2) are large enough during the two years prior to the earthquake that they would be detectable, and during the last few months the changes become extremely large. For points 3 km from the fault, the velocity increases to about 200 mm per year a week before the earthquake, but reach smaller values closer to the fault as comparison of the curves in Figure 2 shows. This is a reflection of the fact that surface points some distance from the fault are more sensitive to the quickly accelerating displacements at depths of about 5 km than points near the fault. At the same time that the velocities are increasing everywhere, the peak in surface velocity is shifting away from the trace of the fault to points progressively farther from the fault, as is clearly shown in Figure 3. At 18 hours before the earthquake the highest surface velocities are at 4.5 km from the fault. This change in the pattern of peak velocity is a manifestation of the fact that the most rapid increases in velocity are occurring at depth due to the growing instability there and this change in the pattern is itself a useful precursor to the earthquake. Although the surface velocities change in ways useful to earthquake prediction, the velocities at depth begin their dramatic increase earlier than those at the surface (Figure 2). Consequently, to obtain an earlier warning and to provide measurements complementary to those at the surface, the ability to monitor the velocity of points within deep wells would be very useful. More details of the results summarized here are presented in Tullis (1987a, b).These calculations indicate that if it were possible to deploy instruments at focal depths, the sensitivity to premonitory changes would be enormously increased. This will be even more true for the more realistic three dimensional situation in which slip on the fault initiates on a patch rather than on an along-strike strip as in the model of Tse and Rice (1986). The current modelling indicates that strain changes at the surface are not large enough to be useful as precursors, but would be useful if they could be measured at depth. Velocities at the surface and the position of the maximum veloctiy are both sensitive indicators of an impending earthquake. If homogeneous strain is assumed within 5 km. of the fault, significant details may be lost.

Reports

Blanpied, M.L. and T.E. Tullis (1986), *The stability and behavior of a frictional system with a two state variable constitutive law*, Pure Appl. Geophys. *124*, 415-444.

Blanpied, M.L., T.E. Tullis, and J.D. Weeks (1986), *Frictional behavior of granite at high slip velocity*, Eos, Trans. AGU *67*, 1186.

Blanpied, M.L., T.E. Tullis, and J.D. Weeks (1987), *Frictional behavior of granite at low and high sliding velocity*, Geophys. Res. Lett. (in press).

Tullis, T.E. (1986), *The relation between surface roughness of laboratory samples and decay distances of friction constitutive laws*, Eos, Trans. AGU *67*, 1187.

Tullis, T. E. (1986) *Friction and faulting, Editor's note*, Pure Appl. Geophys. *124*, 375-381.

Tullis, T. E. (1987a) *Rock friction constitutive behavior from laboratory experiments and its implications for an earthquake prediction field monitoring program*, in *Proceedings of USGS Conference on Physical and Observational Basis for Intermediate-Term Earthquake Prediction*, Open-File Report (U.S. Geol. Surv. National Earthquake Hazards Reduction Program) (in press).

Tullis, T. E. (1987b) *Rock friction constitutive behavior from laboratory experiments and its implications for an earthquake prediction field monitoring program*, Pure Appl. Geophys. (Special Issue on Intermediate-Term Earthquake Prediction) (submitted).

Tullis, T.E. and J.D. Weeks (1986), *Constitutive behavior and stability of frictional sliding of granite*, Pure Appl. Geophys. *124*, 383-414.

Weeks, J.D. (1986), *Constitutive laws for high velocity frictional sliding and their influence on unstable stress drops*, Eos, Trans. AGU *67*, 1186.

Weeks, J.D. (1987), *Constitutive laws for high velocity frictional sliding and their influence on unstable stress drops*, J. Geophys. Res. (submitted).

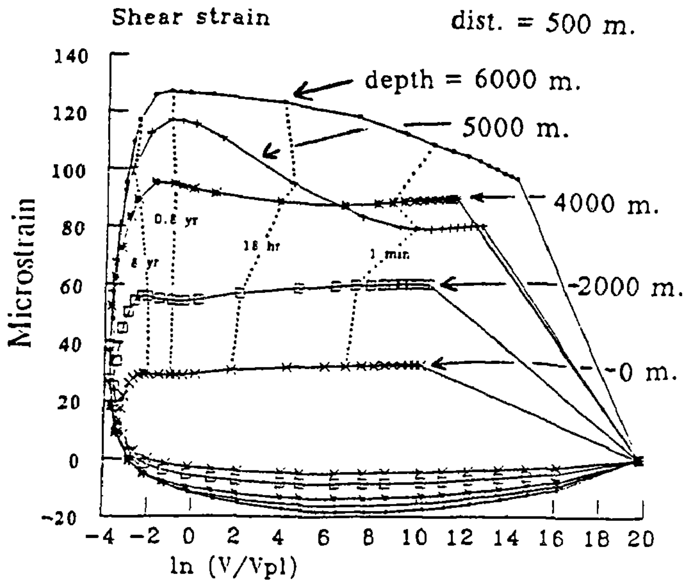

Figure 1. Behavior of the fault for points at a variety of depths, 500 m from the fault, for an entire earthquake cycle, computed from the displacements and velocities in the model of Tse and Rice (1986). V represents the half velocity of the fault with respect to the symmetry point at the fault plane, Vpl represents the total relative plate velocity which is taken to be 35 mm per year. For the boundary element calculations, only 45 representative times have been selected from the much larger number needed by Tse and Rice to model the instability. Times prior to the earthquake for the last part of this sequence of synchronous data points are 28.4, 20, 12.2, 8.1, and 2.8 yr, 297, 174, 88, and 24 days, 17.5 hr, 32, 3.3, and 1 min, and 26, 14, 8.4, 5.6, 3.8, 2.6, 2.0, and 1.4 sec.

Figure 2. Velocities at four different locations on a log-log plot to emphasize the period of time prior to the earthquake and to show the large range in velocities. The velocities are with respect to the symmetry point at the fault as discussed in the caption to Figure 1.

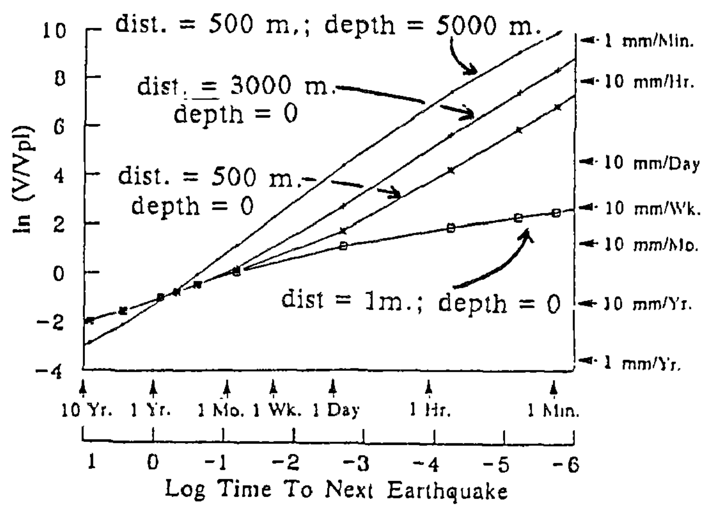

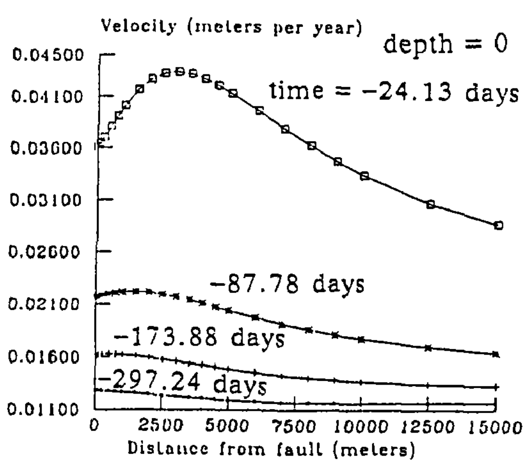

Figure 3. As the earthquake approaches, the velocities at the surface not only increase everywhere, but the pattern changes so that the peak velocities occur away from the fault as a consequence of the increasing slip rate at depth on the fault. By one day before the earthquake the peak velocity has moved even further, to a distance of 4.5 km from the fault. The pattern becomes progressively accentuated as can be seen by study of Figure 2. Beginning a few minutes before the earthquake, the peak in velocity at the surface shifts yet further to 6.5 km from the fault (as the point of highest velocity on the fault at depth rapidly moves to 6.5 km depth) and then jumps to the fault itself as the dynamic rupture occurs. Velocities are with respect to the symmetry point at the fault as discussed in the caption to Figure 1.

Seismic Reflection Investigations of Mesozoic Basins, Eastern U.S.

9950-03869

John D. Unger
Branch of Geologic Risk Assessment
U.S. Geological Survey
922 National Center
Reston, VA 22092
(703) 648-6790

ONGOING INVESTIGATIONS

1. To consolidate and synthesize the available seismic reflection information that pertains to the internal and external structure of Mesozoic basins, with special emphasis on the hypocentral area of the present seismicity of Charleston, South Carolina and the Ramapo fault zone in New Jersey and Pennsylvania.

2. To use 2-D synthetic seismic reflection models of the basement structure along selected seismic reflection traverses in the Charleston and Ramapo regions as an aid to processing and interpretation of the seismic reflection data and to allow the use of ray-tracing algorithms to be used for earthquake relocation.

3. To obtain optimal crustal velocity data from seismic reflection profiles in the hypocentral area by using methods, such as p-t inversion, capable of greater interval velocity resolution than the standard normal-movement techniques.

4. To investigate the role of Mesozoic basins as seismogenic tectonic features in the Eastern U.S.

RESULTS

1. I have collected more than 7,000 km of seismic reflection data over Mesozoic basins in the Eastern United States and summarized these data in a database format. These data show the extent to which the research community and the oil and gas industry have used this method to explore Mesozoic basins. When one examines the geometry of the internal and external structure of the basins the unmigrated reflection profiles are difficult to interpret and it is essential to migrate reflection data in order to understand the details of their features. If only unmigrated data are available, line drawings of them can be migrated quickly and inexpensively with a microcomputer-based program, and the profiles can be more readily interpreted. These results are summarized in Unger, 1986B.

2. I have acquired additional seismic reflection data from offshore eastern Mesozoic basins. Most of these profiles are industry data from the Fundy basin between New Brunswick and Nova Scotia and released to me by the Canadian government. Other data are from the profiles done by Marine Geology in the late 1970's and early 1980's in support of the offshore leasing studies. I have also digitized interpreted line drawings made from many of these profiles and have migrated these data using the line migration program described in Unger, 1986A.

REPORTS

Unger, J. D., 1986, A microcomputer program to migrate line drawings of seismic reflection profiles, U.S.G.S. Open-File Report 86-296, 31 pages.

Unger, J. D., 1986, A simple technique for analysis and migration of seismic reflection profiles from the Mesozoic basins of The Eastern United States, U.S.G.S. Bulletin 1776, in press.

Earthquake Fault Shape and Slip Pattern from Inversion of Geodetic Data

14–08–0001–G1383

Steven N. Ward and Sergio E. Barrientos

C. F. Richter Laboratory
Earth Sciences Board
University of California
Santa Cruz, CA 95064
(408) 429-2480

INVESTIGATIONS

We have continued our studies of fault shape and slip distribution as inferred from geodetic data. We are currently analyzing two Chilean earthquakes: the 1985, ($M_S = 7.8$) Valparaíso, and the great 1960 ($M_W = 9.5$) southern Chile events.

RESULTS

1985 EVENT. The March 3, 1985 Central Chile earthquake (Figure 1) was accompanied by more than 0.5 m of vertical displacement. Using an inversion scheme based on the superposition of elemental point sources and a gradient technique with positivity constraints, we have resolved the dimensions, shape, and slip distribution of the 1985 event. Most of the fault slip is concentrated on two patches at a depth between 30 and 40 km on a plane dipping 18° East. The patch containing the maximum slip has a north–south orientation and it is located close to the reported hypocenter of the mainshock. The overall region of maximum slip (slip $\geq$ 2 m) is more than 140 km long and oriented north–south. The dislocation model obtained from the static field is in good agreement with the mainshock–aftershock distribution, the moment release pattern from analysis of body waves, and the location and fault geometry of the main aftershock. The total moment derived from the dislocation model is 1.6×10^{28} dyne–cm, 30% larger than that obtained from surface wave [*Monfret* and *Romanowicz*, 1986] analysis.

Figure 2 shows contours of equal slip on the fault projected on the Earth's surface. Dashed lines represent the aftershock areas of the 1971 ($M_0 = 5.6 \times 10^{27}$ dyne–cm), the 1973 ($M_0 = 2.8 \times 10^{26}$ dyne–cm) and the 1981 ($M_0 = 6.6 \times 10^{25}$ dyne–cm) events [*Korrat* and *Madariaga*, 1986], and the foreshock area [*Comte et al.*, 1986] of the 1985 main event. The maximum slip of the main shock occurred down–dip of the 1973 and 1985 foreshock sequences along the Nazca and South American plates interface. The second patch of maximum main shock slip took place downdip of the 1981 sequence. This association is interpreted in terms of an asperity model [*Kanamori* and *Stewart*, 1978; *Lay et al.*, 1982; Ruff, 1983]. A primary feature of asperities is their large coseismic displacement. The proximity of the two patches of maximum slip to the aftershock areas of intermediate size earthquakes in the region since 1971 suggests that these compressional events may represent slip prior to failure in the "weaker" surroundings of the main asperities. Prior to the 1985 mainshock, the two patches of slip behave as locked sections on the interface between the two plates. The northern asperity acts as a barrier for the rupture occurring in 1971 and also precludes down–dip propagation of the 1973 event. After the occurrence of these two events, this patch becomes strongly loaded. A similar situation occurs at the southern patch of maximum slip which is loaded by the 1981 event. The absence of large magnitude earthquakes in the region between the 1973 and 1981 events is correlated with a local minimum of slip. This implies that the middle section is able to slip more freely than its northern and southern counterparts during the interseismic period.

Figure 3 contours equal coseismic elevation change. These contours are elongated in a north–south direction reflecting the "ridge" of displacement on the fault. Maximum uplift (600 mm) is concentrated on the sea floor above the epicenter. A small amount of subsidence (100 mm) is predicted for the inland region east of Valparaíso. Three independent observations support the general shape of the vertical elevation change predicted by the model: Two observations of tide gages at Valparaíso and San Antonio and one measurement of tilt at Rapel Lake, 60 to 100 km south of the leveling line.

1960 EVENT. Plafker and Savage [1970] provide detailed descriptions of the sea level changes at more than 150 localities in the region affected by the 1960 earthquake. Extreme values of the vertical movement range from 5.7 m of uplift in Guamblin Island to 2.7 m of subsidence in the city of Valdivia. The sea level data is augmented by a leveling line that runs from the city of Los Angeles to Puerto Montt (north–south orientation) which was surveyed prior to (1959) and after (1963-1964) the 1960 event.

We are currently analyzing this deformation field in terms of variable slip models. Since the surface trace of the fault cannot be recognized on the surface, we suppose that the trench corresponds to the intersection of the fault plane with the Earth's surface. This assumption fixes the strike of the dislocation plane to N7°E (Figure 4).

Preliminary results of the variable slip model for a pure dip–slip event (Figure 5) indicate that most of the moment release was concentrated in a 800 km long narrow band parallel to the coast. The region of maximum slip (> 15 m) varies in width from 100 km in the north to 50 km in the southern extreme. The down–dip region of slip (> 5 m) between 42° and 44° is responsible for the observed inland uplift at those latitudes. At the northern end of the rupture (36° – 38°) there appears to be an independent patch of slip not connected to the main region of moment release.

REPORTS

Barrientos, S. E., R. S. Stein, and S. N. Ward, Comparison of the 1959 Hebgen Lake, Montana, and the 1983 Borah Peak, Idaho, earthquakes from geodetic observations. *Bull. Seis. Soc. Am.*, in press, 1987.

Barrientos, S. E., Slip distribution of the 1985 Central Chile earthquake, submitted to *Tectonophysics*.

Barrientos, S. E., Seismic sources from geodetic observations, Ph. D. dissertation, 105 pp., University of California, Santa Cruz, 1987.

Barrientos, S. E., R. S. Stein, and S. N. Ward, A comparison of the 1959 Hebgen Lake, Montana, and the 1983 Borah Peak, Idaho, earthquakes from geodetic observations, *EOS, 67*, 904, 1986.

Barrientos, S. E. and S. N. Ward, Slip distribution of the 1985 Central Chile earthquake from geodetic observations, *Seismological Research Letters, 58*, 1987.

Ward, S. N. and S. E. Barrientos, Slip distribution and fault shape from geodetic observations of the 1983, Borah Peak, Idaho, and the 1985, Central Chile earthquakes. *XIX International Union of Geodesy and Geophysics*, 1987.

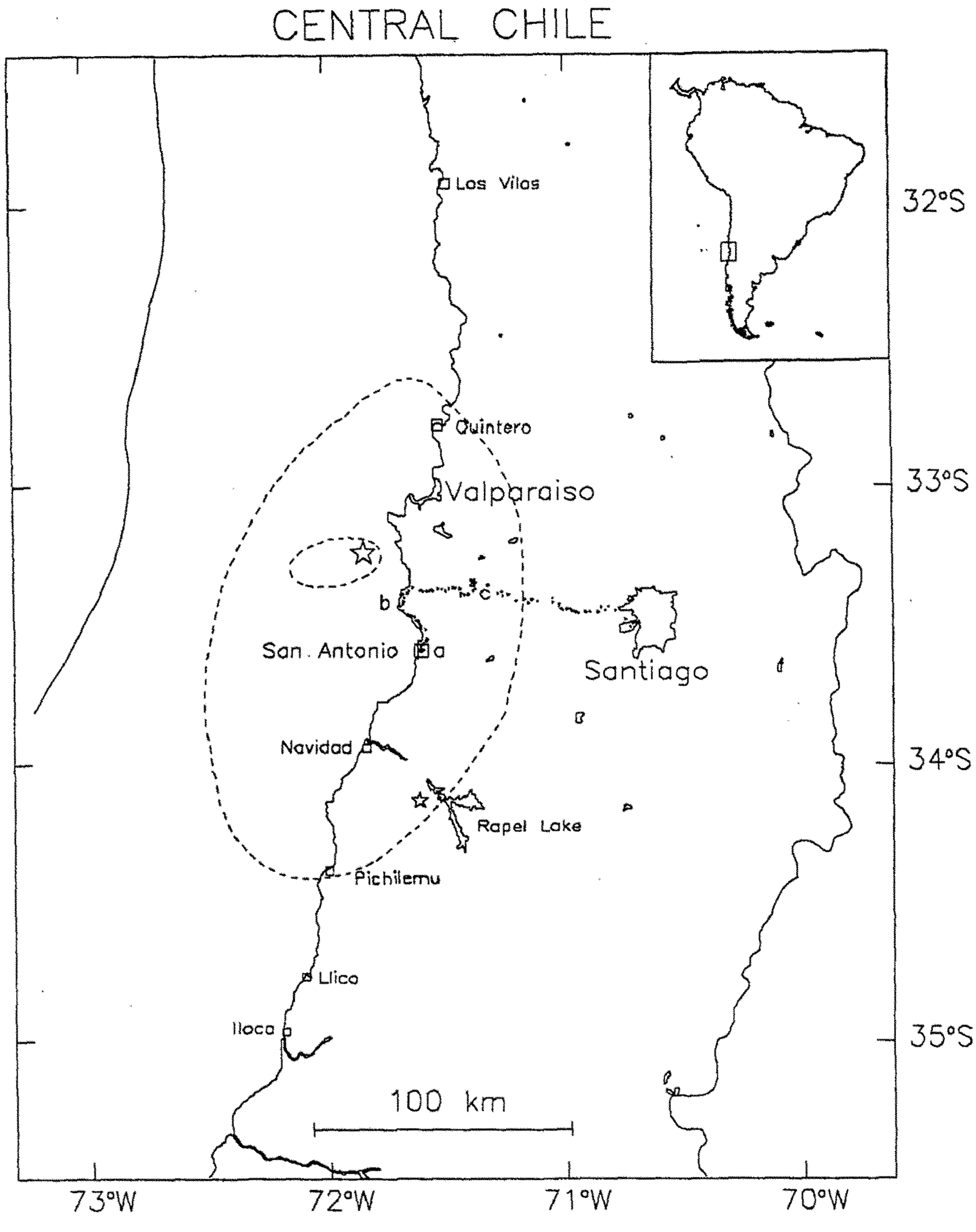

Fig. 1. Map view of Central Chile, site of the 1985 earthquake. The epicenter is the large star, the smaller star is the largest aftershock of the sequence. Foreshock and aftershock regions are the small and large dashed ellipses respectively. The leveling line, represented by small triangles, runs from San Antonio to Santiago.

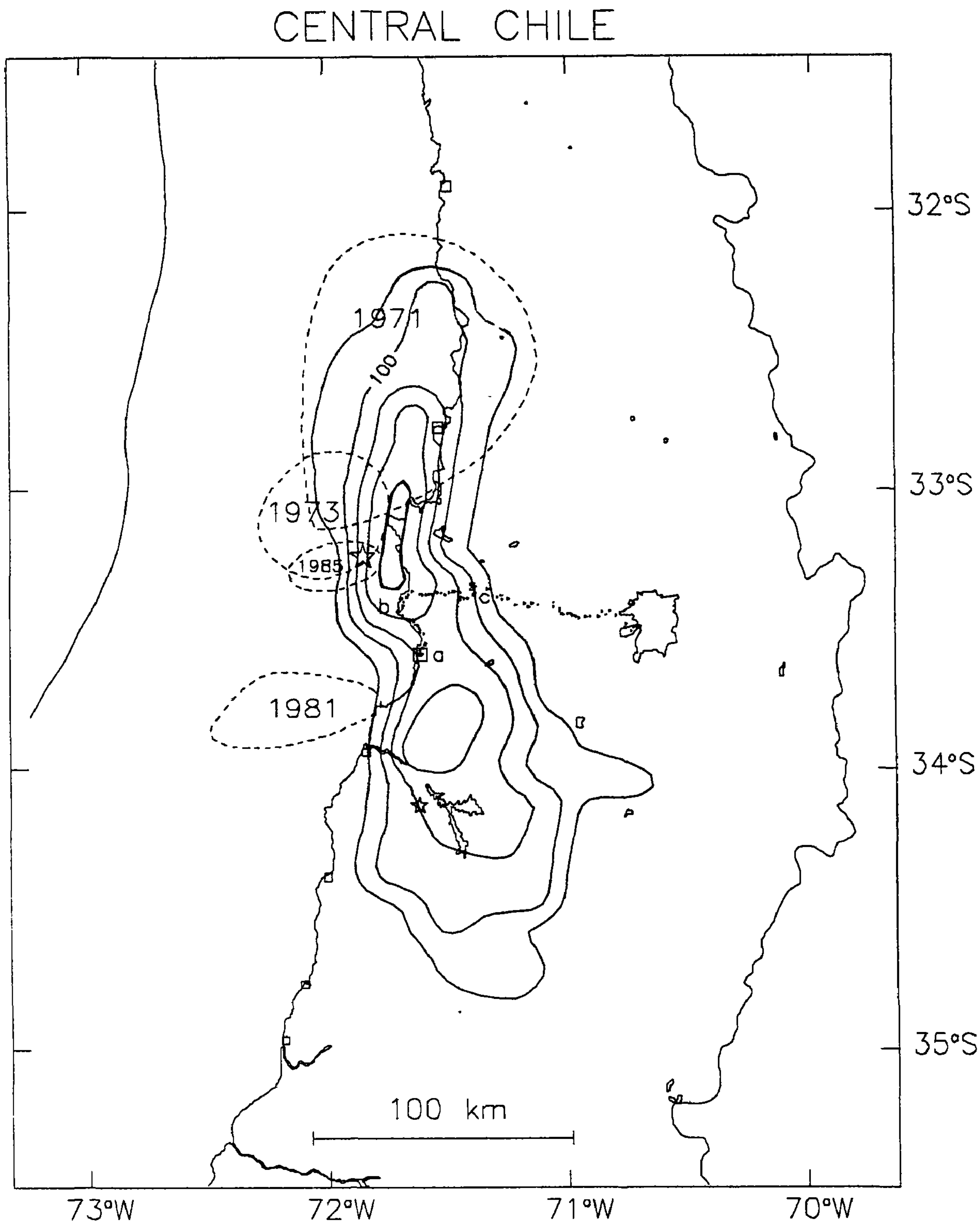

Fig. 2. Contour map of fault slip at 50-cm intervals projected on the Earth's surface superimposed on the aftershock regions of the 1971, 1973, and 1981 earthquakes from *Korrat* and *Madariaga* [1986]. Also the mainshock (large star) and its foreshock region are plotted. Note the correlation of the aftershock areas of the 1973 and 1981 events (plus the 1985 foreshock ellipse) with the regions of maximum slip.

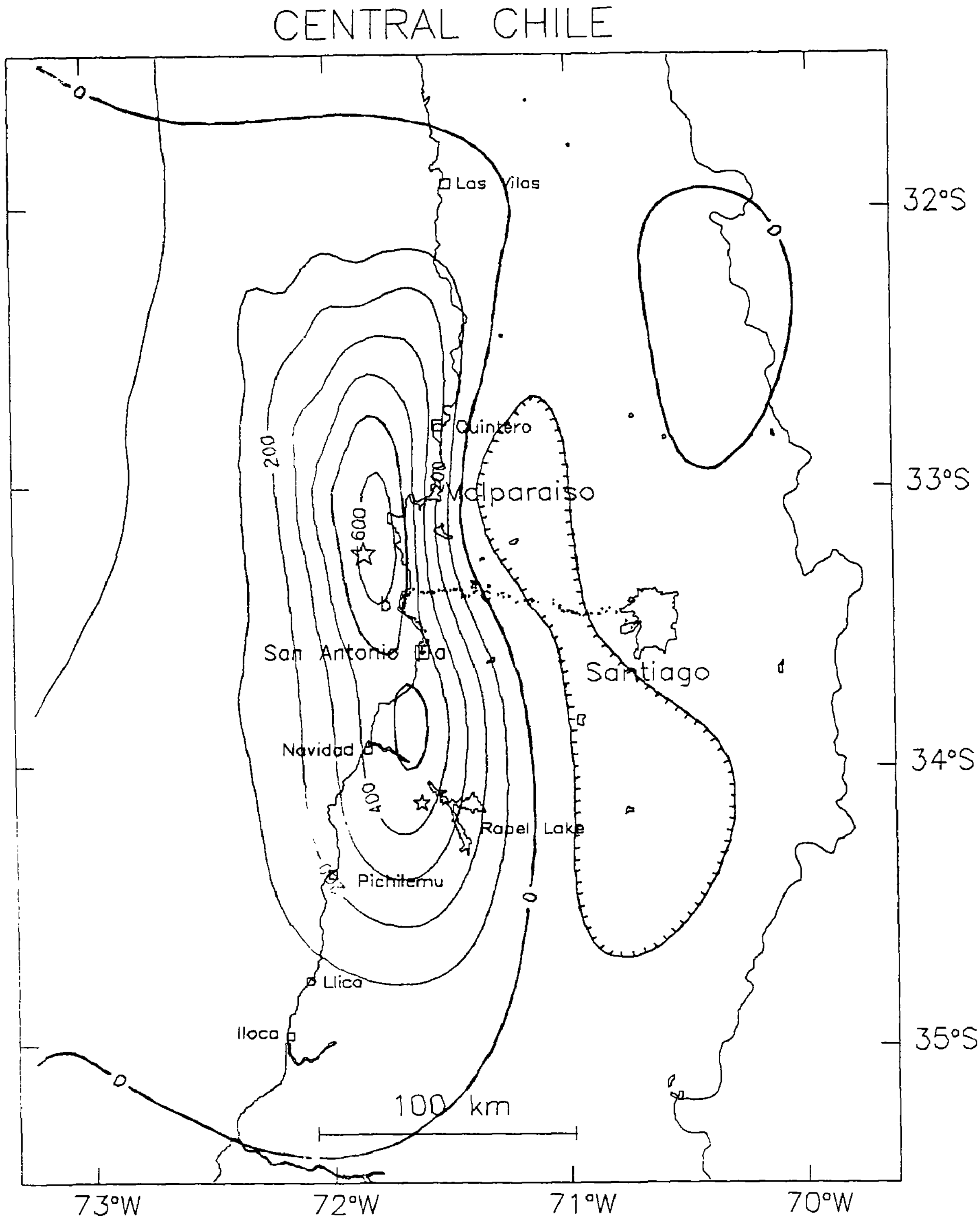

Fig. 3. Contour map at 100 mm interval of the coseismic vertical deformation. The model predicts a general uplift of the coast with maximum values close to Valparaíso and Navidad. An independent estimation of tilt (200 mm over 25 km) between the westernmost and easternmost shores of Rapel Lake agrees with the predicted tilt.

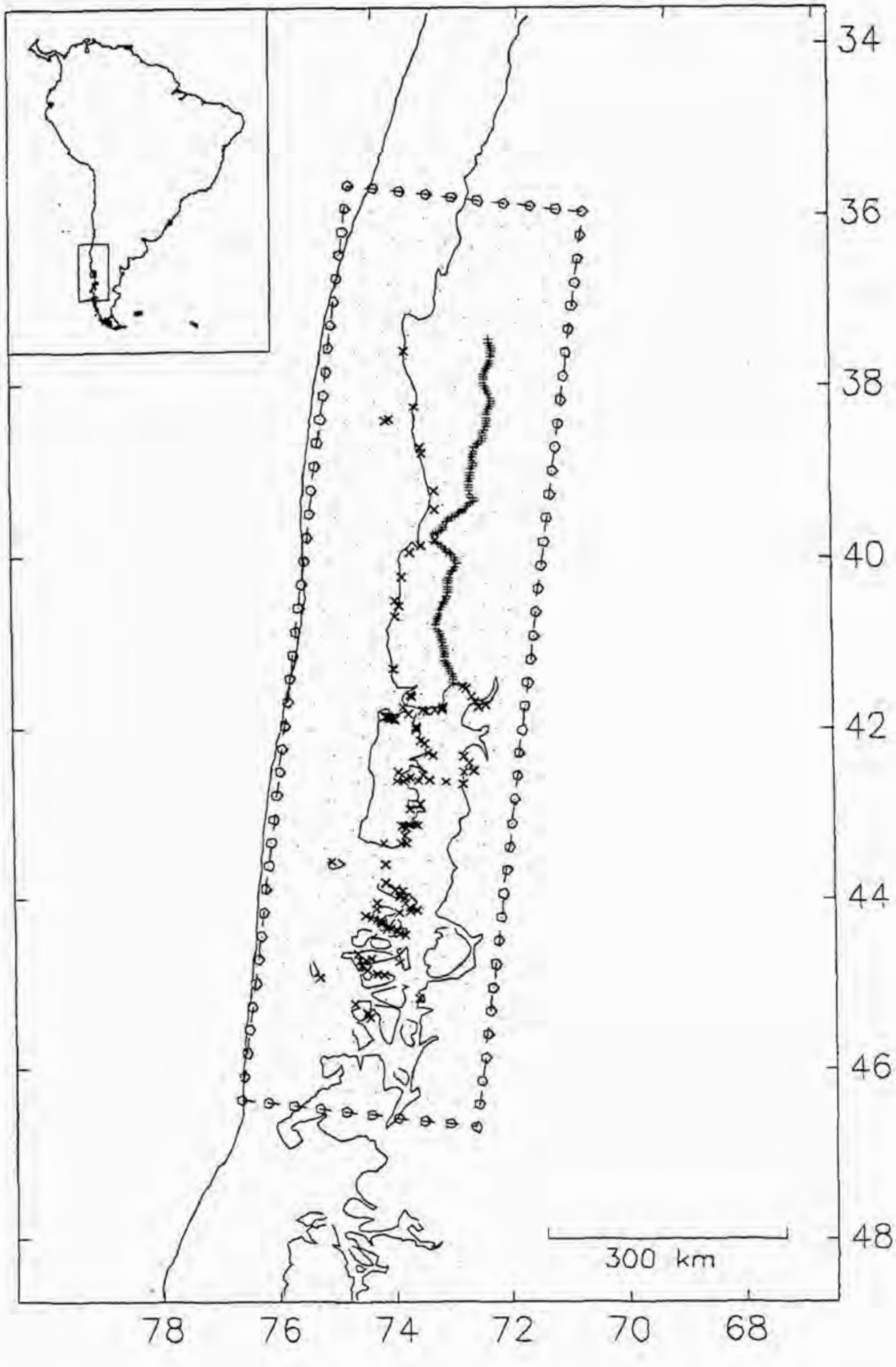

Fig. 4. Map view of South–Central Chile, site of the 1960 earthquake. Vertical crosses represent the leveling line which runs from Los Angeles in the North to Puerto Montt in the South. The inclined crosses represent locations where sea level changes were measured along the coast. The circles and dots represent the surface projection of the dislocation surface.

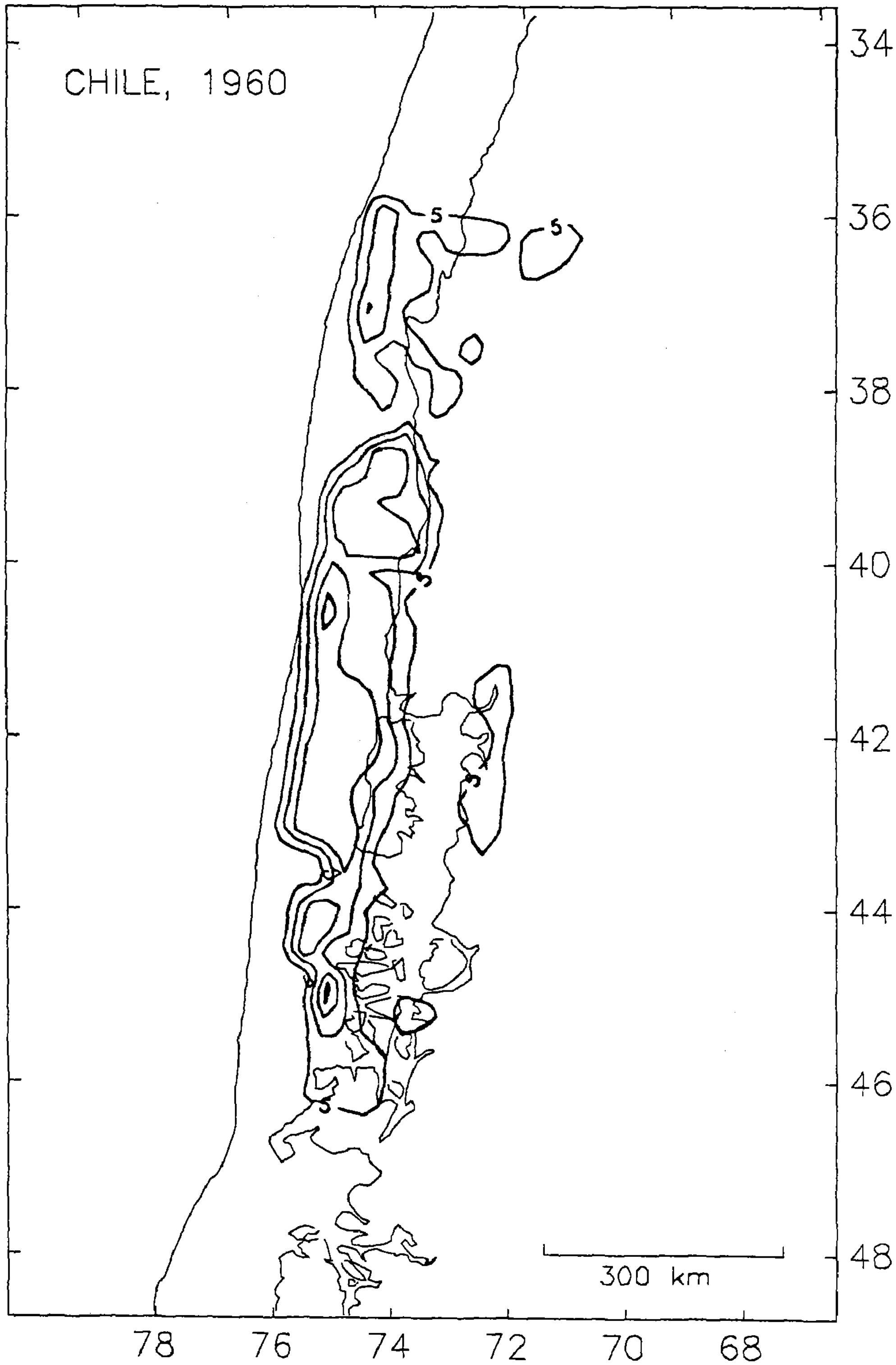

Fig. 5. Contour map of the fault slip at 5-m interval projected on the Earth's surface.

Deep Hole Desalinization of the Dolores River

9920-03464

William Spence
National Earthquake Information Center
U.S. Geological Survey
Denver Federal Center
Box 25046, Mail Stop 967
Denver, Colorado 80225
(303) 236-1506

Investigations

This project relates to monitoring the seismicity of the region of the intersection of the Delores River and Paradox Valley, southwest Colorado. The project is a component of the Paradox Valley Unit of the Colorado River Basin Salinity Control Project and is being performed for the U.S. Bureau of Reclamation with support from the Induced Seismicity Program of the U.S. Geological Survey. In this desalinization project, it is proposed to pump approximately 30,000 barrels/day from brine-saturated rocks beneath the Dolores River through a borehole to the Madison-Leadville limestone formation of Mississippian age, some 15,000 feet below the surface. There is a possibility of seismicity being induced by this desalinization procedure, especially in the long term. The project objectives are to establish a pre-pumping seismicity baseline and, during the pumping phase, to closely monitor the discharge zone for possible induced seismicity. If induced seismicity does occur, it should be possible to relate it to formation characteristics and to the pumping pressure and discharge rates.

Results

A 10-station seismograph network is centered at the location of the proposed injection well. This high-gain network has a diameter of about 80 kilometers, and has been in operation since September 1983. Seismic data are brought to Golden, Colorado, via microwave and phone line transmission. These data are fed through an A/D converter and then through an event detection algorithm. The network has operated at high quality, except for two periods when it was decommissioned by lighting strikes. Analysis procedures have been considerably complicated by a high rate of blasting activity in the region, but means have been developed to distinguish the occurrence of natural earthquakes to good reliability.

Notable regional earthquake activity are a swarm of shallow events (maximum magnitude 3.2) near Carbondale, Colorado, a similar swarm near Crested Butte, Colorado, a magnitude 3.4 shallow earthquake near Blue Mesa Reservoir, Colorado, and a magnitude 2.8 earthquake that was preceded by three events and followed by four events all located about 25 km SE of Grand Junction, Colorado. In the vicinity of the network, the earthquake catalog is complete to about magnitude 2.0, but very few earthquakes have occurred in the immediate vicinity of the proposed injection well. Most of the seismicity in the area of the network is in the shallow crust. However about 25 earthquakes have focal depths greater than 20 km, with several events at the depth intervals 30-35 km and 50-55 km. These results indicate that microearthquakes are distributed throughout the crust of the Colorado Plateau, with an occasional event in the upper mantle. The shallow and deeper earthquakes follow a diffuse north-south trend, parallel to the eastern boundary of the Colorado Plateau. These early results, combined with a lack of historical seismicity at the zone of the Paradox Valley seismic network, indicate that any seismicity induced by deep-well injection near Paradox Valley should be identifiable as such.

Report

Spence, W., and Chang, P-S., 1986, Seismic monitoring in the region of the Paradox Valley, Colorado--Annual Report, July 1985-June 1986: U.S. Bureau of Reclamation, Deep Well Injection Site, Paradox Valley Unit, Colorado River Basin Salinity Control Project, 11 p.

Regional and National Seismic Hazard and Risk Assessment

9950-01207

S. T. Algermissen
Branch of Engineering Geology and Tectonics
U.S. Geological Survey
Denver Federal Center, MS 966
Denver, CO 80225
(303) 236-1611

Investigations

1. Historical reports of damage in Salt Lake City, Utah, from earthquakes were researched and analyzed to assess Modified Mercalli intensity levels historically experienced throughout the city. For sites that experienced damage, the type of damage, type of building, and characteristics and depth of surficial geologic materials were determined to examine the possible contribution of site-response to the sites sustaining damage.

2. Regional attenuation of Modified Mercalli intensity with distance is being investigated for historical earthquakes of Utah, particularly the 1934 Hansel Valley earthquake for which there is the most data.

3. Modified Mercalli intensity values are being assessed on a very refined scale (to a city block) and plotted for the cities of Seattle and Olympia, Washington, for the April 29, 1965, and April 13, 1949, Puget Sound earthquakes.

4. Effects of observational errors in relating various magnitude scales and in fitting the Gutenberg-Richter parameter, β, were investigated and the results summarized in a paper that is in press in the Bulletin of the Seismological Society of America.

5. Liquefaction characteristics and data from the 1886 Charleston, South Carolina, earthquake and the 1811-12 New Madrid, Missouri, earthquakes are being investigated in order to develop a mapping capability of the Liquefaction Severity Index appropriate for the eastern United States. A paper that illustrates the application of the Liquefaction Severity Index to hazard mapping in southern California is in press in the Journal of Geotechnical Engineering.

6. Investigation of the consequences of alternative seismic source zones configurations on probabilistic ground motion hazard estimates along the eastern seaboard has been completed and a paper submitted to Earthquake Spectra, Journal of the Earthquake Engineering Research Institute.

7. Review and updating of seismic source zones used in production of the 1982 national probabilistic ground motion hazard maps was initiated for several parts of the country.

8. Strong motion records from the March 3, 1985 (M_s=7.8) central Chile earthquake and ensuing aftershocks have been processed using AGRAM, a series of computer programs for processing digitized, strong-motion accelerograms.

Results

1. Results of investigations regarding Modified Mercalli intensity levels historically sustained in Salt Lake City, Utah, showed that intensity increases from east-to-west across the city by 2-3 intensity units and north-to-south throughout the city by 1-1.5 intensity units. There is a good correspondence between the distribution of higher Modified Mercalli intensity and increases in measured instrumental site-response for the area.

2. Statistical tests are currently underway to determine if the regional attenuation of Modified Mercalli intensity in northern Utah is significantly different from intensity attenuation in California. Analyses of recorded strong ground motions suggests that northern Utah has lower attenuation than western California. Whether or not this distinction is discernible in the intensity data is not yet established however.

3. Detailed assessment of the Modified Mercalli intensity in the cities of Seattle and Olympia, Washington, will allow assessment of the correlation between observed earthquake damage and measured, instrumental site-response from field studies in the near future. The relation between ground failure effects from the 1965 and 1949 earthquakes and intensity level has been studied and summarized in a paper currently under review.

The Modified Mercalli intensity scale (MMI) places ground-failure phenomena at the highest levels of the scale. However, ground failures, such as liquefaction, have occurred during earthquakes generating intensities one to two units below those levels. Excellent, detailed examples of this type of phenomenon were found in unpublished intensity surveys for the two largest historical Puget Sound earthquakes, April 13, 1949, and April 29, 1965. Both of these important earthquakes had maximum Modified Mercalli intensities of VIII, even though the earlier shock had a larger magnitude (1949 had magnitude 7.1 and 1965 had magnitude 6.5 (m_b)).

Extensive data are available from past intensity surveys that were conducted by the University of Washington immediately after the above earthquake, and from several other primary sources. The total ground failure data base consists of some 314 reports, including 29 liquefaction, 46 slumping, 28 landslides and 211 settling reports. Liquefaction was found from 30 to 120 km from the 1949 epicenter and from 1 to 30 km from the 1965 epicenter. It occurred at intensity levels as low as VII (predicted at VIII). Slumping occurred from 10 to 125 km away from the 1949 epicenter and 5 to 125 km from the 1965 epicenter, while settling occurred at almost all distances for both earthquakes. Landslides occurred from 25 to 185 km in 1949, and 20 to 100 km in 1965. The lowest intensities producing slumping, settling and landslides were VI, V, and VI, respectively (predicted at VII or higher).

4. In order to use historic earthquakes to estimate future seismicity of a region, the analyst usually first converts earthquake sizes that have been recorded in various ways (e.g., m_b, M_S, M_L, I_o) to a common scale (e.g., m_b), by fitting the coefficients a_i and b_i in an assumed linear relationship $m_b=a_i+b_im_i$ between m_b and each of the other size measures m_i. He then combines m_b values (either recorded m_b or fitted $\hat{m}_b$) for all earthquakes to estimate a Gutenberg-Richter rate parameter a_{mb} and distribution parameter β_{mb}. However, even if magnitude scales are linearly related over some range, when observational errors are present and earthquakes have been incompletely recorded at lower magnitudes or terminate abruptly at some finite m_{max}, estimates $\hat{a}_i$, $\hat{b}_i$ may be highly biased and uncertain. Less biased estimates of $\hat{b}_i$ can be obtained if only magnitude values in the interior of the range are used in the fitting. Errors in $\hat{b}_i$ carry over into estimates $\hat{\beta}_{mb}(i)$ obtained using magnitudes converted to $\hat{m}_i$ from m_i. This means that even if a large number N of m_i values are converted to $\hat{m}_b$ values, the variance of $\hat{\beta}_{mb}(i)$ using these magnitudes may depend primarily on the sizes of the observational errors and on the number of n of pairs (m_b,m_i) used to fit $\hat{b}_i$, rather than on N. An estimate $\hat{\beta}_{mb}(i)$ may be obtained without converting magnitudes m_i to m_b by estimating $\hat{\beta}_i$ (the distribution parameter for m_i) using the N m_i values and then setting $\hat{\beta}_{mb}(i)=\hat{\beta}_i$. Individual estimates $1/\beta_{mb}(i)$ for various scales m_i, may be weighted and combined, and then inverted to obtain an estimate of β_{mb} that has a lower variance than does the estimate obtained using all the earthquakes simultaneously. This study particularly considers estimates involving I_o, epicentral intensity, because often I_o is the only size recorded for an earthquake. A relatively large range of magnitudes corresponds to a single intensity, making the analysis more complicated for this case.

5. Coefficient values for an eastern United States attenuation function for Liquefaction Severity Index depend critically on the moment magnitudes assumed for the Charleston and New Madrid earthquakes. When the difference in the two assumed magnitudes is about one unit, the distance coefficient closely matches the values derived from attenuation of Modified Mercalli intensity in the East.

6. Six configurations of regional seismic source zones were used to estimate the ground motion hazard (annual exceedance probability of 1 in 500) along the

eastern seaboard of the United States. The source zones range from being strongly influenced by the regional spatial distribution of earthquakes in the historic record to complete independence of historic seismicity, that is, source zones based solely upon tectonic provinces and basement structure as well as geodetic vertical movement data and geomorphological considerations. Maintaining the same maximum magnitude among all zones and for all source zone models, the results indicate (1) a factor of 3 difference among source zone models for calculated acceleration levels in eastern Massachusetts and coastal Maine; (2) a factor of 2 difference for much of New Jersey, Delaware, and extreme eastern Maryland as well as a broad area of the southeastern seaboard including the Charleston, South Carolina, region; (3) a factor of about 1.4 for much of the interior Appalachian region extending from New Brunswick to the Gulf Coast. Results show that certain source zone models result in considerably lower ground-motion hazard otherwise implied by accepting historical seismicity as a guide to future hazard. Significantly, the highest hazard variability at probability levels of 1 in 500 due to uncertain earthquake causal structures or processes occurs in the highly populated northeast region and not, as often assumed, in the Charleston, South Carolina, area.

7. Insights gained from (7) above, will aid in revising seismic source zones for the eastern United States to estimate regional probabilistic ground motion hazard. Particular attention is needed in defining source zones for areas of the northeastern United States because of particularly high hazard variability resulting from alternate interpretations of source zones. As in previous maps, however, the regional distribution of historical seismicity will play a dominant role in source zone delineation.

8. The usefulness of the AGRAM programs has been enhanced by the application of an innovative technique of more precisely filtering strong-motion data, resulting in more accurate site-specific response spectra for each record. This technique is being used for the first time, on this set of data, and should considerably, improve the usefulness of the products of the AGRAM programs (acceleration, velocity and displacement time histories of each instrument component accelerogram, Fourier spectra, and response spectra).

Reports

Bender, B.K., 1987, Effects of observational errors in relating magnitude scales and fitting the Gutenberg-Richter parameter β: Seismological Society of America Bulletin (in press), 30 ms. p.

Oaks, S.D., 1987, Understanding social realities for effective implementation of earthquake hazard reduction strategies and post-earthquake response and recovery planning [abs.]: Seismological Research Letters, v. 58, no. 1, p. 13.

Oaks, S.D., and Algermissen, S.T., 1986, Site response in the Salt Lake City, Utah, area from intensity data from historic earthquakes [abs.]: Earthquake Notes, v. 57, no. 1, p. 14.

Oaks, S.D., and Algermissen, S.T., in press, Site response in the Salt Lake City urban area determined from historical earthquakes: U.S. Geological Survey Professional Paper chapter.

Oaks, S.D., and Bollinger, G.A., 1986, The epicenter of the December 22, 1875 central Virginia earthquake: New findings from documentary sources: Earthquake Notes, v. 57, no. 3, p. 65-76.

Thenhaus, P.C., Perkins, D.M., Algermissen, S.T., and Hanson, S.L., 1987, Earthquake hazard in the eastern United States: Consequences of alternative seismic source zones: Earthquake Spectra, Earthquake Engineering Research Institute Journal (submitted), 46 ms. p.

Youd, L.T., and Perkins, D.M., 1987, Mapping of Liquefaction Severity Index: Geotechnical Engineering Journal, American Society of Civil Engineers, (in press), 26 ms. p.

Regional and Local Hazards Mapping in the Eastern Great Basin

9950-01738

R. Ernest Anderson
Branch of Geologic Risk Assessment
U.S. Geological Survey
Box 25046, MS 966, Denver Federal Center
Denver, CO 80225
(303) 236-1684

Investigations

1. Summary of tectonic evolution of the intermontane region, including the Colorado Plateau, Basin and Range, and High Lava Plains.

2. Newly acquired fault-slip data from the northwest margin of the Sevier Plateau, Utah, were integrated with existing data and analyzed for paleostress characteristics.

Results

1. Prepared an introductory chapter on the tectonic evolution of the intermontane system for inclusion in a GSA special paper on the geophysical framework of the United States.

2. A total of 235 fault-slip measurements were made on moderately to steeply dipping faults in the upthrown and downthrown blocks along the approximately 4-km-long trace of the Annabella segment of the Sevier fault in the central Sevier Valley area of Utah. Fault strikes are varied and dip directions are skewed toward the uplifted plateau block. Oblique slip is common. The histogram of rake distributions shows a clearly defined minimum at 30°. dip-slip and oblique-slip faults predominate over strike-slip faults.

   The main fault of the Annabella segment was not observed, and therefore, its true attitude is not known. Many measurements were taken from faulted rocks within a few meters of the main fault. The data suggest that the main fault is a sharp break and that normal faults associated with it drop strata down toward the uplifted plateau block. The data show that most of the dip-slip faults in this area are not part of a range-front fault system and may not contribute significantly to plateau uplift.

   Strike-slip faults show an unusually wide range of attitudes (especially dip values). Despite the attitude variability, slip lines show a strong preference for dispersion around a north-south azimuth, but sinistral and dextral faults are not concentrated in separate strike sectors, suggesting that they are not conjugate shears resulting from subhorizontal maximum compressive stress. Therefore, quantitative attempts to resolve paleostress characteristics using strike-slip faults should not be made.

We computed a paleostress orientation from the dip-slip faults with rakes greater than 60° (N=90). It shows σ_3 at 282°, but the value of ϕ is low (0.03). This low value suggests that moderately to steeply dipping faults of any strike are appropriately oriented for dip-slip movement. The dip-slip faulting may be analogous to the strike-slip faulting and may not represent a response to applied remote stresses. Alternatively, a complex and unresolvable history of polyphase deformation could be recorded by the striae we measured.

Reports

None.

Seismic Hazards of the Hilo 7 1/2' Quadrangle, Hawaii

9950-02430

Jane M. Buchanan-Banks
Branch of Geologic Risk Assessment
U.S. Geological Survey
David A. Johnston Cascades Volcano Observatory
5400 MacArthur Boulevard
Vancouver, Washington 98661
(206) 696-7575 FTS 422-7575

Investigations

Preparation of the geologic map and text of the Hilo 7 1/2' quadrangle is nearing completion, and writing of two research papers continues.

Results

Examination of thin sections of all flows within the quadrangle is nearly complete, and the detailed rock descriptions have been incorporated into the map text. A poster on the volcanic hazards of the Hilo quadrangle was prepared and presented at Hawaii Symposium on How Volcanoes Work in Hilo.

While in Hawaii, took the opportunity to field check areas where problematic geologic relationships exist, and collected rock samples for chemical analysis to help resolve the problems. Accompanied Duane Champion, USGS, Menlo Park, to sites chosen for paleomagnetic drilling to complete sample collection from all recognized flows younger than 2,000 years in order to determine the history of secular variation. These data will be incorporated into the map text as they become available.

Reports

Buchanan-Banks, J.M., 1987, Volcanic hazards within the Hilo 7 1/2' quadrangle, Island of Hawaii [abs.]: Hawaii Symposium on How Volcanoes Work Abstract Volume, p. 27.

Buchanan-Banks, J.M., 1987, Structural damage and ground failures from the November 16, 1983, Kaoiki Earthquake, Island of Hawaii, in Decker, R.W., Wright, T.L., and Stauffer, P.H., ed., Volcanism in Hawaii: U.S. Geological Survey Professional Paper 1350, v. 2, p. 1187-1220.

Depth to Bedrock map in the greater Tacoma area, Washington

9950-04073

Jane M. Buchanan-Banks
Branch of Geologic Risk Assessment
U. S. Geological Survey
David A. Johnston Cascades Volcano Observatory
5400 MacArthur Boulevard
Vancouver, Washington 98661
(206) 696-7575 FTS 422-7575

Investigations

Research progresses on determining the thickness and areal extent of unconsolidated sediments, which could produce strong seismic-related ground shaking and slope failures in the greater Tacoma area. Special attention is being given to subsuface geologic units that might amplify ground motion.

Results

Preliminary maps showing the locations of all known water and oil wells with a minimum depth of 60 m have been compiled for the Tacoma and Centralia 30′ by 60′ quadrangles. Deep water wells near the city of Tacoma have been drilled to 680 m without encountering bedrock. Exploratory oil wells, some as much as 1490 m deep, have been drilled mainly in the eastern part of the map area. One oil well drilled northwest of Tacoma reached bedrock at 210 m.

Pleistocene unconsolidated sediments within the Tacoma 30′ by 60′ qaudrangle comprise glacial deposits mainly from the Puget lobe of the Fraser glaciation, but also from glaciers on Mount Rainier to the east and from the Olympic Mountains to the west. Locally, these deposits are underlain by unconsolidated deposits of Tertiary age. Along the northeast edge and southeast corner of the quadrangle, bedrock lies at or near the surface.

GEOLOGY AND TECTONIC EVOLUTION OF THE WESTERN TRANSVERSE RANGES, CALIFORNIA

9950-04063 (Part-time project: 1/4 in FY 1986)

Russell H. Campbell
Branch of Geologic Risk Assessment
U.S. Geological Survey
MS 922, National Center
Reston, Virginia 22092
(703) 648-6784

Investigations

1. Preparation for publication of 1:24,000-scale geologic maps and reports from previous work in the western Santa Monica Mts., California, which was recessed during a sequence of administrative assignments.

2. Compilation of recent geologic mapping in the western Transverse Ranges at 1:100,000 scale, in support of preparation of tectonic maps and overview of geologic history of the region.

Results

1. Preparation of the geologic map and explanation for the Point Dume, 1:24:000 quadrangle for publication as an I-map is complete. It has been reviewed and is with the author for revision.

   Location coordinates (latitude and longitude) for nearly 600 fossil collections in the western Santa Monica have been digitized. A database is being prepared combining the digitized locations with the faunal lists, with the objective of developing a capability to plot selected elements, using the GSMAP program.

2. Stable base map materials at 1:100,000-scale have been acquired for the Los Angeles 1° x 30' quadrangle, for use in compilation of a new geologic map of the area.

   A digital sytem for geologic map compilation and drafting, including hardware and software, has been assembled and tested. The system consists of a PC-driven digitizing pad and 8-pen plotter, configured to use the GSMAP-GSDRAW programs and related software developed by Selner and others (1986). The system will provide the principal tool for the 1:100,000-scale map compilation and drafting.

Reference

Selner, G. I., Taylor, R. B., and Johnson, R. I., 1986, GSDRAW and GSMAP version 3.0: Prototype programs for the IBM PC or compatible microcomputers to assist compilation and publication of geologic maps and illustrations: U.S. Geological Survey Open-File Report 86-447A, 145 p.; and U.S. Geological Survey Open-File Report 86-447B, 3 program disks

Engineering Behavior Study of Sites Affected By Past Seismic Activity in the Charleston, S.C. Area

9900-88807

G.W. Clough
Department of Civil Engineering
Virginia Polytechnic Institute and State University
Blacksburg, Virginia 24061
(703) 961-6637

Investigations

Recent investigations by geologists and geophysicists in the vicinity of Charleston, S.C. have led to new information regarding the seismic history of the area. This work has derived largely from the study of exposures of artifact liquefaction features. These exposures are in many cases found in drainage ditches that are excavated by farmers and developers to lower the ground water table. Through the use of dating of organic materials found in the features, it has been established that the Charleston area has been subjected to a series of major earthquakes, all but one of which predate the recorded history of this location.

The new discoveries are allowing a picture of the seismic recurrence intervals to be developed for the South Carolina Coastal region. Also, it appears that based on the magnitude and nature of the liquefaction features, some information can be derived in regard to the location of the different earthquake epicenters. In addition, the large scope of the exposures has allowed an unusual insight into the nature of the response of soil to liquefaction events.

To date, much effort in the investigations has been expended in the process of simply locating many of the liquefaction features, and mapping the sites and dating of the soils involved. Because of the scope of the work thus far, little time has been allotted to detailed engineering type testing. Work of this nature can usefully supplement that done so far, providing quantitive information which can be used to allow for:

1.) A capability to compare the behavior of the soils to those elsewhere in the US and the world. This will allow one to determine if the soils involved in the Charleston sites are more or less susceptible to liquefaction than elsewhere.

2.) The possibility of quantifying acceleration levels that could have led to the liquefaction events. Such information, if developed systematically and at enough sites can assist in the definition of the seismic regime.

3.) Determination of the lateral extent of the soil conditions that presumably led to the liquefaction features.

4.) Sorting out of the meaning of the range of unusual liquefaction features identified at the field sites.

5.) Definition of the reasons why the liquefaction features are located in certain areas and not others.

For these and other reasons, it was proposed to the USGS to undertake an engineering oriented study of the liquefaction sites in the Charleston area.

Results

The engineering study is intended to consist of field work, laboratory testing, and analytical studies. The investigation was authorized in March of 1987, and, as a result, is only now getting underway. The field work is planned to involve a series of the liquefaction sites. The studies will include drilling, sampling, and standard and cone penetration testing. Sampling will be done both during the conventional drilling process and by undisturbed block sampling in the bottom and walls of the drainage trenches. Sites will be chosen so as to represent situations where liquefaction occurred and did not occur. At sites where liquefaction is not obvious, it will be presumed that the accelerations from the earthquake were too low to cause liquefaction. These sites will be particularly valuable since they can be used to help refine the knowledge of the earthquake epicenters.

During the course of the field work, samples of soils below the liquefaction areas will also be obtained. In Charleston and vicinity, these materials consist mainly of marls. These samples are important to the process of soil profile definition, and the site response analyses.

The laboratory testing will be mainly concerned with the sandy soils of the upper soil layers. In the liquefaction areas, these soils have been identified as the materials which served as the source for the liquefaction phenonmena. The marls also will need to be tested to determine properties for the site response studies. All of the soils will be subjected to classification testing and basic strength and deformation testing. In addition, the sands will be loaded in cyclic undrained triaxial tests, to ascertain their resistance to liquefaction. The marls will be also be loaded in a similar fashion to ascertain their dynamic response.

With the soil parameters and results of the field studies in hand, analytical work can begin. This effort will attempt to back-calculate the accelerations which occurred at each site in order to have caused the phenomena observed at the site (i.e., liquefaction or non-liquefaction). After enough of these analyses are performed, the information on likely accelerations will be coordinated with USGS scientists and others to help refine ideas about the seismic regime in the area.

Earthquake Hazard Investigations in the Pacific Northwest

14-08-0001-G1390

R.S. Crosson
Geophysics Program
University of Washington
Seattle, WA 98195
(202) 543-8020

Investigations

The objectives of this research are to provide fundamental data and interpretations for earthquake hazard investigations. Currently, we are focusing on seismicity, structure, and tectonic questions related to the possibility of a major subduction earthquake on the Juan de Fuca - North American plate boundary. Specific tasks which we have worked on in this contract period are:

1. Tomographic inversion of travel times to determine three-dimensional earth structure.

2. Locations, focal mechanisms and occurrence characteristics of crustal and subcrustal earthquakes beneath western Washington and their relationship to subduction processes.

3. Investigation of offshore earthquakes.

4. Creating an improved catalog of Northwest earthquake locations, magnitudes and dates.

Results

1. A study of crustal velocity in western Washington is being done using tomographic techniques. The study area is divided into a grid of blocks, and travel times from the U. W. network data base are compared to travel-times computed from a starting velocity model. Pseudo three-dimensional inversion is carried out using 2-D methods in horizontal layers. Programs are now being developed for full three-dimensional inversion of a large volume of the earth's crust.

2. Focal mechanisms have been determined for about 275 earthquakes in western Washington. We are implementing FPFIT, a program written by P. Reasenberg and D. Oppenheimer of the USGS (OF-85-739) which automatically determines focal mechanisms given polarity information. This program also provides an estimate of mechanism quality. The objective of this study is to determine the most probable regional tectonic stress in western Washington. Examination of 121 focal mechanisms in the Puget Sound area indicates that systematic differences exist between shallow and deep earthquakes in the Puget Sound region; many more normal mechanisms occur in the deep suite than in the shallow; while thrust events are more common in the shallow suite. The shallow and deep suites also show significantly different distributions of P and T axes. P axes for shallow events are clustered around the North-South direction, while P axes for deep earthquakes scatter in a broad girdle roughly about the E-W equatorial plane. Results are being prepared for publication by Ma Li and others.

By combining high quality hypocenter locations with localized structure form broad band teleseismic P waveform inversion, we have constructed a preliminary structure model of the subducted Juan de Fuca slab beneath Washington. The slab is bent into an eastward plunging arch beneath Puget Sound in which the axis of the arch dips at about 10-12° whereas the "normal" slab dip on both sides of the arch appears to dip at 15-20°. This structure may help explain the localization of slab seismicity beneath Puget Sound and provide a basis for developing a consistent tectonic model for the region.

3. A study of offshore earthquakes occurring in the vicinity of the Juan de Fuca plate was undertaken to examine the possibility that internal deformation of the JDF plate may be in evidence. We found that many offshore earthquakes could be accurately located if both P_n and S_n phases were detected. Although we were able to locate events at least a half magnitude unit lower than the PDE catalog, out of over 135 earthquakes with good locations, only two could be possibly within the plate interior. The remainder were on the Blanco Fracture Zone or at the north end of the JDF plate. We conclude that there is little or no direct evidence of internal deformation of the JDF plate.

4. In cooperation with the USGS, we are preparing a revised catalog of earthquake times, locations, and magnitudes. A national map, and regional seismicity articles are being prepared for the multi-volume "Decade of North American Geology" to be published by the Geological Society of America. Our responsibility is for the catalog and article covering Washington and Oregon. The DNAG catalog for the Pacific Northwest is a compilation of data collected from many sources; we are reviewing the literature to select preferred locations. Previous catalogs for the Pacific Northwest are seriously flawed, and the DNAG catalog represents a significant improvement which allows us to place historical seismicity within the context of seismicity observed with the current network. Seismologists from both the USGS and the U.W. are contributing to both the catalog and an overview article covering seismicity in the Pacific Northwest.

Articles

Ludwin, R. S., S.D. Malone, R.S. Crosson, 1987 (in press), Washington Earthquakes 1983, National Earthquake Information Service.

Ludwin, R. S., S.D. Malone, R.S. Crosson, 1987 (in press), Washington Earthquakes 1984, National Earthquake Information Service.

Ludwin, R. S., S.D. Malone, R.S. Crosson, 1987 (in preparation), Washington Earthquakes 1985, National Earthquake Information Service.

Ludwin, R. S., L.L. Noson, A.I. Qamar, R.S. Crosson, C.S. Weaver, S.D. Malone, W.C. Grant, T.S. Yelin, J.E. Zollweg ,1987 (in preparation), Seismicity in the Pacific Northwest, in Decade of North American Geology, published by Geol. Soc. Am.

Crosson, R.S., 1986, Comment on 'Geodetic Strain Measurements in Washington' by J.C. Savage, M. Lisowski, and W.H. Prescott, JGR, V. 91, No. B7, pp. 7555-7557.

Reports:

Crosson, R. S., 1986, Seismological Setting of the Puget Sound Region, in USGS proceedings of Conference XXXIII, ed. W.W. Hays and P.L. Gori, U.S.G.S. OFR 86-253.

Qamar, Anthony, Anne Rathbun, Ruth Ludwin, Robert S. Crosson, and Stephen D. Malone, 1986, Earthquake Hypocenters in Washington and Northern Oregon - 1980; Washington State Department of Natural Resources, Division of Geology and Earth Resources, Information Circular 82

Qamar, Anthony, Ruth Ludwin, Robert S. Crosson, and Stephen D. Malone, 1987 (in press), Earthquake Hypocenters in Washington and Northern Oregon - 1981; Washington State Department of Natural Resources, Division of Geology and Earth Resources.

Earthquake Hypocenters in Washington and Northern Oregon; 1982-1986, 1987 (in preparation), University of Washington Geophysics Program

Univ. of Wash. Geophysics Program, 1986, Quarterly Network Report 86-C on Seismicity of Washington and Northern Oregon

Univ. of Wash. Geophysics Program, 1986, Quarterly Network Report 86-D on Seismicity of Washington and Northern Oregon

Earthquake Hazard Research in the Pacific Northwest, 1987, Contract 14-08-0001-G1080 Final Technical Report 1987.

Abstracts

Ludwin, R. S., L.L. Noson, A.I. Qamar, R.S. Crosson, C.S. Weaver, S.D. Malone, W.C. Grant, T.S. Yelin, 1986 Seismicity in the Northwestern U.S., EOS, V. 67, No. 44, p. 1084.

Crosson, R. S. and E.L. Crosson, 1986, Preliminary Analysis of Juan de Fuca Plate Seismicity using the Washington Regional Seismograph Network, EOS, V. 67, No. 44, p. 1084.

Ma, Li, and R.S. Ludwin, 1987, Can Focal Mechanisms be used to Separate Subduction Zone from Intra-plate Earthquakes in Washington?, EOS, V. 68, No. 3.

J. Lees, 1987, Tomographic Inversion for Lateral Velocity Variations in western Washington, EOS, V. 68, No. 3.

SITE-RESPONSE AND LIQUEFACTION STUDIES INVOLVING THE CENTRIFUGE

Grant No. 14-08-0001-G1192

C.B. Crouse, B. Hushmand, and G. Martin
Earth Technology Corporation
3777 Long Beach Blvd.
Long Beach, CA 90807
213-595-6611

Ronald F. Scott
California Institute of Technology
Pasadena, CA 91125
818-356-6811

Investigations

A new laminar box apparatus was constructed for use in the centrifuge at the California Institute of Technology. The box was filled with dry and saturated sand samples, which were subjected to earthquake-like excitations while the centrifuge was in flight. Lateral accelerations and displacements, pore-water pressures, and settlements were recorded as a function of time.

Two papers listed below describe the apparatus and test procedures in detail, and present some of the data and analyses.

Future Research

Future research will be devoted to analyzing the remaining data collected during the tests.

Papers Prepared Under this Grant

Hushmand, B., Crouse, C.B., and R.F. Scott, "Centrifuge Liquefaction Tests in a Laminar Box," Geotechnique, submitted, December, 1986.

Hushmand, B., Crouse, C.B., Martin, G.R., and Scott, R.F., "Site Response and Liquefaction Studies Involving the Centrifuge," Proceedings, 3rd International Conference on Soil Dynamics and Earthquake Engineering, Princeton University, Princeton, New Jersey, June, 1987.

Investigations of Intraplate Seismic-Source Zones

9950-01504

W. H. Diment
Branch of Geologic Risk Assessment
U.S. Geological Survey
Box 25046, MS 966, Denver Federal Center
Denver, CO 80225
(303) 236-1574

Investigations

1. Reprocessing and interpretation of seismic-reflection data in upper Mississippi Embayment to investigate deep structure.

2. Quantitative geomorphic study of stream profiles in the southeastern part of the Ozark Mountains.

3. Interpretation of seismic-reflection data recorded on the Mississippi River.

4. Analysis of level line data in the upper Mississippi Embayment and environs.

5. Continued geologic and geophysical investigations of the Meers fault in Comanche County, Okla.

6. Planning and organizing USGS-sponsored workshop on "Directions in Paleoseismology" in Albuquerque, New Mexico, April 22-25, 1987.

7. Analysis of high-resolution reflection data obtained across the Meers fault.

8. Effects of earthquakes on high temperature wells in the Long Valley caldera, Mono County, Calif.

9. Analyses of seismological data from China.

10. Regional studies.

11. Analysis of stream profile data in an area of active faulting immediately west of Pierre, South Dakota, and in the vicinity of the superconducting supercollider site in eastern Colorado.

Results

1. The data from interpretation of seismic-reflection profiles for the seismic-reflection lines in the north part of the New Madrid seismic zone have been submitted to CTR for publication as an MF map. The final interpretation for seismic-reflection lines across the Reelfoot Rift has been completed and manuscript in being reviewed.

2. A draft report entitled "Analysis of stream-profile data for the eastern Ozark Mountains region and their geologic implications," by F. A. McKeown, M. J. Cecil, B. L. Askew, and M. B. McGrath, has been returned to BCTR after making editorial corrections. Publication as a USGS Bulletin has been requested.

3. The interpretation of part of the seismic-reflection data recorded on the Mississippi River has been completed. (Crone and others, 1986) First-cut processing of the data collected along the Mississippi is complete. Major reflectors are being correlated for the entire length of the survey.

4. Compilation and analysis of level line data for the upper Mississippi Embayment and vicinity was completed by Richard Dart and an open-file report is ready for technical review. Completion of this report has been delayed temporarily by other activities (Dart, 1985, 1986, and 1987; Zoback and others, 1985; Dart and Zoback, 1987).

5. Additional geologic field investigations of the Meers fault indicate a significant component of left-lateral slip on the fault in the Quaternary. Field mapping and the morphology of the fault scarp both reveal geologic relationships that are consistent with lateral slip although, at present, it is difficult to quantify the exact amount.

   Radiocarbon dates of organic-rich samples from channel deposits described in the previous summary of technical reports are still pending.

   Crone, Madole, and Luza (Oklahoma Geological Survey) were coleaders of the 1987 South-central cell Friends of the Pleistocene field trip to the Meers fault.

   Geophysical studies of the Meers fault include coordinating efforts with the Branch of Oil and Gas Resources (Denver) to reprocess and reinterpret the pertinent COCORP deep seismic-reflection data across the northern flank of the Wichita uplift and the Meers fault. We have also made field plans to collect detailed gravity data along the COCORP lines and across the fault at selected sites.

6. The workshop on "Directions in Paleoseismology" will be the first scientific gathering dedicated solely to discussing the contributions, uncertainities, problems, and future goals of geologic studies of prehistoric earthquakes. The workshop is being convened by A. J. Crone. The 80 attendees include senior scientists, researchers, and program managers from throughout the United States, Canada, New Zealand, Japan, and France. Proceedings from the workshop will be published as a USGS open-file report.

7. A short, high-resolution seismic-reflection line was conducted across the Meers fault in Oklahoma. This data has been processed and shows a fault at approximately 271 m in depth which can be connected to the surface faulting. This fault has a displacement of about 30 m (Harding, 1985).

8. Temperature logs obtained in Chance No. 1 (south moat of the Long Valley caldera, Mono County, Calif.) in 1976, 1982, 1983, and 1985 show a progressive cooling in the uncased part of the hole. Examination of the rate of change suggests that the cooling began to accelerate about the time of the strong earthquakes of May 1980 (Diment and Urban, 1985). Temperature logs from Mammoth No. 1 (near Casa Diablo Hot Springs, 3 km west of Chance No. 1) obtained in 1979, 1982, and 1983 are also being processed and examined for seismically induced phenomena (Urban and Diment, 1984; 1985).

   More recently, precision temperature logs and gamma-ray logs were also obtained in two other hot wells (PLV-1 and RDO-8) in the south moat 6-11 days before and 3-4 days, and 61-64 days after the Chalfant (50 km ESE of well) earthquake M_S=6.2 PDE, M_L=6.4 BRK) of July 21, 1986. The work in RDO-8 was partially supported by participants in the Continental Scientific Drilling Program.

9. Under the Chinese-American Cooperative Earth Sciences Program, K. A. Shedlock and her colleagues from universities and The Peoples Republic of China have conducted extensive studies of the structure and tectonics of the North China basin (Shedlock and others, 1986; Shedlock and Roecker, 1987). These studies are applicable to the better understanding of similar regimes in the United States.

10. L. C. Pakiser and W. D. Mooney perceived the need for the summary/review volume: "Geophysical framework of the Continental United States." A conference was held in Golden between March 17 and 20, 1986 and 24 papers were presented. To date (3/31/87), 31 chapters have been submitted. GSA has agreed to publish the product in their Memoir series. Most manuscripts have been reviewed and are now being revised. Estimated date of submission to GSA is October 1987. The Memoir is estimated to be at least 650 printed pages.

11. At the request of T. C. Nichols and D. S. Collins (Project 02478, Rock deformation induced by subsurface excavation and use) Meridee Cecil digitized 24 streams within about 50 km west of Pierre, S.D., and made an analysis of several fluvial parameters. Known Holocene faults are readily detected as sharp changes in slope and stream-gradient index.

    Other sharp changes in slope and stream-gradient index are evident on a number of profiles but have not yet been field checked. Anomalous logarithmic slope-stream length plots and low concavity to convex stream profiles are characteristic of the entire area studied to data. The cause of the faulting and presumably other deformation is not known but may be related to glacial rebound.

    Meridee Jones-Cecil digitized and analyzed 15 stream profiles within the area proposed for the superconducting supercollider in eastern Colorado. Several anomalous slopes and stream-gradient indices were observed. One marked alinement of profile anomalies and stream-course changes has been brought to the attention of the Assistant State Geologist. Field checking is necessary to determine if the observed anomalies are due to active tectonics. Stream-profile analysis is proving to be a useful reconnaissance tool.

Reports

Crone, A.J., and Luza, K.V. 1986, Holocene deformation associated with the Meers fault, southwestern Oklahoma, in R.N. Donovan, ed., The Slick Hills of southwestern Oklahoma--Fragments of an Aulacogen?: Oklahoma Geological Survey Guidebook 24, p. 68-74.

Dart, R.L., 1985, Horizontal stress directions in the Denver and Illinois Basins from the orientation of borehole breakouts: U. S. Geological Survey Open-File Report 85-733, 44 p.

______1986, Well-bore breakouts and horizontal stress in the Denver and Illinois Basins: Geological Society of America, Abstracts with Programs, v. 18, p. 350.

______1987, Horizontal stress orientations from well-bore breakouts in the south-central United States [abs.]: Geological Society of America Abstracts with Programs, v. 19, no. 5, p. 269.

Dart, R.L., and Zoback, M.L., 1987, Principal stress directions on the Atlantic Continental shelf inferred from the orientations of borehole elongations: U.S. Geological Survey Open-File Report 87-, 40 p. (Branch review).

______1987, Application of well-bore breakout stress method to areas within the continental United States [abs.]: The Minerals and Geotechnical Logging Society, 2nd International Symposium on Borehole Geophysics. (Director's approval.)

Diment, W.H., and Urban, T.C., 1985, Temperature variations with time in a perennially boiling well in the Long Valley caldera, Mono County, California: Observations in Change No. 1 (1976-83): Geothermal Resources Council Transactions, v. 9, part 1, p. 417-422.

Haller, K.M., and Crone, A.J., 1986, Log of an exploratory trench in the New Madrid seismic zone near Blytheville, Arkansas: U.S. Geological Survey Miscellaneous Field Studies Map MF-1858, 1 oversized sheet with text.

Harding, S.T., 1985, Preliminary results of a high-resolution reflection survey across the Meers fault, Comanche County, Oklahoma: Earthquake Notes, v. 56, p. 2.

Harding, S.T., and Dwyer, Ruth-Ann, 1987, A large fault determined from seismic-reflection data in the New Madrid seismic zone and its relationships to seismicity: Tectonics (Submitted.)

Madole, R.F., 1986, The Meers fault Quaternary stratigraphy and evidence for late Holocene movement, in R. N. Donovan, ed., The Slick Hills of southwestern Oklahoma--Fragments of an Aucacogen?: Oklahoma Geological Survey Guidebook 24, p. 55-67.

Shedlock, K.M., Baranowski, J., Xiao, W., and Hu, X., 1986, The Tangshan aftershock sequence: EOS [Transactions of the American Geophysical Union], v. 67, p. 1381-1383.

Shedlock, K.M., Baranowski, J., Xiao, W., and Ju, X., 1987, The Tangshan aftershock sequence: Journal of Geophysical Research, v. 92, p. 2791-2803.

Shedlock, K.M., and Roecker, S.W., Crust and upper mantle structure of the North China basin: Journal of Geophysical Research. (Submitted for publication in 1987.)

Urban, T.C., and Diment, W.H., 1984, Precision temperature measurements in a deep geothermal well in the Long Valley caldera, Mono County, California: Transactions of the American Geophysical Union [EOS], v. 65, p. 1084-1085.

Urban, T.C., and Diment, W.H., 1985, Convection in boreholes: limits on interpretation of temperature logs and methods for determining anomalous fluid flow, in Proceedings National Water Well Association Conference on surface and borehole geophysical methods in ground-water investigations: National Water Well Association, Worthington, Ohio, p. 399-414.

Zoback, M.L., Zoback, M.D., and Dart, R.L., 1985, Reassessment of the state of stress in the Atlantic Coast region: Geological Society of America, Abstracts with Programs, v. 17, p. 759.

A LIQUEFACTION POTENTIAL MAP FOR CHARLESTON, SC

USGS Grant Award 14-08-0001-G1435

Dr. David Elton
Auburn University
Civil Engineering Department
Auburn University, AL 36849
(205) 826-4321

Dr. Tarik Hadj-Hamou
Civil Engineering Department
Tulane University
New Orleans, LA
(504) 865-5778

Liquefaction of soils during earthquakes can cause great damage. History is replete with examples of extensive damage caused by liquefaction. The public must have a quantitative evaluation of the possibility of liquefaction in order to be adequately protected from this earthquake-induced hazard. Liquefaction potential mapping provides a powerful and effective way to provide this protection. These maps show contours of the probability (risk) of occurrence of liquefaction for different magnitude earthquakes and return periods. This proposal develops a new method of liquefaction potential mapping, and then applies it to Charleston, SC.

Charleston, SC, was chosen for a test of the new method because it is susceptible to liquefaction. Recent geologic discoveries indicate that there have been several very large earthquakes accompanied by liquefaction in the Charleston area. From these conditions, Charleston obviously has a liquefaction risk. The high population density of Charleston makes evaluation of the threat imperative.

The objectives of this proposal are to develop -

1. a new methodology for creating liquefaction potential maps,

2. a liquefaction susceptibility map for peninsular Charleston, SC. This map will give the annual probabilities of exceedance for peninsular Charleston.

3. an understanding of the nature of the ground conditions in Charleston, SC, an area of seismic risk. The soil types, locations, variability, and properties will be studied. This information will be very useful in many other hazard mitigation studies.

The significant results of this study will be -

1. A liquefaction potential map for peninsular Charleston, SC. This map will provide quantitative evaluation of the probability that a particular site will liquefy during an earthquake of a given magnitude. This is very important

in city planning, critical facility siting and general earthquake preparedness. The information gained from this phase of this project may lead to the development of a provision in the local building code concerning liquefaction.

2. A new methodology for evaluating liquefaction potential. The new method is flexible and overcomes shortcomings of current techniques.

3. An understanding of the soil conditions in peninsular Charleston, SC. This understanding will be used to do the liquefaction evaluation. The soil data can be used in important future earthquake hazard mitigation studies, such as lifeline engineering, disaster planning, and site period studies.

The approach used in this study is based on the liquefaction evaluation method of Seed and his co-workers (1971, 1983, 1985). It relies on the use of Standard Penetration Test (SPT) data to evaluate how susceptible the soil is to liquefaction. A knowledge of seismic conditions is also needed in order to evaluate the probability of certain ground accelerations occurring. These two factors are combined to produce a liquefaction potential map.

The following procedure will be used to develop the map of liquefaction potential:

1. Gather geotechnical and geological information about the area of interest by contacting local agencies and consulting firms. This information is used to develop a map of penetration resistance. Several Charleston geotechnical firms have agreed to open their files for this project. Their letters of cooperation are in the Appendix.

2. Convert the values of penetration resistance into threshold accelerations and develop a map of threshold accelerations for liquefaction potential.

3. Perform a seismic risk analysis of the area to evaluate the probability of exceedance of different ground acceleration for all possible earthquake magnitudes.

4. Combine the data from step 2 and 3 to develop the map of probability of exceedance of threshold accelerations for liquefaction. This analysis can be done for each magnitude or for the total risk.

5. Draw contours of equal risk for liquefaction by joining locations on the map that present same probability of exceedance of the threshold acceleration for liquefaction.

The method outlined in this proposal has some distinct advantages over current techniques. One advantage is the use of the simplified Seed and Idriss method (1981), which is very easy to implement. Others are the separation between the geotechnical and seismological analyses, and the development of a map of quantitative probability of occurrences of threshold accelerations, rather than a relative description.

The results of this research have important implications for Charleston and other areas of the country faced with a liquefaction threat. For Charleston, a map of the liquefaction potential will be produced. This map will aid in land use planning, zoning, building code updating, and construction (and retrofitting) of critical facilities. Hospitals, fire stations and other critical facilities can be better protected against the liquefaction threat once the threat is known. Charleston can provide greater public safety as the results of this research are applied.

Other cities will benefit from this research. The flexibility of the new method allows it to be used in any location where there is SPT data. It is possible to develop the map without the use of expensive dynamic soil tests. The new method allows for easy incorporation of new soil or seismic data as such data is produced. The result is greater protection for the public by mitigating this earthquake hazard.

Seismic Hazard Studies, Anchorage, Alaska

9950-03643

A. F. Espinosa
Branch of Geologic Risk Assessment
U.S. Geological Survey
Box 25046, MS 966, Denver Federal Center
Denver, Colorado 80225
(303) 236-1597

Investigations

1. Fifteen earthquakes recorded in the field seismological experiment conducted in Anchorage, Alaska, have been edited and are being analyzed. This topic on "Ground amplification studies in areas damaged by the Alaskan earthquake" will be jointly used in the site-response study obtained on different geologic environments with the damage evaluation along 15 Avenue and DeBarr Avenue.

2. A map showing the surficial geology of the Anchorage B-7 NW quadrangle is being photo copied in preparation for release as USGS Open-File Report 87-168. This product contains 11 pages with a plate at scale of 1:25,000; authors are Lynn A. Yehle and Henry R. Schmoll. During this study, there was extensive consultation with geologic colleagues in the Alaska Division of Geological and Geophysical Surveys as to the location and extent of the bedrock in the mapped area.

3. A paper describing a model for analyzing the subsurface at Anchorage, Alaska, in terms of geology, geotechnical properties, and seismic response of both the Pleistocene glacial deposits and the Tertiary continental sedimentary rocks that overlie metamorphic or plutonic basement was prepared for and delivered at the 5th International Congress of the International Association of Engineering Geology, held in Buenos Aires, Argentina, October 20-25, 1986.

4. A suite of seismicity maps and depth cross sections for the Anchorage and vicinity region in Alaska are being prepared. A technique has been developed to map the subducting plate on a three-dimensional finite-difference display for Alaska and the Aleutian Islands.

5. Initial airphoto interpretation of the surficial geology within the confines of the Anchorage B-7 NE map area is complete (1:24,000-scale airphotos). Initial typescript has been completed of the text that includes surficial geologic unit and area descriptions and references. Revision of this material is about one-third complete. Additional work now underway involves reconciling our estuarine deposits with earlier developed studies in the same region and comparisons with limited recent (1985) NASA photography. Reconciling limits of surficial geology with colleagues of the Alaska Division of Geological and Geophysical Surveys concerning the extent of bedrock is complete for about one-half of the map area and adjoining regions to the east. Some joint (tentatively planned) field investigations (part of July 1987) will be very important in order to achieve a satisfactory completion of this quadrangle map.

6. Review of map units on all existing, partially completed, geologic maps of the Municipality of Anchorage has begun, and from this review material for use in preparation of the Anchorage B-7 NW and B-7 NE quadrangles has been incorporated into the introductory text, the description of map units, and the correlation of map units for the open-file reports on these quadrangles. In addition, an index map for use on these and all subsequently produced geologic maps of the Municipality has been prepared.

7. A digital intensity catalog covering the period 1786 through 1981 for the State of Alaska is being released as a USGS publication.

8. Airphoto interpretation of the surficial deposits of the Anchorage B-7 SE 1:25,000-scale map area is about one-half completed.

9. Previously existing and partially completed compilation of surficial geologic mapping in the Nabesna B-6 quadrangle, Alaska, has been completed and newly plotted using PG-2 equipment, as a contribution to the GQ map of the quadrangle in preparation by D. H. Richter, Branch of Central Mineral Resources, related to TACT/TALI statewide geophysical program work coordinated by Bob Page, USGS, Menlo Park, Calif.

10. Paleontological identification of pollen and spores by Jack Wolfe, Paleontology and Stratigraphy Branch, March 19, 1987, give evidence that rocks suggested by him to be the youngest Tertiary unit (Sterling Formation) do indeed underlie Quaternary deposits and at a depth of about 155 m beneath part of the east-central part of Anchorage (Tikishla Park drill hole, Open-File Report 86-293). This confirms earlier work from the farthest west part of Anchorage (Alaska Geological Society, 1970). It is speculated that a greater total thickness of younger Tertiary rocks may underlie Anchorage than heretofore considered likely.

Results

Brockman, S.R., Espinosa, A.F., and Michael, J.A., 1987, Digital intensity catalog of earthquakes felt in Alaska and the Aleutian Islands, 1797-1981: U.S. Geological Survey Open-File Report 87-68, 15 p.

Espinosa, A.F., 1987, Seismological field experiment in Anchorage and vicinity [abs.]: Geologic Hazard Symposium, Alaska Geological Society, Anchorage, Alaska. (Invited speaker.)

Espinosa, A.F., Brockman, S.R., and Michael, J.A., 1986, Modified Mercalli *intensity distribution for the most significant earthquakes in Alaska*, 1899-1981. U.S. Geological Survey Map 86-203.

Espinosa, A.F., Rukstales, K.S., and Michael, J.A., 1987, Digital seismicity catalog of Alaska and the Aleutian Islands, 1797-1981: U.S. Geological Survey Open-File Report 87, 25 p.

Herraiz, M., and Espinosa, A.F., 1987, Coda Waves: A review: Pure and Applied Geophysics, 125 p. (in press).

Soil Development as a Time-Stratigraphic Tool

9540-03852

Jennifer W. Harden
Branch of Western Regional Geology
U.S. Geological Survey
345 Middlefield Road, MS 975
Menlo Park, California 94025
(415) 329-4949

Investigations

1. Slip-rate studies along the Paicines Fault near Tres Pinos: Jennifer Harden, Kathy Harms, Malcolm Clark.

2. Geochronology-soil chronology-remote sensing study of outwash fans near Independence, California: Jennifer Harden, R.M. Burke, Alan Gillespie.

Results

1. Soils are being used to date Quaternary surfaces along Tres Pinos creek that have been laterally offset by the Paicines fault. In the case of one slip rate, fluvial terraces on either side of the modern, main trace of the fault needed to be correlated in order to estimate slip distances and dated for estimates of slip rates. On the east side of the fault there are four Holocene to late Pleistocene nested terraces derived from Tres Pinos creek. F tests indicate that, overall, the terraces are best distinguished (99.9 % level) by the soil development index, dry consistence, rubification, and total-texture as defined by Harden's soil development index in 1982. Other field properties such as structure, clay films and melanization also are good tools for differentiating the terraces. More specifically, however, two of the terraces apparently are too close in age to be distinguished by soils. On the west side of the fault, there are three nested terraces with very similar soils developed on them. The surfaces probably were eroded and colluviated as as a result of proximity to the fault and cannot be diffentiated by their soils.

   The ages of the terraces on the east side of the fault were approximated by calibration to dated surfaces near Merced, California, which has similar climate, vegetation, slopes, and parent material to Tres Pinos. The ages of terraces on the east side of the fault are 250-to-370, 70-to-190, 14-to-32, and 1-to-13 thousand years old. Terraces on the northwest side of the fault are 13-to-41 thousand years old. A terrace along the San Benito river about 10 km from this study was dated by charcoal at less than 12 thousand years; the soil age on this terrace was 5-to-11 thousand years.

2. Eight outwash fans along the eastern front of the Sierra Nevada were identified by A. Gillespie using multi-spectral imaging. At least 5 of those fans can be dated by their stratigraphic relationship to basalt flows dated by Ar 39-40 and K-Ar methods. Backhoe pits were excavated on each of the 8 fans, and 2-3 replicate soils were described and sampled.

Soils differentiated seven of the eight fans distinguished by remote sensing. Field parameters of the soil development index were used to distinguish the fans. When plotted against age, soil development indices appear to develop at similar rates on the east and west sides of the Sierra Nevada. The implications of these preliminary results are that 1) glacial moraines on the east side have soils that are less well developed than the fans, possibly owing to erosion of the moraines 2) climatic differences today and in the past between the east and west sides of the Sierra are averaged or masked by soil development over long periods (greater than 40 thousand years) of time.

Reports

Harms, K.K., Harden, J.W. and Clark, M.M., 1987, Use of quantified soil development to determine slip rates on the Paicines fault, northern California abs. : Geological Society of America, Abstracts with Programs, in press.

Burke, R.M. and Harden, J.W., 1986, Soil development, a possible relative dating tool for landslides. Assoc. Engineering Geology, Annual Meeting.

Burke, R.M., Lundstrom, S. Harden, J.W., 1986. Soil chronosequence on eastern Sierra Nevada fans, California, supporting remote sensing studies. Geol. Soc. Amer. Abstracts with Programs, Annual Meeting, Nov. 10-13, San Antonio, Texas.

Harden, J.W., McFadden, L.D., Reheis, M.C., Taylor, E.M. and Sowers, J.M., 1987, Soils as time-stratigraphic tools for correlation: results from studies in southern California and Nevada, U.S.A. submitted to International Union for Quaternary Research, XII International Congress, July 31-August 9, 1987.

Investigation of Seismic-Wave Propagation for Determination of Crustal Structure

9950-01896
Samuel T. Harding
Branch of Geologic Risk Assessment
U.S. Geological Survey
Box 25046, MS 966, Denver Federal Center
Denver, Colorado 80225
(303) 236-1572

Investigations

1. Processed results of high-resolution seismic lines that were run across the southern San Andreas fault.

2. Refined processing of seismic-reflection lines conducted in Crater Flat near Beatty, Nev.

3. Interpreted Mississippi Embayment deep-reflection lines.

4. Planned a shallow multi-channel seismic-reflection survey of Puget Sound.

Results

1. An initial interpretation of the results from the southern San Andreas fault seismic-reflection study indicates that the Banning fault, a member of the southern San Andreas fault system, has a northeast dip. The dip of this fault in Whitewater Canyon is near 45° NE and steepens in the vicinity of Desert Hot Spring to a dip of approximately 70° and the southern San Andreas fault near North Shore, California, dips at about 70° east and is a single strand.

2. The seismic-reflection line which crosses the Bare Mountain fault in Crater Flat, Nev., has been reprocessed and the effect of possible velocity variations on the interpretation have been studied. A hint of the Bare Mountain range-bounding fault can be seen. The more spectacular antiform 1 km out from the range front can be correlated with some surface faulting near the line.

3. The paper on our interpretation of the seismic-reflection line across the Realfoot Rift boundary is about ready for review. The Rift boundary appears on the seismic-reflection section as a set of slip faults and has a vertical displacement of approximately 1,000 m. At least two episodes of rifting can be interpreted from these lines.

4. Much of the logistics and ground work have been done for the planned multi-channel marine study for Puget Sound.

References

Harding, S.T., and Dwyer, Ruth-Ann, A large fault determined from seismic-reflection data in the New Madrid seismic zone and its relation to seismicity: Submitted to Tectonics

Seismic Slope Stability

9950-03391

Edwin L. Harp

U.S. Geological Survey
345 Middlefield Road
Menlo Park, California 94025

Investigations

Participated in research fellowship in Japan at National Research Center for Disaster Prevention in Tsukuba and at Kyoto University. Research involves the collection of strong motion data from the Izu-Oshima-Kinkai and Nagano-Ken-Seibu earthquakes in order to calculate Arias intensity values from as many sites as possible and to compare the Arias intensity distribution with the distribution of landslides from the two earthquakes. Good maps of the landslides from these earthquakes have been compiled and can be used to develop relations between Arias intensity, a parameter related to energy of shaking, and the landslide intensity (number of landslides per unit area). The goal is to develop relations between Arias intensity and landslide intensity as a function of earthquake source distance, to compare with Wilson and Keefer's (1986) relation between Arias intensity and the source distance to the furthest landslide in a given earthquake, and to use the relations to predict the intensity of landsliding in an earthquake.

Results

Preliminary calculations of Arias intensities from acceleration records from the Izu-Oshima-Kinkai earthquake indicates that the distribution of Arias intensities is not a simple relation depending only on the source distance but is probably related to local geologic conditions as is also the case in the landslide distribution. The distribution of landslides shows that the landslide intensity attenuates rapidly with source distance and that the distance to the furthest landslides from the source lies at the low edge of the data field compiled by Keefer (1984) for worldwide earthquakes. Preliminary examination of the landslide distribution from the Nagano-Ken-Seibu earthquake indicates that it too attenuates rapidly with distance from source and lies at the lower edge of the Magnitude-Distance data field for worldwide earthquakes.

References

Keefer, David K., 1984, Landslides caused by earthquakes, Geological Society of America Bulletin, v. 95, p. 406-421.

Wilson, R. C., and Keefer, D. K., 1985, Predicting areal limits of earthquake-induced landsliding, in Earthquake Hazards in the Los Angeles Metropolitan Area, J. I. Ziony, editor, U.S. Geological Survey Professional Paper 1360, p. 317-345.

ANALYSIS OF SEISMIC RISK FROM FOCUSING AND RESONANCE IN SALT LAKE VALLEY BY NUMERICAL SIMULATION OF THE WAVE EQUATION

Contract Number: 14-08-0001-G1344
Julie Hill
Harley Benz
Gerard Schuster
Geology and Geophysics Department
University of Utah
Salt Lake City, Utah 84112

Objectives

Focusing and resonance of seismic waves in alluvial-filled basins play a major role in determining which valley locations are most susceptible to severe ground shaking. From an accurate knowledge of the valley's P- and S-wave velocity structure, attenuation and geometry it may be possible to predict the ground shaking potential of a basin by numerical simulation of the wave equation. An accurate prediction of site amplification within the basin can then guide city planners in earthquake mitigation planning.

The objective of this research is to roughly predict the amplification (resonance and focusing) of seismic waves for various sites within the Salt Lake Valley. Seismic wave propagation in a Salt Lake Valley model will be simulated using a finite difference solution to the wave equation. This study will detail the basin response as a function of earthquake source location, source frequency, radiation pattern, and basin geometry. The study area will be limited to the locations in Salt Lake Valley where the subsurface structure is well known from seismic surveys, such as that conducted by USGS (King, personal commun., 1987).

Salt Lake Valley Model

The Salt Lake Valley is a fault-bounded, alluvial-filled valley located between the Oquirrh and Wasatch Mountains (Figure 1). Bounded on the east by the Wasatch fault, it extends roughly 35 kilometers from north to south from the Salt Lake to the Traverse Mountains. Refraction surveys (Bashore, W.M., 1982) indicate that the underlying basin extends to a depth of 3 or 4 kilometers and well log information (Arnow and Mattick, 1968, and Mattick, 1970) shows an extensive unconsolidated surface layer with a thickness of up to one kilometer.

A seismic reflection survey (Smith, R. B., personal commun., 1987) was carried out by Mountain Fuel and an interpreted section derived from line R-11 (see Figure 1) is shown in Figure 2. The reflection data clearly show the contact between the unconsolidated sediments and consolidated valley sediments and the contact between the basin sediments and basement rock. This interpretation is supported by the sonic and density logs at well sites 1, 2 and 3 in Figure 1. From these data, an interpreted cross-section of the northern portion of Salt Lake Valley basin is shown in Figure 3. Although relatively simple, this cross-section delineates some of the key features that are probably responsible for significant amplification of low frequency (0-3 Hz) seismic waves within this basin. The most notable feature is the extreme impedance contrast at the base of the semi-consolidated sediments; this is designated reflector 2 in Figure 2a and is labeled the base of the semi-consolidated layer in Figure 2b. This interface should be an important factor in influencing the resonance of low frequency waves within this basin.

Preliminary Numerical Results

Results are now given for numerically simulating a normally incident SH plane wave impinging from below on the models in Figures 3 and 4. It will be assumed that the basin model is two dimensional and that the basin is homogeneous in the north-south direction. Future simulations will be conducted for plane wave compressional sources, upward propagating faults, and obliquely incident plane waves. Numerical simulation tests will also be conducted for two dimensional basin models appropriate to other locations in Salt Lake Valley. These results will eventually be compared to the data from NTS site amplification studies, such as in Hays and King (1984).

Figure 4 depicts four basin models and Figure 5 depicts the corresponding simulations for SH wave propagation. The simulation technique was by a finite difference method (Benz, 1987) and the dominant frequency of the normally incident SH source was 2.3 Hz (Figure 6). Only Figure 4d corresponds to the basin model deduced from line R-11 in Figures 1 and 2. The other three basin models were used to demonstrate the differences between modeling a plane layer (Figures 4a and 5a), a symmetric homogeneous basin (Figures 4b and 5b), an asymmetric homogeneous basin (Figures 4c and 5c) and the actual layered basin model (Figures 4d and 5d).

Although these results are preliminary, some salient features are to be noted:

1). The symmetrical basin response (Figure 5b) shows significantly more Love wave energy than the plane layer response in Figure 5a. Bard and Bouchon (1980) and others demonstrated that Love waves trapped between the walls of a symmetric two-dimensional basin can introduce significant surface wave energy compared to that produced from a plane layered model. The basin geometry focuses normally incident source energy to oblique angles (guided Love waves) and traps these waves by lateral reflections from the basin walls.

2). The asymmetrical basin response (Figure 5c) appears to be somewhat muted relative to the symmetrical basin response (Figure 5b). The strong SH response generated at the western portion of the basin in Figure 5b is not present in Figure 5c because the asymmetrical basin model pinches out to a thin layer. The thin layer is not conducive to resonance or lateral reflection effects at these low frequencies. Additionally, the apparent source generation at the eastern end of the asymmetrical basin appears to be weaker than that for the symmetrical basin model. Apparently, the dipping nature of the contact between basement and basin lithology may strongly influence focusing of the incident source to the edges of the basin.

3). The layered asymmetrical basin response (Figure 5d) shows longer duration and stronger ground shaking at the eastern edge of the basin than either the symmetrical or asymmetrical basin responses. A preliminary interpretation is that the strong impedance contrasts between the consolidated and unconsolidated layers of the layered basin may play an important role in the focusing and resonance of low frequency SH energy. This effect cannot be adequately modeled with homogeneous symmetrical basin models.

References

Arnow, T. and Mattick, R.E., 1968, Thickness of valley fill in the Jordan Valley east of the Great Salt lake: Utah, U.S.G.S. Prof. Paper, 600-B, B79-B82.

Bard, P.Y., and Bouchon, M., 1980, The seismic response of sediment filled valleys. Part I. The case of incident SH waves: BSSA, 70, 1263-1286.

Bashore, W.M., 1982, Salt Lake Valley and Wasatch Fault crustal structure: University of Utah MS thesis.

Benz, H., 1986, Elastic wave propagation in heterogeneous media from normal faulting earthquakes, in preparation.

Hays, W., and King, K., 1984, The ground shaking hazard along the Wasatch Fault Zone, Utah: USGS Proceedings of Conference XXVI, 133-147.

Mattick, R.E., 1979, Thickness of unconsolidated to semi-consolidated sediments in Jordan Valley, Utah: USGS Prof. Paper, 700-C, C119-124, 1970. 600-B, B79-B82.

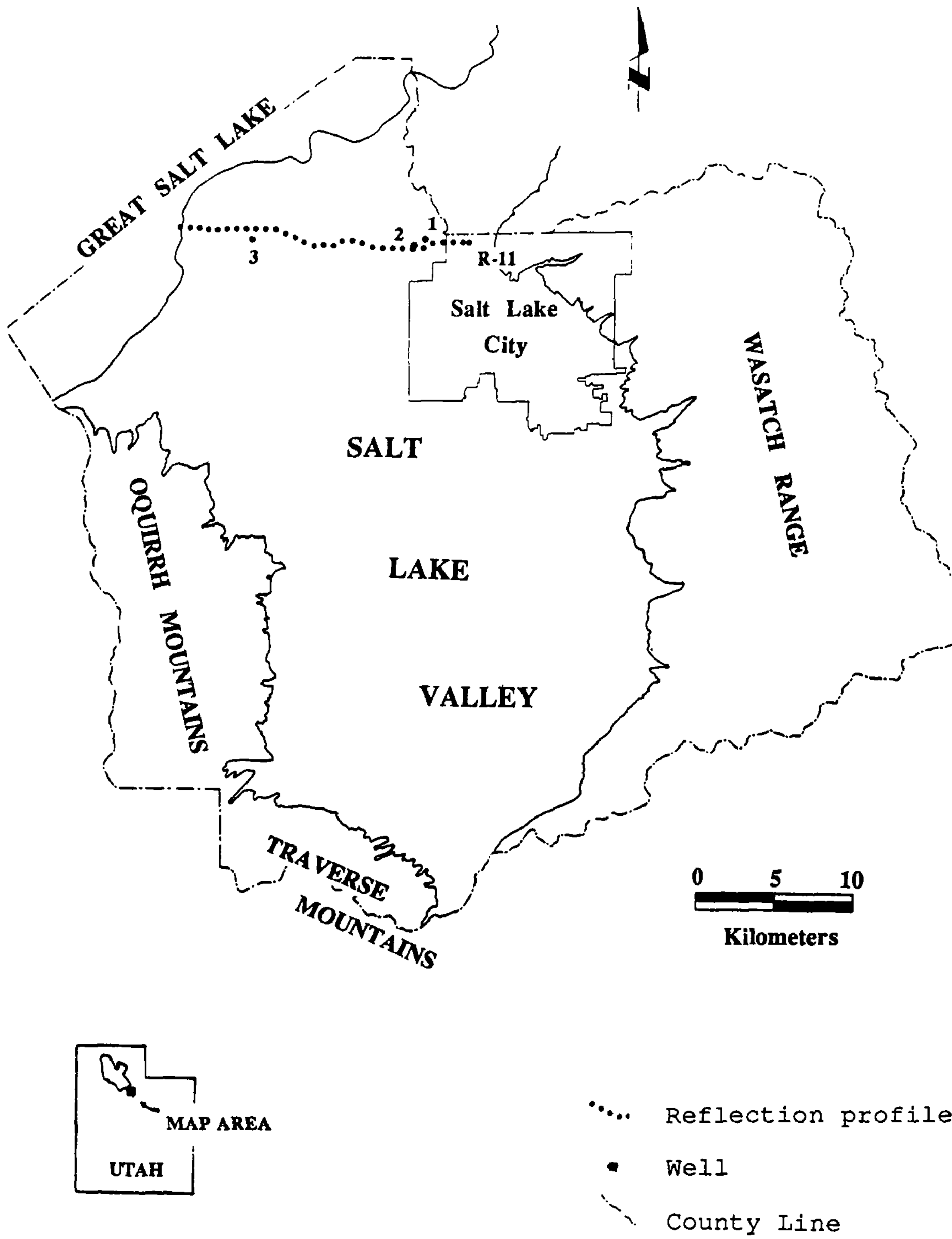

Figure 1. Map of study area with locations of reflection profile, R-11, and wells.

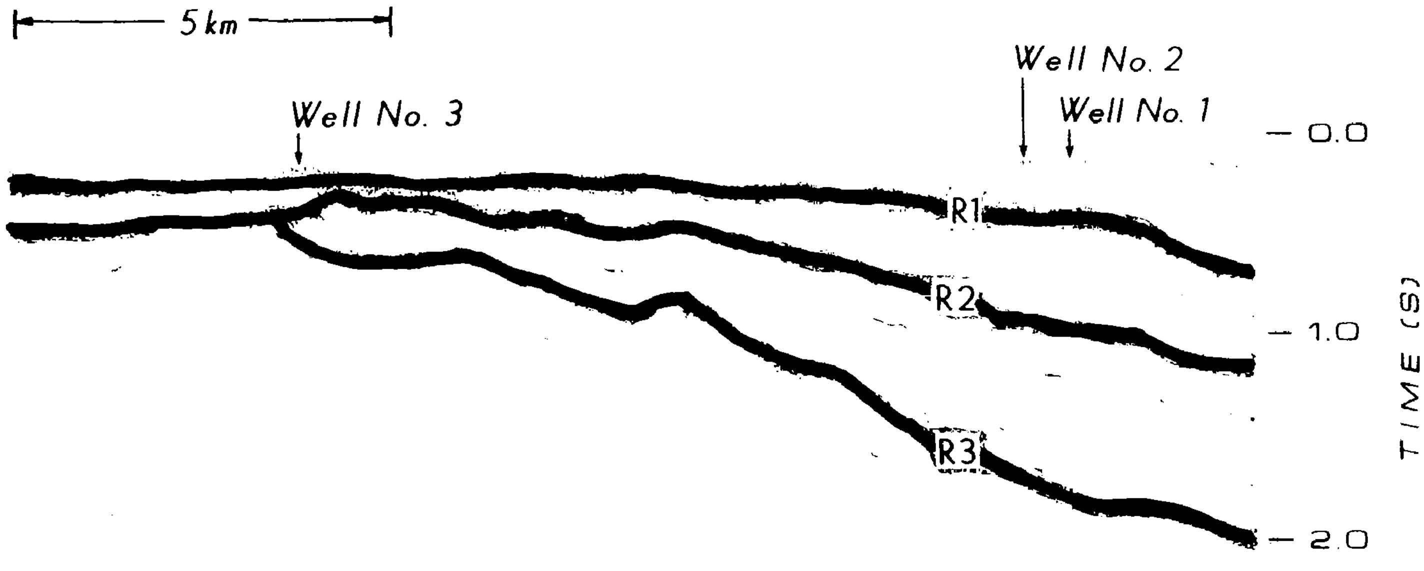

Figure 2a. Interpreted cross-section derived from profile R-11 in Figure 1. The horizons R1, R2, and R3 correspond to, respectively, the base of the unconsolidated sediments, the base of the semi-consolidated sediments, and the base of the consolidated sediments.

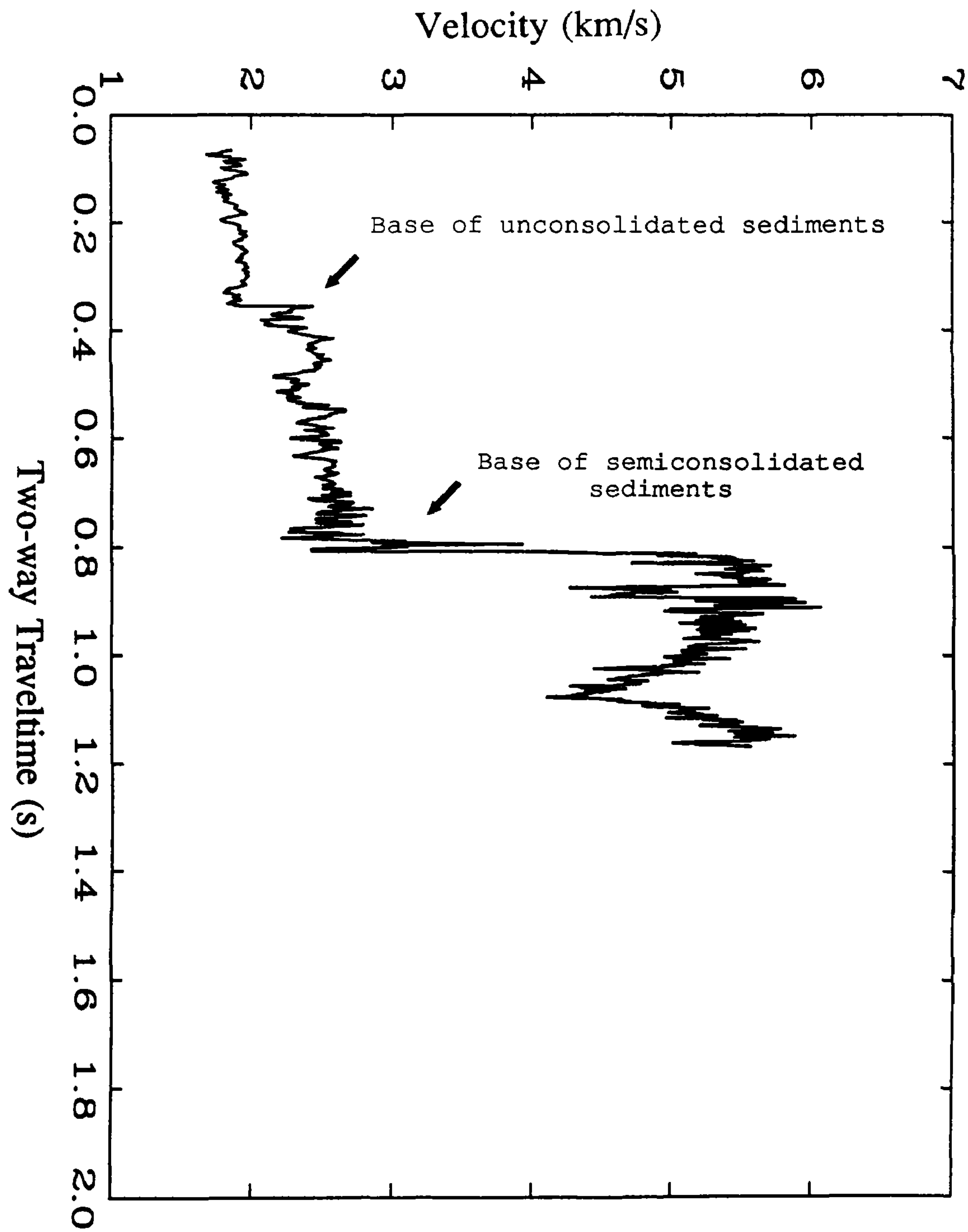

Figure 2b. Sonic log for Western United Mines Gillmar Fee #1, corresponding to well site #2 in Figure 1.

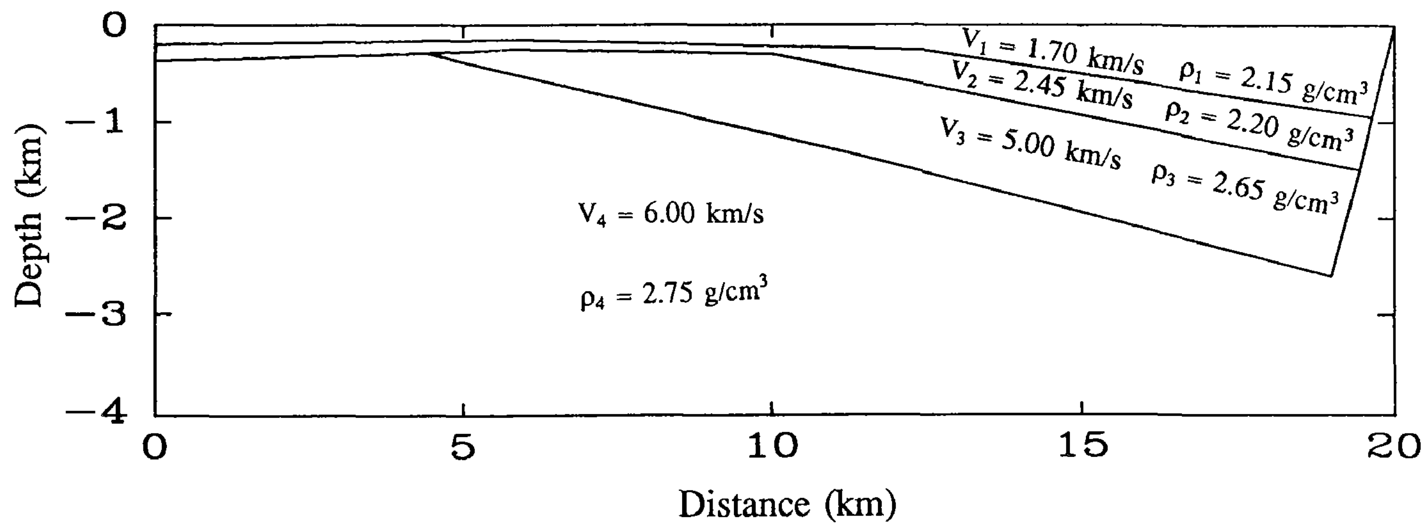

Figure 3. East-west cross section and physical parameters of Salt Lake Valley along line R-11 from reflection and well data. P-wave velocities are shown and are used to estimate S-wave velocites, assuming $V_s = V_p / \sqrt{3}$.

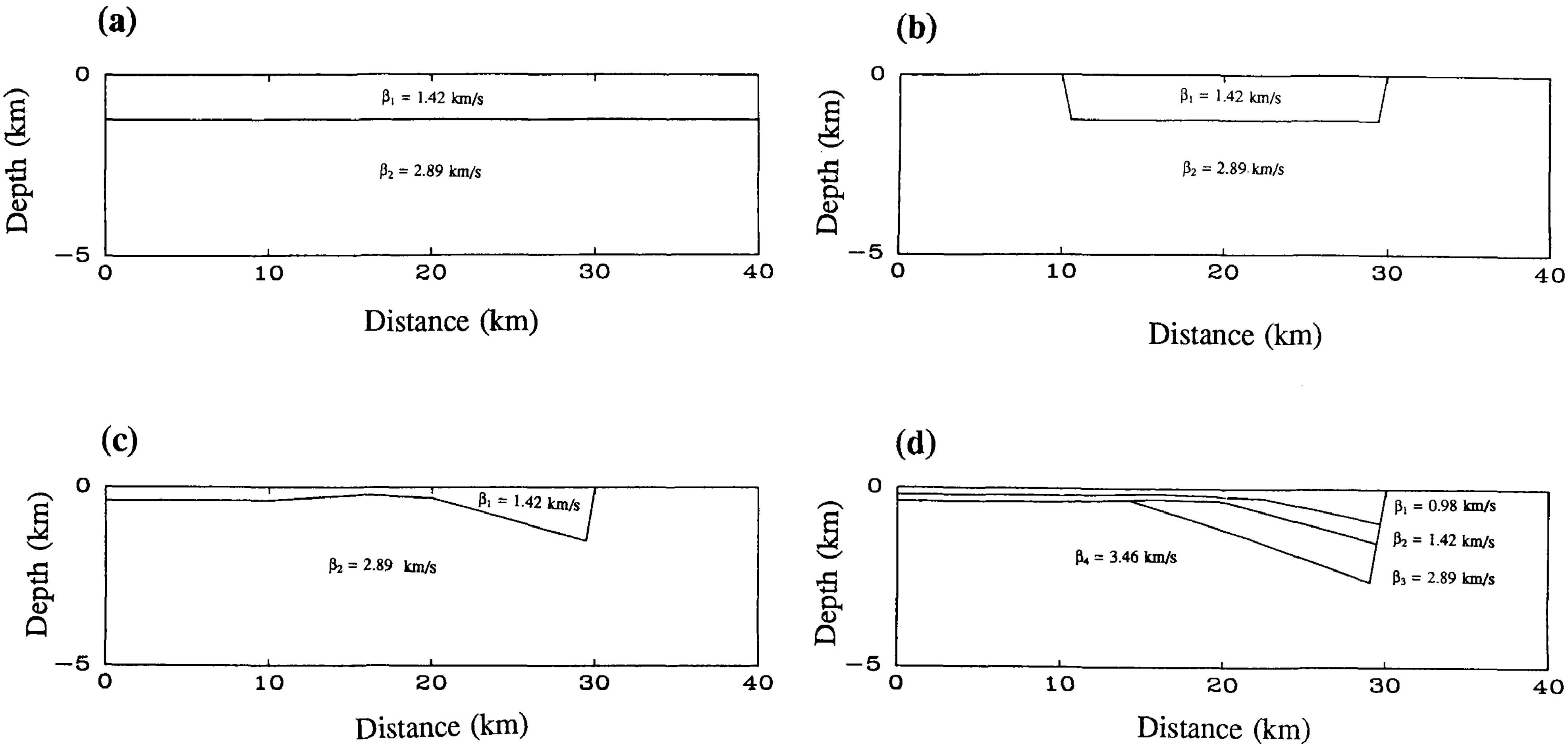

Figure 4. Suite of models used to demonstrate the variation in seismic response with increasing basin complexity. S-wave velocities are shown. (a) Plane layer model. (b) Symmetric, homogeneous basin model. (c) Asymmetric, homogeneous basin model. (d) Asymmetric, multi-layer basin model.

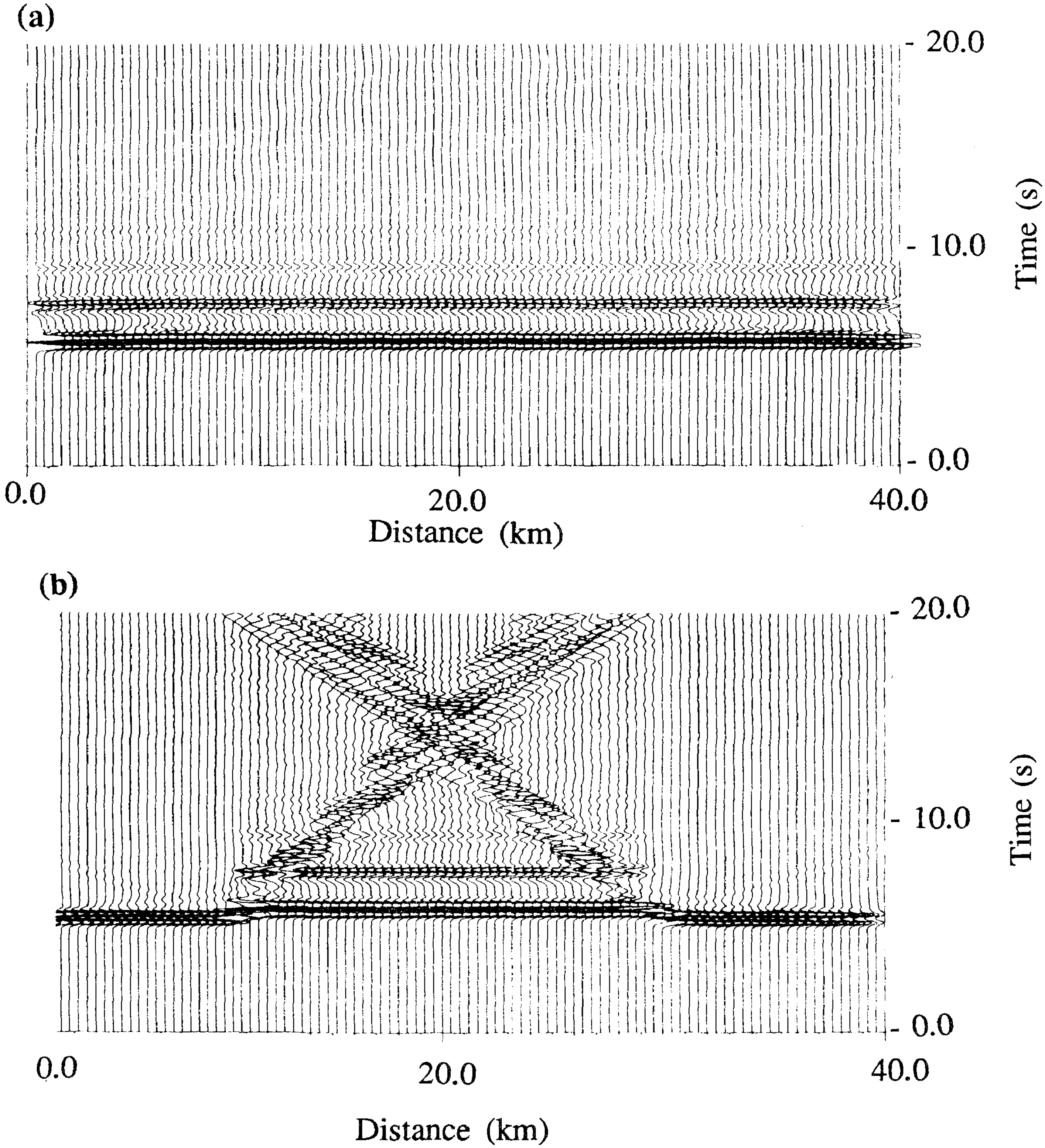

Figure 5. Seismograms for the models shown in Figure 4 for a plane, SH-wave source. (a) Seismic response of the plane layer model. (b) Seismic response of the symmetric, homogeneous model. (cont.)

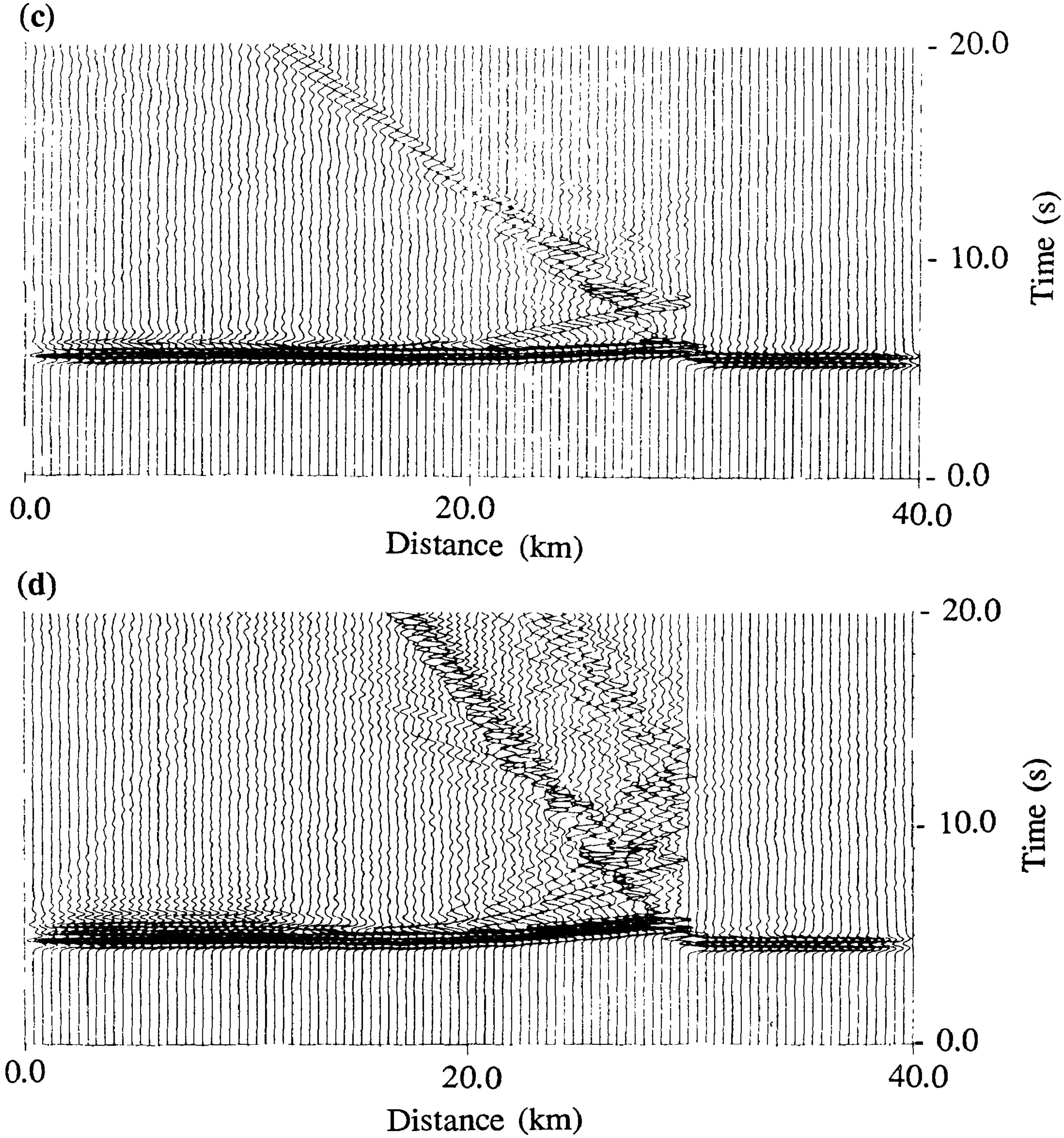

Figure 5. (cont.) (c) Seismic response of the asymmetric, homogeneous basin model. (d) Seismic response of the asymmetric, multi-layer model.

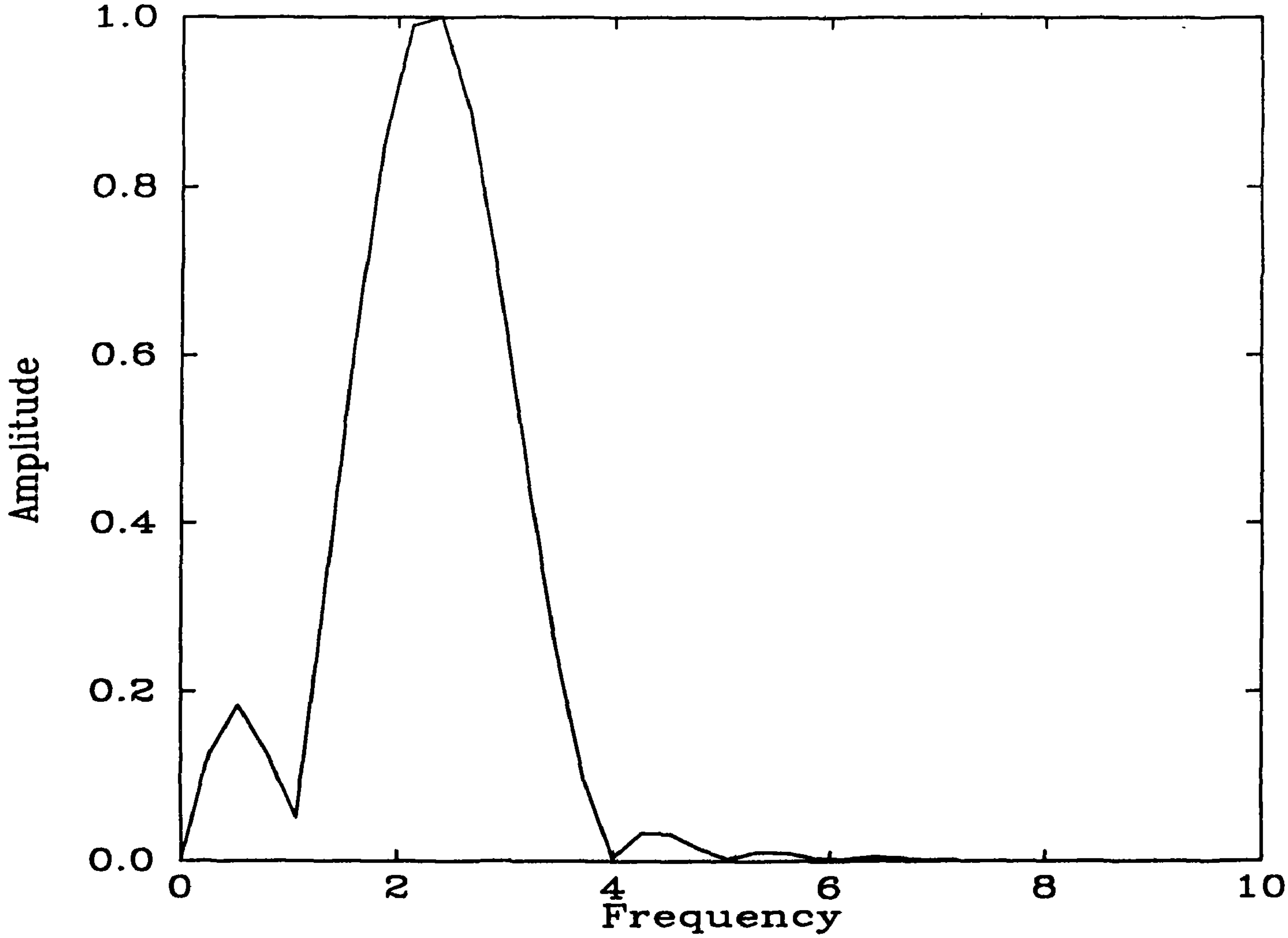

Figure 6. Frequency response of the source wavelet used in calculating the seismograms of Figure 5.

Urban Hazards Seismic Field Investigations and Study of the Effects of Site Geology on Ground Shaking

9950-01919

Kenneth W. King and Arthur C. Tarr
Branch of Geologic Risk Assessment
U.S. Geological Survey, MS 966
Denver Federal Center, Box 25046
Denver, CO 80225
(303) 236-1591 and (303) 236-1605

Investigations

The general objectives of this project are to:

(1) Improve understanding of how shallow geology affects ground shaking;

(2) Devise methodologies and techniques for the efficient acquisition and organization of seismic and geotechnical data for ground response determination.

Specific objectives for this reporting period are:

(1) Continue acquisition of geotechnical data from the Wasatch Front area;

(2) Continue site response and geotechnical data acquistion from the Puget Sound region;

(3) Completion of study related to vibration hazard to archeological ruins at Hovenweep National Monument, Utah-Colorado;

(4) Initiation of study of shallow subsurface geology at a liquid waste disposal area near Farmington, N.M.;

(5) Initiation of study of shallow subsurface geology at site of a proposed dike at Great Salt Lake, Utah;

(6) Continuation of development of computerized data base and mapping systems which will facilitate analysis of ground response data.

Results

Downhole *P*- and *S*-wave velocity measurements were made at 18 boreholes in the Salt Lake City urban area. The analysis of the data is approximately 25% complete. The downhole velocity profiles will be added to a geotechnical data base and will be used in correlations with shallow sesimic reflection results and with values of relative site response.

In December 1986, a field experiment was conducted in Seattle, Washington to acquire ground response and geotechnical data which would augment similar data acquired in September 1986 in Seattle and Olympia. A nuclear explosion at the Nevada Test Site was recorded at five sites in Seattle. Spectral ratios were computed from Fourier amplitude spectra in the 0.5 Hz to 2.0 Hz band; however, ratios at higher frequencies were not possible because ambient background noise masked the explosion signal which had been attenuated by the long path. Ambient background noise was recorded along two five-station lines, one in West Seattle and one in the Brighton district of southeast Seattle. The lines were about two miles long, crossing areas where the underlying soil and glacial till varied in thickness from zero meters to about 100 meters. The noise spectra showed persistent amplification in the 3-5 Hz band, very similar to noise spectra obtained in September 1986. Eight seismic refraction profiles were run near ground response sites to establish velocity and depth to bedrock. Two sites where the surface *P*-wave velocity was in excess of 7000 ft/sec were selected to be reference ground response sites. Eight single-family dwellings were shaken to determine resonant period and damping constant characteristics of the dwelling and chimneys. These data will be used later in comparisons with observed damage patterns (particularly chimneys) from the 1965 earthquake.

A final report was submitted to the National Park Service presenting results of a vibration study of archeological ruins at the Hovenweep National Monument. The study showed that various stone walls in the ruins could amplify ground vibration up to 50 times from traffic, blasting, and construction activities using heavy equipment. A vibration zonation map was proposed to protect the ruins in the future.

A new study was initiated in the Four Corners region, near Farmington, N.M., at the request of Water Resources Division and the Environmental Protection Agency to determine shallow subsurface structure at a liquid toxic waste disposal site. Four seismic refraction profiles were run across the structure. Data analysis continues at present but preliminary results indicate the presence of buried channels which could provide pathways for contamination of the water table.

Another study was begun at the request of the State of Utah to determine seismic response at the location of a proposed dike which is intended to prevent inundation by the rising Great Salt Lake. Recordings of a nuclear explosion and mine blasts were made to extend previous response data from the central Salt Lake Valley westward to the proposed dike location. Preliminary data analysis indicate that seismic response is lower in the western Salt Lake Valley than in the central Valley. Additional ground response recordings are planned for the second half of FY 1987.

This project has taken the lead for the Branch in examining the feasibility of using Geographical Information Systems (GIS) technology for urban hazards studies, with the assistance of National Mapping and Water Resources Divisions. The effort will focus on the Puget Sound–Portland urban hazards study area where GIS is likely to have the most impact. Thus far, several data bases and existing maps have been identified for input to the GIS system for a trial implementation. It is expected that data from the microcomputer-based geotechnical data sets described last reporting period will be easily incorporated into the GIS.

Reports

King, K. W. and Algermissen, S. T., 1987, A vibration study of the archeological ruins Hovenweep National Monument, Utah-Colorado: U.S. Geological Survey Open-File Report, 22 p.

Williams, R. A. and King, K. W., 1987, Detection of mined coal cavities near Boulder, Colo., using high-resolution seismic-reflection methods: G.S.A. Abstracts with Programs, vol. 19, no. 5, March 1987.

Nichols, T. C., King, K. W., Collins, D. S., and Williams, R. A., 1987, Seismic reflection technique used to verify shallow fracture zones in the Pierre Shale of South Dakota: Canadian Geotechnical Journal, File No. 2312.

Quaternary Geology Along the Wasatch Fault Zone, Utah

(New project, no number assigned)

Michael N. Machette
Branch of Central Regional Geology
U.S. Geological Survey
Box 25046, MS 966, Denver Federal Center
Denver, Colorado 80225
(303) 236-1243

Investigations

1. Continued field investigations (mainly trenching) and analysis of data pertaining to earthquake hazards along the Wasatch fault zone. Preliminary results from our trenching efforts will be presented at the May 1987 meeting of the Rocky Mountain section of GSA.

   a. Personius finished field investigations of four trenches across the Wasatch fault zone at Brigham City, Utah, with Hal Gill (UGMS).

   b. Nelson finished field investigations of five trenches across the Wasatch fault zone at Ogden, Utah, with Bob Klauk (UGMS), Mike Lowe (Weber Co. Geologist), and John Garr (Utah State Univ.). Analysis of trenching data continues, and displacement and other fault-scarp measurements from field-scarp profiles are being compared with measurements from several hundred profiles drawn from stereo aerial photographs with the Kern PG-2 (computer-assisted photogrammetric plotter).

   c. Machette finished field investigations of three trenches across the Wasatch fault zone at Brigham City, Utah, with Bill Lund (UGMS). Analysis of trenching data continues pending results of radiocarbon dating.

   d. Machette logged one of two trenches across the Woodland Hills splay of the Spanish Fork segment of the Wasatch fault zone. These trenches were dug by the U.S. Bureau of Reclamation (Provo) as part of a study for the Loafer Mountain water diversion project.

2. The 30 organic carbon samples collected from the exploratory trenchs have been separated and concentrated in the INSTAAR laboratory (University of Colorado) and about a third of them have been submitted for radiocarbon analysis.

   a. Six samples from Brigham City segment trenches were obtained by Personius; three of these samples have been submitted to Steve Robinson (USGS Menlo).

   b. Eighteen samples from the Weber segment trenches (East Ogden) were obtained by Nelson; two charcoal samples have been submitted to the TAMS facility at the University of Arizona--Tucson. All other samples are prepared for dating, but none have been submitted as yet (awaiting budget allotment and approval).

c. Machette obtained six samples from American Fork segment trenches; three samples of organic matter (A horizons) have been submitted to Steve Robinson (USGS Menlo), and three small samples of charcoal have been submitted to the TAMS facility at the University of Arizona--Tucson. In addition, one sample each from the Rock Creek site (Provo segment) and Woodland Hills site (Spanish Fork segment) were submitted for radiocarbon analysis.

3. Continued compilation of data for a series of six 1:50,000-scale maps showing the Quaternary geology along the Wasatch fault zone from Honeyville to Fayette, Utah. These maps form a 10- to 15-km-wide strip along nine segments of the fault zone.

   a. Personius finished the Brigham City segment map and submitted it for technical review.

   b. Nelson and Personius continued compilation of the Weber segment map. The map should reach technical review by late spring.

   c. Machette continued compilation of the Utah Valley map (American Fork, Provo, and Spanish Fork segments). Field checking in early summer should finalize geologic relations shown on map; it should reach technical review by the end of the fiscal year.

   d. Personius, Machette, and Haller started recompilation and reformatting of the 1:24,000-scale maps of the Salt Lake City segment (Scott and Shroba, 1985) for inclusion in the 1:50,000-scale map series. The map area is being expanded to include the West Valley fault zone as mapped by Keaton and others (in press).

4. Haller completed initial fieldwork and aerial-photo reconnaissance of the Lemhi and Beaverhead faults, Idaho, and the Red Rock fault, Montana. Photogrammetric mapping of the fault scarps is near completion. Preliminary interpretation of the segmentation of these three faults will be presented at the May 1987 meeting of the Rocky Mountain section of GSA.

5. Wheeler remained busy routing his comprehensive (267 p.) manuscript on segmentation of the Wasatch fault zone. At the reviewers' exhausted requests, the manuscript was split into two Survey Bulletins (on methods and analyses) and a chapter for a Professional Paper (on results).

Results

1. Completion of our cooperative trenching effort with the Utah Geological and Mineral Survey has given us a much expanded data base for analyzing recency and recurrence intervals of surface rupturing along the Wasatch fault zone. We now have one or more major trench sites on the seven most active segments and will be able to test our hypothesis that the Wasatch fault zone has more segments (10+) than originally suggested by Schwartz and Coppersmith (1984). In addition, the results of radiocarbon analysis will permit us to place tighter constraints on the times of most recent movement along the critical, urbanized parts of the fault zone.

2. A total of 32 samples of organic carbon (organic matter or charcoal) have been processed for concentration, but as yet only one radiocarbon age determination has been received. We anticipate that 40 percent of the samples will be dated by July 1 and hope that the remainder will be completed by October 1. Further interpretations of the fault relations observed in the trenches awaits the age determinations.

3. The 1:50,000-scale map of the Brigham City segment has been through technical review and is ready for branch approval. Personius has spent considerable time on map format, layout, and use of units and symbols because this map will be the prototype for the remaining maps in the series. These maps will provide a comprehensive base for further evaluations of earthquake-hazards potential. We anticipate publishing the maps initially in the MF series (black and white, limited distribution) for early release and later in the I series (color, wide distribution).

4. Nelson has completed analysis of 70 percent of his scarp-profile data from the Weber segment. This analysis indicates that most fault-displacement values measured from aerial photographs with the PG-2 agree within ±10 percent with field mesurements for the same scarps. Especially for higher scarps (>5 m), this measurement error is similar to errors in calculating displacements from field data. The photogrammetric method provides a valuable and time-efficient method for estimating net surface displacement across inaccessible or heavily vegetated portions of the fault zone.

5. Aerial-photo reconnaissance by Haller of the Lemhi and Beaverhead faults, Idaho, and the Red Rock fault, Montana, indicates that only the central portions of each of these faults have been active during the late Quaternary and those parts that have been active show characteristics of segmentation. The central 110 km of the Lemhi fault appears to be composed of five segments, and the central 90 km of the Beaverhead fault appears to be composed of four segments. Only the central 22 km of the Red Rock fault ruptured during the late Quaternary, and the morphology of the scarps indicates that they define a single segment.

6. Stratigraphic relations exposed in the Woodland Hills trench (U.S. Bureau of Reclamation--Provo) reveal a complex history of faulting that probably goes back more than 100,000 years. Machette's interpretation of alluvial-fan deposits that were transgressed by the highest stand of the Lake Bonneville cycle shows about 3 m of stratigraphic offset along the Woodland Hills splay of the Spanish Fork segment of the Wasatch fault zone. Discrete colluvial wedges and rotated blocks of soil indicate at least three times of movement in the past 125,000 yrs. Organic carbon from the A horizon of a rotated and buried block of fault-scarp colluvium has been dated at 1380±60 yrs B.P. This age determination, although suspiciously young, is a maximum <u>limiting</u> date for the most recent movement on the fault. James McCalpin (Utah State Univ.) has submitted several samples of older faulted alluvium from the trench for commercial analyses of thermoluminescence. These data may permit us to document times of late Pleistocene faulting. The small number of faulting events recorded on this splay of the Wasatch fault zone indicates that the splay only participates in 1 of 5 to 10 major events that occur on the main fault segment.

Reports

Crone, A.J., Machette, M.N., Bonilla, M.G., Lienkaemper, J.J., Pierce, K.L., Scott, W.E., and Bucknam, R.C., 1987, Surface faulting accompanying the Borah Peak earthquake and segmentation of the Lost River fault, central Idaho: Seismological Society of America Bulletin, v. 77, no. 3, (in press).

Haller, K.M., 1987, Preliminary interpretation of segmentation of three range-front normal faults in southeastern Idaho and southwestern Montana [abs.]: Geological Society of America Abstracts with Programs, v. 19, no. 5, p. 280.

Machette, M.N., 1987, Recent studies of the Wasatch fault zone, Utah--A review [abs.]: Geological Society of America Abstracts with Programs, v. 19, no. 5, p. 317.

Machette, M.N., 1987, Documentation of benchmark photographs that show the effects of the 1983 Borah Peak earthquake with some considerations for studies of scarp degradation: Seismological Society of America Bulletin, v. 77, no. 3 (in press).

Machette, M.N., and Lund, W.R., 1987, Trenching across the American Fork segment of the Wasatch fault zone, Utah [abs.]: Geological Society of America, Abstracts with Programs, v. 19, no. 5, p. 317.

Machette, M.N., Personius, S.F., Menges, C.M., and Pearthree, P.A., 1986, Map showing Quaternary and Pliocene faults in the Silver City $1^{\circ} \times 2^{\circ}$ quadrangle and Douglas $1^{\circ} \times 2^{\circ}$ quadrangle, southeastern Arizona and southwestern New Mexico: U.S. Geological Survey Miscellaneous Field Studies Map MF-1465-C, scale 1:250,000, 20 p. pamphlet.

Nelson, A.R., Klauk, R.H., Lowe, Michael, and Garr, J.D., 1987, Holocene history of displacement on the Weber segment of the Wasatch fault zone at Ogden, northern Utah [abs.]: Geological Society of America Abstracts with Programs, v. 19, no. 5, p. 322.

Nelson, A.R., and Personius, S.F., 1987, A nonconservative barrier to Holocene rupture propagation in the northern Wasatch fault zone, Utah, USA [abs.]: International Union for Quaternary Research, 12th International Congress, Ottawa, Canada, Abstracts with Program (in press).

Personius, S.F., and Gill, H.E., 1987, Holocene displacement on the Brigham City segment of the Wasatch fault zone near Brigham City, Utah [abs]: Geological Society of America, Abstracts with Programs, v. 19, no. 5, p. 326.

Wheeler, R.L., and Krystinik, K.B., 1987, Persistent segment boundaries on the Wasatch fault zone, central Utah [abs.]: Seismological Research Letters, v. 58, no. 1, p. 31.

Wheeler, R.L., and Krystinik, K.B., 1987, Persistent and nonpersistent seismic segmentation of the Wasatch fault zone, Utah [abs]: Geological Society of America, Abstracts with Programs, v. 19, no. 5, p. 342.

Determining Landslide Ages and Recurrence Intervals

9950-03789

Richard F. Madole
Branch of Geologic Risk Assessment
U.S. Geological Survey
P. O. Box 25046, MS 966
Denver, Colorado 80225
(303) 236-1617

Investigations

1. The feasibility of using soil development to date landslide events by means of calibrated ages was investigated using the Manti slide, Sanpete County, Utah, as the principal study area.

2. Work was completed on dating movement on the Meers fault, southwestern Oklahoma. This work included study of the local fluvial stratigraphy and a review of the regional Quaternary stratigraphy of the Osage Plains.

Results

1. Many large landslides have complex histories of repeated movements that may be recorded by a series of discrete pond deposits that have been translocated from the same pond-forming depression. The location of the pond-forming depression remains fixed from one movement to the next, because it is controlled by the configuration of the failure plane which remains essentially the same from slide to slide. Consequently, repetitive slope movements result in a sequence of pond deposits that are progressively older in a downslide direction.

Once the pond deposits are exposed to the atmosphere, soil formation begins and increases progressively with time. Translocated pond deposits form a type of soil chronosequence not previously described. A chronosequence is a series of soils for which all soil-forming factors other than time--climate, fauna and flora, topography, and parent material--are more or less the same. Such chronosequences provide relative dates for landslide events and, to a degree, the amount of soil development provides a means of estimating ages for landslide deposits. In addition, translocated pond deposits commonly contain ^{14}C-datable materials, mainly charcoal and wood. Because soil formation did not begin in the pond deposits until after they were translocated, the ^{14}C ages make it possible to determine the length of time required to form various soil properties. In turn, this makes it possible to derive calibrated ages based on the degree of soil development for other landslide deposits.

Several soil properties are time dependent, including depth of $CaCO_3$ leaching; accumulation of organic matter, clay, and $CaCO_3$ (measured in g/cm^3); the formation and translocation of iron compounds; rubification (reddening) and melanization (darkening); horizon thickness and profile thickness; and complexity of horizon sequences. The most useful soil properties for determining calibrated ages vary from area to area because of differences in climate, vegetation, and parent material. In the High Plateaus of central Utah, the most useful soil properties for determining calibrated ages for landslides of late Holocene age, which are particularly widespread, are the quantity of soil humus that has accumulated and the thickness of the A horizon.

A horizons are formed by the incorporation of humus into soil parent material (sediment). Accumulation of humus and the formation of A horizons take place relatively fast and reach a steady state more quickly than most other pedogenic processes, generally in time spans of 0.2 to 10 ka (Birkeland, 1984, p. 203).[1] Therefore, the properties of A horizons developed in geologically young deposits have the potential for quantification and use in determining calibrated ages for landslide events.

Translocated pond deposits of at least four ages are recognized on the Manti landslide, Sanpete County, Utah. ^{14}C ages have been obtained for two ages of pond deposits, and age determinations for a third set of deposits are in progress. The fourth set of pond deposits was formed by the 1974 landslide. The latter shows no evidence of soil formation, whereas the next older pond deposit has a weakly developed soil profile consisting of A/2A/2C horizons. The two A horizons have a combined thickness that ranges from 3 to 10 cm, but is typically 6-7 cm. The next older pond deposit has a soil profile consisting of A/2A/2AC/2C horizons in which the combined thickness of the two A horizons is generally 9-11 cm and the AC horizon is about 10 cm thick. This profile is believed to be the product of about 2000 years of soil formation. The oldest translocated pond deposit has an A horizon that is as much as 18-22 cm thick. This deposit is thought to be about 3000 years old. Laboratory analyses of specific soil properties, being done for purposes of determining calibrated ages, have not yet been completed.

[1]Birkeland, P. W., 1984, Soils and geomorphology: New York, Oxford University Press, 372 p.

2. Three manuscripts describing the Quaternary stratigraphy and evidence for Holocene movement on the Meers fault, southwestern Oklahoma, were completed during the first half of FY 87. Two field trips (one national and one sectional) were scheduled to the area during this period. Titles of published documents resulting from this work are included in the list below.

Reports

Madole, R. F., 1986, The Meers fault--Quaternary stratigraphy and evidence for late Holocene movement, in Donovan, R. N., ed., The Slick Hills of southwestern Oklahoma--Fragments of an Aulacogen?: Oklahoma Geological Survey Guidebook 24, p. 55-67.

Madole, R. F., Bradley, W. C., Loewenherz, D. S., Ritter, D. F., Rutter, N. W., and Thorn, C. E., Rocky Mountains, Chapter 7, in Graf, W. L., ed., Geomorphic systems of North America: Boulder, Colorado, Geological Society of America Centennial Special Volume 3 (in press).

Reheis, M. C., Madole, R. F., Mears, Brainerd, Jr., Nelson, A. R., Osborn, G. D., Palmquist, R. C., and Jaworowski, Cheryl, Quaternary history of some Southern and Central Rocky Mountain basins, Chapter 9, in Morrison, R. B., ed., Nonglacial Quaternary Geology--Conterminous United States: Boulder, Colorado, Geological Society of America, Centennial Special Volume (scheduled for publication late 1987).

Madole, R. F., Stratigraphic evidence of Holocene faulting in the midcontinent--The Meers fault, southwestern Oklahoma: Geological Society of America Bulletin. [Director's approval 1/13/87]

Luza, K. V., Madole, R. F., and Crone, A. J., Investigation of the Meers fault, southwestern Oklahoma--Final Report: Nuclear Regulatory Commission. Also to be published in the Special Report Series of the Oklahoma Geological Survey. [Director's approval 1/7/87]

Madole, R. F., Ferring, C. R., Guccione, M. J., and Hall, S. A., Osage plains and Interior Highlands, Chapter 12, in Morrison, R. B., ed., Nonglacial Quaternary Geology--Conterminous United States: Boulder, Colorado, Geological Society of America, Centennial Special Volume (scheduled for publication late 1987).

Madole, R. F., 1987, Quaternary stratigraphy and evidence for late Holocene movement on the Meers fault along Browns Creek and Canyon Creek, in Ferring, C. R., Late Quaternary Stratigraphy, Neotectonics and Geoarchaeology of Southwestern Oklahoma: Fifth Annual Field Trip, Friends of the Pleistocene South-Central Cell, Guidebook, p. 1-15. (Reprinted from Oklahoma Geological Survey Guidebook 24, with permission)

Chronology of Paleoearthquakes on the Wasatch fault zone by Thermoluminescence (TL) Dating

Contract #:14-08-0001-G1396

Principal Investigators: JAMES McCALPIN, Dept. of Geology Utah State University, Logan, Utah 84322, PH:801-750-1220
STEVEN L. FORMAN, INSTAAR and Dept. of Geological Sciences, Univ. of Colorado, Boulder CO. 80309, PH:303-492-1196,

I. OBJECTIVES

This study focuses on developing and applying the relatively new thermoluminescence (TL) technique to date Holocene and Pleistocene surface-faulting events on the Wasatch fault zone. For the TL technique to be useful sediment must have been exposed to light for a sufficient time during sedimentation to reduce previously acquired TL. After deposition, the TL signal accumulates in the mineral grains by exposure to ionizing radiation from the decay of radioactive elements. The TL technique is not dependent on locating dateable fossils but directly dates mineral grains, reflecting the time since deposition of the sediment.

In conjunction with U.S. Geological Survey the Ogden, Provo, Salt Lake and other segments of Wasatch fault zone have been sampled for thermoluminescence dating. Targeted samples for analyses are faulted loess and lacustrine sediment and fault derived colluvial-wedge sediments. The accuracy of the TL method is tested by dating modern and radiocarbon dated sites. These analyses are providing better constraints for defining the timing and re-occurrence of faulting events as well as ascertaining the extent of fault segments.

II. RESULTS

Samples Collected

A total of 54 samples (Table 1) have been collected for TL analyses from 12 trenches excavated by the U.S. Geological Survey and the Utah Geological and Mineral Survey. These samples were collected from a variety of sedimentary settings, which will allow us to ascertain which sedimentary environments are most amenable for TL dating. Large volume samples were taken for more accurate radioactivity measurements.

Table 1: Samples collected from the Wasatch fault zone for TL analysis

Site	Samples	Sediment Type
Brigham City trench	2	colluvial
East Ogden		
trench EO-1	11	colluvial
trench EO-2	7	colluvial/fluvial
trench EO-3	7	colluvial/buried soils
trench EO-4	3	colluvial
trench EO-5	2	colluvial
American Fork		
trench 1	6	Loess/colluvial/buried soils
trench 2	2	Lacustrine
trench 3	2	Loess/colluvial
Salem		
trench WH-2	6	colluvial/buried soils
Dresden Lane		
N trench	2	colluvial
S trench	4	colluvial

Development of Methods

For a TL date to be calculated the U, Th and K content of the sediment has to be accurately determined. With cooperation of Isotope Geology Branch, U.S. Geological Survey-Denver radioactivity determinations by the combined methods of alpha counting and atomic absorption spectroscopy (AAS) are compared to determinations by gamma spectrometry. (Table 2). Gamma spectrometry is the preferred method for radioactivity measurement because determinations are completed on more representative, large volume samples and this method can evaluate the equilibrium status of the U and Th decay chains. For most sediments alpha counting and AAS over-counted compared to gamma spectrometry, resulting in some significant differences in age calculations. In addition we are developing procedures to more accurately measure the radioactivity of diamicts.

Our experiments have addressed whether laboratory ultraviolet (UV) light is an effective simulation of natural light exposure. Results indicate that exposure of sediment to UV light at a 40 cm distance from the lamp with the UV heated-air vented does not result in sensitivity changes and is a close simulation of natural light.

Table 2: Dose Rates (mrad/year) by combined thick source alpha counting and atomic absorption spectroscopy (AAS) and gamma spectrometry*

Sample ID	Alpha & AAS	Gamma spectrometry
ITL2	552.1 ± 27.6	539.6 ± 27.0
ITL3	466.9 ± 23.3	411.0 ± 12.3 (U) 436.4 ± 13.1 (Ra)
ITL11	501.1 ± 20.0	418 ± 21
ITL12	388.5 ± 12.1	254.2 ± 7.6 (U) 249.1 ± 7.5 (Ra)
ITL13	290.9 ± 11.1	204.9 ± 6.2
ITL14	427.3 ± 19.2	362.4 ± 14.5 (U) 372.6 ± 14.9 (Ra)
CTL05	369.9 ± 13.0	340.1 ± 11.9
CTL16	370.3 ± 13.1	351.9 ± 10.6
CTL160	322.1 ± 12.9	240.7 ± 8.4
CTL48	538.3 ± 19.3	531.4 ± 18.6
CTLH2	296.9 ± 8.9	320.8 ± 9.6

* Assuming a = 0.15 ± 0.02 and H20 = 25% ± 3%

Application to Faulted and Fault Derived Sediments

Determining an accurate paleodose for colluvial wedge sediments such as those that accumulated after fault displacement, is predicated on the assumption that the TL signal of mineral grains is reduced by natural light during deposition. Our laboratory experiments on distal-slope sediment from a colluvial wedge indicate that this sediment is adequately bleached by exposure to light and hence dateable. Buried soils within colluvial wedge sequences are also well bleached by light and have produced reliable TL age estimates. Sag pond silts, which are often intercalated within colluvial wedges, and graben lake sediments are well bleached and thus are newly targeted sediments for dating. Loess, lacustrine, and flood-plain sediments that have been tectonically displaced also are amenable for TL dating.

Preliminary TL age estimates (Table 3) are in general agreement with "accepted geological ages". Radiocarbon dating of organic material associated with the above samples will provide a more rigorous test on the accuracy of the TL age estimates.

Table 3: Dose rates, equivalent doses and TL age estimates for samples from the Wasatch fault zone, Utah

Lab #	Sample Type	Dose Rate mrad/y	Equil. Dose (Krads)	TL Age Estimate(ka)	"Geological Age" (ka)
ITL2	loess	540±27	4.4 ± .5	8.2 ± 1	<15
ITL16	soil	302±17	1.1 ± .2	3.2 ± 1	2-4
ITL23	soil	398±19	<.60	<2	1-2
ITL3	sag pond	436±13	<.25	<1	modern
ITL18	sag pond	504±22	ND	ND	3-4

ND= no data

III. REPORTS

Forman, S. L., Jackson, M.J. and McCalpin, J., 1987: Thermoluminescence (TL) dating studies of colluvial and alluvial sediments from Utah and Colorado: preliminary results. Geological Society of America Abstracts with Programs, Rocky Mountain Section, v. 19(5): 275.

Forman, S. L. and Jackson, M. J. in press: The potential of dating by thermoluminescence fluvial and colluvial deposits in the western U.S.A. 5th International Specialist Seminar on Thermoluminescence and Electron-Spin-Resonance Dating Abstracts

Database Management

9910-03975

Charles S. Mueller
Branch of Engineering Seismology and Geology
U.S. Geological Survey
345 Middlefield Road, MS 977
Menlo Park, California 94025
(415) 323-8111, ext. 2989 or (415) 329-5646

Investigations

1. Development of techniques for data playback, processing, management, and export with emphasis on large datasets collected with portable digital event-recording seismographs (*e.g.*, GEOS).

2. Design and implement relational databases for strong-motion, aftershock, and special-experiment data. The goal of the database is to enhance researcher access to diverse Branch datasets.

Results

1a. The following new datasets were played back, processed, and archived:
Calaveras Seismic Investigation: ground motion experiment for Army Corps of Engineers.

1b. The following datasets were exported to other research institutions:
Calaveras Seismic Investigation: Army Corps of Enginners, Vicksburg, Mississippi.
Coalinga aftershock data: S-Cubed, San Diego, California.
Coalinga aftershock data: USGS Seismology Branch, Menlo Park, California.
Borah Peak aftershock data: University of Utah, Salt Lake City, Utah.

1c. FORTRAN software developed to enhance data processing and archival procedures: ASCEXP, XASCII--programs to reformat block binary waveform files to ASCII format for export.

2. Preliminary strong motion database and user's guide completed.

Reports

Converse, April M., 1987, User's guide to ESM: a database for strong-motion information: *U.S. Geological Survey Open-File Report 87-160.*

Earthquake Recurrence and Quaternary Deformation On the Cascadia Subduction Zone--Coastal Oregon

(New project, number not assigned)

Alan R. Nelson
Branch of Geologic Risk Assessment
U.S. Geological Survey
Box. 25046, MS 966, Denver Federal Center
Denver, Colorado 80225
(303) 236-1596

Investigations

1. A thorough study of the late Holocene sea-level record in coastal Oregon is required to evaluate the hypothesis that great plate-interface earthquakes have occurred due to the active subduction of the Juan de Fuca plate beneath western Oregon. Nelson completed a brief field reconnaissance of the Oregon coast north of Bandon looking for salt-marsh sites where coring may reveal evidence of coseismic subsidence during postulated great earthquakes. One or more buried salt-marsh surfaces were found at six of seven investigated sites. Future detailed work at each of these sites and additional sites is required to show when and if the surfaces were buried following coesismic subsidence. Work will begin on several sites in Coos Bay in July. Preliminary studies of marsh foraminifera faunas at selected sites will be made to determine if the faunas can be used to relocate former sea levels more accurately than can be done with marsh plants.

2. Long-term (late and middle Quaternary) deformation styles and rates along transects perpendicular to the coast will be investigated by Steve Personius. Steve will concentrate on mapping and dating fluvial terrace remnants in the larger Coast Range drainages. Reconnaissance investigations and previous mapping by others indicate suitable remnants along the Umpqua, Siletz, Siuslaw, Nestucca, and Nehalem Rivers. Work on the Umpqua and Siuslaw Rivers will begin in July. Attempts will be made to use thermoluminescence analysis and various relative methods to date the terraces. Terrace sequences will be tied to dated marine terraces where possible. Where marine terraces are undated, attempts will be made to date them.

Results

1. Reconnaissance coring at six salt-marsh sites along the Oregon coast north of Cape Arago revealed one to three peaty layers at 0.6-2.5 m depth. Detailed studies will be required to show if these buried marsh surfaces subsided suddenly during great earthquakes.

2. Several river valleys with sufficiently extensive terrace remnants to evaluate long-term deformation rates in coastal Oregon have been selected.

Reports

Nelson, A.R., Atwater, B.F., and Grant, W.C., 1987, Estuarine record of Holocene subduction earthquakes in coastal Oregon and Washington, USA [abs.]: International Union for Quaternary Research, 12th International Congress, Ottawa, Canada, Abstracts with Program. (Branch approval.)

Numerical Modeling of Rupture Mechanisms and Ground Motion of the 1886 South Carolina Earthquake

14-08-0001-G1273

Otto W. Nuttli and Robert B. Herrmann
Department of Earth and Atmospheric Sciences
Saint Louis University
P.O. Box 8099 Laclede Station
St. Louis, MO 63156
(314) 658-3131

Goals

1. Estimate source parameters for the 1886 Charleston earthquake based on historical observations and relationships to earthquake size and scaling laws.

2. Use source parameter estimates to model ground motion for the 1886 earthquake and compare to observations.

Investigations

1. Using Green's functions from a reasonable coastal plain earth model and a variable stress-drop distribution over small fault elements, we have modeled ground motion at regional distances (100 to 600 km) along 16 azimuths for three source models of the 1886 Charleston, South Carolina earthquake. At these distances the location of asperities (points of high stress drop) is found to have little effect on the calculated ground motion. Peak ground acceleration is more sensitive ot the number of fault elements used in the model than are the peak velocity and displacment or the pseudo-velocity respeonse spectra in the 0.05 - 1.0 Hz band.

2. Observational data obtained form Dutton's 1889 report on the earthquake intensity and direction of ground shaking at various cities and towns, when compared to the synthetic seismograms, do not allow us to select a preferred source model from the three considered: 1) a vertical, N-S striking fault with strike-slip motion, 2) a steeply dipping, NW-SE striking fault with reverse motion, and 3) a shallow dipping, NW-SE striking fault with reverse motion.

Results

A six chapter report detailing modeling procedures results and analysis is being prepared for publication.

Determination of the Subduction Geometry beneath Western Washington using Teleseismic Body Waveforms

Contract No. 14-08-001-G1343

Thomas J. Owens
Department of Geology
University of Missouri-Columbia
Columbia, MO 65211
(314) 882-3231

Investigation

This summary covers the period from January 20, 1987 to April 1, 1987; the first two months of this 1 year award. The project is designed to constrain the dip of the subducting Juan de Fuca plate beneath western Washington using broadband teleseismic receiver function analysis on data recorded on a linear east-west profile of digital event recorders located at about 46.8°N. The array was installed by R.S. Crosson of the University of Washington and has been operating since the fall of 1986. The instrumentation for the sites consists of Sprengnether DR-200 digital event recorders and Kinemetrics SV-1/SH-1 intermediate period seismometers. The profile consists of 4 stations extending from the site of a recent study by Owens *et al.* (1987) near Satsop, WA eastward toward Mt. Rainier. The portable instruments are spaced at 20 to 30 km intervals. Data from the intermediate period passband of DWWSSN station LON (Longmire, WA) are also being analyzed for comparison with our data.

Results

We have just begun to assemble and analyze the data set. Progress includes:

1. Collection and processing of 46 teleseismic events from LON. Our original event list consisted of 164 events, $Mb \geq 6.0$ known to be well-recorded in North America. Of these, only 46 actually triggered the intermediate-period passband at LON, due to the low sensitivity of the triggering algorithm. The 46 events that were available are good quality and have been processed to isolate the receiver structure response. These receiver functions tend to have slightly increased noise level near about 1 Hz, possibly due to a peak in the intermediate period instrument response at this frequency. It is immediately obvious that the LON receiver functions are more complex than the receiver functions from the rest of the array. The shallow complexities in structure observed by Langston (1979) in his analysis of LON long-period data clearly dominate the intermediate period response as well. We are presently attempting to deal with these problems so we can proceed with analysis of the deep structural effects.

2. Processing of 30 events recorded by the temporary stations prior to mid-January, 1987. Data from these sites are quite encouraging. Although interpretation is still preliminary, there is strong evidence for the azimuthal variation in Ps converted phase amplitudes that Owens *et al.* (1987) use to model the slab depth and dip at the westernmost array site near Satsop, WA. Our analysis of these effects and their geometric basis continues with the goal of developing improved constraints on the structure and geometry of the Juan de Fuca plate beneath western Washington.

Acknowledgements

We are indebted to John Hoffman, USGS Albuquerque Seismological Laboratory, for assistance in identifying events which triggered the intermediate passband at LON.

References

Langston, C. A. (1979). Structure under Mount Rainier, Washington, inferred from teleseismic body waves, J. Geophys. Res., 84, 4749-4762.

Owens, T.J., R.S. Crosson, and M.A. Hendrickson (1987). Constraints on the subduction geometry beneath western Washington from broadband teleseismic waveform modeling, in preparation, to be submitted to J. Geophys. Res.

Quaternary Framework for Earthquake Studies
Los Angeles, California

9540-01611

John C. Tinsley
Branch of Western Regional Geology
U.S. Geological Survey
345 Middlefield Road, MS 975
Menlo Park, California 94025
(415) 329-4928

Investigations

1. Geology and relative ground motion, Wasatch Region: Project activities included continued analysis of logs of boreholes and samples obtained during the drilling operations conducted in the Salt Lake City area during FY 86. Contract specifications for a second and final phase of site-characterization investigations in the Wasatch region have been forwarded to the U.S. Geological Survey's Contracts Section for presentation and bid. Operations including the drilling and sampling of about 20 additional exploratory boreholes at selected stations in the Provo, Utah and Ogden, Utah areas are scheduled for August and September, 1987. (J. Tinsley, D. Trumm, K. King, and D. Carver).

2. San Gorgonio Pass fault zone: Trenching and soil stratigraphic analyses of faulted fluvial terraces and alluvial fans have emphasized determining the history of fault displacement along reverse faults that bound the south margin of the San Bernardino Mountains. Progress has been stalled while awaiting the results of radiocarbon analyses and chemical analyses of soils sampled during the trenching conducted during June and July, 1986. (J. Tinsley, J. C. Matti, D. Trumm, S. Goldfinger, and R. Versical).

3. Holocene stratigraphy and fold deformation rates near Coalinga, CA: Recent field studies have emphasized detailed mapping and interpretations of selected exposures of Holocene sediments along Los Gatos Creek, from the Pleasant Valley syncline across the Coalinga anticline into the San Joaquin Valley. The studies of surficial geology have been augmented by efforts to map the contact with the underlying Tulare Formation in the subsurface along Los Gatos Creek, using shallow seismic refraction techniques and drillers' descriptions contained in water well records. The mapping of a 5000-year old isochron from the vicinity of the anticlinal fold axis westward into the Pleasant Valley syncline has been frustrated owing to extensive and laterally persistent cut- and-fill relations involving chiefly channel deposits within this critical reach. We are considering the feasibility of a modest truck-mounted augering operation to locate additional, older floodplain facies within the Pleasant Valley syncline and to recover datable material from these horizons. (D. Trumm, R. Versical, R. Stein, and J. Tinsley).

4. Geology of ground motion stations and regional aspects of site-response in the Puget Sound area, Washington:

In late February, 1987, study of the geology beneath ground-motion instrument sites in the Seattle, WA area was initiated. In order to build upon building upon the extensive, ongoing and prior studies of the earthquake hazard of the region, I anticipate involving many local agencies and representatives in the effort to extending the techniques employed in the Los Angeles, CA and Wasatch Front, UT to the Puget Sound area, geologic settings in which the presence or absence of Late Cenozoic glacial ice is a signficant factor in the basinal history. Initial emphasis of this study is on the geology of the Seattle area, specifically those areas where significant damage owing to ground motion accompanied the 1965 earthquake (J. Tinsley, K. King, A. M. Rogers, D. Carver, A. Tarr).

Results:

1. Lithologic logs, 3-inch Shelby-tube-type samples, down-hole shear wave and compressional wave velocity profiles, and soil parameters including bulk density, dry density, consolidation tests, particle size analyses and unconfined compressive strength studies will comprise a suite of geologic data that will be used to characterize ground-motion recording stations in the Provo and Ogden areas, Utah. About 20 sites will be drilled; the selection of sites will be determined chiefly by the accessibility of any site to drilling equipment and of course the permission of the owner. Approximately 60 sites now exist at which ground motion emanating from the Nevada Test Site has been recorded on different site geologies; we will have drilled 40 of these by the end of FY 87. The thickness of various semiconsolidated and unconsolidated key strata and the wave-propagation characteristics of the deposits will enable sites to be classed in terms of site period, frequencies most likely to be amplified during earthquake shaking, and geologic characteristics most useful for predicting site response.

2. Radiocarbon dates obtained using accelerator-mass spectrometer techniques through Beta Analytic, Inc. have been received and the data are being analyzed. At least one event in the past 3000 years has produced 187 cm of dip slip on the lowest and presumably most recent scarp considered in this study. It seems desirable to conduct additional studies of the highest scarp, in order to determine the degree to which changes in scarp profile correspond to the position of reverse faulting that generates the scarp. Landowner relations permitting, additional studies are scheduled for June, 1987. See the previous semi-annual technical report of this project for general information concerning the findings in the trenches.

3. The Holocene history of Los Gatos Creek near Coalinga, CA has been characterized by a series of at least 4 aggradational episodes during the past 5500 radiocarbon years before present. Detailed mapping of outcrops recently exposed by winter discharge along Los Gatos Creek indicates that the oldest Holocene sediments may be exposed near locality C84-101. Fine-grained silt containing 4-inch diameter sections of trees up to 4 ft. in length were mapped

and sampled for radiocarbon analyses. Mapping of the Tulare Formation beneath the Holocene and late Pleistocene (?) deposits bridging and flanking the Coalinga Anticline has been accomplished using shallow seismic refraction techniques. The seismic stratigraphy indicated by profiles at 12 localities along Los Gatos Creek is shown in table 1. Detailed analyses and construction of detailed cross-sections using these relations and relations gleaned from lithologic logs of water wells is in progress at this writing.

4. The initial results of the Puget Sound study are sparse. Initial contacts have been made in the Portland, OR, area, and contacts have also being made in the Seattle-Tacoma-Port Townsend areas. Nine instrument stations have been deployed in the Seattle area; the geologic setting of these stations is being evaluated using a database assembled by James C. Yount (USGS, Menlo Park).

Reports:

1. Morton, D. M., Matti, J. C., and Tinsley, J. C., 198 , Cucamonga fault zone scarps, Day Canyon alluvial fan, Eastern San Gabriel Mountains, Southern California, in Hill, M. (ed.) Decade of North American Geology Volume, approved by the Director, 3/13/87.

2. Morton, D. M., Matti, J. C., and Tinsley, J. C., 198 , Banning Fault, Cottonwood Canyon, San Gorgonio Pass, Southern California: in Hill, M. (ed.) Decade of North American Geology Volume, approved by the Director, 3/13/87.

Seismic-refraction profiles near Coalinga

Line no.	Material	P-wave velocities (m/s)	Location below surface(m)	Total Thickness(m)
RL-1	Unconsolidated alluvium	340	0 - 9	9
RL-2	Unconsolidated alluvium	380	0 - 1	1
	Tulare Formation	1980	1	
RL-3	Unconsolidated alluvium	380-420	0 - 3	3
	Unconsolidated alluvium	470-500	3 - 13	10
	Unconsolidated alluvium	740-770	13 -27	14
RL-4	Unconsolidated alluvium	400	0 - 3	3
	Unconsolidated alluvium	850	3 - 37	34
RL-5	Unconsolidated alluvium	360	0 - 7	7
	Tulare Formation	2060	7	
RL-6	Unconsolidated alluvium	350	0 - 11	11
	Tulare Formation	2020	11	
RL-8	Unconsolidated alluvium	250	0 - 6	6
	Unconsolidated alluvium	600	6 - 18	12
	Unconsolidated alluvium	940	18 - 81	63
	Tulare Formation	4480	81	
RL-9	Unconsolidated alluvium	230	0 - 4	4
	Unconsolidated alluvium	440	4 - 14	10
	Unconsolidated alluvium	1160	14 - 48	34
	Tulare Formation	4570	48	
RL-10	Unconsolidated alluvium	350	0 - 4	4
	Unconsolidated alluvium	700	4 - 6	2
	Unconsolidated alluvium	850	6 - 21	15
	Tulare Formation	2110	21	
RL-11	Unconsolidated alluvium	360	0 - 5	5
	Unconsolidated alluvium	920	5 - 8	8
	Tulare Formation	2770	8	
RL-12	Unconsolidated alluvium	360	0 - 3	3
	Unconsolidated alluvium	590	3 - 11	8
	Unconsolidated alluvium	900	11 - 25	14
	Tulare Formation	1740	25	

This refraction data is used to map the structure contours of the Tulare Formation at depth across the Coalinga Anticline. The Tulare is the youngest folded formation mapped across the Coalinga Anticline. This data shows the Tulare to have a dip of 12 degrees on the western flank and 6 degrees on the eastern flank which shows that the anticline is asymmetric.

GEOLOGIC MAPPING ALONG THE BORDER RANGE FAULT ZONE, ANCHORAGE, ALASKA

14-08-0001-A0237

Randall G. Updike

Engineering Geology Section
Alaska Division of Geological and Geophysical Surveys
P.O. Box 772116
Eagle River, Alaska 99577
(907) 696-0070

Investigations

1. Detailed bedrock and surficial geologic mapping, at 1:25,000 scale, of eight quadrangles located astride the Border Ranges Fault Zone, Chugach Mountains, east and north of the Anchorage metropolitan areas, to determine possible Holocene movement.

2. Three-dimensional engineering geologic mapping of Quaternary deposits in the City of Anchorage, to assess the potential for seismically induced ground failure.

3. Conduct site-specific geotechnical studies of engineering soils in Anchorage, to determine their behavior under static and dynamic loading.

Results

1. Field mapping of the bedrock geology of the Anchorage A-7NW (Temptation Peak) and Anchoarage A-8NE (East Anchoarage) quadrangles completed. Laboratory analyses in progress.

2. Completion of the manuscript versions of the bedrock and surficial geology of the Anchorage B-7NE (Mt. Eklutna) and B-7SE (Mt. Magnificent) quadrangles.

3. A geophysical survey of the Border Ranges Fault Zone in the floor of Eklutna Valley, utilizing seismic reflection (dynamite energy source), gravimetry, and magnetometry. Holocene displacements could not be determined but accurate fault location beneath glaciofluvial deposits was attained. Trenching and seismic reflection surveys are needed.

4. Completion of construction of seven (7) engineering geologic cross-sections north-south and east-west across metropolitan Anchorage, at 1-meter resolution, showing variation in geotechnical properties and subsurface disconformities to 100 m depth.

5. Acquisition of 47 geotechnical consultant reports for sites in Anchorage, containing more than 350 geotechnical borehole logs. These are added to the several thousand technical logs currently on file.

6. Computer processing and interpretation of six electric cone penetrometer test sites completed.

7. Completion of data analyses of a drilling and sampling program on tidal flats in Turnagain Arm (Girdwood and Portage) which has recovered buried peat horizons yielding C-14 age dates to 4200 ybp. THese horizons are believed to record tectonic subsidence events of major earthquakes similar to the 1964 earthquake. Our age dates correlate well with raised beach dates of Prince William Sound (Plafker and Rubin, 1967), and yield an average recurrence interval of 425 to 730 C-14 yrs between 2000 and 4200 ybp.

8. Three site specific geotechnical reports have been prepared and are in various stages of review and edit for publication:

   (1) "Earthquake-induced landslides, Anchorage, Alaska -- a geotechnical re-evaluation", by R.G. Updike, Y. Moriwaki, I.M. Idriss, J.A. Egan, and T.L. Moses, submitted to GSA Bulletin.

   (2) "Geologic and geotechnical conditions adjacent to the Turnagain Heights Landslide, Anchorage, Alaska", by R.G. Updike, H.W. Olsen, H.R. Schmoll, K.H. Stokoe II, and Y.F. Kharaka, in TRU-Denver as a USGS Bulletin.

   (3) "Cyclic triaxial tests of the Bootlegger Cove Formation, Anchorage, Alaska, by P.V. Lade, R.G. Updike, and D.A. Cole, in TRU-Denver as a USGS Bulletin.

Reports recently published

Updike, R.G., 1986, Engineering-geologic maps of southwest Anchorage, Alaska: Alaska Division of Geological and Geophysical Surveys Professional Report 89.

Updike, R.G., 1986, Engineering geologic maps of the Government Hill Area, Anchorage, Alaska: U.S. Geological Survey Map I-1610.

Updike, R.G., and Ulery, C.A., 1986, A geotechnical cross-section of downtown Anchorage -- an assessment using the electric cone penetration test: Alaska Division of Geological and Geophysical Surveys Report of Investigations 86-3, 41 p.

Updike, R.G., and Carpenter, B.A., 1986, Engineering geology of the Government Hill area, Anchorage, Alaksa: U.S. Geological Survey Bulletin 1588, 32 p.

Updike, R.G., and Oscarson, R.C., 1987, An atlas of facies microfabrics of the Bootlegger Cove Formation using the scanning electron microscope: U.S. Geological Survey Open-file Report 87-60, 115 p.

Central California Deep Crustal Study

9540-02191

Carl M. Wentworth
Branch of Western Regional Geology
U.S. Geological Survey
345 Middlefeild Road, MS-975
Menlo Park, California 94025
(415) 329-4950

Tentative Regional Framework of the Parkfield Segment of the San Andreas Fault

A small-scale geologic map of the Parkfield region (fig. 1) and associated topographic map (fig. 2), prepared in cooperation with R.C. Jachens and R. W. Simpson, provide a tentative framework within which to view the Parkfield segment of the San Andreas fault in central California. (The geologic map was compiled from the 1:250,000 and 1:750,000 state geologic maps, locally modified from Dibblee's 1:62,500-scale maps and the present work; the topographic map was prepared by Simpson from a 15-second file of average altitudes.)

The structure and topography for as much as 25 km southwest of the San Andreas fault are relatively simple, and principally involve southwestward tilting of the crystalline basement and Cenozoic sedimentary cover. The basement seems otherwise undeformed except for two reverse faults above which a large chip of basement has been thrust southwestward slightly. These faults are based on a seismic reflection line (SJ-6; see OF 85-22, p. 149) and associated gravity gradients.

Northeast of the San Andreas fault, structure and topography are complex and record extensive crustal shortening, through faulting and folding, that is largely normal to the fault. The greater Cholame Valley (surrounding Gold Hill) marks a low around which structure and topography seem to flow southeastward in an S-shaped pattern. This pattern terminates at the large, east-trending thrusts due east of Cholame. The northern boundary of this Cholame depression seems marked by thrusts that are overlain by Franciscan rock. Similarly, the serpentinite-cored New Idria block farther northwest is underlain on the southwest by thrusts inferred from associated gravity gradients. On the east, this block is bounded by a large structural discontinuity involving right lateral faulting at depth that strikes southward toward the Parkfield preparation zone.

Explanation for Figure 1.

- Quaternary alluvium
- Pliocene and Quaternary sediments
- Upper Tertiary strata
- Lower Tertiary strata
- Tertiary volcanic rocks
- Mesozoic strata
- Plutonic rocks
- Serpentinite
- Franciscan Assemblage

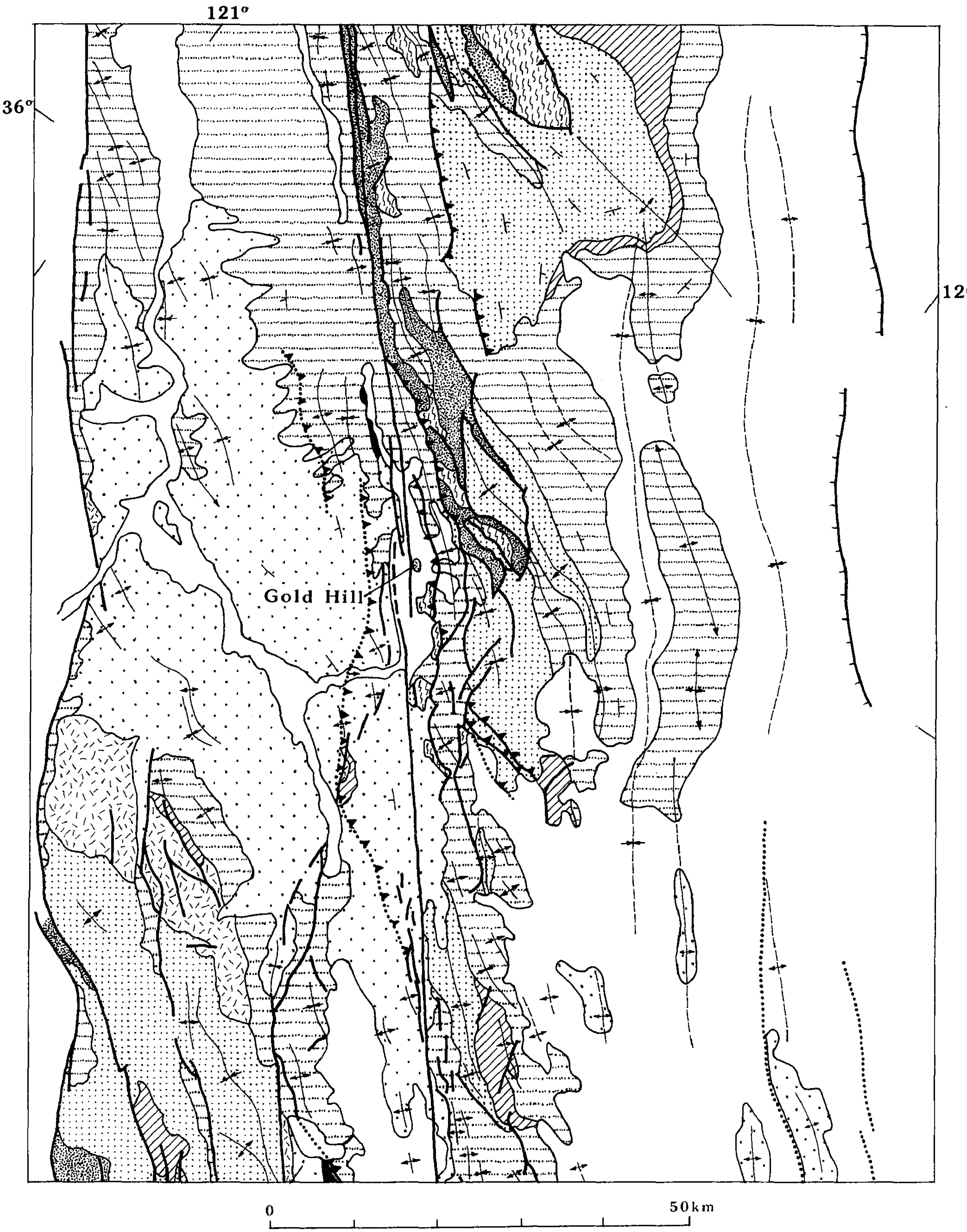

Figure 1.--Tentative geologic map of the Parkfield region.

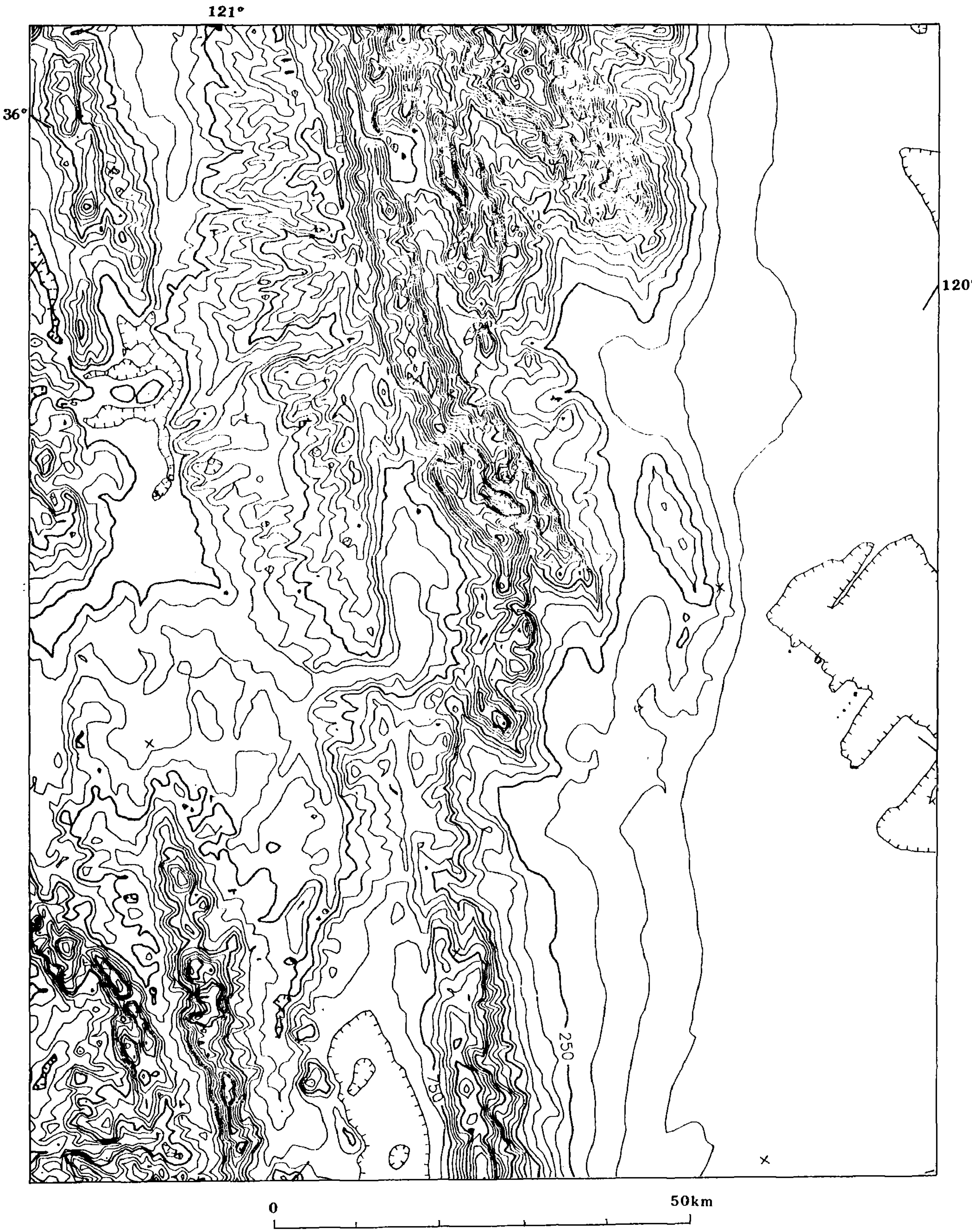

Figure 2.--Smoothed topography of the Parkfield region.

Liquefaction Risk Map for Boston

14-08-0001-G1188

Robert V. Whitman
Herbert H. Einstein
Daniele Veneziano

Department of Civil Engineering
Massachusetts Institute of Technology
Cambridge, MA 02139
(617)253-7127

This study was formally established 1 December 1985, with work commencing 1 February 1986. The study has three major components: 1) the determination of liquefaction susceptibility of different soils; 2) estimation of earthquake intensities, recurrence intervals and based thereupon the shaking hazard at different locations; 3) combining of 1 and 2. The work is divided into 4 tasks.

Task 1: Geologic Classification

Two reports which contain the geologic classification of soils underlying the cities of Boston and Cambridge are going through the final editing at present. They will be completed within the next few weeks.

Report 1 deals with the natural soil deposits. It contains a review of the geologic history of the sediment deposits in the Boston Basin. A number of discrepancies in the geologic literature could be reconciled while others remain and require resolution through further geologic research.

The main body of this report consists of digitized data on Boston subsoil conditions based on the BSCE boring log reports and a computer code which allows its user to specify any line or combinations of lines on the map and to obtain a soil profile along this (these) line(s). The report presents a number of such profiles in Boston and Cambridge to provide a representative picture of the subsoil conditions. Cohesionless soils (which are potentially liquefiable) are identified in these profiles (Note that the digitized data include information on natural soil and artificial fill, as well as on rock). The digitization is continuing and it is estimated that by early summer all boring data in the BSCE reports will be digitized correspondingly.

Report 2 contains detailed descriptions on the fills underlying Boston and Cambridge. The research consisted of a review of historical records updated by recent boring information. Fill areas are distinguished by the time when they were filled, the material and the methods used. The documentation is in the form of maps and associated descriptions. The information allows one to make a first, subjective, estimate on which fills are potentially liquefiable.

Further work regarding task 1 (in addition to the digitizing mentioned above) will consist of collecting more recent data on Boston subsoil conditions (the BSCE reports for this area only contain data up to the year 1969, the Cambridge data go all the way up to 1984). Also, selected areas outside the two cities, notably in zones where liquefaction may be possible, will be included.

It would clearly be desirable to continue the digitizing effort to include all boring data and foundation excavation records which are in the files of local geotechnical firms.

Task 2: Probability Distribution of SPT Value for Each Geologic Class

In order to evaluate earthquake liquefaction potential, one needs to quantify uncertainty on the soil characteristics that are related to the liquefaction phenomenon. In this study, such characteristics are taken to be the geologic class, G, and the corrected blowcount number, N. Corrections of the blowcount number are made to account for depth, water table elevation, and SPT procedure. Other factors, such as age and mode of deposition of the soil, are considered to affect liquefaction potential through the uncorrected blowcount number.

Uncertainty on the geologic class G at each geographical location is assessed judgementally, whereas uncertainty on N is quantified through statistical data analysis. Work to date on N has concentrated on the Back Bay fill. Based on construction records and boring logs, the N values from the Back Bay fill area have been classified according to three factors: type of material (city ashes and refuse, gravel from the hills in the Boston peninsula, sand and gravel from Needham, and material from the Charles River), age (we have distinguished six periods: 1814-1816, 1836-1851, 1858-1861, 1861-1871, 1871-1881, and 1929-1931), and mode of transportation and deposition (material carried by cart, dumped directly from rail cars, hydraulically dredged, excavated from the Charles River and deposited in various ways). We have then searched for the factors with significant influence on N. Our conclusion is that neither age nor mode of deposition are influential. We have further concluded that, for the purpose of charaterizing uncertainty on N, the four material classes can be collapsed into three, by grouping together "gravel from Boston" and "sand and gravel from Needham".

For each of the resulting three material classes, we have performed several statistical analyses on the N values to determine the type of probability distribution, the existence of systematic spatial variations (trends), and the degree of spatial correlation. The last characteristic is important for the quantification of uncertainty on N at sites where no direct determination of N is available.

Results can be summarized as follows:

1. The uncorrected values of N are well fitted by lognormal distributions;

2. Spatial trends on the horizontal plane are small and statistically non significant. For some of the materials, the trend with depth is significant and indicates a decrease of N for increasing depth;

3. Spatial correlation is small. This is especially true for the "gravel and sand" material, for which correlation is practically nil at horizontal distances larger than about 50 feet.

A consequence of the above results is that, for most of the sites in the Back Bay area, uncertainty on N is well expressed by the lognormal distribution obtained by pulling together all the SPT values from the appropriate geologic class. Exceptions are sites very close to blowcount measurements.

The characterization of uncertainty on soil-deposit will be completed by performing the following tasks:

1. Examination of possible nonhomogeneities within the above-mentioned soil classes.

2. Analyses of more recent and better documented blowcount data, mainly to confirm our current findings;

3. Extension of the analyses to fills and natural deposits outside the Back Bay area; and

4. Judgemental quantification of uncertainty on the geologic class G at various sites in the Boston area.

Task 3: Liquefaction Susceptibility as a Function of Soil Parameters

The work under task 1 provides the basis for identifying liquefiable soil on the basis of the geologic and man made history. Amongst the natural soils the fine sands/silts overlying the Boston Blue Clay in some areas are of concern. Also, the sensitive clays in the Alewife Brook area require further study in this respect. Fills consisting of sands and silts which have been placed by the suction pumping-slurry pipeline procedure or by dumping from barges (scows) into deep water are potentially problematic. Cinder and ashes, although usually dumped overhead from the advancing fill front also require further study as to their liquefaction potential. With regard to these fills and some of the natural soils it should be kept in mind that they are often removed before a foundation is placed.

Initial work on a more quantitative identification of liquefaction susceptibility has been performed on the basis of SPT data. SPT values for the fills in the Back Bay area have been plotted on maps and in summary graphs showing SPT value versus depth. The same was done for silts, sands and gravels along a few selected profiles in the Boston peninsula. These plots allow one to identify areas where potentially liquefiable soils exist.

In addition, this information is being used to establish correlations between geologic information and SPT values. Such correlations will be used to extrapolate and interpolate soil conditions in zones where insufficient direct information is available.

Task 4: Seismicity and Attenuation Models

We have continued the analysis of seismicity and attenuation in the Northeastern United States. For the analysis of seismicity, we have developed a new procedure that is insensitive to the specified configuration of earthquake sources. The lack of sensitivity is achieved by the means: 1. the parameters of the Gutenberg-Richter law are allowed to vary on the geographical plane inside the "homogeneous sources", and 2. the degree of smoothness in the spatial variation of the parameters within each source is determined directly from the historical seismicity data, using statistical goodness-of-fit criteria. Using this new procedure, we are now generating recurrence relationships for the region of interest to the project, namely the Northeastern U.S. and adjacent Southeastern Canada, based on the Weston Observatory Catalog. Two brief reports, one concerning seismicity and one about attenuation, will soon become available. These documents will briefly review the methods of analysis and describe the models selected for the evaluation of liquefaction potential.

April 1987

Worldwide Standardized Seismograph Network (WWSSN)

9920-01201

Russ Wilson
WWSSN Project Chief
Branch of Global Seismology and Geomagnetism
U.S. Geological Survey
Albuquerque Seismological Laboratory
Building 10002, Kirtland AFB-East
Albuquerque, New Mexico 87115-5000
(505) 844-4637

Investigations

1. Technical and operational support was provided to each station in the Worldwide Standardized Seismograph Network (WWSSN) as needed and required.

2. Ninty-five (95) modules and components were repaired, and one hundred ninety (190) separate items were shipped to ninety-six (96) separate locations to support the WWSSN network during this period.

Results

1. A continuous flow of high-quality seismic data from the cooperating WWSSN stations within the network was provided to the users in the seismological community.

WWSSN Maintenance and Calibration Visits:

1. South Pole, Antarctica (SPA) - September 29, 1986, through October 10, 1986, Mr. Ken Murphy from Reston, Virginia and Mr. Greg Littin from Phoenix, Arizona were trained to operate the (SPA) WWSSN station during the Antarctic winter-over period.

2. Scott Base Antarctica (SBA) - During November 1986, Mr. Jack Dorneden, field engineer for the Albuquerque Seismological Laboratory (ASL), converted the WWSSN station from photographic recording to hot-pen recording (helicorder). SBA is now operating four channels, three LP at magnitude 750 and one SPZ at magnitude 50K.

3. Nurmijarvi, Finland (NUR) - During March 1987, Mr. Juan Nieto, field engineer from ASL, visited the NUR WWSSN station.

Hot Pen Conversion:

1. March 1987 - Six hot-pen conversion kits (production model prototype) were received from Kinemetrics, Inc. and installed at the ASL WWSSN station (ALQ) for a 30-day evaluation.

2. The first production quantity of heated-pen conversion kits from Kinemetrics are to be shipped to ASL in July 1987.

National Map of Liquefaction Hazard

14-08-0001G1187

T. Leslie Youd
Dept. of Civil Engineering
Brigham Young University
Provo, Utah 84602
(801) 378-6327

Objective:

One of the key tools for evaluating earthquake hazards is a map showing liquefaction hazard. The purpose of this project is to prepare a liquefaction hazard map for the 48 contiguous U.S. states. This map will show contours of a parameter termed liquefaction severity index (LSI) which is a measure of anticipated ground displacement, the damage producing consequence of liquefaction. LSI will be contoured to provide an estimate of severity of expected liquefaction effects with a high degree of probability of not being exceeded in a given period of time. For sites underlain by liquefiable soils, LSI provides an index for estimating probable ground displacement, however, site specific investigation is required to confirm the presence or absence of liquefiable material. The latter information can not be effectively mapped on a national scale.

Results:

1. The basic equations relating LSI, earthquake magnitude, and distance from the earthquake source developed by Youd and Perikins (in press) were evaluated and adopted for this study.

2. The program SEISRISK II was adapted and necessary modifications made to operate on the computers and graphics terminals at Brigham Young University. Some modifications were also made to make the program easier to use and more user friendly.

3. An equation was developed for relating LSI to earthquake magnitude and distance from the energy source in the eastern United States. Reports from the 1811-12 New Madrid, Missouri, earthquakes and the 1886 Charleston, South Carolina, earthquake were reviewed and LSI data compiled to verify the equations developed for the eastern U.S. Crustal attenuation of ground motion is less in the eastern U.S. is smaller than in the western U.S. where the equations of Youd and Perkins were developed. Thus, the LSI equations required adjustment to reflect the greater distances to which strong ground motions are transmitted in the eastern U.S.

4. Using a map of seismic source zones and a tabulation of expected earthquake activity prepared by Algermissen and others (1982), the equations developed in item 3 above, and the SEISRISK II algorithm, maps for the conterminous United States were generated showing contours of LSI values with 90 percent probability of not being exceeded in periods of 10, 50 and 250 years respectively. See map for 50-year exposure time reproduced on next page.

5. A draft report for the project has been prepared and is presently being examined by colleagues to evaluate the validity of data and results and to review text and figures. A 6-month, no-cost extension of the project was granted to make these evaluations and revisions, and to initiate preparation of a journal paper.

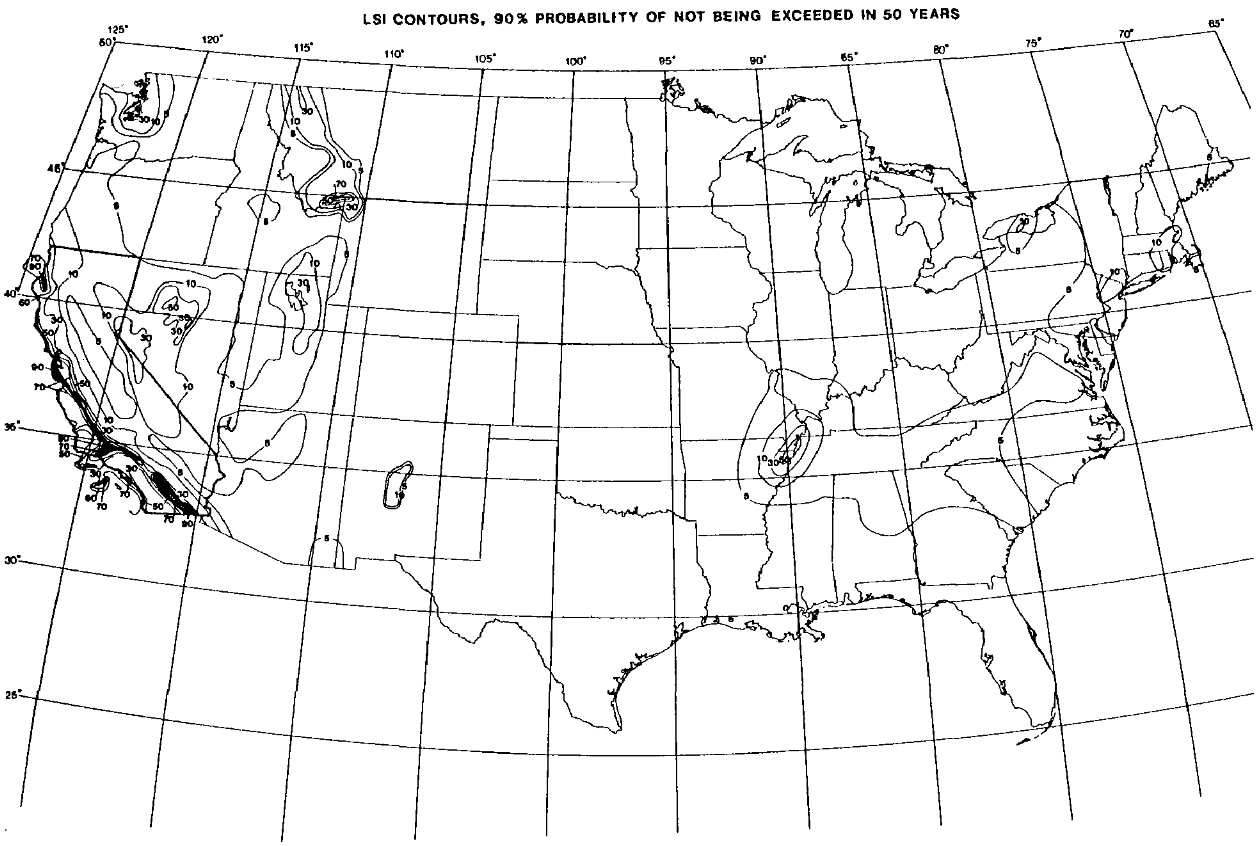

Geophysical and Tectonic Investigations of the Intermountain Seismic Belt

9930-02669
Mary Lou Zoback
Branch of Seismology
U.S. Geological Survey
345 Middlefield Road, Mail Stop 977
Menlo Park, California 94025
(415) 329-4760

Investigations

1. Analysis of seismic reflection, well, and gravity data along the southern Wasatch fault zone near Nephi, Utah.

2. Analysis of the state of stress in the south-central United States (with special emphasis on the vicinity of the Meers fault in Oklahoma) using wellbore elongations or "breakouts".

3. Investigation of the state of stress and style of tectonism within the Walker Lane belt, Western Great Basin.

Results

1) Seismic reflection and gravity data suggest that the overall structure of Juab Valley is an asymmetric sag bounded on the east by the Wasatch fault zone, with beds on both sides of the valley tilting towards the axis of the valley. A central graben defines the deepest part of the basin. Anderson and others (1983) and Zoback and Anderson (1983) have identified this type of basin as commonly being bounded by one or more major, planar, steep normal faults. The maximum valley fill thickness is about 1.60 km based on a combined interpretation of both the reflection and gravity (assuming a density contrast for basin sediments of -0.4 g/cm^3). Possible displacement of a buried thrust(s), truncation of deep reflectors, and absence of reverse drag in basin sediments suggest that the Wasatch fault zone has a planar, high-angle with a dip of 50°-55° (as opposed to a listric or low-angle geometry). However, the lack of reverse drag within basin sediments is the strongest evidence against a listric geometry.

   On a more regional note, structural data suggest the presence of major ramps in the Mesozoic thrust system near the trace of the modern Wasatch fault at several localities along its length. One possible source for this ramping may be major crystalline basement displacements on normal faults formed along a north-trending, west-facing passive margin that developed through the region in late Proterozoic time (Stewart, 1972). Thus, the modern Wasatch fault zone may be localized by a zone of pre-existing extensional faulting in Precambrian crystalline rocks.

2) Dipmeter and fracture-identification well logs from 180 oil and gas wells in a study area extending from the Texas Panhandle to the Mississippi River (including Oklahoma and Arkansas) yield information on the orientation of horizontal crustal stresses. The stress data are inferred from approximately 1,000 directionally oriented well-bore elongations (breakouts) totalling over 26,000 vertical feet. Within this area, the wells are located in nine structural provinces: the Mississippi

Embayment, Arkoma basin, Ouachita fold belt, Anadarko basin, Ardmore-Marietta basins, southern Oklahoma aulacogen, Midland basin, Palo Duro-Dalhart basins, and the Hugoton Embayment.

Wells located in the central part of the study area from Oklahoma to the Mississippi River form a high-quality data set having a consistent NNW- to N-trending orientation indicative of an ENE regional maximum horizontal compressive stress (S_{Hmax}) direction. These data agree with a S_{Hmax} orientation of N 65°E based on a hydrofracture study in central Oklahoma. This high-quality data set includes breakout orientations from wells in south-central Oklahoma in the vicinity of the WNW-striking Meers fault. The ENE regional S_{Hmax} is compatible with evidence of Holocene left-lateral oblique slip on the Meers fault. Possible deviation from this regional stress trend is seen in the orthogonal NW and NE breakouts in wells in the southwestern part of the study area. This apparent local deviation could be related to a complex tectonic and structural history. However, it is possible that drilling-induced hydraulical fractures may appear as borehole elongations on fracture-identification well logs. If this is the case, this orthogonal data might be compatible with the regional S_{Hmax}; that is, the NW-oriented breakouts are normal to the regional S_{Hmax} as expected, while the NE-trending "breakouts" may in fact be hydraulic fractures oriented subparallel to S_{Hmax}. Elsewhere within the study area, highly variable breakout orientations preclude a determination of the current tectonic stress orientations.

3) Late Cenozoic through Holocene deformation in a broad band along the Sierra Nevada - Great Basin boundary zone in eastern California and western Nevada is characterized by a mix of normal, strike-slip, and normal oblique faulting. Earthquake focal mechanisms and detailed observations of fault slip indicate a rather uniform WNW to E-W least principal stress orientation (S_{hmin}) for this faulting. A uniform S_{hmin} orientation imples that the observed normal and strike-slip faulting results from variations in the relative magnitude of the maximum horizontal stress (S_{Hmax}) and the vertical stress (S_V).

Detailed observations of fault slip in the Owens Valley area constrain the magnitude of these variations. Field investigations of the Owens Valley fault zone by Beanland indicate that the dominant sense of Holocene offset is right-lateral strike-slip with an estimated ratio of lateral to vertical offset for the ($M \sim 7.7$) event averaging 6:1 and possibly as great as 10:1. This fault zone lies in the valley 5 to 20 km east of the subparallel Sierra frontal fault zone. Late Pleistocene slip on the Sierran frontal fault is dominantly dip-slip. An analysis of stress and slip directions assuming a regional S_{hmin} orientation of N 80°W indicate the nearly pure normal dip slip along the Sierran frontal zone occurs when $S_{Hmax} \simeq S_{hmin}$. Whereas, the strike-slip offset on the Owens Valley fault zone in 1872 indicates a stress regime in which $S_{Hmax} \simeq S_V$. Thus, there appears to have been large fluctuations in relative magnitude of the ~ N-S oriented S_{Hmax} in late Pleistocene to Holocene time.

Reports

Zoback, M. L., in press, Superimposed Cenozoic, Mesozoic, and possible Proterozoic deformation in central Utah: U.S. Geological Survey

Professional Paper on "Evaluation of Urban and Regional Earthquake Hazards and Risk in Utah", (currently at TRU).

Zoback, M. L., and Beanland, S., 1986, Temporal variations in stress magnitude and style of faulting along the Sierran frontal fault system: Geological Society of America Abstracts with Program, v. 18, p. 801.

Zoback, M. L., and Beanland, S., 1986, Stress and tectonism along the Walker Lane Belt: EOS, Transactions American Geophysical Union, v. 67, p. 1225.

Dart, R. L., 1987, Horizontal stress orientations from well-bore breakouts in the south-central United States: Geological Society of America Abstracts with Programs, v. 19, in press.

Wasatch Front County Hazards Geologist Program

14-08-0001-G991

Gary E. Christenson
Utah Geological and Mineral Survey
606 Black Hawk Way
Salt Lake City, Utah 84108
(801) 581-6831

INVESTIGATIONS:

1) Compilation of basic-data maps for use in deriving translated hazard maps.
2) Review of engineering geologic reports.
3) Aid to planning departments in developing ordinances and master plans.
4) Continued aid to cities and counties for engineering geologic studies.

RESULTS: Compilation of basic-data maps needed to derive translated hazard maps is nearing completion. In some cases, basic-data maps have already been prepared by others. This is true for geology, soils, and depth to shallow ground-water maps. Basic-data maps depicting Quaternary faults and earthquake ground shaking are in preparation by the USGS and hopefully will be available at least in preliminary form for the area during the period of this contract. The principal basic-data maps being compiled from original mapping by the county geologists are landslide, rock-fall, and debris-flow inventory maps. These maps are 75%-80% complete. Digital elevation model tapes to produce slope maps needed to derive slope failure susceptibility maps are on order and negotiations are underway with the Utah State Automated Geographic Reference (AGR) Center to produce maps from the tapes.

Services provided to cities and counties during the second year of the program include aid in developing ordinances, reviews of engineering geologic reports, and memos to planners and developers indicating potential hazards at proposed developments requiring geologic investigations. Major special projects have included preparation of: 1) a gravel resource assessment for county property in Davis County, 2) a surface fault rupture hazard study for a proposed Provo City landfill in Utah County, 3) the geologic hazards portion of the master plan for the city of Washington Terrace in Weber County, 4) site investigation reports for two water tank sites for the city of North Salt Lake in Davis County, 5) a review of a proposed county fire station site along the Wasatch fault in Salt Lake County, 6) the engineering geologic section for the Pineview Reservoir Clean Lakes study to control development near the lakeshore to avoid contamination, Weber County, 7) a geologic hazards evaluation of property owned by Payson City proposed for development in Utah County, and 8) an engineering geologic report regarding geologic hazards, slope stability, and potential for ground-water contamination at the North Davis Refuse Dump and new burn plant in Davis County. The county geologists and UGMS have also given talks to various civic groups and governmental organizations, answered public inquiries, participated in radio talk shows, and been involved in a variety of technical and policy publications (see Publications list) related to the program.

HAZARD MAPS (Phase III): Translated hazard maps planned under Phase III of the program will depict areas subject to: 1) surface fault rupture (1:24,000), 2) ground shaking (1:250,000), 3) tectonic subsidence (1:100,000), 4) liquefaction (1:48,000), 5) dam failure inundation (1:24,000), 6) rock fall (1:24,000), 7) landsliding (1:24,000), 8) debris flows (1:24,000), 9) seismically induced slope failure (1:48,000), 10) shallow ground water (1:48,000),and 11) problem soils and subsidence (1:24,000). Maps 3), 4), 5), 9),and 10) are already completed by others and will be recommended by the county geologists for adoption by the county. Other maps will be compiled during the coming year of the program. An explanatory text will be prepared to accompany all maps to discuss the nature of the hazard, its probability of occurrence, and possible consequences. Maps will be at a scale of 1:24,000 to 1:250,000 as listed above, depending on the scale of the basic-data maps used in the compilation. All of these products are designed for use by planning departments in evaluating where site-specific geologic reports are required.

Publications related to the County Geologist Program

Christenson, G.E., 1987, Suggested approach to geologic hazards ordinances in Utah: Utah Geological and Mineral Survey Circular 79, 16 p.

Christenson, G.E., Lowe, Mike, Nelson, C.V., and Robison, R.M., 1987, Geologic hazards and land-use planning, Wasatch Front, Utah: Geological Society of America Abstracts with Programs, v. 19, no. 5, p. 265.

Nelson, C.V., Christenson, G.E., Lowe, M.V., and Robison, R.M., 1987, The review process and adequacy of engineering geologic reports, Wasatch Front, Utah, in McCalpin, James, ed., Proceedings of the 23rd Symposium on Engineering Geology and Soils Engineering: Utah State University, Logan, Utah, p. 83-86.

Robison, R.M., Christenson, G.E., Knight, R.V., Dewsnup, Wes, and Johnson, Mike, 1987, Earthquake and slope failure hazards, Utah County Comprehensive Hazard Mitigation Project, Utah, in McCalpin, James, ed., Proceedings of the 23rd Symposium on Engineering Geology and Soils Engineering: Utah State University, Logan, Utah, p. 499-521.

Title: Tsunami Threat Analysis for the Pacific Northwest
Number: 14-08-0001-G1346
Investigator: Gerald T. Hebenstreit
Institution: Science Applications International Corporation
Address: 1710 Goodridge Drive
McLean, VA 22102
Phone: 703-827-4975

Numerous investigations in recent years of the seismicity of the Juan de Fuca Plate area of the eastern Pacific have led to the hypothesis that a major subduction-type earthquake in the Plate is a real possibility, despite the absence of historical records of such earthquakes. If this hypothesis is indeed true, then the northwestern regions of the United States and Canada are at risk. If such an earthquake or series of earthquakes were to occur off the western coast of North America, the threat would not only be from ground motions, but also from tsunamis generated by the motion of the sea floor in the outer shelf and slope area. The purpose of this study is to examine the nature of this tsunami risk by conducting numerical simulations of tsunami generation and propagation in the nearshore environment of the Juan de Fuca Plate region.

The first step in this study is to define possible source areas within which thrust earthquakes (the most common tsunami-producing type) could reasonably occur. Examination of recent literature on this subject has lead to the identification of three broad areas of concern. These are delineated in the attached Figure.

Area A covers the region of the Gorda South Plate, which is bounded at its southern end by the Mendocino Fault Zone. Because of the relatively small areal extent of this source zone, the model study will be confined to the indicated area, on the assumption that most of the wave energy produced by an earthquake in the zone would be concentrated on the immediate coastline, and little significant wave energy would escape to the north or south of the zone.

Area B includes the entire Juan de Fuca Plate, from the Gorda South Plate to the northern end of the Explorer Plate. A major earthquake along the entire 900+ km length of this zone would probably produce a tsunami to rival the southern Chile tsunami of May, 1960. In this case, the entire coastline will be included in the simulation. Not indicated on the Figure are several subsets of this source area which will also be examined. The rationale for these smaller zones (which will probably divide the full Juan de Fuca Plate into thirds) is that the Plate could easily break in segments rather than as one block. In each subset case, the full Juan de Fuca area will be included in the

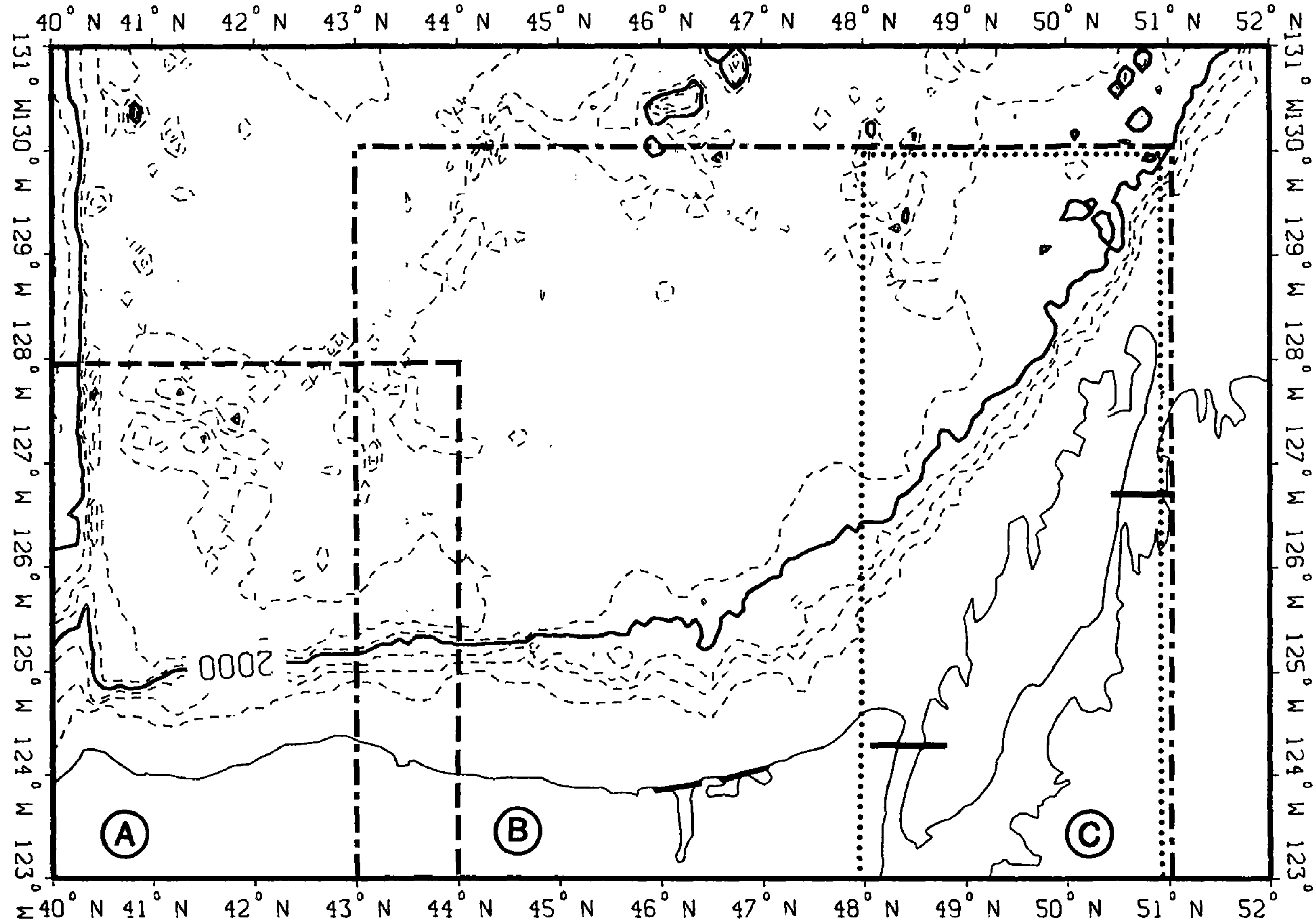

Bathymetry (meters) of the study area and the three major source areas to be examined

model, at least until it becomes clear that the effects of a smaller source motion would produce only a localized threat.

Area C includes the Explorer Plate, located along the northern half of Vancouver Island. Even though the area of the Plate itself is relatively small, the model area will extend far enough south to include the Strait of Juan de Fuca.

The details of the seafloor uplift patterns (which actually drive the wave model) are being developed from available historical information about the relatively few observed large earthquakes in the Juan de Fuca region (see, for example, Heaton and Hartzell, 1986.) Reasonable estimates of fault length and width, focal depth, dip angle, and vertical slip component will be compiled and then used in the Mansinha and Smylie (1971) source displacement model to produce seafloor uplift patterns. These patterns will then be used as initial conditions for a tsunami shelf propagation model based on the hydrodynamic equations for long ocean surface waves. The model topography is derived from the same data set that produced the accompanying Figure. Note that none of the inland estuaries, such as the Strait of Juan de Fuca, Puget Sound, or the Strait of Georgia, are included in the model grid. The limits of the grid in these areas are indicated by solid lines on the Figure. The model will produce estimates of concentrations of wave energy along the open coastlines of the United States and Canada, and succeeding studies can perform detailed threat analyses for coastal locations identified in this study.

One area of concern, which is not addressed by this study, is the interior of the Puget Sound/Strait of Georgia basin. This area has been identified as a region of specific interest in the Earthquake Hazards Reduction Program. Although this present study does not directly examine the possible tsunami threat to the area, a study being conducted concurrently by the Institute of Ocean Sciences in British Columbia is concentrating on the tsunami threat posed by earthquakes within the estuary. A cooperative agreement has been worked out between Dr. Hebenstreit and the IOS Principal Investigator (Dr. T. Murty) to share results of computer runs and analyses in order to broaden the scope of both studies. Of special importance is an agreement to share predictions of the SAIC study concerning wave energies entering the Strait of Juan de Fuca from the outer shelf, since such waves could pose a threat to the interior of the estuary.

As of April, 1987, the bathymetry for the study has been assembled and filtered to meet the needs of the study and hypothetical source motions are being tested. Full model runs will begin in May, 1987, with completion scheduled for late 1987.

References

Heaton, T.H. and S.H.Hartzell, 1986: Source characteristics of hypothetical subduction earthquakes in the northwestern United States. Bulletin of the Seismological Society of America,76(3), 675-708.

Mansinha, L. and D. E. Smylie, 1971: The displacement fields of inclined faults. Bulletin of the Seismological Society of America, 61, 1433-1440.

Earthquake-Resistant Design and Structure Vulnerability

New Project
(No number assigned)

Edgar V. Leyendecker
Branch of Geologic Risk Assessment
U.S. Geological Survey
Denver Federal Center, MS 966
Denver, CO 80225
(303) 236-1601

Investigations

1. A program has been initiated to examine, evaluate, and improve the estimation of casualties and aggregate monetary losses associated with the occurrence of earthquakes in the United States.

2. An investigation is underway to develop improved measures of vulnerability of structures to damage, including the refinement of our understanding of earthquake damage and the applicability of the existing data base on earthquake damage.

3. Investigations continue for development/identification of cost-effective techniques for determining inventory at risk.

Results

1. Plans are being made for development of an improved and consistent loss-estimation methodology that can be applied in a uniform way on a regional basis for the estimation of losses throughout the United States. As a first step in this new project, planning for a USGS Workshop on earthquake losses to be held late FY 87 or early FY 88 has started. Participants will include both USGS and non-USGS researchers and users. Results of this workshop will be useful in guiding the planning and conduct of this project.

An evaluation of risk (losses) for the Seattle urban area is anticipated as part of the initial application of preliminary results of this project.

2. Examination of current vulnerability relationships is underway with a review of existing earthquake damage data bases. Plans for the careful collection of earthquake damage data following significant earthquakes are being made, including development of data collection techniques. Improvement of vulnerability relationships, including parameter variability, depends heavily on the collection of earthquake damage data.

Analysis of vulnerability relationships appropriate for the Seattle area is underway as part of this project.

3. Development of inventory at risk is costly and is a major impediment to accurate loss estimates. Methods are being developed to identify and obtain the critical elements of inventory needed for loss assessment in urban areas, including field inventory techniques. A preliminary field inventory procedure is being developed. Plans for preparation of inventory training procedures are underway. Both the survey and training procedures will be evaluated and revised following a trial use.

A plan for an inventory in the Seattle urban area is being developed for initial application of some of the techniques.

Evaluation of Ground Failure Susceptibility Opportunity and Potential in Anchorage, Alaska Urban Area

14-08-0001-22031

Yoshiharu Moriwaki and Izzat M. Idriss
Woodward-Clyde Consultants
203 North Golden Circle Drive
Santa Ana, California 92705
(714) 835-6886

Investigations

The collection, interpretation, and evaluation of available geological and geotechnical data in Anchorage have been completed. A summary of ground damages in Anchorage due to the 1964 Alaskan earthquake has been made. The liquefaction potential of major sandy formations in Anchorage has been evaluated using a probabilistic method similar to that described in Woodward-Clyde Consultants (1986). Basic engineering properties of soils in Anchorage have been summarized following the facies classification by Dr. R. Updike of Alaska Division of Geological and Geophysical Surveys. A modification to probabilistic seismic hazard analysis to incorporate the effects of seismically-induced displacements is now almost complete. The report covering these results is being prepared at this time.

Results

In this summary, some results of the evaluation for liquefaction potential in Anchorage and some preliminary results of the seismic hazard analysis for Anchorage are presented.

Table 1 presents probabilities of liquefaction for various geological units in Anchorage as a function of various peak ground acceleration levels given a magnitude 7-1/2 earthquake has occurred. As can be seen in Table 1, sandy soils in the Bootlegger Cove Formation have the largest probabilities of liquefaction. However, all the values shown in Table 1 are considered to be low when compared to expected behavior of loose sandy deposits under similar conditions.

In a typical probabilistic seismic hazard evaluation, equal weights are assigned to earthquakes of all magnitudes.

However, although different magnitudes can produce identical levels of peak ground acceleration, the smaller the magnitude the shorter is the duration. A weighting procedure to incorporate these considerations in probabilistic seismic hazard evaluation for liquefaction assessment is presented by Idriss (1985).

For Anchorage, potential for seismically-induced ground movements through mainly clayey parts of the bootlegger Cove Formation may be of more concern than liquefaction. For this reason, a weighting procedure using the data from Makdisi and Seed (1978) and Woodward-Clyde Consultants (1982) was developed in this study. The preliminary weighting relationships are shown in Figure 1 for seismically-induced displacements of 1, 15, and 100 cm. The results of probabilistic seismic hazard analyses for a downtown Anchorage area corresponding to displacements of 1 and 100 cm are shown in Figures 2a and 2b.

As can be seen in Figures 2a and 2b, the displacement of 1 cm is dominated by the Megathrust for acceleration levels lower than about 0.2 g, but by the Border Ranges fault for those higher than about 0.2 g. However, the displacement of 100 cm is completely dominated by the Megathrust. These relationships are being refined at present.

Reports

Idriss, I.M. (1985). Evaluating seismic risk in engineering practice, Theme Lecture, Proceedings of the Eleventh International Conference on Soil Mechanics and Foundation Engineering, San Francisco.

Makdisi, F.I., and Seed, H.B. (1978). Simplified Procedure for Estimating Dam and Embankment Earthquake-Induced Deformations. ASCE J. Geotech. Engr. Div., v. 104, no. GT7, 849-867.

Woodward-Clyde Consultants (1982). Anchorage Office Complex, Geotechnical Investigation, Anchorage, Alaska. Report to Alaska Department of Transportation and Public Facilities, Central Region, Design and Construction, Anchorage, Alaska.

Woodward-Clyde Consultants (1986). Evaluation of Liquefaction Opportunity and Liquefaction Potential in the San Diego, California Urban Area, Final Technial Report, U.S. Geological Survey, Contract No. 14-08-0001-20607.

TABLE 1

ESTIMATED PROBABILITY OF LIQUEFACTION
GIVEN A MAGNITUDE OF 7-1/2 EARTHQUAKE HAS OCCURRED

Geologic Unit	Number of SPT Data	Mean Probabilities of Liquefaction		
		A_{max}* = 0.1g	A_{max}* = 0.2 g	A_{max}* = 0.3g
Alluvium, Q_{al}	32	0.1×10^{-9}	0.0012	0.025
Naptowne Outwash, Q_o	238	0.14×10^{-9}	0.0008	0.019
Bootlegger Cover Formation, Q_{bc}	580	0.0045	0.025	0.089

* Peak horizontal acceleration at ground surface.

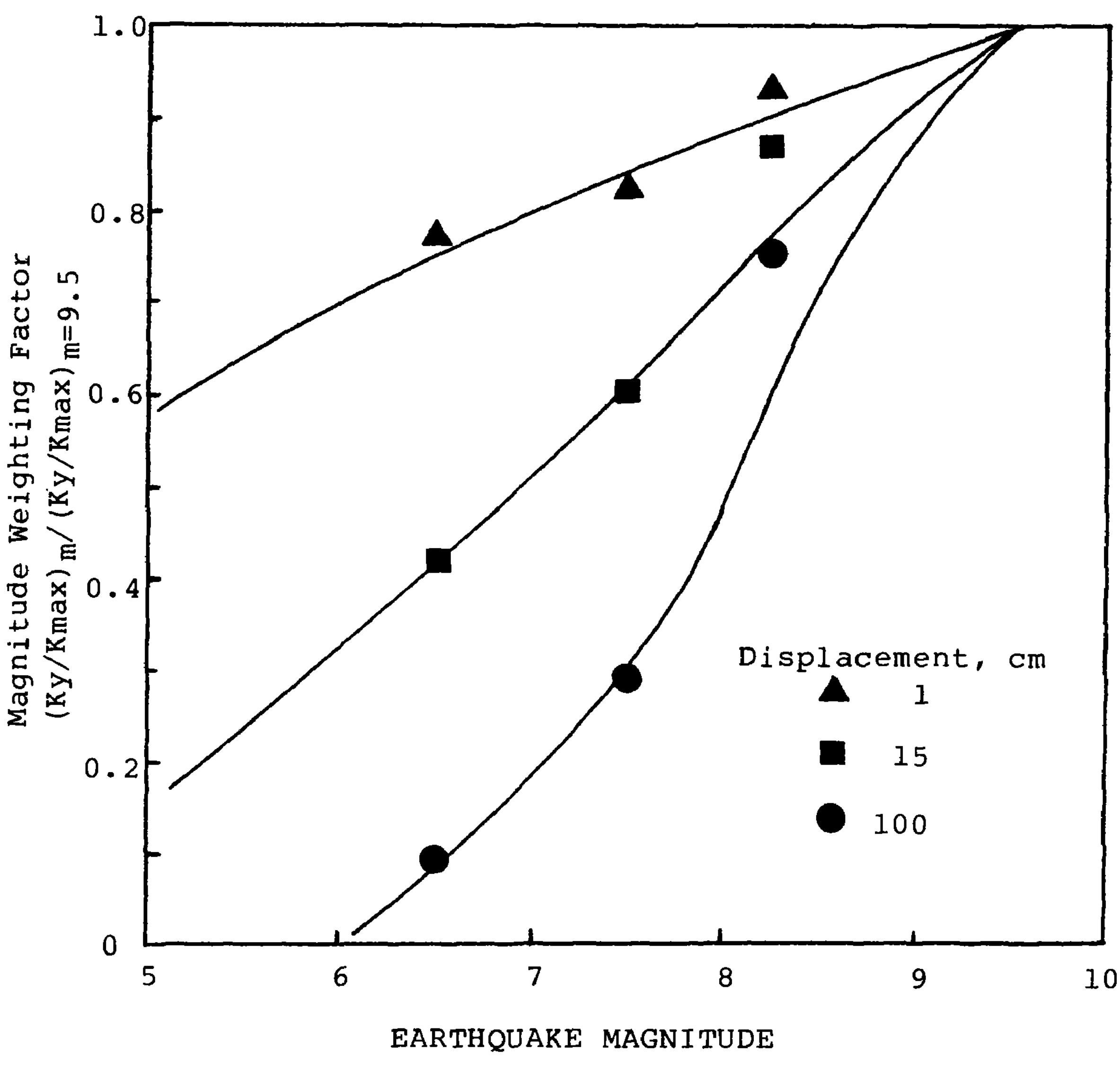

Figure 1 Magnitude Weighting Factors for Seismically-induced Displacements

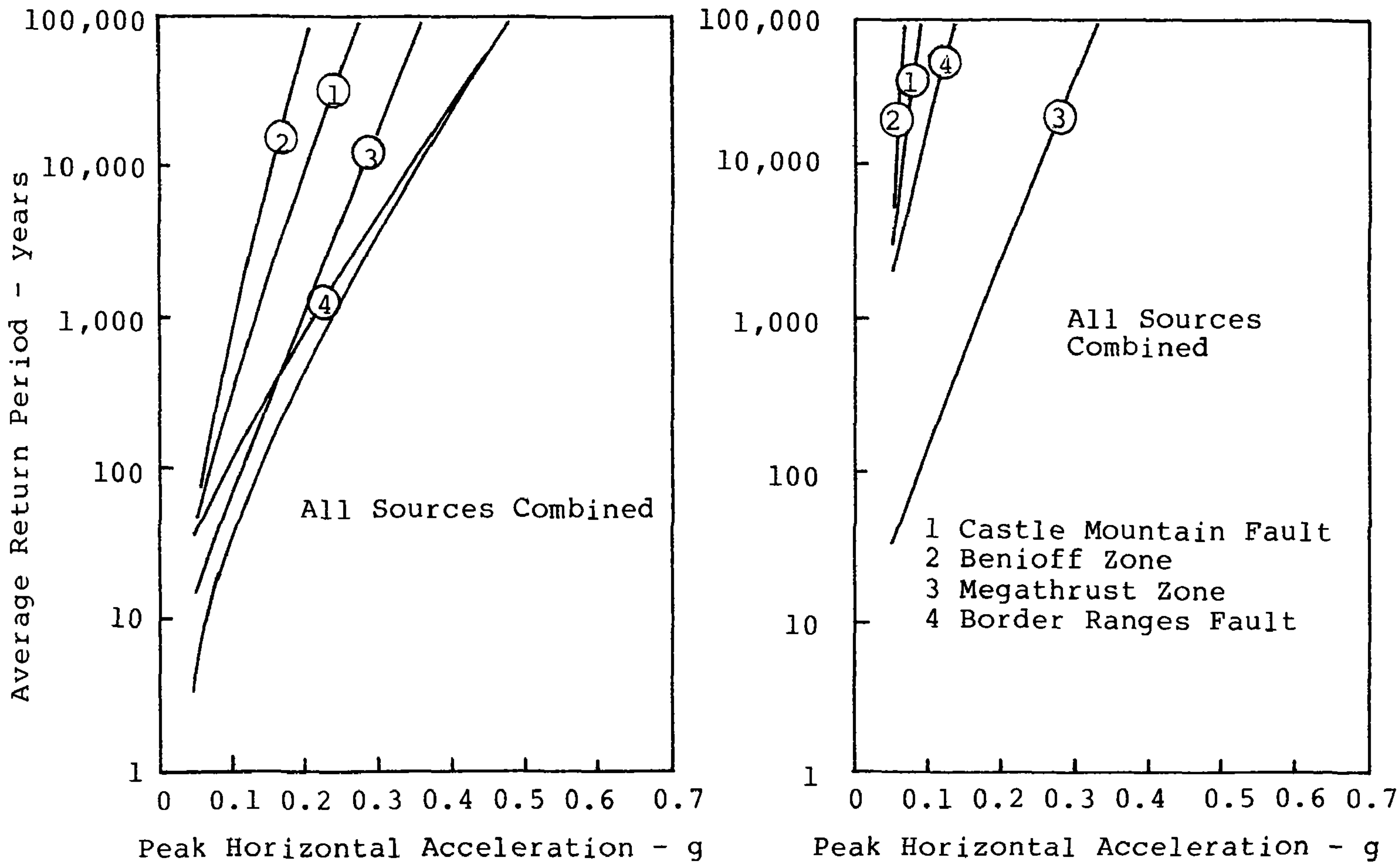

a. 1 cm Displacement Weighting

b. 100 cm Displacement Weighting

Figure 2 Results of Probabilistic Seismic Hazard Evaluation With Magnitude Contributions Weighted With Respect to m=9.5

LATE QUATERNARY FAULTING, SOUTHERN SAN ANDREAS FAULT

9910-04098

Michael J. Rymer

Branch of Engineering Seismology and Geology
U.S. Geological Survey
345 Middlefield Road, MS-977
Menlo Park, CA 94025
(415) 323-8111 ext. 2081

Investigations

1. Late Quaternary history of the Banning and Mission Creek segments of the San Andreas fault zone in the Indio Hills, Riverside County.

2. Late Quaternary history of the San Andreas fault near Bombay Beach, Imperial County.

3. Postearthquake investigations of the 10 October 1986 San Salvador, El Salvador earthquake.

Results

1. Analysis (with Ray Weldon) of a preliminary set of paleomagnetic samples from the Ocatillo Formation between the Banning and Mission Creek faults indicates no block rotation has occurred since deposition of this Pleistocene unit. A more complete sampling was also made in the report period and consists of two sections in the Ocatillo Formation and one in the Palm Spring Formation. These sample sets will test possible fault drag and block rotation, and will construct a magnetostratigraphic section. These samples are being analysed.

Paleosol and Carbonate marker beds were mapped in the Ocatillo and Palm Spring Formations for correlation of magnetstratigraphic ages throughout the Indio Hills.

2. Preliminary trenches were dug (with R.V. Sharp) across the San Andreas fault near Bombay Beach to look for age of deposits and rate of slip. The preliminary trences showed that Holocene lacustrine deposits and sedimentary structures may be correlated across the fault. More extensive trench investigations to start in October will resolve the age of offset features, rate of slip, and continuity of faults that trend southeast, toward the Brawley seismic zone.

3. The San Salvador earthquake struck an area of late Cenozoic volcanic rocks, consisting of basaltic to silicic flows and tuffs. Tuff deposits constitute the upper 30 m of section below San Salvador with thiner sections in the hills surounding the city. Tuffs were important in landslide development during the earthquake and may have amplified strong ground motion. Faults mapped in the area strike east-west, northwest, and less distinctly, northeast and north-south.

No evidence was seen of surface faulting associated with the 10 October main shock or an earthquake on a separate fault 7 km west-northwest of the main shock on 13 October. Numerous cracks were seen in the epicentral areas of both of these earthquakes, but the cracks were easily related to secondary ground failures. Both of the earthquakes occurred on unmapped faults.

The main shock caused several hundred landslides throughout an area at east 200 km^2. The most numerous landslides were soil slides and soil falls, which were especially common in stream banks and road cuts in volcanic tuff. The earthquake also produced rock falls and slides, slumps, earth flows, shattered ridge effects, and compaction. Landslides and related ground failures were triggered as much as 12 km from the epicenter and accounted for about 200 fatalities and at least 100 damaged homes.

Reports

Rymer, M.J., 1987, Geologic aspects of the San Salvador, El Salvador earthquake of 10 October 1986 [abs.]: Seismological Research Letters, v. 58, p. 8-9.

Historical Normal Fault Scarps -- Wasatch Front and Vicinity

9910-04102

David P. Schwartz
Branch of Engineering Seismology and Geology
U.S. Geological Survey
345 Middlefield Road, MS 977
Menlo Park, California 94025
(415) 323-8111, ext. 2689 or (415) 329-5651

Anthony J. Crone
Branch of Geologic Risk Assessment
MS 966, Box 25046
Denver Federal Center
Denver, Colorado 80225
(303) 236-1595

Investigations:

The project goal is to study historical and recent normal fault scarps in the Great Basin in order to calibrate geological techniques used to identify individual past earthquakes and the amount of displacement during each, quantify earthquake recurrence intervals, and evaluate earthquake recurrence models and fault segmentation models. Investigations have concentrated on 1) recurrence and segmentation along the 1983 Borah Peak, Idaho surface rupture and associated scarps of the Lost River Range and 2) recurrence and paleo-displacements at the Dry Creek site near the southern end of the Salt Lake segment of the Wasatch fault zone.

Results:

1. Lost River fault zone (Schwartz and Crone). Results to date were reported in Summaries of Technical Reports, Volume XXIII (USGS Open-File Report 87-63). Trench investigations will resume in July/August 1987.

2. Wasatch fault zone (Schwartz and W.R. Lund of the Utah Geological and Mineral Survey). Trenching and scarp profiling at Dry Creek, 20 km south of Salt Lake City, have provided information on the timing and amount of displacement during the past two surface faulting events at this location. The event prior to the most recent occurred before 2000 to 4000 yr BP. Radiocarbon dating of soil developed on colluvium exposed in trenches suggests a maximum age of 1890 (+50, -60) ^{14}C yr BP for the most recent event and scarp diffusion modeling suggests an age closer to 900 years.

   Topographic profiles of a late-Holocene debris-flow levee that crosses the entire fault zone shows that the net vertical tectonic displacement at this location during the most recent event was 4.75 m.

Reports:

Lund, W.R., and Schwartz, D.P., 1986, Fault behavior and earthquake recurrence at the Dry Creek site, Salt Lake segment, Wasatch fault zone, Utah [abs.] EOS, v. 67, p. 1107.

CONTINUING INVESTIGATIONS OF EARTHQUAKE RISKS TO UTAH WATER AND GAS SYSTEMS

14-08-0001-G1394

Craig Taylor
NTS Engineering
6695 East Pacific Coast Highway
Long Beach, CA 90803
(213) 493-6651

Objectives

In a previous project, we showed how the development of seismic risk estimates for water and gas systems in Salt Lake and Davis Counties can provide materials directly useful to utility management. Extensive hazard studies of the Wasatch Front area, especially with respect to fault systems and subsurface geometry, relative site response, attenuation functions, and liquefaction susceptibility, yielded significant inputs into seismic risk estimates and resulting risk reduction programs. In this project, which has only recently (March 15th) begun, we shall develop similar seismic risk estimates for culinary water and natural gas facilities in Utah and Weber Counties. Project objectives include:

1. Collecting detailed data on culinary water and natural gas systems and on new and improved estimates for geologic hazards;

2. Developing the theoretical framework: defining pertinent seismic source zones, updating attenuation functions, incorporating relative site response factors, enhancing methods for estimating ground displacement probabilities, upgrading seismic pipe vulnerability models, and developing seismic fragility models for wells and other key types of nodes.

3. Developing findings and presenting them: constructing isoseismal maps and damage estimates for the large suite of earthquakes modeled, examining the sensitivity of these estimates to various input parameters, and conveying relevant information to utility representatives to help initiate or else to advance seismic risk reduction programs.

Results

A trip was made to Utah in order to collect data and to discover advances in the geosciences since the previous project. Detailed data have been gathered on natural gas system facilities and on Ogden City water and South Ogden water facilities. Data collection on Utah County water facilities is being coordinated through the County Office of Emergency Services. Background planning documents are being gathered from the Utah State Division of Comprehensive Emergency Management. County geologists have provided materials on local geology. Useful theoretical developments appear to come from work performed at Dames & Moore, Utah State University, the University of Utah, and BYU. Based on an initial examination of a paper by Youd and

Perkins, we may need to revise extensively our previous crude models for estimating liquefaction probabilities.

Although additions and revisions to our previous hazard modeling already appear to be extensive, a trip to Golden, Co. is planned to gather even further pertinent data and insights. We also expect again to make use of raw data on liquefaction susceptibility as collected by Utah State University.

A second trip to Utah is being planned in order to make walk-throughs of key booster stations and wells so that generic seismic fragility models can be produced for such facilities. The Salt Lake County Water Conservancy District and Ogden City Engineering have so far provided drawings and plans as background materials. With the assistance of consultant R. Eguchi, we also expect to be improving models of the vulnerability of various types of piping joints to strong ground motion and its secondary effects.

References

Youd, T. Leslie and David M. Perkins, "Mapping of Liquefaction Severity Index, " accepted for publication in the Journal of Geotechnical Engineering, ASCE.

Taylor, Craig E., Wiggins, John H., Haber, Jerold M. and Ward, Delbert, "A Systems Approach to Wasatch Front Seismic Risk Problems," Redondo Beach, CA: NTS Engineering Report No. 86-1513, U.S.G.S. Contract No. 14-08-001-22013, February 1986.

Earthquake Hazards Studies, Metropolitan Los Angeles-Western Transverse Ranges Region

9540-02907

R. F. Yerkes
Branch of Western Regional Geology
345 Middlefield Road, MS 975
Menlo Park, California 94025
(415) 329-4946

Investigations and results

1. Historic earthquakes (Levine and Yerkes, with W. H. K. Lee). Systematic relocation of hypocenters and derivation of fault-plane solutions for earthquakes ET/GT M_L 1.0. 1/74 through 6/85 (with data gap 5/80 through 9/83), using HYPO71 and interactive processing, is underway. We are concentrating on a 17-minute-wide band along the Anacapa-Santa Monica-Sierra Madre-Cucamonga zone of reverse faults, which marks the south boundary of the Transverse Ranges immediately northwest, north, and northeast of the Los Angeles basin, and along which exploratory well data are available. About 1500 hypocenters have been relocated and 400 single-event fault-plane solutions have been obtained for the reverse-fault zone west of the San Jacinto fault, the most active element of the San Andreas system in the area. Evaluation of apparent depth/local geology/veocity models continues.

2. Quaternary stratigraphy, chronology, and tectonics, Ventura area (Sarna-Wojcicki). This investigation is presently concentrating on: improvement of age control for Quaternary marine deposits in onshore sections such as those of the Ventura basin, developing more detailed oxygen-isotope records, and correlation of marine and continental sequences.

Continued investigations described in semi-annual report of fall, 1986. Results of recent electron microprobe analysis of tephra layers collected from Balcom Canyon in the Ventura area indicate the presence of a newly-identified, thin silicic ash bed stratigraphically below the ca. 2.0 Ma Huckleberry Ridge ash bed, within deformed beds in the lower part of the marine Pico Formation (fig. 1). This ash bed correlates chemically (table 1) with an ash bed in the deformed Waucoba lake beds of eastern Owens Valley, east of Big Pine. The tephra of this ash bed was erupted from the Mono Glass Mountain volcanic source area, and probably correlates with ash layers within the Tuff of Taylor Canyon (Krauskopf and Bateman), proximal equivalents of this tephra. The age of the ash bed in the Balcom Canyon section is bracketed between 2.0 and 2.4 Ma, based on available age control at the localities where it is found.

A sequence of tephra layers stratigraphically lower down in the Balcom Canyon section, within the deformed Modelo Formation, was collected from the north and south limbs of an anticline. Of 24 tephra layers collected from this structure, only one corrlates across it. The other tephra layers must either lens-out laterally, occur in sequences in one limb that are not exposed on the opposite limb, or the anticline may be cut by an unmapped fault. Tentative correlations based on matching the glass compositions of these layers determined by electron probe-analyses correlate some of the layers with several others at localities in the western U.S.: 1) the type section of the marine Monterey formation, near Monterey, Calif., 2) continental beds of the Aldrich Station section in west-central Nevada (west of Walker Lake), old fan alluvium in the vicinity of the Nevada Test Site in southern Nevada (Point of Rocks area), and 3) the China Ranch beds in eastern Mojave Desert. The correlations are preliminary, pending further analysis by more precise X-ray fluorescence and neutron-activation. If the correlations are confirmed, however, then there is some problem either with the age estimates of the tephra layers in the Modelo and Monterey Formations, based on diatom biostratigraphy (J. Barron, written commun., 1986), with their radiometric ages (K-Ar and fission-track) at the correlative localities, or with our stratigraphic interpretation (possible presence of faults within the anticline section at Balcom Canyon). At the localities in Nevada and the eastern Mojave desert, as well as in the Ventura area, the ages of these tephra layers are important in determining the timing of late Cenozoic tectonism.

Completed up to technical review a report summarizing late Cenozoic tephrochronology in the Pacific margin of the U.S., for chapter in DNAG volume on the Quaternary of the non-glaciated U.S. Report contains correlation charts for Pliocene and Quaternary tephra layers in sediments of the western states (Calif., Nev., amd Ore.), and the northeastern Pacific Ocean.

Reports

No reports submitted.

Table 1. Electron microprobe analysis of tephra layer within Pico Formation, Balcom Canyon, Ventura area, strat. beneath the Huckleberry Ridge ash bed. C. E. Meyer, analyst, USGS, Menlo Park. Samples PICO-163Q, 169Q - Balcom Canyon; WAC-6 - Waucoba lake beds.

Oxide	PICO 163Q	PICO 169Q	WAC-6
SiO_2	76.93	77.59	77.20
Al_2O_3	13.52	12.55	12.74
Fe_2O_3	0.60	0.58	0.60
MgO	0.04	0.04	0.04
MnO	0.10	0.10	0.06
CaO	0.32	0.33	0.34
TiO_2	0.07	0.06	0.09
Na_2O	3.86	3.87	3.98
K_2O	4.56	4.87	4.94

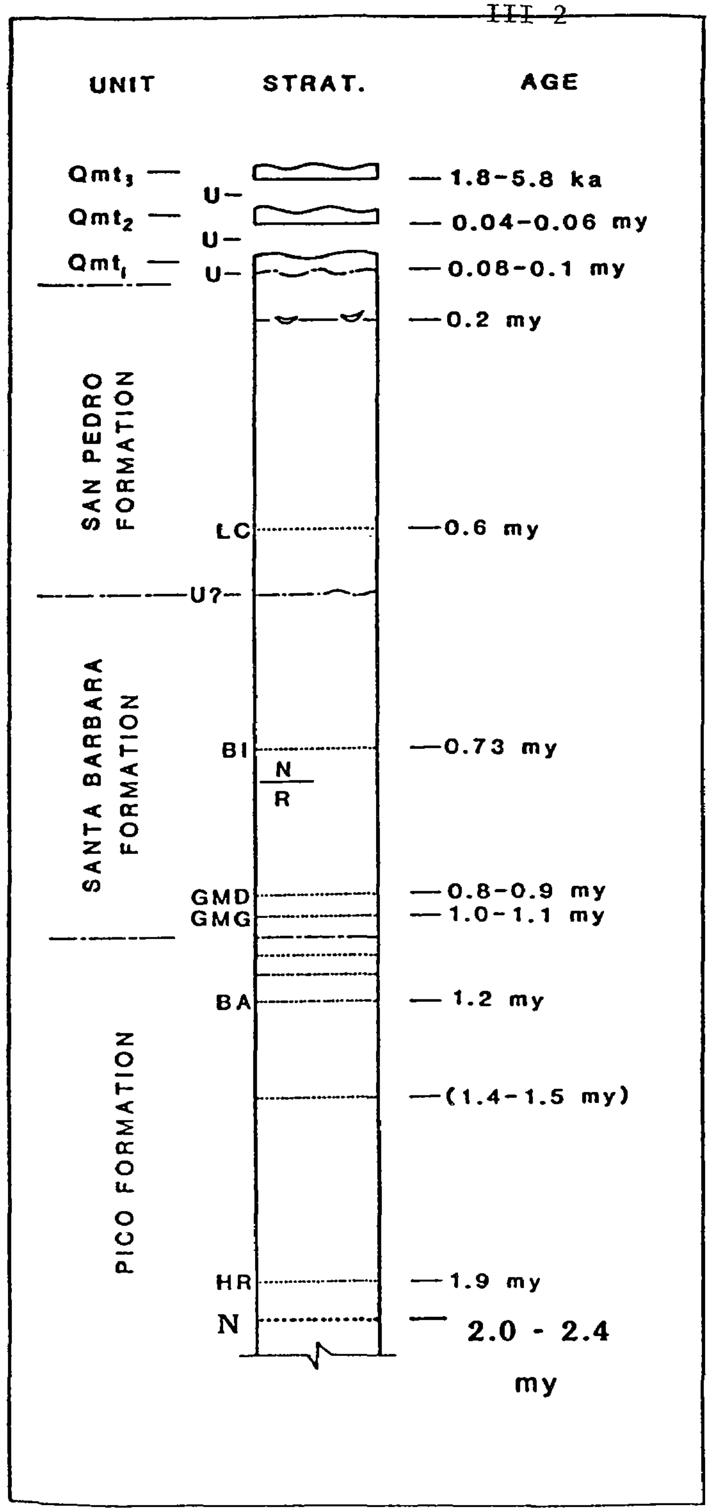

Figure 1 (upper right). Composite, generalized stratigraphic column for the Ventura area, showing available age control. U - unconformity. Upper part of section dated by amino-acid racemization (Lajoie and others, 1982). LC - Lava Creek ash bed; BI - Bishop ash bed; GMD, GMG - Glass Mountain ash beds; BA - Bailey ash bed; HR - Huckleberry Ridge ash bed; N - new ash bed reported here. Figure modified after Lajoie and others, 1982.

A DEMONSTRATION PROJECT WITH SALT LAKE CITY & COUNTY ON SEISMIC RISK ANALYSIS, LAND USE PLANNING AND RISK REDUCTION

14-08-0001-G1202
Philip C. Emmi
Department of Beography
University of Utah
Salt Lake City, Utah 84112
(801) 581-5562

Objectives

This project is the first of two dealing with seismic risk assessment and local public policy for seismic risk mitigation. The objective of this project is to collect the data relevant to a seismic risk assessment and integrate it into a geographic information system for later manipulation and retrival. Data files collected by staff members are detailed below. In some cases, data files were manipulated to produce new results. These are discussed in the subsequent section.

Accomplishments

Prior to data collection, meetings were held with local urban planning officials to gain concensus on data requirements and secure co-operation in data collection. Subsequent to those meetings, officials from the Salt Lake City and County Planning Offices have helped secure maps and digital data files useful to our efforts. Their co-operation is greatly appreciated.

The fifty-eight data and digital map files collected to date are grouped into three categories – data on the geologic environment, data on cultural features in the built environment and boundary files. Boundary files create the spatial context within which mapped data is displayed. The following is a list of the boundary files developed to date:

- Study area file delineating the urbanizable area of Salt Lake County
- Traffic zone file delineating the spatial subdivisions (i.e., parts of Census tracts) used when reporting population and land use data
- Quarter-section file delineating sub-sections of the township and range survey system used when reporting building structural data from the County Assessor's files

Digital maps on the geologic environment are based on studies done by Anderson et al. (1986), Keaton (1986), Scott and Shroba (1985), Hayes et al. (1978), Hayes and King (1982) and our research team. These include:

- Seismic faults in Quaternary deposits
- Probabalistic liquifaction potential
- Probabalistic slope failure potential
- Inundation and ground water ponding areas given tectonic subsidence
- Relative ground shaking response, 0.1-0.2 and 0.2-0.7 second bands
- Modified Mercali Intensity data with 10% exceedence probabilities over 10, 50 and 250 years periods

Digital map and data files on cultural feature are divided into three sub-categories — data on population and land use, data on residential, commercial and industrial structures and data on critical facilities and lifelines. Population and land use data were secured from the Wasatch Front Regional Council (1986). These files include:

- Population per traffic zone, 1985 and projected to the year 2005
- Single and multi-family dwelling units, 1985 and 2005
- Commercial floor area and acreage per traffic zone, 1985 and 2005
- Industrial acreage per traffic zone, 1985 and 2005
- Acreage used for transportation per traffic zone, 1985 and 2005
- Acreage in institutional uses per traffic zone, 1985 and 2005
- Acreage in parks and recreation per traffic zone, 1985 and 2005
- Acreage under institutional use per traffic zone, 1985 and 2005
- Agricultural acreage per traffic zone, 1985 and 2005
- Vacant acreage per traffic zone, 1985 and 2005

Data on residential, commercial and industrial structures were provided by the Salt Lake County Assessor's Office (1986) and the Utah State Tax Commission, Property Tax Division (1986). These include:

- A complete census of residential structures with data on use category, building type, year built, effective age, height, quality of construction, value and replacement cost locationally referenced by Census tract/traffic zone, and by township and range down to the quarter-section
- The total number of commercial and industrial structures by quarter-section
- A 10 to 25 percent random stratified sample of commercial and industrial structures with data on use category, building type, year built, effective age, height, quality of construction, value and replacement cost locationally referenced by quarter-section

These maps represent new map products unique to this project.

Data files on lifelines and critical facilities include:

- A census of all public and major private schools, their locations and 1985 enrollments
- The locations of all hospitals and nursing homes
- The locations of all major hotels
- The locations of police and fire stations
- Major roads and overpasses
- A census of all water tanks, reservoirs, public culinary water wells, and drinking water treatment plants
- Components of the drinking water distribution system
- Components of the sanitary sewer system by size of line
- Components of the storm drain system including surface canals and subsurface drains by size
- Components of the electrical power grid including power stations, substations and power lines by line capacity
- Approximate location of natural gas lines by size

Some of these digital map planes are unique compilations of data from previously unassemble source materials. These include the maps on the drinking water distribution system, the sanitary sewer system, the storm drain system and the system for natural gas distribution.

Results

To date our efforts have focused on data collection, mapping, and digitizing mapped data. The results are a collection of single and composite digital map planes. Several of the digital map planes are unique compilations of data from previously unassemble source materials. Two sets of mapped data planes represents the mapping of new analytical results. New analytical results are presented in a set of Modifies Mercali Intensity (MMI) maps for the study area and in a set of maps depicting projections of densities of residential and commercial/industrial structures in the year 2005. Modified Mercali Intensity maps are needed to later estimate expected damage from seismic events. Maps of future structural densities are needed to assess future seismic risk and mitigation opportunities.

The method used to produce Modifies Mercali Intensity maps relies upon probabalistic estimates of maximum velocity in bedrock (Algermissen et al., 1982, Plate 4) and bedrock-to-soil horizontal transfer functions (Hayes and King, 1982) to generate microzonal values for soil velocity within the study area. A microzonation of MMI values is derived from an MMI-velocity relationship developed by Everenden and Thompson (1985, Figure 68C). The bedrock velocity to MMI conversions used to develop the two sets of MMI maps are shown in the table below.

Table 1.

Conversion of Bedrock Velocity to Modified Mercali Intensity[1]

Site Response Relative to Bedrock	Modified Mercali Intensity Assumming a 10% probability of Exceedence over a: 10-year Period	50-year Period	250-year Period
1.5	5.3	6.8	8.2
2.5	5.9	7.5	8.9
3.7	6.5	8.0	9.4
5.6	7.0	8.6	10.0
8.5	7.6	9.1	10.5
10.0	7.8	9.4	10.8

1. Assumes peak bedrock velocities in Algermissen et al (1982), transfer functions in Hayes & King (1984) and a velocity to MMI relationship in Everenden & Thompson (1985).

Maps depicting the densities of residential and commercial/industrial structures in the year 2005 are based on projections of future land use provided by the Wasatch Front Regional Council (1986). These provide projections of the number of acres dedicated to each of several land use categories. Acreage projections were converted to an estimate of the future number and distribution of structures by structural type by applying current zone-specific densities to the acreage projections. This results in a projection of key structural elements in the future built environment of Salt Lake County.

These efforts have been taken so that the implications of regional seismology might be more clearly articulated in local-level seismic hazard mitigation policies.

References Cited

Algermissen, S. T. et al. 1982. Probabilistic estimates of maximun acceleration and velocity in rock in the contiguous United States, U.S. Geological Survey Open File Report 82-1033.

Anderson, L.R. et al. 1986. Liquifaction potential map for Salt Lake County, Utah. Prepared by the Utah State University Department of Civil and Environmental Engineering and Dames and Moore Consulting Engineers for the U.S. Geological Survey, Contract # 14-08-0001-19910.

Everenden, J. F. and Thomson, J. M. 1985. Predicting seismic intensities. In I. Ziony, ed., Evaluatin Earthquake Hazards in the Los Angeles Region - An Earth Science Perspective. U. S. Geological Survey Professional Paper 1360. U.S. Government Printing Office, Washington, D.C.

Hayes, W. W. et al. 1978. Preliminary ground response maps for the Salt Lake City Area. Proceedings of the Second International Conference on Microzonation, San Francisco, v.2, p. 497-508.

Hayes, W. W. and King, K. W. 1982. Zoning of earthquake shaking hazard along the Wasatch fault zone, Utah. Third International Earthquake Microzonation Conference, Seattle, v.3, p. 1307-1318.

Keaton, J. R. 1986. Potential consequences of tectonic deformation along the Wasatch Fault. U.S. Geological Survey, NEHRP Grant # 14-08-0001-G1174. Dames & Moore Geotechnical Services, Salt Lake City, Utah.

Scott, W. E. and Shroba, R. R. 1985. Surficial geologic map of an area along the Wasatch fault zone in the Salt Lake Valley, Utah. U.S. Geological Survey Open File Report 84-763, p. 73-112.

Salt Lake County Assessor's Office. 1986. State building card system: Assessment information, 1985. Salt Lake City, Utah: Assessor's Office.

Utah State Tax Commission, Property Tax Division. 1986. Stat file: Master file / data base used to derive stratification and valuation models, 1985. Salt Lake City, Utah: Utah State Property Tax Division.

Wasatch Front Regional Council. 1986. Surveillance of Land Use: 1985. Bountiful, Utah.

Experimental Investigation of Liquefaction Potential

9910-01629

Thomas L. Holzer

Branch of Engineering Seismology and Geology
U.S. Geological Survey
345 Middlefield Road, MS 977
Meno Park, CA 94025
(415) 323-8111 Ext. 2760

Investigations

1. Establishment of an instrumented site in Parkfield, California, to monitor pore pressures in sands and strong ground motion during the predicted Parkfield earthquake.

2. Investigation of the cause of ground failure at the Juvenile Hall during the February 9, 1971, San Fernando Valley earthquake.

3. Preparation of National Research Council report on mitigating losses from land subsidence in the United States.

Results

1. Routine maintenance of instrumentation at the USGS-EPRI Parkfield liquefaction array has revealed a high rate of mortalty of the pore-pressure transducers. As of March 31, the array was still functional but all redundancy was lost. These instrument failures have prompted a review of the perfomance of similar arrays at St. Helens, Washington, and in the Imperial Valley, California, in addition to a reappraisal of *in situ* dynamic pore-pressure transducers. Funding for new instrumentation is being discussed with EPRI and installation of new units is planned in June. In addition to the work on instrumentation, preliminary appraisals are being conducted of computer programs to model seismic response and pore pressure build-up and dissipation at soil sites. Geotechnical data from the Parkfield site also are being reviewed as they become available from contractors.

2. A subsurface investigation at the Juvenile Hall ground failure associated with the San Fernando Valley earthquake has revealed a deep-seated layer of saturated sand that is capable of generating excess pore pressures under seismic loading conditions. Analysis of SPT and CPT data at the site suggests that ground failure in 1971 was caused by liquefaction. Results are being prepared for publication in the AEG Bulletin.

3. The first draft of the report of the National Research Council Panel on Land Subsidence was prepared and submitted to the Panel's parent committee for review. The report finds that subsidence losses in the United States are more then $100 million per year. Subsidence has affected an aggregate area of at least 44,00 km^2 in a 45 states. The principal outstanding national problem is a failure to consider the contribution of land subsidence to flooding. This increases the costs of payments from the Federal Flood Insurance Program.

Reports

Holzer, T.L., 1986, Ground failure caused by ground-water withdrawal from unconsolidated sediments, in International Symposium on Land Subsidence, 3rd, Venice, Italy, 1984, Proceeding: International Association of Hydrological Sciences Publication 151, p. 747-756.

Holzer, T.L., 1988, Nontectonic subsidence, in Kiersch, G.A., and Mathewson, C.C., eds., The Heritage of Engineering Geology: Geological Society of America Decade of North American Geology, 41 p., 1 table, 14 figs. (Approved by Director on January 27, 1987).

Holzer, T.L., 1987, Geodetic networks and land subsidence due to withdrawal of underground fluids (abs.): American Geophysical Union Spring Meeting, Baltimore (Approved by Director on February 24, 1987).

Holzer, T.L., and Lluria, M.R., 1987, Selected hydrogeological problems in central Arizona, in Field Trip Guidebook for 1987 Geological Society of America Annual Meeting, 8 p., 4 figs. (Approved by Director on March 3, 1987).

Near-Surface Lithologic and Seismic Properties

9910-01168

W.B. Joyner
J.F. Gibbs

Branch of Engineering Seismology and Geology
U.S. Geological Survey
345 Middlefield Road, MS 977
Menlo Park, California 94025
(415) 323-8111, ext. 2754, 2910 or (415) 329-5640, 5631

Investigations

Measurement of seismic velocity and attenuation to determine the effect of local geology on strong ground motion and to aid in the interpretation of seismic source parameters.

Results

We have done P- and S-wave velocity surveys to depths of 285 and 290 m in two drill holes near Anza, California and to depths of 95 to 180 m in three holes near Parkfield, California, in addition to those previously reported.

Preliminary analysis of data from the previously logged hole at Vineyard Canyon near Parkfield suggests S-wave velocity anisotropy of about 25 percent.

Reports

Joyner, W.B., 1987, Incorporation of site effects in stochastic source models for prediction of earthquake ground motion: Workshop on Ground Motion Estimation in Eastern North America, Electric Power Research Institute, Palo Alto, California.

Joyner, W.B., 1987, Ground-motion attenuation relationships: Earthquake Engineering Research Institute, Course on Strong Ground Motion, San Francisco, California, April 3, 1987.

WEST VALLEY CITY
EARTHQUAKE HAZARDS REDUCTION PROGRAM
PHASE I

14-08-001-G1-79

Joseph L. Moore, AICP
West Valley City Community Development Department
2470 So. Redwood Rd.
West Valley City, Utah 84119
801-974-5501

SCOPE:

To compile and analyze existing geologic/seismic data as part of a citywide effort to understand and hopefully mitigate some of the consequences of a significant seismic event in West Valley City, Utah. This study of a potentially catastrophic earthquake event will be utilized in the planning and emergency management functions within City government.

SPECIFIC OBJECTIVES:

1. **Define the Study Area** - Phase I researched the eastern half of the City, from about 4400 West to the Jordan River and from 2100 South to about 4700 South, encompassing 13 square miles. Many major critical facilities, lifelines and various land uses are found in the study area.

2. **Inventory and Digitally Map Study Area Attributes** - Initially a base map at 1" = 1000' scale was produced showing streets and lot lines. Then overlays of the available geologic/seismologic data were plotted utilizing using a digital mapping system . These overlays included liquefaction (Anderson), faults (USGS), ground shaking (Hays & King), soil types (SCS), water table (SCS), landslides, tectonic subsidence (Anderson & Keaton). In addition, overlays of critical facilities were digitally produced.

3. **The Digital Overlay Mapping of Study Area Attributes** - Once the information for the maps identified in step 2 was complete they were overlayed upon each other with the intent of identifying high risk multi-hazards areas.

4. **Target High Risk Seismic Zones** - This information led to defined areas of greater seismic risk. A separate map was developed displaying the high risk areas.

5. **Damage and Loss Potential** - Critical facilities and lifelines that were considered structurally marginal have been identified for their importance in the urban environment and the consequences of their failure.

FINDINGS:

Our intent was not to generate new information but to compile and synthesize the existing geologic/seismic data. The question that has always concerned the researcher has been whether such information was readily available and usable by local officials. On the whole adequate information exists except in the area of ground shaking and reaction of various soil types at various depths. Some gross information was compiled but it seems quite vague for our effort. It is hoped that during 1988 there will be a new more detailed study of the ground shaking and soil reaction issue which can be incorporated into the Phase II report.

There are three major seismic hazards that are found within the City, namely, fault lines, potential ground shaking and a secondary hazard known as liquefaction. Most Salt Lake Valley residents tend to think of faults only being a problem along the Wasatch Front but there are numerous faults scattered across the Valley floor. Some bisect West Valley City as shown on figure 1. We also tend to believe that since the faults are in the mountains then areas like West Valley City are safe from earthquakes. This is not true. Our valley is somewhat similar to the area around Mexico City, in that large areas of lake bottom materials, called unconsolidated sediments, exist which can amplify a shock wave from a fault rupture in the mountains. During this shaking it is possible for the soils, if they are saturated, to liquefy and lose their bearing capabilities causing heavy structures to topple or cause soil flows, even on very shallow slopes, such as less than 5 %. Much of the study area has slopes capable of generating lateral spreading.

For the study, a map that combines the major hazards is shown as figure 1. This multi-hazard map demonstrates that almost all of the study area is expected to have problems in the event of a major earthquake. Even in the area defined as "low" hazard, the ground shaking is fairly strong, therefore structural damage can be anticipated.

The final section of the report covered possible implementation strategies. Much research had been completed utilizing examples from California and other states. Ordinances, building code modifications, Master Plan elements and other information has been compiled for our purposes. Generally, this section reviewed potential strategies since no strategy will make much sense until the whole City is addressed in Phase II.

Brabb, E. E., ed. Progress on Seismic Zonation in the San Francisco Bay Region, Circular 807. Arlington, Virginia: U.S. Geological Survey, 1979.

Governor's Conference on Geologic Hazards. Utah Geological and Mineral Survey Circular 74, Atwood, Genevieve, Director. Salt Lake City, Utah: Utah Geological and Mineral Survey, December, 1983.

Richins, William D., et al. Earthquake Data for the Utah Region July 1, 1978 to Dec. 31, 1980. Salt Lake City Utah: University of Utah Seismograph Stations, Department of Geology and Geophysics, University of Utah, October 1981.

Mabey, Don R., and Atwood, Genevieve. "Fluctuations of the Level of Great Salt Lake." Survey Notes Vol. 18, No.1. Salt Lake City, Utah: Utah Geological and Mineral Survey, Spring 1984, pp. 3-8.

Mabey, Don R. "Earthquake Hazards in Utah." Survey Notes Vol. 18, No. 4. Salt Lake City, Utah: Utah Geological and Mineral Survey, Winter 1985.

Marine, Wendell and Price, Don. "Geology and Ground-Water Resources of the Jordan Valley, Utah." Water Resources Bulletin #7, Salt Lake City, Utah: Utah Geological and Mineral Survey, (Dec. 1964(, pp. 7-10, 22-27.

Ringholz, Raye C. "The Inevitability of Earthquake." Utah Holiday, January 1981, pp. 54-58.

Anderson, Loren R., et al. Liquefaction Potential map for Davis County, Utah. Eight plates, scale 1:48,000. Logan, Utah: Department of Civil and Environmental Engineering, University of Utah. U.S. Geological Survey, Professional paper, contract: 14-08-001-19127, February, 1982.

Anderson, Loren R., et al. Liquefaction Potential map, Salt lake County, Utah. Eight Plates, scale 1:48,000. Logan, Utah: Department of Civil and Environmental Engineering, Utah State University, and Dames and Moore Consulting Engineers, Salt lake City, Utah. U.S. Geological Survey, Professional paper, 1982.

Bruhn,R.L., et al. Structure of the Salt Lake Segment, Wasatch Normal Fault Zone; Implications for Rupture Propagation during Large Earthquakes. Salt Lake City, Utah: Department of Geology and Geophysics, University of Utah, 1985.

Currey, Donald R. Paleolake History in Reconstructing Neotechtonic History and Assessing Earthquake Hazards: The Special Case of Lake Bonneville and the Wasatch Front. Salt Lake City, Utah: Department of Geography, University of Utah, March, 1986.

Hays, Walter W. Evaluation of Local Site Amplification of Earthquake Ground Motion, An Important Consideration In Earthquake-Resistant Design In Utah. Reston, Virginia: U.S. Geological Survey, 1986.

Keaton, Jeffery R., Currey, Donald R., and Olig, Susan J. Paleoseismicity and Earthquake Hazards Evaluation Salt Lake City, Utah of the West Valley Fault Zone, Salt Lake Urban Area. Salt Lake City, Utah: Department of Geography and Department of Geology and Geophysics, University of Utah, 1985.

King, Kenneth W. Efforts on Site Geology on the Level of Ground Shaking Along the Wasatch Front. Denver, Colorado: U.S. Geological Survey, 1986.

Tingey, James L. and Findlay, Ralph F. Emergency Management in Utah for Earthquakes. Salt Lake City, Utah: Utah Division of Comprehensive Emergency Management, 1986.

FIGURE I

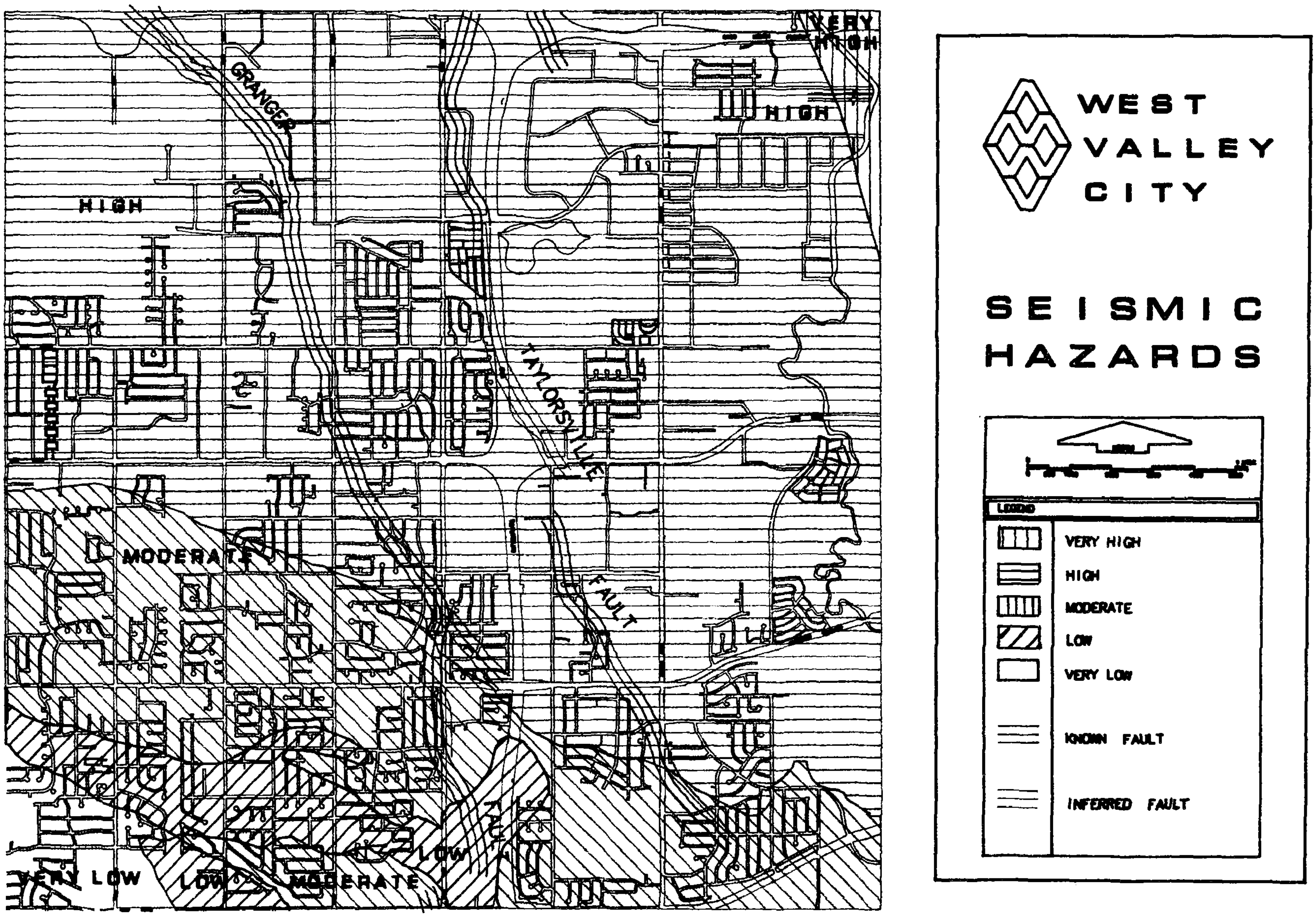
VERY HIGH
GRANGER
HIGH
HIGH
TAYLORSVILLE
MODERATE
FAULT
VERY LOW
LOW
MODERATE
LOW
WEST
VALLEY
CITY
SEISMIC
HAZARDS
LEGEND
VERY HIGH
HIGH
MODERATE
LOW
VERY LOW
KNOWN FAULT
INFERRED FAULT

TECHNIQUES FOR APPLYING EARTHQUAKE HAZARD MAP DATA--
San Francisco Bay Area, California

14-08-0001-G1166

Jeanne B. Perkins
Association of Bay Area Governments
MetroCenter
Eighth and Oak Streets
[P.O. Box 2050--Oakland, CA 94604]
(415) 464-7934

INTRODUCTION

For the past several years, ABAG has been developing computer-based maps and map files of the San Francisco Bay Area depicting earthquake hazards. The information currently is underutilized. ABAG is working to correct this situation. The process consisted of two steps:
(1) conduct a survey to determine how and why ABAG products are and are not used, as well as what ABAG should be doing to correct the situation;
(2) based on the survey, produce a couple of products needed by the user community.

The survey results indicated that the most needed product was well-organized non-technical documentation for the earthquake hazard maps, particularly those relating to ground shaking. The most innovative product desired was a computer analysis of the earthquake hazards associated with the locations of approximately 6000 non-wood buildings in the City of San Francisco. The decision was made to produce these two quite different products. This summary describes the non-technical documentation and the San Francisco work. The survey itself was the subject of the previous summary of this project.

NEW NON-TECHNICAL DOCUMENTATION -- *ON SHAKY GROUND*

The documentation prepared as part of this grant is intended to convey the nature and severity of the ground shaking hazard in the Bay Area, as well as to provide several options for local government actions to mitigate that hazard. Because of past experience, ABAG determined that a Review Committee should be formed to guide the author in the content of the report. This group of local government staff geologists, building inspectors/structural engineers, planners and emergency response personnel met twice to review the outline and final content of the report. Rather than describing the report any further, an excerpt from that report follows.

EXCERPT FROM *ON SHAKY GROUND*

The San Francisco Bay Area is in "earthquake country".

> **In most earthquakes, ground shaking is the greatest hazard, causing the largest percentage of damage.**
>
> Albert M. Rodgers
> U.S. Geological Survey

In some earthquakes, the surface of the ground can rupture along a fault -- or a landslide can be triggered -- or underground sand layers may flow (liquefy) -- or a tsunami (tidal wave) may be generated in water. But in all earthquakes, the ground shakes. In larger magnitude earthquakes, more ground shakes, and it shakes more severely. Ground shaking has and will cause damage tens of miles away from the fault source.

Three major factors affect the severity of ground shaking at a site (that is, its intensity) in an earthquake:

- the size (magnitude) of the earthquake;
- the distance from the site to the fault that generated that earthquake; and
- the geologic materials at the site.

The first map that follows shows the major faults in the Bay region. There are at least thirty faults in this area that can generate earthquakes. The second map shows the geologic materials in the central Bay Area. These materials are grouped into categories of similar susceptibility to shaking from earthquakes. The soils near the Bay (called Bay mud by geologists) are the most susceptible to shaking.

Using this information on fault location and geology, together with assumptions about typical earthquakes, it is possible to generate maps showing the expected severity of ground shaking from hypothetical earthquakes. Maps of two such scenarios, one for the San Andreas fault and a second for the Hayward fault, are included.

ABAG, with funding from the U.S. Geological Survey, has generated such scenario maps for thirty earthquakes. Because using these maps can become unwieldy, they have been combined them into two types of composite maps. The first was generated by looking down through the stack of thirty maps and selecting, for each site, the "worst case" or highest intensity occurring on any of the maps. The resulting map is the maximum ground shaking intensity map. The second type of composite map was generated by weighting the importance of each of the scenario intensity maps based on the recurrence interval of the earthquake and associated damage (for a range of three building types). These three maps are generated by adding the expected damage from all the earthquakes to form "risk" maps.

When the ground shakes, damage occurs to buildings, facilities and their contents. People are injured and killed. Businesses can't function and the economy suffers. A dozen options for avoiding, reducing or otherwise mitigating these results include:

- land use and zoning controls;
- requirements for soils and geotechnical studies;
- special building design requirements;
- special requirements for non-structural components;
- hazardous building retrofitting and abatement;
- special requirements related to hazardous materials;
- infrastructure and lifeline requirements;
- disclosure requirements and posting of signs;
- disaster response planning;
- reconstruction and redevelopment planning;
- public information and education programs; and
- strategies for maximizing political support.

All of these strategies are important and useful in improving safety plans of local governments. We must do a better job of preparing for the ride of our lives.

DATA FOR SAN FRANCISCO'S BUILDINGS

During the past couple of years, the Bureau of Building Inspection of the City/County of San Francisco has been inventorying all of the non-wood buildings built prior to 1951 as a first step in determining how to mitigate potential problems with the older unreinforced masonry buildings in the City. As part of this USGS grant, ABAG obtained a tape of these approximately 6000 buildings, including the more than 2100 unreinforced buildings in the City. One mitigation option would be to phase compliance with a new code based on relative ground shaking hazard. Another option would be to have more severe rehab code standards for buildings in locations with a relatively greater shaking hazard. Implementation of either standard would be the first time that geologic information has played a part in a citywide rehabilitation effort.

ABAG was able to obtain a copy of a tape containing over 6000 building addresses. The next step was to convert these addresses to latitude/longitude listings using the Association's computer-based geographic information system (GIS) operated by Geogroup Corporation, as well as DIME files from the U.S. Bureau of the Census. Finally, the earthquake hazard data for each building location was extracted from the GIS and the results written to a new tape for the City's Bureau of Building Inspection.

The earthquake hazard map data files provided for each building were:

- geologic materials (grouped into categories of similar susceptibility to ground shaking);
- maximum ground shaking intensity;
- risk of damage (or cumulative damage potential) for tilt-up concrete buildings (with damage curves similar to those for unreinforced masonry structures); and
- liquefaction potential.

PUBLICATIONS

Perkins, Jeanne B., July 1986. A Survey of Local Governments - Use of Earthquake Information, 8 p.

Perkins, Jeanne B., October 1986. Results of a Survey of Local Governments - Use of Earthquake Information, 14p.

Perkins, Jeanne B., February 1987. The San Francisco Bay Area - *On Shaky Ground*, 32p.

San Andreas Segmentation Cajon Pass to Wallace Creek

9910-03983

David P. Schwartz, Robert V. Sharp, and Ray J. Weldon
Branch of Engineering Seismology and Geology
U.S. Geological Survey
345 Middlefield Road, MS 977
Menlo Park, California 94025
(415) 323-8111, ext. 2689

Investigations

The project goal is to refine existing and/or develop new segmentation and fault behavior models for the San Andreas fault between Wallace Creek and Cajon Pass.

1. Develop new slip rate and recurrence data from Wallace Creek to south of Cajon Creek.

2. Critically review published and unpublished data and, where possible, existing field relationships to define and quantify uncertainties in: a) timing, displacement, and lateral extent of individual past earthquakes; and b) location-specific slip rate estimates.

3. Map and characterize the style of secondary faulting along the San Andreas, particularly near the junction with the San Jacinto fault on the south and near Liebre Mountain on the north.

Results

1. 96 St. (Littlerock) site. Shallow seismic refraction profiling is in progress to help define the contact between basement and gravel below the offset alluvial fill sequence at this locality. One additional trench was excavated to further define facies relationships that will help to narrow the preliminary slip-rate estimate, which is currently a minimum of 16 mm/yr for the past 1000-1200 years and a maximum of 38 mm/yr for the past 3600 years (Schwartz, Weldon, Fumal).

2. Wrightwood site. Work-to-date has been summarized in Summaries of Technical Reports, Volume XXIII (USGS Open-File Report 87-63). Trenching operations will resume Summer/Fall 1987.

3. Geologic and soils mapping are continuing at several locations to develop a better understanding of the tectonic evolution of the San Andreas fault zone. Localities include:

    a. Cajon Pass in conjunction with DOSECC (Weldon)
    b. Liebre Mountain (Weldon and Alexander)
    c. North branch of San Andreas fault in San Bernardino (Weldon in con junction with L. McFadden, University of New Mexico).

Reports

Alexander, J., and Weldon, R., 1987, Comparison of structural style of the Liebre Mountain and Squaw Peak thrust systems, offset across the San Andreas fault, southern California [abs.]: *Geological Society of America, Abstracts with Programs*, Cordilleran Section, Hilo, Hawaii, in press.

Humphreys, E.D., and Weldon, R.J., (in press), Kinematic constraints on the rifting of Baja California: *AAPG Memoir #* __, (on the Gulf of California).

McFadden, L.D., and Weldon, R.J., 1987, Rates and processes of soil development on Quaternary terraces in Cajon Pass, southern California: *Geological Society of America Bulletin*, v. 98, p. 280-293.

Schwartz, D.P., and Weldon, R.J., 1987, San Andreas slip rates: preliminary results from the 96th Street site near Littlerock, California [abs.]: *Geological Society of America, Abstracts with Programs*, Cordilleran Section, Hilo, Hawaii, in press.

Weldon, R.J., (in press), San Andreas fault, Cajon Pass, couthern California, in Hill, M.L. (ed.), 200 field trips to the North American Cordilleran: *Geological Society of America*, DNAG Volume No. ___.

Weldon, R.D., and Humphreys, E., 1987, Plate model constraints on the deformation of coastal southern California north of the Transverse Ranges [abs.]: *Geological Society of America, Abstracts with Programs*, Cordilleran Section, Hilo, Hawaii, in press.

Bay Area Faults

9910-NEW

David P. Schwartz, Michael J. Rymer,
James J. Lienkaemper, and Katherine K. Harms
Branch of Engineering Seismology and Geology
U.S. Geological Survey
345 Middlefield Road, MS 977
Menlo Park, California 94025
(415) 323-8111, ext. 2689, 2081, 2759, 2172
or (415) 329-5651, 329-5649, 329-5642, 329-5635

Investigations

This is a new project. The goal is to develop slip rate and earthquake recurrence information on the Hayward, Calaveras, and San Andreas (southern part of the 1906 rupture) faults. Plans include:

- Continue cooperative efforts with the California Division of Mines and Geology (CDMG) on Hayward fault slip rate studies.

- Initiate reconnaissance of the northern Calaveras fault with the goal of locating sites for paleoseismic investigations. This will be accomplished using aerial photographs, consultants' reports, and field reconnaissance. Emphasis will be placed on the Alum Rock segment of the fault, which has been proposed as the next Calaveras rupture segment, and on the section through the rapidly developing San Ramon Valley.

- Increase monitoring of consultants' trenches. Many trenches are opened by consultants throughout the Bay Area. With a more organized and systematic approach to monitoring those exposures, we may be able to increase our knowledge of local stratigraphy and soils, find charcoal or other datable material, and observe sites that have the potential to yield important paleoseismic data with additional investigations.

- Initiate reconnaissance along the 1906 rupture, with emphasis on the southern part, to evaluate sites for slip rate and recurrence studies.

Results

During FY 86, USGS amd CDMG worked together on trenches at Fremont City Hall. Trenches excavated parallel to the Hayward fault exposed gravel channels that may be correlative across the fault. Detrital charcoal has been found in deposits above and below the gravels. For FY 87, new and deeper trenches will be excavated at this location to systematically trace the gravels to the fault to better evaluate the tentative correlation. Additional charcoal will be looked for. This locality has the potential to provide the first well-constrained late Holocene slip rate on the Hayward fault.

Reports

None.

Global Digital Network Operations

9920-02398

Howell M. Butler
Branch of Global Seismology and Geomagnetism
U.S. Geological Survey
Albuquerque Seismological Laboratory
Building 10002, Kirtland AFB-East
Albuquerque, New Mexico 87115-5000
(505) 844-4637

Investigations

The Global Digital Network Operations presently consists of 15 SRO/ASRO and 14 DWWSSN stations. The primary objective of the project is to provide technical and operational support to keep these stations operating at the highest percentage of recording time possible to provide high-quality digital seismic data to the seismic research community. This support includes operational supplies, replacement parts, repair service, modification of existing equipment, installation of systems and on-site maintenance, training and calibration. A service contract provides technicians to perform on-site maintenance and installations, as well as to perform repair-and-test of seismometers and all replaceable units that comprise the various network systems. Contract technicians are also provided for special projects such as on-site noise surveys, special telemetered system installations, system renovations, and evaluation and testing of seismological and related instrumentation.

The following on-site station maintenance activity was accomplished:

- ANTO - Ankara, Turkey - SRO - Two maintenance visits
- COL - College, Alaska - DWWSSN - Two maintenance visits
- ANMO - Albuquerque, New Mexico - SRO - Two maintenance visits
- SNZO - Wellington, New Zealand - SRO - Two maintenance visits
- CTAO - Charters Towers, Australia - ASRO - One maintenance visit
- KEV - Kevo, Finland - DWWSSN - One maintenance visit
- TOL - Toledo, Spain - DWWSSN - One maintenance visit
- KBS - Kingsbay, Spitsbergen - DWWSSN - One maintenance visit
- BDF - Brasilia, Brazil - DWWSSN - One maintenance visit
- SCP - State College, Pennsylvania - DWWSSN - One maintenance visit
- BOCO - Bogota, Colombia - SRO - One maintenance visit

Special Activity. Maintenance and recalibration was performed at Scott Base, Antarctica (SBA) during October and November. Photo recorders were replaced with helicorders, installed new data and power cables, WWSSN console was relocated to new lab, installed mini-ups system, installed DWWSSN type filter/amps and modified seismometers to DWWSSN configuration.

Contract Field Engineers were trained on installation and maintenance of Streckeisen seismometer systems.

A second Streckeisen seismometer system was installed at Albuquerque.

Streckeisen seismometer systems were installed at College, Alaska and Kevo, Finland DWWSSN stations.

One Field Engineer was in China four months of this period for on-site maintenance and training of the China Digital Seismograph Network (CDSN)

Results

The Global Digital Network continues with a combined total of 29 SRO/ASRO/ DWWSSN stations. The main effort of this project is to furnish the types of support at a level needed to keep the GSN at the highest percentage of operational time in order to provide the highest quality digital data for the worldwide digital data base.

U.S. Seismic Network

9920-01899

Marvin A. Carlson
Branch of Global Seismology and Geomagnetism
U.S. Geological Survey
Denver Federal Center
Box 25046, Mail Stop 967
Denver, Colorado 80225
(303) 236-1506

Investigations

U.S. Seismicity. Data from the U.S. Seismic Network (USSN) are used to obtain preliminary locations and magnitudes of significant earthquakes throughout the United States and the world.

Results

As an operational program, the U.S. Seismic Network operated normally throughout the report period. Data were recorded continuously in real time at the NEIC main office in Golden, Colorado. At the present time, 120 channels of SPZ data are being recorded at Golden on develocorder film. This includes data telemetered to Golden via satellite from both the Alaska Tsunami Warning Center, Palmer, Alaska, and the Pacific Tsunami Warning Center, Ewa Beach, Hawaii. A representative number of SPZ channels are also recorded on Helicorders to give NEIC real-time monitoring capability of the more active seismic areas of the United States. In addition, 15 channels of LPZ data are recorded in real time on multiple pen Helicorders.

Data from the U.S. Seismic Network are interpreted by record analysts and the seismic readings are entered into the NEIS data base. The data are also used by NEIS standby personnel to monitor seismic activity in the United States and worldwide on a real time basis. Additionally, the data are used to support the Alaska Tsunami Warning Center and the Pacific Tsunami Warning Service. At the present time, all earthquakes large enough to be recorded on several stations are worked up using the "Quick Quake" program to obtain a provisional solution as rapidly as possible. Finally, the data are used in such NEIS publications as the "Preliminary Determination of Epicenters" and the "Earthquake Data Report."

Development is continuing on an Event Detect and Earthquake Location System to process data generated by the U.S. Seismic Network. We expect the new system to be ready for routine operational use by spring of 1987. At that time, the use of develocorders for data storage will be discontinued. Ray Buland and David Ketchum have been doing most of the developmental programming for the new system. A Micro Vax II will be used as the primary computer of the Event Detect and Earthquake Location System. PDP 11/23's and PDP 11/73's are being used as front ends to off load the real-time data collection from the Micro Vax II. A second Micro Vax II has been procured to serve as a backup to the primary system. The two Micro Vaxs share 1.3 gigabytes of disk storage.

During March 1987, installation of a pilot VSAT system was completed at the McMinnville, Tennessee RSTN station. The data is transmitted via satellite to a shared Master Earth Station and on to Golden, Colorado. If this system is successful, it will be the first of many such stations in a VSAT network which will be implemented in the next few years with the goal of completely replacing the use of AT&T Long Lines to transmit seismic data.

Earth Structure and its Effects upon Seismic Wave Propagation

9920-01736

George L. Choy
Branch of Global Seismology and Geomagnetism
U.S. Geological Survey
Denver Federal Center
Box 25046, Mail Stop 967
Denver, Colorado 80225
(303) 236-1506

Investigations

1. Use of body wave pulse shapes to infer attenuation in the Earth. We are developing techniques to determine the depth- and frequency-dependence of attenuation in the earth. Resolution of this frequency dependence requires analysis of a continuous frequency band from several Hz to tens of seconds. It also requires consideration of the contributions of scattering and slab diffraction to apparent broadening of a pulse.

2. Source parameters from broadband data. The extraction of accurate source parameters from digitally recorded data requires the correct application of propagation corrections to waveforms. These corrections are most important for the midband frequencies in which is located the corner frequency of most well-recorded teleseismic events.

3. Use of differential travel-time anomalies to infer lateral heterogeneity. We are investigating lateral heterogeneity in the Earth by analyzing differential travel times of phases that differ in ray path only in very narrow regions of the Earth. Because such phases often are associated with complications near a cusp or caustic, their arrival times can not be accurately read without special consideration of the effects of propagation in the earth as well as additional processing to enhance arrivals.

Results

1. We are attempting to separate intrinsic attenuation from scattering in waveforms. We synthesize waveforms using a method that simultaneously models causal attenuation and source finiteness. Under the assumption that intrinsic attenuation can be described by minimum phase operators, we can attribute discrepancies in the waveforms to scattering.

2. We are incorporating the frequency-dependent Q model derived by Choy and Cormier (1986) into an NEIC energy-computation package. This package is a semi-automated version of the algorithm of Boatwright and Choy (1986) which computes energy directly from broadband data. We expect the package to be ready for routine use on all earthquakes with $m_b > 5.8$ by mid-1987.

3. We have developed a source-deconvolution technique that resolves differential travel times of body waves near cusps and caustics. Application of this algorithm to PKP waves sampling the inner core suggests that regional velocity variations exists within the upper 200 km of the inner core. The regional variations are consistent with those obtained from global inversions of absolute PKP times.

Reports

Choy, G.L., and Cormier, V.F., 1986, Direct measurement of the mantle attenuation operator from broadband P and S waveforms: Journal of Geophysical Research, v. 91, p. 7326-7342.

Cormier, V.F., and Choy, G.L., 1986, A search for lateral heterogeneity in the inner core from differential travel times near PKP-D and PKP-C: Geophysical Research Letters, v. 13, p. 1553-1556.

Systems Engineering

9920-01262

Harold E. Clark, Jr.
Branch of Global Seismology and Geomagnetism
U.S. Geological Survey
Albuquerque Seismological Laboratory
Building 10002, Kirtland AFB-East
Albuquerque, New Mexico 87115-5000
(505) 844-4637

Investigations

1. Installation of the Antarctic Dry Valley Seismograph Project (DVSP) seismic station and data telemetry link from the borehole site in the Wright Valley to Scott Base.

2. Continuation of the development and deployment of the China Digital Seismograph Network (CDSN).

Results

During the time period of October and November 1986, Harold Clark worked with Geotech personnel, Mike Browne and Gayland Shiel, in Antarctica to install the DVSP network. Tasks included installation of large propane tanks at the Wright Valley borehole site and at the Mt. Newall repeater site. The borehole sensors were installed at the Wright Valley borehole site. The telemetry radio systems and towers were installed at the Mt. Newall and Crater Hill sites. The propane powered thermo-electric systems had to be rebuilt and installed. The two-way telemetry link between Scott Base, Crater Hill, Mt. Newall and the Wright Valley borehole site was aligned and made operational. This telemetry link provided voice communication between any site and seismic data transmission from the borehole site to Scott Base.

CDSN System No. 12 parts were ordered and construction/assembly was started. CDSN System No. 12 will provide the same data recording techniques as the other eleven CDSN systems, but will also provide a satellite telemetry channel for data transmission. Work has started on a special satellite data receiving station to record and analyze the CDSN data. The initial satellite link will be tested using parts and equipment from the Sandia RSTN satellite network.

Reanalysis of Instrumentally Recorded United States Earthquakes

9920-01901

J. W. Dewey
Branch of Global Seismology and Geomagnetism
U.S. Geological Survey
Denver Federal Center
Box 25046, Mail Stop 967
Denver, Colorado 80225
(303) 236-1506

Investigations

1. Relocate instrumentally recorded U.S. earthquakes using the method of joint hypocenter determination (JHD) or the master event method, using subsidiary phases (Pg, S, Lg) in addition to first arriving P-waves, using regional travel-time tables, and expressing the uncertainty of the computed hypocenter in terms of confidence ellipsoids on the hypocentral coordinates.

2. Evaluate the implications of the revised hypocenters on regional tectonics and seismic risk.

Results

1. D. W. Gordon has continued to relocate earthquakes and investigate relationships between tectonics and seismicity in central and eastern Wyoming. Gordon is using regionally recorded strip mine blasts to calibrate his use of JHD on the Wyoming shocks. Many of the revised epicenters are within uplifts, such as the Wind River Range, where late Cenozoic, high-angle, faults have been mapped. An east-west trend of the revised epicenters correlates spatially with geologically young faulting along the north flank of the Granite Mountains. In the Hartville uplift, the revised instrumental epicenters and epicenters of felt, but instrumentally unrecorded, shocks are associated with a zone of geologically mapped, late Cenozoic, faults.

2. J. W. Dewey is co-authoring a paper for the Decade of North American Geology project on the seismicity of Mexico, Central America, and the Caribbean. Dewey's contribution focuses on Central America and the Caribbean. In addition to their intrinsic importance in local seismic hazard analysis, several source regions in Middle America are of interest to us because they are similar in some ways to important source regions in the United States. The similarities allow observations from one region to constrain seismotectonic hypotheses in the other region. The northern and southern boundary-regions of the Caribbean plate, for example, contain major strike-slip fault-zones. Like some major strike-slip faults in California, the Caribbean strike-slip faults appear to have seismic cycles that comprise infrequent great earthquakes separated by periods, lasting more than a century, during which the frequency of earthquakes of all magnitudes is low. As is also the case in California, transform plate-boundary zones of the Caribbean commonly contain more than one subparallel strike-slip fault, so that the width of the region in which destructive strike-slip earthquakes might occur exceeds 50 km.

Global Seismology

9920-03684

E. R. Engdahl
and
J. W. Dewey

Branch of Global Seismology and Geomagnetism
U.S. Geological Survey
Denver Federal Center
Box 25046, Mail Stop 967
Denver, Colorado 80225
(303) 236-1506

Investigations

1. Depth Phases. Develop procedures for the global analyses of earthquake depth phases and source characteristics using broadband seismograms of body waves.

2. Earthquake Location in Island Arcs. Develop practical methods to accurately locate earthquakes in island arcs.

3. Subduction Zone Structure. Develop techniques to invert seismic travel times simultaneously for earthquake locations and subduction zone structure.

4. Global Synthesis. Synthesize recent observational results on the seismicity of the earth and analyze this seismicity in light of current models of global tectonic processes.

Results

1. Depth Phases. Displacement and velocity records of body waves with frequency content from 0.01 to 5 Hz can now be routinely obtained for most earthquakes with magnitude greater than about 5.5. These records are obtained either directly or by multichannel deconvolution of waveforms from digitally recording seismograph stations such as those of the GDSN (Global Digital Seismograph Network), RSTN (Regional Seismic Test Network), and GRF-array (Gräfenberg Seismological Observatory). Once the distortion of the seismograph filter is removed, the seismograms often show the source-time functions of the direct and surface-reflected phases, even for shallow events where depth phases may overlap the direct wave. A systematic procedure has been developed for analyzing broadband seismograms that identifies depth phases and subevents (for complex earthquakes). A natural benefit of the procedure is that better resolution of the focal mechanism can be obtained from the polarities of depth phases. In particular, the phase sP, which is also more clearly defined, provides additional valuable constraints on focal mechanism determinations. Because most large earthquakes are complex events, depth phases recorded on conventional seismograms are often incorrectly read and reported. The National Earthquake Information Center

is now utilizing digital waveforms routinely to obtain better estimates of focal depth, to identify subevents in complex earthquakes, and to improve focal mechanism determinations.

Source Parameters. The May 7 Andreanof Islands earthquake (M_w = 8.0) was the largest event to occur in 1986 and the largest to strike this region since the 1957 Great Aleutian earthquake. The aftershock distribution indicates that the main shock ruptured a 250-km portion of the arc between Adak Canyon in the west and the Amlia fracture zone in the east. Centroid-moment tensor (CMT) solutions are computed for the main shock and more than 30 moderate-size ($M_w \geq 5.0$) events in the aftershock sequence, as well as for previous events which have occurred in the main shock source region over the last 10 years. Since the CMT method is relatively insensitive to the hypocentral locations, additional data and complementary methods are used to locate the events and to correlate them with observed tectonic features.

Due to the significant variations in the shallow and deep velocity structure across the subduction zone, catalog epicenters located in a spherical Earth structure are systematically mislocated. All events are relocated in a cylindrically symmetric crustal and deep slab velocity model using both teleseismic and local data. For shallow focus events (h < 45 km) the relocated epicenters systematically lie closer to the trench axis by up to 50 km. Except for events close to the local Adak network, the relocation of shallow earthquakes does not result in well-constrained focal depths, however, and two alternative methods of depth determination are used.

In the first method, broadband P-wave displacement seismograms together with the long-period CMT data set are used in an inversion for the mechanism, depth, and time function of the source. In the second method, arrival times of direct and prominent reflected phases, primarily pwP, from short-period and broadband digital seismograms are read. Detailed models of bathymetry and crustal structure are used in the calculations of synthetic seismograms and depth phase delay times. For events which can be analyzed using both methods, a comparison of the results is made. The agreement in source depth is generally within a few kilometers.

These results show that a majority of moderate-size subduction earthquakes occur as thrust events on the shallow (15-25 km) portion of the slab interface. The main shock epicenter indicates a nucleation depth of approximately 25 km. The deeper (25-45 km) events along the slab interface are also of thrust type, and lie primarily in the western half of the region with a concentration of events south of Adak.

2. Earthquake Location in Island Arcs. A plate model is used to relocate teleseismically well-recorded earthquakes ($m_b \geq 4.9$) in the region of the May 7, 1986, Andreanof Islands earthquake. The relocated earthquakes provide a complete description of the space-time history of earthquakes in the region. The sequence of earthquakes associated with the 1986 mainshock extended over a 250 km long segment of the arc primarily along the updip portion of the active thrust zone. A strong foreshock (M_S 6.3), 2.1 hours before the mainshock, and early aftershocks were apparently confined to a region only 50 km east and west of the mainshock epicenter. A large

earthquake (m_b 5.9) west of that region and near Adak Canyon, 2.4 hours after the mainshock, apparently initiated the extension of the aftershock zone to its full length along the arc. Later strong aftershocks extended the sequence into the overriding plate along the downdip portion of the thrust zone (M_S 6.3 on June 18).

The aftershock zone of the 1986 mainshock is very similar to the spatial distribution of relocated aftershocks of the great 1957 earthquake in this region. Before the 1986 mainshock and since at least 1964, seismicity in this updip portion of the thrust zone has been characterized by localized concentrations of moderate-size earthquakes. Aftershocks of the 1986 earthquake occurred both within these concentrations and within new centers of activity. A striking feature of both the pre- and post-mainshock seismicity is the absence of deeper thrust zone activity east of the 1986 mainshock. A sharp decrease in the rate of microearthquake activity before the 1986 mainshock, that started suddenly in July-August, 1982, apparently was centered within a 100 km segment of the thrust zone just west of the early aftershocks. This quiescence seems to correlate with a near absence of teleseismic activity over the same period in that segment and with the region of major moment release of the 1986 mainshock.

The aftershock sequence for the first 105 days and for $m_b \geq 4.6$ (247 events), as given in the USGS Monthly Listing, fits the modified Omori relation: $n(t)=27.035(t+0.02)^{-0.9}$ events per day. Small departures from this rate of decay are associated with some of the larger aftershocks. The b-value for the entire sequence is 1.36. After 1.6 days, it increased to .15. Following the strong aftershocks of May 15 and 17, the count of earthquakes stayed above that of the Omori relation for about 15 days, with a high b-value. After the aftershock of June 18, the count was below the relation for 45 days, with b=1.2.

3. <u>Subduction Zone Structure</u>. A combined location and velocity inversion technique is applied to travel-time data from 151 well-recorded central Aleutian earthquakes. The data include P- and S-wave arrivals at stations of a local network and P-, pP-, and sP-wave arrivals at teleseismic stations. After correction for upper crustal structure at the reflection points, the depth phases pP and sP provide important constraints on subduction zone structure not ordinarily resolved by other data types. The structure is assumed to vary only across the arc and in depth; it is parameterized with cubic splines that provide a specification of velocity at each point of a gridded arc cross section. To avoid ray tracing, it is assumed that the velocity part of the problem is linear. Preliminary results show that deep earthquakes apparently occur within a narrow downdip zone near the upper surface of the descending slab, in contrast with previous studies which have located them within the presumably stronger and colder inner core of the slab. A slab thickness of 80-100 km and a downdip length of about 400 km, well below the deepest seismic activity, is indicated. The slab is characterized by seismic velocities as much as 11 percent higher than the surrounding mantle in its upper portions and 4-6 percent higher at depth. A sharp velocity gradient and lower velocities occur directly beneath the volcanic arc near the top of the slab. The slab anomaly appears to spread

out and fall off very slowly with depth; these are probably not real effects but consequences of the omission of three-dimensional ray tracing.

4. Global Synthesis. A highlight of the Decade of North American Geology program is four new continent-scale tectonic maps (geothermal, stress, seismicity, and geologic) on a common base. The maps are in color, at a scale of 1:5,000,000, and use a Transverse Mercator projection. Construction of the seismicity map has required the rationalization of more than one-half million earthquake epicenters from global, national, regional, and local catalogs. Duplicate entries were removed regionally based on a comparison of reported origin times, epicentral locations, and magnitudes. The reduced data base spans an interval from A.D. 1500 to 1985. Only those data that exceed the magnitude-completeness threshold for each region and time period were plotted. In all parts of the map, earthquakes of magnitudes less than 4 are represented by small dots, larger earthquakes by filled circles of various sizes in proportion to magnitude, and great earthquakes ($M \geq 7$) by large rings. Different colors are used to distinguish modern from historic data and to show deep ($h \geq 50$ km), intraplate earthquakes in subduction zones. The modern data are more useful than historic data for resolving seismotectonic features, as they have more accurate locations and lower magnitude-completeness thresholds. This scheme of symbols and colors reveals details of the seismotectonic fabric of North America yet preserves a perspective of historical earthquake occurrence.

Reports

Choy, G., and Engdahl, E.R., 1987, Analysis of broadband seismograms from selected IASPEI events: Physics of the Earth and Planetary Interiors, in press.

Engdahl, E.R., and Billington, S., 1986, Focal depth determination of central Aleutian earthquakes: Bulletin of the Seismological Society of America, v. 76, p. 77-93.

Engdahl, E.R., and Kind, R., 1986, Interpretation of broadband seismograms from central Aleutian earthquakes: Ann. Geophysicae, v. 4, p. 233-240.

Engdahl, E.R., and Gubbins, D., 1987, Simultaneous travel-time inversion for earthquake location and subduction zone structure in the central Aleutian Islands: Journal of Geophysical Research, in press.

9920-02384

Jon Peterson
Branch of Global Seismology and Geomagnetism
U.S. Geological Survey
Albuquerque Seismological Laboratory
Building 10002, Kirtland AFB-East
Albuquerque, New Mexico 87115-5000
(505) 844-4637

Investigations

1. Work continued on the China Digital Seismograph Network (CDSN).

2. Work began on the Incorporated Research Institutions for Seismology (IRIS) global seismograph network (GSN).

Results

1. The CDSN is fully operational. Some additional equipment was installed in the data management center to simplify the transfer of data from station cartridges to nine-track tape. Minor work is needed at the stations to repair a software bug in the event detectors, and additional training is planned for network personnel in China and in the U.S. Data flow from the CDSN to ASL has been a little erratic and some of the data have been received too late to place on the ASL network-day tape. This is a procedural problem that will be worked out in the near future.

2. Initial work began on the new GSN sponsored by IRIS. The GSN will ultimately consist of 50 to 100 broadband seismograph stations. Preliminary activities involving the USGS this fiscal year include the installation of broadband sensor systems at five DWWSSN stations, two of which have been installed at COL and KEV, and initial steps in the upgrading of the ASL data collection center. A contract has recently been awarded by IRIS for development of the new digital data system.

Digital Data Analysis

9920-01788

Stuart A. Sipkin
Branch of Global Seismology and Geomagnetism
U.S. Geological Survey
Denver Federal Center
Box 25046, Mail Stop 967
Denver, Colorado 80225
(303) 236-1506

Investigations

1. Moment Tensor Inversion. Apply methods for inverting body phase waveforms for the best point-source description to research problems.

2. Other Source Parameter Studies. Apply methods for inverting body phase waveforms for distributed kinematic and dynamic source properties.

3. Broadband Body-Wave Studies. Use broadband body phases to study lateral heterogeneity, attenuation, and scattering in the crust and mantle.

4. Computation of Free Oscillations. Study the effects of anelasticity on free oscillation eigenfrequencies and eigenfunctions.

5. Earthquake Recurrence Statistics. Use earthquake recurrence statistics and related parameters to better understand the earthquake cycle and study how they can be used for prediction and forecasting purposes.

6. Earthquake Location Technology. Study techniques for improving the robustness, honesty, and portability of earthquake location algorithms.

7. Real-Time Earthquake Location. Experiment with real-time signal detection, arrival-time estimation, and event location for regional earthquakes.

8. Data Collection Center. Develop a state-of-the-art data collection center to handle digital waveform data collection for the next decade.

9. NEIC Monthly Listing. Contribute both fault-plane solutions (using first-motion polarity) and moment tensors (using long-period body-phase waveforms) for all events of magnitude 5.8 or greater when sufficient data exists. Contribute waveform/focal-sphere figures of selected events.

Results

1. Moment Tensor Inversion. A catalog of moment tensors for all sufficiently large events during 1981--1983, including comparisons with the first-motion fault-plane solutions and the Harvard CMT solutions, has been published. The strengths and weaknesses of all three methods are assessed. A paper assessing the large number of non-double-couple

earthquakes occurring in the Nazca plate subduction zone is in press. We find that these earthquakes are caused by slip on non-planar fault surfaces which is, in turn, due to the extreme structural complexity in this region. An anomalous seismic event which occurred off the coast of Japan has been analyzed. The resulting mechanism is consistent with the hypothesis that this event was caused by fluid injection.

2. Other Source Parameter Studies. An method for simultaneously inverting teleseismic long- and short-period waveforms for the distribution of slip on a fault surface has been developed. The long-period waveform data constrains the duration and size of the earthquake, while the short-period data are necessary to resolve the slip distribution.

3. Broadband Body-Wave Studies. High-quality digitally recorded broadband data sets from the Gräfenberg Array in West Germany and the Regional Seismic Test Network in North America have been collected and are being assessed. New software is continuing to be developed.

4. Computation of Free Oscillations. An article on the use of variational methods in geophysics has been completed and will appear as a chapter in an IASPEI sponsored book on seismological algorithms.

5. Earthquake Recurrence Statistics. A computer program implementing a new earthquake forecasting algorithm has been prepared for distribution. Work is underway on applying the algorithm to cases where only one recurrence interval is available, where the recurrence interval must be estimated from other information, and where only paleoseismic information is available.

6. Earthquake Location Technology. A journal article on the statistics of teleseismic body-wave travel-time residuals has been submitted for publication. An outgrowth of follow-up work on robust earthquake location suggested improvements for the Bulletin of the International Seismological Centre which have been installed. These improvements permit better rejection of outlying data and much more precise estimation of error bars (particularly for small events).

7. Real-Time Earthquake Location. Preliminary work on the color graphics workstation has demonstrated the feasibility of this technology as an analyst workstation and has laid the (system interface) cornerstone for subsequent development. The preliminary design of new field stations has been completed. Tentative selection of vendors for the sensors, ADC's, and station processors have been made, as well as selection of a technology for the satellite telemetry.

8. Data Collection Center. Equipment for the development system has been delivered and software conversion/redevelopment is in progress. Additional equipment required to reach operational status has been defined and is being procured. Tentative plans for the enhancement, growth, and operation of the system have been made and approved. Preliminary discussions have been held to define final design goals.

9. NEIC Monthly Listing. Since January 1981, fault-plane solutions for large events have been contributed to the Monthly Listings. Since July 1982, moment tensor solutions and waveform/focal-sphere plots have also been contributed. Fault-plane solutions for the period 1981-1985, and moment tensor solutions for the period 1981-1983, have been compiled and published. In the last six months solutions for approximately 65 events have been published. Detailed regional seismicity maps, covering the time period from 1971 to 1986, for 16 seismogenic areas worldwide have been prepared.

Reports

Buland, R.P., 1987, Residual statistics: Bulletin Seismological Society of America, submitted.

Buland, R.P., and Nishenko, S.P., 1987, Earthquake forecasting along simple plate boundaries [abs.]: Abstracts, 19th IUGG General Assembly, Vancouver, Canada, in press.

Kubas, A., and Sipkin, S.A., 1987, Non-double-couple earthquake mechanisms in the Nazca plate subduction zone [abs.]: EOS (American Geophysical Union, Transactions), v. 68, in press.

______1987, Non-double-couple earthquake mechanisms in the Nazca plate subduction zone: Geophysical Research Letters, v. 14, in press.

Mendoza, C., and Hartzell, S.H., 1987, Inversion for slip distribution using teleseismic body waves: North Palm Springs and Borah Peak earthquakes [abs.]: Seismological Research Letters, v. 58, no. 1, p. 8.

Nishenko, S.P., and Buland, R.P., 1987, A generic recurrence interval distribution for earthquake forecasting: Bulletin Seismological Society of America, v. 77, in press.

Nishenko, S.P., Perkins, D., and Buland, R.P., 1987, Normalized time and precursor reliability: in Proceedings of U.S. Geological Survey Red Book Conference, in press.

Sipkin, S.A., 1986, Estimation of earthquake source parameters by the inversion of waveform data: Global seismicity, 1981-1983: Bulletin Seismological Society of America, v. 76, no. 6, p. 1515-1541.

______1987, Body wave analysis of the anomalous seismic event near Tori Shima, Japan [abs.]: EOS (American Geophysical Union, Transactions), v. 68, in press.

______1987, A comparison of the USGS moment tensor solutions, USGS first-motion focal mechanisms, and Harvard CMT solutions [abs.]: Abstracts, 19th IUGG General Assembly, Vancouver, Canada, in press.

Seismicity and Tectonics

9920-01206

William Spence
Branch of Global Seismology and Geomagnetism
U.S. Geological Survey
Denver Federal Center
Box 25046, Mail Stop 967
Denver, Colorado 80225
(303) 236-1506

Investigations

Studies carried out under this project focus on detailed investigations of large earthquakes, aftershock series, tectonic problems, and earth structure. Studies in progress have the following objectives:

1. Use earthquake focal mechanisms and integrative tectonics to infer the origins of present-day stresses acting at the proposed Cascadia subduction zone (W. Spence).

2. Provide tectonic setting for and analysis of the 1974 Peru gap-filling earthquake (W. Spence and C.J. Langer).

3. Examine the source properties (focal mechanism and depth) of aftershocks following large thrust earthquakes in subduction regions by using digital surface-wave data (C. Mendoza).

4. Determine the maximum depth and degree of velocity anomaly beneath the Rio Grande Rift and Jemez Lineament by use of a 3-D, seismic ray-tracing methodology (W. Spence and R.S. Gross).

Results

1. The seismicity of the Cascadia subduction zone is highly anomalous when compared to other subduction zones. A synthesis of nineteen focal mechanisms for the zone from Cape Mendocino to the Queen Charlotte fault shows that most of the offshore earthquakes are associated with maximum compressive stress axes that trend about N-S. The locations of these earthquakes indicate that much of the offshore plate system is being compressed by the northwestward motion of the Pacific plate. Similarly, there is considerable evidence for N-S compression in the shallow crust of the overriding North American plate. The fact that the South Gorda block is not subducting but is being driven northward (along with the northward movement of the Mendocino triple junction) suggests that a N-S shear traction can be transmitted into the overriding plate, consistent with the observed landward focal mechanism data. Earthquakes with downdip tension axes occur in the subducted Juan de Fuca plate, from southern Vancouver to just south of Puget Sound, indicating that the slab pull force is resisted at shallow depths there. However, the lack of seismicity at the probable interface thrust zone for the entire Cascadia zone, the lack of seismicity

in the subducted Juan de Fuca plate outside the indicated zone, and the known cessation of subduction of the Gorda block and Explorer subplate that if subduction is occurring at the remainder of the Cascadia zone, it is of very limited extent. The dominant N-S stresses observed for shallow earthquakes of the entire Cascadia zone suggest that the collision of the Pacific plate with the Gorda block and southern Juan de Fuca plate dominates the tectonics of the Cascadia region.

2. The great 1974 Peru thrust earthquake (M_S 7.8, M_W 8.1) occurred in a documented seismic gap, between two earthquakes each with magnitude of about 8, occurring in 1940 and 1942. Additional major earthquakes occurred in this region in 1966 and in 1970; all but the 1970 shock represent thrust faulting. The stress release of the October 3, 1974, main shock and aftershocks occurred in a spatially and temporally irregular pattern. The multiple-rupture main shock produced a tsunami with wave heights of 0.6 ft at Hawaii and which was observed, for example, at Truk Island and at Crescent City. The aftershock series essentially was ended with the occurrence of a M_S 7.1 aftershock on November 9, 1974. The several years of preseismicity data to this earthquake include an unusually clear example of the "Mogi donut" pattern.

3. Love and Rayleigh-wave signals recorded by the Global Digital Seismograph Network provide source-parameter information for moderate-magnitude aftershocks that followed the large (M_S 7.7) Colombia earthquake of 12 December 1979. Love/Rayleigh amplitude ratios observed in a 30-80 second passband are compared against theoretical values calculated for a suite of source models fixed at independently determined depths. In addition, a reference earthquake with known focal mechanism and depth is used to calibrate the procedure and to minimize the path and size effects. Source mechanisms compatible with the amplitude data and observed P-wave first motions are obtained. These mechanisms serve to identify subsidiary faulting not associated with the main shock rupture.

Similar surface-wave techniques are being implemented in the analysis of the aftershock sequence that followed the large (M_S 7.8) Chile earthquake of 3 March 1985. The earthquake ruptured about 1/3 of the rupture length inferred for the great (M_S 8.2-8.4) Valparaiso earthquake of 1906. By comparing the spectra observed in a 20-50 second period range, focal depths can be estimated and source mechanisms can be computed for the aftershocks. The aftershock properties should provide additional constraints on the faulting geometry produced by the main shock of 3 March 1985.

4. To a depth of about 160 km, the upper mantle P-wave velocity beneath the Rio Grande rift and Jemez lineament is 4-6 percent lower than beneath the High Plains Province. A 3-D, P-wave velocity inversion shows scant evidence for pronounced low P-wave velocity beneath the 240-km-long section of the Rio Grande rift covered by our array. However, the inversion shows a primary trend of 1-2 percent lower P-wave velocity underlying the northeast-trending Jemez lineament, down to a depth of about 160 km. The Jemez lineament is defined by extensive Pliocene-Pleistocene volcanics and late Quaternary faults. The upper mantle low-velocity segment beneath the Jemez lineament is at most 100 km wide and at least 150-200 km long, extending in

our inversion from Mt. Taylor through the Jemez volcanic center and through the Rio Grande rift. A Backus-Gilbert resolution calculation indicates that these results are well-resolved.

Reports

Mendoza, C., 1986, Source mechanisms of Colombia aftershocks using digital surface-wave data: Bulletin of the Seismological Society of America, Bulletin of the Seismological Society of America, v. 76, p. 1597-1613.

Spence, William, 1986, The 1977 Sumba earthquake series: evidence for slab pull force acting at a subduction zone: Journal of Geophysical Research, v. 91, p. 7225-7239.

______1986, Origins of stresses at the Cascadia subduction zone [abs.]: EOS (American Geophysical Union, Transactions), v. 67, p. 1115.

______1987, Slab pull and the seismotectonics of subducting lithosphere: Reviews of Geophysics, v. 25, p. 55-70.

United States Earthquakes

9920-01222

Carl W. Stover
Branch of Global Seismology and Geomagnetism
U.S. Geological Survey
Denver Federal Center
Box 25046, Mail Stop 967
Denver, Colorado 80225
(303) 236-1500

Investigations

1. One hundred and five earthquakes in 18 states were canvassed by a mail questionnaire for felt and damage data. Forty-one of these occurred in California and 25 in Alaska. The largest magnitude events occurred on January 3 (M_s 6.6) and February 27 (M_s 6.7) in the Fox Islands, Aleutian Islands, Alaska. The February 27 earthquake was felt strongly at Akutan and Unalaska but no damage was reported; however, the volcano on Akutan Island was releasing smoke following the earthquake. No damage caused by earthquakes in the United States has been reported during this reporting period.

2. Hypocenters for earthquakes in the United States for the period October 1, 1986, to March 31, 1987, have been computed and published in the Preliminary Determination of Epicenters (PDE) Weekly and Monthly Listings.

Results

Seismicity maps for the conterminous United States, Alaska, and the world showing earthquakes located during the month of the publication were included in each Monthly Listing of the PDE.

A retrieval system for historical earthquake data has been established on the VAX 780 computer. This system, called the EARTHQUAKE DATA BASE SYSTEM, is available to anyone who has the equipment necessary to login to the VAX 780. The system manager is Glen Reagor.

Reports

Reagor, B.G., Stover, C.W., and Algermissen, S.T., 1987, Seismicity map of the state of Florida: Miscellaneous Field Studies Map MF-1056 (updated through 1983).

______1987, Seismicity map of the state of Tennessee: Miscellaneous Field Studies Map MF-1157 (updated through 1983).

Reagor, B.G., Stover, C.W., Algermissen, S.T., and Long, L.T., 1987, Seismicity map of the state of Georgia: Miscellaneous Field Studies Map MF-1060 (updated through 1983).

Stover, C.W., Reagor, B.G., and Algermissen, S.T., 1987, Seismicity map of the state of Kentucky: Miscellaneous Field Studies Map MF-1144 (updated through 1983).

Data Processing, Golden

9950-02088

Robert B. Park
Branch of Geologic Risk Assessment
U.S. Geological Survey
Box 25046, MS 966, Denver Federal Center
Denver, CO 80225
(303) 236-1638

Investigations

The purpose of this project is to provide the day-to-day management and systems maintenance and development for the Golden Data Processing Center. The center supports Golden-based Office of Earthquakes, Volcanoes, and Engineering investigators with a variety of computer services. The systems include a PDP 11/70, several PDP 11/03's and PDP 11/23's, a VAX/750, a VAX/780, a MicroVAX, and two PDP 11/34's. Total memory is 14 mbytes and disk space will be approximately 6 G bytes. Peripherals include five plotters, ten mag-tape units, an analog tape unit, two line printers, 5 CRT terminals with graphics, a Summagraphic digitizing table, and a laser disk. Dial-up is available on all the major systems and hardwire lines are available for user terminals on the upper floors of the building. Users may access any of the systems through a Gandalf terminal switch. Operating systems used are RSX11 (11/34's), Unix (11/70), RT11 (LSI's) and VMS (VAX's).

The three major systems are shared by the Branch of Global Seismicity and Geomagnetism and the Branch of Geologic Risk Assessment.

Results

Computation performed is primarily related to the Global Seismology and Hazards programs; however, work is also done for the Induced Seismicity and Prediction programs as well as for DARPA, ACDA, MMS, U.S. Bureau of Reclamation and AFTAC, among others.

In Global Seismology and Geomagnetism, the data center is central to nearly every project. The monitoring and reporting of seismic events by the National Earthquake Information Service is 100 percent supported by the center. Their products are, of course, a primary data source for international seismic research and have implications for hazard assessment and prediction research as well as nuclear test ban treaties. Digital time series analysis of Global Digital Seismograph Network data is also 100 percent supported by the data center. These data are used to augment NEIS activities as well as for research into routine estimation of earthquake source parameters. The data center is also intimately related to the automatic detection of events recorded by telemetered U.S. stations and the cataloging of U.S. seismicity, both under development.

In Geologic Risk Assessment, the data center supports research in assessing seismic risk and the construction of national risk maps. It also provides capability for digitizing analog chart recordings and maps as well as analog tape. Also, most, if not all, of the research computing related to the hazards program are supported by the data center. Data from digital networks are input through the microVAX to a multiported data base available to users on the other two VAX systems.

The data center also supports equipment for online digital monitoring of Nevada seismicity. Also, it provides capability for processing seismic data recorded on field analog and digital cassette tape in various formats.

National Earthquake Information Center

9920-01194

Waverly J. Person
Branch of Global Seismology and Geomagnetism
U.S. Geological Survey
Denver Federal Center
Box 25046, Mail Stop 967
Denver, Colorado 80225
(303) 236-1500

Investigations and Results

The Quick Epicenter Determinations (QED) continues to be available to individuals and groups having access to a 300-baud terminal with dial-up capabilities to a toll-free watts number or a commercial telephone number in Golden, Colorado. The time period of data available in the QED is approximately three weeks (from about two days behind real time to the current PDE in production). The QED program is available on a 24-hour basis, 7 days a week. From October 1, 1986 through March 31, 1987, we have had approximately 1737 log-ins.

The weekly publication, Preliminary Determination of Epicenters (PDE) continues to be published, averaging about 100 earthquakes per issue. The QED, PDE Monthly Listing and Earthquake Data Report (EDR) continue to be prepared on the VAX/1180 with very little down time encountered.

Telegraphic data are now being received from the USSR on magnitude 6.5 or greater earthquakes at this time. We had discussion with Aleksei Gvishiani during his visit with us in February.

Data from the People's Republic of China via the American Embassy are being received in a very timely manner and in time for the PDE publication. We continue to receive four stations on a weekly basis from the State Seismological Bureau of the People's Republic of China. The Bulletins with additional data are not being received in time for the Monthly. We have rapid data exchange (alarm quakes) with Centre Seismologique European-Mediterranean (CSEM), Strasbourg, France, and Instituto Nazionale de Geofisica, Rome, Italy, and data by telephone from Mundaring Geophysical Observatory, Mundaring, Western Australia and Japan Meteorological Agency (JMA).

The Monthly Listing of Earthquakes is up to date. As of March 31, 1987, the Monthly Listing and Earthquake Data Report (EDR) were completed through November 1986. A total of 6,354 events were published for the 6-month period. Solutions continue to be determined when possible and published in the Monthly Listing and EDR for any earthquake having an m_b magnitude $\geq$ 5.8. Centroid moment tensor solutions from Harvard University continue to be published in the Monthly Listing and EDR. Moment tensor solutions are being computed by the U.S. Geological Survey and are also published in the above publications. Waveform plots are being published for selected events having m_b magnitudes $\geq$ 5.8. Beginning with the month of October 1985, depths for selected events were obtained from broadband displacement seismograms and waveform plots published in the Monthly.

The Earthquake Early Alerting Service (EEAS) continues to provide information on recent earthquakes on a 24-hour basis to the Office of Earthquakes, Volcanoes, and Engineering, scientists, news media, other government agencies, foreign countries, and the general public. Fifty releases were made from October 1, 1986 through March 31, 1987. The most significant earthquake released in the United States during this reporting period was a magnitude 6.6 on January 5, 1987, in the Fox Islands, Aleutian Islands. Foreign earthquakes: magnitude 5.4 in El Salvador on October 10, 1986; magnitude 8.2 in the Kermadec Islands on October 20, 1986; magnitude 7.8 in Taiwan on November 14; and magnitude 6.9 in Ecuador on March 6, 1987.

Reports

Monthly Listing of Earthquakes and Earthquake Data Reports (EDR); six publications from June 1986 through November 1986. Compilers: W. Jacobs, L. Kerry, J. Minsch, R. Needham, W. Person, B. Presgrave, W. Schmieder.

Person, Waverly J., Seismological Notes: Bulletin of the Seismological Society of America, v. 76, no. 6, January-February 1986; v. 77, no. 1, March-April 1986.

Preliminary Determination of Epicenters (PDE); 26 weekly publications from October 3, 1986 through March 27, 1987, numbers 37-86 through 10-87.

Quick Epicenter Determination (QED) (daily): Distributed only by electronic media.

Person, Waverly J., Earthquake Notes, v. 56, no. 4, Significant Earthquakes of the World 1985.

Monthly Listing of Earthquakes - January, February, March (Microfiche): Seismological Research Letters. Compilers: W. Jacobs, L. Kerry, J. Minsch, R. Needham, W. Person, B. Presgrave, W. Schmieder.

Seismic Review and Data Services

9920-01204

James N. Taggart
Branch of Global Seismology and Geomagnetism
U.S. Geological Survey
Denver Federal Center
Box 25046, Mail Stop 969
Denver, Colorado 80225
(303) 236-1506

Investigations and Results

Technical review and quality control were carried out on 398 station months of seismograms from the Worldwide Standardized Seismograph Network (WWSSN). Photography of the first weekly delivery of seismograms (27 station months) by the new contractor was completed on January 15, 1987, three-and-one-half months after the beginning of the fiscal year. By the end of this reporting period, 126 station months had been photographed. Before photography, the National Earthquake Information Center uses the original seismograms to obtain additional arrival time and amplitude data for a few of the WWSSN stations. The seismograms also are checked for first-motions of earthquakes with magnitudes $\geq$ 5.8.

Over 4,500 microfiche copies of WWSSN seismograms and 58 reels of other microfilmed seismograms were supplied at cost to 24 researchers on special orders. Six standing orders for all films of WWSSN seismograms and two standing orders for Canadian Standard Network Seismograms have been received during FY 1987. Because delivery of the standing orders has not yet begun, only 21,000 copies of seismograms were supplied to the public during this reporting period.

Data Processing Section

9920-02217

John Hoffman
Branch of Global Seismology and Geomagnetism
U.S. Geological Survey
Albuquerque Seismological Laboratory
Building 10002, Kirtland AFB-East
Albuquerque, New Mexico 87115-5000
(505) 844-4637

Investigations

1. Data Management Center for the China Digital Seismograph Network. The Data Management Center in Beijing is completely installed and fully operational. Additional training in Albuquerque is scheduled for the director of the Data Management Center.

2. Installation of the Data Collection Center at the Albuquerque Seismological Laboratory. The Incorporated Research Institutions for Seismology (IRIS) have designated the Albuquerque Seismological Laboratory (ASL) to be the Data Collection Center (DCC) for a new global network of seismograph stations. Some new computer hardware has been installed and software conversion has been started.

3. Data Processing for the Global Digital Seismograph Network. All of the data received from the Global Network and other contributing stations are reviewed and checked for quality.

4. Network-Day Tape Program. Data from the Global Network stations are assembled into network-day tapes which are distributed to regional data centers and other government agencies.

Results

1. Data Management Center for the China Digital Seismograph Network. The Data Management Center, located in Beijing, China, is now processing all of the data received from the China Digital Seismograph Network (CDSN). The system is fully operational and the Chinese are now producing network-day tapes which contain all of the data recorded by the CDSN for a specific calendar day on one digital tape. In February 1987, the final hardware was installed which will copy the data received from the field stations onto small cartridges or 10-1/2 inch diameter magnetic tapes. This provides the Chinese with a backup system of copying the digital data, and also frees the computer system to process the seismic data and assemble it into network-day tapes. During this visit several modifications were made to the software system and all known bugs were eliminated. The Chinese computer operators were carefully trained in all aspects of processing the seismic data, and the operations program for the Data Management Center is basically complete. Maintenance of the system is more a difficult problem as it is only available through the Digital Equipment Corporation office located in

Hong Kong. Although a technician is located in Beijing, it is difficult to arrange for service due to export license restrictions and it is also expensive. The Chinese are forwarding copies of the digital data to the ASL where it is incorporated into the network-day tape program. We will continue to work with and assist the Chinese in the operation of their Data Management Center, but it should be considered fully operational at this time.

2. Installation of the Data Collection Center at the Albuquerque Seismological Laboratory. IRIS is planning to install a network of 50 or more seismograph stations around the world during the next five years. All of the data from this network will be forwarded to the DCC located at the ASL. As part of this program IRIS is funding much of the new hardware required by the DCC to process this large amount of data. During FY86 two MicroVax II computer systems, complete with disk memory and Ethernet communications, were purchased and installed at the ASL. Additional hardware is scheduled for procurement during FY87 consisting of a third MicroVax and more disk memory. The new MicroVax hardware will use the VMS operating system, and considerable software revision is required to upgrade our existing programs and also convert them for operation on VMS. The amount of data received at the ASL will increase by an order of magnitude from 30 megabytes per day to 300 megabytes per day over the next five years and the existing software must be considerably automated to handle this large amount of data. The DCC will be further expanded during the next several years to include a optical/laser disk storage system which will be used both as a online storage system and also as an archive for the seismic data.

3. Data Processing for the Global Digital Seismograph Network. During the past six months, 526 digital tapes (199 SRO/ASRO, 270 DWWSSN, and 120 CDSN) from the Global Network and other contributing stations were edited, checked for quality, corrected when feasible, and temporarily archived at the ASL. The Global Network is presently comprised of 12 SRO stations, 4 ASRO stations, and 14 DWWSSN stations. In addition, there are six contributing stations which include Glen Almond, Canada, plus the five stations from the China Network. The RSTN network which was supported by the Sandia National Laboratories was closed October 23, 1986.

4. Network-Day Tape Program. The network-day tape program is a continuing program which assembles all of the data recorded by the Global Digital Seismograph Network plus the contributing stations for a specific calendar day onto one magnetic tape. This tape includes all the necessary station parameters, calibration data, frequency response and time correction information for each station in the network. Copies of these tapes are distributed to several university and government research groups for detailed analysis.

National Strong-Motion Network: Engineering Data Analysis

9910-02760

A.G. Brady and G.N. Bycroft
Branch of Engineering Seismology and Geology
U.S. Geological Survey
345 Middlefield Road, MS 977
Menlo Park, California 94025
(415) 323-8111, ext. 2881 or (415) 329-5664

Investigations and Results

1. Differential Ground Motions: A method of calculating multi-degree-of-freedom differential spectra is being developed and will be applied to the various records obtained at the El Centro and Hollister differential arrays.

2. Soil Structure Interaction: The problem of the impact of a column on an elastic halfspace has been completed and a paper written. Further solutions to fundamental problems in soil structure interaction are continuing.

Reports

Bycroft, G.N., 1987, Impact of a column on an elastic half-space: to be submitted to the *Journal of Engineering Mechanics*, A.S.C.E.

Bycroft, G.N., and Mork, P.N., 1987, Differential spectra for the 1979 El Centro and the 1984 Morgan Hill earthquakes: *U.S. Geological Survey Pen-File Report 87-94*.

Bycroft, G.N., and Mork, P.N., 1987, Differential displacements and their spectra for the April 26, 1981 Westmorland and the January 26, 1986 Hollister earthquakes: *U.S. Geological Survey Open-File Report 87-63*.

National Strong-Motion Network: Data Processing

9910-02757

A.G. Brady
Branch of Engineering Seismology and Geology
U.S. Geological Survey
345 Middlefield Road, MS 977
Menlo Park, California 94025
(415) 323-8111, ext. 2881 or (415) 329-5664

Investigations

1. Routine Processing. The last of the records from the Chile earthquake and aftershocks, as obtained from Chile, has been processed and the Open-File report containing all the processed data is in final stages of completion.

   The local commercial digitizing company in use for more than ten years has undergone major ownership and managerial changes during the last several months, but recently restarted with effectively the same technical and scientific personnel. The records from the North Palm Springs earthquake (M 5.9, 8 July 1986) have been forwarded to the new company for digitizing.

   A set of records from two of the Coalinga aftershocks (September 9 and 11, 1983) has been selected in a study of topographical amplification--whether records at the crest of Anticline Ridge are significantly larger, and at which frequencies, than those of the surrounding flat ground.

   A course on earthquake engineering based on the routine record processing of this project was given over a two-week span in March, 1987 to participants in the one-year program at the International Institute of Seismology and Earthquake Engineering in Tsukuba, Japan.

2. Database. Work continues for the INGRES database on the DEC VAX. The incorporation of the strong motion permanent network data into the same database as the much more voluminous aftershock database (from temporary station locations) has allowed the main database design to be moved out of this project. As an interim measure, an Open-File Report describing ESM, the database containing descriptions of the strong-motion records acquired from the permanent network of strong motion instruments maintained by the USGS, has been published. The report is primarily a user's guide for the USGS staff but serves to inform non-USGS organizations about the database. An ESM update, maintenance and development guide has also been published.

Results

1. Routing processing, including digitizing (D), computer processing (P), and report preparation (R) of strong-motion accelerograms continues: 1 record (P, R) Chile mainshock of March 3, 1985; 8 records (D) two Coalinga aftershocks September 9 and 11, 1983.

Reports

Converse, April M., 1987, User's guide to ESM: a database for strong-motion information: *U.S. Geological Survey Open-File Report 87-160*.

National Strong Motion Data Center

9910-02085

Howard Bundock
Branch of Engineering Seismology and Geology
U. S. Geological Survey
345 Middlefield Road, MS 977
Menlo Park, California 94025
(415) 323-8111, ext. 2982

INVESTIGATIONS

The objectives of the National Strong Motion Data Center are to:

Maintain a strong capability for the processing, analysis and dissemination of all strong motion data collected on the National Strong Motion Network and data collected on portable arrays;

Support research projects in the Branch of Engineering Seismology and Geology by providing programming and computer support including digitizing, graphics, processing and plotting capabilities as an aid to earthquake investigations;

Manage and maintain computer hardware and software so that it is ready to process data rapidly in the event of an earthquake.

The Center's facilities include a VAX 11/750 computer operating under VMS Version 4.4, a PDP 11/70 running RSX-11M+ and two PDP 11/73 computers. The Center's computers are part of a local area network with other branch, OEVE, Geologic Division, and ISD computers, and we have access to computers Survey-wide over Geonet. Project personnel joined other office branches in the support of the OEVE VAX 11/785.

Investigations during the first six months of FY87 included further research into VAX/VMS compatible laser optical disk technology. A series of programs was further developed that read Digital Elevation Model data and use that data to plot surface contours, fault systems, and earthquake hypocenters for definition of fault planes; this elevation data can now also be plotted as color contour plots on our color graphics stations. Project personnel have developed and documented a complete procedure for digitizing and plotting map features such as fault lines, etc. The project has continued in in planning the forthcoming move to temporary quarters while asbestos fireproofing is removed from Buildings 7 and 8. The project continues its support of the OEVE VAX 11/785 project. As an ongoing policy, the project has kept its hardware up to current revision levels, and operating system, network, and other software at the most recent versions.

RESULTS

As a result of these and previous investigations, the project has:

Tested demonstration optical disk drives on the branch VAX 11/750 and the project is following the progress of both 12" and 5 1/4" disk technology so that we will be ready to purchase wisely when these systems have been fully developed. Compatibility and standardizing problems must be resolved before a purchase can be justified;

Instructed Branch scientists in the use of Digital Elevation Model data for plotting surface topography, faults and hypocenters in the Parkfield area and along the coast of southern California;

Instructed Branch scientists in the use of digitizing and plotting programs for storing and plotting San Francisco Bay Area fault lines and other surface features and data;

Successfully insured that Branch and Office computers remained up and running during asbestos removal from Building 7. No downtime on any Branch or Office computer has occurred as a result of the asbestos removal thus far.

Managed the OEVE VAX 11/785 and has joined with representatives from other Branches in managing the project.

Managed and maintained Branch computer system hardware and software.

REPORTS

none

Instrumentation of Structures

9910-04099

Mehmet Celebi
Branch of Engineering Seismology and Geology
U.S. Geological Survey
345 Middlefield Road, MS 977
Menlo Park, California 94025
(415) 323-8111, ext. 2394

Investigations:

1. The process of selection of structures to be recommended for strong-motion instrumentation has continued in Los Angeles, Orange County, New Madrid area, northeastern United States (Boston), Alaska, Hawaii, and Puget Sound (Seattle).

2. The process of designing instrumentation schemes for selected structures has continued. During this period, we attempted to obtain permits for instrumenting two structures, one in San Bernardino and the other in Alaska. We obtained the permit for San Bernardino Building and designed the instrumentation for it.

3. The process of actual instrumentation of structures has continued in Los Angeles (1100 Wilshire Finance Building) and in Charleston, SC (the Charleston Place). The strong-motion recording sytstems in these two buildings are now operational. Non-destructive testing of 1100 Wilshire Finance Building will take place soon.

4. New advisory committees are being formed. The newest committee formed covers Puget Sound Region (Seattle area). This effort will be extended to Portland, Oregon.

Results:

1. The Charleston Place Building in Charleston, SC -- recommended for strong motion instrumentation by the advisory committee -- is fully implemented.

2. The instrumentation scheme for the 1100 Wilshire Finance Building in Los Angeles -- recommended for strong-motion instrumentation by the advisory committee -- is fully implemented.

3. Report of the New Madrid area advisory committee for strong motion instrumentation has been completed and issued (OFR-87-59).

4. A draft of the report of the Alaska advisory committee for strong motion instrumentation of structures has been prepared. This report is now being reviewed by the committee members.

5. A draft of the report of the Los Angeles advisory committee for strong motion instrumentation of structures has been prepared. This report is now being reviewed by the committee members.

6. A draft of the report of the Boston area advisory committee for strong motion instrumentation of structures has been prepared. This report is now being reviewed by the committee members.

7. The Hawaii committee on strong motion instrumentation of structures is nearing completion of its deliberations.

Reports:

Celebi, M. (Coordinator) and Durbin, W. (Chairman), et. al., 1986, Report on recommended list of structures for seismic instrumentation in New Madrid (St. Louis) area: U.S. Geological Survey Open-File Report 87-59.

STRONG-MOTION INSTRUMENTATION NETWORK DESIGN, DEVELOPMENT, AND OPERATIONS

9910-02763, 02764, 02765

Edwin C. Etheredge
Richard P. Maley

Branch of Engineering Seismology and Geology
345 Middlefield Road, MS 977
Menlo Park, CA 94025
(415) 323-8111, ext. 2881

Investigations

The Strong-Motion laboratory, in cooperation with federal, state, and local agencies and advisory engineering committees, designs, develops, and operates an instrumentation program in 41 states and Puerto Rico. Program goals include: (1) recording of potentially damaging ground motion in regional networks, and in closely spaced sensor arrays; and (2) monitoring the structural response of buildings, bridges and dams using sensors placed in critical locations. The present coordinated network consists of approximately 1,000 recording units installed at 600 ground sites, 27 buildings, 5 bridges, 56 dams, and 2 pumping plants.

New Instrumentation

A 12 channel instrumentation system was completed at the 6-story, plus basement, Veterans Administration Hospital at San Diego (fig. 1). The present instrumentation replaces the former outdated system and includes three new sensors installed at the second floor level. The steel frame building is 450' x 450' square up to the second floor, topped by a cruciform shaped structure for the remaining five floors.

Three interconnected triaxial accelerographs were installed in the recently completed building 100 at the Seattle Veterans Administration Medical Center. The building is a rectangular 7-story steel frame structure, part of a three building complex with seismic separations between the units. Accelerographs are located in the interstitials above the 4th and 7th floors and in a basement tunnel. The instrumentation was jointly contributed by the U.S. Geological Survey and the Veterans Administration.

A five accelerograph system was completed at the Corps of Engineers Bonneville dam on the Columbia River at the Oregon-Washington boundary. Instrumentation is located in the main dam gallery and in two powerhouses.

Recent Earthquake Records

More than one hundred earthquake records were recovered during the past 6 months from instrumentation located in California and Hawaii. The following summarizes some of the more important results.

Earthquake Date	Magnitude	Location	Records	Peak Acceleration
14 January 1986	4.7	Bear Valley, CA Central CA	8	Ground .27 g Bear Valley Fire Station
9 March 1986	3.5	LaVerne, CA Southern CA	5	Ground >.05 g Structure .14 g (Live Oak Reservoir crest)
31 March 1986	5.7	Mt. Lewis, CA Near Fremont	12	Ground .09 g Structure .39 g (Livermore VA Hospital, 7th level)
21 November 1986 2333 GMT	5.1	Humboldt Cty, CA Northern, CA	7	Ground .28 g
2334 GMT	5.1	Humboldt, CA Northern CA	7	Ground .21 g

Figure 2 shows the records from the Livermore VA hospital recovered from the Mt. Lewis earthquake of 31 March 1986. The VA hospital building, completed in 1949, is a rectangular 6-story reinforced concrete structure 48 ft wide by 158 ft long. The foundation consists of spread footings resting on unconsolidated sediments. Triaxial accelerographs, interconnected for starting and time, are installed in the basement and on the 7th level (roof).

Recent Reports

Porcella, R., Etheredge, E., and Maley, R., 1986, Some strong-motion recordings of the 1986 North Palm Springs earthquake, Bull. Seism. Soc. Am. 76, p. 1844-1847.

Porcella, R., Etheredge, E., Maley, R., and Switzer, J., 1987, Strong-motion data from the July 8, 1986 North Palm Springs earthquake and aftershocks, U.S. Geological Survey Open-File Report 87-155, 37 p.

VETERANS ADMINISTRATION HOSPITAL
SAN DIEGO, CALIFORNIA

STRONG-MOTION INSTRUMENTATION

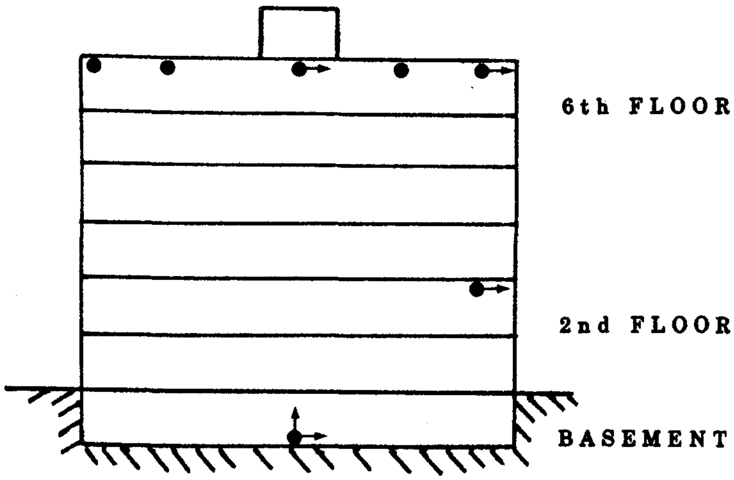

WEST-EAST SECTION

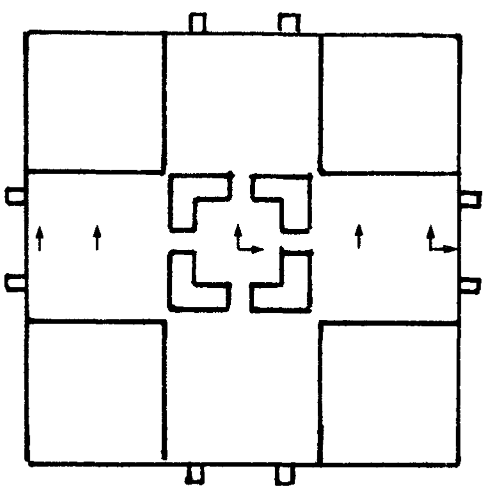

ROOF PLAN

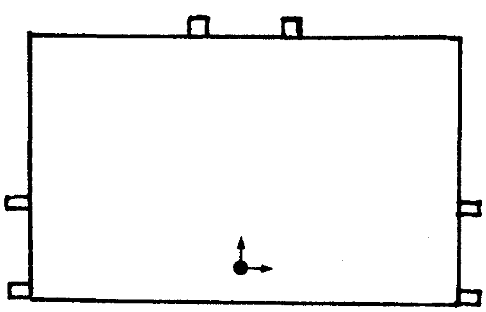

PARTIAL BASEMENT PLAN

ACCELEROMETER DIRECTIONS

● INTO PLANE OF SECTION/PLAN

→ AS SHOWN

FIGURE 1

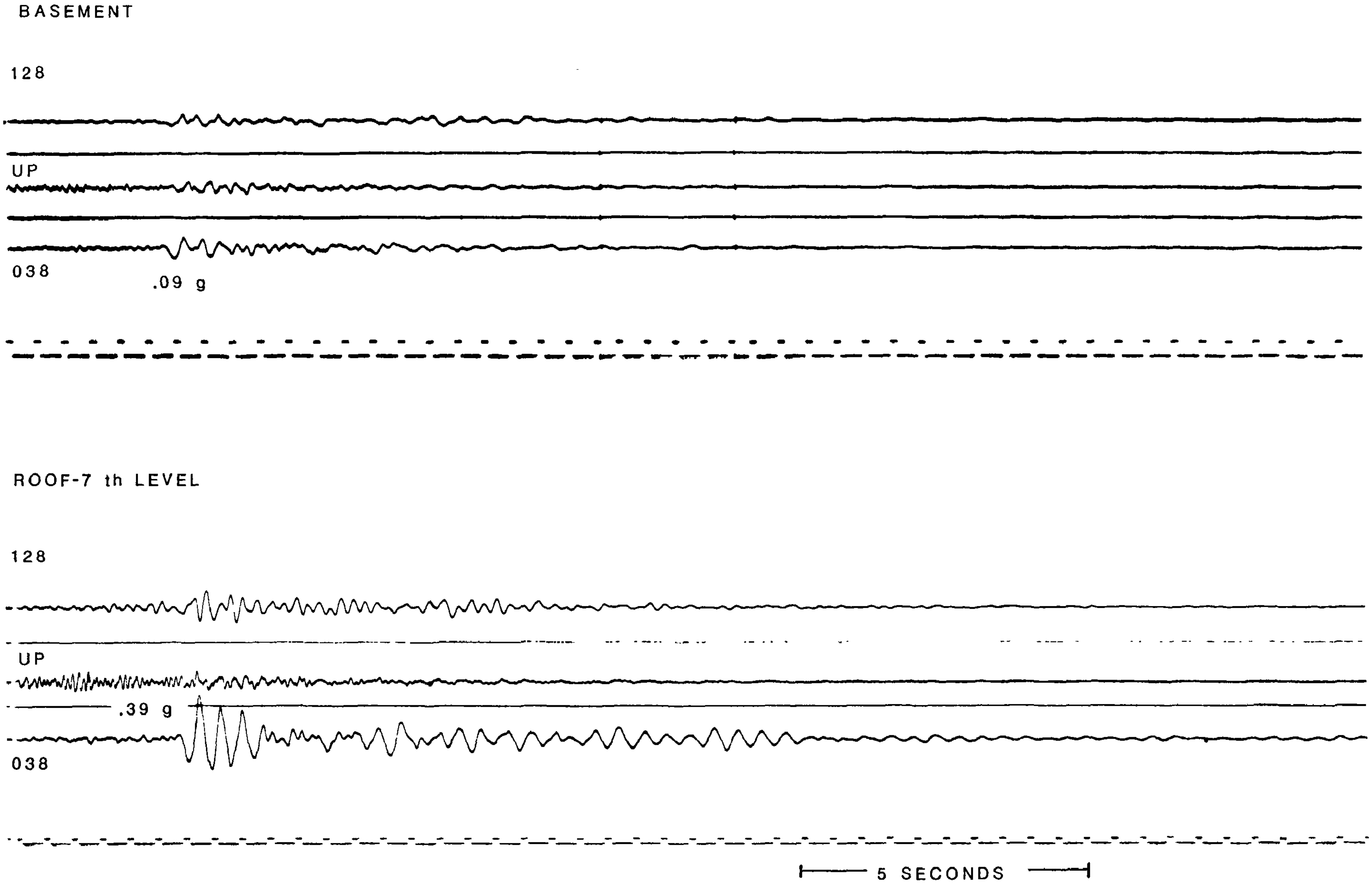

FIGURE 2. Livermore VA hospital. Earthquake of 31 March 1986

General Earthquake-Observation System (GEOS)
GEOS Analysis and Playback Systems (GAPS)

9910-03009

Gary L. Maxwell and Roger D. Borcherdt
Branch of Engineering Seismology and Geology
U.S. Geological Survey
345 Middlefield Road, Mailstop 977
Menlo Park, California 94025
(415) 323-8111 ext. 2318 or (415) 329-5618 (Maxwell)
(415) 323-8111 ext. 2910 or (415) 329-5619 (Borcherdt)

Investigations

1. Development and construction of a portable, low-power, broad band, high-resolution digital data acquisition capability for seismology and engineering (GEOS).

2. Development of mini- and micro-computer systems (hardware and software) for retrieval, processing, and archival of large volumes of digital data (GAPS).

3. Development of hardware and software components to improve functionalilty, versatility, and reliability for digital data acquisition and retrieval systems.

4. Improving methods for digitally recording broadband, low amplitude seismic signals (e.g. dilatational earth strain) at remote locations.

Results

Design features and modifications to the General Earthquake-Observation Systems (GEOS) incorporated or being investigated during this report period with assistance from M. Kennedy, J. Sena, E.G. Jensen, and J. VanSchaack include:

1. Continuation of Request for Proposal contracting process to construct an additional fifty-five recording units. Award and initiation of contract should commence during the next report period.

2. Completed design and test of new "Motherboard" and extended program memory modules intended to improve system reliability

and expand programmable functions within each recording unit.

3. Completion of software enhancement to allow for remote interrogation and parameter selection of each recording unit over a standard RS232C (TTY) connection. This improvement (together with use of new modules described above) will allow technicians to monitor and modify recorder status and parameters from a central location, improving efficiency of operations and reducing costs for travel to remote sites.

4. In-progress design of increasing capacity of semiconductor memory to retain collected seismic data. Improvements in this area will allow recording of seismic data in hostile environments or will facilitate store-and-forward data capture methods in seismic observatory settings.

5. Completed online evaluation of a digital multiple-bandpass seismic event detection algorithm utilizing Finite-Impulse-Response filtering methods developed by J. Evans and R. Cutler. This algorithm is designed to discriminate, detect, and record seismic signals that occur within narrowly defined frequencies.

6. Evaluation of efficient, regulated power components from various manufacturers for use in GEOS systems to improve signal-to-noise ratio at very high gain settings.

Reports (utilizing data recorded by GEOS and processed by GAPS)

Borcherdt, R.D., Glassmoyer, G, On the aftershock sequence of the earthquake of January 31, 1986 in northeastern Ohio; effects of bandwidth and local geology on observed high-frequency motion: Workshop on Earthquake Ground Motion Estimation in Eastern North America.

Structural Response in Support of National Strong Motion Program

9910-02759

Erdal Safak, Mehmet Celebi, A. Gerald Brady, and Richard Maley
Branch of Engineering Seismology and Geology
U.S. Geological Survey
345 Middlefield Road, MS 977
Menlo Park, California 94025
(415) 323-8111, ext. 2133

Investigations

1. Implementation of structural instrumentation and design of instrumentation schemes for structures selected by instrumentation advisory committees.

2. Develop methodologies and computer software to analyze ground motion and structural vibration recordings.

3. Continue on site response studies and structural damage correlation during the 3 March 1985 Chile earthquake.

4. Continue on structural characteristic evaluation during the 19 September 1985 Mexico earthquake.

Results

1. As part of structural response study efforts through strong-motion instrumentation, and in accordance with recommendations of committees, two new structures are now instrumented. These are the 1100 Wilshire Building (33 stories) in Los Angeles and the Charleston Place Building (8 stories) in Charleston, South Carolina. Instrumentation schemes for these two buildings were designed.

2. A computer program is being developed to identify source and site amplification of earthquake motions from ground motion recordings, and frequency, damping, and mode shapes of buildings from the ambient and earthquake vibration recordings.

3. After the 3 March 1985 Chile earthquake (M_s=7.8), and as a result of observation of damages on ridges, as well as alluvial and sandy sites, site response studies were conducted. The results showed that there were topographical and geological amplification and these two factors contributed to the patterns of responses observed during post-earthquake surveys. In addition, data obtained from structures are being studied.

4. Approximately 15 structures in Mexico City were tested in January 1986. Some of these structures were tested in 1962 also. Studies are being finalized on the changes of dynamic characteristics of these structures.

Reports

Safak, E., Celebi, M., Brady, G., and Converse, A., 1986, Recorded seismic response of three structures: ASCE Structures Congress, New Orleans, Louisianna, September 1986.

Scawthorn, C., Celebi, M., and Prince, J., 1986, Performance characteristics of structures, 1985 Mexico City earthquake: ASCE Mexico City Conference, September 19-21, Mexico City, Mexico.

Brady, G. and Celebi, M., 1986, Fundamental modal behavior of an earthquake excited bridge: III U.S. Conference on Earthquake Engineering, Charleston, South Carolina, August 1986.

Celebi, M., and Maley, R., 1986, Strong motion instrumentation of structures in Charleston, South Carolina and elsewhere: III U.S. Conference on Earthquake Engineering, Charleston, South Carolina, August 1986.

Celebi, M., and Safak, E., 1987, Earthquake response of an unique building in Vina del Mar, Chile (invited paper): Spring Conference, Society of Experimental Mechanics, June 14-19, 1987, proceedings.

Safak. E., and Celebi, M., 1987, On identification of site amplification from earthquake records (invited paper): Spring Conference, Society of Experimental Mechanics, June 14-19, 1987, proceedings.

Physical Constraints on Source of Ground Motion

9910-01915

D. J. Andrews
Branch of Engineering Seismology and Geology
U.S. Geological Survey
345 Middlefield Road, MS 977
Menlo Park, California 94025
(415) 329-5606

Investigations

Application of the diffusion equation to scarp degradation.

Implications of fault geometry for earthquake mechanics.

Results

A manuscript on degradation of profiles of shoreline scarps from Lakes Bonneville and Lahontan was revised for publication in J. Geophys. Res.

A computational effort is being planned to model the interaction of many fault segments with arbitrary orientations. Methods applicable to interacting frictional fault surfaces in both quasistatic equilibrium and dynamic motion are being considered and evaluated.

Reports

Andrews, D. J. and R. C. Bucknam, 1987, Fitting scarp degradation by a model with nonlinear diffusion, to appear J. Geophys. Res.

Andrews, D. J., 1987, Implications of energy absorption at rupture branches for the hypothesis of characteristic earthquakes (abs), Seismological Research Letters, 58, p. 24.

Strong Ground Motion Data Analysis

9910-02676

M. Andrews, J. Boatwright, J. Fletcher, and A. McGarr
Branch of Engineering Seismology and Geology
U. S. Geological Survey
345 Middlefield Road, MS 977
Menlo Park, California 94025
(415) 323-8111, exts. 2938, 2485, 2384, 2708
or (415) 329-5607, 329-5609, 329-5628, 329-5645

Investigations

1. Theoretical investigation of the earthquake rupture process.
2. Analysis of underground mine tremors.
3. Analysis of borehole recordings of earthquakes at Coalinga, CA.
4. Analysis of borehole recordings of earthquakes at Anza, CA.
5. Development of a three-component borehole seismometer system.

Results

1. A decomposition of the earthquake reupture process is presented in which the time-dependent rupture area Σ (t) is decomposed into a set of sub-event areas Σ_i which rupture at times τ_i. The slip associated with the stress release on Σ_i is calculated by modeling the sub-event as an asperity with the dynamic stress drop $\Delta\sigma_i$ and setting the stress drop on the complement of the sub-event area $\Sigma(t) - \Sigma_i$ equal to zero. The sub-event failure produces slip on both the sub-event area and the complement area. The moment release of the sub-event is proportional to $\Delta\sigma_i \ \Sigma_i \ \Sigma(\infty)^{1/2}$, while the radiated acceleration spectrum is proportional to $\Delta\sigma_i \ \Sigma_i^{1/2}$. Because the sum of the boundary conditions for the asperity subevents equals the boundary conditions for the composite event, the sum of the sub-event slips equals the slip for the composite event. The slip on the complement areas is proportional to the dynamic loading of the sub-event failure. The non-linearity of the constitutive relation between between traction and slip implies that the sub-event slip directions and healing times must be set equal to those of the composite rupture for the superposition to be exact. Relaxing these constraints gives small errors, how-

ever. Because the model parameters are reduced to the set of sub-event stress drops and rupture times, the decomposition yields a convenient basis for inverting seismograms to obtain the space-time distribution of stress release. to model the sub-event radiation, aftershock recordings are combined with results from 3D dynamic rupture models of the asperity failures. The sub-event models are iteratively refined as the rupture model evolves. The inversion process has been demonstrated for a $M_L = 5.5$ aftershock of the 1983 Coalinga, using a 3.6 M_L aftershock as a Green's function.

2. During November 1986, we deployed GEOS digital-event recorders on the surface and at depths of 1800 m and 300 m within the Western Deep Levels gold mine in South Africa. One hundred fifteen mine tremors ranging from $0 < M(M_0) \leq 3.0$ have been simultaneously recorded. In general, these tremors occur within 1 km of the nearest underground instrument; the propagation path to the surface is roughly 3 km. Using this data set combined with earlier studies of mine tremors, we hope to model the nature near-source, frequency-dependent attenuation and its contribution to the perceived breakdown in earthquake similarity observed as seismic moments decrease beneath 10^{20} dyne-cm. Preliminary analysis suggests that for these small events and thus for higher frequencies, attenuation over several km to the surface is an important factor but not the only one. Peak velocities recorded underground exceed those recorded at the surface typically by a factor of 1.4. But observed underground peak motions remain uniformly less than their theoretical values assuming similarity arguments. Assuming earthquake similarity and stress drops which are not a function of seismic moment, peak velocity scales according to the cube root of seismic moment, $R\underline{v} \propto M_0^{1/3}$. In contrast the underground data define a significantly stronger scaling, $R\underline{v} \propto M_0^{1/2}$. This appears to be a source effect limiting high-frequency radiation.

3. Aftershocks of the Coalinga, California EQ (May 2, 1983; $M_L = 6.7$) showed large frequency-dependent amplitude variations along a linear array extending from a soil site in the City of Coalinga to a rock site in the nearby foothills. To investigate these variations in ground motion, three-component uphole and downhole seismometers were installed in 100-meter-deep boreholes located at both ends of the array. More than 40 earthquakes, 10 to 50 km distant, were detected by the borehole sensors

and recorded on a broad-band system (GEOS). Comparisons of the uphole and downhole ground motions show that P-waves are 3 to 4 times larger at the ground surface than they are at a depth of 100 m. while S-waves are slightly less amplified. Uphole and downhole spectral ratios are dominated by interference peaks which are fairly stable for P and S waves at the alluvium site and for P-waves at the hardrock site; but which are quite variable for S-waves at the bedrock site. To determine near-surface attenuation, we calculated synthetic spectral ratios from simple plane-layered models based on the velocities measured in the boreholes. At the alluvium site, the models replicated the main features of the observed spectral ratios, yielding a Q_p between 5 and 10, and a Q_S of about 15. The modeling was less successful at the alluvium site, but the best fit suggested a Q_p between 10 and 15 and a Q_S between 15 and 20.

4. To study near-surface attenuation and amplifications of seismic body waves, the USGS recently installed two downhole instruments at station KNW of the seismic array at Anza, California. Each instrument contains three orthogonal geophones with natural periods of 0.5 Hz. The horizontal components are levelled to better than 0.1 degrees, which is necessary to prevent spurious resonances and asymmetrical clipping. The boreholes were drilled to depths of 150 and 300 meters in granite and the instruments were emplaced at the bottom of each hole. Co-sited with the boreholes are two surface instruments, which use the same sensors as the borehole instruments. All of the geophones are attached to GEOS digital event recorders, which sample the component 200 times a second with a dynamic range of 96 dB. During the first three months of operation over 30 events with seismic moments ranging from 10^{17} to 10^{20} dyne-cm were recorded on both downhole and surface instruments. Spectral ratios between recordings made at the surface and at 300 m depth show amplifications of up to a factor of 10 in the 10 to 40 Hz range little or no attenuation is apparent. The spectral signature of these ratios is made up of large spikes riding on top of a broader amplification which extends from about 1 to about 40 Hz. Spectral ratios between the 300 m and 150 m recordings are close to one in general, however, which suggests that most amplifications in the 10-40 Hz range raises questions regarding the validity of both attenuation studies and corner frequency estimates in this frequency range.

5. We have developed a borehole-seismometer system that has several advantages over previous designs. Compared to systems that use electronic feedback principles, ours uses simple geophone elements for transducers, has an inherent low noise, is simple to build, and is inexpensive. The disadvantages are a smaller dynamic range and a lack of response at long periods. Our main goal in building a new borehole package was to design an internal system for leveling horizontal geophones. Horizontal moving-coil geophones with a natural period greater than 0.5 s need to be leveled to better than 1.5 degrees in order to avoid nonlinear response and asymmetric clipping. In boreholes, where the axis of the package may well deviate from the vertical by more than 1.5 degrees, a special device is required for leveling. A gimbal stage was adapted from the design of ocean-bottom seismometers for leveling the two orthogonally orriented horizontal geophones: the geophones can be leveled to better than 0.1 degrees from a maximum initial tilt of 10.5 degrees. The external package is 14 cm in diameter and approximately 40 cm in length. The gimbal stage uses bendix cross-flexed hinges and suspends a brass pendulum (when unlocked) that houses the horizontal sensors. Two such seismometers, using Mark Products L-22D 2-Hz geophones, have been installed at the bottom of two boreholes 152 and 304 m deep, in granite at station KNW of the Anza digital array near Keenwild, California. Earthquake data have been gathered to study the effects of near-source spectrum. An experiment for determing near-surface attenuation, amplification, and anisotropy is currently underway using a controlled shear-wave source and the borehole geophones.

Reports

Andrews, M.C., and Borcherdt, R.D., 1987, Response of near-surface geology from uphole-downhole arrays at Coalinga, California [abs.]: EOS.

Bicknell, J., and McGarr, A., 1987, Underground recordings of mine tremors [abs.]: Earthquake Notes.

Boatwright, J., 1987, A dynamic decomposition of the earthquake rupture process [abs.]: EOS, in press.

Boatwright, J., 1987, Seismic radiation from composite models of faulting: Bulletin of the Seismological Society of America, in press.

Haar, L.C., Fletcher, J.B., Liu, H.-P., Warrick, R.E., and Westerlund, R.E., 1987, Near-surface effects at Anza: comparisons of surface and borehole data: Seismolgical Research Letters, v. 58, p. 26.

Haar, L.C., Fletcher, J.B., Liu, H.-P., Warrick, R.E., and Westerlund, R.E., 1987, Preliminary results from a borehole experiment at Anza, California, to investigate near-surface effects of seismic wave propagation: submitted to the Spring AGU meeting, Baltimore, MD.

Liu, H.-P., Warrick, R.E., Fletcher, J.B., and Westerlund, R.E., 1987, A three-component borehole seismometer for controlled-source and earthquake seismology: submitted to the Spring AGU meeting, Baltimore, MD.

Liu, H.-P., Warrick, R.E., Fletcher, J.B., and Westerlund, R.E., 1987, A three-component borehole seismometer for controlled-source and earthquake seismology: Seismolgical Research Letters, v. 58, p. 11.

Wennerberg, L., and Frankel, A., 1987, Site response and spectra of earthquakes determined from the Anza network, Seismolgical Research Letters, v. 58, p. 11.

Ground Motion Prediction for Critical Structures

9910-01913

D. M. Boore
W. B. Joyner

Branch of Engineering Seismology and Geology
U. S. Geological Survey
345 Middlefield Road, MS 977
Menlo Park, California 94025

Investigations Work was started on analyzing two different data sets not previously examined. These are the recordings of the Nahanni, Northwest Territories, Canada earthquakes of October, November, and December 1985, and aftershocks of the Tangshan, China earthquake.

Results

1. We have collected recordings of 9 events in the Nahanni region, ranging in size from M_s 4.9 to 6.9. The data include western Canadian digital network (WCTN), global digital network (GDSN), and strong motion accelerograph records (the latter for 3 events in December, 1985). We are in the process of computing spectral ratios of the events at WCTN stations, the purpose being to remove path effects and thereby illuminate the source scaling of the spectra. We also compared observed and predicted response spectra computed from records obtained at 2 sites within 10 km of the M_s 6.9 earthquake of 23 December 1985. The response spectra for both sites have been computed for the first 7 secs of the record, in order to exclude the contribution from a large but inexplicable burst of energy late in the record from site 1 (this energy is not present at site 2, which is situated 11 km from site 1 and, like site 1, is situated at the northern end of the rupture zone of the earthquake). The predictions have been made from the empirical results, largely using California strong-motion records (Joyner and Boore, 1982), and from the theoretically-based predictions of Boore and Atkinson (1987) for ground motions in eastern North America, who used the theoretical method outline in this paper. For the latter predictions, two distances have been used: the distance to the closest point of the rupture surface and the distance to the approximate center of the rupture surface. Both of the distances rely on my estimate of the location of the rupture surface, which I have based on aftershock locations (e.g., Weichert et al, 1986). The predictions are in reasonable accord with the observations, especially in view of the fact that the predictions are intended to be predictions of mean motions;

any one observation can be more than a factor of 2 from the mean (the standard deviation of individual observations is close to a factor of 1.8)

2. Many aftershocks of the Tangshan earthquake have been collected within a few tens of kilometers on digital instruments purchased and deployed as part of an NSF sponsored project for which David M. Boore was one of 3 principal investigators. Two scientists from the People's Republic of China visited the USGS for 3 months, starting on 5 December 1986, to help in analyzing the data. Of particular concern for this project were recordings made at the surface and at depths of 600 m and 900 m in a coal mine. Comparisons of the spectra and waveforms of these data should provide valuable information about near-surface amplification and attenuation effects. Preliminary processing of the data (including conversion of the data to the proper format, the construction of a catalog of waveforms, and relocation of hypocenters using P- and S-wave times read from the accelerograms) has been completed, and spectral ratios will soon be computed.

Reports

An report on the work being done on this project was presented at a workshop on ground motion estimation in eastern North America, organized by the Lawrence Livermore National Laboratory and held in Cambridge, Massachusetts in October, 1986.

Digital Data Acquisition for Strong Motion Seismology

9910-02089

Roger D. Borcherdt
James F. Gibbs
Branch of Engineering Seismology and Geology
345 Middlefield Road, MS 977
Menlo Park, Caliofrnia 94025
(415) 323-8111, ext. 2910 or (415) 329-5619

Investigations

Cooperative seismological and engineering studies to extend bandwidth and detection thresholds for a variety of active and passive experiments including: near-source strong motion, source mechanisms for aftershock sequences, velocity and Q^{-1} structure for crust and upper mantle, short-period earth strain, high-frequency wave propagation from downhole arrays, local-site amplification studies and earthquake engineering. This project, during the report period, has been responsible for the maintenance, operation, and deployment of wide dynamic range, broad band digital recorders (General Earthquake Observation System, GEOS) to acquire data sets for the cooperative studies indicated. This project has been conducted in conjunction with project 9910-03009 (see Maxwell and Borcherdt) with contributions from G. Sembera, J. Sena, C. Dietel, R. Warrick, G. Jensen, D. Myren, D. Hopkins, and T. Noce.

Results:

1. Maintenance laboratory; several improvements in laboratory maintenance procedures have been implemented by J. Sena. The maintenance lab has been reorganized to facilitate maintenance of the 45 GEOS currently in operation.
2. Cooperative digital array near Parkfield, CA. In cooperation with M. Johnston, A. Lindh, B. Bakun, T. Burdette and T. Noce an array of GEOS have been established to provide on-scale, broad-band, wide dynamic range recordings of volumetric strain and three-component ground motions for local and regional seismic events in the Parkfield region. Instrumentation has been installed at ten sites in the region in preparation for on-scale recordings of seismic radiation fields for events ranging in magnitude from about 2 to 6+.
3. Downhole Material Parameter determinations. In cooperation with M. Johnston, Ed Roth, Ron Porcella, Bob Westerlund and H.-P. Liu, we have made downhole measurements of shear and compressional waves at four locations prior to installation of Sacks'-Evertson dilatometers. The measurements were made at Stockdale Mountain, Jack Canyon, Red Hills and Vineyard Canyon. Data obtained will provide a determination of near-surface velocity structure as well as information Q in shallow materials. An experiment was conducted at the Vineyard Canyon site to see if anistrophy could be detected by rotating the shear-wave source 90° and repeating the downhole measurements. Preliminary analysis of data from Vineyard Canyon shows S-wave velocity variations of approximately 25% [perpendicular directions of the shear-wave source].

Reports

See related projects of Borcherdt, Gibbs, Johnston, and Maxwell.

4/87

Anelastic Wave Propagation

9910-02689

Roger D. Borcherdt
Branch of Engineering Seismology and Geology
U.S. Geological Survey
345 Middlefield Road, MS 977
Menlo Park, California 94025
(415) 323-8111, ext. 2755

Investigations:

1. Effects of an anelastic free surface on the physical characteritsics of inhomogeneous P, elliptical S, and linear S waves as recorded on co-located three-component seismometers and dilatometers.

2. Observation of short period volumetric strain (10^5 - 10^{-1}s).

3. High frequency (20 - 130 Hz) radiation near seismic sources.

Results:

1. Working in conjunction with G. Glassmoyer a general computer code (WAVES) was utilized to calculate anelastic reflection coefficients for displacement and volumetric strain, energy flow, and the physical characteristics of plane waves reflected by general P, type-I S, and type-II S waves incident on an anelastic free surface. The exact anelastic formulation with no low-loss approximations predicts that conversion of S energy to dilatational strain energy by the free surface is largest at angles of incidence for which inhomogeneity of this reflected P wave is near its physical limit (that is, amplitudes vary rapidly along surfaces of constant phase). For such angles of incidence in a low-loss anelastic half-space, the particle motions for the reflected P waves are elliptical, amplitudes increase near the surface with depth and phase propagation is not parallel to the free surface. Volumetric strain for a Rayleigh-type surface wave shows an exponentially damped sinusoidal dependence on depth not evident for a Rayleigh wave on an elastic half-space.

2. Short-period strain - In conjunction with M. Johnston and others (see Borcherdt and Gibbs; 9910-02089) dilatational earth strain, associated with the radiation fields for several hundred local, regional, and teleseismic earthquakes, has been recorded over an extended bandwidth and dynamic range at four borehole sites near the San Andreas fault, California. Catalogs of these data sets are being compiled with initial interpretation efforts concentrating on development of procedures to calibrate the volumetric strain meters at frequencies near the upper limit of the band width (1-10 Hz) for the sensors.

3. High-frequency seismic radiation - In cooperation with G. Glassmoyer, data from the ten-station array of portable digital instrumentation (GEOS) deployed to record the aftershock sequence of the moderate (m_b 4.9) earthquake that occurred on January 31, 1986 near Painesville, Ohio has been analyzed. High-resolution (16-bit; 96 dB), broadband (400 sps; 200 Hz) recordings of two of the larger aftershocks (m_b 2.2; 2.5) show that seismic signals as high as 130 Hz were resolvable above background noise levels at hypocentral distances up to 18 km. Spectral ratios computed with respect to "rock" site to estimate the amplitude response of local soil deposits at a site near Perry, Ohio suggest strong site resonances near 20 Hz and other resonances at frequencies exceeding 60 Hz. Modeling of the soil response based on two-dimensional anelastic wave propagation suggests that the exaggerated levels of shaking near 20 Hz could be due in part to response of near-surface soil layers to S energy incident at angles of incidence near 30 degrees. Accurate prediction of peak acceleration values at the site for the aftershocks requires characterization of the ground motions at frequencies as high as 80 Hz, which are beyond the bandwidth of conventional strong motion recorders and short-period networks.

Reports

Andrews, M., and Borcherdt, R., 1986, Response of near-surface geology as observed on uphole-downhole arrays in and near Coalinga, CA [abs.]: *EOS (American Geophysical Union Transactions)*, p. 1091.

Borcherdt, R.D., 1986, Characteristics of anelastic reflection-refraction coefficients with implications for calculation of synthetic seismograms: Proceedings, Indo-U.S. Workshop on Earthquake Disaster Mitigation Research, January 19-23, 1987, New Delhi, India, v. I, pp. IV-65-75.

Borcherdt, R.D., Fuis, G., and Mooney, W., 1986, Introduction--Three-component digital velocity and acceleration recordings made in conjunction with the PACE refraction experiment, L. Wennerberg (ed.): *U.S. Geological Survey Open-File Report 86-387*, 250 p.

Borcherdt, R.D., and Glassmoyer, G., 1987, On the aftershock sequence of the earthquake of January 31, 1986 in northeastern Ohio: effects of bandwidth and local geology on observed high-frequency ground motion: Proceedings, Workshop on Earthquake Ground Motion Estimation in Eastern North America, Los Altos, California.

Johnston, M.J.S., Borcherdt, R.D., Glassmoyer, G., Gladwin, M.T., and Lindh, A.T., 1986, Static and dynamic strain during and following the January 26, 1986 Quiensabe earthquake [abs.]: *EOS (American Geophysical Union Transactions)*, v. 67, p. 308.

Johnston, M.J.S., Borcherdt, R.D., Gladwin, M.T., and Lindh, A.T., 1986, Fault failure with moderate earthquakes in California [abs.]: *EOS (American Geophysical Union Transactions)*, v. 67, p. 1106.

Johnston, M.J.S., Lindh, A.T., Gladwin, M., and Borcherdt, R.D., 1986, Fault failure for moderate earthquakes (Japan and California): accepted *Tectonophysics*.

Seismic Waveform Analysis Project

7-9930-03790

Thomas H. Heaton
Branch of Seismology
525 S. Wilson Ave.
Pasadena, CA 91106

Investigations

The purpose of this project is to study seismic waveforms that are recorded principally in southern California or from southern California earthquakes. This project was previously called the Northwest U.S. Subduction Zone Risk Assessment Project and most of the work on this problem is complete. Many of the administrative and earthquake monitoring responsibilities of the Pasadena Field Office are also covered under this project.

1. Much of the work done under this project in recent years has involved the inversion of moderately large, discretely sampled, seismological data sets; usually consisting of local strong ground motion records and teleseismic body wave records. The purpose of these inversion studies has been to recover the spatial and temporal dislocation for specific earthquakes. The Householder algorithum (Lawson and Hanson, 1974) has been the work horse in all these matrix inversions. Recently we have tested two iterative schemes to re-evaluate the best numerical method to use with large matrixes.

2. Long and short-period GDSN P-waves are used to invert for three-dimensional dislocation models for the following earthquakes: 1) 1986 North Palm Springs, California, earthquake, 2) 1983 Borah Peak, Idaho, earthquake, and 3) 1985 Michoacan, Mexico, earthquake. These three events span the magnitude range from 5.9 to 8.0 and give us a good indication of how well faulting details can be resolved at different magitude levels.

3. We investigate the nature of seismic radiation from very large subduction earthquakes in the period range from several seconds to twenty seconds by studying teleseismic P-waves from historic earthquakes.

4. We endeavor to obtain the system response characteristics of the telemetered signals recorded on the Southern California Telemetered Seismic Network.

5. We investigate the characteristics of the seismic moment tensor by obtaining the closed-form solution for the problem of an arbitrary moment tensor embedded within two welded, Poisson-solid, half-spaces.

6. We investigate recent seismicity in the San Diego and surrounding area.

Results

1. The inversion of waveform data for a three-dimensional dislocation model can easily lead to a least-squares problem, Ax = b, where the size of the A matrix is several megabytes or much larger. The execution time for the Householder algorithum, which we have mostly used, is proportional to $mn^2 - n^3/3$, where m is the number of data and n is the number of unknowns. As the number of unknowns increases, the executive time increases dramatically. One solution to this problem is to invert in the frequency domain, where a series of smaller inversions can be performed at a set of equally spaced frequencies (Olson and Anderson, 1987). However, frequency domain inversion makes it difficult to apply spatial smoothing and other stabilizing constants. For this reason we prefer time domain inversions.

   In our investigation of other inversion algorithums we have tried the iterative Chebyshev accelerated convergence method of Olson (1986) and an iterative conjugate gradient method (Press et al., 1986). Both of these algorithums were modified to include a positivity constraint on the solution (no negative dislocations). The Chebyshev method and the conjugate gradient method gave nearly identical results as the Householder method for several test cases, but can be significantly faster depending on the size of the matrixes and the accuracy desired.

   A nonlinear parameterization can reduce the number of unknowns in the problem and thus reduce the execution time. Since we have no prior knowledge of when slip occurs on a particular fault segment, we must allow for the possibility of slip occurring over a wide time window. This parameterization leads to a problem with many unknowns. However, if we adopt a nonlinear parameterization where the rupture time as well as the size of the dislocation is solved for, much fewer unknowns are required. A nonlinear inversion code is being written and will be tested on the 1986 North Palm Springs earthquake strong motion and teleseismic data sets.

2. The constrained, least squares inversion technique of Hartzell and Heaton (1983) has been used to recover the distribution of dislocation for the 1986 North Palm Springs earthquake and the 1983 Borah Peak earthquake. Work on the 1985 Michoacan earthquake is presently being completed. The fault strike and dip are fixed from teleseismic focal parameters and we invert for the rake vector as a function of position. The rupture velocity is fixed at 80% of the shear wave velocity. The results for the North Palm Springs and Borah Peak earthquakes are shown in Figure 1. Six frames are displayed for each earthquake in which the dislocation is contoured in centimeters. The frames on the left show the distribution of disloction obtained from inverting just the GDSN long-period P-waves. The frames on the right show the dislocation for the simultaneous inversion of long- and short-period P-waves. The dislocation is broken up into strike-slip and dip-slip conponents

as well as the vectoral sum. The long-period GDSN records are only useful for estimating the duration and overall size of the dislocation (moment). The details in the distribution of dislocation are obtained from the short-period records. Both events are characterized by localized patches or asperities having larger dislocation. The inversion results obtained for North Palm Springs will be checked by an independent inversion of the strong ground motion data.

Figure 2 compares aftershock locations which have been projected perpendicularly onto the dipping fault plane of the North Palm Springs earthquake. Only 'A' quality locations have been used (Given, 1986) that are within 2 km of the fault plane. There is a tendency for the aftershocks to occur where the largest slip did not, such that the aftershocks loosely outline the patch of larger dislocation.

3. We have completed a manuscript (Hartzell and Heaton, 1987) describing our study of radiation of energy from very large subduction earthquakes. We compared teleseismic P-waves from earthquakes in the magnitude range from 6.0 to 9.5 with synthetics for a self-similar omega-squared source model and we found that the energy radiated by the very largest earthquakes (Mw > 8 ½) is not self-similar to that radiated from smaller earthquakes. Furthermore, in the period band from 2 seconds to several tens of seconds, we found that large subduction earthquakes have an average spectral decay rate of omega $^{-1.5}$. This spectral decay rate is consistent with previously noted tendency of the omega-squared model to overestimate Ms for large earthquakes.

4. Components that affect the response of individual stations of the telemetered southern California seismic network were compiled (Given et al., 1986). Computer codes were written to generate nominal instrument responses for each station. In addition, calibration pulses generated at the seismometer were recorded and investigated for some stations.

5. A closed form solution to the static problem of an arbitrary moment tensor located within two welded Poisson-solid half-spaces was derived. The solution has been checked for compatibility with boundary conditions. Future work will report on the behavior of double-couple point sources near interfaces.

6. Seismic activity in the coastal region adjacent to San Diego has increased dramatically since 1983 when compared with previous historic activity. At least two different clusters of seismicity have occurred in the immediate vicinity of San Diego and the largest concentration of activity is located about 70 km to the northwest (often referred to as the Oceanside sequence). The largest recent earthquake is the 13 July 1986 M 5.3 Oceanside earthquake. Similar increases in seismicity, that occurred prior to significant earthquakes in California, are also documented. It is speculated that the tectonic style in the continental borderland off of San Diego is very similar to that in the Basin and Range

Publications

Given, D.G., R. Norris, L.M. Jones, L.K. Hutton, C.E. Johnson, and S.H. Hartzell (1986). The southern California Network Bulletin, January through June, 1986, U.S. Geol. Surv. Open File Report. 86-598.

Hartzell, S.H., and T.H. Heaton (1987). Failure of self-similarity for large (Mw > 8 $\frac{1}{2}$) earthquakes, to be submitted to the Bull. Seism. Soc. Am.

Heaton, T.H. (1987). Anomalous seismicity in the San Deigo coastal region. U.S. Geol. Surv. Open-File Report with proceeding of the conference on intermediate-term earthquake prediction (Redbook), Monterey, CA, Nov., 1986.

Mendoza, C., and S. Hartzell (1987). Inversion for slip distribution using teleseismic body waves: North Palm Springs and Borah Peak Earthquakes, Seismological Research Letters, 58, 8.

References

Given, D. (1986). Master event relocations of the North Palm Springs earthquake sequence of July 1986, EOS, 67, 1089.

Hartzell, S.H., and T.H. Heaton (1983). Inversion of strong-ground motion and teleseismic waveform data for the fault rupture history of the 1979 Imperial Valley, California, earthquake, Bull. Seism. Soc. Am., 73, 1553-1583.

Lawson, L., and R. Hanson (1974). Solving least squares problems, Prentice-Hall, Englewood Cliffs, New Jersey.

Olson, A. (1986). A Chebyshev condition for accelerating convergence of iterative tomographic methods - solving large least squares problems, Phys. Earth Plan. Interiors, (submitted).

Olson, A.H., and J.G. Anderson (1987). Inferred models of earthquake rupture from frequency domain inversion of nearfield ground motions, Seismological Research Letters, 58, 8.

Press, W.H., B.P. Flannery, S.A. Teukolsky and W.T. Vetterling (1986). Numerical Recipes, Cambridge University Press, Cambridge.

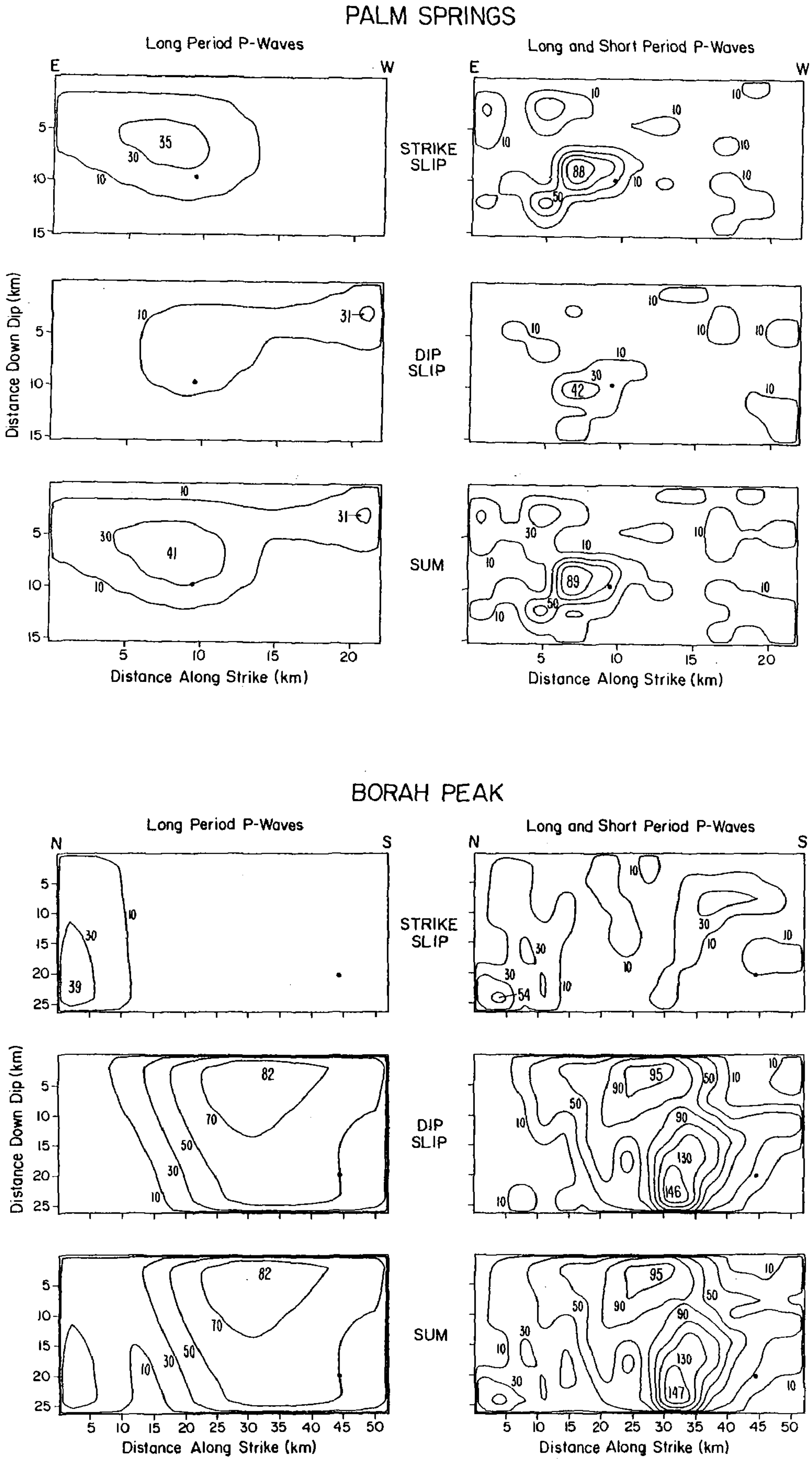

Figure 1. Contoured dislocation in centimeters for the 1986 North Palm Springs and 1983 Borah Peak earthquakes. The hypocenter is indicated by a small solid dot.

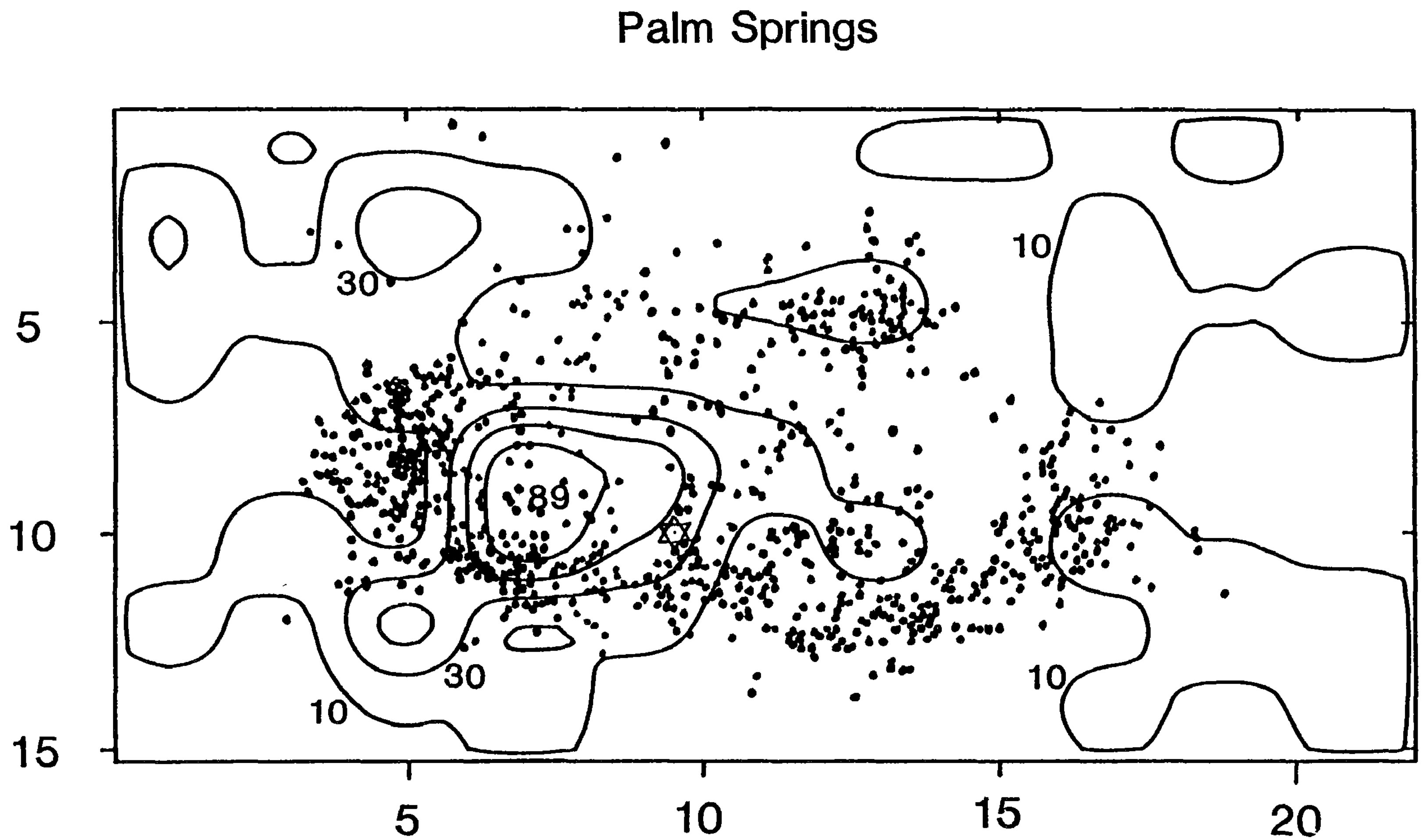

Figure 2. Comparison of aftershock locations, projected onto the plane of the fault, with the distribution of dislocation for the North Palm Springs earthquake. The main shock hypocenter is indicated by a star.

Velocity and Attenuation Measurements in Engineering Seismology

9910-02413

Hsi-Ping Liu
Branch of Engineering Seismology and Geology
U. S. Geological Survey
345 Middlefield Road, MS 977
Menlo Park, California 94025
(415) 853-8300 ext. 5643

Investigations

1. In-situ measurement of seismic shear-wave velocity and attenuation in the San Francisco bay mud. Seismic properties of near-surface earth materials have a significant effect on the earthquake ground motions. The September 19, 1985 Mexican Earthquake provides a striking example. Because of the amplification of ground motions caused by shallow lake deposits, considerable damages were sustained in Mexico City, more than 400 km away from the epicenter. In order to properly characterize the earthquake site response, seismic velocity and attenuation measurements are needed. It is straight forward to measure the compressional- and shear-wave velocities using first arrivals excited by appropriate compressional- or shear-wave sources. Seismic attenuation determination, on the other hand, involves amplitude measurements which can be influenced by many factors; systematic errors must be evaluated in order to obtain meaningful results. Sections of San Francisco bay mud having thickness greater than 20 m can be found on the west San Francisco bay shore from Redwood City to San Francisco. These sections of young bay mud lack horizontal stratification and are suitable for development of methodology for in-situ seismic attenuation measurements. Moreover, the San Francisco bay mud is an important earthquake engineering material whose in-situ physical properties need to be determined. At an undeveloped site in Foster City, California, we have been using a highly repeatable shear-wave generator (Liu et al., 1987a) and a vertical geophone string embedded in the bay-mud for the shear-wave attenuation measurements.

2. Installation of 2-Hz, 3-component borehole seismometers in the San Jacinto fault zone near Idyllwild, California. Several recent studies (e.g. Anderdon, 1986) have suggested that the spectra of small earthquakes can be strongly influenced by attenuation in the shallow crustal layers near the receiver. In oreder to study near-surface attenuation and site resonant-amplification effects on the earthquake spectra, we have installed two borehole seismometers in the San Jacinto fault zone near Idyllwild, California. Each instrument contains three orthogonal geophones having natural periods of 0.5 s. The horizontal geophones are leveled to 0.1 degrees, which is necessary to avoid nonlinear response and asymmetric clipping. The boreholes were drilled to depths of 150 and 300 meters in granite and the instruments were emplaced at the bottom of each hole. Co-sited with the boreholes are two surface instruments which use the same sensors as the borehole seismometers.

Results

1. Data reduction and analysis have been carried out for data collected on Sept. 22, 1986. Current methods of determining seismic attenuation using the first arrival pulse-width and rise-time are found to be in error because source spectra are not included in the analysis. A new method which includes the effect of source spectra has been developed and applied to the determination of shear wave attenuation in bay mud. A preliminary value of the seimic quality factor, Q = 21, has been obtained.

2. During the first three months of operation of the borehole seismometers in the San Jacinto fault zone, more than 30 events with seismic moments ranging from 10^{17} to 10^{20} dyne-cm were recorded on both downhole and surface instruments. Spectral ratios between recordings made at the surface and at 300 m depth show amplification of up to a factor of 10 in the 10 to 40 Hz range; little or no attenuation is apparent.

Reference Cited

Anderson, J. G., 1986, Implication of attenuation for studies of the earthquake source, Geophysical Monograph v. 37 (Maurice Ewing v.6), p.311 - 318.

Liu, H.-P., R. E. Warrick, R. E. Westerlund, J. B. Fletcher, and G. L. Maxwell, 1987a, An air-powered impulsive shear-wave source with repeatable signals, submitted to Bulletin of the Seismological Society of America.

Reports

Liu, H.-P., R. E. Warrick, J. B. Fletcher, and R. E. Westerlund, 1987b, A three-component borehole seismometer for controlled source and earthquake seismology, Seismological Research Letters, v. 58, p.11.

Haar, L. C., J. B. Fletcher, H.-P. Liu, R. E. Warrick, and R. E. Westerlund, 1987, Near surface effects at ANZA: comparison of surface and borehole data, Seismological Research Letters, v. 58, p. 26.

Strong Ground Motion Prediction in Realistic Earth Structures

9910-03010

P. Spudich
Branch of Engineering Seismology and Geology
U.S. Geological Survey
345 Middlefield Road, MS 977
Menlo Park, California 94025
(415) 323-8111, ext. 2395 or (415) 329-5654

Investigations

1. Development of an automated iterative procedure for determining earthquake rupture behavior based on near-source ground motion records.

2. Studies of the S wave coda of aftershocks of the 1984 Morgan Hill earthquake.

Results

1. In collaboration with G. Beroza of MIT, we have developed an iterative procedure for modeling strong motion records and finding rupture mechanisms. Ground motions are linearly related to the amount of slip on the fault but are nonlinearly related to rupture time. Consequently, to invert for rupture time, an iterative procedure is employed. Using the isochron formalism, it is computationally rapid to calculate the partial derivatives of seismograms with respect to rupture time and slip amplitude on the fault. The inverse of this partial derivative matrix is multiplied by 'residual' seismograms to obtain a perturbation to the current slip and rupture time model. We usually obtain convergence in 5-10 iterations. The inversion is stabilized by applying smoothness and positivity constraints to the slip perturbation. The positivity constraint is implemented using a penalty function method. Preliminary results for the 1984 Morgan Hill earthquake indicate that there was significant deceleration of the rupture under Anderson Dam.

2. Using an array analysis technique reported on previously, T. Bostwick and I have examined the composition of waves comprising the S wave coda in aftershocks of the 1984 Morgan Hill earthquakes. We examined the early coda, which is the part of the seismogram between the direct S wave arrival time and twice the S wave arrival time, at three seismic stations on considerably different site geologies. At all stations the early coda is dominated by waves that reverberate in a shallow region beneath the station. Coda-Q, however, is unaffected by the large station-to-station variations in geology, further substantiating the hypothesized deep lithospheric origin for codas waves.

Reports

Beroza, G., and Spudich, P., 1986, Iterative inversion for fault rupture using a high frequency, near source approximation [abs.]: *EOS*, v. 67, p. 1097.

Spudich, P., and Bostwick, T., 1987, Studies of the seismic coda using an earthquake cluster as a buried seismograph array: *Journal of Geophysical Research*, accepted.

Spudich, P., and Archuleta, R., 1987, Techniques for earthquake ground motion calculation with applications to source parameterization of finite faults, *in* Bolt, B.A. (ed.), *Seismic Strong Motion Synthetics*, Academiuc Press, Orlando, Florida, *in press*.

INDEX 1

INDEX ALPHABETIZED BY PRINCIPAL INVESTIGATOR

INDEX 2

INDEX ALPHABETIZED BY INSTITUTION

☆ U.S. GOVERNMENT PRINTING OFFICE 1987—788-412/79200